# Technical Advances in Minimally Invasive Spine Surgery

## Navigation, Robotics, Endoscopy, Augmented and Virtual Reality

Jin-Sung Kim
Roger Härtl
Michael Y. Wang
Adrian Elmi-Terander
*Editors*

MOREMEDIA
Springer

# Technical Advances in Minimally Invasive Spine Surgery

Jin-Sung Kim • Roger Härtl
Michael Y. Wang • Adrian Elmi-Terander
Editors

# Technical Advances in Minimally Invasive Spine Surgery

## Navigation, Robotics, Endoscopy, Augmented and Virtual Reality

Springer

*Editors*
Jin-Sung Kim
Department of Neurosurgery
Seoul St Mary's Hospital
The Catholic University of Korea
College of Medicine
Seoul, Korea (Republic of)

Roger Härtl
Department of Neurological Surgery
Weill Cornell Medicine Center for
Comprehensive Spine Care
New York Presbyterian OCH SPINE
New York, NY, USA

Michael Y. Wang
Department of Neurosurg & Rehab
Medicine
University of Miami Hospital
Miami, FL, USA

Adrian Elmi-Terander
Department of Neurosurgery
Karolinska University Hospital
Stockholm, Sweden

ISBN 978-981-19-0174-4 ISBN 978-981-19-0175-1 (eBook)
https://doi.org/10.1007/978-981-19-0175-1



This Springer imprint is published by the registered company Springer Nature Singapore Pte Ltd.
The registered company address is: 152 Beach Road, #21-01/04 Gateway East, Singapore 189721, Singapore

# Foreword

Publication of *Technical Advances in Minimally Invasive Spine Surgery: 2&3D Navigation, Endoscopy, Robotics, and AR & VR*, by Drs Kim, Hartl, Wang, and Terander, is not only timely, but it is a tremendously important contribution to spine surgery. When considering the current state of spine surgery, one could speculate that "minimally invasive spine surgery" is now relatively mature. "Image guidance" is in its adolescence; currently useful but continuing to develop. "Robotics, augmented and virtual reality," however, are in their infancy. What place they will assume in spine surgery and how they will contribute to the advancement of our discipline are completely unknown! That is why the assembly of these chapters into one tome is critically important. Each chapter is written by that techniques leading surgeon(s) and thought leader(s). By describing "beyond the state of the art" surgeries, and utilizing new and currently developing technologies, each author boldly demonstrates where recent developments are taking spine surgery. In doing so, it begs the reader to ask the questions which will guide us even further into the future. "What else can be done with this technique?" "How can we improve this technology even further?" "How can we utilize these techniques and technologies to make spine surgery safer and more effective for our patients?"

We are fortunate to be living in an exciting time in which our ability to skillfully care for patients with spinal pathology is advancing at a staggering rate. Just a few decades ago, the surgeries we routinely perform today were unimaginable. It is my hope that this book will stimulate the next generation of spine surgeons to continue this creative revolution and take us to the next "unimaginable" plane of spinal surgery.

Richard G. Fessler
Department of Neurosurgery
Rush Medical College
Chicago, IL, USA

# Foreword

Spine surgery continues to evolve at an extremely rapid pace, as spine surgeons strive to incorporate novel technology to advance patient care. Concomitantly, novel technology applied in the medical field is a natural fit for spine surgery given the complexity of the cases, the delicate nature of the neurological anatomical structures, and the importance of precise and accurate surgery, in order to correct spinal pathology with optimal outcomes. This knowledge requires the collection of the most contemporary information in a proper textbook, which grouped together will transfer this critical knowledge to spine surgeons throughout the world. I believe the goals of this comprehensive textbook are to assemble the current thought-leaders on these novel individual topics and combine them in a collection that will serve as an educational reference for the implementation of these novel techniques, for spine surgeon generations to come.

I have known all of the editors of this book for many years, and I highly respect each of them. If I were to create a list of the most cutting-edge spinal surgeons today, utilizing minimally invasive surgical techniques and robotics and navigation, the editors of this book would be at the top of the list. Each has a busy spine surgery practice, utilizing these newer techniques, and has developed a massive amount of expertise in their individual areas. Each is a highly sought-after speaker, educator, and leader in the world of spine surgery today. A project such as this textbook, led by this group of editors, can only be considered a significant work which will be seen as a landmark book for the current and next generation of spine surgeons.

This book comprises 43 chapters on novel techniques, with 94 authors involved, who are at the forefront of the topics being discussed. I am extremely impressed with the assembled author list, and choice of the topics, which lead the reader through the basics of contemporary minimally invasive surgery, all the way into the future of education and predictions of how this will look into the future. The book begins with a history of minimally invasive spinal surgery and how it evolved with the introduction of navigation. The basic foundations of the principles of minimally invasive spinal surgery are brought forth, even delving into applications into anterior and lateral approaches to the spine. The entire spectrum is discussed, from the cervical spine, all the way to the thoracic and lumbar spine. The topic of navigation-guided minimally invasive spinal surgery is then expanded in detail, discussing decompressive techniques with tubular retractors, and evolving into endoscopic approaches. This is then expanded into fusion techniques, using microscopic

and endoscopic approaches. Once again, the entire spine from the cervical down to the lumbar spine, is considered. The topic then progresses into robotics and the application of novel robotic technologies for minimally invasive spinal surgery. Once again, a comprehensive journey of robotics applied to the different areas of the spine, and for degenerative and deformities pathologies. The book finishes the topic of minimally invasive spinal surgery, with a look into virtual reality, and augmented reality for the same treatments, extending into future applications of education of these techniques.

I am personally extremely excited to present this contemporary collection of topics on minimally invasive spinal surgery, using the advances in current technology, to serve as a landmark reference and educational compilation, for spine surgeons today. I am delighted to see this effort led by such a distinguished and well-respected group of editors, and even more excited about the list of authors. I highly recommend this educational collection, for all spine surgeons today, not only to serve as an education on the most novel technologies for minimally invasive spinal surgery today, but also as a peek into the future of spine surgery and education.

In conclusion, the readers of this textbook are going to be treated to the entire gamut of minimally invasive spinal surgery using advances in modern technology, and I believe this will stimulate the younger generation of spine surgeons, to advance this topic into the future. I am confident that this will ultimately result in improved treatment outcomes for our patients suffering from spinal disorders.

Jeffrey C. Wang
USC Spine Center
Keck School of Medicine at
the University of Southern California
Los Angeles, CA, USA

# Preface

In our world of fast-paced technical advances, one may argue that a book on spine surgery relying on today's cutting-edge technologies will be outdated before it is printed. Indeed, technological developments occur at an ever-increasing speed. However, the human body does not, and in surgical specialties it is of great importance to recognize, understand, and implement those technologies which will bring the most benefit to the patients. Minimally invasive surgery, including endoscopy, has matured to become mainstream in spine surgery. Similarly, navigation, robotics, and augmented reality are frequently found in surgical centers. In this textbook, "*Technical Advances in Minimally Invasive Spine Surgery: 2&3D Navigation, Endoscopy, Robotics, and AR & VR*," we have relied on experts, using these technologies in their practices, to present their insights and experiences. The intended audience includes all with a particular interest in advanced spine surgery, ranging from medical students to experienced spine surgeons. To the student, the contents may serve as an introduction to a world where technology and medicine interact to improve outcomes. To the experienced spine surgeon, it may serve as a resource in the development of their own medical practice. The aim is to present a comprehensive and structured summary of the field and suggest what comes next based on current developments and unsolved issues. To this end, we, the editors, believe that the chosen format is best suited.

Seoul, Korea (Republic of) — Jin-Sung Kim
New York, NY, USA — Roger Härtl
Miami, FL, USA — Michael Y. Wang
Stockholm, Sweden — Adrian Elmi-Terander

# Contents

**Part II Navigation Guided MIS Decompressive Spinal Surgery**

**Part IV Augmented and Virtual Reality in Spine Surgery**



**Part V Augmented and Virtual Reality in Spine Surgery Training**

# List of Contributors

**Nicholas Ahye** Department of Neurosurgery, Minimally Invasive and Complex Spine Fellowship Program, Temple University Hospital, Lewis Katz School of Medicine, Temple University, Philadelphia, PA, USA

**Kutbuddin Akbary** Pushpawati Singhania Research Institute (PSRI), Press Enclave Marg, Sheikh Sarai, New Delhi, India

**Michelle Barrera Arreola** Department of Neurosurgery, The Brain and Spine Care, Minimally Invasive Spine Surgery Group, Spine Clinic, Hospital H+ Querétaro, Querétaro City, Mexico, Querétaro, Mexico

**Basar Atalay** Department of Neurological Surgery, Weill Cornell Medical College, New York-Presbyterian Hospital, New York, NY, USA

Department of Neurological Surgery, Weill Cornell Medicine, New York Presbyterian Hospital, New York, NY, USA

**Ufuk Aydinli** Verom Spine and Tumor Center, Bursa, Turkey

**Gregory Basil** Department of Neurological Surgery, University of Miami Miller School of Medicine, Miami, FL, USA

**Nathaniel Brooks** Department of Neurological Surgery, University of Wisconsin, Madison, WI, USA

**Gustav Burström** Department of Clinical Neuroscience, Karolinska Institutet, Stockholm, Sweden

Department of Neurosurgery, Karolinska University Hospital, Stockholm, Sweden

Department of Clinical Neuroscience, Karolinska Institute, Stockholm, Sweden

**Joseph A. Carnevale** Department Neurological Surgery, Weill Cornell Medicine Director, Weill Cornell Medicine Center for Comprehensive Spine Care New York Presbyterian OCH SPINE, New York, NY, USA

**Lung Chan** Department of Orthopedics, Guangzhou Red Cross Hospital Affiliated to Jinan University, Guangzhou, China

**Bo-Lai Chen** Guangdong Provincial Hospital of Chinese Medicine & Second Affiliated Hospital of Guangzhou University of Chinese Medicine, Guangzhou, China

Guangdong Provincial Hospital of Chinese Medicine & Second Affiliated Hospital of Guangzhou University of Chinese Medicine, Guangzhou, China

**Chien-Min Chen** Division of Neurosurgery, Department of Surgery, Changhua Christian Hospital, Changhua, Taiwan

School of Medicine, Kaohsiung Medical University, Kaohsiung, Taiwan

College of Nursing and Health Sciences, Dayeh University, Dacun, Taiwan

**Kuo-Tai Chen** Department of Neurosurgery, Chang Gung Memorial Hospital, Chia-Yi, Taiwan

**Hungtae Chung** Endoscopic Spine Surgery Center, Neurosurgery and Orthopedics, Seoul Bumin Hospital, Seoul, South Korea

**Claudia A. Covarrubias** Department of Experimental Surgery, McGill University, Montreal, QC, Canada

**Davide Croci**, **MD** Neurosurgery Clinic, Neurocenter of Southern Switzerland, Lugano, Switzerland

**Martina Dalolio**, **MD** Neurosurgery Clinic, Neurocenter of Southern Switzerland, Lugano, Switzerland

**Erik Edström** Department of Clinical Neuroscience, Karolinska Institutet, Stockholm, Sweden

Department of Neurosurgery, Karolinska University Hospital, Stockholm, Sweden

Department of Clinical Neuroscience, Karolinska Institute, Stockholm, Sweden

**Umut Elestekin** NOYA Enterprise, Istanbul, Turkey

**Adrian Elmi-Terander** Department of Clinical Neuroscience, Karolinska Institutet, Stockholm, Sweden

Department of Neurosurgery, Karolinska University Hospital, Stockholm, Sweden

Department of Clinical Neuroscience, Karolinska Institute, Stockholm, Sweden

**Haruki Funao** Department of Orthopaedic Surgery, School of Medicine, International University of Health and Welfare (IUHW), Narita, Chiba, Japan

**Danny P. Goel** UBC Department of Orthopedic Surgery, Vancouver, BC, Canada

PrecisionOS, Vancouver, BC, Canada

**Jacob L. Goldberg** Department Neurological Surgery, Weill Cornell Medicine Director, Weill Cornell Medicine Center for Comprehensive Spine Care New York Presbyterian OCH SPINE, New York, NY, USA

Department of Neurological Surgery, Weill Cornell Medical College, New York-Presbyterian Hospital, New York, NY, USA

Department of Neurological Surgery, Weill Cornell Medicine, New York Presbyterian Hospital, New York, NY, USA

**Christopher R. Good** Virginia Spine Institute, Reston, VA, USA

**Erin Graves** Department of Neurosurgery, Minimally Invasive and Complex Spine Fellowship Program, Temple University Hospital, Lewis Katz School of Medicine, Temple University, Philadelphia, PA, USA

**Yong Hai** Department of Orthopedic Surgery, Beijing Chao-Yang Hospital, Capital Medical University, Beijing, China

**Roger Härtl** Department of Neurological Surgery, Weill Cornell Medicine Center for Comprehensive Spine Care New York Presbyterian OCH SPINE, New York, NY, USA

**Dong Hwa Heo** Endoscopic Spine Surgery Center, Neurosurgery and Orthopedics, Seoul Bumin Hospital, Seoul, South Korea

**Young Ho Hong** Neurosurgery and Orthopedics, Bundang Barunsesang Hospital, Seongnam, South Korea

**Ken Ishii** Department of Orthopaedic Surgery, School of Medicine, International University of Health and Welfare (IUHW), Narita, Chiba, Japan

Spine and Spinal Cord Center, International University of Health and Welfare (IUHW) Mita Hospital, Tokyo, Japan

**Norihiro Isogai** Spine and Spinal Cord Center, International University of Health and Welfare (IUHW) Mita Hospital, Tokyo, Japan

**Tokumi Kanemura** Spine Center, Konan Kosei Hospital, Konan, Aichi, Japan

Department of Orthopedic Surgery, Spine Center, Konan Kosei Hospital, Konan, Aichi, Japan

**Siri Sahib S. Khalsa** Department of Neurosurgery, University of Michigan, Ann Arbor, MI, USA

**Bong-Soo Kim** Department of Neurosurgery, Minimally Invasive and Complex Spine Fellowship Program, Temple University Hospital, Lewis Katz School of Medicine, Temple University, Philadelphia, PA, USA

**Jin-Sung Kim** Department of Neurosurgery, Seoul St Mary's Hospital, The Catholic University of Korea, College of Medicine, Seoul, Korea (Republic of)

**Kyoung-Tae Kim** Department of Neurosurgery, School of Medicine, Kyungpook National University, Daegu, Republic of Korea

Department of Neurosurgery, Kyungpook National University Hospital, Daegu, Republic of Korea

**Sertac Kirnaz** Department Neurological Surgery, Weill Cornell Medicine Director, Weill Cornell Medicine Center for Comprehensive Spine Care New York Presbyterian OCH SPINE, New York, NY, USA

Department of Neurological Surgery, Weill Cornell Medical College, New York-Presbyterian Hospital, New York, NY, USA

Department of Neurological Surgery, Weill Cornell Medicine, New York Presbyterian Hospital, New York, NY, USA

**Vit Kotheeranurak** Queen Savang Vadhana Memorial Hospital, Thai Red Cross Society, Sriracha, Chonburi, Thailand

**Arvind G. Kulkarni** Mumbai Spine Scoliosis and Disc Replacement Centre, (Work done at Saifee Hospital), Mumbai, India

**Vignessh Kumar** Department of Neurological Surgery, University of Miami Miller School of Medicine, Miami, FL, USA

**Young-Seok Lee** Department of Neurosurgery, School of Medicine, Kyungpook National University, Daegu, Republic of Korea

Department of Neurosurgery, Kyungpook National University Chilgok Hospital, Daegu, Republic of Korea

**Yong-Jin Li** Guangdong Provincial Hospital of Chinese Medicine & Second Affiliated Hospital of Guangzhou University of Chinese Medicine, Guangzhou, China

**Guang-Xun Lin** Department of Orthopedics, The First Affiliated Hospital of Xiamen University, School of Medicine, Xiamen University, Xiamen, Fujian, China

Department of Clinical Medicine, Fujian Medical University, Fuzhou, Fujian, China

**Yong-Peng Lin** Guangdong Provincial Hospital of Chinese Medicine and Second Affiliated Hospital of Guangzhou University of Chinese Medicine, Guangzhou, China

Guangzhou University of Chinese Medicine, Guangzhou, China

**Jason I. Liounakos** Department of Neurological Surgery, University of Miami, Miami, FL, USA

**Yanting Liu** Department of Neurosurgery, Seoul St Mary's Hospital, The Catholic University of Korea, Seoul, South Korea

**Ryan Lohre** University of British Columbia Department of Orthopaedics, Vancouver, BC, Canada

**Yadhu K. Lokanath** Department of Neurosurgery, Aster RV Hospital, JP Nagar, Bangalore, Karnataka, India

**Xuexiao Ma** Department of Spine Surgery, The Affiliated Hospital of Qingdao University, Qingdao, China

**Akaworn Mahatthanatrakul** Department of Orthopaedics, Naresuan University Hospital, Phitsanulok, Thailand

**Lynn McGrath** Department Neurological Surgery, Weill Cornell Medicine Director, Weill Cornell Medicine Center for Comprehensive Spine Care New York Presbyterian OCH SPINE, New York, NY, USA

Department of Neurological Surgery, Weill Cornell Medicine, New York Presbyterian Hospital, New York, NY, USA

**Branden Medary** Department of Neurological Surgery, Weill Cornell Medical College, New York-Presbyterian Hospital, New York, NY, USA

Department of Neurological Surgery, Weill Cornell Medicine, New York Presbyterian Hospital, New York, NY, USA

Department of Neurological Surgery, New York-Presbyterian Hospital/Weill Cornell Medical Center, New York, NY, USA

**Kobina G. Mensah-Brown** Department of Neurosurgery, University of Pennsylvania Health System Penn Presbyterian Medical Center, Philadelphia, PA, USA

**Hiroaki Nakashima** Department of Orthopaedic Surgery, Nagoya University Graduate School of Medicine, Nagoya, Japan

**Raj Nangunoori** Department Neurological Surgery, New York Presbyterian Hospital/Weill Cornell Medical Center, New York, NY, USA

**Wataru Narita** Department of Orthopedic Surgery, Kameoka Municipal Hospital, Kameoka, Kyoto, Japan

**Lindsay D. Orosz** National Spine Health Foundation, Reston, VA, USA

**Jun Ouchida** Department of Orthopaedic Surgery, Nagoya University Graduate School of Medicine, Nagoya, Japan

**Paul Park** Department of Neurosurgery, University of Michigan, Ann Arbor, MI, USA

**Roberto J. Perez-Roman** Department of Neurological Surgery, University of Miami Miller School of Medicine, Miami, FL, USA

**Oscar Persson** Department of Clinical Neuroscience, Karolinska Institutet, Stockholm, Sweden

Department of Neurosurgery, Karolinska University Hospital, Stockholm, Sweden

Department of Clinical Neuroscience, Karolinska Institute, Stockholm, Sweden

**Eric Quach** Department of Neurosurgery, Minimally Invasive and Complex Spine Fellowship Program, Temple University Hospital, Lewis Katz School of Medicine, Temple University, Philadelphia, PA, USA

**Joseph Queenan** Department of Neurosurgery, Minimally Invasive and Complex Spine Fellowship Program, Temple University Hospital, Lewis Katz School of Medicine, Temple University, Philadelphia, PA, USA

**Diego Quillo-Olvera** Department of Neurosurgery, The Brain and Spine Care, Minimally Invasive Spine Surgery Group, Spine Clinic, Hospital H+ Querétaro, Querétaro City, Mexico, Querétaro, Mexico

**Javier Quillo-Olvera** Department of Neurosurgery, The Brain and Spine Care, Minimally Invasive Spine Surgery Group, Spine Clinic, Hospital H+ Querétaro, Querétaro City, Mexico, Querétaro, Mexico

**Pritem A. Rajamani** Mumbai Spine Scoliosis and Disc Replacement Centre, (Work done at Saifee Hospital),, Mumbai, India

**Si-Yuan Rao** Guangdong Provincial Hospital of Chinese Medicine & Second Affiliated Hospital of Guangzhou University of Chinese Medicine, Guangzhou, China

Guangzhou University of Chinese Medicine, Guangzhou, China

**Pradhyumn Rathi** Mumbai Spine Scoliosis and Disc Replacement Centre, Saifee Hospital, Mumbai, India

**Cameron Rawanduzy** Department of Neurological Surgery, New York-Presbyterian Hospital/Weill Cornell Medical Center, New York, NY, USA

**Javier Quillo Reséndiz** Department of Neurosurgery, The Brain and Spine Care, Minimally Invasive Spine Surgery Group, Spine Clinic, Hospital Star Médica Querétaro, Querétaro, Mexico

**Daiuke Sakai** Department of Orthopaedic Surgery, Surgical Science, Tokai University School of Medicine, Isehara, Kanagawa, Japan

**Kotaro Satake** Department of Orthopedic Surgery, Konan Kosei Hospital, Konan, Aichi, Japan

**Pietro Scarone**, **MD, PD** Neurosurgery Clinic, Neurocenter of Southern Switzerland, Lugano, Switzerland

**Franziska Schmidt** Department of Neurological Surgery, New York-Presbyterian Hospital/Weill Cornell Medical Center, New York, NY, USA

**Ethan Schonfeld** Neurosurgery AI Lab & Department of Neurosurgery, Stanford University School of Medicine, Stanford, CA, USA

**Sagar B. Sharma** Smt. SCL General Hospital, Ahmedabad, India

**Fabian Sommer** Department of Neurological Surgery, Weill Cornell Medical College, New York-Presbyterian Hospital, New York, NY, USA

Department of Neurological Surgery, Weill Cornell Medicine, New York Presbyterian Hospital, New York, NY, USA

Department of Neurological Surgery, New York-Presbyterian Hospital/Weill Cornell Medical Center, New York, NY, USA

**Annelise Sprau** Department of Neurological Surgery, University of Miami Miller School of Medicine, Miami, FL, USA

**Philipp Stefan** Medability GmbH, Munich, Germany

**Martin N. Stienen** Neurosurgery AI Lab & Department of Neurosurgery, Stanford University School of Medicine, Stanford, CA, USA

Department of Neurosurgery and Spine Center of Eastern Switzerland, Kantonsspital St.Gallen, St. Gallen, Switzerland

**Michael J. Strong** Department of Neurosurgery, University of Michigan, Ann Arbor, MI, USA

**Dong-won Suh** Neurosurgery and Orthopedics, Bundang Barunsesang Hospital, Seongnam, South Korea

**Masato Tanaka** Department of Orthopedic Surgery, Okayama Rosai Hospital, Okayama, Japan

**Alexandra E. Thomson** Virginia Spine Institute, Reston, VA, USA

Department of Orthopaedics, University of Maryland School of Medicine, Baltimore, MD, USA

**Takamitsu Tokioka** Institute of Neuroscience and Orthopedics, Okayama Kyokuto Hospital, Okayama City, Okayama Prefecture, Japan

**Luca Valci, MD** Neurosurgery Clinic, Neurocenter of Southern Switzerland, Lugano, Switzerland

**Anand Veeravagu** Neurosurgery AI Lab & Department of Neurosurgery, Stanford University School of Medicine, Stanford, CA, USA

**Sinan Vural** NOYA Enterprise, Oslo, Norway

**Chao Wang** Department of Spine Surgery, The Affiliated Hospital of Qingdao University, Qingdao, China

**Jeffrey C. Wang** Orthopaedic Spine Service, USC Spine Center, Los Angeles, CA, USA

Orthopaedic Surgery and Neurosurgery, USC Spine Center, Los Angeles, CA, USA

**Michael Y. Wang** Department of Neurological Surgery, University of Miami, Miami, FL, USA

Department of Neurological Surgery, University of Miami Miller School of Medicine, Miami, FL, USA

**Simon Weidert** Musculoskeletal University Center of LMU Munich, Munich, Germany

**Derong Xu** Department of Spine Surgery, The Affiliated Hospital of Qingdao University, Qingdao, China

**Andrew I. Yang** Department of Neurosurgery, University of Pennsylvania Health System Penn Presbyterian Medical Center, Philadelphia, PA, USA

**Jang W. Yoon** Department of Neurosurgery, University of Pennsylvania Health System Penn Presbyterian Medical Center, Philadelphia, PA, USA

**Chuanli Zhou** Department of Spine Surgery, The Third Affiliated Hospital of Sun Yat-sen University, Guangzhou, China

Centre for Minimally Invasive Spinal Surgery, Affiliated Hospital of Qingdao University, Qingdao, China

# Part I

# Navigation Guided Spinal Fusion

# History of Navigation Guided Spine Surgery

1

Jacob L. Goldberg, Sertac Kirnaz, Joseph A. Carnevale, Lynn McGrath, and Roger Härtl

## 1.1 Introduction

Spinal surgery has undergone a rapid transformation over the past 30 years largely driven by technological advances in image-based intraoperative navigation. In traditional open instrumented spinal surgery, screw trajectory is estimated after exposing both the screw entry point and the nearby relevant surgical landmarks. For example, in placing cervical lateral mass screws, the surgeon will only be certain of their entry point and trajectory if they have exposed the full extent (including lateral aspect) of the lateral masses and are able to visualize or palpate the superior and inferior articulating processes. This level of assurance is required to ensure instrumentation is durably placed and injury is avoided to the spinal cord, nearby neural elements, and critical vasculature. Unfortunately, this technique is not ideal. It requires large incisions and significant tissue trauma. Further, in cases of severe pathology, trauma, or deformity, the normal trajectories/anatomical relationships can be distorted resulting in screw misplacement. The adaptation and rapid evolution of image-based navigational techniques have allowed spinal instrumentation to move toward minimal exposure as the surgeon's reliance on anatomical knowledge/relationships can be augmented with navigation diminishing the need for direct visualization. The result is less invasive surgery. Minimally invasive spine (MIS) surgery has been demonstrated to decrease blood loss, duration of hospital admission, and decrease postoperative narcotic use [1, 2]. Here we will briefly review the history of navigation guided spinal surgery particularly as it relates to minimally invasive instrumented fusion and discuss the currently available imaging techniques and navigation technologies (Fig. 1.1).

## 1.2 Single and Biplanar Fluoroscopy (Non-navigated)

Early uses of intraoperative fluoroscopy-based MIS percutaneous instrumentation techniques were described in the lumbar spine (wider pedicles and no spinal cord) and later described in the thoracic and cervical segments. C-arm fluoroscopy remains a widely used modality for placement of percutaneous pedicle screws. In these techniques, since anatomic landmarks are not directly visualized, their success and safety depend on visualizing the landmarks via fluoros-

J. L. Goldberg · S. Kirnaz · J. A. Carnevale · L. McGrath · R. Härtl (✉)
Department of Neurological Surgery, Weill Cornell Medicine Center for Comprehensive Spine Care New York Presbyterian OCH SPINE, New York, NY, USA
e-mail: jag9177@nyp.org; sek2024@med.cornell.edu; joc3003@nyp.org; lbm9009@med.cornell.edu; roh9005@med.cornell.edu



J.-S. Kim et al. (eds.), *Technical Advances in Minimally Invasive Spine Surgery*,
https://doi.org/10.1007/978-981-19-0175-1_1

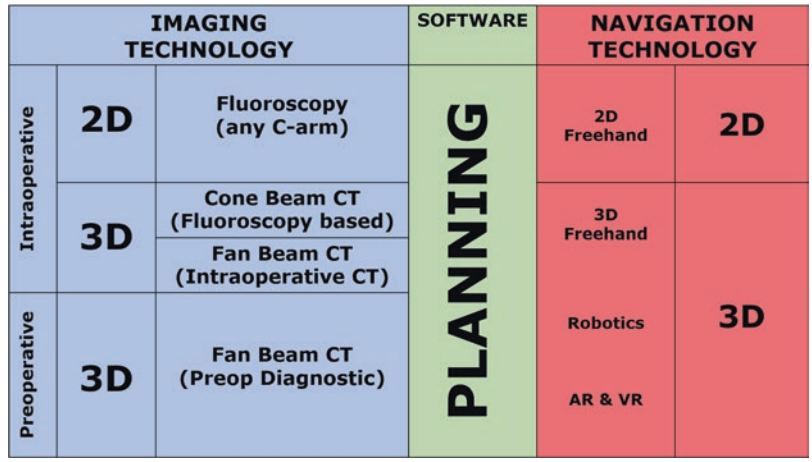


**Fig. 1.1** Imaging techniques and navigation technology in widespread use in minimally invasive spine surgery

copy. For example, when placing lumbar pedicle screws, the anterior-posterior (AP) fluoroscopy is acquired such that the spinous process is midline, vertebral body endplates are even, and pedicles are easily identifiable. Next, using a combination of AP and lateral fluoroscopy, Jamshidi needles are placed on the lateral margin of the pedicle and advanced into the vertebral body and removed leaving behind a k-wire guide allowing the remainder of the procedure to occur via cannulated instrumentation over the k-wire guide.

There are advantages and limitations to the fluoroscopically guided but non-navigated techniques. Important advantages include low upfront costs associated with necessary equipment, relatively fast learning curve, ability to use the equipment in a variety of different procedures across the hospital. In addition, this method (more so than intraoperative CT) involves essentially real-time imaging. A notable limitation with this technique is decreased accuracy in relation to navigated methods. Though accuracy across studies is difficult to compare, a study evaluating 346 screws in 72 patients found "perfect" pedicle screw placement in 65% of cases compared with a rate of 90% in 176 screws placed in 39 patients with the use of a navigated robot [3]. Another limitation is the reliance on k-wires to guide screw placement. Pedicle breach by screw or k-wire can result in serious complications including dural perforations resulting in leakage of cerebrospinal fluid, injuries to the bladder and other abdominal organs, injury to the great vessels, and cardiac tamponade [4, 5]. Another important drawback is increased radiation exposure to the surgical team. A representative meta-analysis examining 785 patients in 11 clinical studies found that radiation exposure time doubled when using fluoroscopic guidance compared with "free hand" pedicle screw placement [6].

## 1.3 Navigated Two-Dimensional Fluoroscopy

Two-dimensional navigation built on the foundations of single and biplanar fluoroscopic methods and incorporated 2D computer-assisted navigational guidance. Similar to frameless navigation techniques employed in cranial surgery, these techniques rely upon the application of a reference frame set in a fixed position to the surgical field with tagged instruments which can be tracked with regard to their relation to the surgical field. After intraoperative fluoroscopic images are acquired the surgical tools, designed with light-emitting diodes, can be detected by a camera and virtually projected onto the fluoroscopy monitor to correspond 2-dimensionally with the imaged anatomy. This technique was well described by Foley et al. [7]. Foley demonstrated an acceptable degree of accuracy in an in vitro model between the tips and trajectories of virtual and the fluoroscopically imaged probes with the mean error being 0.97 mm and 2.7 degrees, respectively. They verified an additional benefit

to this method finding no detectable radiation exposure to the surgeon.

Though this technique represented a significant step forward, it has several limitations. Most notably, this method of application of fluoroscopy supported a two-dimensional "virtual" navigation system which can more easily lend itself to errors and misinterpretations compared with a full three-dimensional rendering. Additionally, this system is susceptible to all of the factors which diminish fluoroscopic image quality such as interference from radio-opaque materials or obesity.

## 1.4 Fan Beam and Cone Beam Computed Tomography-Based Three-Dimensional Navigation

Increases in the availability of fast computer processor speeds, navigational software, and mobile fan beam and cone beam image acquisition platforms have led to widespread adaptation of 3D navigational techniques. With these techniques, an array is rigidly fixed to the patient either via fixation to a pinned skull clamp (cervical) or fixed to a spinous process (any spinal segment) or iliac crest (thoracolumbar) and imaging is acquiring intraoperatively via intraoperative CT (fan beam) or C-arm/O-arm (cone beam) techniques. Figure 1.2 depicts one of the available fan beam intraoperative CT systems available (AIRO ©, Brainlab) with an integrated flat Jackson table. After acquisition of intraoperative CT, a wide variety of surgical tools with arrays rigidly affixed can be visualized in 3D on monitors displaying the intraoperatively acquired scan (Fig. 1.3). This represents an important advance as it decreases reliance on k-wires. Lian et.al described the concept of "total navigation" which is a combination of intraoperative 3D navigation with portable intraoperative CT scanner [8]. Studies have demonstrated an improved workflow and increases in the safety, accuracy, and efficiency of minimally invasive spinal procedures [9–11].

Three-dimensional real-time rendering allows for an easier conceptualization of 3-D anatomy and a high degree of accuracy. During pedicle screw placement, the surgeon can monitor inline axial, sagittal, and coronal views to ensure optimal trajectory (Fig. 1.4). Additionally, the ability to perform scans after instrumentation has been placed but while the patient is still in the operating room allows for misplaced instrumen-

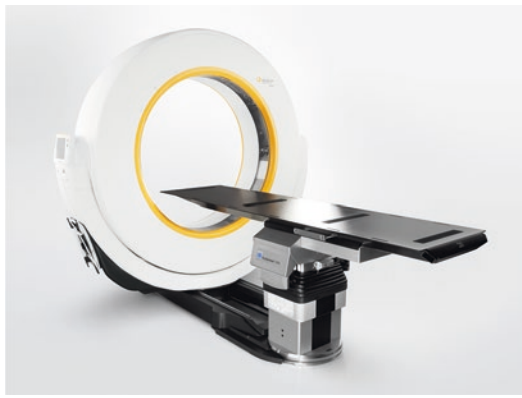

**Fig. 1.2** Intraoperative fan beam CT scanner (AIRO©, Brainlab) with integrated operating table. Image copyright owned by Brainlab, used with permission

**Fig. 1.3** Intraoperative infrared camera, computer, and monitor (Curve@, Brainlab). The infrared camera tracks reflective material placed on surgical instruments as well as a reference array rigidly affixed to the patient. The computer and associated software create 3-D projections depicting the surgical instruments relative to the patient's intraoperatively acquired anatomy. Image copyright owned by Brainlab, used with permission

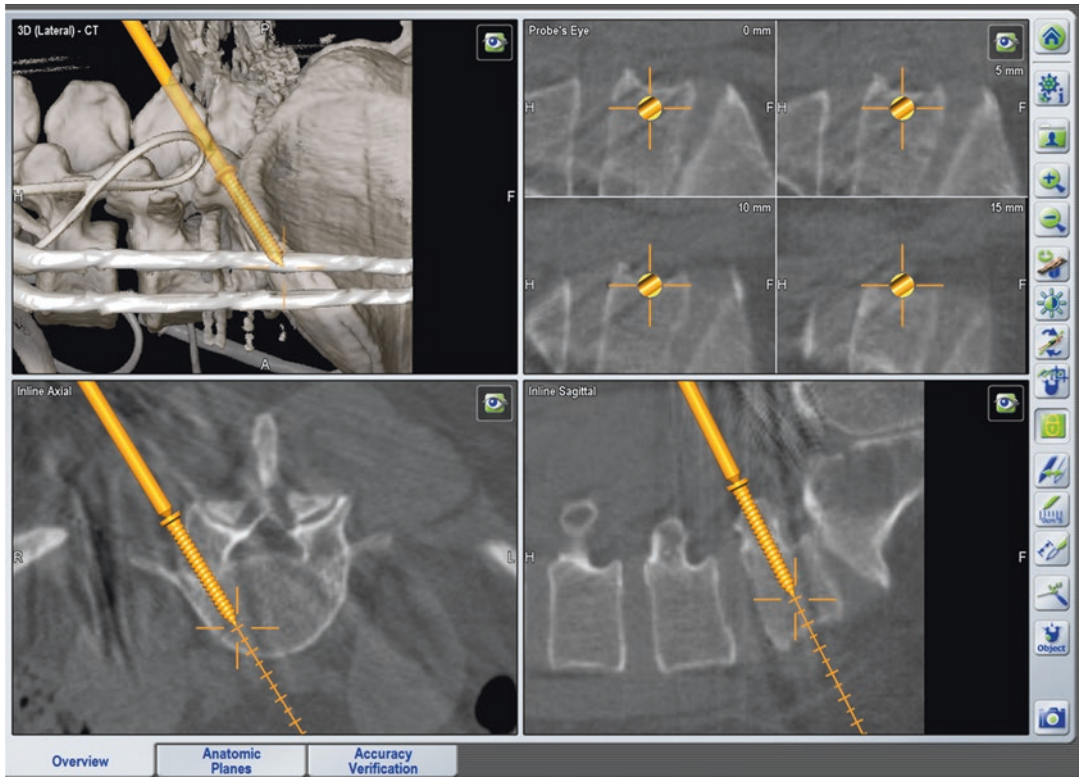


**Fig. 1.4** Display of intraoperative monitor demonstrating the 3-D rendering and instrument tracking during 3-D navigated pedicle screw placement

tation to be revised without a return to the OR (and its associated costs and morbidities) [12]. In all regions of the spine the use of navigation (compared with non-navigated techniques) is associated with a lower risk for pedicle breach [13]. Notable drawbacks include high up-front equipment costs and a surgical workflow learning curve. Sclafani et al. reported a learning curve related to operation speed when using 3D navigation but importantly found that accuracy with these techniques was high and remained high throughout the learning process [14].

## 1.5 Robotics

Robotic spinal surgery builds on the computer generated 3D navigational techniques by employing a robotic arm (fixated to the floor or table) capable of aligning with a planned starting point and trajectory. Reports have described a significant but surmountable learning curve [15] but a high degree of accuracy is achievable for pedicle screw placement [16]. The significant limitation in robotics had been their reliance on preoperative image acquisition and preoperative planning. Next generation robotics capable of integrating intraoperatively acquired images have the potential to broaden the application of robotics. An example of integration with fluoroscopy-based (cone beam) CT and true intraoperative CT (fan beam) is shown in Fig. 1.5.

## 1.6 Augmented Reality and Virtual Reality

Augmented reality systems overlay preoperatively identified anatomical structures, idealized screw locations/trajectories, or lesions, superim-

**Fig. 1.5** Example of intraoperative setup integrating robotic arm with intraoperative imaging. Left panel: Ziehm© cone beam CT and Cirq© Brainlab robotic arm affixed to surgical table. Right panel: robotic arm affixed to surgical table with true intraoperative AIRO© CT in background. Image copyright owned by Brainlab, used with permission

**Fig. 1.6** Intraoperative microscope with rigidly affixed reference array tracked by infrared camera to allow augmented reality projections to be visible in real time in the microscope eye piece. Image copyright owned by Brainlab, used with permission

posed on the anatomy visualized in the OR via projections in operative microscope eyepiece or specialized goggles. Among other capabilities, this technology allows relevant structures to be identified on preoperative MRI scans to be merged with intraoperatively acquired CT. The fixation of a rigid reference array to the microscope (in addition to the patient and surgical instruments) allows these projections to be viewed in 3-dimensions in the correct anatomic place (Fig. 1.6). When applied to minimally invasive spinal surgery, this allows the surgeon to orient themself in terms of trajectory and anatomy which can become obscured while operating through small tubes when the lesion of interest is not encountered in the field of view. For example, trajectory planning and re-orientation can be augmented in tubular transforaminal lumbar interbody fusion projecting anatomical landmarks via microscope eyepiece in their idealized location (Fig. 1.7). Intradural tumors can be identified with their idealized location and borders visible via the microscope eye before the lesion is encountered and throughout the resection (Fig. 1.8). A wide range of applications of this capability are imaginable and actively under investigation [17, 18].

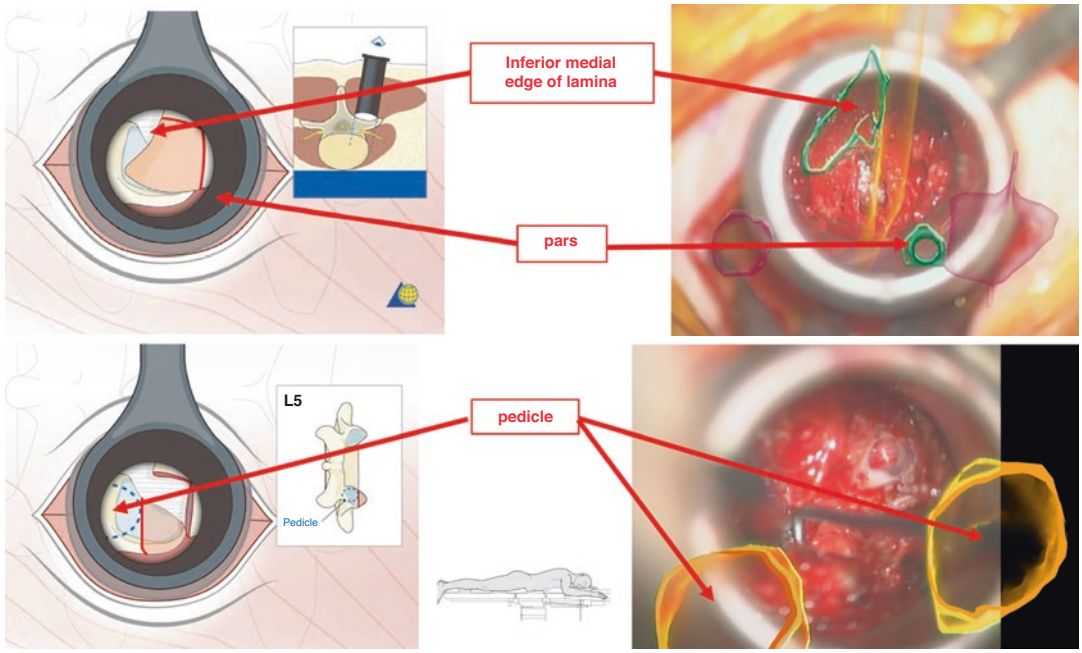


**Fig. 1.7** Visualization of TLIF landmarks. Panel on the left: illustrations highlighting orientation and relation of tubular retractor to important landmarks during tubular TLIF. Right panel: intraoperative view through operative microscope during tubular TLIF with overlay of surgical landmarks via augmented reality

Virtual reality, viewing and manipulating 3D renderings, has been used for simulation, teaching, and training purposes in a variety of medical settings as well as other industries given its ability to simulate real world situations in a safe learning environment. One group has reported the use of VR in preoperative planning transpedicular corpectomy and reported satisfaction with their ability to preoperatively determine degree of necessary bone removal and cage diameter and reported no serious complications [19]. Its educational potential was separately elucidated in a study demonstrating an improvement in accuracy in cervical lateral mass screw placement among trainees participating in a VR simulation compared with those taught in the traditional fashion [20].

## 1.7 Conclusion

Over the past 30 years, spinal surgery has undergone rapid change specifically with the widespread use of instrumentation and push toward minimally invasive techniques which has been made possible in large part due to the evolution of image-based navigation. New technologies have rapidly been synergistically incorporated into the operating room in order to increase the cost effectiveness and efficiency of surgery as well as improve safety with respect to both the patient (with increased accuracy) and the surgical team (with decreased radiation exposure). Augmented reality is now being rigorously tested and showing promise to further enhance spinal surgery and virtual reality is being developed to train the future generation of spinal surgeons.

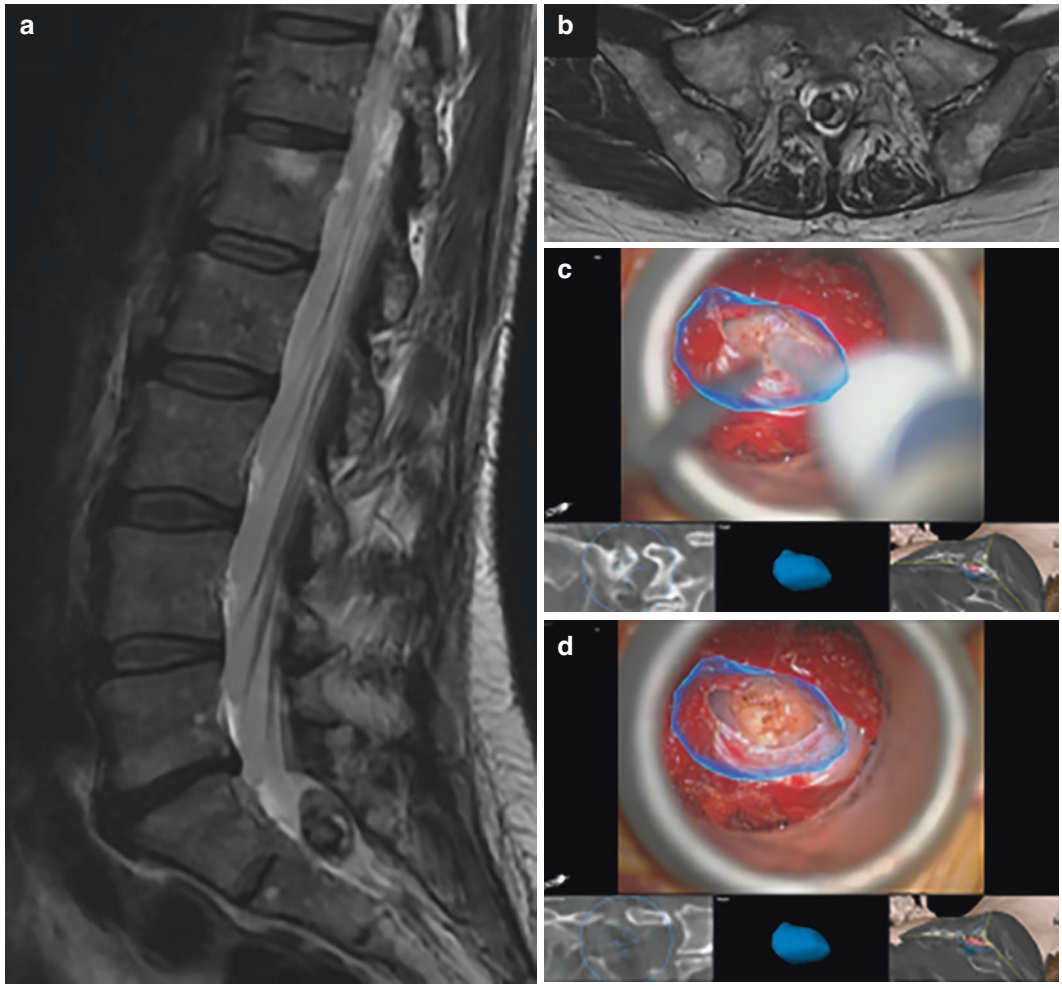


**Fig. 1.8** (**a**) Sagittal and (**b**) Axial T2-weighted MRI demonstrating sacral schwannoma. After these preoperatively acquired scans were co-registered with intraoperatively acquired CT, an augmented reality projection was superimposed. (**c**) Tubular approach to mass with blue projection representing location and borders of mass. (**d**) Microscope view through tube with interval mass resection. Borders and location of preoperatively visualized mass superimposed in blue

## References

1. Imada AO, Huynh TR, Drazin D. Minimally invasive versus open laminectomy/discectomy, transforaminal lumbar, and posterior lumbar interbody fusions: a systematic review. Cureus. 2017;9:e1488.
2. Nerland US, Jakola AS, Solheim O, et al. Minimally invasive decompression versus open laminectomy for central stenosis of the lumbar spine: pragmatic comparative effectiveness study. BMJ. 2015;350:h1603.
3. Fan Y, Du J, Zhang J, Liu S, Xue X, Huang Y, Zhang J, Hao D. Comparison of accuracy of pedicle screw insertion among 4 guided technologies in spine surgery. Med Sci Monit. 2017;23:5960–8.
4. Heini P, Schöll E, Wyler D, Eggli S. Fatal cardiac tamponade associated with posterior spinal instrumentation. A case report. Spine. 1998;23:2226–30.
5. Mobbs RJ, Raley DA. Complications with K-wire insertion for percutaneous pedicle screws. J Spinal Disord Tech. 2014;27:390–4.
6. Tian N-F, Wu Y-S, Zhang X-L, Xu H-Z, Chi Y-L, Mao F-M. Minimally invasive versus open transforaminal lumbar interbody fusion: a meta-analysis based on the current evidence. Eur Spine J. 2013;22:1741–9.

7. Foley KT, Simon DA, Rampersaud YR. Virtual fluoroscopy: computer-assisted fluoroscopic navigation. Spine. 2001;26:347–51.
8. Lian X, Navarro-Ramirez R, Berlin C, Jada A, Moriguchi Y, Zhang Q, Härtl R. Total 3D airo® navigation for minimally invasive transforaminal lumbar interbody fusion. Biomed Res Int. 2016;2016:5027340.
9. Janssen I, Lang G, Navarro-Ramirez R, Jada A, Berlin C, Hilis A, Zubkov M, Gandevia L, Härtl R. Can Fan-beam interactive computed tomography accurately predict indirect decompression in minimally invasive spine surgery fusion procedures? World Neurosurg. 2017;107:322–33.
10. Navarro-Ramirez R, Lang G, Lian X, Berlin C, Janssen I, Jada A, Alimi M, Härtl R. Total navigation in spine surgery; a concise guide to eliminate fluoroscopy using a portable intraoperative computed tomography 3-dimensional navigation system. World Neurosurg. 2017;100:325–35.
11. Hussain I, Navarro-Ramirez R, Lang G, Härtl R. 3D navigation-guided resection of giant ventral cervical intradural schwannoma with 360-degree stabilization. Clin Spine Surg. 2018;31:E257–65.
12. Luther N, Iorgulescu JB, Geannette C, Gebhard H, Saleh T, Tsiouris AJ, Härtl R. Comparison of navigated versus non-navigated pedicle screw placement in 260 patients and 1434 screws: screw accuracy, screw size, and the complexity of surgery. J Spinal Disord Tech. 2015;28:E298–303.
13. Torres J, James AR, Alimi M, Tsiouris AJ, Geannette C, Härtl R. Screw placement accuracy for minimally invasive transforaminal lumbar interbody fusion surgery: a study on 3-d neuronavigation-guided surgery. Glob Spine J. 2012;2:143–52.
14. Sclafani JA, Regev GJ, Webb J, Garfin SR, Kim CW. Use of a quantitative pedicle screw accuracy system to assess new technology: initial studies on O-arm navigation and its effect on the learning curve of percutaneous pedicle screw insertion. SAS J. 2011;5:57–62.
15. Hu X, Lieberman IH. What is the learning curve for robotic-assisted pedicle screw placement in spine surgery? Clin Orthop Relat Res. 2014;472:1839–44.
16. Fan Y, Du JP, Liu JJ, Zhang JN, Qiao HH, Liu SC, Hao DJ. Accuracy of pedicle screw placement comparing robot-assisted technology and the free-hand with fluoroscopy-guided method in spine surgery: an updated meta-analysis. Medicine. 2018;97:e10970.
17. Carl B, Bopp M, Saß B, Nimsky C. Microscope-based augmented reality in degenerative spine surgery: initial experience. World Neurosurg. 2019;128:e541–51.
18. Elmi-Terander A, Burström G, Nachabe R, et al. Pedicle screw placement using augmented reality surgical navigation with intraoperative 3D imaging: a first in-human prospective cohort study. Spine. 2019;44:517–25.
19. Archavlis E, Schwandt E, Kosterhon M, Gutenberg A, Ulrich P, Nimer A, Giese A, Kantelhardt SR. A modified microsurgical endoscopic-assisted transpedicular corpectomy of the thoracic spine based on virtual 3-dimensional planning. World Neurosurg. 2016;91:424–33.
20. Gottschalk MB, Yoon ST, Park DK, Rhee JM, Mitchell PM. Surgical training using three-dimensional simulation in placement of cervical lateral mass screws: a blinded randomized control trial. Spine J. 2015;15:168–75.

# Navigation Guided Single-Stage Lateral Surgery

2

Raj Nangunoori, Jacob L. Goldberg, Joseph A. Carnevale, Lynn McGrath, Sertac Kirnaz, and Roger Härtl

## 2.1 Introduction

Lateral lumbar interbody fusion (LLIF) has become increasingly popular in recent years as a minimally invasive surgery (MIS) option for fusion. In 1997, the first lateral anterior to the psoas approach to the lumbar spine was described by Mayer [1]. In 2006, Ozgur et al. reported on the promising results of a trans-psoas approach [2]. Regardless of the corridor, LLIF is ideal for patients with mechanical back pain with spondylolisthesis, adjacent segment disease in patients with a prior fusion, pseudoarthrosis, as well as for correction of coronal deformity. Advantages to the approach include indirect decompression of neural elements, low large surface area for fusion across the implant surface, and avoidance of soft tissue injury by avoiding injury to the paraspinal musculature and posterior tension band. In addition, this approach avoids the great vessels and manipulation of abdominal organs. With proper cage selection, this approach offers a low risk of subsidence [3]. Lateral approaches have become an attractive option for arthrodesis in the lumbar spine.

The lateral approach allows for placement of a graft with a large footprint and surface area for fusion, spanning the apophyseal ring. However, standalone cage placement without fixation poses the risks of graft migration or extrusion causing visceral or vascular injury. Additionally, standalone cage placement without fixation carries increased risk of pseudoarthrosis [4]. Due to early failures with stand-alone lateral interbody cage placement, many surgeons opt for supplemental fixation including a lateral plate with screws that are inserted into the rostral and caudal vertebral bodies. Other options include integrated cage/screw implants, unilateral, or bilateral pedicle screw fixation. Traditionally, patients undergoing lateral interbody cage placement are initially placed in the lateral position and later placed prone for posterior instrumentation. The prone position, while familiar to most surgeons does confer risks associated with pressure to the anterior body including: cardiovascular and pulmonary compromise, oropharyngeal swelling, abdominal compartment syndrome, and increased bleeding due to increased intra-abdominal pressure [5]. Another disadvantage to

Raj Nangunoori and Jacob L. Goldberg contributed equally with all other contributors.

R. Nangunoori · J. L. Goldberg · J. A. Carnevale · L. McGrath · S. Kirnaz
Department Neurological Surgery, New York Presbyterian Hospital/Weill Cornell Medical Center, New York, NY, USA
e-mail: jag9177@nyp.org; joc3003@nyp.org; lbm9009@med.cornell.edu; sek2024@med.cornell.edu

R. Härtl (✉)
Department of Neurological Surgery, Weill Cornell Medicine Center for Comprehensive Spine Care New York Presbyterian OCH SPINE, New York, NY, USA
e-mail: Roh9005@med.cornell.edu



J.-S. Kim et al. (eds.), *Technical Advances in Minimally Invasive Spine Surgery*,
https://doi.org/10.1007/978-981-19-0175-1_2

changing surgical position intraoperatively is the inherent increase in operative time. For all of the above reasons, placement of the interbody cage as well as posterior pedicle screw placement and posterior direct tubular decompression in a single stage with the patient remaining in the lateral position has emerged as an attractive technique.

## 2.2 Published Reports of Single-Stage Lateral Surgery

The first published case series of patients undergoing single-stage lateral surgery was by Drazin et al. in 2015 [6]. In their series, the authors performed a retrospective review of 20 patients, ten of whom underwent lateral followed by prone positioning and ten who underwent single-stage surgery, controlling the respective cohorts in terms of age, BMI, and pathology treated via LLIF. The authors reported a statistically significant decrease in average operative time (average 60 min/case) when comparing single stage to repositioning. No significant differences were observed with regard to blood loss, length of stay, clinical, or radiographic outcomes. Pedicle screws in this study were placed bilaterally using fluoroscopy. From their experience, the advantages of the single position technique were lost when more than two spinal levels are involved. They also noted that while single position surgery seems advantages in morbidly obese patients, they encountered technical challenges in this population related to poor fluoroscopic visualization. They further recommended against the single position technique in patients with small or rotated pedicles in which case lateral placement of pedicle screws can be a challenge.

Blizzard et al. in 2018 evaluated a consecutive case series of 72 patients who underwent either OLIF or LLIF followed by instrumentation in the lateral position [7]. In their series, the majority of patients (65/72) underwent single level interbody placement followed by bilateral pedicle screw fixation using fluoroscopy. Average operative time was 87.9 min with an average of 5.9 min/screw. Postoperative CTs were obtained in 85% of patients with a screw breach rate of 5.1%, and no clear trend between the "upside" or "downside" (dependent side) pedicles in terms of breach rate. In their series, two patients underwent reoperation for radiculopathy due to a screw breach with resolution of their symptoms at last follow-up. The authors reported that in their experience, they did not find a significant learning curve in pedicle screw placement in the lateral position using fluoroscopy. However, they did that placing screws into S1 may be more challenging in the lateral position due to the lack of a good docking surface compared with higher lumbar levels. Specifically, the inherent difficulty cited by the authors in this study was that the transverse process/facet junction is not as obvious at the lumbosacral junction. Interestingly, in both early case series of single-stage lateral surgery, navigation was not used for pedicle screw fixation despite the perceived challenges of placing pedicle screws in the lateral position, especially in the downside pedicles.

Despite several case series of single-stage surgery, there are few studies comparing patients undergoing single position surgery to those who are repositioned. Ziino et al. compared patients undergoing single position LLIF to lateral followed by prone positioning [8]. Patients were included if they were undergoing LLIF alone without adjunct procedures such as TLIF, PLIF, or ALIF, though patients with fusions above or below the level of interest were not excluded. The single position ($n = 42$) and dual position ($n = 24$) cohorts had no differences in patient demographics, blood loss, length of stay, blood loss, or pre- or postoperative lordosis. However, the authors did find a statistically significant decrease of 44 min between the single position surgery group to the lateral then prone group. An additional 27 min were saved if unilateral rather than bilateral pedicle screw fixation was performed. Compared with earlier studies, this was the first to evaluate the theoretical advantages of single position surgery. As with other single-stage studies, pedicle instrumentation was performed percutaneously without navigation. Importantly, this study also found no difference in preoperative and postoperative lordosis suggesting prone positioning is not required to facilitate lordosis. Despite these encouraging results, additional studies comparing these techniques are needed. The five published studies including 183 patients are summarized in Table 2.1 [6–10].

**Table 2.1** Studies evaluating single position surgery (SPS)

| Author (year) | Study design | # of patients | LLIF vs OLIF for SPS | Imaging modality | Screw placement time or OR time (min) | Screw breaches | Revision surgery for screw breach |
|---|---|---|---|---|---|---|---|
| Drazin 2015 | Retrospective | 10[c] | LLIF | Fluoroscopy | 190.3 min (DP) vs 130.5 min (SP) | 1[a] | 1 pt |
| Blizzard 2018 | Retrospective | 72 | Both | Fluoroscopy | 5.9 min/screw | 13/254 (5.1%) | 2 pts. (2.8%) |
| Ziino 2018 | Retrospective | 42[b] | LLIF | Fluoroscopy | 226 ± 74.9 min (DP) vs 149.2 ± 53.2 min (SP) | Unspecified | 2 pts. (4.7%) |
| Sellin 2018 | Retrospective | 4 | OLIF | Intraoperative CT | 138 ± 16.7[d] | 2 | 1 pt |
| Huntsman 2019 | Retrospective | 55 | LLIF | Intraop CT or preop CT with robotic assistance | 155.7 ± 42 min[d] | 0 | 0 |

*LLIF* lateral lumbar interbody fusion, *OLIF* oblique lumbar interbody fusion, *OR* operating room time, *SPS* single position surgery

[a]Screw breach was in a single patient who underwent dual positioning (lateral then prone)

[b]Forty-two patients underwent single-position, 24 dual position

[c]Ten patients underwent single-position, 10 dual position

[d]No comparison group that was repositioned

## 2.3 Single Position Lateral Surgery with Navigation

Since the era of fluoroscopy-guided pedicle screw insertion, navigation systems have become ubiquitous in spine surgery. Cone beam or fan beam based 3-D navigation systems are in widespread use. In addition, pedicle screw systems now include platforms that facilitate single-step screw insertion with integrated navigation or with robotic assistance [9]. At our institution we use a navigated single-step pedicle screw insertion system. The surgical technique and example cases are summarized below.

## 2.4 General Technique

For single-stage surgery, all procedures are performed under general anaesthesia with neuromonitoring. We use a flat Trumpf table integrated with the intraoperative CT navigation platform. In our standard workflow for single-stage surgery, the patient is placed lateral for the interbody work first with fluoroscopy used for cage planning and placement, followed by an intraoperative CT scan for navigation of pedicle screws.

## 2.5 Positioning and Lateral Interbody Cage Placement

The patient is placed in the lateral decubitus position with the approach side up. Care is taken to safely secure the patient to the operative Table. A small axillary roll is placed to protect the brachial plexus, and a small hip roll is used on the dependent side to induce slight lateral flexion away from the side of the approach (Fig. 2.1). This manoeuvre stabilizes the spine for the navigation part of the procedure, facilitates access to the disc space at L4/5 that can be obstructed by the iliac crest, and higher up in the lumbar spine due to the ribs. The patient's arms are bent at the elbows at a 90-degree angle and appropriately padded to facilitate CT scanning for the preoperative scan needed for navigation of the pedicle screws, which is performed after the interbody work is

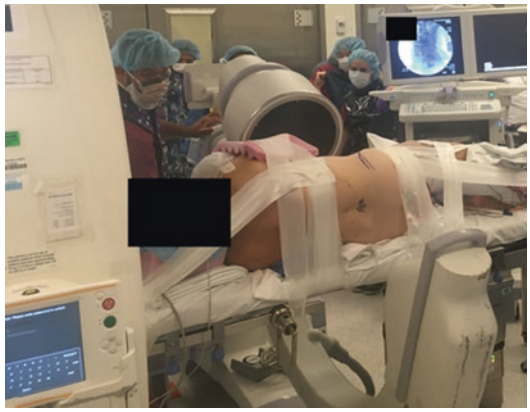

**Fig. 2.1** Intraoperative positioning. Patient is flat on the operating room table and securely taped (and padded) to prevent movement during cage and screw placement. Notice that the entire posterior lumbar surface is left exposed to allow access to both sides for pedicle screws. The patient is placed as close to the table edge as possible to avoid inadvertent malpositioning of the downside pedicle screws due to obstruction by the OR table

complete. In addition, the patient is positioned as close to the edge of the table as possible to ensure the ability to place pedicle screws into the dependent (downside) pedicles without obstruction by the operating room table. The positioning of the patient close to the table edge is also critical for draping, to ensure sterility and to make sure the maximal surface area of the lumbar region is available to obtain the necessary trajectory from lateral to medial for placing pedicle screws into the dependent (downside) pedicles. Once the patient is padded and secured to the operating room table, intraoperative fluoroscopy is brought in and the patient and table are rotated appropriately to obtain orthogonal views of the disc space of interest. LLIF is performed in a standard fashion [11].

Our experience is primarily with direct lateral interbody cage placement using fluoroscopy only and using 3D navigation when placing pedicle screws. LLIF is performed in a standard fashion with fluoroscopy alone. After the interbody cages have been placed, a reference array is attached to the iliac crest and intraoperative CT is acquired for navigated screw placement as well as possible tubular decompression as necessary. Acquisition of intraoperative CT after LLIF allows for intraoperative confirmation of cage placement. In addition, discectomy and cage placement require high-velocity manoeuvres which may shift the reference frame, making navigation inaccurate if the scan is performed before this point.

Optimal timing and use of fluoroscopy and intraoperative CT is debated and remains an area of active study [12]. As with LLIF, some surgeons perform a pre-psoas approach for interbody placement using navigation as posterior pedicle screw placement. In one of the author's (RN) experience, use of navigation is helpful for incision planning if using the pre-psoas corridor and confirming position of the disc space of interest. Annulotomy, discectomy, and endplate preparation are similar as with the direct lateral approach, however the cage may be undersized due to the limitations of the navigation platform in use. Intraoperative fluoroscopy can be used to optimally fit and position the cage to promote fusion.

## 2.6 Navigated Pedicle Screw Placement

Once final fluoroscopic images have been taken, the iliac crest is palpated through the LLIF incision and a reference array for navigation is placed. The patient is tilted away approximately 10–15° away (Fig. 2.2) from the surgeon to bring the downside pedicles into better alignment for screw placement. In addition, patient rotation ensures navigation accuracy as the patient's body is in the same position that it would be for pedicle screw placement into the downside pedicles. In the authors' experience, if the patient is kept neutral for the navigation scan followed by rotation, this can lead to navigation inaccuracies and misplaced screws which carries with it risks of neurologic injury. An intraoperative CT scan is taken, and the data is sent to the navigation system. Depending on the surgeon's preference, uni-or bilateral pedicle screw fixation can be performed using navigation. If performing bilateral fixation, we advise placing screws on the downside pedicles first to mitigate the chances of navigation inaccuracy.

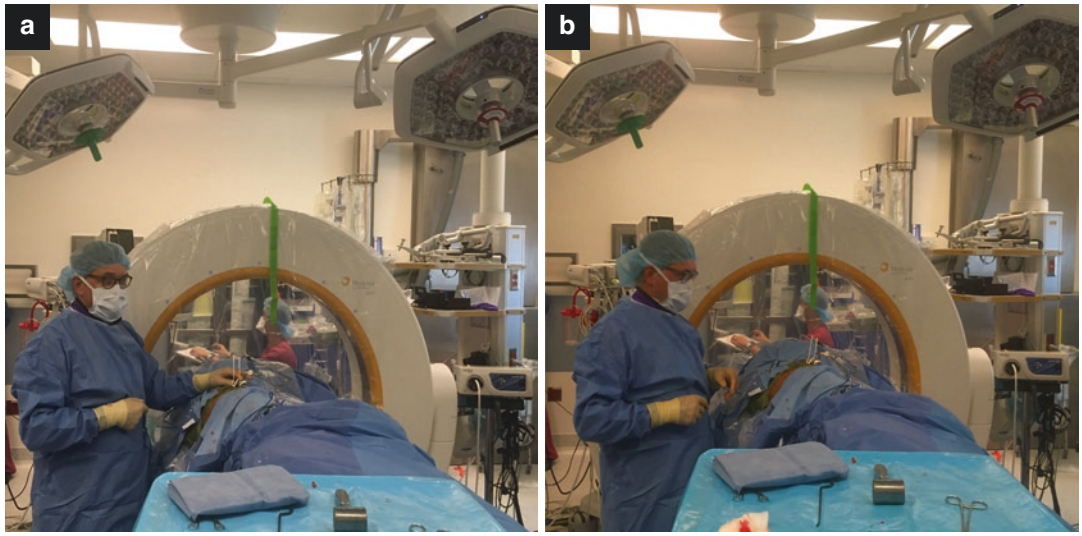


**Fig. 2.2** The iliac crest navigation pins are placed via the same incision as the interbody cages. (**a**) Iliac crest pins placed. (**b**) Operating table tilted 10–15 degrees away from the surgeon prior to obtaining the intraoperative CT scan to bring downside pedicles into optimal alignment for screw placement

Using the navigation pointer, the entry point for each pedicle and the lateral-to-medial trajectory is determined (Fig. 2.3). The optimal trajectory for each pedicle screw can be represented by a marker. For single-stage surgery, we typically use a single-step pedicle screw insertion system with an integrated K-wire. A linear incision through the skin is made, followed by electrocautery. A generous fascial incision longer than the actual skin incision is recommended to prevent the soft tissue pressure from changing screw trajectory. This is especially important in the lateral position as the effects of gravity and soft tissue pressure can inadvertently change the final screw trajectory despite accurate navigation. Blunt finger dissection is used to palpate the facet joint and the transverse process. The navigation wand is used to confirm navigation accuracy by "rolling" the wand above and below the transverse process. The trajectory of the screw is matched to the initial plan and adjustments are made if necessary, and at this point, the screw diameter and length are selected. When starting instrumentation, we typically start with the most caudal, downside pedicle and check for navigation accuracy here. If the navigation on this caudal transverse process is deemed accurate, the rostral pedicles (and therefore furthest away from the navigation array) are also accurate. Alternatively, if unilateral pedicle fixation is utilized, the most rostral transverse process is used to check for accuracy as it is the furthest away from the reference array. For first-time practitioners of this technique, we encourage checking the navigation accuracy of all TPs to ensure accuracy for each pedicle screw. A pedicle screw with an integrated K-wire at the tip (Fig. 2.4) is then introduced into the pedicle using a mallet to drive the wire into the cortical bone. Then, the screw is slowly advanced through the cortical bone into the cancellous bone of pedicle using the navigation screen to determine the depth. Once the tip of the screw enters the vertebral body, the operator removes their hands and performs a "hands-off" test to confirm the trajectory of the pedicle screw. The screw is advanced into its final position and the integrated K-wire and navigation handle are removed. The outlined steps are repeated for all the downside screws and again for the upside screws. If there is any

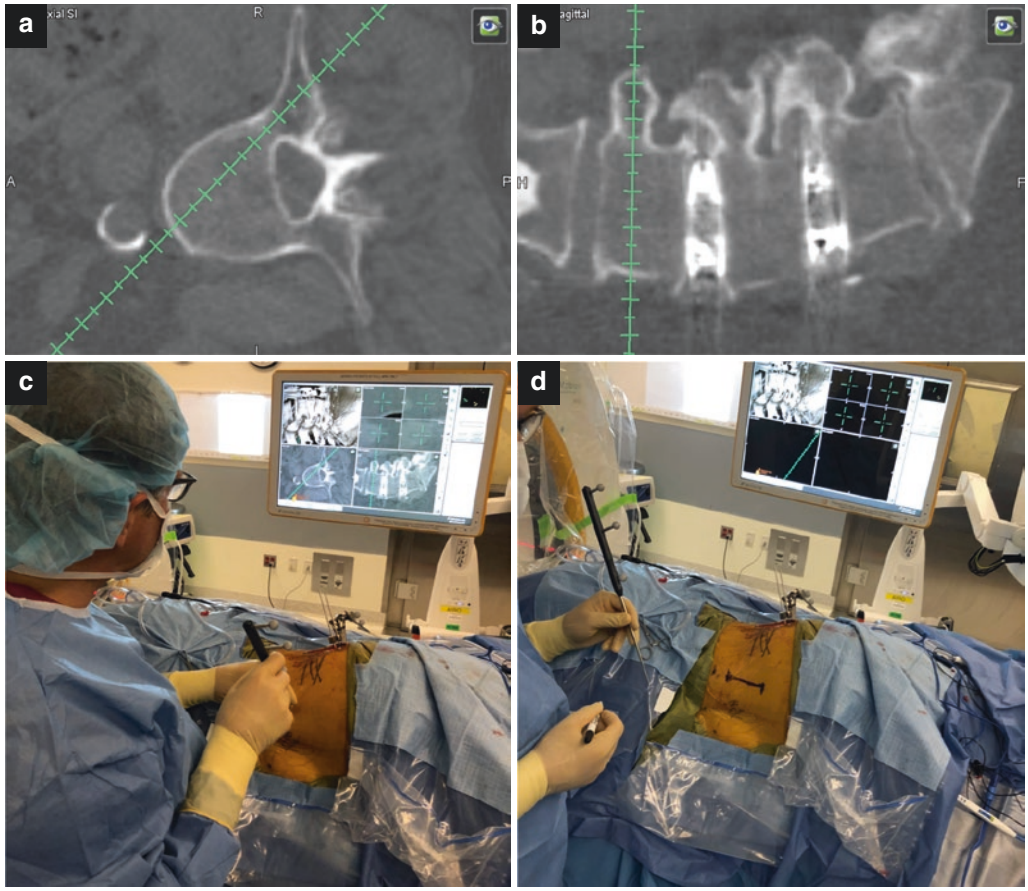


**Fig. 2.3** Intraoperative navigational CT with interbody cages seen at L3–4 and L4–5 with green inline trajectory of pedicle screws. (**a**) Axial. (**b**) Sagittal. (**c**) The navigation pointer is placed on the surface of the skin to determine the screw trajectories for the levels of interest. (**d**) Linear incision is marked

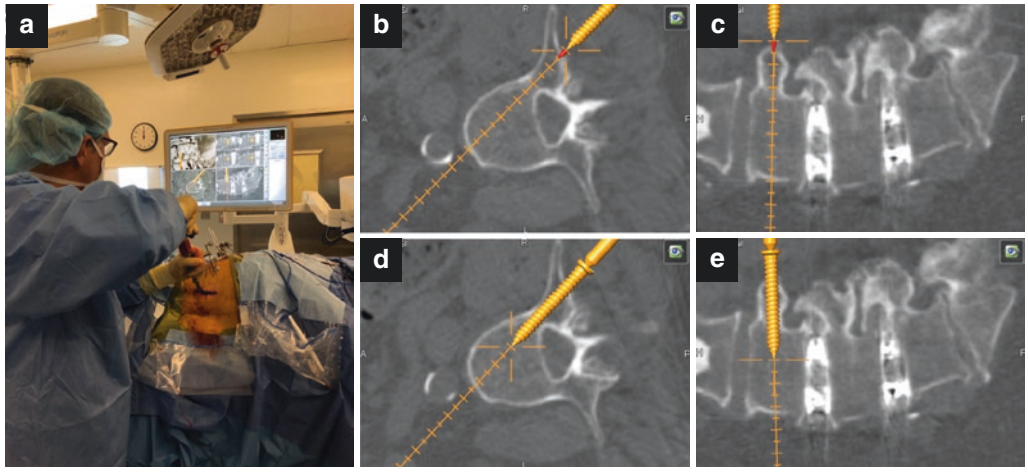


**Fig. 2.4** (**a**) The screw is advanced into the pedicle along with the K-wire. Once the screw enters the vertebral body, the K-wire is withdrawn and the screw is advanced into its final position. The process for placing the pedicle screw is repeated for additional pedicles, as needed. (**b**) Axial and (**c**) Sagittal screw starting point. (**d**) Axial and (**e**) Sagittal navigated screw advancement

question about navigation accuracy, the screw is not placed, and another CT scan can be taken to confirm accuracy.

## 2.7 Illustrative Cases

### 2.7.1 Case 1

A 71-year-old female presented with low back and right lower extremity pain into the dorsum of her foot. Visual analogue scale (VAS) was 10, with an Oswestry Disability Index (ODI) of 48. Surgical history was notable for an L4–5 laminectomy and a spinal cord stimulator placed for her leg pain. The neurological exam was notable for right foot weakness from an old cerebrovascular accident. Due to the presence of the stimulator, a CT myelogram was obtained which demonstrated degenerative disc disease at L3–4, L4–5 with severe neural foraminal stenosis with a disc-osteophyte complex compressing the exiting right L4 nerve (Fig. 2.5). Because of her known cardiac history and to minimize operative time, she underwent a single position L3–4, L4–5 lateral lumbar interbody fusion followed by unilateral pedicle fixation from L3 to L5 on the upside pedicles. The presence of a bony disc-osteophyte complex causing nerve root compression was the rationale for performing a tubular decompression of the exiting L4 nerve using navigation. The patient did well postoperatively, with resolution of her right leg pain. Final anteroposterior (AP) and lateral X-rays demonstrating appropriate cage and screw placement is illustrated in Fig. 2.5.

For one- to two-level fusions unilateral screw placement provides sufficient stabilization in our experience, unless there is significant spondylolisthesis or pars defects (in which case we prefer bilateral pedicle screw placement).

### 2.7.2 Case 2

A 73-year-old male presented with low back and buttock pain. He also complained of left leg weakness. The patient reported exacerbation of his back and leg pain when standing, walking, or with movement and amelioration of his symptoms with sitting or leaning forward. His neurological examination was notable for 4+/5 strength with hip flexion and knee extension, and the diameter of his left thigh was approximately 2.5 cm smaller than his right thigh. A preoperative MRI (Fig. 2.6) demonstrated severe degenerative disc disease spanning from L2 to S1, with bilateral lateral recess stenosis at L2–3 and L3–4. A synovial cyst was also present on the left side at the L2–3 level. Preoperative dynamic X-rays demonstrated

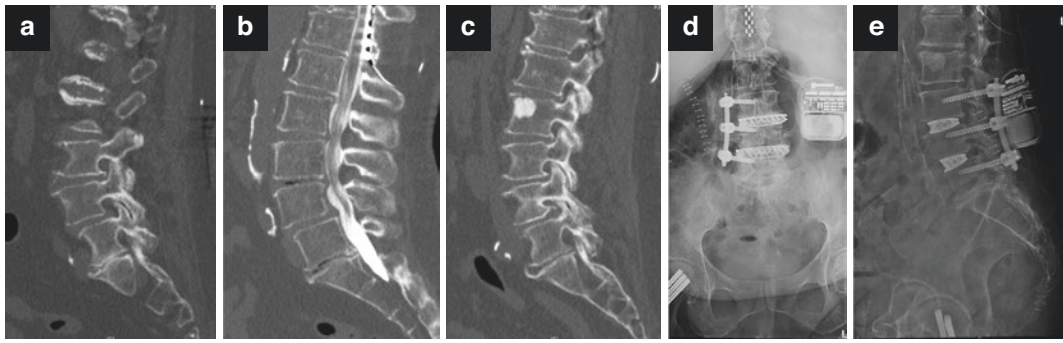


**Fig. 2.5** Preoperative CT myelogram: left foraminal view (**a**), midline (**b**), and right foraminal view (**c**). The scan is notable for disc degeneration with spondylolisthesis at the L4–5 level is present. There is moderate central stenosis at L3–4 and L4–5 with a disc osteophyte causing severe right L4 foraminal stenosis. Immediate postoperative anterior-posterior (**d**) and lateral (**e**) standing radiographs reveal interbody cages at L3–4 and L4–5 with unilateral pedicle screws on the right spanning L3-L5. Note: CT myelogram performed in lieu of MRI due to incompatible spinal cord stimulator

instability at the L2–3 level (Fig. 2.6). His imaging and neurological exam findings were suggestive of mechanical back pain due to instability and radiculopathy with weakness caused by compression of the traversing left L3 nerve by the synovial cyst. As a result, he underwent a 2-level left-sided approach for L2–3, L3–4 LLIF with unilateral pedicle screw fixation and direct left-sided L2–3 laminectomy with resection of the synovial cyst. The tubular retractor is placed with the patient in lateral position producing a microscopic view similar to that seen with the patient in prone position (Fig. 2.7). The patient had resolution of his pain and weakness postoperatively and continued to do well at 1 year postoperatively with no recurrence of symptoms and no hardware complications (Fig. 2.6).

### 2.7.3 Case 3

A 60-year-old male presented with a several-month history of right-sided buttock and anterior thigh pain. He also endorsed significant back pain at rest, worsened with activity. The patient did have a history of a lumbar laminectomy several months prior to presentation for neurogenic claudication. The neurological exam was intact with no motor weakness. MRI of his lumbar spine (Fig. 2.8) demonstrated significant disc degenera-

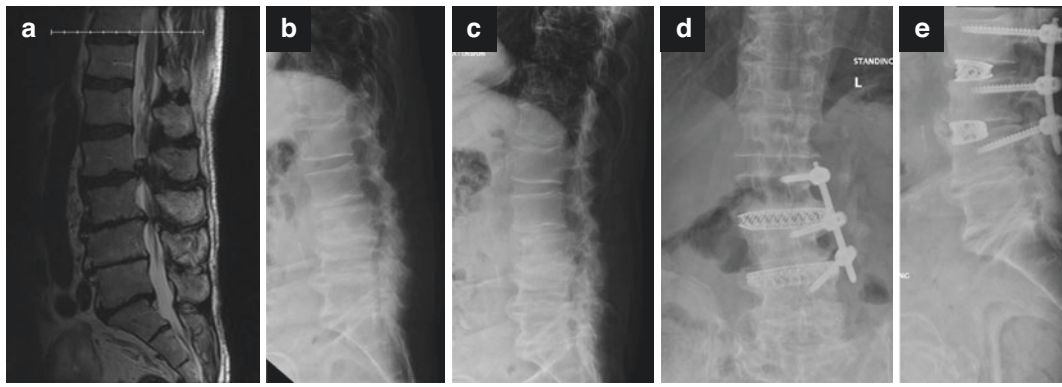


**Figure 2.6** Preoperative T2-weighted MRI scan demonstrates degenerative changes throughout lumbar spine with stenosis most severe at L2–3 and L3–4 levels. Careful inspection of the L2–3 level on axial MRI (not pictured) and (**a**) sagittal MRI reveals fluid in the facet joints bilaterally, a synovial cyst on the left side, and severe stenosis. Dynamic X-rays with flexion (**b**) and extension (**c**) demonstrate a mobile spondylolisthesis at L2–3. Immediate postoperative AP (**d**) and lateral (**e**) demonstrate intact hardware with interbody cages at L2–3 and L3–4 and left-sided posterior pedicle fixation spanning L2–4

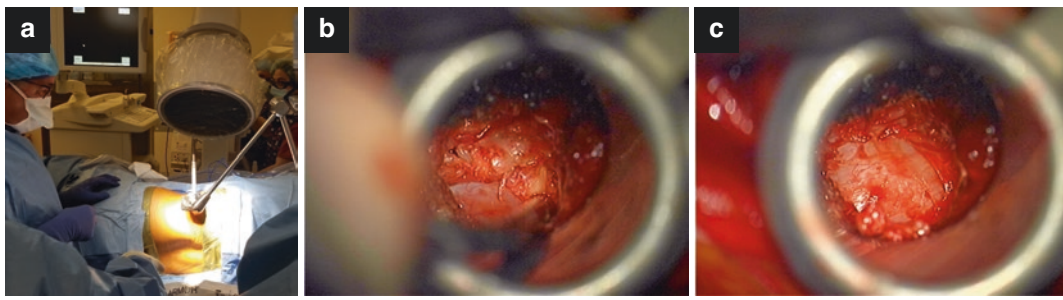


**Figure 2.7** (**a**) Placement of tubular retractor with patient in lateral position. (**b** and **c**) Microscopic view through tubular retractor in the lateral position. The navigation wand is used to make a more medial fascial incision for placement of serial tubular dilators of increasing size. The thecal sac is deformed by a synovial cyst (**b**) and is visible decompressed after cyst drainage (**c**)

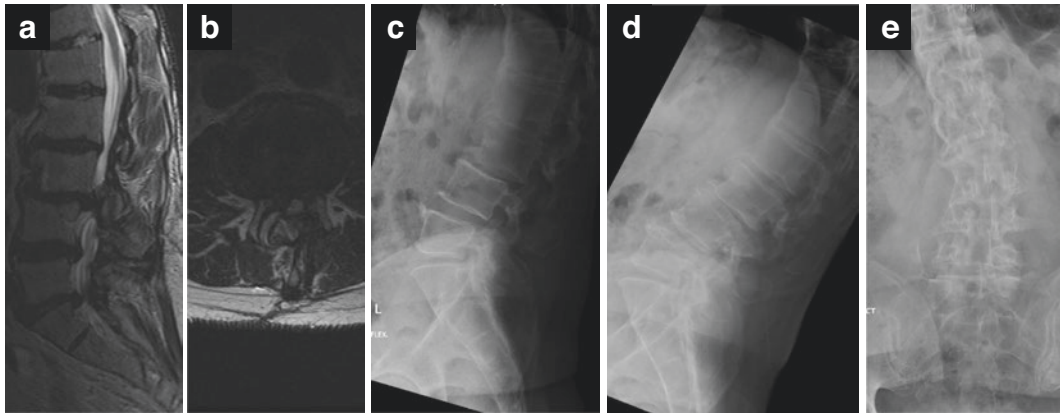


**Fig. 2.8** (**a**) T2-weighted sagittal MRI of the lumbar spine with degenerative changes throughout, most severely involving L3–S1 with significant disc protrusions worst at L3–4 and L5–S1 causing significant lumbar stenosis. (**b**) Axial MRI at L3–4 with facet gapping and evidence of a disc herniation causing severe canal and lateral recess stenosis at that level. Dynamic flexion (**c**) and extension (**d**) radiographs demonstrate mobile listhesis at the L3–4 level. (**e**) Anteroposterior view of the lumbar spine demonstrates a coronal deformity with lateral listhesis at the L3–4 and L2–3 levels

tion at L3–4, L4–5, and L5-S1 with retrolisthesis at the L3–4 level along with a right-sided disc herniation at L3–4. Dynamic X-rays showed instability (Fig. 2.8). The anteroposterior (AP) view demonstrated a coronal deformity at the L3–4 and L2–3 levels with lateral listhesis at both levels. Due to the patient's mechanical back pain, lumbar stenosis with disc herniation and coronal deformity, he underwent a single-stage, right-sided LLIF with navigated pedicle screw placement from L2 to L4. In addition, a direct decompression and microdiscectomy was performed at the L3–4 level. At 1-year post-op (Fig. 2.9), the patient had resolution of his back pain and right leg pain and remained neurologically intact.

### 2.7.4 Case 4

A 68-year-old male presented to the office with a history of low back pain with radiation from the posterior buttocks and alternating between the right and left posterior thigh. He also complained of axial low back pain worse with standing and walking. The patient did have a history of an L4–5 TLIF about 3 years prior for a grade 1 spondylolisthesis of L4 on L5 with an acute disc herniation causing radiculopathy. The neurological exam was intact with no motor weakness. MRI of his lumbar spine (Fig. 2.10) demonstrated degenerative disc disease at L3–4 and L5–S1 with severe neural foraminal stenosis on the left side at L3–4, and severe neural foraminal stenosis on the right side at L5–S1. Dynamic X-rays did not show any instability. Due to the significant disc degeneration above and below the prior fusion, the patient's axial low back pain, and neural foraminal compression at L3–4 and L5–S1, he underwent a single-stage left-sided L5–S1 lateral ALIF, L3–4 LLIF with revision of posterior instrumentation from L3 to S1. The patient did well postoperatively with improvement of his back and leg pain. His 1-year post-op X-rays are demonstrated in Fig. 2.11.

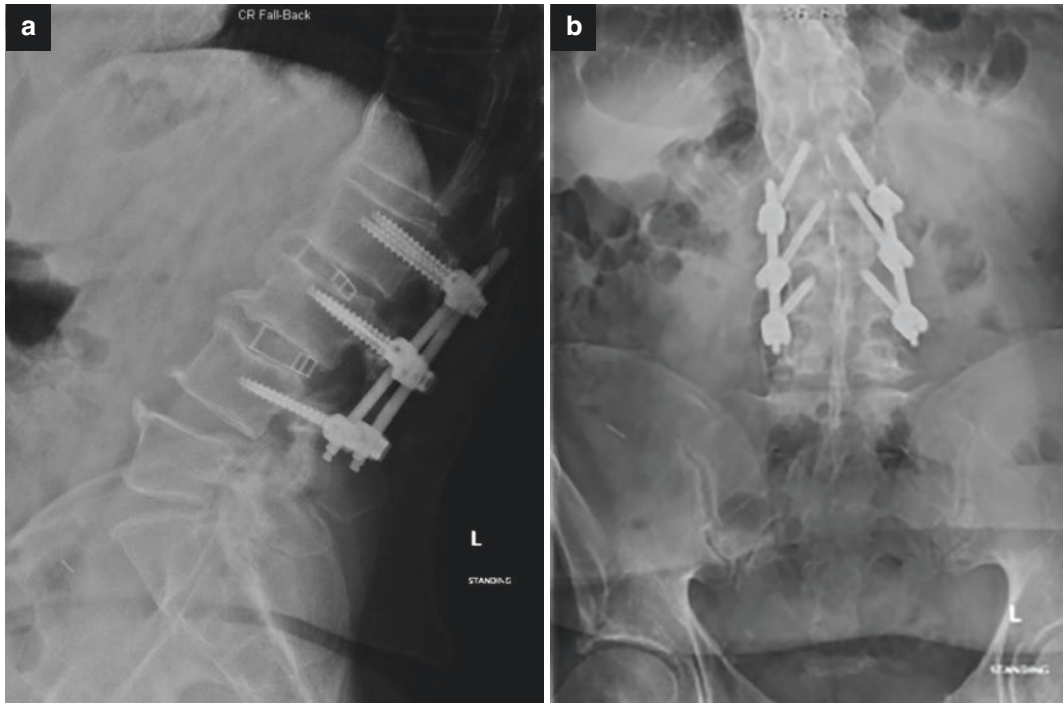


**Fig. 2.9** (**a**) Lateral and (**b**) AP radiographs at 1-year post-op with evidence of interbody fusion across both grafts. On the AP view, improvement in the coronal deformity and reduction of the lateral listhesis as compared with preop can be appreciated

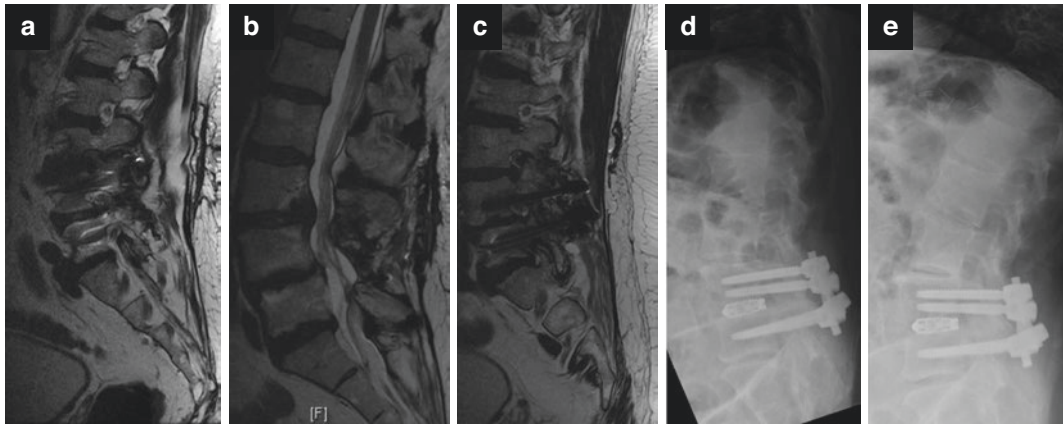


**Fig. 2.10** T2-weighted MRI scans ((**a**) left parasagittal, (**b**) midline sagittal, and (**c**) right parasagittal) demonstrating the degenerative disc disease above and below the previous L4–5 fusion. There is severe left-sided foraminal stenosis at L3–4 and severe right-sided L5–S1 foraminal stenosis. Preoperative flexion (**d**) and extension (**e**) radiographs without evidence of dynamic instability. The prior L4–5 TLIF hardware is visualized without concern for hardware malfunction or graft subsidence

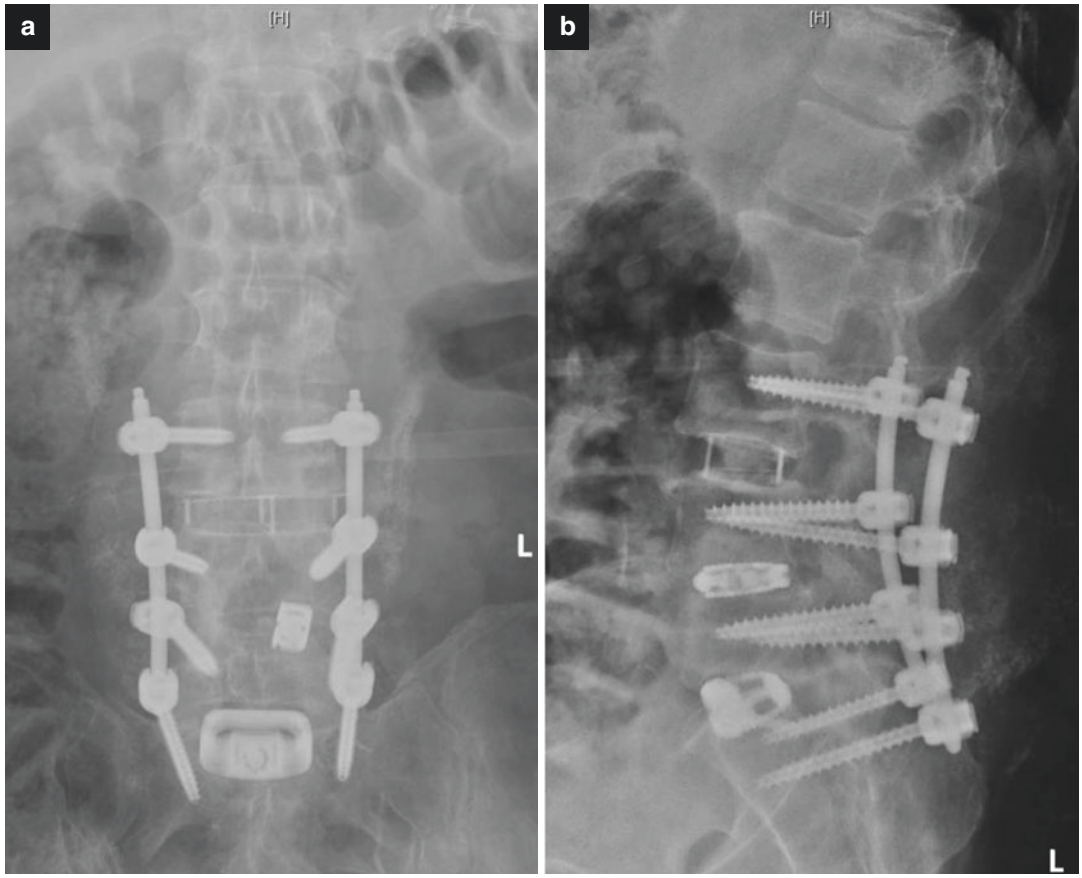


**Fig. 2.11** One-year post-operative (**a**) AP and (**b**) lateral radiographs X-rays with intact hardware and evidence of bony fusion across the interbodies placed during this surgery (L3–4 and L5–S1). Additionally, lumbar lordosis is increased compared with preoperative radiographs

## References

1. Mayer HM. A new microsurgical technique for minimally invasive anterior lumbar interbody fusion. Spine. 1997;22:691–9; discussion 700.
2. Ozgur BM, Aryan HE, Pimenta L, Taylor WR. Extreme lateral interbody fusion (XLIF): a novel surgical technique for anterior lumbar interbody fusion. Spine J. 2006;6:435–43.
3. Lang G, Navarro-Ramirez R, Gandevia L, Hussain I, Nakhla J, Zubkov M, Härtl R. Elimination of subsidence with 26-mm-wide cages in extreme lateral interbody fusion. World Neurosurg. 2017;104:644–52.
4. Cassinelli EH, Wallach C, Hanscom B, Vogt M, Kang JD. Prospective clinical outcomes of revision fusion surgery in patients with pseudarthrosis after posterior lumbar interbody fusions using stand-alone metallic cages. Spine J. 2006;6:428–34.
5. Kwee MM, Ho Y-H, Rozen WM. The prone position during surgery and its complications: a systematic review and evidence-based guidelines. Int Surg. 2015;100:292–303.
6. Drazin D, Kim TT, Johnson JP. Simultaneous lateral interbody fusion and posterior percutaneous instrumentation: early experience and technical considerations. Biomed Res Int. 2015;2015:458284.
7. Blizzard DJ, Thomas JA. MIS single-position lateral and oblique lateral lumbar interbody fusion and bilateral pedicle screw fixation: feasibility and perioperative results. Spine. 2018;43:440–6.
8. Ziino C, Konopka JA, Ajiboye RM, Ledesma JB, Koltsov JCB, Cheng I. Single position versus lateral-then-prone positioning for lateral interbody fusion and pedicle screw fixation. J Spine Surg. 2018;4:717–24.
9. Huntsman KT, Riggleman JR, Ahrendtsen LA, Ledonio CG. Navigated robot-guided pedicle screws

placed successfully in single-position lateral lumbar interbody fusion. J Robot Surg. 2020;14:643–7.
10. Sellin JN, Mayer RR, Hoffman M, Ropper AE. Simultaneous lateral interbody fusion and pedicle screws (SLIPS) with CT-guided navigation. Clin Neurol Neurosurg. 2018;175:91–7.
11. Hood B, Vanni S. Minimally invasive extreme lateral trans-psoas approach to the lumbar spine: applications and techniques. Spine Surg. 2012; https://doi.org/10.5772/36813.
12. Park P. Three-dimensional computed tomography-based spinal navigation in minimally invasive lateral lumbar interbody fusion: feasibility, technique, and initial results. Neurosurgery. 2015;11(Suppl 2):259–67.

# 3 The Six Pillars of Minimally Invasive Spine Surgery

Basar Atalay, Sertac Kirnaz, Fabian Sommer, Jacob L. Goldberg, Lynn McGrath Jr, Branden Medary, and Roger Härtl

Low back pain is the leading cause of years lost to disability globally, a figure which continues to increase along with the average age of our population [1]. Commensurate with the growing pervasiveness of back pain, spine surgical procedures across the spectrum have increased in prevalence—from fusion surgery to minimally invasive outpatient spine surgery [2]. Advances in minimally invasive approaches to the spine have been particularly rapid due to a myriad of published clinical and economic benefits including superior preservation of normal tissue and decreased morbidity which has facilitated a decrease in postoperative pain, hospital stay and ultimately a decrease in short- and long-term complications and associated healthcare costs [3]. MIS approaches have also demonstrated advantages over conventional open surgery in terms of patient satisfaction, a trend which has driven further demand for minimally invasive approaches to a wider range of pathologies [4].

B. Atalay · S. Kirnaz · F. Sommer · J. L. Goldberg
L. McGrath Jr · B. Medary
Department of Neurological Surgery, Weill Cornell Medical College, New York-Presbyterian Hospital, New York, NY, USA
e-mail: fjv4001@med.cornell.edu; jag9177@nyp.org; lbm9009@med.cornell.edu; brm4011@med.cornell.edu

R. Härtl (✉)
Department of Neurological Surgery, Weill Cornell Medicine Center for Comprehensive Spine Care New York Presbyterian OCH SPINE, New York, NY, USA
e-mail: Roh9005@med.cornell.edu

As the number and variety of minimally invasive approaches to the spine increase in complexity so does the nomenclature. In the name of simplicity, we employ the most commonly understood term—Minimally Invasive Spine Surgery (MISS) to describe all approaches that meet the taxonomic guidelines set forth by AOSpine, whereby MISS procedures represent a "suite of technology-dependent techniques and procedures that reduce local surgical tissue damage and systemic surgical stress, enabling an earlier return to function and striving for better outcomes than traditional methods" [5, 6].

## 3.1 The Unmet Potential of Minimally Invasive Spinal Surgery

Approximately one million spine procedures are performed annually in the United States alone [7]. According to Rajaee and Castillo et al., 413,000 spinal fusions, 370,000 discectomies, and 103,000 laminectomies were reported annually in the USA [8, 9]. Demographic and industry trends indicate that these numbers will likely continue to rise and will include increasing numbers of the elderly and vulnerable patient populations who will benefit most from the advantages of MISS techniques.

Compounding the increasing need for spine surgery, these procedures are on average the costliest surgeries routinely performed, rank-



J.-S. Kim et al. (eds.), *Technical Advances in Minimally Invasive Spine Surgery*,
https://doi.org/10.1007/978-981-19-0175-1_3

ing first in percent of aggregate costs for all hospital stays [7]. Fortunately, it is estimated that 50% of fusion operations and 75% of spine surgical procedures in total could be performed using MISS techniques. These figures indicate that our healthcare system has the potential to accrue significant economic and clinical benefits from the ongoing transition to MISS techniques. Even significant multilevel deformities, among the most challenging pathologies to address by any means, are becoming more amenable to MISS principles through the development of technologies like intraoperative navigation, percutaneous and robotic pedicle screw placement, and novel anterior and lateral approaches.

## 3.2 The "6 T's of MISS"

The application and study of MISS methods has led to the emergence of six principles fundamental to the appropriate adoption and utilization of MISS techniques. These basic principles have become known as the "6 T's of MISS" and are crucial to consider throughout the process of learning and employing these techniques [10]. These six principles are as follows:

1. *Target*—selecting the appropriate procedure for the patient and the pathology
2. *Technology*—leveraging technology that facilitates the optimal use of MISS
3. *Technique*—maintaining high-level surgical skills and perioperative best-practices
4. *Training*—career-long training of the surgeon, collaborating team, and trainees
5. *Testing*—critical review and analysis of surgical outcomes (research)
6. *Talent*—nurturing and cultivating surgical talent, decision-making

Ultimately, the goal of the MISS surgeon is to leave the smallest possible "surgical footprint" while achieving short- and long-term results superior to those of conventional open surgery.

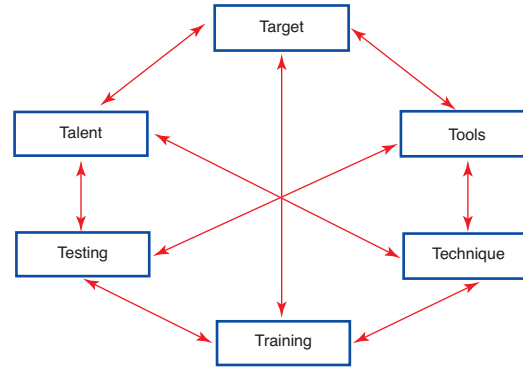


**Fig. 3.1** The six principles "6Ts" should be considered when getting ready and fully equipped for MISS. 6Ts are all interactive with each other and the patient is in the center of our main focus

The 6 T's are fundamental to achieving the goals of the MISS surgeon (Fig. 3.1).

## 3.3 Target

Spine surgery is complex in nature, and therefore surgeons often find themselves with several reasonable options for approaching a given pathology. The first T, Target, represents the process by which a surgeon sifts through all available data and surgical options to select the optimal procedure for a given patient and pathology. Targeting one's approach to achieve maximum benefit with minimal complication is the foundation upon which the MISS philosophy is built.

One frequently encountered decision point most spine surgeons will face is that regarding the need for fusion. Fusion of a spinal level is an inherently pathological process, albeit one that we commonly leverage to treat another pathological process. While in many cases the need for fusion is inevitable, a surgeon trained in MISS principles may find opportunities to avoid a fusion operation through the targeted use of microsurgical decompression of the neural elements while preserving native osseoligamentous structures which may, for example, help to organically stabilize a spondylolisthesis. This decision-making process is one of the most complex

problems in spinal surgery; however, preserving functional tissue should be the ultimate goal for the MISS surgeon.

In tailoring an approach to a patient and pathology, each surgeon must be aware of the role their own training, experience, and skillset play in their surgical decision-making process. This self-awareness must also include an understanding of the influence each patient's expectations, beliefs, knowledge-base, and socioeconomic status can exert on the outcome of a given approach despite the limitations inherent in quantifying these factors.

One of the most nuanced components of target selection is reconciling the often vague correlation between a patient's constellation of symptoms and their imaging findings. In surgical cases where the "target" is not clear and all diagnostic modalities are exhausted, a conservative approach may be the best option.

Target selection is also challenging for the surgeon in cases where the causative pathology may be clear but additional pathology complicates the decision-making process by introducing the need to incorporate consideration of the potential for accelerated future deterioration secondary to an intervention or simply as the result of the patient's natural history. In some cases performing a more extensive surgical approach in order to mitigate this expected future deterioration may be reasonable and by sparing the patient from additional future procedures may ultimately represent the least invasive option.

Selecting the optimal MISS approach relies upon a complete understanding of the individual patient as well as their symptoms, goals, and pathology as seen on imaging. For example, most patients with degenerative disorders will present with pain-related symptoms that may be difficult to localize. A well-trained MISS surgeon must localize these symptoms via history, neurologic exam, and careful review and use of imaging studies.

The perfect surgical approach will typically require consideration of the following steps, as demonstrated by Fig. 3.2:

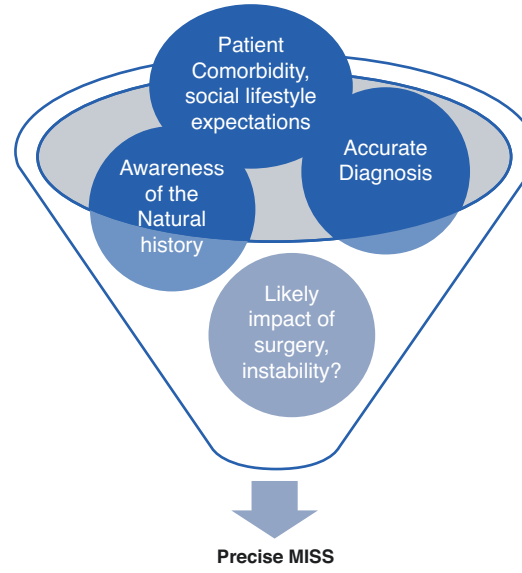


**Fig. 3.2** Requirements for the precise MISS are demonstrated as a combination of definitive diagnosis, understanding the natural history, patient comorbidities, likely impact of the surgery, social life, and expectations of the patients in the figure

1. Definitive diagnosis is critical for the comprehensive and precise surgical decision-making in MISS**.** Different types of pain patterns should be identified and classified. Correlation of physical exam and radiological findings is imperative. Additional testing, such as electromyography (EMG), nerve conduction studies, or diagnostic injections, may be required on some occasions. In more complex cases, using a team-based approach with other subspecialists such as pain anesthesiologists, physiatrists, and neurologists may be considered.
2. Understanding of the natural history of the underlying pathology has crucial importance. As an example, we may consider motion-preserving surgery in a younger patient, but this surgery is not suitable for multiple degenerative conditions. Another example may be the unnecessary utilization of rigid systems in osteoporotic patients.
3. The likely impact of surgery on the disease process. Adjacent segment disease is an

example of the effects of the operation on the ongoing degenerative process. Another example may be improper identification of the instrumentation levels in deformity surgery. Surgery may make an impact on the patient's current biomechanical balance and may accelerate the disease process. These aforementioned surgical approaches may worsen the curve progression and require additional surgical treatments in the future.

4. General medical conditions and expectations of the patient have to be considered in the surgical decision-making process. These are factors such as age, functional status, and comorbidities such as obesity, osteoporosis, cardiopulmonary, and vascular diseases. Additionally, patient's expectations, lifestyle, and social factors (such as support system) should be evaluated and discussed before any surgery including MISS.

### 3.3.1 Tools and Technology

Tools and technology refers to surgical devices and instruments available to perform MISS. Recent innovations and rapidly evolving technology now made it possible to produce high fidelity implants. Pre- and intra-operatively, radiographic imaging with navigation and surgical planning software make it possible for us to understand the exact pathophysiology. Virtual reality is another significant advancement that makes it possible to customize precise surgical plans, and even practicing virtual surgery is possible.

Currently used fundamental tools and technologies for performing MISS include the following:

- Access: Tubular or specular retractors, endoscope tubes, and working channels
- Visualization and illumination: microscope, exoscope, endoscope
- Implants: bioabsorbable cages, expandable cages, hyperlordotic cages, stand-alone cages, cannulated screws, percutaneous single-step pedicle screw system, dynamic implant technology, artificial disks
- MISS surgical instruments: evolving every minute by the needs of the MISS surgeon. Examples may be the curved, bayoneted, and extended instruments like Kerrison rongeurs.
- Radiological innovations: Intraoperative imaging system with 2D and 3D navigation
- Robotics: Robotic guidance systems, screw implantations
- Computer software: Surgical planning and augmented reality software

Although all these tools are not necessary in every surgery, up-to-date knowledge of the newly available technologies allows surgeons to consider all available options when caring for a diverse variety of patients and pathologies.

The surgical microscope is a sine qua non for MISS. Even you are operating via an endoscope or exoscope, a MISS surgeon should always have a backup plan, and the microscope is a primary tool in alternative strategies. The microscope already gives 3D vision, the real sensation of the depth, and illumination when working in fields with limited exposure. Some current surgical microscopes come equipped with integrated navigation technology and high-definition video recording systems. They also allow for easy editing and transfer of videos to handheld devices. Of course, all these innovations are important, but the essential point is the comfort that the microscope provides to the surgeon. The microscope should be very easy to handle. It must give the surgeon a 360 degrees flexibility, and it should be as compact as possible to allow the user to get as close to the patient as possible [11].

High quality imaging is critical in MISS procedures which lack clear visualization of anatomical reference points that can be used as a basis for surgical orientation and implant placement during traditional open approaches. Additionally, Navigation systems are widely utilized to overcome the lack of anatomical reference points in MISS. The Airo® C.T. scanner (Brainlab AG, Feldkirchen, Germany) greatly expands navigation from a tool used solely for

instrumentation navigation to one used for intraoperative planning and guidance throughout the entirety of the MISS. It has introduced an era of "total navigation," that is, the use of navigation for all steps of the process from pathology localization and incision planning to screw placement, tubular decompression, cage placement, and rod measurement without the need for fluoroscopy [12]. 3D navigation has improved the workflow of MISS by increasing the accuracy of localization of the pathology to hardware implantation and decreasing radiation exposure to the surgical staff [13].

The paradigm shift from open surgery to MISS was achieved gradually with the development of new technologies. Figure 3.3 demonstrates the essential tools for a safe MISS.

### 3.3.2 Surgical Technique

Surgical technique is continually evolving in tandem with advances in anatomical studies. Training, motivation, knowledge of anatomy, and experience are crucial factors for the development of surgical techniques. MISS techniques are relatively new techniques, and they are evolving rapidly with the combination of new technologies, thus they are not the standard surgical approaches generally taught in spinal programs. Some of the MISS surgical techniques constitute the vast majority of MISS procedures as we have summarized below:

1. MISS via tubular or specular retractor to achieve a bilateral decompression and a con-

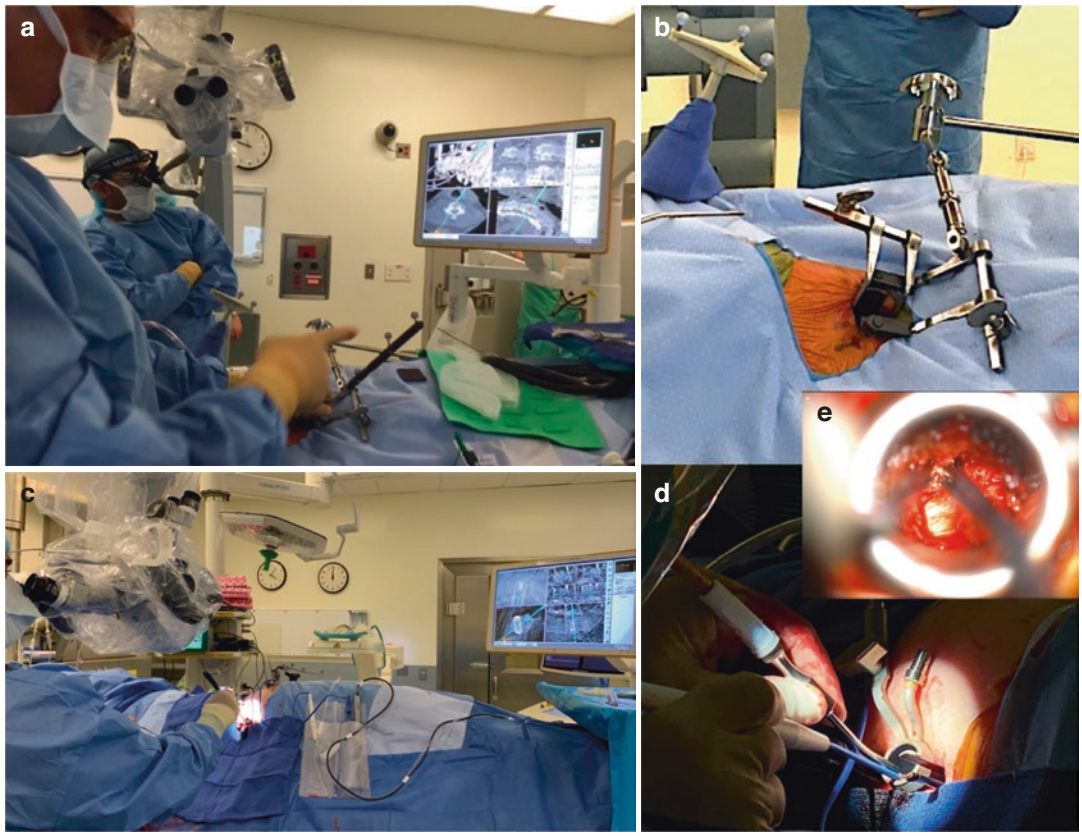


**Fig. 3.3** Some of the currently used fundamental tools for MISS are demonstrated in the figure including; navigation technology (**a**), tubular or specular retractors (**b**), surgical microscope (**c**), tubes, and working channels (**d**, **e**)

tralateral foraminotomy through a unilateral approach. This approach is frequently used in degenerative spinal stenosis, and it is possible to use this technique in all spine locations. The tubular decompression procedure has been named "unilateral laminotomy for bilateral decompression" (ULBD) [8]. As previously mentioned, Yasargil et al. utilized unilateral laminotomy for bilateral decompression for the treatment of 250 spinal tumors and 78 spinal AVMs [14]. This technique minimizes iatrogenic instability and reduces the need for instrumentation and fusion surgery. This technique is excellent for patients with lumbar stenosis and stable grade I spondylolisthesis, for the contralateral approach for decompression of synovial cysts, and contralateral approach for decompression of intraforaminal pathology [15, 16].

2. MISS via the endoscope is a relatively new technique benefiting from advances in camera and visual display technologies. There are endoscopic techniques similar to microdiscectomy popularized by Destandau J [17] and percutaneous endoscopy popularized by Lübbers T [18]. Several other types of endoscopic surgeries are evolving and bringing their tools and technology [19].
3. MISS for the *indirect* decompression of central and foraminal stenosis. In this technique, the surgical approach to the patient may be lateral, oblique, or anterior related to the pathological anatomy. The challenge currently lies in the accurate prediction of successful indirect decompression and the determination of which patients should also undergo a direct decompression. In addition, these approaches also allow a certain degree of deformity correction depending on the type of implants and techniques used.
4. MISS surgical techniques combined with the practical and safe integration of 2D/3D navigation and robotic surgery into the surgical workflow. These techniques require even more tools and technology. They are more commonly involved in routine MISS depending on the hospital's facilities.

### 3.3.3 Teaching/Training

Mastery in every MISS technique necessitates a focused practice and the process of accomplishing surgical proficiency involves a learning curve best addressed by ongoing teaching and training [20–22]. At institutions where MISS is performed frequently, residents are privileged to have a chance to get this training. To be competent in MISS techniques, this training, as mentioned above, is sophisticated and requires the commitment of the residents and/or the surgeons. At this time, training in MISS is not mandatory or considered a core competency. Educating future generations of surgeons on MISS is crucial not only for the advancement of the field but for the safety of the patients.

MISS is rapidly evolving with the involvement of new surgical approaches that require detailed anatomical knowledge, and utilization of new tools and technology necessitates further training. MISS trained surgeons are also responsible for finding ways to effectively keep up with new developments and further contribute to the area. For surgeons who have reached the plateau of the learning curve, it is crucial to understand that this is a lifelong learning process. Innovations in computer technologies make it possible for MISS surgeons to use surgical simulations and utilizing very realistic 3D models to practice surgical anatomy. These computerized tools are available and allow surgeons to train in the necessary skills and procedures in MISS [21]. Last, attending MISS courses aimed at educating surgeons in new processes can be extremely valuable as well as visiting and observing other expert surgeons. Proficient MISS surgeons should continue to be encouraged to train others in these techniques.

### 3.3.4 Curriculum Development

Development of a standardized curriculum is important to promote high quality care and standards across institutions [1]. The AOSpine approach divides MISS into nine necessary

**Table 3.1** AOSpine curriculum [5] for the basic MISS skills and the basic MISS procedures

| Basic MISS Skills | Basic MISS Procedures |
|---|---|
| Using a microscope | Microscopic interlaminar lumbar discectomy (MILD) |
| Using an endoscope | Microscopic posterior cervical foraminotomy (MPCF) |
| Using a burr with an endoscope | Microscopic extraforaminal lumbar discectomy (MELD) |
| Using a drill for MISS | Interlaminar endoscopic lumbar discectomy (IELD) |
| Using 2-D and 3-D navigation and assistive technologies | Transforaminal endoscopic lumbar foraminotomy and discectomy (TELF), (TELD) |
| Managing a dural tear | Endoscopic unilateral laminotomy for bilateral decompression (Endoscopic "over the top" decompression or endoscopic ULBD) |
| Bleeding control | Microscopic unilateral laminotomy for bilateral decompression ("over the top" decomp, ULBD) |
| Maximizing arthrodesis | Percutaneous screw and rod placement |
| What to do when lost | TLIF |

skills and nine basic procedures which are expanded and developed over time as demonstrated in Table 3.1 [1]. The best way to implement a curriculum is to go from "simple" to "complex." "Simple" includes reinforcement of general medical knowledge, reviewing surgical indications, solidifying the anatomical knowledge, building up knowledge of tools and technologies, and then proceeding into "complex" levels, which includes the teaching of surgical techniques. This consists of a stepwise program using videos, surgical simulation, lectures, and online teaching material to minimize the learning curve for surgeons.

### 3.3.5 Testing: Research and Outcomes

Outcome tracking and research have an essential role in the aspect of awareness regarding the results of MISS. Objective data allows surgeons to refine patient selection, counseling, and surgical decision-making. It also drives collaborative innovations. For example, Feng et al. created and implemented an enhanced recovery after surgery (ERAS) protocol for the patients undergoing MIS TLIF and found the ERAS pathway to be associated with decreased blood loss, operative time, intraoperative fluid infusion, postoperative drainage, lower costs, and shorter length of hospital stay [23].

### 3.3.6 Talent

Talent involves innate and learned skills required to perform a surgical operation. Importantly, many surgical skills can be learned. Excellent surgical skills require time and patience. A genuinely successful surgeon is also characterized by traits such as enthusiasm, resilience, caring attitude toward patients, self-discipline, and criticism, physical fitness, and commitment [24]. Gagne argues that innate natural abilities exist but that they need to be actualized and appreciated by a context to flourish [25]. He developed a "Differentiated Model of Giftedness and Talent" that describes how coaching or training can transform skills or natural abilities into true excellence and talent [26]. Figure 3.4 summarizes the talent in the top of the pyramid as a representation of the mastery.

Ericsson et al. suggested "deliberate practice" to reach mastery. Deliberate practice means a focused, wise, and continuous practice which involves a complex combination of many tools, support from mentors, and constant hard work. There is evidence that in many professions, hours of practicing activities are positively correlated with expertise, which is, at least initially, designed by the mentors and coaches [27]. Ericsson et al. cited that the estimated accumulated practice (deliberate practice) in expert violinists, was 10,000 h to achieve expert performance [28]. While training new surgeons, the primary goal

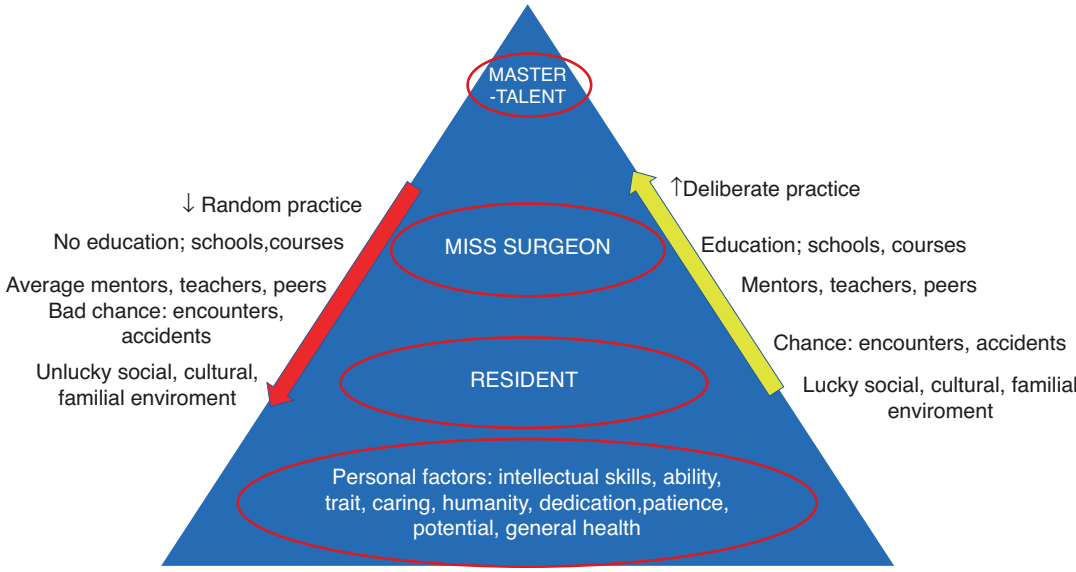


**Fig. 3.4** Talent is developed by one's natural ability, intrapersonal factors, and environmental factors. Figure summarizes the steps to achieve the talent in the top of the pyramid as a representation of the mastery

should be to focus on better understanding the motivational factors encouraging sustained deliberate practice for talent in MISS. Research shows that surgical skills can be improved significantly when using appropriate teaching and learning techniques, independent from a preexisting skill level (37). The environment, including adequate teaching and training, has an essential impact on whether talent can be developed and optimized. As summarized in a study by Jensen et al., "Individual skills make good surgeons, the mixture of skills provides the potential to become talented, while the person-environment fit is what determines if the talent potential can be realized" [29].

## 3.4 Conclusion

MISS is rapidly evolving and advancing the field of spine surgery. It is being enabled by rapidly evolving technology, innovative tools, and the needs of our patients. Future technologic innovations may support 4D and virtual reality technologies by including tactile feedback and other concepts to simulate real surgery on the aspect of training surgeons. The rapid rate of progress over the past decade suggests more innovations to come to the field of MISS. As the role and indications for MISS increase, and the pathologies addressed become more complex, it is essential to consider the six T's to ensure practitioners of MISS maintain high standards.

**Conflicts of Interest and Financial Disclosure**
The authors declare no conflicts of interest related to the material presented with the exception of the following: RH.

## References

1. Grotle M, Småstuen MC, Fjeld O, Grøvle L, Helgeland J, Storheim K, et al. Lumbar spine surgery across 15 years: trends, complications and reoperations in a longitudinal observational study from Norway. BMJ Open. 2019;9(8):1–7.
2. Martin BI, Mirza SK, Spina N, Spiker WR, Lawrence B, Brodke DS. Trends in lumbar fusion procedure rates and associated hospital costs for degenerative spinal diseases in the United States, 2004 to 2015. Spine. 2019;44(5). https://journals.lww.com/spinejournal/Fulltext/2019/03010/Trends_in_Lumbar_Fusion_Procedure_Rates_and.14.aspx
3. Basil GW, Wang MY. Trends in outpatient minimally invasive spine surgery. J Spine Surg (Hong Kong).

2019;5(Suppl 1):S108–14. https://pubmed.ncbi.nlm.nih.gov/31380499
4. Peng H, Tang G, Zhuang X, Lu S, Bai Y, Xu L. Minimally invasive spine surgery decreases postoperative pain and inflammation for patients with lumbar spinal stenosis. Exp Ther Med. 2019;18(4):3032–6. https://pubmed.ncbi.nlm.nih.gov/31555386
5. Schmidt FA, Wong T, Kirnaz S, Taboada N, Assaker R, Hofstetter C, et al. Development of a curriculum for minimally invasive spine surgery (MISS). Glob Spine J. 2020;10(2_suppl):122S–5S.
6. Andersson G, Buvenenadran A, Lauryssen C, Cappuccino A, Garfin S, Pimenta L, et al. Summary statement: minimally invasive spine surgery. Spine. 2010;35(26):S271–3.
7. McDermott KW, Freeman WJ, Elixhauser A. Overview of operating room procedures during inpatient stays in U.S. hospitals, 2014: statistical brief #233. In: Healthcare cost and utilization project (HCUP) statistical briefs. Rockville, MD: Agency for Healthcare Research and Quality (US); 2006. p. 1–14. http://www.ncbi.nlm.nih.gov/pubmed/29578672.
8. Rajaee SS, Bae HW, Kanim LEA, Delamarter RB. Spinal fusion in the United States: analysis of trends from 1998 to 2008. Spine. 2012;37(1):67–76.
9. del Castillo-Calcáneo J, Navarro-Ramirez R, Gimenez-Gigon M, Adjei J, Damolla A, Nakhla J, et al. Principles and fundamentals of minimally invasive spine surgery. World Neurosurg. 2018;119:465–71.
10. Härtl R. The 6 T's of minimally invasive spine surgery. Glob Spine J. 2020;10(2_suppl):5S–7S. https://doi.org/10.1177/2192568220911617.
11. Yaşargil MG, Krayenbühl H. The use of the binocular microscope in neurosurgery. Bibliotheca ophthalmologica : supplementa ad ophthalmologica. 1970;81:62–5.
12. Navarro-Ramirez R, Lang G, Lian X, Berlin C, Janssen I, Jada A, et al. Total navigation in spine surgery; a concise guide to eliminate fluoroscopy using a portable intraoperative computed tomography 3-dimensional navigation system. World Neurosurg. 2017;100:325–35.
13. Fomekong E, Safi SE, Raftopoulos C. Spine navigation based on 3-dimensional robotic fluoroscopy for accurate percutaneous pedicle screw placement: a prospective study of 66 consecutive cases. World Neurosurg. 2017;108:76–83. https://doi.org/10.1016/j.wneu.2017.08.149.
14. Yaşargil MG, Tranmer BI, Adamson TE, Roth P. Unilateral partial hemi-laminectomy for the removal of extra- and intramedullary tumours and AVMs. Adv Tech Stand Neurosurg. 1991;18:113–32.
15. Wipplinger C, Melcher C, Hernandez RN, Lener S, Navarro-Ramirez R, Kirnaz S, et al. "One and a half" minimally invasive transforaminal lumbar interbody fusion: single level transforaminal lumbar interbody fusion with adjacent segment unilateral laminotomy for bilateral decompression for spondylolisthesis with bisegmental stenosis. J Spine Surg (Hong Kong). 2018;4(4):780–6.
16. Boukebir MA, Berlin CD, Navarro-Ramirez R, Heiland T, Schöller K, Rawanduzy C, et al. Ten-step minimally invasive spine lumbar decompression and dural repair through tubular retractors. Oper Neurosurg. 2017;13(2):232–45.
17. Destandau J. A special device for endoscopic surgery of lumbar disc herniation. Neurol Res. 1999;21(1):39–42.
18. Lübbers T, Abuamona R, Elsharkawy AE. Percutaneous endoscopic treatment of foraminal and extraforaminal disc herniation at the L5-S1 level. Acta Neurochir. 2012;154(10):1789–95.
19. Hussain I, Rapoport BI, Krause K, Kinney G, Hofstetter CP, Elowitz E. Transforaminal endoscopic lumbar discectomy and foraminotomy with modified radiofrequency nerve stimulator and continuous electromyography under general anesthesia. World Neurosurg. 2020;137:102–10.
20. Parikh K, Tomasino A, Knopman J, Boockvar J, Härtl R. Operative results and learning curve: microscope-assisted tubular microsurgery for 1- and 2-level discectomies and laminectomies. Neurosurg Focus. 2008;25(2):E14.
21. Son-Hing JP, Blakemore LC, Poe-Kochert C, Thompson GH. Video-assisted thoracoscopic surgery in idiopathic scoliosis: evaluation of the learning curve. Spine. 2007;32(6):703–7.
22. Lau D, Lee JG, Han SJ, Lu DC, Chou D. Complications and perioperative factors associated with learning the technique of minimally invasive transforaminal lumbar interbody fusion (TLIF). J Clin Neurosci. 2011;18(5):624–7.
23. Feng C, Zhang Y, Chong F, Yang M, Liu C, Liu L, et al. Establishment and implementation of an enhanced recovery after surgery (ERAS) pathway tailored for minimally invasive transforaminal lumbar interbody fusion surgery. World Neurosurg. 2019;129:e317–23.
24. Schmidt-Tintemann U. Women in surgery. Der Chirurg; Zeitschrift fur alle Gebiete der operativen Medizen. 1997;68(6):583–5. https://doi.org/10.1007/s001040050233.
25. Gagné F. From genes to talent: the DMGT/CMTD perspective. Rev Educ. 2015; https://doi.org/10.4438/1988-592X-RE-2015-368-289.
26. Gagné F. Nature or nurture? A re-examination of Sloboda and Howe's (1991) interview study on talent development in music. Psychol Music. 1999;27:38–51.
27. Ericsson KA, Nandagopal K, Roring RW. Toward a science of exceptional achievement. Ann N Y Acad Sci. 2009;1172:199–217.
28. Ericsson KA. Deliberate practice and the acquisition and maintenance of expert performance in medicine and related domains. Acad Med. 2004;79(10):S70–81.
29. Jensen RD, Christensen MK, LaDonna KA, Seyer-Hansen M, Cristancho S. How surgeons conceptualize talent: a qualitative study using sport science as a lens. J Surg Educ. 2017;74(6):992–1000.

# MI-TLIF with 3D Navigation

4

Arvind G. Kulkarni, Pradhyumn Rathi, and Pritem A. Rajamani

## 4.1 Introduction

Over the last decade, TLIF (Transforaminal Lumbar Interbody Fusion) has become a popular technique for achieving segmental interbody fusion. The recent advances in minimal access technology have helped to execute the procedure through a minimally invasive approach and provide adequate decompression with a solid fusion. The minimally invasive technique also helps to avoid many of the disadvantages of the traditional posterior open approach [1, 2]. A study by Schwender et al. [3] reported clinically significant improvements in visual analog scores and Oswestry disability index scores along with a 100% fusion rate in a cohort of patients who underwent a minimally Invasive TLIF (MIS-TLIF) procedure. Visualization is through a smaller and narrower dissection in MIS cases. The presence of complex spine pathologies such as rotated spine in degenerative scoliosis, poor anatomy on fluoroscopy, asymmetric and abnormally shaped pedicles can pose serious challenges in MIS-TLIF, resulting in incorrect placement of pedicle screws and cages [4]. Image-guided navigation during spinal surgery can be of an invaluable assistance to MIS surgeons as it allows for a larger area of visualization of bony and soft tissues through a smaller area of surgical dissection. Pedicle screw placement by freehand techniques is primarily based on anatomical landmarks, and various methods have been described so far based on cadaveric studies. The high variability in the morphology of pedicles makes it more challenging in complex spinal deformities. Fluoroscopy can assist screw placement; however, it increases the operative time and radiation exposure to the surgeon and operating room personnel. Misplacement rates of up to 30% in the lumbar spine and up to 50% in the thoracic spine have been reported with freehand and fluoroscopic guided pedicle screw placement. Mal-positioned screws risk potential damage to the spinal cord, nerve roots, and great vessels and also decrease the stability of the fixation. Medico-legal concerns over patient safety have further reinforced the need for image-guided screw placements to improve accuracy [5].

Computer-assisted spine surgery (CASS) is a discipline that uses novel computer-based technologies, including stereotaxy, navigated surgery, and robotics. Navigation-assisted spine surgery is a group of technologies, which allow the surgeon to access real-time, three-dimensional, and virtual images of the spine in relation to the surgical instruments intra-operatively. This is a combination of image acquisition and processing that is followed by intra-operative navigation. The primary goal of navigation is to optimize the surgical intervention by providing the surgeon with

A. G. Kulkarni (✉) · P. Rathi · P. A. Rajamani
Mumbai Spine Scoliosis and Disc Replacement Centre, (Work done at Saifee Hospital), Mumbai, India



J.-S. Kim et al. (eds.), *Technical Advances in Minimally Invasive Spine Surgery*,
https://doi.org/10.1007/978-981-19-0175-1_4

advanced visualization of the operative field and to see the exact position of the handheld instrument in relation to the bony anatomy. The overall benefits include accurate and safe instrumentation, minimal radiation exposure to the surgical team, reduction of surgeon fatigue and surgical duration. Spine navigation was initially used to improve the accuracy of pedicle screw placement. However, over the years, its use has extended into minimally invasive surgical techniques, cervical spine surgery, revision surgery, and spine tumour surgery [5].

## 4.2 Components in Spine Navigation Systems [5]

There are numerous navigation systems available commercially now. The basic fundamentals, however, remain the same and include the following.

### 4.2.1 Image Acquisition and Processing Unit

The first step in spinal navigation is to acquire high-resolution images of the region of interest, either pre-operatively or intra-operatively, which then allows the surgeon to navigate upon these processed images. Intra-operative imaging is currently being used in most navigated surgeries as it involves the acquisition of images after positioning the patient for surgical intervention, and this reduces the rate of errors in matching and registration. Intra-operative imaging can be done either by fluoroscopy, computerized tomography (CT) scan and of late even magnetic resonance imaging (MRI).

### 4.2.2 Referencing System

This includes Dynamic Reference Frame/Array (DRA), Light Emitting Diodes (LEDs), and Tracking system.

#### 4.2.2.1 Dynamic Reference Array

The dynamic reference array (DRA) is usually attached to fixed anatomical landmarks, such as the spinous process. The accuracy of the navigation depends on the stable fixation of this DRA, and, therefore, it must be left undisturbed throughout the surgery.

#### 4.2.2.2 Light-Emitting Diodes

DRA has provisions for attaching three or more spheres known as light-emitting diodes (LEDs). These LEDs emit light which is tracked by an electro-optical camera and are known as active arrays. Specialized surgical instruments are used, which also have LEDs attached to them and are called passive arrays as they reflect the infrared rays emitted from the camera and gives the surgeon a real-time tracking of the exact location of these devices over the surgical field. The 3D orientation between these active and passive LEDs thus facilitates navigation.

#### 4.2.2.3 Tracking System

Various tracking systems are available that include optical, mechanical, acoustic, or electromagnetic systems. Optical tracking systems are the most frequently used due to superiority in terms of accuracy. They use infrared camera devices to actively track the light emitted or reflected from the LEDs, which are attached to the DRA and surgical instruments which requires the “line of sight” maintenance between the LEDs and cameras at all times.

### 4.2.3 Registration Process

The process of establishing the synchronization between virtual images and the real anatomy is called registration. Once the image is acquired, the data is transferred to the navigational system, which then performs an automated registration eliminating the need for manual registration.

## 4.3 Evolution

The methodology of pedicle screws insertion techniques in spine fusion surgery is the most significant advancement, extending from conventional open procedures to accurately placed percutaneous pedicle screws. Numerous studies in literature have highlighted clinically significant sequelae from inaccurate implant placement. For achieving a safe and ideal screw placement, a number of imaging methods and image guidance systems have been used. The use of stereotactic navigation based intra-operative CT is a promising modality offering the benefits of highly accurate pedicle screw placement, reduced operative radiation exposure, and seamless integration into minimally invasive spine surgery. Recently, extensive minimally invasive spinal systems have surged, almost all based on the principle of using a series of dilators of different lengths and increasing diameters to create a path between muscle fascicles to access the posterior spinal elements [6–8]. Initial surgeries using these access portals involved simple decompressive procedures; however, over the last decade, these systems have been expanded to facilitate interbody and posterolateral arthrodesis in addition to the placement of pedicle screws in a less invasive fashion in traumatic to deformity correction cases [9]. Spinal navigation is closely related to intra-operative 3D imaging providing an imaging dataset for navigational use and the opportunity for immediate intra-operative assessment of final screw position giving the option of immediate screw revision if necessary.

## 4.4 Generations of Navigation System [5]

The history of spine navigation systems can be considered to have undergone three generations of evolution as shown in Table 4.1.

**Table 4.1** Comparison between various navigation systems

| Image acquisition | 2D fluoroscopy | 3D fluoroscopy | Preoperative CT | Cone Beam CT | Intra-operative CT |
|---|---|---|---|---|---|
| Generation | 2nd | 2nd | 1st | 2nd | 3rd |
| Registration | Automated | Automated | Manual and time consuming | Automated | Automated |
| Registration duration | Short | Short | Long | Short | Ultra-short |
| Image display | 2D (AP and lateral) | 3D | 3D | 3D | 3D |
| Scan time | Only AP and lateral radiographic images | 2 min | 30 s | 40 s | 30 s |
| Number of vertebrae in single scan | 3–5 vertebrae | 3–5 vertebrae (working corridor 12 × 12 cm) | Whole spine | 6–8 vertebrae (working corridor 30 × 40 cm) | Whole spine |
| Bone image quality | Poor | Poor | Good | Good | Good |
| Imaging in severe deformities | Not possible | Not possible | Possible | Possible | Possible |
| Carbon table and carbon head clamp fixation | Not necessary | Required | Not necessary | Required | Required |
| Ideal area of the spine | Lumbar spine | Whole spine | Whole spine | Whole spine | Whole spine |
| Minimally invasive spine surgery | Difficult | Possible | Not possible | Possible | Possible |
| Real-time imaging | Yes | Yes | No | Yes | Yes |
| Radiation exposure | Patient↓ OT personnel↓ | Patient↓ OT personnel↓ | Patient↑↑ OT personnel↓ | Patient↑ OT personnel↓ | Patient↑↑ OT personnel↓ |

### 4.4.1 First-Generation Spine Navigation

First-generation spine navigation systems employed image acquisition using thin-slice CT scan pre-operatively.

### 4.4.2 Second-Generation Spine Navigation

Second-generation spine navigation managed to overcome the shortcomings noted in the first generation. They offered intra-operative reconstruction images of the spinal anatomy using two-dimensional (2D) and three-dimensional (3D) fluoroscopy. The 2D fluoroscopy system provided images in two planes. Axial reformatting was not available. The advantage of this system was that the computer software and image acquisition system could be paired with routinely used fluoroscopy units available in the operating room.

Further improvement was seen in the form of cone-beam CT that used basic multiplane fluoroscopy to reconstruct three-dimensional CT like images. The drawbacks were that limited segments of the spine could only be scanned during the process. This made multiple level fixation spanning long segments difficult as multiple scans needed to be performed for a single procedure, increasing the radiation exposure, and operative time.

#### 4.4.2.1 3D C-Arm Navigation System

This system depends on the concept of isocentricity. The fluoroscopy unit is coupled with a special reference system and computer software to provide axial, sagittal, and coronal reformatted images. The fluoroscopy unit moves through an arc of 180° while focusing on a solitary point in the spine. The system can be calibrated to a high spatial resolution protocol, which takes multiple fluoroscopy images while the arc moves through the 180° or lower resolution protocol, which may take fewer images during the process. The system allows for automatic reference. The advantage of the system was that it did not require a pre-operative CT scan. Intra-operative image acquisition allowed for a post-operative scan to assess the accuracy of the screw position possible. The 3D C-Arm can be used as a routine fluoroscopy unit and can be paired with image guidance surgery software to work as a navigation system for complex spinal surgery.

However, there are a few disadvantages to this navigation system. It scans patients based on the selected isocentric point. Therefore, all the images obtained are from a segment of the spine in the field of the scan. This limits the scan to 6–7 vertebral segments. Although the images generated by the 3D C-Arm are similar to a reformatted CT scan, the image quality is inferior to conventional pre-operatively performed CT scans.

#### 4.4.2.2 Cone Beam CT

Plenty of Cone Beam CT (CBCT) devices are available commercially, and again they can be used either pre-operatively or intra-operatively. The image quality is superior to 3D C-Arm, and the time for image acquisition is also shorter. Intra-operative CBCT devices allow automatic registration and have a larger field of scan and, therefore, can screen more vertebral segments in a single scan when compared to the 3D-C Arm system. They can provide both routine fluoroscopy images and reformatted CT images in the axial, sagittal, and coronal sections. The radiation dose of the CBCT devices, however, is lower than a conventional CT scanner, and it may be used to assess the accuracy of placement of screws intra-operatively.

#### 4.4.2.3 Third-Generation Spine Navigation Systems

Third-generation spine navigation systems are considered the most recent developments in the field. These navigation systems can perform an intra-operative CT scan with subsequent automatic registration. They provide excellent CT images with a scan field that can screen the entire

spinal column. It offers an opportunity to use the navigation in conjunction with minimal access surgical procedure. The radiation exposure to the patient with the use of such CT based systems can be much higher than fluoroscopy-based navigation systems. These imaging devices have adjustable radiation density thresholds, which provide good images even when the density is reduced by 25–50% of the maximum dosage.

### 4.4.3 Senior Author's MIS Navigation Surgical Technique

The senior author's MIS surgical technique is centred around navigation when performing specific portions of his operations. We will outline the operating room setup, data acquisition for tracking, registration of instrumentation/patient, and operative steps while performing navigated MIS-TLIF.

## 4.5 Indications

1. Degenerative spondylolisthesis with difficult facet morphology.
2. Grade I-III spondylolytic spondylolisthesis and spondyloptosis with narrow pedicles.
3. Degenerative scoliosis with an indication for selective fusion with rotated pedicles.
4. Revision spine surgery—Adjacent segment disease.

### 4.5.1 Operating Room Setup

The senior author (SA) sets up the operating room with the patient prone in the centre of the operating room. The image intensifier comes in from the right side of the room (as seen from the foot of the patient). The monitor with the navigation guide stays above the right side of the patient's right shoulder. The registration camera is above the head of the bed.

### 4.5.2 Anaesthesia

General anaesthesia is used for Navigated TLIF.

### 4.5.3 Positioning

The patient is placed prone on a radiolucent operating table following intubation which allows tilting in all directions and is secured with tapes/belts. The elbows are placed at 90° to decrease traction on the brachial plexus and pads are placed under the ulnar and peroneal nerves. In addition, pillows are placed under the lower extremities (Fig. 4.1). After positioning, the mobility of the Foley catheter is checked, the endotracheal tube is secured, and the fluoroscopic machine is draped into the operative field. Reverse Trendelenburg position is given to make the involved level as vertical as possible to the floor and avoid prolonged abnormal postures with microscope usage.

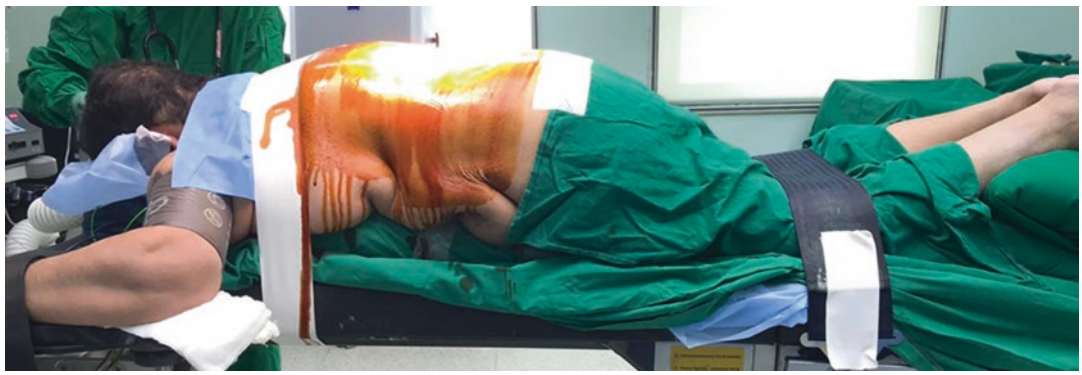

**Fig. 4.1** On table patient positioning

### 4.5.4 3D Navigation Registration

Following standard skin preparation and sterile draping, navigation reference frame is docked on the adjacent spinous process (usually one level above). The 3D C-arm is triggered to spin around the patient and the procured images get formatted into images in all planes (sagittal, coronal, and axial). These images are then transferred to the Stealth monitor. The Stealth™ camera can detect and track anatomy using infrared rays to whichever part/instrument the tracker is attached and registered. At the time of spinning the 3D C-arm, operating team are off the operating room to avoid radiation. The total time taken from draping to registering patients data to 3D navigation takes approximately around 45 min. Authors noticed that anchoring reference frame, static position of patient, and temporary suspension of ventilation to sidestep respiratory movements (generally for a minute) at the time of image capture by the C-arm play a key role to minimize anatomical (registration) errors [10, 11]. Literature suggests that error margins were positive in <1 mm translation and 5° rotation of the patient reference array in all regions of spine [12].

As a first step following verification, navigated Jamshedi needle is registered and tracked to the optical system following which pedicle cannulation is performed using real-time visualization in all the three planes. Percutaneous guide wires are then passed into the pedicles through the Jamshedi needle (11 G) (the authors prefer to place the pedicle guide wires first followed by interbody cage and finally pedicle screws with interconnecting rods. This is because of the change in the real anatomy as a result of disc space preparation and insertion of the cage v/s the virtual anatomy that was captured earlier). Once the placement of the navigated Jamshedi needle within the vertebral body at an appropriate orientation is confirmed, a blunt-tipped threaded guidewire is passed through the cannulated centre of the entry needle. Care should be taken not to advance the guide wire to within 10 mm from the anterior wall of the vertebral body. Following confirmation by lateral view from navigated images, tip of the guidewire from the navigated Jamshedi needle is withdrawn. The steps are repeated for rest of the pedicles and all the guide wires are bent away from the operative field securing them to the draping without introducing sharp bends into them (Fig. 4.2).

### 4.5.5 Decompression

Using the Wiltse's approach, with 3D navigation, successive serial dilators of increasing diameters till 22 mm are inserted. The tubular retractor of appropriate length (5/6/7 cm) is placed over the dilator and accurately docked on the lamina–facet complex (Fig. 4.3). After removal of dilators, the final retractor system can be a fixed rigid tube (METRx), or a split blade tubular retractor (QUADRANT, MARS 3 retractor, etc.) that can be expanded. The surgical microscope

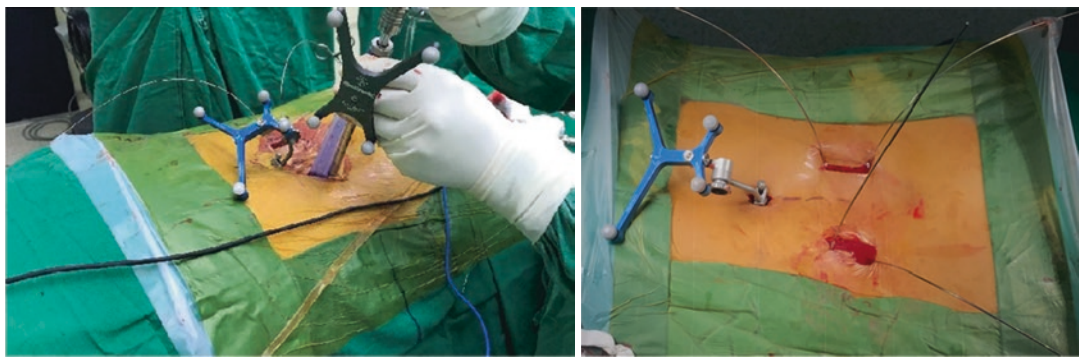

**Fig. 4.2** 3D Navigation with guide wire placement

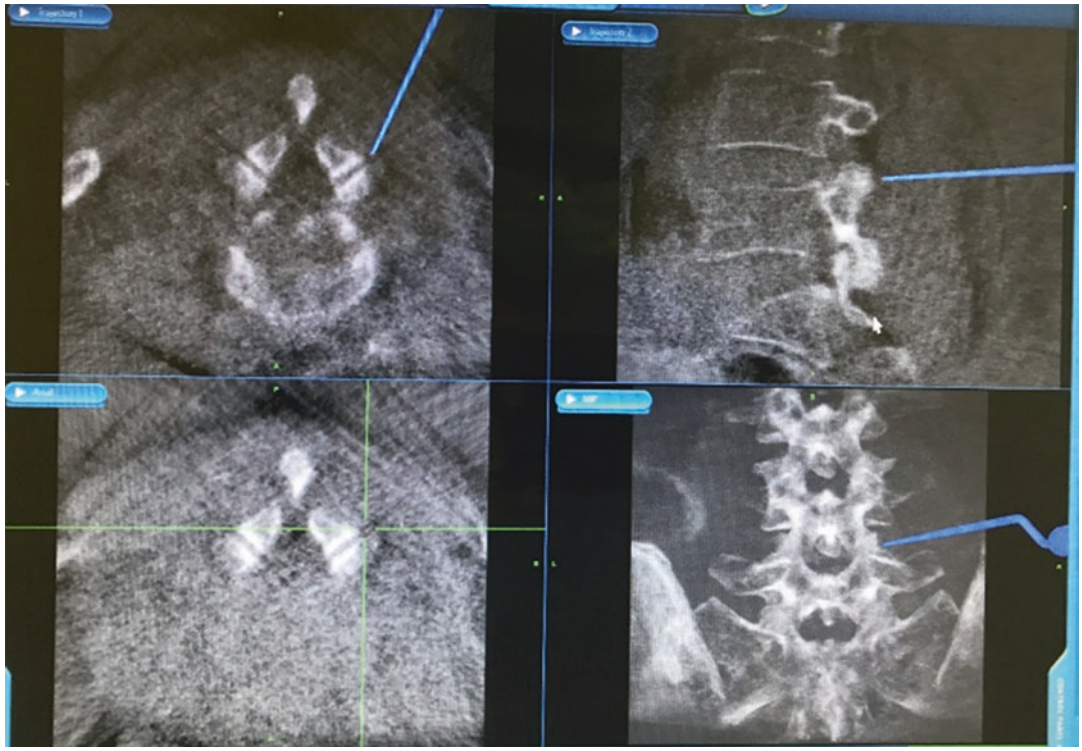

**Fig. 4.3** Planning Tube placement—Navigated Probe

is then moved into the field and decompression and interbody fusion are performed through the tubular retractor with variations in the operative steps as per the demands of the indication. The soft tissue over the facet is removed with a long monopolar cautery and Kerrison rongeur. The facet–lamina junction is delineated using navigated curette. Using an angled curette, the space between the lamina and the ligamentum flavum is defined after thinning out the lamina with a high-speed navigated burr. Using the Kerrison rongeur, the lamina–facet junction is removed. If there is no stenosis, then a small laminotomy can be done to allow the visualization of the neural elements in close proximity to the facet joint. If the patient has stenosis on the ipsilateral side, a complete laminectomy should be performed. In cases of bilateral stenosis, the spinous process is undercut and a contralateral laminectomy and medial-facetectomy accomplished by tilting the tube. If stenosis is severe or there is a significant foraminal component on the contralateral side, we suggest decompressing the lateral recess down to the exit zone by wanding the tube caudally [13]. For confirming adequate decompression, navigated probe is checked into spinal canal and foramina in both ipsilateral and contralateral sides (Fig. 4.4). A navigated burr may be used to drill the lamina and the facets, but this decreases the quantity of bone graft, since the surgeon relies on locally excised bone for fusion.

### 4.5.6 Disc Space Preparation

The next step is identifying the disc space. In general, the traversing root is medial to the pedicle and only minimal retraction is justified. The exiting nerve root hugs the superior pedicle as it exits the neural foramen and is generally cephalad to the level of the disc in the foramen. Although we do not necessarily dissect out the exiting root, it may be protected by placing a patty directed towards the cephalad pedicle in the foramen. Discectomy and disc space preparation are performed with the help of disc forceps,

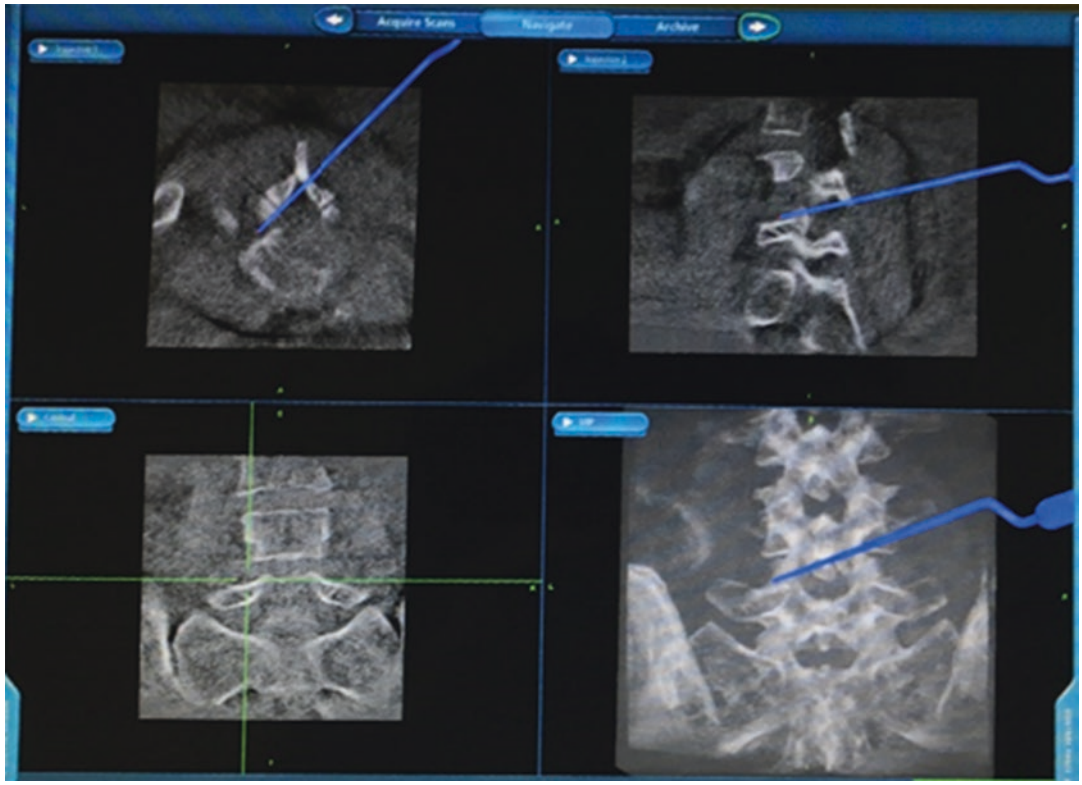

**Fig. 4.4** Evaluation of decompression

Kerrison rongeurs, bayonetted curettes, and rotating end plate shavers. The completeness of excision of the intervertebral disc is evaluated by introducing the navigation array probe in all directions: contralateral-posterior, anterior and ipsilateral-anterior, posterior quadrants of disc space (Fig. 4.5) [14]. Once disc space is cleared of the remnant disc, superior and inferior cartilaginous endplates are curetted till superficial bleeding appears on the bed of endplates to promote fusion. In certain complex situations such as high-grade spondylolisthesis, conditions with collapsed disc spaces, etc., identification of the posterior annulus and intervertebral disc may be difficult and the navigation probe has a role in identifying the precise anatomy.

The appropriate size trial interbody cage is then placed into the disc space. After confirming proper placement on navigated screen, the trial is removed and any fragment of bone and cartilage is removed. Autologous bone graft is then packed into the anterior disc space using a funnel and checked with navigated probe for equal distribution of graft. The interbody structural device (cage filled with bone graft) is then advanced into the disc space. The size and position of the cage to be placed was calculated using calibration applications on the Stealth monitor. Interbody fusions are performed using either titanium/PEEK cage and autograft, the cage being precisely positioned and verified with navigation assistance.

### 4.5.7 Percutaneous Pedicle Screw and Rod Fixation

The skin and underlying fascia are dilated by means of sequential dilators to create a pathway for the pedicle screws over the initially placed guide wires. The largest dilator is left in place to protect surrounding soft tissue. Using navigation

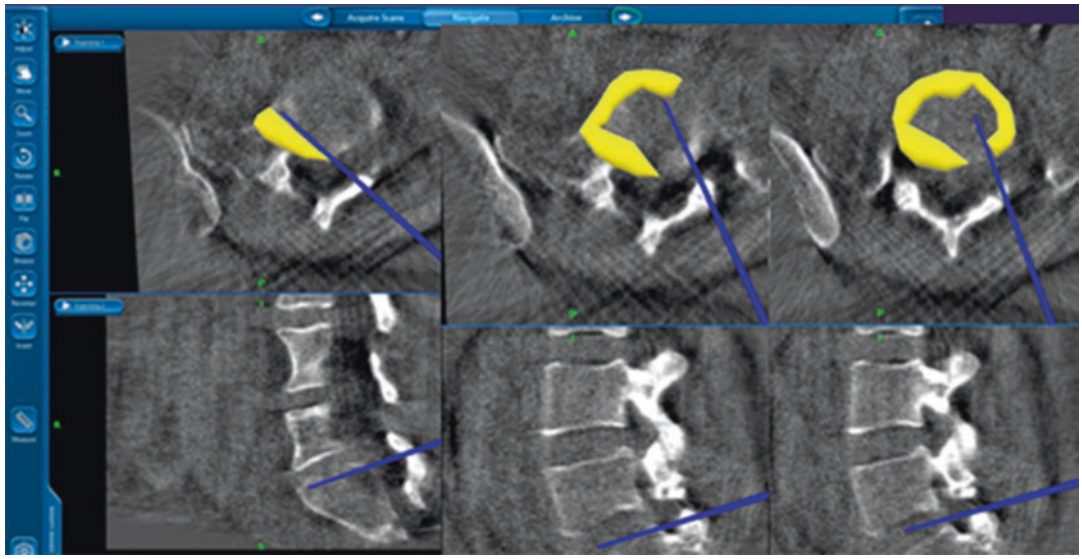

**Fig. 4.5** Cage placement

assistance tracker attached to the handles of cannulated tap, advanced over the guidewire down to the pedicle. Depth and diameter of pedicle can be calculated using navigated measurement software at the end of tapping. Care should be taken to prevent the guidewire from advancing or backing-out. Once the pedicle is tapped, the tap and tissue dilator sleeve are withdrawn while the screwdriver and tower assembly are placed over the guidewire. The pedicle screw is advanced with the navigated assistance polyaxial screwdriver avoiding cranio-facet joint violation until the appropriate depth is achieved (Fig. 4.6). Coronal, axial, sagittal images are checked intraoperatively to confirm the screw's placement within the pedicle, orientation, and overall depth. Care should be taken to avoid advancing the screw head to bone, which would limit the ability to seat the rod. The guidewire is withdrawn as the screw enters the pedicle in order to avoid it getting bent ahead of screw tip and trapped. The screwdriver is withdrawn from the tower assembly. Subsequent pedicle screws are placed with this same technique. It is important to note that all screw tower assemblies should line up in the same orientation and height before the next step of the procedure (Fig. 4.6).

A rod measurement guide is placed to facilitate measurement of the rod size. The rod is passed percutaneously through a separate stab incision (SEXTANT) or placed freehand in other designs leaving adequate lengths at both ends. Once the rod is seated, a cap inserter is placed in the tower assembly. Subsequent screw caps are now placed. Compression can be achieved by system specific methods. Final tightening of the construct is performed with an anti-torque stabilizer and torque-limited driver. The screw tower assemblies are loosened and removed. Final radiograph is obtained to confirm proper positioning of screws, cage, and rod (Fig. 4.7). Dorsolumbar fascia is approximated with absorbable No. 2-0 Vicryl and subcuticular running closure with Monocryl 3-0 done.

### 4.5.8 Post Operative Care

Ambulation usually begins on post-operative day 1. The average hospital stay is 2 days to longer for patients who have additional medical comorbidities with most patients being discharged on POD 4 with assisted ambulation. The scar at 6 weeks follow-up is cosmetic (Fig. 4.8).

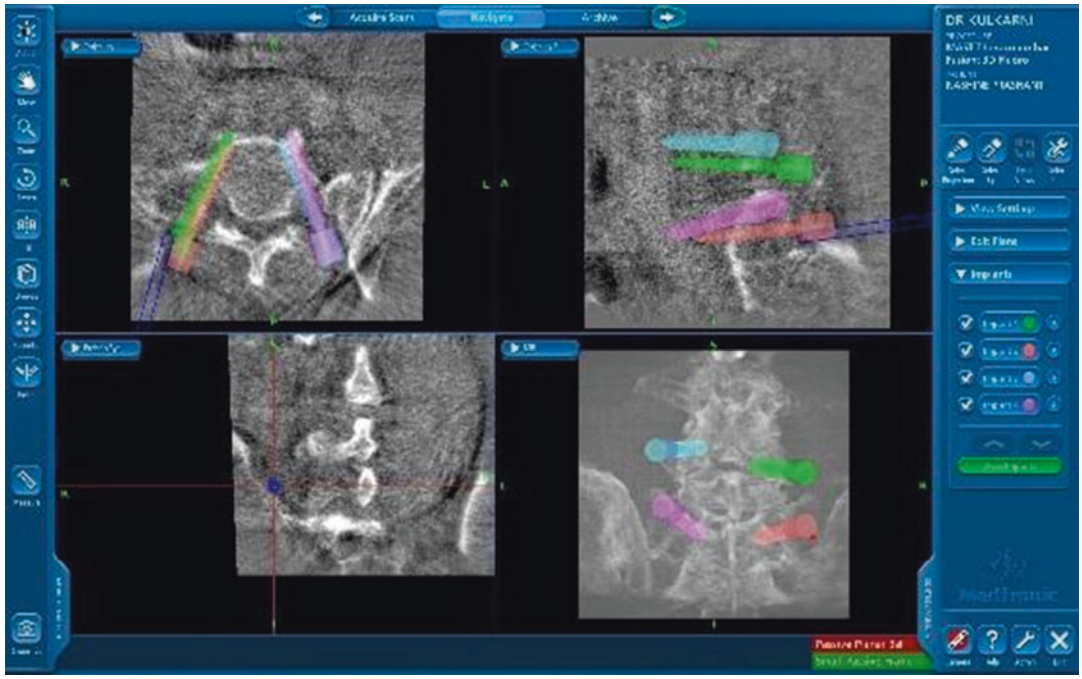

**Fig. 4.6** Pedicle screw placement

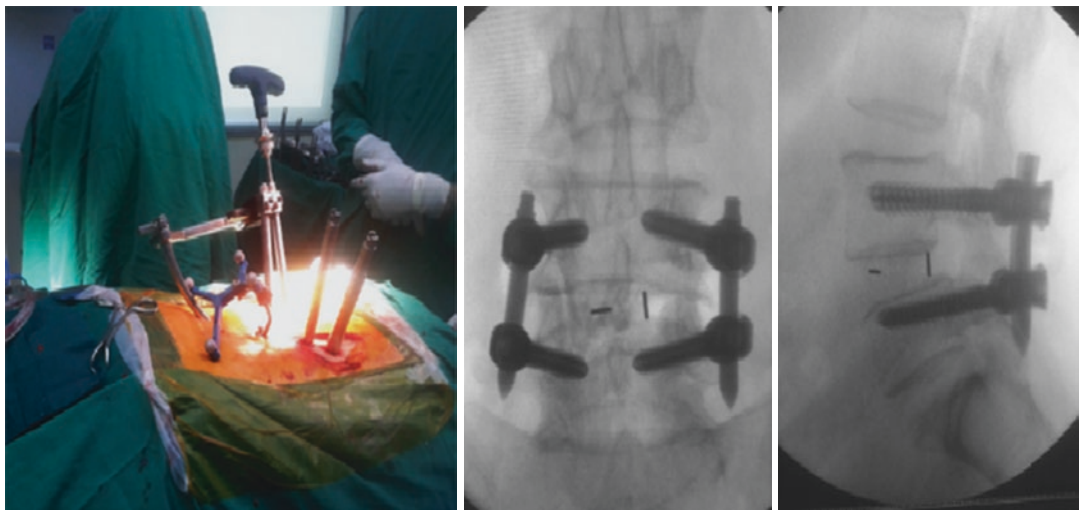

**Fig. 4.7** Placement of screws and rods

### 4.5.9 Advantages of MIS

The conventional open posterior approach contributes to wide soft tissue dissection and leads to localized denervation of muscles, extensive blood loss, fibrous tissue (dead space), persistent back pain, and muscle spasm after the procedure [15–17]. Kawaguchi et al. [18] demonstrated that the duration of muscle retraction during spine surgery, pressure of the retractors, and the number of levels exposed directly correlate with the postoperative elevation of serum creatinine phosphokinase isoenzymes, a marker of muscle injury. The MIS-TLIF procedure has overt advantages

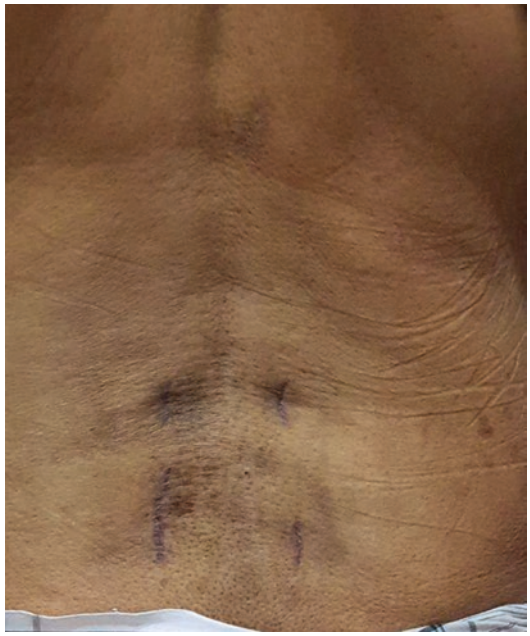

**Fig. 4.8** Scar at 6 weeks post single-level 3D navigated MIS-TLIF

over open TLIF in reducing blood loss (intra-operative and post-operative) thus abolishing need for transfusion, reduced infection rates [19, 20]. These specific advantages can be attributed to fall back of the dilated muscles in the tracts thus collapsing the dead space, which in turn helps to hasten post-operative recovery and early rehabilitation in MIS-TLIF.

## 4.6 Advantages of Navigation-Assisted Surgery

Although MIS-TLIF with fluoroscopy causes lesser damage to the patients, the intra-operative challenges faced by surgeons in inserting percutaneous pedicle screw are spinal alignment, quality/quantity of multifidus muscle, and depth of screw entry point. Furthermore, the pedicle dimensions, facet joint arthritis, screw location (ipsilateral and contralateral), screw length, screw diameter, cortical encroachment, frank penetration, and screw trajectory angle are all uncertainty screw-related variable [4].

### 4.6.1 Accuracy

Navigation-assisted screw positioning has reported lower misplacement rate compared to the freehand placement. Rajasekaran et al. in a recent article have analyzed pedicles and documented an accuracy rate of 96.2% using intra-operative CT based navigation [21]. In addition to pedicle screw placement, navigation helps to classify these non-negotiable pedicles and prevents the surgeon from attempting to instrument it. Navigation has resulted in pedicle perforation rates as low as 1–5%. The accuracy of 3D navigation system is considered to be superior to virtual fluoroscopy and 2D navigation [22]. A meta-analysis of 9019 thoracic pedicle screws established the superiority of CT navigated instrumentation over fluoroscopic guidance [23]. Castro et al. noted a 40% pedicle breach following freehand pedicle screw placement in fluoroscopy-assisted surgery in spite of anatomic visualization of entry points [24]. MISS is likely to have much higher misplacement rates. Navigated spine surgery has the potential to create phantom screw trajectories and helps the surgeon to apply stab incision at the appropriate level through which screws can be placed with ease in correlation with these phantom images. Baaj et al. used intra-operative navigation to apply percutaneous pedicle screws in short constructs in degenerative spine [25]. Kim et al. observed an accuracy rate of 96.6% in MISS using computer aided navigation and intra-operative CT [26].

### 4.6.2 Radiation Safety

It has been noted that for the spine surgeons, radiation exposures are up to 10–12 times greater than in other orthopaedic procedures and may approach or exceed guidelines for cumulative exposure [27]. Minimally invasive spine surgeries (MISS) involve notoriously high amount of radiations to the surgeon and other operating room staff due to the non-visualization of anatomical landmarks for freehand placement of

screws. In such a scenario, navigation-assisted surgery reduces the radiation exposure for the operative team, as all members are protected during the scanning procedure. They also found 87% less exposure time to radiation while using intra-operative CT in comparison to fluoroscopy used in MIS procedures [28]. From the patient's perspective, the radiation exposure for CT based navigation systems is significantly higher when compared to fluoroscopy-based systems, yet they fall within permissible limits.

#### 4.6.3 Surgical Site Infection

A review of MIS-TLIF studies suggest an infection rate of 0–10% [26]. Similar experience has been highlighted by the author's team [20]. O'Toole et al. found that the incidence of surgical wound infection was significantly lower after MIS–TLIF (0.6%) than after open TLIF (4.0%) [29]. To reduce the rate of infection with MIS-TLIF, it is recommended to avoid placing fingers into the surgical wound, which may increase the risk of surgical wound infection if there are microscopic breaks in the surgeons gloves. Nassr A also concluded that MIS-TLIF is associated with lower incidence of surgical site infection than open TLIF [30].

#### 4.6.4 Facet Joint Preservation

There is also a high chance of facet joint violation in MISS which in turn results in adjacent segment degeneration. The real advantage of navigated MIS-TLIF lies in the fact that precise facet joint sparing entry can be taken and optimal trajectory in axial plane can be made with maximal screw length to achieve a near perfect and extremely safe pedicle screw with maximum possible pull-out strength (Fig. 4.9). Lau et al. observed lesser facet joint violations in MISS while using intra-operative navigation [31].

#### 4.6.5 In Obese/Osteoporotic Patients

Instrumentation using MISS in obese patients and frail osteoporotic patients is challenging as manual tactile feel of the pedicles would not be possible, and spinal navigation comes to the rescue in such scenarios.

### 4.7 Concerns with Spine Navigation

#### 4.7.1 Operative Time

The older generation of navigation systems employing manual point matching registration did lead to increased operative times. This drawback has been overcome with newer generation navigation systems that allow for automatic registration and a larger field of scan (BRAINLAB) extending to multiple vertebral segments. Improvement in quality of virtual images, reduction in acquisition time, and automatic registration process have contributed to the reduction in the duration of a surgery over the years. The overall duration is set to improve steadily as the experience of the surgeon and operating room personnel rises resulting in a systematic workflow in the long run.

#### 4.7.2 Wobbling and Motion Related Artefacts

Whilst the entry points and trajectories of instrumentation are clearly defined by image-guided surgery, the wobble created by manually tapping or inserting screws across the trajectories involved might result in inaccuracies due to the maximal radial movement from its centre of axis [10]. This is best avoided by postponing the screw insertion process after creating trajectories of all planned screws. Nowadays, powered pedi-

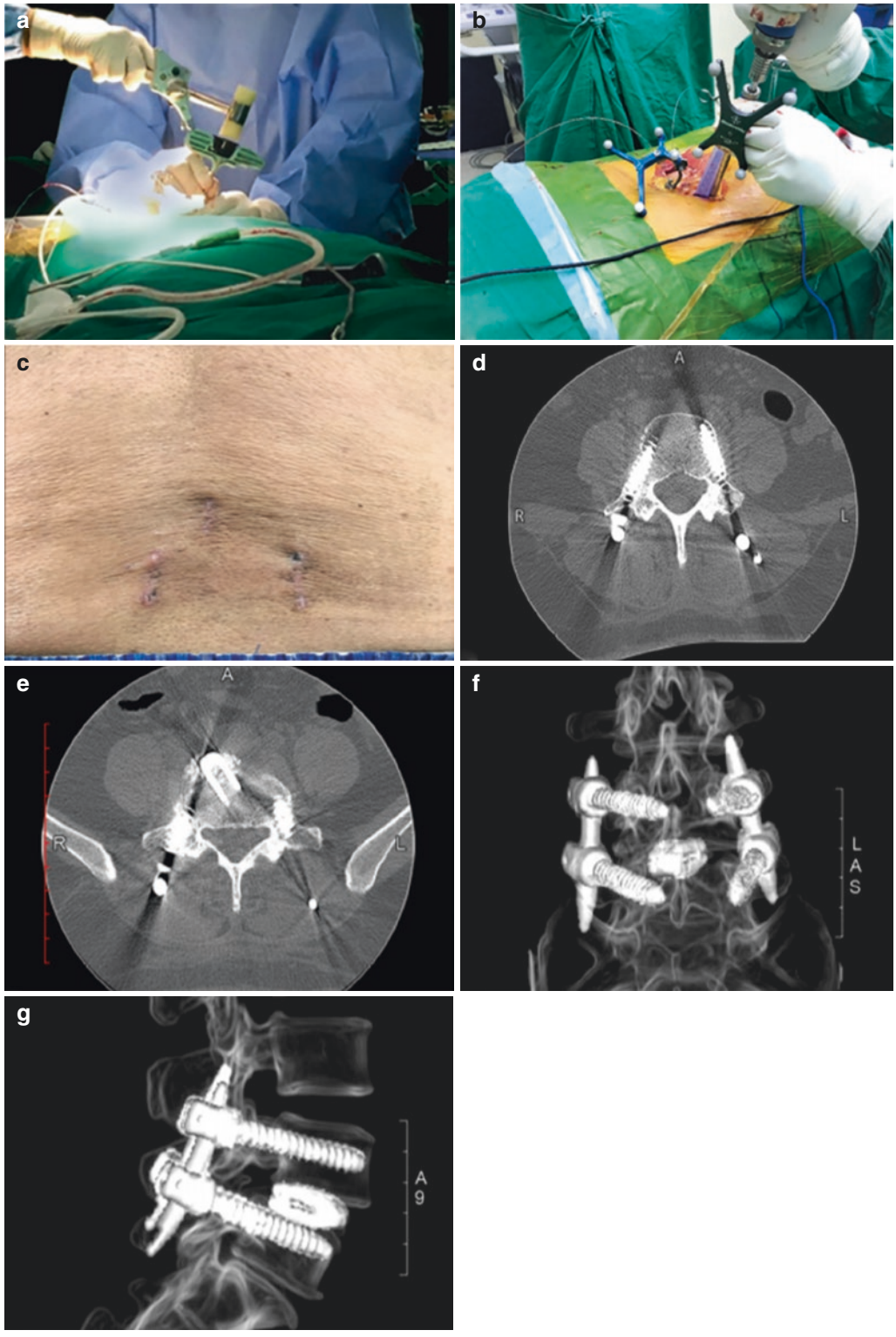


**Fig. 4.9** (**a**, **b**) Set-up of navigation apparatus (**b**, **c**) Healed scar area; (**d**–**g**) CT scan showing good alignment of pedicle screws with interbody cage

cle screw drive systems are available which enhance surgeon experience with faster, accurate screw insertions. In lean and poorly built patients, ventilation related movement of the thoracic spine may hinder the accuracy of navigation. It is better to acquire images in a non-ventilation mode and reduce the tidal volume in such scenarios to reduce motion-related artefacts. More important, all the nursing staff and assisting surgeons who are involved in the handling of instruments around the surgical field must be aware of the fact that the slightest deflection of the fixed reference array might result in severe inaccuracy. In doubtful scenarios, the surgeon needs to re-verify the accuracy. If the tip of the pointer appears to be either underneath the lamina or hanging above in space, one can be sure that there has been a disturbance of the array, and the entire navigation needs to be repeated. Sometimes in spite of placing the surgical instruments and camera in the "line of sight," navigation might be troublesome. It might be due to bloodstain or debris covering the spherical diodes. Care should be taken to gently clear it to avoid disturbing the position of reference array.

### 4.7.3 Distance from Reference Array

The accuracy of instrumentation is directly proportional to the distance of the level of interest from the reference array. Even though the current systems are capable of imaging the whole spine, the accuracy is questionable at the farthest point from the reference array. This can be solved in two ways. Firstly, when the surgeon requires imaging of the entire spine in case of complex deformity and surgery involves more than 12 segments, it would be appropriate to affix the reference array midway between the ends of the surgical incision. On the other hand, where the surgeon is not able to get an adequate fixation point as in paediatric cervical spine, considering the far distance of iliac crest from the area of instrumentation, it would be better to place the reference array on immobile regions such as Mayfield clamp. Whenever instrumentation is attempted at distal levels, it is better to re-verify the accuracy manually.

### 4.7.4 Cost-Effectiveness

The uptake of navigation technology has been limited by start-up, acquisition, and maintenance costs. The opponents of spinal navigation cite this as one of the major drawbacks. The economical evaluations have recognized limitations and challenges as the cost-effectiveness depends on multiple factors such as the number of surgeries performed, the intricateness of surgical procedures undertaken, complications, and the cost of revision surgeries. But a study also concluded that it would actually be a cost-saving surgery for a spine unit that does more than 254 spinal instrumentations yearly [32]. Al-Khouja et al.in his systematic review states that the biggest advantage of image-guided surgery is the prevention of reoperation and four out of seven studies had a zero reoperation rate [33].

### 4.7.5 Learning Curve

As with any new technology and its user experience, navigated spine surgery does have a learning curve. However, here, it requires well-organized operating room personnel to function as a single unit, and the success depends on the learning curve of the entire team. Each of the team needs to understand and execute their roles efficiently to reduce the nuances of surgical duration and technical flaws. Bai et al. in his prospective study analyzed the learning curve of surgeons using image-guided navigation spinal surgery and noticed a steep incline in operating time and screw perforation rate by 6 months and reached a plateau by 12 months [34]. Sasso et al. in his retrospective analysis of 4-year data, noted an average reduction of 40 min in operative time for lumbar fusion using navigation and image-guided surgery [35]. Ryang et al. in his prospective analysis of the

learning curve using 3D fluoroscopy found a learning curve of 4 months in placing lumbar and thoracic pedicle screws [36].

## 4.8 Senior Authors Experience

The authors ventured to assess the impact of 3D navigation in MI-TLIF in evaluating

1. Navigation setting time
2. Radiation exposure
3. Disc space preparation
4. Cage placement
5. Accuracy of pedicle screw placement
6. Cranial facet violation, and
7. Evaluation of canal decompression

### 4.8.1 Results

**3D Navigation Setting Time** Total time taken for setting up of navigation including pre- surgical time, i.e. scrubbing of the parts, draping, initializing the 3D C-arm and the navigation workstation, mounting reference array on the patient, acquiring scans, and transferring the same onto the navigation workstation was 46.65 ± 9.45 min. As displayed in results, the navigation setting up time progressively reduced with increasing experience. Our setting time values were in consensus with a study conducted by Balling et al. Balling [37] recorded an O-arm guided 3D navigation setting time of 46.2 ± 10.1 min in a prospective study of 306 posterior instrumentations. In our study, we experienced navigation error in one case probably due to translation of the reference array while operating. And this caused a medial breach in one patient which was rectified immediately. Rampersaud et al. suggested that error margins were positive in <1 mm translation and 5° rotation of the patient reference array in all regions of spine [38]. Furthermore, a study by Rahmathullah et al., with his experience of 1500 cases in navigation commented that turning on the warmers during registration can cause image artefacts leading to error [39]. Again, while registration and setting up of navigation take additional time, the total operating time may get shorter in patients with complex anatomy, as compared to fluoroscopy-assisted MI-TLIF. To minimize anatomical errors that could be secondary to respiratory movements, the authors temporarily suspend ventilation (generally for a minute) at the time of image capture by the C-arm [40].

**Radiation Exposure** In author's experience, 117 patients were treated with single-level 3D navigated MI-TLIF and 15 have lost to follow-up. A total of 408 pedicle screws were implanted, the mean time for fluoroscopy usage was 97.6 ± 11.67, and mean amount of radiation from fluoroscopy was 4.43 ± 0.87 which was similar to those found by Mendelsohn et al. who reported that radiation exposure to patients using O arm navigation was 2.77 times more when compared to non-navigated surgeries. However, the dose of 5.69 mSv was much lower than a conventional CT (7.5 mSv) and amounts to one-quarter of the total occupational exposure allowed per year. They also found 87% less exposure time to radiation while using intra-operative CT in comparison to fluoroscopy used in MIS procedures. From the patient's perspective, the radiation exposure for CT based navigation systems is significantly higher when compared to fluoroscopy-based systems, yet they fall within permissible limits [28]. Kim et al. have also concluded that the use of navigation-assisted fluoroscopy is feasible and safe for minimally invasive spine surgery. Radiation exposure is decreased to the patient as well as the surgical team [41].

**Volume of Disc Excised** Adequate disc space preparation is extremely vital for optimum fusion. In our study, the amount of disc removed was 75% in the ipsilateral-anterior, 81% in ipsilateral-posterior, 63% in contralateral-anterior, and 43% in contralateral-posterior quadrants. Following discectomy, Hurly et al. [42] compared the area of empty disc space between two techniques; cone beam navigation and open technique using a navigation probe. Disc removed using cone beam navigation was ipsilateral-anterior = 75%, ipsilateral-posterior = 81%,

contralateral-anterior = 63%, and contralateral-posterior = 43%. Rhin et al. showed in his randomized study of 40 lumbar TLIF that the percent disc removed by volume (80% versus 77%, $p = 0.41$), percent disc removed by mass (77% versus 75%, $p = 0.55$), and percent total disc removed by area (73% versus 71%, $p = 0.63$) between the open and MIS approaches were nearly same. The posterior contralateral quadrant was associated with the lowest percent of disc removed compared with the other three quadrants in both open and MIS groups (50% and 60%, respectively). Thus, concluding that navigation can help guide adequate disc space preparation intra-operatively and the surgeon should be generous during discectomy from the posterior contralateral corner to minimize the likelihood of pseudoarthrosis [43].

**Cage Placement** Transforaminal lumbar interbody fusion entails packing the anterior one-thirds of disc space with bone graft and navigation allows assessment of the thickness of this mantle of bone graft using the navigation probe. While the guidelines for exact placement of the cage have not been published, numerous papers show encouraging results with anterior and central placement within the intervertebral disc space [44]. In our study, the cage position was central in 87 patients, contralateral antero-central in six patients, and ipsilateral postero-central in eight patients. The Cohen's kappa statistic test for interobserver co-relation was 0.92 for the two examiners with regard to cage placement. Progressive posterior cage migration was noticed in a patient with initial postero-lateral placement of the cage and this was revised. Schupper et al. had employed navigation in his revision L3L4 case, as an adjunct, to help localize the interspace for cage deployment through minimal exposure. The TLIF cage was able to be appropriately placed in the collapsed disc space, as well as the pedicle screws, which allowed for improvement of lumbar lordosis. Similarly, Lian et al. in his 33 cases had determined the size and orientation of the cage by the navigation and after the cage insertion, a second scan was made to verify the accuracy of all the implants. Navigation also allows the surgeons to place and impact the cage in the desired spot and also most importantly avoid mishaps such as accidental penetration of anterior longitudinal ligament (ALL) and retroperitoneal positioning of the cage [45].

**Blood Loss** The mean intra-operative blood loss was 89.65 ± 23.67 mL which is lower as compared to Xu YF et al. [46] and Foley et al. [47].

**Accuracy of Pedicle Screw Placement** Regarding accuracy 95.6% showed grade 0 and 4.4% had grade 1 pedicle breach. In one case a grade 3 pedicle screw breach occurred; this was suspected intra-operatively on the C-arm images and confirmed by spinning the 3D C-arm again and extracting images before extubating the patient. The Cohen's kappa statistic test with regard to pedicle screw breach was 0.889 which demonstrated high reproducible accuracy. Freehand screw misplacement rates in spine is much higher than other spinal segments, and it becomes much more challenging in dysmorphic pedicles as seen in deformities and in areas where there is distortion of normal anatomical landmarks such as trauma, revision surgeries, and ankylosed spine. Navigation has resulted in pedicle perforation rates as low as 1–5%. The accuracy of 3D navigation system is considered to be superior to virtual fluoroscopy and 2D navigation [22]. A meta-analysis of 9019 pedicle screws established the superiority of CT navigated instrumentation over fluoroscopic guidance [22, 23]. Similarly 94.6% had grade 0 and 5.4% demonstrated grade 1 cranial facet violation as was observed by Lau et al. [31]. Thus, 3D-navigation makes sure that the pedicle screw is implanted in the most precise trajectory in all the 3 planes with added benefit of protection against radiation.

**Cranio-Facet Violation** The facet joint cranial to the level of fixation is a critical anatomic structure and protection of this joint is vital in avoiding adjacent segment disease [48, 49]. In the current study, only 25 out of 408 pedicle screws (6.1%) violated the cranial facet joint, with 94.6% and 5.4% of pedicle screws demonstrated grade 0 and grade 1 cranial facet violation, respectively, reinforcing the advantages of navigation-assisted insertion of pedicle screws. Again, the degree of violation in

these 6.1% of screws appears relatively inconsequential (grade 1), based on the classification of Babu et al. [50]. The Cohen's kappa statistic test with regard to cranial facet violation was 0.878 which demonstrated high reproducible accuracy. Ohba et al. [51] reviewed 194 pedicle screws in 28 consecutive patients and found that 87.5% and 94% of screws inserted using conventional fluoroscopy and 3D navigation group, respectively, did not violate the facet joint. Park et al. [48] reported a high rate of cranial-facet joint violation in fluoroscopic MISS surgery when compared to open surgeries (31.5% vs. 15.2% of all screws, $p < 0.001$).

**Evaluation of Canal Decompression** In our study, the navigation array probe was utilized to verify the adequacy of decompression and to confirm the anatomical landmarks as and when necessary. In their study on 28 patients undergoing MIS-TLIF, Lee et al. [52] found that the Mean spinal canal cross section area at disc spaces have increased significantly at 12 months post-operatively from 157.5 $mm^2$ to 294.3 $mm^2$, ($p = 0.012$) leading to a good clinical outcome, which could easily be evaluated intra-operatively using the navigation like in our study [42].

**Reduced Surgical Site Infection** In the present study of 117 patients, no surgical site infection was seen. In our another study of 1043 patients treated with MIS techniques, 763 underwent non-instrumented surgeries and 280 underwent instrumented fusion. The overall infection rate after MISS was 0.29%, 0% in non-instrumented cases and 1.07% [3 out of 280 cases] in instrumented cases. Nassr A also concluded that MIS-TLIF is associated with lower incidence of surgical site infection than open TLIF [30].

**Example 1**

Figure 4.10 demonstrates the use of navigation in L4L5 MI-TLIF in a patient with adult degenera-

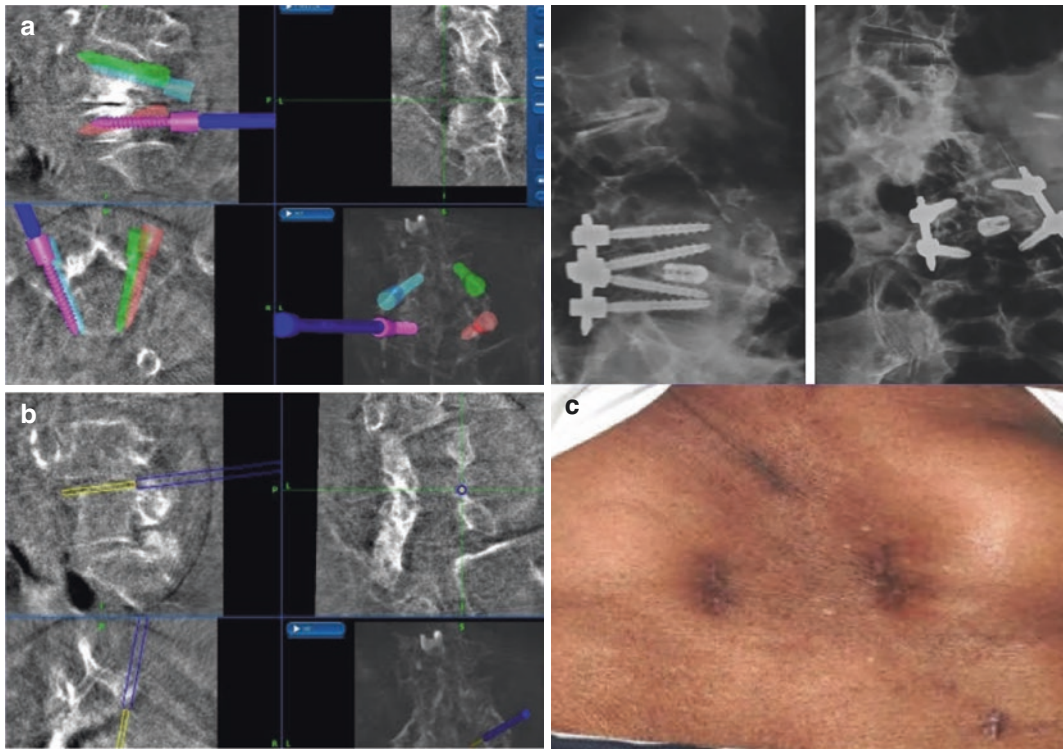


**Fig. 4.10** (**a**) Accurate placement of screws across rotated pedicles with malformed anatomy due to advanced degenerative arthritis is seen. (**b**) The cage can be placed optimally using navigation. (**c**) Post-operative X-ray and healed scar of MI-TLIF

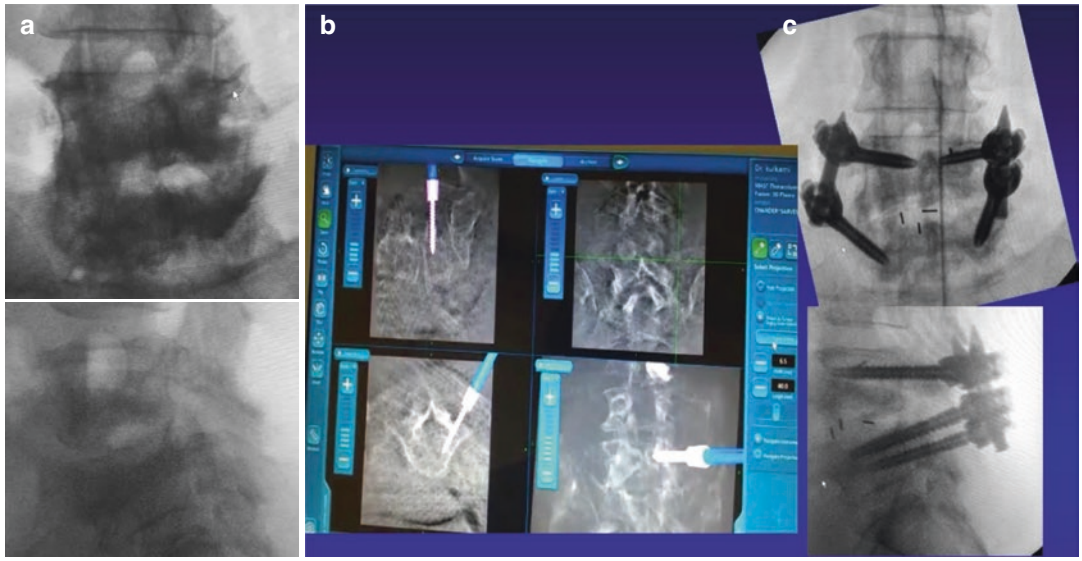


**Fig. 4.11** (**a**) Poorly defined anatomy on 2D fluoroscopy images. (**b**) Pedicle screw insertion using 3D navigation. (**c**) Post operative X-ray of MI-TLIF

tive scoliosis in which only selective fusion of L4 L5 is indicated.

(a) Accurate placement of screws across rotated pedicles with malformed anatomy due to advanced degenerative arthritis is seen.
(b) The cage can be placed optimally using navigation.
(c) Post-operative X-ray and healed scar of MI-TLIF.

**Example 2**
Figure 4.11 demonstrates the use of 3D navigation in ill-defined anatomy at L4L5 in advanced degenerative arthritis

(a) Poorly defined anatomy on 2D fluoroscopy images.
(b) Pedicle screw insertion using 3D navigation.
(c) Post operative X-ray of MI-TLIF.

## 4.9 Conclusions

At author's institution, almost all cases requiring fusion are operated with Minimally Invasive Transforaminal Lumbar Interbody Fusion [MIS-TLIF] technique with fluoroscopy and 3D navigation. With vast experience in minimally invasive techniques, we find MIS to be associated with less post-operative infection rates as compared to open techniques. With 3D navigation, MIS becomes safer and highly accurate. MIS-TLIF with 3D navigation has satisfactory clinical outcomes and fusion rates with the additional benefits of less initial post-operative pain, less blood loss, earlier rehabilitation, and shorter hospitalization. MIS-TLIF with 3D navigation is a more cost-effective treatment than MIS-TLIF with fluoroscopy.

**Conflict of Interest** The authors have no conflicts of interests to disclose.

**Ethical Review Committee Statement** The study is approved by institutional review board (approval vide - SaHo7840), Saifee Hospital, Mumbai.

## References

1. Eliyas JK, Karahalios D. Surgery for degenerative lumbar spine disease. Dis Mon. 2011;57:592–606.
2. Vaccaro AR, Bono CM. Minimally invasive spine surgery. CRC Press; 2007.

3. Phillips FM, Lieberman IH, Polly DW Jr, Wang MY. Minimally invasive spine surgery: surgical techniques and disease management. Springer Nature; 2020.
4. Kim M-C, Chung H-T, Cho J-L, Kim D-J, Chung N-S. Factors affecting the accurate placement of percutaneous pedicle screws during minimally invasive transforaminal lumbar interbody fusion. Eur Spine J. 2011;20:1635–43.
5. Rajasekaran S, Shetty AP. Section 11, Chapter 14: Navigation in spine surgery. In: Lumbar spine online textbook. DT Internet publisher - ISSLS, Wheeless Online; 2020.
6. Jahng T-A, Fu T-S, Cunningham BW, Dmitriev AE, Kim DH. Endoscopic instrumented posterolateral lumbar fusion with Healos and recombinant human growth/differentiation factor-5. Neurosurgery. 2004;54:171–81.
7. Foley KT, Holly LT, Schwender JD. Minimally invasive lumbar fusion. Spine. 2003;28:S26–35.
8. Kambin P. Letters. Spine. 2004;29:598–9.
9. Kim DH, Jaikumar S, Kam AC. Minimally invasive spine instrumentation. Neurosurgery. 2002;51:S15–25.
10. Rahmathulla G, Nottmeier EW, Pirris SM, Deen HG, Pichelmann MA. Intraoperative image-guided spinal navigation: technical pitfalls and their avoidance. Neurosurg Focus. 2014;36:E3.
11. Guha D, Jakubovic R, Gupta S, Fehlings MG, Mainprize TG, Yee A, Yang VXD. Intraoperative error propagation in 3-dimensional spinal navigation from nonsegmental registration: a prospective cadaveric and clinical study. Glob Spine J. 2019;9:512–20.
12. Rampersaud YR, Simon DA, Foley KT. Accuracy requirements for image-guided spinal pedicle screw placement. Spine. 2001;26:352–9.
13. Kulkarni AG, Sagane SS, Kunder TS. Management of spondylolisthesis using MIS techniques: recent advances. J Clin Orthop Trauma. 2020;11(5):839–47. https://doi.org/10.1016/j.jcot.2020.07.015.
14. Hurley RK Jr, Anderson ER 3rd, Lawson BK, Hobbs JK, Aden JK, Jorgensen AY. Comparing lumbar disc space preparation with fluoroscopy versus cone beam-computed tomography and navigation: a cadaveric study. Spine. 2018;43:959–64.
15. Sihvonen T, Herno A, Paljärvi L, Airaksinen O, Partanen J, Tapaninaho A. Local denervation atrophy of paraspinal muscles in postoperative failed back syndrome. Spine. 1993;18:575–81.
16. Styf JR, Willén J. The effects of external compression by three different retractors on pressure in the erector spine muscles during and after posterior lumbar spine surgery in humans. Spine. 1998;23:354–8.
17. Gejo R, Matsui H, Kawaguchi Y, Ishihara H, Tsuji H. Serial changes in trunk muscle performance after posterior lumbar surgery. Spine. 1999;24:1023–8.
18. Kawaguchi Y, Matsui H, Tsuji H. Changes in serum creatine phosphokinase MM isoenzyme after lumbar spine surgery. Spine. 1997;22:1018–23.
19. Kulkarni AG, Patel RS. Is closed-suction drainage essential after minimally invasive lumbar fusion surgery? A retrospective review of 381 cases. J Minim Invasive Spine Surg Tech. 2017;2:27–31.
20. Kulkarni AG, Patel RS, Dutta S. Does minimally invasive spine surgery minimize surgical site infections? Asian Spine J. 2016;10:1000–6.
21. Rajasekaran S, Bhushan M, Aiyer S, Kanna R, Shetty AP. Accuracy of pedicle screw insertion by AIRO intraoperative CT in complex spinal deformity assessed by a new classification based on technical complexity of screw insertion. Eur Spine J. 2018;27:2339–47.
22. Silbermann J, Riese F, Allam Y, Reichert T, Koeppert H, Gutberlet M. Computer tomography assessment of pedicle screw placement in lumbar and sacral spine: comparison between free-hand and O-arm based navigation techniques. Eur Spine J. 2011;20:875–81.
23. Meng X-T, Guan X-F, Zhang H-L, He S-S. Computer navigation versus fluoroscopy-guided navigation for thoracic pedicle screw placement: a meta-analysis. Neurosurg Rev. 2016;39:385–91.
24. Castro WHM, Halm H, Jerosch J, Malms J, Steinbeck J, Blasius S. Accuracy of pedicle screw placement in lumbar vertebrae. Spine. 1996;21:1320–4.
25. Baaj AA, Beckman J, Smith DA. O-Arm-based image guidance in minimally invasive spine surgery: technical note. Clin Neurol Neurosurg. 2013;115:342–5.
26. Kim TT, Drazin D, Shweikeh F, Pashman R, Johnson JP. Clinical and radiographic outcomes of minimally invasive percutaneous pedicle screw placement with intraoperative CT (O-arm) image guidance navigation. Neurosurg Focus. 2014;36:E1.
27. Rampersaud YR, Raja Rampersaud Y, Foley KT, Shen AC, Williams S, Solomito M. Radiation exposure to the spine surgeon during fluoroscopically assisted pedicle screw insertion. Spine. 2000;25:2637–45.
28. Mendelsohn D, Strelzow J, Dea N, et al. Patient and surgeon radiation exposure during spinal instrumentation using intraoperative computed tomography-based navigation. Spine J. 2016;16:343–54.
29. O'Toole JE, Eichholz KM, Fessler RG. Surgical site infection rates after minimally invasive spinal surgery. J Neurosurg Spine. 2009;11:471–6.
30. Nassr A. CORR insights®: does minimally invasive surgery have a lower risk of surgical site infections compared with open spinal surgery? Clin Orthop Relat Res. 2014;472:1725–6.
31. Lau D, Terman SW, Patel R, La Marca F, Park P. Incidence of and risk factors for superior facet violation in minimally invasive versus open pedicle screw placement during transforaminal lumbar interbody fusion: a comparative analysis. J Neurosurg Spine. 2013;18:356–61.
32. Dea N, Fisher CG, Batke J, Strelzow J, Mendelsohn D, Paquette SJ, Kwon BK, Boyd MD, Dvorak MFS, Street JT. Economic evaluation comparing intraoperative cone beam CT-based navigation and conventional fluoroscopy for the placement of spinal pedicle

screws: a patient-level data cost-effectiveness analysis. Spine J. 2016;16:23–31.
33. Drazin D, Al-Khouja L, Shweikeh F, Pashman R, Johnson J, Kim T. Economics of image guidance and navigation in spine surgery. Surg Neurol Int. 2015;6:323.
34. Wang D, Zhang K, Qiang M, Jia X, Chen Y. Computer-assisted preoperative planning improves the learning curve of PFNA-II in the treatment of intertrochanteric femoral fractures. BMC Musculoskelet Disord. 2020; https://doi.org/10.1186/s12891-020-3048-4.
35. Sasso RC, Garrido BJ. Computer-assisted spinal navigation versus serial radiography and operative time for posterior spinal fusion at L5-S1. J Spinal Disord Tech. 2007;20:118–22.
36. Ryang Y-M, Villard J, Obermüller T, Friedrich B, Wolf P, Gempt J, Ringel F, Meyer B. Learning curve of 3D fluoroscopy image–guided pedicle screw placement in the thoracolumbar spine. Spine J. 2015;15: 467–76.
37. Balling H. Time demand and radiation dose in 3D-fluoroscopy-based navigation- assisted 3D-fluoroscopy-controlled pedicle screw instrumentations. Spine (Phila Pa 1976). 2018;43(9):E512–9.
38. Rampersaud YR, Simon DA, Foley KT. Accuracy requirements for image-guided spinal pedicle screw placement. Spine (Phila Pa 1976). 2001;26(4):352–9.
39. Rahmathulla G, Nottmeier EW, Pirris SM, et al. Intraoperative image-guided spinal navigation: technical pitfalls and their avoidance. Neurosurg Focus. 2014;36(3):E3.
40. Guha D, Jakubovic R, Gupta S, et al. Intraoperative error propagation in 3-dimensional spinal navigation from nonsegmental registration: a prospective cadaveric and clinical study. Glob Spine J. 2019;9(5):512–20.
41. Kim CW, Lee Y-P, Taylor W, Oygar A, Kim WK. Use of navigation-assisted fluoroscopy to decrease radiation exposure during minimally invasive spine surgery. Spine J. 2008;8:584–90.
42. Hurley RK, Anderson ER, Lawson BK, et al. Comparing lumbar disc space preparation with fluoroscopy versus cone beam-computed tomography and navigation. Spine (Phila Pa 1976). 2018;43(14):959–64.
43. Rihn JA, Gandhi SD, Sheehan P, Vaccaro AR, Hilibrand AS, Albert TJ, Anderson DG. Disc space preparation in transforaminal lumbar interbody fusion: a comparison of minimally invasive and open approaches. Clin Orthop Relat Res. 2014;472:1800–5.
44. Castellvi AD, Thampi SK, Cook DJ, et al. Effect of TLIF cage placement on in vivo kinematics. Int J Spine Surg. 2015;9:38.
45. Lian X, Navarro-Ramirez R, Berlin C, Jada A, Moriguchi Y, Zhang Q, Härtl R. Total 3D Airo® navigation for minimally invasive transforaminal lumbar interbody fusion. Biomed Res Int. 2016;2016:5027340.
46. Xu Y-F, Le X-F, Tian W, et al. Computer-assisted, minimally invasive transforaminal lumbar interbody fusion. Medicine. 2018;97:e11423.
47. Schwender JD, Holly LT, Rouben DP, Foley KT. Minimally invasive transforaminal lumbar interbody fusion (TLIF): technical feasibility and initial results. J Spinal Disord Tech. 2005;18(Suppl):S1–6.
48. Park Y, Ha JW, Lee YT, et al. Cranial facet joint violations by percutaneously placed pedicle screws adjacent to a minimally invasive lumbar spinal fusion. Spine J. 2011;11(4):295–302.
49. Chen Z, Zhao ÆJ, Xu ÆH, et al. Technical factors related to the incidence of adjacent superior segment facet joint violation after transpedicular instrumentation in the lumbar spine. Eur Spine J. 2008;17(11):1476–80.
50. Babu R, Park JG, Mehta AI, et al. Comparison of superior-level facet joint violations during open and percutaneous pedicle screw placement. Neurosurgery. 2012;71(5):962–70.
51. Ohba T, Ebata S, Fujita K, et al. Percutaneous pedicle screw placements: accuracy and rates of cranial facet joint violation using conventional fluoroscopy compared with intraoperative three-dimensional computed tomography computer navigation. Eur Spine J. 2016;25(6):1775–80.
52. Lee CK, Park JY, Zhang HY. Minimally invasive transforaminal lumbar interbody fusion using a single interbody cage and a tubular retraction system: technical tips, and perioperative, radiologic and clinical outcomes. J Korean Neurosurg Soc. 2010;48:219–22.

# Navigation Guided Oblique Lumbar Interbody Fusion

5

Masato Tanaka and Sagar B. Sharma

Oblique lumbar interbody fusion (OLIF) refers to a technique of lumbar interbody fusion where an interbody cage is inserted through an oblique corridor made through the retroperitoneal space anterior to the psoas major muscle. The pre-psoas or ante-psoas (anterior to psoas muscle) approach for lumbar interbody fusion has been present since more than two decades, described first in 1997 by Mayer. OLIF consists of insertion of a cage with a large footprint through the retroperitoneal approach from the left side via corridor between the anterior border of psoas muscle and the abdominal aorta [1]. It is now the first choice of lumbar interbody fusion for many surgeons around the globe. Being a minimally invasive technique with shorter operative times and better biomechanical attributes, OLIF has been proved in numerous studies to be, at least, as good as, if not better than, TLIF—Transforaminal Lumbar Interbody Fusion [2–4]. One of the major drawbacks of the technique is the unfamiliar oblique approach for disc space preparation and cage insertion leading to repeated fluoroscopic exposures increasing the risk to operating room personnel. The supplementation of navigation to OLIF mitigates many, if not all, the disadvantages and risks of OLIF approach [5, 6].

## 5.1 Indications

OLIF is indicated in the following conditions requiring interbody fusion from L1 to L5. At L5–S1, the high iliac crest, anterior position of the vascular window, and a different set of armamentarium are challenges to OLIF that require sufficient expertise [7]. However, recently, OLIF is also used by many surgeons at L5S1 level as well. Broadly, the indications of OLIF include the following:

1. Degenerative spondylosis with or without Grade I/II listhesis
2. Spondylodiscitis
3. Adult degenerative scoliosis
4. Adjacent segment disease

## 5.2 Advantages of OLIF Over Other Interbody Fusion Techniques [8]

### 5.2.1 OLIF Vs. TLIF

1. Biomechanical—OLIF cages are larger than TLIF cages and are placed along the biomechanical axis of load bearing leading to better

M. Tanaka (✉)
Department of Orthopedic Surgery, Okayama Rosai Hospital, Okayama, Japan

S. B. Sharma
Smt. SCL General Hospital, Ahmedabad, India


J.-S. Kim et al. (eds.), *Technical Advances in Minimally Invasive Spine Surgery*,
https://doi.org/10.1007/978-981-19-0175-1_5

correction of lumbar lordosis and the segmental lumbar lordosis [9].

2. Biological—OLIF provides a large bed for graft, thorough preparation of the end plate of vertebral bodies, and insertion of wide cages which rest on the ring apophysis of the vertebral body (which is the strongest part of the vertebral body). Theoretically, these arguments increase the probability of fusion and decrease the incidence of cage subsidence [10].
3. Indirect decompression—OLIF relies on indirect decompression of the neural canal, that is, via increasing the disc height, it makes the ligamentum flavum taut and also increases the neural foramen diameter. There is no interaction with the dura and hence minimal chance of dural damage [11, 12].
4. Preservation of posterior elements—The back musculature, posterior tension band structures, and posterior bony elements are preserved in the procedure. Moreover, being a minimally invasive approach with minimal abdominal muscle damage, it allows for a faster post-operative recovery and earlier mobilization.

### 5.2.2 OLIF Vs. Direct/Lateral Lumbar Interbody Fusion (DLIF/LLIF)

OLIF approach was introduced to abate the complications associated with LLIF. Damage to lumbar plexus was the primary disadvantage of LLIF. OLIF avoids the exposure through the psoas muscle and decreases the chances of injury to lumbar plexus [13].

## 5.3 Relevant Surgical Anatomy

In order to create a safe corridor for the procedure, it is necessary to be aware of the important structures encountered in the approach [14]. These include the abdominal wall muscles; subcostal, iliohypogastric, and ilioinguinal nerves; psoas muscles; lumbar plexus and genitofemoral and femoral nerves; ureter; sympathetic chain; abdominal aorta and segmental vessels and iliolumbar vessels (Fig. 5.1).

The anterior abdominal wall muscles consist of external oblique, internal oblique, and transverse abdominis. The subcostal, iliohypogastric,

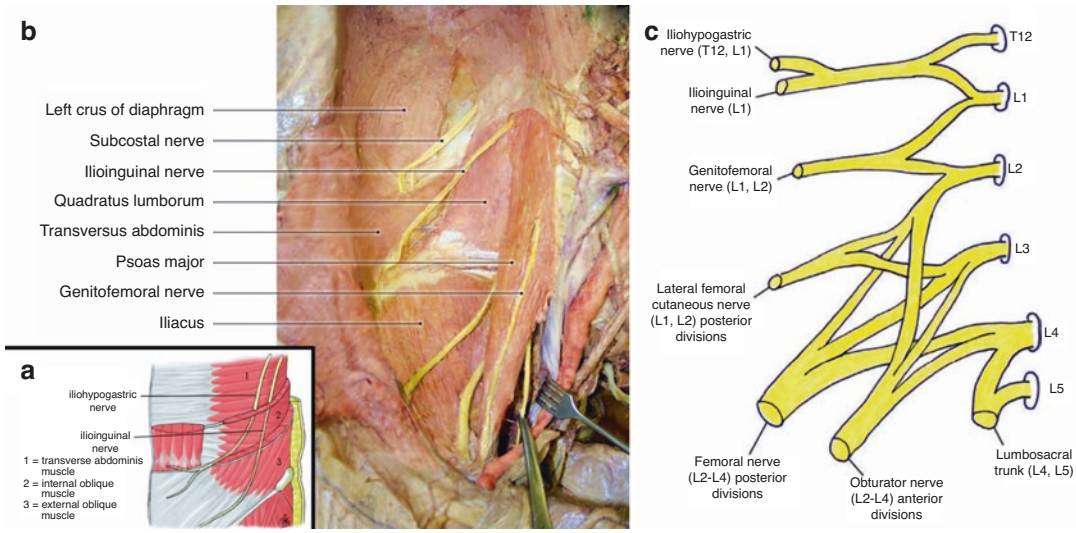


**Fig. 5.1** Anatomy of the anterior abdominal wall. (**a**) Abdominal wall musculature and the related nerves (**b**) Psoas muscle and relation to important nerves (**c**) Anatomy of lumbar plexus

and ilioinguinal nerves run in the substance of these muscles. The psoas muscles arise from the transverse processes of L1 to L5 vertebrae and form an important landmark for the approach. It is anterior to the anterior border of the muscle that the disc space is entered. The lumbar plexus consists of network of nerves derived from the lumbar roots L1–L4. The lumbar plexus lies in the posterior 1/4th of the vertebral bodies in lateral view from L1 to L3 and in the posterior 1/2nd of the vertebral bodies from L4–L5. Important nerves arising from the plexus include iliohypogastric, ilioinguinal, femoral, and obturator nerves. The femoral nerve (L2,3,4) is the largest branch and found deep in the posterior half of substance of the psoas muscle descending in a gradual posterior-to-anterior direction at L4–5 disc space. It passes down between the psoas and the iliacus muscle, beneath the inguinal ligament, and into the thigh. The iliohypogastric and ilioinguinal nerves emerge from the posterolateral border of the psoas and cross obliquely into the retroperitoneal space in front of the quadratus lumborum and the iliacus muscles to reach the iliac crest. The genitofemoral nerve travels obliquely in the substance of the psoas muscle from its origin, crossing the L2–3 disc space and emerges from its medial border at the L3–4 level. It then descends on the surface of the psoas major, underneath the peritoneum, and on the anterior 1/4th of the L4 and L5 vertebral bodies. Another important neural structure to be considered is the lumbar sympathetic chain. It lays anterolateral to the vertebral bodies, just underneath the medial border of psoas major muscle [15].

The ureter is another structure which is encountered in this approach. The ureter is a thin tubular structure which begins from the anteromedial surface of the kidney and passes downwards in the retroperitoneal fat, anterolateral to the psoas muscle. It is attached to the posterior portion of the peritoneum. Identification of the ureter is important in developing a corridor of OLIF. The vena cava is located on the right of the patient while the aorta is located more in midline. This anatomy allows for oblique corridor access from the patient's left side. Therefore, placing the patient in a right lateral decubitus position increases the size of the corridor because great vessels move to the right side with gravity [16]. Bifurcation of the aorta and vena cava is most often found at the lower L4 vertebral body. The segmental lumbar arteries arise at multiple levels and pass laterally over the mid-part of the vertebral bodies. The iliolumbar vein is the segmental vein for the L5 vertebral body. It runs transversely anterior to posterior across the L5 vertebral body and turns cephalad, crossing the L4–L5 disc space posteriorly. If the patient has transitional anatomy, the course of the iliolumbar vein may be observed at the L4–L5 disc space. If that is the case, it can be carefully visualized during the procedure and protected.

## 5.4 Advantages of Navigation in OLIF

In OLIF, fluoroscopy is required at many steps in the procedure from skin marking, to endplate preparation, cage insertion, and percutaneous pedicle screw (PPS) insertion. Also, with beginners, the oblique corridor is confusing leading to increased fluoroscopy times [17–19]. Addition of navigation has numerous advantages compared to fluoroscopy based OLIF which include:

1. No/reduced radiation exposure
2. Reduced operative times
3. Increased accuracy of interbody bed preparation and implant placement
4. Reduced complications related to implant placement [20]
5. Real-time position and depth of the instruments
6. With increasing experience, simultaneous insertion of the interbody cage and percutaneous pedicle screws can be done [21].

Whether this leads to improved patients outcomes/rapid recovery remains to be proven in studies.

## 5.5 Technique of OLIF

1. *Preoperative planning*: As in all fusion procedures, preoperative assessment includes analysis of standing X-rays in AP and lateral views and MRI. X-ray analysis includes assessment of disc height, segmental lordosis, whole lumbar lordosis, degree of listhesis (if present), coronal alignment, heights of iliac crest, etc. MRI evaluation is most important to establish a candidate's suitability to OLIF. The morphology of psoas muscle and the corridor between the psoas muscles and anterior vasculature should be assessed carefully. The surgical corridor between the anterior border of psoas muscle and lateral border of aorta should be at least 1 cm (known as fixed OLIF corridor). The presence of a fat plane between the psoas and the disc means it can be easily retracted. The space created by retraction of the psoas muscle until the middle of the disc is called the flexible OLIF corridor. The bulk of the psoas muscle should also be evaluated. Any abnormality of the abdominal viscera, particularly the kidneys and ureter and the aorta must be noted and carefully evaluated (Fig. 5.2).
2. *Patient positioning*: The standard approach for OLIF25 is from the left side of the patient. For navigation guided OLIF, a radiolucent table (preferably a carbon fibre Jackson table) is used. The patient is positioned in right lateral decubitus with the left side up. The patient is secured to the table with tapes over the chest and iliac crest and supports from dorsal and ventral sides. The operating surgeon stands on the abdominal side of the patient. All the body prominences are padded. An axillary roll in the axilla protects the neurovascular structures. Another pad is placed between the knees. The right hip and knee is kept extended while the left hip and knee is flexed to relax the psoas major muscle. Breaking the table to increase the distance between the rib cage and iliac crest depends upon the personal choice of the surgeon and patient characteristics. While it does ease the access, it may increase the

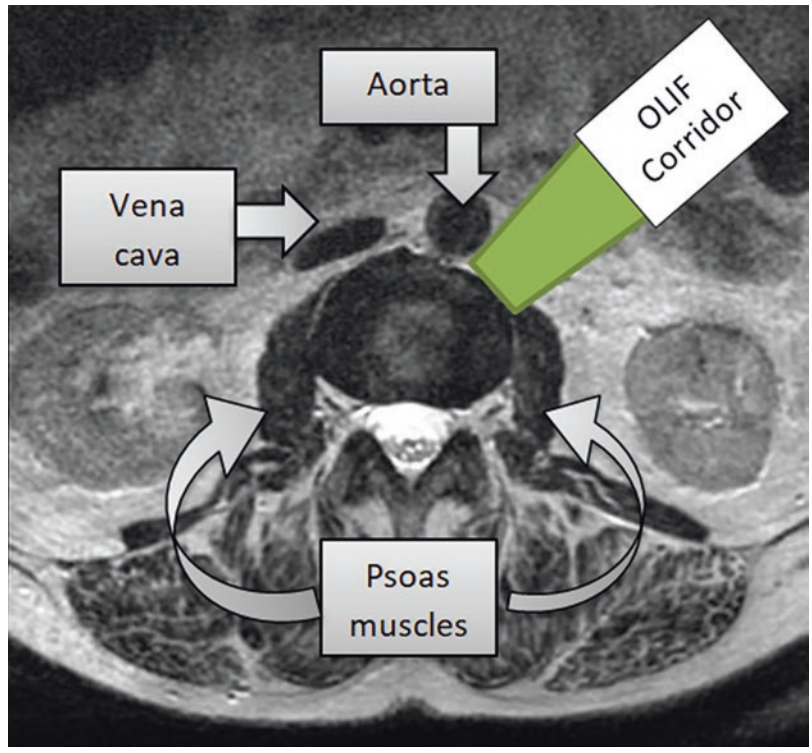


**Fig. 5.2** MRI analysis of the OLIF corridor showing important anatomical structures

chance of lumbar plexus traction injury if continued for longer periods (Fig. 5.3).

3. *Registration of navigation system*: A key step for successful and precise execution of the surgery is insertion of reference frame (also called Patient reference array). An incision is made 3–4 cm proximal to the posterior superior iliac spine over the iliac crest and the reference frame is anchored to the bone. It must be pointed out the greater the distance between the reference frame and the disc space of interest, the lesser is accuracy. Hence, in case of L2–3 OLIF, it is better to attach the reference frame on the spinous process of the cranial vertebra. After attaching the reference frame, a 3D scan is obtained and data registered with the navigation system (Fig. 5.4).
4. *Localization of level*: With navigation, the localization of the disc space becomes very easy. The endplates of the concerned level are drawn over the skin and the inclination of the disc space and midpoint of the disc is marked. A 4–5 cm oblique incision is made starting from the midpoint of the disc space.
5. *Dissection*: After making a skin incision and dissecting the subcutaneous fat, the abdominal musculature is reached. A bipolar cautery is preferred for haemostasis over monopolar. The external oblique fascia is reached and

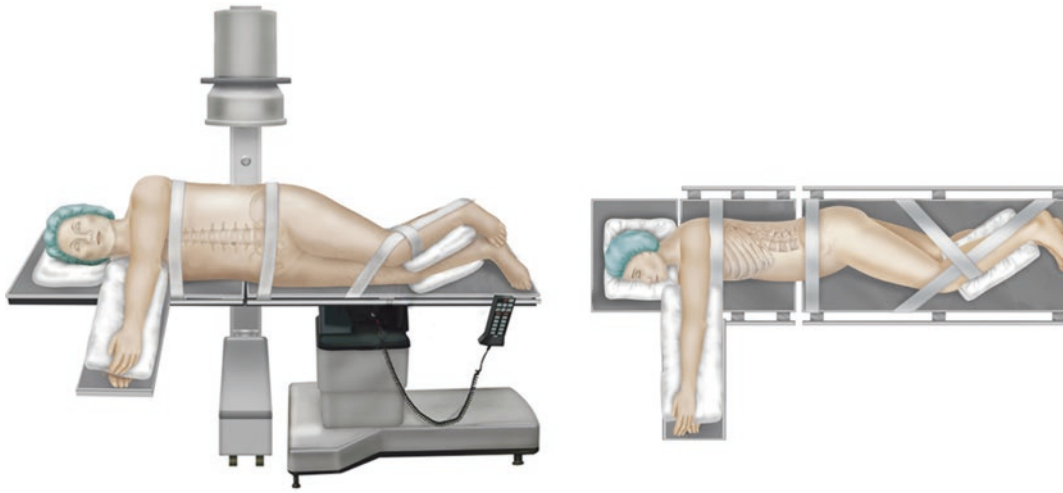

**Fig. 5.3** Positioning of the patient of Jackson table as viewed from front and above

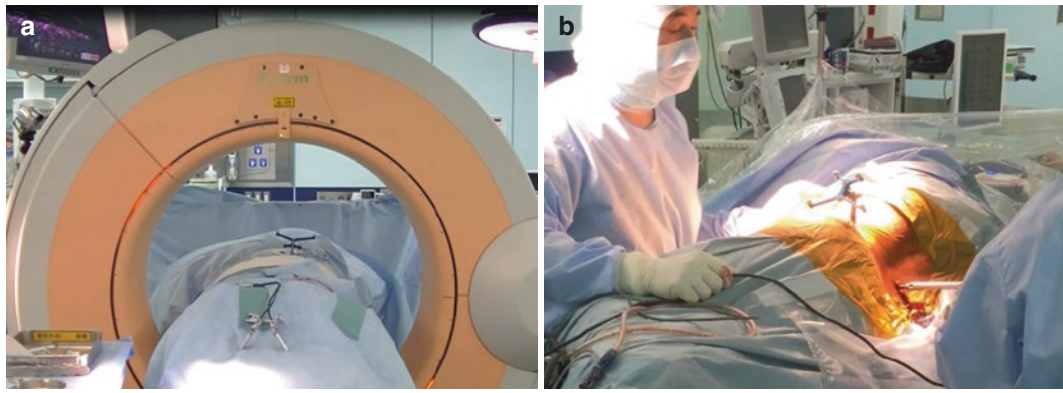


**Fig. 5.4** (**a**) Registration of the navigation system (**b**) Insertion of patient reference array

will need to be sharply incised. After that, the internal oblique and transversus abdominis are dissected. The muscle fibres are dissected in line with the muscle fibres as these muscle layers run in opposite directions. The nerves encountered during this approach should be identified and protected. After bluntly penetrating the transversalis fascia, the yellow retroperitoneal fat is exposed. Care should be taken not to injure the peritoneum at this stage. Once inside the retroperitoneal space, the index finger is directed backwards to follow the internal abdominal wall dorsally down to the psoas muscle, which can be visualized. Entering the transversalis fascia obliquely from anterior in the incision to posterior to the quadratus muscle will prevent inadvertent entry into the peritoneum. Palpating the quadratus muscle, followed by the tip of the transverse process and finally the psoas muscle, will help verify that the correct retroperitoneal plane is being entered and ensures that the peritoneum is not compromised. The finger is used to sweep the peritoneal contents, including the ureter, which reflects with the peritoneum and the retroperitoneal fat anteriorly. It is possible to visualize the structures in addition to tactile feel to ensure a safe approach to the disc space free from vascular, peritoneal, and nerve obstructions. Blunt dissection with finger or a mop is done to clear the psoas major muscles and the antero lateral portion of the vertebral bodies. One can palpate the pulsations of the aorta ventrally [22]. The psoas may be mobilized dorsally till the midpoint of the disc space. (Fig. 5.5).

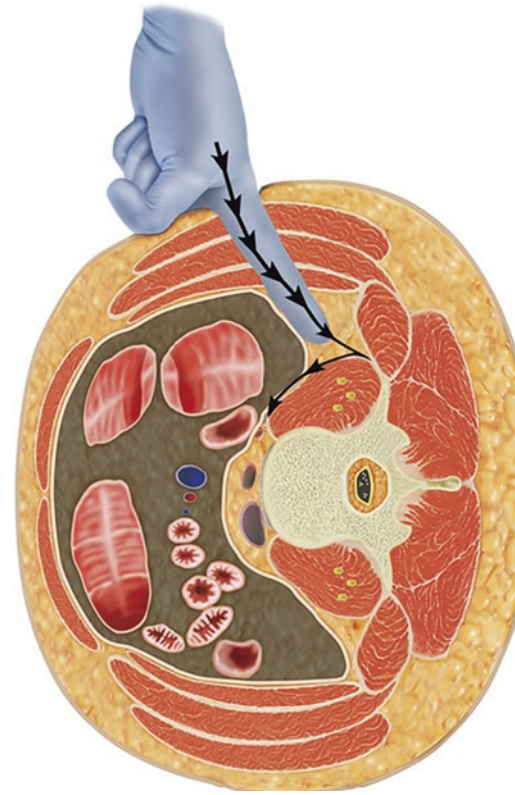

**Fig. 5.5** Pathway for dissection of OLIF corridor by blunt dissection using fingers

6. *Dilatation and retractor placement*: Using a navigated dilator, the anterior portion of the disc space is localized. The initial placement is just anterior to the psoas major muscle. Over the initial dilator, serial dilators are put until a 22 mm expandable retractor is placed and a fibre-optic light source is attached to the retractor system (Fig. 5.6). The retractor is attached to the flexible table arm to maintain the retractor position. It is important to align the retractor blades such that the opening between them is parallel to the disc space. The marking of the endplates done initially over the skin may be utilized for reference. The retractor blades are fixed to the vertebral body using threaded pins. One should avoid injury to the segmental vessels during pin insertion. The iliolumbar vein must be carefully evaluated in preop MRI and identified intraoperatively and protected during insertion of L5 pin. Navigation avoids the use of an initial Jamshidi needle and guide-wire placement into the disc space and thus reduces chances of injury to contralateral nerve root by sharp instruments. Avoiding the posterior half of the psoas major muscle protects the lumbar plexus. Cadaveric studies have identified that the lumbar plexus lies in the posterior one third of the psoas major muscle. The position

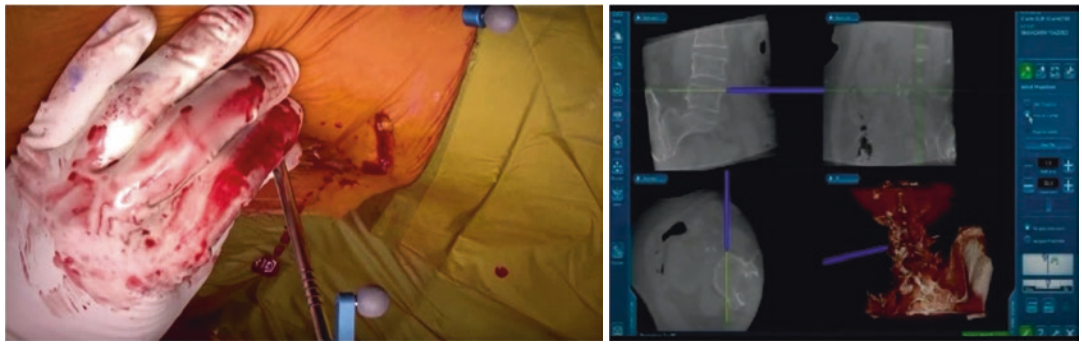

**Fig. 5.6** Marking of the disc space with initial navigated dilator and localization of the disc space

of the retractorblades and the orientation of the corridor can be evaluated in real time using the navigated probe.

7. *Annulotomy and disc space preparation*: Using a Penfield dissector, residual soft tissue is dissected off the annulus. A rectangular annulotomy of about 15–20 mm is made under visualization carefully protecting the aorta ventrally and the psoas muscle dorsally. The psoas muscle can be retracted till the middle of the disc space. Then the disc space is prepared using pituitary forceps, shavers, and endplate curettes. A large Cobb's elevator is passed along both end plates to the contralateral annulus. A mallet is then used to gently release both the superior and inferior aspects of the contralateral annulus. This step is critical to ensure that appropriate distraction so that a larger size cage may be placed. All disc preparation instruments, including the Cobb's elevator and end plate shavers enter obliquely through the retractor and then turned dorsally to allow the surgeon to work orthogonally across the disc space and release the contralateral annulus. The retractor blades should be slightly opened to allow the instruments to turn orthogonally. Adequate preparation of disc space by thorough removal of cartilaginous endplate is essential to achieve proper fusion. It is also essential that the bony endplate is not damaged to prevent cage subsidence.
8. *Trialling*: Serially graduated trials are inserted obliquely and turned orthogonally before impacting into the disc space. The cage with the largest possible height is inserted to obtain adequate indirect decompression. The cage should be centred over the spinous process and span the entire ring apophysis on both sides (Fig. 5.7). Using navigated cages, real-time information about the position of the trail can be obtained. However, it is difficult to judge the disc traction achieved using the trial by navigation and is best judged by the firm fitting of the trial into the disc space.
9. *Implant placement*: After trialling, a polyether ether ketone (PEEK) cage of appropriate height, length, and lordosis is selected and filled with auto graft or bone graft substitute. The cage inserter has retractable sleeves which cover the graft site of the cage and prevent graft dislodgement during insertion. Using navigation, the cage is gently hammered into appropriate direction. The position and angulation of the cage can be monitored in real time using navigation (Fig. 5.8). Once in proper position, the inserter is unscrewed and removed.
10. *Closure*: After removal of the inserter, the retractor pins are unthreaded and the retractor blades are removed. Thorough wash with saline is ensured. The external oblique aponeurosis is closed with interrupted absorbable sutures. The subcutaneous fascia and skin is closed.
11. *Percutaneous pedicle screw (PPS) insertion*: Then the patient is turned prone and again an O-arm or 3D C-arm image is obtained and

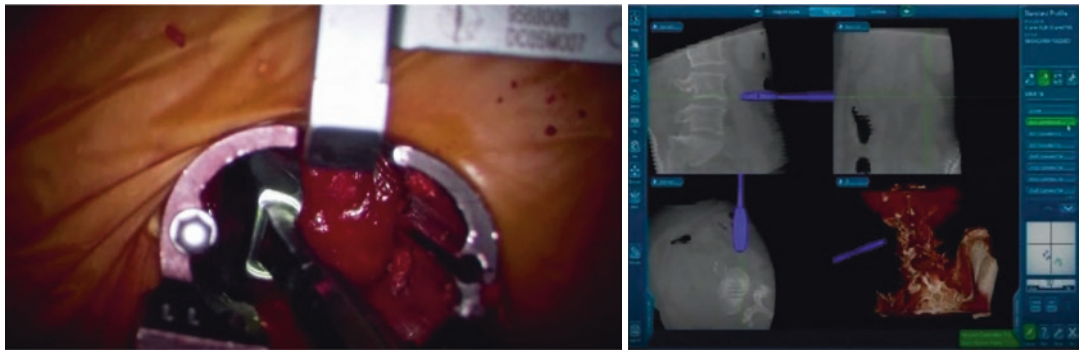

**Fig. 5.7** Trialling under real-time image guidance

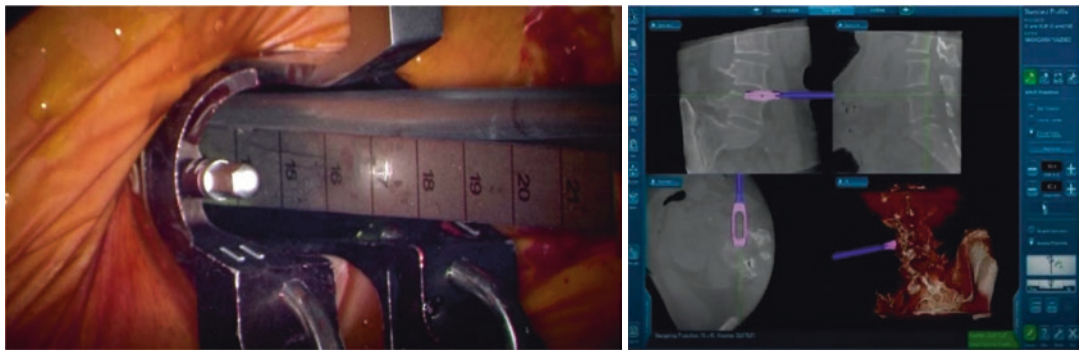

**Fig. 5.8** Insertion of final cage under real-time image guidance

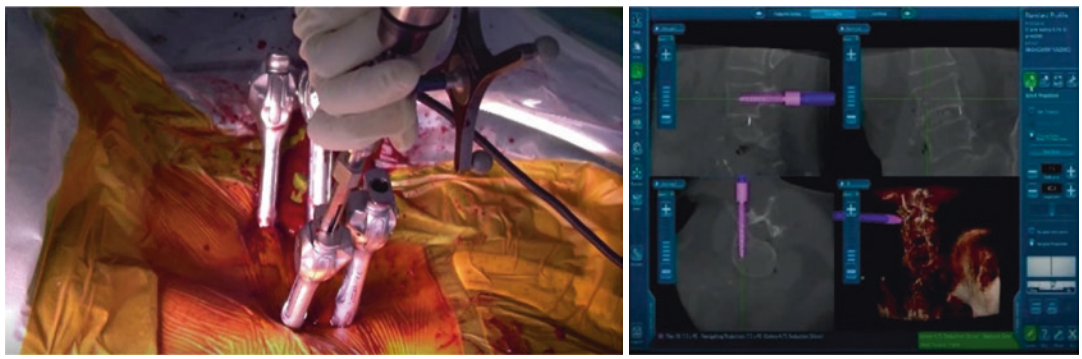

**Fig. 5.9** Insertion of percutaneous pedicle screws (PPS)

registered with the navigation system. Percutaneous pedicle screws are inserted using navigation system. In our institute, we perform a simultaneous insertion of OLIF cage and PPS in lateral position utilizing two teams of surgeons. However, doing simultaneous procedures requires coordination and proficiency but saves the surgical time (Fig. 5.9). A case example is discussed in Figs. 5.10 and 5.11.

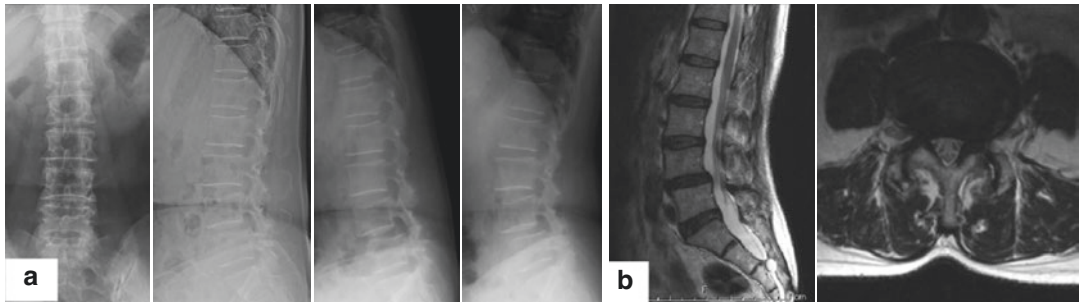


**Fig. 5.10** (**a**) Preoperative radiographs of a patient showing listhesis with dynamic instability at L4–5 level (**b**) MRI image of the same patient showing stenosis at L4–5 level

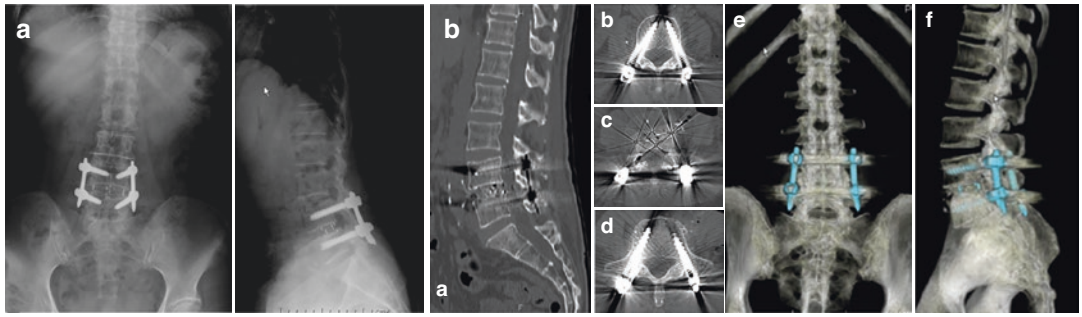


**Fig. 5.11** (**a**) Post-operative radiograph of the same patient after surgery showing implant in situ (**b**) O-arm images taken intraoperatively showing proper position of the screws and cage

## 5.6 Complications of OLIF and Tips to Avoid them

The complications of OLIF can be divided into intraoperative and post-operative complications [23, 24].

| Intraoperative | Immediate post-operative | Late post-operative |
|---|---|---|
| Ilioinguinal/ iliohypogastric nerve injury | Transient hip paresis, anterior thigh numbness | Adjacent segment degeneration |
| Ureteric injury | Deep vein thrombosis | Cage subsidence and pseudoarthrosis |
| Vessel injury—Aorta, segmental vessels, iliolumbar vein | Paralytic ileus | |
| Lower extremity symptoms caused by sympathetic chain injury, lumbar plexus injury | Retrograde ejaculation | |
| Contralateral nerve root damage | Lumbar plexopathy | |
| Peritoneal laceration | Surgical site infection | |
| Endplate fracture | Pedicle screw breach | |
| Ventral dural injury [25] | | |

- Intraoperative:
  1. *Nerve injury*: during the approach, it is possible to damage the ilioinguinal, iliohypogastric nerve during the dissection of the abdominal wall. The genitofemoral nerve which lies on the ventral surface of the psoas major muscle is also liable to get injured during retractor placement. Careful visualization and blunt dissection is essential to avoid these injuries.
  2. *Ureteric injury*: Injury to ureter occurs during dissection through the retroperitoneal fat. In multilevel fixations, manipulation of the retractor blades from one level to another without proper dissection of the retroperitoneal plane can damage the ureter. It requires prompt attention and repair [26].
  3. *Vessel injury*: this is by far the most common injury reported in literature. The aorta, segmental arteries and veins, and the iliolumbar vein have all been reported to be injured. Very rarely, the inferior vena cava may be injured if the approach is from the right side. It is observed that in chronic degenerative changes in the intervertebral disc space, the aorta is adherent to the osteophytes and the rudimentary discs. Very rarely, the aorta may have intrinsic diseases such as aortic aneurysm and aortic dissection which can very well be recognized on preoperative MRI. The lumbar arteries or segmental arteries of corresponding levels run along the middle of the vertebral bodies. These can get damaged during the insertion of Schanz screws of the retractor blades. Hence, while putting these screws should be placed as close to the endplate as possible. At the L5 level, the iliolumbar vein lies very close to the L4–5 disc. The bleeding from this vein can be torrential and difficult to control. Hence, it is essential to identify this vein, if present in the planned level of surgery and it is advisable to avoid putting the L5 pins if this vein is present.
  4. *Sympathetic chain injury and lumbar plexopathy*: The sympathetic chain lies between the aorta and the anterior border of psoas major muscle and is liable to get injured during disc space preparation. Sympathetic chain injury causes post-operative limb paraesthesia and warmness due to loss of vasomotor activity. In some cases, retrograde ejaculation is a possibility. The lumbar plexus is less likely to be injured in the pre-psoas approach. However, prolonged retraction beyond the mid-sagittal plane or breaking the Jackson table for prolonged periods increases the chances of lumbar plexopathy.
  5. *Dural tear and contralateral nerve root injury*: These complications are likely to occur during endplate preparation and cage insertion. The direction of the OLIF corridor is oblique and lies in line with the contralateral nerve root. The ventral dural sac may be damaged if the instruments are inserted too obliquely. Hence, the orthogonal manoeuvre is a very important step in endplate preparation and cage insertion. The orthogonal manoeuvre directs the instruments directly lateral and thus protecting the dural sac and the contralateral nerve root.
  6. *Other rare complications*: Numerous other complications have been described in literature which are infrequent. Endplate disruption can occur with inexperienced hands and osteoporotic bones and lead to suboptimal distraction. Cage subsidence and pseudoarthrosis are rare and late complications related to every fusion technique.

## 5.7 Disadvantages of OLIF

Although there are very few complications associated with the procedure, there are a few disadvantages to the technique. Being a minimally invasive technique with an unfamiliar approach, it has its own learning curve for beginners. Traditional OLIF requires frequent radiation exposure; however, navigation mitigates most of

the disadvantages associated with technique. The setup of navigation has its own technical elements that require training of the OT personnel and the surgeon with increased operative times in the initial cases.

## 5.8 Limitations of OLIF

Although OLIF can be used in any patient where TLIF can be used, there are a few cases in which OLIF cannot be practical. In patients with a bulky psoas, it may be easier to do a trans-psoas approach than an ante-psoas approach. Caution is also warranted in some cases such as spondylodiscitis where anatomical details may be obscure and the bed for interbody graft is inadequate. Although OLIF is reported to improve the spinal sagittal parameters, it may not be adequate in cases with severe deformity and may require additional posterior corrective osteotomies. However, with increasing experience, OLIF can be utilized in almost all patients for interbody fusion.

## 5.9 Conclusion

With increasing utilization of OLIF as an interbody fusion technique, addition of navigation complements its advantages. By providing the surgeon about the real-time location and depth of the instruments, navigation increases the efficacy and safety of the procedure. It also greatly reduces the radiation exposure to the OT personnel. Simultaneous insertion of interbody cage and percutaneous pedicle screws can also be done.

## References

1. Jin C, et al. Outcomes of oblique lateral interbody fusion for degenerative lumbar disease in patients under or over 65 years of age. J Orthop Surg Res. 2018;13:38.
2. Koike Y, Kotani Y, Terao H, Iwasaki N. Comparison of outcomes of oblique lateral interbody fusion with percutaneous posterior fixation in lateral position and minimally invasive transforaminal lumbar interbody fusion for degenerative spondylolisthesis. Asian Spine J. 2021;15:97.
3. Keorochana G, Setrkraising K, Woratanarat P, Arirachakaran A, Kongtharvonskul J. Clinical outcomes after minimally invasive transforaminal lumbar interbody fusion and lateral lumbar interbody fusion for treatment of degenerative lumbar disease: a systematic review and meta-analysis. Neurosurg Rev. 2018;41:755–70.
4. Lin G-X, et al. Clinical and radiologic outcomes of direct versus indirect decompression with lumbar interbody fusion: a matched-pair comparison analysis. World Neurosurg. 2018;119:e898–909.
5. Konieczny MR, Krauspe R. Navigation versus fluoroscopy in multilevel MIS pedicle screw insertion: separate analysis of exposure to radiation of the surgeon and of the patients. Clin Spine Surg. 2019;32:E258–65.
6. Sardhara J, et al. Neuro-navigation assisted pre-psoas minimally invasive oblique lumbar interbody fusion (MI-OLIF): new roads and impediments. Neurol India. 2019;67:803–12.
7. Kim J-S, Sharma SB. HOW I DO IT-SPINE DEGENERATIVE How I do it? Oblique lumbar interbody fusion at L5S1(OLIF51). Acta Neurochir. 2019;161:1079–83.
8. Mobbs R, Phan K, Malham G, et al. Lumbar interbody fusion: techniques, indications and comparison of interbody fusion options including PLIF, TLIF, MI-TLIF, OLIF/ATP, LLIF and ALIF. J Spine Surg. 2015;1:2–18.
9. Lu T, Lu Y. Comparison of biomechanical performance among posterolateral fusion and transforaminal, extreme, and oblique lumbar interbody fusion: a finite element analysis. World Neurosurg. 2019;129:e890–9.
10. Lin G-X, Sharma S, Rui G, Song M-S, Kim J-S. Minimally invasive transforaminal lumbar interbody fusion with intraoperative fluoroscopy for disc space preparation: analysis of fusion rate and clinical results. Oper Neurosurg. 2020; https://doi.org/10.1093/ons/opaa178.
11. Mahatthanatrakul A, Kim HS, Lin GX, Kim JS. Decreasing thickness and remodeling of ligamentum flavum after oblique lumbar interbody fusion. Neuroradiology. 2020;62:971–8.
12. Lin GX, Rui G, Sharma S, Mahatthanatrakul A, Kim JS. The correlation of intraoperative distraction of intervertebral disc with the postoperative canal and foramen expansion following oblique lumbar interbody fusion. Eur Spine J. 2020; https://doi.org/10.1007/s00586-020-06604-3.
13. Jin J, et al. Comparative study of the difference of perioperative complication and radiologic results. Clin Spine Surg. 2018;31:31–6.
14. Uribe JS, Arredondo N, Dakwar E, Vale FL. Defining the safe working zones using the minimally invasive lateral retroperitoneal transpsoas approach: an anatomical study. J Neurosurg Spine. 2010;13:260–6.

15. Wang H, et al. Radiographic study of lumbar sympathetic trunk in oblique lateral interbody fusion surgery. World Neurosurg. 2018;116:e380–5.
16. Ouchida J, Kanemura T, Satake K, Nakashima H, Segi N. Anatomic evaluation of retroperitoneal organs for lateral approach surgery: a prospective imaging study using computed tomography in the lateral decubitus position. Eur Spine J. 2018; https://doi.org/10.1007/s00586-018-5803-x.
17. Zhang YH, White I, Potts E, Mobasser JP, Chou D. Comparison perioperative factors during minimally invasive pre-psoas lateral interbody fusion of the lumbar spine using either navigation or conventional fluoroscopy. Glob Spine J. 2017;7:657–63.
18. Park P. Impact of spinal navigation on the oblique lumbar interbody fusion. Neurospine. 2020;17:268–9.
19. Tajsic T, Patel K, Farmer R, Mannion RJ, Trivedi RA. Spinal navigation for minimally invasive thoracic and lumbosacral spine fixation: implications for radiation exposure, operative time, and accuracy of pedicle screw placement. Eur Spine J. 2018;27:1918–24.
20. Xi Z, Chou D, Mummaneni PV, Burch S. The navigated oblique lumbar interbody fusion: accuracy rate, effect on surgical time, and complications. Neurospine. 2020;17:260–7.
21. Tanaka M, Ruparel S, Fujiwara Y, Uotani K, Yamauchi T. Simultaneous oblique lumbar interbody fusion (OLIF) and lateral percutaneous pedicle screw fixation (lateral PPS): a technical note. Res Arthritis Bone Study. 2019;1:1–8.
22. Molinares DM, Davis TT, Fung DA. Retroperitoneal oblique corridor to the L2-S1 intervertebral discs: an MRI study. J Neurosurg Spine. 2015;24:1–8.
23. Silvestre C, Mac-Thiong JM, Hilmi R, Roussouly P. Complications and morbidities of mini-open anterior retroperitoneal lumbar interbody fusion: oblique lumbar interbody fusion in 179 patients. Asian Spine J. 2012;6:89–97.
24. Quillo-Olvera J, Lin G-X, Jo H-J, Kim J-S. Complications on minimally invasive oblique lumbar interbody fusion at L2-L5 levels: a review of the literature and surgical strategies. Ann Transl Med. 2018;6:101.
25. Chang J, Kim J-S, Jo H. Ventral dural injury after oblique lumbar interbody fusion. World Neurosurg. 2017;98(881):e1–881.e4.
26. Lee HJ, Kim JS, Ryu KS, Park CK. Ureter injury as a complication of oblique lumbar interbody fusion. World Neurosurg. 2017;102:693.e7.

# 6 Navigation-Guided Spinal Fusion: MIS Fusion and Reconstruction in Complex Spine Disease and Deformity

Ken Ishii, Norihiro Isogai, and Haruki Funao

## 6.1 Introduction

Advances in diagnostic technologies [1, 2] and surgical procedures [3–5] in addition to the development of new implants [6, 7] and biological agents [8] in the field of spinal surgery have revolutionized our understanding and treatment of various spinal disorders. In the past, good surgical results for various pathological conditions such as trauma, degenerative diseases, deformation, and inflammatory diseases have been reported. However, difficult surgical procedures are often required for complex conditions such as severe spinal deformity, failed back surgery syndrome, multiple operations on the back, spinal tumor, and congenital deformity. Technically challenging procedures require a high level of skill on part of the surgeon and often involve long operation times, high invasiveness, and increased risk of complications; therefore, a reliable and safe procedure is warranted.

In recent years, the demand for various minimally invasive spine (MIS) surgery has rapidly increased, and the technique has also been popularized against the backdrop of an aging society and extended life expectancy. These MIS techniques include the MIS-TLIF procedure using percutaneous pedicle screws described by Foley et al. [3, 7] and the combination of microendoscopic techniques and percutaneous instrumentation to perform MIS-PLIF through a tubular retractor described by Khoo et al. [9]. A 2001 study by Pimenta [10] reported a new MIS procedure using the lateral endoscopic trans-psoas retroperitoneal approach. Following this study, retractors and spinal monitoring were developed to allow direct visualization, which led to the creation of the extreme lateral interbody fusion (XLIF) procedure [11]. The oblique lateral interbody fusion (LIF) was first described by Mayer [12] in 1987, which provided additional modifications to prevent known complications of the muscle-splitting retroperitoneal approach such as lumbar plexus and femoral nerve palsies [12]. The modified approach diversified the available options for LIF procedures and enabled interbody correction for spinal deformities and indirect decompression for spinal canal stenosis [13]. Minimally invasive spine stabilization (MISt) techniques such as MIS-TLIF, MIS-long fusion,

K. Ishii (✉)
Department of Orthopaedic Surgery, School of Medicine, International University of Health and Welfare (IUHW), Narita, Chiba, Japan

Spine and Spinal Cord Center, International University of Health and Welfare (IUHW) Mita Hospital, Tokyo, Japan

N. Isogai
Spine and Spinal Cord Center, International University of Health and Welfare (IUHW) Mita Hospital, Tokyo, Japan

H. Funao
Department of Orthopaedic Surgery, School of Medicine, International University of Health and Welfare (IUHW), Narita, Chiba, Japan



J.-S. Kim et al. (eds.), *Technical Advances in Minimally Invasive Spine Surgery*,
https://doi.org/10.1007/978-981-19-0175-1_6

percutaneous kyphoplasty, XLIF/DLIF/OLIF, cortical bone trajectory, and total disc replacement have since become popular as they offer immediate stabilization of the spine. Moreover, these techniques can reduce muscle damage, blood loss, recovery time, postoperative pain, hospital stay, the necessary period of bed rest, and motion preservation of the affected level when compared to previously available methods. Thus, MISt offers a promising alternative to conventional open procedures, with emphasis placed on minimizing exposure-related morbidity.

Despite their advantages, MISt procedures pose several difficulties and limitations for surgeons, including small skin incisions leading to narrow working spaces, lack of clear anatomic landmarks, and overall limited visualization. MISt has an inherently shallow learning curve with comparatively fewer complications and provides surgeons an alternative to open procedures. With navigation technology, there has been a remarkable demonstration of safety and accuracy improvement in the placement of spinal instrumentation. Although the use of navigation in spine surgery was by and large initially implemented in the conventional open approach, the increasing adoption of MIS techniques has also prompted the use of navigation in MIS.

## 6.2 CT (O-Arm)-Based Navigation Surgery

In 1981, Japan introduced the world to car navigation technology. This technology would soon be adopted for medical use with computed tomography (CT)-based navigation and has since continued to gain traction worldwide. A major challenge of MIS surgery can be potentially addressed through the implementation of car navigation technology in medicine by reducing the burden on surgeons and at the same time providing a safer and more accurate surgical procedure. The technology creates something of a microcosm in the operating theater when drawing parallels between the infrared sensor of the navigation system and the satellite, the patient's body and the map, and the various surgical instruments and the car. Surgical instruments have been increasingly adopting innovative technology like that of cars, and the introduction of instruments such as pneumatic drills have allowed an expanded range of indications with better accuracy. The newest generation of navigation technology has led to an enormous improvement in imaging resolution of the spine via intraoperative three-dimensional (3D) CT-based navigation using the mobile O-arm (Medtronic, Minneapolis, MN, USA) [14]. CT-based navigation has enabled the surgeon to refine MIS techniques through enhancements of real-time virtual images, mapping of planned trajectories, and visualization of deep spine anatomy. By increasing the accuracy of the pedicle screw and instrumentation placement in the cervical, thoracic, and lumbar spine, CT-based navigation in spine surgery has led to a significant decrease in instrumentation-related morbidity.

With the currently available technology, the use of CT-based navigation can be especially useful in (1) the implantation of cages, pedicle screws, and pelvic anchors [15–17], (2) bone tumors resection [18], and (3) performing the anterior floating method for the ossification of the posterior longitudinal ligament (OPLL). In the insertion of implants, it is also effective for MISt with percutaneous pedicle screws. Application of navigation even for open surgeries such as corrective surgery for spinal deformity, tumor resection, and OPLL resection, the application of navigation can reduce the invasiveness compared to conventional approaches (e.g., less soft tissue exposure, greater precision, and better rate of securing an appropriate resection margin). In the surgical corrections for adult spinal deformity, O-arm navigation allows the physician to place the minimally invasive lateral interbody cages, percutaneous pedicle screws, and S2-alar-iliac screws with precision (Fig. 6.1a–c). It can be applied for three-column osteotomies such as pedicle subtraction osteotomy and vertebral column resection to obtain clear anatomical orientation. In bone tumor resection, navigation enables surgeons to perform resections with appropriate tumor margins. The tumor resection of lumbar osteochondroma under O-arm navigation is shown in Fig. 6.2.

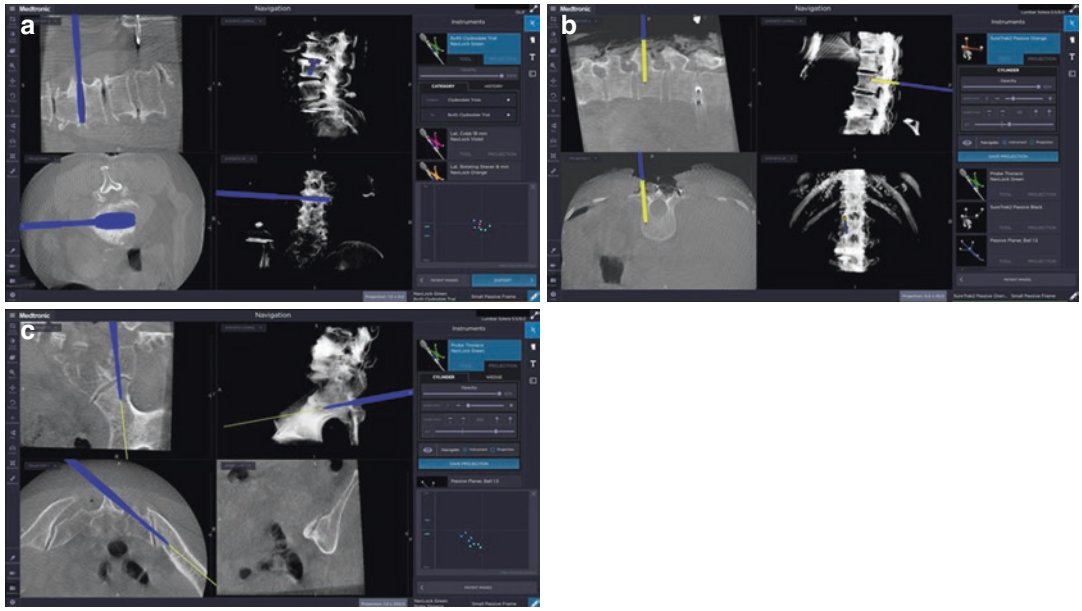


**Fig. 6.1** Computed tomography (O-arm)-based navigation surgery for severe adult spinal deformity. O-arm navigation allows the precise placement of minimally invasive lateral interbody cages (**a**), percutaneous pedicle screws (**b**), and S2-alar-iliac screws (**c**)

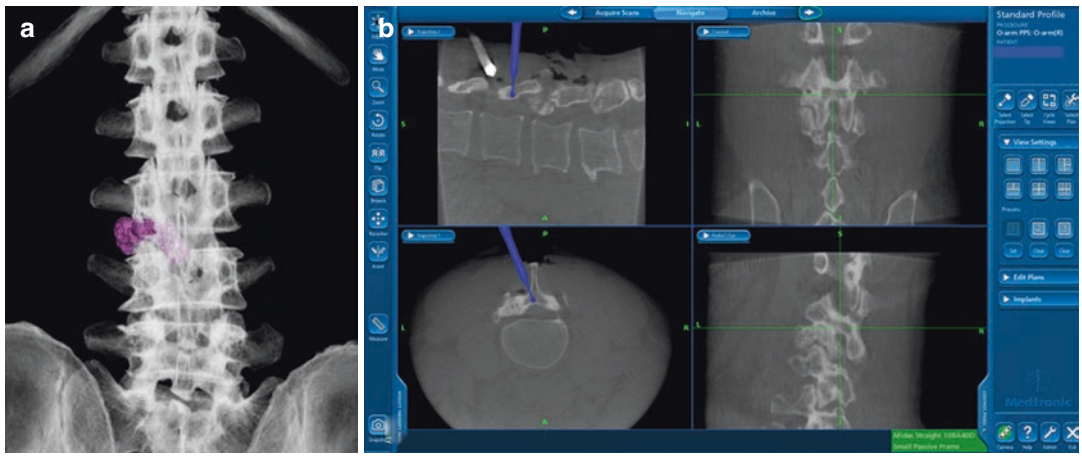


**Fig. 6.2** Computed tomography (O-arm)-based navigation surgery for securing an appropriate resection margin in bone tumor. The bone tumor is shown in purple on preoperative 3D-CT image (**a**). On navigation monitor (**b**), the wide margin can be easily detected to perform en bloc tumor resection

The complete resection of the tumor can be performed with a wide resection margin. On the other hand, some of the limitations noted for the use of navigation include its high cost, medical exposure, interface errors involving the operator, and errors related to reference markers.

## 6.3 Mixed Reality-Based Navigation

In recent years, immersive technologies such as virtual reality (VR), augmented reality (AR), and mixed reality (MR) have been widely applied in the medical field. VR provides a complete sensory

immersion that is experienced through an artificial environment. AR projects an artificial environment onto the physical environment. MR mediates between the extremes of virtuality, with either the artificial environment being projected into the physical environment or the physical environment being completely immersed by the artificial environment. These technologies are now used in the gaming industry and entertainment industry such as film, manufacturing, construction, logistics, advertising, tourism, education, and sports.

We have applied MR technology using Microsoft HoloLens in spinal surgery since 2017. Microsoft HoloLens is a pair of MR smart glasses developed and manufactured by Microsoft Corporation. HoloLens was the first head-mounted display to support the Windows MR platform that was introduced as part of the Windows 10 computer operating system. The HoloLens is equipped with a group of optical sensors, with four peripheral sensors to facilitate environmental perception, a main downward-facing depth camera to detect hand motions, and specialized speakers to simulate the spatialization of sound by capturing the head-related transfer function. The HoloLens also has several microphones, a head-mounted camera, an ambient light sensor, and a custom "Holographic Processing Unit" that Microsoft claims to demonstrate a processing power that exceeds that of an average laptop. The combination of these components permits the device to sense the spatial orientation of the display unit, track walls and objects, and blend holograms into the environment. In actual surgery, polygonal models are created from the volume data of preoperative or intraoperative CT images and installed in HoloLens [19]. MR technology produced by HoloLens can project 3D images of organs, blood vessels, and bones on the patient's body or the actual surgical field (Fig. 6.3a). Devices that use MR technology can be beneficial tools for implant placement as well as understanding the intraoperative orientation of tissues and organs. Moreover, the trajectory and location of pedicle screws can be added to polygonal data (Fig. 6.3a). Another advantage is that the same 3D images can be shared between multiple HoloLens via Wi-Fi (Fig. 6.3b). In our experience, this excellent MR technology can be applied to complex spinal surgery indicated for conditions such as severe spinal deformity and total en bloc spondylectomy. Although the technology is still in a developmental stage, we believe that there is great potential to achieve further strides in the future.

## 6.4 Augmented Reality-Based Navigation

AR is a general term for technologies that add real-time information to moving images of the real world. A familiar example of AR is software

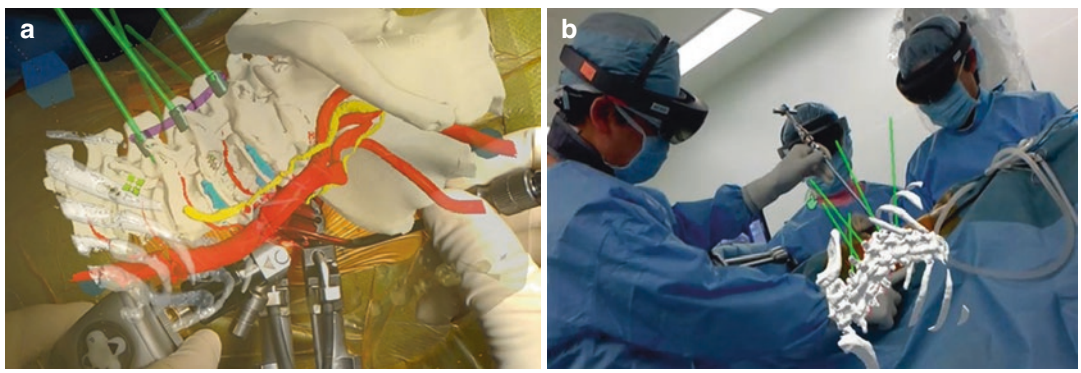


**Fig. 6.3** Mixed Reality (MR)-based navigation for severe spinal deformity. HoloLens can project 3D images of organs, blood vessels, and bones on the patient's body (**a**). The same projection image can be shared intraoperatively between the operator and assistants (**b**)

that adds CG illustrations to facial photographs taken by smartphone cameras. AR technology is defined by three essential characteristics: (1) a combination of the real and virtual, (2) real-time interaction, and (3) 3D registration [20]. AR-based navigation is a novel type of navigation that distinguishes itself from other state-of-the-art navigation systems. Philips N.V. has introduced a next-generation AR system (ClarifEye; Philips, Amsterdam, Netherlands) equipped with a visible light camera that simultaneously captures tracking markers on the body surface via spinal fluoroscopy (Fig. 6.4). The ClarifEye system is a surface referenced, navigation system based on video input from four optical cameras mounted into the frame of a C-arm detector. Acquisition and patient tracking are ensured by continuous video detection of 8–10 sterile, flat, adhesive, circular markers randomly placed on the skin around the surgical field. In addition, instruments equipped with an optical marker, in this case, the bone access needle with an optical marker on the shaft (Galt Medical Corp., Garland, TX, USA), can be tracked by the navigation system in three dimensions. The needle was specifically designed to be tracked by the system and does not require any calibration. During needle insertion, AR views provide real-time feedback to the surgeon (Fig. 6.4c, d). The AR views show the location of the tracked needle and the planned path on the cone beam CT volume reconstruction. The needle position is overlaid on at least one of the optical camera views to indicate the accuracy of the tracked needle. The C-arm enables 3D cone beam CT scans (XperCT; Philips, Amsterdam, Netherlands) for planning screw placement as well as confirming screw position. The vertebrae and corresponding pedicles are automatically segmented with the planning software. The optimal screw path through the vertebra and the physical dimensions of the screw are specified by the operator. The intraoperative CT planned paths for screw placement and needle position-

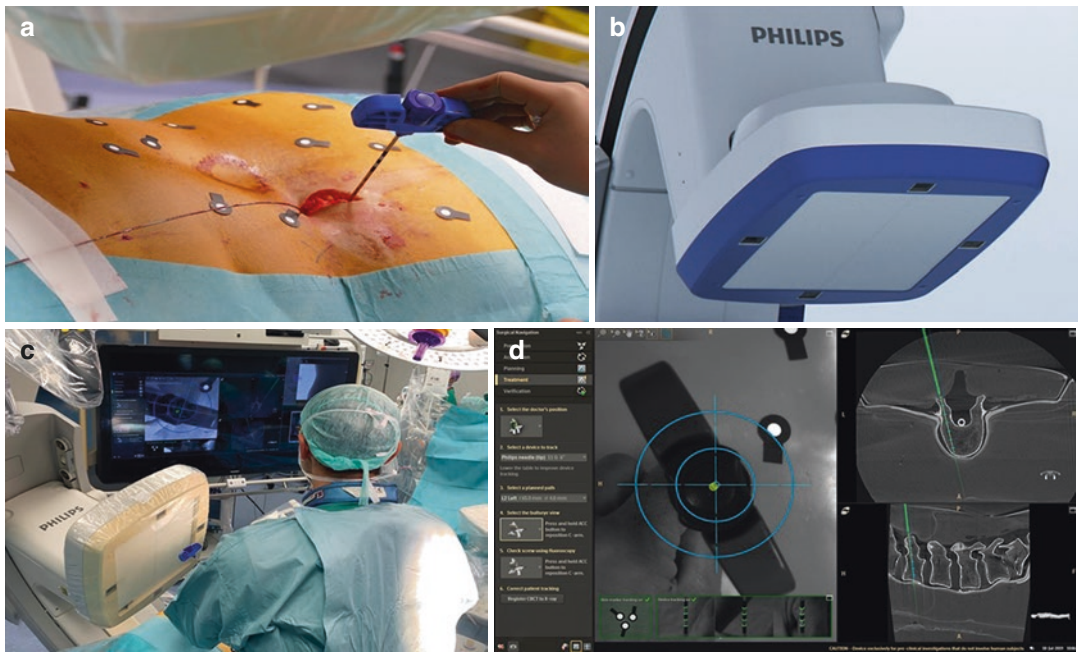


**Fig. 6.4** Augmented Reality (AR) (ClarifEye)-based navigation for spinal deformity. Video cameras integrated into X-ray detector frame cover (**b**) for tracking with non-invasive markers (**a**) placed on the patient's skin. Live display from the video cameras augmented with 3D volume rendering of the spine and planned path of a pedicle screw (**c** and **d**). The left viewport in (**d**) corresponds to a bull's eye view, whereas other viewports display line paths for instrument alignment. (**a**, **c**, **d**): Courtesy of Dr. Scarone, Neurosurgeon, EOC Lugano, Switzerland

ing are added onto the video images of the surgical field. A previous study showed that percutaneous pedicle screw insertion with AR-based navigation with instrument tracking functionality is feasible and results in accuracy compared to the standard fluoroscopy-guided percutaneous method [21]. Another study carried out in a cohort of mostly spinal deformity cases indicated that AR surgical navigation with intraoperative 3D imaging in a hybrid operating room demonstrated a statistically higher screw placement accuracy compared to the free-hand technique [22]. Procedure time, length of hospital stays, and blood loss did not show any statistical difference between surgical techniques. In a comparative study between XperCT and O-arm, the estimated patient dose for small, medium, and large phantoms imaged by O-arm in low, standard, and high doses ranged from 9.4 to 27.6 mGy, 8.9 to 33.3 mGy, and 13.8 to 40.6 mGy, respectively. With XperCT, the estimated patient dose under the same condition was 2.8–4.6 mGy, 5.7–10.0 mGy, and 11.0–15.2 mGy. The contrast-to-noise ratio for the small, medium, and large phantoms was 2.9, 3.7, 2.0–3.0, and 2.5–2.6 times higher with the XperCT system, respectively [23]. Although the utilization of AR-based navigation surgery in the field of spinal surgery is still a developing technology, it has the potential to make significant progress in the future.

## References


1. Ishii K, Isogai N, Shiono Y, Yoshida K, Takahashi Y, Takeshima K, et al. Contraindication of minimally invasive lateral interbody fusion for percutaneous reduction of degenerative spondylolisthesis: a new radiographic indicator of bony lateral recess stenosis using I line. Asian Spine J. 2020. https://doi.org/10.31616/asj.2020.0083. Epub ahead of print.
2. Fujiyoshi T, Yamazaki M, Kawabe J, Endo T, Furuya T, Koda M, et al. A new concept for making decisions regarding the surgical approach for cervical ossification of the posterior longitudinal ligament: the K-line. Spine (Phila Pa 1976). 2008;33(26):E990–3.
3. Foley KT, Gupta SK, Justis JR, Sherman MC. Percutaneous pedicle screw fixation of the lumbar spine. Neurosurg Focus. 2001;10(4):E10.
4. Ishii K, Shiono Y, Funao H, Singh K, Matsumoto M. A novel groove-entry technique for inserting thoracic percutaneous pedicle screws. Clin Spine Surg. 2017;30(2):57–64.
5. Tomita K, Kawahara N, Baba H, Tsuchiya H, Fujita T, Toribatake Y. Total en bloc spondylectomy. A new surgical technique for primary malignant vertebral tumors. Spine (Phila Pa 1976). 1997;22(3):324–33.
6. Ishii K, Kaneko Y, Funao H, Ishihara S, Shinohara A, Nakanishi K, et al. A novel percutaneous guide wire (S-Wire) for percutaneous pedicle screw insertion: its development, efficacy, and safety. Surg Innov. 2015;22(5):469–73.
7. Foley KT, Holly LT, Schwender JD. Minimally invasive lumbar fusion. Spine (Phila Pa 1976). 2003;28(15 Suppl):S26–35.
8. Chiba K, Matsuyama Y, Seo T, Toyama Y. Condoliase for the treatment of lumbar disc herniation: a randomized controlled trial. Spine (Phila Pa 1976). 2018;43(15):E869–76.
9. Khoo LT, Palmer S, Laich DT, Fessler RG. Minimally invasive percutaneous posterior lumbar interbody fusion. Neurosurgery. 2002;51(5 Suppl):S166–81.
10. Pimenta L. Lateral endoscopic transpsoas retroperitoneal approach for lumbar spine surgery. Presented at VIII Brazilian Spine Society Meeting, Belo Horizonte, Minas Gerais, Brazil; May 2001.
11. Ozgur BM, Aryan HE, Pimenta L, Taylor WR. Extreme Lateral Interbody Fusion (XLIF): a novel surgical technique for anterior lumbar interbody fusion. Spine J. 2006;6(4):435–43.
12. Mayer HM. A new microsurgical technique for minimally invasive anterior lumbar interbody fusion. Spine (Phila Pa 1976). 1997;22(6):691–9. discussion 700
13. Berjano P, Lamartina C. Far lateral approaches (XLIF) in adult scoliosis. Eur Spine J. 2013;22(Suppl 2):S242–53.
14. Holly LT, Foley KT. Intraoperative spinal navigation. Spine (Phila Pa 1976). 2003;28(15 Suppl):S54–61.
15. Larson AN, Santos ER, Polly DW Jr, Ledonio CG, Sembrano JN, Mielke CH, et al. Pediatric pedicle screw placement using intraoperative computed tomography and 3-dimensional image-guided navigation. Spine (Phila Pa 1976). 2012;37(3):E188–94.
16. Ray WZ, Ravindra VM, Schmidt MH, Dailey AT. Stereotactic navigation with the O-arm for placement of S-2 alar iliac screws in pelvic lumbar fixation. J Neurosurg Spine. 2013;18(5):490–5.
17. Drazin D, Liu JC, Acosta FL Jr. CT navigated lateral interbody fusion. J Clin Neurosci. 2013;20(10):1438–41.
18. Drazin D, Bhamb N, Al-Khouja LT, Kappel AD, Kim TT, Johnson JP, et al. Image-guided resection of aggressive sacral tumors. Neurosurg Focus. 2017;42(1):E15.
19. Saito Y, Sugimoto M, Imura S, Morine Y, Ikemoto T, Iwahashi S, et al. Intraoperative 3D hologram support with mixed reality techniques in liver surgery. Ann Surg. 2020;271(1):e4–7.

20. Yamada Y, Nakamura T, Yamada M, Maruyama J, Maruyama K, Azuma E. Use of augmented reality to assist teaching for future perfusionists in extracorporeal technology. J Extra Corpor Technol. 2019;51(4):244–7.
21. Peh S, Chatterjea A, Pfarr J, Schäfer JP, Weuster M, Klüter T, et al. Accuracy of augmented reality surgical navigation for minimally invasive pedicle screw insertion in the thoracic and lumbar spine with a new tracking device. Spine J. 2020;20(4):629–37.
22. Elmi-Terander A, Burström G, Nachabé R, Fagerlund M, Ståhl F, Charalampidis A, et al. Augmented reality navigation with intraoperative 3D imaging vs fluoroscopy-assisted free-hand surgery for spine fixation surgery: a matched-control study comparing accuracy. Sci Rep. 2020;10(1):707.
23. Nachabe R, Strauss K, Schueler B, Bydon M. Radiation dose and image quality comparison during spine surgery with two different, intraoperative 3D imaging navigation systems. J Appl Clin Med Phys. 2019;20(2):136–45.

# 7 Single-Stage Lateral Lumbar Interbody Fusion Based on O-arm Navigation

## A Simultaneous Anterior and Posterior Procedure in a Lateral Position

Jun Ouchida, Hiroaki Nakashima, and Tokumi Kanemura

## 7.1 Introduction

Lateral interbody fusion (LIF) has become widely used to treat patients with spinal instability, deformity, or lumbar canal stenosis. The cage used in LIF has the advantage of having a higher height and larger footprint when compared to cages for posterior or posterior-lateral approach methods, thus providing a solid spinal stabilization, alignment correction, and intervertebral disc restoration [1, 2]. In addition, these advantages of the LIF cage profile provide effective indirect decompression and allow less invasive circumferential anterior-posterior spinal fusion with percutaneous pedicle screw (PPS) [3, 4]. On the other hand, the anterior-posterior fixation usually requires repositioning the patients between anterior and posterior fixation procedures, which is associated with the disadvantages of requiring medical staff resources for repositioning and twice surgical materials to create a sterile field compared to a single-position surgery.

We have combined LIF surgery with PPS insertion in a single lateral decubitus position assisted by intraoperative Computed Tomography (CT)-based navigation. The usage of intraoperative CT images for the navigation system provides reliable surgical imaging assistance for patients, especially those with obesity and significant spinal degeneration where there is a difficulty encountered in recognizing anatomical landmarks of the spine using intraoperative fluoroscopy alone. In addition, this surgical procedure reduces radiation exposure to surgeons and medical staff compared to fluoroscopy-guided methods. In this surgical technique, two surgeons perform anterior-posterior surgical procedures simultaneously.

The indications for this single-position anterior-posterior fixation method are the same as for indirect decompression, i.e., lumbar spinal canal stenosis with instability, with mild to moderate (grade 2 or less) spondylolisthesis. Calcification in the foramen, severe (grade 3 or more) spondylolisthesis, and preoperative bladder and rectal disturbance or motor paralysis are not considered indications for this surgical strategy [5]. To perform anterior and posterior surgical procedures simultaneously, two surgeons skilled in spinal fusion surgery are required.

J. Ouchida · H. Nakashima
Department of Orthopaedic Surgery, Nagoya University Graduate School of Medicine, Nagoya, Japan
e-mail: hirospine@med.nagoya-u.ac.jp

T. Kanemura (✉)
Spine Center, Konan Kosei Hospital, Konan, Aichi, Japan
e-mail: spinesho@vmail.plala.or.jp



J.-S. Kim et al. (eds.), *Technical Advances in Minimally Invasive Spine Surgery*,
https://doi.org/10.1007/978-981-19-0175-1_7

## 7.2 Settings and Surgical Techniques

After general anesthesia, the patient is placed in a lateral position on the operating table. The approaching side is determined by preoperative CT to evaluate the bowel, vascular, and ureteral tracts. The side of the body to be entered is turned up, and the hip and knee joints are each flexed 30° and fixed to the operating table with tape (Fig. 7.1). Cushions are placed between the thighs and lower legs and the bed to distribute the weight of the patient in order to prevent skin damage or compressive peripheral nerve disorder at the fibular head. The patient's anterior-posterior position should be adjusted so that the operating table does not interfere with the floor side screw insertion, e.g., leaving a palm space between the patient's back and the table's edge (Fig. 7.1a). An operating table should be bendable at the patient's waist to prevent the iliac bone from interfering with the approach to the lateral space of the low lumbar level (Fig. 7.1b, c). The bending of the operating table should be limited to about 15–20° in the case of using intraoperative CT scanning, any further bending may cause a collision between the operating table and the CT unit. After sterilization, drapes and compressions are placed on the patient's body and a sterile surgical field is established. Because of the proximity of the skin incision for the floor side screw insertion and the table's sterile zone, the drapes are secured to the patient's body with a suture to prevent contamination.

To perform simultaneous anterior and posterior fixation, the surgeon responsible for the anterior fixation component stands on the patient's ventral side while the surgeon undertaking the posterior fixation stands on the patient's dorsal side. Two monitors that display the navi-


**Fig. 7.1** The patient is fixed with tape on the bendable Jackson bed (ProAxis® Spinal Surgery Table, MIZUHO OSI, Union City, CA, USA). The patient's position was adjusted to keep the space between the patient and table edges (double-headed arrow) not too far apart so that the table is not in the way during floor-side screw insertion (**a**). The pictures are from the anterior (**b**) and posterior (**c**) views of the patient

gation images to be referenced should be available and placed on the facing side of each surgeon. An optical navigation camera is placed on the patient's head side. The intraoperative CT unit is located on the patient's foot side and slides to the head side for image acquisition. It is preferable to have one assistant assigned for the anterior and one for the posterior surgeon, respectively (Fig. 7.2).

The surgical procedure is performed by placing the navigation reference frame in the iliac bone on the patient's operative entry side through a small incision in the hip (Fig. 7.3). The placing position and direction of the navigation reference frame is crucial for barrier-free surgical procedure in a lateral single-position surgery with intraoperative CT-based navigation. The reference frame is placed at an angle to avoid interference between the surgical instruments and the infrared receiver during anterior cage placement and posterior screw insertion. After intraoperative CT images are obtained by the O-arm® O2 imaging system (Medtronic Sofamor Danek, Inc., Memphis, TN, USA), the anterior fixation surgeon, referring to the navigation images, makes a skin incision in the patient's lateral side of the abdomen, approaches the lateral area of the anterior disc in a retroperitoneal approach, performs an anterior disc dissection, and inserts the LIF cage.

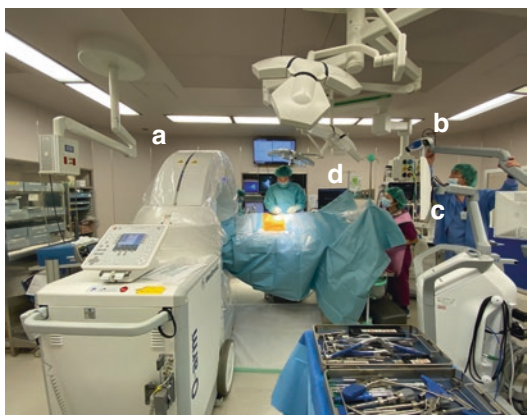


**Fig. 7.2** Position of surgical assistance equipment. (a) O-arm, (b) the navigation optical camera, (c) the navigation monitor for anterior fixation surgeon, (**d**) the navigation monitor for posterior fixation surgeon. This picture was taken from the posterior side of the patient

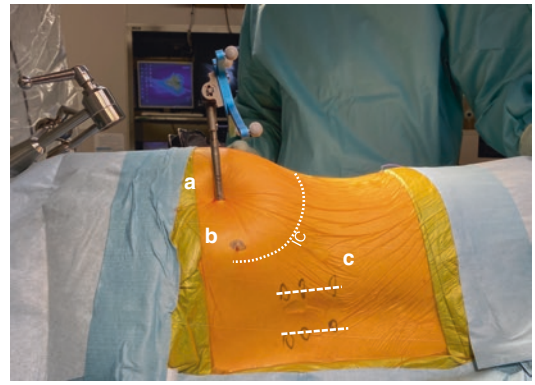


**Fig. 7.3** The navigation reference frame for (a) is placed in the posterior superior iliac crest with a small skin incision. (b) Bone marrow collection site to be mixed with the graft bone, (c) location of the skin incision for percutaneous pedicle screw insertion, *IC* iliac crest

The posterior fixation surgeon places the screws using the PPS insertion technique (Fig. 7.4a, b). Since the two channels of navigation guidance are not available at the same time, two surgeons can perform simultaneous anterior-posterior fixation by alternately referring to the navigation when necessary (Fig. 7.5). Screw insertion for posterior fixation should be performed in sequence starting at the level of the cranial vertebrae that are farther away from the navigation reference since intervertebral manipulation and correction of disc height by cage insertion deteriorate the navigation accuracy of the screw insertion on the far side from the navigation reference (Fig. 7.6). After the placement of the cage in all intervertebral spaces, the rod is connected to the PPS, and circumferential fixation is completed. At this point, it is recommended to use fluoroscopy to detect navigation misalignment or to confirm instrument position. Before finishing the surgery, ensure that there are no signs of visceral or vascular injuries in the anterior surgical site and remove the retractor. After confirming that the anterior and posterior surgical sites are completely clear of persistent bleeding, skin closures are performed.

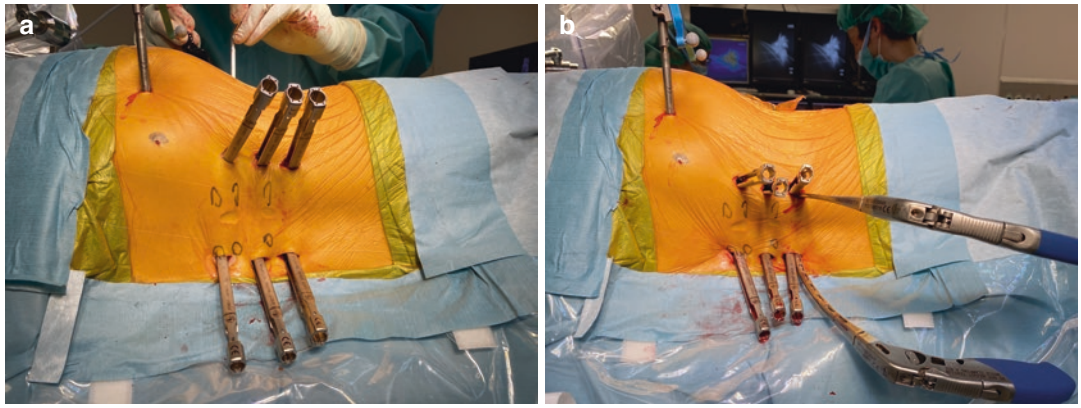


**Fig. 7.4** The screws using the PPS insertion technique in a lateral position. All tabbed screws were inserted (**a**). The rods were installed, and the screws were connected (**b**)

**Fig. 7.5** Simultaneous proceeding of anterior–posterior surgery. Two navigation monitors to which the anterior and posterior fixation surgeons refer. Note: Since only one navigation system is available at a time, each surgeon refers to the navigation alternately

## 7.3 Advantages of Single-Position Anterior and Posterior Lumbar Interbody Fusion

A simultaneous single-position lumbar interbody fusion can reduce operating room occupancy time compared to conventional two-staged surgery with repositioning. A study done at our institution compared single and two-staged anterior-posterior fixation at 1.2 of mean fixed vertebral levels, respectively, where the operating room occupancy of the single position group was reduced to an average of 176 min, compared with 272 min in the repositioning group [6]. This method allows two surgeons to perform the anterior-posterior surgical procedures simultaneously, reducing the operating time and the risk of complications for patients associated with long operation time. In a comparative study, Blizzard et al. also demonstrated that the single-position all-lateral technique with fluoroscopy was feasible in terms of accuracy of screw placement, time-saving on operating time, fluoroscopic image usage, and complication rates being comparable to conventional anterior-posterior surgeries using LLIF [7]. The single-position technique is expected to be cost-effective because it reduces the required number of staff and surgical materials for the position change between the ante-

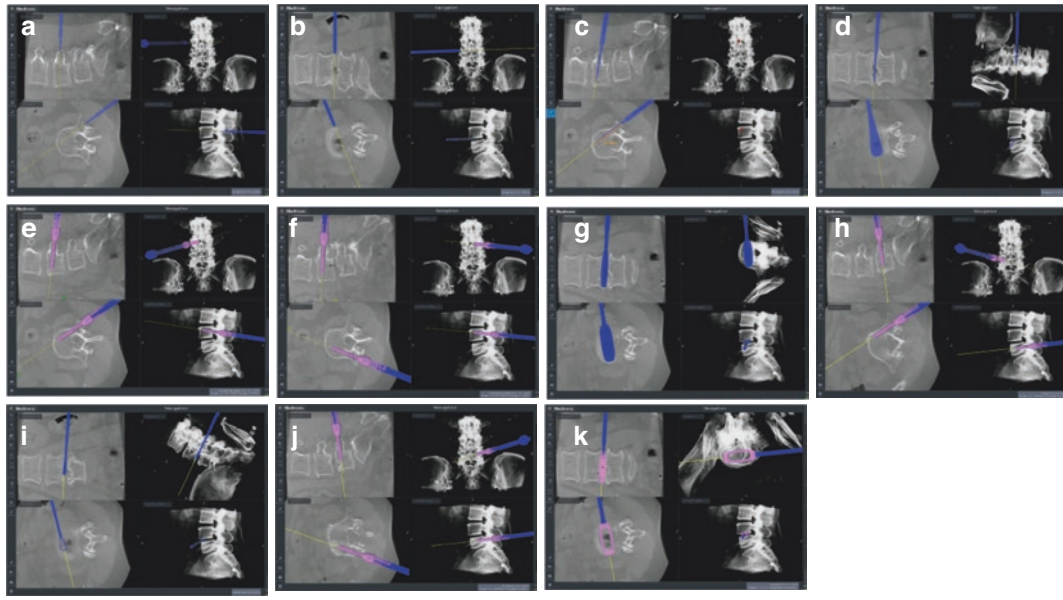


**Fig. 7.6** Simultaneous proceeding of anterior-posterior surgery. The procedures are done in alphabetical order. The navigation screens to which the posterior fixation surgeon refers; the awl for left L4 pedicle (**a**), the screw tap for left L4 pedicle (**c**), the pedicle screw insertion to left L4 pedicle (**e**), to right L4 pedicle (**f**), to left L5 pedicle (**h**), and to right L5 pedicle (**f**). The navigation screens to which the anterior fixation surgeon refers; the probe (**b**), the cobb elevator (**d**), the trial (**g**), the curet (**i**), the pedicle screw insertion (**j**) and the OLIF cage insertion (**k**) to L4/5 disc. Note: Since only one navigation system is available at a time, each surgeon refers to the navigation alternately

rior and posterior surgeries. On the other hand, a tendency to increase intraoperative blood loss has been reported (93.4 vs. 40.9 ml, $p < 0.001$) in our study series [6], and meticulous hemostatic manipulation is therefore recommended.

Although the concern about inadequate lumbar lordosis acquisition in spinal fusion in lateral decubitus position is still controversial, our study showed that the radiographic outcomes in this single position group were comparable to those of the repositioning group with supine screw fixation concerning the acquisition of lumbar lordosis and vertebral height restoration. Furthermore, Hiyama et al. reported that in a comparative study between single-position LLIF and repositioning LLIF, there was no difference between the two groups in terms of radiographic parameter changes and dural sac enlargement on postoperative MRI [8].

Intraoperative CT images in the operative position provide reliable support even for obese patients and patients with severe degeneration where it is challenging to identify anatomical orientation with intraoperative fluoroscopy equipment, thereby reducing radiation exposure to surgeons and medical staff compared to fluoroscopy-based methods [9].

## 7.4 Learning Curve

We conducted a comparative survey to investigate the learning curve of single-position surgery compared to the conventional repositioning technique. Single-position surgeries performed by two surgeons in 39 consecutive cases since the initial introduction was compared with the repositioning method performed by two surgeons in 38 cases since its initial introduction. We investigated the surgery time, occupancy time in the operating room, and the accuracy of screw insertion in postoperative CT scans as variables reflecting the learning curve. A significant reduction of approximately 30 min in the occupancy time of the operating room was observed from the earliest stage (first to tenth cases) of the intro-

duction (83.0 ± 14.7 vs. 110.3 ± 34.8 min), and a reduction of more than 60 min in operating time was observed from the 21st cases and after compared with the conventional method (201.6 ± 60.0 vs. 262.4 ± 42.7 min). In addition, the accuracy of screw insertion was comparable to that of the traditional process from the early stage (first to tenth cases) of introduction. This study suggests that single-position LIF-PPS with O-arm-based navigation exhibits equal surgical outcomes as conventional repositioning LIF-PPS as well as attaining reduction in the occupancy time of the operating room from the initial introduction. Lastly, we noted that the surgery time tended to become shorter with the number of cases. We believe that institutions performing two-stage anterior and posterior spinal fusion using the conventional repositioning method can expect to achieve favorable treatment effects and time benefits by introducing single-position surgery under appropriate indications for surgical strategy.

## 7.5 Future Possibilities of Single-Position Surgery

The efficacy of indirect decompression has been reported in several papers, and Thomas et al. reported a very low failure rate (1.7%) of indirect decompression surgery for the lower lumbar level [10]. Indirect decompression is performed by percutaneous posterior fixation and does not directly manipulate the dural periphery, so it is considered minimally invasive leading to less risk of nerve injury. Because of the reduction in operative time compared to surgery with repositioning, the necessity of direct decompression for the pathology of each case and the need to properly estimate the risks associated with prolonged operative time and increased intraoperative blood loss should be considered in the surgical strategy, and the single position may be one of the solutions to make surgery safer. Due to the minimally invasive nature of PPS, this surgical approach may also be a useful option in patients with comorbidities or those who cannot tolerate massive surgery. We consider the potential of intraoperative CT-based navigation assistance to be highly compatible with single-position spine surgery for patients with such an anatomical complexity. Furthermore, although the case series of our institution included primary spinal fusion surgery by two surgeons, the single-position technique is considered to be feasible compared with the conventional repositioning method, even with a single surgeon situation or revision surgery [11], this surgical technique may become the gold standard for anterior and posterior fusion using LIF in cases that do not require direct decompression.

In addition to surgical indications for short segment spinal fixation for lumbar spondylolisthesis, it is expected that this advantageous surgical technique can be widely applied to other spinal diseases. One example would be the dislocated fractures of the ankylosing spine with severe kyphosis that have difficulty achieving an adequate reduction in the supine position (Fig. 7.7). The increased flexibility of the patient's position may also contribute to the development of reduction techniques for displaced spinal trauma. It may also be beneficial in spinal fixation for malignancy in the spine (e.g., palliative surgery in spinal fixation for metastatic spinal tumors), requiring a minimally invasive intervention or not being tolerant of prolonged surgery under general anesthesia [12].

Intraoperative CT navigation assistance is useful for screw placement in patients with complex anatomical characteristics. Furthermore, navigation-guided robotic surgery in the spine has recently been introduced and is expected to be applied to PPS placement in the decubitus position [13]. Huntsman et al. reported a favorable accuracy rate of 98% for successful screw placement in postoperative radiographic evaluation of single-position pedicle screw placement using robot-assisted technology under intraoperative CT navigation [14]. The development of navigation-assisted surgery is expected to be applied to anatomically complex structures. For example, the lumbosacral junction is still considered challenging to approach using the MIS technique as well as the anterior fixation in the lateral supine position due to their anatomical complexity. However, with the development of navigation

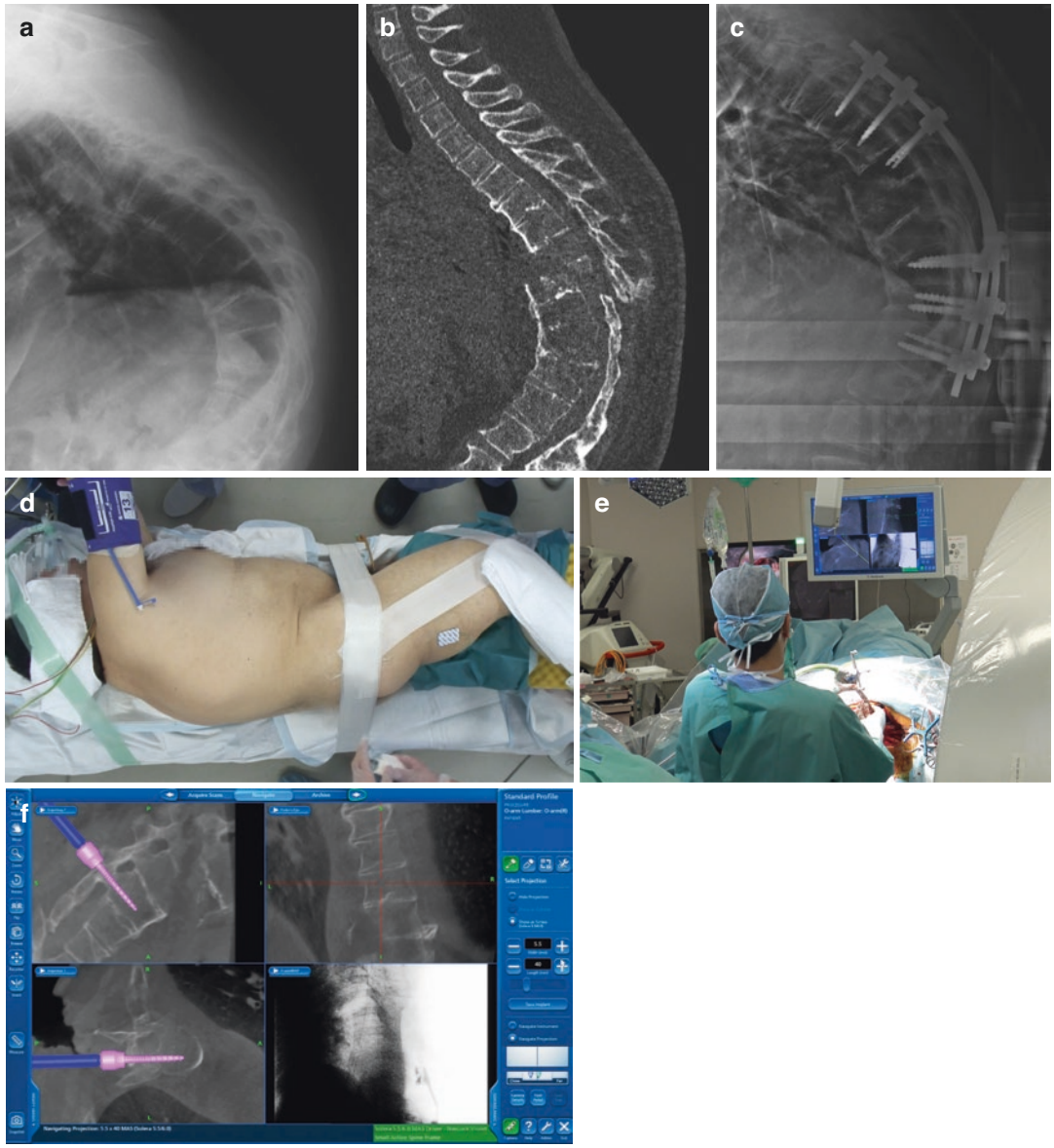


**Fig. 7.7** The dislocation fracture of the ankylosing spine with severe kyphosis. Preoperative lateral radiograph (**a**) and sagittal CT (**b**). Lateral radiograph after posterior fixation in a lateral position with O-arm navigation (**c**). Lateral setting position (**d**). Making a hole for thoracic pedicle screw insertion with a navigated surgical drill (**e**). The navigation screen at thoracic pedicle screw insertion (**f**)

technology, single-position surgery may be feasible for regions that are currently difficult to approach safely [15].

Single-position surgery offers an option for anterior and posterior spine surgery that can be valuable in enhancing medical efficiency through time savings, reducing the risk of surgical complications due to prolonged surgery time, and reducing the amount of personnel and medical resources used for repositioning compared to conventional repositioning methods. We believe that advances in assisted navigation technology, the application of robotic surgery, and the introduction of augmented reality technology to spine

surgery will accelerate the expansion of the application of single-position techniques.

## References


1. Kotwal S, Kawaguchi S, Lebl D, Hughes A, Huang R, Sama A, Cammisa F, Girardi F. Minimally invasive lateral lumbar interbody fusion clinical and radiographic outcome at a minimum 2-year follow-up. J Spinal Disord Tech. 2015;28:119–25.
2. Tormenti MJ, Maserati MB, Bonfield CM, Okonkwo DO, Kanter AS. Complications and radiographic correction in adult scoliosis following combined transpsoas extreme lateral interbody fusion and posterior pedicle screw instrumentation. Neurosurg Focus. 2010;28:E7.
3. Nakashima H, Kanemura T, Satake K, Ito K, Tanaka S, Ouchida J, Segi N, Kobayashi K, Ando K, Ishiguro N. Patient-reported quality of life following posterior lumbar interbody fusion or indirect decompression using lateral lumbar interbody fusion. Spine. 2020;45:E1172–8.
4. Oliveira L, Marchi L, Coutinho E, Pimenta L. A radiographic assessment of the ability of the extreme lateral interbody fusion procedure to indirectly decompress the neural elements. Spine. 2010;35:S331–7. https://doi.org/10.1097/BRS.0b013e3182022db0.
5. Nakashima H, Kanemura T, Satake K, Ishikawa Y, Ouchida J, Segi N, Yamaguchi H, Imagama S. Unplanned second-stage decompression for neurological deterioration caused by central canal stenosis after indirect lumbar decompression surgery. Asian Spine J. 2019;13:584–91. https://doi.org/10.31616/asj.2018.0232.
6. Ouchida J, Kanemura T, Satake K, Nakashima H, Ishikawa Y, Imagama S (2020) Simultaneous single-position lateral interbody fusion and percutaneous pedicle screw fixation using O-arm-based navigation reduces the occupancy time of the operating room. Eur Spine J.
7. Blizzard DJ, Thomas JA. MIS single-position lateral and oblique lateral lumbar interbody fusion and bilateral pedicle screw fixation. Spine. 2018;43:440–6.
8. Hiyama A, Katoh H, Sakai D, Sato M, Tanaka M, Watanabe M. Comparison of radiological changes after single-position versus dual-position for lateral interbody fusion and pedicle screw fixation. BMC Musculoskelet Disord. 2019;20:1–9.
9. Houten JK, Nasser R, Baxi N. Clinical assessment of percutaneous lumbar pedicle screw placement using the O-arm multidimensional surgical imaging system. Neurosurgery. 2012;70:990–5. https://doi.org/10.1227/NEU.0b013e318237a829.
10. Thomas JA, Thomason CI, Braly BA, Menezes CM. Rate of failure of indirect decompression in lateral single-position surgery: clinical results. Neurosurg Focus. 2020;49:E5.
11. Ziino C, Arzeno A, Cheng I. Analysis of single-position for revision surgery using lateral interbody fusion and pedicle screw fixation: feasibility and perioperative results. J Spine Surg. 2019;5:201.
12. Laratta JL, Weegens R, Malone KT, Chou D, Smith WD. Minimally invasive lateral approaches for the treatment of spinal tumors: single-position surgery without the "flip". J Spine Surg. 2020;6:62.
13. Walker CT, Godzik J, Xu DS, Theodore N, Uribe JS, Chang SW. Minimally invasive single-position lateral interbody fusion with robotic bilateral percutaneous pedicle screw fixation: 2-dimensional operative video. Oper Neurosurg. 2019;16:E121.
14. Huntsman KT, Riggleman JR, Ahrendtsen LA, Ledonio CG. Navigated robot-guided pedicle screws placed successfully in single-position lateral lumbar interbody fusion. J Robot Surg. 2020;14(4):643–7.
15. Baum GR, Lin JD, Morr S, Osorio JA, Leung E, Schutzer RW, Lehman RA Jr. Minimally invasive approach to the lumbosacral junction with a single position, 360° fusion. J Spine Surg. 2019;5:S68.

# The Role of 3D Navigation for MIS Cervical Spine Surgery

8

Tokumi Kanemura, Takamitsu Tokioka, and Kotaro Satake

## 8.1 The 3D Navigation for MIS Cervical Spine Surgery

### 8.1.1 Evolution of Posterior Cervical Fixation

In various cervical disorders or trauma, a secure stabilization is required to save the compromised bone- or neural structure. Since the early twentieth century, the methods of anterior and posterior cervical fixation have been developed. Different from an anterior fixation with a simple use of metal plates or cages, the posterior fixation has been upgraded to achieve more secure stabilization for more complicated cases.

Hadra reported the spinous process wiring for Pott's disease in 1891 [1] and thereafter the wiring technique was developed by others [2–6]. Interlaminar clamps for C1–C2 fixation were reported in the 1970s [7]. In fact, the posterior wiring could restore the posterior tension band constructs; however, it could not stabilize the construct against extension, rotation, or lateral bending moments [8]. In addition, wires and clamps could not be used in patients requiring posterior decompression procedures [9]. Consequently, screw systems combined with plates or rods were developed. Roy-Camille reported the lateral mass screws combined with plates for fixation of the unstable cervical spine [10]. Nonetheless, this procedure was later modified by others [11–13] with different entry points and trajectories of the screws.

The screw and rod system was developed to facilitate the application for cases with severe degenerative spondylosis or trauma [14] in the 1980s and 1990s [15, 16]. It also enabled multilevel fixation, including occipitocervical or cervicothoracic lesions [14].

Abumi et al. [17] first reported the cervical pedicle screw (CPS) fixation for subaxial trauma cases. CPS placement offers three-column fixation [18] and is probed to provide great pullout strength in various biomechanical examinations [19–21]. However, the accurate placement of CPS by freehand technique is technically difficult [8] due to its small target [22–24] as well as the large convergent pedicle trajectory [25, 26], seen especially in the subaxial vertebrae. CPS placement contains the potential risk of injuries to the vertebral artery (VA) or the exiting nerve roots [8, 27]. Thus, the navigation system has been expected to solve the technical difficulties faced with CPS placement technique.

T. Kanemura (✉)
Spine Center, Konan Kosei Hospital, Konan, Aichi, Japan
e-mail: spinesho@vmail.plala.or.jp

T. Tokioka
Institute of Neuroscience and Orthopedics, Okayama Kyokuto Hospital, Okayama City, Okayama Prefecture, Japan

K. Satake
Department of Orthopedic Surgery, Konan Kosei Hospital, Konan, Aichi, Japan



J.-S. Kim et al. (eds.), *Technical Advances in Minimally Invasive Spine Surgery*,
https://doi.org/10.1007/978-981-19-0175-1_8

### 8.1.2 Development of Navigation System for Cervical Spine Surgery

Since the beginning of the twenty-first century, a computer-assisted technique such as computed tomography (CT)-based navigation has been applied for cervical spine surgery, particularly for CPS placement [28–30]. The CT-based navigation system significantly improved the accuracy of CPS placement compared to the freehand technique using lateral fluoroscopy alone [28, 31].

The first type of navigation system is based on the CT data acquired preoperatively. The CT data set is transferred to the navigation system; however, the data obtained in a supine position is different from that in the intraoperative prone position in terms of cervical alignment. To adjust the positional gap of each vertebra, a complicated registration procedure with surface-matching is required in the first step of navigation surgery. This is time-consuming and has been thought to be a cause of navigation error especially for the small targets in cervical spine surgery [32, 33]. Thus, fluoroscopy, which can provide 3D CT images intraoperatively, has been replacing the preoperative CT-based navigation system.

Iso-C 3D (Arcadis Orbic 3D®, Siemens Medical Solutions, Erlangen, Germany) (Fig. 8.1) is the first device that can create intraoperative 3D images. It does not require anatomical registration and is able to renew 3D images during surgery repeatedly. It reduces the prevalence of malposition of CPS significantly compared to the conventional technique performed with 2D fluoroscopy alone [31]. The drawbacks are the low-quality images compared to the traditional CT and its potential risk of contamination of the surgical field during intraoperative scanning.

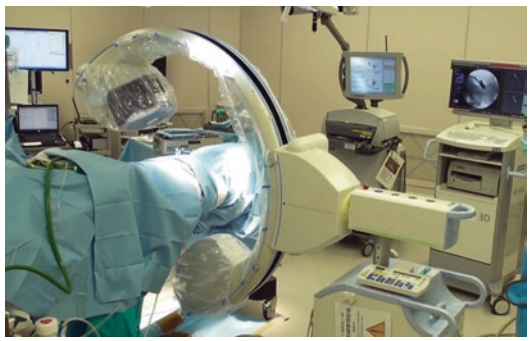

**Fig. 8.1** Iso-C 3D (Arcadis Orbic 3D®, Siemens Medical Solutions, Erlangen, Germany)

Most recently, O-arm (O-arm®, Medtronic Navigation, Littleton, CO, USA), an intraoperative full-rotation and multidimensional image system, was introduced in 2006. In the characteristic O-shaped gantry, the X-ray tube and flat-panel detector are able to turn 360°. Moreover, the image quality is almost the same as the recent multidetector helical CT scans. The gantry is covered with a special plastic sterilized bag that helps avoid contamination of the surgical field. It can provide more clear images than Iso-C 3D with tremendously reduced metallic artifacts and can also easily facilitate the intraoperative detection of the implant position. This is thought to be helpful in reducing the instrumentation error. Although there were no direct comparative reports on the accuracy of CPS placement, O-arm provided a reduced rate of CPS malposition compared to Iso-C 3D in two reports published from the same institute [31, 34]. In 2015, the latest version of O-arm, O-arm2 (Fig. 8.2), was released. It reduces the radiation exposure up to a maximum of 50% of the previous version of O-arm. In addition, the field of view expanded from 20 to 40 cm, and the image transfer time to the navigation system was reduced as well.

### 8.1.3 Development of Navigation Tools

Since the development of 3D navigation systems for spine surgery, there have been reports of improved accuracy of CPS placement [28, 31, 34–44], especially O-arm-based full-rotation image acquisition, which provides a high-quality image and helps to evaluate the CPS position intraoperatively [34, 35]. The reference frame for the cervical spine used to be the same type for the thoracic- or lumbar spine, which includes a clamp to a spinal process. This clamp does not always fit the small cervical spinal process and has a

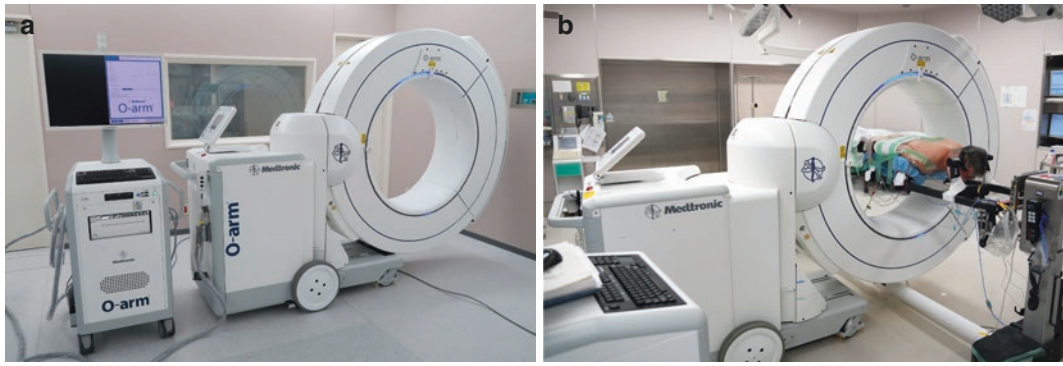


**Fig. 8.2** O-arm2 Imaging System (O-arm2®, Medtronic Navigation, Littleton, CO, USA). (**a**) Image acquisition system (O-typed gantry) and mobile view station. (**b**) O-2arm setting at cervical posterior surgery

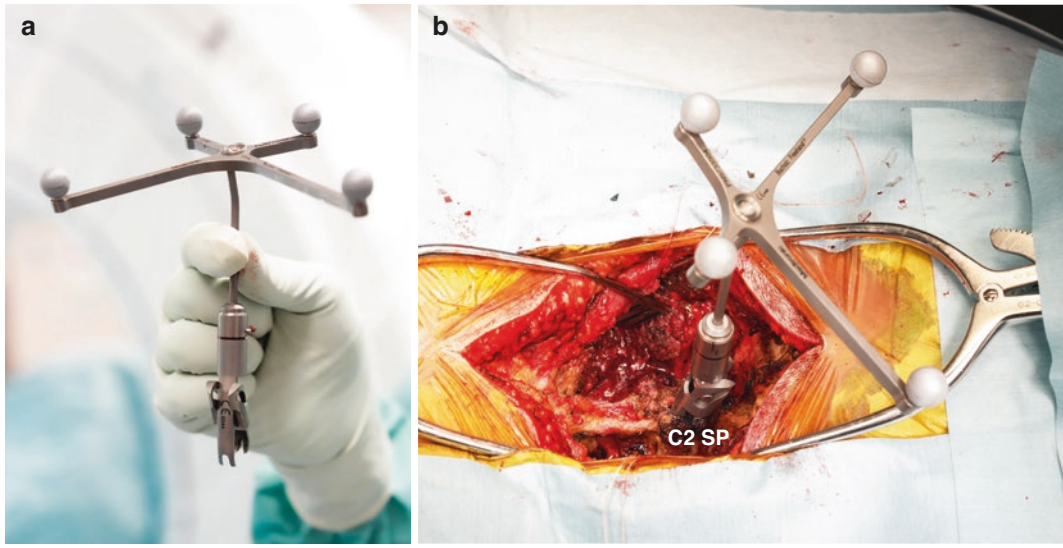


**Fig. 8.3** Navigation reference frames with a 3-point clamp. (**a**) This type is Appropriate for grabbing the spinous process of C2. (**b**) Setting on the spinous process of C2

potential risk to drift accidentally at the touch of surgeons in the small surgical field. Recently, reference frames with a 3-point clamp (for C2) (Fig. 8.3) or a double spine clamp (for subaxial spine) (Fig. 8.4) have improved the stability and the reliability of the navigation system. Various surgical tools (taps or screwdrivers) with the navigation system have been simultaneously developed as well (Figs. 8.5 and 8.6). Based on these navigation tools, each procedure can be projected on the navigation monitor.

## 8.2 Cervical Pedicle Screw Placement with Navigation

Cervical pedicle screw (CPS) fixation provides more excellent segmental stability than other fixation techniques such as sublaminar wiring or lateral mass screw (LMS) fixation [19, 22, 45, 46] and is helpful in the treatment of various disorders or trauma of the cervical spine [47–49]. As mentioned in the introduction, the accurate placement of CPS is technically challenging in the

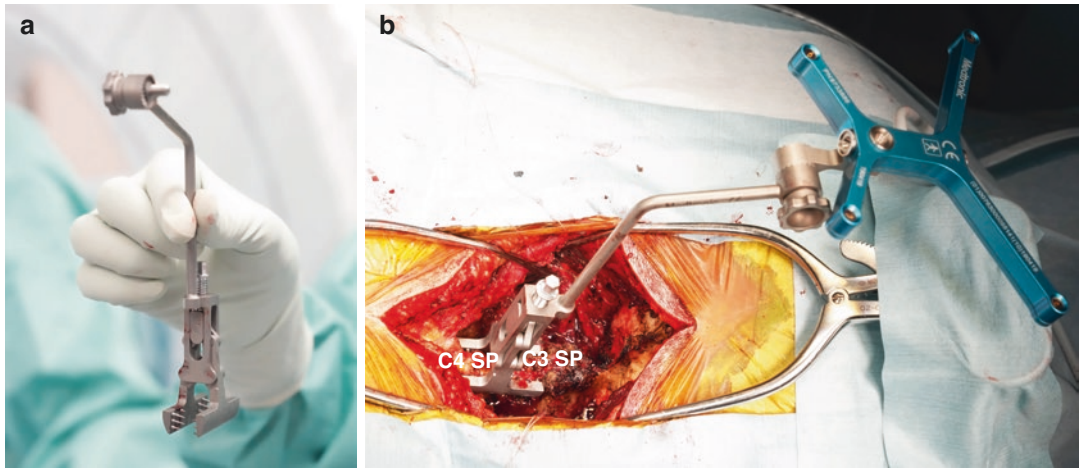


**Fig. 8.4** Navigation reference frames with a double spine clamp. (**a**) This type can grab two or three cervical spinous processes. (**b**) Setting on the spinous processes of C3 and C4. *SP* spinous process

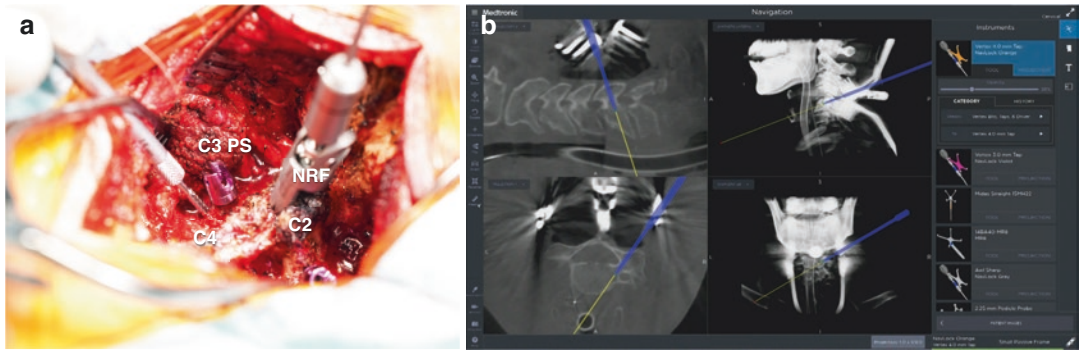


**Fig. 8.5** Navigated screw tap for cervical pedicle. (**a**) Navigated screw tap for C4 pedicle. (**b**) Navigation screen monitor showing navigated screw tap for C5 pedicle. *NRF* navigation reference frame, *PS* pedicle screw

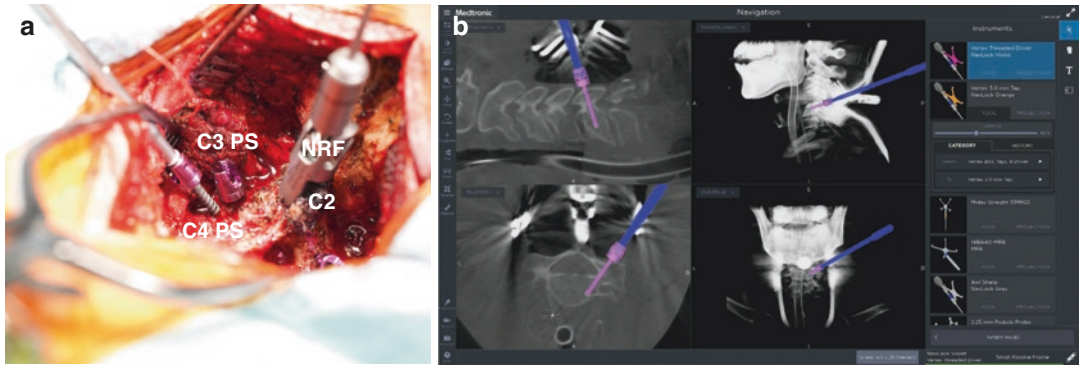


**Fig. 8.6** Navigated screwdriver for cervical pedicle. (**a**) C4 pedicle screw inserted with a navigated screwdriver. (**b**) Navigation screen monitor showing C5 pedicle screw with a navigated screwdriver. *NRF* navigation reference frame, *PS* pedicle screw

freehand technique [8] due to its small target [22–24] as well as the large convergent trajectory [25, 26], encountered especially in the subaxial cervical vertebrae.

The ideal entry point and trajectory for CPS placement are challenging to locate and reproduce intraoperatively. As for the entry point, few anatomical characteristics guide surgeons in the lateral mass of cervical vertebrae. In the case of degenerative or traumatized cervical vertebra, it is much more complex. Lateral fluoroscopy can guide the pedicle trajectory in the sagittal plane. However, an anterior-posterior view of fluoroscopy cannot indicate the accurate trajectory in an axial plane. In terms of CPS misplacement, lateral violation of the pedicle wall contains a potential risk of vertebral artery (VA) injury. The medial or rostral violation has a risk of injury to the spinal cord or exiting nerve root [8, 27]. VA injury, especially, is a critical and life-threatening complication though its incidence is quite low [8]. Nevertheless, previous literature reported the dominance of lateral violation over medial one [27, 50].

Abumi et al. [51] performed CPS placement using lateral fluoroscopy and reported a 6.8% of screw breach rate with 1 VA injury and two nerve root injuries. Yukawa et al. [52] reported the pedicle axis view method using oblique fluoroscopy to identify the entry point simultaneously and the trajectory for CPS placement in cervical trauma cases. Their reported breach rate was 13.1%. Finally, Miyamoto et al. [53] invented a CT cutout technique using the sterilized CT film cutouts of the axial plane indicating the entry point and trajectory, with a breach rate of 3.8%.

In terms of spinal navigation, Kotani et al. described an improved accuracy of CPS placement using a computer-assisted navigation system with a 1.2% reported breach rate [28]. Later, Ito et al. introduced intraoperative 3D-CT-based navigation for CPS and LMS placement and reported their 2.8% of breach rate [39].

### 8.2.1 CPS Placement with Intraoperative 3D-CT Based Navigation System (O-Arm)

Following the induction of general anesthesia, the patient is placed on a radiolucent table such as a Jackson table (Modular Table System, Mizuho OSI®, CA, USA) with the skull fixation using a carbon Mayfield device. The cervical alignment should be checked and adjusted before the surgical draping. The use of an additional bandage is adequate to fix the Mayfield device to the table securely. Following the draping of the surgical field, the O-arm covered with a sterile plastic drape is placed at the caudal end of the table.

Even under navigation surgery, a wide-open exposure of the cervical index vertebrae is required, the same as a conventional freehand technique. This is due to reducing the pressure of paravertebral muscles toward the medial side. Therefore, before obtaining 3D-CT images, a surgeon should roughly estimate the entry point of each vertebra and simulate the trajectory with the use of a pointer or a screwdriver. If the paravertebral muscles are still an obstacle to taking a position to probe in an appropriate trajectory, the exposure should be expanded more rostrally and caudally. In terms of the subaxial cervical spine, each lateral mass of the whole C2–C7 should be exposed up to the lateral edge.

C2 spinous process is the most secure point to dock the reference frame. The retractors are placed so as to not obstruct the communications between the reference and the infrared camera of the navigation system. The position of the intraoperative CT gantry is adjusted to focus on the index cervical spine by its fluoroscopic view in the anteroposterior (AP) and lateral plane. O-arm is moved to the targeted area and 3D scanning is performed. Breathing should be halted during 3D-CT scanning to reduce the image deviation.

The image dataset is transferred to the navigation system and the O-arm is moved back to the caudal position. Registration of various navigation tools (probe, tap, and screwdriver) is performed. Before the CPS placement procedure, the surgeon should verify the surface matching between the actual bone and the virtual image in the navigation monitor.

The probe shall be advanced gradually with rotation torque, not with pushing force. In the axial plane of the navigation monitor, the probe shall go more medially than the anatomical axis toward the medial cortex of the pedicle. This is because a surgeon feels the resistance of the complex cortex of the medial pedicle wall and advances the probe alongside the cortex. A surgeon shall occasionally assess the trajectory in the monitor by releasing the probe. Following the completion of the probing, the length and the diameter are measured in the monitor and the appropriate size of screw is selected. The position of CPS shall be checked intraoperatively by a 3D-CT image.

### 8.2.2 The Problems of the Navigated CPS Placement

There are some theories advocated to explain the reasons why lateral violation is dominant in CPS misplacement. First, the medial cortex of the cervical pedicle is thicker than the lateral one [23, 24, 27, 50], and the anatomical transverse angle of pedicles is very large, especially at C3–C6. [25] Initial probing tends to be repelled laterally. Second, the paravertebral muscle is always forcing the probing tool inward and makes the tip go outward in the direction of the transverse foramen [27, 50]. The insertion trajectory is forced to be more straight-forward from the more medial point of the bony surface than the anatomical pedicle axis. Third, this pressure derived from the paravertebral muscle also obliges surgeons to grasp the insertion tools tightly. This forcible procedure makes the cervical vertebra rotate quickly to the opposite side, even with a Mayfield fixation [27, 34]. This vertebral rotation is likely to lead the trajectory laterally. Finally, in the cervical pedicle with sparse cancellous bone, it is difficult to adjust the course of the following tapping and screwing from the initial probing. The failed initial probing tends to result in the screw malposition.

### 8.2.3 Navigated Surgical Drill for CPS Placement

A navigated high-speed drill (Stealth-Midas®, Medtronic Powered Surgical Solutions, Fortworth, TX, USA) (Fig. 8.7) is a newly developed high-speed drill integrated with a navigation sensor that can be monitored on a navigation screen (Stealth Station S8®, Medtronic Navigation, Littleton, CO, USA) (Fig. 8.8). It

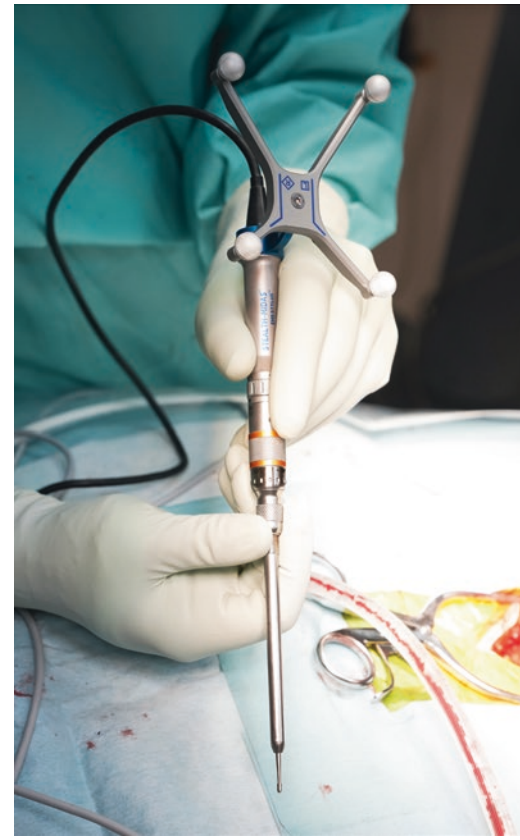

**Fig. 8.7** A navigated high-speed drill (Stealth-Midas®, Medtronic Powered Surgical Solutions, Fortworth, TX, USA)

was released in 2016, and we have used this navigated drill for the initial probing of CPS placement, then combined it with an O-arm-based navigation system. Unfortunately, so far, there have been no clinical reports on the navigated drill application for CPS.

#### 8.2.3.1 CPS Placement with the Use of a Navigated Drill with Use of O-arm

The navigated drill is connected to an electric motor system and is set up at 2000–3000 revolutions per minute (rpm). A 2.2-mm steel burr (match head type) (Fig. 8.9a) is attached to the navigated drill. The burr is maneuvered gently through the pedicle up to the vertebral body (Fig. 8.9b), and after that additional probing up to the anterior vertebral wall, which is completed with a manual probe. Tapping and screw insertion procedures are performed under the navigation guide as well. The most beneficial aspect of the navigated drill in CPS placement is that it can probe the pedicle without forcible maneuver. The drill burr is stiffer than the manual probe due to the short tip (maximal 24 mm from the attachment top). Furthermore, it can advance the pedicle by its rotation torque, not by pushing force. It is also capable of grazing the thick medial cortex

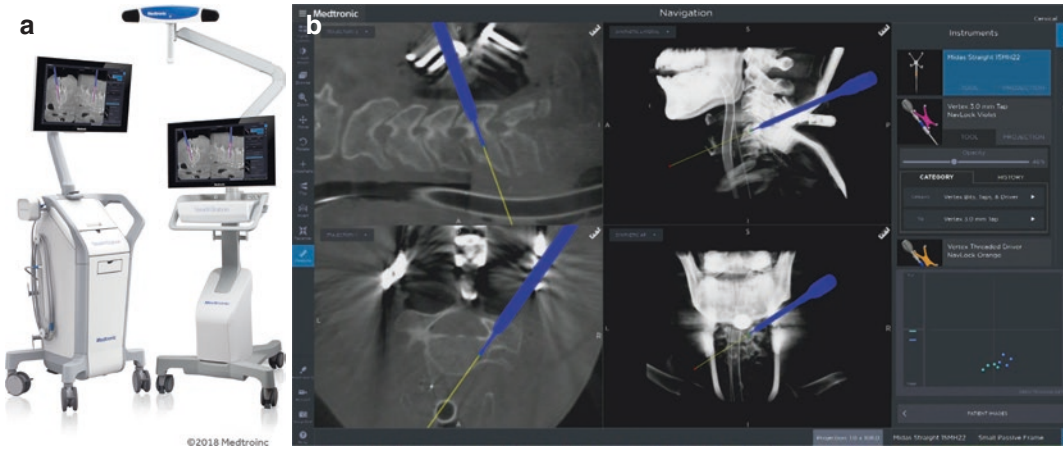


**Fig. 8.8** StealthStation S8® (Medtronic Navigation, Littleton, CO, USA). (**a**) StealthStation S8 navigation system. (**b**) S8 navigation monitor showing the navigated high-speed drill

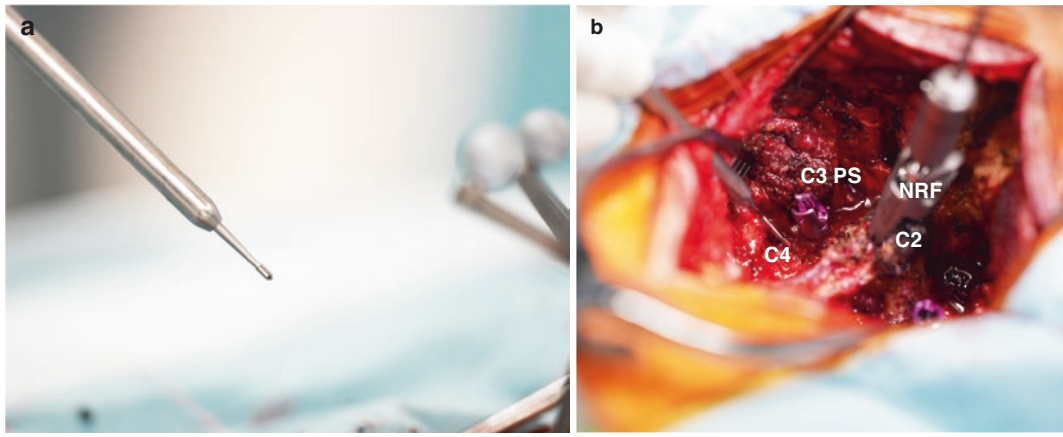


**Fig. 8.9** A navigated high-speed drill. (**a**) A match head typed 2.2-mm steel burr attached to the navigated drill. (**b**) Making a hole for C4 PS inserting with the navigated high-speed drill

of the pedicle even with gentle handling. Thus, even for difficult cases due to various anatomical problems (thick paravertebral muscles, small and largely convergent pedicles, or a hypertrophic VA on the dominant side), and in order to make the CPS pathway along with the anatomical pedicle axis, the navigated drill allows a surgeon to intentionally make the pilot hole medially and to graze the medial cortex gently.

As previously described, the navigated drill is set at a very low speed (2000–3000 rpm). We confirmed that the burr does not penetrate even a surgeon's plastic glove at this speed. This low-speed burr facilitates the surgeons' feel of the subtle resistance of the medial cortex without a forcible maneuver. In addition, it possibly reduces the disorientation in the virtual monitor of the navigation system.

#### 8.2.3.2 Clinical Results

In our data [54] using the Neo grading scale [27] in postoperative CT images, the navigation drill demonstrated a reduced rate of pedicle wall violation compared to the conventional navigated manual probe though the difference was not significant (navigated drill vs. manual probe; Grade 1: 5.9% vs. 10.9%, Grade 2: 1.3% vs. 3.6%, $p = 0.25$). However, the violation rates to the lateral cortex (36.4% vs. 87.5%, $p = 0.037$) were significantly reduced in the navigated drill compared to the conventional manual probe. The dural sac has a space of 2.4–3.1 mm from the medial border of the pedicle [55]. Theoretically, this space allows Grade 2 perforation of CPS. On the other hand, the safe zone for VA in the transverse foramen (the space between the lateral pedicle wall and the VA) is reported as 0.65–1.7 mm, according to a CT angiography study [55].

Mahesh et al. reported a partial drilling technique of the medial cortex in CPS placement under lateral fluoroscopy, and their lateral perforation rates were 13.9% in total [56]. However, it is technically demanding to estimate the accurate axial angle and drill the medial cortex without any guide in the axial plane. Even though the navigated drill might not decrease the total perforation rate of the pedicle wall, it could reduce the incidence of lateral perforation in CPS placement. The navigated drill has the potential to make initial probing easier without forcible manipulation which might provoke vertebral rotation.

#### 8.2.3.3 Case Presentation

A 68-year-old male with a diffuse idiopathic skeletal hyperostosis suffered a C6/C7 dislocation fracture in an accidental fall (Fig. 8.10a). He was overweight (BMI 27.5 kg/m$^2$) and bull-necked. Preoperative CT angiography demonstrated a hypertrophic dominant VA on the left side (Fig. 8.10b). A posterior arthrodesis with CPS fixation was undergone at C4-T2 using an ND. Postoperative CT revealed a Grade 1 violation of the left CPS at the medial pedicles of C4. However, the transverse foramen remained intact, and the left VA was safe (Fig. 8.10c).

## 8.3 Minimally Invasive Cervical Pedicle Screw Fixation (MICEPS) via a Posterolateral Approach

Cervical pedicle screw (PS) fixation provides great mechanical strength; however, it requires wide soft tissue detachment. In the acute phase of injury, a wide posterior exposure also poses a risk for massive bleeding. Although cervical PS fixation can be an essential part of reconstruction in spinal disorders, it has the potential risk of injury to the vertebral artery (VA), as previously described [57]. To avoid lateral misplacement of cervical PS, we developed a new method for minimally invasive cervical pedicle screw (MICEPS) fixation through a posterolateral approach. This chapter describes the novel surgical technique.

### 8.3.1 Minimally Invasive Cervical Pedicle Screw Fixation (MICEPS)

The indications for MICEPS fixation through the posterolateral approach are the same as those for conventional posterior cervical fusion from C2–C7, such as: cervical instability due to trauma,

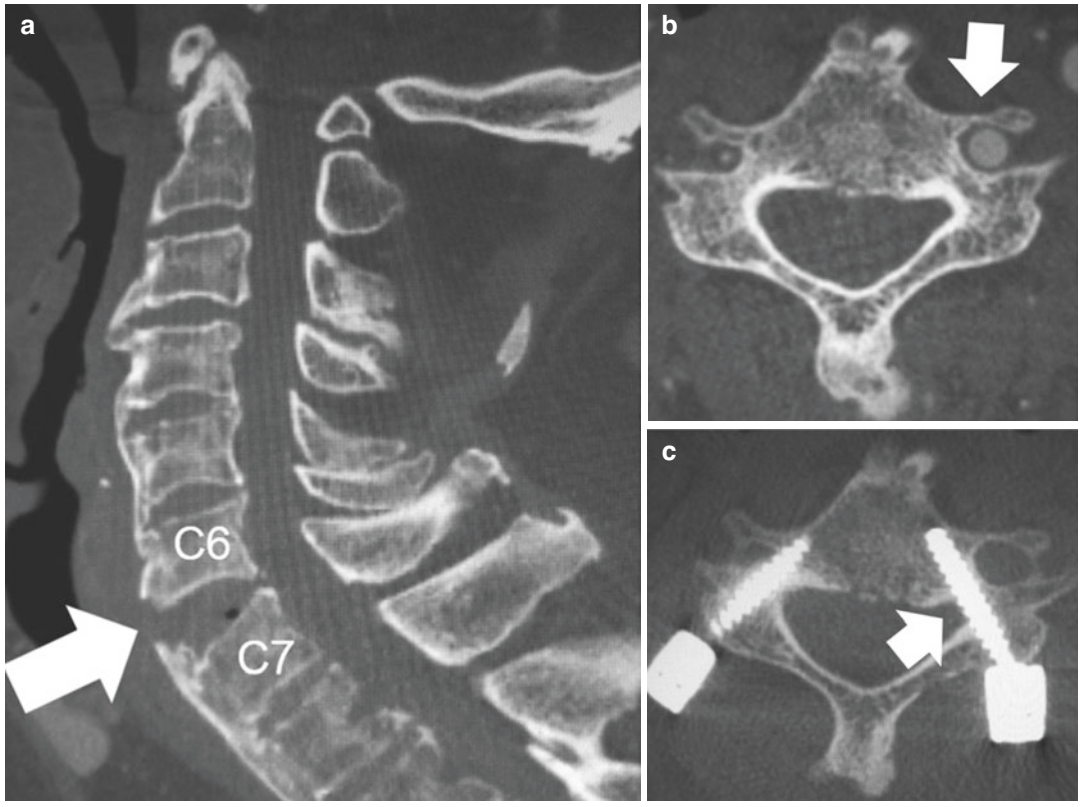


**Fig. 8.10** 68 years old male who suffered a dislocation fracture at C6/C7. (**a**) Preoperative CT sagittal plane (white arrow: fracture site). (**b**) Preoperative CT angiography at C4 (white arrow: the dominant VA in the left transverse foramen). (**c**) Postoperative CT axial plane at C4 (white arrow: medial violation of the left CPS)

metastatic tumor of the cervical spine, infectious spondylitis of the cervical spine, and segmental instability of degenerative cervical spinal disorders.

The contraindications for MICEPS fixation are: congenital anomalies (i.e., defects of the cervical pedicles), traumatic VA aneurysm and bilateral vertebral artery injuries (VAI), and difficulty lying in a prone position. In addition, patients with fracture-dislocations or fractures of the lateral mass of the cervical spine often have concomitant traumatic VAI, which can lead to the brainstem or cerebellar infarction by the maneuver of closed reduction. The ideal situation for the patient is to undergo coil embolization of the injured VA, followed by a reduction of the dislocation. Inserting the PS to the embolized side does not pose a problem; however, close attention must be paid to inserting the screws to the dominant VA side. A posterolateral approach directly visualizes the facet joint and enables us to reduce dislocated facet joints even if closed reduction fails.

#### 8.3.1.1 Instruments and Materials

The following instruments and materials are required when performing MICEPS fixation: a radiolucent operating room table and a carbon Mayfield head holder; intraoperative computed tomography scans and a 3D navigation workstation; intraoperative fluoroscopy; high-speed burr, 1.4-mm guide wires, a 2.9-mm cannulated drill, a power tool, a navigated guide tube, and a cannulated PS and rod system.

#### 8.3.1.2 Surgical Technique

The patient is positioned prone on a radiolucent carbon table with a carbon Mayfield frame. For

patients with cervical facet dislocation, a closed reduction before surgery is performed whenever possible.

The cervical spine is positioned parallel to the floor, and the shoulder girdles are pulled caudally and fixed by taping. An image intensifier is rotated so that an appropriate circular portion of the pedicle cortex wall is identified in the inclination angle from 30° to 45° from the midsagittal plane (pedicle axis view [52]), then the incision lines are marked. The operative field is disinfected widely, close to the ears, and the patient is draped 360° around the neck. A reference frame is attached to the spinous process through a midposterior small skin incision. An isocentric C-arm acquires multiple successive images as it performs an automated 190° rotation around the patient's cervical spine. Afterimage acquisition, the navigation workstation generates axial, sagittal, and coronal reconstructions of the imaging anatomy. CiosSpin (Siemens Healthineers, Munich, Germany) and Kick (BrainlabAG, Germany) for computer navigation are used to place screws in cervical pedicles.

#### 8.3.1.3 Instructions for the Procedure

1. Incision and Exposure
   Bilateral skin incisions are made for screw insertion under navigational guidance. After skin incisions of ~4 cm in length have been made, the underlying subcutaneous tissue and nuchal fascia are divided with electrocautery. The lateral mass is exposed with blunt dissection, and a finger is inserted between the elevator scapulae and splenius muscles (Fig. 8.11a). The posterior rami's medial branches, which often appear on the multifidus muscle, should be retracted (Fig. 8.12a). A self-retaining tubular retractor with illumination applied between the split muscle fibers allows sustained exposure of the lateral mass (Fig. 8.11a). This posterolateral approach involves transmuscular dissection and is often bloodless. To expose the C2 screw entry point, we retract the obliquus capitis inferior muscle medially and the great occipital nerve (C2 posterior nerve root) cranially. The third occipital nerve must be retracted cranially when the C3 screw is inserted.
2. Identification of the Entry Point
   The multifidus muscles are partially separated on the lateral masses. The entry point of the PS is determined using a 3D navigation system (Fig. 8.13) and confirmed by the pedicle axis view of the oblique C-arm image. A starting hole is made from the lateral mass to the cancellous bone in the pedicle by a 5-mm high-speed diamond burr. A pilot hole is drilled using a 3-mm high-speed diamond burr with a 10-mm stop to access the medial cortex of the spinal canal.
3. Direction of the Guide Wire
   A 1.4-mm guide wire is inserted obliquely from the pilot hole in the pedicle to the vertebral body using a navigated guide tube and power drill driver (Fig. 8.11b). The most critical point of this procedure is to direct the guidewire not to the center of the pedicle but to the medial cortex of the spinal canal corresponding to the axial view of the navigation image (Fig. 8.13). Careful attention must be paid to avoid breach of the transverse foramen. We do not use a pedicle probe because it often causes misdirection. When pressure is applied on one side of the vertebra while the pedicle probe is being inserted, the vertebra tends to rotate away from the intended point of placement, causing the probe to be inserted more vertically. The use of a guidewire and a power drill driver can prevent this vertebral rotation. We carefully check for the guide wire's direction and depth using a lateral fluoroscopic image (Fig. 8.14a, b).
4. Placement of the PS
   To avoid VAI, the surgeon should feel the hardness of the medial cortex through the power drill driver. A drill, a tap, and a cannulated PS are inserted sequentially over the guidewire. The diameter of the cannulated PS inserted in this procedure is 4.0 mm, with a length ranging from 26 to 30 mm (Fig. 8.15). Medial perforation of the spinal canal with screws is permitted as it provides mechanical strength and safety compared to lateral devia-

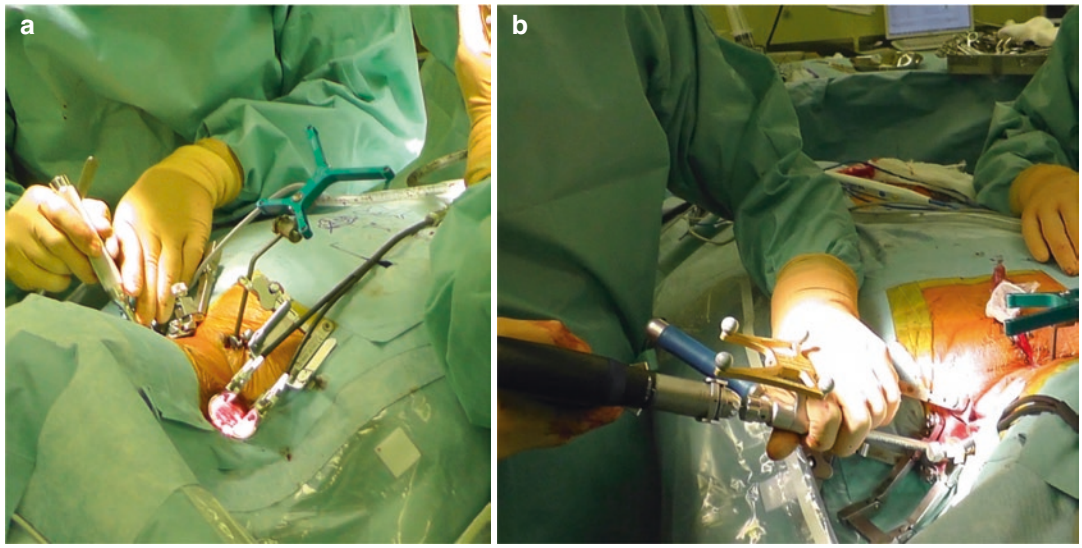


**Fig. 8.11** Positioning and surgical setup. (**a**) Tubular retractor with illumination. (**b**) A guidewire is inserted obliquely in the pedicle using a navigated guide tube and power drill driver

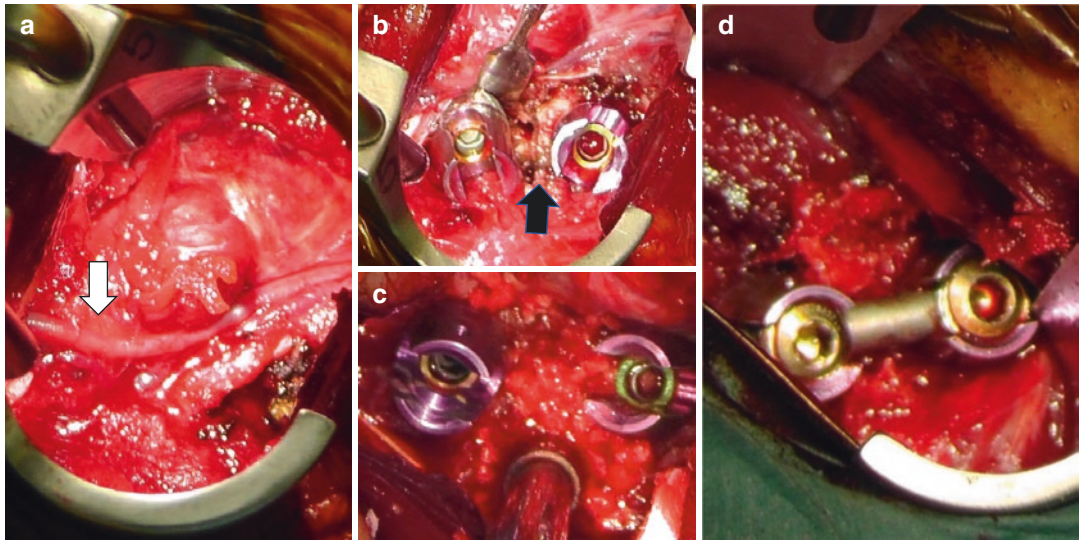


**Fig. 8.12** Intraoperative photographs. (**a**) Multifidus muscle and posterior rami medial branch of spinal nerve (white arrow). (**b**) Inserted pedicle screws and reduced facet joint of C6/7 (black arrow). (**c**) Bone graft on to facet joint. (**d**) A rod was connected to pedicle screws

tion. To insert the Th1 and Th2 PS, we made an additional small midline skin incision and placed them conventionally. After blunt finger dissection through the muscle, we pushed the rod to connect the midcervical and thoracic PS.

5. Facet Fusion

   Facet joints are visible directly through this posterolateral approach (Fig. 8.12b). Open reductions of dislocated facet joints are possible with lifting the inferior articular process by applying a leverage force with a spatula, if

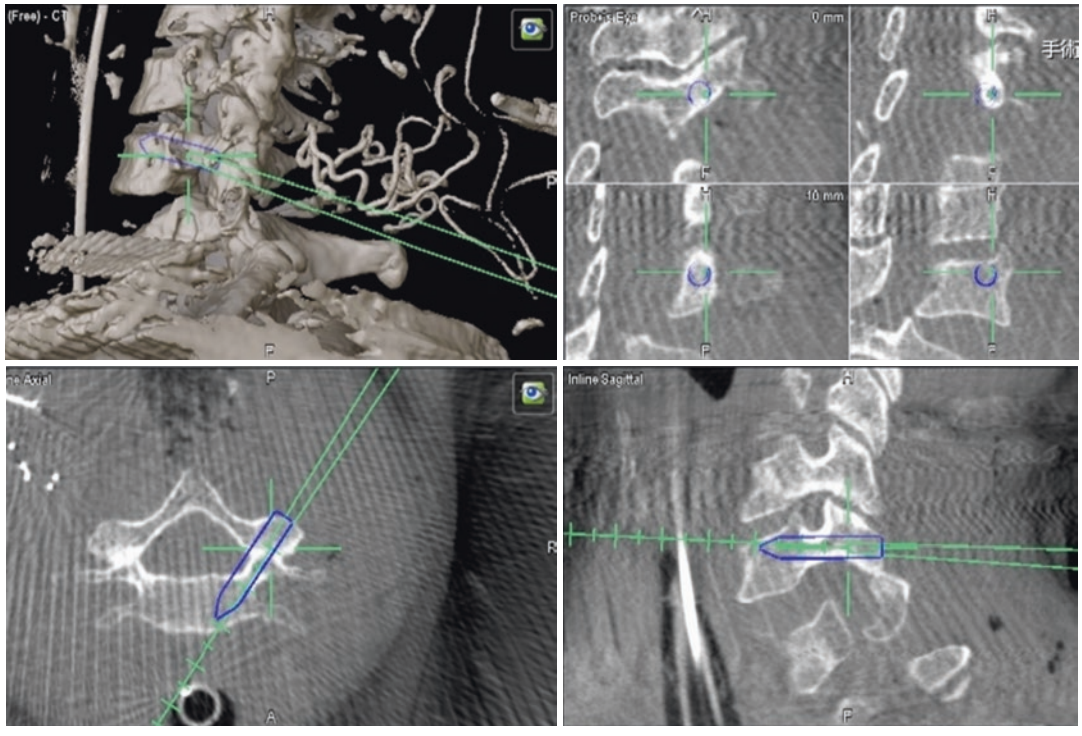

**Fig. 8.13** Intraoperative 3D navigation image of left C6 pedicle

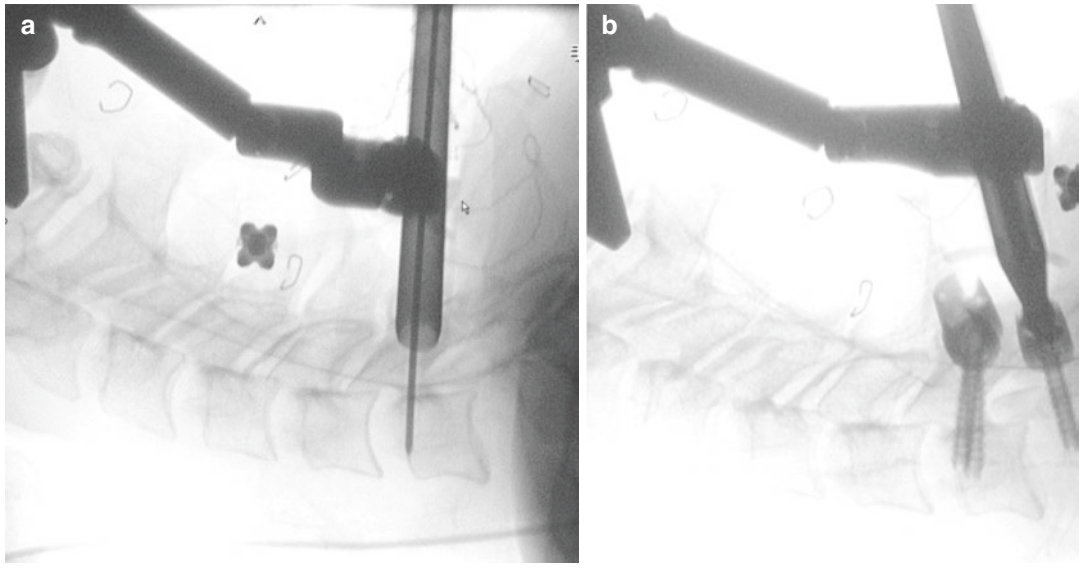


**Fig. 8.14** Intraoperative fluoroscopic image. (**a**) Insertion of guidewire. (**b**) Insertion of cannulated pedicle screw

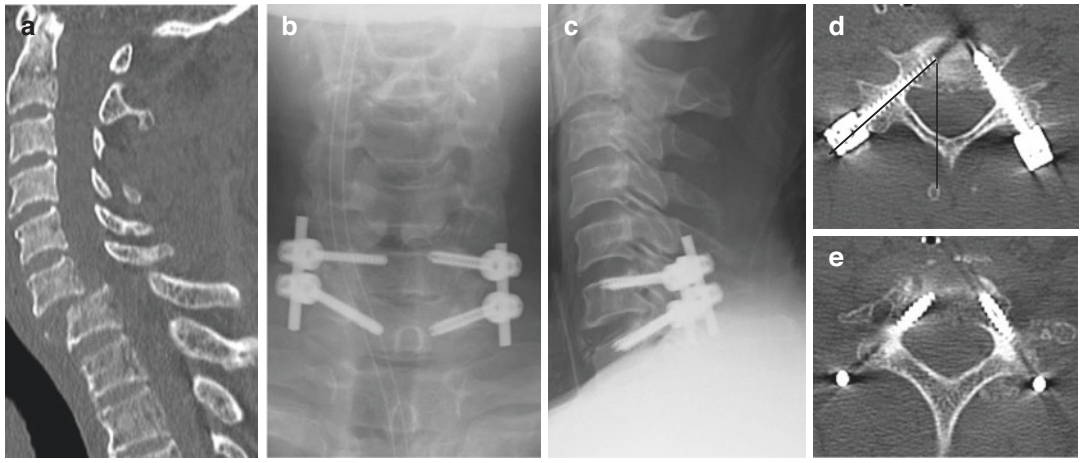


**Fig. 8.15** A 77-year-old man with C6–C7 bilateral facet dislocation. (**a**) Preoperative computed tomography (CT) showed anterior C6 dislocation. (**b**) AP X-ray after operation. (**c**) Lateral X-ray. (**d**) Postoperative CT of C6. Black line showed Alpha-angle. (**e**) Postoperative CT of C7

necessary. Decortication of the facet joints is performed with a diamond burr, and chips of local bone from the spinous processes and artificial bone such as hydroxyapatite are grafted into the facet and onto the lateral masses (Fig. 8.12c).

6. Rod Connection
   Rods are placed onto the screw heads and secured (Fig. 8.12d). A lateral radiograph can be used to verify the alignment. The wound is closed in layers without a suction drainage tube.

#### 8.3.1.4 Complications

Although VAI is rare, it may be critical if it occurs. Surgeons should evaluate VA anatomy before surgery. The posterolateral approach provides the optimum trajectory of the PSs within the shortest distance. PSs should be placed close to the medial cortex of the spinal canal to obtain solid bony fixation and avoid VAI. If a vascular injury occurs during the preparation of the screw track, hemostasis can often be achieved by packing the hole with bone wax.

Nerve root injury can occur if the screw perforates a pedicle caudally and irritates the exiting nerve root. After surgery, any patient with new radicular symptoms should undergo advanced imaging to ensure that the screw is not malpositioned. In addition, close attention must be paid to prevent injury to the medial branch of the posterior rami, especially the great occipital nerve (C2) and the third occipital nerve (C3), when inserting PSs (Fig. 8.16).

#### 8.3.1.5 Clinical Results

Our comparative study included 119 consecutive patients who underwent surgery for cervical fractures (conventional cervical PS, $n = 19$; MICEPS fixation, $n = 100$). We inserted a total of 342 cervical PSs. In the MICEPS fixation group, 32 and 68 patients were treated with unilateral and bilateral fusion, respectively. In total, 82 patients (82%) underwent surgery within 24 hours after injury. In both groups, all PSs were inserted using a spinal navigation system.

The average surgical time was 217 and 152 min with conventional PS and MICEPS fixation, respectively ($P = 0.0014$). The average intraoperative bleeding volume was 560 and 150 ml in conventional and MICEPS fixation, respectively ($P < 0.0001$). We assessed the positions of 434 screws using computed tomography according to the Neo classification as follows: grade 0, no deviation (i.e., the screw was contained in the pedicle); grade 1, deviation <2 mm; grade 2, deviation >2 mm but <4 mm; and grade 3, deviation >4 mm. Grade 2 or 3 screw deviation

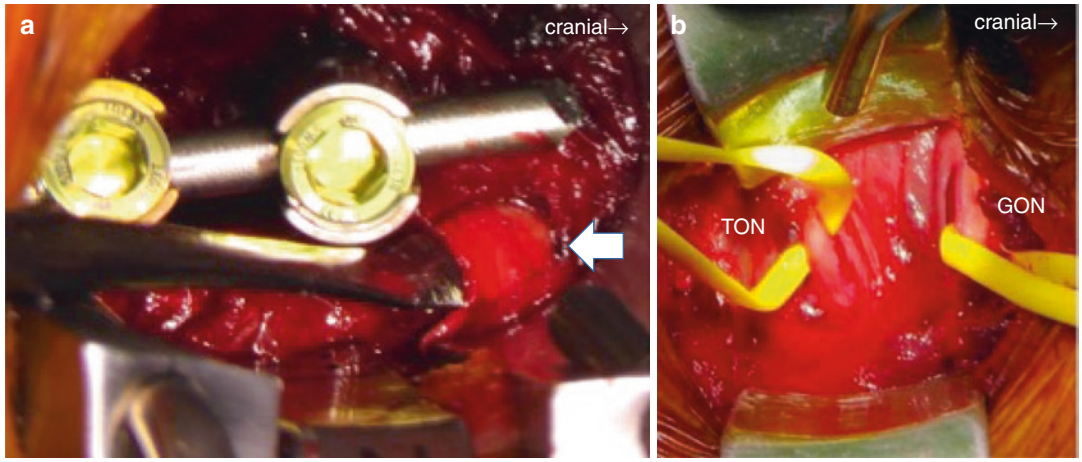


**Fig. 8.16** Posterior rami of the spinal nerve. (**a**) Posterior rami medial branch of C4 (arrow). (**b**) Great occipital nerve (GON) and third occipital nerve (TON)

**Table 8.1** Alpha-angle

| | | C2 | C3 | C4 | C5 | C6 | C7 | Th1 | Total |
|---|---|---|---|---|---|---|---|---|---|
| Conventional CPS | No. of screws | 8 | 6 | 11 | 13 | 18 | 17 | 8 | 81 |
| | Alpha-angle* | 20 | 43 | 44 | 37 | 34 | 27 | 26 | – |
| MICEPS | No. of screws | 18 | 19 | 55 | 91 | 94 | 47 | 29 | 353 |
| | Alpha-angle* | 36 | 48 | 52 | 51 | 48 | 34 | 20 | – |

*Average
*CPS* cervical pedicle screw, *MICEPS* minimally invasive cervical pedicle screw

was considered clinically significant in the present study, and the incidence of grade 2 or 3 screw deviation was significantly lower in the MICEPS group than in the conventional cervical PS group ($P = 0.0039$). In the conventional cervical PS group, 71 screws (87.7%) were classified as grade 0 or 1, and 10 screws (12%) were classified as grade 2 or 3, of which 4 and 6 had lateral and medial deviation, respectively. One patient with a laterally deviated screw had cerebellar infarction but fully recovered. In the MICEPS fixation group, 348 screws (98.0%) were classified as grade 0 or 1, and 7 screws (2.0%) were classified as grade 2 or 3 with medial deviation. There were no neurological complications attributable to medially deviated screws in either group; therefore, no screws were replaced. A significant screw deviation was significantly lower in the MICEPS fixation group than in the conventional cervical PS group ($P = 0.0039$).

The alpha-angles of PSs on postoperative CT scan (Fig. 8.15d) in the MICEPS group were oblique angles compared to those in the conventional group, which means the insertion angle of PSs was close to the horizontal line (Table 8.1).

### 8.3.2 Advantages of MICEPS

Posterior fixation surgery using a PS system ensures good biomechanical stability; however, the considerable posterior exposure poses a risk of massive bleeding and the thick muscles disturb the trajectory of the PS, which leads to lateral misdirection and VA injury. One of the advantages of this MICEPS fixation is horizontal PS fixation at the mid-cervical spine, which can avoid VAI. This technique is helpful because it is minimally invasive and provides an ideal trajectory for the PS to prevent VAI.

A computer 3D navigation system is necessary to achieve this technique [34]. C7 PS should be inserted from a midline posterior approach where the muscles (i.e., trapezius) are thick. If a

surgeon wants to fix the midcervical PS inserted through a posterolateral approach and C7 or Th1, a rod can be connected through the subcutaneous tunnel.

This mini-open intramuscular approach allows for the ideal trajectory of PS insertion using a 3D navigation system and reduces intraoperative bleeding.

## 8.4 Minimally Invasive C1–C2 Posterior Fixation Via a Posterolateral Approach.

The atlantoaxial junction is a highly complicated region with important neurovascular structures, such as the vertebral arteries (VA) and the upper cervical spinal cord, allowing a huge range of motion. Posterior fusion of C1–C2 is a well-known technique for treating traumatic, inflammatory, and congenital instability of the C1–C2 junction. Unfortunately, primary stability following sublaminar wiring is often poor and burdened with a considerable rate of non-union. Transarticular screw fixation described by Magerl [58] has been shown to result in a high fusion rate of nearly 100%, although it is still technically demanding. The C1 lateral mass-C2 pars screw fixation technique described by Goel [59, 60] and Harms [61] has become an effective alternative to transarticular screw fixation; however, it requires extensive posterior exposure, which has been associated with superficial infections and occipital nerve injury. Bleeding from the venous plexus during C1–C2 joint exposure is also frequently encountered. Patients also suffer from an increased risk of intraoperative VA injuries due to anatomical variations in the VA and instability of C1. Spinal navigation techniques are frequently used to perform posterior stabilization of C1–C2 to avoid neurovascular injuries [62].

From the perspective of navigation technology, the surface matching of C1 is hindered by the reduced osseous surface of C1 and the deep screw entry point on the lateral mass of C1. Using an intraoperative CT scan promises to overcome these problems by allowing CT after positioning and reducing the C1–C2 malposition at the same time [62, 63]. To overcome the limitations of the conventional posterior approach, an intramuscular posterolateral approach was applied to the C1–C2 region. A new technique of minimally invasive stabilization of the upper cervical spine via the posterolateral approach using intraoperative CT-guided 3D navigation was introduced.

### 8.4.1 Minimally Invasive C1–C2 Posterior Fixation

The indications for minimally invasive C1–C2 posterior fixation through the posterolateral approach are: fractures, tumors, congenital deformities, and degenerative or inflammatory diseases. Such indications at this level lead to instability, which poses a significant risk to the associated neurovascular structures.

#### 8.4.1.1 Surgical Technique

The same instruments and materials as described in the MICEPS technique of the subaxial cervical spine are required when performing minimally invasive C1–C2 posterior fixation. The patient was positioned prone on a radiolucent carbon table with a carbon Mayfield frame under general anesthesia. The same intraoperative fluoro-CT scan and a computer-navigation system are used as in the MICEPS technique. The operative field is disinfected widely, close to the ears and occiput, and the patient is draped 360° around the neck. A small midline incision is performed to attach the referential frame to the C2 spinous process.

#### 8.4.1.2 Instructions for the Procedure

1. Posterolateral approach
   A posterolateral 4 cm long, longitudinal skin incision is required at the C1–C2 level, which is approximately 4–5 cm lateral from the C2 spinous process. The underlying subcutaneous tissue and nuchal fascia are divided with electrocautery. The fascia is opened, and the semispinalis capitis and splenius capitis muscles are divided bluntly by the fingers. The splenius muscles are split using fingers from the C1 and C2 lateral masses. Blunt dissection

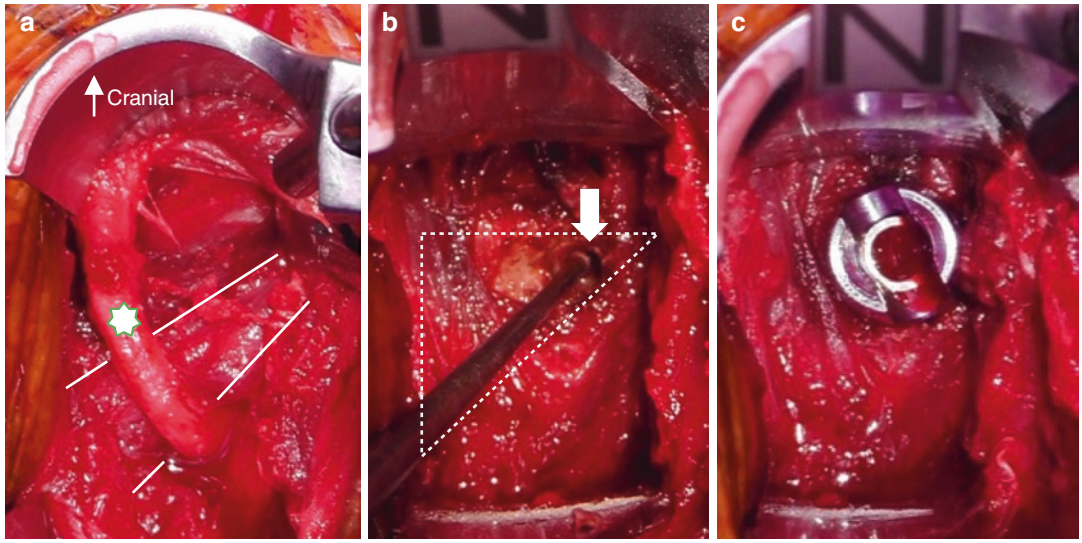


**Fig. 8.17** Entry point of C1 lateral mass screw. (**a**) White star demonstrates great occipital nerve (GON), the muscle surrounded white lines is the oblique capitis inferior (OCI) muscle. (**b**) broken line shows suboccipital triangle. White arrow is the entry point of C1 lateral mass screw; (**c**) C1 lateral mass screw is inserted

is performed along the lower border of the oblique capitis inferior (OCI) muscle (Fig. 8.17a).

The great occipital nerve (GON) is detected on the OCI muscle (Fig. 8.17a), and the third occipital nerve (TON) is often detected in the multifidus muscles at the C3/4 level. Each nerve is hung using vessel tape. The GON is the first landmark of this approach. Large venous plexuses in the lateral intramuscular space must be handled appropriately. Blunt dissection is performed along the upper border of the oblique capitis inferior (OCI) muscle cranially in the suboccipital triangle (Fig. 8.17b). The medial border of the C1 attachment of the OCI muscle is an entry point for the C1 lateral mass screw (Fig. 8.17c). The vertebral artery (VA) is protected cranially by a retractor [64].

This posterolateral approach involves transmuscular dissection and is often bloodless. However, a large venous plexus occasionally appears behind the OCI muscle. Bipolar cautery and hemostatic agents such as a flowable gelatin matrix with thrombin are used to control bleeding from the venous plexus surrounding the C2 nerve and that which surrounds the VA.

2. C2 pedicle screw

The GON was retracted cranially, and the multifidus muscles were split on the C2 lateral mass (Fig. 8.18a, b). The entry point of the C2 pedicle screw was determined using a navigation system (Fig. 8.18c, d). If the patient has an abnormally high position of VA in the C2 vertebrae (Fig. 8.19), screws are inserted parallel to the VA pathway through the spinal canal. This trajectory of the C2 pedicle screw is not the pars screw but the real pedicle screw. A 5-mm entry hole was dug with a 3-mm high-speed diamond bur (Fig. 8.18c). A 1.4-mm K-wire was inserted obliquely through a guide tube with the help of a navigation system and a power drill driver (Fig. 8.18d). Drilling and tapping are performed through this guide pin, and a 4.0-mm diameter cannulated screw is inserted (Fig. 8.18d). Cannulated pedicle screws are aimed at the medial wall of the C2 canal using a 3D navigation system to avoid lateral misplacement. Medial perforation of the C2 canal with screws is permitted as it provides better mechanical strength and

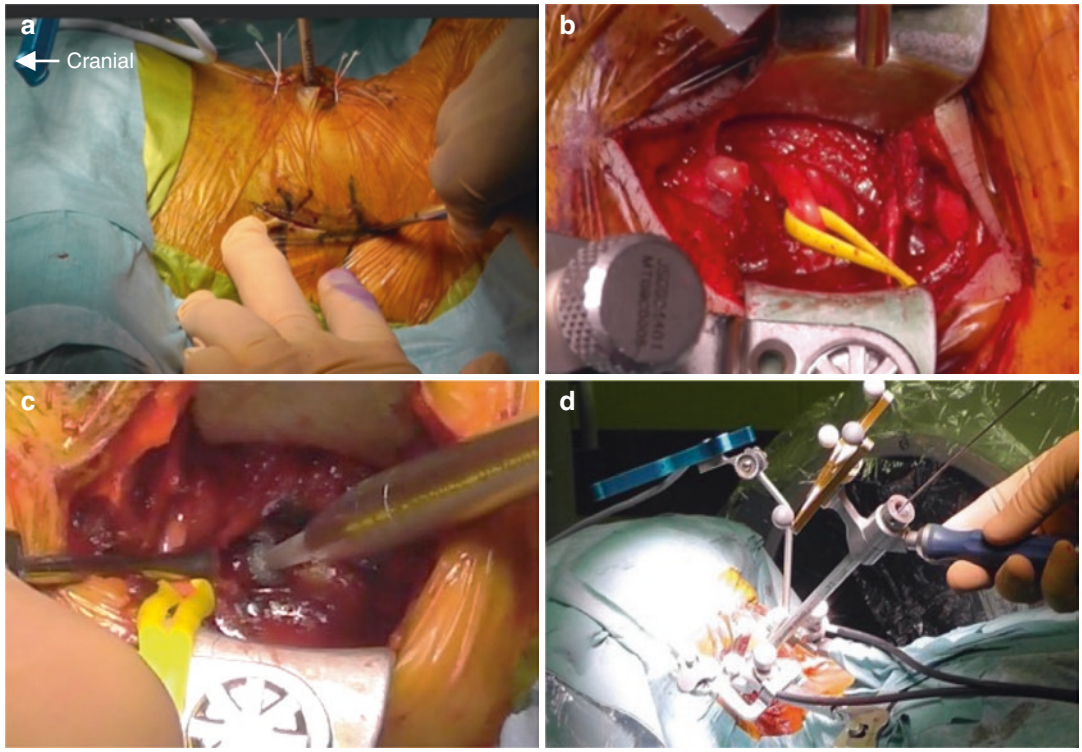


**Fig. 8.18** Surgical technique: C2 pedicle screw. (**a**) Skin incision; (**b**) great occipital nerve; (**c**) entry point of C2 pedicle screw; (**d**) a guidewire is inserted through a navigated guide tube

safety when compared to lateral deviation. If the C2 structure seems to be risky, it is preferred to choose C3 pedicle screws.

3. C1 lateral mass screw
   When the C1 lateral mass is exposed, there are two ways to deal with the OCI muscle. One approach is that the OCI muscle is pulled caudally, and the lateral mass is accessed via the suboccipital triangle. This approach quickly exposes the lateral mass directly; however, VA is often encountered cranially (Fig. 8.19). Another way is that the inferior C1 attachment of the OCI muscle is coagulated and resected, half of the C1 lateral mass is exposed, and VA is protected cranially by the remaining muscle fibers (Fig. 8.20a).

   A self-retaining retractor applied between the C2 pedicle screw and OCI muscle allows sustained exposure of the C1 lateral mass so that the GON is retracted cranially with OCI. The medial border of the OCI attachment of C1 was used as an entry point of the C1 lateral mass screw, and the precise entry point was confirmed by a navigation system (Figs. 8.20b and 8.21). Partial resection of the OCI attachment of C1 helps expose the entry point of the C1 lateral mass screw.

   A 1.4-mm K-wire was inserted through a guide tube to penetrate the anterior arch of C1 (Fig. 8.20c). Unfortunately, C1 is unstable, and the navigation is not as reliable in all cases as in C2, where the reference frame is attached.

   The use of a guidewire and a power drill driver can prevent vertebral rotation from reducing the pressure on unstable C1. We carefully checked the guide wire's direction and depth using a lateral fluoroscopic image (Fig. 8.20c).

   The diameter of the cannulated PS inserted in C1 is 4.0 mm, with a length ranging from 26 to 34 mm, whereas a sufficient length of screws is recommended.

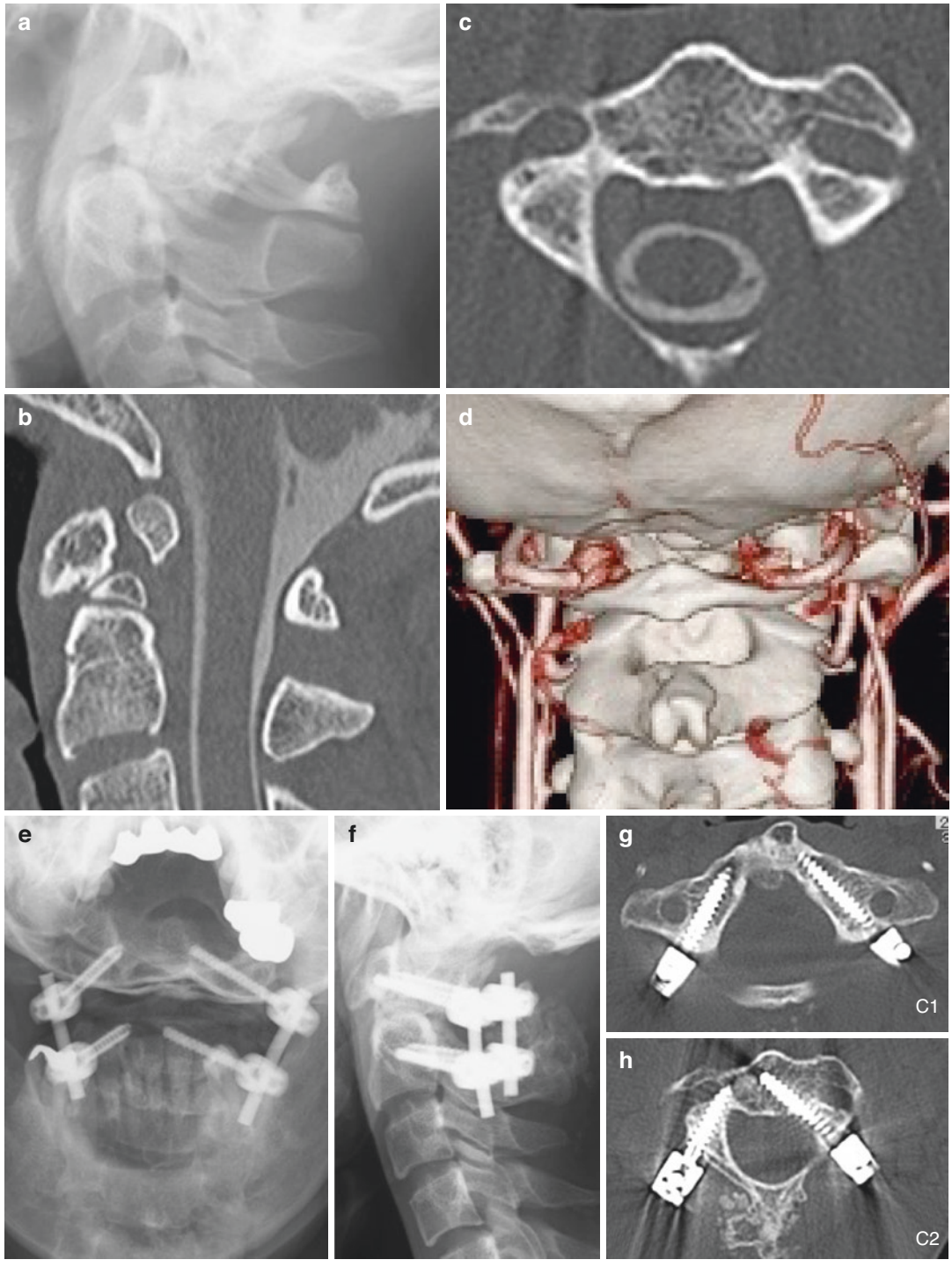


**Fig. 8.19** High position of vertebral artery (36-year-old male, pseudarthrosis of odontoid fracture). (**a**) Plain X-ray of lateral C1–C2; (**b**) CT-myelogram; (**c**) axial view of CT myelogram showed high position of vertebral artery; (**d**) enhanced 3D-CT angiogram. (**e**) Postoperatively (18 months) plain A-P X-ray; (**f**) Postoperatively (18 months) lateral X-ray; (**g**) Postoperatively (18 months) axial CT of C1. C1 α-angle 33° in right screw, 40° in left; (**h**) Postoperatively (18 months) axial CT of C2. α-angle 30° in right screw, 49° in left

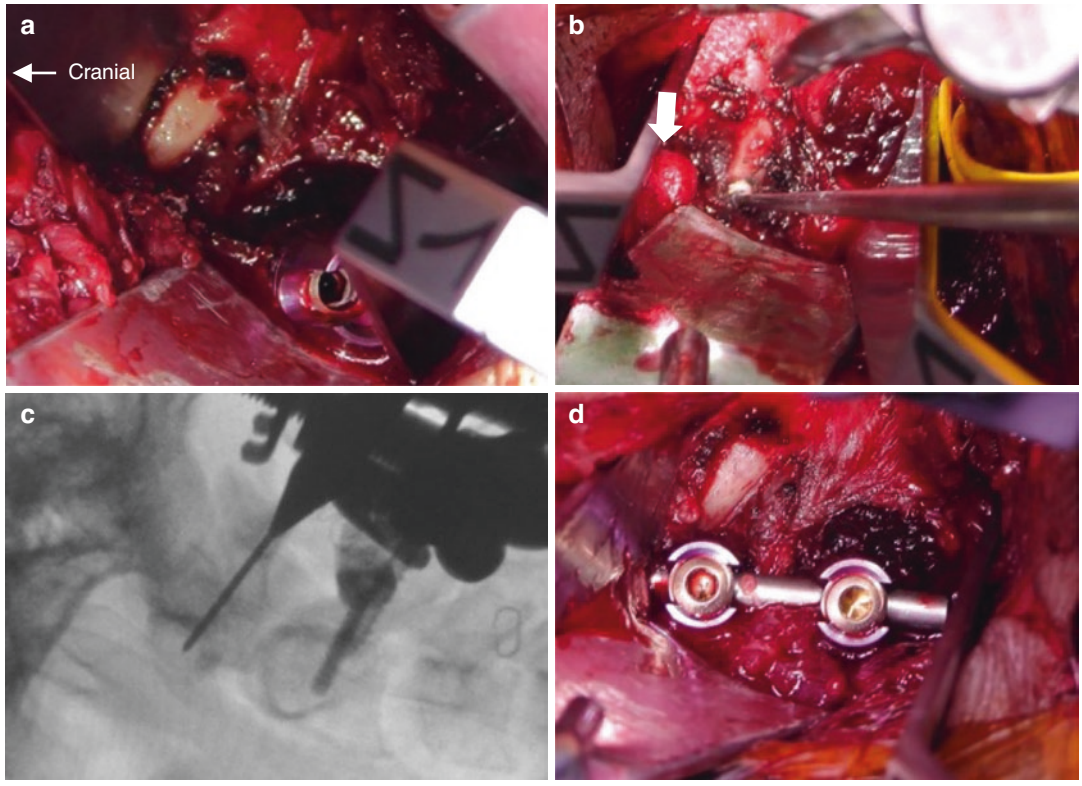


**Fig. 8.20** Surgical technique: C1 lateral mass screw. (**a**) Retractor is applied between C2 pedicle screw and OCI muscle; (**b**) entry point of C1 lateral mass. White arrow indicates vertebral artery; (**c**) intraoperative fluoroscopy of C1 lateral mass inserted a K-wire; (**d**) a rod is connected to C1–C2

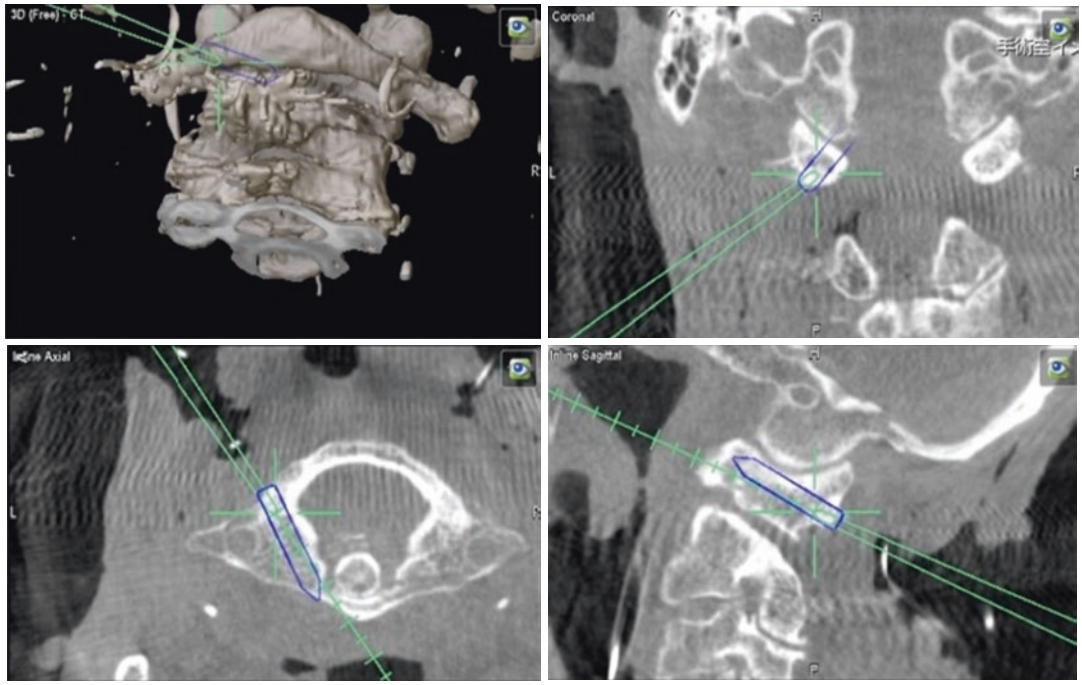


**Fig. 8.21** Navigation view of C1 lateral mass

4. Bone graft
   Decortication is performed around the cortical bone of the C1 and C2 screws to create space for the bone graft. Venous bleeding originates from the extradural venous plexus surrounding the C2 nerve when the facet joint of C1–C2 is widely decorticated using a high-speed diamond bur. A flowable gelatin matrix with thrombin is useful for a quick and reliable hemostatic effect. Allografts, autografts, or artificial bone grafts, such as hydroxyapatite, are used. To gain an effective bone union in cases of pseudoarthrosis of odontoid fracture, a bone graft is added to the C1–C2 region from the mid-posterior approach.
5. Rod connection
   Rods are fixed to maintain the C1–C2 alignment (Fig. 8.20d).

#### 8.4.1.3 Complications

VA injury may be catastrophic if it occurs. Anatomical variation of the VA pathway is not rare in the C1–C2 segment. The VA anatomy should be evaluated using enhancement 3D-CT before surgery (Fig. 8.19d). Screw placement using this technique is easy and safe for VA compared to Magerl's transarticular fixation. If a vascular injury occurs during the preparation of the screw track, hemostasis can often be achieved by packing the hole with bone wax. If VA is injured in the free pathway cranial to C1 [64], hemostasis becomes troublesome. Vascular surgeons or radiologists of catheter intervention must be called immediately while packing gauze with hemostatic agents such as a flowable gelatin matrix with thrombin.

Although the C2 nerve root is sacrificed routinely in the Goel and Harms technique [59, 60], this nerve is preserved using this method. The GON is a posterior ramus of the C2 nerve and is protected medially by the OCI muscle. Neither the C2 nerve ganglion nor the anterior rami of the C2 nerve appear in this technique because of their deep position. If the GON is damaged during surgery, postoperative occipital pain can be a complaint.

#### 8.4.1.4 Clinical Results

Forty patients underwent this new method (MIS group) and were compared to 13 patients who underwent conventional C1LM-C2PS fixation via a mid-posterior approach (P-group) performed at our institute. The mean age at operation was 72 years (range, 27–97 years). The diagnoses were axis fractures in 21 patients, atlas fracture in 1, rheumatoid arthritis (RA) in 4, degenerative subluxation of C1–C2 in 13, and C1–C2 dumbbell tumor in 1 case. The insertion angle of the screws to the sagittal axis (alpha-angle) was measured on postoperative CT (Fig. 8.22).

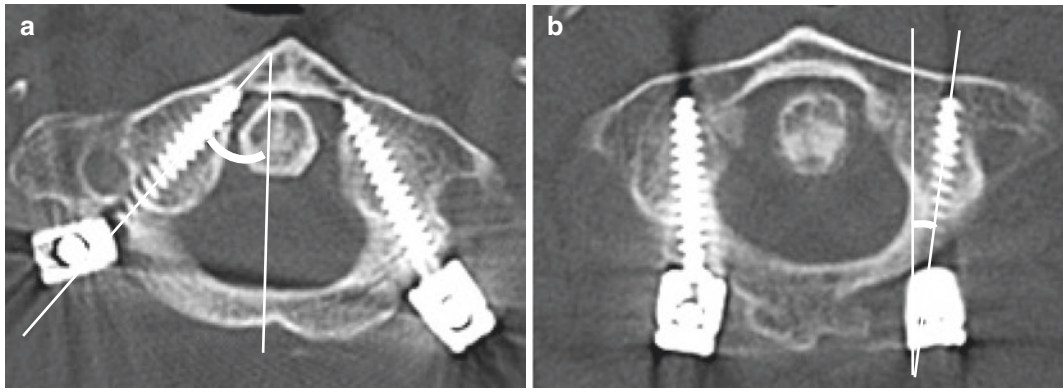


**Fig. 8.22** Insertion angle of screws to sagittal axis (alpha-angle) measured on postoperative CT. (**a**) C1 lateral mass screw of MIS group. α-angle 40°in right; (**b**) C1 lateral mass of Goel–Harms group. α-angle −9° in left

The average bleeding volume in the MIS group was 115 ml relative to 352 ml in the conventional P-group ($p = 0.0102$), and the average surgical time was 198 min in the MIS group versus 260 min in the P group ($p = 0.1190$). Forty-eight screws were inserted in C1 lateral masses, 42 screws in C2 pedicles, 26 screws in C3 pedicles, and 10 screws in opposite transarticular C1/2. No significant complications or screw misplacement occurred. Three screws (7.1%) out of 42 pedicle screws in C2 deviated medially to avoid damage to the high position of the VA. The average alpha-angle of C1 lateral mass screws was 32.0° in the MIS group relative to 7.1° in the P-group, and the alpha-angle of C2 was 38.4° in the PL group versus 14.3° in the P group. The diameter of all screws was 4.0 mm in PL-group and 3.5 mm in P-group. The MIS group's fusion rate, which was followed up for more than 12 months, was 18/18 (100%), compared to 11/13 (84.6%) in the P-group, which showed postoperative subluxation due to loosening of C1 LMS and salvaged transarticular fixation of C1–C2.

### 8.4.2 The Intraoperative 3D Navigation for Minimally Invasive C1–C2 Posterior Fixation

The Goel–Harms technique has become an effective alternative to Magerl's transarticular fixation; however, it requires extensive posterior exposure, which has been associated with superficial infections and occipital nerve injury. The sacrifice of the C2 ganglion provides wide exposure to the region for the conduction of surgery, which enables screw insertion into the center of the C1 lateral mass without a navigation system. Huge venous bleeding and postoperative occipital neuralgia occur because of C2 neurectomy. Another entry point of the C1 lateral mass is suggested at the midpoint of the posterior C1 arch (Tan method [64]) or in the inferior aspect of the C1 arch (notch method). It should be noted that VA often runs in a sulcus on the superolateral aspect of the C1 posterior arch [65], and care should be taken to avoid drilling or tapping in this area. The C1 posterior arch is too small to insert a 3.5-mm screw in some cases. A drill bit rarely breaches the posterior arch or harms the VA [65]. Each conventional method from a posterior approach has disadvantages, which has encouraged the development of a breakthrough idea of a new posterolateral approach to the C1–C2 region, attained with the help of intraoperative 3D-CT navigation.

The posterolateral approach directly visualizes the C1 and C2 lateral masses and the best screw placement trajectory to avoid VA injury (Fig. 8.23). The venous plexus appears behind the OCI muscle, whereas bleeding is completely controlled. VA is superior to the C1 sulcus and is protected by a retractor and OCI muscle fibers. The 4.0-mm cannulated screws are placed in all C1 because the exposed lateral mass is wider from this approach. If the patients have a high position pathway of VA in C2, the pedicle screw is inserted obliquely, parallel to the VA from this approach.

Spinal navigation systems can reduce the VAI risk during posterior instrumentation surgery of C1–C2; however, C1 is unstable, and C1 navigation is unreliable compared to C2. Therefore, to verify the accuracy of the navigation, meticulous intraoperative control of anatomical landmarks should be performed (Fig. 8.5). Nevertheless, the highly accurate screw positioning for the placement of C1 and C2 is demonstrated despite the complicated anatomy, owing to the intraoperative 3D navigation system and a new posterolateral approach [62, 63].

This method using an intraoperative 3D navigation system provided a direct, oblique exploration of C1 lateral masses. It allowed the correct oblique angle of the screw position, resulting in less lateral deviation and reduced muscle damage and bleeding from the venous plexus.

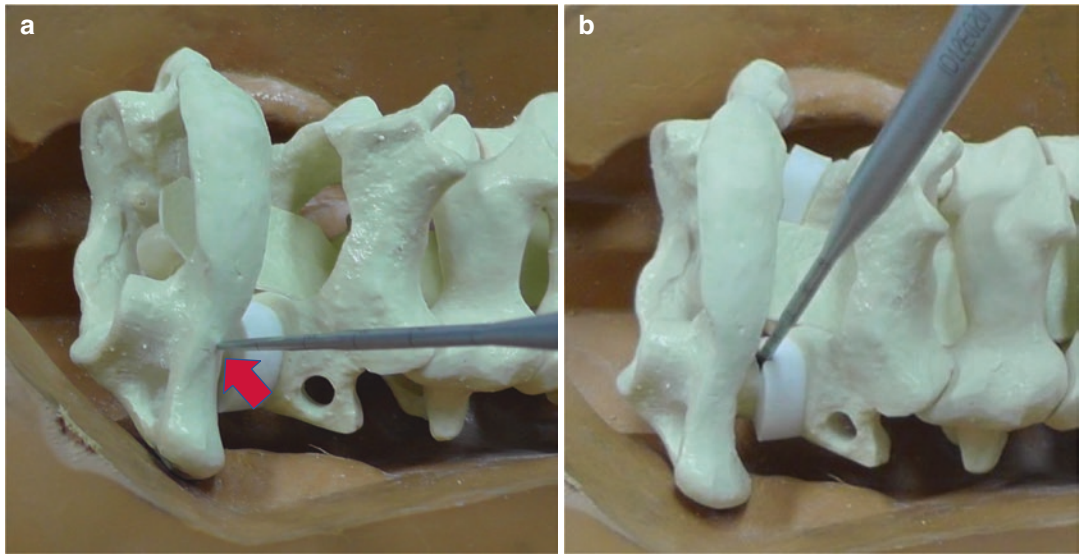


**Fig. 8.23** Entry points of C1 lateral mass screw. (**a**) A new entry point of C1 lateral mass screw from a posterolateral approach (red arrow). This new method provides direct exploration of C1 lateral mass; (**b**) conventional entry point of Goel–Harms technique

## References


1. Hadra BE. Wiring of the vertebrae as a means of immobilization in fractures and Pott's disease. Med Times Reg. 1891;2:1–8.
2. Abdu WA, Bohlman HH. Techniques of subaxial posterior cervical spine fusions: an overview. Orthopedics. 1992;15(3):287–95.
3. Whitehill R, Stowers SF, Fechner RE, Ruch WW, Drucker S, Gibson LR, et al. Posterior cervical fusions using cerclage wires, methylmethacrylate cement and autogenous bone graft. An experimental study of a canine model. Spine (Phila Pa 1976). 1987;12(1):12–22.
4. Benzel EC, Kesterson L. Posterior cervical interspinous compression wiring and fusion for mid to low cervical spinal injuries. J Neurosurg. 1989;70(6):893–9.
5. Rogers WA. Treatment of fracture-dislocation of the cervical spine. J Bone Joint Surg Am. 1942;24:245–58.
6. Rogers WA. Fractures and dislocations of the cervical spine: an end-result study. J Bone Joint Surg Am. 1957;39A:341–76.
7. Tucker HH. Technical report: method of fixation of subluxed or dislocated cervical spine below C1-C2. Can J Neurol Sci. 1975;2(4):381–2.
8. Ghori A, Le HV, Makanji H, Cha T. Posterior fixation techniques in the subaxial cervical spine. Cureus. 2015;7(10):e338.
9. Tukkapuram VR, Kuniyoshi A, Ito M. A review of the historical evolution, biomechanical advantage, clinical applications, and safe insertion techniques of cervical pedicle screw fixation. Spine Surg Relat Res. 2019;3(2):126–35.
10. Roy-Camille R, Saillant G, Mazel C. Internal fixation of the unstable cervical spine by a posterior osteosynthesis with plates and screws. In: Cervical Spine Research Society Editorial Committee, editor. The cervical spine. 2nd ed. Philadelphia: JB Lippincott; 1989. p. 390–403.
11. Jeanneret B, Gebhard JS, Magerl F. Transpedicular screw fixation of articular mass fracture-separation: results of an anatomical study and operative technique. J Spinal Disord. 1994;7(3):222–9.
12. Anderson PA, Henley MB, Grady MS, Montesano PX, Winn HR. Posterior cervical arthrodesis with AO reconstruction plates and bone graft. Spine (Phila Pa 1976). 1991;16(3 Suppl):S72–9.
13. An HS, Coppes MA. Posterior cervical fixation for fracture and degenerative disc disease. Clin Orthop Relat Res. 1997;335:101–11.
14. Omeis I, DeMattia JA, Hillard VH, Murali R, Das K. History of instrumentation for stabilization of the subaxial cervical spine. Neurosurg Focus. 2004;16(1):E10.
15. Fielding JW. The status of arthrodesis of the cervical spine. J Bone Joint Surg Am. 1988;70(10):1571–4.
16. Jeanneret B. Posterior rod system of the cervical spine: a new implant allowing optimal screw insertion. Eur Spine J. 1996;5(5):350–6.
17. Abumi K, Itoh H, Taneichi H, Kaneda K. Transpedicular screw fixation for traumatic lesions of the middle and lower cervical spine: description of the techniques and preliminary report. J Spinal Disord. 1994;7(1):19–28.

18. Jung YG, Jung SK, Lee BJ, Lee S, Jeong SK, Kim M, et al. The subaxial cervical pedicle screw for cervical spine diseases: the review of technical developments and complication avoidance. Neurol Med Chir (Tokyo). 2020;60(5):231–43.
19. Johnston TL, Karaikovic EE, Lautenschlager EP, Marcu D. Cervical pedicle screws vs. lateral mass screws: uniplanar fatigue analysis and residual pullout strengths. Spine J. 2006;6(6):667–72.
20. Kowalski JM, Ludwig SC, Hutton WC, Heller JG. Cervical spine pedicle screws: a biomechanical comparison of two insertion techniques. Spine (Phila Pa 1976). 2000;25(22):2865–7.
21. Kotani Y, Cunningham BW, Abumi K, McAfee PC. Biomechanical analysis of cervical stabilization systems. An assessment of transpedicular screw fixation in the cervical spine. Spine (Phila Pa 1976). 1994;19(22):2529–39.
22. Jones EL, Heller JG, Silcox DH, Hutton WC. Cervical pedicle screws versus lateral mass screws. Anatomic feasibility and biomechanical comparison. Spine (Phila Pa 1976). 1997;22(9):977–82.
23. Karaikovic EE, Daubs MD, Madsen RW, Gaines RW. Morphologic characteristics of human cervical pedicles. Spine (Phila Pa 1976). 1997;22(5):493–500.
24. Panjabi MM, Shin EK, Chen NC, Wang JL. Internal morphology of human cervical pedicles. Spine (Phila Pa 1976). 2000;25(10):1197–205.
25. Onibokun A, Khoo LT, Bistazzoni S, Chen NF, Sassi M. Anatomical considerations for cervical pedicle screw insertion: the use of multiplanar computerized tomography measurements in 122 consecutive clinical cases. Spine J. 2009;9(9):729–34.
26. Chazono M, Soshi S, Inoue T, Kida Y, Ushiku C. Anatomical considerations for cervical pedicle screw insertion: the use of multiplanar computerized tomography reconstruction measurements. J Neurosurg Spine. 2006;4(6):472–7.
27. Neo M, Sakamoto T, Fujibayashi S, Nakamura T. The clinical risk of vertebral artery injury from cervical pedicle screws inserted in degenerative vertebrae. Spine (Phila Pa 1976). 2005;30(24):2800–5.
28. Kotani Y, Abumi K, Ito M, Minami A. Improved accuracy of computer-assisted cervical pedicle screw insertion. J Neurosurg. 2003;99(3 Suppl):257–63.
29. Holly LT, Foley KT. Intraoperative spinal navigation. Spine (Phila Pa 1976). 2003;28(15 Suppl):S54–61.
30. Tjardes T, Shafizadeh S, Rixen D, Paffrath T, Bouillon B, Steinhausen ES, et al. Image-guided spine surgery: state of the art and future directions. Eur Spine J. 2010;19(1):25–45.
31. Ishikawa Y, Kanemura T, Yoshida G, Ito Z, Muramoto A, Ohno S. Clinical accuracy of three-dimensional fluoroscopy-based computer-assisted cervical pedicle screw placement: a retrospective comparative study of conventional versus computer-assisted cervical pedicle screw placement. J Neurosurg Spine. 2010;13(5):606–11.
32. Hott JS, Deshmukh VR, Klopfenstein JD, Sonntag VK, Dickman CA, Spetzler RF, et al. Intraoperative Iso-C C-arm navigation in craniospinal surgery: the first 60 cases. Neurosurgery. 2004;54(5):1131–6. discussion 6–7
33. Rajasekaran S, Vidyadhara S, Shetty AP. Iso-C3D fluoroscopy-based navigation in direct pedicle screw fixation of Hangman fracture: a case report. J Spinal Disord Tech. 2007;20(8):616–9.
34. Ishikawa Y, Kanemura T, Yoshida G, Matsumoto A, Ito Z, Tauchi R, et al. Intraoperative, full-rotation, three-dimensional image (O-arm)-based navigation system for cervical pedicle screw insertion. J Neurosurg Spine. 2011;15(5):472–8.
35. Chachan S, Bin Abd Razak HR, Loo WL, Allen JC, Shree KD. Cervical pedicle screw instrumentation is more reliable with O-arm-based 3D navigation: analysis of cervical pedicle screw placement accuracy with O-arm-based 3D navigation. Eur Spine J. 2018;27(11):2729–36.
36. Ludwig SC, Kramer DL, Balderston RA, Vaccaro AR, Foley KF, Albert TJ. Placement of pedicle screws in the human cadaveric cervical spine: comparative accuracy of three techniques. Spine (Phila Pa 1976). 2000;25(13):1655–67.
37. Richter M, Cakir B, Schmidt R. Cervical pedicle screws: conventional versus computer-assisted placement of cannulated screws. Spine (Phila Pa 1976). 2005;30(20):2280–7.
38. Bredow J, Oppermann J, Kraus B, Schiller P, Schiffer G, Sobottke R, et al. The accuracy of 3D fluoroscopy-navigated screw insertion in the upper and subaxial cervical spine. Eur Spine J. 2015;24(12):2967–76.
39. Ito Y, Sugimoto Y, Tomioka M, Hasegawa Y, Nakago K, Yagata Y. Clinical accuracy of 3D fluoroscopy-assisted cervical pedicle screw insertion. J Neurosurg Spine. 2008;9(5):450–3.
40. Liu YJ, Tian W, Liu B, Li Q, Hu L, Li ZY, et al. Comparison of the clinical accuracy of cervical (C2-C7) pedicle screw insertion assisted by fluoroscopy, computed tomography-based navigation, and intraoperative three-dimensional C-arm navigation. Chin Med J. 2010;123(21):2995–8.
41. Mason A, Paulsen R, Babuska JM, Rajpal S, Burneikiene S, Nelson EL, et al. The accuracy of pedicle screw placement using intraoperative image guidance systems. J Neurosurg Spine. 2014;20(2):196–203.
42. Rajasekaran S, Kanna PR, Shetty TA. Intraoperative computer navigation guided cervical pedicle screw insertion in thirty-three complex cervical spine deformities. J Craniovertebr Junction Spine. 2010;1(1):38–43.
43. Tian W, Liu Y, Zheng S, Lv Y. Accuracy of lower cervical pedicle screw placement with assistance of distinct navigation systems: a human cadaveric study. Eur Spine J. 2013;22(1):148–55.
44. Zhang HL, Zhou DS, Jiang ZS. Analysis of accuracy of computer-assisted navigation in cervical pedicle screw installation. Orthop Surg. 2011;3(1):52–6.
45. Kothe R, Rüther W, Schneider E, Linke B. Biomechanical analysis of transpedicular screw

fixation in the subaxial cervical spine. Spine (Phila Pa 1976). 2004;29(17):1869–75.
46. Barnes AH, Eguizabal JA, Acosta FL, Lotz JC, Buckley JM, Ames CP. Biomechanical pull-out strength and stability of the cervical artificial pedicle screw. Spine (Phila Pa 1976). 2009;34(1): E16–20.
47. Kast E, Mohr K, Richter HP, Börm W. Complications of transpedicular screw fixation in the cervical spine. Eur Spine J. 2006;15(3):327–34.
48. Pelton MA, Schwartz J, Singh K. Subaxial cervical and cervicothoracic fixation techniques--indications, techniques, and outcomes. Orthop Clin North Am. 2012;43(1):19–28, vii
49. Abumi K, Ito M, Sudo H. Reconstruction of the subaxial cervical spine using pedicle screw instrumentation. Spine (Phila Pa 1976). 2012;37(5):E349–56.
50. Uehara M, Takahashi J, Ikegami S, Mukaiyama K, Kuraishi S, Shimizu M, et al. Screw perforation features in 129 consecutive patients performed computer-guided cervical pedicle screw insertion. Eur Spine J. 2014;23(10):2189–95.
51. Abumi K, Shono Y, Ito M, Taneichi H, Kotani Y, Kaneda K. Complications of pedicle screw fixation in reconstructive surgery of the cervical spine. Spine (Phila Pa 1976). 2000;25(8):962–9.
52. Yukawa Y, Kato F, Ito K, Horie Y, Hida T, Nakashima H, et al. Placement and complications of cervical pedicle screws in 144 cervical trauma patients using pedicle axis view techniques by fluoroscope. Eur Spine J. 2009;18(9):1293–9.
53. Miyamoto H, Uno K. Cervical pedicle screw insertion using a computed tomography cutout technique. J Neurosurg Spine. 2009;11(6):681–7.
54. Satake K, Kanemura T, Ito K, Tanaka S, Morita Y, Nakashima H, et al. Pedicle screw placement with use of a navigated surgical drill at subaxial cervical spine. J Clin Neurosci. 2021;88:28–33.
55. Tomasino A, Parikh K, Koller H, Zink W, Tsiouris AJ, Steinberger J, et al. The vertebral artery and the cervical pedicle: morphometric analysis of a critical neighborhood. J Neurosurg Spine. 2010;13(1):52–60.
56. Mahesh B, Upendra B, Mahan RS. The medial cortical pedicle screw--a new technique for cervical pedicle screw placement with partial drilling of medial cortex. Spine J. 2014;14(2):371–80.
57. Komatsubara T, Tokioka T, Sugimoto Y. Minimally invasive cervical pedicle screw fixation by a posterolateral approach for acute cervical injury. Clin Spine Surg. 2017;30:466–9.
58. Magerl F, Seeman P. Stable posterior fusion of the atlas and axis by transarticular screw fixation. In: Kehr P, Weidner A, editors. Cervical spine I. Wien, New York: Springer; 1987. p. 322–7.
59. Goel A, Laheri V. Plate and screw fixation for atlanto-axialsubluxation. Acta Neurochir (Wien). 1994;129:47–53.
60. Goel A, Desai KI, Muzumdar DP. Atlantoaxial fixation using plate and screw method: a report of 160 treated patients. Neurosurgery. 2002;51:1351–6.
61. Harms J, Melcher RP. Posterior C1-C2 fusion with polyaxial screw and rod fixation. Spine (Phila Pa 1976). 2001;26:2467–71.
62. Yang YL, Zhou DS, He JL. Comparison of isocentric C-Arm 3-dimensional navigation and conventional fluoroscopy for C1 lateral mass and C2 pedicle screw placement for atlantoaxial instability. J Spinal Disord Tech. 2013;26:127–34.
63. Hur JW, Kim JS, Ryu KS, et al. Accuracy and safety in screw placement in the high cervical spine: retrospective analysis of O-arm based navigation-assisted C1 lateral mass and C2 pedicle screws. Clin Spine Surg. 2019;32(4):E193–9.
64. Tan M, Wang H, Wang Y, et al. Morphometric evaluation of screw fixation in atlas via posterior arch and lateral mass. Spine. 2003;28:888–95.
65. Yeom JS, Buchowski JM, Park KW, et al. Undetected vertebral artery groove and foramen violations during C1 lateral mass and C2 pedicle screw placement. Spine. 2008;33(25):942–9.

# 9 Minimally Invasive Lateral Transpsoas Approach with Intraoperative CT Navigation

Martina Dalolio, Davide Croci, Luca Valci, and Pietro Scarone

## 9.1 Introduction

### 9.1.1 Background

The morbidity related to anterior and posterior approaches for interbody fusion led, in the late 1990s and 2000s, to the development of other techniques with the aim to find new anatomical corridors, that could allow for a better bony fusion.

Driven by the development of endoscopic techniques, a new anterolateral approach to the lumbar spine through the psoas muscle was initially proposed [1]. The endoscopic approach has been then largely abandoned, mainly because of a higher incidence of new postoperative neurological deficits that occurred in 30% of cases [2], the main reason being the absence of intraoperative neuromonitoring.

The mini-open lateral retroperitoneal approach was then pioneered by Luiz Pimenta in the early 2000s [3], as a minimally invasive surgical technique to perform a complete discectomy and an interbody fusion through a new surgical corridor, without the need for dissection of aorta and vena cava. Because of the easier anatomical pathway and the possibility to treat a wider spectrum of spine pathologies compared to the anterior lumbar interbody fusion (ALIF), the use of this approach increased dramatically in the following decade.

The original technique, later introduced in the literature as lateral transpsoas interbody fusion [4], was designed as a minimally invasive, muscle-sparing lateral approach to the vertebral column. Compared to posterior approaches, the technique allows for an indirect decompression of neural structures with ligamentotaxis [5], avoiding any nerve retraction or manipulation, and also for the possibility to insert a large anterior support through different types of interbody cages specifically designed [6].

In 2004 Bergey et al. [2] published the first experience of a minimally invasive lateral transpsoas approach supported by triggered EMG to identify the position of the lumbar plexus. The results were encouraging, but 30% of thigh numbness and pain was reported.

Only in 2010, Uribe et al. [7] standardized the approach describing the safe working zone. From 2011 on, intraoperative neuromonitoring (IONM) has been extensively applied during lateral approach, reducing the risk of postoperative paresthesias secondary to lumbosacral plexus injury from 30% to 0.7% [8].

Nowadays, several different platforms for minimally invasive lateral transpsoas approach exist, that include the Direct Lateral Interbody

M. Dalolio · D. Croci · L. Valci · P. Scarone (✉)
Neurosurgery Clinic, Neurocenter of Southern Switzerland, Lugano, Switzerland
e-mail: martina.dalolio@eoc.ch; davide.croci@hsc.utah.edu; luca.valci@eoc.ch; pietro.scarone@eoc.ch



J.-S. Kim et al. (eds.), *Technical Advances in Minimally Invasive Spine Surgery*,
https://doi.org/10.1007/978-981-19-0175-1_9

Fusion (DLIF®, Medtronic Sofamor Danek, Memphis, TN), Lateral Lumbar Interbody Fusion (LLIF®, Globus Medical Inc., Audubon, PA), and Extreme Lateral Interbody Fusion (XLIF®, NuVasive Inc., San Diego, CA).

Procedural recommendations for all these platforms include the use of fluoroscopic imaging to confirm the surgical level and to check intraoperative implant positioning during surgery. In many situations, it is recommended that the operating room setup during the approach provide the surgeon the ability to obtain an adequate visualization of the lumbar spine in the lateral as well as in the frontal plane. In fact, patient rotation before or during surgery could prevent surgeons to visualize the correct trajectory to access disc space and potentially cause injury to contralateral vascular structures during disc preparation [6, 9].

Apart from the need for intraoperative fluoroscopic imaging, many differences exist between the different surgical platforms, including the design of retractor used during the approach and the technique used for intraoperative monitoring.

The present chapter will focus on the LLIF approach done with the so-called shallow docking technique, originally described by Acosta et al. [10]. Briefly, this approach relies on the direct visualization of the lateral aspect of the psoas muscle, prior to dissection down to the spine. The surface of the psoas muscle is explored using a neuro-stimulating probe to confirm the location of the neural elements. Compared to the original technique [10], at this stage navigation is used to identify the safe working zone where the tubular expandable retractor will be placed through the psoas, and the neuro-stimulating probe is again used through this working window to confirm that the neural elements are not on the way of the retractor. Psoas muscle fibers are not dissected; instead, sequential dilators are placed to transverse the muscle and dock the working tube on the lateral aspect of the disc space.

### 9.1.2 3D Navigation with an Intraoperative CT

In recent years, intraoperative image-guided systems that allow for real-time, 3D navigation of different surgical instruments have been introduced in spinal procedures. A substantial body of literature in recent years has shown improved accuracy during pedicular screw positioning [11–16], with potential reduction of surgical time [13, 17], intraoperative blood losses [13, 18–20], hospital stay [21], and radiation exposure [22]. Many of these studies have used navigation technology coupled with a cone-beam CT (O-arm®, Medtronic Sofamor Danek, Memphis, TN) or a portable, 32-slice helical CT scanner more recently developed (Airo®, Brainlab AG, Feldkirchen, Germany).

Much of the literature studying the impact of 3D navigation on surgical efficiency is focused on the evaluation of the accuracy of pedicle screw positioning either in the cervicothoracic or in the lumbar spine. In general, many studies have evaluated the position of the implants on intraoperative and/or postoperative CT scans, using different methods [23, 24]. However, the clinical impact of these radiological measurements is not obvious. Other studies have tried to evaluate the impact of 3D navigation in spinal surgery, focusing on the rate of postoperative neurological deficits or reoperation for mispositioned screws [25]. However, probably because of the very low reported incidence of these events, evidence from the literature showing a better clinical outcome using spinal navigation is still lacking. In a meta-analysis including more than 5000 screws in 1288 patients, Verma et al. were not able to show a benefit of spinal navigation over traditional techniques in reducing neurological complications or improving clinical outcomes, while there was a significant advantage in terms of accuracy [26]. This is also consistent with recent data reported from our own experience with two different 3D navigation systems in 263 consecutive patients submitted to spinal fusion procedures in the thoracic and lumbar spine [16].

However, even in the absence of evidence-based data, a common experience of surgical teams using spinal navigation on an everyday basis show that intraoperative CT (iCT) 3D navigation could be particularly useful in case of anatomical landmark modifications (e.g., scoliosis, degenerative spine disease, ankylosing spondylitis) and in obese patients [27].

This technology, moreover, could ameliorate surgical efficiency and workflow compared to traditional 2D fluoroscopic imaging. In a recent retrospective analysis [28] Khanna et al. were able to show a reduction in surgical time using iCT navigation compared to free-hand technique, despite a similar setup time. Moreover, the surgical time showed a decrease over time in the authors' experience, suggesting a learning curve effect. Together with reported personal experiences of other authors [29], these data suggest that spinal navigation coupled with an iCT could significantly ameliorate the surgical workflow of complex spinal procedures, and have a role also in surgical procedures including lateral approaches.

Indeed, the use of navigation in lateral approaches for degenerative diseases has been previously described. Webb et al. [30] in a cadaveric study first showed a significant reduction in time of surgery and radiation exposure with the use of spinal navigation with C-Arm fluoroscopy.

Drazin [31] in 2013 introduced the use of 3D navigation based on a cone-beam CT (O-Arm®). In the following years, case reports and retrospective case series of patients submitted to lateral approaches with O-arm navigation confirmed higher accuracy of implant positioning without a significant increase in radiation exposure for patients [32, 33]. In 2018, Jiang et al. [34] retrospectively compared the outcome and complication rate of patients treated with navigated (O-Arm) and not navigated DLIF, showing similar clinical outcomes, but a reduction of radiation exposure with navigation.

Strong et al. [35] more recently reported a series of 59 patients operated for spinal deformity with posterior instrumentation combined with lateral interbody cage positioning. One-hundred seventy-five lateral cages were positioned using 3D navigation, with 2 patients (3.4%) showing a complication related to navigation inaccuracy and 1 misplaced cage (0.6%) requiring intraoperative revision.

Yu et al. [36] firstly introduced the use of 3D spinal navigation coupled with a mobile iCT (AIRO®, Brainlab AG, Feldkirchen, Germany) during lateral thoracolumbar corpectomies in a series of 20 patients, showing similar results compared to 2D fluoroscopic guidance in terms of blood losses, operative time, hospital stay, and need for revision but reduced radiation exposure with navigation. Experiences with mini-open lateral access through a tubular dilator retractor guided by 3D navigation remain however scarce, and as far as we know, no author has reported on this technique guided by navigation coupled with a mobile iCT.

### 9.1.3 Main Indications and Contraindications

The spectrum of spinal pathologies treatable with a lateral approach is typically those requiring interbody fusion in L1–L5. These may include mild to moderate degenerative spondylolisthesis (Meyerding [37] Grade I), adult scoliosis, degenerative disc disease, pseudarthrosis/nonunion, spondylodiscitis/postoperative infection after posterior lumbar interbody fusion (PLIF) or transforaminal lumbar interbody fusion (TLIF), and revision surgery for adjacent disc disease after PLIF/TLIF. However, the level L5/S1 still remains inaccessible from a lateral trajectory because of the impendence of the iliac crest. Major contraindications are previous extensive retroperitoneal surgery or abdominal trauma, history of retroperitoneal infection (e.g., diverticulitis), poor bone quality, and/or osteoporosis (risk factor for interbody cage subsidence). A relative contraindication exists at level L4/5 because of the reported higher risk of thigh motor deficits, particularly in case of L5 sacralization for the anterior displacement of lumbar plexus. At this level, moreover, the anatomy of the iliac crest should be carefully evaluated preoperatively.

### 9.1.4 Preoperative Assessment and Planning

A preoperative lumbar spine CT scan may be useful in case of significant spinal deformity, to assess the vascular anatomy in relation to the anterior longitudinal ligament (ALL) and the vertebral bodies. This evaluation is, in some cir-

cumstances, necessary to determine the safest side of the approach, given the fact that the great vessels and especially the inferior vena cava migrate posteriorly and laterally as they travel from L1 to L5 [9]. We usually avoid performing the procedure at L4/L5, because this level is the most difficult to gain access and the most vulnerable to neural injury, and in most cases prefer a left-sided approach, as the aortic wall is thicker and more elastic than vena cava, therefore more resistant in case of an encounter with the surgical instruments. However, the side of the approach might change depending on the spine pathology, the clinical picture, and the indication (e.g., high-level foraminal stenosis on the right, previous neurological deficits in right thigh, inaccessible disc space on the left side in the case of vertebral rotation). Anatomical variations like situs inversus should also be verified.

Lumbar spine MRI is also essential for the planning. Particular attention should be paid to the dimensions and shape of the psoas muscle to assess the neurological risk for the patient and choose the safest surgical corridor. As shown by previous anatomical and radiological studies [38, 39] the choice of the trajectory through the psoas muscle is critical to avoid damage to the lumbar plexus. Moreover, patients with a higher anterior-posterior to latero-lateral ratio of psoas muscle on axial view show a higher risk of postoperative pain and neurological deficits [40]. Hu et al. [39] performed a preoperative evaluation of the anatomy of the psoas muscle and abdominal vessels on 48 patients and divided the lumbar intervertebral disc spaces into six zones from the anterior to the posterior according to Moro's [38] method, showing that the approach is safe through zones II–II at L1/L2 and L2/L3, and only via zone II at L3–L4 (Fig. 9.1). The anterior one-third of the vertebral body should therefore be the aim of the surgical corridor in order to avoid possible neuronal injuries as the nerves run in the posterior two-third of the vertebral body [7].

Some authors have also advocated the need to verify the real position of the psoas muscle with a preoperative lumbar spine MRI in a sitting position, that can simulate the lateral side position with flexed legs [41]. However, there is no clear evidence to support the need to perform such an MRI scan in every case.

Magnetic resonance neurography of the lumbar plexus has also been advocated as a preoperative imaging modality useful to surgical plans

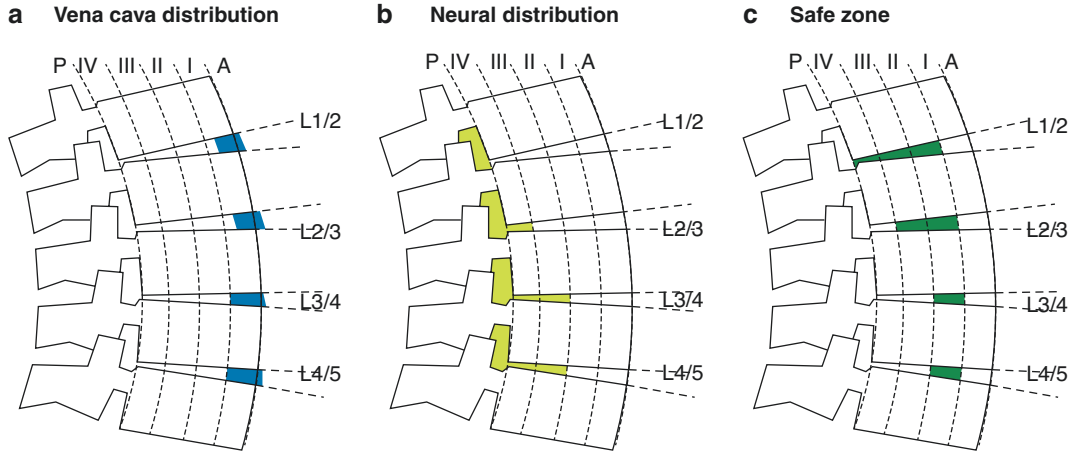


**Fig. 9.1** Illustration of the left side (upper quadrants) and right side (lower quadrants) LLIF approach as related to anatomical structures: (**a**) vascular structures distribution (**b**) lumbar plexus distribution (**c**) safe zone, i.e. the zone where tubular retractors, instruments for disc preparation and interbody cages can be safely positioned. The safe zone is narrower and more anterior progressing from cranial to caudal levels. Taken from [39]

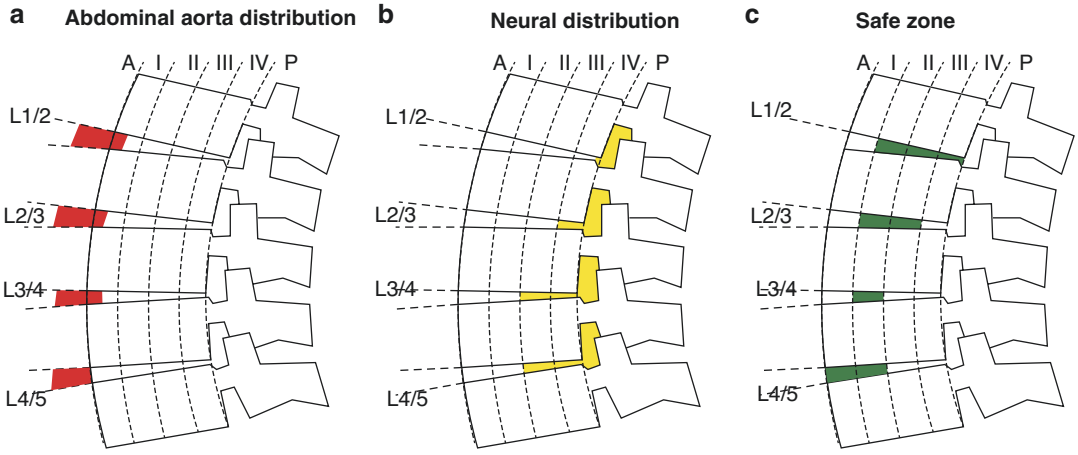


**Fig. 9.1** (continued)

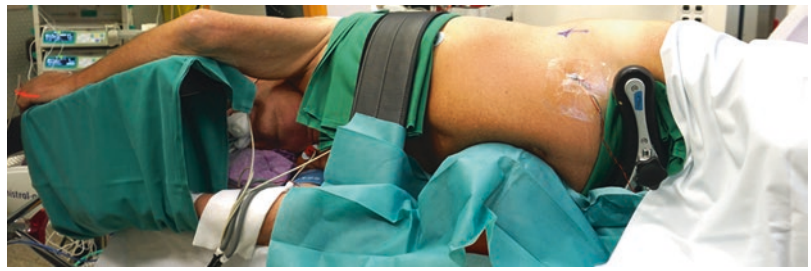

**Fig. 9.2** Patient in right lateral position secured with supports and strains. A blow-up pillow is positioned below the patient. The arms are toward the head and the legs are flexed

[42], but its use is limited by the inadequate visualization of the nerves in the region of interest in many cases, particularly in overweight patients.

## 9.2 Description of the Procedure

### 9.2.1 Surgical Technique

#### 9.2.1.1 Patient Positioning

Correct positioning of the patient is the first fundamental step of any surgical procedure and even more in the case of a lateral approach to the spine. The patient, under general anesthesia, is positioned on the side on an unbroken, not bendable mobile radiolucent carbon fiber table (Trumpf TruSystem 7500, Trumpf Inc., Farmington, Connecticut, USA) that is linked to the mobile scanner, with appropriate pressure points padded. Regarding laterality, a preoperative choice is made to approach the side that allows the best access to the target disc and pathology as previously stated. An axillary roll is positioned to protect the brachial plexus. A blow-up pillow positioned below the patient is used to indirectly open the contralateral space between the 12th rib and the iliac crest, in order to facilitate the surgical exposure. The legs are slightly flexed, and the arms are put toward the head with flexed elbows. The patient is then secured in this position with supports and strains (Fig. 9.2). Not opening enough the subcostal space could prevent reaching the disc space easily, the surgical corridor being too long or narrow to use the instruments safely. Equally, the surgeon should provide that the patient is as perpendicular as possible to the surgical table, in order to avoid rotation of the spine, which can reduce the safe zone to access the disc space. IONM electrodes are positioned by a trained neurophysiology technician to allow

for motor evoked potentials (MEPs) and spontaneous electromyography (sEMG).

**Key Points**

- *Ensure adequate protection for brachial plexus and pressure points.*
- *Inflate a blow-up pillow contralaterally in order to augment the distance between the iliac crest and the rib cage on the side of the approach.*
- *Ensure that there is no rotation of the spine. However, performing radiographs at this stage is not necessary if iCT is used during the procedure.*

### 9.2.1.2 Room and Navigation Setup

The patient on the table is positioned with the head toward the intraoperative CT (iCT) (AIRO®, Brainlab AG, Feldkirchen, Germany), while anesthesia is located at the head of the surgical bed, the scrub nurse at the feet, and the surgeon on the lateral back side (Fig. 9.3). An infrared tracking camera (Brainlab Curve, Brainlab AG, Feldkirchen, Germany), connected to the scanner, is positioned at the feet of the patient.

The surgical field is disinfected and sterile draped, taking care to ensure that the anterior superior iliac spine (ASIS) is kept in the sterile field. Alternatively, the posterior superior iliac spine (PSIS) can be used. MEPs are tested as baseline acquisition. The iCT is covered with a transparent drape that allows moving the iCT scan on the patient under sterile conditions. Then, two stab incisions are made over either the ASIS or PSIS, and two pins are introduced to fix the reference array for navigation system (BrainLAB®, Brainlab AG, Feldkirchen, Germany) (Fig. 9.4). An initial scan of the region of interest is acquired and automatically transferred to the image-guidance system (Brainlab Curve, Brainlab AG, Feldkirchen, Germany); the accuracy of the navigation system is then verified checking the head–feet orientation and using anatomical landmarks (such as iliac crest).

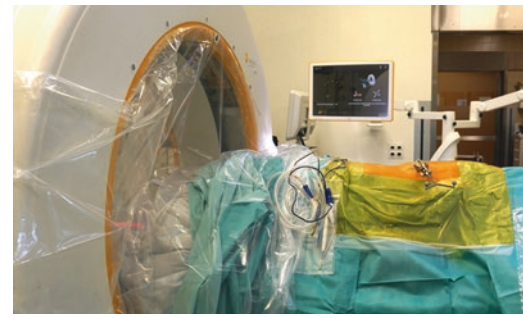

**Fig. 9.4** Patient in right lateral position, surgical field is draped, the navigation star is fixed on the left anterior superior iliac spine, a sterile transparent plastic drape covers the iCT and the head of the patient to make a barrier from anesthesia side and to allow patient and iCT translations maintaining the sterility

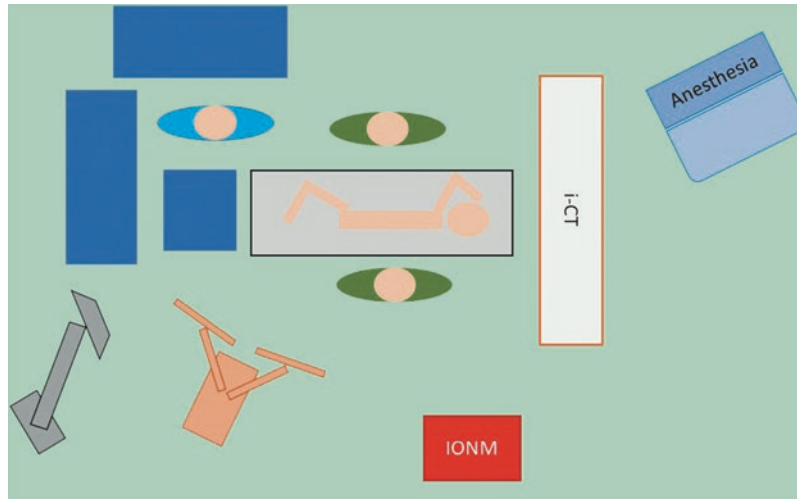


**Fig. 9.3** Anesthesia is located behind the iCT, the patient lays on the carbon table with the head toward the iCT, the surgeon and the assistant (green) are on both sides of the patient, the scrub nurse (blue), the navigation screens (orange), and the navigation camera (gray) are at the patient's feet, and IONM machine is at the back of surgeon

Registration of surgical instruments such as navigated drill-guide (Brainlab AG, Feldkirchen, Germany) is then performed before skin incision.

**Key Points**

- *Ensure the draping in order to allow movement of the surgical table toward the scan gantry and vice-versa.*
- *Verify the absence of any obstruction under the surgical table, that may prevent adequate movement of the iCT.*
- *Verify perfect fixation of the pins for the reference star on the anterior iliac crest, and the absence of any obstruction of the infrared camera sight.*

#### 9.2.1.3 Planning Skin Incision and Performing Initial Dissection

A one-incision approach is preferred by the senior author (PS). Using the sagittal and coronal view of the image-guided navigation system, we mark the anterior and posterior margins of the vertebral bodies as well as the target disc space. The skin incision usually spans approximately 3 cm on an oblique line centered over the disc space (Fig. 9.5), and connects these margins previously identified with the navigation. When two levels are addressed, the incision is centered between the two target discs.

Subcutaneous and fat layers are bluntly dissected without electrocautery, to avoid injury to

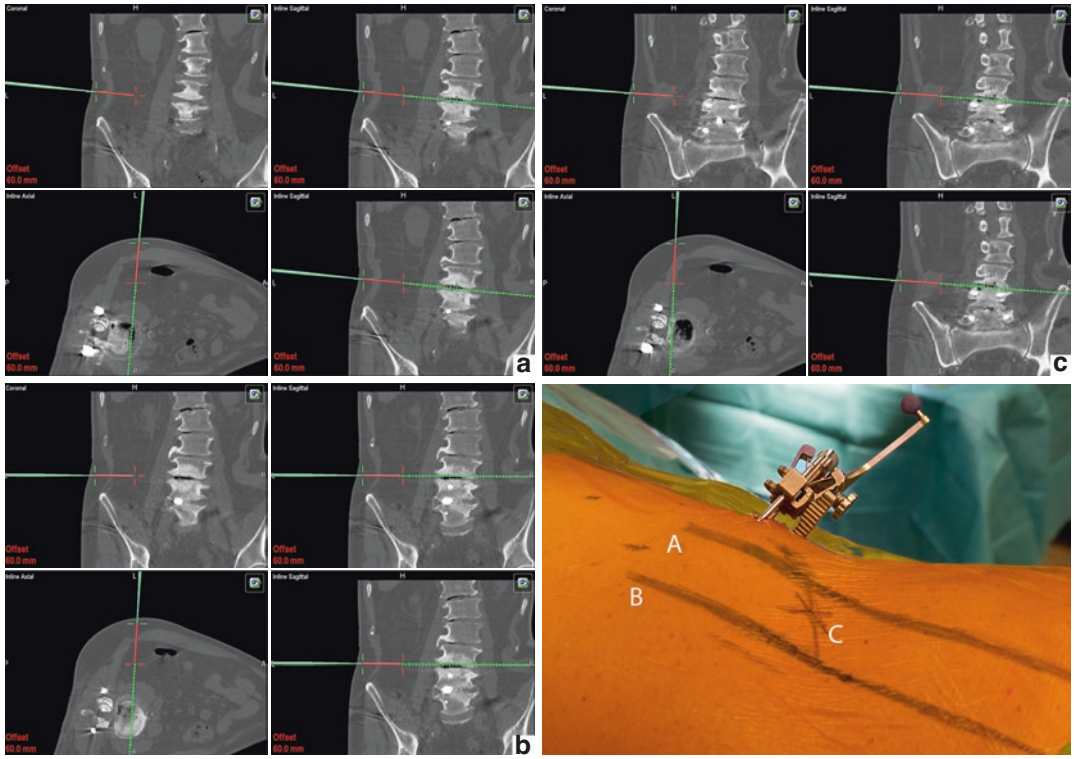


**Fig. 9.5** *Lower right*: Skin projections of (**a**) anterior border of the spine, (**b**) posterior limit of vertebral body, (**c**) the middle point of vertebral body on lateral side at the disc level. The skin incision is an oblique line connecting **a** to **b** passing through **c** at the level of interest (L3–4 in this case). Panel **a**, **b**, and **c** are the navigation screenshots referring to the corresponding landmarks; in each panel the navigated pointer (green) on the skin surface and its virtual tip extension of 60 mm (red) are pointing to the target in different planes

subcostal nerves, which may lead to denervation of abdominal wall muscles. The fascia is divided and the abdominal wall muscles (external oblique, internal oblique, and transversus abdominis) are split following the fiber direction of each layer to reach the retroperitoneum space. The abdominal and retroperitoneal contents are carefully moved from posterior to anterior with a curved blade until the lateral aspect of the psoas muscle can be seen.

**Key Points**

- *A single oblique incision is planned with help of the image-guided navigation system at a level of the disc space.*
- *The use of electrocautery during dissection should be avoided in order to reduce the risk of injuries to the lateral cutaneous branches of iliohypogastric nerve.*

#### 9.2.1.4 Deep Dissection and Crossing of the Psoas Muscle

The transpsoas entry point for the surgical corridor to the anterior one-third of the vertebral body is identified with navigation (Fig. 9.6). Prior to dilation through the muscle, the entry point is then tested by stimulating with a handheld EMG probe (Inomed, Emmendingen, Germany) on the surface of psoas muscle with different thresholds (from 15 to 5 mA intensity) to map the region and identify the motor nerves of lumbar plexus. The lower the threshold required to evoke a response, the closer is the motor nerve to the probe. We usually start from the anterior margin of the muscle, and then proceed posteriorly, trying to obtain in every case a mapping of the neuroanatomy to allow for a safe positioning of the retractor. In most cases, stimulating the posterior part of the muscle results in low response thresholds (at 5 mA), while anterior stimulation results in higher response thresholds (>15 mA). The dilation is not started until a complete absence of responses is obtained in the anterior part of the muscle.

In a safe region, a navigated drill guide (Brainlab AG, Feldkirchen, Germany) is then inserted through the muscle fibers and placed on the lateral surface of the target disc space (Fig. 9.7). A Kirchner wire is then inserted through the drill guide manually into the disc and the drill guide is retrieved. Sequential dilators are then inserted over the wire, and finally, a minimally invasive expandable tubular retractor (MARS™ 3VL, Globus Medical, Audubon, PA) composed of 3 or 4 independent blades and illumination system, that allows for a good direct visualization of surgical field (Fig. 9.7), is placed.

The retractor is opened under sEMG monitoring to control and decide the range of muscle retraction. In case of muscle fibrillations or if a decrease in response thresholds is noted, the retractor is closed to some mm or grades to avoid

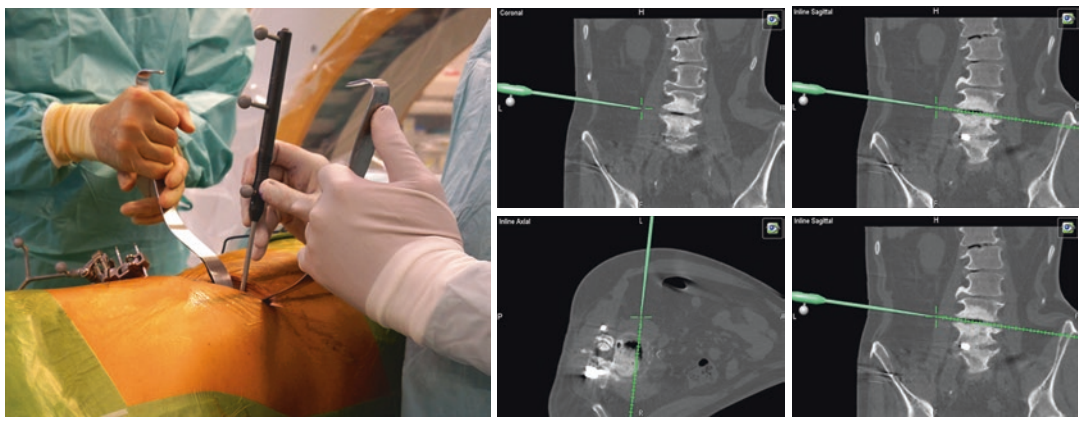

**Fig. 9.6** *Left*: Identification of the entry point on psoas muscle corresponding to the anterior one-third of the vertebral body with navigated pointer. *Right*: navigation screenshot of corresponding point in different planes (top, coronal and sagittal; bottom, axial and sagittal)

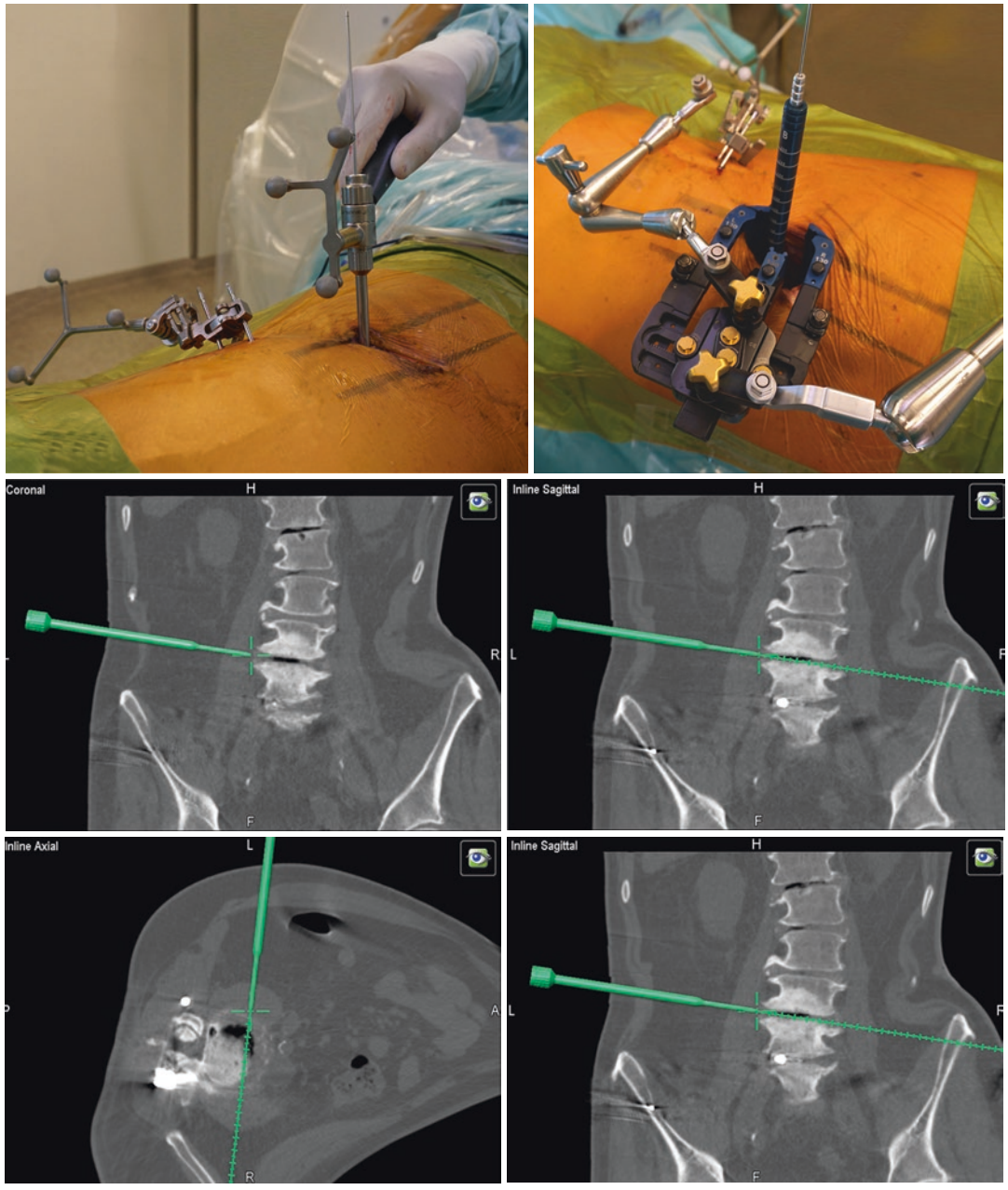


**Fig. 9.7** *Upper left*: A navigated drill guide is used to place a guidewire at entry point to disc surface. *Upper right*: a minimally invasive retractor (MARS™ 3VL, Globus Medical, Audubon, PA) fixed at the table with a flexible metallic arm is used to expose the lateral surface of the psoas muscle *Lower left and right*: navigation screenshots during wire positioning in different planes

them. MEPs are checked and in case of reduction >50% or loss of response on thigh or leg muscles the retractor position needs to be changed.

**Key Points**

- *Try to avoid any manipulation and dissection through the psoas muscle before EMG mapping.*
- *If a traversing nerve is encountered, gently retract it dorsally.*
- *Retraction has to be performed primarily anteriorly and in cephalocaudal orientation: use navigation to confirm the position of the target disc during retraction, and avoid unnecessary exposure of lateral surface of vertebral bodies.*

#### 9.2.1.5 Discectomy and Implant Insertion

Once the disk and the superior and inferior endplates are well represented, an anulotomy is performed with a scalpel, and disc material is removed using a pituitary rongeur. In case of the presence of lateral osteophytes, these can be carefully removed with drill and Leksell rongeurs, in order to guarantee a complete exposure of the lateral surface of the disk. Blunt shavers of different dimensions are used to detach disc material from the endplates. Finally, contralateral anulus is carefully opened with a 5-mm-high, 20-mm-wide blunt tip trial under X-Ray control. Any use of Cobb elevators is avoided to reduce the risk of damage to contralateral psoas muscle or vascular structures. The length of interbody cage is decided on X-ray using the markers on the trial, while the height and the eventual lordosis are decided on intraoperative CT performed at the beginning of the procedure. An expandable cage (ELSA®-ATP, Globus Medical, Audubon, PA) filled with a bioactive graft material (Signify®, Globus Medical, Audubon, PA) is inserted into the disc space and expanded under X-Ray and sEMG control (Fig. 9.8). In case of muscle fibrillations on sEMG that are not self-reducing, the range of expansion can be decreased.

This cage is then fixed with screws on adjacent vertebral bodies. Direction of screws is planned with navigation (Fig. 9.9). In case of previous posterior fusion with pedicular screws, navigation is essential to plan screws trajectory and to avoid the posteriorly placed screws.

Finally, the retractor is gently removed, a confirmation scan is performed to verify the correct position of the interbody implant (Fig. 9.10). MEPs are checked at the end of procedure to be compared with the baseline acquisition. In our series, the minimum surgical time reached for the whole procedure on 1 level, comprehensive of initial and final verification scan, is 100 min.

**Key Points**

- *Minimize use of curettes and Cobb elevators during discectomy, to avoid inadvertent damage to the endplates.*
- *More frequent use of navigation could be necessary when the disc space is severely collapsed, to avoid violation of endplates during trial insertion.*
- *Do not over-expand the implant to avoid postoperative subsidence: in general, the final height is decided by taking the adjacent discs as a reference, if not degenerated.*

### 9.2.2 Use of Intraoperative CT Navigation

Intraoperative CT (iCT) navigation relies on a portable 32 slice helical CT scanner (Airo®, Brainlab AG, Feldkirchen, Germany), that is used during the intervention to obtain thin-cut CT through the region of interest. Compared to a cone-beam CT scanner (CBCT), the iCT emits a "fan type" X-ray and is detected by a linear detector array [43]. This translates into a greater soft tissue definition and bone resolution compared to other intraoperative imaging modalities. The higher intraoperative image quality results in a better evaluation of vertebral pedicles and bodies, especially in difficult anatomical conditions, like in spinal deformity, or in certain regions like the cervicothoracic junction [44]. The technical features of the mobile iCT, including the extended scan volume capacity, that eliminates the need to re-center the device, make it perfectly suitable for

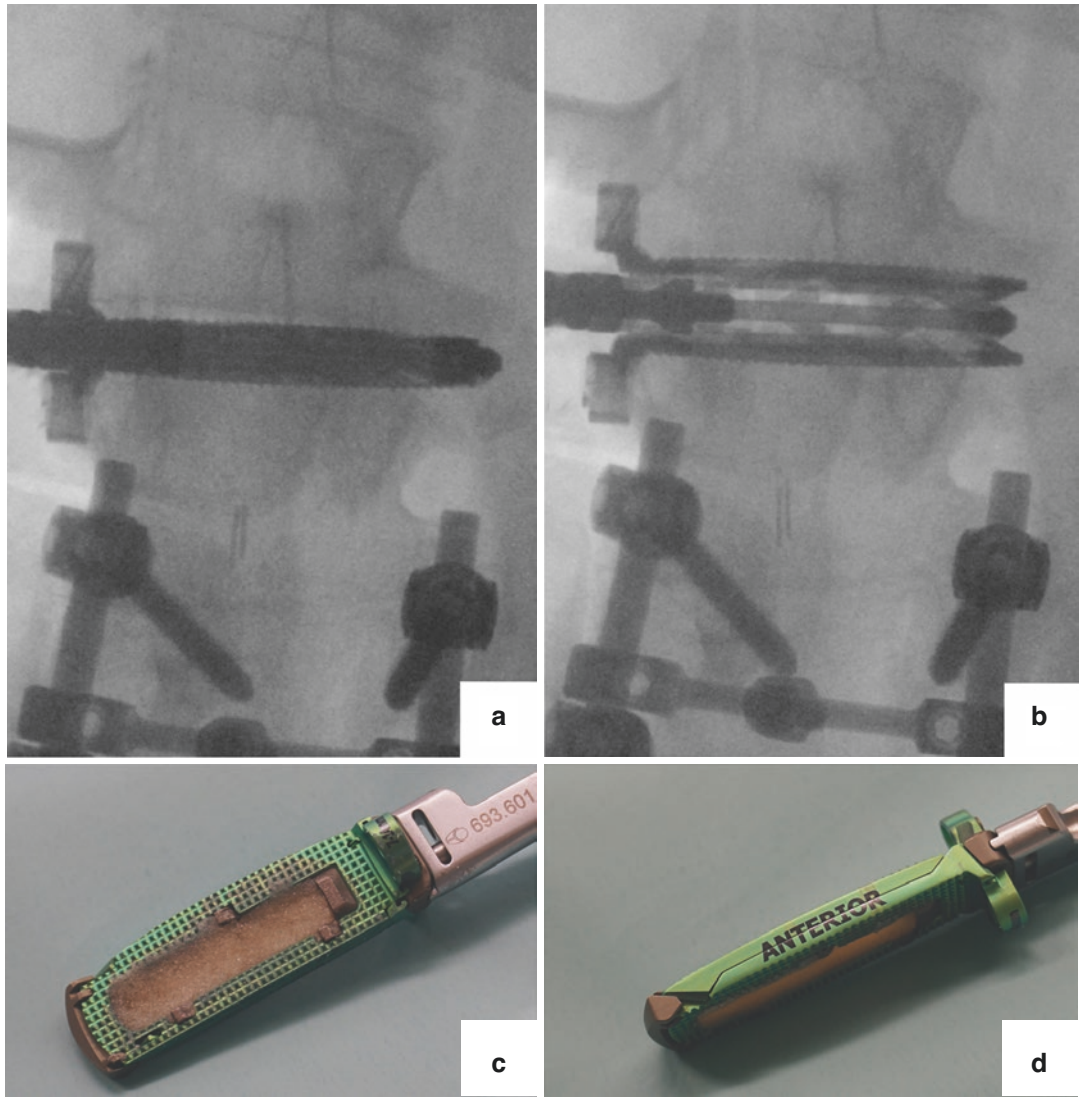


**Fig. 9.8** (**a**) X-ray image showing an interbody expandable cage (ELSA®-ATP, Globus Medical, Audubon, PA) inserted at level L3-L4, (**b**) the cage is expanded under fluoroscopic control, (**c**, **d**) the expandable cage filled with bone expander

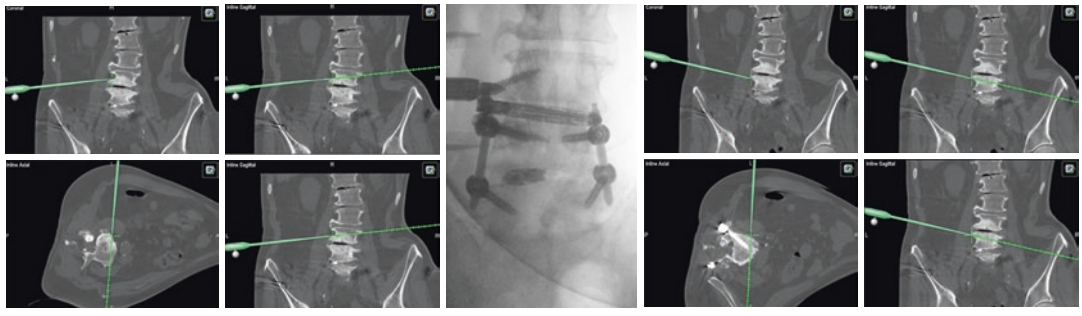

**Fig. 9.9** Navigation screenshots and intraoperative fluoroscopic images taken during fixation of the implant to the upper and lower vertebral bodies with screws. Navigation is used to plan the direction of each screw, particularly in the presence of posterior pedicular screws in adjacent levels, like in this case at L4–L5

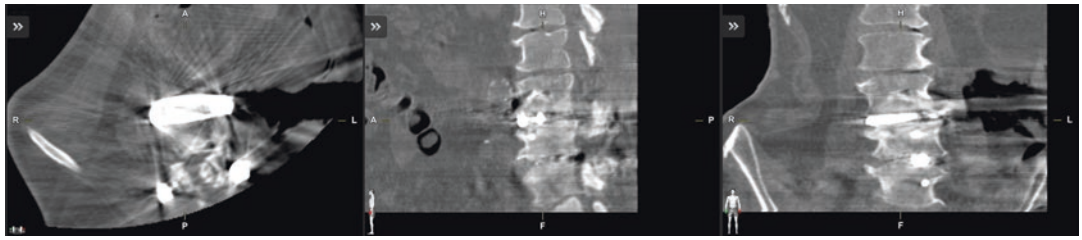

**Fig. 9.10** Control scan made with the mobile iCT after cage positioning at L3–L4

lateral approach surgery, including the transpsoas approach described in the present chapter.

The scanner usually translates from caudal to rostral and creates 3D images that are automatically registered and then transferred to a navigation workstation with a software specifically designed for spinal surgery (Brainlab Curve, Brainlab AG, Feldkirchen, Germany). Using special instruments that are pre-calibrated, like a navigation pointer, and a drill guide, the surgeon is able to plan the surgical incision, evaluate the correct trajectory to the target disc space and measure any implant that needs to be positioned, like an interbody cage or a screw.

At the end of the procedure, the iCT allows for an immediate survey of interbody cage positioning. In case of misplacement, the surgeon is able to correct the position. As a general rule, we perform a scan of the region of interest (ROI) after any changement in the position of the implant.

Moreover, similar to what happens with cone-beam CT devices, like the O-arm® (Medtronic Sofamor Danek, Memphis, TN), the OR staff is not exposed to radiation. The use of the ICT however could be associated with an increase in radiation exposure for patients during the procedure. Even if a previous comparative study [16] did not show higher radiation exposure for patients with the use of a mobile iCT compared to a cone-beam CT during posterior screw fixation of thoracolumbar spine, more studies focusing on the lateral approach are needed.

### 9.2.3 IONM Tools

IONM, based on sEMG, triggered EMG (tEMG) and MEPs, is used during a surgical procedure to identify neural elements and detect inadvertent injury.

Registration leads are placed at different muscles that are representative of the femoral nerve, genitofemoral nerve, and ilioinguinal and ilioipogastric nerves. These include vastus medialis, vastus lateralis, tibialis anterior, tight adductor at both sides, cremaster muscle in men, inguinal muscle in women, and external oblique abdominal muscle ipsilateral to the approach side. Muscle of thenar eminence of both hands is registered too, to have a control parameter.

Stimulation electrodes are placed on the scalp in C3–4 and C1–2 positions (based on the international 10–20 system electroencephalography scalp electrodes position). In our experience, SSEPs are not reliable in this surgery. Some authors advocated the use of saphenous SSEPs, which is unfortunately difficult to read and interpreted [45].

Triggered electromyography (tEMG) has been proven to be particularly useful during the lateral transpsoas approach to the spine [4, 46]. This technique uses a direct electrical stimulation on a nerve ("mapping" technique) to elicit responses in distal muscles and can provide surgeons rapid information about the proximity of neural structures, particularly when the psoas muscle has to be dissected to identify the target disc. Previous studies demonstrated that a direct stimulation on a healthy nerve elicits a distal response at approximately 2 mA [46].

The mapping technique can help to confirm the correct entry point through the psoas muscle already defined by navigation. As the accuracy of navigation is extremely high in our experience, in most cases the mapping does not change the surgeon's choice of entry point through the psoas

muscle. However, the use of tEMG must be considered as a real-time, intraoperative measure to reduce errors in case of navigation inaccuracy or in the presence of anatomical variabilities.

As previously described by other authors [47, 48], we use a threshold of 1–5 mA as a value that indicates close proximity to a nerve, and a threshold greater than 10 mA as a safe value to be considered distant from the nerve.

The genitofemoral nerve can be occasionally seen on the psoas muscle surface, at L3–4 level, and its direct stimulation gives answer only on cremasteric/inguinal muscle. This is useful to be sure to confirm the location of this nerve. If this nerve is visible much more attention in its mobilization should be taken to avoid damage.

MEPs are not delivered continuously because of the high intensity needed to induce inferior limb muscles response, which may provoke movements of the patient and disturb the surgeon during delicate phases, eventually reducing navigation accuracy. In our institution, MEPs are tested at different stages: before skin incision after lateral patient positioning, after the mapping of the entry zone in psoas muscle, after retractor positioning, after interbody implant positioning, after any change in retractor or cage positioning, and before skin closure. Once the psoas has been dissected and the retractor positioned, sEMG is used throughout the procedure. Responses like burst trains and discharges, that reflect severe irritation to a neural structure due to traction or manipulation, are communicated to the surgeon. In those cases, it is our practice to reposition the retractor confirming its position with navigation, and to repeat a mapping of the surgical field.

Moreover, an MEPs loss or a persistent amplitude change superior to 50% after retractor positioning is always reported to the surgeon, who is asked to exclude a change in retractor position.

In general, during a lateral transpsoas approach every attempt should be made to reduce the total time of distraction through the muscle. In our experience, the reduction of MEPs response is not directly correlated with a postoperative motor deficit, but a loss of one or two muscles innervated by the same nerve (i.e., femoral nerve) is a negative prognostic factor.

### 9.2.4 Postoperative Management

Patients are usually mobilized on first postoperative day and a standing X-ray of the lumbar spine is performed the same day or the day after. Postoperative pain is managed with anti-inflammatory drugs and muscle spasms are treated with muscle relaxants. Side effects of the approach may include thigh pain and hip flexion weakness due to psoas irritation and sensory changes in the anterior thigh and groin region. All these effects, in our experience, typically resolve within 3 months. A recent qualitative retrospective analysis of more than 100 patients reported a complete resolution of pain, strength, and sensation changes within 3 months after the procedure in 84.1% of patients and within 6 months in 93.2% [49]. Patients are discharged home after a complete evaluation from a physical therapist and in case of normal bowel function. Follow-up includes clinical evaluations at 1, 3, 6, and 12 months. A lumbar CT scan is performed at 6 and 12 months.

## 9.3 Outcomes

One of the main reasons for the increasing use of LLIF is the higher fusion rate that has been described compared to standard posterior approaches (?). Berjano et al. [50] reported a 97.4% rate of fusion, assessed with lumbar CT scan with a mean follow-up of 34.5 months, while Rodgers et al. [51] reported a rate of 97% at 12 months. Improvements in lumbar pain and disability as reported in the literature are also considerable [51].

Moreover, the technique has been shown to be effective in cases of spondylolisthesis [52] and also capable to obtain a good correction of sagittal and coronal imbalance in complex deformity cases [53, 54].

One of the main advantages of the technique consists in its power to provide a solid anterior support without any disruption of the posterior tension band [55]. Several supplemental fixation materials, like posterior pedicular screws, facet screws, or plate fixation can also be applied and integrated into the approach.

In recent years, LLIF has been proposed also for patients with central canal stenosis. This condition was initially considered a contraindication by some authors [4], while others recommended leaving posterior decompression to the surgeon's choice [55]. In a prospective study on 21 patients with central and foraminal stenosis, Oliveira et al. [56] looked at the ability of lateral interbody fusion to indirectly decompress neural structures. They noted substantial dimensional improvement on all radiographic parameters with stand-alone XLIF, even if indirect decompression was less effective in patients with congenital stenosis or locked facets.

In a recent retrospective study, Beng et al. [57] evaluated the effect of indirect neural decompression with lateral interbody fusion through a prepsoas approach in adult patients with spinal deformity. The authors reported greater improvement with indirect decompression in patients with more severe central stenosis and higher lumbar lordosis, concluding that indirect neural decompression has not to be limited by the severity of spinal stenosis and should be considered an option in place of conventional direct neural decompression.

Newer manufacturing technologies in recent years have led to the development of a new generation of expandable cages, like the one described in the present chapter, that are suited to be positioned from a lateral approach. Theoretical advantages of using an expandable implant are the possibility to position the implant through a smaller window, to increase disc and foraminal height, and to obtain a more effective indirect decompression in cases of central stenosis. Previous retrospective studies [58, 59] have already demonstrated the impact of these particular features in patients submitted to minimally invasive TLIF, even if a recent review of the literature [60] showed limited evidence directly comparing postsurgical outcomes of expandable and static devices.

Future prospective investigations comparing outcomes of expandable and static devices following lateral lumbar interbody fusion are required.

## 9.4 Complications

LLIF, as any retroperitoneal approach, comes with the risk of vascular and visceral injuries. The risk of vascular injuries reported in the literature ranges from 0.10% to 0.56%, compared to 3% in ALIF [53, 61, 62]. On the other hand, the rate of visceral injuries is very low in LLIF (0.08% reported in a large retrospective series [62], compared to 1.6% in ALIF [63]) and mostly due to inadequate release and anterior mobilization of the peritoneum, making an injury possible as the initial dilator and guidewire are passed through the psoas muscle. On the other hand, the risk of retrograde ejaculation in men, reported in 2% of cases in retroperitoneal and 25% in laparoscopic ALIF [53], is absent in LLIF.

Abdominal wall hernia has been reported in the literature as a rare event and is generally due to a lesion of subcostal nerves during initial exposure and consecutive possible muscle atrophy (?). A blunt dissection of the abdominal wall muscle is therefore recommended.

Specific complications of LLIF are mainly peripheric neurological and due to potential lesion of the lumbar plexus located between the psoas muscle fibers during the approach. Based on an anatomical study by Moro et al. [38], it is possible to encounter the femoral nerve mostly below the L4–5 level, while the genitofemoral nerve cross from posterior to anterior and from deep to surface of psoas muscle at level L3–4. A lesion to the genitofemoral nerve is generally due to an inadvertent erroneous positioning of the retractor during the approach and may happen very rarely. In most cases, the nerve, along with the femoral nerve that usually remains posterior to the retractor, is submitted to a tension during the expansion of the minimally invasive retractor. This causes a typical thigh numbness (which involves both sensory territory of genitofemoral and femoral nerve, the medial and lateral part of thigh, respectively) in the immediate postoperative period. In the literature, this transient sensory deficit is reported in 0.7% to 30% of cases [8, 64–66].

The risk of motor deficits, in the majority of literature reported without differentiation in hip

flexion and thigh muscles, ranges instead from 3.4% to 23.7% [53, 66].

While a clear qualitative description of postoperative neurological complications after LLIF appears to be now clear, being the obvious consequence of a partial or complete lesion to branches of the lumbar plexus, the time to obtain a resolution of these symptoms has not been investigated.

Nunley et al. [49] recently conducted a prospective analysis to characterize adverse postoperative neurological changes after transpsoas approach, and compared provider reported changes to patients reported. One-hundred-fifteen subjects were included: the authors reported objective neurological exam changes in 14.8% of subjects, all resolved between 6 weeks and 3 months. Approximately 20% of patients reported thigh pain, which was resolved in all cases at 3 months, while 38% of patients reported hip flexion or extension weakness, which resolved in more than 90% of cases at 6 months.

The variability in the rate of postoperative neurological deficits that is described in the literature seems to correlate with at least two factors. First of all, good anatomical knowledge and surgeons experience, which induces the choice of a safer surgical corridor, the reduction in time of surgery and therefore the time of psoas retraction, that has been correlated with the risk of postoperative distal motor weakness [67]. Periodic posterior blade stimulation has also been advocated by some authors to reduce this risk [67]. In our institution, the use of iCT navigation allows for an intraoperative planification of the exact entry point through the psoas (the "safe zone"), avoiding any manipulation of the posterior one-third of the muscle, where motor nerves are located [55]. Moreover, the use of iCT and the reduction of surgical time avoids any extensive or unnecessary retraction to the muscle.

## 9.5 General Considerations

In our opinion, the biggest advantages of using iCT 3D spinal navigation during LLIF are to improve the accuracy of the procedure and to widen the indications (e.g., obese patients). Moreover, the choice of the safe zone during transpsoas approach is the fundamental step in LLIF surgery. This zone can be difficult to identify in lateral position only with X-ray, and anatomical variabilities can also increase this task. iCT 3D spinal navigation helps the surgeon to have a better understanding of patient anatomy in real time.

The correct positioning of the distractor also plays a fundamental role in reducing neurological damage and in positioning the interbody cage correctly. In some situations, depending on patient's anatomy, BMI, and individual pathology, choosing the ideal position could be difficult under X-ray control, even with the guidance of tEMG, and repositioning always brings a higher risk of lumbar plexus damage. iCT 3D spinal navigation can be safely used in all these circumstances, making the approach safer and also reducing the radiation exposure for the surgical team.

Intraoperative CT 3D navigation gives also the advantage of precisely planning the dimensions of the cage and verifying the cage position at the end of the procedure, potentially reducing the risk of non-fusion and subsidence.

## 9.6 Conclusion

The mini-open lateral transpsoas approach is an effective technique that provides minimally invasive lumbar interbody fusion and indirect decompression of spinal canal and foramens. Its inherent risks, related to the anatomical relationships between the target discs and the lumbar plexus, can be significantly reduced with the use of spinal navigation coupled with an intraoperative mobile CT.

## 9.7 Summary

Thanks to an easier surgical corridor and the possibilities to treat a wider spectrum of lumbar spine pathologies compared to ALIF, resulting at the same time in comparable high fusion rates,

the use of lumbar lateral interbody fusion has significantly increased in the last decade, resulting at the same time in comparable high fusion rates.

However, even if the risk of vascular and visceral damage is reported to be lower than in ALIF, the risk of postoperative neurological deficit due to lumbar plexus injuries is still considerable, even with the introduction of intraoperative neuromonitoring.

Intraoperative planning and identification of the safer surgical corridor through the psoas is one of the crucial aspects to reduce neurological risk.

Intraoperative CT coupled with spinal navigation provides:

- A more precise real-time surgical trajectory planning and verification in 3D, with any anatomical variances, reducing the mispositioning of the retractor and possibly the risk of neurological deficits.
- Real-time planning of the cage dimension, controlled cage positioning and verification on CT scan, reducing the rate of mispositioning and reposition of the cage, and possibly the risk of subsidence.
- Reduction of radiation exposure for the surgical team.

## References


1. Pimenta L. Lateral endoscopic transpsoas retroperitoneal approach for lumbar spine surgery. VIII Brazilian Spine Soc. Meet. 2001 - Belo Horizonte, Minas Gerais Brazil.
2. Bergey DL, Villavicencio AT, Goldstein T, Regan JJ. Endoscopic lateral transpsoas approach to the lumbar spine. Spine (Phila Pa 1976). 2004;29:1681–8.
3. Pimenta L. Approach retroperitoneal endoscopic transpsoas of the lumbar spine. 2004;18(3):91-95. Acta Ortop Mex. 2004;18(3):91–5.
4. Ozgur BM, Aryan HE, Pimenta L, Taylor WR. Extreme Lateral Interbody Fusion (XLIF): a novel surgical technique for anterior lumbar interbody fusion. Spine J. 2006;6:435–43.
5. Elowitz EH, Yanni DS, Chwajol M, Starke RM, Perin NI. Evaluation of indirect decompression of the lumbar spinal canal following minimally invasive lateral transpsoas interbody fusion: radiographic and outcome analysis. Minim Invasive Neurosurg. 2011;54:201–6.
6. Salzmann SN, Fantini GA, Okano I, Sama AA, Hughes AP, Girardi FP. Mini-open access for lateral lumbar interbody fusion indications, technique, and outcomes. JBJS Essent Surg Tech. 2019;9:1–10.
7. Uribe JS, Arredondo N, Dakwar E, Vale FL. Defining the safe working zones using the minimally invasive lateral retroperitoneal transpsoas approach: an anatomical study. J Neurosurg Spine. 2010;13:260–6.
8. Rodgers WB, Gerber EJ, Patterson J. Intraoperative and early postoperative complications in extreme lateral interbody fusion: an analysis of 600 cases. Spine (Phila Pa 1976). 2011;36:26–32.
9. Assina R, Majmundar NJ, Herschman Y, Heary RF. First report of major vascular injury due to lateral transpsoas approach leading to fatality. J Neurosurg Spine. 2014;21:794–8.
10. Acosta FL, Drazin D, Liu JC. Supra-psoas shallow docking in lateral interbody fusion. Neurosurgery. 2013;73:48–52.
11. Kosmopoulos V, Schizas C. Pedicle screw placement accuracy: a meta-analysis. Spine (Phila Pa 1976). 2007;32:E111–20.
12. Tian N-F, Xu H-Z. Image-guided pedicle screw insertion accuracy: a meta-analysis. Int Orthop. 2009;33:895–903.
13. Shin BJ, James AR, Njoku IU, Härtl R. Pedicle screw navigation: a systematic review and meta-analysis of perforation risk for computer-navigated versus freehand insertion. J Neurosurg Spine. 2012;17:113–22.
14. Shimokawa N, Takami T. Surgical safety of cervical pedicle screw placement with computer navigation system. Neurosurg Rev. 2017; https://doi.org/10.1007/s10143-016-0757-0.
15. Cordemans V, Kaminski L, Banse X, Francq BG, Detrembleur C, Cartiaux O. Pedicle screw insertion accuracy in terms of breach and reposition using a new intraoperative cone beam computed tomography imaging technique and evaluation of the factors associated with these parameters of accuracy: a series of 695 screws. Eur Spine J. 2017;26:2917–26.
16. Scarone P, Vincenzo G, Distefano D, Del Grande F, Cianfoni A, Presilla S, Reinert M. Use of the Airo mobile intraoperative CT system versus the O-arm for transpedicular screw fixation in the thoracic and lumbar spine: a retrospective cohort study of 263 patients. J Neurosurg Spine. 2018;29:397–406.
17. Richter M, Cakir B, Schmidt R. Cervical pedicle screws: conventional versus computer-assisted placement of cannulated screws. Spine (Phila Pa 1976). 2005;30:2280–7.
18. Ito H, Neo M, Yoshida M, Fujibayashi S, Yoshitomi H, Nakamura T. Efficacy of computer-assisted pedicle screw insertion for cervical instability in RA patients. Rheumatol Int. 2007;27:567–74.
19. Laine T, Lund T, Ylikoski M, Lohikoski J, Schlenzka D. Accuracy of pedicle screw insertion with and without computer assistance: a randomised controlled clinical study in 100 consecutive patients. Eur Spine J. 2000;9:235–40.

20. Rajasekaran S, Vidyadhara S, Ramesh P, Shetty AP. Randomized clinical study to compare the accuracy of navigated and non-navigated thoracic pedicle screws in deformity correction surgeries. Spine (Phila Pa 1976). 2007;32:E56–64.
21. Xiao R, Miller JA, Sabharwal NC, Lubelski D, Alentado VJ, Healy AT, Mroz TE, Benzel EC. Clinical outcomes following spinal fusion using an intraoperative computed tomographic 3D imaging system. J Neurosurg Spine. 2017;26:628–37.
22. Villard J, Ryang YM, Demetriades AK, Reinke A, Behr M, Preuss A, Meyer B, Ringel F. Radiation exposure to the surgeon and the patient during posterior lumbar spinal instrumentation: a prospective randomized comparison of navigated versus non-navigated freehand techniques. Spine (Phila Pa 1976). 2014;39:1004–9.
23. Gertzbein SD, Robbins SE. Accuracy of pedicular screw placement in vivo. Spine (Phila Pa 1976). 1990;15:11–4.
24. Heary RF, Bono CM, Black M. Thoracic pedicle screws: postoperative computerized tomography scanning assessment. J Neurosurg. 2004;100:325–31.
25. Bydon M. Safety and efficacy of pedicle screw placement using intraoperative computed tomography: consecutive series of 1148 pedicle screws. J Neurosurg Spine. 2014;21:320–8.
26. Verma R, Krishan S, Haendlmayer K, Mohsen A. Functional outcome of computer-assisted spinal pedicle screw placement: a systematic review and meta-analysis of 23 studies including 5,992 pedicle screws. Eur Spine J. 2010;19:370–5.
27. Epstein N. Commentary: utility of the O-Arm in spinal surgery. Surg Neurol Int. 2014;5:517.
28. Khanna AR, Yanamadala V, Coumans J-V. Effect of intraoperative navigation on operative time in 1-level lumbar fusion surgery. J Clin Neurosci. 2016;32:72–6.
29. Kochanski RB, Alahmadi H, O'Toole JE. Image guidance in minimally invasive spine surgery. In: Minim. Invasive Spine Surg. Cham: Springer International Publishing; 2019. p. 83–92.
30. Webb JE, Regev GJ, Garfin SR, Kim CW. Navigation-assisted fluoroscopy in minimally invasive direct lateral interbody fusion: a cadaveric study. SAS J. 2010;4:115–21.
31. Drazin D, Liu JC, Acosta FL Jr. CT navigated lateral interbody fusion. J Clin Neurosci. 2013;20:1438–41.
32. Park P. Three-dimensional computed tomography-based spinal navigation in minimally invasive lateral lumbar interbody fusion: feasibility, technique, and initial results. Neurosurgery. 2015;11(Suppl 2):259–67.
33. Joseph JR, Smith BW, Patel RD, Park P. Use of 3D CT-based navigation in minimally invasive lateral lumbar interbody fusion. J Neurosurg Spine. 2016;25:339–44.
34. Jiang J, Gan F, Tan H, Xie Z, Luo X, Huang G, Li Y, Huang S. Effect of computer navigation-assisted minimally invasive direct lateral interbody fusion in the treatment of patients with lumbar tuberculosis: a retrospective study. Medicine (Baltimore). 2018;97:e13484.
35. Strong MJ, Yee TJ, Khalsa SSS, Saadeh YS, Swong KN, Kashlan ON, Szerlip NJ, Park P, Oppenlander ME. The feasibility of computer-assisted 3D navigation in multiple-level lateral lumbar interbody fusion in combination with posterior instrumentation for adult spinal deformity. Neurosurg Focus. 2020;49:1–8.
36. Yu JYH, Fridley J, Gokaslan Z, Telfeian A, Oyelese AA. Minimally invasive thoracolumbar corpectomy and stabilization for unstable burst fractures using intraoperative computed tomography and computer-assisted spinal navigation. World Neurosurg. 2019;122:e1266–74.
37. Meyerding HW. Spondylolisthesis; surgical fusion of lumbosacral portion of spinal column and interarticular facets; use of autogenous bone grafts for relief of disabling backache. J Int Coll Surg. 1956;26:566–91.
38. Moro T, Kikuchi S, Konno S, Yaginuma H. An anatomic study of the lumbar plexus with respect to retroperitoneal endoscopic surgery. Spine (Phila Pa 1976). 2003;28:423–7.
39. Hu WK, He SS, Zhang SC, Liu YB, Li M, Hou TS, Ma XL, Wang J. An MRI study of psoas major and abdominal large vessels with respect to the X/DLIF approach. Eur Spine J. 2011;20:557–62.
40. Buric J. Relationship between psoas muscle dimensions and post operative thigh pain. A possible preoperative evaluation factor. Int J Spine Surg. 2015;9:27.
41. Buckland AJ, Beaubrun BM, Isaacs E, et al. Psoas morphology differs between supine and sitting magnetic resonance imaging lumbar spine: implications for lateral lumbar interbody fusion. Asian Spine J. 2018;12:29–36.
42. Quinn JC, Fruauff K, Lebl DR, Giambrone A, Cammisa FP, Gupta A, Chazen JL. Magnetic resonance neurography of the lumbar plexus at the L4–L5 disc. Spine (Phila Pa 1976). 2015;40:942–7.
43. Luís A, Navarro-Ramirez R, Kirnaz S, Nakhla J, Härtl R. Navigated spinal fusion. In: Minim. Invasive spine surg. Cham: Springer International Publishing; 2019. p. 355–74.
44. Habib N, Filardo G, Distefano D, Candrian C, Reinert M, Scarone P. Use of intraoperative CT improves accuracy of spinal navigation during screw fixation in Cervico-Thoracic Region. Spine (Phila Pa 1976). 2020;45:1–9.
45. Silverstein J, Mermelstein L, DeWal H, Basra S. Saphenous nerve somatosensory evoked potentials. Spine (Phila Pa 1976). 2014;39:1254–60.
46. Gupta M, Taylor SE, O'Brien RA, Taylor WR, Hein L. Intraoperative neurophysiology monitoring. In: Minim. Invasive spine surg. Cham: Springer International Publishing; 2019. p. 69–81.
47. Uribe JS, Vale FL, Dakwar E. Electromyographic monitoring and its anatomical implications in minimally invasive spine surgery. Spine (Phila Pa 1976). 2010;35:S368–74.

48. Tohmeh AG, Rodgers WB, Peterson MD. Dynamically evoked, discrete-threshold electromyography in the extreme lateral interbody fusion approach. J Neurosurg Spine. 2011;14:31–7.
49. Nunley PD, Hill CP, Strenge KB, Malloy J (Sean) P, Kunwar S, Stone M (2020) A prospective, in-depth analysis of perioperative anterior thigh symptoms associated with a direct lateral access approach for lumbar interbody fusion. Spine J 20:S21–S22.
50. Berjano P, Langella F, Damilano M, Pejrona M, Buric J, Ismael M, Villafañe JH, Lamartina C. Fusion rate following extreme lateral lumbar interbody fusion. Eur Spine J. 2015;24:369–71.
51. Rodgers WB, Gerber EJ, Patterson JR. Fusion after minimally disruptive anterior lumbar interbody fusion: analysis of extreme lateral interbody fusion by computed tomography. SAS J. 2010;4:63–6.
52. Rodgers WB, Lehmen JA, Gerber EJ, Rodgers JA. Grade 2 spondylolisthesis at L4–5 treated by XLIF: safety and midterm results in the "worst case scenario". ScientificWorldJournal. 2012;2012:356712.
53. Xu DS, Walker CT, Godzik J, Turner JD, Smith W, Uribe JS. Minimally invasive anterior, lateral, and oblique lumbar interbody fusion: a literature review. Ann Transl Med. 2018;6:104.
54. Arnold P, Anderson K, McGuire R. The lateral transpsoas approach to the lumbar and thoracic spine: a review. Surg Neurol Int. 2012;3:198.
55. Chomba D, Rodgers WC, Rodgers WB. Minimally disruptive lateral transpsoas approach for thoracolumbar anterior interbody fusion. In: Minim. Invasive Spine Surg. Cham: Springer International Publishing; 2019. p. 277–315.
56. Oliveira L, Marchi L, Coutinho E, Pimenta L. A radiographic assessment of the ability of the extreme lateral interbody fusion procedure to indirectly decompress the neural elements. Spine (Phila Pa 1976). 2010;35(26 Suppl):S331–7. https://doi.org/10.1097/BRS.0B013E3182022DB0.
57. Beng TB, Kotani Y, Sia U, Gonchar I. Effect of indirect neural decompression with oblique lateral interbody fusion was influenced by preoperative lumbar lordosis in adult spinal deformity surgery. Asian Spine J. 2019;13:809–14.
58. Kim CW, Doerr TM, Luna IY, Joshua G, Shen SR, Fu X, Wu AM. Minimally invasive transforaminal lumbar interbody fusion using expandable technology: a clinical and radiographic analysis of 50 patients. World Neurosurg. 2016;90:228–35. https://doi.org/10.1016/J.WNEU.2016.02.075.
59. Kucharzyk DW, Miller LE. Two-year clinical and radiographic results with a multidimensional, expandable interbody implant in minimally invasive lumbar spine surgery. Cureus. 2020;12:e7070.
60. Jenkins NW, Parrish JM, Khechen B, Block AM, Lalehzarian SP, Brundage T, Hrynewycz N, Iyer S, Singh K. Outcomes of expandable interbody devices in lumbar fusion: a systematic review and meta-analysis. Clin Spine Surg. 2020;33(6):230–43. https://doi.org/10.1097/BSD.0000000000000959.
61. Kueper J, Fantini GA, Walker BR, Aichmair A, Hughes AP. Incidence of vascular complications during lateral lumbar interbody fusion: an examination of the mini-open access technique. Eur Spine J. 2015;24:800–9.
62. Uribe JS, Deukmedjian AR. Visceral, vascular, and wound complications following over 13,000 lateral interbody fusions: a survey study and literature review. Eur Spine J. 2015;24:386–96.
63. Rajaraman V, Vingan R, Roth P, Heary RF, Conklin L, Jacobs GB. Visceral and vascular complications resulting from anterior lumbar interbody fusion. J Neurosurg Spine. 1999;91:60–4.
64. Abel NA, Januszewski J, Vivas AC, Uribe JS. Femoral nerve and lumbar plexus injury after minimally invasive lateral retroperitoneal transpsoas approach: electrodiagnostic prognostic indicators and a roadmap to recovery. Neurosurg Rev. 2017;41:457–64.
65. Houten JK, Alexandre LC, Nasser R, Wollowick AL. Nerve injury during the transpsoas approach for lumbar fusion. J Neurosurg Spine. 2011;15:280–4.
66. Lehmen JA, Gerber EJ. MIS lateral spine surgery: a systematic literature review of complications, outcomes, and economics. Eur Spine J. 2015;24:287–313.
67. Uribe JS, Isaacs RE, Youssef JA, Khajavi K, Balzer JR, Kanter AS, Küelling FA, Peterson MD. Can triggered electromyography monitoring throughout retraction predict postoperative symptomatic neuropraxia after XLIF? Results from a prospective multicenter trial. Eur Spine J. 2015;24:378–85.

# Part II

# Navigation Guided MIS Decompressive Spinal Surgery

# Navigation Guided MIS Tubular Decompression in Cervical Spine

10

Kutbuddin Akbary and Jin-Sung Kim

## 10.1 Introduction

MIS surgery has been defined by the AO Foundation as an approach to spine surgery that helps in reducing muscle damage, blood loss, and postoperative pain [1]. With the advent of newer instruments and imaging technologies, the application of MIS approaches to all areas of spine, both pathologically and anatomically, has expanded at an enormous pace. The presence of real-time image guidance and navigation capabilities along with the computing ability to process and reconstruct these data into an interactive three-dimensional spinal "model" has helped improve the precision targeting of specific anatomical structures with minimal collateral damage to the surrounding tissues. Emphasis can now be laid on decreasing postoperative morbidity and faster recovery times due to the inherent surgical advantages as described in the definition of MIS surgery. One of the areas it has expanded into is the cervical spine.

Posterior cervical microforaminotomy (PCM) for decompression of cervical nerve roots is a well-established procedure among operative treatments for degenerative cervical spine diseases associated with radiculopathy. It is mainly reserved for posterolateral soft discs causing unilateral upper limb radiculopathy not amenable to treatment via conservative methods. It was first described by Spurling and Scoville [2] and Frykholm in 1947 [3] and was further modified by Scoville et al. in 1951 [4].

After the description of the Smith-Robinson anterior approach to the cervical spine for discectomy and fusion, posterior foraminotomy approach was restricted in its use. But there has been recent renewal of interest in the posterior foraminotomy surgical technique, both in part to its avoidance of fusion and approach related morbidity and the improvement in precision targeting of anatomical structures in the cervical spine via intra-operative navigation assistance. Cost-analysis studies also favour posterior foraminotomy over ACDF [5, 6].

Nevertheless, the anterior approach is associated with risk of injury to the oesophagus, trachea, carotid artery, jugular vein, recurrent laryngeal nerve, superior laryngeal nerve, and thoracic duct. Moreover, the sacrifice of motion with anterior cervical fusion predisposes patients to accelerated degeneration of adjacent motion

**Supplementary Information** The online version contains supplementary material available at [https://doi.org/10.1007/978-981-19-0175-1_10].

K. Akbary
Pushpawati Singhania Research Institute (PSRI), Press Enclave Marg, Sheikh Sarai, New Delhi, India

J.-S. Kim (✉)
Department of Neurosurgery, Seoul St Mary's Hospital, The Catholic University of Korea, College of Medicine, Seoul, Korea (Republic of)



J.-S. Kim et al. (eds.), *Technical Advances in Minimally Invasive Spine Surgery*,
https://doi.org/10.1007/978-981-19-0175-1_10

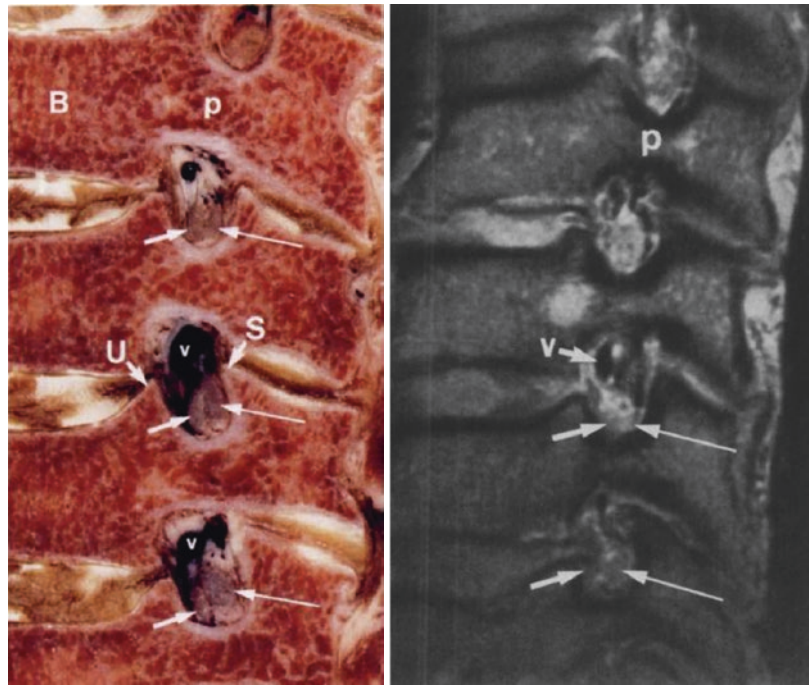


**Fig. 10.1** 45° sagittal oblique sections at the level of the foramen (Comparison of anatomical specimen and MRI T1-weighted image). *B* vertebral body, *p* pedicle, *U* uncinate process, *S* superior articular process, *v* transforaminal veins. The nerve roots (dorsal and ventral roots) are depicted by the short and long arrows, respectively [10]

segments. These risks are clearly avoided with the posterior approach.

The minimal invasiveness of the tubular retractor system, such as the METRx system (Medtronic Sofamor Danek, Memphis, TN) enables muscle-splitting dissection without the traditional extensive subperiosteal stripping of the paraspinal muscles in open posterior approaches which may lead to postoperative neck pain [7]. However, minimally invasive PCM (MI-PCM) may be difficult for obese patients with a short neck, especially in the lower cervical spine or the cervico-thoracic junction.

In this chapter, we will describe the surgical anatomy, indications and contraindications, and surgical technique of MI-PCM with intraoperative navigation guidance. Readers can also go through these articles previously published for further reference [8, 9].

## 10.2 Anatomical Considerations

The cervical foramen is bounded by the inferior aspect of the cranial vertebral pedicle to the superior aspect of the pedicle of the caudal vertebra. The anterior wall of the foramina is formed by the uncinate process, the posterolateral aspect of the intervertebral disc, and the adjoining vertebral body. The posterior wall of the foramen is formed by the facet joint and superior articular process of the caudal vertebra. The nerve root enters from the medial margins of the cranial and caudal pedicles and exits the foramen at the lateral margins of the cranial and caudal pedicles. The nerve foramen exits obliquely at 45° from the sagittal plane. In the sagittal oblique plane, the nerve roots are seen to lie below a line drawn from the tip of the uncinate process to the tip of the superior articular process (Fig. 10.1) [10].

When approaching the foramen posteriorly, the most important landmark to visualise is the laminofacet junction, which is formed by the confluence of the inferior laminar margin of the cranial vertebra and the superior laminar margin of the caudal vertebra with the medial aspect of the facet joint (Fig. 10.2).

## 10.3 Indications

MI-PCM is mainly indicated for cases of lateralized disc herniation (prolapsed disc being lateral to the edge of the thecal sac) or for

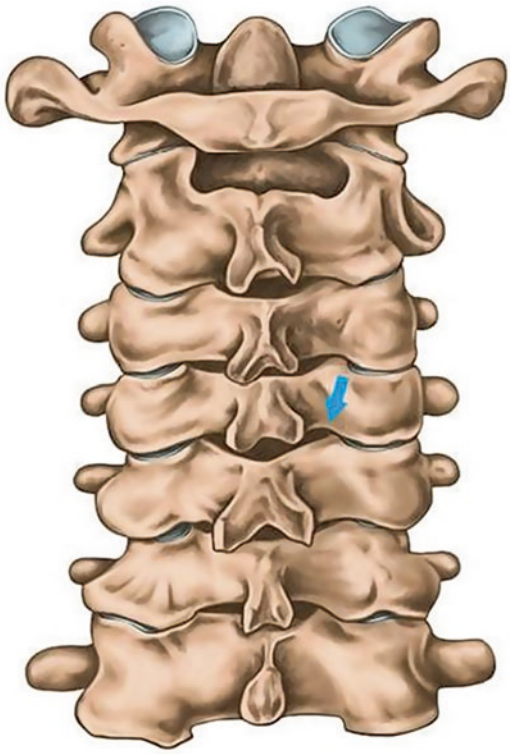

**Fig. 10.2** The laminofacet junction, depicted as the blue arrow, which is the junction of the inferior laminar margin of the cranial vertebra and the superior laminar margin of the caudal vertebra with the medial aspect of the facet joint

foraminal stenosis due to facet degeneration and osseoligamentous hypertrophy. Patients usually present with painful cervical radiculopathy. Their MRI findings correlate with the neurological findings in terms of sensory distribution patterns and, in some cases, motor deficits. Contraindications include pure axial neck pain without correlating neurologic symptoms, gross cervical instability on dynamic imaging, symptomatic large central disc herniation, anterior diffuse pathological processes such as ossification of posterior longitudinal ligament (OPLL), or a kyphotic cervical spine deformity that would make posterior decompression ineffective [11].

In cases of equivocal clinicoradiological findings, getting an EMG study and/or supplementing with a selective nerve root block can help in localising the levels at which the intervention is required.

## 10.4 Surgical Technique

### 10.4.1 Patient Positioning, Anaesthesia, and Operating Room Set-Up

The patient is positioned prone with the head in slight flexion with a Mayfield three-point fixation under adequate general anaesthesia. All the bony prominences are adequately padded. The whole procedure is monitored with somatosensory-evoked potentials (SSEP) and myotomal electromyography (EMG) (NIM-Spine System, Medtronic, Inc., Memphis, TN). Before draping, a spinal needle is inserted into the skin and a radiograph is obtained to locate the level that will be decompressed.

The operating room is set-up for an image-based navigation using the StealthStation Treon system (Medtronic Surgical Navigation Technologies, Louisville, CO) consisting of an infrared camera positioned at the caudal end of the surgical table with its monitor placed on the opposite side from the surgeon to facilitate visualisation during the procedure. The dynamic reference base (DRB) is attached over the cervico-thoracic junction or over the upper thoracic levels and contains passive markers that reflect light from the infrared light source integrated with the tracking camera system (Fig. 10.3).

As soon as surgical preparation is complete, with the patient's position fixed on the operating table, an intra-operative CT image set is obtained with the O-arm equipment (Medtronic, Inc., Memphis, TN) and transferred to the StealthStation Treon image guidance workstation, where it is automatically registered. The operative level is now again confirmed using the navigation system.

### 10.4.2 Surgical Procedure

With the aid of the sagittal CT and the fluoroscopy mode reconstructions aimed at the target facet joint and the axial CT views pointing over the laminofacet junction, the proper entry point is defined which is 1.5 cm away from the midline (Fig. 10.4). A 1.6- to 2.0-cm long incision is


**Fig. 10.3** Operating room setting. (**a**) Intra-operative CT scan being performed with O-arm; (**b**) navigation monitor; (**c**) Surgeon performing CT-guided navigation with dynamic reference base (DRB)

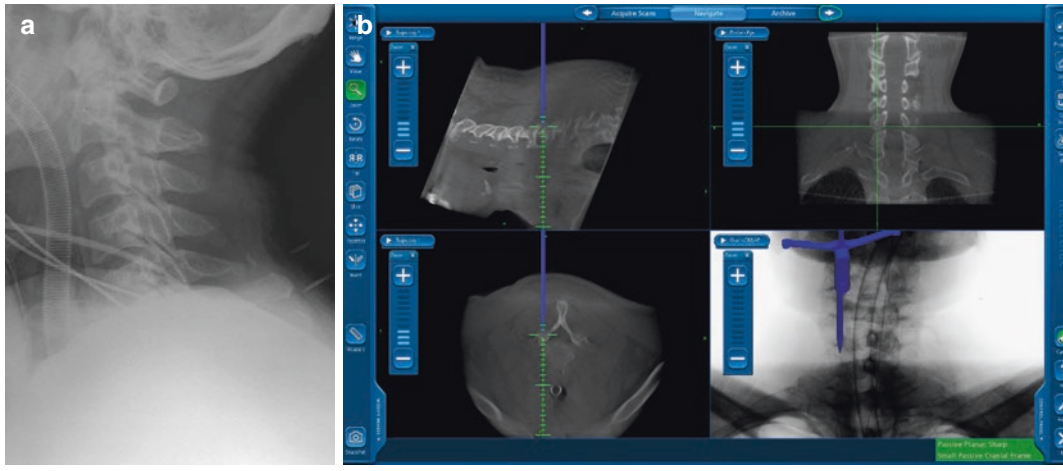


**Fig. 10.4** (**a**) Pre-operative radiograph showing the difficulty in finding the correct level (C6–7 level) for the surgical approach. (**b**) O-arm navigation images allowing proper localization of the level and laminofacet junction

made in the skin as well as the cervical fascia. For a two-level procedure, the incision is placed midway between the levels to be approached. Finger dissection is used to split the paravertebral muscles, then sequential dilators are serially inserted, and the METRx tubular retractor is placed over

the cortical bone at the laminofacet junction. It is imperative to land on bone and avoid penetrating the interlaminar space, as the lateral ligamentum flavum is thinned out and may lead to iatrogenic dural or spinal cord injury.

At this point, it is necessary to check the matching accuracy between the patient's anatomy and the images provided by the navigation system on the monitor. For this purpose, specific osseous landmarks inside the operative field are selected as references with the pointer probe and are then compared to decide if safe navigation is possible. If the accuracy is not acceptable, the matching procedure must be repeated. Once the proper level has been reconfirmed with navigation, the METRx retractor is fixed in the selected position with a table-mounted flexible retractor arm. All surgical procedures following the positioning of the tubular retractor are performed under the operating microscope.

Remaining soft tissues are cleared from the field, so that the facet joint, both ipsilateral lateral masses and laminofacet junction, can be viewed satisfactorily. Subsequently, the pointer probe is used to determine the shape and size of the drill hole according to the pre-operative plan. A 4-mm diamond burr with a high-speed drill is preferred both to provide some safety for neural structures and for its hemostatic effect on the bone. In cases where only a small foraminotomy is necessary, a 3-mm diamond burr can also be used instead. Bone removal begins with the lateral part of the superior and inferior hemilaminae and then progresses to the medial portion of the descending facet. The drilling continues until the entire medial aspect of the ascending facet is exposed. The opened foraminotomy defect is then checked again with the navigation probe to determine whether any adjustment is needed. Upto 50% of the facet joint can be drilled to make a foraminotomy hole without significantly affecting the stability of the cervical spine [12].

Subsequently, the ascending facet and the remaining hemilaminae are drilled until a thin layer of the deep cortical bone is visualized. Then, with a small 45° angled curette and a 1-mm Kerrison punch, the soft tissues covering the neural foramen and the lateral spinal canal are exposed. Using dissecting hooks and the same 1-mm Kerrison punch, the ligamentum flavum is removed from lateral to medial direction, and now the lateral dural sac as well as the nerve root can be seen. In the event of epidural bleeding, the source can be filled with gelatin foam embedded with a thrombin activator component or Floseal (Baxter Healthcare Corporation, Deerfield, IL). We discourage the frequent use of bipolar cauterization, and its use should be limited, keeping it in a low-intensity mode. After this, the features of the foraminotomy defect are reviewed visually, with a small probe to search for the cranial and caudal pedicles, and reconfirmed with the navigation probe. The disc space is then identified and the discectomy is done, either via fragmentectomy of the loose extruded fragment or via an annulotomy followed by a disc excision. Since the nerve root exits the thecal sac at roughly 45° angle, the bulk of the discectomy is done at the axilla of the nerve root. After the discectomy is completed, both the axilla and the shoulder of the nerve root are inspected with a blunt tip right-angled probe for any loose fragments and adequacy of decompression via gentle excursion of the nerve root in the foramen (see Video 1).

Care should be taken to avoid injuring the vertebral artery as the nerve root passes in close proximity to it laterally. Instruments should not be passed beyond the bony posterior margin of the foramen transversarium. The dense venous plexus surrounding the vertebral artery, if damaged, produces a brisk dark venous bleeding. This kind of bleeding can be construed as a useful warning to avoid further lateral dissection to prevent iatrogenic vertebral arterial injury.

To assure complete decompression of the nerve root, O-arm scanning is always performed in all cases at this point in the procedure. After this, we remove any residual compression in the foramen, whenever indicated. After checking that the decompression is adequate, the surgical wound is closed. During the follow-up period, a 3D CT scan can be done to evaluate the grade of laminofacet resection (Fig. 10.5).

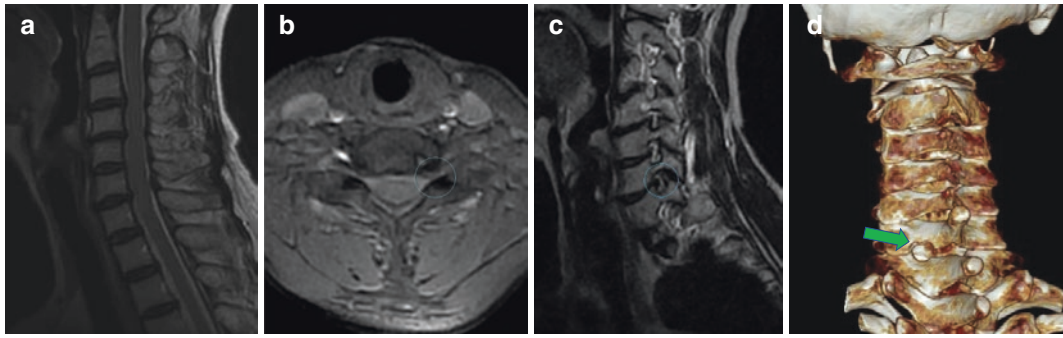


**Fig. 10.5** Pre-operative MRI (**a**, **b**, **c**) showing severe foraminal stenosis at C6–C7 level on the left side (circled). Post-operative posterior view of a 3D CT (**d**) scan showing the small keyhole for decompression of a C6–7 left foraminal stenosis and demonstrating adequate preservation of facet joints (arrow)

### 10.4.3 Post-operative Care

Most patients can be discharged and sent home within 24 h. Patients having spasmodic muscular neck pain due to surgical incision, or patients with residual paraesthesias in the upper limb, presumably due to nerve root handling, can be observed in the hospital setting for 1–2 days for adequate pain management. Anti-inflammatory medications can be prescribed as per institutional standards. Neuromodulatory drugs such as gabapentin or pregabalin can be added to help alleviate the residual mild radicular symptoms, if any.

Wound inspection is performed at post-operative day 3, with care being taken to exclude the presence of any signs of infection. Rapid mobilisation is promoted and physical therapy is started after wound healing. Use of soft collar is optional and depends on the surgeon's preference. No follow-up imaging is usually required.

### 10.4.4 Complications

This procedure is generally very safe, and complications reported are very few. One of the earliest reports by Adamson et al. [13] showed operative complications in 3 out of their 100 patients (two dural punctures needing no intervention and one superficial wound infection). A recent meta-analysis [14] has also reported lesser complication rates of MI-PCM compared to conventional ACDF (4% versus 7.8%).

The potential complications associated with MI-PCM are due to error in accurate localisation of the surgical level, especially in the lower cervical spine. This is one of the main advantages of using navigation, wherein the surgical level can be confirmed in real time with a very little margin of error.

Nerve root injury can occur due to its misidentification as a disc or due to its duplication, or both, or due to crowding of surgical instruments around the nerve root in a stenotic foramen. These risks may be avoided by fully visualizing the nerve root and then decompressing it. The surgeon should also look for signs of double roots at the index level on the pre-operative MRI.

Iatrogenic dural tears can generally be managed with dural sealants and usually resolve without complications in the post-operative period. Occasionally persistent leakage from a larger dural tear may require a lumbar drain along with a direct dural repair. Use of bipolar diathermy should be kept to a minimum, and a 45° angled diathermy probe may be more useful in coagulating the bleeding vessels from the foraminal venous plexus.

Post-operative instability can be avoided by evaluating the pre-operative dynamic X-rays, avoiding of bilateral surgery at the same level and preserving up to 50% of the facet joint [12]. Patients having a kyphotic spine or a straight spine may be better treated via an anterior approach with or without fusion.

As previously mentioned, intra-operative vertebral artery injury may occur if the facetectomy

followed by soft tissue dissection extends too far laterally. This can be avoided with the intra-operative O-arm navigation which can delineate the extent of foraminotomy and consequently avoid lateral extension of the foraminotomy. Pre-operative imaging should be carefully studied to detect any anatomical abnormalities of the vertebral artery.

Recurrence of radicular symptoms should be managed aggressively, as they may be indicative of incomplete decompression of the foramen, a nerve injury, or the presence of a post-operative epidural hematoma or an abscess. An intra-operative O-arm imaging can usually confirm the adequacy of decompression, and any residual osteophytes, if seen, can be removed before wound closure. A post-operative epidural hematoma or abscess should be evacuated surgically to relieve the compression.

## 10.5 Conclusion

MI-PCM assisted by O-arm-based navigation is a safe, effective, and minimally invasive procedure for the treatment of lateral disc herniations and foraminal stenosis of the lower cervical spine and C-T junction, offering the advantage of more accurate targeting of the pathology, avoidance of residual foraminal stenosis, and a reduced risk of segmental instability.

## References


1. Hartl R, Korge A. Minimally invasive spine surgery – techniques, evidence and controversies. 1st ed. New York: Georg Thieme; 2013.
2. Spurling RG, Scoville WB. Lateral rupture of the cervical intervertebral disc. A common cause of shoulder and arm pain. Surg Gynecol Obstet. 1944;798:350–8.
3. Frykholm R. Deformities of dural pouches and strictures of dural sheaths in the cervical region producing nerve-root compression: a contribution to the etiology and operative treatment of brachial neuralgia. J Neurosurg. 1947;4:403–13.
4. Scoville WB, Whitcomb BB, MacLaurin RL. The cervical ruptured disc: report of 115 operative cases. Trans Am Neurol Assoc. 1951;56:222–4.
5. Tumialán Luis M, Ponton Ryan P, Gluf Wayne M. Management of unilateral cervical radiculopathy in the military: the cost effectiveness of posterior cervical foraminotomy compared with anterior cervical discectomy and fusion. Neurosurg Focus. 2010;28(5):E17.
6. Witiw CD, Smieliauskas F, O'Toole JE, et al. Comparison of anterior cervical discectomy and fusion to posterior cervical foraminotomy for cervical radiculopathy: utilization, costs, and adverse events 2003-2014. Neurosurgery. 2018;5:1–8.
7. Won S, Kim CH, Chung CK, et al. Clinical outcomes of single-level posterior percutaneous endoscopic cervical foraminotomy for patients with less cervical lordosis. J Minim Invasive Spine Surg Tech. 2016;1(1):11–7.
8. Del Curto D, Kim JS, Lee SH. Minimally invasive posterior cervical microforaminotomy in the lower cervical spine and C-T junction assisted by O-arm-based navigation. Comput Aided Surg. 2013;18(3–4):76–83.
9. Zhang C, Wu J, Xu C, et al. Minimally invasive full-endoscopic posterior cervical foraminotomy assisted by O-arm-based navigation. Pain Physician. 2018;21(3):E215–23.
10. Czervionke LF, Daniels DL, Ho PS, et al. Cervical neural foramina: correlative anatomic and MR imaging study. Radiology. 1988;169(3):753–9.
11. O'Toole JE, Sheikh H, Eichholz KM, et al. Endoscopic posterior cervical foraminotomy and discectomy. Neurosurg Clin N Am. 2006;17:411–22.
12. Raynor RB, Pugh J, Shapiro I. Cervical facetectomy and its effect on spine strength. J Neurosurg. 1985;63(2):278–82.
13. Adamson TE. Microendoscopic posterior cervical laminoforaminotomy for unilateral radiculopathy:results of a new technique in 100 cases. J Neurosurg. 2001;95(1 Suppl):51–7.
14. Sahai N, Changoor S, Dunn CJ, et al. Minimally Invasive Posterior Cervical Foraminotomy as an Alternative to Anterior Cervical Discectomy and Fusion for Unilateral Cervical Radiculopathy: A Systematic Review and Meta-analysis. Spine (Phila Pa 1976). 2019;44(24):1731–9.

# 11 Navigation-Guided Tubular Decompression in the Lumbar Spine

Sertac Kirnaz, Basar Atalay, Jacob L. Goldberg, Branden Medary, Lynn McGrath, Fabian Sommer, and Roger Härtl

## 11.1 Introduction

Intraoperative navigation for spinal surgery has rapidly evolved since the turn of the century. With new functionalities supported by advancements in technology, its utility in a variety of surgical settings is expanding [1]. Navigation is widely used in lumbar spine surgery to assist in the placement of implants such as intervertebral cages/spacers and with percutaneous pedicle screw instrumentation [2–4]. Usage of intraoperative navigation for lumbar decompression-only surgery has been slowly adapted by spine surgeons for a variety of reasons including high purchase and maintenance costs of the intraoperative imaging technology, increased radiation exposure to the patient, and longer setup and OR turnover times [5–8]. In general, both open and MIS approaches for lumbar decompression surgery can be performed successfully without intraoperative navigation. Fluoroscopy is only required for localization of the surgical level, and the remainder of the procedure can be guided using anatomical landmarks. Nonetheless, utilization of intraoperative navigation can facilitate surgical workflow and provide benefits in certain clinical situations when performing traditional open, endoscopic, or tubular decompression in lumbar spine surgery [9–12].

In the literature, numerous case series were published showing favorable clinical outcomes via the utilization of intraoperative navigation guidance for lumbar decompression-only surgery [13–16]. In a prospective study in 2013, Sembrano et al. found intraoperative navigation using an O-arm to be helpful in assessing the adequacy of decompression of the lumbar spine in 38 patients [16]. In another study including 50 patients who underwent a MIS unilateral laminotomy with a crossover decompression, Cardali et al. demonstrated that a better control of the radicular symptoms was achieved when they used intraoperative 3D fluoroscopy and navigation to determine the degree of decompression [13]. They found a correlation between the extent of bone decompression and improvement in VAS and ODI scores. We have previously published a step-by-step surgical technique for the minimally invasive laminotomy for contralateral "over-the-top" foraminal decompression using a portable intraoperative computed tomography scanner [15]. Several other authors have demonstrated the advantages

S. Kirnaz · B. Atalay · J. L. Goldberg · B. Medary
L. McGrath · F. Sommer
Department of Neurological Surgery, Weill Cornell Medicine, New York Presbyterian Hospital, New York, NY, USA
e-mail: jag9177@nyp.org; brm4011@med.cornell.edu; lbm9009@med.cornell.edu; fjv4001@med.cornell.edu

R. Härtl (✉)
Department of Neurological Surgery, Weill Cornell Medicine Center for Comprehensive Spine Care New York Presbyterian OCH SPINE, New York, NY, USA
e-mail: roh9005@med.cornell.edu



J.-S. Kim et al. (eds.), *Technical Advances in Minimally Invasive Spine Surgery*,
https://doi.org/10.1007/978-981-19-0175-1_11

of intraoperative navigation guidance during anatomically complex decompressive procedures [17, 18]. Our group described navigation-guided extraforaminal decompression of the L5 nerve root via a minimally invasive tubular approach in 10 patients with foraminal stenosis or extraforaminal disc herniation [18]. Hartmann et al. showed navigation-guided decompression of the L5 nerve root ganglion and safe removal of the extraforaminal extravasation of cement in a patient after L5 vertabroplasty [17].

Navigation guidance may provide additional benefits when performing MIS decompression in the upper lumbar spine due to the more challenging anatomy [19]. For example, the interlaminar space is significantly smaller, the facet joints are oriented in a more sagittal plane, and the lamina are steeply sloped in these levels compared to the lower lumbar levels. As we demonstrate in Case 2, the intraoperative navigation pointer can localize the pars and facet joint precisely to guide the extent of laminotomy in an effort to avoid iatrogenic instability. MIS approaches generally have a steep learning curve due to lack of broad visualization of anatomical structures [20–22]. Intraoperative navigation can be beneficial for surgeons inexperienced with MIS techniques, and it can prevent wrong-level surgery [23].

Radiation exposure is frequently studied and discussed in relation to navigation-guided spinal procedures [23–25]. The use of intraoperative navigation eliminates fluoroscopy; therefore, radiation exposure is significantly reduced to the surgeon and other OR staff. Although patients are exposed to higher radiation during initial intraoperative CT scan, this shortcoming can be overcome by obtaining low-dose CT scans which is now readily available using newer imaging technologies [1]. Nevertheless, the use of intraoperative navigation streamlines the surgical workflow particularly in cases involving patients with obesity, multi-level disease, and other complex anatomy (overgrown facet joints, deformity, scar formations due to previous surgery) where excessive fluoroscopy usage is usually needed if intraoperative navigation is not available [12].

## 11.2 Indications and Contraindications

In our institution, we perform navigation-guided decompression for the management of various lumbar pathology including central stenosis, lateral recess stenosis, foraminal stenosis, epidural lipomatosis, and thecal sac compression due to facet joint cysts. Patients typically present with neurogenic claudication, leg, foot, or buttock symptoms, as well as radiculopathy or neurological deficits. Contraindications to navigation-guided tubular decompression include high-grade spondylolisthesis, significant spinal instability, and symptoms predominantly of mechanical back pain.

## 11.3 Operating Room Setup and Localization

After intubation, the patient is positioned prone on the radiolucent table, which is perpendicular to the intraoperative CT scanner (iCT). All pertinent cables, such as the intubation tube, monopolar cautery, and suction, are fed through the gantry of the iCT. After carefully padding pressure points, the patient is taped to the table to ensure immobilization and to increase the accuracy of navigation. The reference array is fixed rigidly to the iliac crest. Two sterile half sheets are clipped around the incision and mark the scan range. To begin scanning, all staff leave the OR, including the radiologic technologist, who brings the CT scanner's touch screen outside the door to control the scanner. Therefore, no lead apron is necessary for the surgeon or the rest of the OR staff. When the scan is completed, the images are automatically transferred to the stereotactic navigation system (BrainLab Curve, Brainlab AG, Feldkirchen, Germany). Schematic depiction of the OR setup and navigation instruments are illustrated in Figs. 11.1 and 11.2.

A stereotactic navigation pointer aids with the localization of the pathology, planning of the incision, and the proper surgical trajectory (Fig. 11.3). Skin incision is marked using naviga-

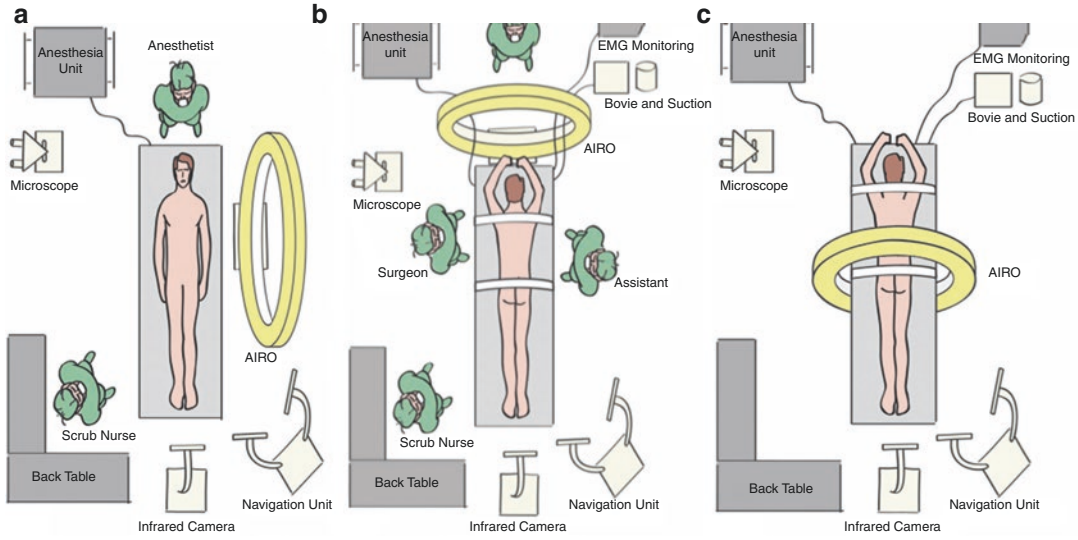


**Fig. 11.1** Schematic depiction of OR setup and navigation instruments

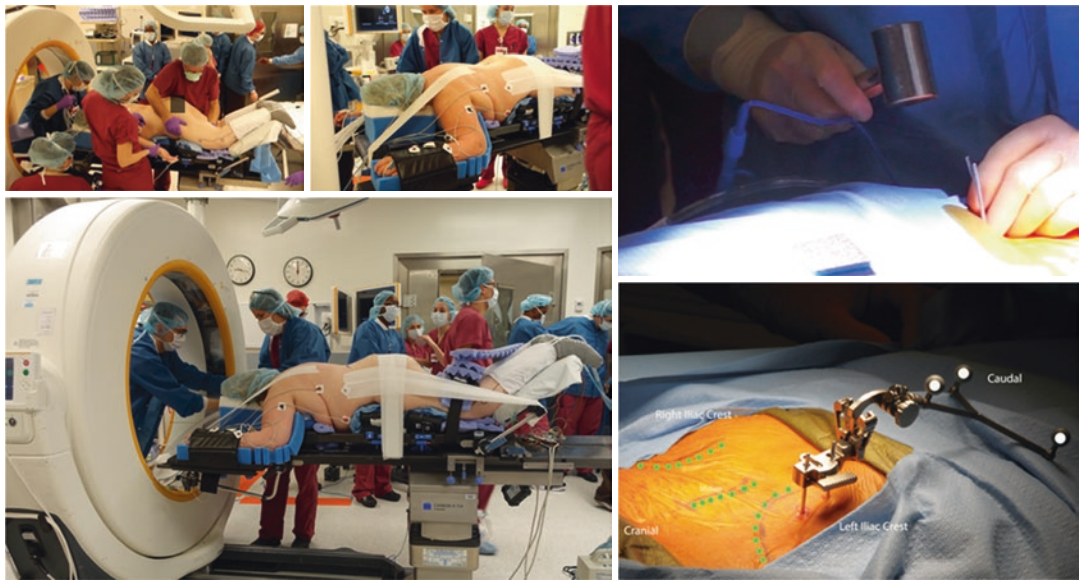


**Fig. 11.2** Key elements of the OR setup include the following: Positioning of the anesthesia unit and team close to the patient's head; neuro-monitorization unit positioning; positioning of the intraoperative CT; positioning of the surgical team on both sides of the patient; positioning of the intraoperative microscope; positioning of the scrub nurse and surgical instruments; positioning of the navigation unit and infrared cameras

tion guidance to identify the site of incision and its proper trajectory, which help in obtaining the best exposure with the smallest possible access so prevent fighting the fascia to get a suitable trajectory for our target point. After skin incision has been made, accuracy is confirmed using the navigation pointer by palpating a transverse process at a distance from the reference array.

With the assistance of the pointer, the tubular retractor scope of vision is predicted. We use 15 mm and 18 mm tubular retractors for lumbar discectomy and laminectomy, respectively. We

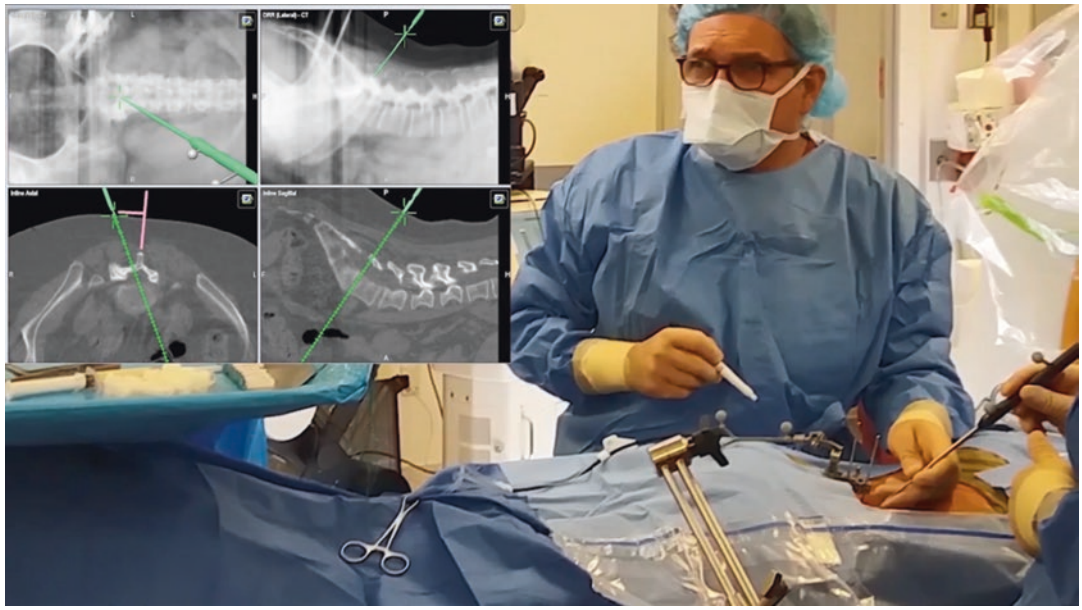

**Fig. 11.3** Intraoperative navigation is used for the localization of the pathology, planning of the incision, and the proper surgical trajectory

aim to show the working zone, which includes the pars and the inferior laminar border of the upper level and the superior articular process of the lower level, forming the facet joint (Fig. 11.4). The bony anatomy is then re-confirmed with the pointer and the tubular retractor is adjusted as needed.

## 11.4 Surgical Technique

After adequate exposure of the bony anatomy is achieved, the intersection of the inferior edge of the cranial lamina and the base of the spinous process is identified using pointer as it is the drilling start point. Ipsilateral laminotomy is performed up to the cranial insertion of the ligamentum flavum (LF) using a 3-mm curved matchstick drill bit and bayonet-shaped 2- and 3-mm Kerrison punches. A ball-tip probe or blunt nerve hook is used to lift up and strip the cranial attachment of the LF. Then, the ipsilateral LF is removed using a 2–3 mm Kerrison punch. In order to visualize the contralateral side, the operating table is tilted away from the surgeon and the tubular retractor is angled medially. The base of the spinous process is identified via the pointer. Next, the spinous process and the contralateral lamina are undercut. During this step, contralateral LF is left intact to protect the dura during contralateral laminotomy. Exposure and decompression of the exiting nerve root is completed by subarticular undercutting until the nerve root passes the contralateral inferior pedicle. It may be necessary to undercut ventrally to the facet joint to access the contralateral foramen. At the end, adequate contralateral decompression can be confirmed using stereotactic navigation. Hemostasis is achieved with repeated irrigation with saline solution, bipolar coagulation, or the use of hemostatic/sealing agents. The tubular retractor is slowly removed while identifying and addressing any bleeding. After closure of the fascia and adaptation sutures of the subcutaneous tissue, the skin is closed by resorbable intracutaneous running suture. The muscle can be injected with local anesthetic for postoperative pain control (Fig. 11.5).

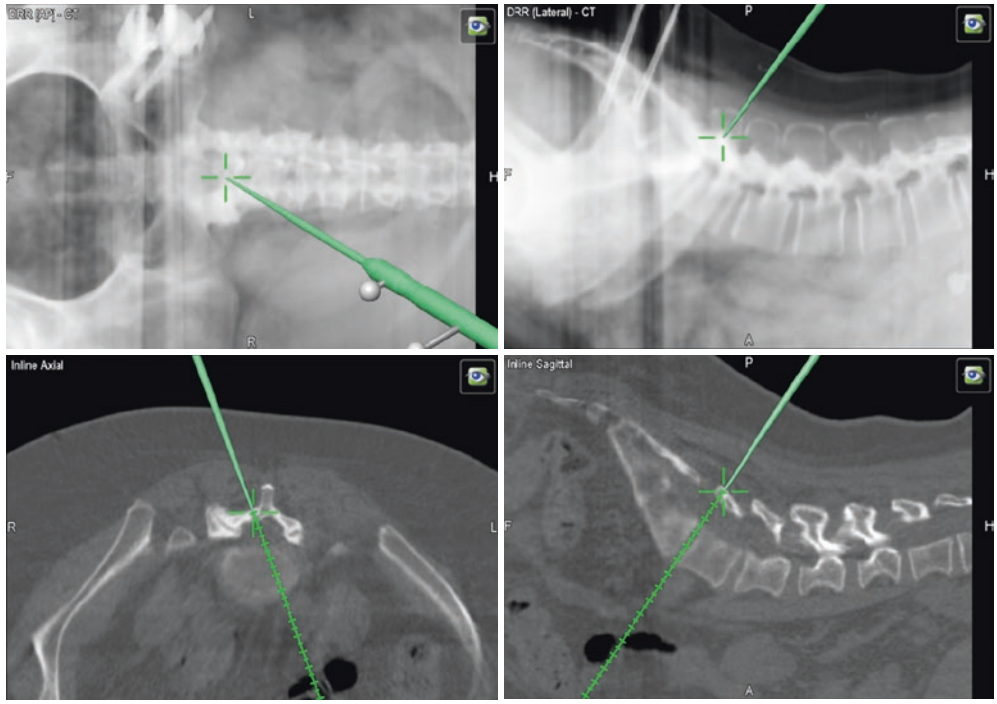


**Fig. 11.4** Confirming the position of tubular retractor and the starting point of laminotomy

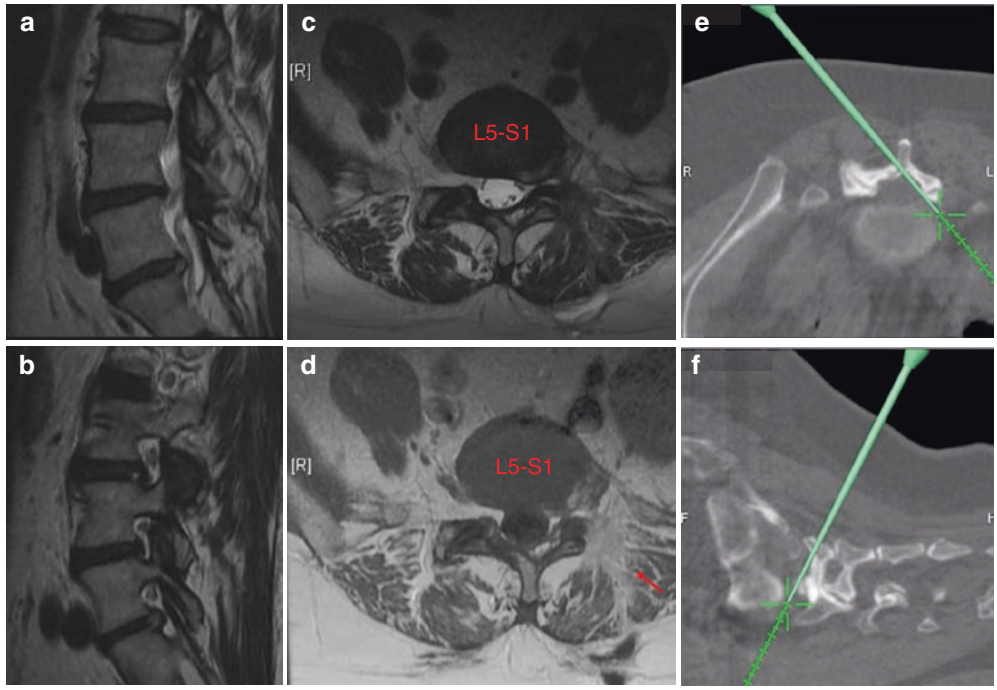


**Fig. 11.5** Large superiorly extruded left L5-S1 foraminal greater than posterolateral disc herniation resulting in compression of the left L5 nerve root. (**a**, **b**) Sagittal T2-weighted MR images; (**c**, **d**) Axial T2-weighted MR images; (**e**, **f**) Adequate decompression is confirmed using intraoperative navigation

## 11.5 Case Example 1: Revision Case

A 51-year-old female patient with a past medical history of left-sided L5-S1 microdiscectomy 10 months prior presented to the clinic with residual/recurrent foraminal disc herniation at L5-S1 compressing the left L5 nerve root. The patient had left lower extremity pain in the left hip and thigh that radiated down the front and side of the leg, as well as tingling and numbness in the left foot. She failed multiple steroid injections and other non-surgical treatments. Her neurological exam was intact except a positive straight leg raise test on the left and numbing of the left foot at L5 nerve distribution. She underwent an MRI of the lumbar spine which demonstrated foraminal and extraforaminal L5/S1 recurrent/residual disc herniation. T1-weighted post-contrast images showed postoperative changes from the first surgery with extensive scar formation along the extraforaminal approach area and discectomy side. The decision was made to offer a right-sided minimally invasive laminotomy for contralateral "over-the-top" foraminal decompression using intraoperative 3D navigation due to the presence of extensive extraforaminal scar tissue on the left side and partial removal of the left facet joint from the first surgery. The main advantage of this technique is the direct "over-the-top" trajectory to the foraminal pathology that minimizes the need for facet joint resection. The inferior facet contralateral to the approach side as well as its outer capsular surroundings can be preserved with the help of intraoperative navigation. The patient did well and was discharged at postoperative day 1. She reported resolution of symptoms during postoperative follow-up at 6 months (Fig. 11.6).

## 11.6 Case Example 2: Upper Lumbar Level

A 52-year-old male presented with right-sided lower back pain with radiation into proximal right buttock, groin, and right anterior thigh to the level of the knee which started 6 weeks prior. He had had sciatic pain for years on and off but had managed to deal with his symptoms with

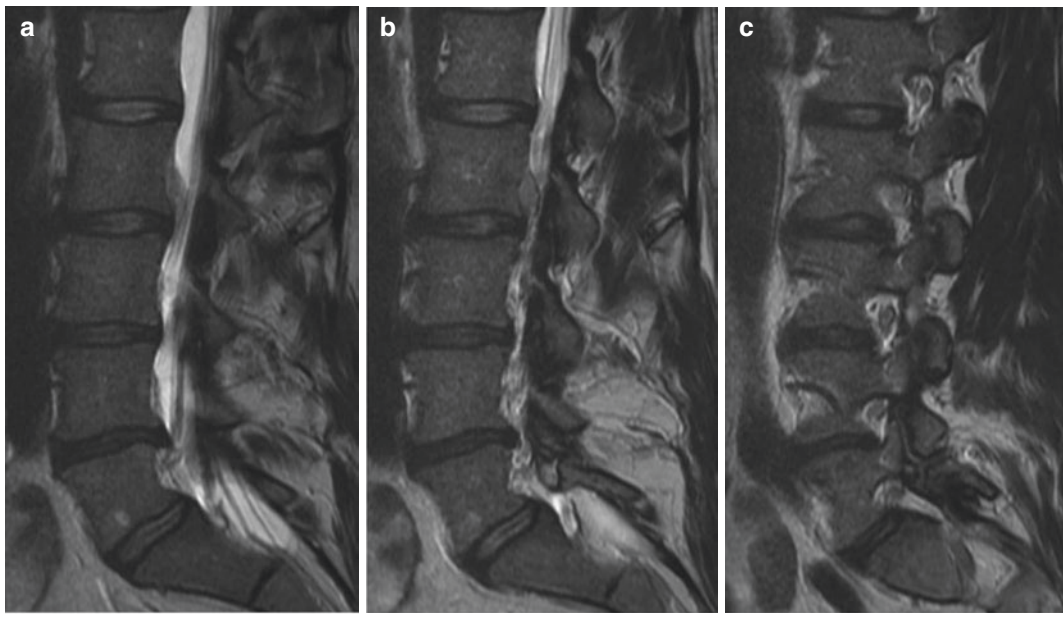


**Fig. 11.6** Right L2–L3 foraminal disc extrusion with superior migration into the neural foramen compressing the exiting right L2 nerve root. (**a**, **b**, **c**) Sagittal T2-weighted MR images; (**d**, **e**) Axial T2-weighted MR images

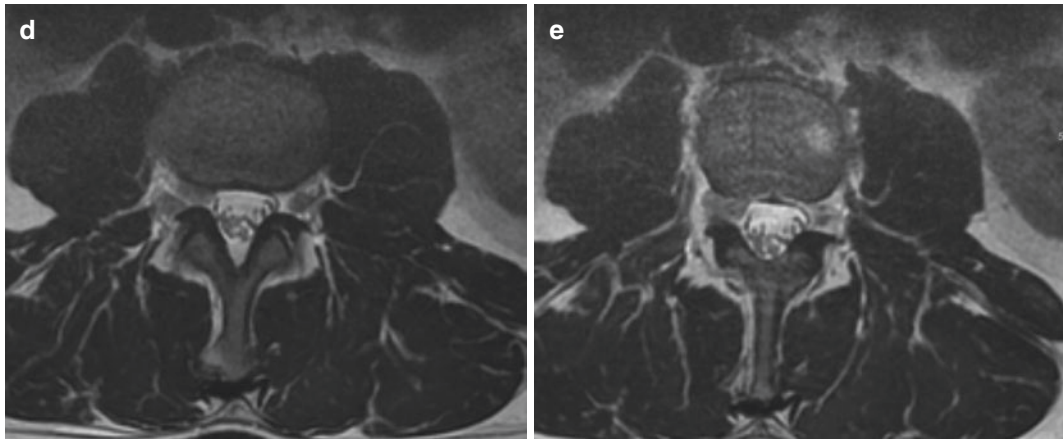


**Fig. 11.6** (continued)

conservative treatments. His most recent symptoms were of acute onset and significantly more severe than his previous symptoms. He underwent an MRI of the lumbar spine which demonstrated a disc herniation at L2–3 with rostral migration and compression of the exiting L2 nerve on the right side, consistent with his symptoms. His neurological exam was intact except a positive straight leg raise test. The decision was made to offer a left-sided minimally invasive laminotomy for contralateral "over-the-top" foraminal decompression to get a better exposure of the L2–3 foramen. When operating at the upper lumbar segments (e.g., L1–L2, L2–L3), the incision should be placed more medially, and the tubular retractor should be oriented more vertically to avoid excessive ipsilateral as well as contralateral facet removal or pars violation due to the narrow lamina window and more sagittally oriented facet joints of the upper lumbar spine. The stereotactic navigation pointer facilitates the planning of the incision and the proper surgical trajectory in such a case and ensures to preserve facet joints. Navigation can be very important in these cases in order to avoid accidently violating the pars. Finally, adequate contralateral decompression was confirmed using intraoperative navigation. The patient's leg pain was resolved immediately postop and was discharged same day (Fig. 11.7).

## 11.7 Case Example 3: Complex Anatomy

An 85-year-old female patient presented to our clinic with low back pain which radiated to her right buttock. Her symptoms started 3 weeks prior without any inciting event. She failed steroid injections, physical therapy, and oral pain medication. Her MRI revealed foraminal narrowing at L5/S1 level on the right side with compression of the exiting L5 nerve root. She underwent a CT scan which demonstrated advanced facet arthropathy with hypertrophy, hook osteophytes, and a disc ridge complex causing severe right-sided L5-S1 foraminal stenosis (Fig. 11.8). The patient was treated with a right-sided L5/S1 far lateral discectomy and decompression via a minimally invasive tubular approach using intraoperative total navigation (Fig. 11.9). An excellent decompression of the nerve root was achieved by removing medial bone and lateral bone which was subsequently confirmed with intraoperative 3D navigation. The use of intraoperative 3D navigation allows for safe and efficient decompression by facilitating surgical planning and minimizing facet joint compromise in such cases with complex anatomy including facet arthropathy, bony hook osteophytes, and deformity. The patient did well and was discharged on the same day (Fig. 11.10).

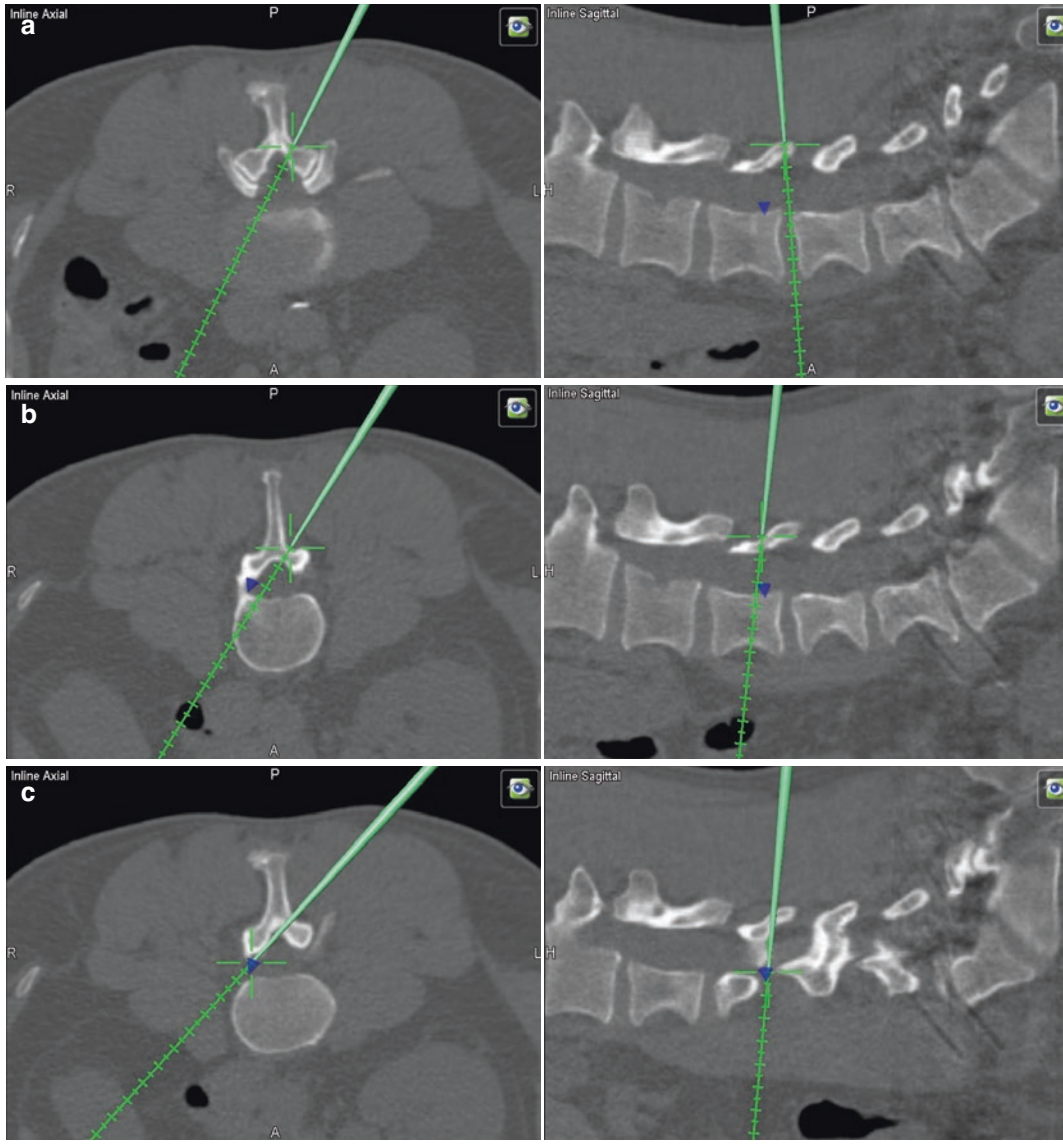


**Fig. 11.7** Minimally invasive laminotomy for contralateral "over-the-top" foraminal decompression. (**a**) Inferior edge of the L2 lamina: started laminotomy; (**b**) Ipsilateral pars: preserved to avoid iatrogenic instability; (**c**) Contralateral foramen: confirmed adequate decompression

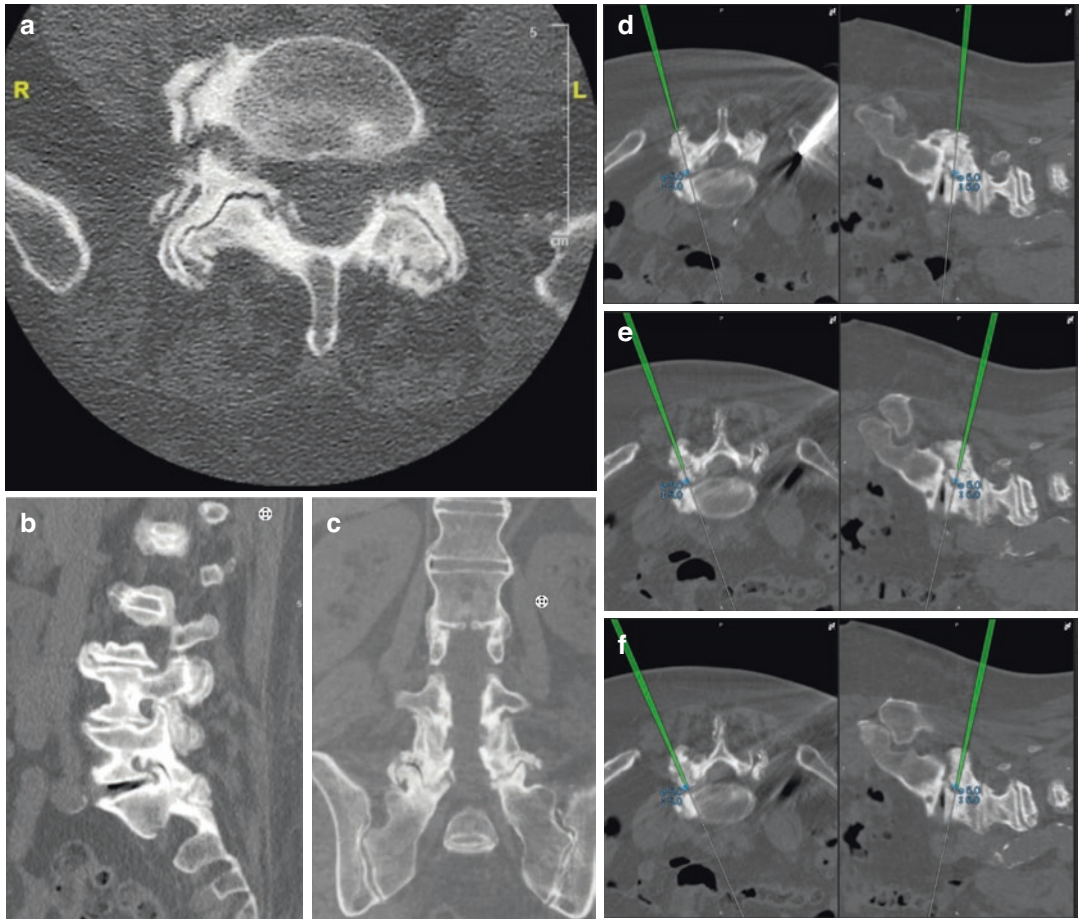


**Fig. 11.8** Advanced facet arthropathy with hypertrophy, hook osteophytes, and a disc ridge complex causing severe right-sided L5-S1 foraminal stenosis. (**a**) Axial CT images; (**b**) Sagittal CT images; (**c**) Coronal CT images; (**d**, **e**, **f**) Intraoperative navigation aids removal of the lateral aspect of the facet joint; (**f**)

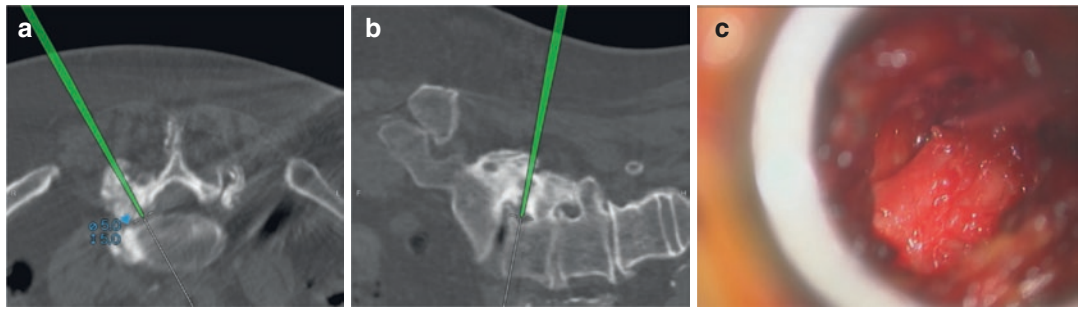


**Fig. 11.9** Adequate decompression is confirmed using intraoperative navigation. (**a**, **b**) Intraoperative navigation screenshots; (**c**) Microscope view through tubular retractor

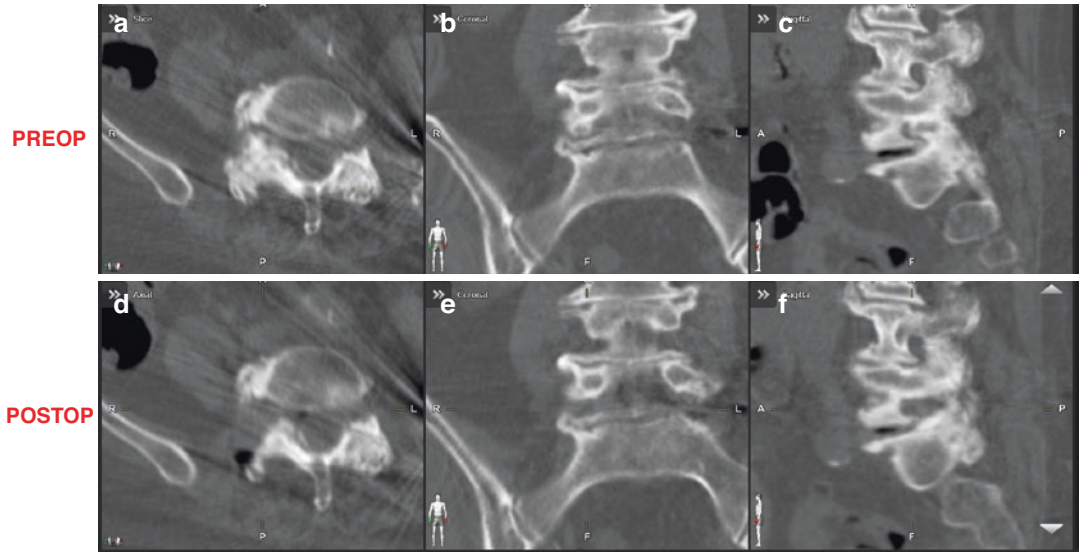


**Fig. 11.10** Right L5/S1 far lateral discectomy and decompression. (**a**, **b**, **c**) Preoperative CT Images; (**d**, **e**, **f**) Postoperative CT images

## 11.8 Conclusion

Navigation-guided MIS tubular decompression in the lumbar spine safely augments tubular decompression and may prevent iatrogenic spinal instability. In addition, utilization of navigation for lumbar decompression minimizes the risk of injury to neurological elements, reduces radiation exposure to surgical staff, and improves surgical workflow. These capabilities are especially useful in more complex decompression cases such as patients with obesity, multi-level disease, and complex anatomy.

We believe that there is true benefit to the use of navigation not only for instrumented spine cases but also for cases that require decompression or microsurgical resection of pathology without fusion. However, in order for navigation to expand into non-instrumented spine cases and maybe even into pain management procedures it will be necessary to improve our ability to match preoperative MRI scans with intraoperative imaging studies while minimizing radiation.

## References

1. Hussain I, Cosar M, Kirnaz S, et al. Evolving navigation, robotics, and augmented reality in minimally invasive spine surgery. Global Spine J. 2020;10(2 Suppl):22s–33s.
2. Kirnaz S, Navarro-Ramirez R, Wipplinger C, et al. Minimally invasive transforaminal lumbar interbody fusion using 3-dimensional total navigation: 2-dimensional operative video. Oper Neurosurg (Hagerstown, Md). 2020;18(1):E9–e10.
3. Lian X, Navarro-Ramirez R, Berlin C, et al. Total 3D Airo® navigation for minimally invasive transforaminal lumbar interbody fusion. Biomed Res Int. 2016;2016:5027340.
4. Navarro-Ramirez R, Lang G, Lian X, et al. Total navigation in spine surgery; a concise guide to eliminate fluoroscopy using a portable intraoperative computed tomography 3-dimensional navigation system. World Neurosurg. 2017;100:325–35.
5. Huang M, Tetreault TA, Vaishnav A, York PJ, Staub BN. The current state of navigation in robotic spine surgery. Ann Transl Med. 2020;9(1):86.
6. Jenkins NW, Parrish JM, Sheha ED, Singh K. Intraoperative risks of radiation exposure for the surgeon and patient. Ann Transl Med. 2020;9(1):84.
7. Rawicki N, Dowdell JE, Sandhu HS. Current state of navigation in spine surgery. Ann Transl Med. 2020;9(1):85.

8. Weiner JA, McCarthy MH, Swiatek P, Louie PK, Qureshi SA. Narrative review of intraoperative image guidance for transforaminal lumbar interbody fusion. Ann Transl Med. 2020;9(1):89.
9. Kochanski RB, Lombardi JM, Laratta JL, Lehman RA, O'Toole JE. Image-guided navigation and robotics in spine surgery. Neurosurgery. 2019;84(6):1179–89.
10. Overley SC, Cho SK, Mehta AI, Arnold PM. Navigation and robotics in spinal surgery: where are we now? Neurosurgery. 2017;80(3s):S86–s99.
11. Sembrano JN, Yson SC, Theismann JJ. Computer navigation in minimally invasive spine surgery. Curr Rev Musculoskelet Med. 2019;12(4):415–24.
12. Virk S, Qureshi S. Navigation in minimally invasive spine surgery. J Spine Surg (Hong Kong). 2019;5(Suppl 1):S25–s30.
13. Cardali SM, Cacciola F, Raffa G, Conti A, Caffo M, Germanò A. Navigated minimally invasive unilateral laminotomy with crossover for intraoperative prediction of outcome in degenerative lumbar stenosis. J Craniovertebr Junction Spine. 2018;9(2):107–15.
14. Ho TY, Lin CW, Chang CC, et al. Percutaneous endoscopic unilateral laminotomy and bilateral decompression under 3D real-time image-guided navigation for spinal stenosis in degenerative lumbar kyphoscoliosis patients: an innovative preliminary study. BMC Musculoskelet Disord. 2020;21(1):734.
15. Kirnaz S, Wipplinger C, Schmidt FA, Hernandez RN, Hussain I, Härtl R. Minimally invasive laminotomy for contralateral "over-the-top" foraminal decompression using 3-dimensional total navigation: 2-dimensional operative video. Oper Neurosurg (Hagerstown). 2020;19(3):E296.
16. Sembrano J, Santos EG, Polly D. New generation intraoperative three-dimensional imaging (O-arm) in 100 spine surgeries: Does it change the surgical procedure? J Clin Neurosci. 2014;21:225–31.
17. Hartmann S, Kavakebi P, Tschugg A, Lener S, Stocsits A, Thomé C. Navigation for tubular decompression of the L5 nerve root ganglion after cement leakage via a wiltse approach. Asian J Neurosurg. 2019;14(2):565–7.
18. Stavrinou P, Härtl R, Krischek B, Kabbasch C, Mpotsaris A, Goldbrunner R. Navigated transtubular extraforaminal decompression of the L5 nerve root at the lumbosacral junction: clinical data, radiographic features, and outcome analysis. Biomed Res Int. 2016;2016:3487437.
19. Sugimoto Y, Ito Y, Tomioka M, et al. Upper lumbar pedicle screw insertion using three-dimensional fluoroscopy navigation: assessment of clinical accuracy. Acta Med Okayama. 2010;64(5):293–7.
20. Ao S, Wu J, Tang Y, et al. Percutaneous endoscopic lumbar discectomy assisted by O-arm-based navigation improves the learning curve. Biomed Res Int. 2019;2019:6509409.
21. Bai YS, Zhang Y, Chen ZQ, et al. Learning curve of computer-assisted navigation system in spine surgery. Chin Med J. 2010;123(21):2989–94.
22. Tian W, Liu B, He D, et al. Guidelines for navigation-assisted spine surgery. Front Med. 2020;14(4):518–27.
23. Rahmathulla G, Nottmeier EW, Pirris SM, Deen HG, Pichelmann MA. Intraoperative image-guided spinal navigation: technical pitfalls and their avoidance. Neurosurg Focus. 2014;36(3):E3.
24. Edström E, Burström G, Omar A, et al. Augmented reality surgical navigation in spine surgery to minimize staff radiation exposure. Spine. 2020;45(1):E45–e53.
25. Nachabe R, Strauss K, Schueler B, Bydon M. Radiation dose and image quality comparison during spine surgery with two different, intraoperative 3D imaging navigation systems. J Appl Clin Med Phys. 2019;20(2):136–45.

# EM-Based Navigation-Guided Transforaminal Endoscopic Lumbar Discectomy

12

Bo-Lai Chen, Yong-Peng Lin, and Si-Yuan Rao

## Abbreviations

| | |
|---|---|
| PN | percutaneous nucleotomy |
| APLD | automated percutaneous lumbar discetomy |
| PELD | percutaneous endoscopic lumbar discectomy |
| YESS | Yeung endoscopic spine system |
| THESSYS | Thomas Hoogland Endoscopic Spine System |
| TELD | transforaminal endoscopic lumbar discectomy |
| EM | electromagnetic |
| LDH | lumbar disc herniation |
| 2D | two-dimensional |
| 3D | three-dimensional |
| CT | computed tomography |

**Key Points**

1. Transforaminal endoscopic lumbar discectomy (TELD) is one of the most minimally invasive techniques for the treatment of lumbar disc herniation. It is completed under local anesthesia and is attributed with less bleeding and soft tissue trauma. The working channel enters the intervertebral disc through the natural foramen and hardly damages the normal anatomical structure. Thus, the patient can resume normal social activities soon after surgery. However, this minimally invasive technique has a steep learning curve. Especially for beginners, without good intraoperative guidance, serious complications may occur, such as dural sac tear and nerve injury.
2. Electromagnetic (EM) navigation is a frameless stereotactic navigation technology, which integrates electromagnetic technology, modern diagnostic radiology technology, stereotactic technology, and minimally invasive surgery. With the assistance of a high-performance computer, it can accurately display the anatomical structure of the spine, the three-dimensional spatial position, and adjacent relationship of lesions.
3. EM-based navigation-guided TELD has the advantages of good positioning accuracy, real-time monitoring, and great reduction of X-ray perspective. The new technique is especially helpful for inexperienced spinal surgeons. Its application prospect is very broad

B.-L. Chen (✉)
Guangdong Provincial Hospital of Chinese Medicine and Second Affiliated Hospital of Guangzhou University of Chinese Medicine, Guangzhou, China
e-mail: chenbolai@gzucm.edu.cn

Y.-P. Lin · S.-Y. Rao
Guangdong Provincial Hospital of Chinese Medicine and Second Affiliated Hospital of Guangzhou University of Chinese Medicine, Guangzhou, China

Guangzhou University of Chinese Medicine, Guangzhou, China



J.-S. Kim et al. (eds.), *Technical Advances in Minimally Invasive Spine Surgery*,
https://doi.org/10.1007/978-981-19-0175-1_12

in the future, and EM-based navigation will further promote the development of percutaneous endoscopic spinal surgery.

## 12.1 Introduction

In 1975, Hijikata et al. [1] performed mechanical percutaneous nucleotomy (PN) via posterolateral access to treat lumbar disc herniation for the first time. Under local anesthesia, the working channel was inserted into the intervertebral disc through a small skin incision via posterolateral access for nucleus pulposus resection. However, since the position of the working cannula is determined under C-arm fluoroscopy rather than under microscopic guidance, the cannula cannot enter the spinal canal, so this is an indirect decompression technique without direct vision. Similarly, automated percutaneous lumbar discectomy (APLD) [2] was also applied to remove nuclear material in the following years. Nonetheless, later studies have demonstrated that the success rate of this technique was no more than 65%, which is not different from that of conservative treatment. In addition, the surgical indications of these two methods are relatively narrow and mainly suitable for inclusive lumbar disc herniation, a relatively rare type of lumbar disc herniation. Following Hijikata's experience, Schreiber [3] improved the original instruments and developed a series of cannulas and a modified arthroscopic technique, which help to remove nucleus pulposus more accurately and effectively, with a reported success rate of 72.5%. One year later, Hausmann et al. [4] also reported that a detailed and risk-free observation of the intervertebral disc space could be performed through improved arthroscopy.

Kambin et al. [5] described the anatomic boundaries of the "safe working zone" of a lumbar intervertebral foramen in the 1990s, which laid the theoretical foundation for the development of percutaneous endoscopic lumbar discectomy (PELD). In 1997, Yeung [6] successfully developed the third-generation spinal endoscope, the Yeung endoscopic spine system (YESS), which emphasized access to the intervertebral disc through the "Kambin's triangle," thereby removing the nucleus pulposus tissue from the inside out under direct vision and achieving indirect decompression under vision. Yeung's technique of "inside out," carried out with a 2.8 mm surgical channel, is relatively simple and safe for use in cases including inclusive, subligamentous lumbar disc herniation and some discogenic back pain. Yeung and Tsou [7] performed at least a one-year retrospective analysis of 307 patients undergoing PELD. The postoperative satisfaction rate was 90.7%, and the excellent and good rate was 89.3% according to the improved Macnab evaluation criteria, while the incidence of complications was 3.5%. The surgical results were comparable to that of intervertebral fenestration discectomy. However, since this technique warrants decompression inside the disc, its indication is relatively narrow, and it is difficult to work for expelled nucleus and sequestered disc. Furthermore, the nerve root and dural sac cannot be exposed under the microscope, and it is highly vulnerable to damage to the nerve root when entering and exiting through the Kambin's triangle.

To address the shortcomings of the YESS technique, Hoogland [8] developed the Thomas Hoogland Endoscopic Spine System (THESSYS) in 2003 with a wider range of indications compared to the YESS technique. Hoogland described the "outside-in" approach for transforaminal endoscopic technique by cutting the facet and direct landing into the epidural space so that the ligamentum flavum, dural sac, nerve root, and herniated nucleus pulposus can be seen under a microscope. However, this technique has high technical requirements and a steep learning curve, so beginners are prone to damage spinal nerve roots, blood vessels, and dural sac, which may lead to serious complications. Hoogland et al. [9] reported that 262 patients with recurrent lumbar disc herniation were treated by THESSYS, among which 238 patients (90.84%) completed a 2-year follow-up, with a reported 3.8% complication rate which included 3 cases of nerve root stimulation, 7 cases of early recurrent herniation

(<3 months), and no postoperative infection and discitis. Likewise, Schubert et al. [7] performed foraminoplasty by cutting part of the upper facet joint with Hoogland-designed bone reamers to directly insert the c into the spinal canal, and then remove the migrated nucleus pulposus tissue with endoscopic assistance. The postoperative excellent and good rate was 95.3% and the recurrence rate was 3.6%. Furthermore, he believed that the greatest advantage of the THESSYS technique was that the extruded and sequestered nucleus pulposus tissue inside the spinal canal could be directly removed. However, he deemed it relatively difficult to deal with the necrotic and broken nucleus pulposus tissue due to the difficulty of entering the disc, which increased the risk of postoperative recurrence.

Although transforaminal endoscopic lumbar discectomy (TELD) is the most advanced and minimally invasive surgical method for the treatment of lumbar disc herniation, there are still several complications [10–15]. These complications include the following: (1) Nerve root injury: the process of puncture, expansion, and working tube insertion without direct vision may result in nerve root injury due to the anatomic variation. (2) Dural sac rupture: It is a rare but serious complication, mainly related to mechanical wear of surgical instruments or radiofrequency thermal injury during operation. (3) Incomplete decompression and postoperative recurrence: Incomplete decompression is often due to incomplete removal of protrusions, stenosis of a nerve root canal, or insufficient foraminoplasty. Postoperative recurrence is mainly related to the incomplete removal of compressive factors, improper postoperative nursing strategy, early stooping, or sneezing. (4) Abdominal and vascular injury: The blood vessels may be damaged during the process of establishing working channels and the puncture needle may enter the abdominal cavity, resulting in viscera (intestinal canal, kidney, and large blood vessel) injury. The occurrence of these complications is mainly related to factors such as poor technical proficiency and inexperience. Moreover, the routine TELD process not only needs to be carried out under the guidance of repeated X-ray fluoroscopy but also needs dynamically detection of the location of the surgical instruments to ensure the safety of patient, which is especially complicated for beginners and may pose additional radiation damage to both doctors and patients.

Electromagnetic (EM) navigation is a frameless stereotactic navigation technology, which integrates electromagnetic technology, modern diagnostic radiology technology, stereotactic technology, and minimally invasive surgery [16–21]. It can accurately show the anatomical structure of the spine and the three-dimensional spatial position and adjacent relationship of lesions with the assistance of a high-performance computer [20, 21]. The system is based on powerful computer technology and image processing software, obtaining the relative position of the patient's vertebral body, articular process, intervertebral disc, and surgical instruments through infrared remote sensing technology and electromagnetic principle, and **calculates** and displays the relationship between the real-time process of the operation, the accurate location of the lesion, and the surrounding structures. In a word, electromagnetic-based (EM-based) navigation-guided TELD has the advantages of good positioning accuracy and real-time monitoring and is capable of greatly reducing X-ray perspective

## 12.2 Components of the Electromagnetic Navigation System

The electromagnetic navigation system (Fiagon GmbH, Germany) for TELD consists of a navigation screen (Fig. 12.1), navigation module, and tracking pointer (Fig. 12.2). There are three windows in the navigation screen, two of which display the position and dynamic changes of surgical tools simulated on anteroposterior and lateral views and the third window displaying the video image of the surgical field as visualized by the endoscope. The navigation module is equipped with a DVD drive, USB port, plug points for navigation sensor, patient localizer, virtual endos-

copy planning software, and pointer system. The pointer system is equipped with a connecting plug, pointer, and sensor cable that allows for precise tracking of both position and orientation throughout the electromagnetic field. The special I-See endoscopic spine surgical system (Joimax, IseeU, Germany) (Fig. 12.3) is the instrument dedicated to matching the EM navigation.

**Fig. 12.1** The EM navigation screen

## 12.3 Indications and Contraindications

### 12.3.1 Indications

1. Central, paracentral, extreme-lateral, or prolapsed lumbar disc herniation.
2. Radiation pain in a single lower limb with or without back pain, positive Lasegue sign.
3. Mono-segment of lumbar disc herniation or prolapsed suggested by MRI or CT scans.
4. Failure of strict conservative treatments for at least 3 months.
5. Patients who fail to remit or who relapse after other minimally invasive interventional surgery.

### 12.3.2 Contraindications

1. Clinical symptoms or physical examination signs that do not match the radiographic results
2. Cauda equina syndrome
3. Lumbar segmental instability and lumbar spondylolisthesis
4. Lumbar infections, tumors, or deformities
5. Poor local skin condition or wounds at the surgical incision site
6. Patients who are unable to tolerate surgery or cannot cooperate for other reasons

## 12.4 Surgical Procedure

The patient is placed in the prone position on a special, non-metallic, carbon fiber operating (OR) table to prevent electromagnetic interfer-

**Fig. 12.2** The EM navigation module and tracking pointer

ence. The magnetic field generator is fixed on the OR table close to the patient's hip so that the frame encompasses the entire surgical field. After preparation of the operation site, the k-wire is drilled into the spinous process of the caudal vertebral body adjacent to the operative segment to a depth of 2 cm to make it firmly fixed, and the locator is placed on the skin 5–10 mm away from the k-wire. Thereafter, the tracker is firmly connected with the spinous process, and a mapper bridge is placed next to the locator which is identified by the landmarks in the anteroposterior and lateral X-ray images (Fig. 12.4).

After the perspective image is transmitted to the navigation system via the USB driver, the system automatically performs registration by loading the data. Upon confirmation of registration, intraoperative two-dimensional (2D) images are used to match preoperative computed tomography (CT) image data, and the three-dimensional (3D) data sets enable virtual real-time navigation. The target point (the superior articular process or the herniated disc is usually selected as the target point) of puncture must be set on the EM navigation system at the beginning of the operation (Fig. 12.5).

The operation is performed under local infiltration anesthesia by injecting lidocaine into soft tissue. Firstly, the inner core of the 18-gauge puncture needle is removed, which is replaced by the IseePointer sensor. Consequently, the puncture needle is maintained on the multifunctional board for calibration until the needle symbol appears in the upper right corner of the navigation display. After that, the needle is inserted by a posterolateral approach to the target disc under the guidance of real-time navigation view until it reaches the target. During the process, the changes of the puncture needle angle and depth can be seen in real time (Fig. 12.6).

When the angle is correct, it remains green and only turns red if the puncture angle deviates significantly from the design path. Subsequent surgical procedures are as follows: (1) The needle is replaced with a 0.8-mm guidewire, and (2) then a 1.5 cm skin incision is made along the guidewire. (3) After calibration, a gentle sequential dilatation technique is performed to protect the exiting nerve root and to prevent access pain. (4) The semi-serrated outer working cannula is inserted into a navigation rod consisting of IseePointer and adapters, and (5) then into the

**Fig. 12.3** The special I-See endoscopic spine surgical system matching the EM navigation

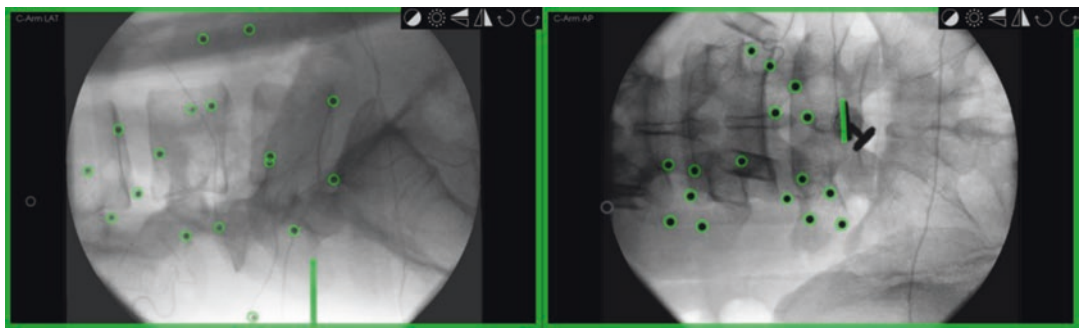

**Fig. 12.4** The intraoperative images are taken by the 3D C-arm and sent to the EM navigation system

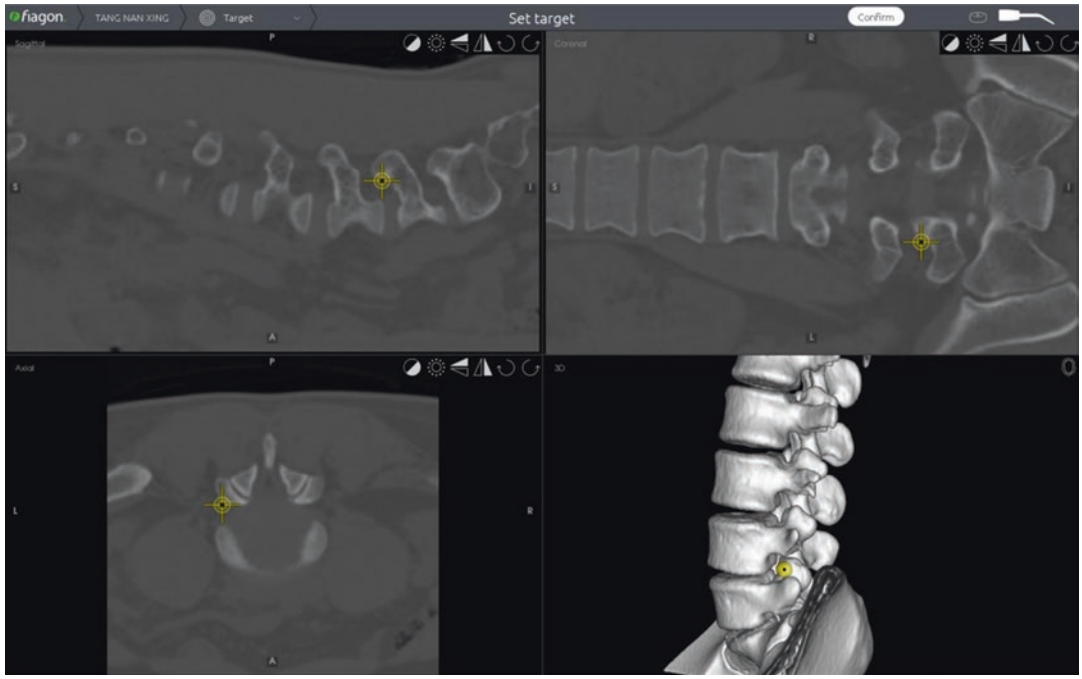


**Fig. 12.5** Target point setting

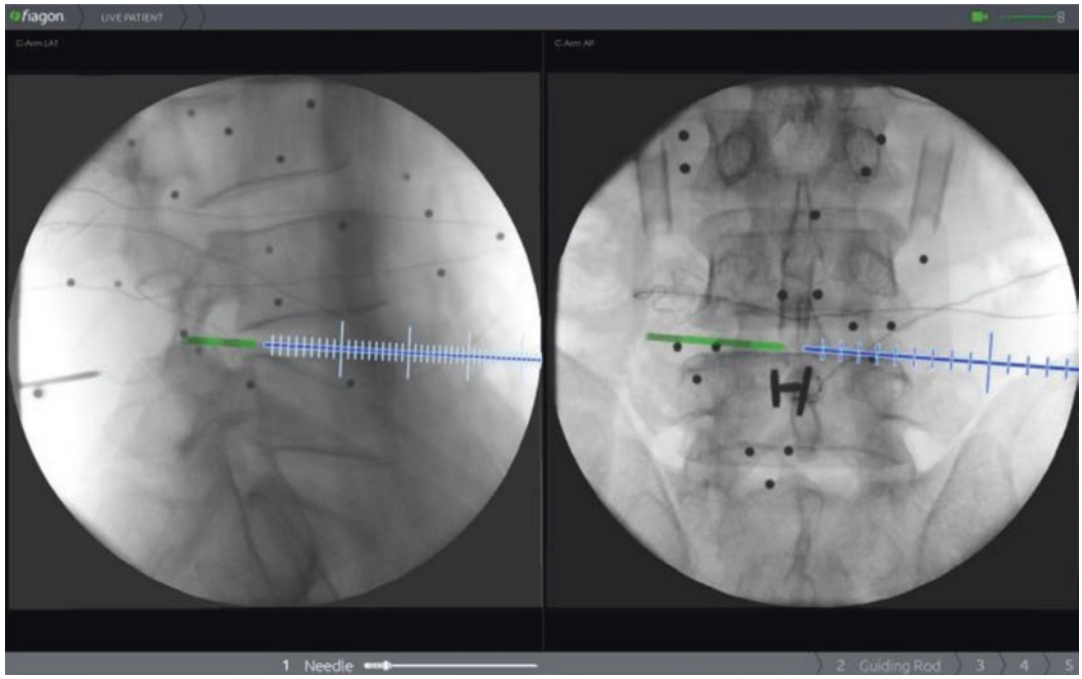


**Fig. 12.6** Puncture under the EM navigation

calibrated trephine. (6) A rigid, rod-lens endoscope with a working channel is introduced, and selective foraminoplasty and discectomy are performed under continuous normal saline irrigation. (7) The depth of endoscope entry and the position of surgical instruments can be visualized in real time under navigation monitoring. At this time, the lateral border of the ipsilateral ligamentum flavum is resected, the degenerative and protruding intervertebral disc is removed, and the nerve roots are decompressed appropriately. Finally, the end-point is determined with the free mobilization of the exiting nerve root and the dural sac.

Both the preoperative MRI and CT determine and confirm the location of the disc herniation and guide the working channel placement and decompression: (1) for the most common type of LDH, paracentral type, the first task is to find the space between ligamentum flavum and intervertebral disc after foraminoplasty and then to explore the rupture of a disc in the abdominal direction. Remove the protruding nucleus pulposus around the rupture until the ventral side of the nerve root can be seen. If the nerve root can easily fluctuate in water pressure, it indicates that the nerve root has been decompressed successfully and radiofrequency ablation can be used to treat the rupture of annulus fibrosus. (2) For prolapse or sequestration, adequate foraminoplasty is needed to remove part of the bony structure of the superior articular process so that the working channel can enter the target. Generally speaking, after removing the prolapsed nucleus pulposus in the spinal canal, it is necessary to swing the working channel to explore the rupture of the intervertebral disc and remove the degenerative nucleus pulposus in the disc to reduce probability of recurrence. (3) For the extreme-lateral LDH, the working tube is not needed to enter the intervertebral foramen, but it is needed to reach the lateral edge of the articular process in the anterior-posterior view and the posterior edge of the intervertebral disc in the lateral view, simultaneously. After that, the protruding disc and exiting nerve root can be detected. (4) For the completely contained LDH, the working channel can be directly placed into the intervertebral disc without foraminoplasty if the intervertebral foramen is large enough, and the degenerative nucleus pulposus is directly removed. Then, the working channel is gradually withdrawn to the intervertebral foramen area and the nerve root is subsequently explored.

There is no need to place drainage tubes after an operation, and the patient does not need to take antibiotics or painkillers. After 3-h observation postoperatively, the patient is allowed to walk on the ground wearing protective equipment if they have no obvious discomfort. Patients are discharged on the day of surgery or the first day after surgery, but they are informed of precautions in the first 6 weeks, such as reducing strenuous activities, avoiding overwork, or stooping with long hours.

## 12.5 Case Study

Male, 54 years old.

Symptoms: Radiation pain from the low back area, down to the left leg and into the left feet for more than 2 years, aggravated in the past 3 months. Activities such as bending, lifting, twisting, and sitting increased the pain. Patient had undergone repeated conservative treatment and steroid blockade with unsuccessful clinical response.

Physical examination: The Lasegue sign was positive on the left side.

The visual analog scale (VAS) was 7/10 (Figs. 12.7, 12.8, 12.9, and 12.10).

## 12.6 Discussion

The key prerequisite for a successful TELD is to establish a working channel accurately and safely. The Kambin's triangle is small because of the occlusion of the superior articular process of the lumbar vertebrae, especially for patients with long and narrow intervertebral foramen, which

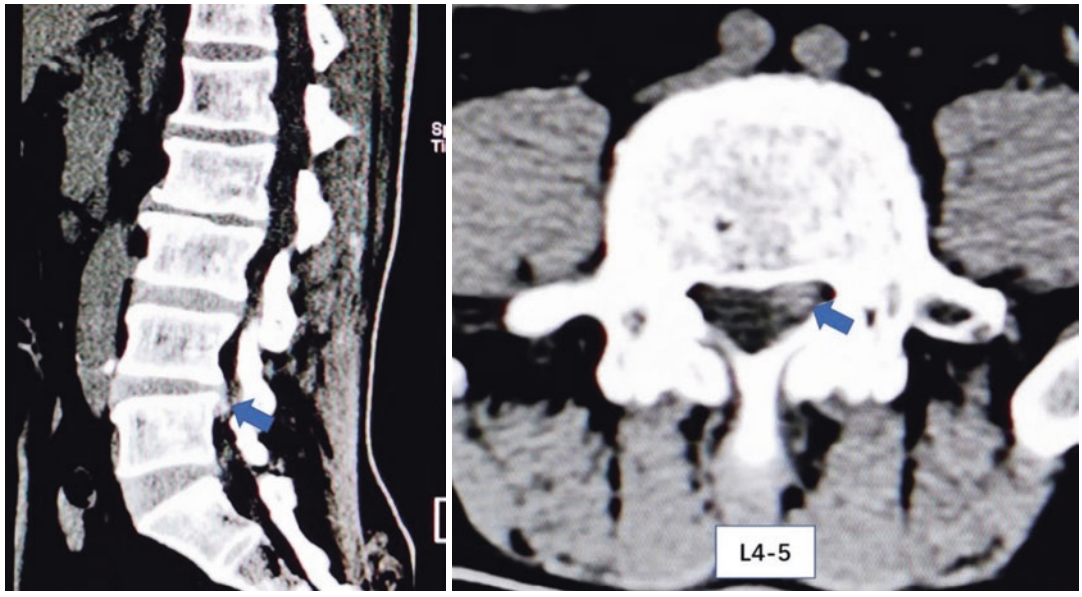


**Fig. 12.7** Preoperative CT scan showed LDH on the L4–5 left side

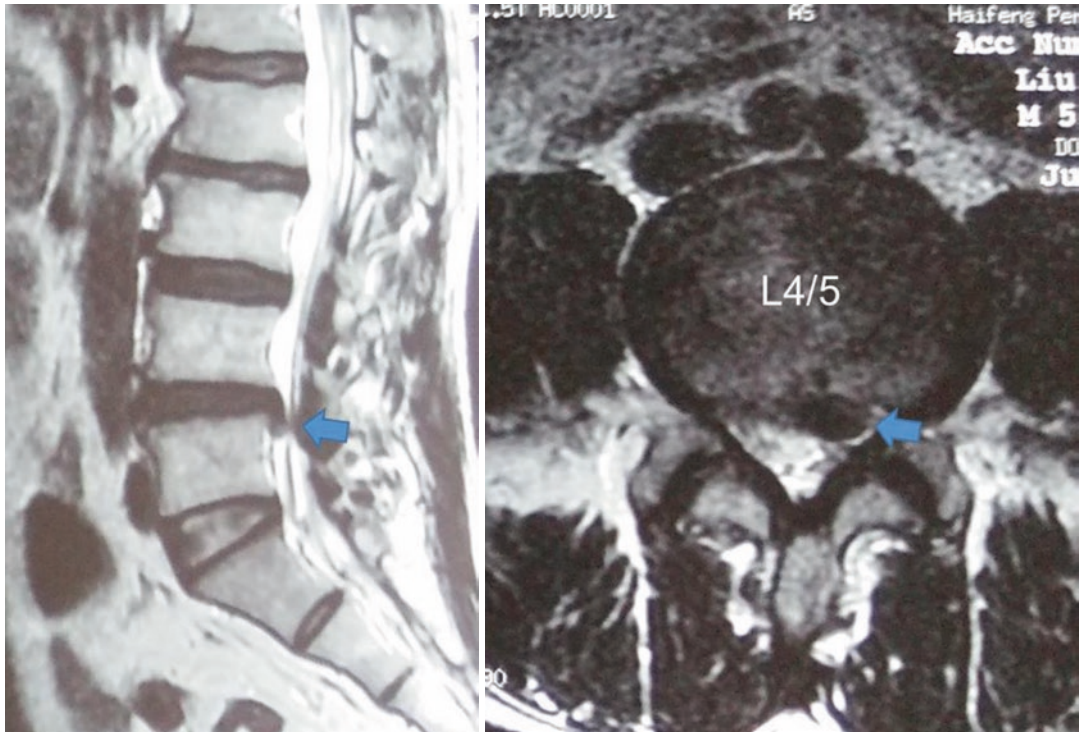


**Fig. 12.8** Preoperative MRI showed LDH on the L4–5 left side

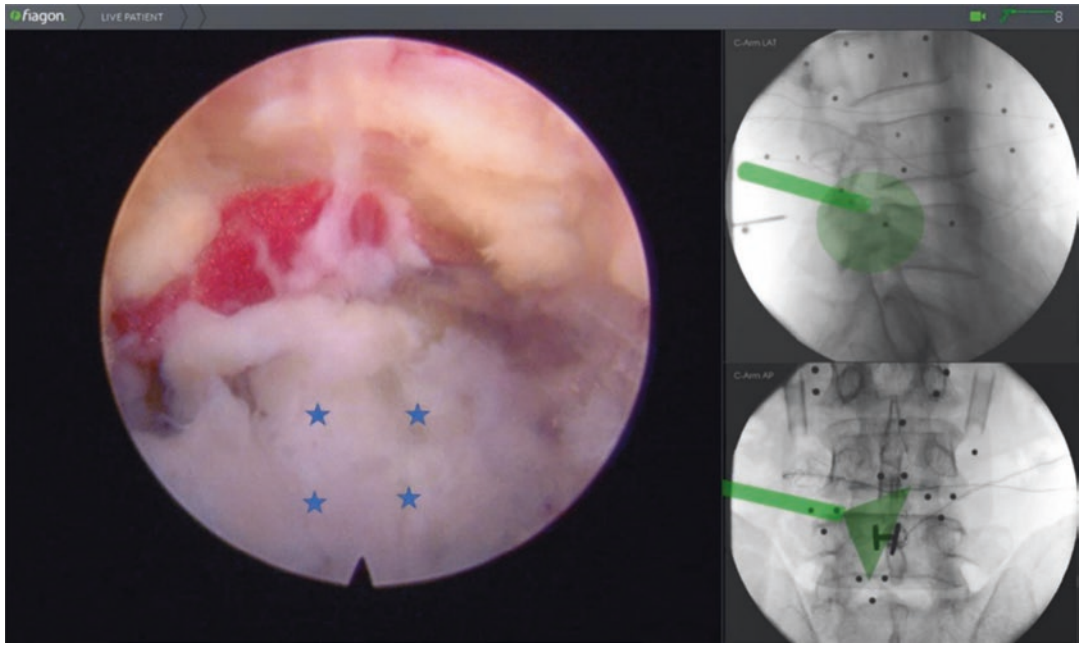


**Fig. 12.9** The real-time position of the working channel and the herniated disc can be clearly observed

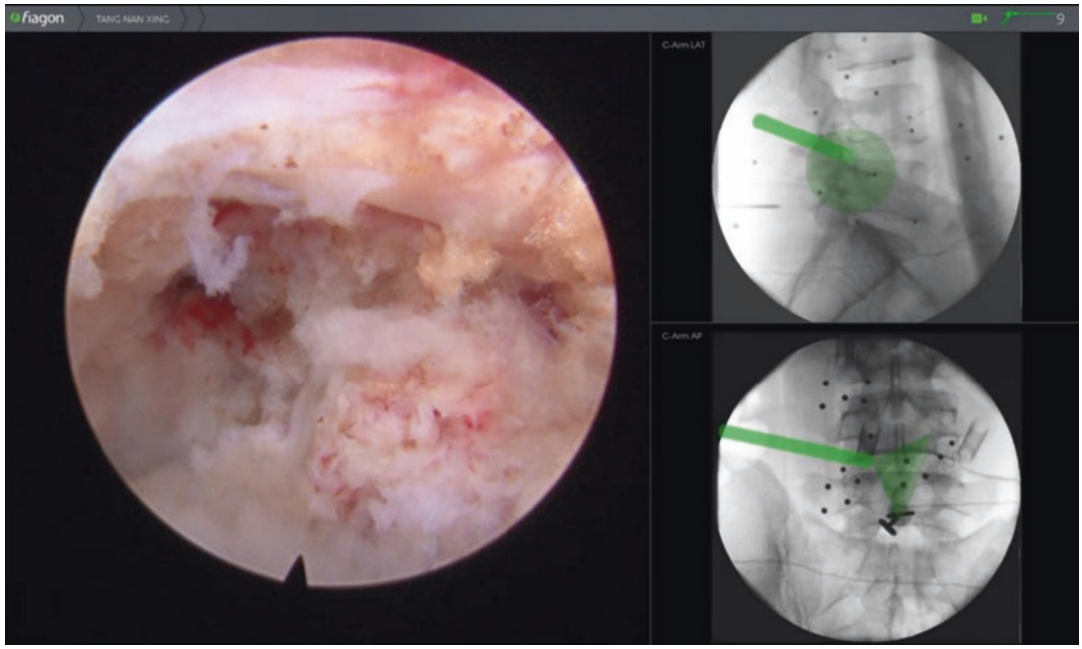


**Fig. 12.10** After the herniated disc is removed, the nerve root is completely decompressed

greatly increases the difficulty of accurate insertion of working cannulas during TELD. For beginners with poor 3D sense and inexperience, the difficulty of performing TELD will be magnified, and the risk of nerve injury will increase as well. In order to ensure operational safety, the working cannulas are inserted under the monitoring of C-arm X-ray fluoroscopy, which virtually increases the radiation exposure of both patients and doctors. Increasing studies have shown that different doses of radiation exposure can induce tumors, cataracts, cardiovascular diseases, etc., posing a serious threat to the health of patients and medical staff [1].

Computer navigation technology is a manifestation of minimally invasive and accurate medical treatment. Navigation technology can accurately locate the lesions, help to select the best surgical approach reasonably, and effectively reduce surgical injury and complications. According to the space position of the instrument, the signals can be divided into optics (infrared ray), magnetism (electromagnetism), and acoustic (ultrasound), and the corresponding navigation is called photoelectric, electromagnetic, and acoustic navigation systems, respectively [21–27].

The different navigation systems have diverse advantages and disadvantages [2]: (1) Optoelectronic navigation has the highest accuracy, but the signal may be blocked by surgical instruments and operators, and it is expensive. (2) Although ultrasound navigation has the advantages of non-invasive, radiation-free, and real-time tracking, it has not been widely used in clinical practice. (3) Electromagnetic navigation is not restricted by visual field and sightline, especially suitable for minimally invasive spinal surgery, but it is easily affected by environmental ferromagnetic effects. Due to the poor penetrability of ultrasound signals in bone, the guiding performance of the deep spine and spinal canal cannot meet the clinical requirements. The current navigation applications used in spine surgery are mainly optoelectronic navigation and electromagnetic navigation. Optoelectronic navigation is traditional navigation. As a traditional navigation technology, photoelectric navigation has strong anti-interference ability, stable signal, no obvious influence on other equipment in an operating room, and low cost, but there are unfavorable factors such as large size and heavy equipment. In addition, optical navigation may cause navigation interruption through the blocking of light source by surgeons or surgical instruments. Under the guidance of intraoperative imaging (C-arm, O-arm), spinal surgeons perform operations based on their clinical experience and skills.

On the contrary, electromagnetic navigation is a relatively new technology, which has the characteristics of safe and accurate operation under direct vision, ensuring the accurate and real-time reproduction of intraoperative images. It is not susceptible to light occlusion, has no blind area, and can accurately record surgical procedures, improving the accuracy and security of the spinal surgery. Additionally, it is widely used in pedicle screw implantation [20–25]. Hahn et al. [3] implanted pedicle screws with the assistance of electromagnetic navigation technology. In their study, there were 37 (77.1%) thoracic pedicle screws with maximum cortical penetration less than 2 mm and only 9 screws with dislocation, indicating that pedicle screws placement under electromagnetic navigation is an ideal method.

Compared with other optoelectronic navigation systems, electromagnetic navigation has the advantages of accurate positioning and no intraoperative occlusion, and the continuity of operation is generally not disturbed. In addition, the advantages of electromagnetic navigation systems are listed as follows: (1) The navigation device is small in size and easy to move. A single person can complete equipment preparation and debugging, reducing the pressure of insufficient operating room space as it is easy to transfer the equipment within the operating room. (2) The entire surgical area is located in the magnetic field, and the objects that do not emit magnetic field signals are not imaged, so it is unchallenging to use during the operation. There is no need to adjust the direction of the instrument repeatedly, improving the operation efficiency and saving operation time. (3) Computer control is not manual control, improving the operation simplicity, accuracy, and stability. (4) It supports hot

start, which can be closed or opened at any time, thus avoiding the influence among systems. It has no obvious impact on other equipment in the operating room, and the accuracy of the system is not affected by the various instruments found in the operating room. (5) There is no need for reference to the environment installation and commissioning, no visual field barrier encountered during operation, and is attributed to low infection rate [4].

TELD has the advantages of a bright and clear surgical field, precise discectomy, and fewer complications, albeit still with some limitations, which include as follows: (1) The 2-dimensional (2D) images under percutaneous endoscopy lack depth perception. (2) The anatomical structure under the endoscope is different from that of conventional microanatomy, and lack of experience can easily lead to localization deviation. (3) The narrow operation space and the hand-eye separated operation bring more difficulties to the surgeons. (4) Sometimes, it is difficult to stop bleeding under a microscope, and the position of endoscopy and surgical tools cannot be clearly determined because of the blurred surgical field of vision, which may warrant suspension of the operation. However, the combination of TELD and electromagnetic navigation can reduce the difficulties caused by the above conditions, and can also bring more assistance to doctors who lack surgical experience by aiding in the reduction of the learning curve.

Electromagnetic navigation-assisted percutaneous endoscopic spinal surgery has the following advantages: (1) Improving the surgical safety and accuracy of lesion resection, which are beneficial to the postoperative recovery of patients. (2) It can determine the positional relationship between intervertebral disc lesions and peripheral blood vessels and the range of decompression, effectively avoiding the damage of normal tissue. (3) It is beneficial to individualized puncture design, avoiding the key structural and functional areas in the spinal canal, and reducing surgical trauma. (4) Combined with percutaneous spinal endoscopy, it can expand surgical indications and effectively avoid trauma and complications caused by routine open surgery. However, the electromagnetic field may be affected by iron during the operation, and electromagnetic navigation cannot be used if the patient has iron objects intact. Additionally, the locator must be fixed stable during operation, and the accuracy of navigation will decrease if the locator is unstable or shifted. Therefore, in order to achieve more accurate and occlusion-free stable positioning, further studies are required. However, with the miniaturization of magnetic field transmitters and the improvement of the accuracy of automatic recognition and registration of detectors, electromagnetic navigation is expected to become one of the main gateways of spinal surgical navigation.

There are some points for attention in electromagnetic navigation-assisted TELD: (1) Surgeons and relevant technologists should be professionally trained and familiar with the operation process of a navigation system in order to reduce the operation time of establishing navigation. With the accumulation of experience and familiarity with a navigation system, the time to establish navigation configuration will be gradually shortened, generally within five to ten minutes. (2) The electromagnetic navigation sensor frame and needle positioner must be firmly fixed, generally fixed on the adjacent surgical segment spinous process. On the other hand, the depth of K-wire insertion is required to reach 2 cm, so as to avoid serious errors caused by image drift. (3) Although the direction of puncture needle and reamers and the depth of the insertion and the position of the surgical tools can be monitored in real time during the operation, surgeons should still be familiarized with the anatomical structures under the microscope and should be careful when operating around nerve roots and blood vessels so as to avoid inevitable damage. (4) Although electromagnetic navigation can largely reduce the learning curve of PELD to young surgeons, navigation itself has a steep learning curve. It is necessary to be fully familiar with the applicable specifications of navigation and accumulate the experience of 20–30 cases in order to better combine electromagnetic navigation technology with TELD and improve the efficiency of surgery.

## 12.7 Conclusions

EM-based navigation-guided TELD is an effective and safe minimally invasive technology for the treatment of various types of lumbar disc herniation. The TELD assisted by electromagnetic real-time navigation is more accurate and safer, as well as providing a reduction in X-ray radiation damage. The new technique is especially helpful for inexperienced spinal surgeons. Its application prospect for the future is broad-ranging, and EM-based navigation will further promote the development of percutaneous endoscopic spinal surgery.

## References


1. Hijikata S. Percutaneous nucleotomy. A new concept technique and 12 years' experience. Clin Orthop Relat Res. 1989;238(238):9.
2. Onik G, Helms CA, Ginsberg L, et al. Percutaneous lumbar diskectomy using a new aspiration probe: porcine and cadaver model. Radiology. 1985;155(1):251–2.
3. Hahn P, Oezdemir S, Komp M, Giannakopoulos A, Kasch R, Merk H, Liermann D, Godolias G, Ruetten S. Navigation of pedicle screws in the thoracic spine with a new electromagnetic navigation system: a human cadaver study. Biomed Res Int. 2015;2015:183586. https://doi.org/10.1155/2015/183586. PMID: 25759814; PMCID: PMC4339821.
4. Hausmann B, Forst R. Nucleoscope. Instrumentarium for endoscopy of the intervertebral disc space. Arch Orthop Trauma Surg. 1983;102(1):57–9.
5. Kambin P, NASS. Arthroscopic microdiscectomy. Spine. 2003;3(3 Suppl):60S–4S.
6. Yeung AT. Minimally invasive disc surgery with the yeung endoscopic spine system (YESS). Surg Technol Int. 1999;8:267–77.
7. Yeung AT, Tsou PM. Posterolateral endoscopic excision for lumbar disc herniation: Surgical technique, outcome, and complications in 307 consecutive cases. Spine (Phila Pa 1976). 2002;27(7):722–31. https://doi.org/10.1097/00007632-200204010-00009. PMID: 11923665.
8. Hoogland T, Schubert M, Miklitz B, et al. Transforaminal posterolateral endoscopic discectomy with or without the combination of a low-dose chymopapain: a prospective randomized study in 280 consecutive cases. Spine (Phila Pa 1976). 2006;31(24):E890–7.
9. Hoogland T, van den Brekel-Dijkstra K, Schubert M, et al. Endoscopic transforaminal discectomy for recurrent lumbar disc herniation: a prospective, cohort evaluation of 262 consecutive cases. Spine (Phila Pa 1976). 2008;33(9):973–8.
10. Pan M, Li Q, Li S, Mao H, et al. Percutaneous endoscopic lumbar discectomy: indications and complications. Pain Physician. 2020;23(1):49–56.
11. Tacconi L, Baldo S, Merci G, et al. Transforaminal percutaneous endoscopic lumbar discectomy: outcome and complications in 270 cases. J Neurosurg Sci. 2018;26:531–6.
12. Panagiotopoulos K, Gazzeri R, Bruni A, et al. Pseudoaneurysm of a segmental lumbar artery following a full-endoscopic transforaminal lumbar discectomy: a rare approach-related complication. Acta Neurochir. 2019;161(5):907–10.
13. Ahn Y. Transforaminal percutaneous endoscopic lumbar discectomy: technical tips to prevent complications. Expert Rev Med Devices. 2012;9(4):361–6.
14. Kapetanakis S, Gkantsinikoudis N, Chaniotakis C, et al. Percutaneous transforaminal endoscopic discectomy for the treatment of lumbar disc herniation in obese patients: health-related quality of life assessment in a 2-year follow-up. World Neurosurg. 2018;113:e638–49.
15. Hilbert T, Boehm O, Pflugmacher R, et al. Rare complication after endoscopic discectomy. Anaesthesist. 2014;63(1):41–6.
16. Hsu PK, Wu YC. Electromagnetic navigation-guided one-stage dual localization of small pulmonary nodules. Chest. 2018;154(6):1462–3.
17. Arenberg D. Electromagnetic navigation guided bronchoscopy. Cancer Imaging. 2009;9(1):89–95.
18. Putzer D, Arco D, Schamberger B, et al. Comparison of two electromagnetic navigation systems for ct-guided punctures: a phantom study. Rofo. 2016;188(5):470–8.
19. Durand P, Moreau-Gaudry A, Silvent AS, et al. Computer assisted electromagnetic navigation improves accuracy in computed tomography guided interventions: a prospective randomized clinical trial. PLoS One. 2019;12(3):e0173751.
20. von Jako RA, Carrino JA, Yonemura KS, et al. Electromagnetic navigation for percutaneous guidewire insertion: accuracy and efficiency compared to conventional fluoroscopic guidance. NeuroImage. 2009;47(Suppl 2):T127–32.
21. von Jako R, Finn MA, Yonemura KS, et al. Minimally invasive percutaneous transpedicular screw fixation: increased accuracy and reduced radiation exposure by means of a novel electromagnetic navigation system. Acta Neurochir. 2011;153(3):589–96.
22. Allison RR. The electromagnetic spectrum: current and future applications in oncology. uture. Oncologia. 2013;9(5):657–67.

23. Mehta AC, Hood KL, Schwarz Y, et al. The evolutional history of electromagnetic navigation bronchoscopy: state of the art. Chest. 2018;154(4):935–47.
24. Komune N, Matsushima K, Matsuo S, et al. The accuracy of an electromagnetic navigation system in lateral skull base approaches. Laryngoscope. 2017;127(2):450–9.
25. Cai K, Yang R, Lin Q, et al. Near-infrared camera calibration for optical surgical navigation. J Med Syst. 2016;40(3):67.
26. Diana M, Soler L, Agnus V, et al. Prospective evaluation of precision multimodal gallbladder surgery navigation: virtual reality, near-infrared fluorescence, and X-ray-based intraoperative cholangiography. Ann Surg. 2017;266(5):890–7.
27. Kapoor R, Ramasamy S, Gardi A, et al. Acoustic sensors for air and surface navigation applications. Sensors (Basel). 2018;18(2):499.

# 13 Navigation-Guided Endoscopic Lumbar Laminotomy

Akaworn Mahatthanatrakul, Yanting Liu, Claudia A. Covarrubias, and Jin-Sung Kim

## Abbreviations

| | |
|---|---|
| CT | Computed tomography |
| EM | Electromagnetic |
| EMTS | Electromagnetic tracking system |
| IR | Infrared |
| LE-ULBD | Lumbar endoscopic unilateral laminotomy for bilateral decompression |
| MRI | Magnetic resonance imaging |
| OTS | Optical tracking system |
| PECD | Posterior endoscopic cervical discectomy |
| TELD | Transforaminal endoscopic lumbar discectomy |
| ULBD | Unilateral laminotomy for bilateral decompression |

A. Mahatthanatrakul
Department of Orthopaedics, Naresuan University Hospital, Phitsanulok, Thailand

Y. Liu
Department of Neurosurgery, Seoul St Mary's Hospital, The Catholic University of Korea, Seoul, South Korea

C. A. Covarrubias
Department of Experimental Surgery, McGill University, Montreal, Quebec, Canada
e-mail: claudia.covarrubias@mail.mcgill.ca

J.-S. Kim (✉)
Department of Neurosurgery, Seoul St Mary's Hospital, The Catholic University of Korea, College of Medicine, Seoul, Korea (Republic of)

## 13.1 Introduction

Surgical decompression is undertaken for patients with lumbar spinal stenosis when conventional treatments are no longer effective. Direct decompression such as open laminotomy and laminectomy with or without fusion are the standard procedures taught during orthopedics and neurosurgery residency training. Lumbar endoscopic unilateral laminotomy for bilateral decompression (LE-ULBD) is an alternative minimally invasive surgery used for decompression of lumbar spinal stenosis. The advantages of LE-ULBD include decreased blood loss, shortened operative time, shorter hospital stay, decreased early postoperative pain scores, and minimal spinal muscle injury [1]. In contrast, some LE-ULBD disadvantages include unfamiliarity with endoscopic view and instrument handling, bleeding control, radiation exposure, and a significant learning curve [2].

Navigation using intraoperative 3D imaging is commonly used in instrumented spinal surgery. It is proven to have shortened operative time, reduced radiation exposure to surgical teams, and higher instrument insertion accuracy such as the pedicle screws or cortical screws [3–6]. Navigation is often combined with endoscopic spine surgery in various situations. Presently, posterior endoscopic cervical discectomy (PECD) with navigation is an effective method to treat cervical radiculopathy [7]. Additionally, there are reports that navigated transforaminal endoscopic lumbar



J.-S. Kim et al. (eds.), *Technical Advances in Minimally Invasive Spine Surgery*,
https://doi.org/10.1007/978-981-19-0175-1_13

discectomy (TELD) and navigation-guided interlaminar endoscopic foraminotomy reduce radiation exposure and learning curve [8–11]. In the LE-ULBD procedure, navigation has the potential to reduce the learning curve and radiation exposure, while also confirming the adequacy of decompression, which is advantageous during the resident and fellowship training, especially in cases with distorted anatomy [12].

## 13.2 Indications

General indications for LE-ULBD are similar to unilateral laminotomy for bilateral decompression (ULBD) using an operating microscope. LE-ULBD is a surgical treatment for patients suffering from spinal canal stenosis with bilateral symptoms related to dorsal pathologies, such as lumbar spondylosis with facet joint hypertrophy, ligamentum flavum hypertrophy, facet cyst, mild grade spondylolisthesis, or degenerative scoliosis [13].

## 13.3 Operative Procedures

### 13.3.1 Equipment and Instruments

- General equipment for interlaminar endoscopic surgery: monitor, light source, irrigation fluid, bipolar radiofrequency generator, endoscope, working sheath, endoscopic burr, rongeur, and forceps (Fig. 13.1).
- Surgical navigation system: optical tracking camera, reference frame, calibration probe, and endoscopic attachable tracker.
- An intraoperative 3D fluoroscopy or mobile CT scanner.

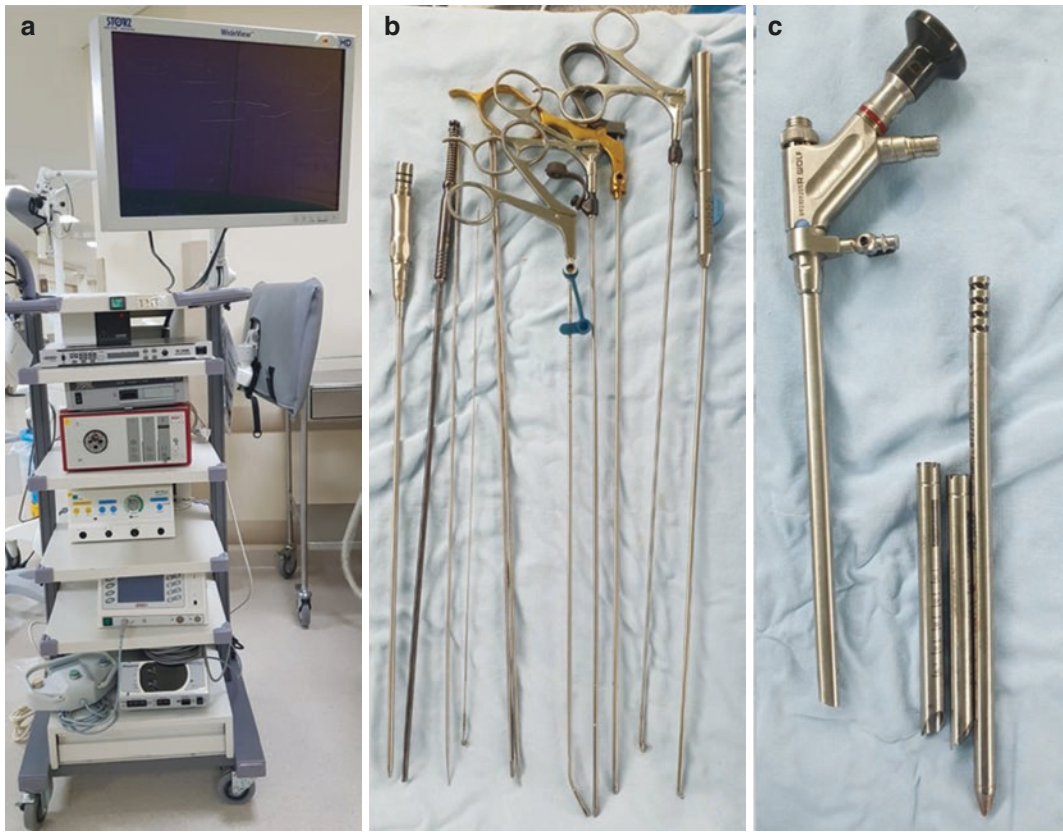


**Fig. 13.1** Equipment for endoscopic surgery. Endoscopic workstation (**a**), endoscopic instruments (**b**), spinal endoscope (**c**)

## 13.4 Operative Setting

Put the patient under general anesthesia and place in a prone position on the operating table (Fig. 13.2). Attach the reference frame to the operating table (Fig. 13.3). Place the endoscopic monitor opposite to the surgeon. Set the optical tracking cameras and the navigation monitor at the end of the operating table.

## 13.5 Surgical Technique

Perform aseptic skin routine and drape at the surgical site. Obtain the three-dimensional images by deploying an intraoperative 3D fluoroscopy. Register the endoscope and the trackers to the reference frame (Fig. 13.4). Use a navigation probe to locate the surgical landmark instead of two-dimensional fluoroscopy (Fig. 13.5). Insert the dilators and working sheath according to the standard interlaminar endoscopic approach. Examine the location of the working sheath with the navigation probe (Fig. 13.6). The surgeon maneuvers the endoscope at the index level and then utilizes the C-arm fluoroscopy to check the location of the endoscope and to ensure the correct operative level. Start the standard LE-ULBD procedure, coagulate the bleeding muscle, and create a working space by extracting the soft tissues to expose the lamina. Use a burr and bone punch to

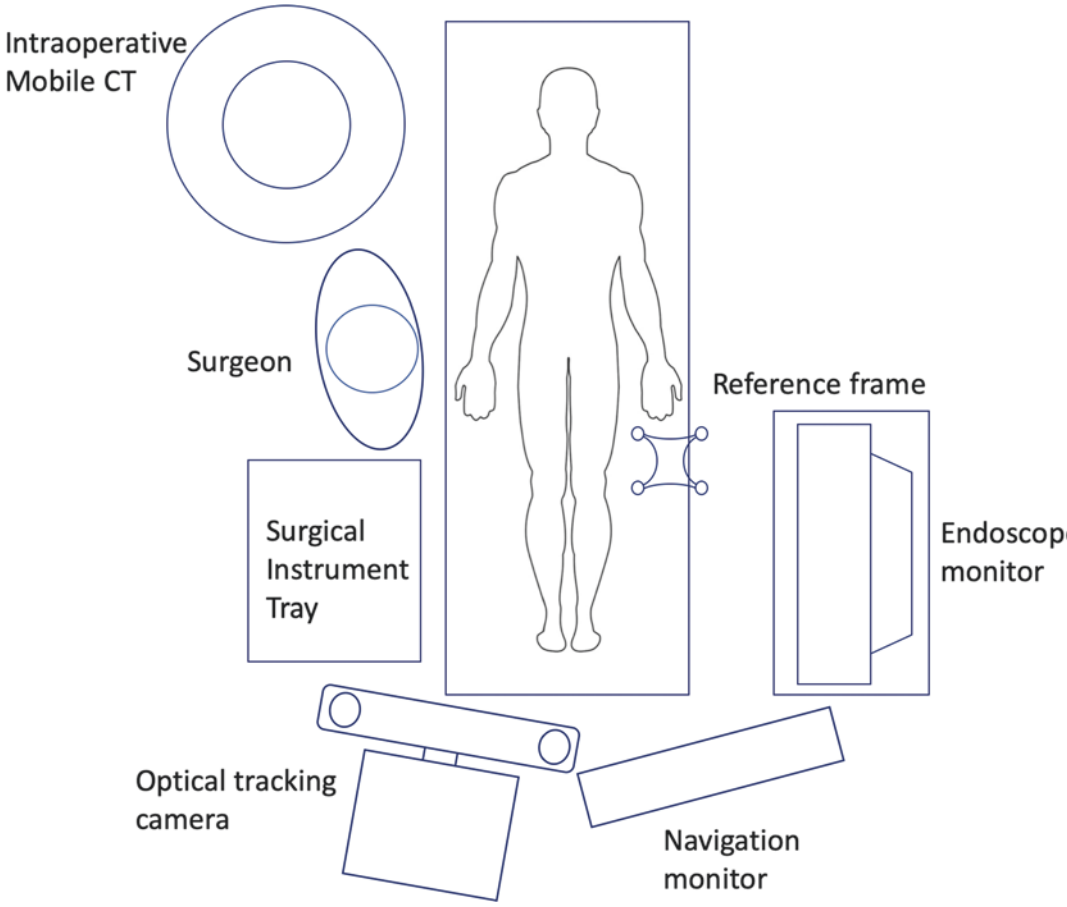


**Fig. 13.2** Operating room setup. The patient was prone positioned on the operating table. The optical camera and monitor were set at the end of the table. The reference frame was attached to the operating bed rail. The endoscopic monitor was placed opposite to the surgeon

**Fig. 13.3** Reference frame placement

remove the upper end of the lower lamina, then the medial side of the inferior articular process, and lastly the lower end of the upper lamina until the margin of the ligamentum flavum is exposed. Drill the contralateral lamina keeping the ligamentum flavum intact to prevent injury to the dura. Resect the ligamentum flavum and facet joint to decompress contralateral lateral recess and to ensure bilateral decompression of the spinal canal. Utilize endoscopic view and navigation view to confirm the adequacy of decompression without excessive facetectomy. An intraoperative 3D fluoroscopy or CT confirms the degree of decompression (Fig. 13.7).

## 13.6 Case Illustration

A 59-year-old male patient with a previous diagnosis of ankylosing spondylitis visited the hospital with a chief complaint of lower back pain and right thigh tingling sensation at 6 months of onset. Physical examination revealed decreased

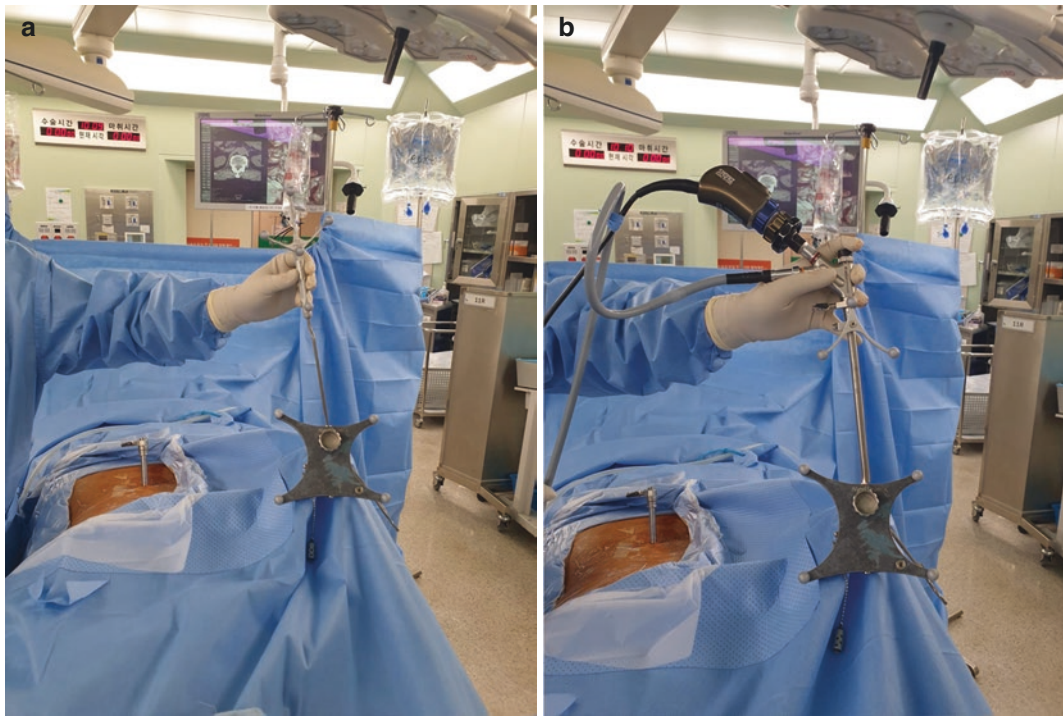


**Fig. 13.4** Registration of the navigated probe (**a**) and the endoscope (**b**)

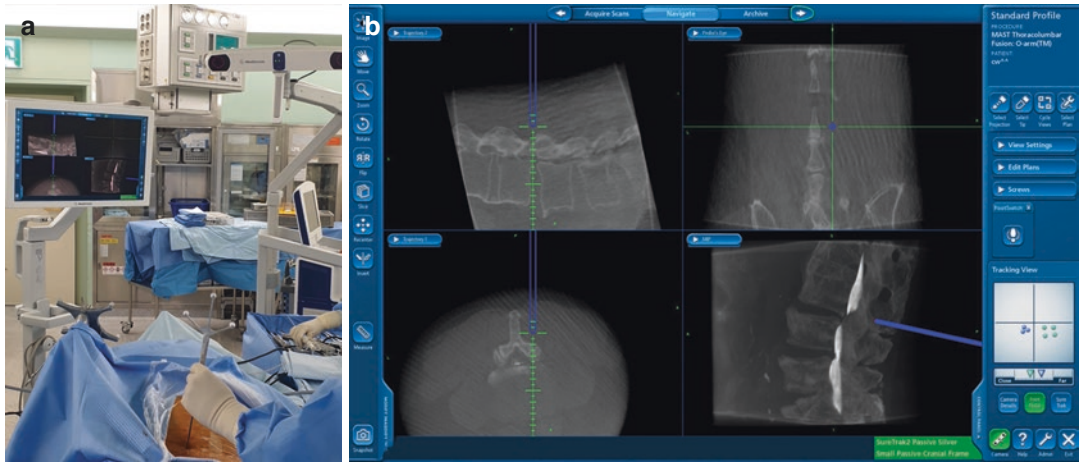


**Fig. 13.5** Landmarking for the working sheath insertion was done with navigated probe (**a**). The navigation view (**b**) shows the position of the probe

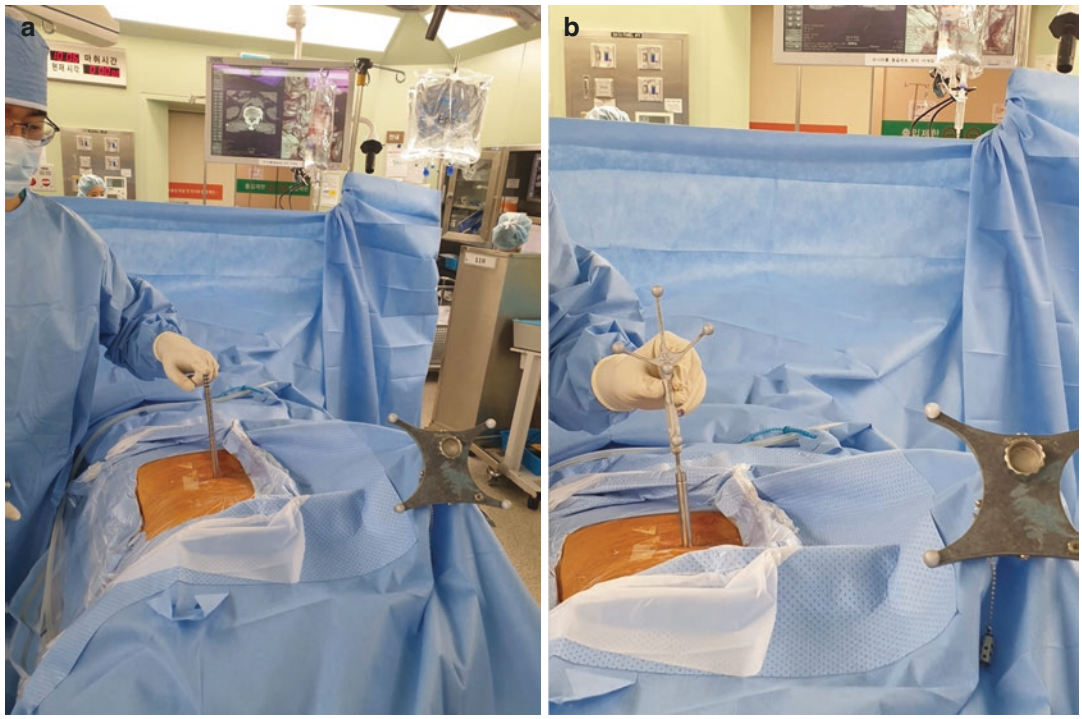


**Fig. 13.6** Insertion of the dilators and working sheath (**a**) Position of the working sheath were confirmed with a navigated probe (**b**)

motor power of right knee extension and grade IV ankle dorsiflexion. Dynamic plain radiographs showed static retrolisthesis of L3–4 vertebrae (Fig. 13.8). MRI displayed central spinal stenosis of L3–4 with facet cyst of the right L3–4 facet joint and lateral recess stenosis of left L4–5 level (Fig. 13.9). However, the patient had no symptoms of the left L4 or L5 nerve root compression. He underwent navigation-guided LE-ULBD at the right L3–4 level (Fig. 13.10). Postoperative CT and MRI showed decompression of the spinal canal (Fig. 13.11).

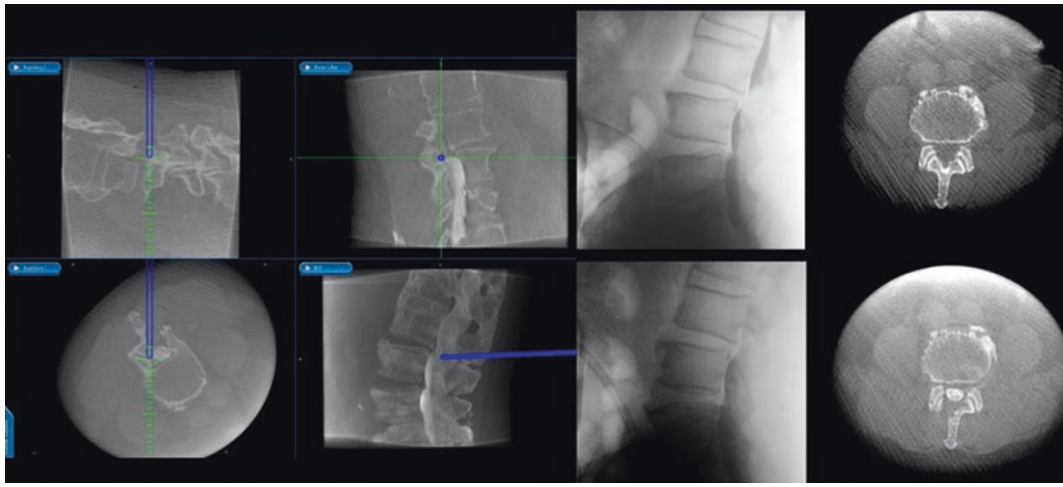

**Fig. 13.7** Intraoperative images show the adequacy of decompression and preservation of the facet joint

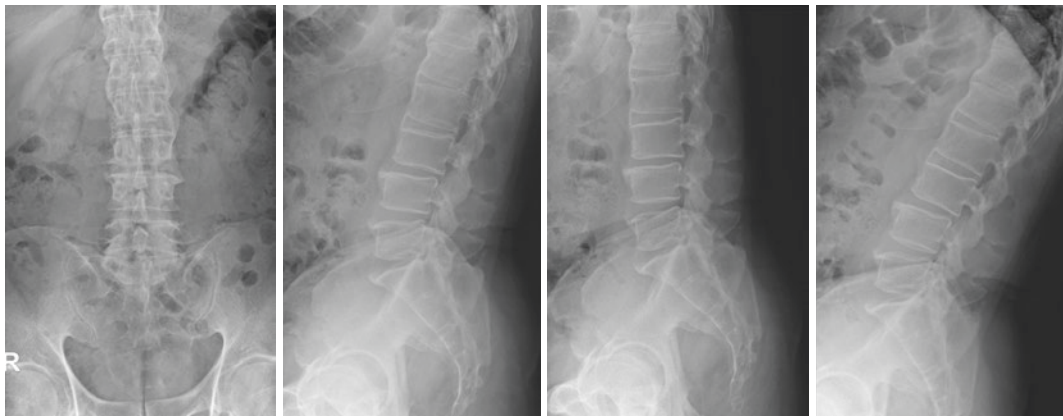

**Fig. 13.8** Dynamic plain radiograph shows stable retrolisthesis L3–4 level and ankylosing spine

Advantages of navigation-guided endoscopic lumbar laminotomy

- Reduce radiation exposure to the technician and the surgical team.
- Assess the adequacy of decompression with endoscopic view and navigation.
- Track the amount of facet joint removal with the navigated endoscope.
- Offer schematic mastery of the procedure to residents and fellows.
- Shorten the learning curve of surgeons performing the LE-ULBD.
- Navigate any straight instrument with the SureTrack system.

Disadvantages of navigation-guided endoscopic lumbar laminotomy

- Longer setup time.
- Increased radiation exposure to the patient.
- Sensitivity to the position change of the patient.
- More training and familiarization of the equipment.
- Drawbacks to cost-effectiveness.

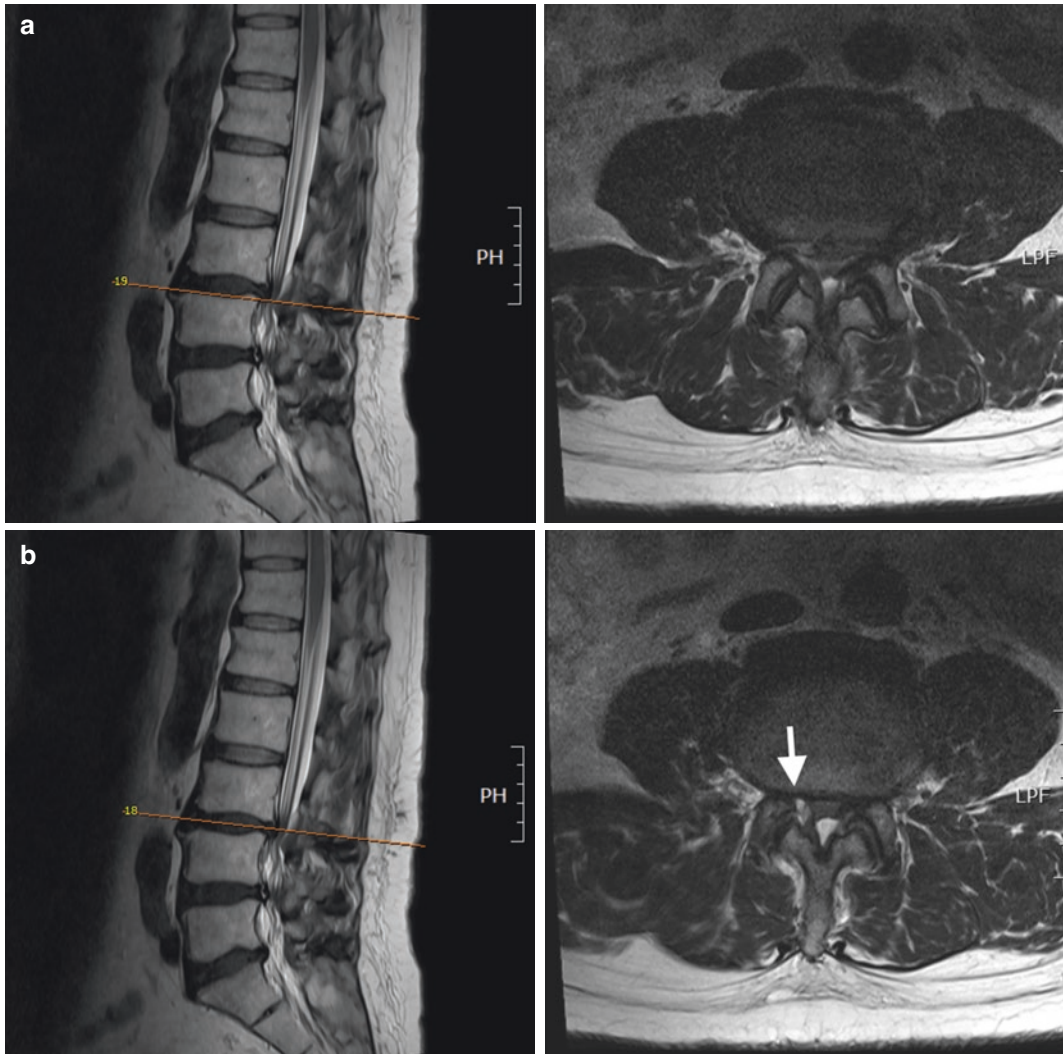


**Fig. 13.9** Preoperative MRI (**a**) shows central canal stenosis and (**b**) a right facet joint cyst (arrow)

## 13.7 Discussion

Current surgical navigation systems rely on the optical tracking system (OTS), the electromagnetic tracking system (EMTS), or a combination of both. The OTS usually utilizes the infrared (IR) beam and IR camera to detect the location of the marker attached to the patient reference frame and the navigated instruments. This OTS needs the IR camera and the marker to be in the line of sight for accurate navigation. The EMTS consists of the electromagnetic (EM) field produced by the generator, EM patient reference, and EM sensor at the navigated instrument. Both systems have comparable accuracy [14, 15]. OTS is more commonly used in neurosurgery, spinal surgery, and orthopedic surgery because they are less affected by metal artifacts. EMTS provides a specific advantage since the sensor does not require a line of sight with the tracking source; hence, it is suitable to be placed at the tip of the flexible endoscope [14].

Obesity is considered one of several risk factors for postoperative complications after spinal surgery [16, 17]. Spinal endoscopy may reduce postoperative complications, such as infection, in

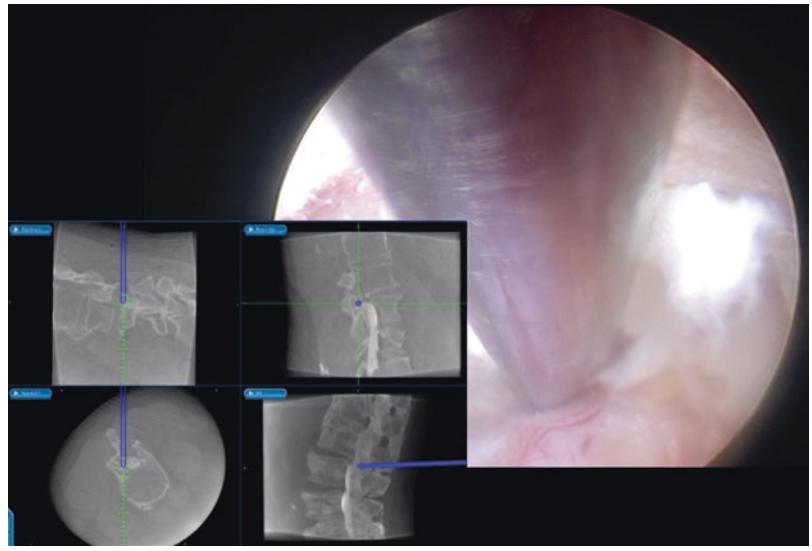

**Fig. 13.10** Video shows intraoperative findings and a step-by-step approach for lumbar endoscopic unilateral laminotomy for bilateral decompression (Video available in electronic supplementary material)

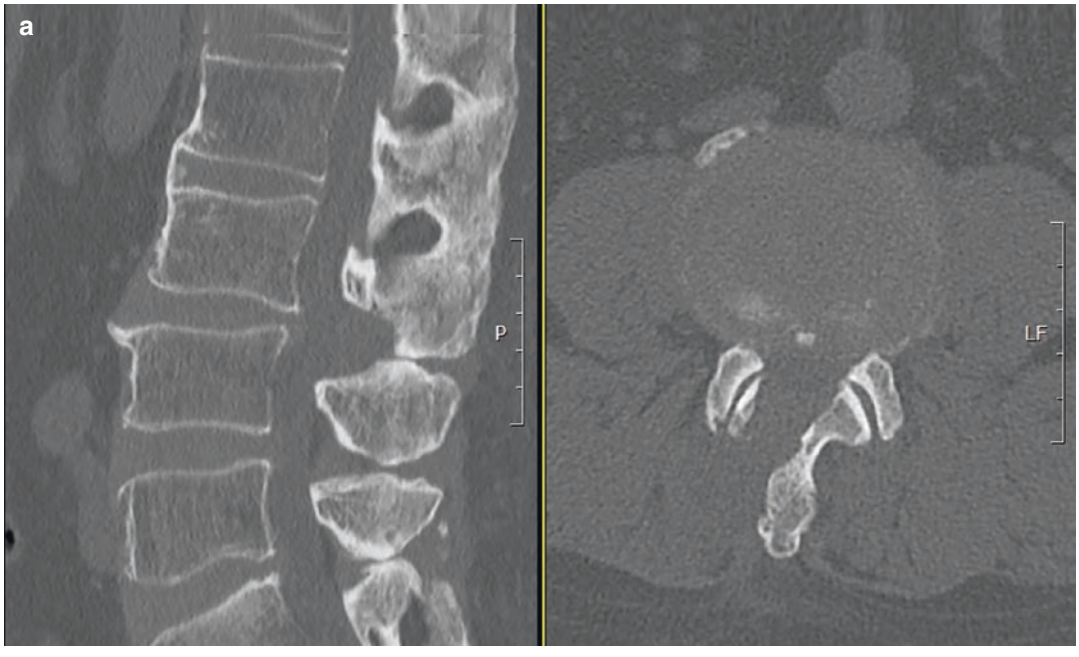


**Fig. 13.11** Postoperative imaging. Postoperative CT (**a**) shows the extent of bone cutting and facet joint preservation. Postoperative MRI (**b**) shows the adequacy of decompression

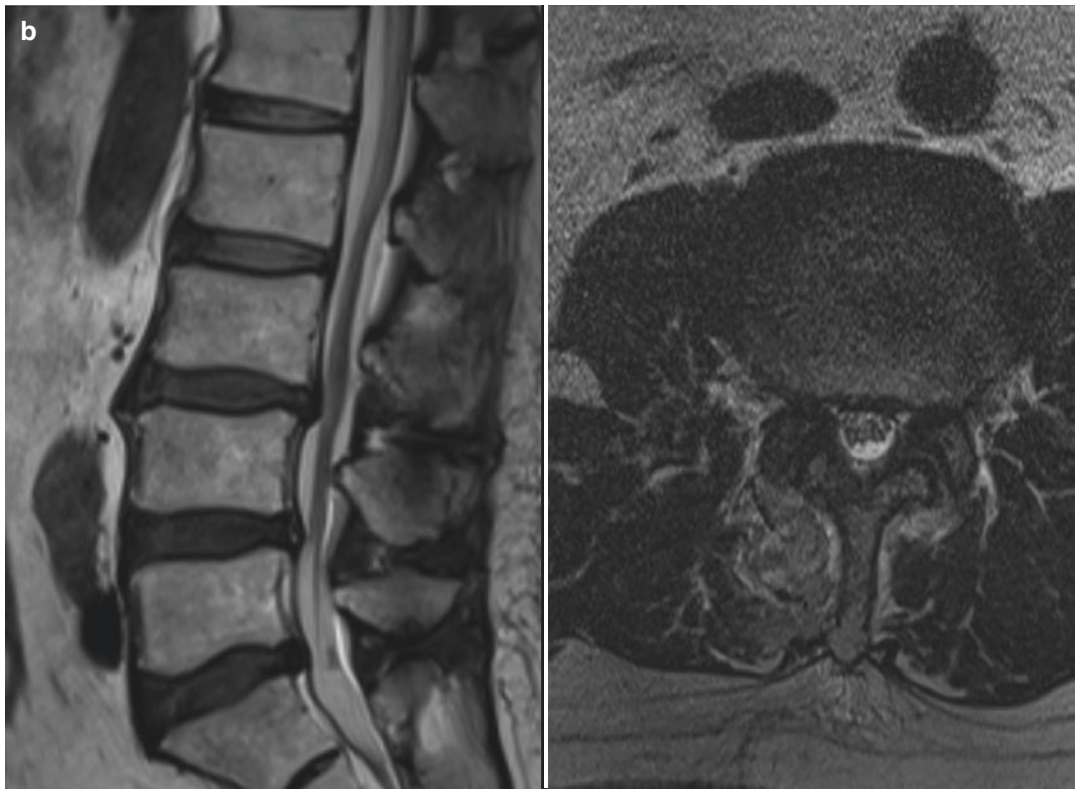


**Fig. 13.11** (Continued)

obese patients. However, this procedure also poses many challenges in this population [18]. The fluoroscopic image is usually non-optimal due to the thickness of subcutaneous tissue. Furthermore, the incision site varies as the distance from the initial site of the incision to the disc or lamina is deeper in the obese population. Navigation is especially helpful when surgeons perform the LE ULBD in an obese patient. It assists in planning the location for needle insertion in contralateral decompression and eliminates the haziness of soft tissue in two-dimensional fluoroscopy.

Adequacy of decompression and excessiveness of the facet joint resection may be difficult to assess in LE ULBD, particularly during the first part of the learning curve [2, 19]. Intraoperative CT myelogram reveals the level of stenosis (Fig. 13.5) and ensures sufficient decompression in the operating theater to prevent reoperation caused by inadequate surgical decompression (Fig. 13.6).

Reoperation significantly increases the cost of treatment. Although the initial equipment cost is high, intraoperative navigation has demonstrated a reduction of reoperation rates and an increase in its cost-effectiveness, specifically in high-volume centers [20, 21]. Navigation also indicates a reduced operating time in instrumented spinal fusion, although the reduction in operative time can offset the high initial cost of the navigation system [5].

The interlaminar spinal endoscope has evolved to its current third generation. With a larger outer diameter and working channel, surgeons can efficiently decompress the central canal, lateral recess, and neural foramen simultaneously in the same incision [22]. Endoscopes specifically designed for navigation, e.g., the addition of EM sensor to the tip of the flexible instrument or the

bipolar radiofrequency, with the combined utilization of OTS and ETMS navigation system, can improve the accuracy of the surgical procedure, shorten the learning curve of surgeons, and enhance the overall safety of LE-ULBD.

## 13.8 Conclusion

LE-ULBD is a minimally invasive procedure to decompress bilateral spinal canal stenosis. Intraoperative navigation is an auxiliary tool that increases the accuracy of bone removal and facet joint sparing, shortens the learning curve of surgeons, and reduces radiation exposure to the surgical team.

## References


1. Komp M, Hahn P, Oezdemir S, Giannakopoulos A, Heikenfeld R, Kasch R, Merk H, Godolias G, Ruetten S. Bilateral spinal decompression of lumbar central stenosis with the full-endoscopic interlaminar versus microsurgical laminotomy technique: a prospective, randomized, controlled study. Pain Physician. 2015;18(1):61–70.
2. Lee CW, Yoon KJ, Kim SW. Percutaneous endoscopic decompression in lumbar canal and lateral recess stenosis - the surgical learning curve. Neurospine. 2019;16(1):63–71. https://doi.org/10.14245/ns.1938048.024.
3. Johnson N. Imaging, navigation, and robotics in spine surgery. Spine (Phila Pa 1976). 2016;41(Suppl 7):S32. https://doi.org/10.1097/BRS.0000000000001437.
4. Kochanski RB, Lombardi JM, Laratta JL, Lehman RA, O'Toole JE. Image-guided navigation and robotics in spine surgery. Neurosurgery. 2019;84(6):1179–89. https://doi.org/10.1093/neuros/nyy630.
5. Hussain I, Cosar M, Kirnaz S, Schmidt FA, Wipplinger C, Wong T, Hartl R. Evolving navigation, robotics, and augmented reality in minimally invasive spine surgery. Global Spine J. 2020;10(2 Suppl):22S–33S. https://doi.org/10.1177/2192568220907896.
6. Kotheeranurak V, Lin GX, Mahatthanatrakul A, Kim JS. Endoscope-assisted anterior lumbar interbody fusion with computed tomography-guided, image-navigated unilateral cortical bone trajectory screw fixation in managing adjacent segment disease in L5/S1: technical note. World Neurosurg. 2019;122:469–73. https://doi.org/10.1016/j.wneu.2018.10.029.
7. Zhang C, Wu J, Xu C, Zheng W, Pan Y, Li C, Zhou Y. Minimally invasive full-endoscopic posterior cervical foraminotomy assisted by O-arm-based navigation. Pain Physician. 2018;21(3):E215–23.
8. Qin H, Huang S, Xu L, Wei P, Jiang J, Xie Z, Luo X, Tan H, Huang W. Radiation exposure and operation time in percutaneous endoscopic lumbar discectomy using fluoroscopy-based navigation system. World Neurosurg. 2019;127:e39–48. https://doi.org/10.1016/j.wneu.2019.01.289.
9. Ao S, Wu J, Tang Y, Zhang C, Li J, Zheng W, Zhou Y. Percutaneous endoscopic lumbar discectomy assisted by O-arm-based navigation improves the learning curve. Biomed Res Int. 2019;2019:6509409. https://doi.org/10.1155/2019/6509409.
10. Fan G, Han R, Gu X, Zhang H, Guan X, Fan Y, Wang T, He S. Navigation improves the learning curve of transforamimal percutaneous endoscopic lumbar discectomy. Int Orthop. 2017;41(2):323–32. https://doi.org/10.1007/s00264-016-3281-5.
11. Chen KT, Song MS, Kim JS. How I do it? Interlaminar contralateral endoscopic lumbar foraminotomy assisted with the O-arm navigation. Acta Neurochir. 2020;162(1):121–5. https://doi.org/10.1007/s00701-019-04104-y.
12. Shin Y, Sunada H, Shiraishi Y, Hosokawa M, Koh Y, Tei R, Aketa S, Motoyama Y, Yonezawa T, Nakase H. Navigation-assisted full-endoscopic spine surgery: a technical note. J Spine Surg. 2020;6(2):513–20.
13. Hasan S, McGrath LB, Sen RD, Barber JK, Hofstetter CP. Comparison of full-endoscopic and minimally invasive decompression for lumbar spinal stenosis in the setting of degenerative scoliosis and spondylolisthesis. Neurosurg Focus. 2019;46(5):E16. https://doi.org/10.3171/2019.2.FOCUS195.
14. Sorriento A, Porfido MB, Mazzoleni S, Calvosa G, Tenucci M, Ciuti G, Dario P. Optical and electromagnetic tracking systems for biomedical applications: a critical review on potentialities and limitations. IEEE Rev Biomed Eng. 2020;13:212–32. https://doi.org/10.1109/rbme.2019.2939091.
15. Koivukangas T, Katisko JP, Koivukangas JP. Technical accuracy of optical and the electromagnetic tracking systems. Springerplus. 2013;2(1):90. https://doi.org/10.1186/2193-1801-2-90.
16. Jackson KL II, Devine JG. The effects of obesity on spine surgery: a systematic review of the literature. Global Spine J. 2016;6(4):394–400. https://doi.org/10.1055/s-0035-1570750.
17. Katsevman GA, Daffner SD, Brandmeir NJ, Emery SE, France JC, Sedney CL. Complexities of spine surgery in obese patient populations: a narrative review. Spine J. 2020;20(4):501–11. https://doi.org/10.1016/j.spinee.2019.12.011.
18. Kapetanakis S, Gkantsinikoudis N, Chaniotakis C, Charitoudis G, Givissis P. Percutaneous transforaminal endoscopic discectomy for the treatment of lumbar disc herniation in obese patients: health-related quality of life assessment in a 2-year follow-up. World Neurosurg. 2018;113:e638–49. https://doi.org/10.1016/j.wneu.2018.02.112.
19. Lim KT, Nam HGW, Kim SB, Kim HS, Park JS, Park CK. Therapeutic feasibility of full endoscopic decompression in one- to three-level lumbar canal

stenosis via a single skin port using a new endoscopic system, percutaneous stenoscopic lumbar decompression. Asian Spine J. 2019;13(2):272–82. https://doi.org/10.31616/asj.2018.0228.

20. Al-Khouja L, Shweikeh F, Pashman R, Johnson JP, Kim TT, Drazin D. Economics of image guidance and navigation in spine surgery. Surg Neurol Int. 2015;6(Suppl 10):S323–6. https://doi.org/10.4103/2152-7806.159381.
21. Costa F, Porazzi E, Restelli U, Foglia E, Cardia A, Ortolina A, Tomei M, Fornari M, Banfi G. Economic study: a cost-effectiveness analysis of an intraoperative compared with a preoperative image-guided system in lumbar pedicle screw fixation in patients with degenerative spondylolisthesis. Spine J. 2014;14(8):1790–6. https://doi.org/10.1016/j.spinee.2013.10.019.
22. Chen KT, Jabri H, Lokanath YK, Song MS, Kim JS. The evolution of interlaminar endoscopic spine surgery. J Spine Surg. 2020;6(2):502–12. https://doi.org/10.21037/jss.2019.10.06.

# O-arm Navigation-Guided Lumbar Foraminotomy

14

Kuo-Tai Chen, Jin-Sung Kim, and Nathaniel Brooks

## Abbreviations

| | |
|---|---|
| CT | Computed tomography |
| DRG | Dorsal root ganglion |
| ICELF | Interlaminar contralateral endoscopic lumbar foraminotomy |
| LFS | Lumbar foraminal stenosis |
| MRI | Magnetic resonance imaging |
| SAP | Superior articular process |
| TELF | Transforaminal endoscopic lumbar foraminotomy |
| VAS | Visual analogue scale |

## 14.1 Introduction

Lumbar spinal stenosis refers to the narrowing of the spinal canal or intervertebral foramen, causing the compression of neural structure. Lumbar foraminal stenosis (LFS) is one of the subgroups and usually causes entrapment of exiting nerve roots. Patients with LFS usually present with radiating pain over the unilateral leg in a dermatomal pattern with or without motor weakness [1, 2]. Surgical treatment is indicated if conservative treatment fails.

The current surgical strategies for treating LFS can be classified into decompression only and decompression with fusion. Fusion is usually reserved for patients with significant spinal deformity, such as scoliosis or spondylolisthesis, or potential risk of iatrogenic instability after an operation. Traditional open and minimally invasive posterior approaches for LFS entail performing a modest laminotomy or laminectomy with partial removal of the medial facet joint to decompress the nerve root [3]. The risk with the traditional approach is in further destabilizing the facet joint complex. Additionally, if the stenosis extends into the lateral aspect of the foramen, then complete decompression from a medial approach may not be possible. In 1988, Wiltse and Spencer reported the paraspinal approach for microsurgical decompression of LFS [4]. This technique preserved stability while decompressing the nerve root. It has been standard operation for treating LFS and far-out syndrome (i.e., far lateral disc herniations). However, there is some limitation with traditional microsurgical decompression. The excessive manipulation of dorsal root ganglion may result in postoperative dysesthesia. Instrument reach, and visualization which

K.-T. Chen
Department of Neurosurgery, Chang Gung Memorial Hospital, Chia-Yi, Taiwan

J.-S. Kim
Department of Neurosurgery, Seoul St Mary's Hospital, The Catholic University of Korea, College of Medicine, Seoul, Korea (Republic of)

N. Brooks (✉)
Department of Neurological Surgery, University of Wisconsin, Madison, WI, USA
e-mail: brooks@neurosurgery.wisc.edu



J.-S. Kim et al. (eds.), *Technical Advances in Minimally Invasive Spine Surgery*,
https://doi.org/10.1007/978-981-19-0175-1_14

are limited in larger patients. The limited view of the surgical field may cause incomplete decompression.

The initial development of full-endoscopic lumbar surgery mainly treated soft lumbar disc herniation via a posterolateral trajectory through the intervertebral foramen. Surgeons can also achieve decompression of hard bony stenosis using a trephine or drill. The endoscopic view is extremely focused, making anatomic localization challenging. Therefore, the standard full-endoscopic spine surgery is guided by intraoperative fluoroscopy. This two-dimensional imaging modality requires significant experience to master because integrating the surgical skills and fluoroscopy-guided concepts requires cognitively translating two-dimensional images onto three-dimensional navigation. This is similar to using a paper topographic map and a compass to navigate through the mountains. This translational skill can be learned but lengthens the learning curve of full-endoscopic spine surgery for this procedure. Recently, intraoperative computerized stereotactic navigation with CT-based image modalities has been applied in minimally invasive spine surgery (e.g., O-Arm-Medtronic, Brain-Lab, and others) [5, 6]. Navigation systems constantly provide computer reconstructed information in three dimensions. Continuing the metaphor, this is similar to transitioning from using the paper map to smartphone-based navigation. Computerized stereotactic navigation has been widely used for the placement of spine surgery instrumentation. For endoscopic spine surgery, computerized stereotactic navigation has been shown to shorten the learning curve by decreasing the experience needed to gain competence in endoscopic procedures [7, 8]. This chapter describes the principles and technical considerations of computerized stereotactic navigation-guided lumbar foraminotomy.

### 14.1.1 Anatomy

The intervertebral foramen is an ovoid window lateral to the spinal canal, containing the exiting nerve root originating from the dural sac. The ventrodorsal boundary of the intervertebral foramen is composed of multiple components. The posterior margin of the vertebral bodies and intervertebral disc is the ventral boundary of the foramen. The dorsal boundary is composed of ligamentum flavum and facet joints. The inferior vertebral notch of the cranial vertebra and the superior vertebral notch of the caudal vertebra form the craniocaudal boundary of the intervertebral foramen (Fig. 14.1). The foraminal dimension varies from 40 to 160 $mm^2$, and foraminal height ranges from 20 to 23 mm [9]. The exiting nerve root and dorsal root ganglion (DRG) are in the foramen's superior region, usually occupying approximately 30% of the foraminal area in the sagittal plane [10]. There is variation in the location of DRG relative to the foramen. The L4 and L5 DRG are more commonly intraforaminal, and the first sacral DRG is in a more cephalad or intraspinal location [11–13].

The common pathologies of the LFS can be the hypertrophic superior articular process (SAP), ligamentum flavum hypertrophy, or these pathologies in combination with a herniated intervertebral disc. The degenerative changes of

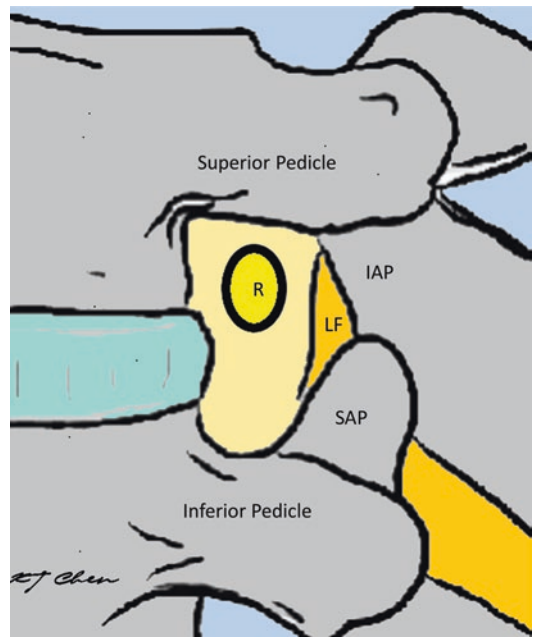


**Fig. 14.1** The anatomy of foramen (*R* nerve root, *SAP* superior articular process, *IAP* inferior articular process, *LF* ligamentum flavum)

the above structures determine the dimension of the foramen. The radicular pain usually originates from the compression of DRG and exiting root due to the narrowing foramen. Lee et al. proposed a practical MRI grading system for LFS in the sagittal plane [14]. The MRI grading system with concordant symptoms is essential for surgical decision making. As for technical consideration, it is crucial to determine the critical point of stenosis along the nerve root in the lateral zone of the spinal canal. The lateral zone can be subdivided into three zones on the horizontal plane (Fig. 14.2). The classification is similar to the disc herniation nomenclature. The subarticular zone is the area between the medial edge of the facet joint and the medial pedicle line. The foraminal zone is the area between medial and lateral pedicle lines. The hypertrophic facet joint and ligamentum flavum often block both areas and compress the exiting root. Bony hard spurs can also narrow the intervertebral foramen. The extraforaminal zone is lateral to the foraminal zone. Sometimes, calcified bone spurs and herniated disc can be pathologies in this area.

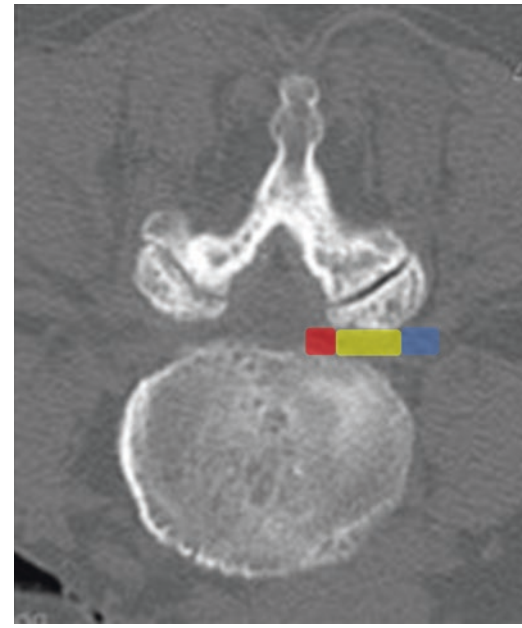

**Fig. 14.2** The lateral zone of the spinal canal on the axial CT image can be classified into three zones. From the medial to lateral are subarticular zone (red), foraminal zone (yellow), and extraforaminal zone (blue)

### 14.1.2 Options of Full-Endoscopic Lumbar Foraminotomy

The full-endoscopic foraminotomy can be classified as transforaminal endoscopic lumbar foraminotomy (TELF) and interlaminar contralateral endoscopic lumbar foraminotomy (ICELF) (Fig. 14.3). There are some differences between the two approaches. The entry point of TELF is posterolateral, and decompression is from the lateral to medial intervertebral foramen. However, the ICELF begins from a paramedian entry point contralateral to the target. The foramen is decompressed in a medial to lateral fashion with ICELF.

The decision making is mainly based on anatomical features of pathologies and the surgeon's experience. TELF is a common approach for pure LFS at the L2–5 level. As for LFS at L5-S1, ICELF might be beneficial if there is a high iliac crest. The foraminal stenosis sometimes combines with other pathologies, such as extraforaminal disc, bone spur, lateral recess stenosis, or central canal stenosis. Solving combined stenosis is technically demanding and requires a modified

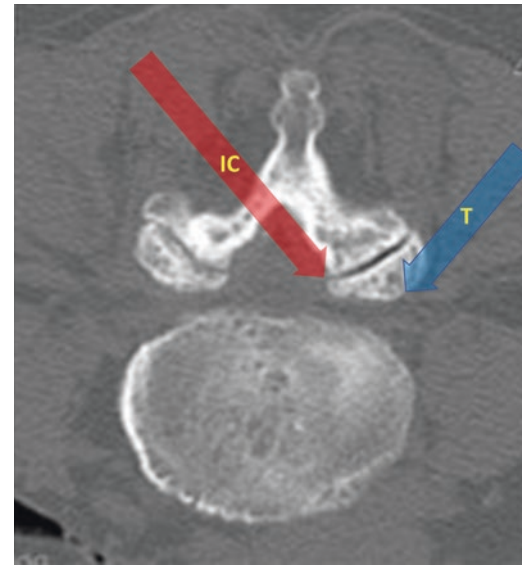


**Fig. 14.3** The two trajectories for lumbar foraminotomy include the transforaminal (T, blue arrow) and interlaminar contralateral (IC, red arrow) approaches

technique. TELF is more conducive to decompression of both foraminal stenosis and extraforaminal disc herniation. If the foraminal stenosis combines with a significant lateral recess or even central canal stenosis, ICELF might be favorable for complete decompression. The ICELF cannot reach extraforaminal pathologies. At the upper lumbar level with the narrowed interlaminar window, bony work might be time-consuming. The experience with endoscopic decompression for spinal stenosis is mandatory to perform ICELF efficiently. Therefore, the intraoperative navigation system is beneficial while performing the advanced technique of decompressing combined stenosis.

### 14.1.3 Indications

Unilateral radicular pain with or without motor weakness results from LFS and fails to improve with at least 6 weeks of conservative treatment, including transforaminal epidural steroid injection. Radiographic evaluation with both CT and MRI is mandatory for preoperative planning. The radicular symptoms are concordant with moderate to severe foraminal stenosis presented by perineural fat obliteration or nerve root collapse on MRI images. The patients with concomitant intracanalicular stenosis, segmental instability, or coexisting pathological conditions such as infection and tumor should be excluded.

## 14.2 Surgical Technique

The technique will describe the use of the preferred imaging and navigation equipment of the authors. This preference is biased by the high expense of acquiring multiple competing technologies to perform these procedures. Other comparable navigation systems exist. It is important to note, however, that current spine endoscopes do not have integrated navigation trackers. Therefore, if a system other than the one presented is to be used, it must have adapters to attach navigation trackers to the endoscope and other tools. The accuracy of the navigation must be verified when using these tools throughout the case. This can be done by palpating known landmarks or using fluoroscopic imaging. The surgeon (not the computer) is responsible at all times to know where the tools are and to avoid injuring the patient.

### 14.2.1 Operating Room Setup

The O-arm navigation setup is similar between the two different endoscopic approaches to foraminal decompression. The O-arm navigation operating suite includes an O-arm CT scanner, a computer-assisted guidance system (O-arm Surgical Imaging System and Stealth-Station S7, Medtronic, Minneapolis, MN) with the tracking instruments (SureTrak™ II Universal Instrument Adaptor), endoscopic equipment, and a radiolucent table with an anti-lordotic frame. The patient is positioned prone on the table. The operation can be performed under local or general anesthesia. General anesthesia is preferred to decrease the navigation error from the motion of the patient during the operation.

After sterile preparation and draping, the reference frame should be set up before the intraoperative CT scan. The reference frame is usually fixed on the spinous process or iliac crest as in other minimally invasive spine surgery. An additional incision is necessary if the reference frame is mounted on the spinous process. If the surgical level is at the upper lumbar spine, the reference frame on the iliac crest may be too far from the target, increasing the navigation error. The alternative is to attach the reference frame on the skin near the surgical site by one or two levels (Fig. 14.4). The skin-referencing technique improves surgical efficiency and reduces the number of incisions. An O-arm machine obtains a helical CT scan in the lumbar region. The intraoperative images are integrated with the navigation workstation (Stealth-Station S7; Medtronic, Minneapolis, MN). The workflow for registration

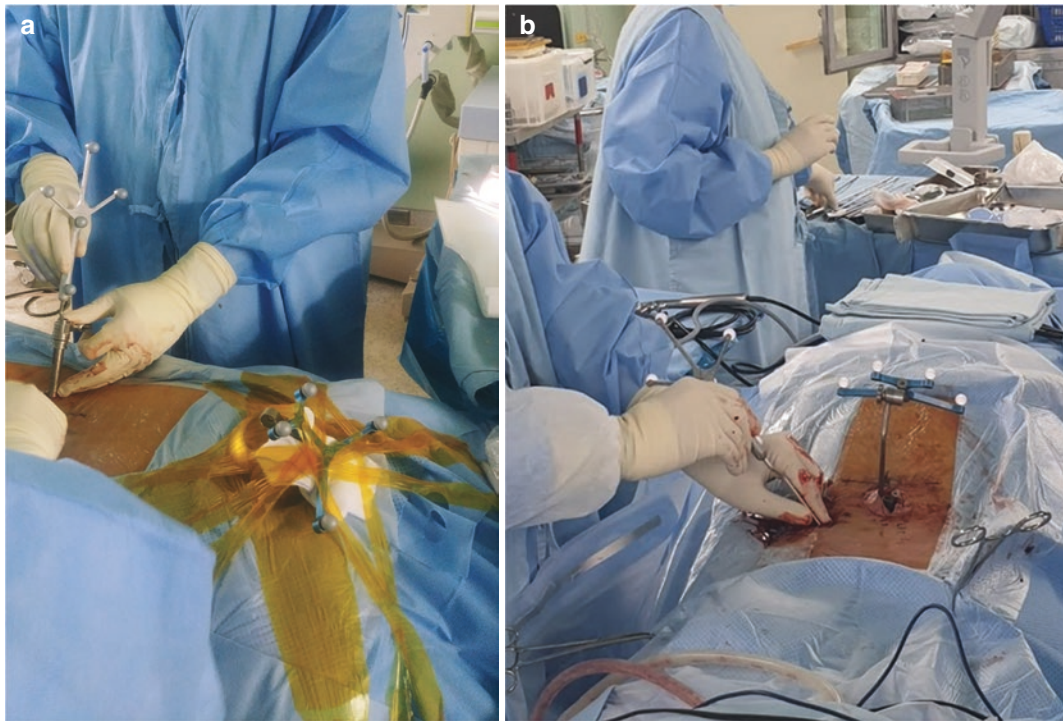


**Fig. 14.4** Common methods of a mounting reference frame. (**a**) Skin-fixed reference frame. (**b**) A reference frame is mounted on the spinous process

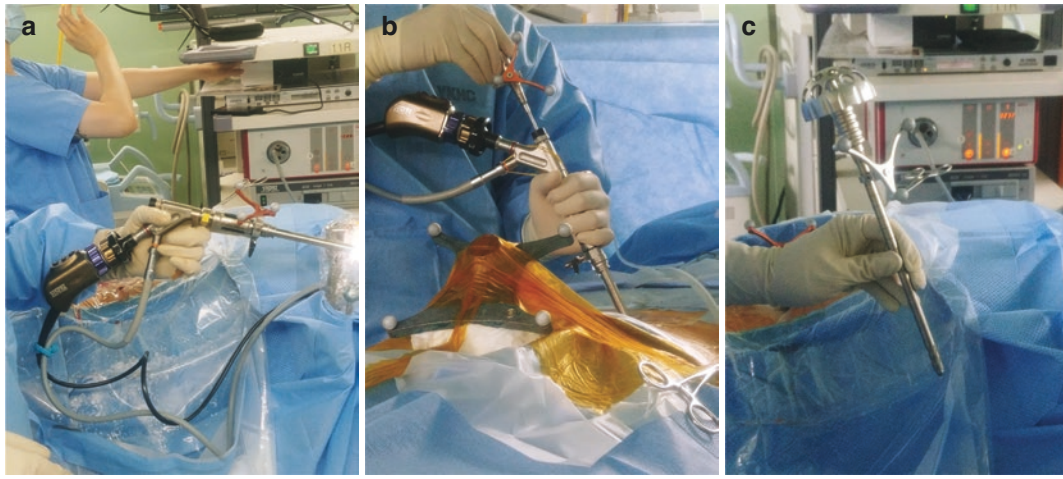


**Fig. 14.5** The tracker can be mounted on different instruments as needed. (**a**) The tracker on the working cannula. (**b**) The tracker on the handpiece of endoscopic drill. (**c**) The tracker on the reamer

and reconstruction of intraoperative three-dimensional images are processed in the computer program. The tracker (SureTrak™ II Universal Instrument Adaptor) is fixed on endoscopic instruments and registered for intraoperative navigation (Fig. 14.5).

#### 14.2.1.1 O-arm Navigation-Guided Transforaminal Endoscopic Lumbar Foraminotomy

After registering instruments, the surgeon can use a pointer probe to confirm the surgical level and plan the entry point accordingly. The trajec-

tory targets the superior articular process (SAP) on the axial and sagittal in-line plane. A stab incision is made with a blade through fascia by 8 mm. The navigated obturator is inserted to dock on the SAP of index level under navigation guidance. At this point, the surgeon can verify the navigation by palpating the instrument landing location and visualizing the corresponding images of the navigation system. Typically, palpation and visualization are performed in *x*, *y*, and *z* planes on the surface of easily palpated landmarks (facet and transverse process are the most common). An 8-mm beveled working cannula is introduced over the obturator, and then the obturator is replaced with the endoscope. Then, the radiofrequency coagulator is used to remove the soft tissue of the ventrolateral facet joint. The navigation tracker on the endoscope or working cannula can help to identify the target before foraminotomy. There are mainly two tools to perform foraminotomy. The surgeon can use a navigated reamer or endoscopic burr with the tracker fixed to the handpiece. Therefore, the surgeon can remove the SAP tip with a 3.0 mm diamond burr under both endoscopic visualization and intra-operative navigation (Fig. 14.6). After removing the SAP tip, foraminal ligaments are dissected meticulously and removed with micropunch and forceps. The whole course of exiting root from lateral foraminal region to medial border of pedicle should be visible and freely mobilized after decompression. The intra-operative CT scan can be repeated to evaluate the extent of foraminotomy. Hemostasis is done with the aid of bipolar radiofrequency coagulation. Then, the wound is closed with one subcutaneous stitch.

#### 14.2.1.2 Case Illustration

A 56-year-old woman had a history of posterior lumbar interbody fusion at L4–5 level in 2008. Then, she underwent L3–4 laminotomy and removal of L4–5 screws in 2013. She had suffered from progressive pain over the buttock with radiation to her left leg since 2015. The pain was mainly located at the left anterolateral thigh, accompanied by abnormal temperature sensation and mild knee extension weakness. The dynamic lumbar radiography showed no instability at the L3–4 level. The magnetic resonance images revealed stenosis of the left L3–4 foramen and lateral recess. Her symptoms had waxed and waned with medical treatment and nerve blocks. Later, she complained of walking intolerance due to aggravated pain after a walk of fewer than 3 min. She underwent O-arm navigation-guided left L3–4 TELF. The next day after the operation, her leg pain improved from 8 to 2 by VAS score. She could walk more than 10 min independently, and there was no back pain reported. The immediate postoperative computed tomography showed widened intervertebral foramen and decompressed nerve roots (Fig. 14.7a, b). The

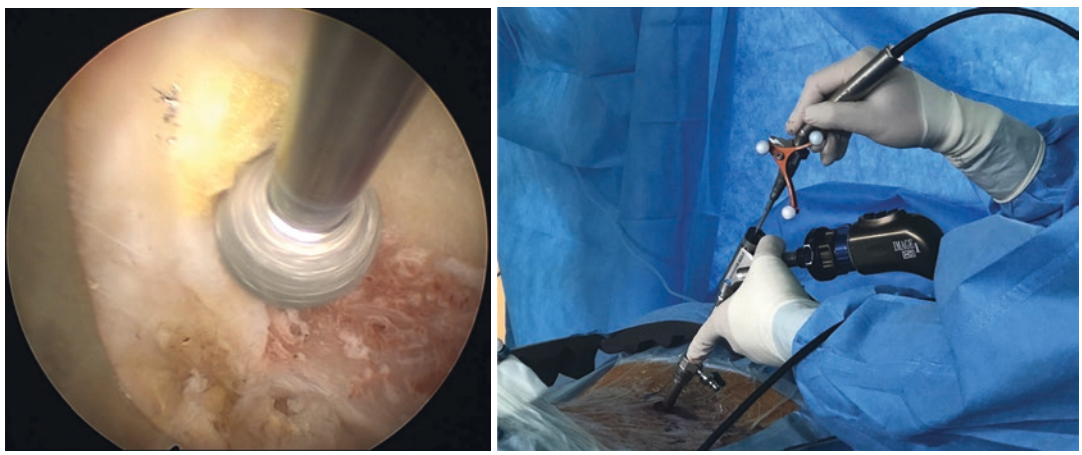

**Fig. 14.6** A tracker-mounted endoscopic instrument can assist foraminotomy with real-time navigation

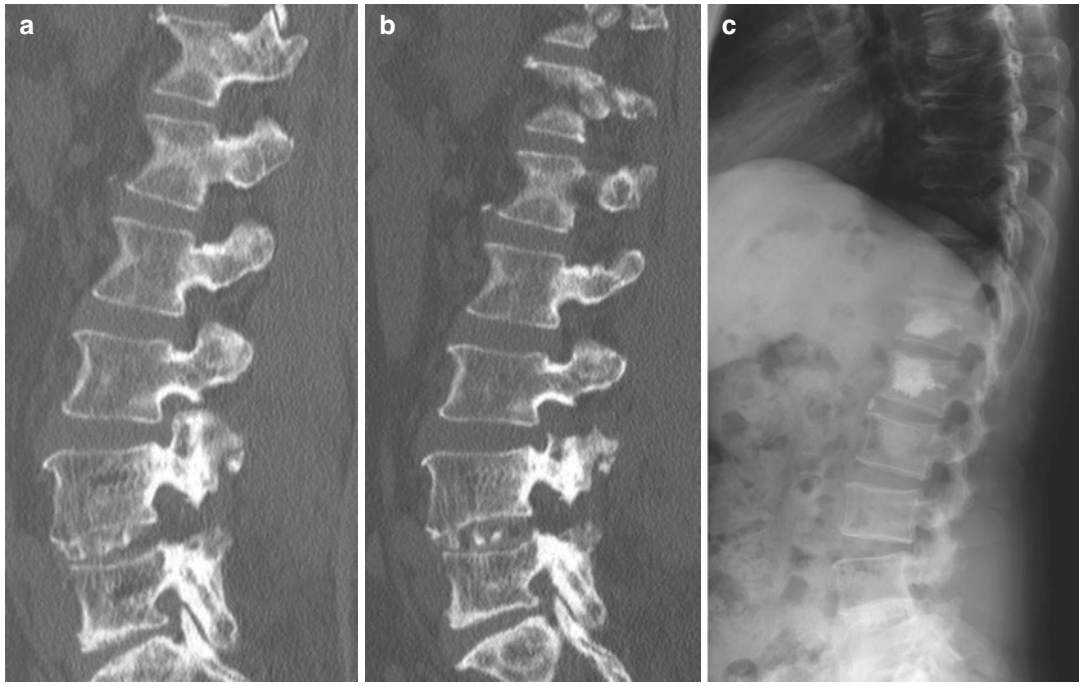


**Fig. 14.7** A 56-year-old woman underwent O-arm navigation-guided left L3-4 TELF. (**a**) The preoperative CT image. (**b**) The postoperative CT image. (**c**) Postoperative lateral radiograph showed no iatrogenic spondylolisthesis

follow-up X-ray also showed no iatrogenic instability (Fig. 14.7c).

#### 14.2.1.3 O-arm Navigation-Guided Interlaminar Contralateral Endoscopic Lumbar Foraminotomy

The surgeon stands opposite to the symptomatic side and uses a pointer probe to confirm the surgical level and plan the entry point with the navigation system. The entry point is usually 1–2 cm lateral to the midline. The trajectory is determined by aiming at the target SAP on the sagittal in-line plane and spinolaminar junction of the cranial lamina on the axial in-line plane. A stab incision by 1 cm is made at the planned entry point with navigation. The navigated obturator is inserted and docked at the spinolaminar junction of the cranial lamina. The 10-mm working cannula is inserted through the obturator, and then the endoscope with a 9.5 mm outer diameter is used at the initial phase.

After clearance of soft tissue, the bone at the spinolaminar junction of the ipsilateral cranial laminae is exposed. A 3.5-mm endoscopic drill was used to widen the middle interlaminar window by middle laminotomy (Fig. 14.8). The middle laminotomy range includes the inferior margin of the cranial lamina, the superior margin of the caudal lamina, and the base of the spinous process. The range of laminotomy can be tailored with intraoperative navigation.

Then, the contralateral laminotomy is performed with a burr in a sublaminar fashion. Disorientation may happen at this phase due to a lack of landmark in the endoscopic view. Therefore, intraoperative navigation can help with guiding the direction of the endoscopic trajectory. After contralateral laminotomy, the medial surface of the contralateral facet can be visualized (Fig. 14.9). The ligamentum flavum can be removed with the micro-punch and forceps and after that the endoscope with a smaller diameter for easier access to lateral recess and foramen.

The endoscope of 8 mm diameter with a 4.2 mm working channel is used at the second phase to conduct contralateral foraminotomy. An

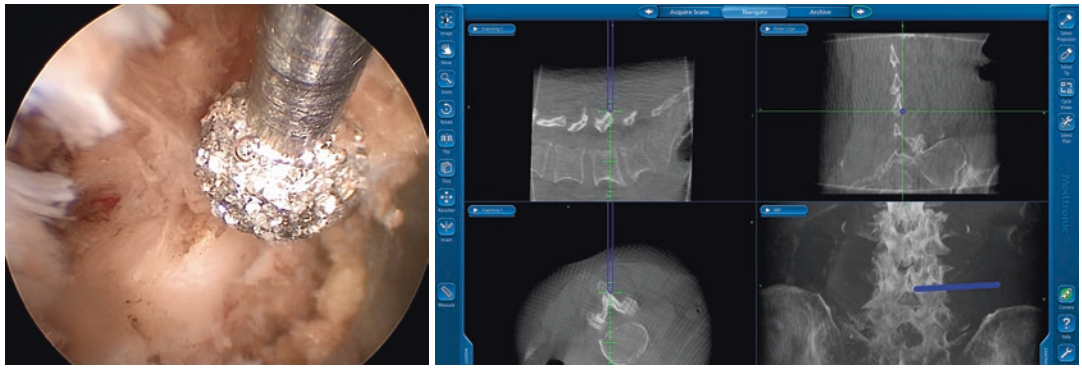

**Fig. 14.8** Navigation-guided middle laminotomy

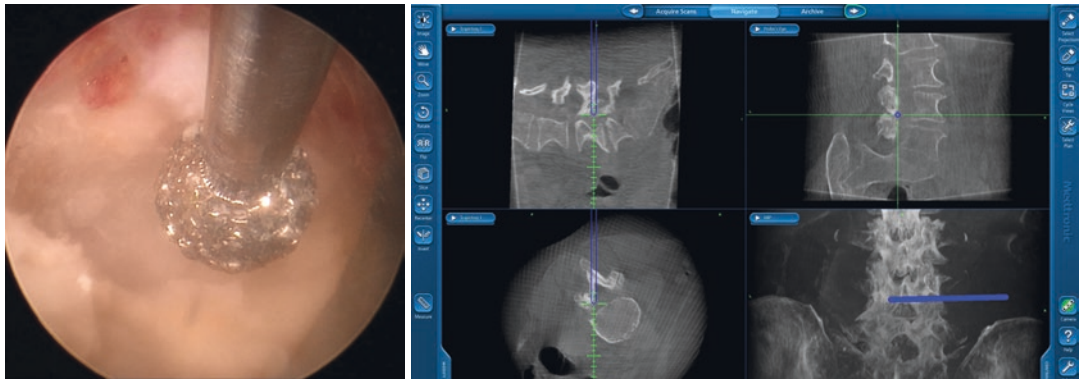

**Fig. 14.9** The contralateral laminotomy is performed until reaching the contralateral subarticular zone

endoscope with a smaller diameter for contralateral foraminotomy can improve endoscopic visualization and flexibility of instruments in the limited space. The target at this phase is the tip of SAP. The tip-control articulated burr can be used to widen the foramen by undercutting the tip of SAP. The soft tissue such as hypertrophic ligamentum flavum or the herniated intervertebral disc can be removed under endoscopic visualization. After gross decompression of the exiting root, the operator could confirm the procedure's endpoint with the navigation system (Fig. 14.10). A drainage tube can be considered to prevent epidural hematoma. After hemostasis, the wound was closed with a subcutaneous suture.

#### 14.2.1.4 Case Illustration

A 64-year-old woman had suffered from progressive left leg radiating pain through posterolateral thigh to her dorsal foot for more than 6 months before visiting the outpatient clinic. The tingling sensation of the left foot was accompanied with the subjective weakness of dorsiflexion. Her symptom was aggravated by walking and relieved with rest. The dynamic lumbar radiography showed no instability at the lumbar spine. The magnetic resonance images revealed stenosis at the left L4–5 foramen and subarticular zone. She had temporary relief with a transforaminal epidural block at the index level. She underwent O-arm navigation-guided ICELF at left L4–5.

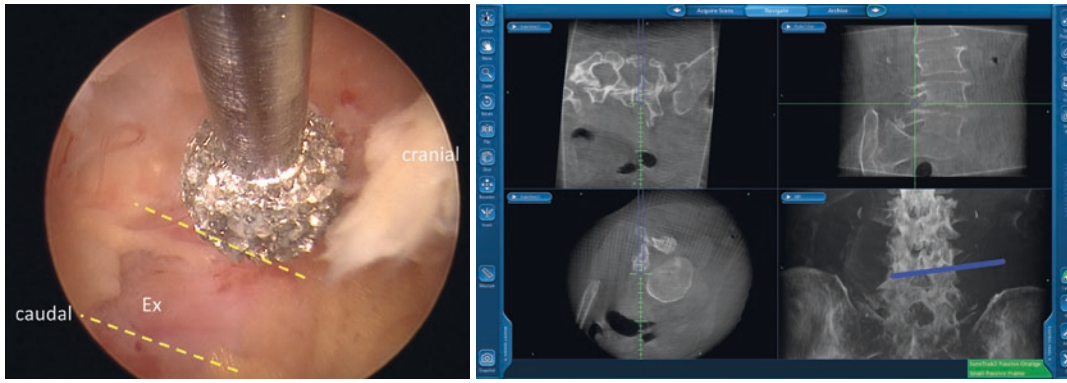


**Fig. 14.10** Confirm the decompression of the exiting root with both endoscopic visualization and intraoperative navigation

Her leg pain improved from 7 to 2 by VAS score. The immediate postoperative CT images showed widened intervertebral foramen (Fig. 14.11).

## 14.3 Pitfalls and Complication Avoidance

Though the operation is conducted by integrating endoscopic visualization and O-arm navigation, there are potential risks to complications, including infection, epidural hematoma, postoperative dysesthesia, dural tear, nerve injury, and iatrogenic instability [15]. To avoid complications, the operator needs to ensure that the computer navigation system works appropriately. The navigation error may cause neural injury or iatrogenic instability when performing the foraminotomy. Inaccurate navigation usually happens when the device is not secure. The reference frame fixed far away from the index level by more than two levels is not recommended. Therefore, the reference frame and the navigating tracker on instruments should be fixed firmly without dislodging during operation. General anesthesia and gentle manipulation during operation can decrease the risk of inaccurate navigation.

While performing TELF, excessive irritation of the dorsal root ganglion may cause postoperative dysesthesia. As for ICELF, incidental durotomy may happen while performing laminotomy with endoscopic drilling. Preservation of ligamentum flavum during sublaminar drilling may decrease the risk of dural tear.

Bleeding control is an essential technique to maintain clear endoscopic visualization. Bloody oozing from a rough bone surface or epidural vein can blur the endoscopic view and pose a risk to dural tear during flavectomy. The endoscopic diamond burr can easily control bleeding from the bone surface during laminotomy or foraminotomy. During the interlaminar approach, hemostasis of identified bone bleeders can also be performed by crushing the bleeding point with a Kerrison punch. The epidural venous bleeders can be coagulated with bipolar tip. When the surgical field is oozing without identified bleeders, temporary packing with Gelfoam or Floseal can be considered to control the bleeding.

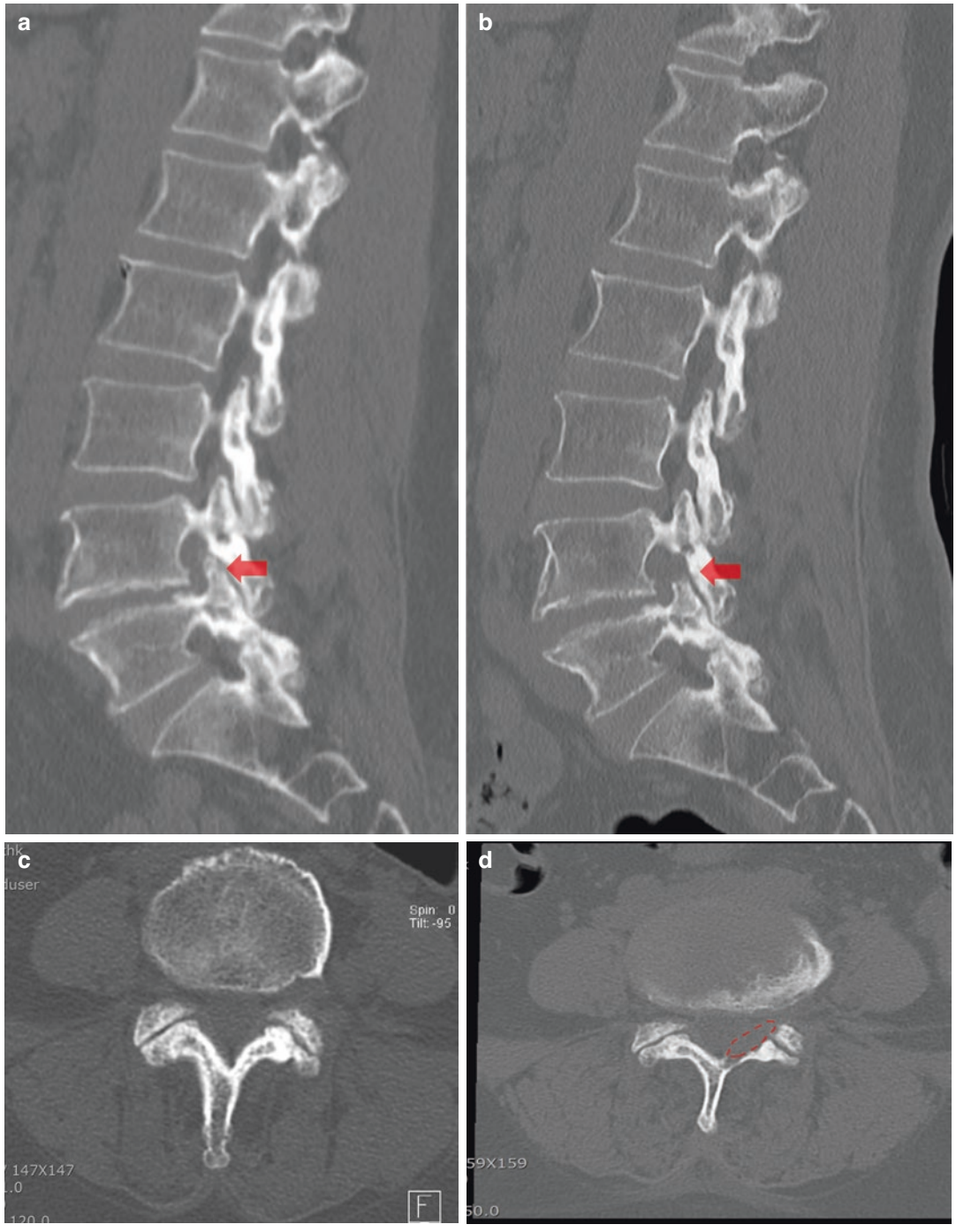


**Fig. 14.11** The CT images from a 64-year-old woman underwent O-arm navigation-guided ICELF at the left L4–5 level. Comparing the preoperative images (**a**, **c**), postoperative CT images (**b**, **d**) showed a widened left L4–5 foramen and subarticular zone after the operation

## 14.4 Conclusion

Image-guided procedures have been applied extensively in minimally invasive spine surgery. The ready availability of intraoperative image acquisition and computerized stereotactic navigation has contributed to the evolution of minimally invasive surgery. Our prior experience and results demonstrated a reliable integration between endoscopic spine surgery and computerized stereotactic navigation. Computerized stereotactic navigation can help reshape the learning curve of advanced endoscopic techniques. Surgeons with limited experience can perform navigation-guided endoscopic foraminotomy safely and confidently. The application of computerized stereotactic navigation can avoid occasional disorientation that occurs due to the focused endoscopic visualization. The constantly updated navigation can confirm the extent of decompression and decrease the risk of facet joint violation and subsequent iatrogenic instability. Therefore, endoscopic spine surgeons can utilize well-developed technology to achieve a favorable outcome more safely and comfortably.

## References


1. Porter RW, Hibbert C, Evans C. The natural history of root entrapment syndrome. Spine (Phila Pa 1976). 1984;9(4):418–21. https://doi.org/10.1097/00007632-198405000-00017.
2. Kunogi J, Hasue M. Diagnosis and operative treatment of intraforaminal and extraforaminal nerve root compression. Spine (Phila Pa 1976). 1991;16(11):1312–20. https://doi.org/10.1097/00007632-199111000-00012.
3. Jenis LG, An HS, Gordin R. Foraminal stenosis of the lumbar spine: a review of 65 surgical cases. Am J Orthop (Belle Mead NJ). 2001;30(3):205–11.
4. Wiltse LL, Spencer CW. New uses and refinements of the paraspinal approach to the lumbar spine. Spine (Phila Pa 1976). 1988;13(6):696–706.
5. Kim JS, Eun SS, Prada N, Choi G, Lee SH. Modified transcorporeal anterior cervical microforaminotomy assisted by O-arm-based navigation: a technical case report. Eur Spine J. 2011;20(Suppl 2):S147–52. https://doi.org/10.1007/s00586-010-1454-2.
6. Kim TT, Johnson JP, Pashman R, Drazin D. Minimally invasive spinal surgery with intraoperative image-guided navigation. Biomed Res Int. 2016;2016:5716235. https://doi.org/10.1155/2016/5716235.
7. Fan G, Feng C, Xie W, Wang D, Liu F, Yuan C, et al. Isocentric navigation for the training of percutaneous endoscopic transforaminal discectomy: a feasibility study. Biomed Res Int. 2018;2018:6740942. https://doi.org/10.1155/2018/6740942.
8. Ao S, Wu J, Tang Y, Zhang C, Li J, Zheng W, et al. Percutaneous endoscopic lumbar discectomy assisted by O-arm-based navigation improves the learning curve. Biomed Res Int. 2019;2019:6509409. https://doi.org/10.1155/2019/6509409.
9. Stephens MM, Evans JH, O'Brien JP. Lumbar intervertebral foramens. An in vitro study of their shape in relation to intervertebral disc pathology. Spine (Phila Pa 1976). 1991;16(5):525–9.
10. Hasue M, Kunogi J, Konno S, Kikuchi S. Classification by position of dorsal root ganglia in the lumbosacral region. Spine (Phila Pa 1976). 1989;14(11):1261–4. https://doi.org/10.1097/00007632-198911000-00021.
11. Kikuchi S, Sato K, Konno S, Hasue M. Anatomic and radiographic study of dorsal root ganglia. Spine (Phila Pa 1976). 1994;19(1):6–11. https://doi.org/10.1097/00007632-199401000-00002.
12. Hasegawa T, Mikawa Y, Watanabe R, An HS. Morphometric analysis of the lumbosacral nerve roots and dorsal root ganglia by magnetic resonance imaging. Spine (Phila Pa 1976). 1996;21(9):1005–9. https://doi.org/10.1097/00007632-199605010-00001.
13. Silav G, Arslan M, Comert A, Acar HI, Kahilogullari G, Dolgun H, et al. Relationship of dorsal root ganglion to intervertebral foramen in lumbar region: an anatomical study and review of literature. J Neurosurg Sci. 2016;60(3):339–44.
14. Lee S, Lee JW, Yeom JS, Kim KJ, Kim HJ, Chung SK, et al. A practical MRI grading system for lumbar foraminal stenosis. AJR Am J Roentgenol. 2010;194(4):1095–8. https://doi.org/10.2214/AJR.09.2772.
15. Sairyo K, Sakai T, Higashino K, Inoue M, Yasui N, Dezawa A. Complications of endoscopic lumbar decompression surgery. Minim Invasive Neurosurg. 2010;53(4):175–8. https://doi.org/10.1055/s-0030-1262814.

# 15 EM-based Navigation-Guided Percutaneous Endoscopic Lumbar Foraminoplasty

Yong-Jin Li, Yong-Peng Lin, and Si-Yuan Rao

## Abbreviations

| | |
|---|---|
| CT | Computerized tomography |
| EM | Electromagnetic |
| LDH | Lumbar disc herniation |
| MRI | Magnetic resonance imaging |
| SAP | Superior articular process |
| SEESSYS | I-See (Full Visualization Endoscopic System) Electromagnetic navigation Endoscopic Spinal Surgery System |
| TESSYS | Transforaminal endoscopic surgical system |
| VAS | Visual analog scale |
| YESS | Yeung Endoscopic Spine System |

**Key Points**

(1) Electromagnetic navigation helps surgeons find the target through the most accurate path.
(2) Remove the lesion tissue accurately after reaching the target point, which reduces the risk of nerve injury.
(3) It has the advantages of navigation path preset, real-time positioning, and X-ray radiation damage reduction.

## 15.1 Introduction

### 15.1.1 Development of Foraminoplasty

In 1983, Kambin P [1] defined a triangle area posterolateral to the intervertebral disc as a safe working area for intervention called "safety triangle" or "Kambin triangle," which consists of three sides: the upper edge of the caudal vertebral body, the outer edge of the dural sac or the traversing nerve root, and the inner edge of the exiting nerve root. In 1999, Yeung AT [2] firstly reported the application of Yeung Endoscopic Spine System (YESS) through the safe triangle for completing minimally invasive discectomy and achieving a good outcome. However, this technology is mainly applicable to the contained lumbar disc herniation (LDH) with a relatively limited range of indications. On this foundation,

Y.-J. Li (✉)
Guangdong Provincial Hospital of Chinese Medicine & Second Affiliated Hospital of Guangzhou University of Chinese Medicine, Guangzhou, China

Y.-P. Lin · S.-Y. Rao
Guangdong Provincial Hospital of Chinese Medicine & Second Affiliated Hospital of Guangzhou University of Chinese Medicine, Guangzhou, China

Guangzhou University of Chinese Medicine, Guangzhou, China



J.-S. Kim et al. (eds.), *Technical Advances in Minimally Invasive Spine Surgery*,
https://doi.org/10.1007/978-981-19-0175-1_15

Hoogland T et al. [3] introduced the concept of foraminoplasty to expand the safe triangle operation space. This technique, known as TESSYS method (transforaminal endoscopic spine system), can remove part of the articular process by special reamers, which provides more space for operation and expands the scope of application of transforaminal endoscopic lumbar discectomy.

### 15.1.2 Anatomical Basis of Lumbar Foraminoplasty

The boundary of the intervertebral foramen includes the adjacent vertebral pedicles superiorly and inferiorly, posteroinferior margin of the superior vertebral body disc, and posterosuperior vertebral notch of the inferior vertebral body and facet joint. The upper part of intervertebral foramen is the exit of the nerve root, which is wide. While the lower part of intervertebral foramen is narrow due to the space occupying the superior articular process. However, there is no important tissue such as nerves or vessels in this area, so it is considered a safe channel for transforaminal endoscopic surgery.

### 15.1.3 The Key Steps of TESSYS Technique

Precise puncture and foraminoplasty directly determine the position of the working channel and the operability of subsequent exploration and decompression, which are key to the success of the operation. Without foraminoplasty, the working channel can only be punctured to the intervertebral foramen about 20° on the coronal plane and reach the posterior annulus fibrosis, encountering difficulty getting into the spinal canal. Through foraminoplasty, part of the superior articular process can be removed by trephine, reamer, or high-speed drill to enlarge the lower part of the narrow intervertebral foramen. It can not only open up the channel for the endoscope to enter the spinal canal, but also effectively achieve the decompression of the foramen and lateral recess, which expands the indications for percutaneous transforaminal endoscopic surgery.

However, due to the narrow safety triangle, occlusion of anatomical structure, or poor three-dimensional sense of beginners with little surgical experience, it is sometimes difficult to puncture and perform foraminoplasty precisely. According to previous reports, the average incidence of complications after percutaneous transforaminal endoscopic surgery was 4.89–17.00% [4, 5]. Therefore, repeated X-ray fluoroscopy is needed throughout the surgery to ensure the thoroughness of the operation and the patient's safety. However, repetitive X-ray fluoroscopy not only increases the operation time, but also conveys more radiation damage to the operating room staff and patients, which may induce diseases such as tumors, cataracts, and cardiovascular diseases [6]. In order to establish a good working channel and improve the accuracy of surgery, aiming devices or computer navigation technology are introduced for spinal surgery to improve the operation efficiency, enhance the surgical effect, and reduce the incidence of risk.

### 15.1.4 Application of Navigation System in Spinal Surgery

At present, the main application of the navigation system in spinal surgery is for pedicle screw implantation, which greatly improves the accuracy and safety [7, 8]. The error rate of pedicle screw implantation can be reduced to 1% to 3% by using the surgical navigation systems, while the incidence of pedicle screw misplacement caused by traditional techniques (e.g., surgeon's perception, anatomical markers, and X-ray fluoroscopy, etc.) ranges from 3% to 55%, depending on the surgeon's experience. There are still few reports on navigation-assisted spinal endoscopic surgery. Huang [9] designed a navigation rod to guide puncture and to establish the working channel, Ye [10] developed a laser navigator combined with preoperative three-dimensional image measurement, and Fu [11] used ultrasound volume navigation to guide posterolateral puncture in percutaneous endoscopic transforaminal discectomy.

Electromagnetic (EM) navigation-guided technique is an exciting innovative procedure,

which provides navigational assistance coupled with steer ability and movability. It is more valuable and exciting, but lacks radiation. EM navigation has been applied in neurosurgery [12, 13], otolaryngology [14, 15], and oral and maxillofacial surgery [16–18], and previous studies have shown that it can decrease the operation time and reduce the risk of complications. Here, we introduce the technique of EM-based navigation-guided percutaneous endoscopic lumbar foraminoplasty.

## 15.2 Working Principle of EM-Based Navigation

The surgical navigation system is based on the input of the preoperative image information (CT, MRI, C-arm X-ray, etc.) obtained by digital scanning technology into the workstation through the media (MO magnetic disc, CD-R disc, DAT tape, etc.), while the workstation reconstructs the three-dimensional images of the patient after high-speed processing and forms a three-dimensional point-to-point relationship with the patient. According to these images, surgeons can then design preoperative plans and simulate the process. During the operation, the spatial position of surgical instruments relative to anatomical structure can be tracked in real time and displayed on the three-dimensional images. Surgeons can observe the real-time surgical approach and various parameters (angle, depth, etc.) from all directions (axial, sagittal, coronal) through the high-resolution monitor, so they can avoid the dangerous area to the maximum extent, reach the target lesion in the shortest time, and consequently complete the operation.

## 15.3 Indications and Contraindications

### 15.3.1 Indications

(1) Various types of lumbar disc herniation: paracentral type, extreme lateral type, prolapse type, and giant type
(2) Lumbar lateral nerve root canal stenosis and lumbar lateral recess stenosis
(3) Epidural abscess
(4) Pyogenic discitis

### 15.3.2 Contraindications

(1) Spondylolisthesis
(2) Lumbar instability
(3) Serious adhesion in spinal canal
(4) Spinal fracture and deformity
(5) Spinal metastases, intradural or intramedullary tumors

## 15.4 Surgical Tools

(1) Electromagnetic Navigation System (Fiagon, GmbH, Germany) including magnetic field generator, MultiPad, MaperBrige, localizer, computer mainframe and monitor, and Kirschner wire (Fig. 15.1a–f).
(2) I-See (Full Visualization) Endoscopic Spine Surgical System (Joimax®, IseeU, Germany) including IseePointer, puncture needle, guide rod, endoscopy, and Isee-reamer with IseePointer (Fig. 15.1g–k).
(3) Multifunctional plasma radiofrequency electrode system (Xi'an Surgical Medical Technology Co., Ltd., China).

## 15.5 Surgical Procedure

The patient is placed prone on a special non-metallic carbon fiber operating table (MAQUET holding GmbH & Co.KG Rasstadt, Germany) to prevent signal interference. The magnetic field generator is fixed on the operating table near the operation site, which does not interfere with the operation (Fig. 15.2a). After routine disinfection and towel spreading, the Kirschner wire is firmly fixed on one of the spinous processes of the operative segment, and then the patient localizer is put on the Kirschner wire and connected to the computer mainframe (Fig. 15.2b). Next, the MaperBrige is placed above the localizer and on

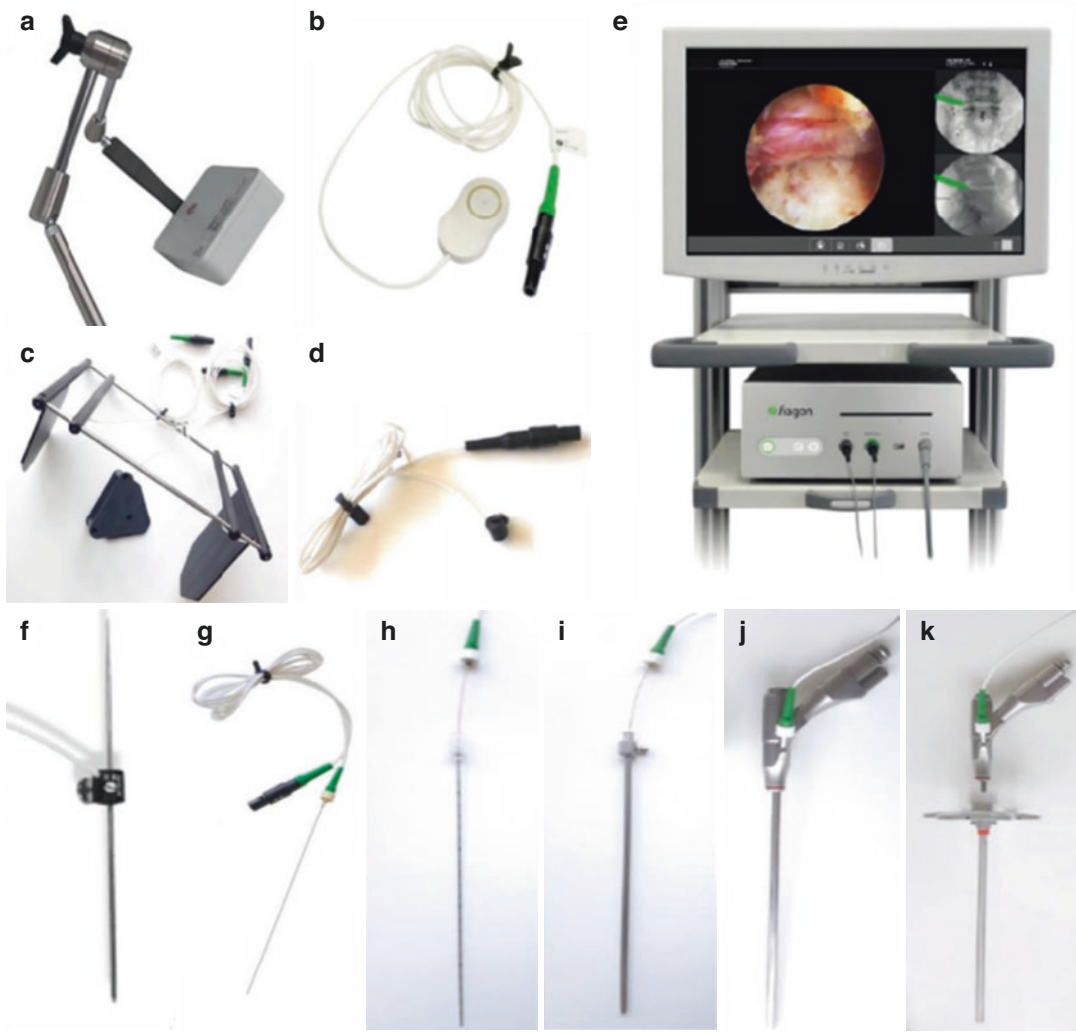


**Fig. 15.1** Instrument of EM-based navigation system for lumbar foraminoplasty. (**a**) magnetic field generator, (**b**) MultiPad, (**c**) MaperBrige, (**d**) Localizer, (**e**) computer mainframe and monitor, (**f**) Kirschner wire, (**g**) IseePointer, (**h**) puncture needle with IseePointer, (**i**) guide rod with IseePointer, (**j**) endoscopy with IseePointer, (**k**) reamer with IseePointer

both sides of the waist (Fig. 15.2c). Anterior-posterior and lateral lumbar X-ray are measured by the C-arm and those images are transmitted to the computer mainframe and matched with pre-operative 3D CT reconstruction (Fig. 15.2d and e). Then, the MaperBrige is removed, and the MultiPad is connected to the magnetic field generator for automatic calibration and identification (Fig. 15.2f).

The puncture target point is then set (Fig. 15.3). This target can be customized according to different conditions. For example, if more articular processes need to be removed for spinal stenosis, it can be set on the superior articular processes of the lower vertebrae. For prolapsed disc herniation, the puncture target is appropriately shifted to the cranial or caudal region of the intervertebral foramen.

The puncture is performed under the guidance of the electromagnetic navigation system. The path and depth of the guide wire can be adjusted at any time during the puncture (Fig. 15.4).

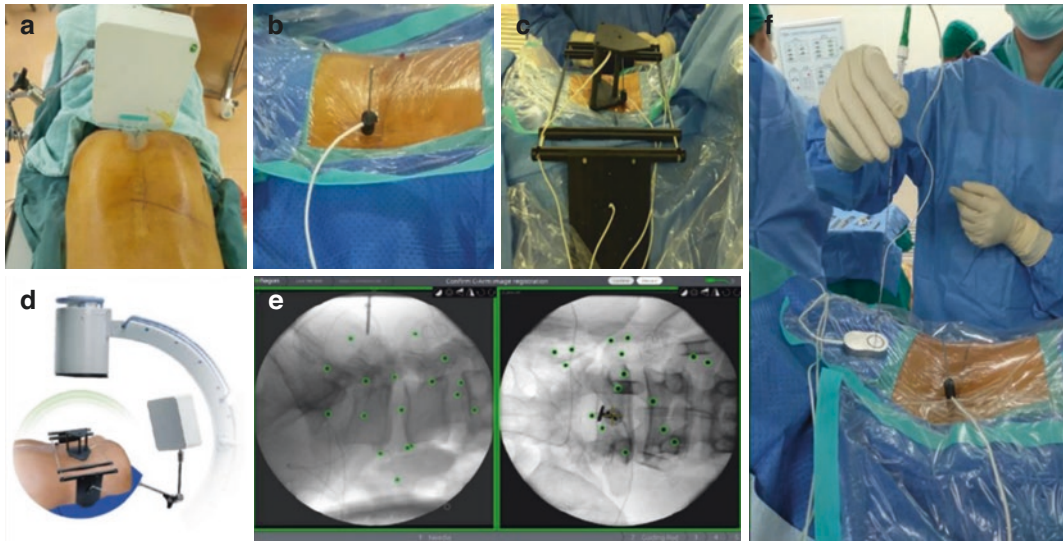


**Fig. 15.2** The procedure of EM-based navigation system for lumbar foraminoplasty. (**a**) Magnetic field generator is fixed to the frame near the surgical site; (**b**) Kirschner wire is fixed to the adjacent spinous process of the surgical segment, and the localizer is connected; (**c**) MaperBrige is placed smoothly near the surgical section; (**d**) positive side perspective of C-arm image transferred to the navigation host; (**e**) auto-complete registration; (**f**) magnetic navigation function can be used after the surgical instruments are paired on the MultiPad

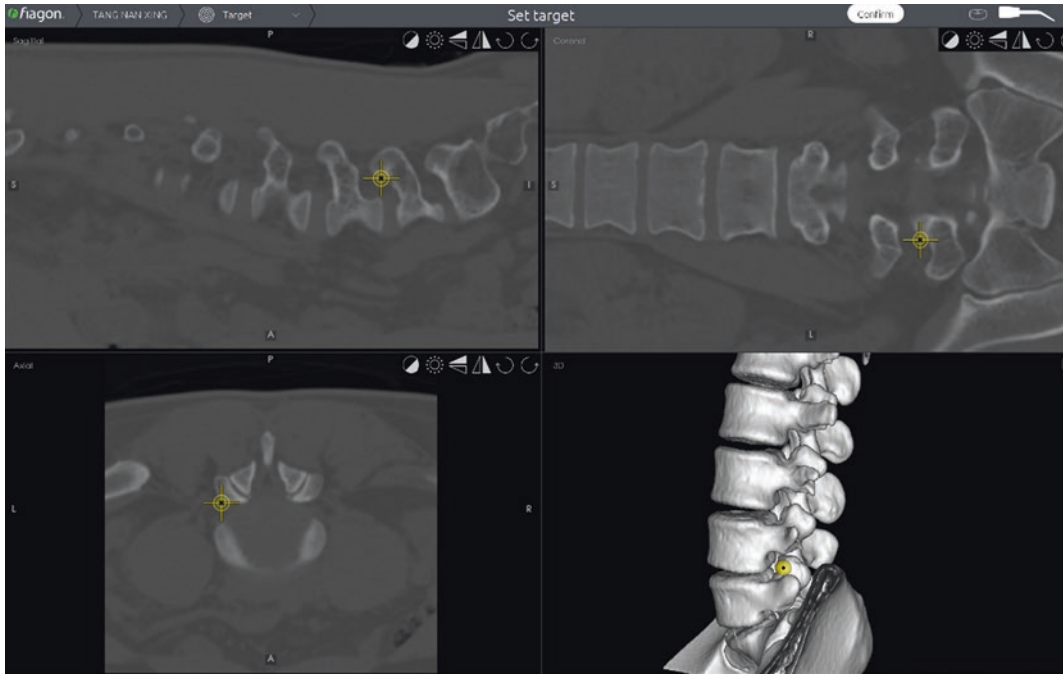


**Fig. 15.3** Surgical target was set to locate the L5 superior articular process

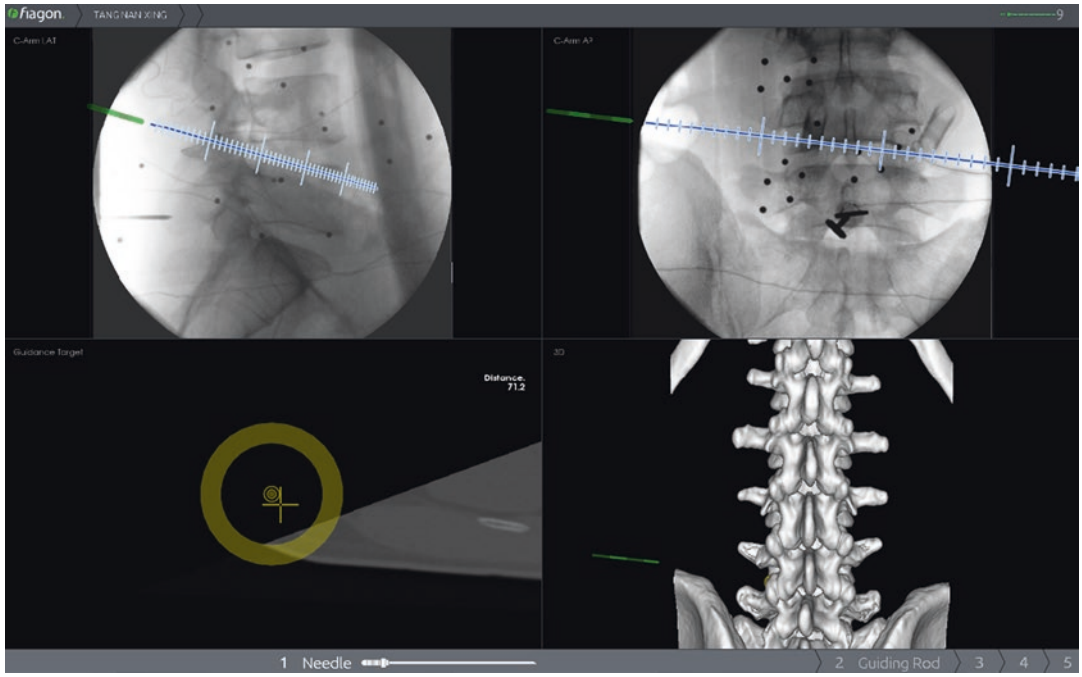


**Fig. 15.4** Direction of the needle in real time under the guidance of the EM-based navigation system was observed and adjusted

After the guide wire reaches the target position (Fig. 15.5), the stepwise dilatation guiding rods are inserted to expand the soft tissue and the protective sheath tube is inserted. Set the warning line of the inner side of the pedicle.

Full visualization foraminoplasty is performed by an identified and calibrated reamer under the guidance of electromagnetic navigation (Fig. 15.6). If the reamer is close to the inner side of the pedicle, a yellow warning line will appear on the monitor. When the warning line changes from yellow to red, it means the reamer has completely crossed the inner side of the pedicle, where there is a risk of nerve damage.

After the foraminoplasty, nerve decompression is performed immediately under endoscope. The decompression technology is the same as TESSYS technology. However, under electromagnetic navigation guidance, the real-time position of the endoscope and the range of decompression can be clearly identified on the monitor without any additional X-ray fluoroscopy(Fig. 15.7).

## 15.6 Case Study

*Case Study starts*

Female, 41

Chief complaint: Numbness and weakness of buttock and left lower limb with over 5 years of evolution.

Physical examination: The straight leg raise test was positive at 60°, and hypoesthesia was present in the S1 dermatome on her left side. The left Achilles tendon reflex was slightly weakened. No pathological neural reflex found. The muscle strength and tension of limbs were normal. The preoperative visual analog scale (VAS) score was 7 points.

Imaging examination: Preoperative MRI and CT scan indicated L5/S1 foraminal stenosis and disc herniation on the left side. Preoperative X-ray showed no instability at L5-S1 level (Fig. 15.8).

Diagnosis: Lumbar foraminal stenosis and disc herniation (L5/S1)

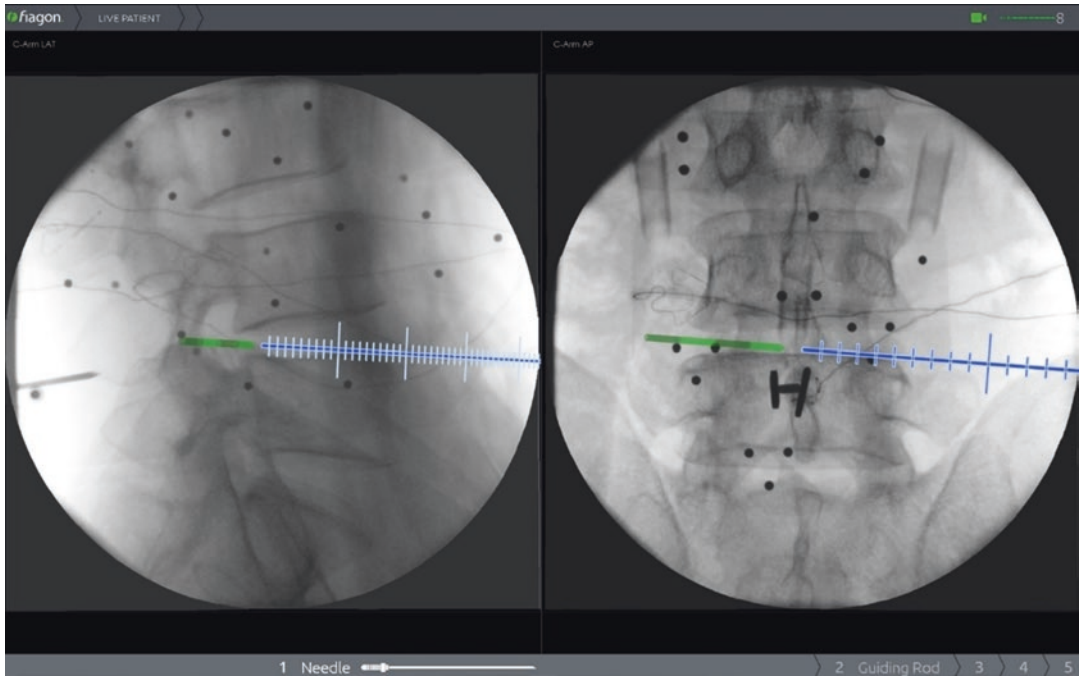


**Fig. 15.5** Position of the guide rod was observed when the expansion guide rod was placed

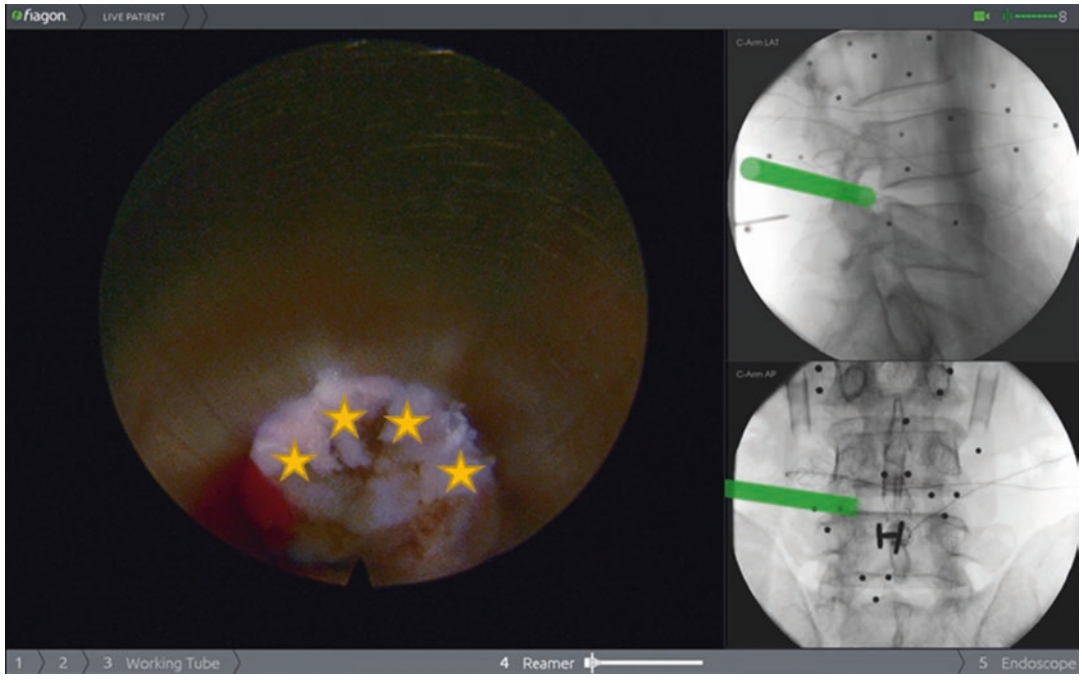


**Fig. 15.6** With EM-based navigation guidance, the position of the reamer was observed in real time. The entire foraminoplasty process is visualized under the endoscope. Superior articular process (the yellow star) is clearly identified under endoscopy

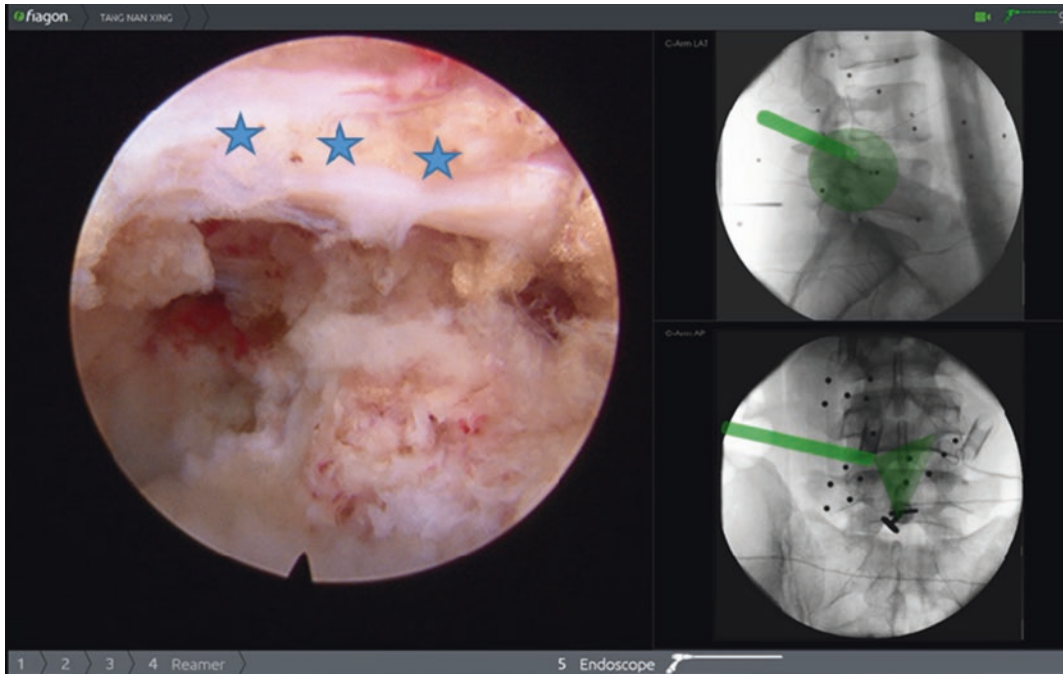


**Fig. 15.7** The position of the surgical instruments into the spinal canal can also be observed in real time, and the nerve root (blue stars) is relieved completely

Surgical treatment: EM-based navigation-assisted L5/S1 percutaneous endoscopic transforaminal foraminoplasty and discectomy under local anesthesia (Fig. 15.9).

*Case Study ends* (Fig. 15.10)

## 15.7 Discussion

Before the advent of surgical navigation technology, surgeons mainly relied on preoperative CT tomographic images or intraoperative X-ray fluoroscopy to obtain intraoperative patient anatomical information [19, 20]. Although these methods have played a certain role in guiding the operation, surgeons need to construct a three-dimensional imagination in their own mind through these images. The quality of surgery largely depends on the clinical experience of surgeons, but there is no objective basis for whether the operation is correct or not. Moreover, repeated intraoperative X-ray fluoroscopy increases the radiation exposure of surgeons and patients, and also increases the operation time and the risk of infection.

Iprenburg [21] measured patient radiation exposure during single-level transforaminal endoscopic lumbar discectomy procedures, and the results showed that for the discectomy procedures at L4-5 and above, the average duration of fluoroscopy was 38.4 s and the mean calculated patient radiation exposure dose was 1.5 mSv. For the L5-S1 procedures, average fluoroscopy time was 54.6 s and the mean calculated radiation exposure dose was 2.1 mSv. Although the consequences of long-term radiation exposure are still unclear, how to avoid radiation exposure as much as possible is undoubtedly a concern, especially those minimally invasive techniques that require repeated fluoroscopy.

Surgical navigation technology was born to solve the above problems. It is based on medical image data and combined with virtual reality technology and 3D visualization technology to

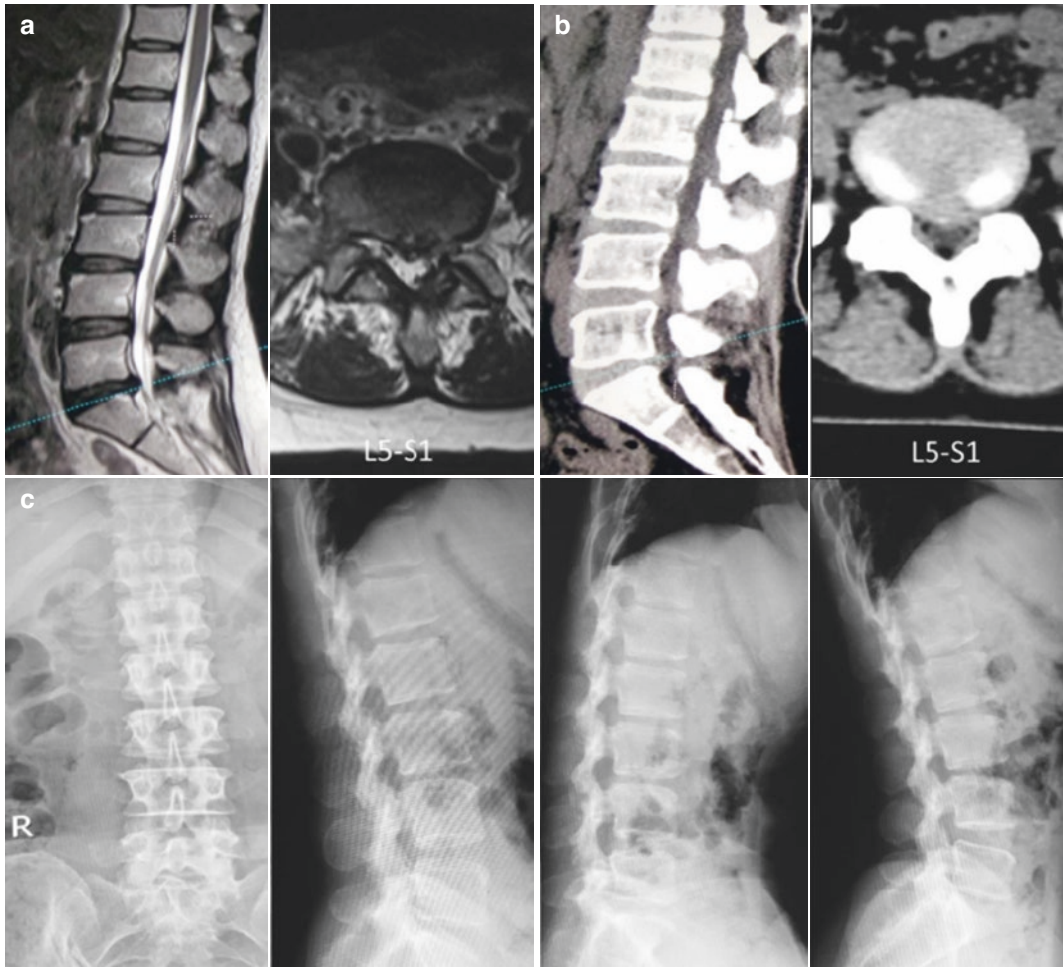


**Fig. 15.8** (**a**) and (**b**) Preoperative MRI and CT scan indicated L5/S1 foraminal stenosis and disc herniation on the left side. (**c**) Preoperative X-ray showed no instability at L5-S1 level

simulate the key steps in the operation and to track the position relationship of the surgical instrument relative to the anatomical structure, so as to realize the guidance of surgery [22–24]. This technology has important clinical application value in reducing radiation exposure, improving surgical positioning accuracy, reducing surgical damage, and reducing surgical error rate.

Electromagnetic navigation-assisted spinal surgery is a new technology developed in recent years, which is helpful to make the preoperative plan, select the best surgical approach, and design the surgical incision [25, 26]. With real-time navigation assistance, surgeons can accurately locate and reach the lesion through the best path, which can avoid the loss of direction, minimize the iatrogenic trauma, and reduce the difficulty and risk of operation.

There was no difference between the time of working channel establishment and foraminoplasty under the assistance of electromagnetic navigation technology compared with the standard TESSYS technology. The reason may be that the version of the navigation system in the study is new to surgeons, and with the further familiarity with the navigation system and instrument improvement, shorter operation time can be expected.

Although electromagnetic navigation is not the only navigation technology that can assist

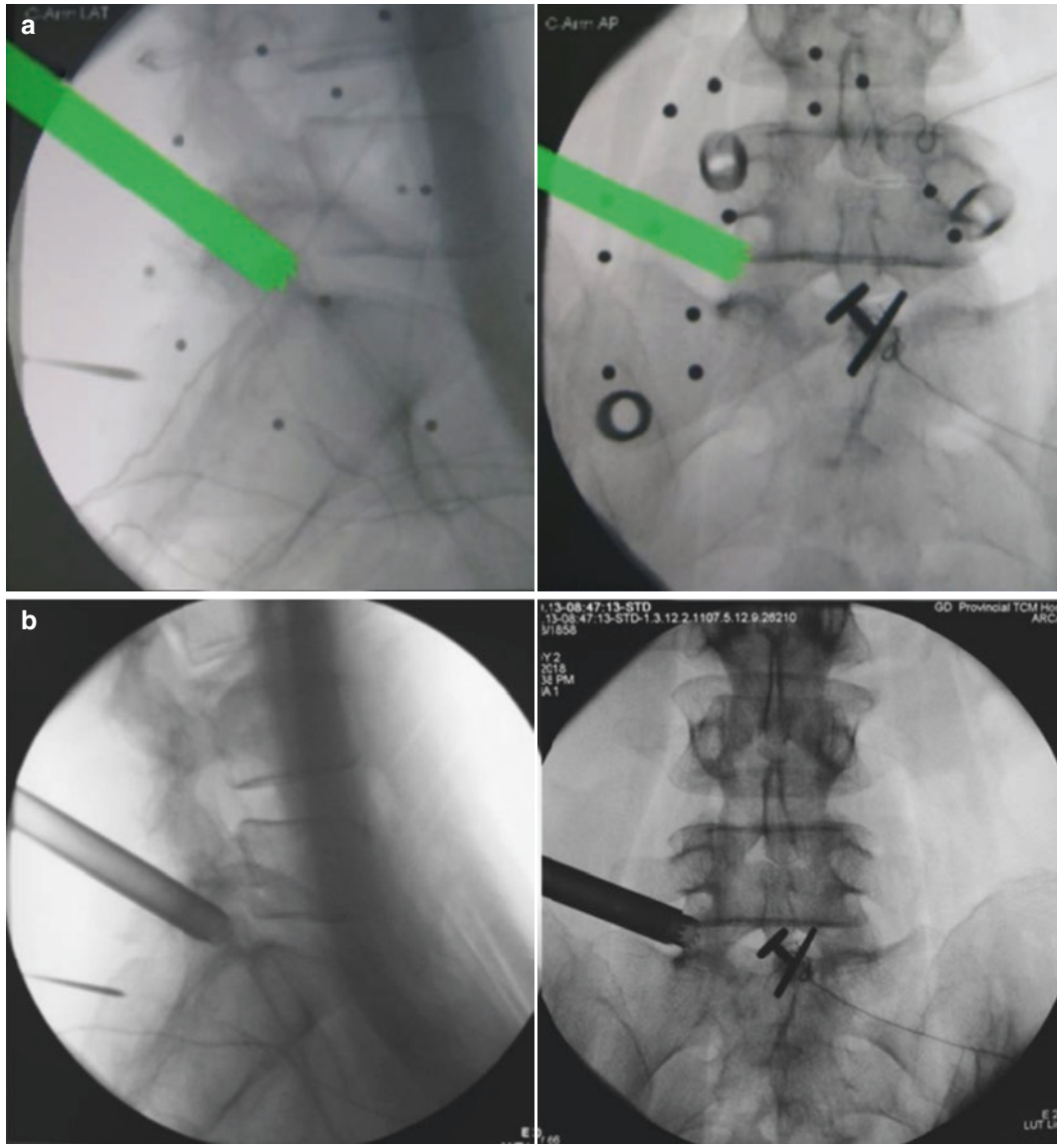


**Fig. 15.9** (**a**) Foraminoplasty by EM-based navigation, the position of endoscopic reamer can be observed in real time; (**b**) The location of the actual reamer, as indicated by the electromagnetic navigation

minimally invasive spinal surgery, it has its unique advantages. Compared with optical navigation systems, electromagnetic navigation does not need to establish a direct line of sight between the optical markers and the camera sensor, so it does not warrant avoidance for shelter on part of the surgeons and nurses [27]. In addition, the electromagnetic navigation system is small in size, which occupies a compact space in the operating room, making it easily removable and portable.

Compared with traditional technology, the disadvantages of an electromagnetic navigation system may include increased system setup and registration time as well as the possibility of software failure. Moreover, an additional incision is required to place the spinous process localizer, making it a challenge to perform revision surgery

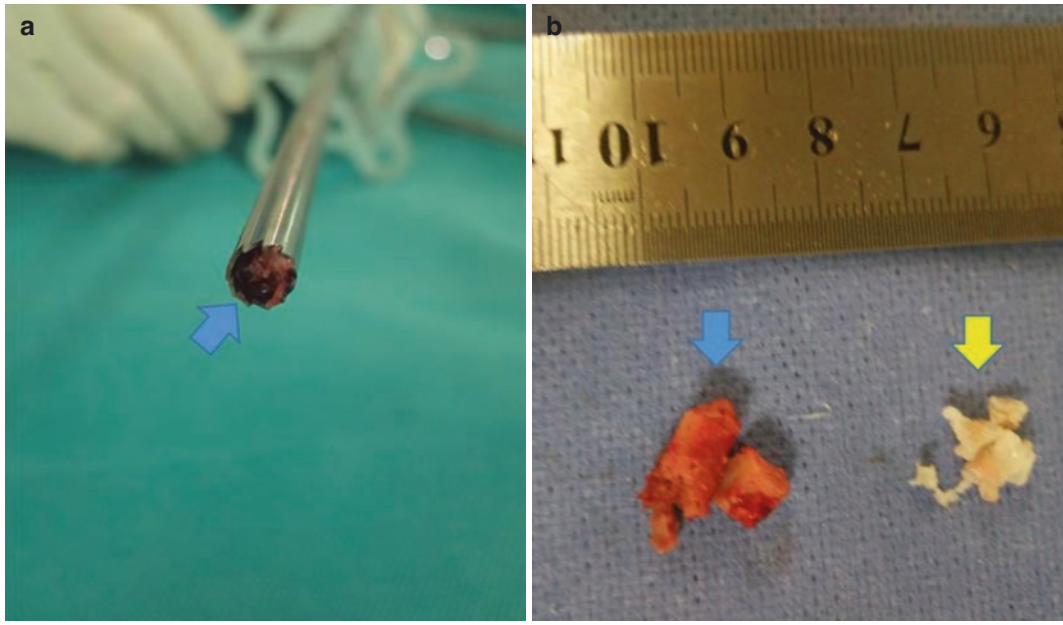


**Fig. 15.10** The excised (**a**) The part of the SAP (blue arrow) excised by the reamer and (**b**) the removed herniated disc (yellow arrow)

on those patients who have previously removed spinous processes. In addition, in order to prevent the indication deviation caused by the patient's positional movement during the operation, the surgeons should verify the accuracy of the navigation system at any time. Once the deviation occurs, a re-registration is required. The small error of electromagnetic navigation (less than 3 mm) may have limited effect on the lower lumbar spine surgery, but it may have some influence on the thoracolumbar junction or thoracic spine surgery.

## 15.8 Conclusion

Electromagnetic navigation is helpful for making the preoperative plan, selecting the best surgical approach, and designing the surgical incision for lumbar foraminoplasty. With real-time navigation assistance, surgeons can accurately locate and reach the lesion through the best path, which can avoid the loss of direction, minimize the iatrogenic trauma, and reduce the difficulty and risk of operation. At present, the results of EM-based navigation-guided lumbar foraminoplasty are still preliminary, albeit encouraging. We believe that the combined use of electromagnetic navigation and endoscopic surgery will further develop the accuracy, safety, and efficiency of lumbar foraminoplasty.

## References

1. Kambin P, Sampson S. Posterolateral percutaneous suction-excision of herniated lumbar intervertebral discs. Report of interim results. Clin Orthop Relat Res. 1986;207:37–43.
2. Yeung AT. Minimally invasive disc surgery with the Yeung Endoscopic Spine System (YESS). Surg Technol Int. 1999;8:267–77.
3. Hoogland T, Schubert M, Miklitz B, et al. Transforaminal posterolateral endoscopic discectomy with or without the combination of a low-dose chymopapain: a prospective randomized study in 280 consecutive cases. Spine (Phila Pa 1976). 2006;31(24):E890–7.
4. Li X, Hu Z, Cui J, et al. Percutaneous endoscopic lumbar discectomy for recurrent lumbar disc herniation. Int J Surg. 2016;27:8–16.
5. Zhou C, Zhang G, Panchal RR, et al. Unique complications of percutaneous endoscopic lumbar discectomy and percutaneous endoscopic interlaminar discectomy. Pain Physician. 2018;21:E105–12.
6. Narain AS, Hijji FY, Yom KH, et al. Radiation exposure and reduction in the operating room: perspectives

and future directions in spine surgery. World J Orthop. 2017;8:524–30.
7. von Jako RA, Carrino JA, Yonemura KS, et al. Electromagnetic navigation for percutaneous guidewire insertion: accuracy and efficiency compared to conventional fluoroscopic guidance. Neuroimage. 2009;47:T127–32.
8. Sagi HC, Manos R, Benz R, et al. Electromagnetic field-based image-guided spine surgery part one: results of a cadaveric study evaluating lumbar pedicle screw placement. Spine. 2003;28:2013–8.
9. HT T, SB H, ZL X, et al. Application of navigation rod for puncture and positioning in percutaneous endoscopic lumbar discectomy. Chin J Spine Spinal Cord. 2017;27(04):339–44.
10. Zhu HY, Ye B, Duan W, et al. Preoperative three-dimensional image measurement combined with laser navigator assisted puncture for percutaneous endoscopic transforaminal discectomy. J Spinal Surg. 2019;017(001):11–7.
11. Fu Q, Liu YB, Li J, et al. Ultrasound volume navigation technology in transforaminal puncture of minimally invasive lumbar surgery with full-endoscopic techniques. Chin J Orthop. 2016;36(001):1–8.
12. Shurkhay VA, Goryaynov SA, Kutin MA, et al. Application of intraoperative electromagnetic frameless navigation in transcranial and endoscopic neurosurgical interventions. Zh Vopr Neirokhir Im N N Burdenko. 2017;81(5):5–16.
13. Takenaka T, Toyota S, Kuroda H, et al. Freehand technique of an electromagnetic navigation system emitter to avoid interference caused by metal neurosurgical instruments. World Neurosurg. 2018;118:143–7.
14. Tsang RK, Chung JCK. Adapting electromagnetic navigation system for transoral robotic-assisted skull base surgery. Laryngoscope. 2020;130(8):1922–5.
15. Soteriou E, Grauvogel J, Laszig R, et al. Prospects and limitations of different registration modalities in electromagnetic ENT navigation. Eur Arch Otorhinolaryngol. 2016;273(11):3979–86.
16. Berger M, Kallus S, Nova I, et al. Approach to intraoperative electromagnetic navigation in orthognathic surgery: a phantom skull based trial. J Craniomaxillofac Surg. 2015;43(9):1731–6.
17. Bouchard C, Magill JC, Nikonovskiy V, et al. Osteomark: a surgical navigation system for oral and maxillofacial surgery. Int J Oral Maxillofac Surg. 2012;41(2):265–70.
18. Ohya T, Iwai T, Luan K, Kato T, et al. Analysis of carotid artery deformation in different head and neck positions for maxillofacial catheter navigation in advanced oral cancer treatment. Biomed Eng Online. 2012;4(11):65.
19. Kochanski RB, Lombardi JM, Laratta JL, et al. Image-guided navigation and robotics in spine surgery. Neurosurgery. 2019;84(6):1179–89.
20. Klingler JH, Sircar R, Scheiwe C, et al. Comparative study of C-arms for intraoperative 3-dimensional imaging and navigation in minimally invasive spine surgery Part I: applicability and image quality. Clin Spine Surg. 2017;30(6):276–84.
21. Ankur S, Narain, Fady Y, et al. Radiation exposure and reduction in the operating room: perspectives and future directions in spine surgery. World J Orthop. 2017.
22. Shin S, Kim Y, Kwak H, et al. 3D tracking of surgical instruments using a single camera for laparoscopic surgery simulation. Stud Health Technol Inform. 2011;163:581–7.
23. Jaeger HA, Nardelli P, O'Shea C, et al. Automated catheter navigation with electromagnetic image guidance. IEEE Trans Biomed Eng. 2017;64(8):1972–9.
24. Zamorano L, Jiang Z, Kadi AM. Computer-assisted neurosurgery system: Wayne State University hardware and software configuration. Comput Med Imaging Graph. 1994;18(4):257–71.
25. Gauvin G, Yeo CT, Ungi T, et al. Real-time electromagnetic navigation for breast-conserving surgery using NaviKnife technology: a matched case-control study. Breast J. 2020;26(3):399–405.
26. Pishnamaz M, Wilkmann C, Na HS, et al. Electromagnetic real time navigation in the region of the posterior pelvic ring: an experimental in-vitro feasibility study and comparison of image guided techniques. PLoS One. 2016;11(2):e0148199.
27. Sorriento A, Porfido MB, Mazzoleni S, et al. Optical and electromagnetic tracking systems for biomedical applications: a critical review on potentialities and limitations. IEEE Rev Biomed Eng PP. 2019;99:1–1.

# 16 O-Arm Navigation-Guided Endoscopic Cervical Laminoforaminotomy

Vit Kotheeranurak and Jin-Sung Kim

## 16.1 Introduction

Computer-based spinal navigation systems have been developed during the past decade, and the indications for use have been broadened [1–4]. These systems facilitate real-time and accurate instrument placement, help improve correct localization, and evaluate the adequacy of spinal decompression [5]. When compared with fluoroscopy, the foremost advantages are reduction of intraoperative radiation exposure to both patient and operating room staff, and three-dimensional (3D) information reconstructed either from a cone-beam computed tomography (CBCT) or computed tomography (CT) that provides image projections of the operative field and instruments in three dimensions.

When integrating the spinal navigation system into the endoscopic cervical laminoforaminotomy, a number of prerequisites need to be met:

1. Intraoperative imaging platforms—The most commonly used are the O-arm™ (Medtronic©, Minneapolis, MN, USA), Ziehm Vision RFD 3D™ (Ziehm Imaging©, Orlando, FL, USA), and the Airo® mobile intraoperative CT (Brainlab©, Feldkirchen, Germany).
2. Navigation software—Typically StealthStation S8 (Medtronic©, Minneapolis, MN, USA), Stryker Spinal Navigation with Spine Mask© (Stryker©, Kalamzoo, MI, USA), and 7D Surgical System (7D Surgical©, Toronto, ON, Canada).
3. The endoscopic system—Cervical (smaller diameter) integrated with navigation instrumentation (lens, probe, burr).

## 16.2 Goal of the Surgery

This is one of the motion-preserving procedures of the cervical spine, which aims to achieve direct visualization of the decompressed exiting nerve root from its origin to the lateral margin of the caudal pedicle (Fig. 16.1), either from a soft disc herniation or any degenerative changes causing foraminal stenosis (foraminal osteophyte, facet arthritis, etc.) (Fig. 16.2a–c) [6].

## 16.3 Patient Selection and Indications [7–10]

1. Unilateral cervical radicular symptoms resulting from nerve root compression within the neural foramen by soft disc herniation, bony

V. Kotheeranurak
Queen Savang Vadhana Memorial Hospital, Thai Red Cross Society, Sriracha, Chonburi, Thailand

J.-S. Kim (✉)
Department of Neurosurgery, Seoul St Mary's Hospital, The Catholic University of Korea, College of Medicine, Seoul, Korea (Republic of)



J.-S. Kim et al. (eds.), *Technical Advances in Minimally Invasive Spine Surgery*,
https://doi.org/10.1007/978-981-19-0175-1_16

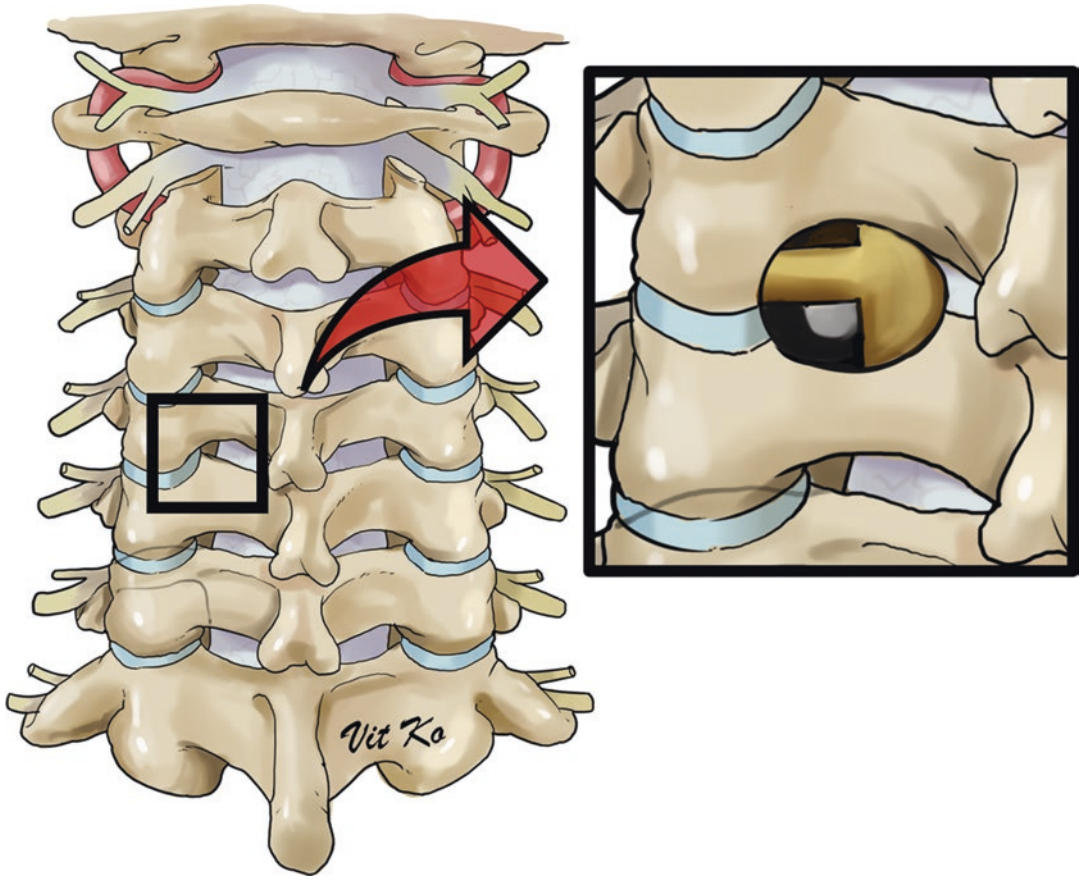


**Fig. 16.1** An illustration showing the area of cervical laminoforaminotomy

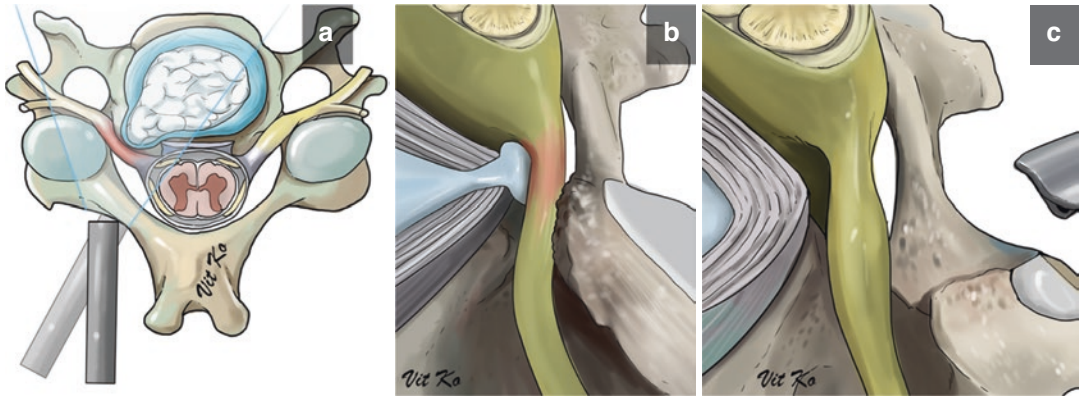


**Fig. 16.2** The trajectory of working tube endoscopy (**a**), A compromised cervical nerve root caused by the intervertebral disc herniation (anterior) and hypertrophic facet joint spur (posterior) (**b**), and a decompressed cervical nerve root after an endoscopic cervical laminoforaminotomy (**c**)

spur, ligamentum hypertrophy, ossification, or facet joint cyst.
2. Progressive muscle weakness or no improvement in symptoms despite a minimum of 6 weeks of an appropriate trial of conservative care.
3. Symptoms correlate with findings on advanced imaging (Magnetic resonance imaging [MRI], CT scan, CT myelogram) which indicate the laterally located herniated disc or foraminal stenosis.

## 16.4 Contraindications [7–10]

1. Segmental instability or kyphosis.
2. Purely axial neck pain without any neurologic symptoms.
3. Centrally located disc herniation.
4. Evidence of spinal cord compression, myelomalacia, or symptoms of myelopathy.
5. Symptoms not correlated with the findings of recent imaging studies.
6. Multilevel pathology.
7. Infection, tumor, and fracture in the region of the cervical segment.

## 16.5 Setup

### 16.5.1 Information for the Patient

Apart from the general risks of prone position surgery and general anesthesia, all patients need to be informed of the potential risks and possible complications from the surgical techniques. An informative statement is provided describing the differences in the technique from the standard microsurgical approach. Neural structures are the most concerning issue when dealing with posterior cervical surgery with the potential for a nerve root, spinal cord, or dural injury. These should be fully reviewed with patients. Possible injuries that could occur during the procedure as well as any consequences should be addressed. Patients should be aware that unintended outflow obstruction of the irrigation fluid could give rise to increased epidural pressure, resulting in postoperative symptoms of increased intracranial pressure, such as headache, blurred vision, and vomiting. The risks and complications of bleeding should be reviewed. Concealed bleeding from the raw surface of the bone or epidural vessels can cause postoperative hematoma or wound problems. The patients should be informed of the possibility of switching to an open procedure in case of any uncontrolled major bleeding or obvious neural structure injuries. Wound infection is considered a very rare complication following cervical endoscopic procedures. However, patients should be informed of wound infection potential. Lastly, patients should be aware of potential iatrogenic instability due to over resection of the facet joint, and that progressive or persistent neck pain could lead to subsequent cervical fusion surgery.

### 16.5.2 Preparation for Surgery

All patients should have recent radiographic images completed prior to surgery including plain cervical radiograph, MRI, and CT scan of the cervical spine. CT scan can add informative data regarding the bone osteophytes or calcified discs, and can be used as a baseline to compare the postoperative bone resection.

The operation is performed under general anesthesia with the patient intubated. The patient is positioned prone on the radiolucent table, with a silicone gel pad under the thorax and pelvis. The Mayfield® headrest and skull clamp system is essential and used for securing the patient's head position. The neck is flexed to open the interlaminar spaces and stretch the ligamentum flavum. The arms are strapped at the sides of the body. The cranial end of the operative table is inclined until the cervical spine is parallel to the floor. Adhesive tape or strap at the buttock can prevent the patient from sliding downwards when

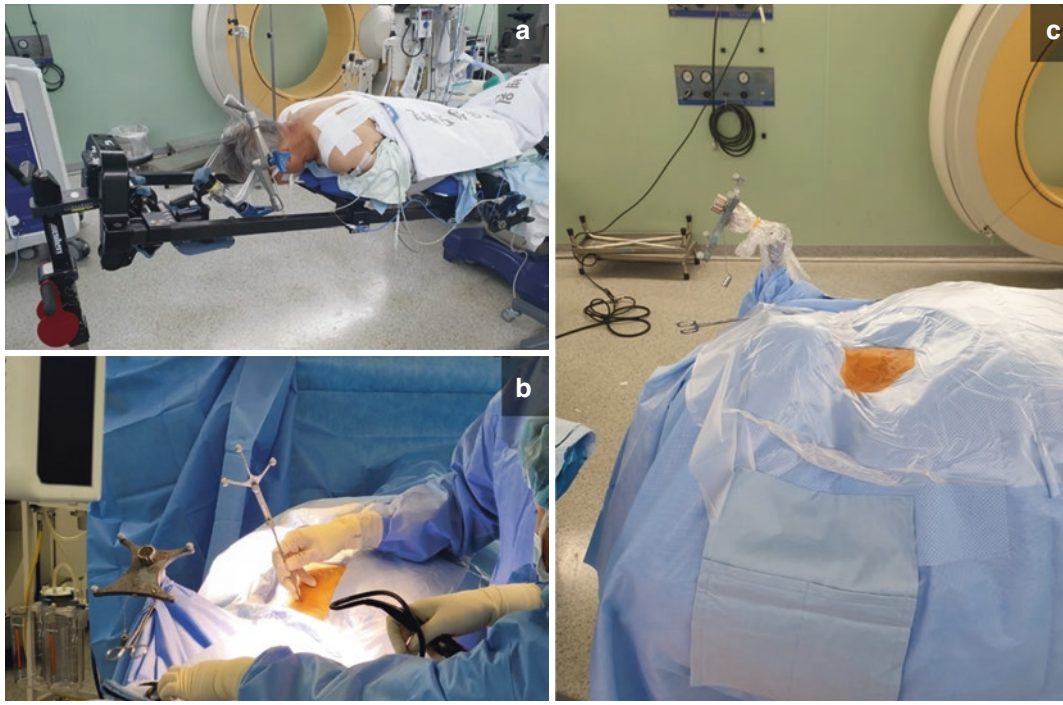


**Fig. 16.3** Operating room set up (**a**) The patient is positioned prone on a Jackson table with the head fixed with the Mayfield® headrest and skull clamp system. (**b**) A proper entry point is determined after verification by the navigating system. (**c**) An alternative attachment of reference array/frame is securely fixed on the extension of the Mayfield® headrest and skull clamp system and the surgical field is prepped and draped

adjusting to a proper position (Fig. 16.3a–c). Neuromonitoring should be performed. Somatosensory-evoked potentials and myotomal electromyography are monitored.

### 16.5.3 Instruments

A basic set of a cervical endoscopic set is required. For the technique described herein, lenses and instruments were obtained from the firm RIWOSpine (Knittlingen, Germany). Note that this device has a smaller diameter (working channel diameter of 3.1 mm, a working length of 122 mm, and a viewing angle of 25°) than the standard interlaminar equipment. However, standard interlaminar equipment can be applied. Modification of the endoscope instruments is a crucial step for integrating the endoscopic system into the navigation system (Fig. 16.4a–c).

## 16.6 Surgical Technique

### 16.6.1 Data Acquisition and Registration

Data acquisition and registration refer to registering equipment and patient position after prepping/draping the patient. We utilize a skin-based navigation system using the StealthStation S8 (Medtronic©, Minneapolis, MN, USA) system to yield a registration point for the navigation software. The reference array/frame is securely fixed on the extension of the Mayfield® headrest and skull clamp system, which the authors prefer rather than using a bony area of the patient, such as the skull or spinous process. Then, the O-arm™ (Medtronic©, Minneapolis, MN, USA) is incorporated and the CBCT (medium dose) is performed. The obtained CT data are registered and transferred to the Stealth navigation system.

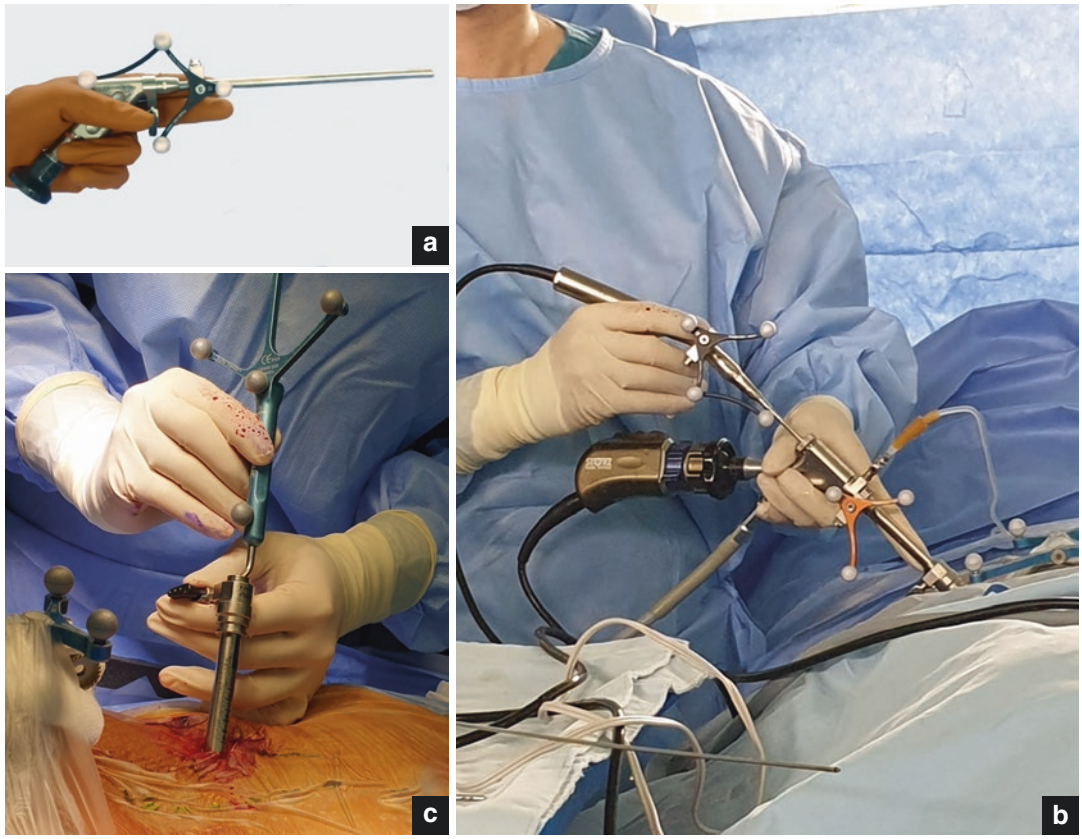


**Fig. 16.4** The modification of various instruments attached to the navigation system is shown. (**a**) Endoscope/Lens, (**b**) high-speed burr, and (**c**) probe

Imaging reconstructions of the cervical spine are generated and ready for navigation. Registration is verified when a sterile navigation probe is placed on known anatomic landmarks, such as the spinous process (Fig. 16.3b).

### 16.6.2 Access

Once the location is validated with navigation, the entry point is determined by the proper trajectory aiming at just medial to the facet joint, and a 6–9 mm skin incision is made. A one-step blunt-tip-navigated dilator is directly placed over the facet joint, which is visualized on the navigation screen (Fig. 16.5a). This is followed by the working sleeve insertion, and subsequent dilator removal. A navigated endoscope is inserted in a working sleeve and the soft tissue is removed using bipolar radiofrequency cautery and pituitary rongeur until the V-point (the junction of the superior and inferior laminae, and the medial part of the facet joint) (Fig. 16.6a) is clearly seen. Attention should be paid to the endoscopic screen, which should be switched to the navigation screen if a surgeon is unsure about or loses orientation.

### 16.6.3 Decompression (Laminoforaminotomy)

The surgeon initiates bone work decompression under endoscopic visualization using either a diamond-tip or a side cutting high-speed burr, beginning at the V-point junction with an even

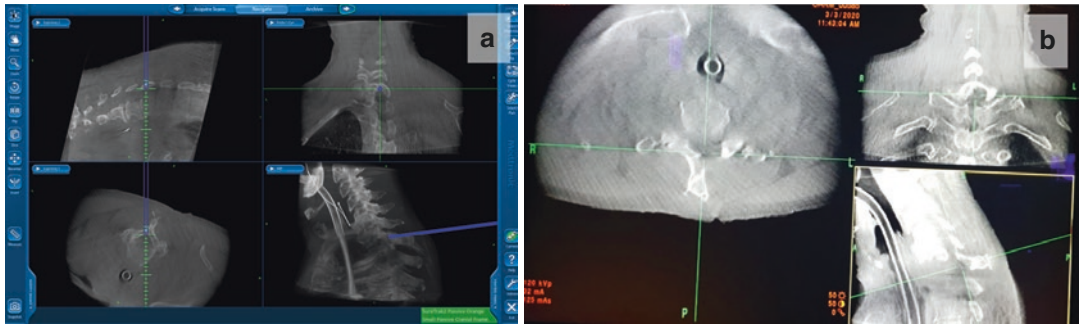


**Fig. 16.5** Navigation display. (**a**) A real-time navigation showing proper localization of the soft tissue dilator. (**b**) An intraoperative computed tomography scan after operation which confirms the location and amount of bony decompression

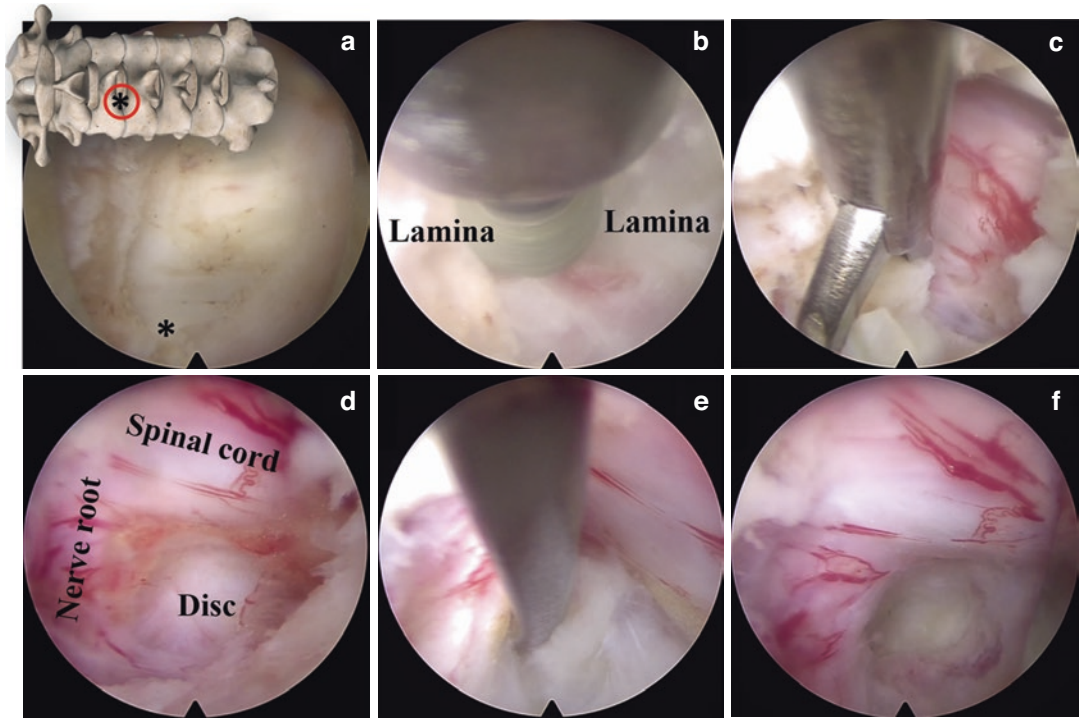


**Fig. 16.6** Intraoperative endoscopic pictures of a navigated cervical laminoforaminotomy procedure. (**a**) Starting landmark; lamina-facet junction or "V" area (asterisk), (**b**) Diamond burr is used to extend the decompression area and expose the ligamentum flavum underneath, (**c**) Cutting of the ligamentum flavum to enter the epidural space, (**d**) Neural structures and intervertebral disc are seen after removing epidural fat and vessels, (**e**) Gentle retraction of nerve root by a probe exposing the herniated intervertebral disc fragment, (**f**) Pulsatile neural structures after decompression

amount of the superior and inferior laminae removed, moving from medial to lateral toward the facet joint (Fig. 16.6b). The laminoforaminotomy is extended toward the lateral or superior direction until the inferior-medial margin of the pedicle is seen and the lateral margin of the ligamentum flavum is reached. The amount of facet joint resection is measured by using the size of the diamond tip high-speed burr (3 mm). It should not be resected more than 50% of its diameter to

prevent further instability [11]. The ligamentum flavum is removed and the epidural space is entered (Fig. 16.6c). Special attention is needed when bleeding occurs from the epidural plexus, which is closed or attached to the neural structures. The laminoforaminotomy is enlarged by thinning down the bone using a diamond tip high-speed burr (leaving a thin layer of bone), then a Kerrison punch rongeur is used to remove the remaining bone, to help reduce bleeding from the epidural plexus compared to a blinded-fashion cut. The overlying epidural fat and vessels are removed and cauterized to gain direct visualization of the intervertebral disc and neural structures (Fig. 16.6d). The ventral aspect of the spinal cord and nerve root should be seen and thoroughly decompressed as well as the axilla and shoulder of the nerve root. The nerve root should be carefully palpated and mobilized to look for any dorsal pathology, such as disc herniation or bulging (Fig. 16.6e). Complete foraminal decompression is checked from the medial to lateral border of the caudal pedicle. After adequate decompression is performed (Fig. 16.6f), the presence of bleeding is checked and coagulated as needed. The drain is not necessary unless ongoing bleeding is encountered. The skin is then closed in a subcutaneous fashion. An intraoperative CT scan should be used to confirm the amount of bony decompression after the procedure (Fig. 16.5b).

## 16.7 Pearls and Pitfalls

### 16.7.1 Neural Structure Injury

Although the procedure involves having real-time image guidance, surgeons need to focus on the endoscopic screen in order to avoid neural injuries. Since the anatomical neural structure is different from the lumbar region, surgeons should be cautious and avoid excessive mobilizing of the spinal cord. The cervical nerve roots are vulnerable and can tolerate only minimal traction and mobilization. Furthermore, inserting a large diameter of the working cannula could result in overstretching of the nerve root. Intraoperative neuromonitoring should be used to ensure the safety of the neural structures.

### 16.7.2 Intraoperative Bleeding Control

When performing procedures involving bone, it is important to be able to control or minimize bleeding. Obtaining an optimum blood pressure or performing hypotensive analgesia is helpful for bone bleeding, thereby improving the field visualization. Various techniques can be used to control bleeding. Examples are temporally increasing the flow and pressure of water irrigation, radiofrequency cauterizing using a diamond tip burr at the bleeding spot (bone bleeding), applying direct pressure over the spongy bone bleeding, or using a gel foam or bone wax to plug the bleeding point. When there is obvious epidural bleeding under the lamina, surgeons may need to extend the procedure involving bone work to address the source of the bleeding.

### 16.7.3 Maintaining Navigation Accuracy

In order to maintain navigation accuracy, surgeons should be mindful and ensure that the reference arc/frame is securely fixed to the Mayfield® headrest and skull clamp extension or patient's anatomy after CT registration. Surgeons and assistants are responsible for avoiding accidentally hitting or bumping the reference arc throughout the operation. Prompt repetition of the CT registration is warranted in any case of reference arc/frame detachment.

## 16.8 Conclusion

A combination of intraoperative CT navigation and the endoscopic cervical laminoforaminotomy procedure yields improved accuracy and safety for the patients. It is one of the modern and cutting-edge spine surgeries, and success is based on understanding and handling of the equipment

appropriately. However, surgeons should be prompted to prepare for a conversion to the backup traditional open surgery in the case of uncontrolled events.

## References


1. Curto DD, Kim JS, Lee SH. Minimally invasive posterior cervical microforaminotomy in the lower cervical spine and CT junction assisted by O-arm-based navigation. Comput Aided Surg. 2013;18(3–4):76–83.
2. Shin Y, Sunada H, Shiraishi Y, Hosokawa M, Koh Y, Tei R, Aketa S, Motoyama Y, Yonezawa T, Nakase H. Navigation-assisted full-endoscopic spine surgery: a technical note. J Spine Surg. 2020;6(2):513.
3. Virk S, Qureshi S. Navigation in minimally invasive spine surgery. J Spine Surg. 2019;5(Suppl 1):S25.
4. Rahmathulla G, Nottmeier EW, Pirris SM, Deen HG, Pichelmann MA. Intraoperative image-guided spinal navigation: technical pitfalls and their avoidance. Neurosurg Focus. 2014;36(3):E3.
5. Guha D, Moghaddamjou A, Jiwani ZH, Alotaibi NM, Fehlings MG, Mainprize TG, Yee A, Yang VX. Utilization of spinal intra-operative three-dimensional navigation by canadian surgeons and trainees: a population-based time trend study. Can J Neurol Sci. 2019;46(1):87–95.
6. Hofstetter CP, Ahn Y, Choi G, Gibson JN, Ruetten S, Zhou Y, Li ZZ, Siepe CJ, Wagner R, Lee JH, Sairyo K. AOSpine consensus paper on nomenclature for working-channel endoscopic spinal procedures. global. Spine J. 2020;10(2_suppl):111S–21S.
7. Zhang C, Wu J, Zheng W, Li C, Zhou Y. Posterior endoscopic cervical decompression: review and technical note. Neurospine. 2020;17(Suppl 1):S74.
8. Murayama Y, Irie K, Saguchi T, Ishibashi T, Ebara M, Nagashima H, Isoshima A, Arakawa H, Takao H, Ohashi H, Joki T. Robotic digital subtraction angiography systems within the hybrid operating room. Neurosurgery. 2011;68(5):1427–33.
9. McAnany SJ, Qureshi SA. Minimally invasive cervical foraminotomy. JBJS Essent Surg Tech. 2016;6(2)
10. Kim CH, Kim KT, Chung CK, Park SB, Yang SH, Kim SM, Sung JK. Minimally invasive cervical foraminotomy and diskectomy for laterally located soft disk herniation. Eur Spine J. 2015;24(12):3005–12.
11. Zdeblick TA, Zou D, Warden KE, et al. Cervical stability after foraminotomy. A biomechanical in vitro analysis. J Bone Joint Surg Am. 1992;74:22–7.

# 17 Feasibility of Endoscopic Transforaminal Lumbar Interbody Fusion

Nicholas Ahye, Eric Quach, Erin Graves, Joseph Queenan, and Bong-Soo Kim

## 17.1 Introduction

The spinal endoscope has gained popularity as a versatile tool in neurosurgery. It provides minimally invasive access to deep-seated regions with excellent visualization and less tissue dissection. Techniques for performing a laminectomy, discectomy, and foraminotomy with an endoscopic transforaminal approach have been well established [1–6]. The feasibility and safety of these operations have been studied in the literature [7, 8]. One drawback to minimally invasive approaches, especially for less experienced surgeons, is the lack of direct visualization of most anatomical landmarks used in traditional open procedures. A need for easily identifiable landmarks and boundaries for safe dissection was met with the description of Kambin's triangle. This chapter will focus on this widely used anatomical zone, and its modifications, through which lumbar pathology can be treated surgically with a transforaminal approach.

N. Ahye · E. Quach · E. Graves · J. Queenan
B.-S. Kim (✉)
Department of Neurosurgery, Minimally Invasive and Complex Spine Fellowship Program, Temple University Hospital, Lewis Katz School of Medicine, Temple University, Philadelphia, PA, USA
e-mail: Nicholas.Ahye@tuhs.temple.edu; Eric.Quach2@tuhs.temple.edu; Erin.Graves@tuhs.temple.edu; Joseph.Queenan@tuhs.temple.edu; Bong-Soo.Kim@tuhs.temple.edu

The techniques of endoscopic transforaminal lumbar surgery, along with development of innovative tools and hardware, have been applied to the transforaminal lumbar interbody fusion (TLIF). The endoscopic TLIF minimizes the amount of bone removal required, sometimes avoiding it completely. This helps to preserve the bony, muscular, and ligamentous structures that give the spine its stability. Decompression of the foramen, preparation of the endplates, and placement of an interbody cage can be accomplished with this endoscopic method [9, 10]. The zone established by Kambin's triangle provides enough room to perform these maneuvers, and respecting its anatomical boundaries is critical to performing a safe endoscopic lumbar fusion. With an endoscopic approach, the typical landmarks visualized during open surgery are not readily seen, which could potentially increase the risk of the nerve root and dural injury. Reports of endoscopic lumbar discectomies have demonstrated nerve root irritation rates as high as 2–8% [11–14]. Postoperative dysesthesias have been reported as high as 8.9% in transforaminal decompressions [15]. A series of 907 transforaminal procedures had a 0.4% rate of unintentional durotomy [16]. While these complications are well recognized, their rate tends to decrease with surgeon experience [17, 18]. The following overview of safe anatomical zones for performing an endoscopic lumbar fusion will demonstrate the feasibility of this operation.



J.-S. Kim et al. (eds.), *Technical Advances in Minimally Invasive Spine Surgery*,
https://doi.org/10.1007/978-981-19-0175-1_17

## 17.2 Anatomical Description of Kambin's Triangle

Parviz Kambin recognized the need for anatomical landmarks to perform safe endoscopic spine surgery. Over a series of papers on a technique for percutaneous lateral discectomy, he described a safety zone for transforaminal lumbar approaches, known today as "Kambin's triangle." [19–22] It is defined by three anatomic structures: the superior endplate of the caudal vertebral body, the thecal sac, and the exiting nerve root (Fig. 17.1). This anatomical right triangle has been used to guide the spine surgeon within the neural foramen, allowing access to the pathology while avoiding nerve and dural injury. Even with modern techniques, spine surgeons continue to apply Kambin's principles to today's ever-evolving minimally invasive and endoscopic approaches.

The superior endplate of the caudal vertebral body is the inferior boundary of Kambin's triangle. A true anteroposterior (AP) X-ray shows the endplate as a single line, and once this view is obtained, identification of the endplate can be done easily and early in the approach. The angle at which a true AP view is seen at each level can be obtained and recorded before the procedure begins, thereby minimizing the amount of time spent finding it as the operation proceeds. This landmark approximates the inferior aspect of the neural foramen, which is bounded by the pedicles of the level above and below. Staying above the superior endplate will correctly guide the surgeon toward the foramen so that an adequate decompression can be performed, and increase safety of the dissection by avoiding nearby nerve roots.

The thecal sac serves as the medial boundary of Kambin's triangle. In the lumbar spine, at the level of the neural foramen, the thecal sac contains the traversing nerve root. Both the traversing nerve and the thecal sac are at risk if this boundary is crossed. CSF leaks are not common, but they can complicate completion of the surgery as well as the postoperative course.

The exiting nerve root forms the hypotenuse of Kambin's triangle. The exiting nerve root in the lumbar spine is closely associated with the inferior aspect of the pedicle of the rostral

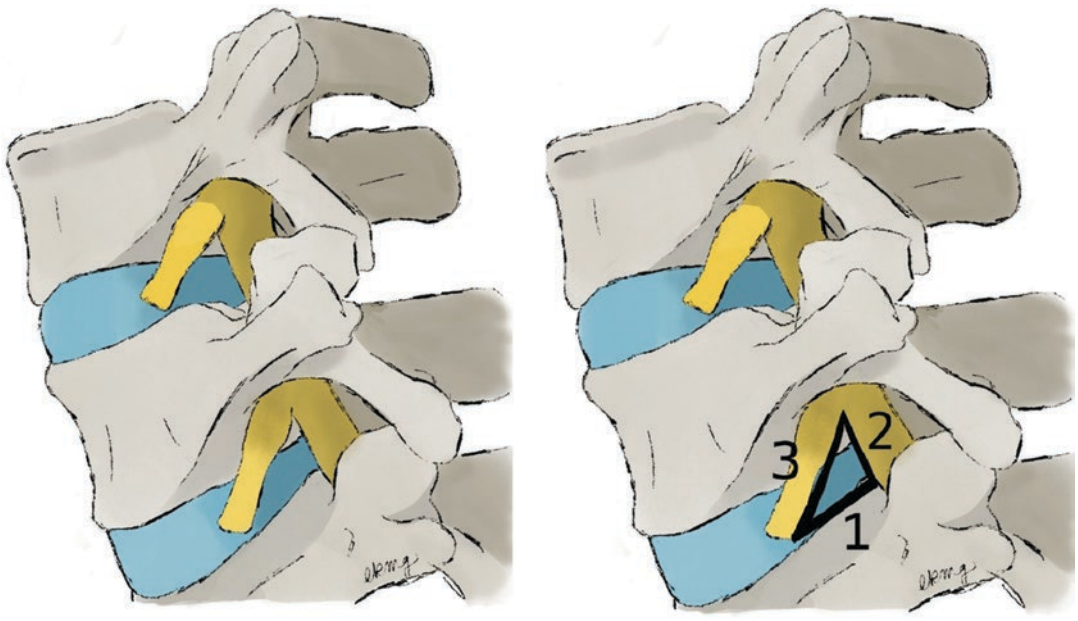


**Fig. 17.1** Side view of the lumbar neural foramen. Kambin's triangle highlighted on the right. This diagram has partial removal of the superior articulating process to better illustrate the relationship between the borders of Kambin's triangle: (1) Sup endplate, (2) Thecal sac, (3) Exiting nerve root

vertebral body. This constant relationship is a reliable indicator of the nerve root's location. Not only can manipulation of the nerve cause direct injury, which may manifest as transient or permanent weakness or paresthesias, but indirect stretch injury can also be inflicted by the endoscope. Understanding the location of this boundary will help the surgeon to protect a critical structure during this operation.

These boundaries collectively define the triangle as described by Kambin. In the original descriptions, the superior articulating process (SAP) was mentioned as a dorsal border of the zone, but not assigned as one of the triangle borders [23]. Subsequent anatomical studies on this region have produced a variety of newer definitions or iterations of Kambin's triangle, incorporating the SAP, which makes it a three dimensional zone. This has been a source of confusion with regard to the true definition of Kambin's triangle, and the actual safe borders for the procedure. Sakane described several approaches for a percutaneous endoscopic lumbar discectomy, of which the transforaminal corridor was suggested primarily for intracanal and foraminal disc herniations [6, 24]. He presents Kambin's triangle as "a three-dimensional anatomical right triangle over the dorsolateral intervertebral disc of the lumbar spine." Subsequently, authors group defined the borders of the triangle as the superior endplate of the inferior vertebral body, the exiting nerve root, and the superior articulating process [25, 26].

Pairaiturkar introduced the concept of a separate neural and bony Kambin's triangle [27]. The neural triangle matches the original definition of Kambin's: the superior endplate of the caudal vertebral body, the thecal sac, and the exiting nerve root. The bony Kambin's triangle, which is also referred to as the "working triangle," is formed by the superior endplate of the caudal vertebral body, exiting nerve root, and the facet joint. Hardenbrook defined a separate working zone and safe zone [28]. The intention was to distinguish an area in which it is safe to introduce the endoscope and instruments, and the area to which the actual dissection should be restricted to avoid injury to critical structures. The working zone lies between the exiting nerve root and traversing nerve root, above the superior margin of the inferior pedicle. The safe zone is defined by the widths of the superior and inferior pedicles between the exiting root and traversing roots.

## 17.3 The Working Zone and Safe Zone

The concept of a working zone and safe zone was originally proposed by Kambin for the minimally invasive transforaminal approach [10, 29]. While the boundaries of the triangle can permit access to the foramen, the surgeon should still avoid dissecting near those boundaries since they are at risk for causing injury to the nerve root or dura. This can come in the form of sharp injury, thermal injury, or traction injury. The surgeon must understand that the area fully visualized with the endoscope is larger than the area in which the dissection should be performed (Fig. 17.2). The working zone is the area through which instruments can be introduced to perform the procedure. The safe zone, which is smaller, is the only area in which dissection should be performed to reduce risk of nerve and dural injury. Due to the small size of these anatomic zones, cadaveric studies have performed measurements of their dimensions so properly design instruments and hardware for this approach.

Cadaveric analysis of Kambin's triangle in the context of performing a endoscopic transforaminal lumbar fusion found the area of the safe zone in the neural foramen, bound by the superior and inferior pedicles, traversing root and exiting root, to have an average of 1.2 $cm^2$. L5–S1 had the largest safe zone area of 1.26 $cm^2$ (Fig. 17.3) [28]. The working triangle, defined as the space between the exiting and traversing nerve roots above the superior margin of the pedicle inferiorly, was found to have an average surface area of 1.83 $cm^2$, with L5–S1 again having the largest area at 2.19 $cm^2$ (Fig. 17.3). Exiting nerve roots have been found to have an average width of 1.79 cm from the medial aspect of the inferior pedicle, 1 cm from the lateral border of the pedicle, with the nerve coming closest to the superior pedicle, with a minimum distance of 0.39 cm

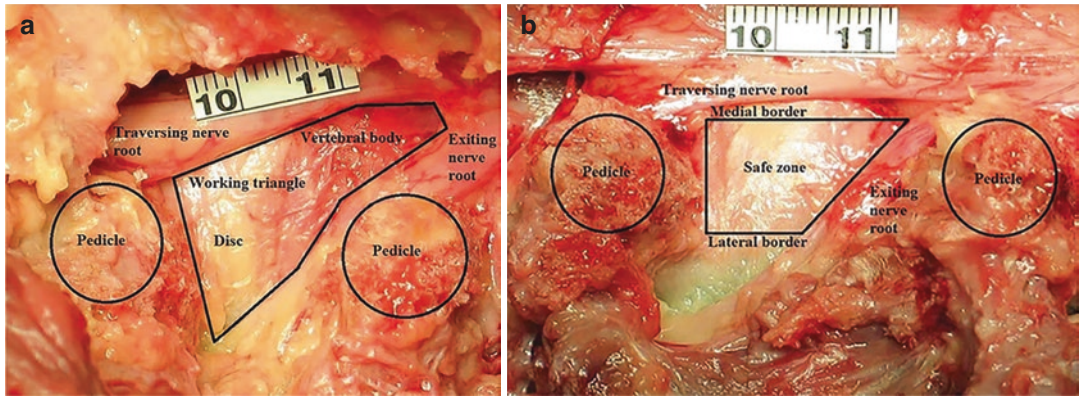


**Fig. 17.2** Cadaveric dissection demonstrating the working zone (**a**) and safe zone (**b**). The area of the safe zone is smaller than the working zone. From Hardenbrook et al. (2016). Used with permission

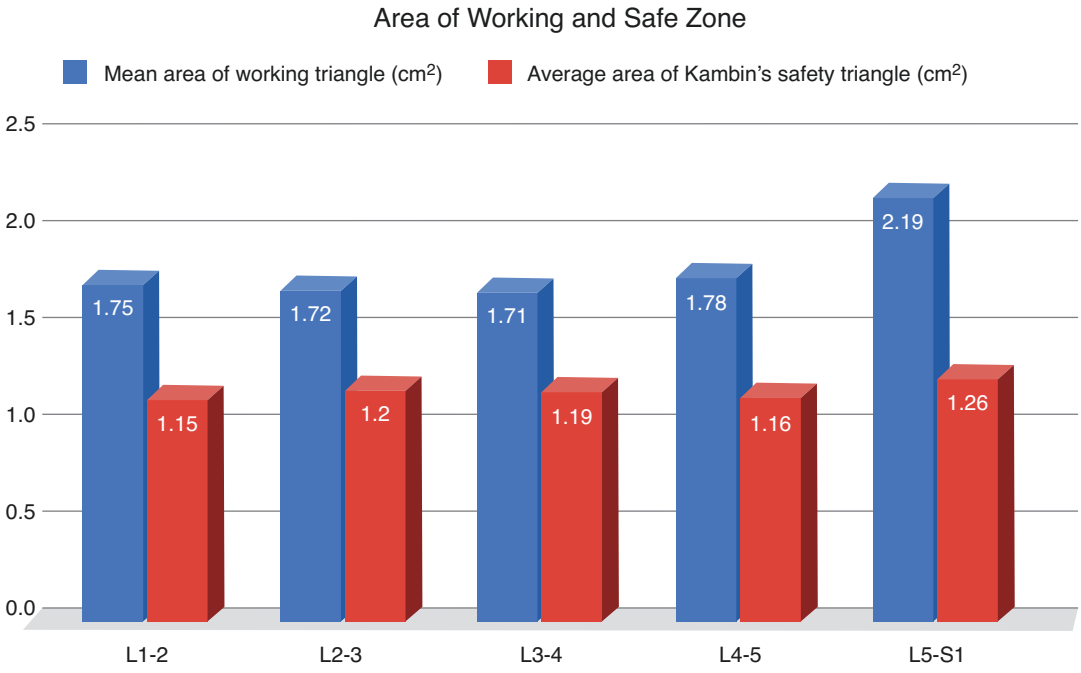


**Fig. 17.3** Bar graph representing the difference in area between the working zone and safety zone [28]

(Table 17.1). Overall, the safe and working zone areas gradually increases from L2–L3 to L5–S1, with L5–S1 having the largest area.

CT-based studies found that the distance of the exiting nerve root to the thecal sac was closest at the L2–L3 and L3–L4 levels when evaluating levels from L2–S1, thus bringing instruments and interbody graft into closer proximity with the exiting nerve roots at these levels than at more inferior levels [31]. In the intervertebral foramen, the exiting nerve root lies in the superior aspect of the foramen, with the dorsal aspect of the foramen limited by the superior articular process. Removal of the superior articular process, particularly at the L2–L3 and L3–L4 levels enlarges the working zone, allowing for a larger working channel up to 10 mm, and larger placement of an expandable interbody cage.

Awareness of the size limits for a port and instruments that can be used for an endoscopic TLIF is critical to planning for the procedure. Knowing the maximum size of an interbody cage and the limits of safe decompression will help avoid an intraoperative complication, and might help improve fusion rates. Injury to the nerve root could result in permanent neurological deficit, and the surgeon should be aware that retraction on the nerve root by the endoscope can also produce injury. If the surgery is performed with general anesthesia, changes in neuromonitoring should be taken seriously. In an awake setting, a patient complaint of paresthesias should be considered a sign of nerve root irritation. In these circumstances, there should be consideration of a maneuver to reduce manipulation of the nerve root.

**Table 17.1** Mean distances between the nerve roots at disc space and disc height within Kambin's triangle at different levels in the lumbar spine [30]

| | Mean distance between thecal sac and nerve root at inferior level of disc space (mm) | Mean distance between thecal sac and nerve root at superior level of disc space (mm) | Mean disc height within Kambin's triangle (mm) |
|---|---|---|---|
| L1–2 | 12.42 | 9.62 | 5.83 |
| L2–3 | 12.04 | 9.53 | 6.97 |
| L3–4 | 12.48 | 8.85 | 9.3 |
| L4–5 | 15.16 | 11.13 | 8.89 |
| L5–S1 | 16.12 | 12.01 | 6.61 |

## 17.4 Technical Considerations and Limitations

The endoscopic transforaminal lumbar interbody fusion requires additional technical considerations compared to an endoscopic discectomy alone, due to the need to prepare the endplates and place an interbody cage through the working channel into the disc space (Fig. 17.4). Improper channel selection or placement may result in a poorly placed graft or damage to the nerve root. The size of the working triangle and safe zone in Kambin's triangle is variable depending on the particular level, a consideration that may affect dissection technique, especially in a smaller space. Due to the aforementioned area of the safe zone, we recommend limiting the size of the port to 10 mm, which will help to ensure the surgeon is limiting dissection within the safe zone. Larger ports may theoretically increase the risk of indirect nerve injury by causing stretch as it is introduced or manipulated.

Difficulty accessing the disc space via the transforaminal approach may occur due to neural

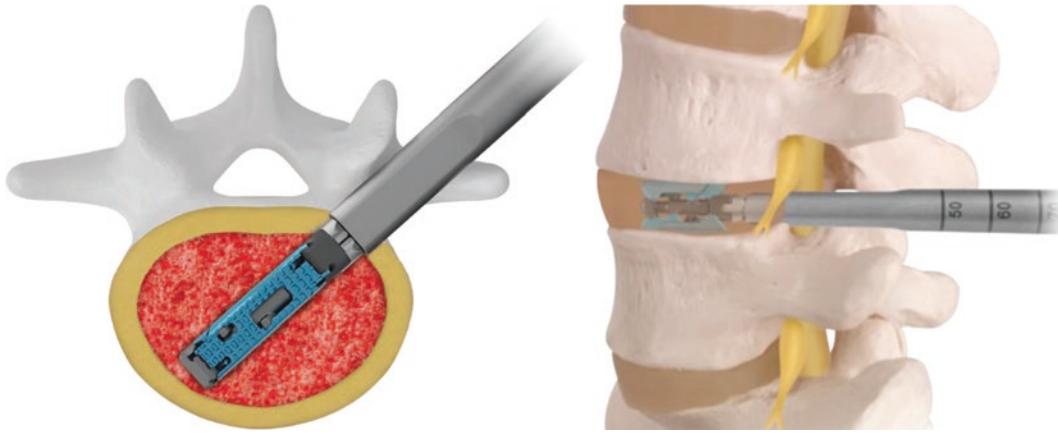


**Fig. 17.4** Demonstration of interbody cage being introduced to the disc space through the working channel. Courtesy of Globus Medical Inc.

foraminal stenosis. Degenerative disease processes that result in a collapsed disc space or, more commonly, superior articulating process hypertrophy, can make it difficult to identify all the boundaries of Kambin's triangle [8, 32]. Performing a foraminoplasty is one option to improve access to the space and reduce risk of exiting nerve root injury due to working channel compression. [32–34] A transforaminal foraminoplasty can be performed utilizing endoscopic tools such as a bone reamer, trephine, or high speed drill, to remove the superior articular process and expand the foramen [35, 36]. Additional bony decompression can be done if necessary, however, this may result in bleeding, and diminishes the benefit of minimal bony removal. Another technique, which helps to avoid a foraminoplasty, is to use a steeper angle with the spinal needle to help enter the disc space, and then adjust to a more lateral angle if difficulty accessing the disc space persists [32].

Additional strategies to further enlarge the working space once access has been obtained include retracting the thecal sac in order to expand the area of the safety zone. Under direct visualization, rotatory maneuvers of the working channel can provide this retraction [37]. The lumbar thecal sac can tolerate retraction since it contains freely mobile nerve roots and no spinal cord, and this maneuver can increase the working space of the safe zone.

## 17.5 Conclusion

Technological advances have facilitated the creation of less invasive approaches to the spine. Minimally invasive spinal surgery offers multiple advantages, including less disruption of supporting structures of the spine, faster recovery times and lower complication rates [18, 38, 39]. The application of endoscopic techniques required development of anatomical corridors and dedicated instruments to safely perform these procedures. Kambin's triangle describes anatomical boundaries necessary to keep these approaches safe. Familiarity with the limits of this zone allows confidence that injury of critical structures can be avoided. The distinction of a safe zone, to which dissection should be limited, is an important concept in performing this procedure to improve its safety.

The original definition of Kambin's triangle has been modified and expanded by several authors, as the endoscopic transforaminal technique has evolved and been applied for different procedures. While the classic Kambin's triangle was initially designed to be applied to endoscopic lumbar decompression, the endoscopic TLIF can also be accomplished safely using these boundaries. The studies and cadaveric dissections presented here show that the necessary anatomical regions can be accessed to safely perform the procedure. We have reviewed evidence from the literature that there are readily identifiable boundaries of the safe zone, and that all the steps of a lumbar interbody fusion can be achieved endoscopically.

## References

1. Ahn Y, Lee S-H, Park W-M, Lee H-Y, Shin S-W, Kang H-Y. Percutaneous endoscopic lumbar discectomy for recurrent disc herniation: surgical technique, outcome, and prognostic factors of 43 consecutive cases. Spine (Phila Pa 1976). 2004;29(16):E326–32.
2. Ahn Y, Oh H-K, Kim H, Lee S-H, Lee H-N. Percutaneous endoscopic lumbar foraminotomy: an advanced surgical technique and clinical outcomes. Neurosurgery. 2014;75(2):124–33.
3. Musacchio M, Patel N, Bagan B, Deutsch H, Vaccaro AR, Ratliff J. Minimally invasive lumbar laminectomy via a dual-tube technique: evaluation in a cadaver model. Surg Neurol. 2007;67(4):348–52.
4. Heo DH, Son SK, Eum JH, Park CK. Fully endoscopic lumbar interbody fusion using a percutaneous unilateral biportal endoscopic technique: technical note and preliminary clinical results. Neurosurg Focus. 2017;43(2):E8.
5. Wang MY, Grossman J. Endoscopic minimally invasive transforaminal interbody fusion without general anesthesia: initial clinical experience with 1-year follow-up. Neurosurg Focus. 2016;40(2):E13.
6. Sakane M. Anatomical relationship between Kambin's triangle and exiting nerve root. Mini-Invasive Surg. 2017;1(1):99–102.
7. Yang J, Liu C, Hai Y, Yin P, Zhou L, Zhang Y, et al. Percutaneous endoscopic transforaminal lumbar interbody fusion for the treatment of lumbar spinal stenosis: preliminary report of seven cases with 12-month follow-up. Biomed Res Int. 2019;2019

8. Choi I, Ahn J-O, So W-S, Lee S, Choi I-J, Kim H. Exiting root injury in transforaminal endoscopic discectomy: preoperative image considerations for safety. Eur Spine J. 2013;22(11):2481–7.
9. Ahn Y, Youn MS, Heo DH. Endoscopic transforaminal lumbar interbody fusion: a comprehensive review. Expert Rev Med Devices. 2019;16(5):373–80.
10. Kambin P, Casey K, O'Brien E, Zhou L. Transforaminal arthroscopic decompression of lateral recess stenosis. J Neurosurg. 1996;84(3):462–7.
11. Sairyo K, Sakai T, Higashino K, Inoue M, Yasui N, Dezawa A. Complications of endoscopic lumbar decompression surgery. Minim Invasive Neurosurg. 2010;53(04):175–8.
12. Sairyo K, Matsuura T, Higashino K, Sakai T, Takata Y, Goda Y, et al. Surgery related complications in percutaneous endoscopic lumbar discectomy under local anesthesia. J Med Investig. 2014;61(3–4):264–9.
13. Epstein NE. More nerve root injuries occur with minimally invasive lumbar surgery, especially extreme lateral interbody fusion: a review. Surg Neurol Int. 2016;7(Suppl 3):S83.
14. Ahn Y, Jang I-T, Kim W-K. Transforaminal percutaneous endoscopic lumbar discectomy for very high-grade migrated disc herniation. Clin Neurol Neurosurg. 2016;147:11–7.
15. Yeung A, Lewandrowski K-U. Five-year clinical outcomes with endoscopic transforaminal foraminoplasty for symptomatic degenerative conditions of the lumbar spine: a comparative study of inside-out versus outside-in techniques. J Spine Surg. 2020;6(Suppl 1):S66.
16. Telfeian AE, Shen J, Ali R, Oyelese A, Fridley J, Gokaslan ZL. Incidence and implications of incidental durotomy in transforaminal endoscopic spine surgery: case series. World Neurosurg. 2020;134:e951–5.
17. Hsu H-T, Chang S-J, Yang SS, Chai CL. Learning curve of full-endoscopic lumbar discectomy. Eur Spine J. 2013;22(4):727–33.
18. Lee JC, Jang H-D, Shin B-J. Learning curve and clinical outcomes of minimally invasive transforaminal lumbar interbody fusion: our experience in 86 consecutive cases. Spine (Phila Pa 1976). 2012;37(18):1548–57.
19. Kambin P. Posterolateral percutaneous lumbar discectomy and decompression. Arthrosc Microdiscectomy Minimal Interv Spinal Surg. 1991;
20. Kambin P, Sampson S. Posterolateral percutaneous suction-excision of herniated lumbar intervertebral discs. Report of interim results. Clin Orthop Relat Res 1986;(207):37–43.
21. Kambin P, Gellman H. Percutaneous lateral discectomy of the lumbar spine a preliminary report. Clin Orthop Relat Res. 1983;174:127–32.
22. Kambin P, Brager MD. Percutaneous posterolateral discectomy. Anatomy and mechanism. Clin Orthop Relat Res 1987;(223):145–54.
23. Tumialán LM, Madhavan K, Godzik J, Wang MY. The history of and controversy over Kambin's triangle: a historical analysis of the lumbar transforaminal corridor for endoscopic and surgical approaches. World Neurosurg. 2019;123:402–8.
24. Abe T, Sakane M, Harabayashi H, Noguchi H, Tsukada A, Ochiai N. Comparison of clinical outcomes of percutaneous endoscopic discectomy and open surgery for lumbar disc herniation. J Japan Spine Res Soc. 2009;20(3):653–5.
25. Hoshide R, Feldman E, Taylor W. Cadaveric analysis of the Kambin's triangle. Cureus. 2016;8(2)
26. Sinkemani A, Hong X, Gao Z-X, Zhuang S-Y, Jiang Z-L, Zhang S-D, et al. Outcomes of microendoscopic discectomy and percutaneous transforaminal endoscopic discectomy for the treatment of lumbar disc herniation: a comparative retrospective study. Asian Spine J. 2015;9(6):833.
27. Pairaiturkar PP, Sudame OS, Pophale CS. Evaluation of dimensions of Kambin's triangle to calculate maximum permissible cannula diameter for percutaneous endoscopic lumbar discectomy: a 3-dimensional magnetic resonance imaging based study. J Korean Neurosurg Soc. 2019;62(4):414.
28. Hardenbrook M, Lombardo S, Wilson MC, Telfeian AE. The anatomic rationale for transforaminal endoscopic interbody fusion: a cadaveric analysis. Neurosurg Focus. 2016;40(2):E12.
29. Kambin P. Percutaneous lumbar discectomy: current practice. Surg Rounds Orthop. 1988;2:31–5.
30. Lertudomphonwanit T, Keorochana G, Kraiwattanapong C, Chanplakorn P, Leelapattana P, Wajanavisit W. Anatomic considerations of intervertebral disc perspective in lumbar posterolateral approach via Kambin's triangle: cadaveric study. Asian Spine J. 2016;10(5):821.
31. Zhang L, Yang J, Hai Y, Yin P, Ding Y, Xu C, et al. Relationship of the exiting nerve root and superior articular process in Kambin's triangle: assessment of lumbar anatomy using cadavers and computed tomography imaging. World Neurosurg. 2020;
32. Basil G, Wang MY. Technical considerations of endoscopic Kambin's triangle lumbar interbody fusion. World Neurosurg. 2020;
33. Lee W, Park J-Y, Kim KH, Kuh SU, Chin DK, Kim KS, et al. Minimally invasive transforaminal lumbar interbody fusion in multilevel: comparison with conventional transforaminal interbody fusion. World Neurosurg. 2016;85:236–43.
34. Li Z, Hou S, Shang W, Cao Z, Zhao H. Percutaneous lumbar foraminoplasty and percutaneous endoscopic lumbar decompression for lateral recess stenosis through transforaminal approach: technique notes and 2 years follow-up. Clin Neurol Neurosurg. 2016;143:90–4.
35. Sang-Ho L, Erken HY, Bae J. Percutaneous transforaminal endoscopic lumbar interbody fusion: clinical and radiological results of mean 46-month follow-up. Biomed Res Int. 2017;2017
36. Li X, Jin L, Lv Z, Su X, Wang K, Shen H, et al. Efficacy of percutaneous transforaminal endoscopic decompression treatment for degenerative lumbar

spondylolisthesis with spinal stenosis in elderly patients. Exp Ther Med. 2020;19(2):1417–24.
37. Soo ES, Sourabh C, Ho LS. Posterolateral endoscopic lumbar decompression rotate-to-retract technique for foraminal disc herniation: a technical report. Biomed Res Int. 2019;2019
38. McGirt MJ, Parker SL, Lerner J, Engelhart L, Knight T, Wang MY. Comparative analysis of perioperative surgical site infection after minimally invasive versus open posterior/transforaminal lumbar interbody fusion: analysis of hospital billing and discharge data from 5170 patients. J Neurosurg Spine. 2011;14(6):771–8.
39. Wang J, Zhou Y, Zhang ZF, Li CQ, Zheng WJ, Liu J. Comparison of one-level minimally invasive and open transforaminal lumbar interbody fusion in degenerative and isthmic spondylolisthesis grades 1 and 2. Eur Spine J. 2010;19(10):1780–4.

# 18 O-Arm Navigation-Guided Biportal Endoscopic Transforaminal Lumbar Interbody Fusion

Javier Quillo-Olvera, Diego Quillo-Olvera, Javier Quillo Reséndiz, Michelle Barrera Arreola, Claudia A. Covarrubias, and Jin-Sung Kim

## Abbreviations

| | |
|---|---|
| AP | Anteroposterior |
| Cau | Caudal. |
| Cra | Cranial |
| CT | Computed tomography |
| Dor | Dorsal |
| EN | Exiting nerve |
| IAP | Inferior articular process |
| IEP | Inferior endplate |
| ILS | Interlaminar space |
| IST | Isthmus |
| L | Lamina |
| Lat | Lateral |
| Med | Medial |
| MISS | Minimally invasive spine surgery |
| ODI | Oswestry disability index |
| RF | Radiofrequency |
| SAP | Superior articular process |
| SEP | Superior endplate |
| SP | Spinous process |
| TLIF | Transforaminal lumbar interbody fusion |
| TN | Traversing nerve |
| TP-SAP | Transverse process superior articular junction |
| TS | Thecal sac |
| UBE | Unilateral biportal endoscopy |
| ULBD | Unilateral laminotomy bilateral decompression |
| VAS | Visual analog scale |
| Ven | Ventral |

J. Quillo-Olvera · D. Quillo-Olvera · J. Q. Reséndiz M. B. Arreola
Department of Neurosurgery, The Brain and Spine Care, Minimally Invasive Spine Surgery Group, Spine Clinic, Hospital H+ Querétaro, Querétaro City, Mexico

C. A. Covarrubias
Department of Experimental Surgery, McGill University, Montreal, Quebec, Canada

J.-S. Kim (✉)
Department of Neurosurgery, Seoul St Mary's Hospital, The Catholic University of Korea, College of Medicine, Seoul, Korea (Republic of)

## 18.1 Introduction

Real-time intraoperative navigation applied to spinal surgery has been associated with shorter operative time, reduced anesthetic consumption, less radiation exposure from the surgical team, and higher accuracy in the placement of pedicle screws [1, 2]. These advantages lead to less damage of adjacent spinal tissues directly resulting in highly specific approaches addressed to the pathology, allowing spine surgeons to offer safer and less aggressive procedures. In this sense, minimally invasive spine surgery (MISS) is considered a set of surgical techniques dependent on technology to reduce damage to local tissues and systemic stress, allowing a faster return to a



J.-S. Kim et al. (eds.), *Technical Advances in Minimally Invasive Spine Surgery*,
https://doi.org/10.1007/978-981-19-0175-1_18

functional life. Therefore, when the appropriate technology is available, concepts such as location, accuracy, and visualization of the pathology make sense, and the integration of these concepts allows the surgeon to choose between the MISS technique closest to them. Among the MISS procedures that could benefit from the precision gained from intraoperative navigation, endoscopic surgery is one of them. This technique offers the spine surgeon a direct and magnified view of the anatomical landmarks. Endoscopic spinal surgery has been employed to manage several degenerative diseases with acceptable outcomes that have been documented in scientific literature such as randomized trials and meta-analyses [3–11].

Endoscopic techniques also have evolved, where presently the total removal of the intervertebral disc, translating to significant bone decompression, and assisting lumbar fusion, are possible through these highly specific procedures [12, 13]. Biportal unilateral endoscopy (UBE) for decompression and fusion is a variant in the portfolio of endoscopic approaches to the spine. Through unilateral access with two ports (one for the endoscope and the other as a working channel), it is attainable to perform the whole fusion technique [13, 14].

This chapter aims to describe the stepwise intraoperative navigation-assisted unilateral biportal endoscopic transforaminal lumbar interbody fusion (UBE-TLIF) technique.

## 18.2 Basic Concepts

Since the introduction of the transforaminal technique for lumbar interbody fusion (TLIF), reported by Harms in 1998 [15], the objectives that can be achieved are the following:

1. The technique is performed through a unilateral posterior approach that reaches the trapezoid Kambin's space to work the intervertebral disc [16].
2. Total facetectomy allows direct decompression of exiting and traversing nerves and the feasibility of extending the approach to achieve direct central and contralateral decompression of the spinal canal through an extended laminectomy if required [15, 17–19].
3. Proper placement of an intersomatic spacer allows indirect decompression of the neural elements [20].
4. Stabilization and fusion [19].
5. Preservation of segmental and lumbar lordosis. However, other variables may influence this result, such as the cage's design and characteristics, location within the intervertebral space, the trajectory of the pedicle screws, and the maneuvers performed to achieve more lordosis as bilateral facetectomy [21].

Therefore, the different modifications that the TLIF has undergone during the last 22 years have made it possible to achieve these objectives with less transgression to the lumbar native tissues.

Since the reported use of tubular retractors in 2005 by Foley [18] to the introduction of the use of endoscopic lenses to assist the fusion process, reported firstly by Osman in 2012 [22] the technology has accompanied the advancement and development of the TLIF and intraoperative navigation in real time has not been the exception [23–25]. Specifically, water-based spinal endoscopy grants two ways to assist the decompression and fusion procedure during TLIF:

1. Transforaminal fusion assisted by uniportal endoscopy may be excellent for patients with axial pain and moderate discogenic or facet degeneration [26–29]. In this procedure, indirect decompression is achieved through an intersomatic spacer's placement through Kambin's trapezoid. However, irritation to the exiting nerve has been reported with a frequency of 0–22%, depending on the author [26–34]. This may result from excessive manipulation of the foramen with the various instruments used for the technique as well as insufficient bone remodeling.
2. Endoscopic transforaminal fusion can be performed through a unilateral biportal endoscopic (UBE) approach, which is the subject of this chapter. This approach is carried out posterior or posterolaterally and reaches the already mentioned goals of the TLIF [14, 35–

39]. In the UBE-TLIF, the surgeon uses two ports to introduce the endoscope and the working instruments. Despite being a transmuscular technique, this procedure maximizes the virtual space between the muscles and the posterior bone elements' periosteum, also called the epiperiosteal space, filled with loose connective tissue and fat (Fig. 18.1). Therefore, it does not pose great significance concerning soft tissue injury. In this technique, the anatomy visualized through the endoscope is similar to the microsurgical one, but the structures' details are exceptional due to continuous saline. This provides greater safety and accuracy.

The UBE-TLIF can be used in cases where the patient requires a direct, extensive bone decompression due to major degenerative changes that cause unilateral or bilateral radicular symptoms in the patient but in a minimally invasive way. Their indications will be discussed in another section. The UBE-TLIF also allows working with surgical tools with which the surgeon is accustomed within their daily practice, and therefore there is greater confidence in their performance. An advantage observed with UBE procedures is the freedom with which the instruments can be used in the surgical field, resulting in less retraction of neural structures.

Both uniportal and biportal techniques have a role in endoscopic spine surgery due to the following premises:

1. Not all patient needs to justify large bone decompressions during TLIF.
2. Some patients can benefit from indirect decompression only.
3. There is another group of patients with severe degenerative changes, complex stenosis, or high-grade instabilities that will require more aggressiveness through the selected technique.

These points can be used to opt between an endoscopic (uniportal or biportal) approach or another way to resolve the disease in a given case.

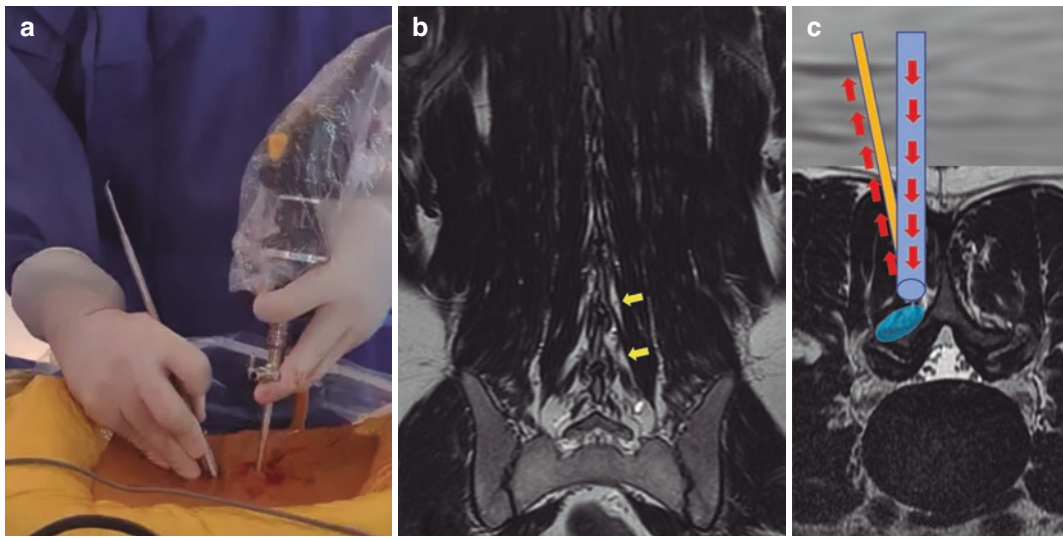


**Fig. 18.1** UBE procedure. (**a**) Two ports are created to introduce the endoscope and common spinal surgical instruments, with which the surgeon is familiar. (**b**) Coronal view of lumbar MRI. The yellow arrows are located in the multifidus muscles pointing toward a hyperintense triangular area known as the multifidus triangle, which corresponds to the epiperiosteal space. (**c**) Fluid circuit created by two channels during the UBE technique. The saline (red arrows) entry is through the endoscope (blue bar), and its exit is through the working channel used for the spinal instruments (yellow bar). The blue circle represents the space created by the saline in the epiperiosteal space

## 18.3 Advantages of Navigation-Guided UBE-TLIF

The integration between the surgical target location through intraoperative navigation and the visual integration through the endoscope offers accuracy, safety, and confidence to the surgeon. The following advantages have been observed during UBE-TLIF under intraoperative navigation:

(A) The accurate location of the superior articular process (SAP) can be accessed through intraoperative navigation, which is further recognized with the endoscope, leading to mark off the bone decompression and thus reducing the risk of injury to the exiting and traversing nerves.
(B) Navigation-guided central and contralateral endoscopic decompression is feasible and safe—granting the surgeon orientation to recognize where they are within the spinal canal.
(C) The navigation-guided endplates preparation reduces the risk of removing the anterior annulus or of causing more damage to the anterior longitudinal ligament, avoiding catastrophic vascular complications. It also avoids insufficient or overpreparation of the endplates.
(D) The intersomatic spacer can be navigated to determine the trajectory, while the cage can be visualized within the intervertebral space using the endoscope, thus preventing malposition of the cage.
(E) Intraoperative navigation has proven to be a facilitator for the precise placement of pedicle screws in various pathologies of the lumbar spine, while additionally reducing the exposure of the surgical team to intraoperative radiation secondary to the cumulative use of the C-arm [1, 2, 24, 40–45].

## 18.4 Surgical Anatomy

The referred bone structures serve as anatomical landmarks that guide the surgeon throughout the whole fusion process. These structures can be identified by intraoperative radiology (C-arm) or more easily by intraoperative navigation (O-arm). The anatomical structures identified through the endoscope initially will depend on the approach chosen by the surgeon.

The surgeon can select between two approaches:

(A) The unilateral biportal endoscopic (UBE) paramedian lumbar approach.

The epiperiosteal space filled with loose connective tissue and fat, located medial to the multifidus muscle, can be reached. The bone landmark that the surgeon recognizes through the endoscope is the spinous process base and lamina (spinolaminar) junction (Fig. 18.2).

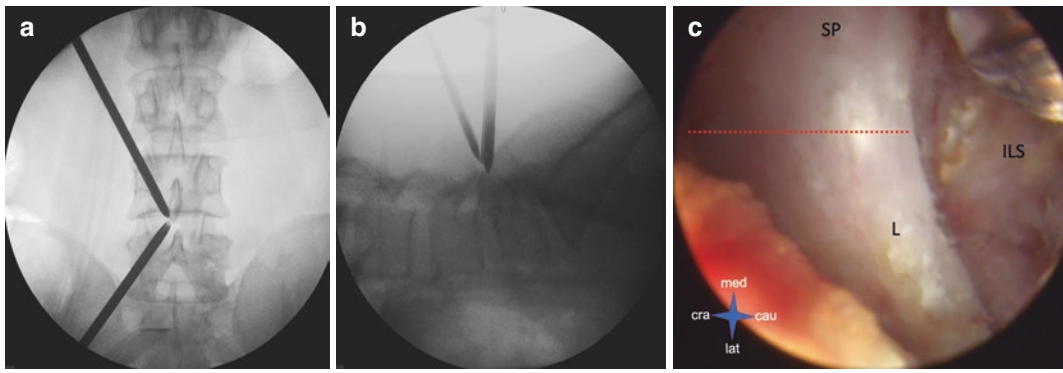


**Fig. 18.2** UBE paramedian approach. (**a**) C-arm AP view showing dilators joining in the spinolaminar junction. (**b**) The UBE paramedian approach is directed to the interlaminar space in the C-arm lateral view. (**c**) Intraoperative endoscopic imaging demonstrating the bone landmarks during the paramedian approach. *SP* spinal process, *L* lamina, *ILS* interlaminar space

This approach grants the interlaminar space control and provides access for performing medial facetectomies to reach the intervertebral disc's lateral surface. The endoscopic anatomy is similar to that seen when performing a PLIF [46, 47].

(B) The unilateral biportal endoscopic (UBE) paraspinal lumbar approach.

This approach is a modification of the oblique paraspinal approach [48]. It aims to reach the foramen through a more lateral plane than the Wiltse approach, along the intermuscular plane between the longissimus and iliocostalis muscles (Fig. 18.3) [49–51]. The access to the intertransverse space, which is limited cranially and caudally by transverse processes, with the intertransverse muscle acting as a floor, and limited medially by the lumbar foramen.

Through this approach, and the patient in prone position, the surgeon can recognize different structures depending on the foraminal craniocaudal height. In the most upper part, the isthmus, in the middle, the apex of the superior articular process (SAP), and inferiorly the SAP transverse process junction (Fig. 18.4) [52].

These landmarks allow orientation and can be found during the paraspinal approach with intraoperative navigation for later direct endoscopic visualization. It can prevent damage to the exiting nerve.

The paraspinal approach also allows working on the intervertebral disc through Kambin's trapezoid after the SAP removal [16]. Therefore, the surgeon can opt for performing a complete or partial facetectomy to reach the intervertebral space (Fig. 18.5) [14]. When a complete facetectomy is required, and the inferior articular process (IAP) is removed, the access to the interlaminar space for a bilateral neural decompression through a single approach (ULBD) is feasible [36].

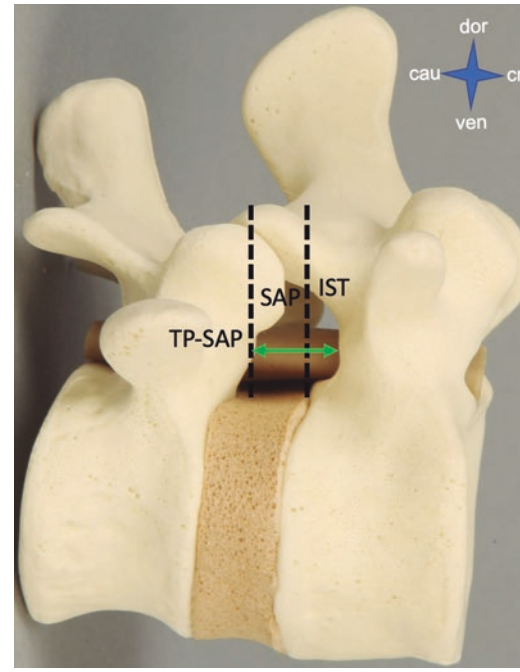


**Fig. 18.4** Depending on where the biportal endoscopic paraspinal approach is being addressed in the foramen, different landmarks can be reached. *IST* isthmus, *SAP* superior articular process, *TP-SAP* transverse process superior articular process junction

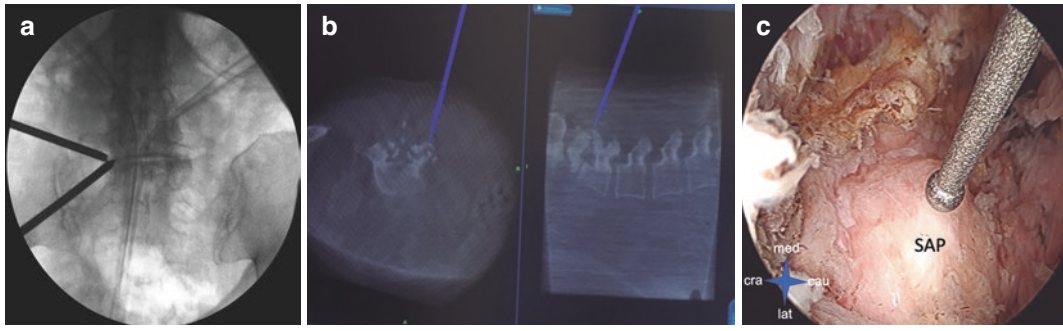


**Fig. 18.3** UBE paraspinal approach. (**a**) C-arm AP view demonstrating a UBE paraspinal procedure with dilators landing over SAP. (**b**) Intraoperative navigation showing the approach oblique trajectory. (**c**) Intraoperative endoscopic imaging of the SAP dorsolateral surface

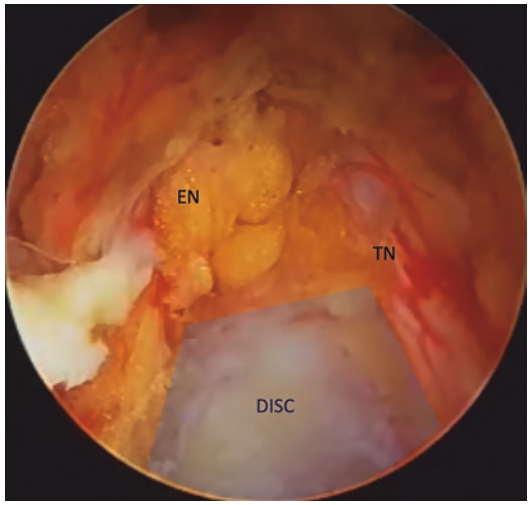


**Fig. 18.5** Intraoperative endoscopic imaging after complete facetectomy and ligamentum flavum removal. The blue shadow represents the Kambin's trapezoid area exposed and the disc within it. The EN and TN were decompressed. *EN* exiting nerve, *TN* traversing nerve

## 18.5 Indications and Contraindications

The meta-analysis-based [53] inclusion and exclusion criteria for deciding on performing a water-based endoscopic TLIF are as follows:

1. Degenerative spondylolisthesis grade 1 or 2.
2. Isthmic spondylolisthesis.
3. Instability.
4. Central stenosis with instability.
5. Foraminal stenosis.
6. End-stage degenerative disc disease.
7. Recurrent lumbar disc herniation.

And, contraindications are:

1. Tumor or neoplasm.
2. Bony fracture.
3. Infection.
4. Metabolic disease.
5. Intraspinal pathology.
6. Systemic disease.
7. High-grade spondylolisthesis (slips greater than 50%).
8. Severe osteoporosis.
9. Cauda equina syndrome.
10. Congenital spinal deformity.
11. Bleeding disorders.
12. Serious calcified fragments.
13. Previous lumbar operation (revision).
14. Multilevel instability.

Relative contraindications for performing only subtotal SAP removal and indirect decompression are:

1. Severe foraminal stenosis.
2. Severe central stenosis.
3. Severely collapsed disc height.

## 18.6 Operative Technique

1. *Operative Room Setup*
   Endoscopic and navigation displays should stay in front of the surgeon to facilitate information integration during the procedure. An assistant should be across from the surgeon to assist him when performing maneuvers that require other hands to hold, support, or guide instruments. The rest of the assistants can be on each side of the surgeon. The anesthesiologist can stay at the head of the patient (Fig. 18.6).
2. *Patient Positioning*
   General anesthesia is recommended. The patient is placed prone over the abdominal support frame. The surgeon staff needs to pay attention to the proper patient position to avoid complications such as brachial plexus traction, lower limb venous stasis or deep vein thrombosis, and soft tissue edema or ocular injury related to facial compression (Fig. 18.7).
3. *CT-based Navigation Setup*
   After clamping the navigation reference to the L1 spinous process through an 18-mm skin incision, an intraoperative CT scan with cone-beam CT (Medtronic Sofamor Danek, Memphis, TN) is performed. Then the verification of surgical instruments that track screw and cage placement is done. Finally, real-time navigation of the index level can be accessed

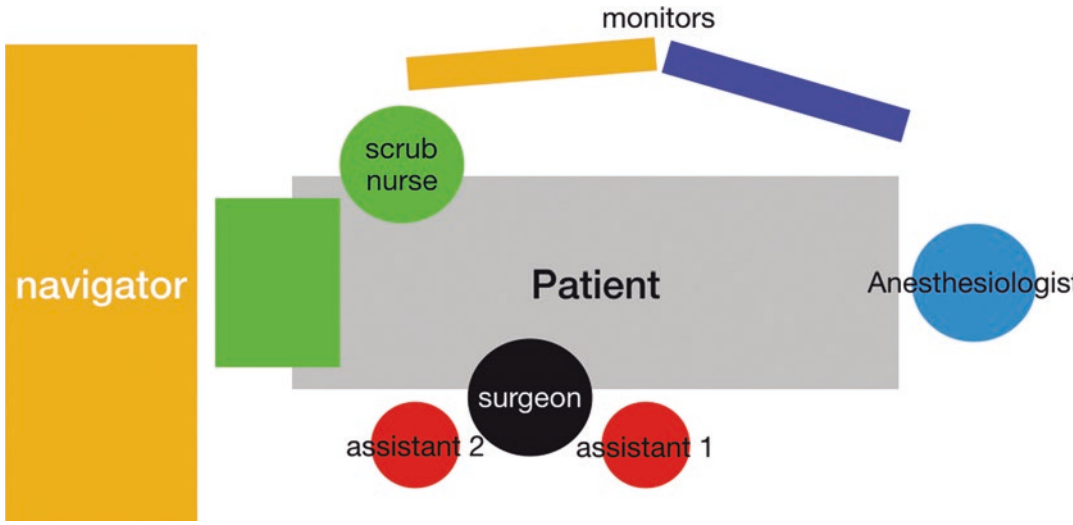


**Fig. 18.6** Operative room setting

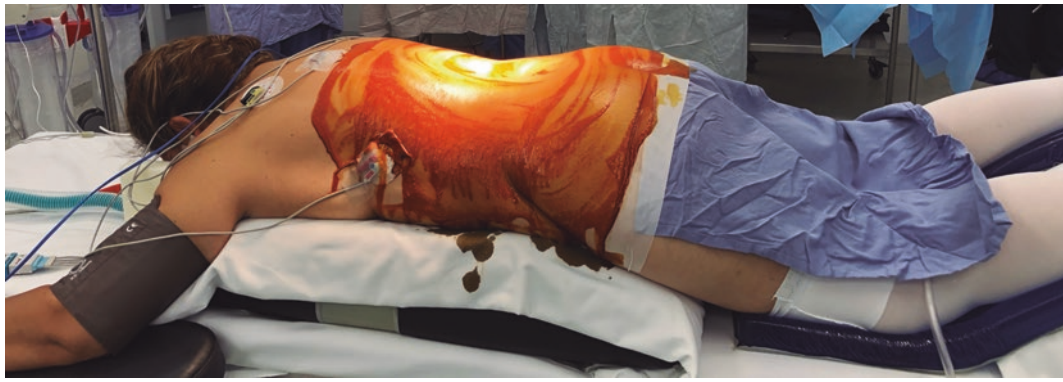

**Fig. 18.7** Patient positioning

throughout the procedure with the registered probe and observed in the StealthStation display (Medtronic Sofamor Danek, Memphis, TN) in axial, sagittal, and coronal planes (Fig. 18.8).

4. *Navigation-Based Paraspinal Approach*

   Two 16-mm skin incisions are navigated and planned ipsilateral to the symptoms' side of the patient. Both incisions are made 25-mm in a paraspinal fashion to the lateral pedicular line of the superior and inferior pedicles of the index level. The underlying fascia should be opened to allow a continuous inside–outside flow of the saline irrigated by the endoscope. Sequential dilation with progressive dilators is performed through the incisions. Before the dilation, the navigated pointer can confirm the correct trajectory of the paraspinal approach. The dilation is performed in an oblique way to allow for a proper angle for the cage's delivery within the intervertebral space after neural decompression. The dilator tips should join in the facet joint, and the surgeon should feel the bone with the dilators. For a right-handed surgeon working on the patient's left side, the endoscope is introduced through the cranial incision, and the caudal incision is used as a working channel. At the instance of a left-sided approach, this would be contrary (Fig. 18.9).

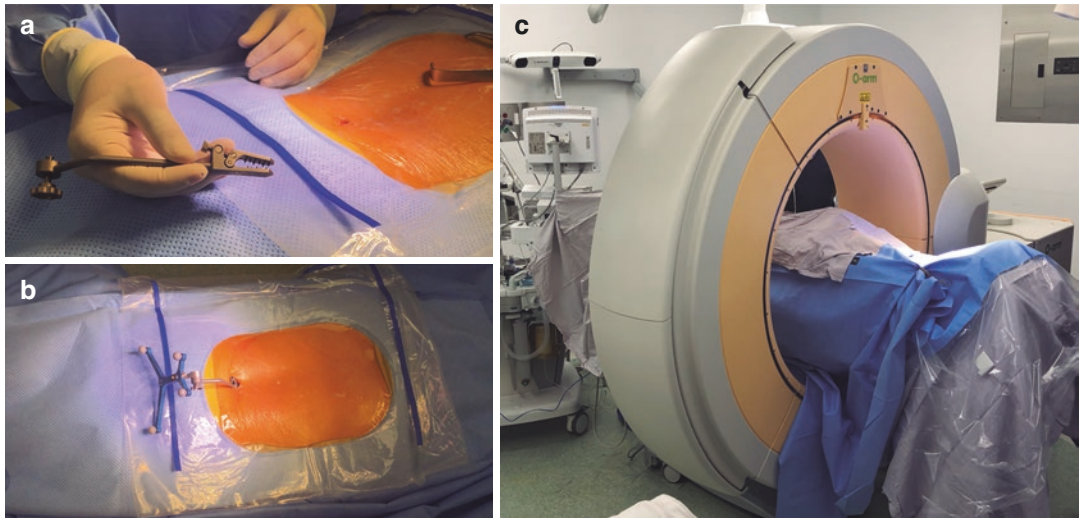


**Fig. 18.8** The navigation reference is clamped at the L1 spinous process (**a** and **b**). (**c**) An intraoperative spin is done to obtain real-time navigation throughout the procedure

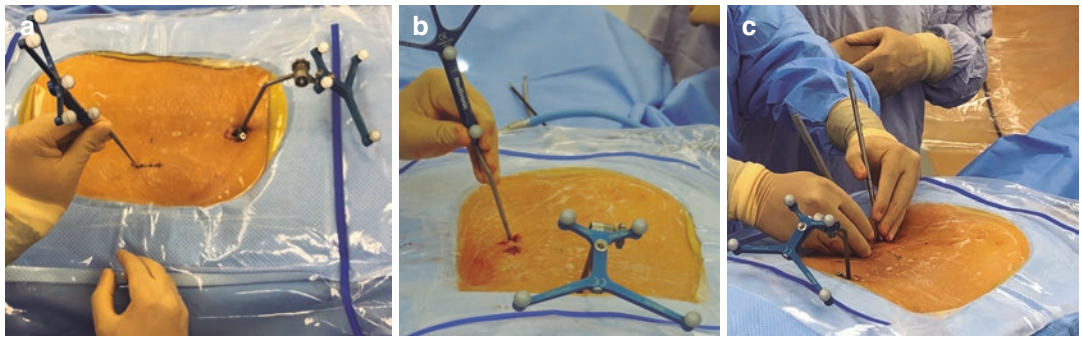


**Fig. 18.9** Navigation-based paraspinal approach. (**a**) Skin incisions planning under navigation. (**b**) Oblique paraspinal trajectory planning with the navigated pointer. (**c**) Sequential dilation through both incisions

5. *Biportal Endoscopic Bone Removal Under Intraoperative Navigation*

   A 4-mm outer diameter with a 30° angulated lens endoscope is introduced through the cranial incision pointed toward the facet joint with continuous saline irrigation. A radiofrequency (RF) probe with a 3.75-mm shaft and 90° of angulation is introduced through the caudal incision to ablate and coagulate the tissue overlying the facet joint (Fig. 18.10). The facetectomy is completed using different sized chisels and a high-speed drill with a 3-mm diamond burr. Like an open or microscopic foraminotomy, the SAP is removed from the base to the apex under endoscopic visualization. Below the SAP, a foraminal fat and the disc will be found. The surgeon can be oriented during bone removal by real-time intraoperative navigation (Fig. 18.11).
6. *Biportal Endoscopic Neural Decompression*

   If the case requires it, the IAP could also be drilled to detach the lateral insertion of ligamentum flavum. The foraminal extension of the ligamentum flavum is removed with 2- and 3-mm Kerrison punches, and the exiting and traversing nerves can be identified. Using the RF probe, the epidural vessels below ligamentum flavum can be coagulated, and the saline pressure displaces the dura, avoiding

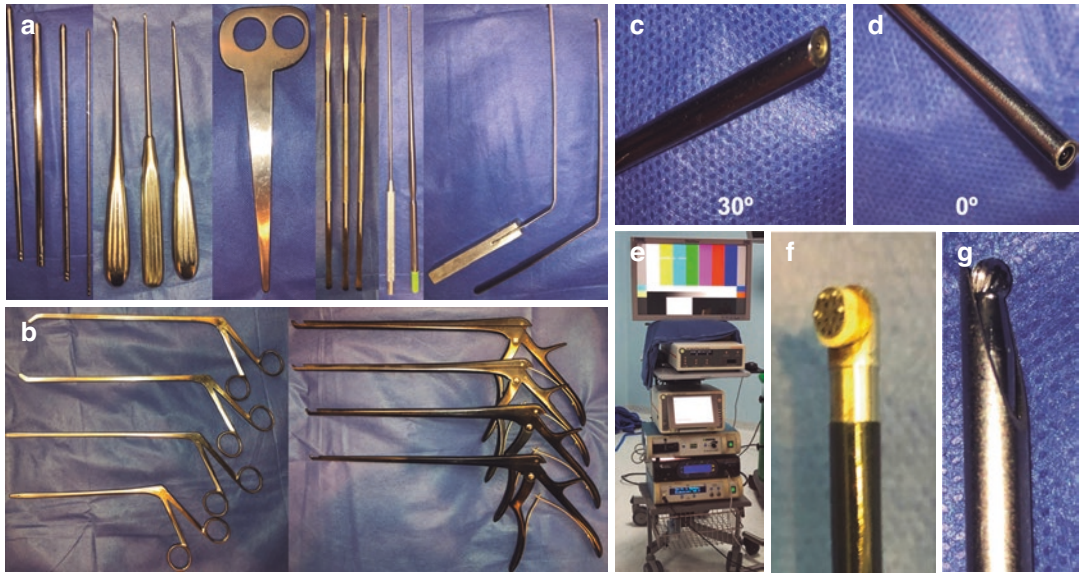


**Fig. 18.10** Surgical instruments used during UBE-TLIF. (**a**, **b**) Different sized dilators, directors, nerve retractors, pituitary forceps, and Kerrison punches. (**c**) 30° angulated lens endoscope. (**d**) 0° angulated lens endoscope. (**e**) Endoscopic display. (**f**) RF probe. (**g**) High-speed drill

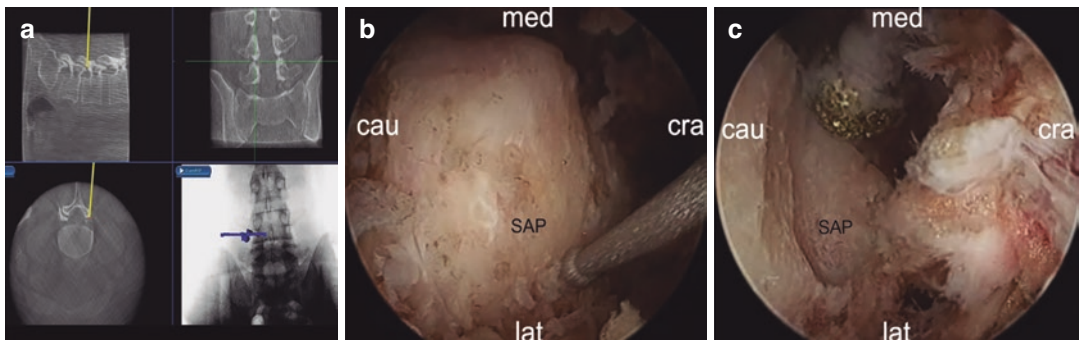


**Fig. 18.11** (**a**) Intraoperative navigation of the SAP. (**b**) Endoscopic visualization and navigation of the SAP at the same time. (**c**) Facetectomy using high-speed drill under endoscopic guidance. *SAP* superior articular process, *cau* caudal, *cra* cranial, *med* medial, *lat* lateral

an injury. Complete flavectomy in an over-the-top way can be attained if the surgeon addresses the approach more medially (Fig. 18.12). During central or contralateral decompression, the surgeon can be guided by using the intraoperative navigated pointer.

7. *Biportal Endoscopic Discectomy and Endplates Preparation*

After cleaning the soft tissue and coagulating the vessels located in the ventral epidural space over the disc using the RF probe, this can be removed under endoscopy. The accuracy of landmarks can be ensured with intraoperative navigation (Fig. 18.13). Discectomy is performed using different sized pituitary forceps. The endplates are prepared meticulously with different curettes, shavers, and rasps to remove the cartilage overlying. The endoscope, together with a navigated pointer, will avoid the anterior annulus' violation and

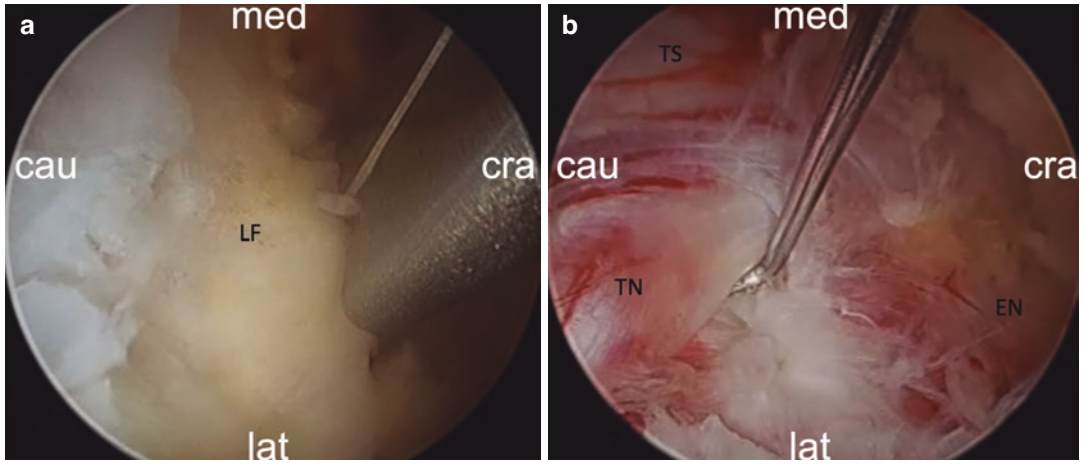


**Fig. 18.12** Intraoperative endoscopic images demonstrated neural decompression. (**a**) Ligamentum flavum (LF) is removed with Kerrison punch. (**b**) Extended neural decompression can be reached through the paraspinal approach. *TS* thecal sac, *TN* traversing nerve, *EN* exiting nerve

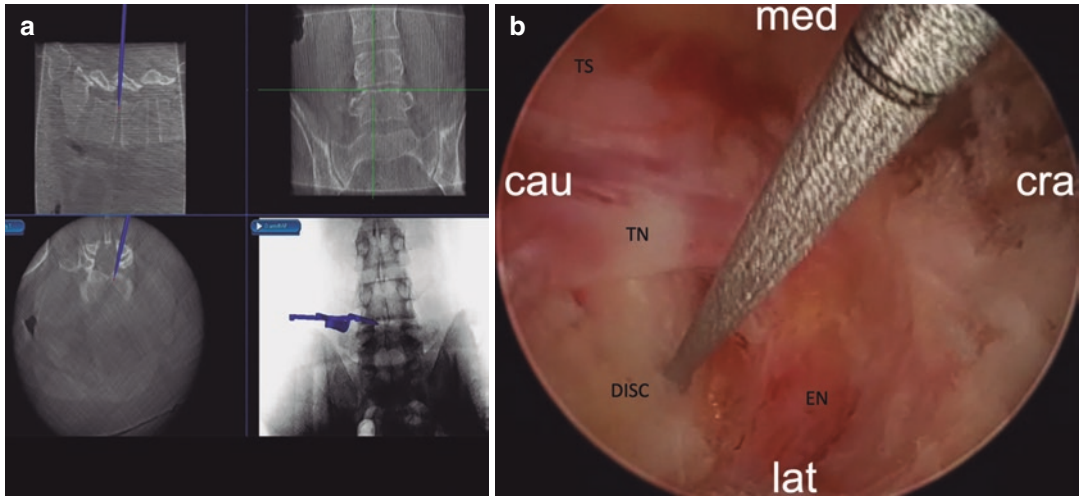


**Fig. 18.13** Confirmation of the disc space under the intraoperative navigation (**a**) and endoscopic guidance (**b**). *TS* thecal sac, *TN* traversing nerve, *EN* exiting nerve

transgression, preventing a catastrophic vascular complication during the intervertebral space preparation (Fig. 18.14).

8. *Biportal Endoscopic Fusion (Graft and Cage Insertion)*

   Autologous bone mixed with a bone matrix is delivered within the intervertebral space. A special neural retractor is placed to protect the traversing and exiting nerves during cage insertion, placed under direct endoscopic and navigation guidance. It improves the trajectory and the final cage position (Fig. 18.15).

9. *Transpedicular Screw Fixation*

   The ipsilateral skin incisions are used to guide the placement of the transpedicular screws. Contralateral fixation requires new incisions made in the same way as the firsts. Intraoperative navigation during transpedicular fixation was carried out as is usually done. The construct is completed with bilateral rods of appropriate length (Fig. 18.16).

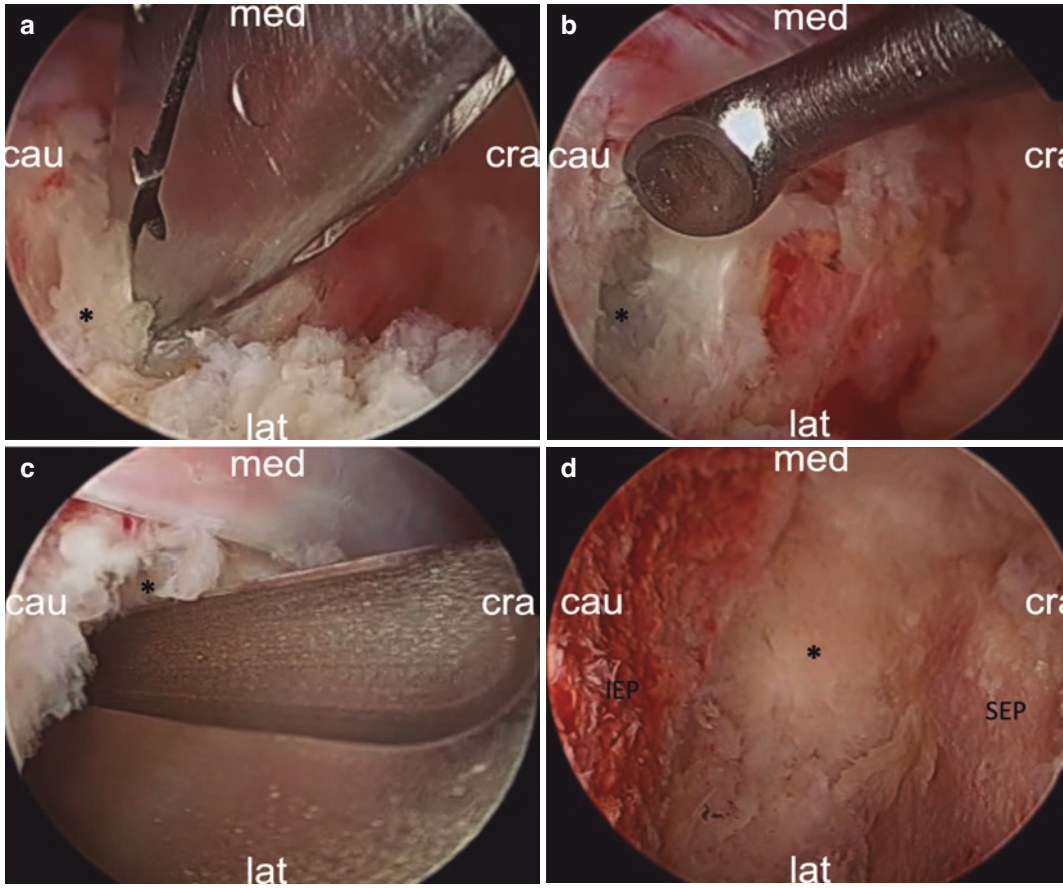


**Fig. 18.14** Unilateral biportal endoscopic discectomy and endplates preparation. (**a**, **b**, **c**) Different surgical tools used for achieving semi-total discectomy. (**d**) Intervertebral space view with the endoscope after endplate preparation. Asterisk intervertebral disc space, *SEP* superior endplate, *IEP* inferior endplate

10. *Wound Closure*

    The navigation tracker is removed, and the skin incisions are closed with a single suture. Depending on the situation, a drain could be inserted in the caudal, ipsilateral incision to evacuate residual fluid from irrigation or avoid an epidural hematoma (Fig. 18.17).

## 18.7 Discussion

There is a considerable amount of scientific literature on intraoperative navigation in spinal surgery. It is associated with high accuracy in the pedicle screws placement in various pathologies, especially in scoliosis, trauma, and degenerative. In addition to reducing the exposure time and the amount of radiation derived from intraoperative fluoroscopy for the surgical team [1, 2, 24, 40–45].

However, intraoperative navigation underestimated use is real-time guidance through the precise location of surgical instruments during the procedure. The orientation and location relationship plays an essential role in obtaining good surgical results in spinal surgery.

If, in addition to this "orientation-location" relationship achieved through intraoperative navigation, we add the clear and direct "observation" of the anatomical pathology generator through water-based endoscopy, we can perform highly precise procedures, with the lesser transgression of biomechanically essential elements in the spine, as well as a lower risk profile to neural tissues.

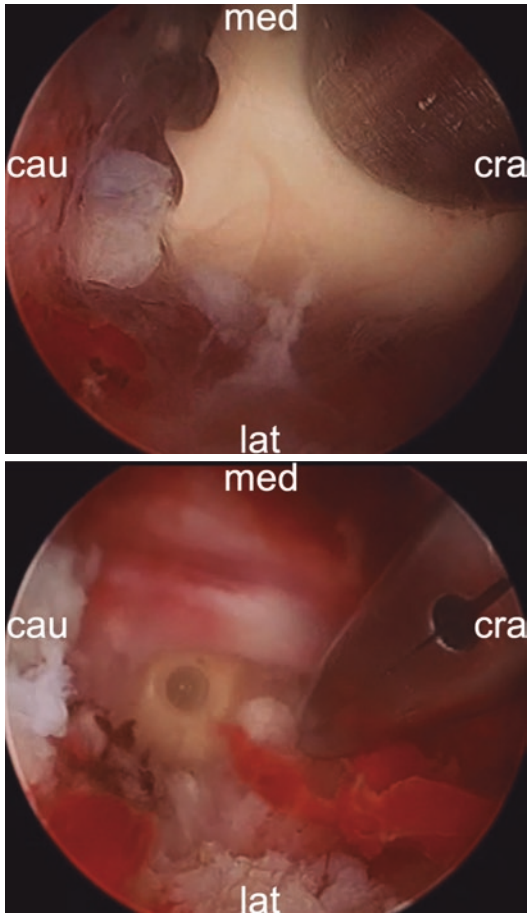


**Fig. 18.15** Cage insertion through direct endoscopic guidance

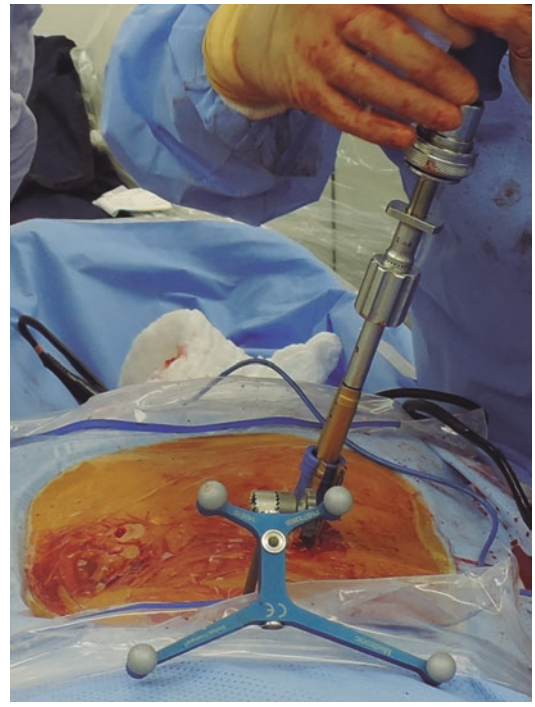

**Fig. 18.16** Navigation-guided screw placement

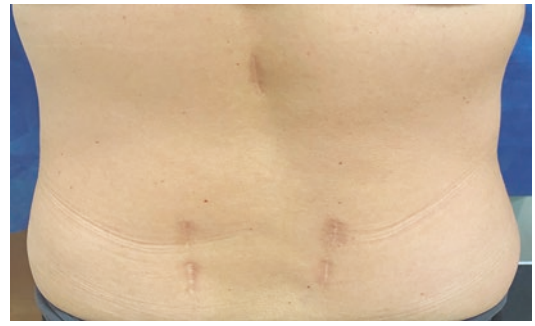

**Fig. 18.17** Postoperative wounds after 1 year

This makes sense, especially when the surgeon faces severe degenerative changes that modify the anatomical landmarks or is not familiar with them, so it is not easy to orient even through the endoscope.

Both technologies used together can provide precision, safety, and confidence, and therefore less tissue damage. Key concepts to define minimally invasive procedures in spinal surgery.

In unilateral biportal endoscopic (UBE) surgery for the spine, an arthroscope without an integrated working channel is used as a means of vision. It is a water-based technique, similar to uniportal endoscopic surgery. The angulation of the working lenses varies from 0° to 30°. They provide clear visibility similar to that obtained by endoscopes specifically designed for uniportal spine surgery [54].

The biportal technique consists of two ports placed, one for the endoscope and the other for the working instruments. Both ports are joined at the desired target through triangulation. This confluence allows a continuous irrigation system.

The technique has been widely used for various pathologies such as lumbar disc herniations and lumbar spinal stenosis. The results achieved

are similar to those obtained through microsurgical procedures in terms of decompression of the neuronal elements [56, 57].

Other associated advantages have been reported, such as facet joint preservation, less injury to the paravertebral muscles, short hospital stays, decreased intraoperative bleeding, and a quick return to daily activities [55–57].

The TLIF has evolved since the first report by Harms et al. [15]. The clear visualization offered by the endoscope of the previously planned target through intraoperative spinal navigation could be another step in the evolution of TLIF and could be called UBE-TLIF under intraoperative spinal navigation.

The following are the most notable advantages of the UBE-TLIF observed: (A) The articular facet was located utilizing navigation. Therefore, the planning of the approach was fast and straightforward. (B) The same structure located and seen in intraoperative CT images was immediately later recognized by endoscopy. (C) The limits of bone decompression and orientation during ipsilateral, central, or contralateral neural decompression were feasible, supported by intraoperative navigation and recognition of anatomical structures with the endoscope (Fig. 18.18).

Recently a meta-analysis on the results and complications of endoscopic lumbar transforaminal fusion was published. The authors report a significant improvement in the ODI and VAS scores for the leg and back. Complications associated with endoscopic TLIF were postoperative hematoma, dural tear, infection, transient nerve palsy, injury to the anterior longitudinal ligament, implant loosening, cage subsidence, cage migration, and endplate violation, with a presentation range of 0–28.6% depending on the series, and with most of these complications having a lower impact on the lives of the reported patients, treated by conservative measures [53].

We consider that the safety profile could improve if, in addition to direct observation obtained through the endoscope, we add prior planning and extensive knowledge of the pathological anatomy through intraoperative spinal navigation, which will grant more significant guidance during surgery.

The limitations associated with biportal transforaminal endoscopic fusion and in general with any endoscopic fusion procedure to date are the limited indications, a steep learning curve, limited interbody fusion, and exposure to excessive radiation [13]. However, through technological advancement, new technique reports, these limitations will be overcome.

This chapter fulfills the objective of providing a modification through intraoperative navigation and water-based spinal biportal endoscopy to overcome in a certain sense these limitations exposed concerning endoscopic TLIF.

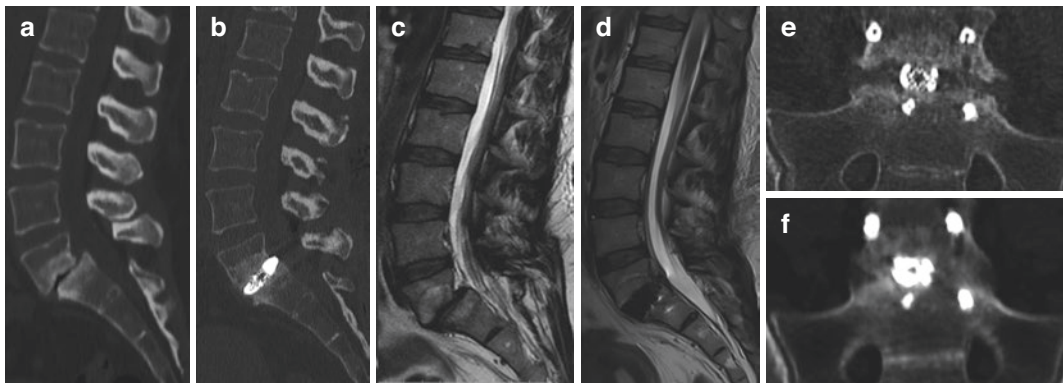


**Fig. 18.18** Demonstrative pictures regarding L5–S1 UBE-TLIF. (**a**) A L5–S1 spondylolisthesis grade 1 with endplates swelling is observed in the sagittal view of the lumbar CT. (**b**) First-week postoperative lumbar CT on a sagittal view. The interbody device was placed at L5–S1. (**c**) Sagittal view of preoperative MRI. (**d**) First-week postoperative MRI with the spondylolisthesis reduced. (**e**) Coronal view of the first-week lumbar CT. (**f**) Solid bone fusion at L5–S1 is shown in the 12-mos lumbar CT

## 18.8 Conclusions

Intraoperative CT-based navigation with the O-arm system provides the UBE-TLIF procedure spatial information for preoperative planning, orientation, and safety. The early experience with both technologies together has demonstrated acceptable clinical outcomes [36]. Extensive bone decompression and endplate preparation can be reached accurately with the UBE-TLIF assisted by intraoperative spinal navigation.

## References


1. Boon Tow BP, Yue WM, Srivastava A, et al. Does navigation improve accuracy of placement of pedicle screws in single-level lumbar degenerative spondylolisthesis?: a comparison between free-hand and three-dimensional O-arm navigation techniques. J Spinal Disord Tech. 2015;28(8):E472–7. https://doi.org/10.1097/BSD.0b013e3182a9435e.
2. Parker SL, McGirt MJ, Farber SH, et al. Accuracy of free-hand pedicle screws in the thoracic and lumbar spine: analysis of 6816 consecutive screws. Neurosurgery. 2011;68(1):170–8. https://doi.org/10.1227/NEU.0b013e3181fdfaf4.
3. Mayer HM, Brock M. Percutaneous endoscopic discectomy: surgical technique and preliminary results compared to microsurgical discectomy. J Neurosurg. 1993;78(2):216–25. https://doi.org/10.3171/jns.1993.78.2.0216.
4. Hermantin FU, Peters T, Quartararo L, Kambin P. A prospective, randomized study comparing the results of open discectomy with those of video-assisted arthroscopic microdiscectomy. J Bone Joint Surg Am. 1999;81(7):958–65. https://doi.org/10.2106/00004623-199907000-00008.
5. Hoogland T, Schubert M, Miklitz B, Ramirez A. Transforaminal posterolateral endoscopic discectomy with or without the combination of a low-dose chymopapain: a prospective randomized study in 280 consecutive cases. Spine (Phila Pa 1976). 2006;31(24):E890–7. https://doi.org/10.1097/01.brs.0000245955.22358.3a.
6. Ruetten S, Komp M, Merk H, Godolias G. Full-endoscopic interlaminar and transforaminal lumbar discectomy versus conventional microsurgical technique: a prospective, randomized, controlled study. Spine (Phila Pa 1976). 2008;33(9):931–9. https://doi.org/10.1097/BRS.0b013e31816c8af7.
7. Nellensteijn J, Ostelo R, Bartels R, Peul W, van Royen B, van Tulder M. Transforaminal endoscopic surgery for symptomatic lumbar disc herniations: a systematic review of the literature. Eur Spine J. 2010;19(2):181–204. https://doi.org/10.1007/s00586-009-1155-x.
8. Nellensteijn J, Ostelo R, Bartels R, Peul W, van Royen B, van Tulder M. Transforaminal endoscopic surgery for lumbar stenosis: a systematic review. Eur Spine J. 2010;19(6):879–86. https://doi.org/10.1007/s00586-009-1272-6.
9. Cong L, Zhu Y, Tu G. A meta-analysis of endoscopic discectomy versus open discectomy for symptomatic lumbar disk herniation. Eur Spine J. 2016;25(1):134–43. https://doi.org/10.1007/s00586-015-3776-6.
10. Li XC, Zhong CF, Deng GB, Liang RW, Huang CM. Full-endoscopic procedures versus traditional discectomy surgery for discectomy: a systematic review and meta-analysis of current global clinical trials. Pain Physician. 2016;19(3):103–18.
11. Ruan W, Feng F, Liu Z, Xie J, Cai L, Ping A. Comparison of percutaneous endoscopic lumbar discectomy versus open lumbar microdiscectomy for lumbar disc herniation: a meta-analysis. Int J Surg. 2016;31:86–92. https://doi.org/10.1016/j.ijsu.2016.05.061.
12. Kim M, Kim HS, Oh SW, et al. Evolution of spinal endoscopic surgery. Neurospine. 2019;16(1):6–14. https://doi.org/10.14245/ns.1836322.161.
13. Ahn Y, Youn MS, Heo DH. Endoscopic transforaminal lumbar interbody fusion: a comprehensive review. Expert Rev Med Devices. 2019;16(5):373–80. https://doi.org/10.1080/17434440.2019.1610388.
14. Heo DH, Hong YH, Lee DC, Chung HJ, Park CK. Technique of biportal endoscopic transforaminal lumbar interbody fusion. Neurospine. 2020;17(Suppl 1):S129–37. https://doi.org/10.14245/ns.2040178.089.
15. Harms JG, Jeszenszky D. Die posteriore, lumbale, interkorporelle fusion in unilateraler transforaminaler Technik. Oper Orthop Traumatol. 1998;10(2):90–102. https://doi.org/10.1007/s00064-006-0112-7.
16. Lertudomphonwanit T, Keorochana G, Kraiwattanapong C, Chanplakorn P, Leelapattana P, Wajanavisit W. Anatomic considerations of intervertebral disc perspective in lumbar posterolateral approach via Kambin's triangle: cadaveric study. Asian Spine J. 2016;10(5):821–7. https://doi.org/10.4184/asj.2016.10.5.821.
17. Khan NR, Clark AJ, Lee SL, Venable GT, Rossi NB, Foley KT. Surgical outcomes for minimally invasive vs open transforaminal lumbar interbody fusion: an updated systematic review and meta-analysis. Neurosurgery. 2015;77(6):847–74. https://doi.org/10.1227/NEU.0000000000000913.
18. Schwender JD, Holly LT, Rouben DP, Foley KT. Minimally invasive transforaminal lumbar interbody fusion (TLIF): technical feasibility and initial results. J Spinal Disord Tech. 2005;18(Suppl):S1–6. https://doi.org/10.1097/01.bsd.0000132291.50455.d0.
19. Rosenberg WS, Mummaneni PV. Transforaminal lumbar interbody fusion: technique, complications, and early results. Neurosurgery. 2001;48(3):569–75. https://doi.org/10.1097/00006123-200103000-00022.
20. Kim MC, Park JU, Kim WC, et al. Can unilateral-approach minimally invasive transforaminal lumbar interbody fusion attain indirect contralateral decom-

pression? A preliminary report of 66 MRI analysis. Eur Spine J. 2014;23(5):1144–9. https://doi.org/10.1007/s00586-014-3192-3.
21. Rothrock RJ, McNeill IT, Yaeger K, Oermann EK, Cho SK, Caridi JM. Lumbar lordosis correction with interbody fusion: systematic literature review and analysis. World Neurosurg. 2018;118:21–31. https://doi.org/10.1016/j.wneu.2018.06.216.
22. Osman SG. Endoscopic transforaminal decompression, interbody fusion, and percutaneous pedicle screw implantation of the lumbar spine: a case series report. Int J Spine Surg. 2012;6:157–66. https://doi.org/10.1016/j.ijsp.2012.04.001.
23. Tian W, Xu YF, Liu B, et al. Computer-assisted minimally invasive transforaminal lumbar interbody fusion may be better than open surgery for treating degenerative lumbar disease. Clin Spine Surg. 2017;30(6):237–42. https://doi.org/10.1097/BSD.0000000000000165.
24. Xiao R, Miller JA, Sabharwal NC, et al. Clinical outcomes following spinal fusion using an intraoperative computed tomographic 3D imaging system. J Neurosurg Spine. 2017;26(5):628–37. https://doi.org/10.3171/2016.10.SPINE16373.
25. Wang Y, Hu Y, Liu H, Li C, Li H, Yi X. Navigation makes transforaminal lumbar interbody fusion less invasive. Orthopedics. 2016;39(5):e857–62. https://doi.org/10.3928/01477447-20160517-01.
26. Wang MY, Grossman J. Endoscopic minimally invasive transforaminal interbody fusion without general anesthesia: initial clinical experience with 1-year follow-up. Neurosurg Focus. 2016;40(2):E13. https://doi.org/10.3171/2015.11.FOCUS15435.
27. Morgenstern C, Yue JJ, Morgenstern R. Full percutaneous transforaminal lumbar interbody fusion using the facet-sparing, trans-kambin approach. Clin Spine Surg. 2020;33(1):40–5. https://doi.org/10.1097/BSD.0000000000000827.
28. Lewandrowski KU, Ransom NA, Ramírez León JF, Yeung A. The concept for a standalone lordotic endoscopic wedge lumbar interbody fusion: the LEW-LIF. Neurospine. 2019;16(1):82–95. https://doi.org/10.14245/ns.1938046.023.
29. Jin M, Zhang J, Shao H, Liu J, Huang Y. Percutaneous transforaminal endoscopic lumbar interbody fusion for degenerative lumbar diseases: a consecutive case series with mean 2-year follow-up. Pain Physician. 2020;23(2):165–74.
30. Ao S, Zheng W, Wu J, et al. Comparison of preliminary clinical outcomes between percutaneous endoscopic and minimally invasive transforaminal lumbar interbody fusion for lumbar degenerative diseases in a tertiary hospital: Is percutaneous endoscopic procedure superior to MIS-TLIF? A prospective cohort study. Int J Surg. 2020;76:136–43. https://doi.org/10.1016/j.ijsu.2020.02.043.
31. Wu J, Liu H, Ao S, et al. Percutaneous endoscopic lumbar interbody fusion: technical note and preliminary clinical experience with 2-year follow-up. Biomed Res Int. 2018;2018:5806037. https://doi.org/10.1155/2018/5806037.
32. Wu PH, Kim HS, Lee YJ, et al. Uniportal full endoscopic posterolateral transforaminal lumbar interbody fusion with endoscopic disc drilling preparation technique for symptomatic foraminal stenosis secondary to severe collapsed disc space: a clinical and computer tomographic study with technical note. Brain Sci. 2020;10(6):373. https://doi.org/10.3390/brainsci10060373.
33. Yang J, Liu C, Hai Y, et al. Percutaneous endoscopic transforaminal lumbar interbody fusion for the treatment of lumbar spinal stenosis: preliminary report of seven cases with 12-month follow-up. Biomed Res Int. 2019;2019:3091459. https://doi.org/10.1155/2019/3091459.
34. Kolcun JPG, Brusko GD, Basil GW, Epstein R, Wang MY. Endoscopic transforaminal lumbar interbody fusion without general anesthesia: operative and clinical outcomes in 100 consecutive patients with a minimum 1-year follow-up. Neurosurg Focus. 2019;46(4):E14. https://doi.org/10.3171/2018.12.FOCUS18701.
35. Heo DH, Park CK. Clinical results of percutaneous biportal endoscopic lumbar interbody fusion with application of enhanced recovery after surgery. Neurosurg Focus. 2019;46(4):E18. https://doi.org/10.3171/2019.1.FOCUS18695.
36. Quillo-Olvera J, Quillo-Reséndiz J, Quillo-Olvera D, Barrera-Arreola M, Kim JS. Ten-step biportal endoscopic transforaminal lumbar interbody fusion under computed tomography-based intraoperative navigation: technical report and preliminary outcomes in Mexico. Oper Neurosurg (Hagerstown). 2020;19(5):608–18. https://doi.org/10.1093/ons/opaa226.
37. Heo DH, Son SK, Eum JH, Park CK. Fully endoscopic lumbar interbody fusion using a percutaneous unilateral biportal endoscopic technique: technical note and preliminary clinical results. Neurosurg Focus. 2017;43(2):E8. https://doi.org/10.3171/2017.5.FOCUS17146.
38. Kim JE, Yoo HS, Choi DJ, Park EJ, Jee SM. Comparison of minimal invasive versus biportal endoscopic transforaminal lumbar interbody fusion for single-level lumbar disease. Clin Spine Surg. 2021;34(2):E64–71. https://doi.org/10.1097/BSD.0000000000001024.
39. Park MK, Park SA, Son SK, Park WW, Choi SH. Correction to: clinical and radiological outcomes of unilateral biportal endoscopic lumbar interbody fusion (ULIF) compared with conventional posterior lumbar interbody fusion (PLIF): 1-year follow-up. Neurosurg Rev. 2019;42(3):763. https://doi.org/10.1007/s10143-019-01131-2.
40. Dusad T, Kundnani V, Dutta S, Patel A, Mehta G, Singh M. Comparative prospective study reporting intraoperative parameters, pedicle screw perforation, and radiation exposure in navigation-guided versus non-navigated fluoroscopy-assisted minimal invasive transforaminal lumbar interbody fusion. Asian Spine J. 2018;12(2):309–16. https://doi.org/10.4184/asj.2018.12.2.309.

41. Kleck CJ, Johnson C, Akiyama M, Burger EL, Cain CJ, Patel VV. One-step minimally invasive pedicle screw instrumentation using O-arm and stealth navigation. Clin Spine Surg. 2018;31(5):197–202. https://doi.org/10.1097/BSD.0000000000000616.
42. Liu Z, Jin M, Qiu Y, Yan H, Han X, Zhu Z. The superiority of intraoperative o-arm navigation-assisted surgery in instrumenting extremely small thoracic pedicles of adolescent idiopathic scoliosis: a case-control study. Medicine (Baltimore). 2016;95(18):e3581. https://doi.org/10.1097/MD.0000000000003581.
43. Pitteloud N, Gamulin A, Barea C, Damet J, Racloz G, Sans-Merce M. Radiation exposure using the O-arm® surgical imaging system. Eur Spine J. 2017;26(3):651–7. https://doi.org/10.1007/s00586-016-4773-0.
44. Tajsic T, Patel K, Farmer R, Mannion RJ, Trivedi RA. Spinal navigation for minimally invasive thoracic and lumbosacral spine fixation: implications for radiation exposure, operative time, and accuracy of pedicle screw placement. Eur Spine J. 2018;27(8):1918–24. https://doi.org/10.1007/s00586-018-5587-z.
45. Chan A, Parent E, Narvacan K, San C, Lou E. Intraoperative image guidance compared with free-hand methods in adolescent idiopathic scoliosis posterior spinal surgery: a systematic review on screw-related complications and breach rates. Spine J. 2017;17(9):1215–29. https://doi.org/10.1016/j.spinee.2017.04.001.
46. Nomura K, Yoshida M. Microendoscopic decompression surgery for lumbar spinal canal stenosis via the paramedian approach: preliminary results. Global Spine J. 2012;2(2):87–94. https://doi.org/10.1055/s-0032-1319774.
47. Choi CM. Biportal endoscopic spine surgery (BESS): considering merits and pitfalls. J Spine Surg. 2020;6(2):457–65. https://doi.org/10.21037/jss.2019.09.29.
48. Kim JS, Lee SH, Moon KH, Lee HY. Surgical results of the oblique paraspinal approach in upper lumbar disc herniation and thoracolumbar junction. Neurosurgery. 2009;65(1):95–9. https://doi.org/10.1227/01.NEU.0000348299.89232.C2.
49. Ahn JS, Lee HJ, Choi DJ, Lee KY, Hwang SJ. Extraforaminal approach of biportal endoscopic spinal surgery: a new endoscopic technique for transforaminal decompression and discectomy. J Neurosurg Spine. 2018;28(5):492–8. https://doi.org/10.3171/2017.8.SPINE17771.
50. Choi CM, Chung JT, Lee SJ, Choi DJ. How I do it? Biportal endoscopic spinal surgery (BESS) for treatment of lumbar spinal stenosis. Acta Neurochir. 2016;158(3):459–63. https://doi.org/10.1007/s00701-015-2670-7.
51. Kim JE, Choi DJ, Park EJ. Clinical and radiological outcomes of foraminal decompression using unilateral biportal endoscopic spine surgery for lumbar foraminal stenosis. Clin Orthop Surg. 2018;10(4):439–47. https://doi.org/10.4055/cios.2018.10.4.439.
52. Quillo-Olvera J, Soriano-Solis S, Ortiz-Leyva RU, Gutiérrez-Partida CF, Rodríguez-García M, Soriano-Sánchez JA. Microsurgical landmarks in minimally invasive transforaminal lumbar interbody fusion. Coluna/Columna. 2015;14(4):317–9. https://doi.org/10.1590/S1808-185120151404152838.
53. Heo DH, Lee DC, Kim HS, Park CK, Chung H. Clinical results and complications of endoscopic lumbar interbody fusion for lumbar degenerative disease: a meta-analysis. World Neurosurg. 2021;145:396–404. https://doi.org/10.1016/j.wneu.2020.10.033.
54. Hwa Eum J, Hwa Heo D, Son SK, Park CK. Percutaneous biportal endoscopic decompression for lumbar spinal stenosis: a technical note and preliminary clinical results. J Neurosurg Spine. 2016;24(4):602–7. https://doi.org/10.3171/2015.7.SPINE15304.
55. Park SM, Kim GU, Kim HJ, et al. Is the use of a unilateral biportal endoscopic approach associated with rapid recovery after lumbar decompressive laminectomy? A preliminary analysis of a prospective randomized controlled trial. World Neurosurg. 2019;128:e709–18. https://doi.org/10.1016/j.wneu.2019.04.240.
56. Heo DH, Lee DC, Park CK. Comparative analysis of three types of minimally invasive decompressive surgery for lumbar central stenosis: biportal endoscopy, uniportal endoscopy, and microsurgery. Neurosurg Focus. 2019;46(5):E9. https://doi.org/10.3171/2019.2.FOCUS197.
57. Choi KC, Shim HK, Hwang JS, et al. Comparison of surgical invasiveness between microdiscectomy and 3 different endoscopic discectomy techniques for lumbar disc herniation. World Neurosurg. 2018;116:e750–8. https://doi.org/10.1016/j.wneu.2018.05.085.

# 19 O-Arm Navigation-Guided Endoscopic Oblique Lumbar Interbody Fusion

Yadhu K. Lokanath, Yanting Liu, Jin-Sung Kim, and Claudia A. Covarrubias

## Abbreviations

| | |
|---|---|
| ALL | Anterior longitudinal ligament |
| AP | Anterior posterior |
| CT | Computed tomography |
| MRI | Magnetic resonance imaging |
| OLIF | Oblique lumbar interbody fusion |
| PSIS | Posterior superior iliac spine |

## 19.1 Introduction

Interbody fusion is accepted as the standard of care in treating various conditions of the lumbar spine and can be accessed in different ways. The ideal approach should be the least invasive with added patient satisfaction rates and good clinical outcomes. The lateral approach has emerged with its potential benefits.

The strategy behind the oblique approach, which is a variant of the lateral approach, is to preserve the posterior ligamentous architecture and minimize the injury to muscle and soft tissue. The oblique lumbar interbody fusion (OLIF) requires a working zone through an oblique blind corridor that runs through the retroperitoneal space between the psoas and major blood vessels (Fig. 19.1).

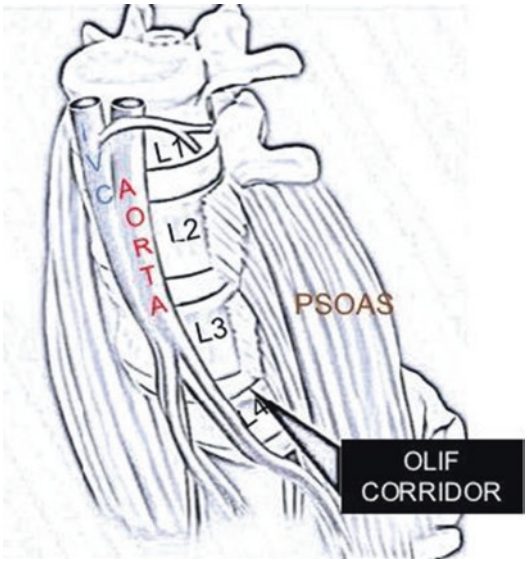


**Fig. 19.1** Boundaries of the OLIF corridor

Y. K. Lokanath
Department of Neurosurgery, Aster RV Hospital, JP Nagar, Bangalore, Karnataka, India

Y. Liu
Department of Neurosurgery, Seoul St Mary's Hospital, The Catholic University of Korea, Seoul, Korea

J.-S. Kim (✉)
Department of Neurosurgery, Seoul St Mary's Hospital, The Catholic University of Korea, College of Medicine, Seoul, Korea (Republic of)

C. A. Covarrubias
Department of Experimental Surgery, McGill University, Montreal, QC, Canada
e-mail: claudia.covarrubias@mail.mcgill.ca



J.-S. Kim et al. (eds.), *Technical Advances in Minimally Invasive Spine Surgery*,
https://doi.org/10.1007/978-981-19-0175-1_19

One of the limitations in lateral access surgery is direct visualization and orientation of the surrounding anatomy, which obviates the need for fluoroscopy for localization and thus adding the risk of radiation exposure. This limitation can be avoided by thorough knowledge of anatomy, intraoperative image guidance by O-arm, navigation assisstance for better delineation of intraoperative lateral anatomy, trajectory planning, and real-time depth assessment. The aforementioned principles allow the surgeon to correct for the unfamiliar oblique trajectory and to decrease radiation exposure to the operative team [1–3].

In addition, when an endoscope is added to the surgeon's armamentarium, the added advantage of accessing hidden areas and endoscope-guided endplate preparation has shown promising results. With O-arm and navigation in hand, interbody cage insertion and percutaneous screw insertion can be performed in the lateral position, limiting the operative time and allowing it to be a single-stage procedure. We describe our technique of O-arm-guided endoscopic oblique lumbar interbody fusion.

## 19.2 Indications

- OLIF can be adopted for a wide array of pathological conditions requiring interbody fusion ranging from degenerative spondylosis with instability to trauma, scoliosis, infection, and spondylolisthesis from D12 to S1.
- Extruded, migrated (inferior/superior), foraminal disc prolapse can be addressed with an endoscope without an additional posterior approach.

## 19.3 Contraindications

- High-grade spondylolisthesis (> grade 3).
- Bony lateral recess stenosis.
- Facet fusion.
- Prior history of retroperitoneal surgery.
- Lack of an operative corridor due to iliac vessel position seen on imaging (variant anatomy and transitional anatomy).

## 19.4 Operative Procedure

### 19.4.1 Preoperative Planning

Preoperative workup should include:

(1) X-ray
   - Full-length 36-inch standing film and dynamic X-rays to identify abnormal motion segment.
   - Assessment of spinal curvature and alignment.
   - Location of iliac crest and rib in relation to an index level of surgery.

(2) Magnetic resonance imaging
   - Position of anterior vasculature (aorta, inferior vena, iliac arteries, and vein) in relation to disc space of interest and its relation to the psoas muscle.
   - The oblique angle of entry and working distance between left side of common iliac artery, vein, and anterior border of the psoas muscle.
   - Size, shape of psoas, and position of the kidney.
   - Anatomical course of the ureter.
   - Anatomical abnormalities of peritoneal content.

### 19.4.2 Equipment and Instruments

- OLIF Retractor system.
- Endoscopy unit—Monitor, light source, irrigation fluid, bipolar radiofrequency probe, endoscope working sheath, beveled working cannula, and a 30-degree endoscope.
- Semi flexible/straight forceps.
- Angled hook.
- Tip control endoscopic burr.
- Surgical navigation system—Optical tracking camera, reference frame, calibration probe,

and endoscopic attachable tracker (SureTrack—Medtronics).
- An intraoperative 3D fluoroscopy or mobile computed tomography (CT) scanner.

### 19.4.3 Operative Flow

(1) Positioning—Right lateral position (Fig. 19.2).
   - Axillary roll protecting the axillary neurovascular structure.
   - Leg flexed—To relax the psoas and lumbar plexus.
   - Padding of all bony prominences.
   - The operating surgeon and scrub team should be positioned to work on the abdominal side of the patient. The assistant, C-arm, and endoscopy unit should be positioned posterior to the patient. Lastly, navigation should be positioned at the foot end.

(2) Reference frame insertion
   - Reference frame can be inserted directly on to posterior superior iliac spine (PSIS) or secured to a table-mounted clamp.
   - The ideal position for reference frame insertion is 5 cm superior, slightly lateral to the PSIS. It should be inserted into the thickest aspect of the iliac bone, so it is firmly secured, out of the surgeon and operative field. The previously mentioned set-up prevents it from being inadvertently moved during the procedure (Fig. 19.3).
   - After securing the reference frame, the O-arm is positioned to acquire the images necessary for 3D reconstruction, the latter is then registered to the navigation software.

(3) Approach
   - A routinely left-sided approach is preferred given that the right side inferior vena cava obstructs the right-sided approach angle.
   - The left-sided approach is much safer as there is a natural corridor between the aorta and the psoas muscle.

(4) Localization and incision planning
   - Under navigation guidance using navigable probe, the diseased disc level is marked, and its midportion is located.
   - The desired trajectory can be assessed with the virtual extension of the probe and a vertical or horizontal incision of the desired length is marked 5 cm from the anterior mid-portion of disc space.

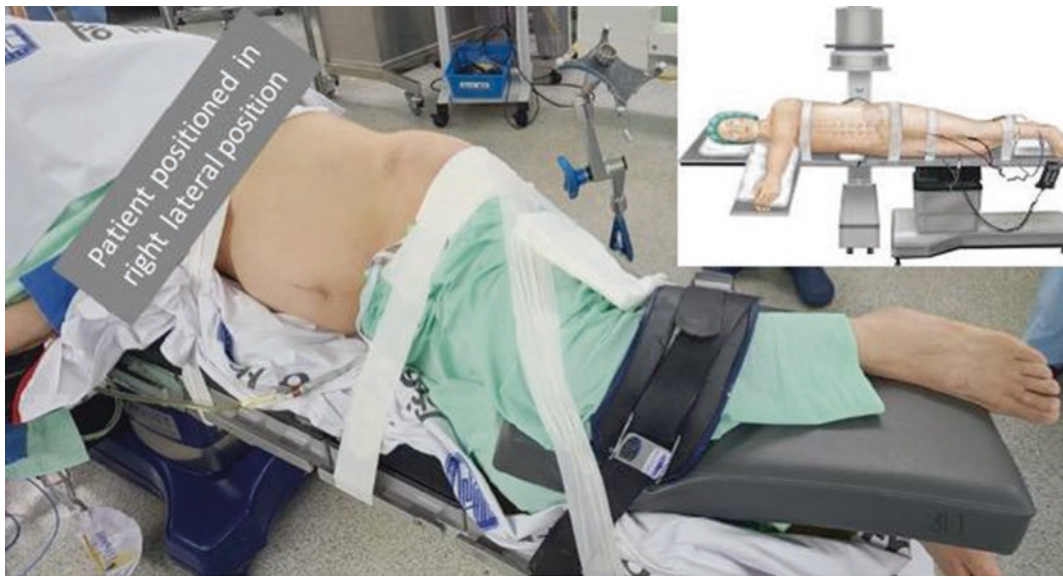


**Fig. 19.2** Patient positioning for navigated OLIF

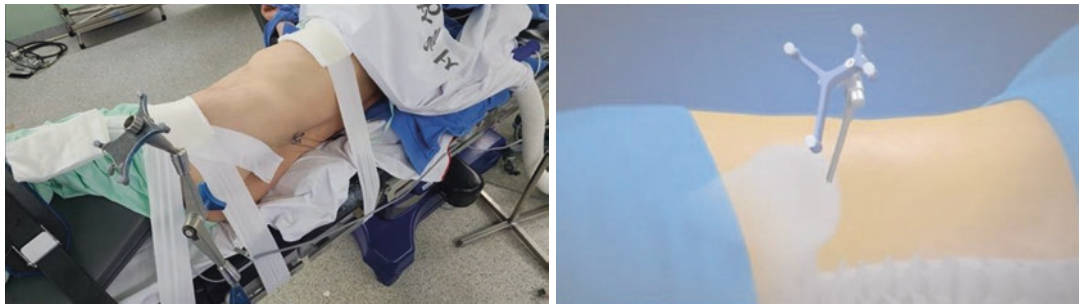

**Fig. 19.3** Placement of reference frame

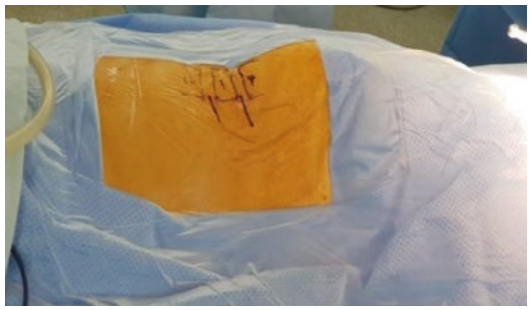

**Fig. 19.4** Level marking and planning of skin incision for a two-level case

Simultaneously, pedicle entry points for pedicle screw insertion can be marked based on the system images.

- For two-level cases, an incision is marked at the midsection of the intervening vertebral body (Fig. 19.4).

(5) Percutaneous pedicle screw insertion

- Using image guidance, pedicles are cannulated using guide wires and pedicle screws are inserted in a percutaneous manner.
- It is advisable to insert screws first prior to the insertion of the interbody cage as the latter might affect the alignment of a cranial and caudal vertebra reducing the navigational accuracy.
- Pedicle screw insertion can be performed in lateral position only.

(6) Dissection

- The dissection follows: Skin, subcutaneous tissue, and muscles (external oblique, internal oblique, and transverse abdominal muscle with its fascia). It is split parallel to the trajectories of the abdominal wall nerve roots with oblique trajectory directed towards the lumbar spine (Fig. 19.5).
- Beyond this, yellow retroperitoneal fat is identified deep in the transverse abdominal muscle.
- Using finger dissection, the retroperitoneal fat and peritoneal contents are circumferentially swept away from the posterior abdominal wall, and the index finger is used to follow and approach the disc space.
- Navigation is routinely used to verify trajectory, correct level, and anterior border of the psoas.

(7) Psoas identification

- The anterior border of the psoas muscle and diseased disc level is identified using navigation guidance. If required, the anterior border of the psoas muscle can be gently mobilized posteriorly.
- In addition to navigation aid, direct visualization may be employed in order to ensure a safe approach to the disc space free from vascular, peritoneal, and neural structures.
- Once disc space is reached, surrounding soft tissue is cleared to gain access for discectomy.

(8) Index level targeting

- After a safe retroperitoneal dissection to identify the anterior portion of the psoas, a probe (X-PAK Probe or the first dilator)

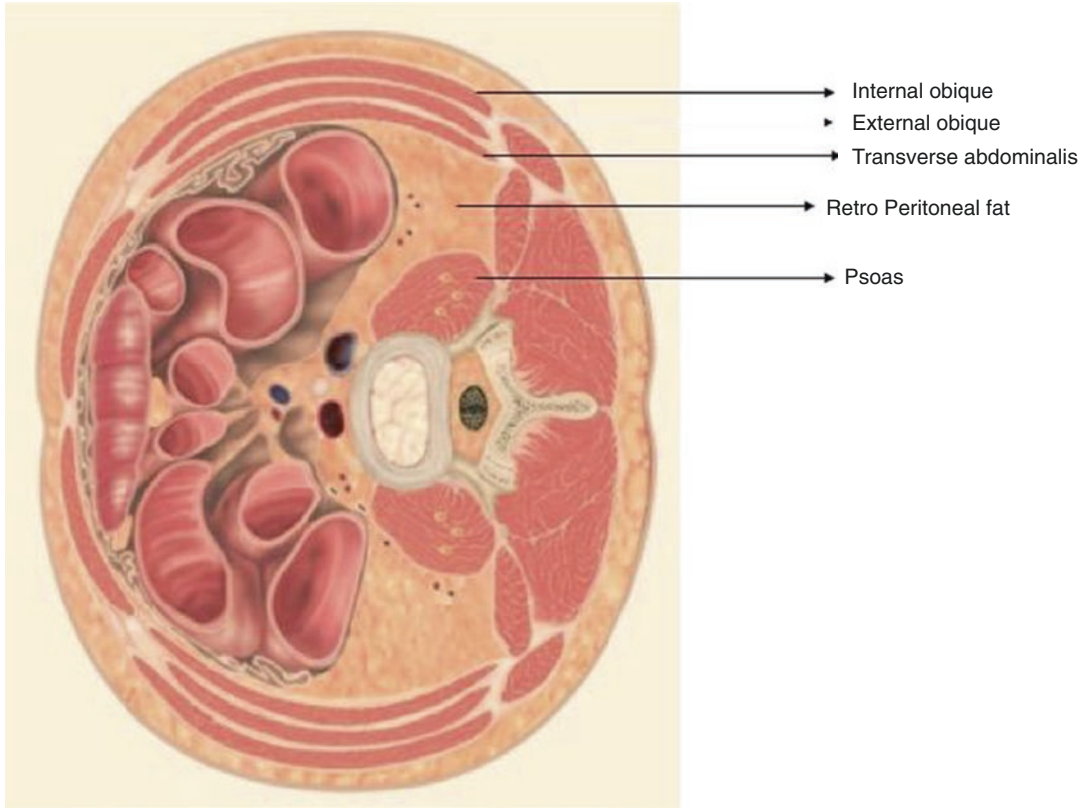


**Fig. 19.5** Layers of lateral abdominal wall

is directed down to the disc space in front or on the anterior portion of the psoas while using the finger or handheld retractors to protect the peritoneal contents and retract retroperitoneal fat (Fig. 19.6).

- Probe position is confirmed under image guidance in both axial and sagittal reconstructed system images.
- The entry point of the probe into the disc should be more anterior than the midpoint of the disc. This will not only minimize the risk of injury to the contralateral foramen due to the oblique trajectory of disc preparation instruments and cage placement, but also to the motor nerve roots as motor nerves are typically located in the posterior one-third of the psoas muscle.

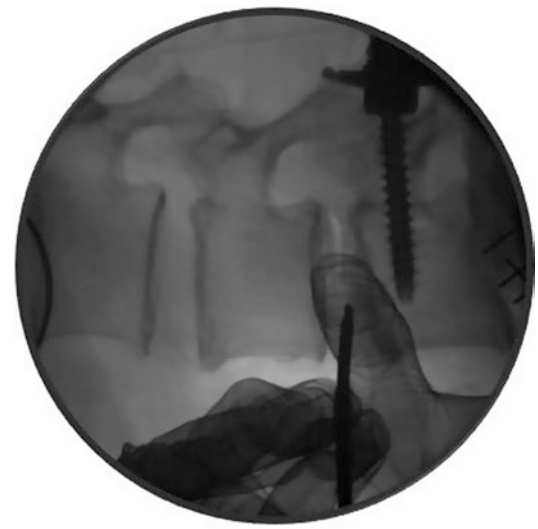

**Fig. 19.6** X–PAK probe in disc space

- A guidewire is then inserted through the probe, which guides into the desired disc space. Positioning is confirmed with fluoroscopy.

(9) Retractor placement, discectomy, and endplate preparation.
- Sequential dilatation is performed and a retractor of appropriate length is selected and placed.
- A table-mounted retractor is then inserted and locked into place, maintaining alignment of retractor blades so that the opening between them is parallel to the disc space (Fig. 19.7).
- Stability pin is inserted through the retractor to prevent displacement throughout the procedure.
- Under navigation, disc space and trajectory are confirmed, and annulotomy followed by discectomy are performed (Fig. 19.8).
- Contralateral release of annulus is then performed. It must be taken into account that the contralateral nerve root could be injured during contralateral release, so an oblique trajectory is required. This is gained by moving the hand dorsally during this maneuver, thereby avoiding injury to the foraminal area. The maneuver can be imaged in real-time using the navigation system (Fig. 19.9).
- Navigation can be used to assess the extent of discectomy and end plate preparation. Adequacy of end plate preparation can be checked intraoperatively not only with navigation but also with injection of dye into the disc space (red circle) (Fig. 19.10).

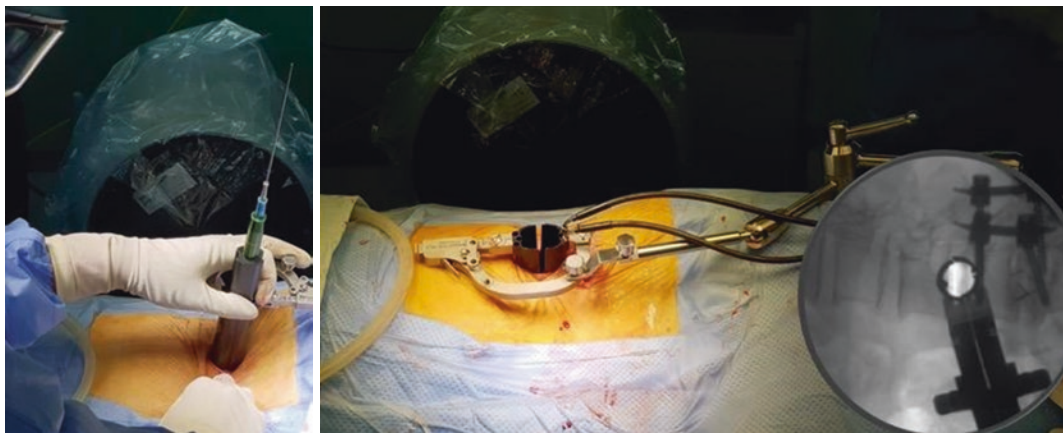

**Fig. 19.7** Sequential dilatations and placement of retractor fixed to table-mounted attachment

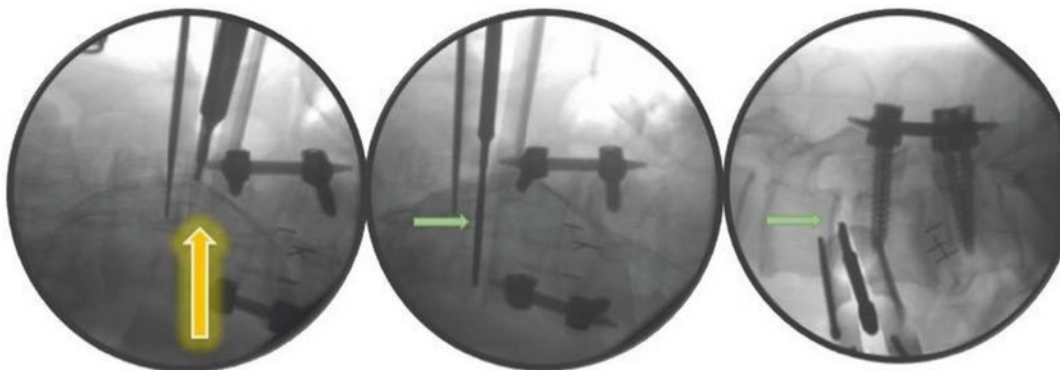

**Fig. 19.8** Annulotomy and sequential discectomy

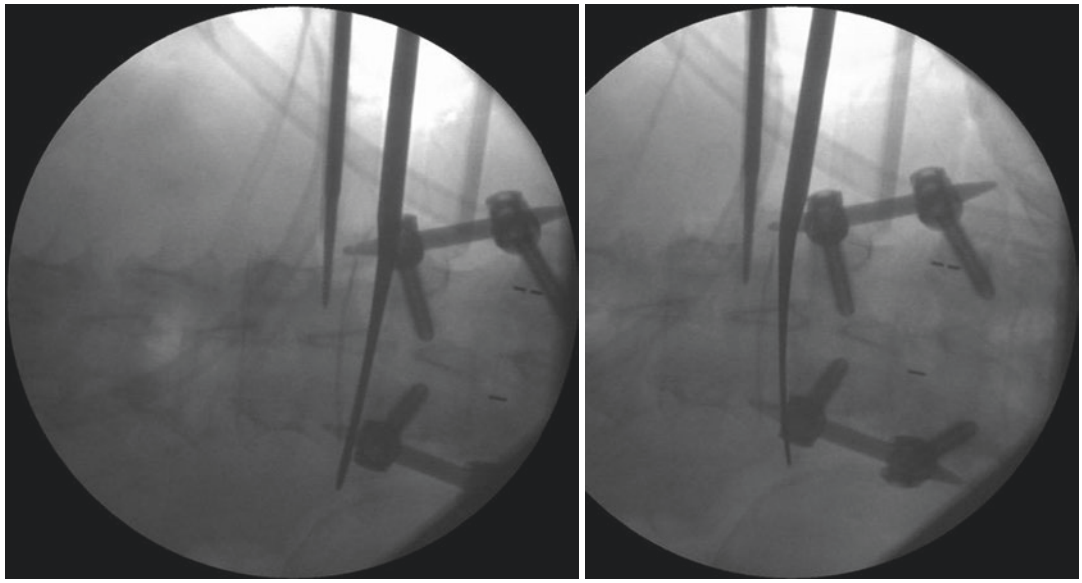

**Fig. 19.9** Fluoroscopic image showing Cobb's elevator used for contralateral release of annulus

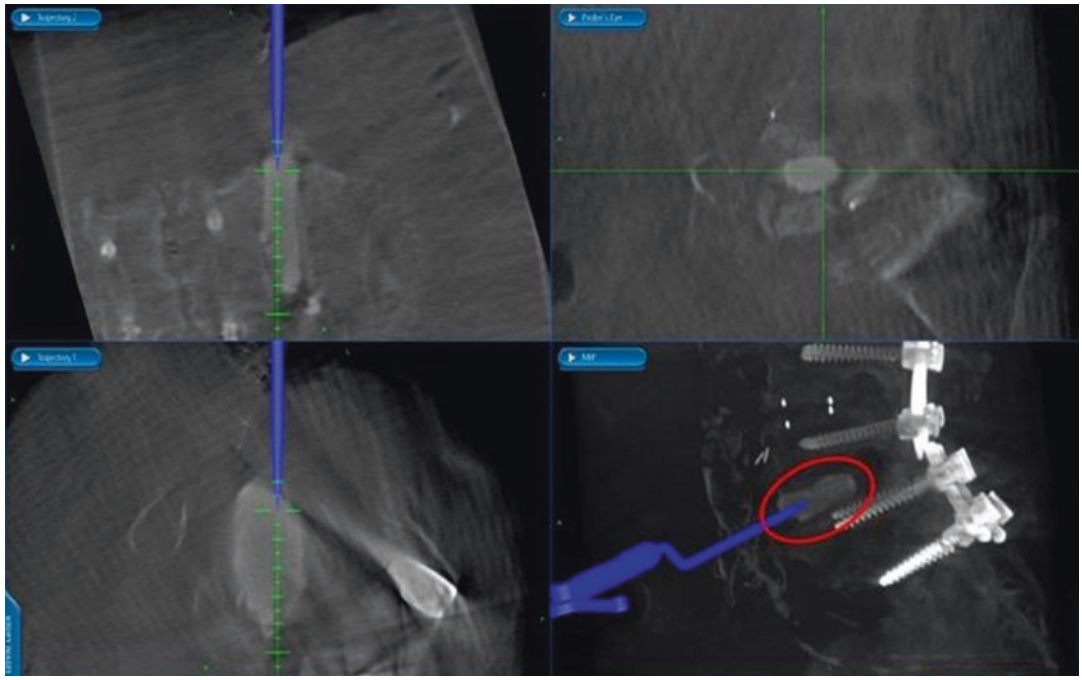

**Fig. 19.10** Intraoperative navigation assistance and use of dye to confirm adequate end plate preparation. Red circle indicated injection of dye into the disc space

- Navigated endoscope can be used to access the foraminal area (Fig. 19.11).

(10) Implant trialing and cage insertion

- After preparing the interbody area, navigated interbody cage template trials are used to assess the accurate size and lordotic angle (Fig. 19.12).
- After selecting an appropriately sized interbody cage, the interbody implant is loaded with a bone graft.

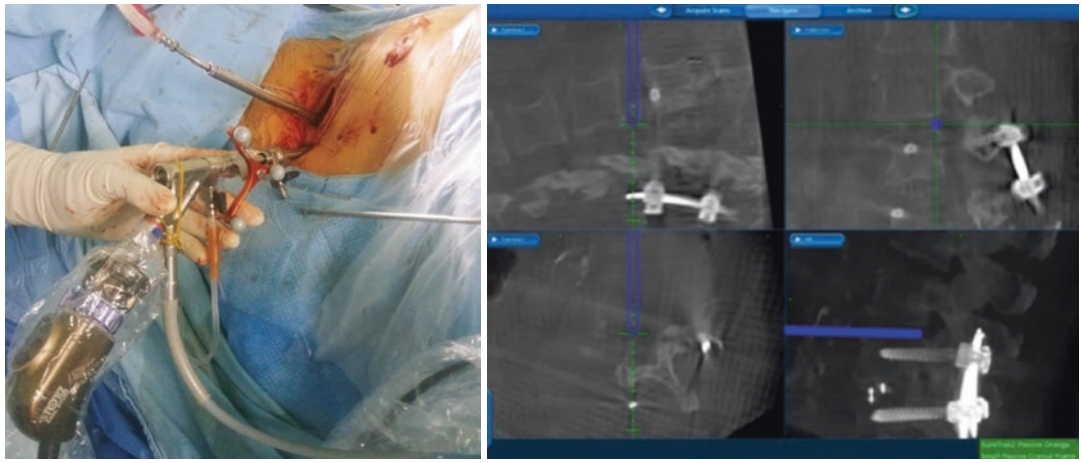

**Fig. 19.11** Combination of navigation and endoscope for discectomy

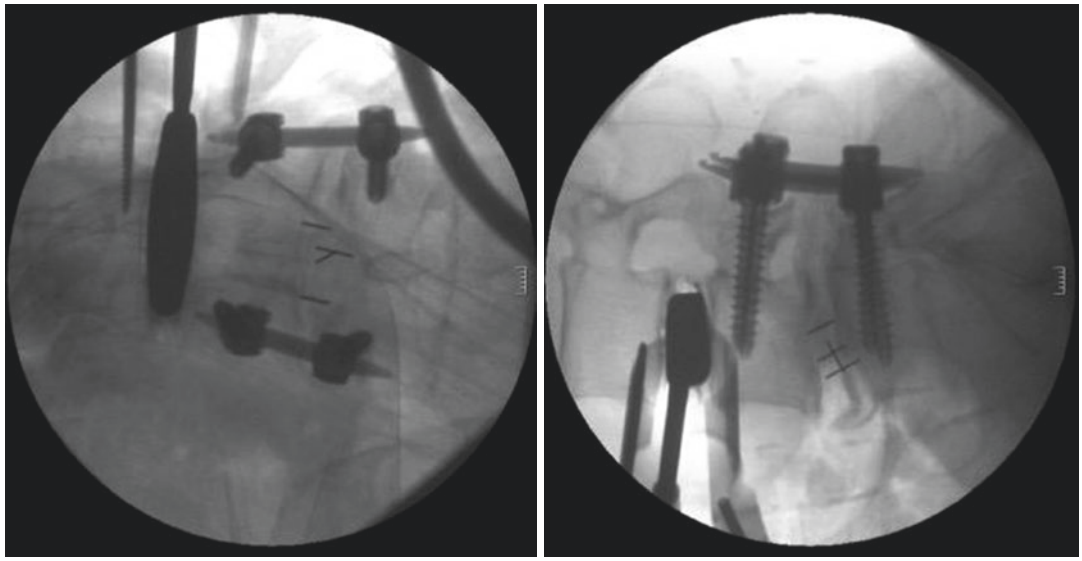

**Fig. 19.12** Fluoroscopic images showing implant trail being inserted into prepared disc space

- The cage inserter is advanced obliquely, which is then turned and placed orthogonally across the disc space.
- The placement of the cage, cage position, and trajectory can be planned and monitored using navigation guidance.
- Final confirmation of cage positioning is performed using the navigation guidance.

(11) Instrumentation
- Pedicle screws are interconnected with rods depending upon the required degree of lordosis needed.

(12) Wound closure
- Tranversalis fascia should always be closed meticulously followed by closure of muscles and fascia in a standard fashion.

### 19.4.4 Endoscope and Its Role in OLIF

(1) Can be used to visualize the path of the genitofemoral nerve on the anterior border of the psoas before docking the retractor.
(2) Can be used to visualize the disc surface before placing the retractor.

(3) A navigable endoscope can be inserted into disc space for discectomy under endoscopic guidance and can help with inspecting the amount of discectomy performed (Fig. 19.13).
(4) Can be used to remove up-/down-migrated or foraminal disc fragment and contralateral release of an anterior longitudinal ligament (ALL).
(5) Assisting in endplate preparation as well as verifying the integrity of end plates.
(6) Can be used to assess hemostasis after removal of tubular retractor.

Schonauer et al. have reported the usefulness of endoscope in extreme lateral interbody fusion [4].

## 19.5 Advantages

- OLIF is both muscle-sparing and posterior ligamentous band preserving as iatrogenic damage to the muscle is avoided.
- In revision cases, the lumbar spine can be addressed through a virgin area.
- Decreased radiation exposure to both surgeon and patient.
- Injury to nerves within the psoas muscle is reduced in comparison to transpsoas approach. Before docking the retractor, the pathway of neural structure can be endoscopically visualized, thereby further reducing the risk of neural injury.
- Although intraoperative image guidance (O-arm + navigation) can be used for a single level, 3D navigation becomes more useful when operating on deformed spine and multilevel cases. Only one intraoperative image acquisition is needed for 4 levels [5] reducing fluoroscopic exposure
- Xi Z et al. reported a 94.86% accuracy rate for cage placement using navigated OLIF [6], which usually requires a series of X-ray in non-navigated cases.
- Correction of both coronal and sagittal alignment is superior in OLIF.

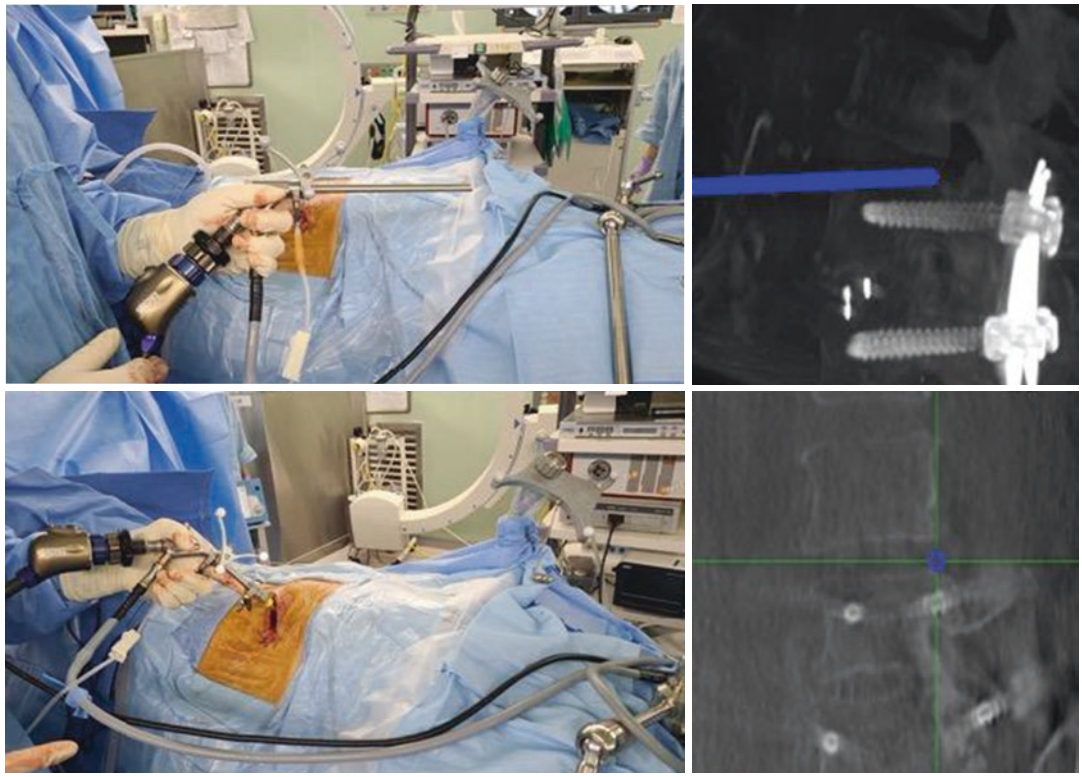

**Fig. 19.13** Sure track navigable device attached to endoscope

## 19.6 Disadvantages

- Regarding approach, it is always necessary to understand lateral oblique anatomical access and related orientation. To facilitate this and the orthogonal maneuver, there is an increased use of radiation. The use of intraoperative imaging with navigation can overcome these specific disadvantages.
- The angle of approach can become obstinate as surgeons must sustain an oblique angle to avoid injuring surrounding nerves, especially the contralateral nerve root. Navigation can diminish this risk through real-time visualization of angle and depth of the approach [7].
- Risk of injury to major vessels, ureter, and bowel in small percentages of cases due to anatomical variation.
- Inaccuracy of navigation may lead to malpositioning of interbody cage and screws.

## 19.7 Discussion

The lateral approach, referred to as OLIF or prepsoas or ante-psoas or retroperitoneal approach, has undergone tremendous changes with recent innovations in imaging and instrumentation technology.

With respect to approch realted complications, some surgeons favor the -pre-psoas approach as it offers the same advantages of the -trans-psoas approach. Additionally, the risk of injury to the psoas muscle and lumbar plexus is nullified as OLIF is performed anterior to the psoas.

Accessing through a virgin corridor in revision cases along with indirect foraminal decompression and the possibility to correct both sagittal and coronal imbalance, which is an added advantage [8]. Other benefits include low risk of injury to the dural sac and unneeded facetectomy, laminectomy, or stripping of paraspinal muscle, hence decreasing the incidence of postoperative pain.

Use of endoscopes into the operative field offers improved visualization of the deep surgical field, decreasing damage to lumbar plexus and vertebral endplates.

As the lumbar spine is approached anterior to the psoas, the technique avoids dissecting the psoas thereby decreasing chance of iatrogenic damage to the psoas muscle and to lumbar plexus [9]. Moreover, a meta-analysis showed that with the transpsoas lateral approach there is a chance of 9.4% temporary and 2.5% probability of permanent neurological deficits [10] that can lead to sensory or motor changes to the thigh and leg [11–14].

Orthogonal orientation in OLIF necessitates the need for radiation, leading to increased radiation usage. However, the use of navigation helps in reducing radiation exposure [15].

Although navigation is a boon to surgeons, hardware and software systems failure may cause added inaccuracy. Movement of reference frame and changes in alignment from surgical manipulation can also lead to inaccuracy as the orthogonal maneuver can have considerable torque on the patient and retractor system if not appropriately performed. Finally, there are added anatomical constraints due to bulky psoas, rib cage, and iliac crest pushing the retractor system, which might affect the surgical flow and potentially increase operative time [16–19].

When comparing intraoperative CT-navigated OLIF versus conventional OLIF with 2D fluoroscopy, Zhang et al. reported significantly lower radiation exposure to both the patient and the surgeon in the CT-navigated OLIF group. However, operative time was slightly longer in the navigated group but was not deemed statistically significant [20].

## 19.8 Conclusion

Endoscopic navigated OLIF technique might be considered an adjunct in cases that require both direct and indirect decompression, offering the surgeon additional visual information. Navigation is therefore a safe alternative to fluoroscopy for OLIF. Navigation obviates the need for intraoperative fluoroscopy during the procedure, aids in planning a proper trajectory, and reduces radiation exposure to the patient and operative team.

## 19.9 Case Illustration

A 71-year-old female presented with long-standing leg and axial back pain affecting her daily activities. Patient had a history of posterior lumbar interbody fusion at L4-L5,14 years ago with L3 and L4 laminectomy 3 years back at an outside hospital. She had intractable leg pain and had failed conservative therapy. X-ray lumbosacral spine showed L3-L4 grade 2 spondylolisthesis with collapsed disc space and foraminal narrowing as well as an interbody cage at L4-L5 with pedicle screw in situ (Fig. 19.14). MRI showed L3-L4 grade 2 spondylolisthesis with pseudo disc bulge, bilateral foraminal and lateral recess narrowing with CT showing L3-L4 grade 2 spondylolisthesis with vacuum disc phenomenon (Fig. 19.15). Patient underwent L3-L4 OLIF navigated endoscopic OLIF with pedicle screw fixation at L2, L3, L4, and removal of pedicle screw at L5 (Fig. 19.16). Postoperative image demonstrated L3-L4 interbody cage pedicle screw construct at L2, L3, L4 with reduction of spondylolisthesis (Fig. 19.17).

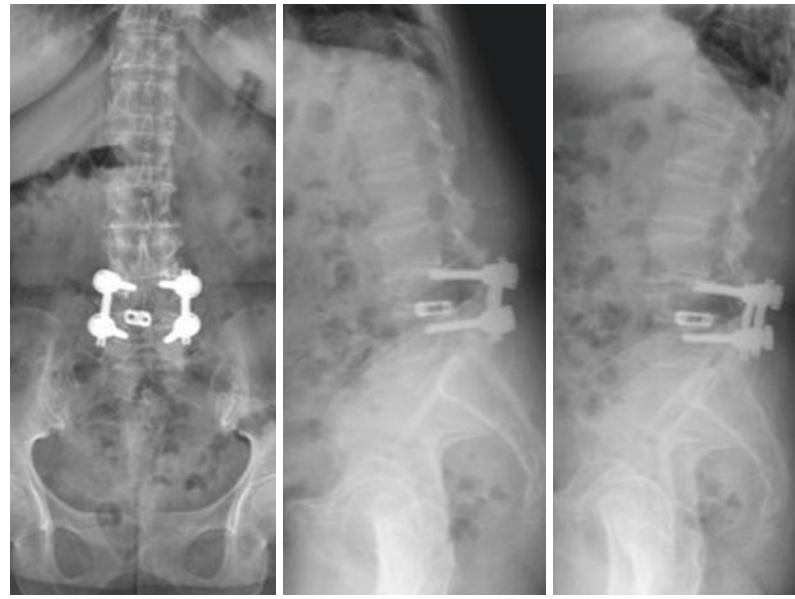

**Fig. 19.14** AP/lateral X-ray showing Grade 2 spondylolisthesis at L3-L4 with interbody cage L4-L5 with pedicle screw

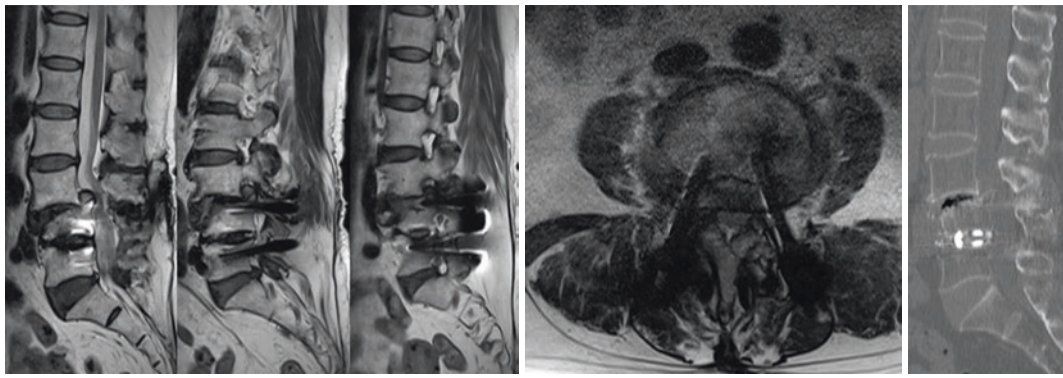

**Fig. 19.15** MRI T2 sagittal and axial views showing grade 2 spondylolisthesis with bilateral foraminal, lateral recess narrowing, lumbar canal stenosis, and interbody cage at L4-L5. CT showing vacuum disc phenomenon at L3-L4 with L4-L5 interbody cage (prior fusion surgery)

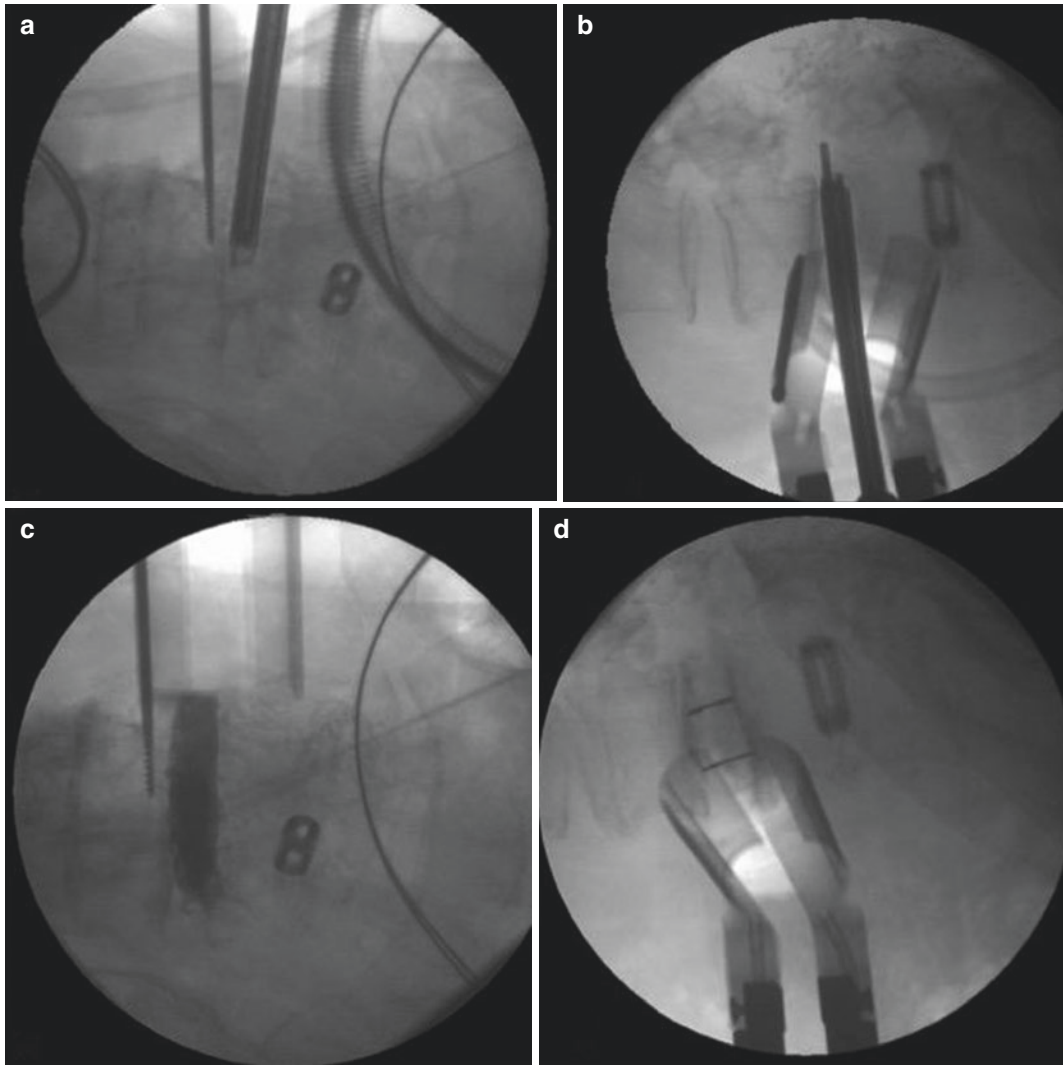


**Fig. 19.16** Intraoperative images **a** and **b**—using endoscope to remove foraminal and central disc **c**—checking endplate preparation using dye **d**—insertion of interbody cage

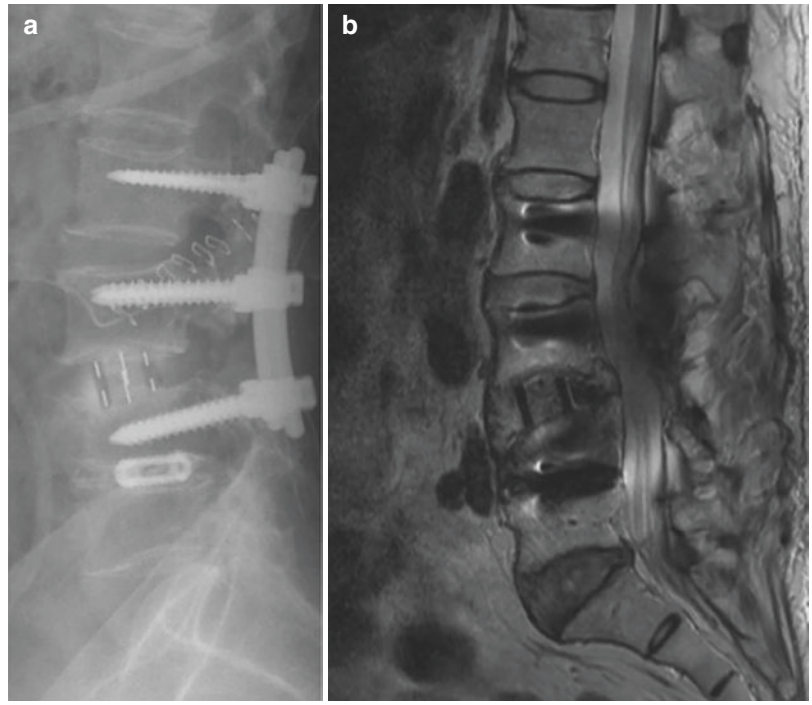


**Fig. 19.17** Post-operative imaging, (**a**) X-ray and (**b**) MRI showing reduction of spondylolisthesis at L3-L4 with restoration of disc height

## References


1. DiGiorgio AM, Edwards CS, Virk MS, et al. Stereotactic navigation for the prepsoas oblique lateral lumbar interbody fusion: technical note and case series. Neurosurg focus. 2017;43(2):E14.
2. Villard J, Ryang YM, Demetriades AK, et al. Radiation exposure to the surgeon and the patient during posterior lumbar spinal instrumentation: a prospective randomized comparison of navigated versus non-navigated freehand techniques. Spine. 2014;39(13):1004–9.
3. Zhang YH, White I, Potts E, et al. Comparison perioperative factors during minimally invasive prepsoas lateral interbody fusion of the lumbar spine using either navigation or conventional fluoroscopy. Glob Spine J. 2017;7(7):657–63.
4. Schonauer C, Stienen MN, Gautschi OP, Schaller K, Tessitore E. Endoscope assisted extreme-lateral interbody fusion (XLIF) – preliminary experience and technical note. World Neurosurg. 2017; https://doi.org/10.1016/j.wneu.2017.04.110.
5. Park P. Impact of spinal navigation on the oblique lumbar interbody fusion. Neurospine. 2020;17(1):268–9. https://doi.org/10.14245/ns.2040518.059.
6. Xi Z, Chou D, Mummaneni PV, Burch S. The navigated oblique lumbar interbody fusion: accuracy rate, effect on surgical time, and complications. Neurospine. 2020;17(1):260–7. https://doi.org/10.14245/ns.1938358.179. Epub 2020 Feb 5. PMID: 32054142; PMCID: PMC7136090
7. DiGiorgio AM, Edwards CS, Virk MS, Mummaneni PV, Chou D. Stereotactic navigation for the prepsoas oblique lateral lumbar interbody fusion: technical note and case series. Neurosurg Focus. 2017;43(2):E14.
8. Berjano P, Gautschi OP, Schils F, Tessitore E. Extreme lateral interbody fusion (XLIF(R)): how I do it. Acta Neurochirurgica. 2015;157(3):547–51.
9. Mobbs RJ, Phan K, Malham G, Seex K, Rao PJ. Lumbar interbody fusion: techniques, indications and comparison of interbody fusion options including PLIF, TLIF, MI-TLIF.
10. Joseph JR, Smith BW, La Marca F, Park P. Comparison of complication rates of minimally invasive transforaminal lumbar interbody fusion and lateral lumbar interbody fusion: a systematic review of the literature. Neurosurg Focus. 2015;39(4):E4.
11. Moller DJ, Slimack NP, Acosta FL Jr, Koski TR, Fessler RG, Liu JC. Minimally invasive lateral lumbar interbody fusion and transpsoas approach-related morbidity. Neurosurg Focus. 2011;31(4):E4.
12. Ohtori S, Orita S, Yamauchi K, Eguchi Y, Ochiai N, Kishida S, et al. Mini-open anterior retroperitoneal lumbar interbody fusion: oblique lateral interbody

fusion for lumbar spinal degeneration disease. Yonsei Med J. 2015;56:1051–9.
13. Ozgur BM, Aryan HE, Pimenta L, Taylor WR. Extreme lateral interbody fusion (XLIF): a novel surgical technique for anterior lumbar interbody fusion. Spine J. 2006;6:435–43.
14. Rodgers WB, Gerber EJ, Patterson J. Intraoperative and early postoperative complications in extreme lateral interbody fusion: an analysis of 600 cases. Spine (Phila Pa 1976). 2011;36:26–32.
15. Villard J, Ryang YM, Demetriades AK, Reinke A, Behr M, Preuss A, et al. Radiation exposure to the surgeon and the patient during posterior lumbar spinal instrumentation: a prospective randomized comparison of navigated versus non-navigated freehand techniques. Spine (Phila Pa 1976). 2014;39:1004–9.
16. Van de Kelft E, Costa F, Van der Planken D, et al. A prospective multicenter registry on the accuracy of pedicle screw placement in the thoracic, lumbar, and sacral levels with the use of the O-arm imaging system and StealthStation Navigation. Spine (Phila Pa 1976). 2012;37:E1580–7.
17. Abdullah KG, Bishop FS, Lubelski D, et al. Radiation exposure to the spine surgeon in lumbar and thoracolumbar fusions with the use of an intraoperative computed tomographic 3-dimensional imaging system. Spine (Phila Pa 1976). 2012;37:E1074–8.
18. Nottmeier EW, Bowman C, Nelson KL. Surgeon radiation exposure in cone beam computed tomography-based, image-guided spinal surgery. Int J Med Robot. 2012;8:196–200.
19. Gelalis ID, Paschos NK, Pakos EE, et al. Accuracy of pedicle screw placement: a systematic review of prospective in vivo studies comparing free hand, fluoroscopy guidance and navigation techniques. Eur Spine J. 2012;21:247–55.
20. Zhang YH, White I, Potts E, Mobasser JP, Chou D. Comparison perioperative factors during minimally invasive pre-psoas lateral interbody fusion of the lumbar spine using either navigation or conventional fluoroscopy. Global Spine J. 2017;7(7):657–63.

# 20 Virtu4D Navigation-Guided Endoscopic Transforaminal Lumbar Interbody Fusion and Percutaneous Pedicle Screw Fixation

Xuexiao Ma, Chuanli Zhou, Chao Wang, and Derong Xu

## 20.1 Historical Perspective

Endoscopic transforaminal lumbar interbody fusion (Endo-TLIF) was reported to address a variety of spinal disorders using percutaneous endoscopic lumbar discectomy (PELD) technique combined endoscopic visualization, expandable or normal cage technology, and interbody fusion technique through Kambin's triangle [1–3]. As reported, the Endo-TLIF technique can achieve not only bilateral direct decompression, interbody cage insertion, and pedicle implantation but also less dissection of normal structures. In other words, the muscle, soft tissue, and nerve roots can be significantly protected because of the access to procedures and the direct visualization under endoscopy. In recent years, research on the Endo-TLIF technique has become a hot topic. A great many spine surgeons put more attention into the clinical application of the technology, which is an important field.

In 2012, G Osman [4] reported 60 patients with endoscopic transforaminal decompression, interbody fusion, and percutaneous pedicle screw implantation of the lumbar spine, and patients were followed up for a minimum of 6 months, The mean time in the operating room is 2 h 54 min. Estimated blood loss averaged 57.6 ml. The duration of the hospital stay averaged 2.6 days. Preoperative back pain and leg pain were significantly reduced. It is concluded that the endoscopic transforaminal lumbar decompression, interbody fusion, and percutaneous pedicle screw instrumentation consistently produced satisfactory results in all demographics.

In 2013, Frederic Jacquot and Daniel Gastambide [5] developed a percutaneous endoscopic lumbar fusion technique based on the principles of Kambin and an original titanium cage to treatment of 57 cases, eight patients had a postoperative radicular pain with paresthesias. Asymptomatic migration of the cages occurred in two cases and symptomatic migration required a conventional secondary reoperation in 13 cases after a mean delay of eight months (range 3 to 36 months). They concluded that the technique is introduced in our practice to take care of difficult or grave comorbidity patients, and some patients had excellent lasting results following a very short procedure and hospital

X. Ma (✉) · C. Wang · D. Xu
Department of Spine Surgery, The Affiliated Hospital of Qingdao University, Qingdao, China

C. Zhou
Centre for Minimally Invasive Spinal Surgery, Affiliated Hospital of Qingdao University, Qingdao, China



J.-S. Kim et al. (eds.), *Technical Advances in Minimally Invasive Spine Surgery*,
https://doi.org/10.1007/978-981-19-0175-1_20

stay. However, considering the 36% complication rate in this series, we do not recommend it unless decisive technical improvements are made.

## 20.2 Terminology

Endoscopic lumbar interbody fusion (Endo-LIF), could be divided into endoscopic transforaminal lumbar interbody fusion (Endo-TLIF) and endoscopic posterior lumbar interbody fusion (Endo-PLIF) according to surgical approach. The surgical procedures of Endo-TLIF are fairly close to that of minimally invasive transforaminal lumbar interbody fusion (MIS-TLIF) on the treatment of lumbar spondylolisthesis, with the obvious differences of working channel (endoscopy in Endo-TLIF and expandable channel in MIS-TLIF) and surgical environment (aqueous medium in Endo-TLIF and air medium in MIS-TLIF).

Clinically available navigation systems can be classified into optoelectronic navigation, robot-assisted surgery, and electromagnetic navigation [6, 7]. The navigation systems that work on the basis of detecting optical sensors have been widely used in the past several years with obvious superiority in pedicle screw placement. However, the disadvantage is that the line of sight can never be interrupted, which limits the operator's degree of freedom during the procedure, thus also limits the intuitive use of the operation instruments. In addition, the trackers must be designed so they extend beyond the operation site in order to be detected by the navigation camera. Even very small changes in position due to accidental contact with the reference base can lead to faulty positioning and subsequent complications.

A new electromagnetic navigation system (fiagon GmbH, Hennigsdorf, Germany) based on electromagnetic field (EMF) and adapted for spine surgery is used. A special field generator is used to generate the EMF. All required and specially developed instruments are free of ferromagnetic substances to prevent measuring and instrument errors, so the navigable screwdrivers with titanium alloy are developed.

## 20.3 Patient Selection

### 20.3.1 General Indications

The inclusion criteria consist of the following: (1) single or two-segment lumbar spondylolisthesis with Meyerding stage I or II; (2) persistent, severe low back pain and sciatica or neurogenic intermittent claudication, no response to standardized conservative treatment and severely affect daily life and work; (3) preoperative flexion-extension radiographs, computed tomography (CT) and magnetic resonance imaging (MRI) show isthmic or degenerative type with instability, lateral recess, foraminal stenosis; (4) no obvious decline of muscle strength and cauda equina syndrome. The exclusion criteria are as follows: (1) revision history in the duty level; (2) spondylolisthesis combined with infection, trauma, scoliosis, osteoporosis, kyphosis, and tumors; (3) severe central canal stenosis or bilateral recess stenosis; (4) cerebrovascular and cardiovascular diseases that make the patients intolerance of long-term operation; and (5) severe osteoporosis.

### 20.3.2 Indications for Endo-TLIF

(1) Single or two-segment lumbar spondylolisthesis with Meyerding stage I or II; (2) persistent, severe low back pain and unilateral sciatica without neurogenic intermittent claudication, no response to standardized conservative treatment and severely affected daily life and work; (3) preoperative flexion-extension radiographs, computed tomography (CT), and magnetic resonance imaging (MRI) showed isthmic or degenerative type with instability, lateral recess, foraminal stenosis; (4) no obvious decline of muscle strength and cauda equina syndrome.

## 20.4 Pros and Cons of Endo-LIF

### 20.4.1 Pros

(1) Eliminating the fear of open surgery; (2) Minimizing the trauma of surgery and preservation of lumbar motion segments; (3) Reduction of

operating time, surgical blood loss, postoperative infection rate, hospital stay, postoperative narcotic medication, convalescence, and complication rates; (4) Bringing down health care costs; and (5) Early return to physical activities.

### 20.4.2 Cons

(1) Long learning curve; (2) Requirement of foundation of open spine surgery, endoscopic experiences, percutaneous techniques, and systematic lumbar anatomy; (3) Longer radiation exposure times; (4) Excessive requirements for surgical tools and equipment; (5) Only a few hospitals and surgeons can carry out; and (6) The revision surgery for Endo-TLIF is much more difficult, due to the paracentral incision.

## 20.5 Preoperative Planning

### 20.5.1 Examinations

Comprehensive imaging data should be prepared. Lumbar dynamic radiographs are used to determine the presence of lumbar instability. The anteroposterior and lateral radiograph of the lumbar spine are used to determine whether there is a developmental deformity, like sacral lumbarization and lumbar sacralization. Lumbar three dimensional reconstruction CT scans are indispensable to make sure the dislocation types and the degree of intervertebral foramen stenosis. MRI is also necessary to accurately judge the extent and location of the stenosis. Spine whole length anteroposterior and lateral radiograph is suggested for differential diagnosis of hip joint disorders and developmental deformity.

The other examinations like chest CT, cerebrovascular function detector, lower extremity vascular ultrasound, cardiac ultrasound, arterial blood gas analysis are also essential to eliminate the taboo of general anesthesia.

### 20.5.2 Preparation

Before the surgery, 3-dimensional constructed CT scans with a slice thickness of less than 1 mm are made for the two groups, which are used to match with the intraoperative X-ray. EMsys needs intraoperative anteroposterior and lateral X-ray films for image matching. The CT data set is stored in DICOM format and copied into the workstation for further processing. Intraoperative spinal monitoring is also necessary to avoid nerve root injury at an early stage. Before Endo-TLIF, the guide wire of percutaneous pedicle screw would be inserted firstly with the help of EMsys via a Jamshidi needle. After guide wire placement and X-ray confirmation, canal decompression, discectomy, reduction, and interbody fusion under full-endoscopy would be done in sequence, then percutaneous pedicle screws are inserted along the guide wire to pull the dislocation again and fix the duty level.

### 20.5.3 Anesthesia

General anesthesia is recommended. Controlled hypertension is a good method to decrease intraspinal bleeding. As for reducing peripheral bleeding due to soft tissue, mixed liquor with 1 mg adrenaline diluted to 0.9% saline can be injected from skin to soft tissues. For the patient with general anesthesia contraindication, local anesthesia using a mixed solution with 2% lidocaine 20 ml, 1% ripovacaine 10 ml, and normal saline 30 ml is also suggested.

### 20.5.4 Positioning

The surgery is performed in the operating room in a strictly sterile environment. Patients are kept in prone position with the abdomen unsupported.

### 20.5.5 Technical Equipment

The Endo-TLIF instruments which are called Endo-Surgi Plus® and Endo-TLIF system are designed and manufactured by Unintech® company from China, and all the procedures are visualized under the endoscope. Endo-Surgi Plus® is an advanced system of Endo-Surgi series. Its application covers the entire spine by using four surgical suites: Lateral Suite, Posterior Suite, Cervical Suite, and Fusion Suite. Compared with the traditional endoscope, the view of Endo-Surgi Plus endoscope is increased by 50%, which increases the surgery efficiency by 30%.

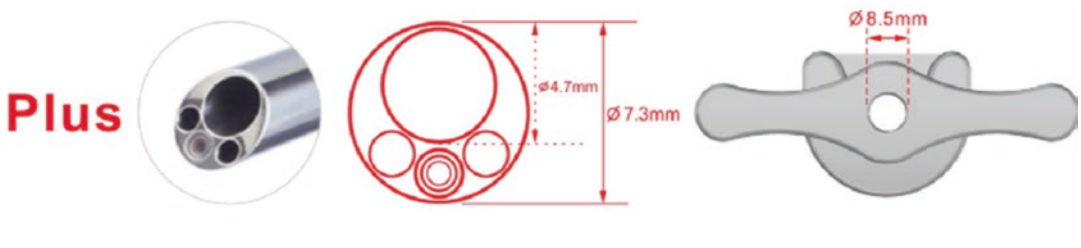



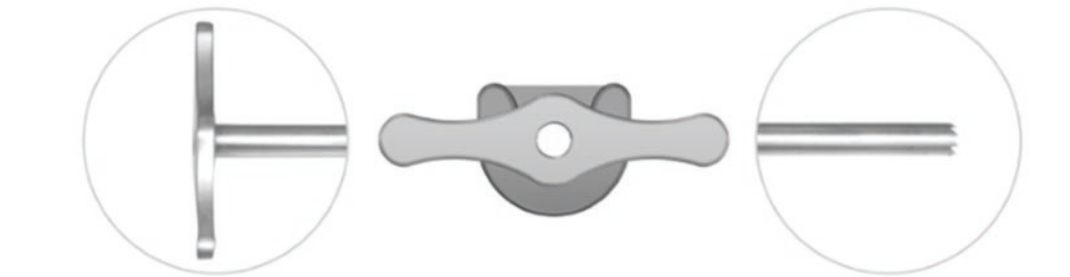

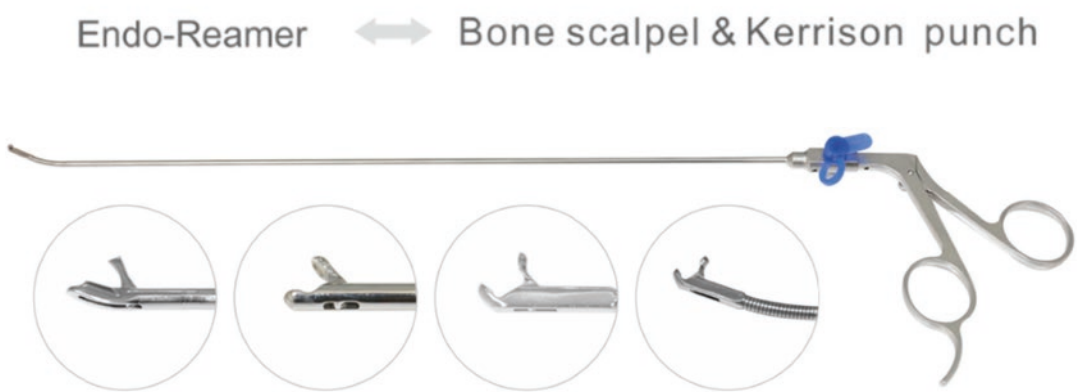

## 20.6 Surgical Procedures

### 20.6.1 Surface Localization of the Surgical Area and Incision Planning

Preoperative surface localization of the pedicle under X-ray is important to verify indirectly the accuracy of electromagnetic navigation. The distance between the two pedicles is called one "L" with a length of 4–6 cm, and the average incision of Endo-TLIF is just one L distance. Four longitudinal incisions about 1 cm are always made for percutaneous pedicle screw placement. One of the incisions is selected as the working channel for decompression and interbody fusion cage placement.

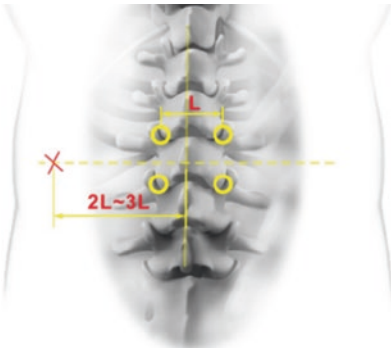


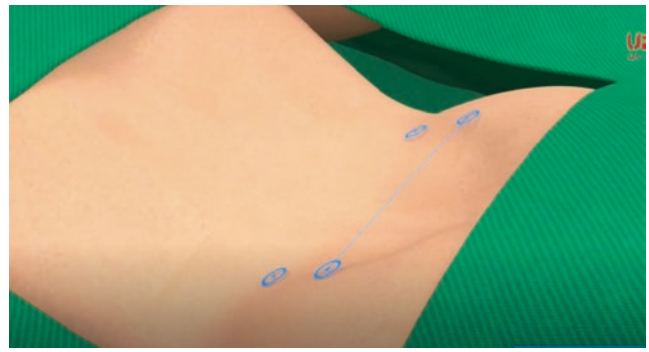

### 20.6.2 Electromagnetic Navigation Registration

A special field generator is used to generate the electromagnetic field (EMF). All required and specially developed instruments are free of ferromagnetic substances to prevent measuring and instrument errors, so the navigable screwdrivers with titanium alloy are developed. The magnetic field generator is placed close to the buttom (nonsterile area) so that the frame can encompass the entire surgical field (Fig. 20.1). The EM field has a spherical size of 500 mm field generator in which the instruments in the field fitted with signal coils can be detected. To match the generated electromagnetic field with the image data set and the spine of the cadaver, a reference coil called the patient tracker is inserted firmly into the spinous process by a short thin K-wire like the bone pin (Fig. 20.2). Mapper bridge with 17 mapping points is put on the low back and standard anteroposterior and lateral X-rays are done to match with the preoperative 3-D CT scans (Fig. 20.3). MultiPad should be placed close to the patient tracker and all the navigable instruments would be identified and registered (Fig. 20.4). Specialized pedicle opener and bone awl are percutaneously placed at the entry point, and inserted into the soft tissues to touch the anatomical landmark following the route designed by the navigation (Fig. 20.5). Four percutaneous pedicle screws are placed accurately and safely under purely navigated guidance. The depth of the screw entry could also be monitored by the navigation system. The incision is independently designed according to the pedicles and decompression procedure, which could be much shorter and more beautiful (Fig. 20.6). AP and LAT radiographs would be checked again to make sure the position is reasonable.

### 20.6.3 Anatomical Identification and Exposure

Blunt guiding rod instead of needle puncturing is inserted along the percutaneous pedicle incision and used to detach the soft tissue around the facet joint. Electromagnetic navigation is also helpful to guide the direction and make sure the position

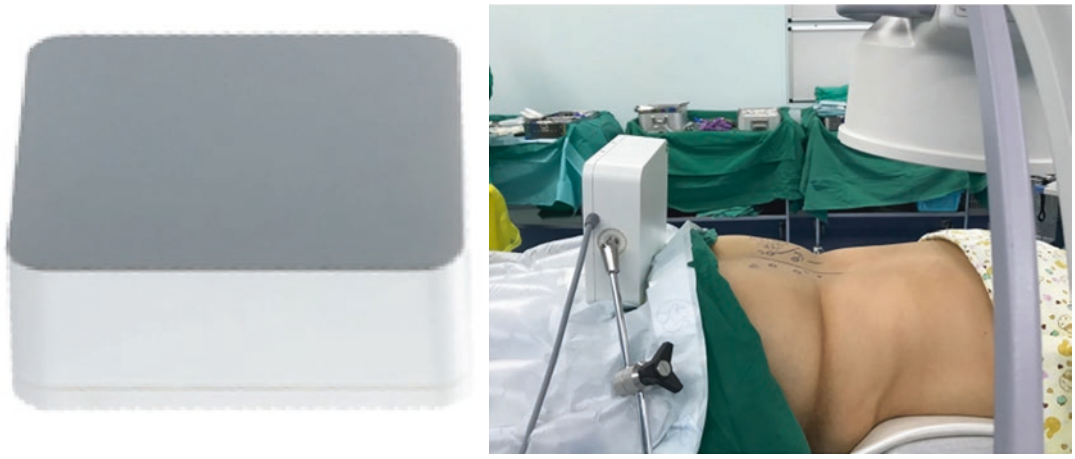

**Fig. 20.1** EM field generator and its position close to the button

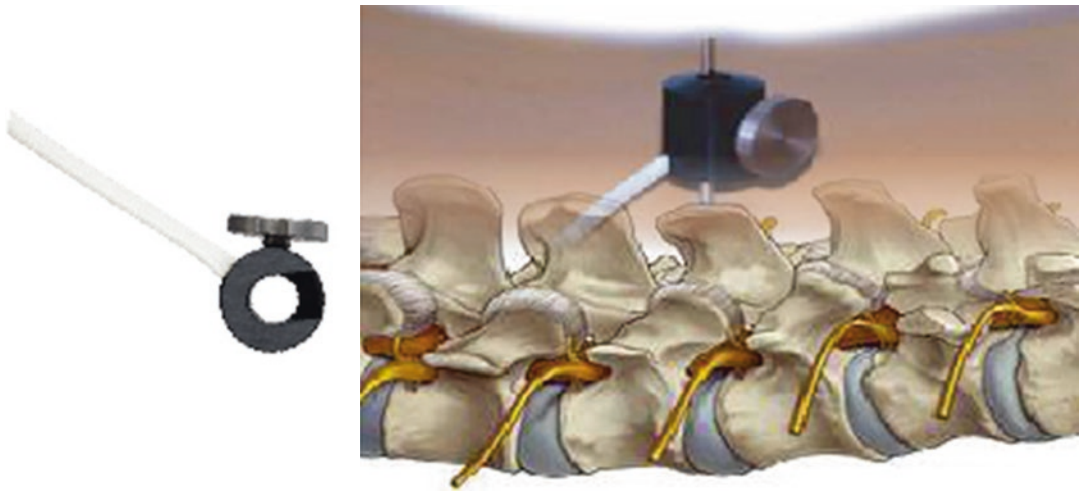

**Fig. 20.2** The reference coil called the patient tracker is attached to the spinous process

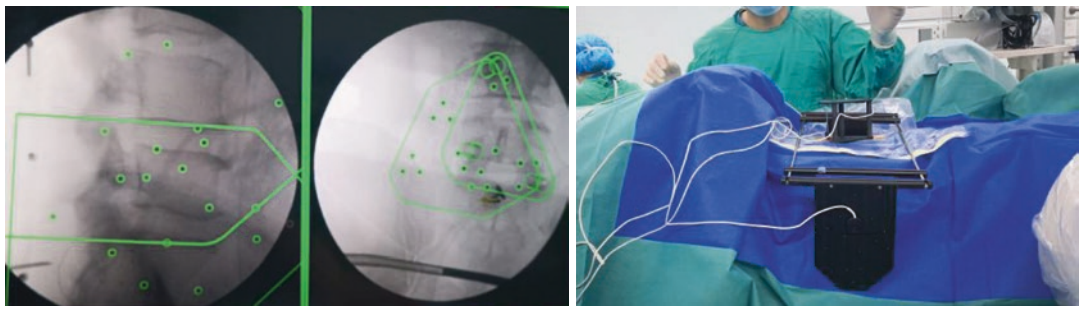

**Fig. 20.3** Mapper bridge is putted on the low back and standard anteroposterior and lateral X-rays are done to match with the preoperative 3-D CT scans

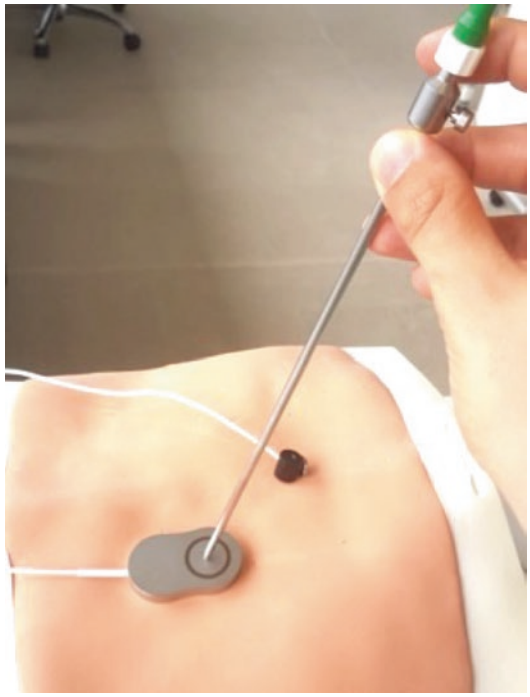

**Fig. 20.4** MultiPad should be placed close to the patient tracker and all the navigable instruments would be registrated

of unidentifiable facet joint because of osteoproliferation. U-T tubes and uniportal endoscope are placed. Radiofrequency electrocoagulation and a bit larger forceps are used interchangeably to clean soft tissues and expose the facet joint clearly.

### 20.6.4 Endoscopic Decompression

Endo-reamer with an inner diameter of 7.5 mm and outer diameter 8.5 mm is powerful and safe for unilateral foraminotomy and laminectomy. If possible, unilateral laminotomy for bilateral decompression (ULBD) can also be done by reamer and laminectomy punch. The first reamer position is very important and should be distinguished clearly. The tip of superior articular process (SAP) and corresponding lateral border of inferior articular process (IAP) are the reasonable points that should be resected firstly. When the facet joint is partially removed, ligamentum flavum is founded. The second reamer position would be the main body of SAP. The base of SAP

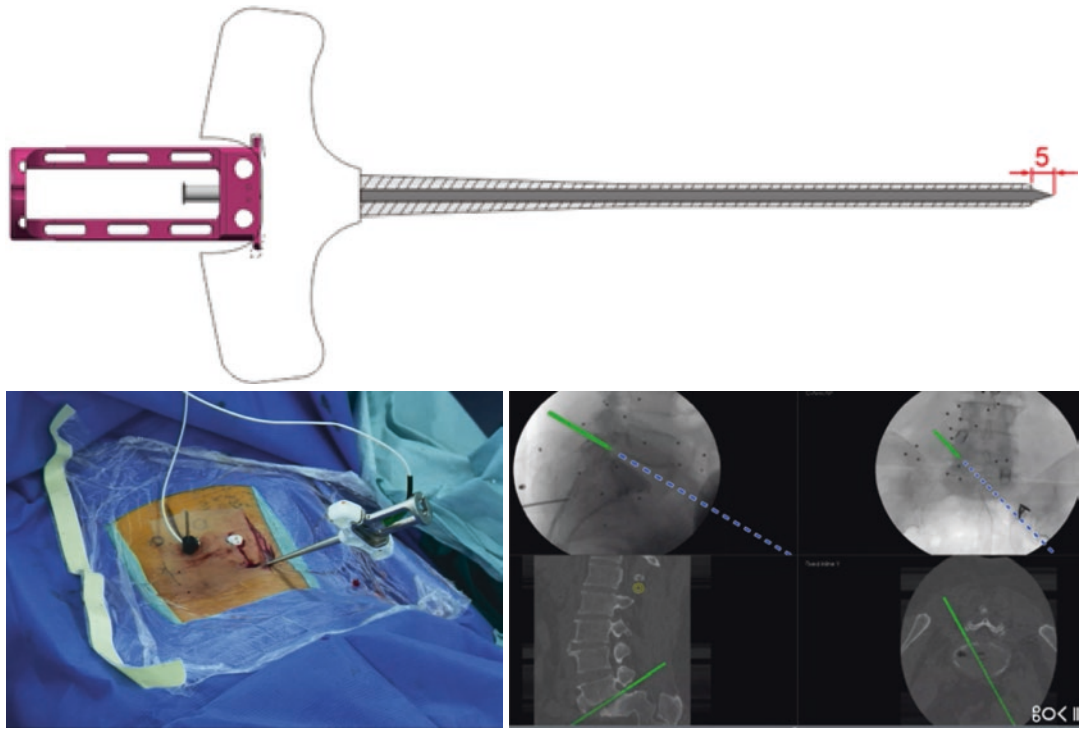


**Fig. 20.5** Specialized pedicle opener and bone awl are percutaneously placed at the entry point, and inserted into the soft tissues to touch the anatomical landmark following the route designed by the navigation

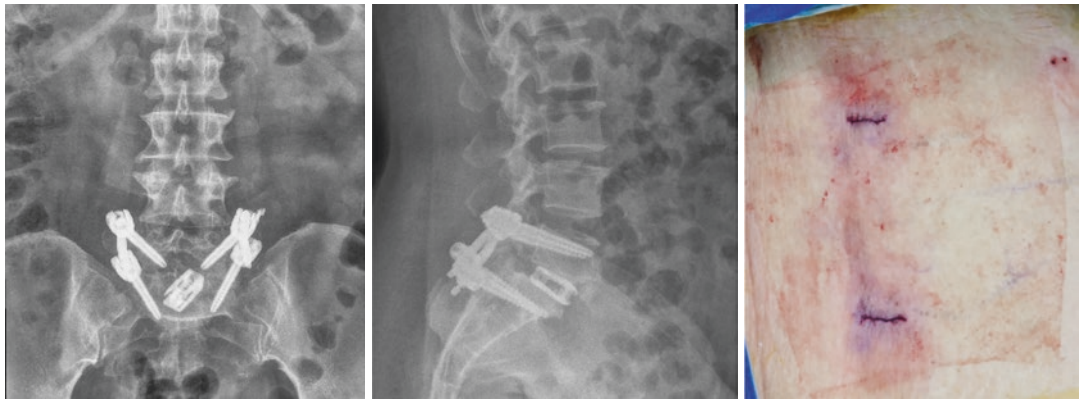

**Fig. 20.6** Four percutaneous pedicle screws are placed accurately and safely under purely navigated guidance and the incision is always much shorter

and superior edge of lower lamina should be the third part. Interlaminar space has appeared clearly and the fourth reamer position is IAP, and inferior edge of upper lamina. After several reamers, the unilateral foramen, caudal, and cephalic stop of ligamentum flavum are visualized. Then dural sac and L5 nerve root are exposed but protected by working tube for spinal canal decompression.

### 20.6.5 Intervertebral Disc Space Treatment

The AccessPointer in the Electromagnetic navigation system makes the location and direction of intervertebral disc clear (Fig. 20.3). The operator could remove the intervertebral disc tissues by using endo-chisel, biopsy forceps, inside and outside reamer, firme chisel, scraper, and flexible scraper. After the upper and lower cartilage plates are scraped off to the oozing of the blood, the AccessPointer could evaluate the depth of processed intervertebral space (Fig. 20.3).

### 20.6.6 Intervertebral Bone Grafting and Cage Implantation

The trial cage was inserted to an appropriate location under the channel and confirmed by anteroposterior and lateral fluoroscopic views or electromagnetic navigation. After removing the model and filling the intervertebral space with autograft and allograft, the cage is implanted via the working cannula to restore lumbar lordosis and the height of the intervertebral space.

### 20.6.7 Percutaneous Pedicle Screws Implantation

At last, the pedicle screws are installed to replace 4 guide wires, the position of screws and cage should be verified under C-arm fluoroscopy.

### 20.6.8 Cleaning the Operating Field

## 20.7 Postoperative Care

In most cases, no drainage tube is necessary and only two or four small incisions are left. The antibiotics should not be overused for more than 24 or 48 h. If possible, all the patients could get out of bed on the second day after surgery with the help of thoracolumbar brace.

## 20.8 Complications

8.1. Nerve root injury or dural tear.
8.2. Percutaneous pedicle screw entering the spinal canal.

8.3. The length of the rod is too long or short, and slipped from the screw.
8.4. Superficial wound or deep incision infection.
8.5. Postoperative hematoma formation.
8.6. Incomplete reduction.
8.7. Nonunion of intervertebral disc space.
8.8. Contralateral symptoms after surgery.
8.9. Persistent low back pain
8.10. Cage migration, subsidence.

## References

1. Wu J, Liu H, Ao S, et al. Percutaneous endoscopic lumbar interbody fusion: technical note and preliminary clinical experience with 2-year follow-up. Biomed Res Int. 2018;2018:5806037.
2. Yang J, Liu C, Hai Y, et al. Percutaneous endoscopic transforaminal lumbar interbody fusion for the treatment of lumbar spinal stenosis: preliminary report of seven cases with 12-month follow-up. Biomed Res Int. 2019;2019:3091459.
3. Syed H, Voyadzis JM. True percutaneous transforaminal lumbar interbody fusion: case illustrations, surgical technique, and limitations. J Neurol Surg A Cent Eur Neurosurg. 2016;77:344–53.
4. Osman SG. Endoscopic transforaminal decompression, interbody fusion and percutaneous pedicle screw implantation of the lumbar spine: a case series report. Int J Spine Surg. 2012;6:157–66.
5. Jacquot F, Gastambide D. Percutaneous endoscopic transforaminal lumbar interbody fusion: is it worth it? Int Orthop. 2013;37(8):1507–10.
6. Tian W, Han X, Liu B, Liu Y, Hu Y, Han X, Xu Y, Fan M, Jin H. A robot-assisted surgical system using a force-image control method for pedicle screw insertion. PLoS One. 2014;9(1):e86346.
7. Overley SC, Cho SK, Mehta AI, Arnold PM. Navigation and robotics in spinal surgery: where are we now? Neurosurgery. 2017;80(3S):S86–99.

# 21 Three-dimensional Endoscopic Spine Surgery Using the Biportal Endoscopic Approach

Dong Hwa Heo, Young Ho Hong, Dong-won Suh, and Hungtae Chung

## 21.1 Introduction

Three-dimensional (3D) imaging or videos has been widely applied in various fields such as movies, television, virtual reality, and mobile applications. In the medical aspect, 3D images have been used in radiological examinations, 3D exoscopy, robotic surgery, and endoscopic surgery. Among them, 3D endoscopic surgery has been attempted in general surgery, gynecology, otolaryngology, neurosurgery, and joint surgery [1–7]. Recently, we performed 3D endoscopic spine surgery using the biportal endoscopic approach [8–11]. Depth sensation and stereognosis of the 3D endoscopic system were the most important advantages during surgery [6, 12]. We introduced the technique and advantages of 3D biportal endoscopic spine surgery.

## 21.2 Surgical Instruments and Equipment

Recently, 3D endoscopic spine surgery is available in only biportal endoscopic approach. There was no 3D endoscopy of uniportal endoscopic approach. We used the 3D endoscopic system of Stoltz (Fig. 21.1a). A specialized 3D monitor and its console system were needed for 3D biportal endoscopic surgery (Fig. 21.1b) and specialized glasses were worn for 3D visualization during surgery (Fig. 21.2a).

The basic operation setting was similar to that of biportal endoscopic surgery except for the 3D endoscopy system and its console. The toolkit set of usual biportal endoscopic surgery was need [8–11]. Specialized biportal surgical instruments as well as general spinal surgical instruments were available for the 3D biportal endoscopic spine surgery. Radiofrequency (RF) probes were useful for soft tissue dissection and bleeding control [9–11]. A continuous saline irrigation system was used to maintain a clear surgical view and bleeding control [9–11].

## 21.3 Surgical Procedure

The patient was placed in the prone position after general endotracheal or epidural anesthesia. We preferred a Wilson flame or Jackson surgical table. Customized waterproof endoscopic surgery drapes were applied to prevent the patient from getting wet due to leakage of the irrigation saline [9–11]. Two portals were needed to perform 3D biportal endoscopic surgery (Fig. 21.2a and b). One was the endoscopic portal for 3D endoscopy

D. H. Heo · H. Chung
Endoscopic Spine Surgery Center, Neurosurgery and Orthopedics, Seoul Bumin Hospital, Seoul, South Korea

Y. H. Hong (✉) · D.-w. Suh
Neurosurgery and Orthopedics, Bundang Barunsesang Hospital, Seongnam, South Korea



J.-S. Kim et al. (eds.), *Technical Advances in Minimally Invasive Spine Surgery*,
https://doi.org/10.1007/978-981-19-0175-1_21

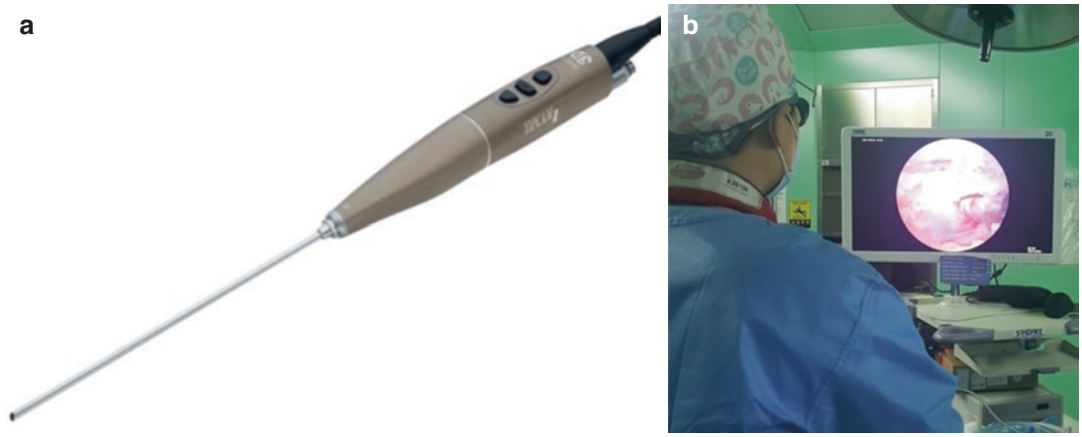


**Fig. 21.1** The 3D endoscopic system. For 3D endoscopic spine surgery, a 3D endoscopy (**a**), a 3D monitor (**b**), its console system (**b**), and customized glassed are necessary

and its trocar. The other was the working portal for surgical instruments such as the drill, RF, Kerrison punch, and forceps. A working sheath was inserted at the working portal Fig. 21.2c). A working sheath helped to smoothly insert the surgical instruments and drain the irrigation saline [9–11].

Based on the mid-portion of the disc space, the endoscopic portal was made 1 cm above the mid-portion of the disc, and the working portal was made 1 cm below the mid-portion of the disc in the left-side approach for a right-handed surgeon (Fig. 21.3). In the anteroposterior view, two portals were made at the medial border of the pedicle for lumbar laminotomy or discectomy [9–11].

Serial dilators were inserted under C-arm fluoroscopic guidance, and then a working sheath was inserted at the working portal area. A specialized trocar for 3D endoscopy was inserted through a 5-mm long skin incision. A 3D endoscopy was put into a trocar. Continuous saline irrigation was started. The soft tissue over the lamina was dissected and removed using RF probes. 2D images were simply converted to 3D images by the button control of the 3D endoscopy without changing the endoscopic system. We usually used 2D images. A working distance between the lens and object is necessary for 3D visualization. 3D demonstration was available from flavectomy (Table 21.1). During soft tissue dissection and bone work (drilling), the 3D vision was poor due to the slight depth. After exposure of the dura, clear 3D visualization was achieved (Table 21.1). The 3D operation videos were recorded in 3D video file top and bottom (Fig. 21.4a) and side-by-side formats (Fig. 21.4b).

## 21.4 Clinical Application

We performed 3D endoscopic surgery for lumbar laminotomy with discectomy, lumbar unilateral laminotomy with bilateral decompression, lateral foraminotomy for exiting nerve root decompression, lumbar interbody fusion, and cervical posterior foraminotomy. The 3D operation video was recorded in top and bottom or side-by-side format types.

(1) **Lumbar decompressive laminectomy**

When the 3D endoscopic system was used, the traversing nerve roots were clearly demonstrated by the 3D endoscopy. Additionally, stereoscopic vision of the 3D endoscope helped to safely decompress the nerves and clearly show the degree of decompression (Fig. 21.5).

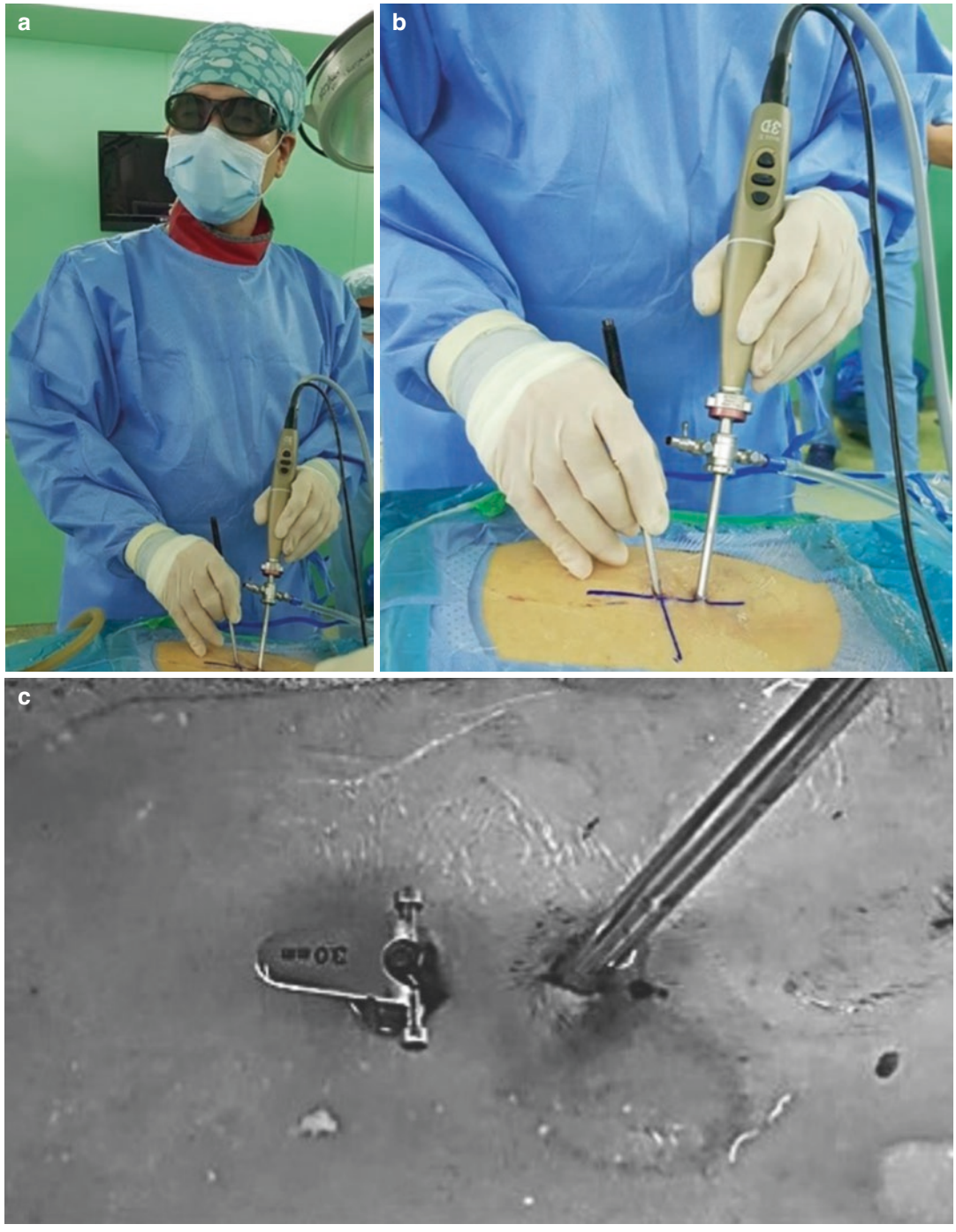


**Fig. 21.2** Overview of 3D endoscopic spine surgery using the biportal endoscopic approach (**a** and **b**). There were two portals. The first was the endoscopic portal for a 3D endoscopy, and the second was the working portal for the surgical instruments (**c**)

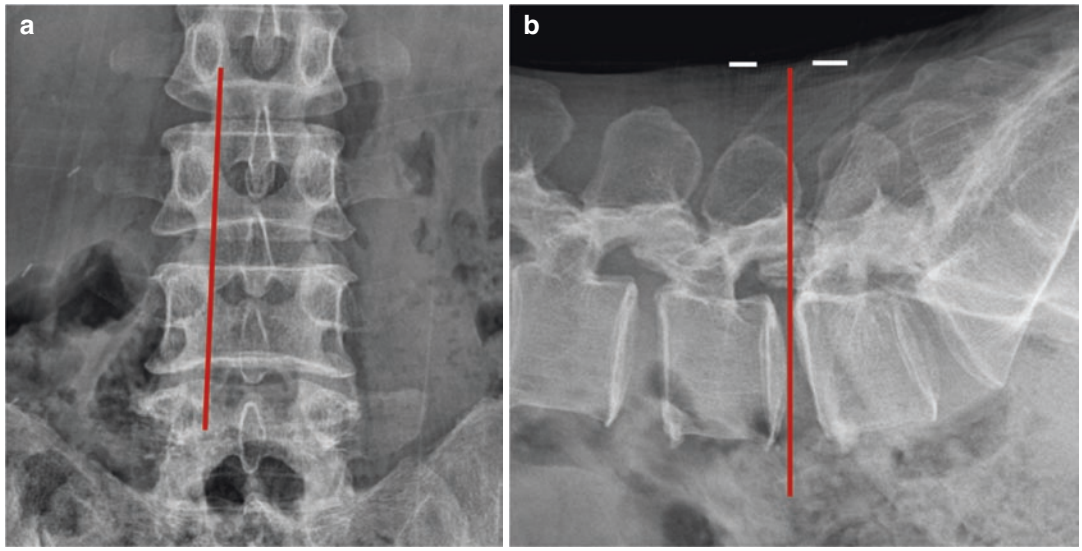


**Fig. 21.3** Making two channels for biportal 3D endoscopic spine surgery. Two portals were made on the medial border (red line) of the pedicle (anteroposterior view, **a**). Based on the intervertebral disc (red line), an endoscopic portal was made upper 1 cm and working portal was below 1 cm for left side approach (lateral view, **b**)

**Table 21.1** Degree of 3D demonstration according to the surgical procedures

| Procedures | 3D demonstration |
|---|---|
| Muscle dissection | Poor |
| Laminotomy | Poor |
| Removal of ligamentum flavum | Good |
| Lateral recess decompression (Ipsilateral nerve root decompression) | Good |
| Dural exposure and retraction | Good |
| Discectomy | Good |
| Contralateral nerve root decompression | Good |

### (2) Contralateral sublaminar approach for ruptured disc particle removal

3D endoscopic surgery was useful in the case of a contralateral sublaminar approach (Fig. 21.6). 3D endoscopy could clearly distinguish between the contralateral nerve root and the ruptured disc particles. Ruptured disc particles were safely removed without injury to the nerve root.

### (3) Cervical posterior foraminotomy

When performing posterior cervical foraminotomy, cervical nerve root decompression is important. Sometimes, a cervical nerve root consisted of sensory and motor nerve roots (Fig. 21.7), In some cases, the disc fragments and nerve roots were difficult to distinguish. The 3D endoscope clearly showed the nerve roots and helped to separate the disc pieces from the nerve roots (Fig. 21.7).

## 21.5 Discussion

All endoscopic surgical images including the arthroscopy, laparoscopy, and thoracoscopy images were 2D images and there was no depth sensation [13]. It is difficult to learn endoscopic surgery and the technique requires a long training period due to the narrow view of the endoscopic field, difficulty in handling surgical instruments, and no depth sensation. In particular, 2D images without depth sensation hinder the understanding

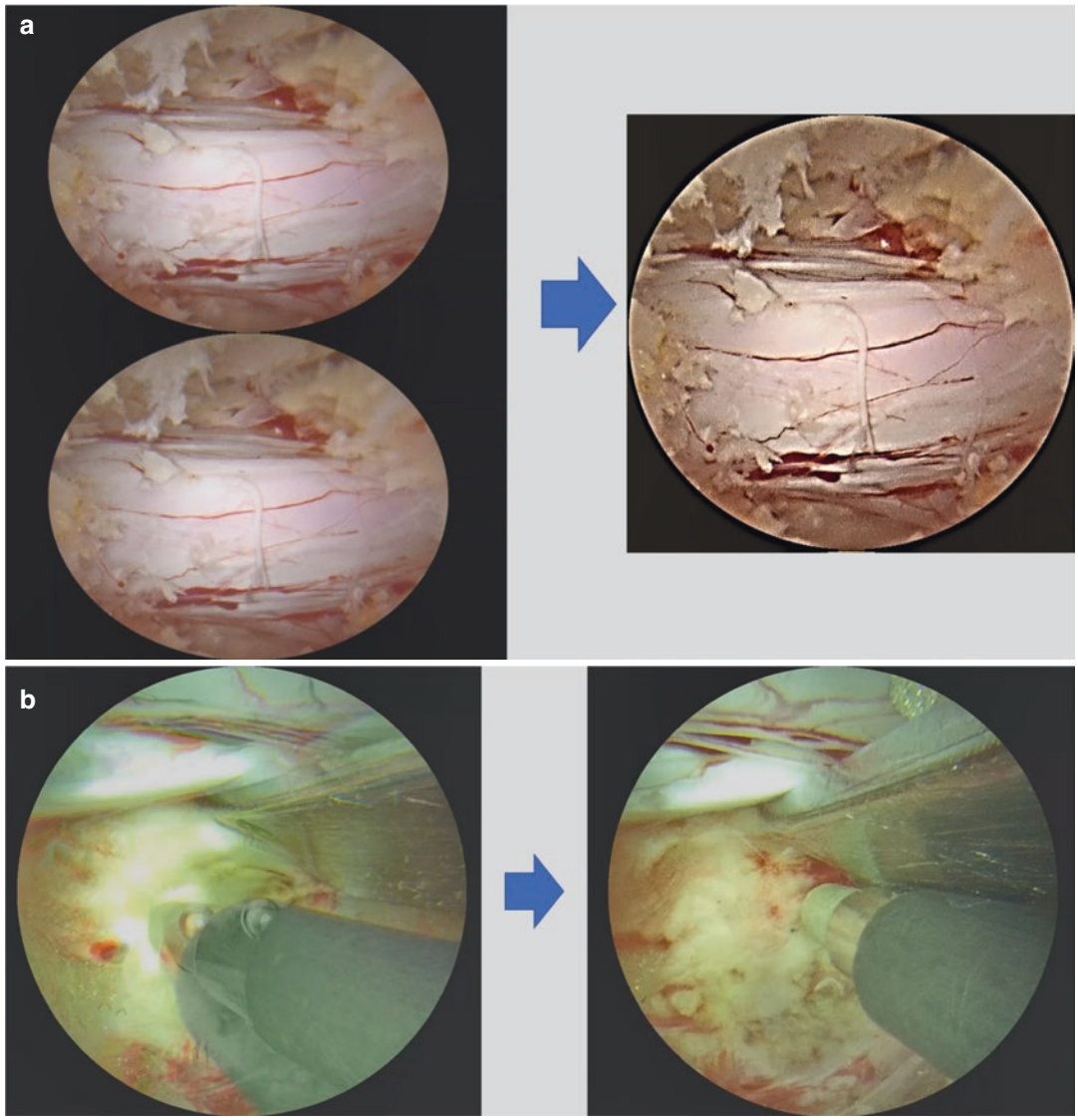


**Fig. 21.4** 3D video file formats. The top and bottom type (**a**) and the side-by-side type (**b**). These 3D video formats presented 3D images and stereognosis during surgery

of surgical anatomy. Moreover, since it is not a stereoscopic view of endoscopic surgery, there is a possibility of damaging normal tissue during endoscopic surgery. For this reason, 3D endoscopes have recently been developed. 3D endoscopy has mainly been used for joint surgery and abdominal surgery and was not yet used for spinal surgery.

Biportal endoscopic spine surgery uses an endoscopic system with a relatively large lance 4-mm in diameter compared to one portal endoscopy. Currently, 3D optical technology is only applicable to endoscopy with 4-mm diameter endoscopic lenses. Therefore, 3D endoscopic spine surgery is only possible with biportal endoscopic approaches.

- **3D images demonstration**

To accomplish stereoscopic vision, there must be some depth. Therefore, it is better to perform 2D surgery when doing muscle dissection or

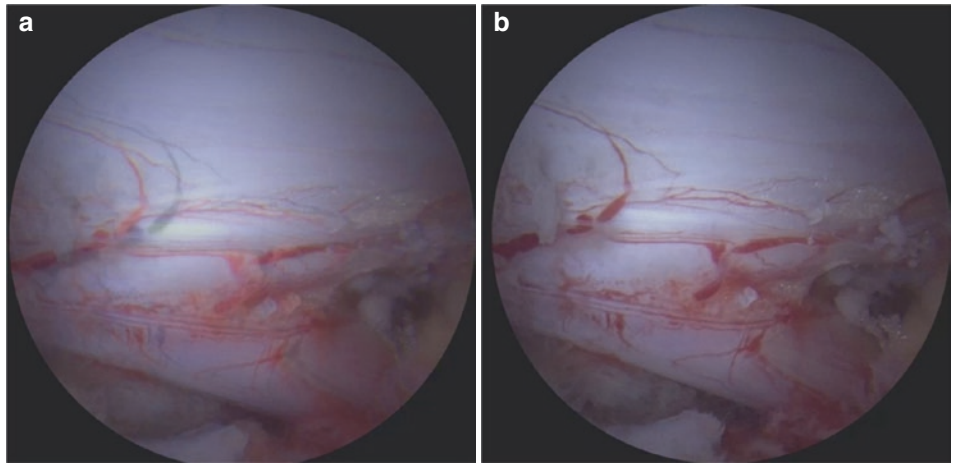


**Fig. 21.5** Intraoperative 3D (**a**) and 2D (**b**) images of the left L5 nerve root after partial hemilaminectomy

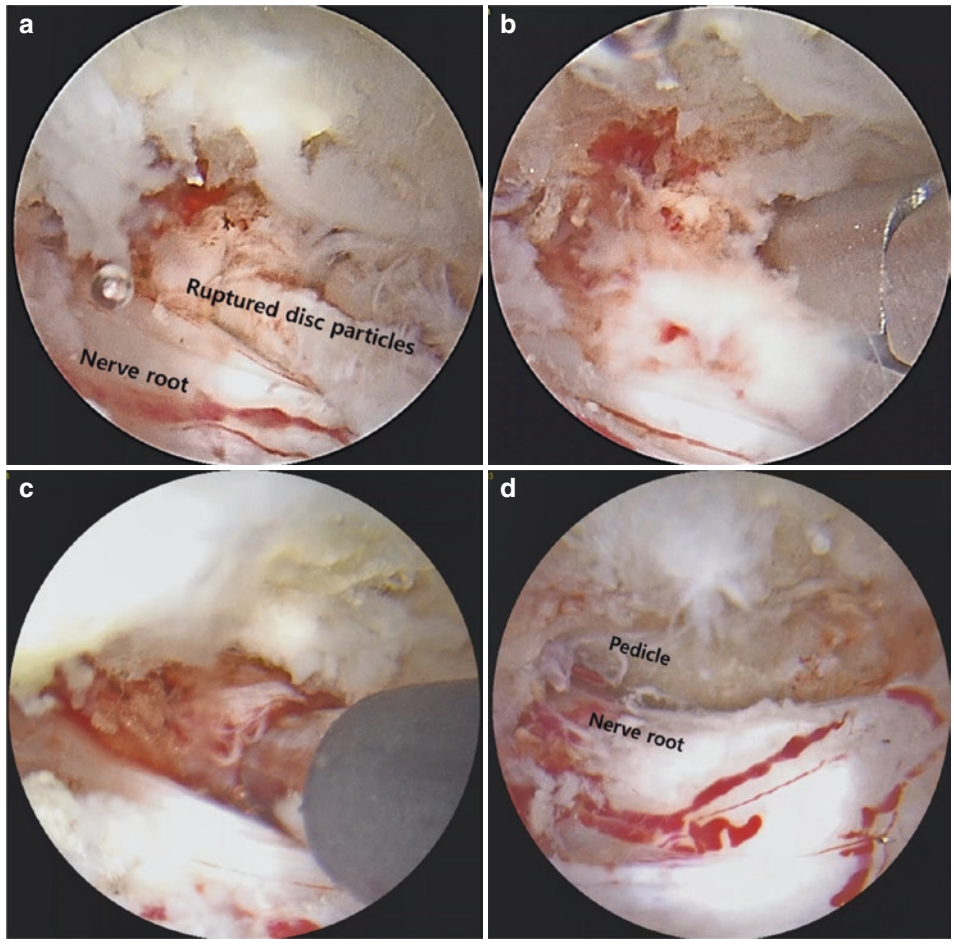


**Fig. 21.6** A case of the contralateral sublaminar approach for disc particle removal at L2-3 left. 3D endoscopy could clearly distinguish between the contralateral nerve root and the ruptured disc particles (**a**). Ruptured disc particles were safely removed without injuring the nerve root (**b**). Bleeding from the epidural vein could be controlled by RF without nerve root injury (**c**). The final endoscopic image demonstrated complete decompression of the contralateral L3 nerve root and medial border of the pedicle (**d**)

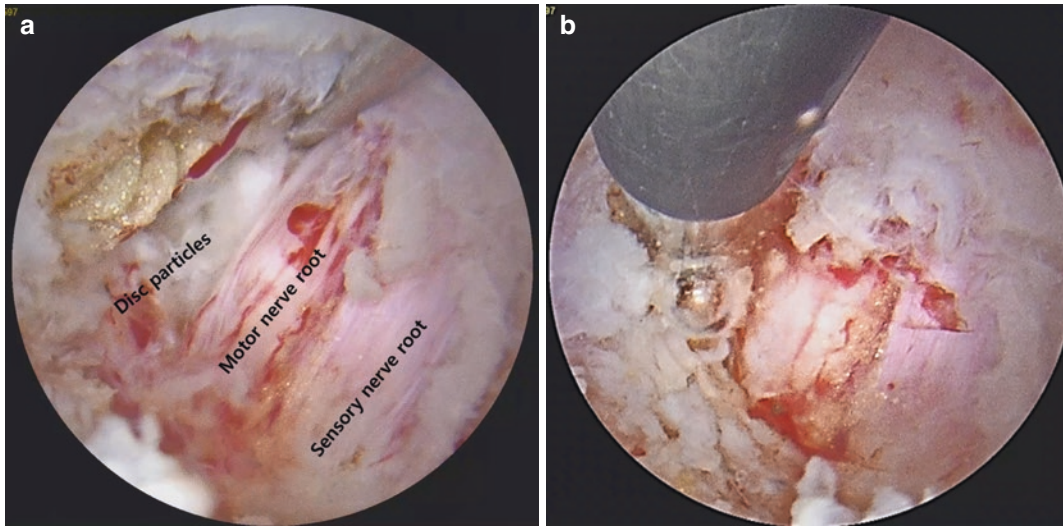


**Fig. 21.7** A case of cervical posterior foraminotomy of the right C6-7. 3D endoscopy demonstrated dual nerve roots of the right C7 (**a** and **b**). Also, disc particles were clearly visible (**a**). Epidural bleeding could be safely controlled by RF under 3D visualization (**b**)

bone work. As the ligamentum flavum is exposed, the advantage of the 3D endoscope is realized when the ligamentum flavum is removed while protecting the dura. When removing the ligamentum flavum, the interface between the dura and ligament can accurately be seen by 3D visualization. After full exposure of the dura, the 3D anatomy of the dura and nerve roots can be seen. In particular, it has depth, so the opposite side such as the contralateral foramen, dura, and the nerve root is also well-demonstrated in the 3D images.

- **Advantages**

3D visualization makes it easy to understand surgical endoscopic anatomy, and 3D images seem to be a great help in endoscopic spine surgery training and education. In the personal experience of the author, 3D endoscopic surgery was very useful for teaching fellows who wanted to learn endoscopic surgery [14].

The sense of depth and stereoscopic vision of the 3D endoscope distinguished normal tissues and lesions well and seem to reduce damage to the normal tissues during surgery. Stereoscopic vision in 3D biportal endoscopic spine surgery may be related to the safety during endoscopic spine approaches. Since it provides depth sensation, it seems that it can reduce dural damage during surgery. Nervous structures such as the dura and nerve roots were well-distinguished from ruptured disc particles, vessels, and ligamentous structures. Therefore, the hypertrophied ligamentum flavum and ruptured disc particles were safely removed without neural structure injury. In addition, epidural veins could be easily cauterized without thermal damage to the dura.

- **Disadvantages**

We need to wear glasses (Fig. 21.2) specially designed for 3D visualization during 3D biportal endoscopic surgery. However, these special glasses produce slightly darkened vision. The 3D endoscope is slightly larger and heavier than the conventional biportal endoscope. Dizziness may be experienced until the is adapted to 3D vision [15].

## 21.6 Conclusion

Presently, the 3D endoscopic spine approach is available only in biportal endoscopic spine surgery systems. Depth sensation was a great advantage in 3D endoscopic surgery, and the stereognosis of 3D biportal endoscopy was related to the safety of surgery and the prevention of perioperative complications. Also, 3D endoscopic spine surgery may have advantages in the education and training of endoscopic spine surgery.

## References


1. Mulder E, Janki S, Terkivatan T, Klop KWJ, Ijzermans JNM, Tran TCK. 3D endoscopic donor nephrectomy versus robot-assisted donor nephrectomy: a detailed comparison of 2 prospective cohorts. Transplantation. 2018;102(6):e295–300.
2. Shoakazemi A, Evins AI, Burrell JC, Stieg PE, Bernardo A. A 3D endoscopic transtubular transcallosal approach to the third ventricle. J Neurosurg. 2015;122(3):564–73.
3. Altieri R, Tardivo V, Pacca P, Pennacchietti V, Penner F, Garbossa D, et al. 3D HD endoscopy in skull base surgery: from darkness to light. Surg Technol Int. 2016;29:359–65.
4. Nomura K, Kikuchi D, Kaise M, Iizuka T, Ochiai Y, Suzuki Y, et al. Comparison of 3D endoscopy and conventional 2D endoscopy in gastric endoscopic submucosal dissection: an ex vivo animal study. Surg Endosc. 2019;33(12):4164–70.
5. Zheng ZF, Wu LM, Jian CX, Liu W. Comparison of 3-dimensional and 2-dimensional endoscopic thyroid lobectomy via the trans-thoracoareolar approach. Saudi Med J. 2018;39(2):142–6.
6. Harada H, Kanaji S, Hasegawa H, Yamamoto M, Matsuda Y, Yamashita K, et al. The effect on surgical skills of expert surgeons using 3D/HD and 2D/4K resolution monitors in laparoscopic phantom tasks. Surg Endosc. 2018;32(10):4228–34.
7. Singh A, Saraiya R. Three-dimensional endoscopy in sinus surgery. Curr Opin Otolaryngol Head Neck Surg. 2013;21(1):3–10.
8. Heo DH, Lee DC, Kim HS, Park CK, Chung H. Clinical results and complications of endoscopic lumbar interbody fusion for lumbar degenerative disease: a meta-analysis. World Neurosurg. 2021;145:396–404.
9. Heo DH, Park CK. Clinical results of percutaneous biportal endoscopic lumbar interbody fusion with application of enhanced recovery after surgery. Neurosurg Focus. 2019;46(4):E18.
10. Heo DH, Lee DC, Park CK. Comparative analysis of three types of minimally invasive decompressive surgery for lumbar central stenosis: biportal endoscopy, uniportal endoscopy, and microsurgery. Neurosurg Focus. 2019;46(5):E9.
11. Heo DH, Hong YH, Lee DC, Chung HJ, Park CK. Technique of biportal endoscopic transforaminal lumbar interbody fusion. Neurospine. 2020;17(Suppl 1):S129–s37.
12. Sinha R, Chawla L, Raje S, Rao G. A retrospective comparative analysis of 2D versus 3D laparoscopy in total laparoscopic hysterectomy for large uteri (>/= 500g). Surg Technol Int. 2018;33:38–43.
13. Zundel S, Lehnick D, Heyne Pietschmann M, Trück M, Szavay P. A suggestion on how to compare 2D and 3D laparoscopy: a qualitative analysis of the literature and randomized pilot study. J Laparoendosc Adv Surg Tech. 2019;29(1):114–20.
14. Bickerton R, Nassimizadeh A, Ahmed S. Three-dimensional endoscopy: the future of nasoendoscopic training. Laryngoscope. 2019;129(6):1280–5.
15. Montanari E, Schwameis R, Veit-Rubin N, Kuessel L, Husslein H. Basic laparoscopic skills training is equally effective using 2D compared to 3D visualization: a randomized controlled trial. J Clin Med. 2020;9(5)

# Navigation in Spinal Tumor Surgery

22

Kuo-Tai Chen, Guang-Xun Lin, Jin-Sung Kim, and Chien-Min Chen

## Abbreviations

CT Computed tomography
MRI Magnetic resonance imaging

## 22.1 Introduction

A spinal tumor is a possible source of pain or neurological dysfunction. Primary tumors of the vertebral column are rare in comparison to metastatic spine tumors. Less than 10% of all primary bony tumors arise from the vertebral column.[1] In contrast, metastatic tumors are the most common neoplasm of the spine. Autopsy studies have shown that spinal metastasis was found in as many as 30% of patients with malignancy [2]. Of all potential sites of bone metastasis, spine metastasis accounts for 70% of all osseous metastasis [3–5]. The spinal metastasis can cause pain by the destruction of the bony structure. Besides, metastatic epidural spinal cord compression occurs in 5–10% of cancer patients, causes debilitating dysfunction, and requires operative management [6]. With the aging population and improvements in cancer diagnosis and therapies, the number of patients with symptomatic spinal metastases has increased. Most spinal metastases are incurable and usually reserved for chemotherapy and radiotherapy. The advancements in surgical techniques and clinical outcomes following multidisciplinary treatments have extended the overall survival of patients with metastatic spine disease.

Surgical strategies of spinal tumors usually incorporate biopsy for diagnosis, resection for decompression of neural structures, or instrumentation for reconstruction and stabilization of vertebral column. Management of spinal tumors depends on the tumor's histology. For benign spinal tumors, complete resection is the aim of surgery. The goal of surgical treatment in spinal metastasis is largely palliative. The surgical strat-

K.-T. Chen
Department of Neurosurgery, Chang Gung Memorial Hospital, Chia-Yi, Taiwan

G.-X. Lin
Department of Orthopedics, The First Affiliated Hospital of Xiamen University, School of Medicine, Xiamen University, Xiamen, Fujian, China

Department of Clinical Medicine, Fujian Medical University, Fuzhou, Fujian, China

J.-S. Kim
Department of Neurosurgery, Seoul St Mary's Hospital, The Catholic University of Korea, College of Medicine, Seoul, Korea (Republic of)

C.-M. Chen (✉)
Division of Neurosurgery, Department of Surgery, Changhua Christian Hospital, Changhua, Taiwan

School of Medicine, Kaohsiung Medical University, Kaohsiung, Taiwan

College of Nursing and Health Sciences, Dayeh University, Dacun, Taiwan
e-mail: 96015@cch.org.tw



J.-S. Kim et al. (eds.), *Technical Advances in Minimally Invasive Spine Surgery*,
https://doi.org/10.1007/978-981-19-0175-1_22

egy can be variable according to the extent and location of metastasis, tumor histology, and performance status of patients. For most spinal metastasis, surgical resection can only achieve local tumor control, and adjuvant chemotherapy or radiotherapy is mandatory for systemic control to prolong survival. Fast recovery time is crucial for metastatic spine disease patients to reduce the period between surgery and postoperative adjuvant chemotherapy or radiotherapy. For epidural metastasis, the goal is adequate decompression of neural structure to restore neurological function. Instrumentation to restore or maintain stability is sometimes necessary while instability after wide resection. The decision of optional treatment for these patients is often a complex and challenging process because of the numerous issues involved and requires multidisciplinary evaluation by the oncologist, radiation oncologist, and surgeon.

Surgical techniques of spine surgeries have evolved and increasingly become minimally invasive. With the advent of different technologies, the surgeon can decrease tissue damage and the incidence of subsequent morbidities. Image-guided procedures are the basis of modern spinal surgeries. The C-arm fluoroscopy is the most common tool during spinal procedures. However, fluoroscopy is a two-dimensional image. Surgeons need to rotate C-arm repeatedly to localize the target in the three-dimensional structure during spinal surgery. The computer-assisted navigation system has been increasingly applied in spinal surgery. Navigation in spinal surgery is exclusively performed using an infrared navigation system combined with an intraoperative CT scanner or three-dimensional fluoroscopy. The navigation system and CT images can directly output images of multiple anatomical planes and provide a three-dimensional real-time localization without interruption for image acquisition. This chapter will introduce the application of CT-based navigation in spinal tumor surgery.

## 22.2 Applications of Navigation in Spinal Tumor Surgery

The role of navigation can be variable in different surgical interventions. It depends on the available equipment and experience of surgeons to apply the technology. Because navigation has been widely used in percutaneous instrumentation procedures, there are customized surgical instruments with a built-in navigation tracker. For other purposes, the tracker with a universal adaptor can be helpful to be anchored on the surgical instruments. The operator can easily apply the accessories to customize the navigating instruments.

### 22.2.1 Localization with Intraoperative CT Scanography

The thoracic spine is the most common site of metastasis. The thoracic spinal metastases compose 70% of all metastases, followed by the lumbar spine (20%) and cervical spine (10%) [7–9]. Unlike a degenerative spinal disease, spinal tumor surgery is more common at the thoracic level. However, localization of thoracic level on fluoroscopic images is technically demanding due to the complex radiological anatomy compared with the lumbar or cervical spine. Because the navigation error is related to the distance between the reference arc and the index level, the reference arc should be docked less than three levels away from the index level. The surgeon can do CT scanography with radiopaque markers on the skin, such as coins or suction catheters (Fig. 22.1). Then, the target can be localized by looking at the CT scanography, and skin incision can be designed accordingly. Compared with the standard CT scan, scanography can be obtained quickly and cause less radiation exposure.

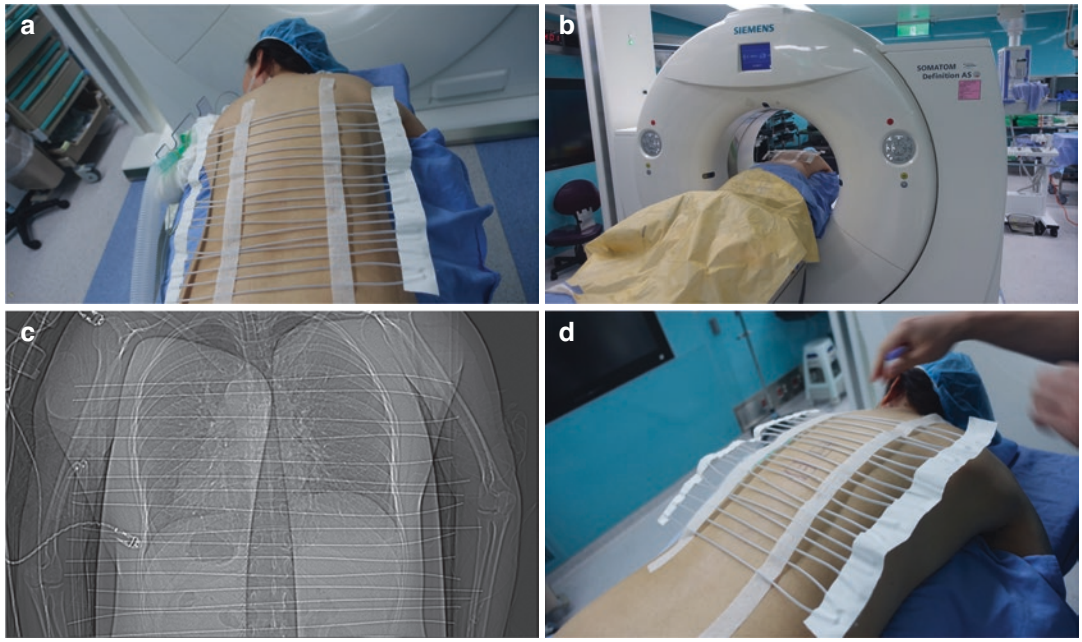


**Fig. 22.1** The CT scanography can help to localize index level with low-dose radiation. (**a**) The radio-opaque tubes were pasted on the skin. (**b**) Perform intraoperative CT scan. (**c**) The index level at the thoracic spine can be identified in the CT scenography. (**d**) Markings on the skin

### 22.2.2 Tracking During the Surgical Procedures

Surgical treatment of spinal metastases is associated with a high risk of intraoperative complications, including injury to the spinal cord or nerves and large vessels during tumor resection and implantation of pedicle screws [10–15]. The familiar spinal navigation is CT-based and valuable to identify bony landmarks. The operator may sometimes have difficulty identifying the anatomical vertebrae features on fluoroscopy due to osteolytic lesion or pathological fracture with deformity. The CT images can delineate vertebral anatomy in detail. The software of current computer-assisted navigation is available to merge preoperative MRI with intraoperative CT images. Then, the tumor can be marked in the merged intraoperative images of the navigation system. Besides, the vascular structure, dural sac, or extent of bone resection can also be identified with spinal navigation. Therefore, spinal navigation might benefit percutaneous procedures such as biopsy, cement augmentation [16], or radiofrequency ablation [17, 18] because the navigated needle can be displayed on the screen simultaneously during procedures. When the lesion is near the major vessels or neural structures, the operator can reach the target with navigated instruments and avoid injury to vessels or neural structures.

While surgical treatment in epidural metastasis, surgeons may identify the epidural tumor first before encountering the dural sac. Therefore, dural or even cord injury may happen while detaching the tumor away from the epidural space, especially in tumors with high vascularity. With spinal navigation, the operator can design skin incisions and plan the extent of resection preoperatively. During the operation, intraoperative navigation can guide the surgeon to confirm the laminotomy to an adequate extent before removing the tumor. After vertebral resection or circumferential decompression with separation surgery, spinal instrumentation is mandatory to restore stability. There are various interbody

devices for the reconstruction of the anterior column after resecting the vertebral body. Pedicle screw fixation is usually necessary to reinforce spinal stability. The instrumentation procedures with computer-assisted navigation in the cervical, thoracic, and lumbar spine have lower rates of pedicle screw misplacement [19, 20]. There is a pitfall in navigation-guided procedures. Spinal navigation is not a real-time image-guided device. It usually works according to the registered intraoperative images. Once the spine is unstable during instrumentation procedures, manipulation during pedicle screw placement may cause the shift of anatomical structures. The navigation error might happen due to the mismatch of actual anatomy and images on the navigation display screen. Therefore, pedicle screws are usually inserted first before tumor resection (Fig. 22.2).

A crucial advantage of computer-assisted navigation is to provide three-dimensional information with reconstruction images. Therefore, the operator can work smoothly without interruption for the acquisition of multi-plane C-arm fluoroscopy. Moreover, the scanner can move out of the surgical table. The operator can work comfortably without the interference of an X-ray tube or intensifier. The workflow can be simplified, and the radiation exposure of the surgical team can be minimized [21, 22]. Once localizing the tumor location, spinal navigation may be limited during the tumor resection procedure. After the tumor removal, an intraoperative CT scan can be repeated to evaluate the resection margin to ensure radical resection and good instrument position.

## 22.3 Case Illustration

Endoscopic spine surgery has evolved with the development of technologies and techniques. There have been several case reports about endoscope-assisted spinal tumor resection [23–25]. The full-endoscopic surgery is conducted with continuous saline irrigation. Therefore, the application of full-endoscopic surgery for the spinal tumor is limited to an extradural tumor with low vascularity and less adhesion or invasion to the dura. The benign extradural tumor with a well-defined margin could be potentially treated with a full-endoscopic technique.

A 52-year-old man had suffered from progressive pain over the buttock with radiation to his left lower leg for one year. The pain was mainly in the left calf and plantar foot, accompanied by numbness and abnormal temperature sensation. The dynamic lumbar radiography showed no instability. The MRI revealed a mass lesion in the left S1 lateral recess. He underwent a full-endoscopic interlaminar approach for tumor removal under general anesthesia. The operation was assisted with Robotic C-arm (ARTIS Pheno,

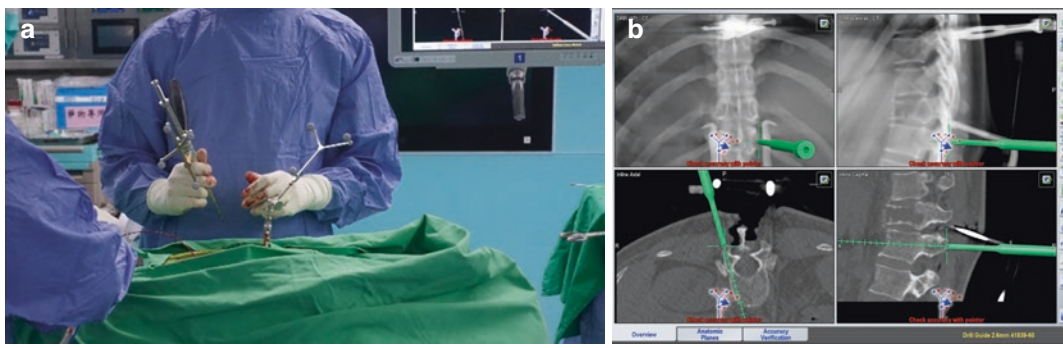


**Fig. 22.2** (**a**) Reference arc was fixed on the spinous process. The pedicle screw entry point and trajectory were planned by a drill guide with a navigation tracker. (**b**) The navigation display screen showed the simulation of the pedicle screw trajectory for planning the instrumentation

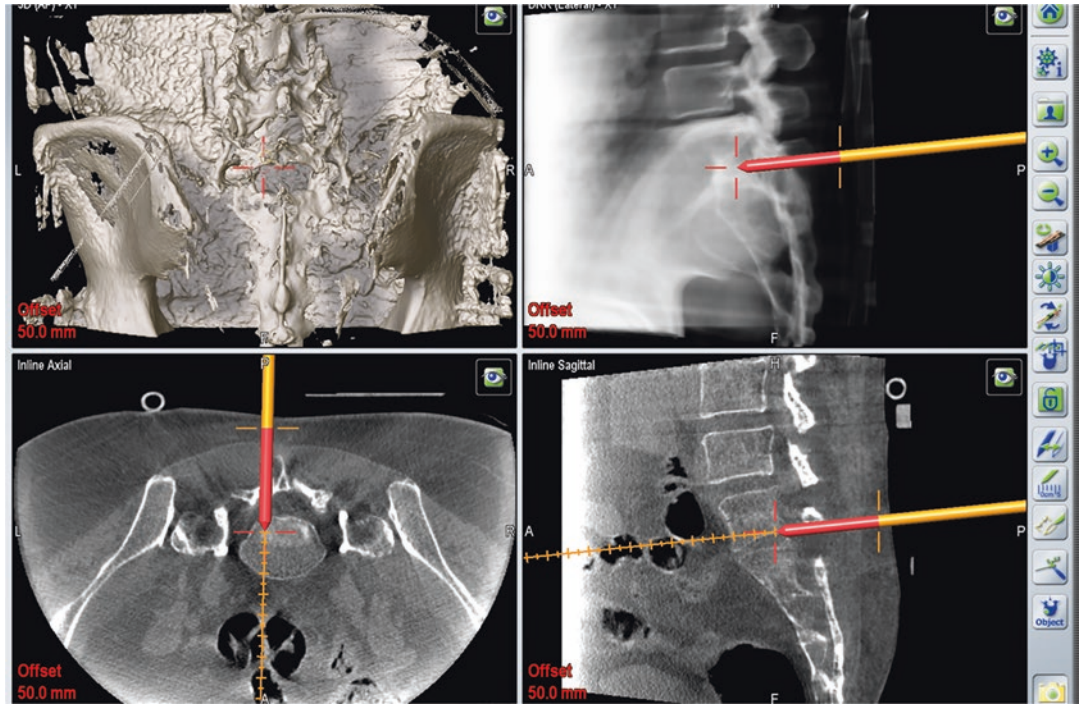


**Fig. 22.3** Robotic C-arm navigation guided the endoscopic trajectory to reach the tumor

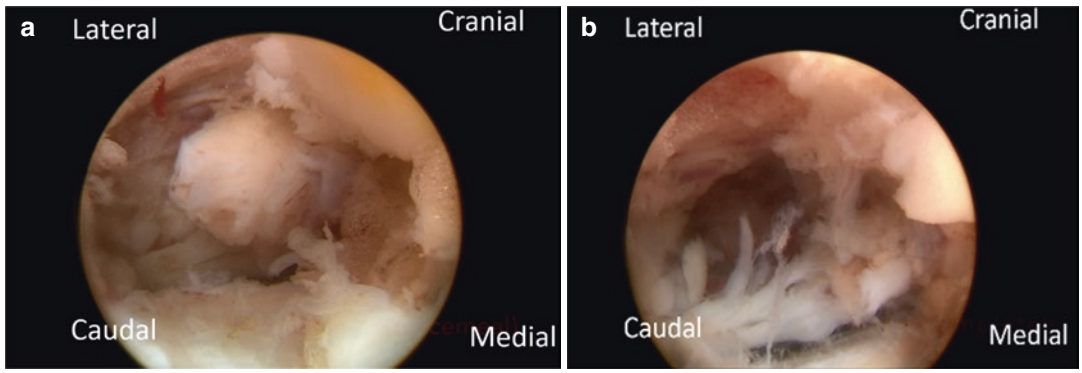


**Fig. 22.4** (**a**) Tumor was identified at left S1-2 lateral recess and attached to the nerve root. (**b**) The endoscopic view after removing the tumor

Simens) navigation (Fig. 22.3). The spinal navigation can guide the endoscope during the initial phases to reach the tumor in the S1-2 lateral recess. The trajectory tracking can provide real-time information to avoid disorientation. The low-vascularized benign tumor attaching to the nerve root was removed under endoscopic visualization (Fig. 22.4). After the operation, his leg pain improved from 8 to 2 by VAS score. There was no neurological deficit, such as motor weakness, dysesthesia, or urinary incontinence. The pathologic diagnosis was ganglioneuroma. There was no residual tumor in the postoperative MRI (Fig. 22.5).

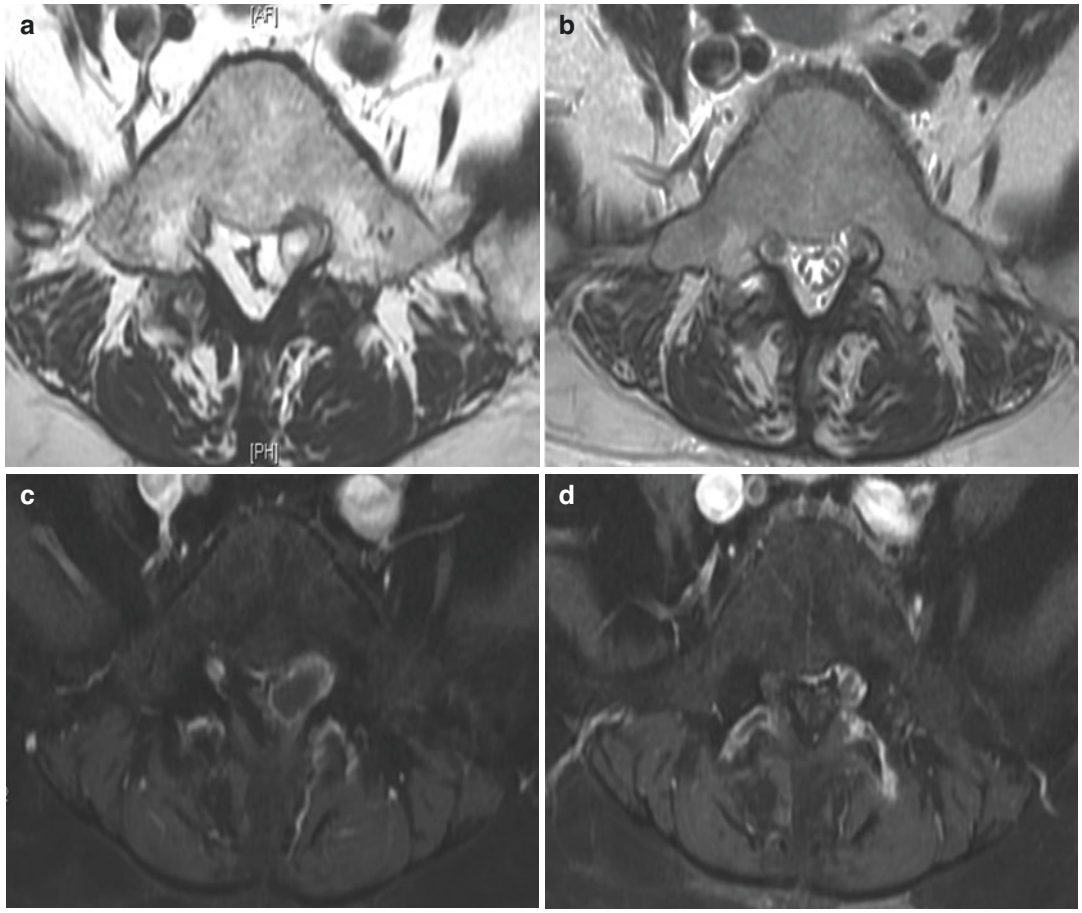


**Fig. 22.5** Comparison of preoperative and postoperative three months MRI findings. (**a**, **c**) Preoperative MRI T2WI images and T1WI images with contrast; (**b**, **d**) Postoperative MRI T2WI images and T1WI images with contrast

## 22.4 Conclusion

With the advancement of technology and techniques, spine surgeries have tended to be minimally invasive. The basis of minimally invasive spine surgery is image-guided procedures. Compared with fluoroscopic guidance, computer-assisted navigation can provide three-dimensional images and real-time tracking of instruments. In general, spinal navigation can help localization of target, orientating surgical trajectory, and instrumentation. The goal of spinal tumor surgery can vary due to the nature of the tumor and disease stage. The navigation is applicable in all kinds of surgical strategies and even minimally invasive approaches. It assists the surgeon in maximal resection in debulking and separation surgeries, instrumentation accuracy, and precisely targeting local ablative therapies. While the navigation device and techniques continuously develop, spinal navigation will be an indispensable tool for spinal oncologic surgeries.

## References

1. Chi JH, Bydon A, Hsieh P, Witham T, Wolinsky JP, Gokaslan ZL. Epidemiology and demographics for primary vertebral tumors. Neurosurg Clin N Am. 2008;19(1):1–4. https://doi.org/10.1016/j.nec.2007.10.005.
2. Sundaresan N, Boriani S, Rothman A, Holtzman R. Tumors of the osseous spine. J Neurooncol.

2004;69(1–3):273–90. https://doi.org/10.1023/b:neon.0000041888.33499.03.
3. Sutcliffe P, Connock M, Shyangdan D, Court R, Kandala NB, Clarke A. A systematic review of evidence on malignant spinal metastases: natural history and technologies for identifying patients at high risk of vertebral fracture and spinal cord compression. Health Technol Assess. 2013;17(42):1–274. https://doi.org/10.3310/hta17420.
4. Prasad D, Schiff D. Malignant spinal-cord compression. Lancet Oncol. 2005;6(1):15–24. https://doi.org/10.1016/S1470-2045(04)01709-7.
5. Wewel JT, O'Toole JE. Epidemiology of spinal cord and column tumors. Neurooncol Pract. 2020;7(Suppl 1):i5–9. https://doi.org/10.1093/nop/npaa046.
6. Sciubba DM, Gokaslan ZL. Diagnosis and management of metastatic spine disease. Surg Oncol. 2006;15(3):141–51. https://doi.org/10.1016/j.suronc.2006.11.002.
7. Gilbert RW, Kim JH, Posner JB. Epidural spinal cord compression from metastatic tumor: diagnosis and treatment. Ann Neurol. 1978;3(1):40–51. https://doi.org/10.1002/ana.410030107.
8. Gerszten PC, Welch WC. Current surgical management of metastatic spinal disease. Oncology (Williston Park). 2000;14(7):1013–24; discussion 24, 29–30
9. Byrne TN. Spinal cord compression from epidural metastases. N Engl J Med. 1992;327(9):614–9. https://doi.org/10.1056/NEJM199208273270907.
10. Konovalov NA, Nazarenko AG, Asyutin DS, Onoprienko RA, Korolishin VA, Cherkiev IU, et al. The use of intraoperative neuroimaging tools and a navigation system in surgical treatment of primary and metastatic tumors of the spine. Zhurnal voprosy neirokhirurgii imeni N N Burdenko. 2016;80(2):5–14. https://doi.org/10.17116/neiro20168025-14.
11. Fehlings MG, Nater A, Tetreault L, Kopjar B, Arnold P, Dekutoski M, et al. Survival and clinical outcomes in surgically treated patients with metastatic epidural spinal cord compression: results of the Prospective Multicenter AOSpine Study. J Clin Oncol. 2016;34(3):268–76. https://doi.org/10.1200/JCO.2015.61.9338.
12. Ohashi M, Hirano T, Watanabe K, Hasegawa K, Ito T, Katsumi K, et al. En bloc spondylectomy for spinal metastases: detailed oncological outcomes at a minimum of 2 years after surgery. Asian Spine J. 2019;13(2):296–304. https://doi.org/10.31616/asj.2018.0145.
13. Vazifehdan F, Karantzoulis VG, Igoumenou VG. Surgical treatment for metastases of the cervical spine. Eur J Orthop Surg Traumatol. 2017;27(6):763–75. https://doi.org/10.1007/s00590-017-2002-0.
14. Jeremy CW, Patrick B, Nandita M, Yoshiya Y, Eric L, Michael S, et al. Single-stage posterolateral transpedicular approach for resection of epidural metastatic spine tumors involving the vertebral body with circumferential reconstruction: results in 140 patients. J Neurosurg: Spine. 2004;1(3):287–98. https://doi.org/10.3171/spi.2004.1.3.0287.
15. Quraishi NA, Arealis G, Salem KMI, Purushothamdas S, Edwards KL, Boszczyk BM. The surgical management of metastatic spinal tumors based on an Epidural Spinal Cord Compression (ESCC) scale. Spine J. 2015;15(8):1738–43. https://doi.org/10.1016/j.spinee.2015.03.040.
16. Cianfoni A, Distefano D, Chin SH, Varma AK, Rumboldt Z, Bonaldi G. Percutaneous cement augmentation of a lytic lesion of C1 via posterolateral approach under CT guidance. Spine J. 2012;12(6):500–6. https://doi.org/10.1016/j.spinee.2012.05.012.
17. Kavakebi P, Freyschlag CF, Thome C. How I do it-optimizing radiofrequency ablation in spinal metastases using iCT and navigation. Acta Neurochir (Wien). 2017;159(10):2025–8. https://doi.org/10.1007/s00701-017-3267-0.
18. Moussazadeh N, Evans LT, Grasu R, Rhines LD, Tatsui CE. Laser interstitial thermal therapy of the spine: technical aspects. Neurosurg Focus. 2018;44(VideoSuppl2):V3. https://doi.org/10.3171/2018.4.FocusVid.17732.
19. Shin BJ, James AR, Njoku IU, Hartl R. Pedicle screw navigation: a systematic review and meta-analysis of perforation risk for computer-navigated versus freehand insertion. J Neurosurg Spine. 2012;17(2):113–22. https://doi.org/10.3171/2012.5.SPINE11399.
20. Han W, Gao Z, Wang J, Li Y, Peng X, Rui J. Pedicle screw placement in the thoracic spine: a comparison study of computer-assisted navigation and conventional techniques. 2010;33.
21. Klingler JH, Sircar R, Scheiwe C, Kogias E, Kruger MT, Scholz C, et al. Comparative study of C-arms for intraoperative 3-dimensional imaging and navigation in minimally invasive spine surgery Part II: radiation exposure. Clin Spine Surg. 2017;30(6):E669–E76. https://doi.org/10.1097/BSD.0000000000000187.
22. Mendelsohn D, Strelzow J, Dea N, Ford NL, Batke J, Pennington A, et al. Patient and surgeon radiation exposure during spinal instrumentation using intraoperative computed tomography-based navigation. Spine J. 2016;16(3):343–54. https://doi.org/10.1016/j.spinee.2015.11.020.
23. Tsai SH, Wu HH, Cheng CY, Chen CM. Full endoscopic interlaminar approach for nerve root decompression of sacral metastatic tumor. World Neurosurg. 2018;112:57–63. https://doi.org/10.1016/j.wneu.2018.01.075.
24. Ying GY, Yao Y, Shen F, Ren YC, Chen CM, Zhu YJ. Percutaneous endoscopic removal of a lumbar epidural angiolipoma via interlaminar approach: a technical report. World Neurosurg. 2017;99:59–62. https://doi.org/10.1016/j.wneu.2016.11.088.
25. Ying GY, Yao Y, Shen F, Wu ZY, Chen CM, Zhu YJ. Percutaneous endoscopic removal of cervical foraminal schwannoma via interlaminar approach: a case report. Oper Neurosurg (Hagerstown). 2018;14(1):1–5. https://doi.org/10.1093/ons/opx088.

# 23 The Usefulness of Navigation in Thoracic Endoscopic Discectomy and Decompression

Kuo-Tai Chen, Jin-Sung Kim, and Chien-Min Chen

## Abbreviations

| | |
|---|---|
| CT | computed tomography |
| OLF | ossification of ligamentum flavum |
| OPLL | ossification of the posterior longitudinal ligament |
| TDH | thoracic disc herniation |

## 23.1 Introduction

Compared with the cervical and lumbar spine, surgical disorders of the thoracic spine are less common. These disorders may present neurological manifestations such as upper back pain; sensory deficit; gait disturbance; bowel, bladder, or sexual dysfunction; paraparesis, or paraplegia. The clinical presentation results from compression of the thoracic spinal cord. Except for trauma-related injuries, the etiologies of spinal canal stenosis include thoracic disc herniation (TDH), ossification of ligamentum flavum (OLF), or posterior longitudinal ligament (OPLL), and tumor invasion into the central canal.

The epidemiologic study of thoracic spinal stenosis showed that OLF was the most common etiology and accounted for 41.5% of the cases. The rest was mainly comprised of TDH and OPLL at 32.4% and 18.7%, respectively. Thoracic OPLL occurs mostly in the middle-thoracic spine, while OLF predominantly occurs in the lower-thoracic spine [1]. The TDH is commonly located in both the middle and lower thoracic spine. Although the incidence of TDH ranges from 7% to 37%, only 0.25–0.57% of all TDH are symptomatic [2–4].

Thoracic spine surgeries comprise less than 10% of spine surgeries [5]. A surgeon's experience may be variable due to the small number of cases, especially for endoscopic thoracic surgery. Besides, wrong-level surgery is more common in the thoracic region due to difficulty in localization. The thoracic spine on fluoroscopy might be obscure due to lung shadow, ribs, or scapula. These factors affect the quality of images and make interpretation challenging. The above prob-

K.-T. Chen
Department of Neurosurgery, Chang Gung Memorial Hospital, Chia-Yi, Taiwan

J.-S. Kim
Department of Neurosurgery, Seoul St Mary's Hospital, The Catholic University of Korea, College of Medicine, Seoul, Korea (Republic of)

C.-M. Chen (✉)
Department of Neurosurgery, Chang Gung Memorial Hospital, Chia-Yi, Taiwan

Division of Neurosurgery, Department of Surgery, Changhua Christian Hospital, Changhua, Taiwan

School of Medicine, Kaohsiung Medical University, Kaohsiung, Taiwan

College of Nursing and Health Sciences, Dayeh University, Dacun, Taiwan
e-mail: 96015@cch.org.tw



J.-S. Kim et al. (eds.), *Technical Advances in Minimally Invasive Spine Surgery*,
https://doi.org/10.1007/978-981-19-0175-1_23

lems can be solved easily by CT-guided technique. CT images integrated with a navigation system have been available and adopted extensively in minimally invasive spine surgery. The previous application of the CT-based navigation system mainly focused on instrumentation. In this chapter, the authors will introduce the application of CT-based navigation in full-endoscopic thoracic decompression surgeries.

## 23.2 Anatomical Considerations

The rib cage stabilizes the thoracic spine and increases its rigidity by two- to threefold [6]. Except for the 11th and 12th ribs, the ribs articulate anteriorly with the sternum anteriorly and posteriorly with the associated thoracic vertebrae. Besides, these ribs also articulate with the vertebral body above via an inferior facet. The 11th and 12th vertebrae articulate with their associated ribs only. These vertebrae contain no inferior facets. Ribs 11 and 12 are floating without an anterior articulation with the rib cage. Besides, facets of the thoracic spine are more coronally oriented, which limits rotation. This configuration spares most of the thoracic decompression above T10 level instrumentation and fusion.

The thoracic spinal canal is more narrowed than the cervical and lumbar regions. The epidural space between the dura and pedicle is also relatively smaller in the thoracic regions. Thus, surgical manipulation in the canal can have significant neurological consequences. The surgical approaches to the thoracic spine are limited and cannot cross the canal region. The surgical corridor decompresses the thoracic spinal cord or roots through posterior or posterolateral approaches. The laminae of the thoracic vertebrae are broad, thick, and imbricated (Fig. 23.1a). Unlike the lower lumbar region, there is no natural interlaminar window in the thoracic region. Therefore, laminotomy is necessary while adopting the posterior route for decompression. The only natural orifice in the thoracic region is the intervertebral foramen. The foramen is large and

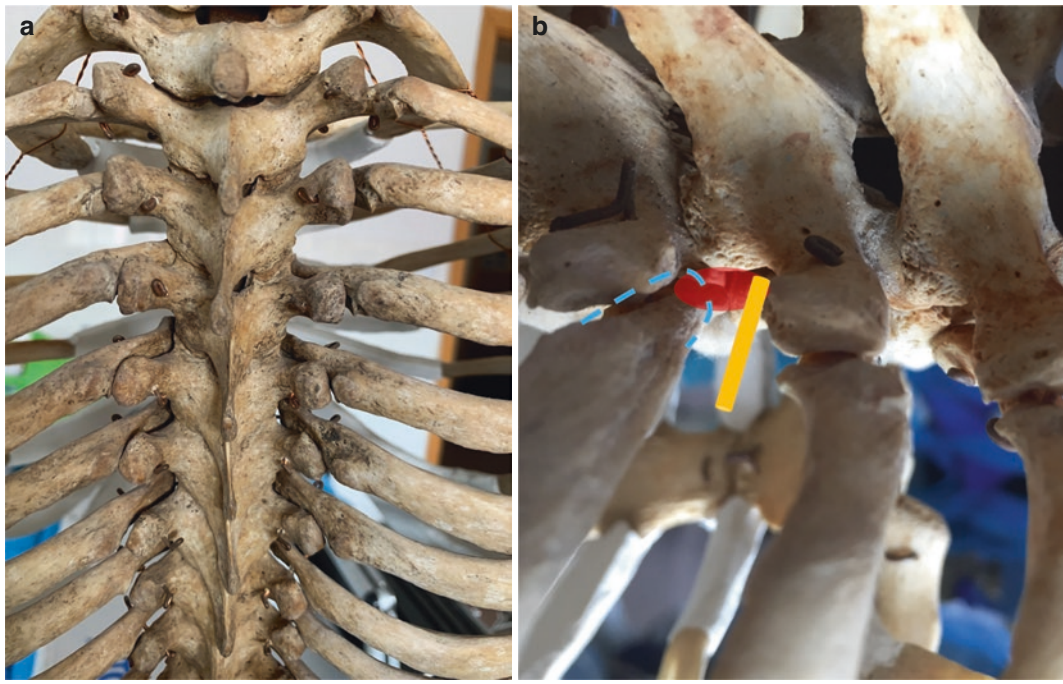


**Fig. 23.1** (**a**) The dorsal view of the thoracic vertebrae shows imbricated laminae without interlaminar window. (**b**) The inline view of the transforaminal corridor shows the rib head (blue dotted line) occupies the caudal part of the foramen (red zone) and decreases the safe zone area during operation. (Orange line: nerve root)

oval from cephalad to caudal. The rib head is located at the lateral and caudal part of the foramen and decreases the working space during the posterolateral approach [7] (Fig. 23.1b).

## 23.3 Indications and Contraindications of Full-Endoscopic Thoracic Decompression

Indications:

- Pain in the upper back with radiation to the neck, chest, or arm is refractory with conservative treatment. The numbness and paresthesia in an intercostal distribution may accompany.
- MRI and CT scans show soft disc herniation or central canal stenosis due to OLF consistent with the distribution of present symptoms

Contraindications:

- Severe cord compression or total block on radiographic studies
- Calcified disc

## 23.4 Options of Full-Endoscopic Thoracic Decompression

Several techniques have been proposed to approach thoracic spine lesions. The traditional thoracotomy or thoracoscopic techniques from an anterior or lateral trajectory can get good visualization and direct access to the vertebral body and intervertebral disc. However, potential injury to lungs or great vessels is a crucial safety issue. Besides, neurosurgeons and orthopedic surgeons might require thoracic surgeons' assistance to provide adequate access to the transthoracic approach. The anterior or lateral approach is usually considered when corpectomy or vertebrectomy is indicated in trauma, deformity, or cancer surgery. Reconstruction with instrumentation is usually necessary after complete resection of the vertebral body. Thus, for the direct decompression of the thoracic spinal cord in minimally invasive ways, especially degenerative etiologies, the authors recommend posterior or posterolateral approaches to minimize complications of the thoracic visceral organs.

The choice of surgical approach depends on the target lesion. For the thoracic spinal canal, the interlaminar approach is an effective and safe way to decompress the thoracic spinal cord. For TDH, the paramedian type can be reached by interlaminar or translaminar approach. If the disc herniation is located at the central portion, a transforaminal or transthoracic retropleural approach can be an alternative to remove the lesion [8] (Fig. 23.2). The current concept of full-endoscopic discectomy has evolved as a target-oriented trajectory regardless of how to approach the lesion. Therefore, preoperative CT and MRI are mandatory to plan the surgical approach before the operation. In most circumstances, the transforaminal or interlaminar approach can achieve adequate thoracic spinal cord decompression with minimal visceral or vascular injury risk.

The imbricated thoracic lamina and a lack of a true interlaminar window make the thoracic interlaminar endoscopic approach challenging. The landmarks of the thoracic spine on the lateral

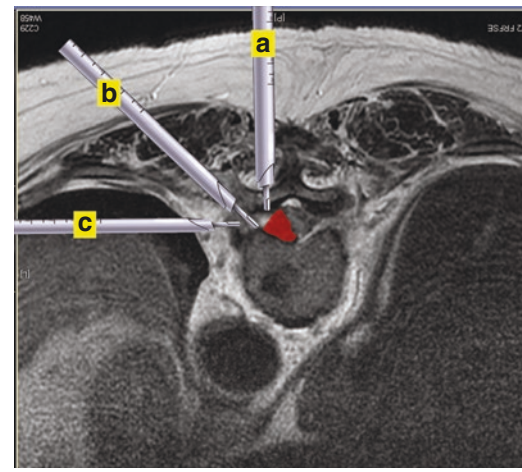


**Fig. 23.2** Different trajectories of full-endoscopic approach for paramedian TDH. (**a**) Interlaminar; (**b**) Transforaminal; (**c**) Transthoracic retropleural

view of fluoroscopy might not be shown clearly, mostly blurred by scapula at the upper thoracic level (T3-7). Currently, intraoperative navigation is available for minimally invasive surgeries. The authors will demonstrate how to combine the technologies for navigated full-endoscopic thoracic spinal surgery in the following paragraphs.

## 23.5 Surgical Technique

### 23.5.1 Operating Room Setup

The navigation system is usually integrated with different kinds of image acquisition suites. The typical image suites include 3D C-arm, portable CT scanner, or MRI scanner. For most spinal surgeries, bone landmarks are an essential reference during the procedure. Therefore, the 3D C-arm or portable CT scanner is ideal for acquiring intraoperative images. The hybrid operating room equipped with advanced medical imaging devices has been available and enabled minimally invasive surgeries (Fig. 23.3). The hybrid operating room integrating navigation and advanced imaging technologies can improve the workflow and efficiency of full-endoscopic spine surgery.

The full-endoscopic equipment and instruments can be tailored according to different approaches regardless of the spine level. The original interlaminar endoscopic set equipment with an 8-mm endoscope can be applied for the interlaminar approach to remove the paramedian disc or OLF. When transforaminal or transthoracic approaches are planned, the original transforaminal endoscopic set with a 7-mm endoscope will help remove the paramedian or central disc herniation.

### 23.5.2 Navigation Setup

The navigation setup is the same between different procedures. Patients should be intubated under general anesthesia, either with a single- or a double-lumen tube. The patient is placed on a radiolucent table in a prone position. CT scanogram is performed to localize the index level and anchor site of the reference array, usually the spinous process 1–2 levels rostral or caudal to the index level. Sterile prepping and draping are conducted after skin marking of the surgical level. A 2-cm incision is made to mount the adaptor of the reference array on the spinous process (Fig. 23.4). Hereafter, registration scanning is performed, and the surgical staff leaves the room and avoids unnecessary radiation exposure. The CT images are synchronized and processed in the navigation system computer, and the registration is complete automatically.


**Fig. 23.3** The hybrid operating room is equipped with a 3D robotic C-arm (the Artis pheno by Siemen Healthineers), a CT scanner, and a navigation system

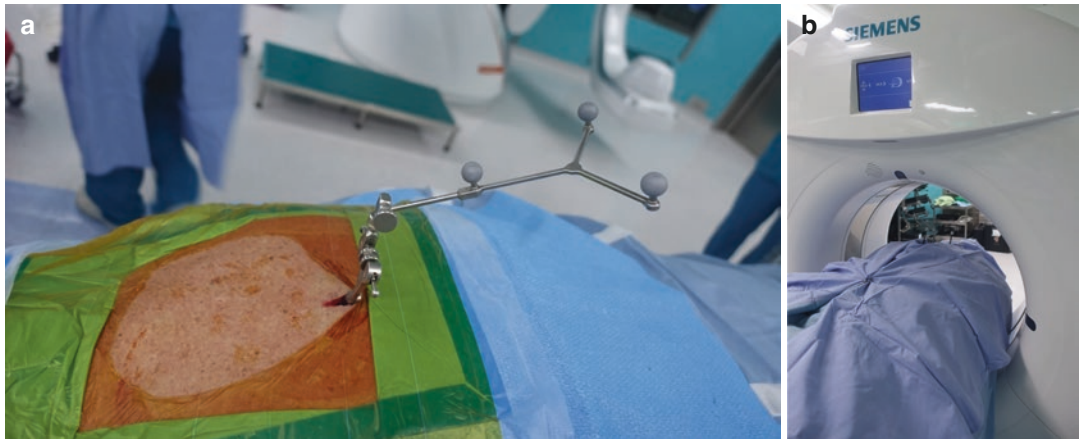


**Fig. 23.4** (**a**) The reference array is mounted on the spinous process before intraoperative CT scan. (**b**) Registration scan with intraoperative CT

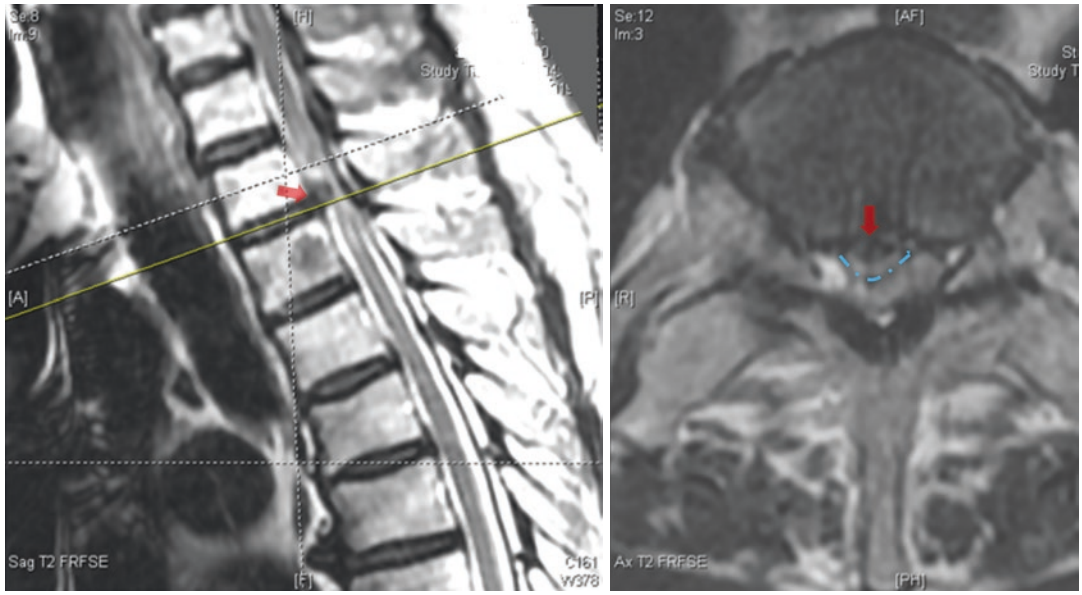


**Fig. 23.5** The preoperative MRI showed a right paramedian TDH combined with dural hypertrophic ligamentum flavum. (Red arrow: herniated disc; blue dotted line: margin of herniated disc)

### 23.5.3 Case Illustration: Full-Endoscopic Interlaminar Thoracic Decompression

A 77-year-old male patient had sustained progressive weakness of bilateral lower limbs and gait disturbance for more than 3 months. The numbness sensation below the nipple accompanied. The MRI showed thoracic spinal cord compression by right paramedian TDH at T3-4 level combined with hypertrophic ligamentum flavum (Fig. 23.5).

### 23.5.4 Determine Entry Point and Docking the Endoscope

After registration of navigation, the entry point could be determined by simulation on the navigation screen (Fig. 23.6). The landing point was at the lateral margin of the lamina. The trajectory was parallel to the target disc. After infiltration with local anesthetics, an 8-mm stab incision was made through the fascia at the planned entry point. The navigated instrument, such as an obturator or dissector, could guide the endoscopic device to the target during the procedure (Fig. 23.7). Then, the endoscope was brought into the field through the working cannula.

### 23.5.5 Full-Endoscopic Discectomy and Decompression

After confirming the surgical field with a navigation system, soft tissue was removed from the laminae with a bipolar probe and forceps. Then, the second step was to create an interlaminar window with a laminotomy. We used the endoscopic burr to drill the lamina down to the ligamentum flavum (LF) under endoscopic visualization. Meanwhile, a tracker-mounted dissector or handpiece of burr could guide the surgical corridor's direction and depth. The drilling began from the inferior margin of the cephalad lamina (T3) and the superior margin of the caudal lamina (T4). The LF was kept intact while doing a laminotomy.

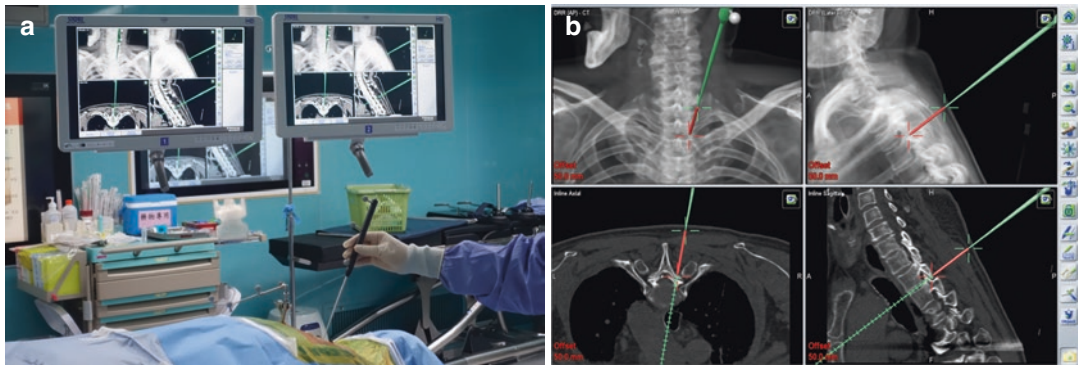


**Fig. 23.6** (**a**) Determine the entry point by simulation on the navigation screen. (**b**) Screenshot of entry point and trajectory planning

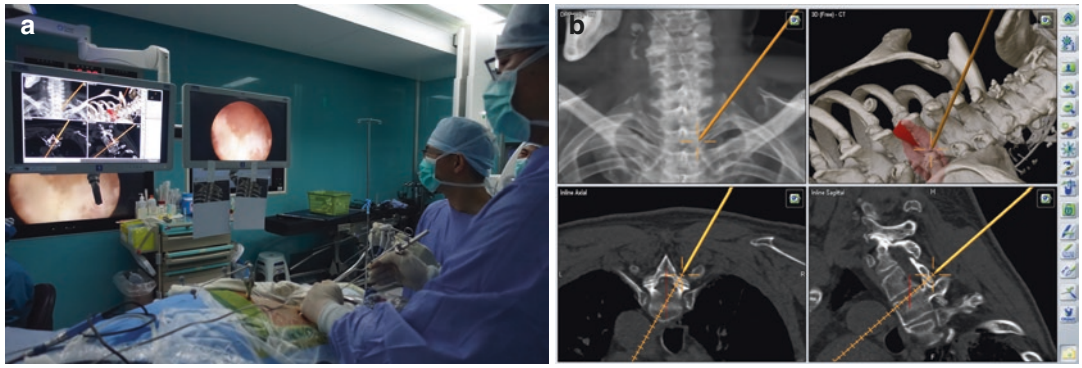


**Fig. 23.7** (**a**) Docking the endoscope with navigation. The tracker was mounted on the dissector to guide the position of the endoscope. (**b**) The screenshot of the navigation guided procedure to dock the endoscope

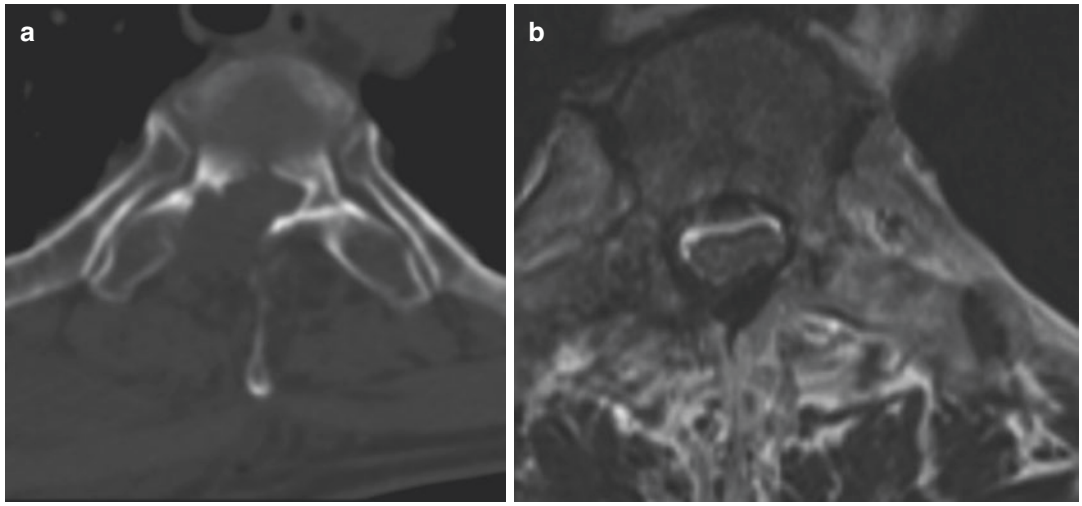


**Fig. 23.8** (**a**) The postoperative CT image showed a surgical corridor to decompress the spinal canal by right hemilaminectomy and partial medial pediculectomy. (**b**) The postoperative MRI showed well decompression of the spinal cord after discectomy and removal of hypertrophic ligamentum flavum

After ipsilateral hemilaminectomy, there was a midline opening or fold in the LF that could access the epidural space. Then, the LF was removed to expose the dura and herniated disc. The epidural space was checked with a hook for a possible remnant, and the dura was pulsatile at the end of decompression. After hemostasis, the wound was closed in one stitch without placing a drainage tube. The postoperative image showed an interlaminar corridor and a well-decompressed thoracic spinal cord (Fig. 23.8). The patient's symptoms improved, and there was no new neurological deficit after the operation.

## 23.6 Pitfalls and Avoidance of Complications

Thoracic spinal procedures carry risks different from lumbar and cervical spinal surgeries. The decision of surgical strategy plays an essential role in the safety issue. The transthoracic approach may put great vessels and visceral organs such as the heart, lungs, or diaphragm at risk for injury. Although posterior or posterolateral approaches still pose a risk to injure the ventral organs and great vessels if reaching too far forward, the incidence is fewer than that of the anterolateral approach. A lack of experience in the anterolateral approach for most spine surgeons is also a crucial factor. The precise localization and orientation during surgical procedures are the core of a safe, minimally invasive approach. The navigation technology can reshape the learning curve and help surgeons recognize orientation quickly, even in complex or distorted anatomical structures. Therefore, intraoperative navigation technology has gradually caught the attention of modern minimally invasive spine surgery.

Although navigation brings many benefits to patient safety and decreases radiation exposure to the surgical team, there are some potential risks regarding navigation error. The navigation accuracy depends on many factors, including explicit images acquired intraoperatively, rigidly fixed reference array or instrument tracker, and patient immobilization. In lean and poorly built patients, ventilation-related movement of the thoracic spine may cause a navigation shift. Thus, acquiring images in a non-ventilation mode and reducing the tidal volume to reduce motion-related navigation shifts is recommended. Moreover, all the staff must be aware that the deflection of the fixed reference array might result in severe inaccuracy. If the tactile feedback or endoscopic visu-

alization is not compatible with the navigation information, one can be sure that there has been an inaccuracy and a repeated registration scan is necessary. Navigation is based on the patient's position while acquiring the images. Navigation errors might happen if patients move. Thus, we recommend fixing the reference array on the spinous process of the adjacent level. The thoracic cage provides excellent stability to the structure and minimizes inaccuracy. Besides, general anesthesia also helps with the immobilization of patients.

## 23.7 Conclusion

Minimally invasive spine surgeries are based on image-guided procedures to remove pathology accurately or restore stability by instrumentation. More precise and detailed imaging information ensures the safety and effectiveness of MISS. The navigation is useful during each step of the thoracic spine surgery. It helps precise localization and avoids wrong-level surgery. The surgeon can use it to design the surgical corridor and trajectory directly toward the target pathology. During the procedure, the navigated instrument can minimize the risk of injury to the vulnerable thoracic spinal cord, thoracic visceral organs, or great vessels. This technology can further help surgeons overcome the learning curve of thoracic spine surgeries, which are relatively uncommon in minimally invasive spinal surgery. Although the intraoperative navigation system can provide practical guidance during procedures, surgeons should set up the proper workflow and be aware of error risks. With increasing devotion to navigation techniques and technologies, surgeons can safely decompress the thoracic spinal cord, either neoplastic or degenerative etiologies, with minimally invasive techniques.

## References

1. Chen G, Fan T, Yang X, Sun C, Fan D, Chen Z. The prevalence and clinical characteristics of thoracic spinal stenosis: a systematic review. Eur Spine J. 2020;29(9):2164–72. https://doi.org/10.1007/s00586-020-06520-6.
2. Bilsky MH. Transpedicular approach for thoracic disc herniations. Neurosurg Focus. 2000;9(4):e3. https://doi.org/10.3171/foc.2000.9.4.4.
3. Carson J, Gumpert J, Jefferson A. Diagnosis and treatment of thoracic intervertebral disc protrusions. J Neurol Neurosurg Psychiatry. 1971;34(1):68–77. https://doi.org/10.1136/jnnp.34.1.68.
4. Stillerman CB, Chen TC, Couldwell WT, Zhang W, Weiss MH. Experience in the surgical management of 82 symptomatic herniated thoracic discs and review of the literature. J Neurosurg. 1998;88(4):623–33. https://doi.org/10.3171/jns.1998.88.4.0623.
5. Kobayashi K, Ando K, Nishida Y, Ishiguro N, Imagama S. Epidemiological trends in spine surgery over 10 years in a multicenter database. Eur Spine J. 2018;27(8):1698–703. https://doi.org/10.1007/s00586-018-5513-4.
6. Andriacchi T, Schultz A, Belytschko T, Galante J. A model for studies of mechanical interactions between the human spine and rib cage. J Biomech. 1974;7(6):497–507. https://doi.org/10.1016/0021-9290(74)90084-0.
7. Gkasdaris G, Tripsianis G, Kotopoulos K, Kapetanakis S. Clinical anatomy and significance of the thoracic intervertebral foramen: a cadaveric study and review of the literature. J Craniovertebr Junction Spine. 2016;7(4):228–35. https://doi.org/10.4103/0974-8237.193266.
8. Bouthors C, Benzakour A, Court C. Surgical treatment of thoracic disc herniation: an overview. Int Orthop. 2019;43(4):807–16. https://doi.org/10.1007/s00264-018-4224-0.

# Part III

# Robot-Assisted MISS

# Currently Available Robot Systems in Spinal Surgery

24

Kobina G. Mensah-Brown, Andrew I. Yang, and Jang W. Yoon

## 24.1 Introduction

### 24.1.1 Brief History of Robotic Surgery

The term robot would evoke imagery of an entirely autonomous artificial intelligence housed in a physical body that we may interact with. However, in the twenty-first century, the most common approximation to this may indeed be an autonomous Roomba®. Notwithstanding, robotics is advancing and expanding rapidly as is readily observed in the introduction of automated transportation, such as drones and self-driving cars [1]. Importantly, the field of medicine has not been immune to this expansion.

Surgical robots may be defined as "computer-controlled manipulators with artificial sensing that can be reprogrammed to move and position tools to carry out a range of surgical tasks." [2]. While this concept of robotic surgery is readily envisioned, current applications of robotic surgery diverge slightly from this. Coined by the Czech writer Karel Capek in his play *Rossom's Universal Robots* and derived from the Czech word, *robota*, which refers to forced labor or chores, three major robotic systems may be readily described: active, semi-active and master-slave systems. Respectively, these refer to either autonomous, surgeon-driven with complementary pre-programmed elements or entirely surgeon-driven systems as emblemized by the da Vinci system. In reality, within the realm of minimally invasive spine surgery, the more prevalent, semi-active robot may be more appropriately described as a "robotic assistant" or "cobot" [3, 4].

While the history of minimally invasive spine surgery stems from nineteenth-century accounts by Virchow, the introduction of robotics into the surgical arena was much more recent and, unsurprisingly, spearheaded by innovations within Neuro- and Orthopedic surgery [5, 6]. Indeed, the first implementation of robotic surgery occurred in the form of the Programmable Universal Machine for Assembly (PUMA®) for CT-guided brain tumor biopsy, followed by the resection of thalamic astrocytomas in children with the same system [7, 8]. However, despite earlier works, it would seem that robotic surgery has been more applicable to spine surgery likely owing to repetitive movements, lengthy operations, and constricted surgical corridors often featured in this subspecialty [9].

In 1992, the *PUMA 260* had been adapted for the first spine-related surgical application—drilling of holes into the vertebrae of a plastic spine model. This early application involved a robot

K. G. Mensah-Brown · A. I. Yang · J. W. Yoon (✉)
Department of Neurosurgery, University of Pennsylvania Health System Penn Presbyterian Medical Center, Philadelphia, PA, USA
e-mail: kobina.mensah-brown@pennmedicine.upenn.edu; andrew.yang@pennmedicine.upenn.edu; jang.yoon@pennmedicine.upenn.edu



J.-S. Kim et al. (eds.), *Technical Advances in Minimally Invasive Spine Surgery*,
https://doi.org/10.1007/978-981-19-0175-1_24

carrying a laser optical guide superimposed on a planned surgical trajectory; thereby, conferring submillimeter accuracy to the surgeon [10]. By the early 2000s, robotic surgery had become a feasible option in pedicle screw placement. In 2004, the Mazor SpineAssist was approved by the FDA for pedicle screw placement paving the way for more sophisticated systems in minimally invasive pedicle screw placement. The remainder of this chapter will elaborate on major advances and trends in robotic surgery specific to minimally invasive spine surgery.

## 24.2 Currently Available Technologies

In 2021, the surgical arena is replete with minimally invasive spine surgery (MISS) and accruing robotic adjuncts for this widely adopted technique. For pedicle screw placement, in particular, several enabling technologies have been implemented. In the United States, seven robotic systems across four different companies have gained FDA approval for their robotic spine surgery systems. In general, these systems are comprised of three major components: the tracking system, mounting system, and robotic arm with varying degrees of freedom modeled after the human arm's seven degrees (Table 24.1) [11].

### 24.2.1 Medtronic/Mazor Robotics: Mazor Spine Assist, Renaissance, X

*Mazor Robotics* (Caesarea, Israel) is a medical device company involved in the development and manufacture of surgical guidance and related systems. In 2004, the *Mazor Spine Assist* became the first robotic system to be FDA-approved for spine surgery. The system consisted of a manipulator with six degrees of freedom for orientation of surgical tools during cases coupled to a navigation software, which was superior to traditional computer-assisted navigation [12, 13]. Following preoperative planning of surgical trajectories

**Table 24.1** Summary of available technologies for Robot-Assisted Minimally Invasive Spine Surgery

| Device | Year of FDA approval | Robot arm | Imaging data sets |
|---|---|---|---|
| *Mazor Spine Assist* (Mazor Robotics) | 2004 | Semi-active<br>6 degrees-of-freedom<br>Mounted via spinous process clamp OR Hover-T frame | Preoperative CT and intraoperative fluoroscopy |
| *Mazor Renaissance* | 2011 | Semi-active<br>6 degrees-of-freedom<br>Mounted via spinous process clamp OR Hover-T frame | Preoperative CT and intraoperative fluoroscopy |
| ROSA | 2012 | Semi-active<br>6 degrees-of-freedom<br>Mounted on mobile floor fixed base | Intraoperative CT and fluoroscopy |
| *Mazor X* | 2017 | Semi-active<br>6 degrees-of-freedom<br>Mounted on mobile floor fixed base | Preoperative CT and intraoperative fluoroscopy |
| ExcelsiusGPS | 2017 | Semi-active<br>6 degrees-of-freedom | Either preoperative CT, intraoperative CT, or fluoroscopy |
| Mazor X Stealth Edition | 2018 | Semi-active<br>6 degrees-of-freedom<br>Mounted near foot of the bed | Either preoperative CT or intraoperative CT |
| Cirq (Brainlab) | 2019 | Passive[a]<br>7 degrees-of freedom<br>Mounted on OR table rail | Either preoperative or intraoperative CT/fluoroscopy |

[a]Surgeon controlled

using their custom navigation software, the device could then be mounted to the patient through the use of a spinous process clamp or Hover-T minimally invasive frame [12]. Subsequently, the robotic system and surgical blueprint would be registered to the patient through a fiducial array attached to the spine and concurrent fluoroscopy. The surgeon could then select a target vertebra for screw placement, which the SpineAssist arm will automatically guide with 1 mm accuracy [14]. However, early iterations of SpineAssist were not without their challenges. Amidst software crashes, registration issues at the S1 level, the robotic guide arm being unable to reach the planned trajectory, or excessive force causing deviation from the plan, there were aspects of the device that required refinement [14, 15].

More advanced systems, such as the *Mazor Renaissance* and *Mazor X* have arisen since the SpineAssist and their general components (arm, tracking system, and mounting configuration) have been iterated and improved upon. Following FDA approval in 2011, the Rennaissance® replaced the SpineAssist thereby conferring a more ergonomic design to surgeons through its upgraded image recognition and allowing them to flatten bone around entry points prior to drilling. However, screw misplacement due to skiving remained a problem [13].

In 2017, the Mazor X became the latest iteration from this line of robotic systems to gain FDA approval. Much like its predecessors, the Mazor X robotic device consists of a workstation for surgical planning and a detachable surgical arm. However, in contrast to the spinal process clamp or Hover-T frame, the arm is attached to the Jackson table bedframe through a mount near the foot of the bed rather than to a spinous process. Moreover, the robotic arm includes an integrated linear optic camera for volumetric assessment and collision avoidance [13]. Additionally, the Mazor SpineAssist and Mazor Rennaissance both required preoperative CT to plan the trajectory and intraoperative fluoroscopy to register to the patient. However, the Mazor X could also rely on intraoperative CT to both plan the trajectory and scan for registration purposes obviating the need for intraoperative fluoroscopy [16, 17]. Soon thereafter, the Mazor Robotics was acquired by Medtronic and by 2018, they had developed the Mazor X Stealth Edition: a combination of the Stealth Intraoperative Navigation system and the Mazor X system.

In this time, several studies evaluating the accuracy of these systems have been conducted. Ringel et al. provided the first randomized controlled study evaluating the accuracy of robot-assisted implantation of pedicle screws in comparison with freehand conventional technique. At the time, they concluded that robotic placement of pedicle screws was inferior to conventional technique in terms of surgical time to screw placement and accuracy [18]. However, further studies demonstrated similar or better accuracy in robotic spinal surgery, in addition to less proximal facet violations with robotic placement [19–22].

### 24.2.2 Zimmer Biomet/Medtech: ROSA® Spine

In addition to Mazor Robotics, Medtech (Montpellier, France) is a European company that has also been heavily involved in the development of robotic systems for surgical procedures. In 2007, Medtech developed the ROSA ® Brain system and gained FDA approval in 2012 for cranial surgery [23]. This initial system had been harnessed for sEEG implantation and deep brain stimulation. In 2018, Medtech extended their technology to spinal surgery and it is now used in 29 US facilities. Like the prementioned robotic systems, the ROSA® Spine device consists of a robotic arm with six degrees of freedom, an optical camera and navigation system. However, in contrast to Mazor robotics, the ROSA® system consists of two stands: A robot stand comprised of a mobile floor-fixed base bearing the robotic arm and main monitor of the workstation and camera stand bearing the optical navigation camera and second monitor showing the same details as the first. Uniquely, the robotic arm is with a haptic sensor and touchscreen-operated surgical workstation and is not mounted

to the patient or operating table side-rail like prior systems. Moreover, it can function solely on intraoperative fluoroscopy or CT instead of preoperative imaging for 3D planning [24].

The ROSA® Spine device has demonstrated a higher rate of precision compared to freehand screw placement. In a study by Lonjon et al., accurate placement of implants (grades A and B Gertzbein Robbins classification) was achieved in 97.3% of patients under robotic guidance compared to 92% in the freehand group [25]. However, this study was a prospective case-matched study and was limited by its small and unrandomized sample of 20 patients. Indeed, in addition to feasibility studies and early evaluations of the ROSA spine device through case series and case-control studies, there have not been a significant number of studies evaluating this device [23, 26, 27]. In 2016, Medtech was acquired by Zimmer Biomet with the hope of providing this innovative technology to a much greater range of patients suffering from neurosurgical disorders.

### 24.2.3 Globus Medical: ExcelsiusGPS

The ExcelsiusGPS® gained FDA approval in 2017 and would be the most recent next-generation robotic system applied to spinal surgery. While several of the aforementioned systems had garnered evidence of improved accuracy in screw placement with the use of robotics during spinal surgery, they had often suffered from misregistration and skiving of screw hole preparation tools [28]. The ExcelsiusGPS® addresses several of these limitations. Like the ROSA® Spine device, it is a floor-mounted robot with foot pedal activation and positioning of the robot arm to the planned pedicle trajectory. Furthermore, instead of interspinous clamps, it harnesses reference arrays (termed the dynamic reference base) secured to the iliac crest and robotic arm to identify and alter the surgeon from skiving, obviating the need for K-wires or table/patient mounting [29, 30]. Unfortunately, at this time, no prospective, randomized studies of the ExcelsiusGPS® have been reported; however, initial insights from case reports assessing its accuracy have been very promising [29, 31, 32].

### 24.2.4 Brainlab: Cirq

As recently as 2019, the Brainlab Cirq system received FDA approval in the United States. The system consists of a passive robotic arm with 7 degrees of freedom, mounted on the operating table rail, in conjunction with Brainlab *Curve* navigation software as opposed to the automatically aligning arms to preplanned trajectories featured in the prementioned systems (Fig. 24.1). While prior systems have all involved thoracolumbar instrumentation, the Cirq® robotic assistance environment has been able to extend its scope of intervention to cervical fractures as well. Unique in its small size, lightweight, and table-mounted design and reference array system being affixed to a Mayfield head holder as opposed to cervical vertebra, it may also circumvent issues that arise due to reference frames being on the patient's bony anatomy. While these findings are promising, only a single case of posterior cervical screw fixation has been assessed at present [33].

### 24.2.5 Other Technologies

With RMISS continuing to show increasingly promising results for spinal procedures. It would follow that several other systems will soon penetrate the robotic spine market. As an example, NuVasive has received 510(k) clearance for their Pulse spinal surgical automation platform. However, the release of this system is pending. Similarly, the TiRobot (TINAVI Medical Technologies, Beijing, China) received China FDA approval in 2016 and continues to be the most popular platform in China [34]. The platform consists of a mobile six degree of freedom manipulator, optical tracking system, and navigation system. Moreover, it is a unified platform designed for use in multiple neurosurgery and orthopedic subspecialties [34]. Furthermore, in a prospective randomized controlled trial of 234

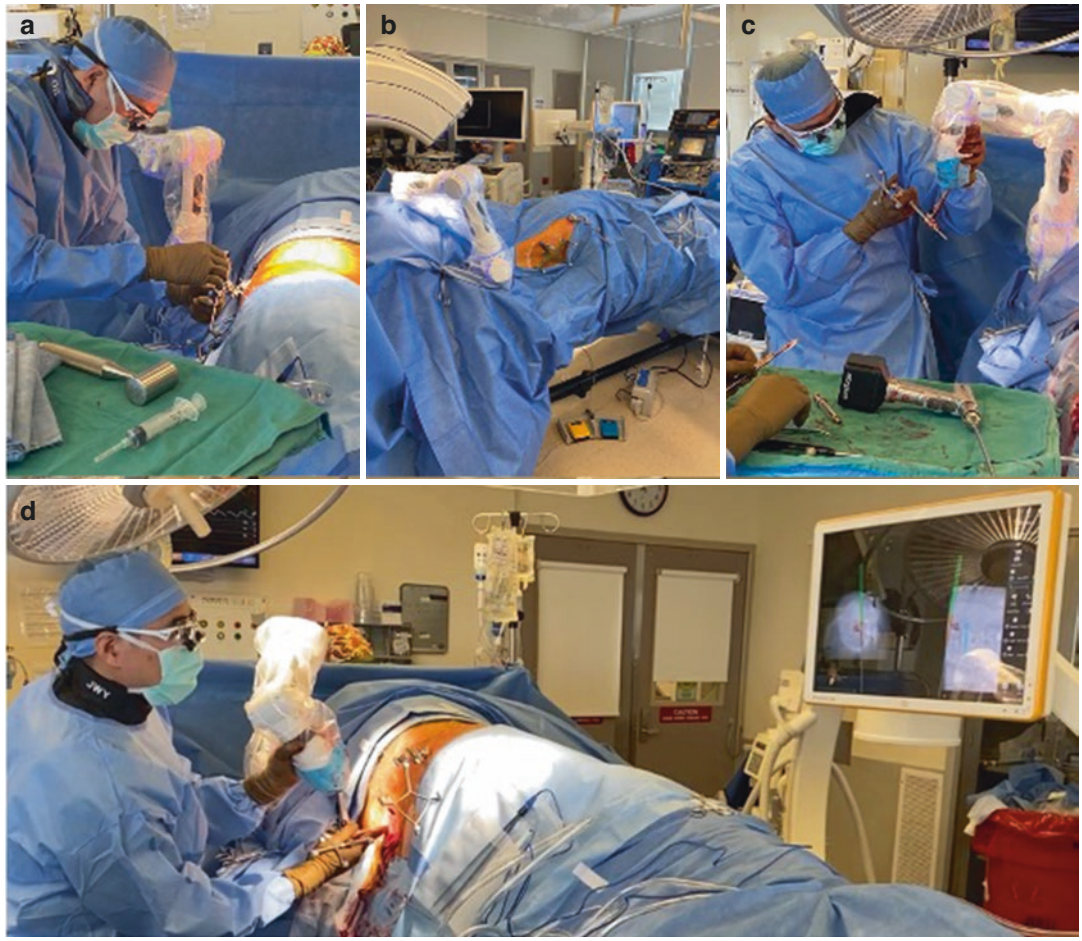


**Fig. 24.1** Intraoperative photographs (**a**–**d**) showing the passive manipulation of the Cirq® robotic arm

patients, the TiRobot system involved better accuracy, significantly less blood loss, and lower mean cumulative radiation exposure than freehand fluoroscopy-assisted surgery [35]. In 2019, Johnson & Johnson entered a co-marketing distribution and R&D agreement with TINAVI medical systems to bring their system to the Chinese orthopedics implant market.

## 24.3 Where We Are

Robotic assistance in minimally invasive spine surgery provides clear improvements in the accuracy of spinal instrumentation. Similarly, owing to this improved accuracy, complication rates of RMISS have been reported to be comparable or lower than conventional freehand procedures. Furthermore, robotic surgery has been shown to reduce mean fluoroscopy time, and general radiation exposure [19–21, 36–38]. While these advantages are readily documented, others are not demonstrably clear. For example, postoperative recovery times in RMISS have been reported to be shorter than their conventional freehand counterparts [19–21, 36–38]. However, whether this can be attributed to robotic assistance instead of the minimally invasive nature of these procedures remains unclear—an observation which is harder to clarify given that the freehand procedures involved in these are typically open procedures as opposed to endoscopic or laparoscopic cases. Similarly, overall complication rates in RMISS appear to not be significantly different

from conventional open surgery; however, this may be due to a scarcity of data evaluating outcomes in RMIS in addition to the associated learning curve [37, 39].

Unique challenges also exist for RMISS. Given the novelty of this technology, there continues to be a learning curve in its implementation. Hu et al. report improved consistent success in robotic-assisted pedicle screw placement after 30 patients [40]. Other studies also suggest a period of acclimatization to the robotic procedure but do provide detailed assessments of this experience [41]. Finally, the benefit of these systems has yet to adequately demonstrate counterbalance to their cost. Menger et al. demonstrate lower rates of infection and revision surgery along with reduced length of stay and operative time [42]. However, they note the limited dataset to which they applied their cost-effectiveness analysis. Ultimately, RMISS would appear to be within the acceptable standard of care but the early nature of robotic technology necessitates further work to better evaluate its impact on MISS.

## 24.4 Where We Are Going

The use of robots within spine surgery would seem limited to transpedicular fixation; however, this is steadily changing. For example, Ponnusamy et al. describe a porcine model in which they apply the da Vinci Surgical Robot for bony decompressions [43]. However, at this stage they required an open dissection of the spine. For RMISS, advances in navigation software and robotic instrumentation may one day allow for robotic spinal decompressions [9, 44]. For decortications, Robots may also be harnessed for facet decortication by employing a burr to the end effector instead of a pedicle screw [45]. Even robotic uses in anterior spinal fusions may be on the horizon with feasibility of the da Vinci system being demonstrated for anterior lumbar interbody fusions and graft placements [46–48]. More, robots may also eventually see consistent use in needle-based interventions such as percutaneous biopsy, facet blocks, and vertebroplasty [49–53].

## 24.5 Conclusion

Robotic systems are readily reshaping the surgical landscape. In its current form, robotic surgery involves increasingly complex cobots with expanding applications. While further work is needed to clarify the impact of these different systems on surgical outcomes, the introduction of so many robotic systems to minimally invasive spine surgery has ushered in a very exciting era for this field.

## References

1. Graetz G, Michaels G. Robots at work. Rev Econ Stat. 2018;100(5):753–68.
2. Davies B. A review of robotics in surgery. Proc Inst Mech Eng H. 2000;214(1):129–40.
3. Lane T. A short history of robotic surgery. Annals. 2018;100(6 Suppl):5–7.
4. Wang MY, Goto T, Tessitore E, Veeravagu A. Introduction. Robotics in neurosurgery. Neurosurg Focus. 2017;42(5):E1.
5. Love JG. PROTRUDED INTERVERTEBRAL DISKS: REPORT OF ONE HUNDRED CASES IN WHICH OPERATION WAS PERFORMED. JAMA. 1938;111(5):396.
6. Love JG. Protrusion of the intervertebral disk (fibrocartilage) into the spinal canal. In: Proc Staff Meet, Mayo Clin. 1936. p. 529–535.
7. Kwoh YS, Hou J, Jonckheere EA, Hayati S. A robot with improved absolute positioning accuracy for CT guided stereotactic brain surgery. IEEE Trans Biomed Eng. 1988;35(2):153–60.
8. Drake JM, Joy M, Goldenberg A, Kreindler D. Computer- and robot-assisted resection of thalamic astrocytomas in children. Neurosurgery. 1991;29(1):27–33.
9. Vo CD, Jiang B, Azad TD, Crawford NR, Bydon A, Theodore N. Robotic spine surgery: current state in minimally invasive surgery. Glob Spine J. 2020;10(2 Suppl):34S–40S.
10. Sautot P, Cinquin P, Lavallée S, Troccaz J. Computer assisted spine surgery: a first step toward clinical, application in orthopaedics. In: 1992 14th Annual International Conference of the IEEE Engineering in Medicine and Biology Society. 1992. p. 1071–2.
11. Prokopenko RA, Frolov AA, Biryukova EV, Roby-Brami A. Assessment of the accuracy of a human arm model with seven degrees of freedom. J Biomech. 2001;34(2):177–85.
12. Lieberman IH, Togawa D, Kayanja MM, Reinhardt MK, Friedlander A, Knoller N, et al. Bone-mounted miniature robotic guidance for pedicle screw and translaminar facet screw placement: Part I—Technical

development and a test case result. Neurosurgery. 2006;59(3):641–50.
13. D'Souza M, Gendreau J, Feng A, Kim LH, Ho AL, Veeravagu A. Robotic-assisted spine surgery: history, efficacy, cost, and future trends. Robot Surg. 2019;6:9–23.
14. Sukovich W, Brink-Danan S, Hardenbrook M. Miniature robotic guidance for pedicle screw placement in posterior spinal fusion: early clinical experience with the SpineAssist®. Int J Med Robot Computer Assisted Surg. 2006;2(2):114–22.
15. Barzilay Y, Liebergall M, Fridlander A, Knoller N. Miniature robotic guidance for spine surgery—introduction of a novel system and analysis of challenges encountered during the clinical development phase at two spine centres. Int J Med Robot Computer Assisted Surg. 2006;2(2):146–53.
16. Khan A, Meyers JE, Yavorek S, O'Connor TE, Siasios I, Mullin JP, et al. Comparing next-generation robotic technology with 3-dimensional computed tomography navigation technology for the insertion of posterior pedicle screws. World Neurosurg. 2019;123:e474–81.
17. O'Connor TE, O'Hehir MM, Khan A, Mao JZ, Levy LC, Mullin JP, et al. Mazor X stealth robotic technology: a technical note. World Neurosurg. 2021;145:435–42.
18. Ringel F, Stüer C, Reinke A, Preuss A, Behr M, Auer F, et al. Accuracy of robot-assisted placement of lumbar and sacral pedicle screws: a prospective randomized comparison to conventional freehand screw implantation. Spine. 2012;37(8):E496.
19. Hyun S-J, Kim K-J, Jahng T-A, Kim H-J. Minimally invasive robotic versus open fluoroscopic-guided spinal instrumented fusions: a randomized controlled trial. Spine. 2017;42(6):353–8.
20. Kim H-J, Jung W-I, Chang B-S, Lee C-K, Kang K-T, Yeom JS. A prospective, randomized, controlled trial of robot-assisted vs freehand pedicle screw fixation in spine surgery. Int J Med Robot Computer Assisted Surg. 2017;13(3):e1779.
21. Kantelhardt SR, Martinez R, Baerwinkel S, Burger R, Giese A, Rohde V. Perioperative course and accuracy of screw positioning in conventional, open robotic-guided and percutaneous robotic-guided, pedicle screw placement. Eur Spine J. 2011;20(6):860–8.
22. Roser F, Tatagiba M, Maier G. Spinal robotics: current applications and future perspectives. Neurosurgery. 2013;72(Suppl 1):A12–8.
23. Lefranc M, Peltier J. Evaluation of the ROSA™ Spine robot for minimally invasive surgical procedures. Expert Rev Med Devices. 2016;13(10):899–906.
24. Wagner C, Raber M, Simpson V, Khanna O, Gupta B, Wu C. Overview of robotics in neurosurgery. 14.
25. Lonjon N, Chan-Seng E, Costalat V, Bonnafoux B, Vassal M, Boetto J. Robot-assisted spine surgery: feasibility study through a prospective case-matched analysis. Eur Spine J. 2016;25(3):947–55.
26. Chenin L, Peltier J, Lefranc M. Minimally invasive transforaminal lumbar interbody fusion with the ROSA(TM) Spine robot and intraoperative flat-panel CT guidance. Acta Neurochir. 2016;158(6):1125–8.
27. Snyder LA. Integrating robotics into a minimally invasive transforaminal interbody fusion workflow. Neurosurg Focus. 2018;45(VideoSuppl1):V4.
28. Ahmed AK, Zygourakis CC, Kalb S, Zhu AM, Molina CA, Jiang B, et al. First spine surgery utilizing real-time image-guided robotic assistance. Computer Assisted Surg. 2019;24(1):13–7.
29. Jiang B, Karim Ahmed A, Zygourakis CC, Kalb S, Zhu AM, Godzik J, et al. Pedicle screw accuracy assessment in ExcelsiusGPS® robotic spine surgery: evaluation of deviation from pre-planned trajectory. Chin Neurosurg J. 2018;4(1):23.
30. Fayed I, Tai A, Triano M, Sayah A, Makariou E, Voyadzis J-M, et al. Robot-assisted percutaneous pedicle screw placement: evaluation of accuracy of the first 100 screws and comparison with cohort of fluoroscopy-guided screws. World Neurosurg. 2020;143:e492–502.
31. Walker CT, Godzik J, Xu DS, Theodore N, Uribe JS, Chang SW. Minimally invasive single-position lateral interbody fusion with robotic bilateral percutaneous pedicle screw fixation: 2-dimensional operative video. Operative Neurosurg. 2019;16(4):E121.
32. Godzik J, Walker CT, Theodore N, Uribe JS, Chang SW, Snyder LA. Minimally invasive transforaminal interbody fusion with robotically assisted bilateral pedicle screw fixation: 2-dimensional operative video. Operative Neurosurg. 2019;16(3):E86–7.
33. Farah K, Meyer M, Prost S, Dufour H, Blondel B, Fuentes S. Cirq® robotic assistance for minimally invasive C1-C2 posterior instrumentation: report on feasibility and safety. Operative Neurosurg. 2020;19(6):730–4.
34. Huang M, Tetreault TA, Vaishnav A, York PJ, Staub BN. The current state of navigation in robotic spine surgery. Ann Transl Med [Internet]. 2021;9(1). https://www.ncbi.nlm.nih.gov/pmc/articles/PMC7859750/
35. Han X, Tian W, Liu Y, Liu B, He D, Sun Y, et al. Safety and accuracy of robot-assisted versus fluoroscopy-assisted pedicle screw insertion in thoracolumbar spinal surgery: a prospective randomized controlled trial. J Neurosurg Spine. 2019;30(5):615–22.
36. Moses ZB, Mayer RR, Strickland BA, Kretzer RM, Wolinsky J-P, Gokaslan ZL, et al. Neuronavigation in minimally invasive spine surgery. Neurosurg Focus. 2013;35(2):E12.
37. Fan Y, Du J, Zhang J, Liu S, Xue X, Huang Y, et al. Comparison of accuracy of pedicle screw insertion among 4 guided technologies in spine surgery. Med Sci Monit. 2017;23:5960–8.
38. Keric N, Eum DJ, Afghanyar F, Rachwal-Czyzewicz I, Renovanz M, Conrad J, et al. Evaluation of surgical strategy of conventional vs. percutaneous robot-assisted spinal trans-pedicular instrumentation in spondylodiscitis. J Robot Surg. 2017;11(1):17–25.
39. Yu L, Chen X, Margalit A, Peng H, Qiu G, Qian W. Robot-assisted vs freehand pedicle screw fixation in spine surgery – a systematic review and a meta-

analysis of comparative studies. Int J Med Robot Computer Assisted Surg. 2018;14(3):e1892.
40. Hu X, Lieberman IH. What is the learning curve for robotic-assisted pedicle screw placement in spine surgery? Clin Orthop Relat Res. 2014;472(6):1839–44.
41. Devito DP, Kaplan L, Dietl R, Pfeiffer M, Horne D, Silberstein B, et al. Clinical acceptance and accuracy assessment of spinal implants guided with SpineAssist surgical robot: retrospective study. Spine (Phila Pa 1976). 2010;35(24):2109–15.
42. Menger RP, Savardekar AR, Farokhi F, Sin A. A cost-effectiveness analysis of the integration of robotic spine technology in spine surgery. Neurospine. 2018;15(3):216–24.
43. Ponnusamy K, Chewning S, Mohr C. Robotic approaches to the posterior spine. Spine (Phila Pa 1976). 2009;34(19):2104–9.
44. Virk S, Qureshi S. Narrative review of intraoperative imaging guidance for decompression-only surgery. Ann Transl Med [Internet]. 2021;9(1). https://www.ncbi.nlm.nih.gov/pmc/articles/PMC7859763/
45. Staub BN, Sadrameli SS. The use of robotics in minimally invasive spine surgery. J Spine Surg. 2019;5(Suppl 1):S31–40.
46. Lee JYK, Bhowmick DA, Eun DD, Welch WC. Minimally invasive, robot-assisted, anterior lumbar interbody fusion: a technical note. J Neurol Surg A Cent Eur Neurosurg. 2013;74(04):258–61.
47. Beutler WJ, Peppelman WCJ, DiMarco LA. The da Vinci robotic surgical assisted anterior lumbar interbody fusion: technical development and case report. Spine. 2013;38(4):356–63.
48. Troude L, Boissonneau S, Malikov S, Champsaur P, Blondel B, Dufour H, et al. Robot-assisted multilevel anterior lumbar interbody fusion: an anatomical study. Acta Neurochir. 2018;160(10):1891–8.
49. Tovar-Arriaga S, Tita R, Pedraza-Ortega JC, Gorrostieta E, Kalender WA. Development of a robotic FD-CT-guided navigation system for needle placement-preliminary accuracy tests. Int J Med Robot. 2011;7(2):225–36.
50. Ju H, Zhang J, An G, Pei X, Xing G. A robot-assisted system for minimally invasive spine surgery of percutaneous vertebroplasty based on CT images. In: 2008E Conference on Robotics, Automation and Mechatronics. 2008. p. 290–295.
51. Melzer A, Gutmann B, Remmele T, Wolf R, Lukoscheck A, Bock M, et al. INNOMOTION for percutaneous image-guided interventions. IEEE Eng Med Biol Magazine. 2008;27(3):66–73.
52. Tehranzadeh J, Tao C, Browning CA. Percutaneous needle biopsy of the spine. Acta Radiol. 2007;48(8):860–8.
53. Stoianovici D, Cleary K, Patriciu A, Mazilu D, Stanimir A, Craciunoiu N, et al. AcuBot: a robot for radiological interventions. IEEE Trans Robot Autom. 2003;19(5):927–30.

# Evidence of Navigation-Guided/ Robot-Assisted Spinal Surgery

25

Young-Seok Lee and Kyoung-Tae Kim

## 25.1 Introduction

Spine surgery has witnessed a series of technological innovations over several decades. As the field has expanded, many developments have occurred in spinal surgical instruments, operative techniques, and implants. Specifically, navigation and robotic systems have rapidly expanded in the spine surgery field.

Stereotactic techniques have been widely used in neurosurgical procedures. In 1908, Horsley and Clarke performed for the first time lesion targeting using stereotactic frames in monkey brains [1]. Subsequently, frameless stereotaxy along with real-time image guidance/navigation gradually developed. In the 1990s, it was widely used in cranial surgery [2]. In addition, stereotaxy, as applied to the spine, has engendered the development of commercially available image guidance navigation systems, such as the O-Arm (Medtronic Navigation, Medtronic Inc, Dublin, Ireland) with Stealth Station Navigation (Medtronic Navigation). These systems provide real-time, navigational feedback on surgical instruments.

Robotic systems employ a fully automated robotic arm and depend on radiographic imaging and stereotaxis for trajectory planning. Navigation and robotics systems for spine surgery enable a spine surgeon to determine the orientation of non-visualized anatomy during surgery with multiplanar CT or fluoroscopic images. This helps improve accuracy during spine surgery, especially for screw fixation. Also, it can help to reduce radiation exposure to patients and surgeons by minimizing the need for conventional fluoroscopy.

The surgical robotic system is divided into three main methods, which are as follows: supervisory controlled system, telesurgical system, and shared-control system [3]:

1. The supervisory controlled system is where the operator plans the operation and then the robot undergoes the operation autonomously under close supervision.
2. The telesurgical system is where the operator remotely controls the robot in real time.
3. The shared-control system is where simultaneous control of surgical instruments is done by the surgeon and a robot.

Y.-S. Lee
Department of Neurosurgery, School of Medicine, Kyungpook National University, Daegu, Republic of Korea

Department of Neurosurgery, College of Medicine, Chung-ang University Hospital, Seoul, Republic of Korea
e-mail: leeys1026@cau.ac.kr

K.-T. Kim (✉)
Department of Neurosurgery, School of Medicine, Kyungpook National University, Daegu, Republic of Korea

Department of Neurosurgery, Kyungpook National University Hospital, Daegu, Republic of Korea



J.-S. Kim et al. (eds.), *Technical Advances in Minimally Invasive Spine Surgery*,
https://doi.org/10.1007/978-981-19-0175-1_25

Among these three methods, the robotic system in spine surgery is a shared-control system. This method is used to determine the position and trajectory of the screw system. It is a method for using a robotic arm to apply a stereotactic trajectory with imaging before and during surgery. Also, a virtual augmented reality (AR) system is a promising technology using dedicated software and hardware that can show images directly onto special monitors, which allows the surgeon to visualize crucial information about the patient and the procedure in real time.

The da Vinci Surgical System (Intuitive Surgical, Sunnyvale, CA) was approved by the Food and Drug Administration (FDA) in 2000 for complex and minimally invasive intracavitary surgical procedures [4]. While spinal surgery robotics has the potential for improving spinal surgery, it remains important to demonstrate its superiority in comparison to traditional techniques before widespread use amongst surgeons. The development of navigation and robotic systems in spine surgery is limited to pedicle screw placement. Therefore, spine surgery remains insufficient for robotic systems [5, 6].

## 25.2 Computer-Assistant Navigation

Intraoperative navigation and image-guided robotics are often used in spinal column and intradural tumors, infection, revision spine surgery, and deformity. Also, using navigation can reduce radiation exposure generated during minimally invasive surgery. In the field of spine surgery, various computer-assistant navigation platforms are currently available. The three-dimension computer-assistant navigation platform available are as follows: Airo Mobile Intraoperative computer tomography-based Spinal Navigation (Brainlab©, Feldkirchen, Germany), Stryker Spinal Navigation with SpineMask© Tracker and SpinalMap Software (Stryker©, Kalamazoo, Michigan), Stealth Strarion, Spine Surgery Imaging and Surgical Navigation with O-arm (Medtronic©, Minneapolis, Minnesota), and Ziehm VisionFD Vario 3-D with NaviPort integration (Ziehm Imaging©, Orlando, Florida).

O-arm (Medtronic©, Minneapolis, Minnesota) provides real-time three-dimensional surgical imaging. During a surgical procedure, 3-D images of the spine can be presented simultaneously on the screen, thereby eliminating the need to account for the patient's position [7]. In theory, the O-arm technique appears to have more advantages than the C-arm system. But, the O-arm system displayed a similar efficiency outcome compared to conventional C-arm fluoroscopy in pedicle screw placement (Fig. 25.1).

For surgeons using robot assistance, several computer-assistant navigation systems can be integrated with the robots currently available. In addition, the Mazor and ROSA robots can have their native navigation software optimized for spinal operations.

## 25.3 Telesurgical Robot System

### 25.3.1 da Vinci

The da Vinci has been approved for laparoscopic surgery by the FDA. Moreover, the field of use has gradually expanded to cardiac surgery, thoracic surgery, obstetrics, gynecology, and urology surgery. The da Vinci is a system where the operator controls the system at a station away from the operatory room. This system allows the operator to control the operatory field by employing three-dimensional vision with a magnification of 10 times, which allows detailed adjustment. In addition, it has tremor filtering and a limitless wrist range of motion. However, the application of da Vinci to spine surgery is limited to a laparoscopic anterior lumbar interbody fusion [8]. da Vinci's use has improved visualization compared to traditional surgical approaches but has disadvantages of high costs of the surgical setup, a steep learning curve, long operating time, and limited surgical indications for spine surgery. Therefore, the da Vinci system has not yet been approved by the FDA for spine surgery, as evidence is still insufficient (Fig. 25.2).


**Fig. 25.1** O-arm (Medtronic©, Minneapolis, Minnesota) as the three-dimension computer-assistant navigation


**Fig. 25.2** da Vinci Surgical System (Intuitive Surgical, Sunnyvale, CA). The da Vinci is a system where the operator controls the device at a station away from the operatory room

## 25.4 Robotic-Assisted Navigation Systems

### 25.4.1 Mazor: SpineAssist

SpineAssist (Mazor Robotic Inc., Caesarea, Israel) was developed in 2004, and FDA approval for spine surgery has been obtained for the first time. After fixing the frame to the patient's spinous process, this system uses a percutaneous screw using a guidewire. This system allows planning with preoperative CT and gradually determines the position of the pedicle and trajectory of the instrument. Further, this system can be combined with preoperative CT and intraoperative fluoroscopy. The accuracy of SpineAssist is very high. Van Dilk JD et al. demonstrated that the accuracy of pedicle screws is 97.9% (477 out of 487 screws) [9]. Moreover, Devito DP et al. showed a 98% screw position accuracy and an additional reduction in neurologic risk [10]. However, one limitation of SpineAssist is that specific anatomical landmarks may need to be fixed. Skidding and other dislocations of the cannula also have been reported.

### 25.4.2 Mazor: Renaissance

Renaissance is a second-generation robotic system for spine surgery developed by Mazor Robotic Inc. (Caesarea, Israel). It was replaced by Renaissance in SpineAssist in 2011. Compared to SpineAssist, Renaissance is smaller and lighter, and sensitivity is improved. This system is capable of selecting the desired position of the vertebral body, along with the characteristics and types of instrumentation, using a three-dimensional reconstruction of the spine during preoperative CT. Hyun et al. compared the classical fluoroscopy-guided technique with transpedicular screw placement using Renaissance [11]. The robotic-guided screw showed 100% accuracy in screw placement, while the fluoroscopy-guided technique had two pedicle branches and one facet violation. Also, the radiation exposure and length of hospital stay were significantly reduced using a robotic system (Fig. 25.3).

### 25.4.3 Mazor: Mazor X

Mazor X was most recently released by Mazor Robotics Inc. It is a robotic system for spine surgery developed by Caesarea (Israel). This model upgraded the previous version of the product. Both intraoperative fluoroscopy and 3D surface scanning are used, though there are still limitations in performing bone mounting on the operative bed and patient. Recently, Mazor X showed 98.7% accuracy of screw placement and reduced operative time and radiation exposure [12].

### 25.4.4 ROSA

The ROSA system (Medtech, Montpellier, France) is a mobile, floor-fixable base system with a robotic arm attached. ROSA is a system that attaches to the patient's bone anatomy. The ROSA robot is a freestanding robotic assistant with a rigid robotic arm and a floor-fixable base. These features may help reduce concerns of fixation strength to the bony anatomy. Additionally, the robotic arm moves along with the patient. Based on camera monitoring tracking, several percutaneously tracking pins are placed in real time to the patient's bony anatomy in reference to tracking spheres affixed to the robot. Lonjon et al. reported an accuracy rate of 97.3% for pedicle screw instrumentation compared to 92% in the freehand group, although this difference was not statistically significant [13].

### 25.4.5 ExcelsiusGPS

ExcelsiusGPS (Globus Medical, Inc., Audubon, PA, USA) is a robotic system approved by FDA and CE-marked for spine surgery. Preoperative or intraoperative CT images are employed under the guidance of a rigid robotic arm. The core of this system is a real-time visualization of instrument positioning and screw placement with respect to the patient's anatomy. Moreover, the system is equipped with sensors that can detect drill skiving or sliding of the reference frame. In addition, they can automatically compensate for

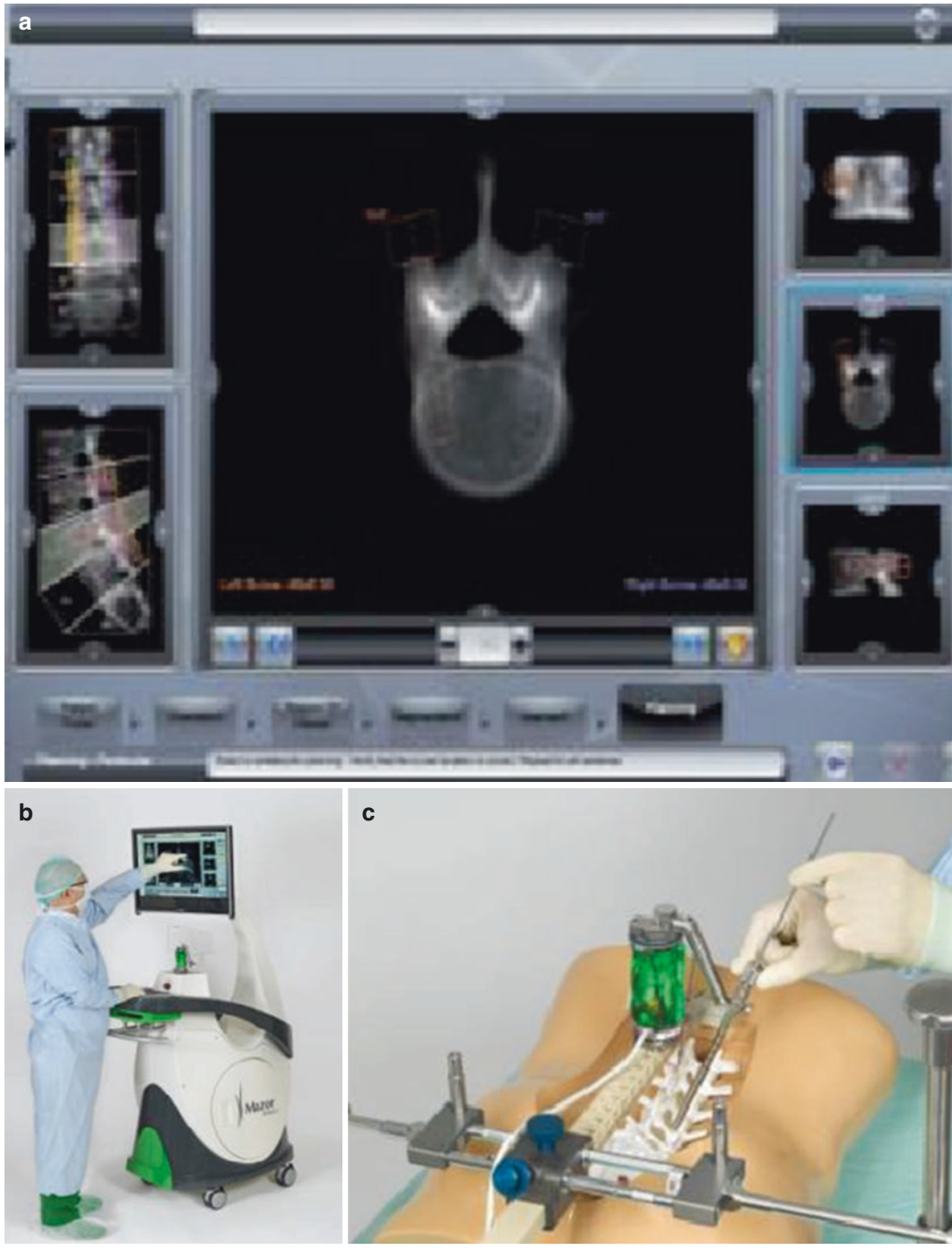


**Fig. 25.3** Renaissance is a second-generation robotic system for spine surgery developed by Mazor Robotic Inc. (Caesarea, Israel). Renaissance consists of three components. (**a**) CT-based 3D planning software, (**b**) Workstation, and (**c**) Miniature robot

patient movements. Huntsman et al. showed that the accuracy of the pedicle screw in 100 cases was 99% [14]. Godzik et al. showed an accuracy of 96.6% of 116 screws in 28 patients [15]. Benech et al. showed accuracy in Gertzbein and Robbins classification of 98.3% in 53 spine surgery [16]. Vaediman et al. showed an accuracy of 97.7% [17].

### 25.4.6 CUVIS-Spine

The CUVIS-spine pedicle screw guide system (CUVIS-spine; Curexo Inc. Republic of Korea) (Fig. 25.4) allows surgical instruments and screws to be inserted into a planned path created by a surgeon using intraoperatively scanned 2D or 3D images. The robotic manipulator guides and supports the surgical instruments or screws. One feature of the robotic system is force navigation which provides a level and orientation of lateral force applied to the surgical instrument in real time while it contacts the bone surface. It makes it possible to insert surgical instruments more safely and accurately. Another feature is that it significantly reduces the radiation dose to patients and medical staff because there is no need for a preoperative CT scan or intraoperative scan to confirm and correct the insertion path. It provides intraoperative C-arm image-based planning with a virtual axial view and an assisted user interface. According to unpublished data, when evaluated by the Gertzbein and Robbins classification in a cadaveric study, GRS A or B showed a high accuracy of 95.45% (21/22) (Table 25.1).

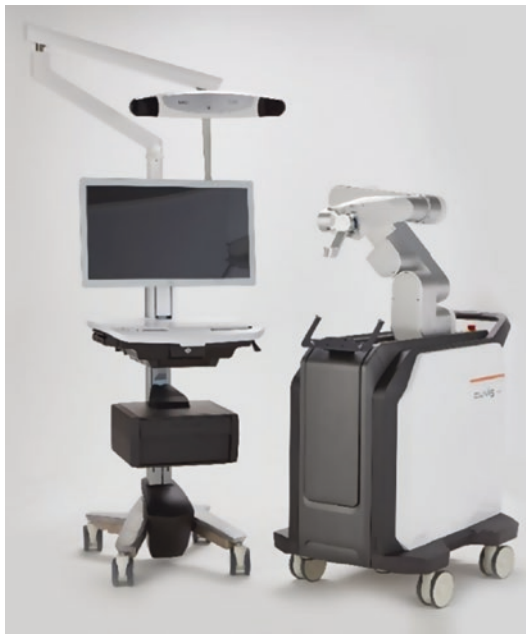

**Fig. 25.4** The CUVIS-spine system (Curexo Inc. Republic of Korea) allows surgical instruments and screws to be inserted into the planned path generated by a surgeon using intraoperatively scanned 2D or 3D images. The main console and robotic arm make a trajectory for the insertion of the screw

## 25.5 Advantages of Robotics and Navigation Systems

The advantages of robotic and navigation systems in spine surgery are as follows: (1) increased pedicle screw placement accuracy; (2) minimally invasive approach (small incision, bleeding and infection, and minimal muscle dissection and retraction); and (3) decreased radiation exposure. Furthermore, the robotic system offers advantages in comparison to the human hand, such as the elimination of hand and wrist fatigue, tremors, and precise repetition.

## 25.6 Accuracy of Pedicle Screw Placement

Pedicle screws are employed in many spine surgeries to create stable spinal fixation. While there is a freehand technique that uses anatomical landmarks, fluoroscopy is needed for greater stability and accuracy. According to recent literature, the accuracy of robotic-assistant pedicle screw placement is not significantly better than fluoroscopic-guided or conventional freehand techniques, though it is reportedly equivalent or slightly superior. The accuracy of pedicle screw placement was determined in most studies using the Gertzbein–Robbins scale (GRS) [18].

Several studies have retrospectively analyzed the accuracy of pedicle screw placement using robotic systems [10, 19–21]. Robotic-guided

**Table 25.1** Robotic systems for spine surgery

| | Mazor (SpineAssist, Renaissance, Mazor X) | ROSA | ExcelsiusGPS |
|---|---|---|---|
| Preoperative CT | Need | No need | No need |
| Mount | Bone, table | Floor | Floor |
| Instrument tracking | Yes | Yes | Yes |
| K-wires required | Yes | Yes | No |
| Clinical application | Pedicle screw placement, tumor biopsy, vertebroplasty | Pedicle screw placement | Pedicle screw placement |
| Accuracy | 98~100% | 96% | 96.6~99% |
| Limitations | Need for rigid bone fixation, skiving of the torch or drill tip | Need for rigid bone fixation | Need for rigid bone fixation |

screw placement demonstrates an accuracy from 94.5 to 98.4%, so it was safe and effective. On the other hand, freehand or fluoroscopy-guided screw placement was 91.4~91.6% accurate, so robotic-guided screw placement was more accurate, though it was not statistically superior.

There are three prospective, randomized controlled trials (RCTs) that have evaluated robot-guided pedicle screw placement. Kim et al. [22] compared the accuracy and safety of robot-assisted minimally invasive PLIF versus freehand screw placements. No significant differences were shown between the groups for accuracy of pedicle screw placement, although, the robot-assisted group had significantly less proximal facet violations (0% vs 15.9%, $P < 0.001$). A three-arm prospective RCT by Roser et al. [23] evaluated pedicle screw insertion techniques using three different modalities: fluoroscopically guided freehand, navigation-guided, and robotic-assisted. However, the study was significantly underpowered with only 10 patients in the fluoroscopy group, 9 patients in the navigation group, and 18 patients in the robot (SpineAssist) group. They found an accuracy rate of 92.0%, 97.5%, and 97.5% for freehand, fluoroscopy-guided, and robot-assisted placement, respectively. In addition, Ringel and colleagues [24] reported significantly poorer screw placement in the robot group compared to the fluoroscopy (85% vs 93%), along with significantly more screws requiring intraoperative revision in the robot group compared to the fluoroscopy group (10 vs 1). In this study, the accuracy of the freehand technique was demonstrated to be superior to the robot-assisted technique. Most malpositioned screws used in the robot-assisted group showed a lateral deviation. Attaching the robot to the spine seems vulnerable to potential screw malposition as well as slipping of the implantation cannula at the screw entrance point. Robot-assisted pedicle screw placement still lacks evidence-based effectiveness and accuracy compared to traditional freehand or fluoroscopy-guided screw placement. Therefore, it is necessary to develop a more advanced robot system.

## 25.7 Radiation Exposure

Spine surgery using fluoroscopy helps to determine the position and trajectory of instrumentation. As a consequence, harmful radiation exposure is given to patients, operators, and the surgical staff in the operating room. Robotic spine surgery helps to minimize and eliminate radiation exposure during surgery. In robotic spine surgery, intraoperative CT and fluoroscopy are occasionally used, though preoperative CT is mainly used [24]. In several studies, radiation exposure was evaluated in robot-assisted screw placement. Gao et al. significantly reduced intraoperative radiation time and intraoperative radiation dosage when using a robotic assistance system. The important point is that when using a robotic-assisted system, the radiation time slowly decreases according to a learning curve effect, so the more familiar the operator is with a developed system, the more the radiation risk will be reduced [25].

## 25.8 Expansion of the Field of Use of Robotic Systems in Spine Surgery

Robotic systems are mostly researched on pedicle screw placement in spine surgery. However, the application field of the robot system has gradually expanded. It is being applied to the S2-alar-iliac screw [26, 27] and metastasis spine tumor [28] using a robotic system. As a result, it is expected to help reduce revision surgery and operation time.

## 25.9 Augmented Reality in Spine Surgery

Augmented reality (AR) is based on computer-generated data that is superimposed on the real world through projecting digital images on special screens or wearable devices. It is thus able to "augment" the quantity of information that can be detected by the surgeon. AR helps in real time to determine the orientation of the bony anatomy and trajectory when the operator performs pedicle screw placement. Elmi-Terander et al. performed pedicle screw placement using augmented reality surgical navigation (ARSN) with both navigation and AR. When using ARSN, higher accuracy was demonstrated in comparison with the freehand technique (ARSN: 85% vs. freehand technique: 64%, $P < 0.05$) [29]. Since then, various AR systems have been developed by the following companies: Google (Mountain View, CA, USA), HoloLens (Microsoft Corp., Redmond, WA, USA), xcision (Augmedics, Arlington Heights, IL, USA), and MicroOptical (MicroOptical Corp., Westwood, MA, USA) [4].

## 25.10 Conclusion

The field of robot-assisted spine surgery still has weak indications limited to pedicle screw placement. Most studies so far have compared robot-assisted pedicle screw placement using freehand or fluoroscopy. Robot-assisted spinal surgery should show a clear improvement in results for clinical effects. Further, there remains a lack of studies on the cost-effectiveness of these procedures. Nevertheless, the next generation of innovative navigation and robotic systems will have the potential to improve spine surgery.

## References

1. Horsley V, Clarke RH. THE STRUCTURE AND FUNCTIONS OF THE CEREBELLUM EXAMINED BY A NEW METHOD. Brain. 1908;31(1):45–124.
2. Kochanski RB, Lombardi JM, Laratta JL, Lehman RA, O'Toole JE. Image-guided navigation and robotics in spine surgery. Neurosurgery. 2019;84(6):1179–89.
3. Overley SC, Cho SK, Mehta AI, Arnold PM. Navigation and robotics in spinal surgery: where are we now? Neurosurgery. 2017;80(3s):S86–s99.
4. Vadalà G, De Salvatore S, Ambrosio L, Russo F, Papalia R, Denaro V. Robotic spine surgery and augmented reality systems: a state of the art. Neurospine. 2020;17(1):88–100.
5. Joseph JR, Smith BW, Liu X, Park P. Current applications of robotics in spine surgery: a systematic review of the literature. Neurosurg Focus. 2017;42(5):E2.
6. Vo CD, Jiang B, Azad TD, Crawford NR, Bydon A, Theodore N. Robotic spine surgery: current state in minimally invasive surgery. Global Spine J. 2020;10(2 Suppl):34s–40s.
7. Feng W, Wang W, Chen S, Wu K, Wang H. O-arm navigation versus C-arm guidance for pedicle screw placement in spine surgery: a systematic review and meta-analysis. Int Orthopaed. 2020;44(5):919–26.
8. Beutler WJ, Peppelman WC Jr, DiMarco LA. The da Vinci robotic surgical assisted anterior lumbar interbody fusion: technical development and case report. Spine (Phila Pa 1976). 2013;38(4):356–63.
9. van Dijk JD, van den Ende RP, Stramigioli S, Köchling M, Höss N. Clinical pedicle screw accuracy and deviation from planning in robot-guided spine surgery: robot-guided pedicle screw accuracy. Spine (Phila Pa 1976). 2015;40(17):E986–91.
10. Devito DP, Kaplan L, Dietl R, Pfeiffer M, Horne D, Silberstein B, et al. Clinical acceptance and accuracy assessment of spinal implants guided with SpineAssist surgical robot: retrospective study. Spine (Phila Pa 1976). 2010;35(24):2109–15.
11. Hyun SJ, Kim KJ, Jahng TA, Kim HJ. Minimally invasive robotic versus open fluoroscopic-guided spinal instrumented fusions: a randomized controlled trial. Spine (Phila Pa 1976). 2017;42(6):353–8.
12. Khan A, Meyers JE, Siasios I, Pollina J. Next-generation robotic spine surgery: first report on feasibility, safety, and learning curve. Oper Neurosurg (Hagerstown). 2019;17(1):61–9.
13. Lonjon N, Chan-Seng E, Costalat V, Bonnafoux B, Vassal M, Boetto J. Robot-assisted spine surgery:

feasibility study through a prospective case-matched analysis. Eur Spine J. 2016;25(3):947–55.
14. Huntsman KT, Ahrendtsen LA, Riggleman JR, Ledonio CG. Robotic-assisted navigated minimally invasive pedicle screw placement in the first 100 cases at a single institution. J Robot Surg. 2020;14(1):199–203.
15. Godzik J, Walker CT, Hartman C, de Andrada B, Morgan CD, Mastorakos G, et al. A quantitative assessment of the accuracy and reliability of robotically guided percutaneous pedicle screw placement: technique and application accuracy. Oper Neurosurg (Hagerstown). 2019;17(4):389–95.
16. Benech CA, Perez R, Benech F, Greeley SL, Crawford N, Ledonio C. Navigated robotic assistance results in improved screw accuracy and positive clinical outcomes: an evaluation of the first 54 cases. J Robot Surg. 2020;14(3):431–7.
17. Vardiman AB, Wallace DJ, Crawford NR, Riggleman JR, Ahrendtsen LA, Ledonio CG. Pedicle screw accuracy in clinical utilization of minimally invasive navigated robot-assisted spine surgery. J Robot Surg. 2020;14(3):409–13.
18. Gertzbein SD, Robbins SE. Accuracy of pedicular screw placement in vivo. Spine (Phila Pa 1976). 1990;15(1):11–4.
19. Kantelhardt SR, Martinez R, Baerwinkel S, Burger R, Giese A, Rohde V. Perioperative course and accuracy of screw positioning in conventional, open robotic-guided and percutaneous robotic-guided, pedicle screw placement. Eur Spine J. 2011;20(6):860–8.
20. Pechlivanis I, Kiriyanthan G, Engelhardt M, Scholz M, Lücke S, Harders A, et al. Percutaneous placement of pedicle screws in the lumbar spine using a bone mounted miniature robotic system: first experiences and accuracy of screw placement. Spine (Phila Pa 1976). 2009;34(4):392–8.
21. Togawa D, Kayanja MM, Reinhardt MK, Shoham M, Balter A, Friedlander A, et al. Bone-mounted miniature robotic guidance for pedicle screw and translaminar facet screw placement: Part 2–Evaluation of system accuracy. Neurosurgery. 2007;60(2 Suppl 1):ONS129–39. discussion ONS39
22. Kim HJ, Lee SH, Chang BS, Lee CK, Lim TO, Hoo LP, et al. Monitoring the quality of robot-assisted pedicle screw fixation in the lumbar spine by using a cumulative summation test. Spine (Phila Pa 1976). 2015;40(2):87–94.
23. Roser F, Tatagiba M, Maier G. Spinal robotics: current applications and future perspectives. Neurosurgery. 2013;72(Suppl 1):12–8.
24. Ringel F, Stüer C, Reinke A, Preuss A, Behr M, Auer F, et al. Accuracy of robot-assisted placement of lumbar and sacral pedicle screws: a prospective randomized comparison to conventional freehand screw implantation. Spine (Phila Pa 1976). 2012;37(8):E496–501.
25. Gao S, Lv Z, Fang H. Robot-assisted and conventional freehand pedicle screw placement: a systematic review and meta-analysis of randomized controlled trials. Eur Spine J. 2018;27(4):921–30.
26. Hyun SJ, Kim KJ, Jahng TA. S2 alar iliac screw placement under robotic guidance for adult spinal deformity patients: technical note. Eur Spine J. 2017;26(8):2198–203.
27. Laratta JL, Shillingford JN, Lombardi JM, Alrabaa RG, Benkli B, Fischer C, et al. Accuracy of S2 alar-iliac screw placement under robotic guidance. Spine Deform. 2018;6(2):130–6.
28. Hu X, Scharschmidt TJ, Ohnmeiss DD, Lieberman IH. Robotic assisted surgeries for the treatment of spine tumors. Int J Spine Surg. 2015;9
29. Elmi-Terander A, Skulason H, Söderman M, Racadio J, Homan R, Babic D, et al. Surgical navigation technology based on augmented reality and integrated 3D intraoperative imaging: a spine cadaveric feasibility and accuracy study. Spine (Phila Pa 1976). 2016;41(21):E1303–e11.

# Workflows for Robotic Surgery in the Lumbar Spine: MIS TLIF

26

Siri Sahib S. Khalsa, Michael J. Strong, and Paul Park

## 26.1 Case History

A 65-year-old man with a remote history of L5-S1 laminectomy presents with progressive low back pain radiating to bilateral lower extremities. The pain is associated with subjective bilateral lower extremity weakness, which worsens with prolonged standing or ambulation. The pain improves with rest and leaning forward. His symptoms have progressed in spite of conservative therapies.

On exam, he has full strength in bilateral lower extremities. Sensation is subjectively diminished in bilateral distal lower extremities. There are no pathologic reflexes. BMI is 27.5 kg/m$^2$.

MRI demonstrates severe central stenosis at L4-5 due to hypertrophy of the ligamentum flavum and the facet joints. There is a grade 1 L4-5 spondylolisthesis, which worsens on standing. Dynamic X-rays demonstrate mobility of the L4-5 spondylolisthesis on flexion and extension. Representative preoperative images are shown in Fig. 26.1.

## 26.2 Surgical Decision-Making

The patient's presentation is consistent with refractory neurogenic claudication due to L4-5 central canal stenosis, in the setting of a mobile L4-5 spondylolisthesis. A decompression and instrumented fusion at L4-5 is indicated. A minimally invasive TLIF offers the advantage of decreased exposure-related morbidity while achieving direct decompression and interbody fusion with posterior fixation [1].

The workflow presented in this chapter uses a robotic-assisted spinal navigation system to plan and insert pedicle screws, position the tubular retractor with navigation, ensure adequate decompression, and place an interbody cage optimized for size and position. Registration of the navigation system is completed with a single intraoperative computed tomography (CT) scan, which reduces radiation exposure to the operative staff, and streamlines workflow by decreasing the need for serial intraoperative fluoroscopic images [2–8].

## 26.3 Surgical Workflow

- Position prone on a Jackson Frame.
- Placement of iliac pin, with attachment of dynamic reference array and intraoperative CT array.

S. S. S. Khalsa · M. J. Strong · P. Park (✉)
Department of Neurosurgery, University of Michigan, Ann Arbor, MI, USA
e-mail: skhalsa@umich.edu; mistrong@umich.edu; ppark@umich.edu



J.-S. Kim et al. (eds.), *Technical Advances in Minimally Invasive Spine Surgery*,
https://doi.org/10.1007/978-981-19-0175-1_26

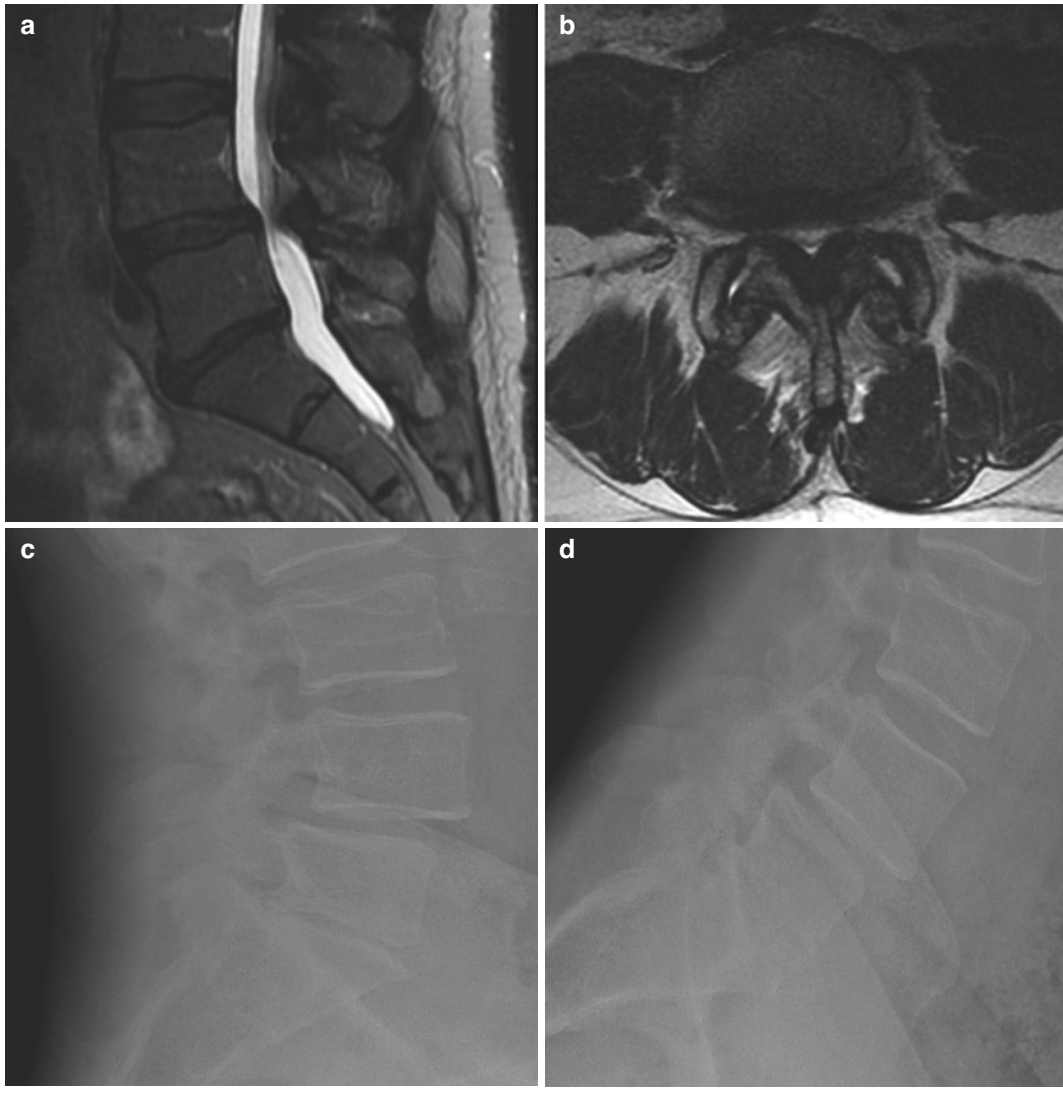


**Fig. 26.1** Preoperative images of the lumbosacral spine. Sagittal (**a**) and axial (**b**) T2 MRI showing central and lateral recess stenosis at L4-5. Extension (**c**) and flexion (**d**) X-rays demonstrate a mobilize spondylolisthesis at L4-5

- Intraoperative CT scan to acquire 3D imaging data for registration. Alternatively, a preoperative CT may be registered with intraoperative fluoroscopy.
- Planning of L4 and L5 pedicle screws on the robotic navigation system.
- Robotic-assisted placement of pedicle screws at L4 and L5 bilaterally, without screwheads on the right side.
- Placement of tubular retractor overlying L4-5 in a muscle-splitting manner utilizing the robotic navigation platform to minimize fluoroscopy.
- Right L4-5 laminotomy, facetectomy, contralateral laminectomy via a unilateral approach.
- L4-L5 discectomy, preparation of end plates.
- Placement of autograft, allograft, and L4-5 expandable interbody cage.

- Placement of screw heads on right L4-5 pedicle screws.
- Percutaneous insertion of bilateral rods and tightening of set screws.
- Confirmatory X-rays.

## 26.4 Procedure Description

The patient is brought to the operating room where he undergoes initiation of general anesthesia and placement of an endotracheal tube. Neuromonitoring leads are placed for somatosensory evoked potentials (SSEP) and electromyography (EMG). The patient is turned prone onto a Jackson frame. Arms are positioned and protected. All pressures points are padded (Fig. 26.2).

In general, fluoroscopy is minimized for a robotic-assisted procedure. The first step, after prep and sterile draping, is to make a small incision overlying the posterior superior iliac spine (PSIS). An iliac pin is then impacted into the bone. The side that the pin is placed is opposite the side of the TLIF. A dynamic reference array is then fixated to the iliac pin. In this workflow, the intraoperative imaging unit, O-arm (Medtronic, Dublin, Ireland), is not directly compatible with the robotic navigation unit, ExcelsiusGPS (Globus Medical, Audubon, Pennsylvania). Consequently, a separate intraoperative CT array is positioned over the region of interest (L4-5) so that the 3D imaging data can be used by the robotic navigation unit (Fig. 26.3). The O-arm fluoroscopic unit is brought into the operative field (Fig. 26.4) to obtain a three-dimensional CT scan of the spine. This imaging data is then transferred to the robotic navigation unit.

Attention is turned to planning the pedicle screw placement. Phantom L4 and L5 pedicle screws are positioned appropriately for size and trajectory on the working station of the robotic unit (Fig. 26.5). The robotic unit is then brought into the operative field. Small paramedian incisions are made to accommodate the planned pedicle screw trajectories. The robotic arm autonomously positions itself at L4 on the left according to the screw plan. A navigated drill is then inserted through the now rigid robotic effector tube to create a pilot hole and the screw tract. This is followed by a navigated tap. A navigated screwdriver is used to insert a pedicle screw connected to a screw extender (Fig. 26.6). This process is repeated at L5 on the left and at L4 and L5 on the right; however, pedicle screw posts (no screw head or extender) are placed on the right so as to not obstruct the subsequent tubular retractor placement. Note that fluoroscopy is not generally used for navigated screw insertion; however, fluoroscopy should be used if there is a concern for navigation error.

Attention is then turned to placing the tubular retractor overlying the L4-5 segment. This

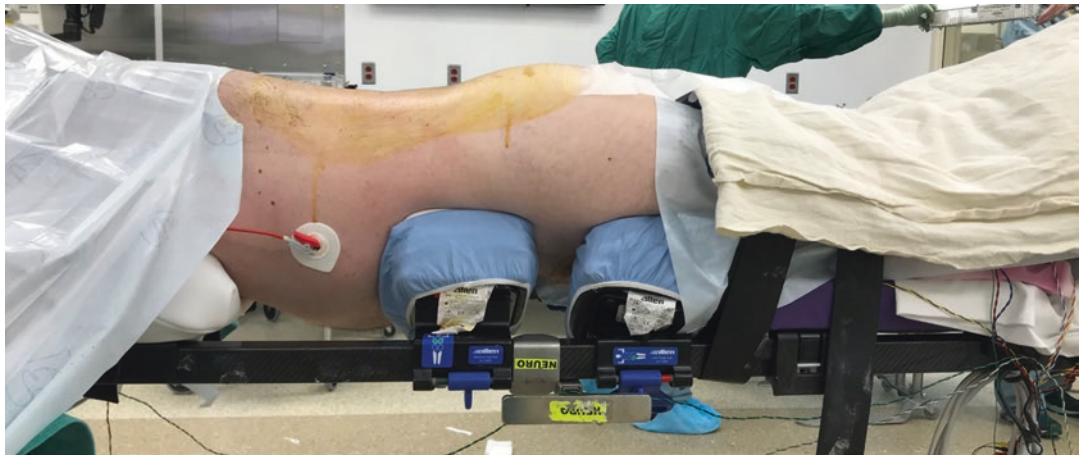

**Fig. 26.2** Prone positioning on a Jackson Frame with pressure points padded

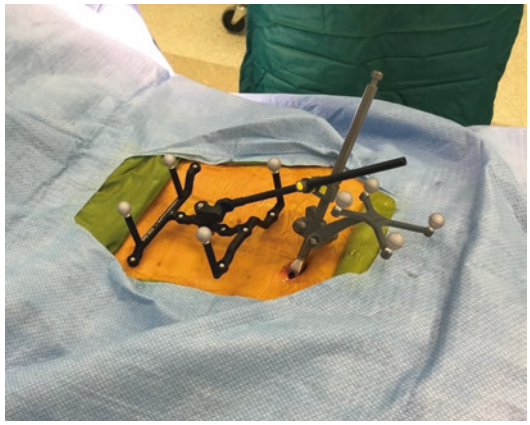

**Fig. 26.3** A dynamic reference array and a separate intraoperative CT array are attached to the iliac pin


**Fig. 26.4** Acquisition of intraoperative CT scan for registration of navigation system

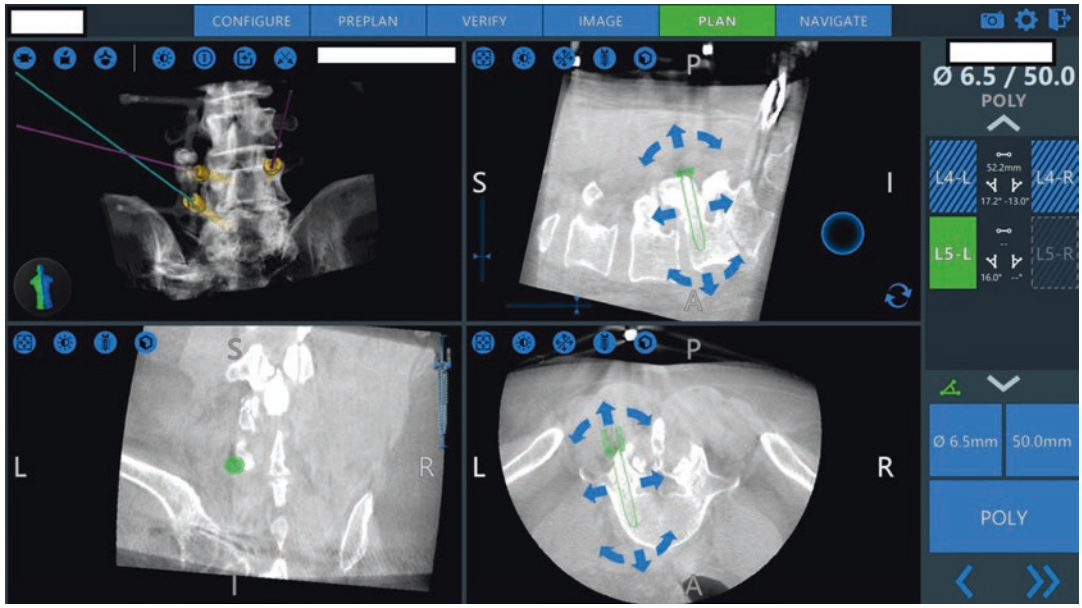


**Fig. 26.5** Planning of pedicle screw sizes and trajectories using the computer interface of the robotic navigation unit

is performed through the same right paramedian incision guided by the robotic navigation system without the need for fluoroscopic imaging (Fig. 26.7). After appropriate positioning of the tubular retractor, the microscope is brought into the operative field. Under microscopic visualization, an L4 laminotomy is created using a high-speed drill and Kerrison rongeurs. A transverse cut through the right L4 pars interarticularis is made. The inferior articular process of L4 is removed and saved as autograft bone. The superomedial portion of remaining superior articular process of L5 is removed. The tubular retractor is then tilted contralaterally. The con-

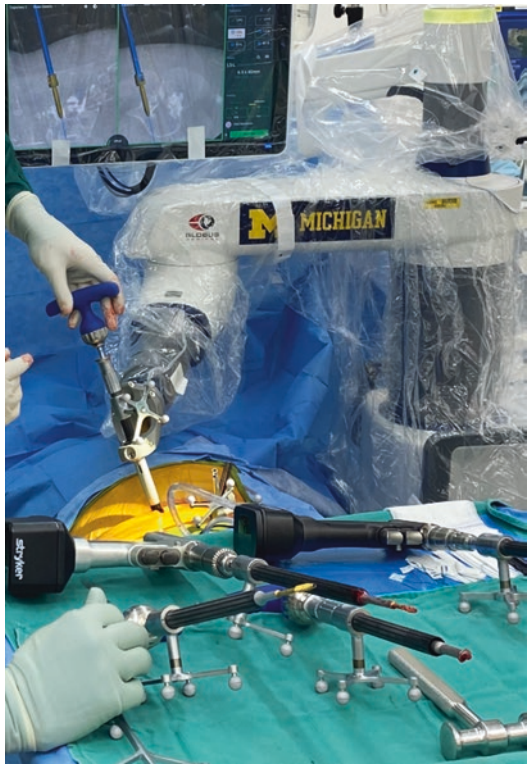


**Fig. 26.6** Navigated instruments passed through the robotic arm's effector tube for pedicle screw placement

tra-lateral laminar bone is then undercut with a high-speed drill and Kerrison rongeurs. The hypertrophic ligamentum flavum is removed initially in the central region and then laterally with undercutting of the contralateral facet. The navigation system is used to confirm that an adequate bony decompression is achieved contralaterally (Fig. 26.8).

After the dorsal decompression is completed, attention is turned to the discectomy. The traversing nerve root is carefully mobilized and retracted. The L4-5 disk space is identified. The navigation system can be used to localize the disc space and optimize the trajectory (Fig. 26.9). A bayoneted knife is utilized to open the annulus. Standard discectomy is performed. The endplates are prepared for grafting. Allograft bone, as well as local autograft bone, is placed in the disk space. The robotic navigation unit can also be used to plan and insert an expandable cage (Fig. 26.10). In this particular case, navigation is not used to insert the cage. Instead, the navigation pointer is used to ascertain the trajectory and then the cage is impacted into the disk space. The cage is expanded and

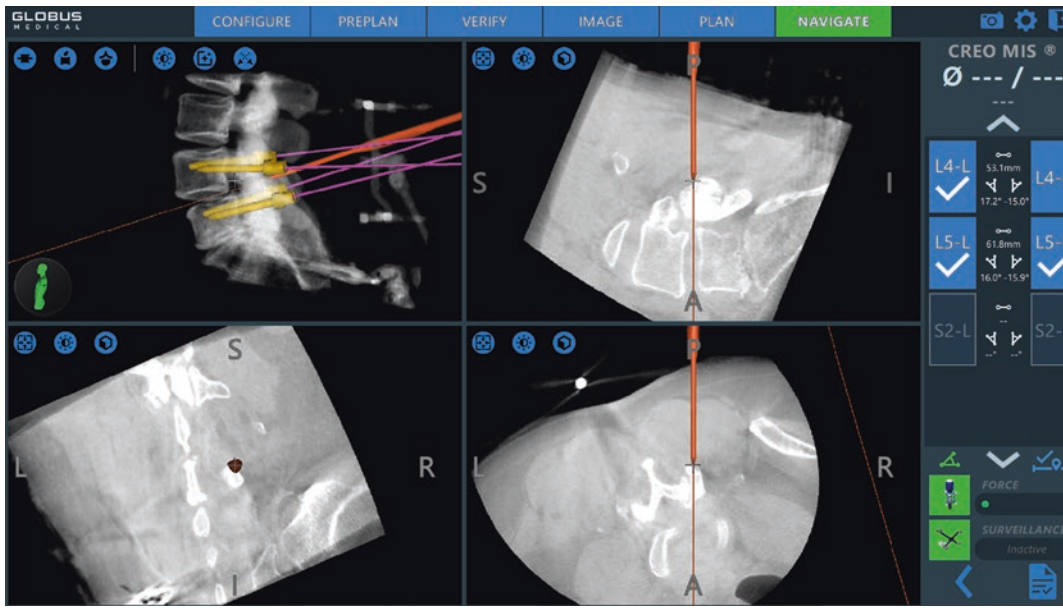


**Fig. 26.7** Robotic-assisted placement of navigated tubular retractor over L4-5

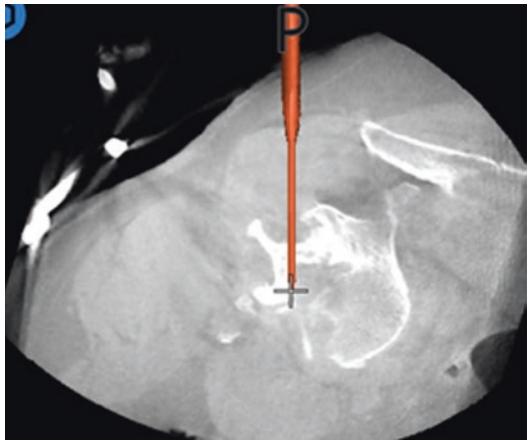

**Fig. 26.8** Use of navigation system to confirm adequate contralateral decompression

final positioning is confirmed with fluoroscopy. The tubular retractor is removed. Screw heads connected to screw extenders are attached to the L4 and L5 pedicle screw posts on the right. A precut and contoured rod is inserted through screw heads on the left. Set screws are placed. A second precut and contoured rod is inserted through screw heads on the right. Set screws are placed and tightened to the manufacturer-specified torque. Extended screw tabs are removed. The iliac pin is removed. Incisions are closed in layers and the skin is closed with tissue glue. Clean dressings are applied.

Postoperative X-rays are shown in Fig. 26.11, revealing adequate positioning of the screws and interbody cage.

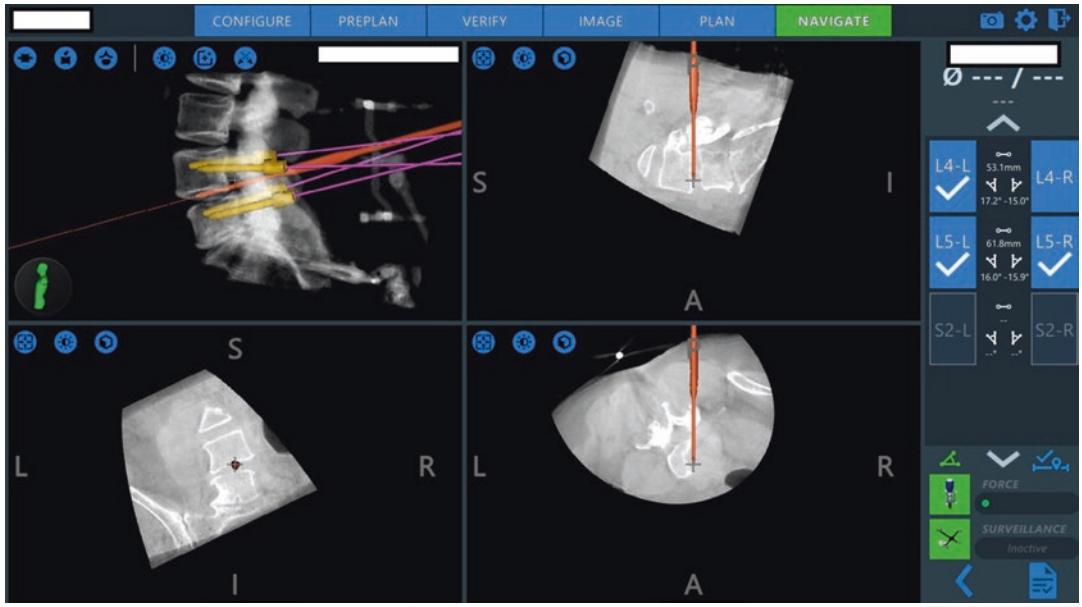


**Fig. 26.9** Navigation system used to assess disc space trajectory in preparation for discectomy

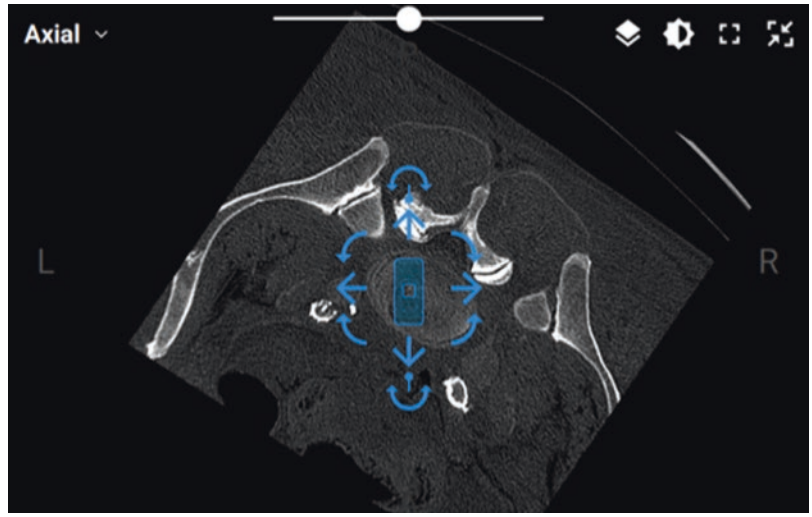


**Fig. 26.10** Optimization of interbody cage size and position using navigation system

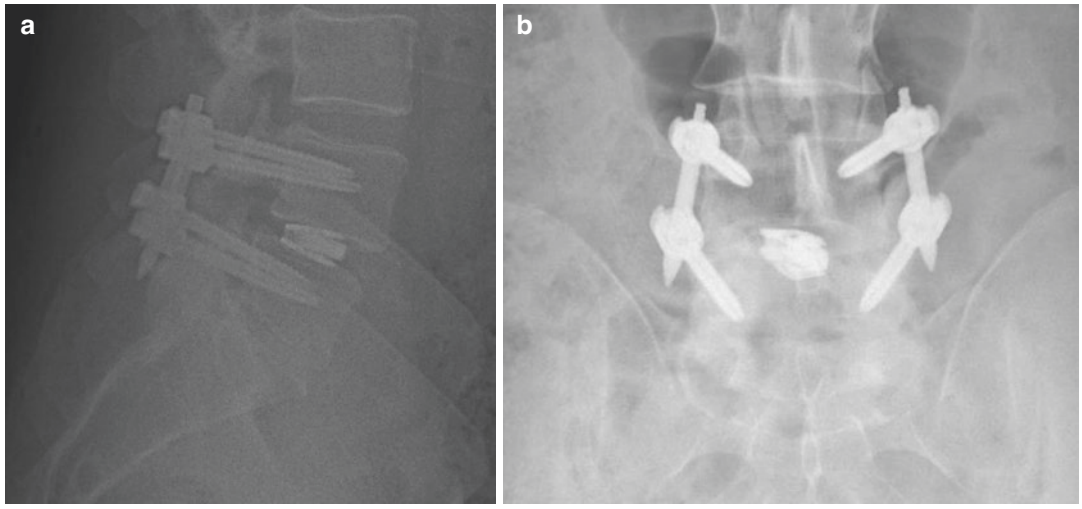


**Fig. 26.11** Postoperative lateral (**a**) and AP (**b**) X-rays confirm adequate positioning of pedicle screws and interbody cage

## References

1. Hammad A, Wirries A, Ardeshiri A, Nikiforov O, Geiger F. Open versus minimally invasive TLIF: literature review and meta-analysis. J Orthop Surg Res. 2019;14(1):229.
2. Ghasem A, Sharma A, Greif DN, Alam M, Maaieh MA. The arrival of robotics in spine surgery: a review of the literature. Spine (Phila Pa 1976). 2018;43(23):1670–7.
3. Elswick CM, Strong MJ, Joseph JR, Saadeh Y, Oppenlander M, Park P. Robotic-assisted spinal surgery: current generation instrumentation and new applications. Neurosurg Clin N Am. 2020;31(1):103–10.
4. Joseph JR, Smith BW, Liu X, Park P. Current applications of robotics in spine surgery: a systematic review of the literature. Neurosurg Focus. 2017;42(5):E2.
5. Khalsa SSS, Mummaneni PV, Chou D, Park P. Present and future spinal robotic and enabling technologies. Operative Neurosurg. 2020. In Press.

6. Srinivasan D, Than KD, Wang AC, La Marca F, Wang PI, Schermerhorn TC, et al. Radiation safety and spine surgery: systematic review of exposure limits and methods to minimize radiation exposure. World Neurosurg. 2014;82(6):1337–43.
7. Jiang B, Pennington Z, Azad T, Liu A, Ahmed AK, Zygourakis CC, et al. Robot-assisted versus freehand instrumentation in short-segment lumbar fusion: experience with real-time image-guided spinal robot. World Neurosurg. 2020;136:e635–e45.
8. Rampersaud YR, Foley KT, Shen AC, Williams S, Solomito M. Radiation exposure to the spine surgeon during fluoroscopically assisted pedicle screw insertion. Spine (Phila Pa 1976). 2000;25(20):2637–45.

# 27 Recent Advancements in Robot-Assisted Spinal Surgery in China and Future Perspective

Yong Hai and Lung Chan

## 27.1 Introduction

In August 2015, the first case of robot-assisted C1-C2 transarticular screw fixation was performed at Beijing Jishuitan Hospital [1] (technical support by TINAVI Medical Technologies Co., Ltd. Beijing, China). At the end of the same year, the Renaissance® (second-generation spine robot-assisted system by Mazor Robotics Ltd., Caesarea. Israel) went public in China [2]. Currently, only the above two robot-assisted systems are used for clinical application in China (TiRobot® & Mazor Renaissance®).

To the author's knowledge, TiRobot® has been installed and applied in 86 hospitals since 2016 and has performed over 10,000 spinal operations. Renaissance® robots were installed and applied in about 20 hospitals. Both robot-assisted systems are shared-control robots that simultaneously allow both the surgeon and robot the ability to control instruments and motions [3, 4].

Synopsis
As we all know, robot-assisted technology is becoming more and more widely used in spinal surgery. Meanwhile, it has become a trend in China. However, the application of robot-assisted in spinal surgery is still in its infancy. In this chapter, the author focuses on the situation of robot-assisted spinal surgery in mainland China.

Y. Hai (✉)
Department of Orthopedic Surgery, Beijing Chao-Yang Hospital, Capital Medical University, Beijing, China
e-mail: yong.hai@ccmu.edu.cn

L. Chan
Department of Orthopedics, Guangzhou Red Cross Hospital Affiliated to Jinan University, Guangzhou, China

## 27.2 Clinical Outcomes and Accuracy

To describe the clinical outcome and accuracy of the robot's application in China, a literature review was performed using PubMed and China National Knowledge Infrastructure (CNKI) via the following keywords: "robot-assisted," "spine surgery," "screw placement," "China." The languages and dates of publication are unlimited (Mainly English, the rest in Chinese). TiRobot® and Mazor Renaissance® are described separately below.

## 27.3 TiRobot®

China does not make its own equivalent of the da Vinci system, but it is starting to catch up. TiRobot® is the third-generation spine and trauma robot-assisted system by TINAVI Medical Technologies Co., Ltd. Beijing, China. In 2016, CFDA (China Food and Drug Administration) approved TiRobot® for use in spinal surgery in China. It has a single arm that



J.-S. Kim et al. (eds.), *Technical Advances in Minimally Invasive Spine Surgery*,
https://doi.org/10.1007/978-981-19-0175-1_27

can conduct spinal surgery (Figs. 27.1, 27.2 and 27.3). Tian et al. reported the first case of atlantoaxial screw fixation by the TiRobot® system for complex upper cervical deformity. The deviation between the actual position and the expected position was 0.8798 mm. C1-2 transarticular fixation is a reliable procedure. However, the procedure is high risk because of the important structures and frequent anatomical variation around the atlantoaxial region. Navigation improves the accuracy, but it might require repeated adjustments of the trajectories, which is inconvenient. TiRobot-assisted surgery can make this process easier and has the potential to improve safety and accuracy. It shows significant potential in spinal surgery [1]. Tian et al. also noted a clinical comparative study about pedicle screws placement by TiRobot® system with more accuracy [5].

**Fig. 27.1** TiRobotic-assisted screw placement system

Han et al. demonstrated that TiRobot-assisted pedicle screw placement is a safer and more accurate way for the insertion of thoracolumbar pedicle screw via a prospective randomized controlled trial [6]. The robot-assisted group has more perfectly placed screws (9.2% than the free-hand fluoroscopy-assisted group). None of the screws violated the proximal facet joint in the robot-assisted group, significantly less blood loss (186.0 ± 255.3 ml: 217.0 ± 174.3 ml; $p < 0.05$) and less radiation exposure (21.7 ± 11.5 μSv: 70.5 ± 42.0 μSv; $p < 0.01$) than the free-hand fluoroscopy-assisted group.

One of the essential effects of traditional TILF (Transforaminal Lumbar Interbody Fusion) is the risk of superior-level facet joint violations (FJV). Zhang et al. noted that minimally invasive robot-assisted TLIF decreased the FJV than the tradi-

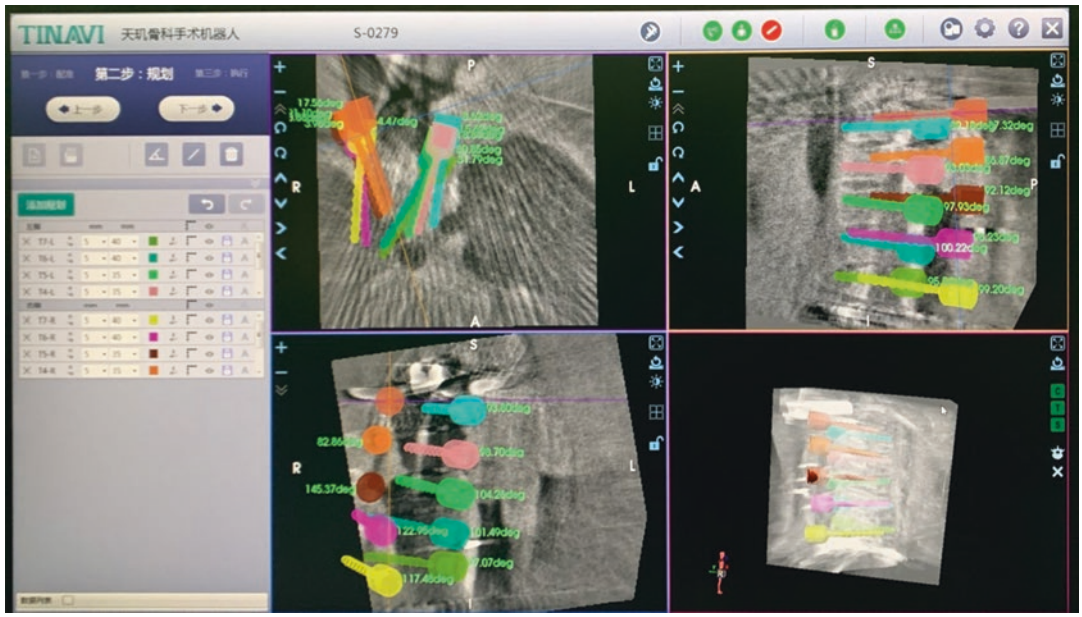


**Fig. 27.2** TiRobotic-assisted screw placement system

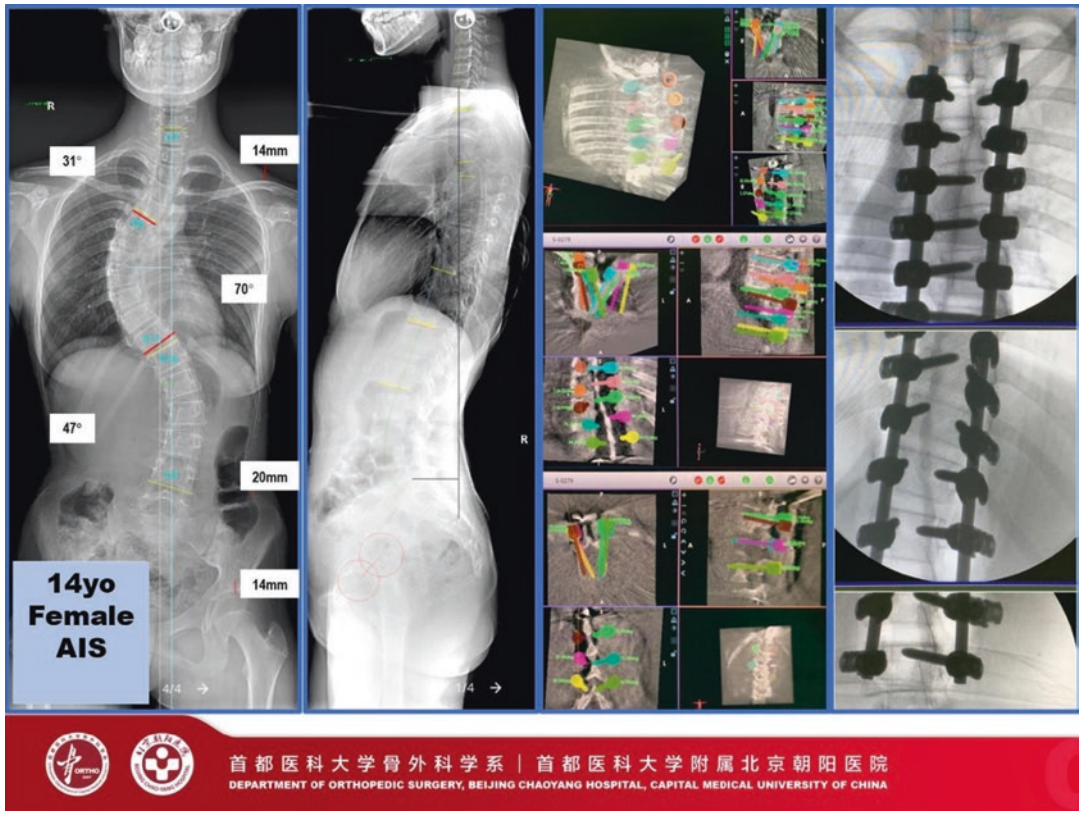


**Fig. 27.3** 14-year-old female adolescent idiopathic scoliosis corrective surgery by TiRobot® system

tional open fluoroscopic-guided group (0.05 vs 0.38, $p = 0.000$) [7].

In 2020, Fan et al. demonstrated using the TiRobot® system to improve the accuracy of cervical screws insertion and clinical outcomes in their prospective randomized controlled trial [8]. Feng et al. reported the clinical outcomes of OLIF (Oblique Lateral Interbody Fusion) by percutaneous robot-assisted minimally invasive pedicle which shows effectiveness for elderly patients with lumbar degenerative diseases [9].

## 27.4 Mazor Renaissance®

Since the Mazor Renaissance® entered the Chinese hospitals at the end of 2016, Hai et al., the first batch of Chinese hospitals to use Mazor Renaissance®, has reported a comparative study between robot-assisted pedicle screws insertion and conventional technique. Mazor Renaissance® group was more accurate than the conventional free-hand group (8.2% with statistical significance), with a lower radiation dosage of intraoperative fluoroscopy. However, for one of the patients with congenital extremely severe scoliosis, the robot-assisted matching failed due to abnormal anatomical structure, and the conventional nail placement was used instead [2] (Figs. 27.4, 27.5, 27.6 and 27.7).

Yang et al. demonstrated robot-assisted percutaneous pedicle screw placement combined with MIS-TLIF is an effective minimally invasive method for treating lumbar spondylolisthesis via a comparative cohort study. The control group (under fluoroscopic guidance) has more violations of the pedicle wall (20% than the robot-assisted group), also with higher incidences of invasion of the facet joints [10].

Zhang et al. indicated that obesity, osteoporosis, and congenital scoliosis were risk factors for dissatisfaction with robot-assisted screw place-

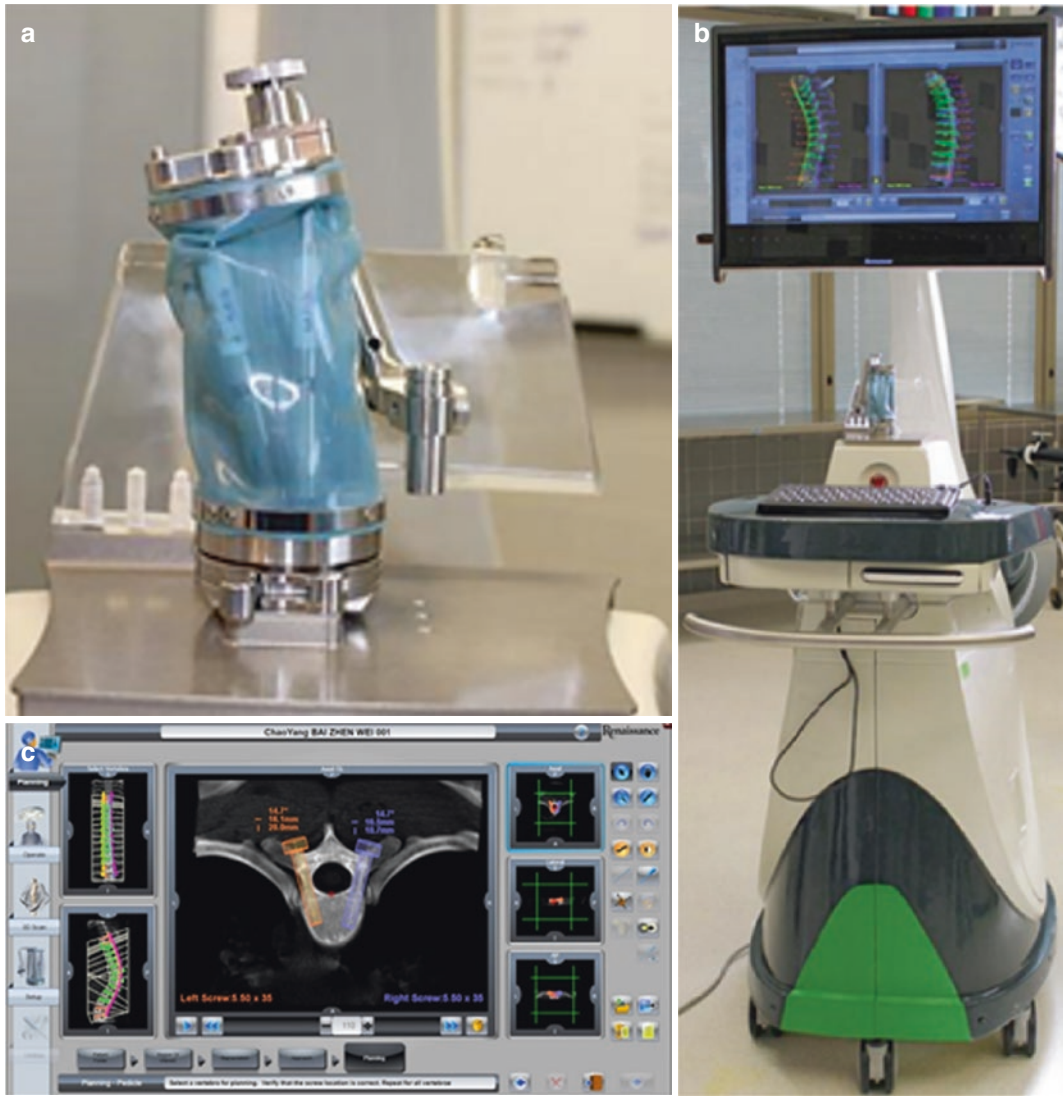


**Fig. 27.4** (**a**) Mazor Renaissance system. (**b**) Robotic work station. (**c**) Screws are planned in the software before the operation

ment. They recommend that it is best to avoid cases involving these risk factors in robotics applications [11].

Tian et al. reported a comparative study of spinal robot-assisted (group A) and traditional fluoroscopy-assisted (group B) percutaneous reduction and internal fixation for thoracolumbar fractures with 12–24 months of follow-up. There were no complications such as neurovascular injury, screw loosening, and fracture in both groups. The accuracy rate of screw placement in groups A and B was 93.75% and 84.71% [12].

## 27.5 Cost-Effectiveness Analysis

There is a leak of studies analyzing the cost-effectiveness of robots in spine surgery. As far as the author knows, the average cost will be increased by ¥13,000–16,000 Chinese Yuan

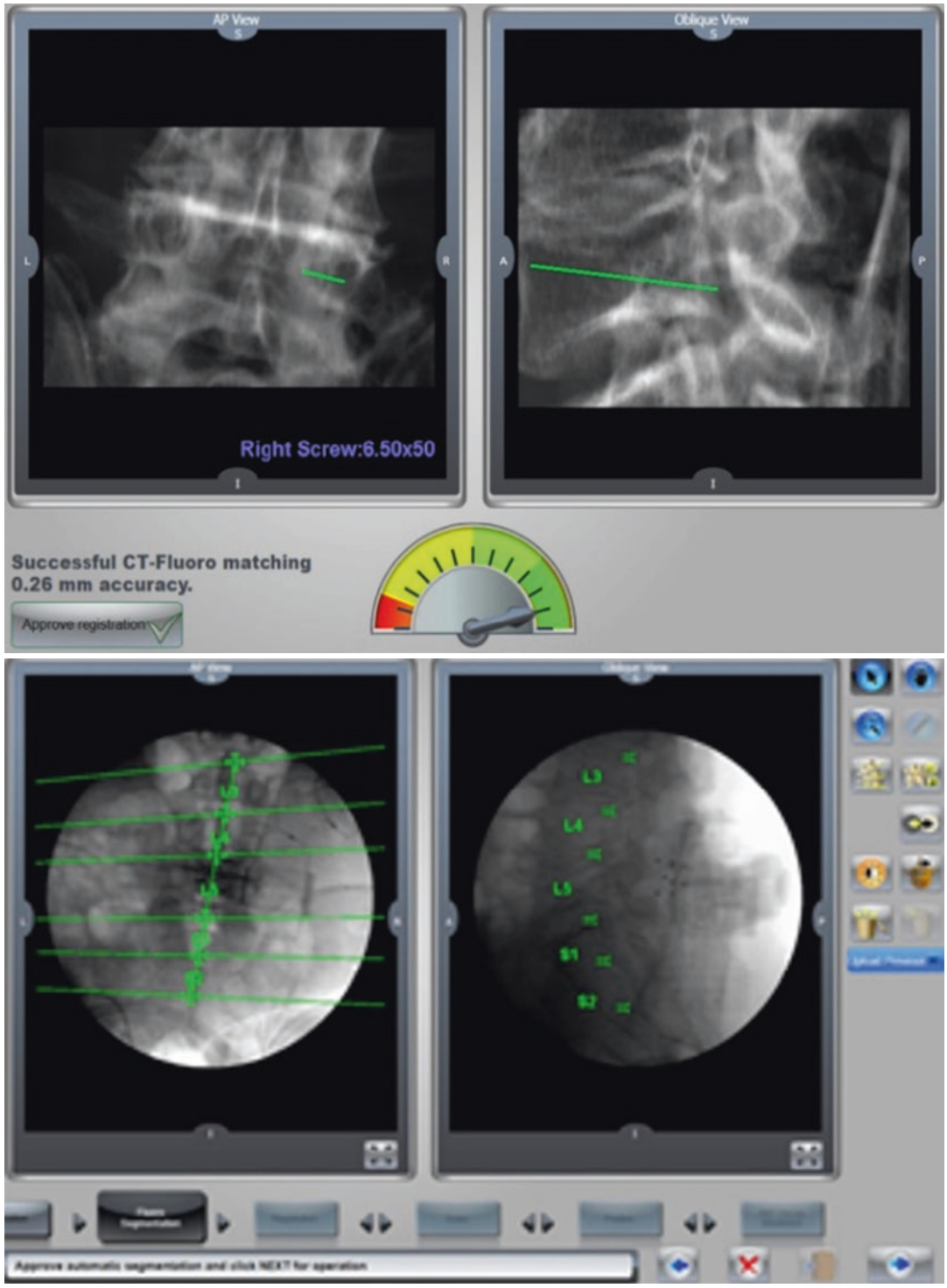


**Fig. 27.5** Auto-registration

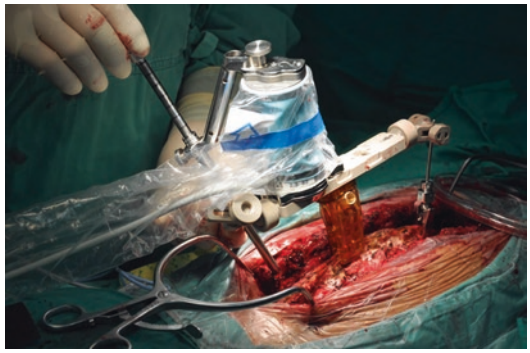

**Fig. 27.6** Robotic-assisted drilling of a channel was used for the placement of a pedicle screw over a guidewire

(equivalent to US$1800–2200), based on the apportioned cost of using TiRobot® system and consumables. It has high initial and maintenance costs. Likewise, Mazor Renaissance® also required expensive installation and maintenance costs. According to Tian et al., the cost of treating a single-level spine fracture increased by about ¥7500 Chinese Yuan (equivalent to US$1300) [12]. In the near future, it is expected that the application and consumables costs will be covered by Chinese health insurance systems to reduce the financial burden on patients. We expect to reduce the incidence of complications through more accurate screws placement and less facet violations, thereby shortening the operation time, reducing revision, lower infection rate, and reduced length of stay to achieve the maximum cost-benefit.

## 27.6 Future Perspective

In China, with rapid development and improvement, robotics in spinal surgery has great promise. The following technologies are currently under research and development.

Li et al. revealed a novel robotic system for pedicle screw fixation named "Orthbot." The "Orthbot" system has a power arm for automatic drilling stead of manual operation. It offers a new option for screw placement, bone cement, and vertebral biopsy [13].

For most spine surgeries, not only the placement of screws but also decompression. Sun et al. is committed to developing a robot-assisted system for decompressive laminectomy. They reveal a state recognition system to monitor the grinding and drilling process to avoid spinal nerves damage [14, 15].

2020 is an era of 5G (fifth-generation mobile network), meaning an era of ultra-high-speed connectivity. Currently, China as a developing country with genuine 5G technology is full of possibilities. Low-latency 5G connectivity allows a surgeon to do operations remotely. Long-distance patients can acquire more professional and accurate treatment.

## 27.7 Conclusion

China has a large population base, and a number of patients with spinal diseases required surgical treatment. Robot-assisted spinal surgery currently has better clinical outcomes. However, further clinical evaluation is needed to be verified. Combined with novel development technology, robot-assisted spinal surgery has great potential in China. With 5G technology, remote operation and presentation can be achieved without any obstacles.

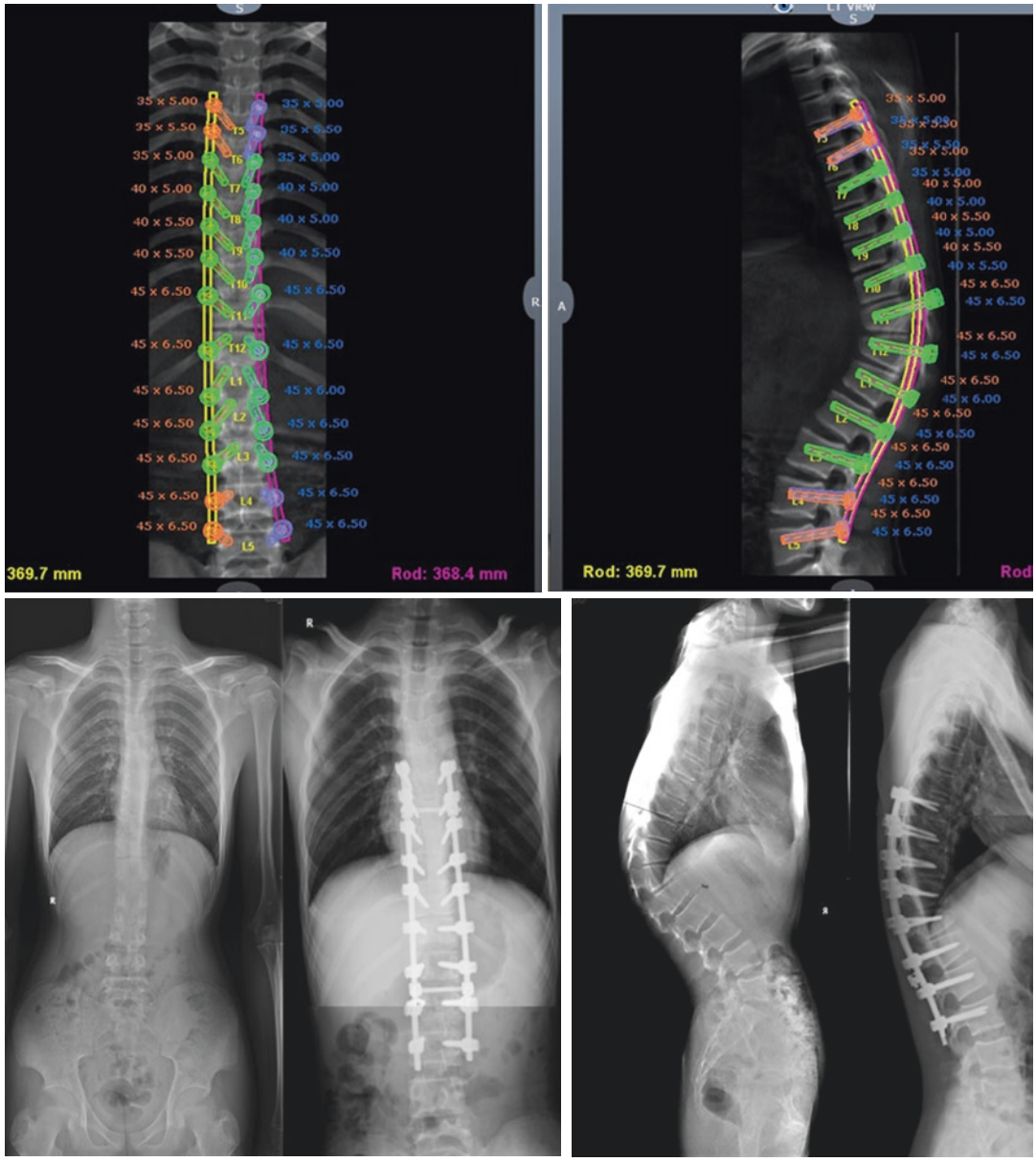


**Fig. 27.7** A 14-year-old male, kyphosis for 5 years. Planning for pedicle screw placement via a Robotic-assisted system before the procedure. Postoperative X-ray demonstrated spinal deformity was corrected

## References

1. Tian W. Robot-assisted posterior C1-2 transarticular screw fixation for atlantoaxial instability: a case report. Spine (Phila Pa 1976). 2016;41 Suppl 19:B2–5. https://doi.org/10.1097/BRS.0000000000001674 [published Online First: 2016/05/05].
2. Long C, Yong H. A comparative study of robot assisted insertion and traditional free-hand pedicle screw technique. Chin J Bone Joint. 2017;6(10):7. https://doi.org/10.3969/j.issn.2095-252X.2017.10.003.
3. D'Souza M, Gendreau J, Feng A, et al. Robotic-assisted spine surgery: history, efficacy, cost, and future trends. Robot Surg. 2019;6:9–23. https://doi.org/10.2147/RSRR.S190720. [published Online First: 2019/12/07]

4. Tian W, Liu YJ, Liu B, et al. Guideline for thoracolumbar pedicle screw placement assisted by orthopaedic surgical robot. Orthop Surg. 2019;11(2):153–9. https://doi.org/10.1111/os.12453. [published Online First: 2019/04/27]
5. Tian W, Fan M, Han X, et al. Pedicle screw insertion in spine: a randomized comparison study of robot-assisted surgery and fluoroscopy-guided techniques. J Clin Orthop Res. 2016;1(1):7. https://doi.org/10.19548/j.2096-269x.2016.01.003.
6. Han X, Tian W, Liu Y, et al. Safety and accuracy of robot-assisted versus fluoroscopy-assisted pedicle screw insertion in thoracolumbar spinal surgery: a prospective randomized controlled trial. J Neurosurg Spine. 2019:1–8. https://doi.org/10.3171/2018.10.SPINE18487. [published Online First: 2019/02/10]
7. Zhang Q, Xu YF, Tian W, et al. Comparison of superior-level facet joint violations between robot-assisted percutaneous pedicle screw placement and conventional open fluoroscopic-guided pedicle screw placement. Orthop Surg. 2019;11(5):850–6. https://doi.org/10.1111/os.12534. [published Online First: 2019/10/31]
8. Fan M, Liu Y, He D, et al. Improved accuracy of cervical spinal surgery with robot-assisted screw insertion: a prospective, randomized, controlled study. Spine (Phila Pa 1976) 2020;45(5):285–91. doi: https://doi.org/10.1097/BRS.0000000000003258 [published Online First: 2019/10/01].
9. Feng S, Tian W, Wei Y. Clinical effects of oblique lateral interbody fusion by conventional open versus percutaneous robot-assisted minimally invasive pedicle screw placement in elderly patients. Orthop Surg. 2020;12(1):86–93. https://doi.org/10.1111/os.12587. [published Online First: 2019/12/28]
10. Yang JS, He B, Tian F, et al. Accuracy of robot-assisted percutaneous pedicle screw placement for treatment of lumbar spondylolisthesis: a comparative cohort study. Med Sci Monit. 2019;25:2479–87. https://doi.org/10.12659/MSM.913124. [published Online First: 2019/04/05]
11. Zhang JN, Fan Y, Hao DJ. Risk factors for robot-assisted spinal pedicle screw malposition. Sci Rep. 2019;9(1):3025. https://doi.org/10.1038/s41598-019-40057-z. [published Online First: 2019/03/01]
12. Tian Y, Zhang J, Chen H, et al. A comparative study of spinal robot-assisted and traditional fluoroscopy-assisted percutaneous reduction and internal fixation for single-level thoracolumbar fractures without neurological symptoms. Chin J Reparative Reconstruct Surg. 2020;34(1):7. https://doi.org/10.7507/1002-1892.201905057. [published Online First: 2020/01/16]
13. Li Z, Chen J, Zhu QA, et al. A preliminary study of a novel robotic system for pedicle screw fixation: a randomised controlled trial. J Orthop Translat. 2020;20:73–9. https://doi.org/10.1016/j.jot.2019.09.002. [published Online First: 2020/01/08]
14. Sun Y, Wang L, Jiang Z, et al. State recognition of decompressive laminectomy with multiple information in robot-assisted surgery. Artif Intell Med. 2020;102:101763. https://doi.org/10.1016/j.artmed.2019.101763. [published Online First: 2020/01/26]
15. Zhang Q, Han XG, Xu YF, et al. Robotic navigation during spine surgery. Expert Rev Med Devices. 2020;17(1):27–32. https://doi.org/10.1080/17434440.2020.1699405. [published Online First: 2019/11/30]

# The Role of Robot-Assisted MIS Spinal Deformity Surgery

28

Lindsay D. Orosz, Alexandra E. Thomson, and Christopher R. Good

## 28.1 Case History

A female patient in her 40s had a history of adolescent idiopathic scoliosis in the thoracic and lumbar regions that was initially asymptomatic and treated with observation. Although she remained fit and active, she developed low back pain in her 30s. At that time, her right thoracic and left thoracolumbar curves were balanced at 30 degrees. Despite years of non-operative treatments such as physical therapy, injections, medications, rest, and time, she continued to have low back pain radiating to the left lateral thigh and anterior shin, with a 60:40 back-to-leg ratio, and an average pain of 7/10 on a visual analog pain scale. She developed progressive coronal imbalance to the left and worsening radiculopathy secondary to spondylolisthesis at L5/S1. Lumbar discography revealed concordant pain provocation at lumbar disc levels L2-S1, while her thoracic curve remained asymptomatic. Based on her declining quality of life and increased opioid medication demand imposed by her pain combined with her progressive spinal deformity, she elected to proceed with surgical intervention.

Her past medical history includes GERD, hypothyroidism, and anxiety. Her past surgical history includes an orthopedic knee procedure, gynecologic procedure, and ENT procedure. She does not use nicotine products and her family history is noncontributory.

On scoliosis plain films, Cobb angles are 30 degrees to the right T5-T10, 30 degrees to the left T10-L3, she stands 5.7 cm to the left of the CSVL, with the right shoulder elevated 2.2 cm and the right hemipelvis elevated 1.3 cm. In the sagittal plane, there is 64 degrees of lumbar lordosis, 65 degrees of pelvic incidence, and 17 degrees of pelvic tilt (Fig. 28.1). Flexion and extension X-rays demonstrate translatory instability at L5/S1. Lumbar MRI showed stenosis at L5/S1.

## 28.2 Key Challenges

- Achieving fusion and deformity correction in an MIS approach
- Improving the pelvic tilt and shoulder asymmetry without overcorrecting the alignment
- Treating all causes of instability, mechanical back pain, and radiculopathy to avoid residual postoperative pain

L. D. Orosz
National Spine Health Foundation, Reston, VA, USA
e-mail: lorosz@spinehealth.org

A. E. Thomson
Virginia Spine Institute, Reston, VA, USA

Department of Orthopaedics, University of Maryland School of Medicine, Baltimore, MD, USA

C. R. Good (✉)
Virginia Spine Institute, Reston, VA, USA



J.-S. Kim et al. (eds.), *Technical Advances in Minimally Invasive Spine Surgery*,
https://doi.org/10.1007/978-981-19-0175-1_28

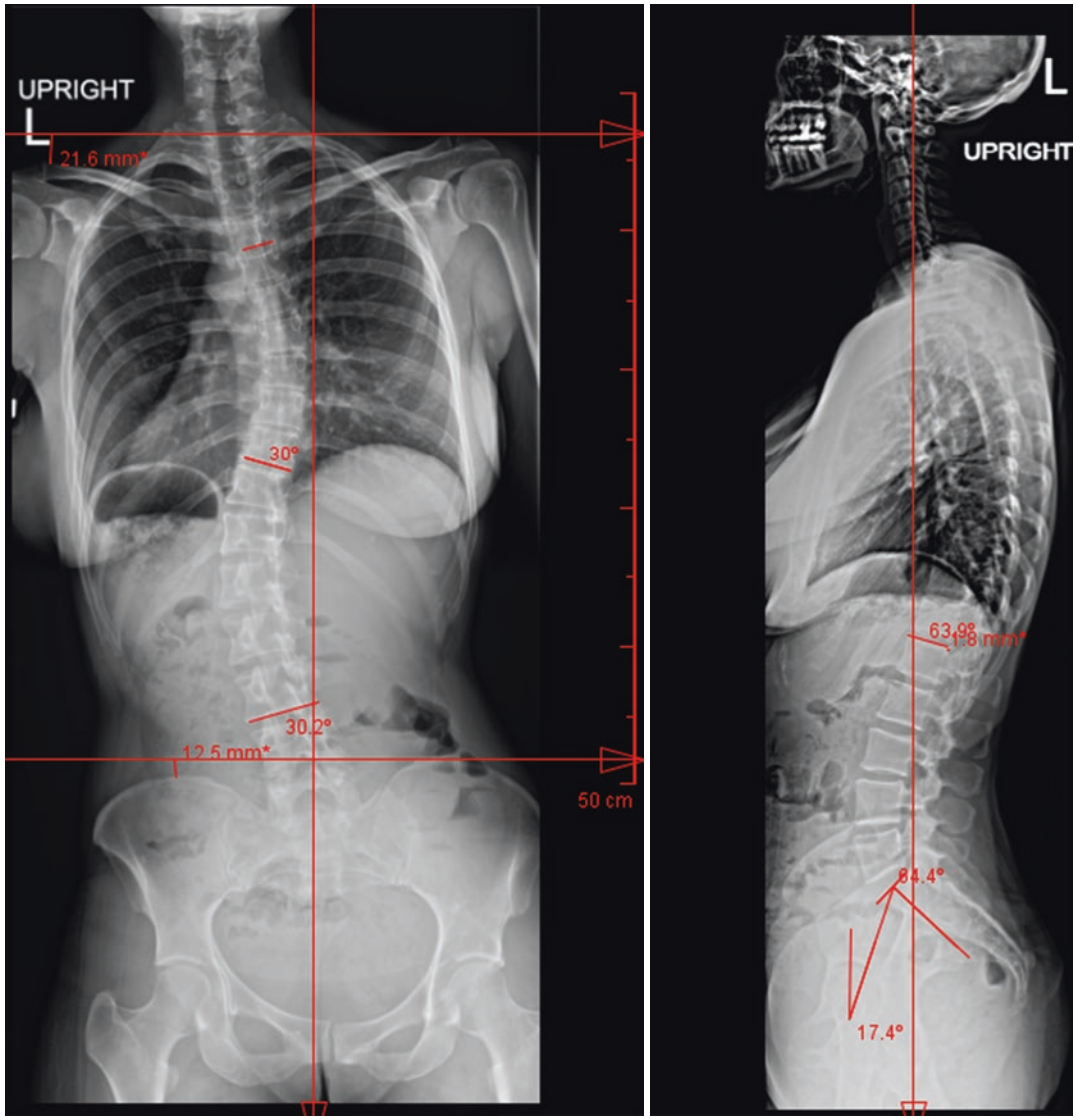


**Fig. 28.1** Preoperative AP and Lateral Scoliosis X-rays demonstrating coronal deformity and sagittal alignment assessment

## 28.3 Surgeon's Rationale

This is a highly unusual situation because spinal deformities of this size typically do not lead to symptoms that require surgical intervention. This very motivated patient had undergone extensive and exhaustive non-operative treatment for years; however, despite this, she continued to have debilitating symptoms of back pain with radiculopathy stemming from the coronal imbalance and instability at L5/S1. Traditionally, this surgery would have been accomplished through an open approach; however, the morbidity is significant with increased estimated blood loss (EBL), increased tissue dissection, higher postoperative pain levels, concerns for future adjacent level issues due to tissue disruption, and a potential need for initial recovery in the intensive care unit. Alternatively, achieving the surgical

goals using a minimally invasive, muscle-sparing technique dramatically reduces morbidity. In the setting of multilevel interbody fusions that cross the lumbosacral junction combined with pelvic fixation, the option opens for a minimally invasive approach to the posterior thoracolumbar instrumented fusion for alignment correction and indirect neurologic decompression. The patient's young age and desired activity level were also factors in the decision-making for this robotic-assisted MIS spinal deformity surgery.

In the literature, robotic-guided spine surgery has been associated with a reduction in complications, revision rates, and intraoperative radiation exposure. In addition to these advantages, precise preoperative planning is made possible by the high-resolution, three-dimensional, CT-based planning software. Preoperative planning allows for optimization of implant size and trajectory matched to the patient's specific anatomical features and planning of facet decortication and fusion through the same incision; the software allows for simulation of deformity correction which allows for optimization of screw head cadence for rod placement and pelvic fixation.

## 28.4 Procedural Steps

- On day 1 of planned staged surgery, OLIF was performed at L2/3, L3/4, L4/5, L5/S1 (Fig. 28.2).
- After the anterior surgery, CT scan of the thoracic and lumbar spine down to S3 with robotic protocol and standing AP and Lateral Scoliosis X-rays were obtained (Fig. 28.3). The results confirmed excellent correction of global coronal and sagittal balance and reduction of the L5/S1 spondylolisthesis. The patient's preoperative neurologic symptoms completely resolved after the anterior approach. Combined, these confirmed the approach for the posterior stage would be MIS rather than open.
- Posterior implants and incisions were planned using the 3D planning software (Figs. 28.4, 28.5, 28.6 and 28.7). Implant sizes are shared with the OR team. In addition, the software allows for planning facet trajectories for decortication to be performed through the same MIS incisions (Fig. 28.8). Finally, deformity correction is simulated

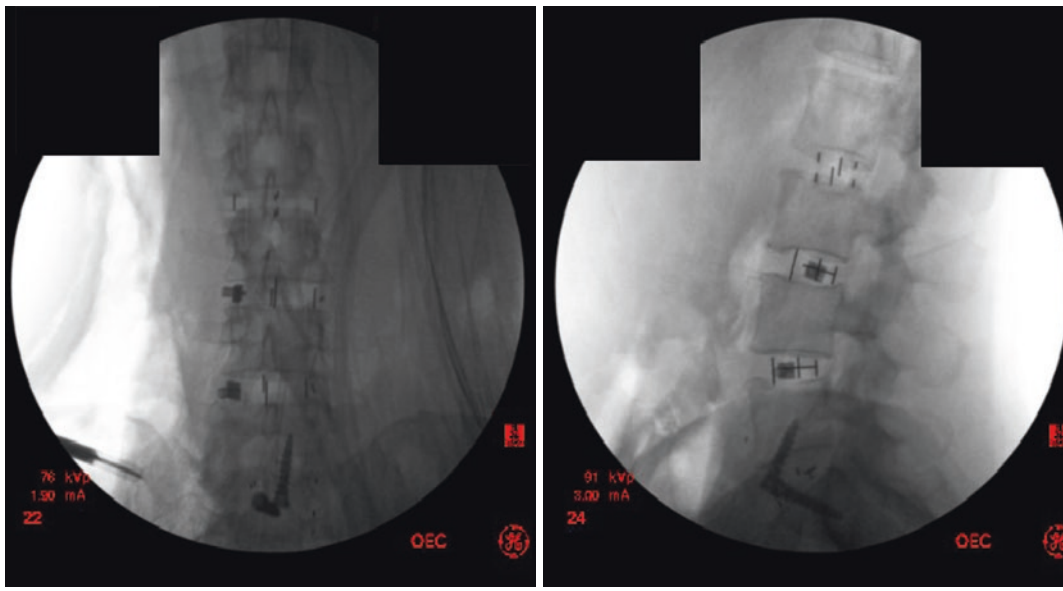


**Fig. 28.2** Intraoperative AP and Lateral fluoroscopic images after day 1 of surgery demonstrating OLIFs L2-sacrum, excellent correction of coronal and sagittal deformity, and reduction of spondylolisthesis

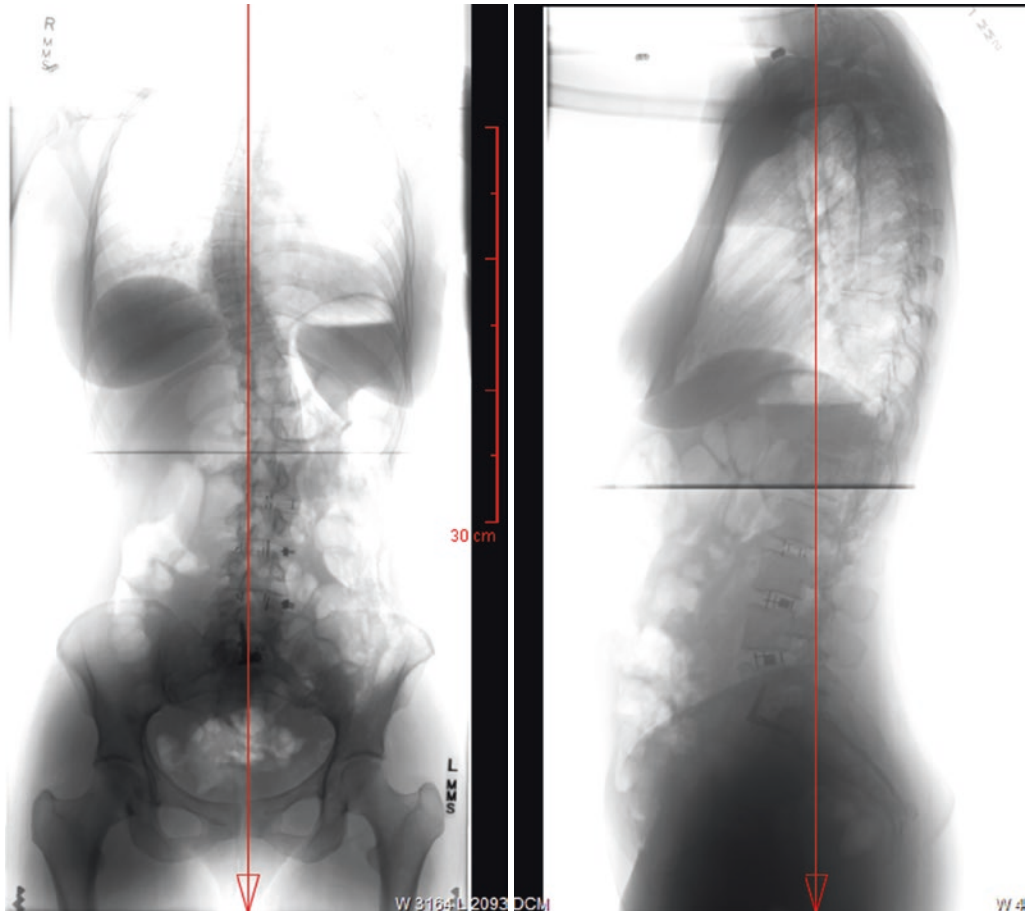


**Fig. 28.3** Postoperative AP and Lateral Scoliosis X-rays after anterior reconstruction demonstrate OLIFs L2-sacrum, excellent correction of coronal and sagittal deformity, and reduction of spondylolisthesis

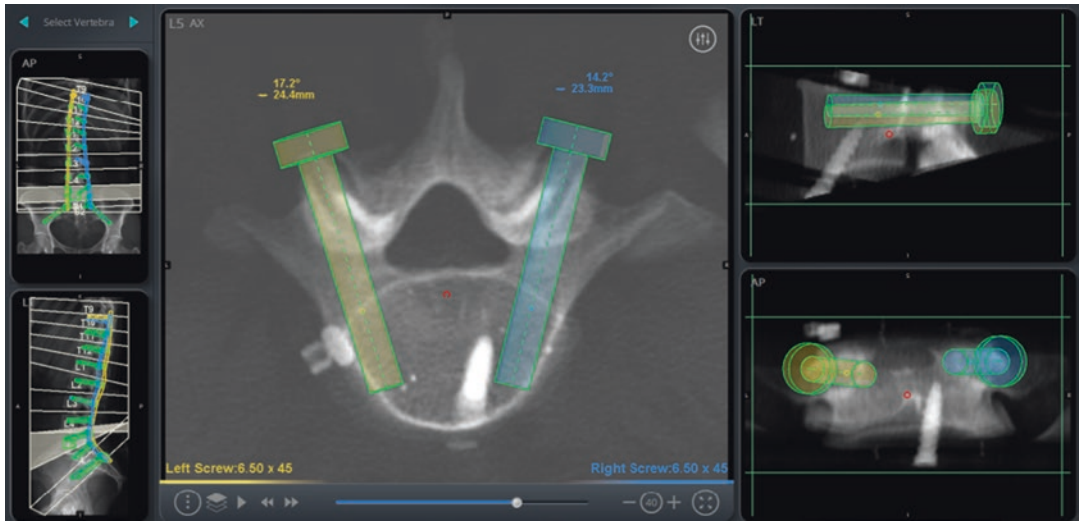


**Fig. 28.4** Screenshot of robotic planning software showing the ability to simultaneously view global construct parameters and perform three-dimensional segmental planning of pedicle screws. This allows for optimization of safe screw trajectories and screw head alignment for rod placement

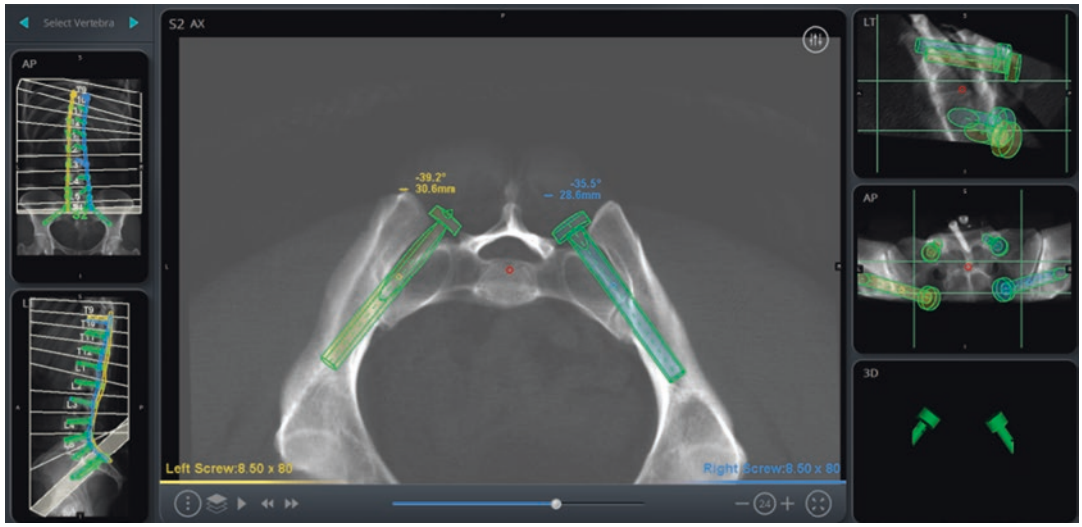


**Fig. 28.5** Screenshot of robotic planning software demonstrating an axial view with the planning of S2AI pelvic fixation

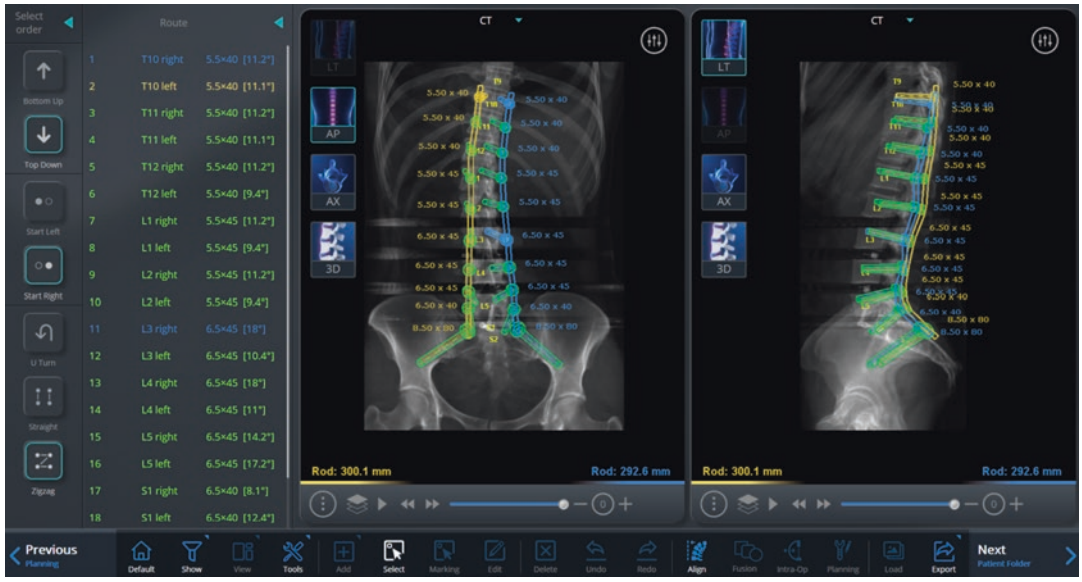


**Fig. 28.6** Screenshot of final construct planning demonstrating placement of all implants with visualization of straight coronal rod placement and desired rod lordosis in the sagittal plane

and screw cadence can be modified to facilitate rod placement (Fig. 28.9).

- On day 2 of planned staged surgery, MIS PIF T11-S1, bilateral percutaneous S2AI fixation, and facet decortication with fusion was performed using the Mazor X Robotic System for guidance.
- The patient was placed in the prone position on a Jackson table.
- The robotic system was attached to the PSIS through two stab incisions with a threaded pin.
- Registration was performed correlating intraoperative fluoroscopic images to the preopera-

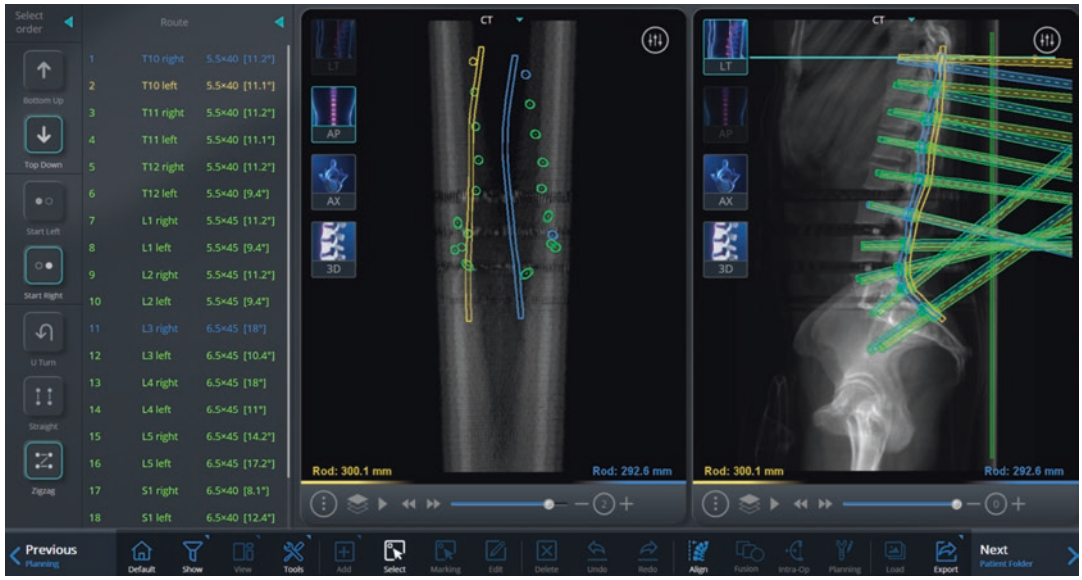


**Fig. 28.7** Screenshot of robotic plan demonstrating the final size of each planned implant and also demonstrating anticipated skin incisions for each of the percutaneous screw trajectories

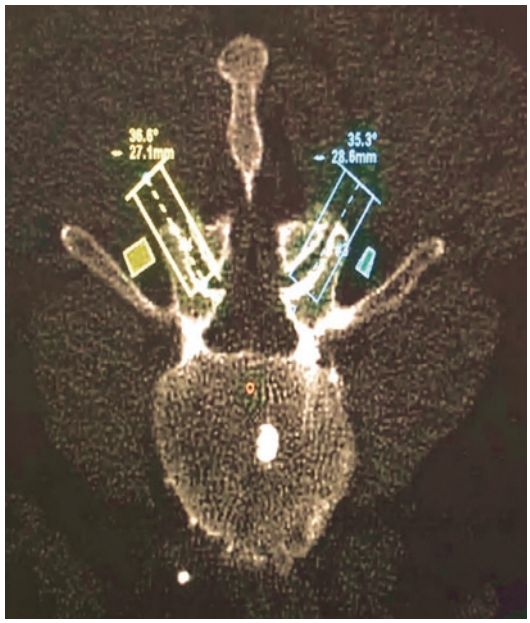


**Fig. 28.8** Axial view of robotic plan demonstrating 9-mm trajectory across the facet joint for the purposes of decortication and bone grafting. The drill is not advanced beyond a depth of 10 mm and extreme care must be taken to avoid advancing the drill deeper toward the spinal canal (example image from another case)

tive CT scan with a high degree of accuracy (first round, L3-S2).

- A 3-cm midline incision was used for the placement of pelvic fixation.
- Muscle-splitting lateral incisions were used for the pedicle screw instrumentation, facet decortications, and MIS bone grafting. The incisions were pre-planned to ensure all screw trajectories would converge allowing for very small skin incisions.
- First, bilateral S2AI screws were placed using the robot to guide the trajectory combined with fluoroscopic verification, followed by drilling, placing K-wires, tapping over K-wires, and then placing the screws. Of note, the current addition of navigation to the robotic system (Mazor X Stealth Edition) is felt to obviate the need for K-wires in the workflow.
- Next, the pedicle screw tracks were made L3-S1 using robotic guidance followed by placing the robotic-guided scalpel, placing a dilator, drilling, placing K-wires, and verifying with fluoroscopy (Fig. 28.10).
- Prior to screw placement, facet decortication was performed at each level bilaterally by

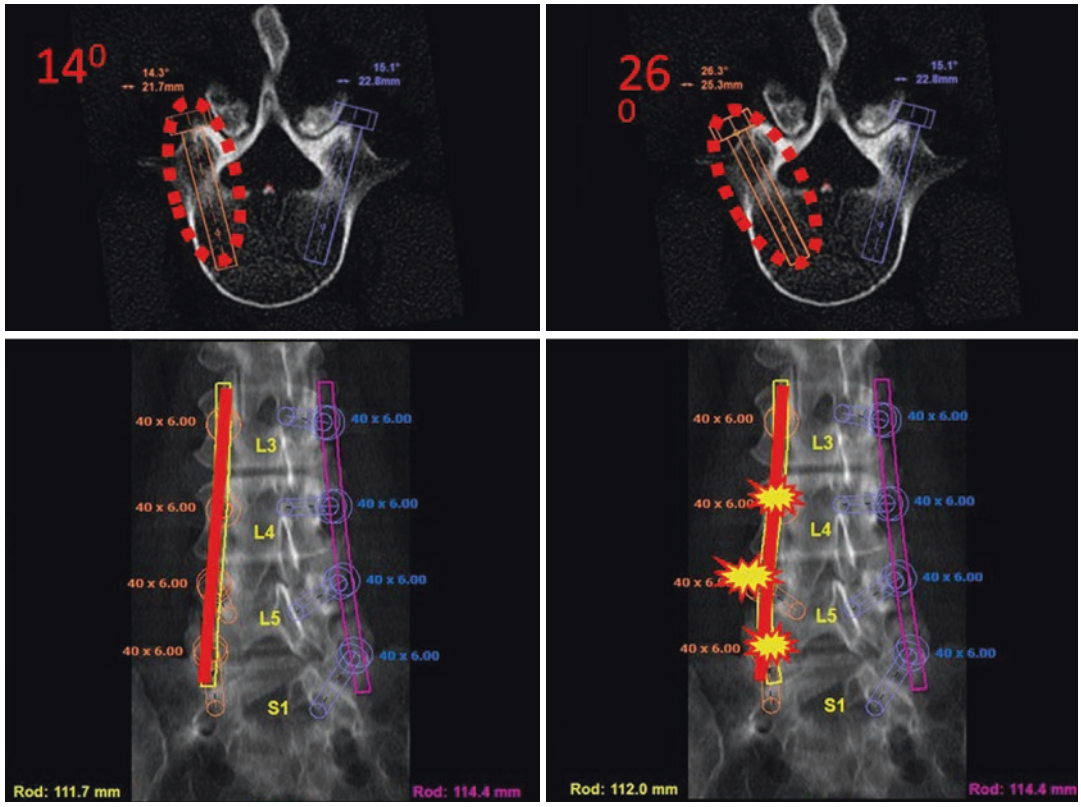


**Fig. 28.9** The same axial cut on both the right and left but with two very different screw trajectories. This demonstrates how a small change in screw trajectory translates into the difference of the rod being aligned in the coronal view or not, leading to potential difficulties placing a rod or perhaps increased risk for screw pull out (example image from another case)

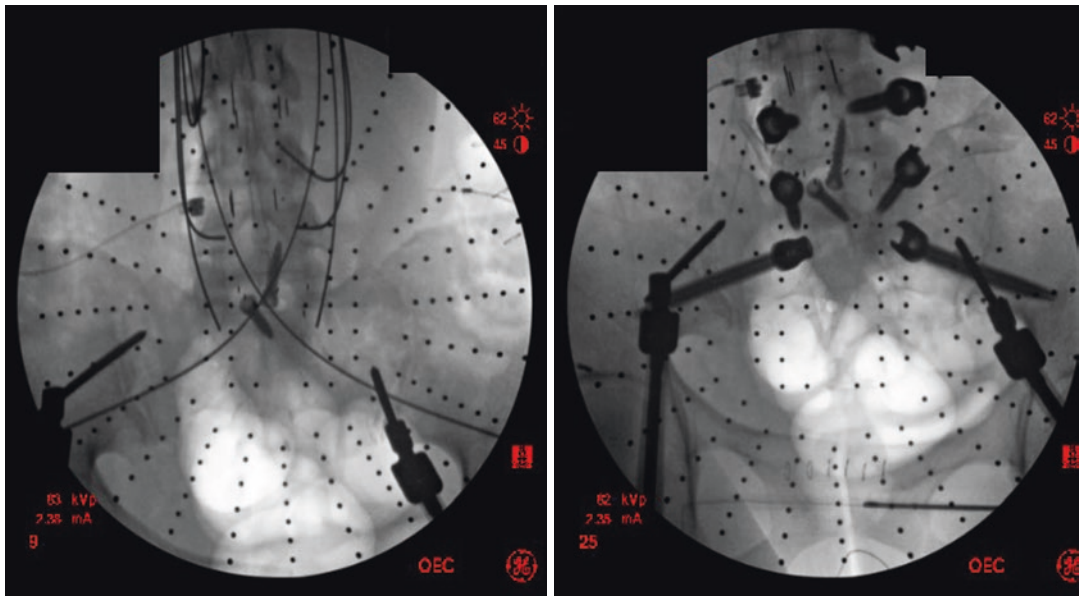


**Fig. 28.10** Intraoperative fluoroscopic images demonstrating percutaneous trajectories with K-wires (left) and screws (right)

sending the robotic system to a pre-planned trajectory through the same skin incision. Using a 9-mm drill through the robotic arm, the drill is advanced to a depth of 10 mm to decorticate each facet (Fig. 28.11). Then the robotic-guided funnel was used to place a mixture of demineralized bone matrix (DBM) and morselized BMP sponges into each facet through the MIS trajectory.

- Pedicle screws were then inserted by placing a dilator, tapping over the K-wires, placing pedicle screws, removing the K-wires, and verifying with neuromonitoring stimulation (Fig. 28.10).
- The second registration was performed by correlating intraoperative fluoroscopic images to the preoperative CT scan with a high degree of accuracy (second round, T11-L2).
- Using the same sequencing as above, pedicle screws were placed T11-L2 using robotic guidance, facets were decorticated, and a bone graft was placed posterolaterally.
- Rods were measured, contoured, and placed cephalad to caudad in a minimally invasive fashion, coronal and sagittal alignment correction was achieved, and set plugs were tightened.
- Final AP and lateral scoliosis X-rays taken intraoperatively confirmed appropriate deformity correction, optimized lumbar lordosis, and appropriate implant placement.
- Postoperative standing AP and lateral X-rays are compared to preoperative X-rays demonstrating excellent correction of global coronal and sagittal balance, reduction of the L5/S1 spondylolisthesis, and appropriate implant placement (Fig. 28.12).

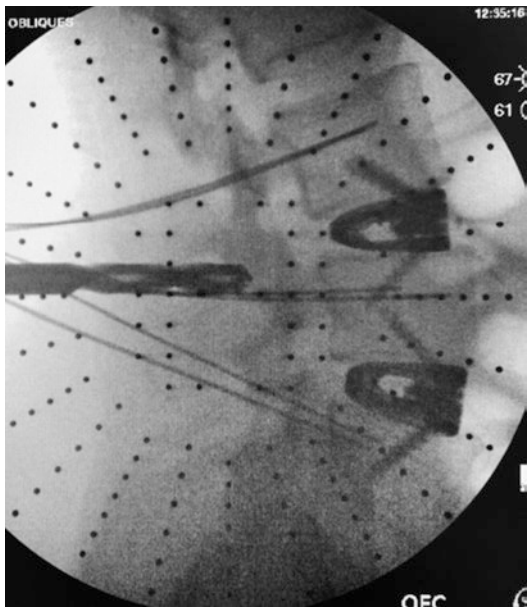


**Fig. 28.11** Intraoperative fluoroscopic view demonstrating facet decortication using a 9-mm drill with robotic guidance. Of note, the drill is only advanced to a depth of 10 mm, verified fluoroscopically, and is not advanced to additional depth to avoid the potential of advancing toward the spinal canal (example image from another case)

## 28.5 Pearls and Tips to Optimize Surgical Planning

- Multilevel interbody fusions particularly crossing the lumbosacral junction, combined with pelvic fixation such as S2AI screws, increase the surface area and provide stability for fusion which remain essential to achieving the goals of spinal deformity surgery.
- Separating surgery into anterior and posterior stages allows for the assessment of changes in the patient's preoperative symptoms. In this case, symptoms of L5 radiculopathy resolved after indirect anterior decompression and realignment of the L5/S1 spondylolisthesis with OLIF, which avoided the need for additional open posterior decompression.
- Obtaining the CT scan with robot protocol (thin 1-mm slices) and standing scoliosis X-rays after day 1 of surgery allows for extensive preoperative planning as outlined in the procedural steps above and review of any new alignment changes after interbody implant placement.
- Expect to perform two registrations for constructs up to the T9/10 level, rather than attempting to include all levels in one registration.

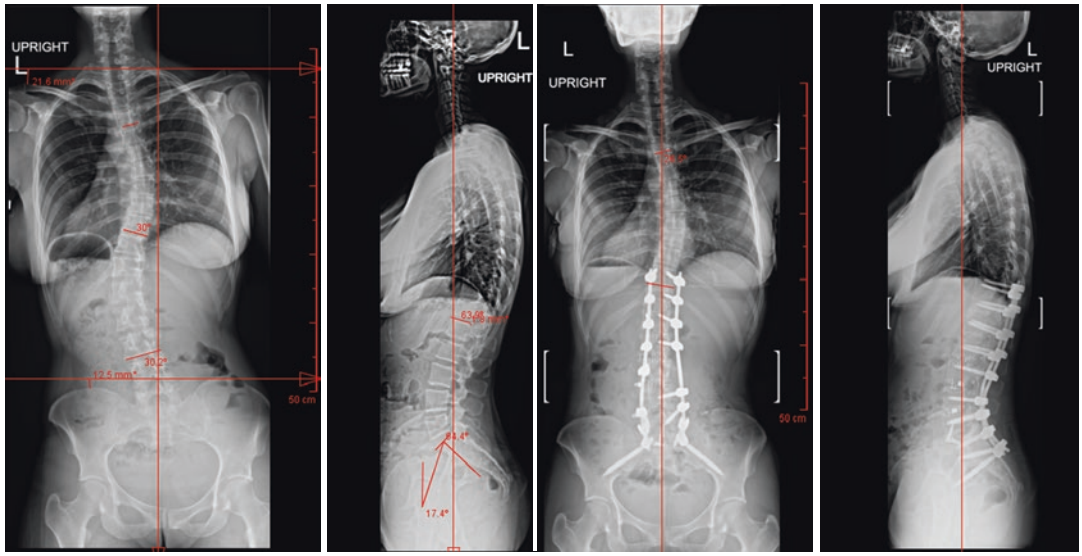


**Fig. 28.12** Preoperative standing AP and Lateral Scoliosis X-rays (left) and postoperative standing AP and Lateral Scoliosis X-rays (right) demonstrating coronal alignment correction and maintenance of sagittal balance

- The MIS exposure allows for reduction of incision size, muscle dissection, and lower EBL. Postoperative pain is also expected to be reduced, which may limit opioid needs.
- Of note, K-wires are not felt to be needed as part of the workflow for screw placement when current systems which incorporate navigation are utilized in combination with robotic guidance.
- Achieving posterior fusion is enhanced by using the preoperative planning software and robotic guidance to facilitate facet decortication and precise placement of bone grafting through the same MIS incision as pedicle screws.
- The software also allows for deformity correction simulation. With this knowledge, screws can be modified to line up the screw heads and decisions on depth choice can be made to optimize lumbar lordosis. Adjusting the depth of the distal screws (some deeper and some more superficial) maintains the lordotic alignment of the lumbar spine but requires less lordotic rod contouring, which ultimately makes the rod easier to pass. It is critical to avoid the creation of a flat back deformity, which can happen with placing a straight rod.
- Deformity correction simulation also allows the surgeon to visualize the changes in pelvic tilt, shoulder asymmetry, and avoid overcorrection.
- With in-line pedicle and S2AI screws, rods are placed with ease after gentle contouring, which previously had been challenging in MIS for deformity.

## 28.6 Key Points

- The minimally invasive surgical approach to deformity spine surgery has the potential to decrease both short- and long-term complications compared to the traditional open techniques without sacrificing the priorities of achieving fusion and alignment correction.
- Deformity correction becomes more predictable with the many tools provided by the robotic preoperative planning software package.
- The prospective comparative MIS ReFRESH study showed that robotic-guided surgery had 5.8 times fewer surgical complications related to screw placement and 11.0 times fewer revision surgeries when compared to

fluoroscopic-guided surgery. The study also showed a reduction of intraoperative radiation exposure by 80% with robotic guidance.

- Robotic guidance allows for predictable and accurate placement of S2AI screws through the otherwise challenging sacropelvic region.
- The advantages of less tissue dissection, less blood loss, less radiation exposure, and less time under anesthesia have great potential to achieve shortened hospital stays, faster recoveries, less opioid use, and less overall economic burden on the healthcare system.

## References


1. Good CR, Orosz L, Schroerlucke SR, et al. Complications and revision rates in minimally invasive robotic-guided versus fluoroscopic-guided spinal fusions. SPINE. 2021; https://doi.org/10.1097/BRS.0000000000004048.
2. Buza JA, Good CR, Lehman RA, Pollina J, Chua RV, Buchholz AL, Gum JL. Robotic-assisted cortical bone trajectory (CBT) screws using the Mazor X Stealth Edition (MXSE) system: workflow and technical tips for safe and efficient use. J Robot Surg. 2020;1:1.
3. Jamshidi AM, Massel DH, Liounakos JI, Silman Z, Good CR, Schroerlucke SR, Cannestra A, Hsu V, Lim J, Zahrawi F, Ramirez PM. Fluoroscopy time analysis of a prospective, multi-centre study comparing robotic-and fluoroscopic-guided placement of percutaneous pedicle screw instrumentation for short segment minimally invasive lumbar fusion surgery. Int J Med Robot Computer Assisted Surg. 2020:e2188.
4. Liounakos JI, Kumar V, Jamshidi A, Silman Z, Good CR, Schroerlucke SR, Cannestra A, Hsu V, Lim J, Zahrawi F, Ramirez PM, Sweeney TM, Wang MY. Reduction in complication and revision rates for robotic-guided short-segment lumbar fusion surgery: results of a prospective, multi-center study. J Robot Surg. 2021;
5. Kochanski RB, Lombardi JM, Laratta JL, Lehman RA, O'Toole JE. Image-guided navigation and robotics in spine surgery. Neurosurgery. 2019;84(6):1179–89.
6. Christopher R, Good LD, Orosz AE, Thomson TC, Schuler CM, Haines FR, Bhatt D, Boyd KM, Grossman R, Roy E. Jazini Robotic-guidance allows for accurate S2AI screw placement without complications. J Robot Surg. https://doi.org/10.1007/s11701-021-01345-x.

# 29 Endoscopic Robotic Spinal Surgery: Current Status and Future

Jason I. Liounakos and Michael Y. Wang

## 29.1 Introduction

Minimally invasive spine surgery (MISS) aims to accomplish the same or better clinical results as traditional open spine surgery, while minimizing soft tissue disruption, intraoperative blood loss, postoperative pain, and hospital length of stay. These techniques continue to be viewed more favorably by surgeons and patients alike, as the economic, social, and psychological burdens of surgery become ever more important in the current healthcare environment. Two major advancements in MISS over recent years include spinal endoscopy and robotic spine surgery. These two techniques are typically described separately, however, recent advancements have allowed for the synergistic combination of these two burgeoning technologies [1]. This chapter will discuss the specific abilities of robotics and endoscopy when utilized in conjunction and speculate as to the future of these techniques in the practice of spine surgery.

## 29.2 Localization and Access

Safe, efficient, and reproducible access to the surgical target is the cornerstone of any MISS operation. Access may take various forms, including transforaminal or translaminar needle localization for an endoscopic discectomy or pedicle localization for transpedicular procedures like vertebral body augmentation (kyphoplasty/vertebroplasty) or percutaneous pedicle screw insertion. Image guidance in the form of fluoroscopy, CT navigation, or robotic guidance is necessary for these procedures. The steep learning curves associated with minimally invasive spine surgery typically stem from localization and access with errors potentially resulting in surgical complications. In order to increase the safety and efficiency of MISS, advancements in image guidance have been a primary focus of research and development for the past two decades.

Fluoroscopic guidance has traditionally been utilized for percutaneous endoscopic spine surgery [2, 3]. The need for highly accurate localization, given the critical nearby neurologic structures, accounts for a large portion of the learning curve and reports range between 10 and 72 surgeries to develop a stable working proficiency [4, 5].

The safe working corridor through which transforaminal endoscopic discectomy is performed is known as Kambin's triangle and was originally described in 1972 (Fig. 29.1) [6]. Kambin's triangle is bounded by four structures: the exiting nerve root anteriorly, the superior articulating process posteriorly, the thecal sac and traversing nerve root medially, and the superior end-plate of the inferior vertebral body inferiorly.

J. I. Liounakos · M. Y. Wang (✉)
Department of Neurological Surgery, University of Miami, Miami, FL, USA
e-mail: mwang2@med.miami.edu



J.-S. Kim et al. (eds.), *Technical Advances in Minimally Invasive Spine Surgery*,
https://doi.org/10.1007/978-981-19-0175-1_29

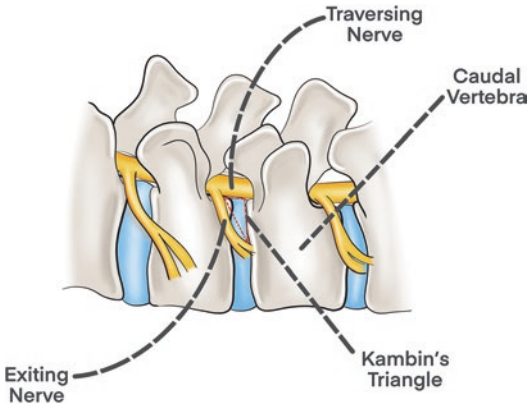


**Fig. 29.1** Kambin's triangle represents a safe working corridor for transforaminal access to the disc space as seen here

Variations in individual anatomy, as well as general anatomic differences in foraminal size depending on the level must be taken into account when gaining access [7]. Care must be taken to avoid the dorsal root ganglion (DRG) associated with the exiting nerve root and the thecal sac during initial localization. Conducting these procedures under local rather than general anesthesia allows for immediate patient feedback if any neurologic structures are disturbed, prompting reevaluation of access [8, 9]. Along with meticulous fluoroscopic localization, this real-time patient feedback is critical. Given the challenges of fluoroscopic localization for spinal endoscopy, the utilization of robotic guidance in lieu of fluoroscopy may prove to be an effective alternative.

Since the US Food and Drug Administration clearance of the first robotic guidance system for spine surgery in 2004, innovation in robotic spine surgery has surged. The recent incorporation of real-time navigation into robotic systems has further increased their efficacy and safety [10]. Unlike the "master-slave" robotic systems used in other surgical fields, developers of spine surgery robots have focused their efforts on developing "semi-active" robotic guidance systems. These "cobot" systems function to assist the surgeon in performing discrete tasks, most notably the placement of spinal instrumentation. Multiple studies suggest superior accuracy of screw insertion, while minimizing radiation burden and complications, associated with robotic guidance as compared to CT navigation and fluoroscopic guidance [11–15]. While minimal literature exists on the subject of robotic guidance for spinal endoscopy, it is likely that the benefits of its use are similar, including increased accuracy of localization, improved learning curve, and reduced radiation exposure.

## 29.3 Robotic Endoscopic Technique

We first described the utilization of robotic guidance for minimally invasive endoscopic transforaminal lumbar interbody fusion [16]. In addition to guiding the placement of percutaneous pedicle screws, the surgeon may use the robot's planning software to plan multiple access trajectories to the disc space of interest through Kambin's triangle (Fig. 29.2). One critical difference from traditional fluoroscopic guidance and a resulting consideration exists at this step. Because robotic procedures require general anesthesia due to the requirement for rigid fixation of the robot to the patient (through a Schanz pin placed in the posterior superior iliac spine), the typical patient feedback is seen in cases performed under local anesthesia is unavailable. Special consideration must then be given to an access trajectory that balances the risk of violation of the exiting nerve root and DRG with an ideal target for discectomy, end-plate preparation, and interbody delivery. Two trajectories (safe and ideal) are planned with this in mind (Fig. 29.2). An ideal trajectory aims to target the center of the disc space, but requires a more lateral trajectory with increased proximity to the exiting nerve root. A safe trajectory through the most medial portion of Kambin's triangle (the largest safe zone) at the expense of a more anterior target is also planned. Owing to the speed and efficiency of the robotic system, both trajectories may be taken and evaluated with triggered electromyography before selecting the most appropriate trajectory for insertion of the endoscope. Discectomy, end-plate preparation, and interbody delivery then proceed as previously described [17].

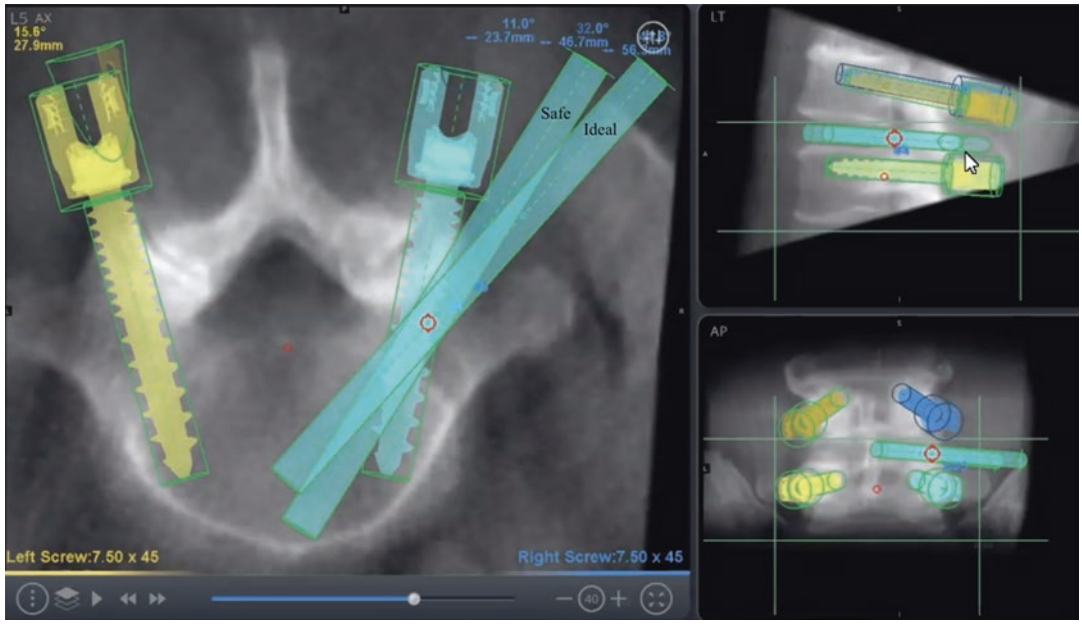


**Fig. 29.2** Intraoperative planning for robotic endoscopic transforaminal lumbar interbody fusion including pedicle screw trajectories and safe and ideal trajectories for disc space access through Kambin's triangle

One other important consideration in the combination of robotic guidance and endoscopy is the potential to streamline and standardize such operations, increasing surgical efficiency. A primary directive of robotic surgery, in general, is to increase consistency and reproducibility of surgical procedures despite varying complexity between cases. This may not only improve clinical outcomes and reduce complications, but optimize operating room efficiency from a logistics and scheduling point of view and effectively reducing healthcare costs.

Few other descriptions of robotic endoscopic surgery exist in the literature. Kolcun et al. has described robotic guidance for an endoscopic transpedicular approach to the thoracic 4–5 disc space for disc biopsy, cultures, and washout for thoracic discitis in a critically ill patient [18]. More recently the DaVinci robotic system was successfully utilized to perform retroperitoneal access and robot-assisted Lumbar 3 corpectomy, serving as a proof of concept for its utilization in spine procedures [19].

## 29.4 Future Outlook

The recent explosion of interest and innovation in minimally invasive spine surgery is not without reason. Multiple studies have reinforced the conclusion that MISS appears to deliver equivalent or better clinical outcomes compared to open surgery, while decreasing recovery times and complication rates [20–22]. As a result, many patients actively seek out minimally invasive options for their ailments. In addition, the upward shift in the global age structure will also undoubtedly lead to an increased number of spine operations being performed on an increasingly aged population with more medical comorbidities. The end result is an ideal environment for MISS to flourish and advance.

With respect to robotic localization for foraminotomy, discectomy, or fusion operations we will likely see improvements in workflow or even miniaturized robotic systems focused on this task. It is also likely that some of the initial steps of surgery will become fully automated. A recent

report describes a dedicated robotic system for percutaneous endoscopic lumbar discectomy that incorporates preoperative planning, navigation, and a fully automated foraminoplasty system utilizing a robotic arm with six degrees of freedom [23]. Devices like this may further increase the safety, efficiency, and accessibility of complex minimally invasive spine procedures. Furthermore, we may see an increased utilization of "master-slave" robotic systems such as the DaVinci system for anterolateral approaches to the thoracic and lumbar spine.

## 29.5 Conclusions

Spinal robotics and endoscopy are two burgeoning minimally invasive technologies that are aptly suited to complement one another. Robotic guidance in its present form may serve to temper the learning curve associated with localization and access that represents a significant barrier to widespread adoption. The general benefits of navigation and robotics are also likely translatable including improved safety, efficiency, and reduced complication profile. The future will likely bring robotic navigation systems specific to endoscopic spine surgery with the goal of increasing safety, improving workflow, and broadening accessibility of these complicated procedures.

## References


1. Liounakos JI, Wang MY. Lumbar 3-lumbar 5 robotic-assisted endoscopic transforaminal lumbar interbody fusion: 2-dimensional operative video. Operat Neurosurg (Hagerstown, Md). 2020;19(1):E73–E4. https://doi.org/10.1093/ons/opz385.
2. Fan G, Guan X, Zhang H, Wu X, Gu X, Gu G, et al. Significant improvement of puncture accuracy and fluoroscopy reduction in percutaneous Transforaminal endoscopic discectomy with novel lumbar location system: preliminary report of prospective hello study. Medicine. 2015;94(49):e2189. https://doi.org/10.1097/MD.0000000000002189.
3. Ahn Y, Kim CH, Lee JH, Lee SH, Kim JS. Radiation exposure to the surgeon during percutaneous endoscopic lumbar discectomy: a prospective study. Spine. 2013;38(7):617–25. https://doi.org/10.1097/BRS.0b013e318275ca58.
4. Morgenstern R, Morgenstern C, Yeung AT. The learning curve in foraminal endoscopic discectomy: experience needed to achieve a 90% success rate. SAS J. 2007;1(3):100–7. https://doi.org/10.1016/SASJ-2007-0005-RR.
5. Hsu HT, Chang SJ, Yang SS, Chai CL. Learning curve of full-endoscopic lumbar discectomy. Eur Spine J. 2013;22(4):727–33. https://doi.org/10.1007/s00586-012-2540-4.
6. Kambin P, Schaffer JL. Percutaneous lumbar discectomy. Review of 100 patients and current practice. Clin Orthopaedics Rel Res. 1989;238:24–34.
7. Hurday Y, Xu B, Guo L, Cao Y, Wan Y, Jiang H, et al. Radiographic measurement for transforaminal percutaneous endoscopic approach (PELD). Eur Spine J. 2017;26(3):635–45. https://doi.org/10.1007/s00586-016-4454-z.
8. Kambin P, Brager MD. Percutaneous posterolateral discectomy. Anat Mech Clin Orthopaedics Rel Res. 1987;223:145–54.
9. Yeung AT, Tsou PM. Posterolateral endoscopic excision for lumbar disc herniation: surgical technique, outcome, and complications in 307 consecutive cases. Spine. 2002;27(7):722–31. https://doi.org/10.1097/00007632-200204010-00009.
10. Godzik J, Walker CT, Hartman C, de Andrada B, Morgan CD, Mastorakos G, et al. A quantitative assessment of the accuracy and reliability of robotically guided percutaneous pedicle screw placement: technique and application accuracy. Operat Neurosurg (Hagerstown, Md). 2019;17(4):389–95. https://doi.org/10.1093/ons/opy413.
11. Jiang B, Pennington Z, Azad T, Liu A, Ahmed AK, Zygourakis CC, et al. Robot-assisted versus freehand instrumentation in short-segment lumbar fusion: experience with real-time image-guided spinal robot. World Neurosurg. 2020;136:e635–e45. https://doi.org/10.1016/j.wneu.2020.01.119.
12. Kochanski RB, Lombardi JM, Laratta JL, Lehman RA, O'Toole JE. Image-guided navigation and robotics in spine surgery. Neurosurgery. 2019;84(6):1179–89. https://doi.org/10.1093/neuros/nyy630.
13. Schatlo B, Molliqaj G, Cuvinciuc V, Kotowski M, Schaller K, Tessitore E. Safety and accuracy of robot-assisted versus fluoroscopy-guided pedicle screw insertion for degenerative diseases of the lumbar spine: a matched cohort comparison. J Neurosurg Spine. 2014;20(6):636–43. https://doi.org/10.3171/2014.3.SPINE13714.
14. Fichtner J, Hofmann N, Rienmuller A, Buchmann N, Gempt J, Kirschke JS, et al. Revision rate of misplaced pedicle screws of the thoracolumbar spine-comparison of three-dimensional fluoroscopy navigation with freehand placement: a systematic analysis and review of the literature. World Neurosurg. 2018;109:e24–32. https://doi.org/10.1016/j.wneu.2017.09.091.
15. Siccoli A, Klukowska AM, Schroder ML, Staartjes VE. A systematic review and meta-analysis of perioperative parameters in robot-guided, navigated, and freehand thoracolumbar pedicle screw instrumenta-

tion. World Neurosurg. 2019;127:576–87.e5. https://doi.org/10.1016/j.wneu.2019.03.196.
16. Liounakos JI, Urakov T, Wang MY. Head-up display assisted endoscopic lumbar discectomy-A technical note. Int J Med Robot Comput Assisted Surg. 2020;16(3):e2089. https://doi.org/10.1002/rcs.2089.
17. Kolcun JPG, Brusko GD, Basil GW, Epstein R, Wang MY. Endoscopic transforaminal lumbar interbody fusion without general anesthesia: operative and clinical outcomes in 100 consecutive patients with a minimum 1-year follow-up. Neurosurg Focus. 2019;46(4):E14. https://doi.org/10.3171/2018.12.Focus18701.
18. Kolcun JPG, Wang MY. Endoscopic treatment of thoracic discitis with robotic access: a case report merging two cutting-edge technologies. World Neurosurg. 2019;126:418–22. https://doi.org/10.1016/j.wneu.2019.03.036.
19. Lippross S, Junemann KP, Osmonov D, Peh S, Alkatout I, Finn J, et al. Robot assisted spinal surgery - a technical report on the use of DaVinci in orthopaedics. J Orthop. 2020;19:50–3. https://doi.org/10.1016/j.jor.2019.11.045.
20. Wang X, Borgman B, Vertuani S, Nilsson J. A systematic literature review of time to return to work and narcotic use after lumbar spinal fusion using minimal invasive and open surgery techniques. BMC Health Serv Res. 2017;17(1):446. https://doi.org/10.1186/s12913-017-2398-6.
21. Patel AA, Zfass-Mendez M, Lebwohl NH, Wang MY, Green BA, Levi AD, et al. Minimally invasive versus open lumbar fusion: a comparison of blood loss, surgical complications, and hospital course. Iowa Orthop J. 2015;35:130–4.
22. Goldstein CL, Macwan K, Sundararajan K, Rampersaud YR. Perioperative outcomes and adverse events of minimally invasive versus open posterior lumbar fusion: meta-analysis and systematic review. J Neurosurg Spine. 2016;24(3):416–27. https://doi.org/10.3171/2015.2.SPINE14973.
23. Fan N, Yuan S, Du P, Zhu W, Li L, Hai Y, et al. Design of a robot-assisted system for transforaminal percutaneous endoscopic lumbar surgeries: study protocol. J Orthop Surg Res. 2020;15(1):479. https://doi.org/10.1186/s13018-020-02003-y.

# 30 Robot-Assisted Posterior Endoscopic Cervical Decompression

Bo-Lai Chen and Yong-Peng Lin

## Abbreviations

| | |
|---|---|
| PCF | Posterior cervical foraminotomy |
| MED | Micro-endoscope |
| PECD | Posterior endoscopic cervical decompression |
| CT | Computed Tomography |
| MRI | Magnetic Resonance Imaging |

**Key Points**

1. Since the advantages of minimally invasive, posterior endoscopic cervical decompression (PECD) is increasingly applied in clinical. The indications of PECD include unilateral cervical foraminal stenosis and paracentral disc herniation, and cervical spinal cord compression by ossified ligamentum flavum or atlantoaxial dysplasia.
2. Robot-assisted PECD shows the characteristics of precise and minimally invasive. Precise catheterization under the guidance of the robot cannot only reduce the risk of neurovascular injury, but also avoid repeated fluoroscopy to confirm the location of the working channel, and effectively reducing the operator's exposure to X-ray radiation.
3. Artificial intelligence in the medical field will further develop in the direction of highly precise, intelligent, personalized, digitized, and integrated in the future. The deep integration of robots and spinal endoscopy will show a growing advantage.

B.-L. Chen (✉)
Guangdong Provincial Hospital of Chinese Medicine & Second Affiliated Hospital of Guangzhou University of Chinese Medicine, Guangzhou, China
e-mail: chenbolai@gzucm.edu.cn

Y.-P. Lin
Guangdong Provincial Hospital of Chinese Medicine & Second Affiliated Hospital of Guangzhou University of Chinese Medicine, Guangzhou, China

Guangzhou University of Chinese Medicine, Guangzhou, China

## 30.1 Introduction

Posterior cervical foraminotomy (PCF), which was applied to decompress the lateral recess and the intervertebral foramen, was initially described by Spurling and Scoville [1] in 1944. In 2001, Adamson [2] first reported the use of microendoscope for PCF. Then Fessler and Khoo [3] further described the technique of microendoscopic PCF in 2002, demonstrating its equivalent results to traditional open PCF. With the development of minimally invasive theory and technology in spinal surgery, Ruetten et al. [4] introduced a new full-endoscopic technique for cervical posterior foraminotomy in the treatment of lateral disc herniations using 6.9-mm endoscopes in 2007,



J.-S. Kim et al. (eds.), *Technical Advances in Minimally Invasive Spine Surgery*,
https://doi.org/10.1007/978-981-19-0175-1_30

which showed that sufficient decompression can be achieved under continuous visualization and the advantages of a minimally invasive procedure were obvious.

At present, posterior endoscopic cervical decompression (PECD) has been very mature in the treatment of cervical lateral disc herniation. And with the accumulation of surgeons' experience, this minimally invasive technique can also be used to treat spinal cord compression injury mainly caused by the pathological factors from the dorsal spinal cord [5]. However, due to the limitation of visual field and operating space caused by the small working channel, high-quality images, and superb surgical skills are required for precise operation. Moreover, the around anatomical structure is also very complicated, such as the spinal cord, nerves and vertebral arteries, and any carelessness during the operation may cause serious complications. These factors are the main reasons for the steep learning curve of PECD [6–8].

For beginners, effective methods for safely through the learning curve periods include precise positioning of the surgical segment to establish the working channel which suitable for decompression, and getting a clear anatomical identification under the endoscope. The key steps of surgical procedures often need to be assisted by intraoperative fluoroscopy of imaging equipment (e.g., C-arm, G-arm, or O-arm) to obtain accurate positioning. However, the long-term and high-dose X-ray radiation poses a potential threat to the health of medical staff and patients. Fortunately, robot-assisted technology can solve the problems of intraoperative precise positioning and X-ray radiation damage [9, 10]. A robot is defined as an instrument composed of sensors and actuators that can be programmed autonomously and controlled by computer programs [11, 12]. With the collaborative development of robotics, computer-aided medical technology, medical image processing technology and minimally invasive surgical technology, the research on surgical robots has also been rapidly developed [10–13].

Orthopedic surgery robot closely integrates design automation, artificial intelligence, electronic information, medical image processing, and other engineering machineries, to extend the range of surgeons' visual and tactile, improve the accuracy and security of the operation and repeatability [13]. Therefore, it can be applied to assist physicians to perform some high-risk and complex surgeries, and decrease operative trauma and reduce radiation damage caused by X-ray fluoroscopy.

Early applications of spinal robots focused on improving the accuracy of pedicle screw placement, and more recently [13], they have been applied to pathological biopsies [14], vertebroplasty [15], and local sealing operations. However, there are still few reports on the application of orthopedic robots in spine endoscopic surgery [16, 17], especially in cervical endoscopic surgery. This chapter mainly introduces the application and exploration of robot-assisted PECD.

## 30.2 The Composition of the TiRobot

The main structure of the TiRobot is composed of the robotic arm, the doctor's workstation, and the coordinate positioning board. The surgical manipulator is composed of a six-joint robotic arm, an intelligent bone drill, and a binocular recognition camera. The doctor's workstation is composed of a workstation matrix, an operation panel, and a double display screen.

## 30.3 The Key Principle of the TiRobot

TiRobot's workstation mainly completes image acquisition, surgical path planning, and three-dimensional coordinate calculation. The surgical control software system is used for surgical image processing, robot control, data storage, etc. The positioning system includes a navigation bracket and a positioning rod. The robot tracking bracket and the patient tracking bracket are installed at the end of the robot and the patient's surgical site, respectively, with a reflective ball. The optical positioning device is stented to track

the space position of the robotic arm. The image calibrator obtains the mapping relationship between the image space and the operative space through the image coordinates of the calibrator and the actual coordinate registration. The navigation robot inputs the image information of the patient's surgical site into the computer and performs three-dimensional modeling. Then doctor designs the direction, length, thickness, etc. of the guide needle, and conduct real-time navigation and tracking of the operation.

## 30.4 Indications and Contraindications

### 30.4.1 Indications

1. Cervical disc herniations with radiculopathy.
2. Cervical stenosis with myelopathy caused by ossification of the ligamentum flavum.
3. Cervical spinal cord compression by an abnormal posterior arch of the atlas.

### 30.4.2 Contraindications

1. Cervical spondylotic myelopathy with the compression at the front of the spinal cord.
2. Multiple-level severe cervical spinal stenosis.
3. Ossification of posterior longitudinal ligament of neck.
4. Cervical instability.

## 30.5 Surgical Procedure

After general anesthesia, the patient is placed in the prone position, and the head is fixed with Mayfield frame to make the cervical spine slightly kyphotic and increase the interlaminar space. The surgical area is disinfected and spread sterile surgical towels.

TiRobot is connected and installed with an aseptic cover. The robotic arm is placed on the left side of the patient, the three-dimensional C-arm machine is placed on the right side, the optical tracking system of the robot is placed on the cranial, and the doctor's workstation is placed next to the display screen. The connecting rod on the fixing frame is installed and extended from the side of the operative table to ensure not interfere with the C-arm X-ray perspective.

The tracer is installed at the end of the connecting rod to integrate the tracer with the surgical segment. A positioning scale is installed at the end of the robotic arm. The positioning scale is a rigid plate of approximately 100 × 30 × 5 mm, with five regularly distributed steel balls of the same size in the plate. The robotic arm is moved to the surgical area, and the positioning scale is located directly above the skin of the surgical segment. The C-arm machine front-to-side fluoroscopy requires a simultaneous display of surgical segments and the five steel balls in the images. Three-dimensional scanning of surgical segments with a C-arm machine may take about 60 s (scan time varies depending on C-arm type).

The scanned image is sent to the mobile operating platform, and automatic registration is conducted when the robot normally recognized the robotic arm tracker and the patient reference array. After the successful registration, data with registration accuracy will pop up on the interface of the mobile operating platform. The registration is completed when the error of precision data value is less than 0.5 mm.

Then the CT image can be processed, and the cross-section, sagittal and coronal plane, and 3D reconstruction image can be displayed simultaneously on the computer system. Surgeons can switch tomographic images at any level, and there will be corresponding linkages on the three levels. According to the needs of the surgeons, the cross-section can be selected at any angle to reconstruct the tomographic image. Then the surgeon plans the ideal working channel position, adds the plan, and then can run the robotic arm.

Replace the positioning ruler with a guide, and run the robotic arm to the position of the working channel. Place the guide rod through the robotic arm guider, and then cut the skin, and stick the rod to the bone surface. The expansion sleeve and working tube are placed along the guide rod to the target step by step. And the remainder is the endoscopic operation.

## 30.6 Case Study

**Case 1**

Male, 66 years old.

Symptoms: Neck pain with numbness in the arms, hands, and fingers for more than seven months. He had trouble grasping and holding on to items, loss of fine motor skills and had difficulty with handwriting, and aggravated and had trouble in walking for one month.

Physical Examination: Hyperreflexia. Hoffmann sign (+). Lossolimo sign (+). Trouble walking, loss of balance. No condition in which muscles deteriorate and shrink in size.

Japanese Orthopaedic Association (JOA) was 8/17.

The visual analog scale (VAS) was 4/10 (Figs. 30.1, 30.2, 30.3, 30.4, 30.5, 30.6, and 30.7).

**Case 2**

Male, 36 years old.

Symptoms: Neck pain, and radicular pain of the left arm down to the hand and fingers. Certain positions or movements of the neck can intensify the pain.

Physical examination. The neck was tenderness and pain. The neck's range of motion was limited. Neurological deficits in the arms, such as issues with reflexes, numbness, and/or weakness were normal.

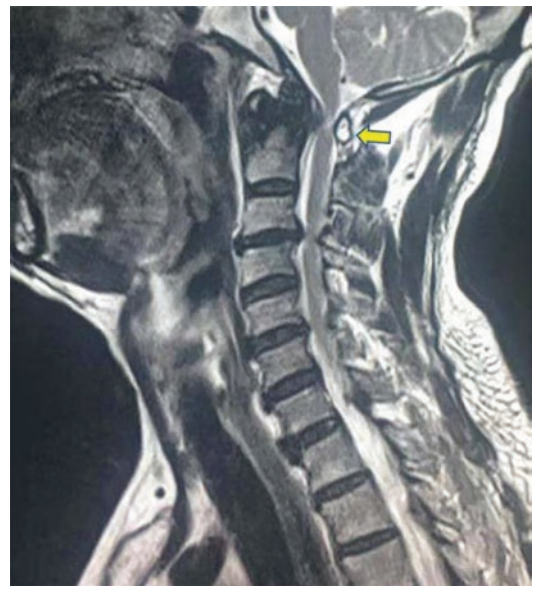

**Fig. 30.1** Preoperative MRI

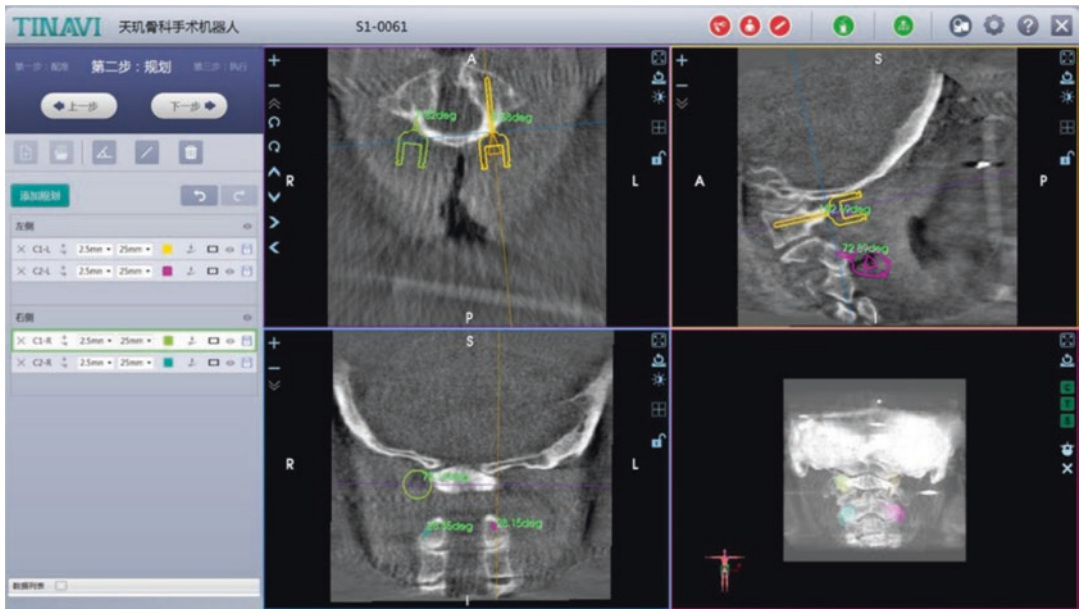


**Fig. 30.2** The anchor point and catheterization route are planned on the robot computer

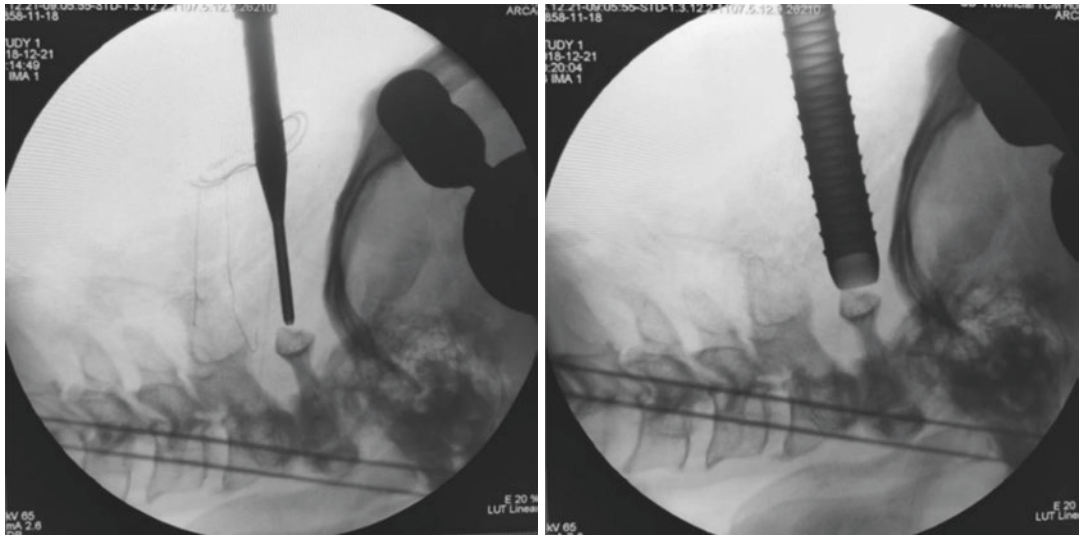

**Fig. 30.3** Robot-assisted precise catheterization

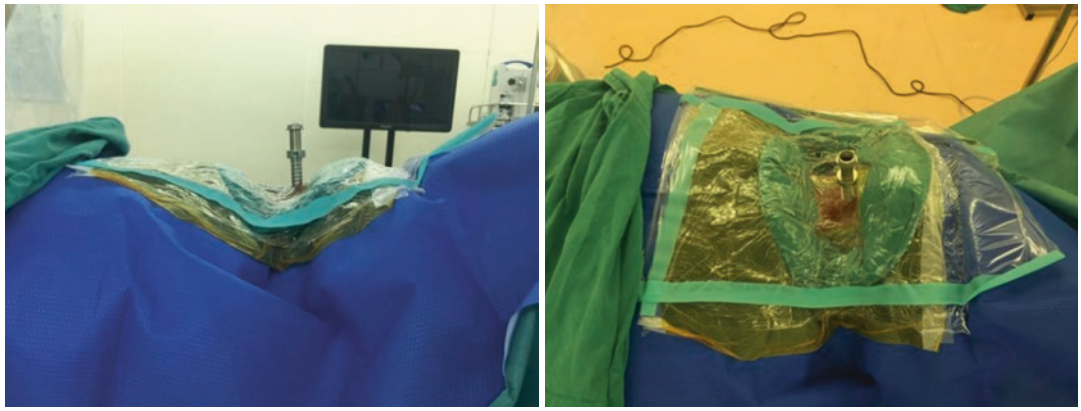

**Fig. 30.4** Working tube of a full-endoscopic laminectomy of C1

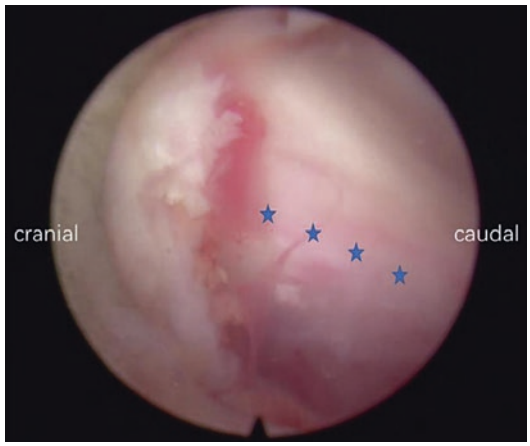


**Fig. 30.5** Adequate decompression of the spinal cord (blue stars)

Neck Disability Index (NDI) was 41/50.

The visual analog scale (VAS) was 8/10 (Figs. 30.8, 30.9, 30.10, 30.11, 30.12 and 30.13).

## 30.7 Discussion

Since the advantages of less trauma, less bleeding, less postoperative pain and faster recovery, etc., PECD is increasingly applied in clinical. Generally, its best indications are unilateral cervical foraminal stenosis and paracentral disc herniation. PECD can also be used for effective decompression when the pathological factors that compress the spinal cord or nerves come from the

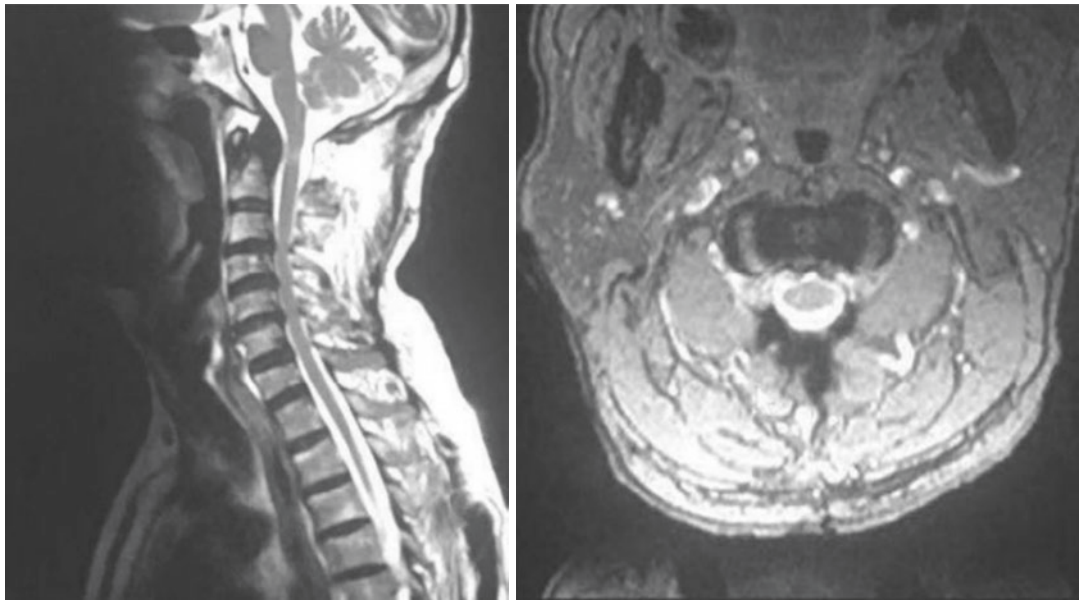

**Fig. 30.6** Postoperative MRI

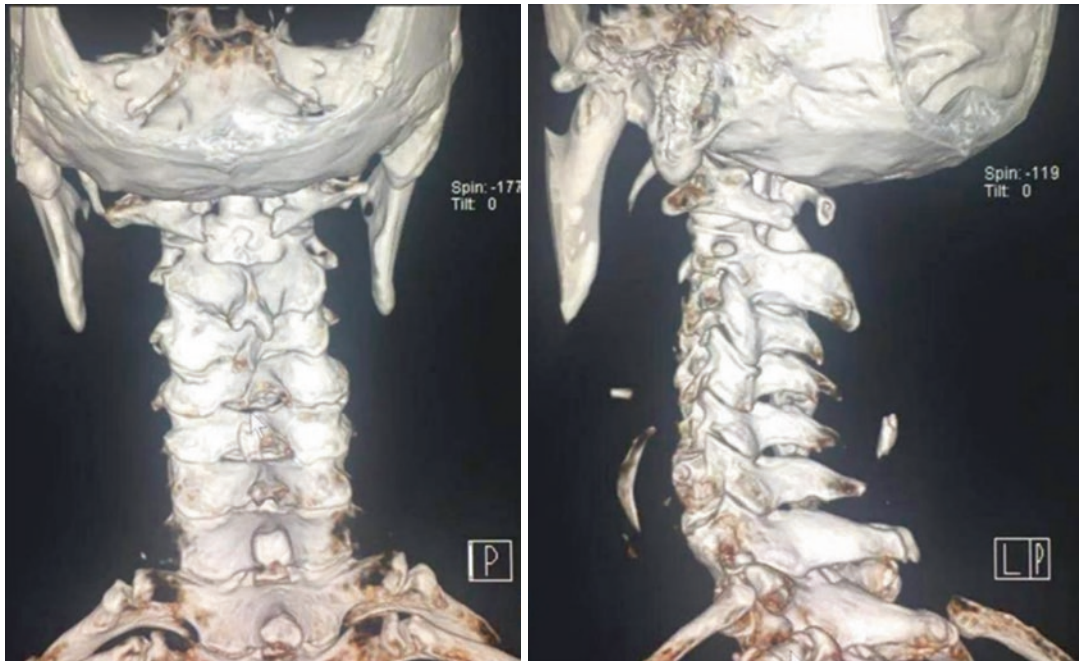


**Fig. 30.7** Postoperative CT Scan

dorsal side of the spinal cord, such as ossified ligamentum flavum or atlantoaxial dysplasia.

Despite the outstanding advantages of PECD as a minimally invasive technique, its learning curve is steep, and the complications mainly occurred during this period. Ruetten et al. [4] reported 87 cases of P-PECD and followed up for 2 years, 3.4% of the patients had transient nerve injury, and 3% of the patients had a recurrence.

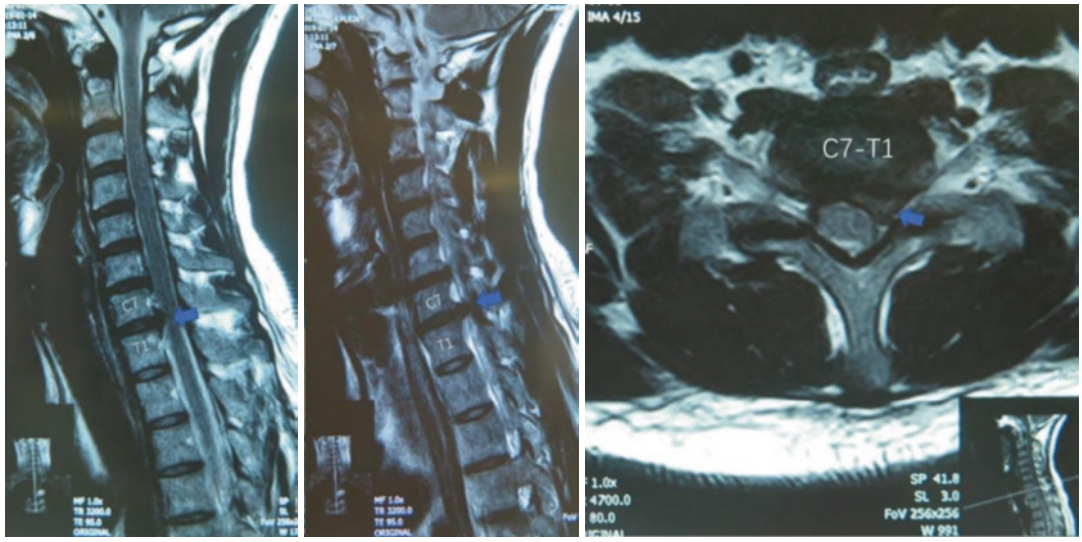


**Fig. 30.8** Preoperative MRI

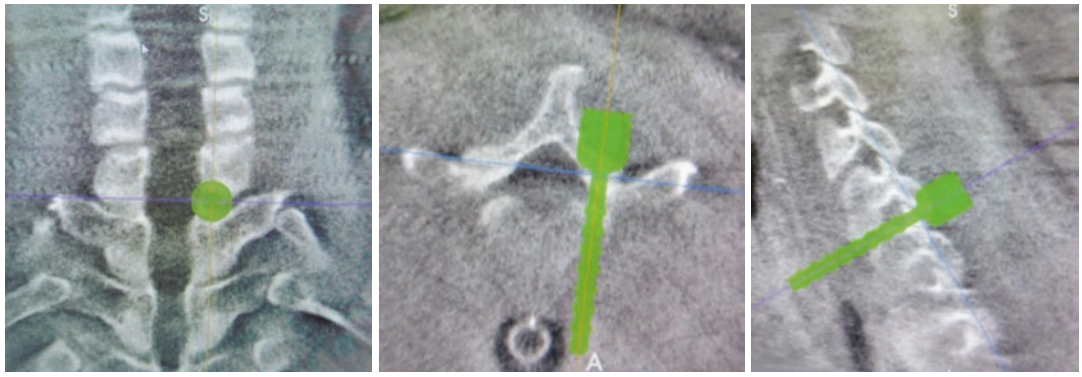

**Fig. 30.9** The anchor point and catheterization route are planned on the robot computer

Spine surgeons typically require a long time of specialized training and experience accumulation to be competent enough to perform minimally invasive surgery [18, 19]. Percutaneous endoscopic spinal surgery requires extreme accuracy since the slightest error causes catastrophic consequences [20, 21]. In terms of the puncture method, 1–2 cm paracentric posterior midline incision is generally selected for PECD. After the establishment of the working passage, soft tissue often covers under the endoscope, and sometimes it is difficult for the inexperienced surgeon to find the iconic anatomical structures. In addition, due to the small size of the working channel and the thinness of cervical muscle, the anatomical mark cannot be found under the endoscope when the angle of the working channel is slightly changed.

With the development of robotics, it is possible for ordinary surgeons to perform some of the most difficult operations that would otherwise require a senior one, and robots shorten the growth curve of young doctors. Orthopedic robots, with their minimally invasive and precise characteristics, provide personalized, intelligent, and precise treatment programs for orthopedic diseases, and have become an important direction in the development of orthopedic clinical treatment [22, 23, 25]. Due to the rigid structure and non-deformation characteristics of bone, the

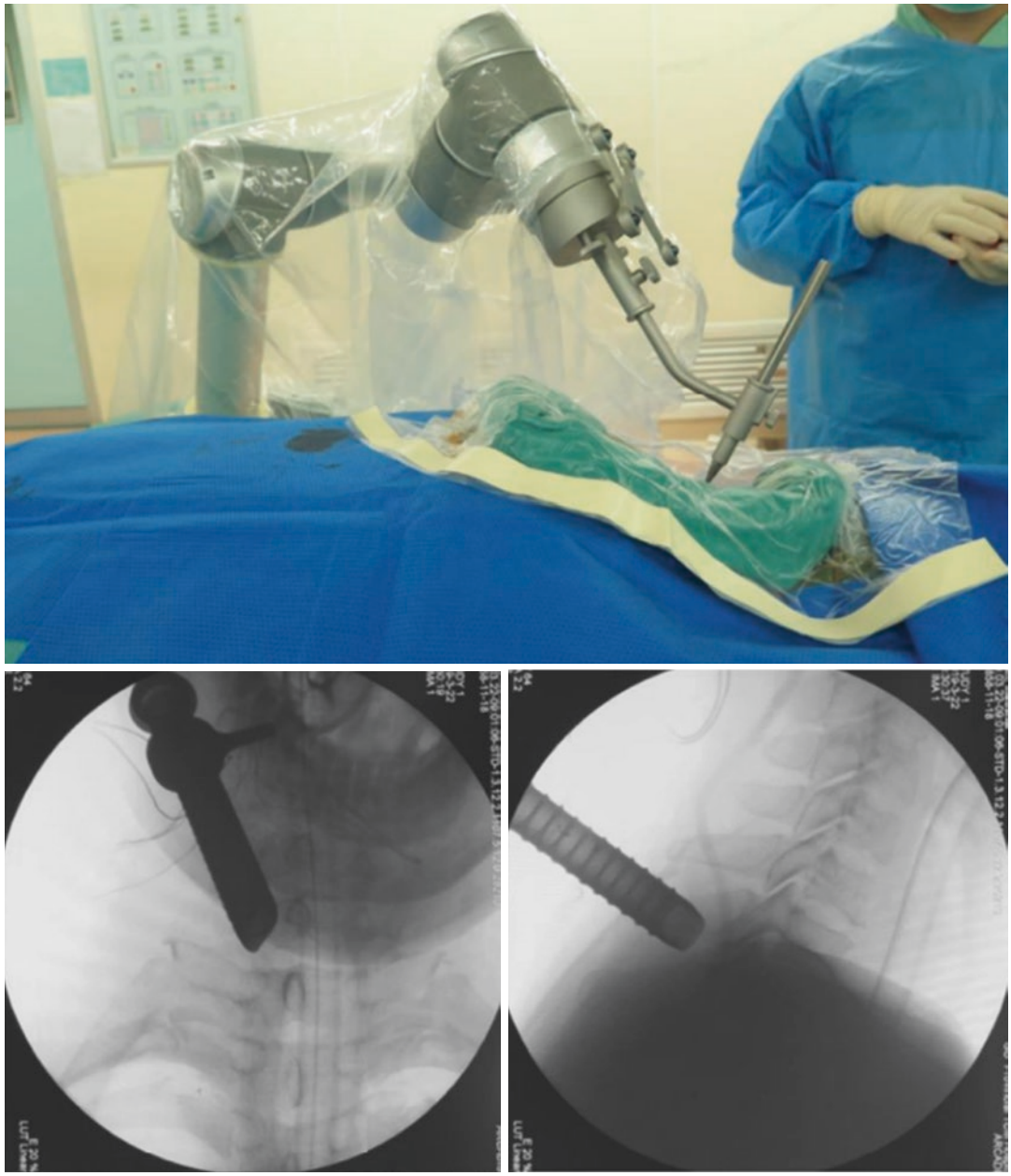

**Fig. 30.10** Precise catheterization is accomplished with the assistance of the robot

intraoperative computer-captured image has a high coincidence rate with the actual anatomical structure and good repeatability [23, 24]. Therefore, the robot-assisted surgical technique is particularly suitable for orthopedic operations.

Currently, there are mainly two types of spinal surgical robots. The first type is mainly used to provide a working channel for surgical instruments and ensure the stability of the instruments with their induction role, such as SpineBot [26] and TiRobot. The second type of robotic system can establish a working channel on its own and automatically perform drilling steps, such as the SpineAssist [27]. Since the cervical spine is

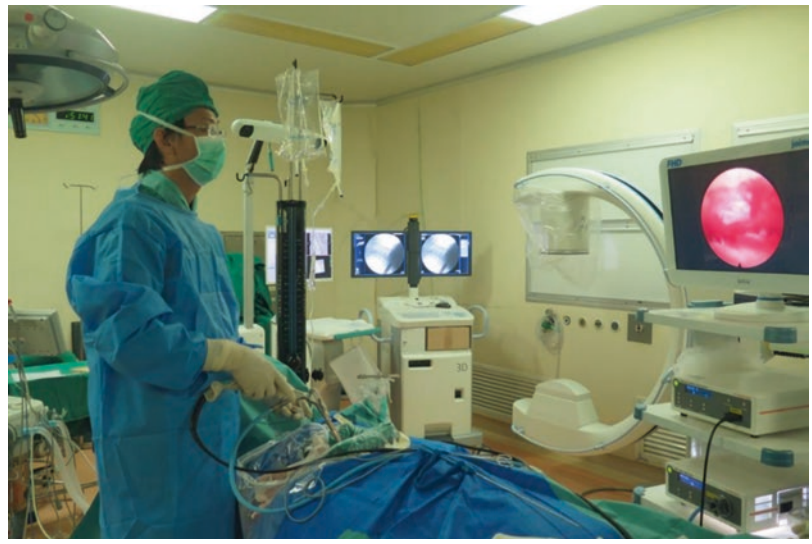

**Fig. 30.11** Surgical procedure of robot-assisted PECD

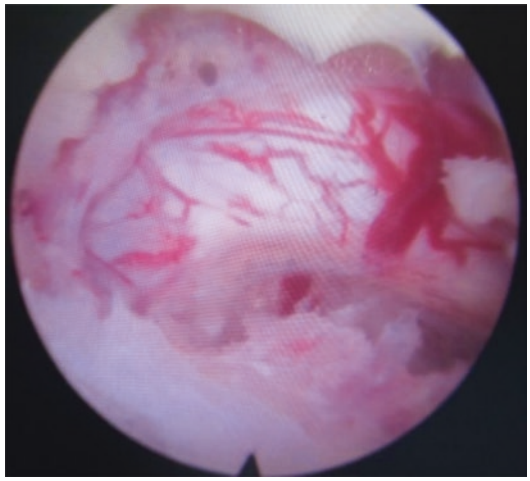

**Fig. 30.12** The nerves are fully decompressed

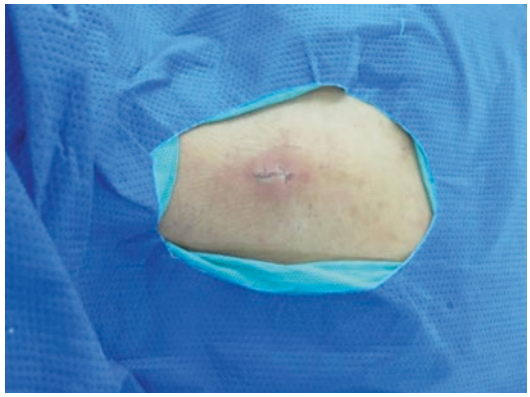

**Fig. 30.13** The incision is about 1 cm

surrounded by important nerves and blood vessels, a slight indiscretion can lead to catastrophic complications. So, the first type of robot is more commonly applied and safer for spinal surgery.

The obvious advantages of utilizing robotics include (1) High precision accuracy. The surgical robot has a motion control system and the flutter filtering system. The robotic arm can approach the target from all angles. With the assistance of the guide, it can effectively reduce the surgeon's movement range and improve the accuracy of operations. Accurate operation is of much concern to percutaneous endoscopic cervical surgery, which can effectively avoid segmental errors. Especially in the upper cervical spine, the posterior arch of the atlas (C1) is so small, which may cause the wrong position of the working tube, and even risk the injury of the spinal cord and nerve. Precise catheterization can also make the soft tissue cleaned easily, and reveal the iconic bone anatomy such as the "V" point easier, which will help to reduce the operation time. (2) The precise Kirschner wire guided by the robot will leave a depression on the bone surface, which can serve as a temporary anatomical reference mark. For example, the midpoint of the atlas posterior arch can be taken as a bone structure marker when doing percutaneous endoscopic C1 laminectomy, and approximately 1 cm of bone can be removed from this point to each side to get

adequate decompression of the spinal cord. Or, the junction of lamina and the articular process is often designed as the anchor point when doing PECD, regarding this point as the center to reveal the "V" point, ligamentum flavum and nerve roots are faster, safer, and more reliable for the operation. These anchor points can be designed on the robot computer and guided by the robotic arm for precise anchoring. Then the working tube can be established by progressive expansion along the anchored Kirschner wire. (3) Robot-assisted surgery can provide accurate and effective solutions to the operation in conventional dangerous areas and blind spots. The advantages of robotic image navigation are particularly prominent in the anatomically complex spinal segments, such as the atlas. It can visualize the anatomical structure, carry out detailed preoperative planning, and improve the accuracy of the operation. Rigorous preoperative planning by robots is of great significance. Through preoperative planning, endoscopic working pipeline positions can be designed at various angles and levels in the coronal, sagittal, and cross-sectional views, and insertion points can be accurately selected according to the requirements of the operation, so as to make the operation more accurate and reasonable. Precise catheterization under the guidance of the robot can not only reduce the risk of neurovascular injury, but also avoid repeated fluoroscopy to confirm the location of the working tube, and effectively reducing the operator's exposure to X-ray radiation.

## 30.8 Conclusion

Since percutaneous cervical spine endoscopic surgery requires high precision, the deep integration of robots and digital orthopedics will provide great assistance to doctors in diagnosis and treatment. In general, robot-assisted PECD shows the characteristics of precise and minimally invasive. And artificial intelligence in the medical field will further develop in the direction of highly precise, intelligent, personalized, digitized, and integrated in the future.

## References


1. Spurling RG, Scoville WB. Lateral rupture of cervical intervertebral disc: a common cause of shoulder and arm pain. Surg Gynecol Obstet. 1944;78:350–8.
2. Adamson TE. Microendoscopic posterior cervical laminoforaminotomy for unilateral radiculopathy: results of a new technique in 100 cases. J Neurosurg. 2001;95:51–7.
3. Khoo LT, Fessler RG. Microendoscopic decompressive laminotomy for the treatment of lumbar stenosis. Neurosurgery. 2002;51(5 Suppl):S146–54.
4. Ruetten S, Komp M, Merk H, et al. A new full-endoscopic technique for cervical posterior foraminotomy in the treatment of lateral disc herniations using 6.9-mm endoscopes: prospective 2-year results of 87 patients. Minim Invasive Neurosurg. 2007;50:219–26.
5. Lin Y, Rao S, Li Y, Zhao S, et al. Posterior percutaneous full-endoscopic cervical laminectomy and decompression for cervical stenosis with myelopathy: a technical note. World Neurosurg. 2019;12:S1878–8750(19)30051–8.
6. Quillo-Olvera J, Lin GX, Kim JS. Percutaneous endoscopic cervical discectomy: a technical review. Ann Transl Med. 2018;6(6):100.
7. Ahn Y. Percutaneous endoscopic cervical discectomy using working channel endoscopes. Expert Rev Med Devices. 2016;13(6):601–10.
8. Visocchi M, Di Martino A, Maugeri R, et al. Videoassisted anterior surgical approaches to the craniocervical junction: rationale and clinical results. Eur Spine J. 2015;24(12):2713–23.
9. Yang C, Guo S, Bao X, et al. A vascular interventional surgical robot based on surgeon's operating skills. Med Biol Eng Comput. 2019;57(9):1999–2010.
10. Overley SC, Cho SK, Mehta AI, et al. Navigation and robotics in spinal surgery: where are we now? Neurosurgery. 2017;80(3S):S86–99.
11. Leal Ghezzi T, Campos Corleta O. 30 years of robotic surgery. World J Surg. 2016;40(10):2550–7.
12. Umedachi T, Vikas V, Trimmer BA. Softworms: the design and control of non-pneumatic, 3D-printed, deformable robots. ioinspirBiomim. 2016;11(2):025001.
13. Elswick CM, Strong MJ, Joseph JR, et al. Robotic-assisted spinal surgery: current generation instrumentation and new applications. Neurosurg Clin N Am. 2020;31(1):103–10.
14. Smith JS, Shaffrey CI, Ames CP, et al. Treatment of adult thoracolumbar spinal deformity: past, present, and future. J Neurosurg Spine. 2019;30(5):551–67.
15. Dreval' ON, Rynkov IP, Kasparova KA, et al. Results of using spine assist Mazor in surgical treatment of spine disorders. ZhVoprNeirokhirIm N NBurdenko. 2014;78(3):14–20.
16. Boškoski I, Costamagna G. Endoscopy robotics: current and future applications. Dig Endosc. 2019;31(2):119–24.

17. Gifari MW, Naghibi H, Stramigioli S, et al. A review on recent advances in soft surgical robots for endoscopic applications. Int J Med Robot. 2019;15(5):e2010.
18. McAfee PC, Phillips FM, Andersson G, et al. Minimally invasive spine surgery. Spine (Phila Pa 1976). 2010;35(26 Suppl):S271–3.
19. Spetzger U, Schilling AV, Winkler G, et al. The past, present and future of minimally invasive spine surgery: a review and speculative outlook. Minim Invasive Ther Allied Technol. 2013;22(4):227–41.
20. Lee S, Kim SK, Lee SH, et al. Percutaneous endoscopic lumbar discectomy for migrated disc herniation: classification of disc migration and surgical approaches. Eur Spine J. 2007;16(3):431–7.
21. Choi G, Prada N, Modi HN, et al. Percutaneous endoscopic lumbar herniectomy for high-grade down-migrated L4–L5 disc through an L5-S1 interlaminar approach: a technical note. Minim Invasive Neurosurg. 2010;53(3):147–52.
22. Bargar WL. Robots in orthopaedic surgery: past, present, and future. Clin Orthop Relat Res. 2007;463:31–6.
23. Picard F, Deakin AH, Riches PE, et al. Computer assisted orthopaedic surgery: past, present and future. Med Eng Phys. 2019;72:55–65.
24. Mont MA, Khlopas A, Chughtai M, et al. Value proposition of robotic total knee arthroplasty: what can robotic technology deliver in 2018 and beyond? Expert Rev Med Devices. 2018;15(9):619–30.
25. Berlemann U, Langlotz F, Langlotz U, et al. Computer-assisted orthopedic surgery. From pedicle screw insertion to further applications. Orthopade. 1997;26(5):463–9.
26. Pechlivanis I, Kiriyanthan G, Engelhardt M, et al. Percutaneous placement of pedicle screws in the lumbar spine using a bone mounted miniature robotic system: first experiences and accuracy of screw placement. Spine (Phila Pa 1976). 2004;34(4):392–8.
27. Sukovich W, Brink-Danan S, Hardenbrook M. Miniature robotic guidance for pedicle screw placement in posterior spinal fusion: early clinical experience with the SpineAssist. Int J Med Robot. 2006;2(2):114–22.

# 31 Robot-Assisted Percutaneous Endoscopic Lumbar Interbody Fusion

Bo-Lai Chen and Yong-Peng Lin

## Abbreviations

| | |
|---|---|
| 3D | Three-dimensional |
| ALIF | Anterior lumbar interbody fusion |
| CT | Computed tomography |
| IAP | Inferior articular process |
| LLIF | Lateral lumbar interbody fusion |
| MIS | Minimally invasive surgery |
| OLIF | Oblique lateral interbody fusion |
| PELIF | Percutaneous endoscopic lumbar interbody fusion |
| PLIF | Posterior lumbar interbody fusion |
| SAP | Superior articular process |
| TLIF | Transforaminal lumbar interbody fusion |

**Key Points**

1. Percutaneous endoscopic lumbar interbody fusion (PELIF) is a minimally invasive technique to treat lumbar degenerative disease combined with instability, it has the advantages of less trauma, less bleeding, shorter hospital stays, and faster recovery.
2. Robot-assisted PELIF mainly embodies the planning of the path of the working channel and Percutaneous pedicle screw, and automatically guides the establishment of the working tube and insertion of the pedicle screw.
3. Robot-assisted PELIF improves the accuracy of operation and helps to shorten the operation time and reduce complications.

## 31.1 Introduction

Lumbar spinal fusion is the golden standard of a surgical therapeutic regimen in the stage-wise treatment of symptomatic degenerative lumbar disease. Variety of techniques exist for fusing lumbar spine vertebrae to help alleviate pain and restore stability, including anterior lumbar interbody fusion (ALIF) [1, 2, 7], posterior lumbar interbody fusion (PLIF) [3], transforaminal lumbar interbody fusion (TLIF) [4, 9, 10], oblique lateral interbody fusion (OLIF) [5, 7] and lateral lumbar interbody fusion (LLIF) [1, 6, 7], etc. The muscles and soft tissues are retracted to expose the lateral aspect of the lamina and facet joint during PLIF and TLIF, which may cause postoperative intractable back pain. Although ALIF, OLIF, and LLIF can reduce muscle and

B.-L. Chen (✉)
Guangdong Provincial Hospital of Chinese Medicine & Second Affiliated Hospital of Guangzhou University of Chinese Medicine, Guangzhou, China
e-mail: chenbolai@gzucm.edu.cn

Y.-P. Lin
Guangdong Provincial Hospital of Chinese Medicine & Second Affiliated Hospital of Guangzhou University of Chinese Medicine, Guangzhou, China

Guangzhou University of Chinese Medicine, Guangzhou, China



J.-S. Kim et al. (eds.), *Technical Advances in Minimally Invasive Spine Surgery*,
https://doi.org/10.1007/978-981-19-0175-1_31

soft tissue damage, these surgical methods, as indirect decompression techniques, cannot remove herniated discs and hypertrophic ligamentum flavum [8].

Precise, intelligent, and minimally invasive treatments for orthopedic surgery are changing from trend to reality. Minimally invasive spine surgery (MIS) has experienced rapid development in the past few decades [9, 10]. The goal of the operation is to obtain reasonable surgical planning, an accurate position and operation, and minimal operative trauma with the best therapeutic effect. Percutaneous endoscopic lumbar interbody fusion (PELIF) is a newly developed MIS technique in recent years, which is more minimally invasive compared with microscopic or microendoscopic operation. Although its application time is relatively short, the preliminary clinical results have shown that PELIF has the advantages of less trauma and bleeding, shorter hospital stays, faster postoperative recovery, and lower risk of wound infection because the whole process is completed under continuous saline perfusion [11–16, 19, 20].

Despite the huge minimally invasive advantages, PELIF requires great skill, careful planning, and the ability to implant percutaneous pedicle screws accurately and smoothly. In obtaining the desired radiographic visualization of anatomy-specific views to place surgical instrumentation and implants, repeated C-arm fluoroscopy images are often acquired, which will cause radiation exposure damage to the patients as well as surgeons [17, 18]. Meanwhile, the surgeon's fatigue and scant operating accuracy limit the further improvement of surgical efficiency and safety. How to find effective tools helping doctors to improve the accuracy of surgery has become an important research direction. To save time and radiation dose in the operating procedure, the method proposed in this work is using a robot to assist the surgeon.

Medical robotics technology is a new interdisciplinary field integrating medicine, biomechanics, mechanics, materials science, computer science, and robotics. It provides sufficient information supports for doctors in operation and decision-making, in terms of vision, tactics, and auditory. Also, it efficiently improves doctors' operating skills and the quality of surgical diagnosis, evaluation, target positioning, and operation preciseness. This chapter mainly introduces the surgical indications, contraindications, and technical points of robot-assisted PELIF.

## 31.2 The Key Working Principle of Orthopedic Robot

At the beginning of the operation, an intraoperative three-dimensional image is established through the CT scan data to reflect the accurate mapping relationship among the reconstruction space, the patient's actual physical space, and the robot space. After that, the doctor will plan the surgical path in the three-dimensional space reconstructed from the intraoperative images. Then, the optical tracking camera and tracer control the robot to accurately place the guide to the planned path. The doctor uses the robot planning system to place the endoscopic working tube accurately and find the most accurate path for pedicle screw implantation.

The robotic arm system can automatically calculate the actual spatial position of the predetermined path of the pedicle screw, and control the robotic arm together with the guide tool attached to the end of the robotic arm to locate the predetermined path with the cooperation of the optical tracking system, and guide the operation through the guider. The surgeon can inserts the endoscopic working pipe and pedicle screw accurately.

The optical tracking system can detect the actual position of the patient and changes of the patient's position due to various reasons in real-time, and cooperate with the robotic arm system for real-time motion compensation that the robotic arm system can always locate the predesigned implant path accurately.

## 31.3 The Composition of the Robot

### 31.3.1 Robotic Arm System

The robotic arm system is mainly composed of the robotic arm and its controller. The system

adopts a 6-joint mechanical arm, the range of motion of each joint is −360° ~ 360°, and the maximum working radius of the mechanical arm is 850 mm. A multipurpose universal tool base is installed at the end of the robotic arm to support the installation and fixation of various supporting tools such as guides, tracers, and surgical instruments. The robotic arm is installed on the base of the mobile platform and is equipped with an automatic balance support system to ensure that the positional relationship between the robotic arm system and the patient remains stable, and to ensure the safety, stability, and repeatability of the robotic arm system. The overall mechanical positioning accuracy of the robotic arm system is 1.0 mm.

### 31.3.2 Optical Tracking System

The optical tracking system consists of an infrared stereo camera and two sets of corresponding tracers. The two groups of tracers are of a passive reflective type and are respectively installed on the end of the manipulator and the spinous process of the patient. During the operation, the optical tracking system can monitor the position changes of the end of the robotic arm and the patient in real time, and automatically compensate for the displacement to ensure a fixed relative position relationship between the robotic arm system and the patient. Relevant accurate information can be displayed on the display screen of the optical tracking system in real time, providing a basis for doctors to perform pedicle screw implantation.

### 31.3.3 Surgical Planning and Navigation System

The path planning for the implantation of the puncture guide needle or pedicle screw is completed by computer software. The software can receive the 3D original image data generated by the 3D C-arm machine scanning, and realize the automatic matching of the image space and the working space of the robot system based on the marker point technology, to complete the registration process of the robot system, which allows the doctor to use the above-mentioned matching 3D original image data to plan the puncture path, set the pedicle screw implant parameters and select the model. After the doctor's reconfirmation, the relevant content is transmitted to the robotic arm system through the computer for execution. In order to ensure the safety of the operation, the operation planning and navigation system also provide the virtual simulation of the pedicle screw's implantation path and emergency stop functions to prevent obvious errors when the robotic arm system touches obstacles during operation.

## 31.4 Indications and Contraindications

### 31.4.1 Indications

(a) Lumbar disc herniation accompanied by instability.
(b) Lumbar central canal stenosis, nerve root canal stenosis, or lateral recess stenosis with instability.
(c) Lumbar spinal instability.
(d) I° or II° lumbar degenerative spondylolisthesis or isthmic spondylolisthesis.
(e) Revision after the lumbar disc herniation surgery.

### 31.4.2 Contraindications

(a) Severe spondylolisthesis (>III°)
(b) Spinal kyphosis or scoliosis deformity.
(c) Multi-segmental disease (>2 segments)
(d) Suppurative spondylitis, spinal tuberculosis, spinal tumors, or traumatic fractures.
(e) Cauda equina syndrome.

## 31.5 Surgical Procedure

After general anesthesia, the patient is placed in a prone position on a surgical frame and the position is adjusted to increase the laminar space. At the beginning of the operation, the robot is wrapped in a disposable protective cover for the medical device and moved to a suitable position beside the operating table to ensure that the robotic arm can reach the lumbar surgical section. The optical tracking camera is placed on the head of the patient, which can be adjusted instantly according to the need for intraoperative navigation. The fixator, linker, and tracer are fixed on the spinous process adjacent to the surgical segment. The C-arm (Siemens Medical Solutions, Erlangen, Germany) is placed on the same side of the robot. After ensuring that the C-arm running track does not conflict with the surrounding environment and the robotic arm, perform orthographic imager and lateral fluoroscopy, and make sure that the robot ruler is in the center of the C-arm field. The three-dimensional CT image data of the patient's lumbar spine is obtained by C-arm circular scan and transmitted to the robot workstation for automatic registration of the marked points, and based on this data, the working channel of the endoscope and the path of the pedicle screws are planned, and the screw specifications can also be set on the computer system.

After that, the non-decompression side pedicle screw implantation and the decompression side guide wire implantation are carried out under the guidance of the robot. Then the robotic arm system runs to the planned path automatically and performs fine-tuning to ensure that the operation error is less than 1 mm before giving a prompt. The surgeon makes a 1–2 cm skin incision along with the designated position of the robotic arm, and inserts the guide sleeve directly to the bone surface, and uses an electric drill to drive the guide needles. Percutaneous pedicle screws are placed along the guide needle on the non-decompression side, and the guide wires are temporarily left on the decompression side.

The Kirschner wire is fixed at the junction of the lamina and the inferior articular process on the decompression side under the guidance of the robot. Then the dilator is inserted through the Kirschner wire to expand the soft tissue before the working channel and the endoscopic system (Joimax, Karlsruhe, Germany) are introduced sequentially. The procedure of nerve decompression, discectomy, and cage implantation are all performed under continuous saline irrigation.

The soft tissue around the surgical lamina space is first cleaned, and then the transitional part of the lamina and the inferior articular process (IAP) is exposed. Regarding it as a center, part of the lamina and IAP are resected by the high-speed drill, reamer, and Kerrison rongeur. And the outer edge of the ligamentum flavum, the disc, and tip of the superior articular process (SAP) are revealed successively. After the apex and medial part of the SAP were cut off, the lateral recess and nerve root canal were decompressed. The small blood vessel and soft tissue covering the disc are separated to clearly identify the boundaries of the annulus fibrosus, dural sac, and nerve root. The nerve is pushed to the medial side by the oblique opening of the working tube. After exposure of the posterior annulus, a complete discectomy is performed using endoscopic rongeurs, disc shavers, and down-biting curved curettes. Completely removing the disc and denuding the cartilaginous endplates can be observed clearly under the endoscope. After confirming the intervertebral space is cleaned up, exit the endoscope and replace the working tube with an assembled working sheath. Ensure that there are no nerves and blood vessels in the channel, the long oblique opening of the rotating sheath blocks the nerve roots, and the bone grafting funnel is inserted. The autologous fragments and allogeneic bone are implanted into the intervertebral space, and then the cage is implanted. The endoscope is introduced again to observe the position of the cage (about 3~5 mm away from the posterior edge of the vertebral body). The ligamentum flavum is then removed and the central canal decompression is performed. Clinically significant bilateral neural element compression can also get an adequate decompression by using the over-the-top technique. Before exiting the working channel, reconfirm that there is no obvious bleeding point. On the decompression side, the percutaneous pedicle screws are then inserted

along the reserved guidewire, and the connecting rod is applied and locked by compression.

Antibiotics are applied for 24 h after surgery. On the first day after the operation, the patient can wear a waistline or a brace for activities and be discharged home 3 days after the operation. No special rehabilitation treatment is required after surgery.

## 31.6 Case Study

Female, 62 years old. Main complaint: low back pain for 2 years, aggravated with right leg pain for 6 months. L4 radiculopathy right side, neurogenic claudication, walking distance 500 m (Figs. 31.1, 31.2, 31.3, 31.4, 31.5, 31.6, 31.7, 31.8, 31.9, 31.10, 31.11 and 31.12).

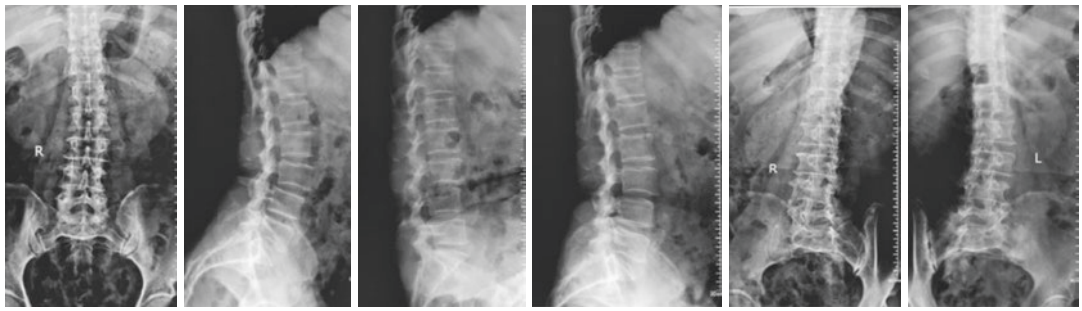


**Fig. 31.1** Preoperative X-ray

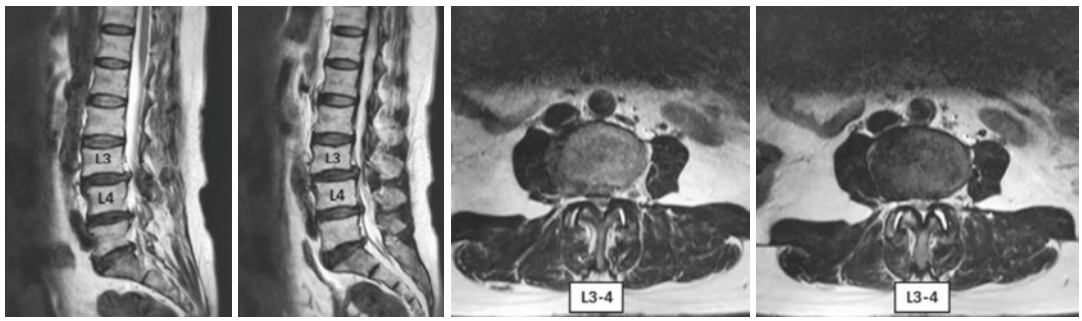


**Fig. 31.2** Preoperative MRI

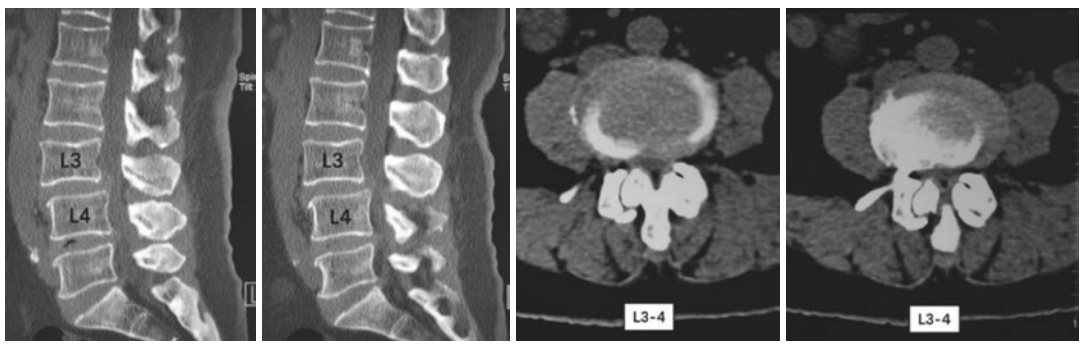


**Fig. 31.3** Preoperative CT scan

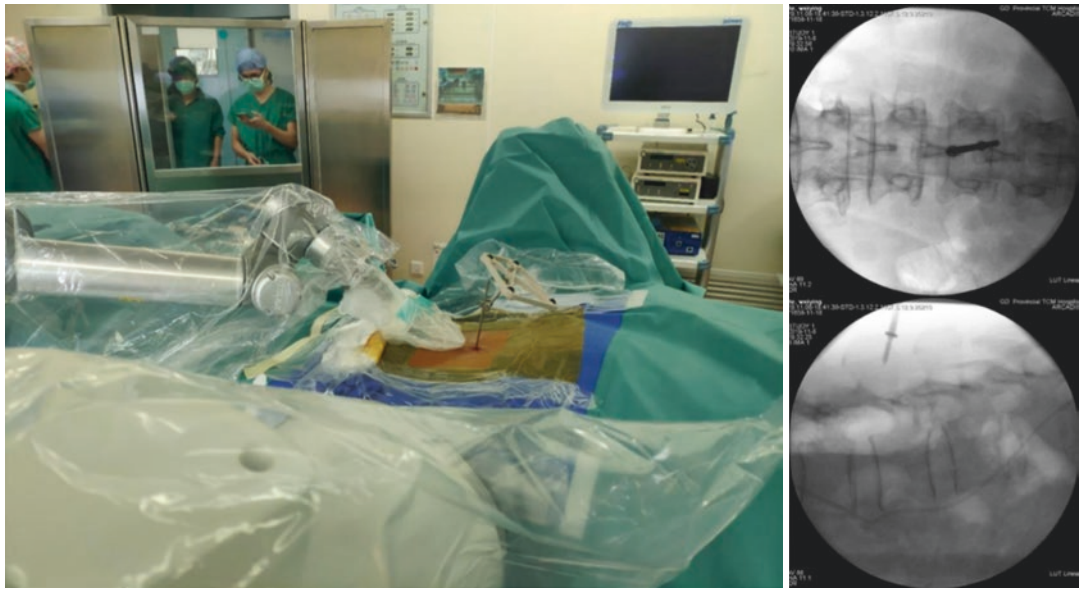

**Fig. 31.4** Linker and tracer are fixed on the adjacent cranial spinous process of the surgical segment

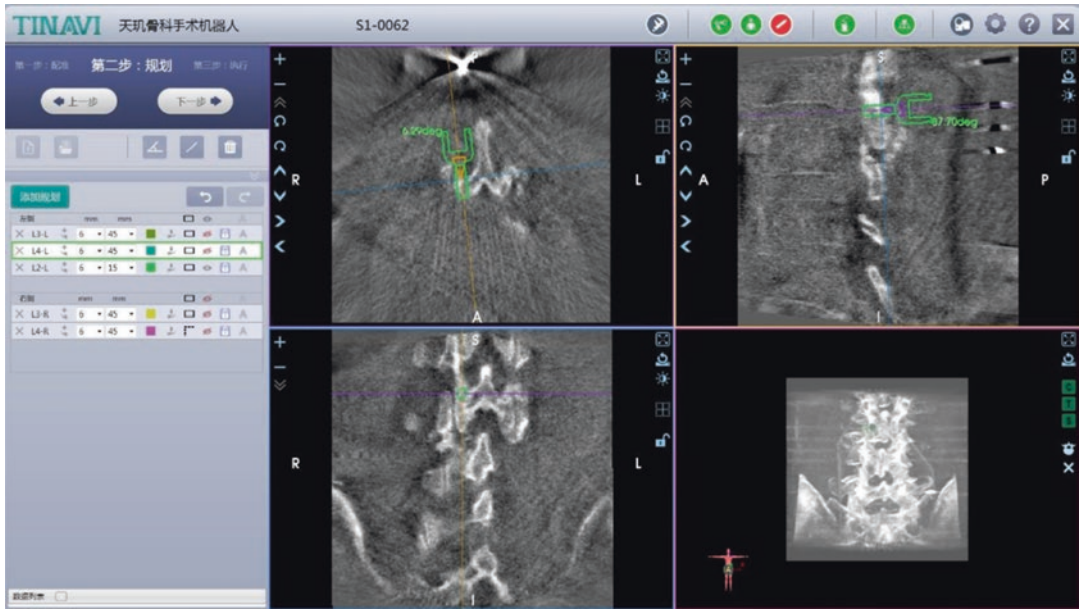


**Fig. 31.5** Working channel of the endoscope and the path of the pedicle screws are planned on the robotic computer system

## 31.7 Discussion

For those lumbar degenerative diseases with segmental instability that need fusion and fixation to restore stability and lordosis, PELIF is a new surgical method. Compared with traditional open PLIF or TLIF, PELIF has obvious advantages in minimally invasive: (1) Smaller surgical incision and less postoperative painful or unsightly scars. Single-segment PELIF requires only four 1-cm

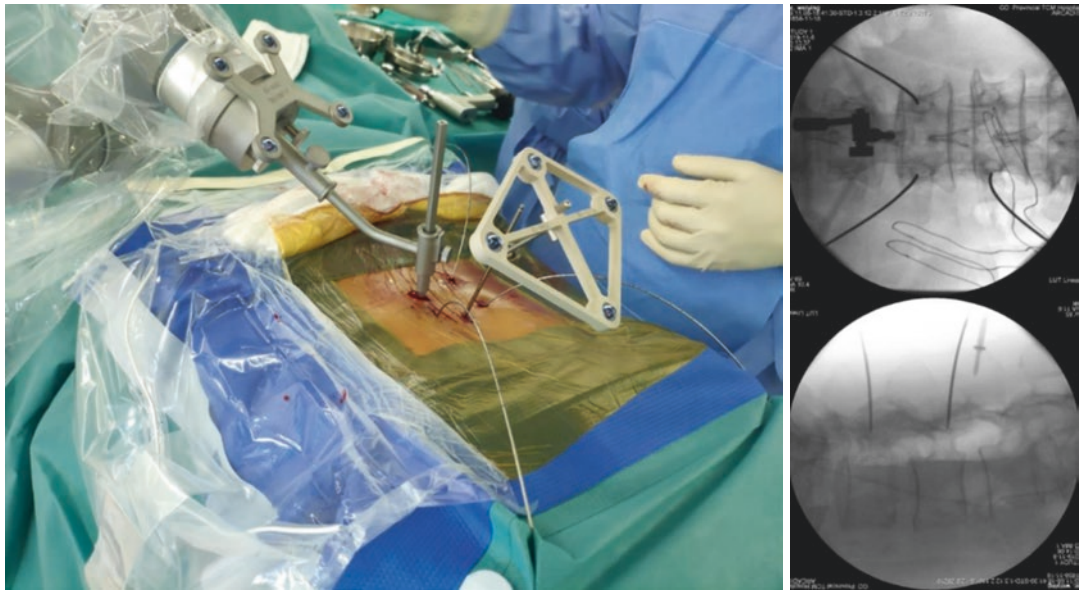

**Fig. 31.6** Robot-assisted precise placement of the endoscopic working channel and pedicle Kirschner wire

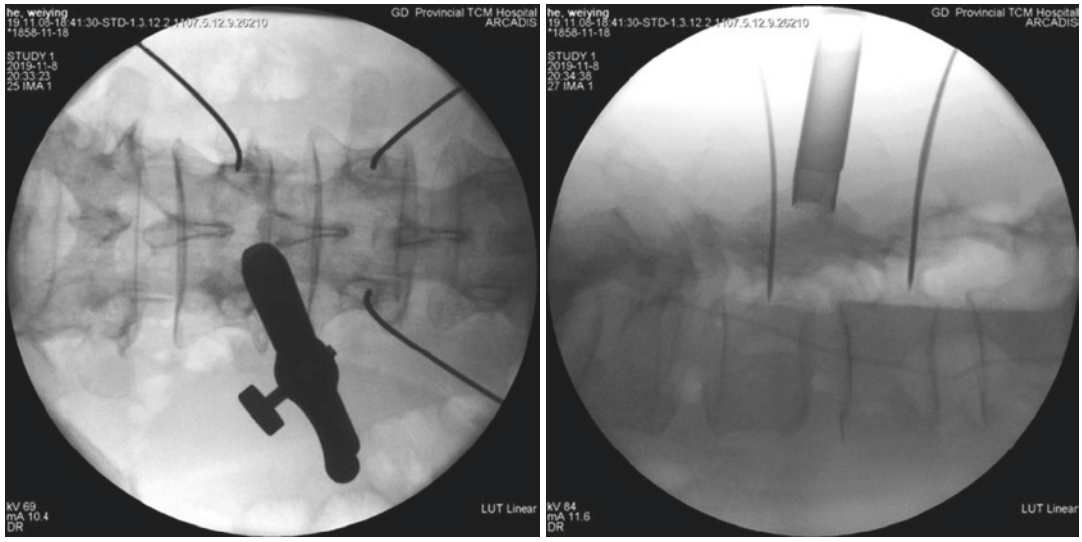


**Fig. 31.7** Position of the working tube and Kirschner wires confirmed by fluoroscopy

incisions, and double-segment needs six small incisions. (2) Less soft tissue damage. The establishment of the working tube and the implantation of percutaneous pedicle screws are completed by soft tissue expansion, so there is no need to extensively strip the spinal fascia and muscles, and the multifidus isotonic is retained to the greatest function. In addition, precise decompression is completed in the effective space under the working channel, and how much the bone resection is needed for decompression and the cage implantation is determined according to the specific situation observed under the endoscope, which can avoid excessive bone resection. Using over-the-top technology, bilateral decompression can be accomplished easily in one approach.

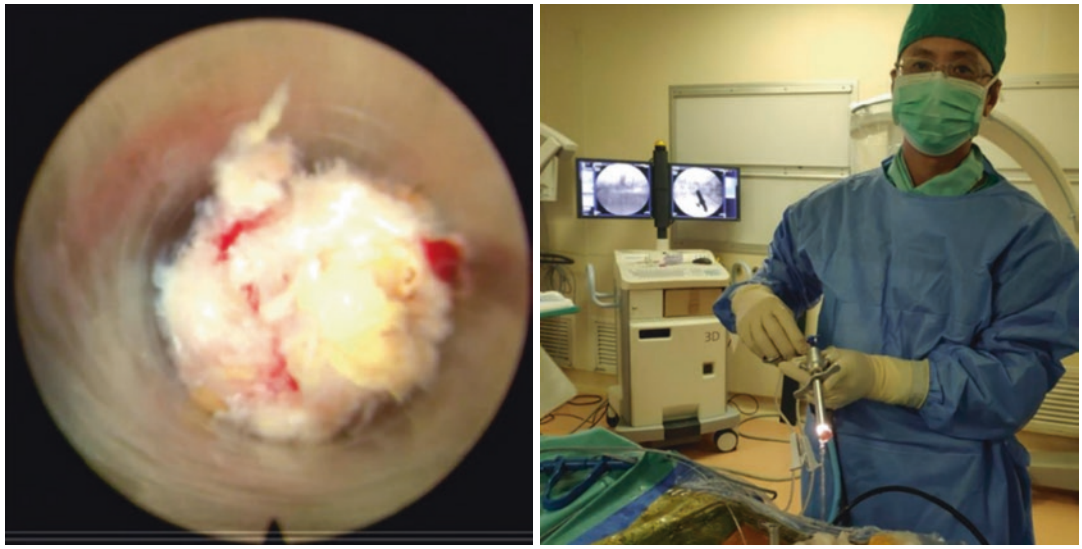

**Fig. 31.8** Part of the lamina and facet joint bony structures are cut by endoscopic reamer for bone grafting in the intervertebral space

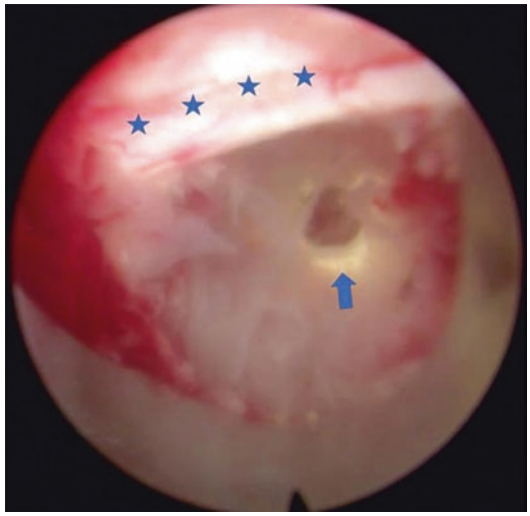

**Fig. 31.9** The nerve (blue star) and cage (blue arrow) can be clearly observed under the endoscope

Combined with percutaneous pedicle screw implantation technology, all operations can be completed percutaneously, which significantly reduces soft tissue trauma. (3) Less bleeding. Decompression under the continuous flushing of the water medium requires the maintenance of a blood-free environment, so even slight bleeding must be stopped in time. Generally speaking, the bleeding volume of single-segment PELIF is less than 30 ml, and in double-segment surgery that is less than 50 ml. (4) More adequate endplate preparation is conducive to promoting rapid fusion. The endplate preparation of PELIF is better than the TLIF or PLIF which cannot be directly displayed when the endplate is being prepared using a reamer or spatula. In addition, the available range of endplate preparation for TLIF or PLIF may not be enough to promote fusion in some cases. Subchondral bone injury or incomplete preparation of the endplate may cause cage subsidence or fusion failure. In contrast, the endoscopic visualization can help confirm the adequacy of the endplate preparation and expand the scope of endplate preparation. (5) Faster postoperative recovery. Back pain after open surgery is related to excessive stripping of the multifidus muscle and damage to the posterior branch of the spinal nerve, resulting in postoperative muscle fiber scarring and decreased muscle function. Patients of PELIF do not need drainage and they have mild postoperative back pain, shorter hospital stay, and faster return to normal life.

Although PELIF has the above advantages, it is a challenging and complicated operation [15], (1) For patients with narrow intervertebral disc space and Kambin triangle, it is difficult to obtain enough space to insert the cage safely, and it may

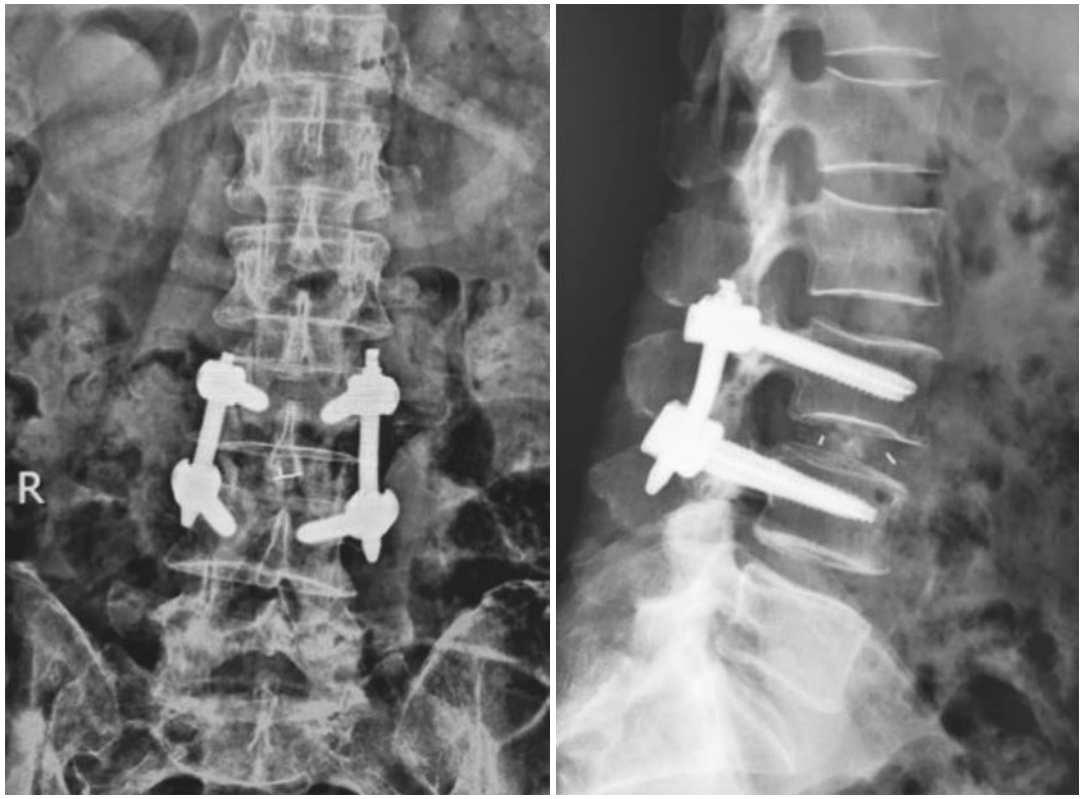


**Fig. 31.10** Postoperative X-ray

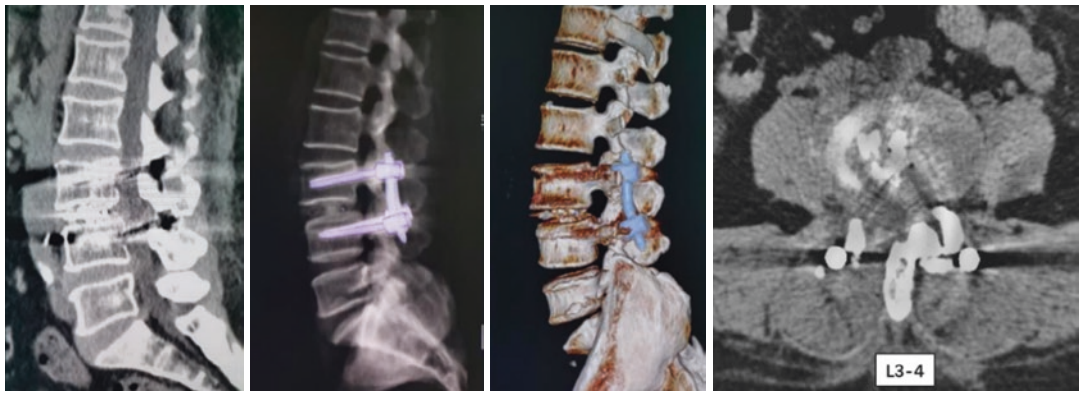


**Fig. 31.11** Postoperative CT scan

cause exiting nerve root damage [21]. (2) Due to the limitation of the working tube, there is a restriction on the size of the cage. For some cases with high intervertebral disc space, the small cage does not match, and the risk of fusion failure is significantly higher. New implants and techniques like B-Twin and other expandable spinal spacer cages are designed for endoscopic lumbar interbody fusion, however, these technologies also have risks such as endplate rupture, intervertebral space subsidence, less bone graft, and cage displacement [3, 16]. And they require specialized tools. (3) PELIF has a steep learning curve [3, 22]. This operation requires the surgeons to

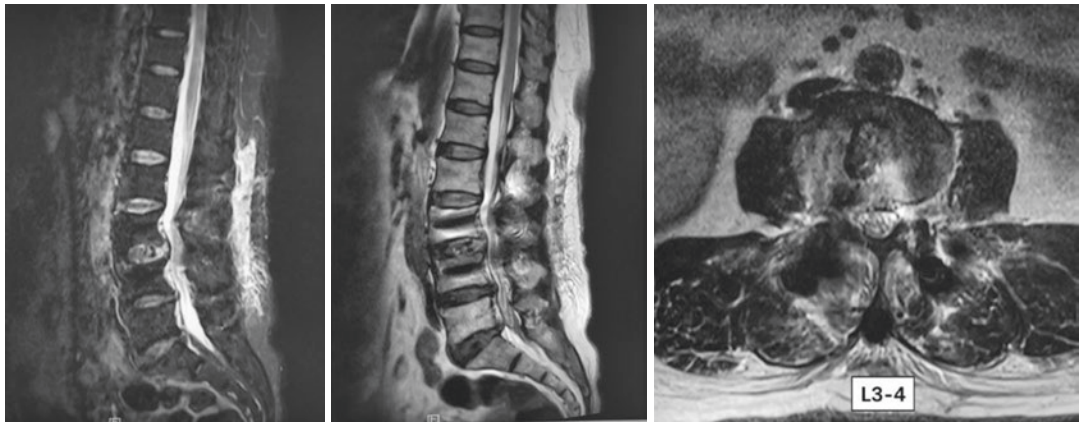


**Fig. 31.12** Postoperative MRI

have the mature experience of percutaneous endoscopic lumbar decompression and TLIF or PLIF, a good understanding of the endoscopic lumbar anatomical structure, and excellent endoscopic hemostasis skills.

In recent years, thanks to the rapid development of advanced robot technology, navigation technology, and computer technology, the application of robot-assisted orthopedic surgery has become increasingly widespread. Orthopedic robots can help to make a reasonable surgical plan, effectively improve the accuracy of implants, reduce the risk of neurogenic injury and other intraoperative complications [23–26]. More importantly, robot-assisted technology reduces intraoperative fluoroscopy, and makes it possible that doctors and patients can be freed from supernumerary X-ray radiation damage [25, 26]. Compared with the freehand technology by the traditional fluoroscopy guidance, the robot-assisted placement not only achieves real-time intraoperative image acquisition and visual evaluation of the actual intraoperative path but also reduces the operator's perceived error during the operation [27]. In addition, the robot also has the advantages of repeatability and fatigue resistance, which can break through the limitations of doctors' freehand ability and further improve the accuracy and safety of the surgery [24, 26, 28].

In addition to joint surgical robot systems such as Robodoc system [29], CASPAR system [30], Arthrobot system [31], and Praxiteles system [32], the commonly used spine surgical robot systems in clinical practice including the Israeli SpineAssist system [33], the Korean SPINEBOT system [34], the German MIS Robot system [35], and China TiRobot System [36].

Orthopedic robots have promoted the development of precise, minimally invasive, and intelligent surgery, but they are not flawless, and there are still certain limitations in large-scale clinical promotion [25, 26, 37, 38]. At present, the common disadvantages of orthopedic robots are complicated operation, expensive equipment, and difficulty for medical maintenance. Robotic surgery also requires a certain learning curve, mainly the preparation of the operation and the precise design of the surgical path. The robotic arm is not as flexible as a human hand, which cannot detect important tissue structures such as critical blood vessels and nerves in the surgical area, and cannot think and judge based on the information feedback replied from the receptors. Even if the automatically designed robot performs operations according to a predetermined program, most of the steps in the operation still need to be controlled by the physician requires controlling of the surgeon.

Points to note when using the orthopedic robots include the following: (1) The tracer should be firmly fixed on the bony structure to ensure that the position always remains unchanged between the tracer and the patient's limb, otherwise, the spatial positioning coordi-

nates may change and it causes the failure of the surgery. (2) The patient's reference array, image device tracker, and position detector during the operation should be placed reasonably to avoid errors caused by collisions during use. (3) The intraoperative image provided by the robot navigation software is a highly accurate virtual image synthesized by a computer, not a real-time image during the operation. The surgeon should conduct a review based on the internal anatomical landmarks of the surgical field. (4) If the space between the image device tracker and the optical camera is blocked by the operator or surgical instruments, it will be impossible to determine the position of the instrument in real time, which will increase the number of repeated adjustments, and prolong the operation time.

## 31.8 Conclusion

In general, PELIF is an innovative, safe, and effective surgical technique, which has the advantages of less trauma and bleeding, shorter hospital stays, lighter postoperative pain, and quicker recovery. Robot-assisted PELIF improves the accuracy and efficiency of the surgery and it is an important trend in future development. However, this new technology has a certain learning curve and requires surgeons to undergo sufficient theoretical learning and operational skills training. Its long-term efficacy also needs to be verified by a large-sample multicenter prospective randomized controlled trial.

## References

1. Buckland AJ, Ashayeri K, Leon C, et al. Single position circumferential fusion improves operative efficiency, reduces complications and length of stay compared with traditional circumferential fusion. Spine J. 2020;13:S1529-9430(20)31217-1.
2. Chan AY, Lien BV, Choi EH, et al. Back pain outcomes after minimally invasive anterior lumbar interbody fusion: a systematic review. Neurosurg Focus. 2020;49(3):E3.
3. Choi UY, Kim KT, Kim KG, et al. Safety and tolerability of stromal vascular fraction combined with β-tricalcium phosphate in posterior lumbar interbody fusion: phase I clinical trial. Cell. 2020;9(10):2250.
4. Chang CC, Chou D, Pennicooke B, et al. Long-term radiographic outcomes of expandable versus static cages in transforaminal lumbar interbody fusion. J Neurosurg Spine. 2020;13:1–10.
5. Li HM, Zhang RJ, Shen CL. Radiographic and clinical outcomes of oblique lateral interbody fusion versus minimally invasive Transforaminal lumbar interbody fusion for degenerative lumbar disease. World Neurosurg. 2018;122:e627–38.
6. Kudo Y, Okano I, Toyone T, et al. Lateral lumbar interbody fusion in revision surgery for restenosis after posterior decompression. Lateral lumbar interbody fusion in revision surgery for restenosis after posterior decompression. Neurosurg Focus. 2020;49(3):E11.
7. Xu DS, Walker CT, Godzik J, et al. Minimally invasive anterior, lateral, and oblique lumbar interbody fusion: a literature review. Ann Transl Med. 2018;6(6):104.
8. Heo DH, Kim JS. Clinical and radiological outcomes of spinal endoscopic discectomy-assisted oblique lumbar interbody fusion: preliminary results. Neurosurg Focus. 2017;43(2):E13.
9. Lin EY, Kuo YK, Kang YN. Effects of three common lumbar interbody fusion procedures for degenerative disc disease: a network meta-analysis of prospective studies. Int J Surg. 2018;60:224–30.
10. Parajón A, Alimi M, Navarro-Ramirez R, et al. Minimally invasive transforaminal lumbar interbody fusion: meta-analysis of the fusion rates. What is the optimal graft material? Neurosurgery. 2017;81(6):958–71.
11. Heo DH, Son SK, Eum JH, et al. Fully endoscopic lumbar interbody fusion using a percutaneous unilateral biportal endoscopic technique: technical note and preliminary clinical results. Neurosurg Focus. 2017;43(2):E8.
12. Nagahama K, Ito M, Abe Y, et al. Early clinical results of percutaneous endoscopic transforaminal lumbar interbody fusion: a new modified technique for treating degenerative lumbar spondylolisthesis. Spine Surg Relat Res. 2018;3(4):327–34.
13. Wu J, Liu H, Ao S, Zheng W, et al. Percutaneous endoscopic lumbar interbody fusion: technical note and preliminary clinical experience with 2-year follow-up. Biomed Res Int. 2018;19(2018):5806037.
14. Kolcun JPG, Brusko GD, Basil GW, et al. Endoscopic transforaminal lumbar interbody fusion without general anesthesia: operative and clinical outcomes in 100 consecutive patients with a minimum 1-year follow-up. Neurosurg Focus. 2019;46(4):E14.
15. Jacquot F, Gastambide D. Percutaneous endoscopic transforaminal lumbar interbody fusion: is it worth it? Int Orthop. 2013;37(8):1507–10.
16. Yao N, Wang W, Liu Y. Percutaneous endoscopic lumbar discectomy and interbody fusion with B-twin expandable spinal spacer. Arch Orthop Trauma Surg. 2011;131(6):791–6.

17. Overley SC, Cho SK, Mehta AI, et al. Navigation and robotics in spinal surgery: where are we now? Neurosurgery. 2017;80(3S):S86–99.
18. Ganguly R, Minnema A, Singh V, et al. Retrospective analysis of pedicle screw accuracy for patients undergoing spinal surgery assisted by intraoperative computed tomography (CT) scanner AIRO® and BrainLab© navigation. Clin Neurol Neurosurg. 2020;198:106113.
19. Heo DH, Lee DC, Kim HS, et al. Clinical results and complications of endoscopic lumbar interbody fusion for lumbar degenerative disease: a meta-analysis. World Neurosurg. 2020;145:396–404.
20. Jin M, Zhang J, Shao H, et al. Percutaneous transforaminal endoscopic lumbar interbody fusion for degenerative lumbar diseases: a consecutive case series with mean 2-year follow-up. Pain Physician. 2020;23(2):165–74.
21. Morgenstern C, Yue JJ, Morgenstern R. Full percutaneous transforaminal lumbar interbody fusion using the facet-sparing. Trans-Kambin Approach Clin Spine Surg. 2020;33(1):40–5.
22. Ao S, Zheng W, Wu J, et al. Comparison of preliminary clinical outcomes between percutaneous endoscopic and minimally invasive transforaminal lumbar interbody fusion for lumbar degenerative diseases in a tertiary hospital: is percutaneous endoscopic procedure superior to MIS-TLIF? A prospective cohort study. Int J Surg. 2020;76:136–43.
23. Jacofsky DJ, Allen M. Robotics in arthroplasty: a comprehensive review. J Arthroplast. 2016;31(10):2353–63.
24. Lustig S, Magnussen RA, Dahm DL, et al. Patellofemoral arthroplasty, where are we today? Knee Surg Sports Traumatol Arthrosc. 2012;20(7):1216–26.
25. D'Souza M, Gendreau J, Feng A, et al. Robotic-assisted spine surgery: history, efficacy, cost. And Future Trends Robot Surg. 2019;7(6):9–23.
26. Chang KD, Raheem AA, Rha KH. Novel robotic systems and future directions. Indian J Urol. 2018;34(2):110–4.
27. Li W, Li G, Chen W, et al. The safety and accuracy of robot-assisted pedicle screw internal fixation for spine disease: a meta-analysis. Bone Joint Res. 2020;9(10):653–66.
28. Luo J, Yan Y, Wang X, et al. Accuracy and safety of robot-assisted drilling decompression for osteonecrosis of the femoral head. Orthop Surg. 2020;12(3):784–91.
29. Liow MHL, Chin PL, Pang HN, et al. THINK surgical TSolution-One® (Robodoc) total knee arthroplasty. SICOT J. 2017;3:63.
30. Prymka M, Vogiatzis M, Hassenpflug J. Primary rotatory stability of robot-assisted and manually implanted hip endoprosthesis stems. Unfallchirurg. 2004;107(4):285–93.
31. Monfaredi R, Iordachita I, Wilson E, et al. Development of a shoulder-mounted robot for MRI-guided needle placement: phantom study. Int J Comput Assist Radiol Surg. 2018;13(11):1829–41.
32. Plaskos C, Cinquin P, Lavallée S, et al. Praxiteles: a miniature bone-mounted robot for minimal access total knee arthroplasty. Int J Med Robot. 2005;1(4):67–79.
33. Molliqaj G, Schatlo B, Alaid A, et al. Accuracy of robot-guided versus freehand fluoroscopy-assisted pedicle screw insertion in thoracolumbar spinal surgery. Neurosurg Focus. 2017;42(5):E14.
34. Kim ER, Lim C, Kim DJ, et al. Robot-assisted cardiac surgery using the da vinci surgical system: a single center experience. Korean J Thorac Cardiovasc Surg. 2015;48(2):99–104.
35. Jin X, Zhao J, Feng M, et al. Snake-like surgical forceps for robot-assisted minimally invasive surgery. Int J Med Robot. 2018;14(4):e1908.
36. Han X, Tian W, Liu Y, et al. Safety and accuracy of robot-assisted versus fluoroscopy-assisted pedicle screw insertion in thoracolumbar spinal surgery: a prospective randomized controlled trial. J Neurosurg Spine. 2019;8:1–8.
37. Mancuso F, Pandit H. Robotics accuracy in orthopaedics: is it enough for a well-working knee replacement? Ann Transl Med. 2016;4(Suppl 1):S39.
38. Lang JE, Mannava S, Floyd AJ, et al. Robotic systems in orthopaedic surgery. J Bone Joint Surg Br. 2011;93(10):1296–9.

# 32 Future Perspective of Robot-Assisted Minimally Invasive Spine Surgery

Ethan Schonfeld, Martin N. Stienen, and Anand Veeravagu

## 32.1 Introduction

With the first ever FDA approval of a spine robot in 2004, Mazor's SpineAssist became a new frontier in the field of open and minimally invasive spine surgery (MISS). Newer generation robots, e.g., the Mazor X, ROSA One, Cirq, and Excelsius GPS, use improved navigation technology, controlled drilling, and improvements in their range of motion [1]. These robots have already benefited spine surgeons in a plethora of ways. They allow for precise stereotactic control by rigid degrees of freedom. Their computer navigation systems aid in collision avoidance, which is especially pertinent in the MISS setting where paths to navigate to and reach deep structures can be difficult for the surgeon. They further offer tremor filtering technology and lower radiation exposure for the surgeon during the procedure. Lastly, a benefit of recent spine robots to the field has come in improving remote surgery.

Considering the aforementioned benefits, it comes as no surprise that research has demonstrated considerable improvements in both accuracy and outcome in spine procedures done using surgical robots. Compared to conventional pedicle screw placements, the use of robotics during these surgeries resulted in more accurate screw placement, lowered neurologic complication rates, decreased fluoroscopy time, lowered infection rates, lowered operative time, and reduced length of stay [2–9]. While most robotic-assisted MISS surgeries have focused on screw placements, many of these benefits are starting to be realized in other procedural domains including robotic-assisted spinal tumor operations [10].

Yet, the more that robotics enter as assistive tools for MISS, the more challenges we see remain. Their high costs, high training requirements, and low portability currently prohibit their large-scale adoption. Long calculation times and difficulties in image synchronization (complicated by patient movements) still prohibit their application to a broader range of procedures. Today's robots cannot or only with difficulty be used for patients with poor bone quality, complex deformities, and high body mass. The lack of sensory feedback, specifically haptic, reduces the ability of the robot, compared to a trained surgeon, to operate in environments with different tissues and densities. The combination of these

E. Schonfeld · A. Veeravagu (✉)
Neurosurgery AI Lab & Department of Neurosurgery, Stanford University School of Medicine, Stanford, CA, USA
e-mail: eschon22@stanford.edu; anand.veeravagu@stanford.edu

M. N. Stienen
Neurosurgery AI Lab & Department of Neurosurgery, Stanford University School of Medicine, Stanford, CA, USA

Department of Neurosurgery and Spine Center of Eastern Switzerland, Kantonsspital St.Gallen, St. Gallen, Switzerland



J.-S. Kim et al. (eds.), *Technical Advances in Minimally Invasive Spine Surgery*,
https://doi.org/10.1007/978-981-19-0175-1_32

challenges culminates in the ability of today's spine robots to assist in limited domains of MISS, namely surgeon-controlled pedicle screw placements and in more recent work some resections and ablations. Either semi or full, robotic autonomy in MISS would be transformative in the field of remote surgery. By developing the robotics mature enough to predict the next steps, this would avoid the limitation of distance due to signal speed. Autonomy would further transform decision-making in the operating room where the surgeon is faced with many choices. Robots, equipped with artificial intelligence (AI) and machine learning (ML) could gather experience from past cases. Hereby they could become helpful agents in working with the surgeon in real-time surgical decision-making, specific to not just the patient's anatomy but their clinical history as well.

We have identified six areas of focus for the future: (1) remote surgery, (2) haptic and auditory feedback for increased precision, (3) nonlinear trajectories and the expansion of procedures for robotic assistance, (4) reductions and eliminations of radiation and fluoroscopy in navigation, (5) artificial intelligence for decision-making assistance, (6) and the large-scale intraoperative data collection by robotics. There are three ways to predict the future of these six areas in MISS: current products in the corporate pipeline, new advances in robotics in non-spine surgical domains, and what the field of MISS itself needs.

## 32.2 Current Products in the Corporate Pipeline

### 32.2.1 NuVasive: Pulse

The NuVasive Pulse, including both the Pulse system, and the Pulse robot will offer innovative improvements including an expansion of procedures that the system can assist in. The Pulse system itself received FDA clearance and is integrated with the mobile C-arm machine from Cios Spine to combine in a single platform: neuromonitoring, surgical planning, rod bending, radiation reduction, imaging, and navigation for MISS [11, 12]. Its radiation reduction of up to 80% comes in the form of LessRay, which uses ML algorithms to take low-dose and low-quality images and augment them to appear conventional [12–15]. However, the true innovation is expected to come in the form of NuVasive's Pulse Robot, which will integrate with the system when it becomes available for first in human use in 2022. It is expected, from initial reports but not peer-reviewed literature, that surgeons can operate the control arm within certain degrees of freedom even when it is locked in place, thereby allowing for better methods of slight adjustments and improvements in screw trajectories during procedures [16]. The robot will have real-time feedback for clinical decision-making. This has been a challenge in the field, as in the earlier robots, when a new approach or trajectory had to be designed during the procedure, the systems were unable to update right away and the procedure had to continue without robotic support. The Pulse Robot also seeks to improve on the accessibility and applicability of robots in spine surgery by using an easier setup, a flexible mobile cart [16]. Apart from these aspects, very little is known about the Pulse Robot that NuVasive intends to integrate with the Pulse system. To warrant an educated guess into novel features that the robot will introduce, recent NuVasive patents show research focus in MISS trauma correction, determining nerve proximity and direction in real-time surgery, MISS spine fixation systems, and methods for predicting spinal corrections by generating rod solution outputs [17–20]. From this analysis it seems that the Pulse Robot may bring novel advances in the range of procedures that it is equipped to assist in, especially as it comes in conjunction with the Pulse system for navigation and collision avoidance.

### 32.2.2 Medtronic: Mazor X Stealth

Medtronic, who acquired Mazor Robotics in 2018, is now a leader in robotics for MISS with their latest product Mazor X Stealth Edition. In December 2020, Medtronic acquired the AI company Medicrea; this acquisition bodes real innovation to their line of MISS robots [21]. Jacob Paul, the senior vice president of Medtronic

Cranial and Spatial Technologies stated that they now have all the pieces necessary to build a comprehensive spinal surgery system driven by AI including surgical planning, personalized spine implants, and robotic-assisted surgical delivery [21]. This system will likely look very different from that of the Pulse System due to the predictive modeling capabilities of Medicrea. Medtronic is now focused on robotic technologies that can be used in more roles during the surgery, and that have greater decision-making capability. Medicrea systems focus on surgical planning and predictive modeling tools, with the ability to create personalized implants, including 3D printed patient-specific rods and cages, compatible with MISS [22–25]. During surgery, surgeons must make decisions regarding how to align the spine and what degree of curvature to choose. Medicrea's AI engine, the UNiD HUB program that uses the ML IB3D Adaptive Spinal Intelligence to learn from patient cases, is trained on 6000 3D patient cases and can predict optimal curvature and predict how selection of the rods and screws will affect adjacent regions. Its output is a set of 3–4 options from which the surgeons can choose their preferred approach [21, 25]. Combined with Mazor's 2020 patent for spine deformity correction by ML segmentation and alignment optimization, integration of this technology into the Mazor robot can show increases in robotic decision-making assistance during real-time surgery [26]. Learning from past patient outcomes can help to better select appropriate curvature, cages, rods, screws, and trajectories.

### 32.2.3 Globus: Excelsius GPS

Similar to Medtronic's focus on planning software, Globus seeks to develop their Excelsius GPS robot for MISS with planning software for higher complexity procedures. A current challenge of robots in MISS is their inability to be used in patients with complex deformities. To address this, Globus acquired Nemaris, developer of Surgimap, in 2018; Surgimap products simulate surgical procedures and outcomes, predict alignments, and share medical images globally, allowing for big data approaches to assist in predictive modeling [27–30]. Surgimap technologies equip Globus with state-of-the-art simulation tools, specialized for the treatment of complex deformities. Furthermore, the ability to aggregate the medical data puts the Excelsius GPS robot in a position for big data analytics and the move toward higher complexity of robotic procedures.

### 32.2.4 Zimmer Biomet: Rosa ONE

Zimmer Biomet, like its competitors, is moving toward expanding the horizon of MISS procedures that its ROSA One robot can be used for. The company acquired A&E Medical in late 2020, including their massive portfolio of sternal closure devices [31]. Capabilities for sternal closure by robotics may extend their ability to address the cervico-thoracic region from anterior, e.g. for robotic assistance in discectomy or corpectomy procedures in the setting of complex degenerative, neoplastic, infectious, or traumatic spine diseases.

### 32.2.5 Discussion

The current state of the corporate pipeline for robotics in MISS is focused on the expansion of procedures that the robots can be used for, reductions in radiation, and the use of AI for patient-specific surgical decision-making. Medtronic is well positioned with their UNiD HUB for learning from previous patient cases to recommend to the surgeon possible curvatures and assist in the selection of rods and screws. To use UNiD HUB, first the patient undergoes a pre-operative imaging analysis with detailed alignment values by a lab engineer. Then the lab engineer uses the HUB software to develop personalized surgical strategies based on surgeon feedback. Next, based on the selected strategy, a TEK implant is designed by the lab engineer and 3D printed. During surgery, there is no need to size and fit standard implants, decreasing the overall surgery time. Anonymized data from the images, surgery, and patient outcome is collected and used by ML algorithms to improve the HUB software and learn from every case. The data is incorporated to

help the surgeon predict patient-specific outcomes, based on what the HUB system has learned. There is not yet much data available to support this innovative concept with scientific evidence, however patient-specific rods implanted with UNiD assistance were found to have a lower rate of rod breakage compared to non-patient specific [32]. Medtronic has the opportunity to equip their Mazor robot with such technologies, thereby transforming the robot to an assistive decision-making agent for the surgeon. As more data is collected, it is likely that the number and degree of complexity of procedures that the technology can be used in will likely expand.

In a similar lens to Medtronic's ability to learn from patient cases to better future predictions, Globus's acquisition of Surgimap allows for large-scale data collection. Companies that buy into big data collection earlier will likely be at a significant advantage to incorporate AI for the improvement of navigation, trajectory planning, and both rod and screw selections.

However, incorporating sensory, specifically haptic and auditory feedback for these robots appears to be notably absent from the corporate leaders. The absence of haptic feedback significantly limits robotic assistive value in different tissue settings. It further remains to be seen as to what degree these companies will commit to artificial and virtual reality (AR/VR) solutions for navigation and imaging during surgery. Lastly, the companies discussed above have yet to enter serious products for remote surgeries. We expect all these areas to be of focus of current research as these novel research areas burgeon. As we move to focus on novel advances in robotics as a way of predicting the future advances in robots for MISS, it is largely these areas that we will discuss.

## 32.3 New Advances in Robotics

### 32.3.1 Remote Surgery

Just recently, remote MISS seemed a faraway possibility due to serious limitations in system delay and network instability. If the robot were to lose contact with the control branch mid-surgery, the patient would be put at an incredible risk. A study testing different delays in telesurgery, by artificially adding latency, found that surgeons' comfort zone upper boundary is at 330 ms [33]. This upper bound, in the domain of challenging spine surgeries, is suggested to be 200 ms in order to avoid fatal consequences [34].

But with recent advances and implementations of 5G, remote MISS becomes much closer to reality. The 5G network is characterized by low latency and ultra-high reliability. The first group to study remote robotic 5G spinal surgery used the TiRobot system for pedicle screw implants on 12 patients [34]. On this network, the mean latency was 28 ms, far below the upper bound. The deviation between planned versus actual screw placement was 0.76 +/− 0.49 mm with no intraoperative adverse effects. The acceptable rate of pedicle screws (grades A and B according to the Gertzbein–Robbins criteria) was 100%. They further validated the approach in a one-to-many surgeon-to-patient setup, demonstrating capabilities with the improved bandwidth of 5G [34].

The success of the study raises the possibility for patients, in isolated areas, requiring advanced spine surgeries to have access to experienced surgeons in large cities. However, this is a long way away from the grandiose visions for remote surgery, including but not limited to battlefield and outer space uses. For distances of 1500 km, delays are commonly less than 10 ms, but for the distances in battlefield and outer space contexts, delays must still be reduced. One emerging method to reduce the delay requirement is by having the robot predict what the next action will be before receiving the signal from the surgeon. By starting the action earlier the robot indirectly reduces the signal-to-action delay bottleneck. To do such predictions, AI stands as a promising tool. Machine learning techniques such as imitation learning, reinforcement learning, and deep learning can learn situational and patient-dependent actions from past cases. In turn, using such learning techniques, the robot can predict for the current patient and the current surgical state what the next surgical step will be. As robots

are now collecting intraoperative data, sufficient data may soon become available for research into the above techniques.

Fully remote spinal surgery has yet to be demonstrated. The above study required a surgical team to be present at the local setting to perform bone grinding and nerve decompression [34]. In a recent editorial, John Adler from Stanford University elaborates on the mechanical innovation that is still required for remote robots: "*While the accurate placement of spinal screws is a specialized and critical task by itself, properly anesthetizing, positioning and monitoring a patient for intricate spinal surgery as well as surgically exposing, inserting hardware and then wound closure are significantly more complex intellectual and mechanical challenges*" [35]. The robotic technique is not yet advanced enough for fully remote applications. The robots are used most commonly for pedicle screw placements, and in more recent work, guidance of percutaneous transforaminal endoscopy, vertebroplasty surgery, transdiscal screw trajectories, anterior odontoid screw fixation, posterior C1–2 transarticular screw fixation, the cortical trajectory for pedicle fixation, and translaminar lag screw fixation [36–45]. However, the limitation of straight-line trajectories and lack of haptic and auditory feedback restricts the mechanics of robots and leaves tasks such as nerve decompressions currently remotely infeasible.

### 32.3.2 Haptic and Auditory Feedback

The absence of advanced haptic feedback limits robotics in both remote and non-remote surgeries. Incorporation of real-time haptic feedback could increase precision and reliability for improvements of robots' surgical skill. As for the current state of the art for haptic feedback in spine robots, the Mazor X functions in a way to require re-registration when sensing too much pressure on the arm [46]. This feedback is of limited value as it requires stopping the surgical procedure; more valuable tools would involve having the robot use haptic and auditory information to alter the pressure applied. Other surgical fields involve robotics with more advanced uses of haptic information. In the arthroplasty domain, robots alert the surgeon during bone cuts, when sensing too much pressure, without requiring re-registration, yet spine robots have been slow to adopt such advances [46].

However, non-visual feedback for surgical robotics in the spine is currently developing to include much more advanced technology. An especially promising advance is the Functionally Accurate Robotic Surgery (FAROS) project. FAROS, a research consortium, funded through European Union's Horizon 2020 Research and collaborating with SpineGuard, began with the identification that humans make use of their entire collection of senses during surgery, especially when vision is limited [47]. However, robots have largely been limited to understanding the surgical state only through computer vision. By using wide field mapping, auditory, and haptic sensors, FAROS collects multimodal, non-visual, information regarding the surgical setting. In turn, this multimodal information is, through deep learning, modeled to functional parameters [48]. These functional parameters include tissue type, tissue or bone quality, condition of tissue or fluid, tissue damage, perfusion, implant stability, among others [48]. FAROS uses these functional parameters to not only supplement the robotic vision of the state, but also to, through reinforcement learning, model reasonable actions that the robot can take in its current environment. With the development of such intelligent feedback, not only can functional accuracy be improved, but also feedback-supplemented computer assisted navigation systems can be developed to further reduce radiation [49]. FAROS is intended to be showcased and validated for pedicle screw placement and endoscopic lumbar discectomy [48].

Further potential for the future of haptic feedback in spine surgery comes from Stryker. Their Mako robot is state of the art for knee and hip replacements, in large part due to its haptic feedback by AccuStop. First, the robot uses data from a CT scan to construct a 3D model for presurgical planning and fine tuning. Using this model, during surgery AccuStop incorporates haptic feedback to be precise in cutting exactly what was

planned, thereby preserving soft tissue and healthy bone [50]. This feedback involves auditory beeps, color changes on screen, and tactile vibrations while the surgeon is making incisions and cutting [51]. Stryker, in 2019, acquired Mobius Imaging and Cardan Robotics which, as Stryker's Group President in Orthopaedics and Spine states, will increase its presence in orthopedics, spine, and neurotechnology [52]. In this way, we may see state-of-the-art haptic technology on surgical robots enter the spine domain.

### 32.3.3 Expanding Procedures for Robotics in MISS

Many of the advances discussed above have serious implications to broaden the array of procedures that robots are able to assist in MISS. Specifically, development of haptic feedback can expand to more complicated tissue procedures, ML incorporation can increase complexity of current procedures including cases of severe deformities, and improved radiation-free navigation can allow for object avoidance for deeper surgeries. However, robotics is unable to assist to a large degree for procedures involving bone cutting and manipulation, such as osteotomies in the spine domain. Yet, with future improvements in mechanical technique, this area stands to massively benefit from robotics in MISS, in both improved accuracy and lowered radiation. For fracture reductions, open surgery resulted in low accuracy, low postoperative recovery, and damages to soft tissues [53]. As a consequence, more minimally invasive approaches were used, leading to high radiation exposure. This poses an opportunity for robotic assistance to improve accuracy while decreasing the necessary amount of radiation. However, there is currently no validated robot for reduction in the fractured spine, for guiding osteotomy cuts in the deformed spine, or for other surgical steps involving bone work.

With the advent of computer aided manufacturing (CAM) technology, bone volume reduction by robotics becomes more of a possibility. CAM technology uses software to generate toolpaths, then these toolpaths are converted into a language that a machine can use as instruction. These instructions are again used to take a prespecified raw material and manufacture a finished product. In the domain of bone cutting, the finalized product is the finished bone with a desired area removed. Packages such as PowerMILL, FeatureCAM, and Robotmaster use inputs of the desired starting and ending bone states as well as robotic arm details to automatically determine the pattern of robotic arm movement necessary to remove a prespecified volume of bone [54]. These CAM solutions are able to be involved in minimally invasive approaches [55]. Thereby, procedures involving bone volume reduction including laminectomies, corpectomies, or osteotomies appear to be possible in the near future, as spine robots begin to incorporate CAM technology [56].

Furthermore, developments in small robotics for specialized procedures are developing, made possible by advances in CAN. The founder of Mazor has created a new start up, XACT Robotics, focused on minimally invasive procedures. XACT Robotics systems have non-linear steering capacity, thereby leading to an expansion of surgical procedures able to assist in [57]. While early stage, having only completed testing on animals, the technology involves narrow penetrative devices capable of precise deep biopsies, injections, ablations, and drainages [58]. Other novel approaches to deep injections have attempted to avoid high radiation levels by using robotic ultrasound and force data. These data are then combined by a deep learning network to model the probabilities of vertebra locations [59]. For both approaches, the reduction of radiation for these complex navigational tasks is centered around ML.

### 32.3.4 Machine Learning (ML) for MISS

#### 32.3.4.1 What Is Machine Learning?

At its core, ML is the ability for a computer to learn from experience. Imagine you are faced with thousands of berries, some are purple and

round, some blue and prickled, and yet some others speckled with stripes. There are infinite possibilities as to the form of these berries, yet common patterns amongst them exist. You are now faced to determine which are sweet and good for food, and which contain poison. Naturally, the human solution is to examine a berry and note its pattern, what other patterns it resembles from the entire group, then eat it and observe the outcome. If the outcome is tasting a sweet berry, then we predict those berries with similar patterns have a higher probability of being themselves sweet. If we get ill, we can similarly adjust the probabilities. This is the same way ML uses its experience to learn.

As an example in the MISS domain, ML can be used for cage fitting. Having been trained on thousands of previous patient cases, imaging a patient's spinal anatomy, and combining this with clinical information and sensory feedback serves as observing the patterns for a new unseen berry. From the computer's experience as to the surgical outcomes of other cases with similar patterns, the computer is able to make a prediction as to what the most appropriate cage is for this specific patient in order to optimize their surgical outcome. This prediction gets stronger as more data is used to train the model.

#### 32.3.4.2 Radiation- and Fluoroscopy-Free Navigation

NuVasive's use of LessRay will reduce radiation levels by around 80%, using less radiation to get a noisy image and using ML methods to enhance the image quality [12]. But recent work has shown that even a future of radiation- and fluoroscopy-free navigation is a possibility.

One of the largest challenges in navigation is from patient movements and shifts during surgery. Current optical tracking systems use reference frames attached to the spine for patient movement tracking by AR to avoid 2D fluoroscopy [60]. However, the intrinsic movements impact the accuracy of navigation systems. These intrinsic movements disrupt the synchronization of preoperative matching to intraoperative navigation. As a solution, ML may be used to identify spine landmarks to match in camera views and synchronize regions unaffected by patient shifts [61]. To accomplish this requires two gray-scale cameras to identify the spinal landmarks, ML to preprocess the spine images and match image regions. Validated in 23 patients, the procedure supports spine feature detection for fluoroscopy-free navigation [61]. The challenge will be in developing such methods for MISS approaches, as they usually do not involve exposing the anatomy for the system to allow for the identification of bony landmarks.

Similarly, to eliminate radiation for navigation, visible light can be used as a replacement. The first and only navigation system that can do this today is 7D Surgical Machine Vision Image Guided Surgery [62]. Reducing registration time down to <20 s, a reference frame is placed and identifies 3D location points. With visible light the surface scan is aligned to a pre-operative CT scan and after an accuracy check the surgeon can use the image guided navigation [63]. A minimally invasive approach with the 7D system was shown in a case study using a 3.5 cm mini-open incision. With a radiation exposure estimated to be in range of 85–94%, a minimally open lumbar fusion under 7D navigation was successfully performed using 372 points to match the preoperative CT scan to intraoperative surface digitization [64]. These improving computer vision approaches may help speed up surgeries and thereby reduce infection rates and prolonged anesthesia times. Additionally, these approaches may make soft tissue procedures, such as tumor resection and disk work, possible without the need for MRI-based intraoperative navigation [46]. For this specific case of MRI navigation, current machine learning has allowed for the transformation of MRI scans to CT imaging [65, 66]. Future work can investigate the feasibility of converting from CT imaging to MRI scans which could expand the uses of robotics in MISS to further procedures.

At the center of many of these reduced radiation and fluoroscopy systems is AR. AR, the bridging of real-world environments with computer generated objects, already stands to improve not only the accuracy of MISS navigation, but also surgical outcomes. In recent work, AR was used in conjunction with ultrasound

assisted navigation in pedicle screw placement, further avoiding radiation [67]. However, AR is not limited to navigation, but also can be used for path planning by virtual roadmaps that superimpose on the surgical site for pedicle screw insertion [68]. This overlaying of virtual images in the surgeon's field of view was found to enhance the surgeon's operating experience [69]. Specifically, with Microsoft's HoloLens 3D reconstruction of CT scan for lumbar facet joint injections—projected in the surgeon's view, needle placements were successful at 97% rate and were significantly faster than CT-guided injections [70]. This same technology for lumbar pedicle screw placements simulated by Kirschner wires similarly led to faster insertion times; however, in a cadaveric study HoloLens resulted in major medial or inferior pedicle wall breaches for 3 and 4 out of 19 screws, respectively [71, 72]. For specifically the MISS domain, 3D structures obtained by O-arm imaging can be transferred and merged into the surgical microscope for live view. Such AR uses have entered transvertebral anterior cervical foraminotomy and posterior foraminotomy [73]. AR projected into the microscope has been used to display vertebrae and implants onto real-time video imaging for neoplastic and degenerative spine disease, culminating in a 70% reduction of radiation dose [74]. However, dose reduction is limited by a threshold when lowered resolution and increased image noise prevent the nonlinear registration of pre- and intraoperative imaging [74]. Such failure for registration would inhibit useful applications of AR, thereby necessitating improved ML algorithms for segmentation, registration, and projection in high-noise environments.

For robotics in MISS, the challenge is to move from an AR navigation system to the harder task of equipping robots with AR. The integration of AR with robotics opens the door to uses that extend toward automation of procedures, voice controlled surgeries, and weak supervision by the surgeon [1, 75].

#### 32.3.4.3 Collision Avoidance and Path Planning

Specifically under radiation- and fluoroscopy-free navigation, collision avoidance becomes a major consideration. As robotics gather large amounts of intraoperative data, robotic surgical decision-making support may have an expanded role. Autonomously controlled robots are starting to develop collision avoidance algorithms that take into consideration both instrumentation and surrounding tissue in deep and narrow spaces [76]. Combined with improvements in computer vision, robotic assistance may aid the surgeon in deep spaces under reduced quality of navigation images.

Further roles of robotic decision-making support come in increasing path planning involvement. This domain, which uses reinforcement learning to decide what actions to take in specific environments, requires large amounts of data. Within research projects, robots have used 3D path planning algorithms based on CT images to allow them to learn paths to lesion sites, avoiding vital organs—even without prior knowledge of the environment. This is heavily reliant on segmentation to construct a 3D model of the spine and vessels [77]. With improvements to such models as more data becomes available, the robot may earn a larger role in surgical assistance, working with the surgeon to decide optimal paths, which can reduce operative adverse effects, shorten hospital stays, and avoid revision surgeries due to postoperative complications.

#### 32.3.4.4 Outcome predictions

With the robot's ability to collect intraoperative data, it becomes possible to learn what actions lead to specific outcomes. This is already seen in the Medicrea system, which learns to suggest optimal implants for individual patients, but can expand to include, e.g., trajectories and path planning besides screw placement [25]. Collecting big data based on the software and haptic feedback features without any work required by either the patient or the surgeon (team), robots can learn how the individual treatment plan relates to desired outcomes such as infection minimization, complication avoidance (e.g., skiving, pedicle breach or fracture), and reduced recovery time. Connecting the robot to the hospital IT system, they could take information from the patient's clinical history (e.g., comorbidities such as osteoporosis, prior surgical

procedures, etc.) into account, to augment decision-making even more. Already demonstrated in practice, ML was given 35 input variables, selected from the clinical history and surgical procedure. Trained on 3034 cases, the algorithm predicted the site of postoperative surgical site infection with high positive (92%) and negative predictive values (98%) [78]. These results support the need for ML in clinical decision-making and can be expanded to study such algorithms in intraoperative contexts. Knowledge with high certainty of, e.g., infection sites, other complications or even long-term outcomes can help determine the optimal surgical strategy including trajectory planning in real-time.

## 32.4 Necessity Dictates Innovation: What the Field of MISS Needs

### 32.4.1 Reduction of Cost

While previous reports have demonstrated that robotic assistance can be cost-effective by its ability to reduce revision rate, lower infections, reduce length of stay, and sometimes even shorten operative times, the cost-effectiveness of robots in spine surgery remains an open question [1]. There is little doubt that—when correctly advertised—centers offering robotic-assisted spine surgery have indisputable advantages to attract demanding patient customers. However, current robots, costing in the range of about a million dollars, are still infeasible for many surgical centers to obtain, limiting MISS on a global scale from benefiting from robotic assistance [1]. To address this, future developments need to factor in economic efficiency. Driving factors for cost reduction include the open competitive market, improved benefits of surgical outcomes such as lowered hospital stay and decreased complication rates, and development of new polymers and material technology [79]. Advances by material science, such as replacing metals with plastics, are being developed to reduce both the weight and costs of equipment for surgical robots [80].

### 32.4.2 Increased Portability

Emerging material science to incorporate plastics into robotic design will lower weight and increase portability. This can be especially important for remote surgical uses if the future of battlefield or space applications is ever to be realized. In fact, efforts to increase surgical robotic portability extend far beyond material science and is an emerging area of development. Auris Surgical Robots, which recently acquired Hansen Medical, is developing smaller robots capable of minimally invasive surgeries. While currently outside the spine domain, this effort uses small robotic catheter systems and 3D visualization with 3D catheter controls to steer guidewires during minimally invasive endovascular procedures [81, 82]. Virtual Incision is another promising company outside the spine domain in minimally invasive surgery that seeks to increase portability of robotic surgical aid. Their robot, about the size of the hand, requires setup time of just a few minutes, and functions to filter the surgeon's unintended movements. Equipped with auto tracking capability, it is currently intended for mainly laparoscopic procedures to increase access to minimally invasive surgery. As robotics gain portability for minimally invasive surgeries, these should soon enter the spine domain.

### 32.4.3 Better Generalization

Currently, patients with low bone quality, high body mass, and severe deformities are poor candidates for robotic-assisted MISS. Furthermore, many current robotic assistance systems in MISS are not applicable for the cervical spine as it is more mobile and the anatomical structures are smaller. A data-driven approach, with the advent of the many ML tools discussed, can develop lower variance navigation and more generalizable path planning algorithms for these more complex cases. Improved generalization is crucial to expand the role that robotics can play in MISS. Robotic assistance is becoming particularly valuable in not only its improved accuracy, lower radiation, and better outcomes, but also its

suitability for pandemics in reducing the risk for both patients and physicians [83]. It is of highest importance to broaden the applicability of robots in MISS to not only more procedures, but also to more patients as these novel systems develop.

## 32.5 Conclusion

As novel advances in robotics, ML, AR/VR, material science, and medicine make their way into robotic solutions and applications for MISS, it will be the responsibility of the surgeon to incorporate these novel techniques to aid their procedures and patients. Typically, some leading academic hospitals per region closely collaborate with the industrial partners to develop, test, validate, and safely introduce the novel technology into patient care. These hospitals serve as educational hubs, where through residency or fellowship training interesting numbers of surgeons are made familiar with the robotic technology and the advantages and challenges of their application in the operative environment.

Ongoing research is needed as robotics continues to make its way into MISS [84]. First, large studies of efficacy and cost–benefit analysis will be necessary to merge the technological developments with the best interests of both the patient and the hospital [85]. Besides long-term patient outcomes, these analyses should ideally include quality outcomes such as operative time, length of stay, fluoroscopic and radiation exposure, operative time, complication-, infection-, and revision rates, indirect costs of patient disabilities, and long-term opioid needs, just to mention some of particular interest. Challenges to this analysis include the fast growing nature of this field. Continuous and rapid changes to the above indicators will pose a challenge to analyze their standing versus costs. However, such an analysis is particularly crucial in order to direct the growth of the technological sector in how best to contribute to modern-day MISS. Another important area of research is the expansion of surgical types for robotic assistance in MISS. Current approaches include agar models pushing the boundaries of robotic use. Such models are good candidates in their ability to study precision of the procedures. However, as we move toward tissue and bone procedures, agar models may no longer suffice due to the biomedical complexity of the different human systems. Cadaveric models remain promising models to study the performance of MISS robots and as technology develops, AR simulation approaches can develop for not only educational tools but also to investigate new uses for the robots in procedures. A bottleneck for the latter is to properly develop models for individual responses to surgical actions, especially those that may result in adverse effects. With such models, detailed studies of surgical complications due to robotics use can be led. These studies will be crucial to determine necessary modifications in the robotic technology and to develop standardizations of procedures involving their uses. Lastly, research to study factors that increase or decrease the likelihood of adoption of robotic assistance in MISS will be necessary [84]. With already significant benefits of robotics for pedicle screw procedures, large efforts to train both experienced and new surgeons in the field, as well as encourage the use of robotics will be worth the required academic and social effort. With improved technology and more autonomously deciding robots, adverse effects can increasingly result as consequences to robotic, and not surgeon, actions. Who will be responsible if such adverse effects happen, what regulations are necessary, which procedural subroutines require varying degrees of supervision, become pertinent questions for the field to consider.

Lumbar spinal fusion surgery has been traced back to the Greeks of the Classical era in the fifth century BC [86]. Even the modern MISS approach can trace its roots to 1967, only 64 years after the first airplane flight [87]. Yet, airplanes are highly automated with weak supervision during most parts of their flight, including both takeoff and landing [88, 89]. In fact, this automation makes use of many of the same computer vision components that are now starting to make their way into navigation of MISS [89, 90]. To automate a plane requires learning how actions differ in adverse weather conditions, descent patterns

for landing based on plane type and carrying capacity, as well as actions in emergency situations. Similarly, automation of components of spinal procedures can involve learning such actions for emergency situations, subroutines such as suturing, path planning based on patient anatomy, and pressure patterns based on surgical state. But why is one field so much more developed than the other? At the backbone of all these predictive tasks is learning from large amounts of data. For data collection in aviation, cameras and flight data recorder devices are sufficient. Yet, in the surgical domain, surgeons cannot gather the same amount of intraoperative data and there is no surgical data recorder. However, now with robotics involved in more and more procedures, the ability for surgical data recorders to capture the operative experience live, and later allow algorithms to learn from such, becomes a real possibility. Tracking surgical state by methods like FAROS, the actions of the supervising surgeon, the robotic behavior of the arms, and mapping these to patient outcomes provides learnable information for later systems to use. Requiring no attention by the surgeon, just as flying requires no data collection by the pilot, can bridge the benefits of the computer with the benefits of the 2000 years of experience humans have in spinal operations. Whether MISS will ever, or can ever, be fully automated, advances in robotics make it absolute: it has come time for MISS' data revolution.

**Conflicts of Interest to Disclose** Anand Veeravagu: NuVasive, Medtronic—consulting.

## References


1. D'Souza M, Gendreau J, Feng A, Kim LH, Ho AL, Veeravagu A. Robotic-assisted spine surgery: history, efficacy, cost, and future trends. Robot Surg Res Rev. 2019;6:9–23. https://doi.org/10.2147/rsrr.s190720.
2. Devito DP, Kaplan L, Dietl R, et al. Clinical acceptance and accuracy assessment of spinal implants guided with SpineAssist surgical robot. Spine. 2010;35(24):2109–15. https://doi.org/10.1097/brs.0b013e3181d323ab.
3. Hu X, Ohnmeiss DD, Lieberman IH. Robotic-assisted pedicle screw placement: lessons learned from the first 102 patients. Eur Spine J. 2012;22(3):661–6. https://doi.org/10.1007/s00586-012-2499-1.
4. Le X, Tian W, Shi Z, et al. Robot-assisted versus fluoroscopy-assisted cortical bone trajectory screw instrumentation in lumbar spinal surgery: a matched-cohort comparison. World Neurosurg. 2018;120 https://doi.org/10.1016/j.wneu.2018.08.157.
5. Ringel F, Stüer C, Reinke A, et al. Accuracy of robot-assisted placement of lumbar and sacral pedicle screws. Spine. 2012;37(8) https://doi.org/10.1097/brs.0b013e31824b7767.
6. Schatlo B, Molliqaj G, Cuvinciuc V, Kotowski M, Schaller K, Tessitore E. Safety and accuracy of robot-assisted versus fluoroscopy-guided pedicle screw insertion for degenerative diseases of the lumbar spine: a matched cohort comparison. J Neurosurg Spine. 2014;20(6):636–43. https://doi.org/10.3171/2014.3.spine13714.
7. Schroerlucke SR, Good CR, Wang MY. A prospective, comparative study of robotic-guidance versus freehand in minimally invasive spinal fusion surgery: first report from MIS ReFRESH. Spine J. 2016;16(10) https://doi.org/10.1016/j.spinee.2016.07.166.
8. Kim H-J, Jung W-I, Chang B-S, Lee C-K, Kang K-T, Yeom JS. A prospective, randomized, controlled trial of robot-assisted vs freehand pedicle screw fixation in spine surgery. Int J Med Robot Comput Assist Surg. 2016;13(3) https://doi.org/10.1002/rcs.1779.
9. Menger RP, Savardekar AR, Farokhi F, Sin A. A cost-effectiveness analysis of the integration of robotic spine technology in spine surgery. Neurospine. 2018;15(3):216–24. https://doi.org/10.14245/ns.1836082.041.
10. Volpe K. Robotic-assisted surgery for spinal tumors shows low complication rate. SpineUniverse. https://www.spineuniverse.com/professional/news/robotic-assisted-surgery-spinal-tumors-shows-low-complication-rate. Accessed March 3, 2021
11. NuVasive Unveils Spine's First Integrated Surgical Automation Platform. NuVasive. https://www.nuvasive.com/news/nuvasive-unveils-spines-first-integrated-surgical-automation-platform/. Published July 27, 2018. Accessed March 3, 2021.
12. NuVasive Launches Pulse™-The First Integrated Technology Platform to Enable Better Spine Surgery. NuVasive. https://www.nuvasive.com/news/nuvasive-launches-pulse-the-first-integrated-technology-platform-to-enable-better-spine-surgery/. Published July 11, 2019. Accessed March 3, 2021.
13. Wang TY, Farber SH, Perkins SS, et al. Internally randomized control trial of radiation exposure using ultra-low radiation imaging versus traditional c-arm fluoroscopy for patients undergoing single-level minimally invasive transforaminal lumbar interbody fusion. Spine. 2017;42(4):217–23. https://doi.org/10.1097/brs.0000000000001720.
14. Isaacs RE, Karikari IO, Anderson DG. Reducing radiation an order of magnitude during X-ray intensive spine procedures using a standard fluoroscope.

Spine J. 2014;14(11) https://doi.org/10.1016/j.spinee.2014.08.206.
15. Nayar G, Blizzard DJ, Wang TY, et al. Pedicle screw placement accuracy using ultra-low radiation imaging with image enhancement versus conventional fluoroscopy in minimally invasive transforaminal lumbar interbody fusion: an internally randomized controlled trial. J Neurosurg Spine. 2018;28(2):186–93. https://doi.org/10.3171/2017.5.spine17123.
16. Kirsh D. NASS 2019 roundup: NuVasive unveils Pulse robot and more: Page 2 of 8. Medical Design and Outsourcing. https://www.medicaldesignandoutsourcing.com/nass-roundup-2019/2/. Published October 4, 2019. Accessed March 3, 2021.
17. Aug 16 2017- NV. Spinal trauma correction and fixation. Justia. https://patents.justia.com/patent/10898239. Accessed March 3, 2021.
18. Apr 3 2018- NV. System and methods for determining nerve proximity, direction and pathology during surgery. Justia. https://patents.justia.com/patent/10716509. Accessed March 3, 2021.
19. Feb 14 2018- NV. Minimally invasive spinal fixation system. Justia. https://patents.justia.com/patent/10716600. Accessed March 3, 2021.
20. Jun 17 2015- NV. Systems and methods for planning, performing, and assessing spinal correction during surgery. Justia. https://patents.justia.com/patent/10709509. Accessed March 3, 2021.
21. Medtronic to Acquire Medicrea. Medtronic. https://newsroom.medtronic.com/news-releases/news-release-details/medtronic-acquire-medicrea. Accessed March 3, 2021.
22. Amelot A, Colman M, Loret J-E. Vertebral body replacement using patient-specific three–dimensional-printed polymer implants in cervical spondylotic myelopathy: an encouraging preliminary report. Spine J. 2018;18(5):892–9. https://doi.org/10.1016/j.spinee.2018.01.019.
23. IB3D-TB™. Medicrea. https://www.medicrea.com/usa/th-lumbar-range-usa/ib3d-tb/#:~:text=The%20IB3D%E2%84%A2%20TLIF%2DBanana,through%20a%20self%2Darticulating%20mechanism.&text=The%20system%27s%20full%20range%20of,with%20MIS%20technologies%20and%20techniques. Accessed March 3, 2021.
24. Fiere V, Szadkowski M, D'Astorg H. Patient-specific rods improve radiological outcomes in adult spinal deformity early results from a prospective study.
25. Floyd E, Cohn P, Ferguson J, Kalantar SB. A review of preoperative planning technologies for spinal deformity correction. Semin Spine Surg. 2020;32(2):100787. https://doi.org/10.1016/j.semss.2020.100787.
26. Patents Assigned to Mazor Robotics Ltd. - Justia Patents Search. Justia. https://patents.justia.com/assignee/mazor-robotics-ltd. Accessed March 3, 2021.
27. Globus Medical acquires Surgimap developer Nemaris. NS Medical Devices. https://www.nsmedicaldevices.com/news/globus-medical-surgimap-nemaris/#. Published September 18, 2018. Accessed March 3, 2021.
28. Langella F, Villafañe JH, Damilano M, et al. Predictive accuracy of surgimap surgical planning for sagittal imbalance. Spine. 2017;42(22) https://doi.org/10.1097/brs.0000000000002230.
29. Lafage R, Ferrero E, Henry JK, et al. Validation of a new computer-assisted tool to measure spino-pelvic parameters. Spine J. 2015;15(12):2493–502. https://doi.org/10.1016/j.spinee.2015.08.067.
30. Wang Y. Surgical treatment of ankylosing spondylitis deformity. Singapore: Springer; 2019.
31. Zimmer Biomet Completes Acquisition of A&E Medical Corporation. – Zimmer Biomet. https://investor.zimmerbiomet.com/news-and-events/news/2020/12-01-2020-120239474. Accessed March 3, 2021.
32. Fiere V, Fuentes S, Burger E, et al. Patient-specific rods show a reduction in rod breakage incidence.
33. Butner SE, Ghodoussi M. Transforming a surgical robot for human telesurgery. IEEE Trans Robot Autom. 2003;19(5):818–24. https://doi.org/10.1109/tra.2003.817214.
34. Tian W, Fan M, Zeng C, Liu Y, He D, Zhang Q. Telerobotic spinal surgery based on 5g network: the first 12 cases. Neurospine. 2020;17(1):114–20. https://doi.org/10.14245/ns.1938454.227.
35. Adler JR. Remote robotic spine surgery. Neurospine. 2020;17(1):121–2. https://doi.org/10.14245/ns.2040088.044.
36. Fan N, Yuan S, Du P, et al. Design of a robot-assisted system for transforaminal percutaneous endoscopic lumbar surgeries: study protocol. 2020. doi:https://doi.org/10.21203/rs.3.rs-43531/v1.
37. Wang H, Liu Y, Fan M, Jiang J, Tian W. Robot assisted transforaminal percutaneous endoscopic lumbar discectomy. doi:10.29007/34nd.
38. Bertelsen A, Melo J, Sánchez E, Borro D. A review of surgical robots for spinal interventions. Int J Med Robot Comput Assist Surg. 2012;9(4):407–22. https://doi.org/10.1002/rcs.1469.
39. Onogi S, Morimoto K, Sakuma I, et al. Development of the needle insertion robot for percutaneous vertebroplasty. Lect Notes Comput Sci 2005:105–113. doi:https://doi.org/10.1007/11566489_14.
40. Ho AL, Varshneya K, Medress ZA, et al. Grade II spondylolisthesis: reverse bohlman procedure with transdiscal S1-L5 and S2 Alar Iliac screws placed with robotic guidance. World Neurosurg. 2019;132 https://doi.org/10.1016/j.wneu.2019.07.229.
41. Tian W, Wang H, Y-jun L. Robot-assisted anterior odontoid screw fixation: a case report. Orthop Surg. 2016;8(3):400–4. https://doi.org/10.1111/os.12266.
42. Tian W. Robot-assisted posterior c1–2 transarticular screw fixation for atlantoaxial instability. Spine. 2016;41(19B) https://doi.org/10.1097/brs.0000000000001674.
43. Tian W, Liu Y, Liu B, et al. Guideline for posterior atlantoaxial internal fixation assisted by orthopae-

dic surgical robot. Orthop Surg. 2019;11(2):160–6. https://doi.org/10.1111/os.12454.
44. Agyei JO, Khan A, Jowdy PK, et al. Robot-assisted cortical bone trajectory insertion of pedicle screws: 2-dimensional operative video. Oper Neurosurg. 2019;18(5) https://doi.org/10.1093/ons/opz216.
45. Cui G, Wang H, Tian W. Robot-assisted translaminar lag screw fixation of spondylolysis Navigation Assisted Robotics in Spine and Trauma Surgery 2020:105–113. doi:https://doi.org/10.1007/978-981-15-1846-1_14.
46. Sayari AJ, Pardo C, Basques BA, Colman MW. Review of robotic-assisted surgery: what the future looks like through a spine oncology lens. Ann Transl Med. 2019;7(10):224. https://doi.org/10.21037/atm.2019.04.69.
47. SpineGuard collaborates with the European project FAROS (Functional Accurate RObotic Surgery) Make orthopedic surgical robots smarter and less dependent on x-rays.
48. https://cordis.europa.eu/project/id/101016985.cordis.europa. Accessed March 3, 2021.
49. Vadalà G, Accoto D, Russo F, et al. A new surgical positioning system for robotic assisted minimally invasive spine surgery and transpedicular approach to the disc. J Biol Regul Homeost Agents. 2017;31(4 suppl 1):159–65.
50. Mako SmartRobotics Overview. Stryker. https://www.stryker.com/us/en/joint-replacement/systems/Mako_SmartRobotics_Overview.html#know-more. Accessed March 3, 2021.
51. Ginoya T, Maddahi Y, Zareinia K. A historical review of medical robotic platforms. J Robot. 2021;2021:1–13. https://doi.org/10.1155/2021/6640031.
52. Stryker completes acquisition of Mobius Imaging and Cardan Robotics. Stryker. https://www.stryker.com/tn/en/about/news/2019/stryker-completes-acquisition-of-mobius-imaging-and-cardan-robot.html. Accessed March 3, 2021.
53. Bai L, Yang J, Chen X, Sun Y, Li X. Medical robotics in bone fracture reduction surgery: a review. Sensors. 2019;19(16):3593. https://doi.org/10.3390/s19163593.
54. Siri Sahib S. Khalsa. The future of robot-assisted spine surgery. AANS Neurosurgeon. https://aansneurosurgeon.org/features/the-future-of-robot-assisted-spine-surgery/. Accessed March 3, 2021.
55. Mitsuishi M, Sugita N, Fujiwara K, et al. Development of a medical CAD/CAM system for orthopedic surgery. CIRP Ann. 2007;56(1):405–10. https://doi.org/10.1016/j.cirp.2007.05.094.
56. Couldwell WT, MacDonald JD, Thomas CL, et al. Computer-aided design/computer-aided manufacturing skull base drill. Neurosurg Focus. 2017;42(5) https://doi.org/10.3171/2017.2.focus16561.
57. Homepage. XACT Robotics. https://xactrobotics.com/. Published February 3, 2021. Accessed March 3, 2021.
58. Ben-David E, Shochat M, Roth I, Nissenbaum I, Sosna J, Goldberg SN. Evaluation of a CT-guided robotic system for precise percutaneous needle insertion. J Vasc Interv Radiol. 2018;29(10):1440–6. https://doi.org/10.1016/j.jvir.2018.01.002.
59. Tirindelli M, Victorova M, Esteban J, et al. Force-ultrasound fusion: bringing spine robotic-US to the next "level". IEEE Robot Autom Lett. 2020;5(4):5661–8. https://doi.org/10.1109/lra.2020.3009069.
60. Burström G, Nachabe R, Persson O, Edström E, Elmi TA. Augmented and virtual reality instrument tracking for minimally invasive spine surgery. Spine. 2019;44(15):1097–104. https://doi.org/10.1097/brs.0000000000003006.
61. Manni F, Elmi-Terander A, Burström G, et al. Towards optical imaging for spine tracking without markers in navigated spine surgery. Sensors. 2020;20(13):3641. https://doi.org/10.3390/s20133641.
62. 7D surgical – image guided surgery. https://7dsurgical.com/. Accessed March 3, 2021.
63. 7D Surgical – Image Guided Surgery. https://7dsurgical.com/spine-navigation/. Accessed March 3, 2021.
64. The 7D surgical system minimally invasive cortical screw placement using novel machine vision image guided system. https://7dsurgical.com/wp-content/uploads/2020/01/7D-Surgical-Minimally-Invasive-Case-Study-scaled.jpg. Accessed March 3, 2021.
65. Staartjes VE, Seevinck PR, Vandertop WP, van Stralen M, Schröder ML. Magnetic resonance imaging–based synthetic computed tomography of the lumbar spine for surgical planning: a clinical proof-of-concept. Neurosurg Focus. 2021;50(1) https://doi.org/10.3171/2020.10.focus20801.
66. Jans LB, Chen M, Elewaut D, et al. MRI-based synthetic CT in the detection of structural lesions in patients with suspected sacroiliitis: comparison with MRI. Radiology. 2021;298(2):343–9. https://doi.org/10.1148/radiol.2020201537.
67. Ma L, Zhao Z, Chen F, Zhang B, Fu L, Liao H. Augmented reality surgical navigation with ultrasound-assisted registration for pedicle screw placement: a pilot study. Int J Comput Assist Radiol Surg. 2017;12(12):2205–15. https://doi.org/10.1007/s11548-017-1652-z.
68. Nguyen NQ, Priola SM, Ramjist JM, et al. Machine vision augmented reality for pedicle screw insertion during spine surgery. J Clin Neurosci. 2020;72:350–6. https://doi.org/10.1016/j.jocn.2019.12.067.
69. Yoon JW, Chen RE, Kim EJ, et al. Augmented reality for the surgeon: systematic review. Int J Med Robot Comput Assist Surg. 2018;14(4):e1914. https://doi.org/10.1002/rcs.1914.
70. Gibby JT, Swenson SA, Cvetko S, Rao R, Javan R. Head-mounted display augmented reality to guide pedicle screw placement utilizing computed tomography. Int J Comput Assist Radiol Surg. 2018;14(3):525–35. https://doi.org/10.1007/s11548-018-1814-7.
71. Liu H, Wu J, Tang Y, et al. Percutaneous placement of lumbar pedicle screws via intraoperative CT image–based augmented reality–guided technology. J Neurosurg Spine. 2020;32(4):542–7. https://doi.org/10.3171/2019.10.spine19969.

72. Urakov TM, Wang MY, Levi AD. Workflow caveats in augmented reality–assisted pedicle instrumentation: cadaver lab. World Neurosurg. 2019;126 https://doi.org/10.1016/j.wneu.2019.03.118.
73. Umebayashi D, Yamamoto Y, Nakajima Y, Fukaya N, Hara M. Augmented reality visualization–guided microscopic spine surgery: transvertebral anterior cervical foraminotomy and posterior foraminotomy. J Am Acad Orthop Surg Glob Res Rev. 2018;2(4) https://doi.org/10.5435/jaaosglobal-d-17-00008.
74. Carl B, Bopp M, Saß B, Nimsky C. Microscope-based augmented reality in degenerative spine surgery: initial experience. World Neurosurg. 2019;128 https://doi.org/10.1016/j.wneu.2019.04.192.
75. Madhavan K, Kolcun JP, Chieng LO, Wang MY. Augmented-reality integrated robotics in neurosurgery: are we there yet? Neurosurg Focus. 2017;42(5) https://doi.org/10.3171/2017.2.focus177.
76. Ueda H, Suzuki R, Nakazawa A, et al. Toward autonomous collision avoidance for robotic neurosurgery in deep and narrow spaces in the brain. Proc CIRP. 2017;65:110–4. https://doi.org/10.1016/j.procir.2017.04.027.
77. Zhang Q, Li M, Qi X, Hu Y, Sun Y, Yu G. 3D path planning for anterior spinal surgery based on CT images and reinforcement learning*. 2018 IEEE international conference on cyborg and bionic systems (CBS). 2018. doi:https://doi.org/10.1109/cbs.2018.8612190.
78. Hopkins BS, Mazmudar A, Driscoll C, et al. Using artificial intelligence (AI) to predict postoperative surgical site infection: a retrospective cohort of 4046 posterior spinal fusions. Clin Neurol Neurosurg. 2020;192:105718. https://doi.org/10.1016/j.clineuro.2020.105718.
79. Koukourikis P, Rha KH. Robotic surgical systems in urology: what is currently available? Investig Clin Urol. 2021;62(1):14. https://doi.org/10.4111/icu.20200387.
80. Bertasa AM. A look at specialty polymers for surgical robots. mddionline.com. https://www.mddionline.com/materials/look-specialty-polymers-surgical-robots. Published February 19, 2020. Accessed March 3, 2021.
81. Hu X, Chen A, Luo Y, Zhang C, Zhang E. Steerable catheters for minimally invasive surgery: a review and future directions. Comput Assist Surg. 2018;23(1):21–41. https://doi.org/10.1080/24699322.2018.1526972.
82. Yu A. Vascular remote catheter manipulator. January 2020.
83. Zemmar A, Lozano AM, Nelson BJ. The rise of robots in surgical environments during COVID-19. Nat Mach Intell. 2020;2(10):566–72. https://doi.org/10.1038/s42256-020-00238-2.
84. Stumpo V, Staartjes VE, Klukowska AM, et al. Global adoption of robotic technology into neurosurgical practice and research. Neurosurg Rev. 2020; https://doi.org/10.1007/s10143-020-01445-6.
85. Staartjes VE, Molliqaj G, van Kampen PM, et al. The European Robotic Spinal Instrumentation (EUROSPIN) study: protocol for a multicentre prospective observational study of pedicle screw revision surgery after robot-guided, navigated and freehand thoracolumbar spinal fusion. BMJ Open. 2019;9(9) https://doi.org/10.1136/bmjopen-2019-030389.
86. Tarpada SP, Morris MT, Burton DA. Spinal fusion surgery: a historical perspective. J Orthop. 2017;14(1):134–6. https://doi.org/10.1016/j.jor.2016.10.029.
87. Oppenheimer JH, DeCastro I, McDonnell DE. Minimally invasive spine technology and minimally invasive spine surgery: a historical review. Neurosurg Focus. 2009;27(3) https://doi.org/10.3171/2009.7.focus09121.
88. Zollitsch AW, Mumm NC, Wulf S, et al. Automatic takeoff of a general aviation research aircraft. 2017 11th Asian control conference (ASCC). 2017. doi:https://doi.org/10.1109/ascc.2017.8287427.
89. Krammer C, Mishra C, Holzapfel F. Testing and evaluation of a vision-augmented navigation system for automatic landings of general aviation aircraft. AIAA Scitech 2020 Forum 2020. doi:https://doi.org/10.2514/6.2020-1083.
90. Kanellakis C, Nikolakopoulos G. Survey on computer vision for UAVs: current developments and trends. J Intell Robot Syst. 2017;87(1):141–68. https://doi.org/10.1007/s10846-017-0483-z.

# Part IV

# Augmented and Virtual Reality in Spine Surgery

# Current Status of Augmented Reality in the Spine

33

Gustav Burström, Oscar Persson, Erik Edström, and Adrian Elmi-Terander

## 33.1 Introduction

While a surgical procedure is dependent on the performance of the individual surgeon, it is not entirely performed in the OR. The process begins when first evaluating a patient and is supplemented by input from imaging investigations such as CT and MRI. By creating a synthesis of the information gathered preoperatively, the experienced surgeon can make correct choices about on whom to operate and how. For the best surgical outcome, this synthesis of information should carry over into the OR. In the OR the surgeon leads the team and must communicate effectively with all other team members. Everyone's focus needs to be on the patient and the correct execution of all the tasks needed for a safe surgery. Despite these preparations, surgery involves the manipulation of complex and dynamic 3D structures, and human errors do occur. Having access to relevant imaging data in the OR is a common way to reduce stress and minimize the risk of surgeon-based error. Radiological imaging data can be provided on printouts, old-fashioned X-ray display cabinets, and monitors or through customized 3D-printed models accessible in the OR. Surgical navigation systems present radiological images and allow the surgeon to view and manipulate imaging data, as well as plan and simulate the surgery (Fig. 33.1). They are also ideally suited to improve surgical precision through the alignment of 3D radiological information, obtained preoperatively or intraoperatively, with the patient in the OR. Once the match between imaging data and the patient has been made, accurate navigation is often maintained indirectly via a reference with a fixed spatial relation to the patient (Fig. 33.2). Radiological imaging data is typically displayed in standardized views such as axial, sagittal, and coronal. In addition, a perspective in line with the instrument, a probe's view, can be used to simulate the path ahead of the instrument. However, while these presentations reflect familiar radiological representations of medical imaging or the angle and position of the tracked instrument, none of them truly matches the perspective of the surgeon.

Augmented-reality solutions differ from other navigation setups in that they can present visual information in this perspective. AR solutions were initially developed for non-medical use via computers and mobile devices (Fig. 33.3). However, the possibility to superimpose virtual data on the surgeon's view of the surgical field

G. Burström · O. Persson · E. Edström
A. Elmi-Terander (✉)
Department of Clinical Neuroscience, Karolinska Institutet, Stockholm, Sweden

Department of Neurosurgery, Karolinska University Hospital, Stockholm, Sweden
e-mail: gustav.burstrom@ki.se; oscar.persson.1@ki.se; erik.edstrom.1@ki.se; adrian.elmi.terander@ki.se



J.-S. Kim et al. (eds.), *Technical Advances in Minimally Invasive Spine Surgery*,
https://doi.org/10.1007/978-981-19-0175-1_33

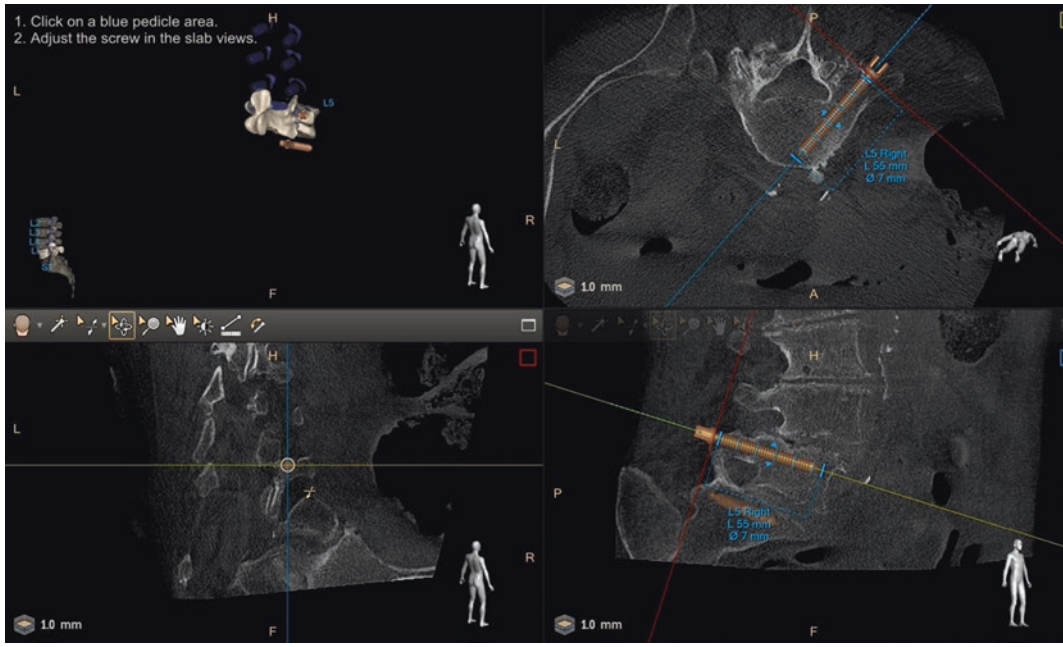


**Fig. 33.1** Pedicle screw planning on intraoperative images using augmented-reality surgical navigation/ClarifEye (Philips). Image courtesy of authors

**Fig. 33.2** Dynamic reference frame (DRF) attached to a vertebral model. The four spheres are identified by infrared cameras for positioning. Image courtesy of Brainlab

**Fig. 33.3** Augmented-reality game "Pokemon Go," one of the first widely used AR games, for mobile phone. Photo by David Grandmougin on Unsplash.com

offers a new dimension to surgical navigation, and technological advancements have ushered AR into the OR (Fig. 33.4). Using AR, the surgeon can concentrate on the surgical procedure aided by comprehensive radiological imaging data integrated with the real-world view and presented on a monitor, in a head-mounted device (HMD), in the microscope view, or projected onto the patient.

## 33.2 Historical Background

Adding lateral radiographs to the surgeon's use of intraoperative anatomical landmarks was the initial step toward navigation and increased surgical accuracy in spine surgery [1–3] Fig. 33.5). The first technical aid in spine navigation was 2D fluoroscopy [5]. Since then, image-guided and minimally invasive technologies have success-

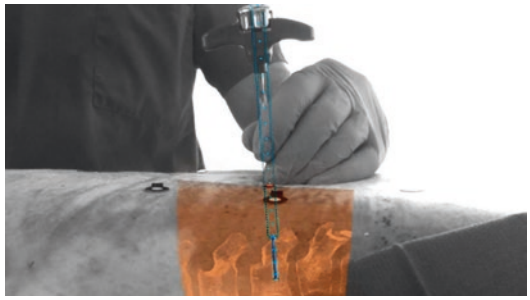

**Fig. 33.4** Example of augmented-reality imagery being superimposed on a patient during surgery. Image courtesy of Philips Healthcare

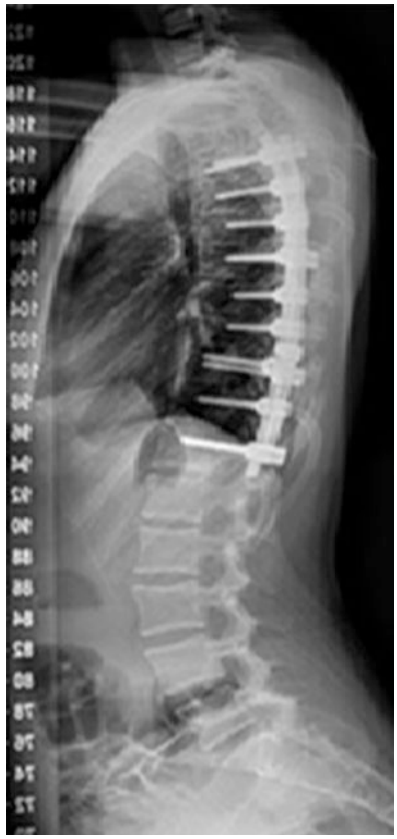

**Fig. 33.5** Lateral radiograph used for instrumentation in scoliosis surgery. Image originally published by Suk et al. [4]. Republished with permission by Springer Nature

fully been applied to spinal surgery [6]. During the past 30 years, there has been a rapid evolution of technical solutions for navigation in general. Fluoroscopy has been replaced with 3D imaging techniques, and intraoperative imaging has replaced preoperative imaging in many situations ([6]; Fig. 33.6). Despite the known advantages of navigated surgery, the development of solutions for spinal surgery has progressed somewhat more slowly than for corresponding cranial applications. One possible reason is the relatively complicated and time-consuming setup of spinal navigation devices [8, 9]. Although the bulk of development has involved cranial navigation, spinal navigation is rapidly catching up. This adaptation has been accelerated by the introduction of minimally invasive spine surgery (MISS) techniques. Since the small incisions used in MISS preclude the use of anatomical landmarks, surgical navigation solutions have become a prerequisite for the implementation and development of MISS ([8]; Fig. 33.7). AR is the latest addition to the navigation arsenal and provides visualization of internal radiological imaging superimposed on the surgical view ([11]; Fig. 33.8). Like the microscope revolutionized neurosurgical microsurgery, AR has the potential to change spine navigation. One great advantage involves a positive effect on the learning curve of the spine surgeon. Using AR navigation and robotics, complex surgical procedures can be performed accurately by less experienced surgeons, freeing the experienced surgeons to supervise and devote attention to improving and developing surgical techniques and approaches to expand the boundaries of spine surgery.

In the early 2000s, researchers at the Institute for Process Control and Robotics at the University of Karlsruhe, Germany published a series of articles regarding augmented reality for intraoperative visualization of surgical planning data using video projectors ([12–17]; Figs. 33.9 and 33.10). The setup involved an off-the-shelf video camera and a 3D surface scanner, which used light pulses to scan and create a representation of the surface of the patient. Preoperatively segmented regions of interest could be projected directly back onto the patient. This system allowed dynamic tracking of the patient without the need for rigid frames. It also offered high accuracy by reaching a resolution of 0.33 mm for an area of interest of 200 × 250 mm, thereby providing an

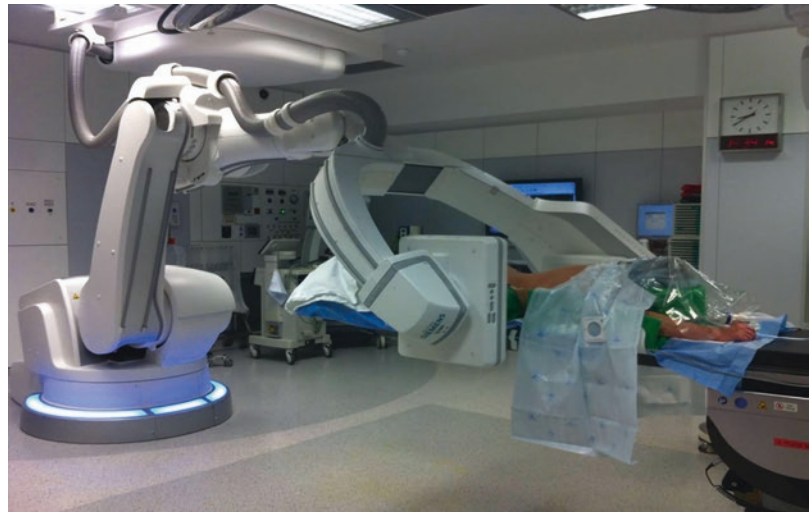

**Fig. 33.6** The Artis zeego imaging system (Siemens) during simulated intraoperative use. Image originally published by Cordemans et al. [7]. Republished with permission by Springer Nature

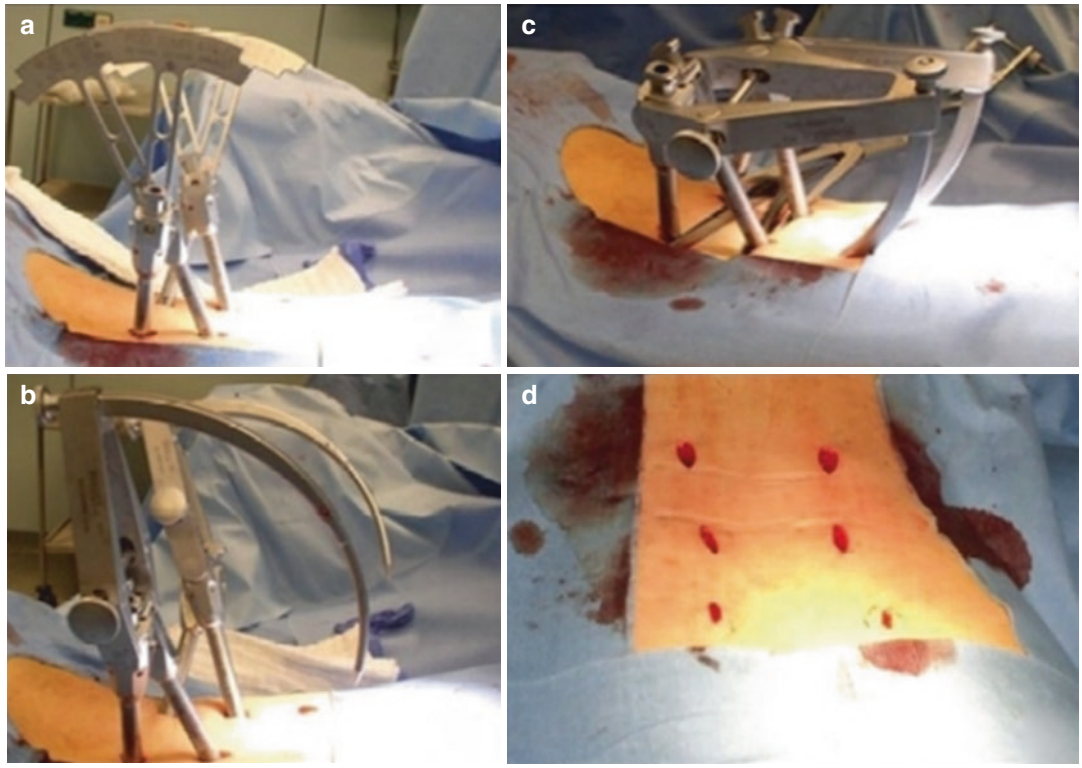


**Fig. 33.7** Minimally invasive spine fixation during acute thoracic and lumbar spine trauma. Intraoperative photographs show simultaneous insertion of two Sextant Fixators. Use of rod templates to determine the length of the rod (**a**) inserted via stab incisions. Conventional rod distractors are used for added distraction force to the posterior wall fragment (**b**) and Rods are attached to the Sextant Introducer (**c**). Final approach-related injury is minimal as demonstrated by these < 2 cm long stab incisions for a bisegmental internal fixator (**d**). Image originally published by Schmidt et al. [10]. Republished with permission by Springer Nature

accuracy of 1.5 mm. This system did not require a head-mounted device or monitor and was quite user friendly [13]. The system has been used for radiotherapy and in craniofacial surgery but no clinical implementation in the spine has ever been published [18].

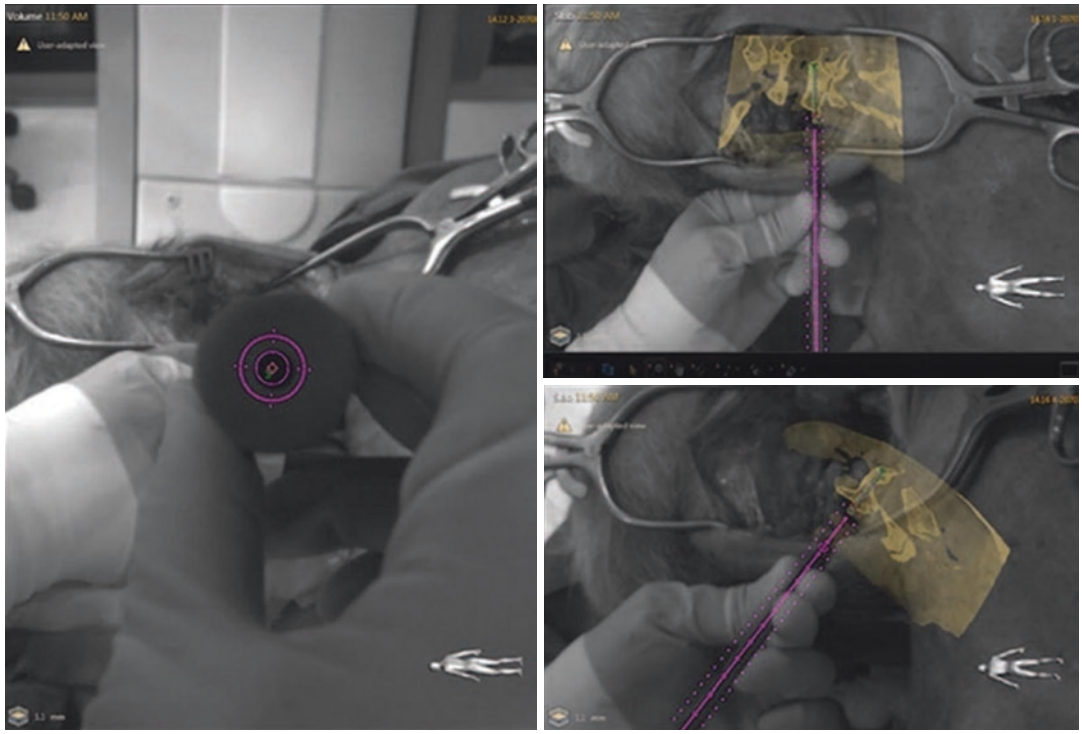

**Fig. 33.8** Intraoperative visualization of internal radiological imaging superimposed on the surgical view. Image courtesy of Philips Healthcare

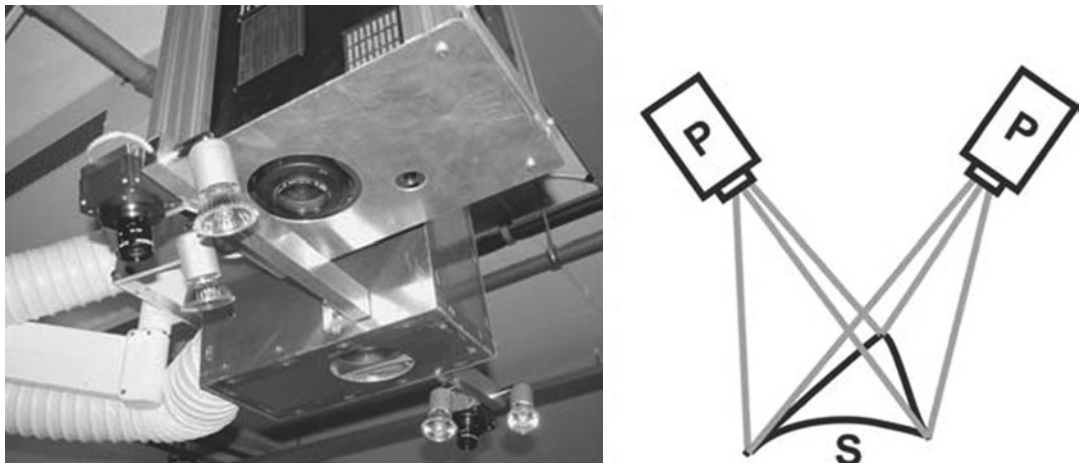


**Fig. 33.9** Video projector setup for enabling augmented-reality imagery superimposed on the patient. To the left, the camera setup is shown. To the right, the projection-based localization concept for a bone segment is shown. Image originally published by Kahrs et al. [16]. Republished with permission by IOS Press

The first use of AR navigation in an orthopedic setup was reported in 2012 by Liang et al. who used a Fluoro-laser navigation system to support pedicle screw insertions in phantoms of the femoral bone, achieving an accuracy of 2.40 ± 1.23 mm ([19]; Fig. 33.11). In 2016, the first study was published using a novel AR surgical navigation technology that was specifically

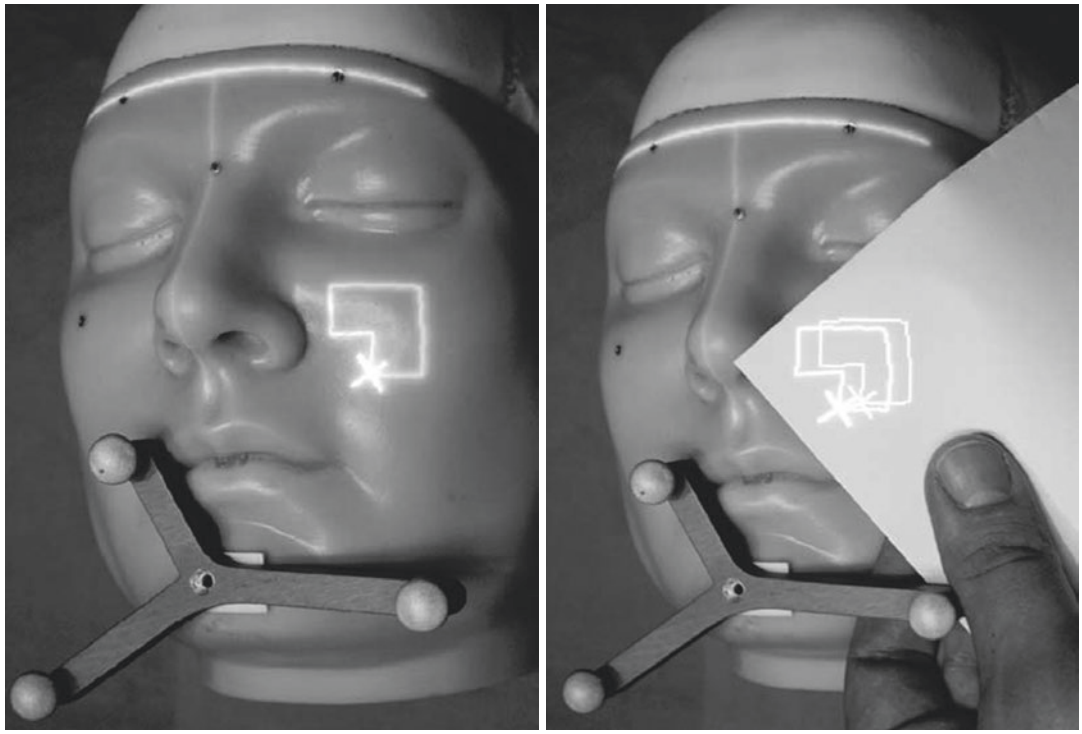

**Fig. 33.10** Projector-based AR superimposed on a doll's head. Image originally published by Kahrs et al. [16]. Republished with permission by IOS Press

designed for spine surgery, comparing its effectiveness to the conventional free-hand technique [11]. The system used four video cameras for patient tracking and image augmentation. The navigational images, a 3D reconstructed and segmented view, and AR visualization of the surgical field were presented on a medical monitor (Fig. 33.12). Since then, technology has evolved rapidly, and several different AR solutions have been designed and adopted for preclinical and clinical use. In this chapter, a summary of the state-of-the-art AR navigation solutions for spine surgery will be presented.

## 33.3 Terminology

- Virtual reality

  Virtual reality is the term used to indicate an interactive 3D representation that is separate from the real world. Most surgical navigation systems present preoperative imaging data on a screen. To represent a virtual reality navigation setup, there must be a co-registration (i.e., a match) of the patient's real-world position in space to the imaging information. This allows real-world navigation with a virtual representation in the corresponding 3D-imaging data. Generally, the interaction is managed with a pointer tool that is seen by the system and uses the co-registration information to move in both the real and the virtual world. The output is presented on a separate screen; it helps guide the surgeon and allows repeated confirmation of the location of the tooltip relative to the imaging data. However, it necessitates the shift of attention back and forth between the surgical field and the virtual representation.

  Virtual reality also describes interactive 3D representations used in surgical teaching tools. An immersive teaching experience can be

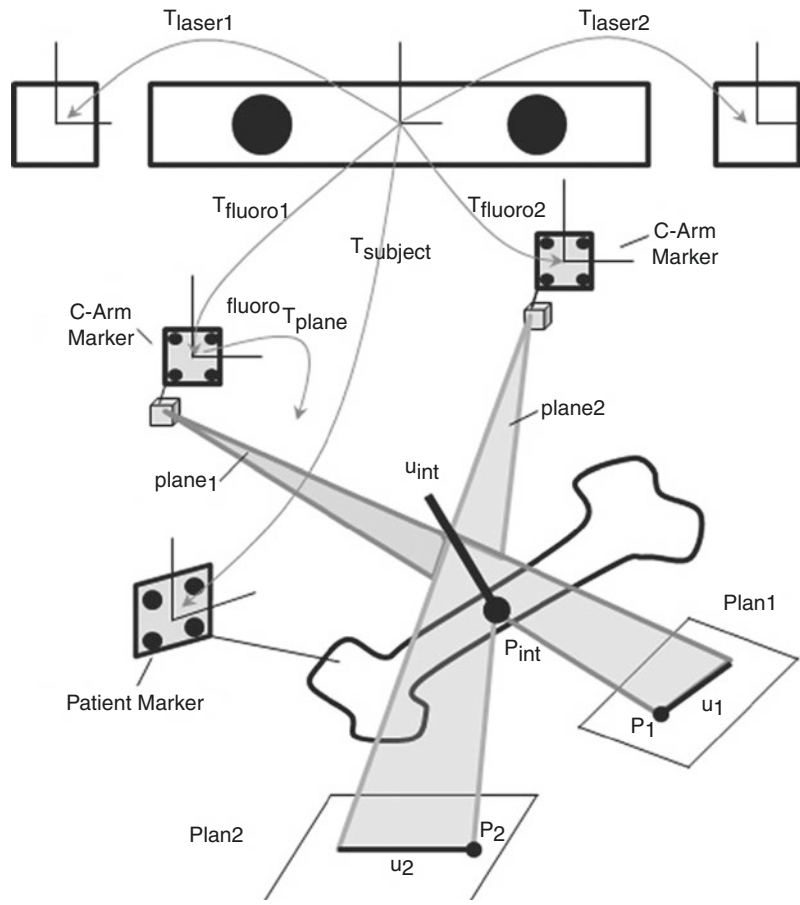


**Fig. 33.11** The design of a fluoro-laser navigation system to aid in pedicle screw insertions in phantoms. Image originally published by Liang et al. [19]. Republished with permission by Springer Nature

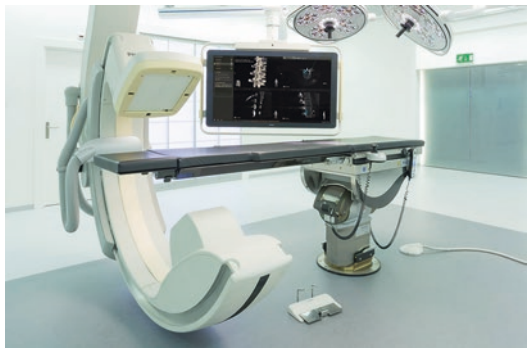

**Fig. 33.12** OR setup of the augmented-reality surgical navigation system (ClarifEye) with 4 patient-tracking cameras integrated into the C-arm. The AR view is presented on the monitor. Photo courtesy of Philips Healthcare

achieved when the virtual reality representation is provided through a head-up display where the content reflects the user's movements.

- Augmented reality

  Augmented reality is the combination of virtual representations with real-world objects, typically adding objects to the viewed environment. To accomplish this objective, the environment and the added objects are superimposed. This necessitates the use of video cameras and the technology and computational power to integrate virtual objects and their relative movement in a real-world representation in real-time. The output is presented on screens, which can be handheld, mounted, or integrated into special glasses or microscope eye pieces. The real-time integration of relevant information reduces the need to shift attention between the surgical field and screens.
- Mixed reality

  The combination of virtual and augmented-reality techniques is referred to as mixed real-

ity. In a surgical context, AR can be used to project navigational guides onto the patient when surgery is performed within the line of sight, while VR is more useful inside the body where the surgical targets are hidden from vision and instead represented by 3D imaging information [20]. Mixed reality makes use of the advantages of both techniques; however, the term sometimes refers to two distinct solutions in the literature. One common use of the term mixed reality is where the navigation interface is presented both as a pure AR interface on part of the screen and as a pure VR experience on another part of the screen. The other definition concerns a traditional AR interface in which the system also adapts the virtual world to changes in the real world. For example, a mixed-reality system may remove parts of the virtual representation of a tumor while the surgeon operates on it, reflecting the progress of the surgery in real-time.

## 33.4 Why Do We Need AR Navigation in Spine Surgery?

Traditionally, spine surgery has been performed as "open surgery." The posterior aspect of the spine is exposed by using a large incision and detaching the musculature to render visual access to the spinal surface anatomy and corresponding landmarks. In recent years, technological advances have allowed minimally invasive treatment of several spine conditions. The concept of minimally invasive spine surgery (MISS) includes minimal incisions to avoid damage to muscles and surrounding tissues, thereby reducing blood loss, postoperative pain, and surgical site infections and resulting in faster recovery after surgery [21–24]. Indications for MISS are rapidly increasing and may amount to more than half of all spinal procedures by 2020 [25]. However, when performing MISS, the surgeon cannot navigate by landmarks, making image guidance crucial for this kind of surgery. Few studies evaluate advanced imaging techniques and surgical navigation in MISS. They show the technology and techniques are feasible but general adoption is still lacking [26, 27]. AR solutions that seek to promote a simplified workflow and ease of use may contribute to the increased use of MISS [28].

Spinal fixation surgery is synonymous with pedicle screw placement, and most complications in spinal fixation surgery result from erroneously placed pedicle screws. In the United States, 1.62 million instrumented spinal procedures are performed each year, and even a small reduction in the complication rate would have a tremendous impact (iData Research, www.idataresearch.com). A meta-analysis by Gelalis et al. in 2012 reported that 1–6.5% of pedicle screws placed using a free-hand technique had a cortical violation greater than 4 mm [29]. When relying only on fluoroscopy in MISS, which is the current gold standard, the pedicle perforation rate is in the range of 12.5–13.5% [30–32]. Accuracy rates for pedicle screw placement vary from 60–97% for lumbar and 27–96% for thoracic spine surgery [33]. There are reports of intraoperative revision rates of 7.5% with the MISS screws resulting in prolonged OR time, 7–12% of cases resulting in neurological injuries due to mispositioned screws, and reoperation for screw revision in 1.5–8.8% of surgeries, reflecting the need for an avoidable extra surgery [34]. Consequently, based on the inherent lack of anatomical clues available to the surgeon, it can be argued that image guidance has a natural role in MISS [35]. However, image guidance implies radiation.

With the introduction of new image-based technologies, it is important to consider their propensity to increase radiation exposure. Patient exposure is normally limited to a single or a few lifetime occurrences but should nonetheless follow the ALARA ("as low as reasonably achievable") principle. Staff exposure, however, is long-term and associated with a risk of radiation-induced cancer [36] and cataracts [37]. The occupational exposure of spine surgeons is a concern, as it is second only to that of trauma/limb deformity surgeons [38].

The continuous development of navigation has significantly improved the accuracy of MISS procedures while eliminating the need for periprocedural radiation [32, 39]. In a review by

Fichtner et al., navigation reportedly reduced the rate of secondary revision surgery to 1.35% compared to 4.38% with a free-hand approach [40]. Notably, despite inter-rater agreement on which screws are misplaced, opinions vary among spine surgeons on which screws should be revised. Surgeons tend to recommend revision less frequently after rod placement or postoperatively [41]. Hence, early intraoperative identification of mispositioned screws using intraoperative imaging has significant clinical value [42]. The first clinical study using AR for pedicle screw placement reported 1% intraoperative and zero later revisions [43]. Thus, AR-navigated surgery has the potential to increase the adoption of navigation in open and minimally invasive spine surgeries through simplified and intuitive workflows, improved accuracy, and minimized staff radiation exposure [28, 44–46].

## 33.5 How to Design a Surgical Navigation System: The Necessary Components

1. **Acquisition of 3D imaging data**

   All spine navigation is image-based. Before starting any navigation, high-resolution 3D-imaging of the spine—and preferably the surrounding neurovascular structures—is necessary.

   Preoperative CT and MRI spine images are the most frequently used modalities for navigation. CT is the gold standard, offering excellent visualization of bony structures, while MRI has the advantage of visualizing soft tissues, including the critical neurovascular structures. Most currently available navigation systems for spine surgery utilize preoperative imaging in some fashion. Planning and subsequent navigation can be performed entirely on preoperative images that are later co-registered to the patient. Alternatively, the preoperative imaging can be fused with intraoperative imaging for co-registration and navigation. Preoperative images, irrespective of modality, are obtained with the patient in the supine position. However, most surgeries are performed in the prone position. Thus, normal spinal mobility may introduce errors and inaccuracies in navigated procedures based on preoperative imaging. Without technology to track each vertebra, the normal movements of the spine need to be compensated for to allow accurate image fusion [47]. A solution based on non-linear matching has been proposed with excellent results [48].

   An alternative to navigation based on preoperative imaging is provided by the integration of intraoperative imaging capability. Most current intraoperative imaging modalities are radiation-based. Intraoperative 3D-fluoroscopy, cone beam CT (CBCT), or CT can be used as a single source for navigation or be combined with preoperative imaging (Fig. 33.6). Intraoperative 2D fluoroscopy, using images taken in orthogonal projections, can be aligned with preoperative imaging for navigation [49]. Thus, intraoperative imaging simplifies patient registration and provides data that is unbiased regarding the patient's position.

   Although there are several commercially available intraoperative MR solutions, no reports on the use of intraoperative MR for spinal navigation have been published. This may be due to the time-consuming and complex process of intraoperative MR imaging, including the need for MR-compatible instruments and substantial training of the OR staff. Currently, the easiest way to incorporate MR image information for navigation, without the cumbersome intraoperative procedure, involves the fusion of preoperative MR images with intraoperatively obtained CT or CBCT images. This solution, which has long been available for cranial navigation, may be the best way to combine information on bony anatomy with soft tissue. The resulting datasets can help augment bony structures, vessels, and nerves onto the surgical field to achieve the best possible AR navigation aid.

   Ultrasound has recently emerged as a new and interesting modality to obtain intraoperative imaging of the spine. Although

still in an experimental phase regarding spine navigation, the technology may offer fast, easy, and radiation-free intraoperative imaging and applications in AR-image generation [50].

Unlike cranial navigation, in which the skull can be fixed in a surgical clamp, rigid fixation of the spine for navigated surgery is not feasible. Even with great efforts to minimize motion, intrinsic spine movements and surgical manipulation during pedicle screw insertion and deformity correction may cause movements that render the navigation inaccurate. This problem may be addressed by using intraoperative imaging, but it comes at the cost of additional radiation. A prerequisite for this solution to be useful involves the ability of the navigation system to update an existing plan with new images to avoid a time-consuming re-planning of the surgery. All intraoperative image updating requires software solutions for image fusion and a capacity to handle large datasets in real-time. Although updated and accurate imaging is quintessential for navigation, ionizing image modalities subject both the patient and the OR staff to radiation [46]. Hence, efforts must be made to provide other solutions for image updating. Ultrasound could be an ideal modality for fast and radiation-free image updates [51, 52].

2. **Patient tracking and co-registration**

In the next step, the 3D imaging data must be co-registered to the patient's position in the OR and reliably tracked by the navigation system to compensate for movements. While different patient-tracking solutions have been proposed, the principal technology is essentially unchanged. It allows the surgeon to track a surgical instrument in three dimensions and in relation to the patient's anatomy, based on co-registration of preoperative CT or MRI images with a dynamic reference frame [53, 54]. The dynamic reference frames are mostly comprised of a star-shaped metal frame, attached to an index vertebra, and equipped with multiple optical spheres that are recognized by an infra-red (IR) camera (Fig. 33.2). This simplifies the computational task of the navigation system, as it does not need to see and track the patient itself. Similarly, reflective spheres on instruments or a pointer can help identify their position in space and their relation to the corresponding imaging data. This information is presented to the user on monitors. This method is applied in several AR systems [48, 55–59].

In classic stereotactic navigation using fixed frames—such as the Leksell stereotactic frame for cranial biopsy and gamma knife treatment [60]—imaging is performed with the frame firmly attached to the patient, and the coordinates of the frame are included in the subsequent imaging. In this way, a highly accurate patient registration is achieved, which is reflected in the submillimeter accuracy obtained with these systems. Although these systems are regularly used for various cranial applications, there are few corresponding spinal solutions because the spine is mobile. Without the use of continuous imaging or individually fixing or tracking every vertebra, some degree of inaccuracy must be accepted.

(a) Spinal reference frames

Spinal reference frames are mostly attached to a spinous process within the surgical field; consequently, they may interfere with the procedure. In addition, to ensure optimal accuracy the reference frame should be repositioned for each new level. This strategy will significantly prolong the OR time [61]. To simplify the workflow, the choice can be made not to reposition the dynamic reference frame. However, at worst the screw misplacement rate may double with every vertebral level away from the index vertebra [61, 62]. A system presented by Thomale et al. aimed to reduce spine movements during surgery to decrease the impact of distance to the reference marker. They introduced a spine-fixation clamp attached to the surgical table to enhance the rigidity of the spine [63, 64]. It took 6 min to install and could reach four lumbar levels. Nevertheless, the navigation accuracy still decreased from 0.35 mm at the index vertebra (L3) to 2.5 mm two vertebral levels away (L5), and mono-segmental registration for navigated procedures was still deemed necessary (Fig. 33.13).

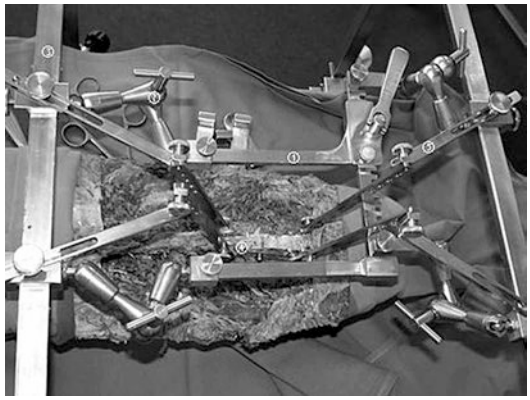

**Fig. 33.13** Depiction of the spine frame, a spine-fixation system designed for increasing the rigidity of the spine and boosting navigation accuracy. Image originally published by Thomale et al. [63]. Republished with permission by Taylor & Francis Ltd (www.tandfonline.com)

(b) Vertebral identification

An alternative method, employed in several AR systems using head-mounted devices, consists of surface tracking combined with manual adjustments,: the camera system identifies the patient's surface anatomy or exposed spinal anatomy [65–70]. In current systems, hand gestures are first used to align the AR image manually with the surgical view of the vertebrae. The system then relies on surface tracking to keep the image in the correct position even if the head and HMD are moving. Soon, these solutions could move toward automatically identifying surface anatomy and correlating it to the preoperative or intraoperative imaging so that the AR image can be automatically aligned. This would minimize the impact on workflow from setting up the system. However, in order to confirm the automatic identification has been correctly performed, systems would likely need to employ verification steps before the start of surgery.

(c) Virtual reference grids: optical markers

Efforts have been made to design patient-tracking methods based on unobtrusive markers or no markers at all. One such system uses an optical tracking system (OTS), consisting of four small high-resolution video cameras embedded in the flat-panel X-ray detector of a motorized C-arm [11]. Flat adhesive skin markers (ASM), which are randomly placed around the surgical field, are tracked by the video cameras [11, 28, 43–46, 71–74]. The OTS uses triangulation and creates a 3D point pattern based on the individual markers' relative positions to each other, which is called the virtual reference grid (VRG; [75, 76]). The relation between the OTS and the intraoperative CBCT coordinates is known based on initial manufacturing calibrations. Therefore, CBCT coordinates can be converted to OTS coordinates and vice versa. The VRG is designed to have redundancy and accepts the occlusion or removal of several ASMs, as long as at least five are still in position. This feature allows maintained navigation accuracy despite manipulation during surgery.

A similar non-invasive optical marker (SpineMask, Stryker, Kalamazoo, Michigan, USA) has been described by Malham et al. ([77, 78]; Fig. 33.14). The system enables the high-accuracy placement of minimally invasive lumbar pedicle screws. It is a rectangular skin-adhesive stereotactic tracking device, covering four to five spinal levels. The system consists of 31 battery-powered LED lights in the frame border. For accurate registration and tracking, 28 of 31 LED lights

**Fig. 33.14** The SpineMask, an example of a non-invasive optical marker system for tracking a patient during navigated spine surgery. Image courtesy of Stryker

need to be visible to the scanner. However, this rigid grid does not tolerate deformation in the surgical field; for incisions larger than stab wounds, it is suggested that tracking should be performed using a bone-anchored tracker.

3. **Instrument tracking**

Enabling the tracking of surgical instruments used during the operation provides the surgeon with visual feedback of the relationship between the instrument and the anatomical structures. A key step in placing a pedicle screw minimally invasively involves the location of the correct bone entry point [79]. Using instrument tracking allows a virtual visualization of the instrument position with respect to the deep bony anatomy, simplifying the localization of the bone entry point and adherence to the planned path [80].

(a) Alignment, depth, width

Tracking an instrument requires its recognition by the navigation system. Currently, this is achieved using different types of optical markers attached to rigid instruments and recognized by the same camera system (IR or conventional) used for patient tracking (Fig. 33.15). Initial registration in relation to the dynamic or virtual reference grid is needed to establish the relationship between the tracked instrument and the surgical field.

**Fig. 33.15** Surgical instruments with integrated markers (3–4 spheres per instrument) for continuous instrument tracking during surgery. Image courtesy of Brainlab

A tracked instrument can be aligned with a pre-planned path, and the position of the tip of the instrument in relation to the path can be visualized on a monitor, offering the possibility to adjust the depth of the instrument in relation to the patient's anatomy [73].

(b) Instrument identification

Instruments can either be registered one by one at the time of use or automatically recognized by the system. Industrial development has moved toward custom-made instruments for each navigation system to minimize the time required for registration and increase accuracy by removing a registration step with inbound errors.

(c) Recognizing instrument deformation

Although many improvements to instrument-tracking features have been made, a limitation remains: only rigid instruments can be accurately tracked. Unfortunately, most systems cannot visualize and warn about instrument deformation due to the use of force or adaptation of the instrument to the anatomical conditions. Thus, a huge advantage of AR instrument tracking is that any malalignment between the real and virtual image of the instrument will be visible in the AR interface.

4. **Interfaces for AR Navigation**

To display an AR view to the surgeon, an appropriate interface is required. Four main types of AR user interfaces have been described in published studies. The most common ones are monitor-based (Monitor-AR) and head-mounted displays (HMD-AR). Monitor-AR solutions typically capture the real-world view using video cameras directed toward the surgical field [43] and display the video feed with an AR overlay of the corresponding radiological imaging (Fig. 33.1). This solution provides everyone in the OR with the same navigational information, simplifying multiple-surgeon procedures and teaching sessions. However, the real-world perspective provided by the cameras will differ from that of the surgeon. HMD-AR

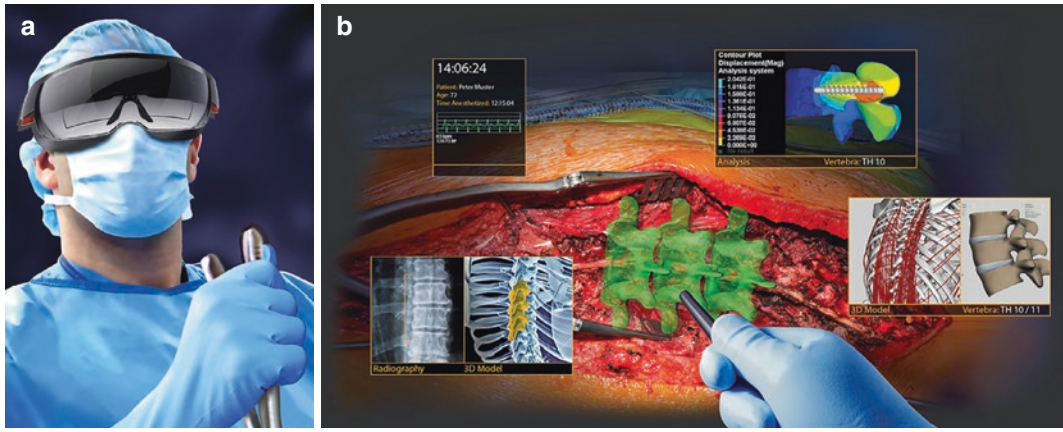


**Fig. 33.16** Example of an AR-enabled HMD to the left (**a**) with the surgeon's view on the right (**b**). Image originally published by Muller et al. [59]. Republished with permission by Elsevier


**Fig. 33.17** Multiple examples of HMD-devices used for augmented-reality applications: (**a, b**)—Google Glass; (**c**)—Optinvent; (**d, e**)—Vufine; (**f**)—Microsoft Hololens; (**g**)—Oculus Rift; (**h**)—Vuzix M300; (**i**)—Vuzix iWear. Images in A (Google Glass), F (Microsoft Hololens), and G (Oculus Rift) are from http://flickr.com, and no changes were made to these originals. License: https://creativecommons.org/ licenses/by/2.0. Image originally published by Yoon et al. [81]. Republished with permission by Wiley

devices resemble goggles and are worn on the surgeon's head [58, 66], and the AR representation is overlaid in the surgeon's field of view (Figs. 33.16 and 33.17). The HMD option uses surface recognition and needs manual adjustment to overlay the AR images accurately. The HMD solution is ideal for 3D presentations of imaging data since the software can provide information to the left and right eye separately. Conversely, because the view in the HMD is unique to the wearer, other OR staff are excluded from that information. The use of multiple HMDs in the OR may ameliorate this situation but will also create an additional computational load on the navigational system. Microscope-based AR-interfaces (microscope-

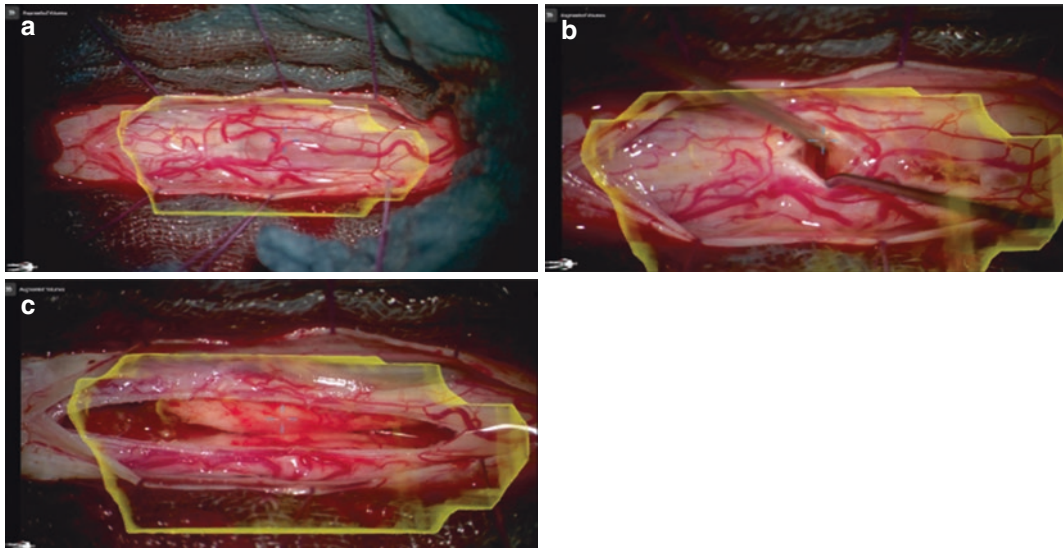


**Fig. 33.18** The surgeon's view during microscope-based augmented-reality navigation. The yellow field outlines the tumor boundaries (**a**, immediately after dural opening; **b**, at the beginning of resection; **c**, at the end of resection). Image originally published by Carl et al. [48]. Republished with permission by Springer Nature

AR) project AR objects in the microscope view during microsurgery (Fig. 33.18). Typically, both the patient and the microscope are tracked using dynamic reference frames (DRFs), and the AR image is adapted based on their relative positions [56]. Due to their limited application, microscope-based systems are often combined with conventional navigational setups. Projector-based AR-interfaces (projector-AR) provide holographic AR overlays on glass screens situated between the surgical area and the surgeon (Fig. 33.19). This solution, albeit elegant, may limit the surgeon's freedom of movement since the screen otherwise should be repositioned to match the surgeon's movements and maneuvers during a surgery. Thus far, projector-AR interfaces have mostly been used for spinal injections and interventional radiology [83].

## 33.6 Current Applications of VR, AR, MIXR Navigation

- Cervical

  Up to now, there have been only two publications on the use of AR for cervical spine surgery. Microscope-based AR has been used in both studies. Intraoperative CBCT (O-Arm) and CT (AIRO) were used in these studies. In the first study, the authors claimed successful use for minimally invasive anterior and posterior cervical approaches without providing technical data [84]. The second study reports a target registration error (TRE) of 0.80 ± 0.28 mm for all spinal cases without specifying the number and type of cervical procedures [85]. Accurate tracking is the major concern regarding all types of navigation including AR in the cervical spine. The inherent movement of the cervical spine, especially the risk for rotation when pressure is applied, constitutes an obstacle for accurate navigation across multiple levels.
- Thoracolumbar applications

  Most AR publications on the spine address thoracolumbar applications. Apart from a few reports on the use of AR for tumor surgery, the rest constitute different approaches for fusion surgery. The use of microscope-based AR for degenerative spine surgery has been discussed in a paper by Carl et al. The authors conclude that reliable AR projections can be obtained and predict that the technology has a great

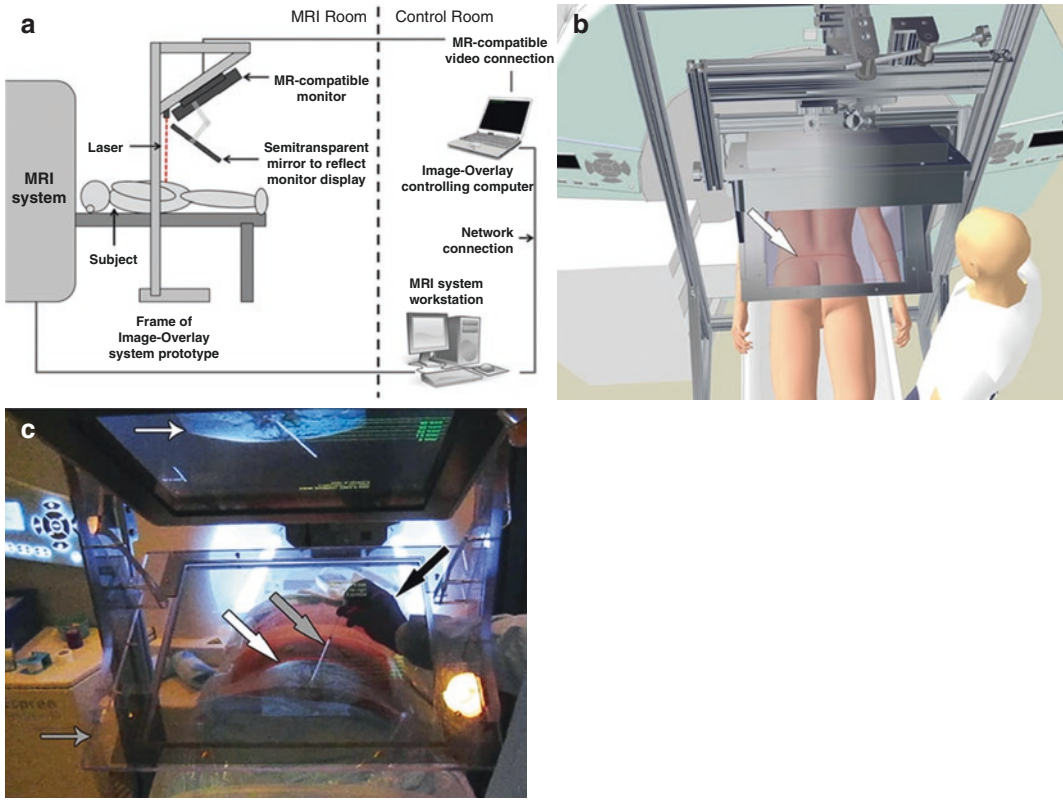


**Fig. 33.19** Augmented-reality visualization using an overlay system for MR-guided interventions: (**a**)—a schematic overview of the system; (**b**)—a schematic of the surgical setup and viewpoint; (**c**)—the surgeon's view during surgery. Image originally published by Fritz et al. [82]. Republished with permission by Springer Nature

potential in cases with complex anatomy and for educational purposes ([56]; Figs. 33.20 and 33.21).

Current research on AR navigation is at an early stage [86]. However, AR-assisted pedicle screw placement is the most common procedure. Six studies have compared AR to free-hand (FH) with or without fluoroscopy for pedicle screw placement [11, 44, 45, 68, 87, 88]. A matched control study compared a prospective cohort of 20 patients treated by AR to 20 retrospectively enrolled patients where FH with or without fluoroscopy had been used [44]. The study found a higher accuracy in the AR vs the FH group (AR: 93.9% vs FH: 89.6%, $p < 0.05$). The same authors used Gertzbein grading to compare AR-navigated and FH pedicle screw accuracies without fluoroscopic guidance in a cadaveric setup. AR had a superior accuracy (AR: 85% vs. FH: 64%, $p < 0.05$) in this comparison [11]. In a cadaveric, minimally invasive study comparing AR to FH with fluoroscopy, no significant difference between the groups could be detected (AR: 94% vs FH: 88%, p = 0.50). However, the trend was toward increased accuracy using AR, and the authors noted the study could have been underpowered [88]. In a small study of HMD-AR with no statistical analysis, more major breaches were observed when using AR (HMD-AR: 36.8% vs FH: 0%; [68]). In a similar study on phantom models, no significant difference was found (HMD-AR: 94% vs FH: 100%, p = 0.106; [87]).

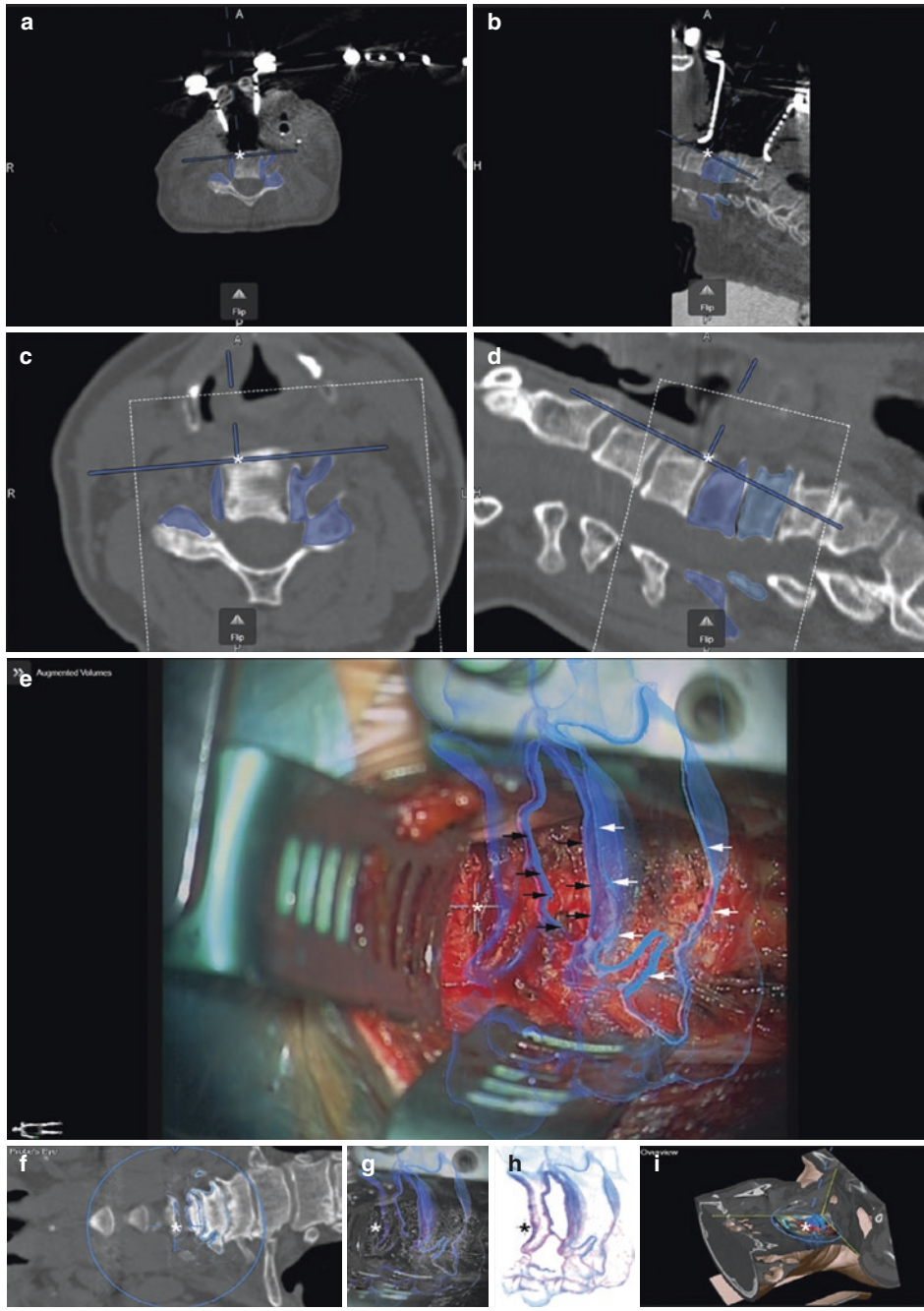


**Fig. 33.20** Microscope-based AR during thoracolumbar surgery. A 73-year-old female patient with cervical myelopathy undergoing vertebral body replacement of C5 and C6 via an anterior approach. Intraoperative computed tomography (CT) images used for augmented reality (AR) registration, showing the viewing axis of the operating microscope: (**a**) axial, (**b**) sagittal view. Nonlinearly registered preoperative CT; the dotted white box marks the region of interest used for the nonlinear image registration: (**c**) axial, (**d**) sagittal view. (**e**) AR visualization of the outline of the vertebral bodies C5 and C6 in different tones of blue; the crosshair in the image center corresponds to the position of the microscope focus point, which is marked by an asterisk in all views; the black arrows depict the AR outline of C5 in the focus plane visualized thicker than the structures beyond the focus plane; the white arrows delineate the C6 outline in the focus plane. (**f**) The probe's-eye view of the preoperative CT images. (**g**) AR visualization over a grayed video frame. (**h**) AR visualization with a white background. (**i**) Overview depicting how the video frame is aligned to the 3-dimensional image data. Image originally published by Carl et al. [56]. Republished with permission by Elsevier

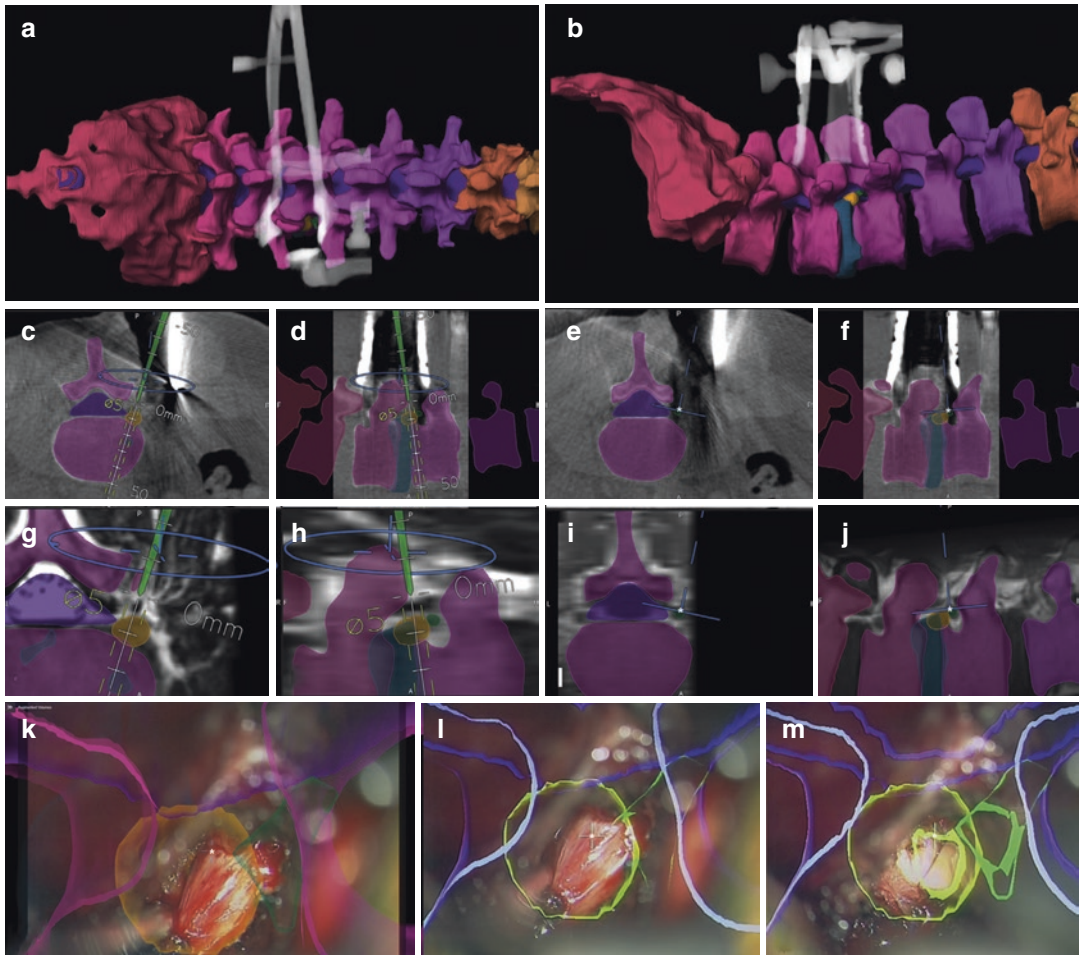


**Fig. 33.21** Microscope-based AR used during thoracolumbar surgery. A 44-year-old male patient with a right-sided lateral disc herniation at the level L3/L4, which is removed via a paramedian lumbar approach. (**a**) Posterior and (**b**) lateral views of a 3-dimensional rendering based on the intraoperative computed tomography (iCT) images depicting the position of the retractor, the vertebras are colored individually, the disc L3/L4 is segmented in dark green, the disc fragment in yellow, and the nerve root is colored green. (**c**) Axial and (**d**) sagittal view of iCT images, additionally to the operating microscope the navigation pointer is placed in the surgical field allowing to point at certain structures and offering the possibility for intraoperative distance measurements, corresponding to (**e**) axial; (**f**) sagittal view of iCT images; (**g**) axial and (**h**) sagittal views of T2-weighted magnetic resonance images with the navigation pointer in place; (**i**) axial and (**j**) sagittal views of T2-weighted magnetic resonance images without the navigation pointer. (**k**) Augmented reality visualization on screens; (**l**) augmented reality visualization applying the microscope head-up display, the nerve root is still covering the direct view of the disc fragment. (**m**) After mobilizing the nerve root, the disc fragment is visible (the crosshair in the center of panels k, l, and m corresponds to the microscope focus position in panels e, f, i, and j, all marked with an asterisk). Image originally published by Carl et al. [56]. Republished with permission by Elsevier

So far, only one study has compared AR navigation to another navigation modality based on pose tracking (PT, e.g., DRF and IR-tracking). In that study, there were no significant differences in translational (AR: 3.4 ± 1.6 mm vs PT: 3.2 ± 2.0 mm, p = 0.85) or angular errors (AR: 4.3 ± 2.3° vs PT: 3.5 ± 1.4°, p = 0.30) between the systems [59].

- Vertebroplasty

A few studies have used AR applications for vertebroplasty. A randomized controlled trial with 10 patients in each arm compared

**Fig. 33.22** Kyphoplasty performed with AR guidance using Microsoft's Hololens. Image originally published by Wei et al. [70]. Republished with permission by Springer Nature

the pedicle cannulation phase for percutaneous vertebroplasty between AR and FH with fluoroscopy [71]. Although there was no significant difference in accuracy between the groups, AR required a longer time for trocar placement while reducing the radiation exposure significantly. In a similar randomized controlled trial on percutaneous kyphoplasty, HMD-AR was compared to FH with fluoroscopy [70]. No accuracy data was reported, but the AR group had larger amounts of bone cement injected, increased postoperative vertebral height, and lower patient-reported pain at a year postoperatively ($p < 0.05$ for all; Fig. 33.22).

- Radiological approaches: spinal injections

  Spinal injection procedures (e.g., selective spinal nerve root blocks, facet joint injections, epidural injections, and discography) are commonly used techniques for the diagnosis and treatment of back pain [89–91]. These procedures are often performed under X-ray fluoroscopy or CT guidance, exposing the operator to ionizing radiation and related health concerns [90, 92–96]. Ultrasound (US) guidance is an alternative. Although US is widely available and lower cost, it offers limited visualization of deep structures, especially underneath bones [97]. Interventional MR imaging techniques have been developed to guide spinal injections because of their unparalleled soft-tissue contrast, multiplanar capabilities, and lack of ionizing radiation [91, 98–107]. The addition of AR solutions to these injection techniques has further improved surgical accuracy and workflow [82]. Different AR interfaces have been utilized. Monitor-based AR was used initially [108]. HMD has also been implemented, but safety and technical reasons require the patient to be treated outside the magnetic field [109]. Image overlay systems (IOS) are often incorporated, and the radiological image is superimposed using projector-based AR.

  The adoption of interventional MRI techniques requires a balance between patient access and image quality. While open systems improve patient access, they have a lower field strength, less homogeneity, and poorer image quality. However, closed-bore high-field sys-

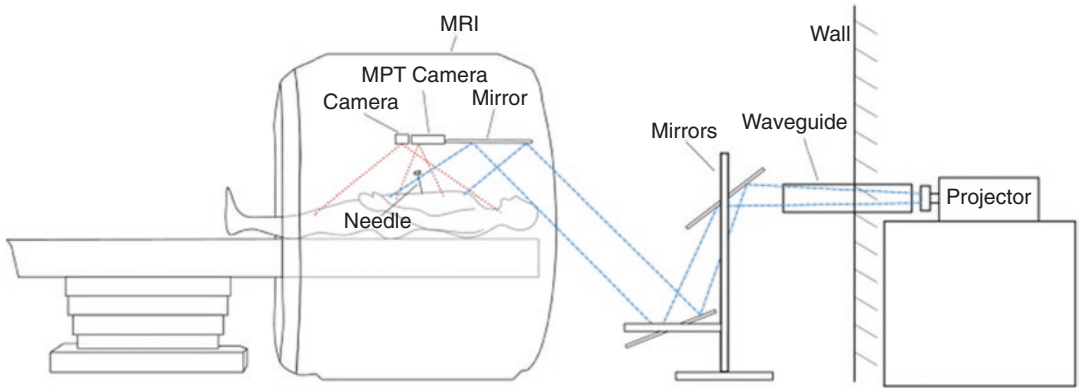


**Fig. 33.23** A schematic drawing of the projector-based AR systems originally published by Mewes et al. [112]. Republished with permission by Wiley

tems provide excellent image quality but limited patient access. AR systems can potentially bridge this barrier between patient access and high-quality imaging by allowing the projection of acquired image data onto a patient outside the bore [110].

Several such systems have been reported in the literature; however, their respective accuracies vary widely, and the clinical usefulness of some systems could be questioned. Wacker et al. used an HMD-AR system in combination with 1.5-T closed-bore MRI as a navigation tool for needle biopsies. In a porcine model, 20 biopsies were performed, and an accuracy of 9.6 ± 4.9 mm was achieved [109]. Weiss et al. described a low-cost system where axial MR images were depicted on a liquid crystal display (LCD) and appeared on a semitransparent mirror projected on the patient outside of the scanner bore. Sixty needles were directed toward the facet joints in a spine phantom, and a mean targeting error of 4.7 mm was achieved [110]. Fritz et al. described the use of a projector-based AR for lumbosacral injections in a cadaveric model. An accuracy of 94.1% was achieved. Needle repositioning was required in 26.7% of the injections without any inadvertent puncture of vulnerable structures ([82]; Fig. 33.19). Mewes et al. presented a projector-based AR system, providing accurate and reliable visualization directly in the MR scanner for in-bore interventions. Using this system, a clinically acceptable accuracy of 1.7 ± 0.5 mm could be achieved ([111, 112]; Fig. 33.23).

## 33.7 Currently Available AR Navigation Systems

The field of AR navigation is rapidly evolving, and new products are introduced and retired, bought, merged, and modified in rapid succession. In the following section, we summarize the current field of established products to give a general idea of items that are available on the market.

- Augmented-Reality Surgical Navigation/ClarifEye (Philips).

  The Augmented-Reality Surgical Navigation (ARSN) system, which is currently registered as the ClarifEye™ system, was an early entrant in the market [11, 72, 73]. This system relies on a combination of a monitor-based AR interface and a hybrid-OR solution with a C-arm (AlluraClarity) plus integrated cameras. Skin fiducials are used for tracking the patient. Intraoperative imaging (CBCT) supports planning and navigation, and patient tracking is automatically performed during the initial imaging. The interface consists of both true AR overlays on the

**Fig. 33.24** Microsoft's Hololens. Image courtesy of Microsoft

**Fig. 33.25** Augmedic's xvision HMD with AR capabilities. Image courtesy of Augmedics

surgical field and traditional VR representations of axial, sagittal, and in-line views when using instrument tracking (Fig. 33.12).

- HoloLens (Microsoft) navigation

  Microsoft's HoloLens is a professional and developer-grade product for general AR use. The headset has been adapted by several different research groups for spine surgery [59, 66, 68, 69, 87, 113]. Although the implementation has varied slightly from case to case, some commonalities are shared by most researchers. The HoloLens uses surface recognition to track the surrounding world without specific markers (i.e., no DRF or skin fiducials are necessary). However, most implementations have required manual patient-to-image co-registration, meaning that the AR overlay first needed to be adjusted manually to fit the position of the patient. The imaging used by these systems has typically been preoperative since no commercial OR solution can integrate the workflow at present (Fig. 33.24).

**Fig. 33.26** Magic Leap 1 by Magic Leap Inc. Image courtesy of Magic Leap

- XVision (Augmedics)

  XVision by Augmedics is an HMD-AR system based on proprietary HMD technology. Unlike the HoloLens, however, it relies on DRFs on instruments and the patient for tracking [58]. The tracking camera is built into the headset, preventing the line-of-sight loss that can occur with external cameras. Patient registration is performed by attaching a registration marker before performing an intraoperative CT scan. The interface consists of both true AR overlays on the surgical field and traditional VR representations of axial and sagittal views (Fig. 33.25).

- Mixed reality by Brainlab

  Brainlab and Magic Leap, the producer of a mixed-reality headset, have combined their technologies to enable an AR/mixed-reality headset. Although mixed reality is mentioned, chiefly conventional AR adaptations have been presented so far. The Magic Leap headset (Magic Leap One, Magic Leap, Plantation, Florida, USA) can either rely on surface recognition to track the surrounding world without specific markers (i.e., no DRF or skin fiducials are necessary) or identify DRFs


**Fig. 33.27** Microscope-based AR solution by Brainlab. Operating room setting: (**a**) for automatic registration, the navigation camera tracks the scanner (black arrows) and the reference array that is attached to the patient (white arrows); (**b**) the operating microscope enabling AR is tracked during surgery (black arrows); (**c**) setting during surgery with the operating microscope where the AR information is superimposed by the integrated heads-up display, additionally the microscope video is shown on screens with an AR overlay, and the autofocus position of the microscope is displayed in co-registered CT and MR images in the spinal navigation application. Image originally published by Carl et al. [57]. Republished with permission by Springer Nature

attached to the patient to perform patient registration procedures with high accuracy. Multiple headsets can be worn by different staff members who can see the same AR projections and interact with the objects at the same position in the room as if they were physically there (Fig. 33.26) [114].

- Microscope-Based Augmented Reality by Brainlab

  Brainlab has integrated its navigation system with multiple microscope manufacturers to enable AR overlays in the microscope view. The system relies on a DRF in the surgical field to track the patient and a separate DRF attached to the microscope to track the surgical viewpoint [48, 56]. Both DRFs are tracked by an IR camera system. The interface in the microscope consists of displaying segmented 3D structures from the preoperative planning, in which the vertebrae are automatically segmented and included, and tumors are manually defined preoperatively. The interface consists of both true AR overlays over the surgical field and traditional VR representations of axial and sagittal views (Fig. 33.27).

## References


1. Odgers CJ, Vaccaro AR, Pollack ME, Cotler JMJCSS. Accuracy of pedicle screw placement with the assistance of lateral plain radiography. J Spinal Disord. 1996;9(4):334–8.
2. Whitecloud TS, Skalley TC, Cook SD, Morgan EL. Roentgenographic measurement of pedicle screw penetration. Clin Orthop Relat Res. 1989;245:57–68.
3. Weinstein JN, Spratt KF, Spengler D, Brick C, Reid SJS. Spinal pedicle fixation: reliability and validity of roentgenogram-based assessment and surgical factors on successful screw placement. Spine (Phila Pa 1976). 1988;13(9):1012–8.
4. Suk S-I, Kim J-H, Kim S-S, Lim D-J. Pedicle screw instrumentation in adolescent idiopathic scoliosis (AIS). Eur Spine J. 2012;21(1):13–22.
5. Hartl R, Lam KS, Wang J, Korge A, Kandziora F, Audige L. Worldwide survey on the use of navigation in spine surgery. World Neurosurg. 2013;79(1):162–72.
6. Bourgeois AC, Faulkner AR, Pasciak AS, Bradley YCJAotm. The evolution of image-guided lumbosacral spine surgery. Ann Transl Med. 2015;3(5)
7. Cordemans V, Kaminski L, Banse X, Francq BG, Cartiaux O. Accuracy of a new intraoperative cone beam CT imaging technique (Artis zeego II) compared to postoperative CT scan for assessment of pedicle screws placement and breaches detection. Eur Spine J. 2017;26(11):2906–16.
8. Hussain I, Cosar M, Kirnaz S, Schmidt FA, Wipplinger C, Wong T, et al. Evolving navigation, robotics, and augmented reality in minimally invasive spine surgery. Global Spine J. 2020;10(2 Suppl):22S–33S.
9. Burström G, Nachabe R, Homan R, Hoppenbrouwers J, Holthuizen R, Persson O, et al. Frameless patient tracking with adhesive optical skin markers for augmented reality surgical navigation in spine surgery. Spine (Phila Pa 1976). 2020;
10. Schmidt OI, Strasser S, Kaufmann V, Strasser E, Gahr RH. Role of early minimal-invasive spine fixation in acute thoracic and lumbar spine trauma. Indian J Orthop. 2007;41(4):374.
11. Elmi-Terander A, Skulason H, Söderman M, Racadio J, Homan R, Babic D, et al. Surgical navigation technology based on augmented reality and integrated 3D intraoperative imaging: a spine cadaveric feasibility and accuracy study. Spine (Phila Pa 1976). 2016;41(21):E1303–E11.
12. Hoppe HDS, Raczkowsky J, Wörn H, Moctezuma JL. Intraoperative visualization of surgical planning data using video projectors. Stud Health Technol Inform. 2001;81:206–8.
13. Hoppe HDS, Kübler C, Raczkowsky J, Wörn H. A new, accurate and easy to implement camera and video projector model. Stud Health Technol Inform. 2002;85:204–6.
14. Däuber SHH, Krempien R, Hassfeld S, Brief J, Wörn H. Intraoperative guidance of pre-planned bone deformations with a surface scanning system. Stud Health Technol Inform. 2002;85:110–5.
15. Eggers GST, Hoppe H, Kahrs L, Ghanai S, Raczkowsky J, Dillman R, Wörn H, Hassfeld S, Marmulla R. Intraoperative augmented reality: the surgeons view. Stud Health Technol Inform. 2005;111:123–5.
16. Kahrs LHH, Eggers G, Raczkowsky J, Marmulla R, Wörn H. Visualization of surgical 3D information with projector-based augmented reality. Stud Health Technol Inform. 2005;111:243–6.
17. Marmulla R, Hoppe H, Muhling J, Eggers G. An augmented reality system for image-guided surgery. Int J Oral Maxillofac Surg. 2005;34(6):594–6.
18. Wörn H, Aschke M, Kahrs LA. New augmented reality and robotic based methods for head-surgery. Int J Med Robot Comput Assist Surg. 2005;01(03)
19. Liang JT, Doke T, Onogi S, Ohashi S, Ohnishi I, Sakuma I, et al. A fluorolaser navigation system to guide linear surgical tool insertion. Int J Comput Assist Radiol Surg. 2012;7(6):931–9.
20. McKnight RR, Pean CA, Buck JS, Hwang JS, Hsu JR, Pierrie SN. Virtual reality and augmented reality-translating surgical training into surgical technique. Curr Rev Musculoskelet Med. 2020;
21. Vazan M, Gempt J, Meyer B, Buchmann N, Ryang YM. Minimally invasive transforaminal lumbar interbody fusion versus open transforaminal lumbar interbody fusion: a technical description and review of the literature. Acta Neurochir. 2017;159(6):1137–46.
22. Goldstein CL, Macwan K, Sundararajan K, Rampersaud YR. Perioperative outcomes and adverse events of minimally invasive versus open posterior lumbar fusion: meta-analysis and systematic review. J Neurosurg Spine. 2016;24(3):416–27.
23. Lu VM, Kerezoudis P, Gilder HE, McCutcheon BA, Phan K, Bydon M. Minimally invasive surgery versus open surgery spinal fusion for spondylolisthesis: a systematic review and meta-analysis. Spine (Phila Pa 1976). 2017;42(3):E177–E85.
24. Wu MH, Dubey NK, Li YY, Lee CY, Cheng CC, Shi CS, et al. Comparison of minimally invasive spine surgery using intraoperative computed tomography integrated navigation, fluoroscopy, and conventional open surgery for lumbar spondylolisthesis: a prospective registry-based cohort study. Spine J. 2017;
25. Phillips FM, Cheng I, Rampersaud YR, Akbarnia BA, Pimenta L, Rodgers WB, et al. Breaking through the "glass ceiling" of minimally invasive spine surgery. Spine (Phila Pa 1976). 2016;41(Suppl 8):S39–43.
26. Park P, Foley KT, Cowan JA, Marca FL. Minimally invasive pedicle screw fixation utilizing O-arm fluoroscopy with computer-assisted navigation: feasibility, technique, and preliminary results. Surg Neurol Int. 2010;1:44.

27. Kim TT, Johnson JP, Pashman R, Drazin D. Minimally invasive spinal surgery with intraoperative image-guided navigation. Biomed Res Int. 2016;2016:5716235.
28. Edström E, Burström G, Nachabe R, Gerdhem P, Elmi-Terander A. A novel augmented-reality-based surgical navigation system for spine surgery in a hybrid operating room: design, workflow, and clinical applications. Oper Neurosurg (Hagerstown). 2020;18(5):496–502.
29. Gelalis ID, Paschos NK, Pakos EE, Politis AN, Arnaoutoglou CM, Karageorgos AC, et al. Accuracy of pedicle screw placement: a systematic review of prospective in vivo studies comparing free hand, fluoroscopy guidance and navigation techniques. Eur Spine J. 2012;21(2):247–55.
30. Schizas C, Michel J, Kosmopoulos V, Theumann N. Computer tomography assessment of pedicle screw insertion in percutaneous posterior transpedicular stabilization. Eur Spine J. 2007;16(5):613–7.
31. Kim MC, Chung HT, Cho JL, Kim DJ, Chung NS. Factors affecting the accurate placement of percutaneous pedicle screws during minimally invasive transforaminal lumbar interbody fusion. Eur Spine J. 2011;20(10):1635–43.
32. Bourgeois AC, Faulkner AR, Bradley YC, Pasciak AS, Barlow PB, Gash JR, et al. Improved accuracy of minimally invasive transpedicular screw placement in the lumbar spine with 3-dimensional stereotactic image guidance: a comparative meta-analysis. J Spinal Disord Tech. 2015;28(9):324–9.
33. Kosmopoulos V, Schizas C. Pedicle screw placement accuracy: a meta-analysis. Spine (Phila Pa 1976). 2007;32(3):E111–20.
34. Santos ER, Sembrano JN, Yson SC, Polly DW Jr. Comparison of open and percutaneous lumbar pedicle screw revision rate using 3-D image guidance and intraoperative CT. Orthopedics. 2015;38(2):e129–34.
35. Del Castillo-Calcáneo J, Navarro-Ramirez R, Gimenez-Gigon M, Adjei J, Damolla A, Nakhla J, et al. Principles and fundamentals of minimally invasive spine surgery. World Neurosurg. 2018;119:465–71.
36. International Commission Radiological Protection: Statement on tissue reactions/early and late effects of radiation in normal tissues and organs - threshold doses for tissue reaction in a radiation protection context. ICRP Publication 118. 2012.
37. International Commission Radiological Protection: Occupational intakes of radionuclides: Part 1. ICRP Publication 130. 2015.
38. Gausden EB, Christ AB, Zeldin R, Lane JM, McCarthy MM. Tracking cumulative radiation exposure in orthopaedic surgeons and residents: what dose are we getting? J Bone Joint Surg Am. 2017;99(15):1324–9.
39. Fomekong E, Safi SE, Raftopoulos C. Spine navigation based on 3-dimensional robotic fluoroscopy for accurate percutaneous pedicle screw placement: a prospective study of 66 consecutive cases. World Neurosurg. 2017;108:76–83.
40. Fichtner J, Hofmann N, Rienmuller A, Buchmann N, Gempt J, Kirschke JS, et al. Revision rate of misplaced pedicle screws of the thoracolumbar spine-comparison of three-dimensional fluoroscopy navigation with freehand placement: a systematic analysis and review of the literature. World Neurosurg. 2018;109:e24–32.
41. Floccari LV, Larson AN, Crawford CH, Ledonio CG, Polly DW, Carreon LY, et al. Which malpositioned pedicle screws should be revised? J Pediatr Orthop. 2018;38(2):110–5.
42. Bauer JM, Moore JA, Rangarajan R, Gibbs BS, Yorgova PK, Neiss GI, et al. Intraoperative CT scan verification of pedicle screw placement in AIS to prevent malpositioned screws: safety benefit and cost. Spine Deform. 2018;6(6):662–8.
43. Elmi-Terander A, Burström G, Nachabe R, Skulason H, Pedersen K, Fagerlund M, et al. Pedicle screw placement using augmented reality surgical navigation with intraoperative 3D imaging: a first in-human prospective cohort study. Spine (Phila Pa 1976). 2019;44(7):517–25.
44. Elmi-Terander A, Burström G, Nachabe R, Fagerlund M, Ståhl F, Charalampidis A, et al. Augmented reality navigation with intraoperative 3D imaging vs fluoroscopy-assisted free-hand surgery for spine fixation surgery: a matched-control study comparing accuracy. Sci Rep. 2020;10(1):707.
45. Edström E, Burström G, Persson O, Charalampidis A, Nachabe R, Gerdhem P, et al. Does augmented reality navigation increase pedicle screw density compared to free-hand technique in deformity surgery? Single surgeon case series of 44 patients. Spine (Phila Pa 1976). 2020;45(17):E1085–E90.
46. Edström E, Burström G, Omar A, Nachabe R, Söderman M, Persson O, et al. Augmented reality surgical navigation in spine surgery to minimize staff radiation exposure. Spine (Phila Pa 1976). 2020;45(1):E45–53.
47. Mularski S, Picht T, Kuehn B, Kombos T, Brock M, Suess OJCAS. Real-time tracking of vertebral body movement with implantable reference microsensors. Comput Aided Surg. 2006;11(3):137–46.
48. Carl B, Bopp M, Sass B, Pojskic M, Nimsky C. Augmented reality in intradural spinal tumor surgery. Acta Neurochir. 2019;161(10):2181–93.
49. Buza JA, Good CR, Lehman RA, Pollina J, Chua RV, Buchholz AL, et al. Robotic-assisted cortical bone trajectory (CBT) screws using the Mazor X Stealth Edition (MXSE) system: workflow and technical tips for safe and efficient use. J Robot Surg. 2020:1–11.
50. Ungi T, Greer H, Sunderland K, Wu V, Baum ZM, Schlenger C, et al. Automatic spine ultrasound segmentation for scoliosis visualization and measurement. IEEE Trans Biomed Eng. 2020;

51. Chen F, Cui X, Liu J, Han B, Zhang D, Zhang X, et al. Tissue structure updating for in situ augmented reality navigation using calibrated ultrasound and two-level surface warping. IEEE Trans Biomed Eng. 2020;67(11):3211–22.
52. Saß B, Bopp M, Nimsky C, Carl BJWn. Navigated 3-dimensional intraoperative ultrasound for spine. Surgery. 2019;131:e155–e69.
53. Citardi MJ, Agbetoba A, Bigcas JL, Luong A. Augmented reality for endoscopic sinus surgery with surgical navigation: a cadaver study. Int Forum Allergy Rhinol. 2016;6(5):523–8.
54. Spetzger U, Laborde G, Gilsbach J. Frameless neuronavigation in modern neurosurgery. Minim Invasive Neurosurg. 1995;38(04):163–6.
55. Abe Y, Sato S, Kato K, Hyakumachi T, Yanagibashi Y, Ito M, et al. A novel 3D guidance system using augmented reality for percutaneous vertebroplasty: technical note. J Neurosurg Spine. 2013;19(4):492–501.
56. Carl B, Bopp M, Sass B, Nimsky C. Microscope-based augmented reality in degenerative spine surgery: initial experience. World Neurosurg. 2019;128:E541–E51.
57. Carl B, Bopp M, Sass B, Voellger B, Nimsky C. Implementation of augmented reality support in spine surgery. Eur Spine J. 2019;28(7):1697–711.
58. Molina CA, Theodore N, Ahmed AK, Westbroek EM, Mirovsky Y, Harel R, et al. Augmented reality-assisted pedicle screw insertion: a cadaveric proof-of-concept study. J Neurosurg Spine 2019:1–8.
59. Muller F, Roner S, Liebmann F, Spirig JM, Furnstahl P, Farshad M. Augmented reality navigation for spinal pedicle screw instrumentation using intraoperative 3D imaging. Spine J. 2020;20(4):621–8.
60. Leksell L. A stereotaxic apparatus for intracerebral surgery. Acta Chir Scand. 1950;99(3):229–33.
61. Jin M, Liu Z, Qiu Y, Yan H, Han X, Zhu Z. Incidence and risk factors for the misplacement of pedicle screws in scoliosis surgery assisted by O-arm navigation-analysis of a large series of one thousand, one hundred and forty five screws. Int Orthop. 2017;41(4):773–80.
62. Uehara M, Takahashi J, Ikegami S, Kuraishi S, Shimizu M, Futatsugi T, et al. Are pedicle screw perforation rates influenced by distance from the reference frame in multilevel registration using a computed tomography-based navigation system in the setting of scoliosis? Spine J. 2017;17(4):499–504.
63. Thomale UW, Kneissler M, Hein A, Maetzig M, Kroppenstedt SN, Lueth T, et al. A spine frame for intra-operative fixation to increase accuracy in spinal navigation and robotics. Comput Aided Surg. 2005;10(3):151–5.
64. Fitzpatrick JM, West JB, Maurer CR Jr. Predicting error in rigid-body point-based registration. IEEE Trans Med Imaging. 1998;17(5):694–702.
65. Liu H, Wu J, Tang Y, Li H, Wang W, Li C, et al. Percutaneous placement of lumbar pedicle screws via intraoperative CT image-based augmented reality-guided technology. J Neurosurg Spine 2019:1–6.
66. Gibby JT, Swenson SA, Cvetko S, Rao R, Javan R. Head-mounted display augmented reality to guide pedicle screw placement utilizing computed tomography. Int J Comput Assist Radiol Surg. 2019;14(3):525–35.
67. Liebmann F, Roner S, von Atzigen M, Scaramuzza D, Sutter R, Snedeker J, et al. Pedicle screw navigation using surface digitization on the Microsoft HoloLens. Int J Comput Assist Radiol Surg. 2019;14(7):1157–65.
68. Urakov TM, Wang MY, Levi AD. Workflow caveats in augmented reality-assisted pedicle instrumentation: cadaver lab. World Neurosurg. 2019;
69. Wanivenhaus F, Neuhaus C, Liebmann F, Roner S, Spirig JM, Farshad M. Augmented reality-assisted rod bending in spinal surgery. Spine J. 2019;19(10):1687–9.
70. Wei P, Yao Q, Xu Y, Zhang H, Gu Y, Wang L. Percutaneous kyphoplasty assisted with/without mixed reality technology in treatment of OVCF with IVC: a prospective study. J Orthop Surg Res. 2019;14(1):255.
71. Auloge P, Cazzato RL, Ramamurthy N, de Marini P, Rousseau C, Garnon J, et al. Augmented reality and artificial intelligence-based navigation during percutaneous vertebroplasty: a pilot randomised clinical trial. Eur Spine J. 2019;
72. Elmi-Terander A, Nachabe R, Skulason H, Pedersen K, Söderman M, Racadio J, et al. Feasibility and accuracy of thoracolumbar minimally invasive pedicle screw placement with augmented reality navigation technology. Spine (Phila Pa 1976). 2018;43(14):1018–23.
73. Burström G, Nachabe R, Persson O, Edström E, Elmi-Terander A. Augmented and virtual reality instrument tracking for minimally invasive spine surgery: a feasibility and accuracy study. Spine (Phila Pa 1976). 2019;44(15):1097–104.
74. Peh S, Chatterjea A, Pfarr J, Schafer JP, Weuster M, Kluter T, et al. Accuracy of augmented reality surgical navigation for minimally invasive pedicle screw insertion in the thoracic and lumbar spine with a new tracking device. Spine J. 2019;
75. Hartley R, Zisserman A. Multiple view geometry in computer vision. Cambridge University Press; 2003.
76. Umeyama S. Least-squares estimation of transformation parameters between two point patterns. IEEE Trans Pattern Anal Mach Intell. 1991;4:376–80.
77. Malham GM, Parker RM. Early experience of placing image-guided minimally invasive pedicle screws without K-wires or bone-anchored trackers. J Neurosurg Spine. 2018;28(4):357–63.
78. Virk S, Qureshi S. Navigation in minimally invasive spine surgery. J Spine Surg. 2019;5(Suppl 1):S25–s30.
79. Su BW, Kim PD, Cha TD, Lee J, April EW, Weidenbaum M, et al. An anatomical study of the mid-lateral pars relative to the pedicle footprint in

the lower lumbar spine. Spine (Phila Pa 1976). 2009;34(13):1355–62.
80. Miller CA, Ledonio CG, Hunt MA, Siddiq F, Polly DW Jr. Reliability of the planned pedicle screw trajectory versus the actual pedicle screw trajectory using intra-operative 3D CT and image guidance. Int J Spine Surg. 2016;10:38.
81. Yoon JW, Chen RE, Kim EJ, Akinduro OO, Kerezoudis P, Han PK, et al. Augmented reality for the surgeon: systematic review. Int J Med Robot. 2018;14(4):e1914.
82. Fritz J, U-thainual P, Ungi T, Flammang AJ, Fichtinger G, Iordachita II, et al. Augmented reality visualisation using an image overlay system for MR-guided interventions: technical performance of spine injection procedures in human cadavers at 1.5 Tesla. Eur Radiol. 2013;23(1):235–45.
83. Ma L, Zhao Z, Chen F, Zhang B, Fu L, Liao H. Augmented reality surgical navigation with ultrasound-assisted registration for pedicle screw placement: a pilot study. Int J Comput Assist Radiol Surg. 2017;12(12):2205–15.
84. Umebayashi D, Yamamoto Y, Nakajima Y, Fukaya N, Hara M. Augmented reality visualization-guided microscopic spine surgery: transvertebral anterior cervical foraminotomy and posterior foraminotomy. J Am Acad Orthop Surg Glob Res Rev. 2018;2(4):e008.
85. Carl B, Bopp M, Sass B, Pojskic M, Gjorgjevski M, Voellger B, et al. Reliable navigation registration in cranial and spine surgery based on intraoperative computed tomography. Neurosurg Focus. 2019;47(6)
86. Kipper G, Rampolla J. Augmented reality: an emerging technologies guide to AR. Elsevier; 2012.
87. Liu H, Wu JL, Tang Y, Li HY, Wang WK, Li CQ, et al. Percutaneous placement of lumbar pedicle screws via intraoperative CT image-based augmented reality-guided technology. J Neurosurg Spine. 2020;32(4):542–7.
88. Peh S, Chatterjea A, Pfarr J, Schafer JP, Weuster M, Kluter T, et al. Accuracy of augmented reality surgical navigation for minimally invasive pedicle screw insertion in the thoracic and lumbar spine with a new tracking device. Spine J. 2020;20(4):629–37.
89. Fletcher-Sandersjöö A, Edström E, Kuntze Söderqvist A, Grane P, Elmi-Terander A. Long-term pain relief following percutaneous steroid treatment of spinal synovial cysts: a population-based cohort study. J Neurointerv Surg. 2020;
90. Fritz J, Niemeyer T, Clasen S, Wiskirchen J, Tepe G, Kastler B, et al. Management of chronic low back pain: rationales, principles, and targets of imaging-guided spinal injections. Radiographics. 2007;27(6):1751–71.
91. Carrino JA, Morrison WB, Parker L, Schweitzer ME, Levin DC, Sunshine JH. Spinal injection procedures: volume, provider distribution, and reimbursement in the U.S. medicare population from 1993 to 1999. Radiology. 2002;225(3):723–9.
92. Krombach GA, Schmitz-Rode T, Wein BB, Meyer J, Wildberger JE, Brabant K, et al. Potential of a new laser target system for percutaneous CT-guided nerve blocks: technical note. Neuroradiology. 2000;42(11):838–41.
93. Nawfel RD, Judy PF, Silverman SG, Hooton S, Tuncali K, Adams DF. Patient and personnel exposure during CT fluoroscopy-guided interventional procedures. Radiology. 2000;216(1):180–4.
94. Paulson EK, Sheafor DH, Enterline DS, McAdams HP, Yoshizumi TT. CT fluoroscopy--guided interventional procedures: techniques and radiation dose to radiologists. Radiology. 2001;220(1):161–7.
95. Wagner LK. CT fluoroscopy: another advancement with additional challenges in radiation management. Radiology. 2000;216(1):9–10.
96. Wagner AL. Selective lumbar nerve root blocks with CT fluoroscopic guidance: technique, results, procedure time, and radiation dose. AJNR Am J Neuroradiol. 2004;25(9):1592–4.
97. Weiss CR, Nour SG, Lewin JS. MR-guided biopsy: a review of current techniques and applications. J Magn Reson Imaging. 2008;27(2):311–25.
98. Blanco Sequeiros R, Carrino JA. Musculoskeletal interventional MR imaging. Magn Reson Imaging Clin N Am. 2005;13(3):519–32.
99. Fritz J, Henes JC, Thomas C, Clasen S, Fenchel M, Claussen CD, et al. Diagnostic and interventional MRI of the sacroiliac joints using a 1.5-T open-bore magnet: a one-stop-shopping approach. AJR Am J Roentgenol. 2008;191(6):1717–24.
100. Fritz J, Clasen S, Boss A, Thomas C, Konig CW, Claussen CD, et al. Real-time MR fluoroscopy-navigated lumbar facet joint injections: feasibility and technical properties. Eur Radiol. 2008;18(7):1513–8.
101. Fritz J, Thomas C, Tzaribachev N, Horger MS, Claussen CD, Lewin JS, et al. MRI-guided injection procedures of the temporomandibular joints in children and adults: technique, accuracy, and safety. AJR Am J Roentgenol. 2009;193(4):1148–54.
102. Fritz J, Thomas C, Clasen S, Claussen CD, Lewin JS, Pereira PL. Freehand real-time MRI-guided lumbar spinal injection procedures at 1.5 T: feasibility, accuracy, and safety. AJR Am J Roentgenol. 2009;192(4):W161–7.
103. Fritz J, Tzaribachev N, Thomas C, Carrino JA, Claussen CD, Lewin JS, et al. Evaluation of MR imaging guided steroid injection of the sacroiliac joints for the treatment of children with refractory enthesitis-related arthritis. Eur Radiol. 2011;21(5):1050–7.
104. Ojala R, Klemola R, Karppinen J, Sequeiros RB, Tervonen O. Sacro-iliac joint arthrography in low back pain: feasibility of MRI guidance. Eur J Radiol. 2001;40(3):236–9.

105. Ojala R, Vahala E, Karppinen J, Klemola R, Blanco-Sequeiros R, Vaara T, et al. Nerve root infiltration of the first sacral root with MRI guidance. J Magn Reson Imaging. 2000;12(4):556–61.
106. Smith KA, Carrino JA. MRI-guided interventions of the musculoskeletal system. J Magn Reson Imaging. 2008;27(2):339–46.
107. Moche M, Trampel R, Kahn T, Busse H. Navigation concepts for MR image-guided interventions. J Magn Reson Imaging. 2008;27(2):276–91.
108. Gering DT, Nabavi A, Kikinis R, Hata N, O'Donnell LJ, Grimson WE, et al. An integrated visualization system for surgical planning and guidance using image fusion and an open MR. J Magn Reson Imaging. 2001;13(6):967–75.
109. Wacker FK, Vogt S, Khamene A, Jesberger JA, Nour SG, Elgort DR, et al. An augmented reality system for MR image-guided needle biopsy: initial results in a swine model. Radiology. 2006;238(2):497–504.
110. Weiss CR, Marker DR, Fischer GS, Fichtinger G, Machado AJ, Carrino JA. Augmented reality visualization using image-overlay for MR-guided interventions: system description, feasibility, and initial evaluation in a spine phantom. AJR Am J Roentgenol. 2011;196(3):W305–7.
111. Mewes A, Heinrich F, Hensen B, Wacker F, Lawonn K, Hansen C. Concepts for augmented reality visualisation to support needle guidance inside the MRI. Healthc Technol Lett. 2018;5(5):172–6.
112. Mewes A, Heinrich F, Kagebein U, Hensen B, Wacker F, Hansen C. Projector-based augmented reality system for interventional visualization inside MRI scanners. Int J Med Robot. 2019;15(1):e1950.
113. Kochanski RB, Lombardi JM, Laratta JL, Lehman RA, O'Toole JE. Image-guided navigation and robotics in spine surgery. Neurosurgery. 2019;84(6):1179–89.
114. Frisk H, Lindqvist E, Persson O, Weinzierl J, Bruetzel LK, Cewe P, Burström G, Edström E, Elmi-Terander A. Feasibilityand accuracy of thoracolumbar pedicle screw placement using an augmented reality head mounted device. Sensors (Basel). 2022;22(2):522.

# 34 Optimizing Visualization in Endoscopic Spine Surgery

Gregory Basil, Annelise Sprau, Vignessh Kumar, Roberto J. Perez-Roman, and Michael Y. Wang

## 34.1 A Global View of Spinal Endoscopy

Proper lighting and visualization have always been critical to safe surgical interventions for the very reason that, in general, *one cannot operate if one cannot see*. To this end, there has been tremendous innovation over the past century in developing enhanced lighting techniques to aid in visualization and anatomic identification. These enhanced lighting techniques take on special importance in endoscopic surgery given two fundamental departures from traditional, open surgery: (1) the narrowed minimally invasive apertures with which to get light in and light out and (2) the indirect nature of visualization, a result of optical manipulation and digital image transformation.

Indeed, as we move toward ever smaller operative windows, the necessity of maximizing light utilization and therefore visual reconstruction are of the utmost importance. This is especially true given the differences between spinal endoscopy and other endoscopic procedures—namely the creation of a novel working corridor in spinal endoscopy compared to the insufflation of preexisting potential spaces. This difference poses unique challenges for multiple reasons, not least of which is the proximity of critical neural elements with surrounding non-deformable structures (bone).

Additionally, although endoscopy in spinal surgery has well-established benefits such as less soft-tissue dissection (and associated muscle trauma), reduced hospital stay, and early functional recovery, practicing this technique is not without challenges [1–5]. Several distinct obstacles exist for widespread adoption of spinal endoscopy, not least of which is a steep learning curve. This learning curve is at least partially related to the novel challenges posed by endoscopic visualization when compared to traditional open surgical approaches. These challenges include the need for a strong three-dimensional anatomic understanding, potentially distorted anatomy secondary to the imperfect resolution, difficult working angles, and less freedom of movement due to the small working aperture.

While improved training and surgeon comfort with endoscopic approaches represent one avenue for improved outcomes in endoscopic spinal surgery, technologic advancement is equally as compelling. In this book chapter, we aim to investigate the concept of enhancing endoscopic optics by modification of the patient's tissue in response to the lighting method, manipulation of

G. Basil · A. Sprau · V. Kumar
R. J. Perez-Roman (✉) · M. Y. Wang
Department of Neurological Surgery, University of Miami Miller School of Medicine, Miami, FL, USA
e-mail: gregory.basil@jhsmiami.org; annelise.sprau@med.miami.edu; vignessh.kumar@jhsmiami.org; roberto.perezroman@jhsmiami.org; mwang2@med.miami.edu



J.-S. Kim et al. (eds.), *Technical Advances in Minimally Invasive Spine Surgery*,
https://doi.org/10.1007/978-981-19-0175-1_34

light within visible spectrum, and enhancement of digitalization to improve image quality.

## 34.2 A Brief History of Light and Endoscopy

Prior to an in-depth discussion of enhanced endoscopic visualization techniques, a discussion of light itself is mandatory. The concept of light and its properties has been mainstay within scientific research for centuries. In the seventeenth century, there was a vigorous global intellectual discourse regarding the true nature of light. On one hand, a Dutch physicist, Christiaan Huygens, postulated that light was a wave [6]. Huygens' work was based on previous findings by the English physicist Robert Hooke and was published in 1690 in the *Traité de la lumière* (*Treatise on Light*) [7–9]. Newton, however, disagreed, suggesting that light was instead composed of "corpuscles" (particles) [10]. Each of these theories centered around differing explanations for the concepts of reflection and refraction [8]. While Newton's theory found favor at the time, the concept of light as a wave was re-invigorated first by the work of Thomas Young and Augustin Fresnel, who explained the concepts of interference and diffraction via the wave-nature of light, and then by James Maxwell who mathematically demonstrated that light was an electromagnetic wave [9]. Until the mid-1800s the "wave theory" of light persisted, but it was Einstein who posited that light was composed of *Lichtquanten* (photons). In later years, he argued that light retained its wave-like properties, thus proposing light acts as both a wave and a particle [8].

Consequently, we have adopted the "dual theory of light," which stands to this day.

The dual theory of light not only constitutes how we perceive the surrounding world, but also suggests a basis for manipulating light and maximizing visualization. Along the electromagnetic spectrum, the human eye can perceive electromagnetic radiation with wavelengths of about 380–750 nm, also known as "visible light" [11]. We process colors of objects relative to the specific wavelength of the light source, coupled with the absorptive and reflective properties of the illuminated object [11]. Specifically, light initially strikes an object as a mixed wavelength, and subsequently, the object absorbs certain wavelengths and reflects the remaining [11]. The human eye absorbs the reflected light, which determines the ultimate perception the object's color. Light perception can be altered through optical filters, which filter the reflection to only specific wavelengths, or enhanced by fluorescence, which intensifies visualization by emitting shorter wavelengths, thus higher energy light [12].

While it is difficult to determine exactly where and when light and surgery first crossed paths in a thoughtful manner, it has been suggested that Hippocrates (460–370 BC) was the first to use a speculum-like instrument to peer into orifices within the human body [13, 14]. A similar but slightly more advanced device was conceived of around 1000 AD, when an Arabian physician by the name of Albukasim used reflected light in combination with a speculum to visualize the cervix [13, 15]. Although Albukasim's device remained little more than a novelty, it is notable that the ideological forefathers of endoscopic surgery had already begun to understand the value of light manipulation.

The next significant advance in endoscopic surgery came in 1806, when the first semblance of a modern endoscope was conceived by Phillip Bozzini [16, 17]. Bozzini's "Lichtleiter" (light conductor) was an endoscope-like instrument illuminated by a candle [13]. While still crude compared to modern standards and never clinically utilized, Bozzini's implement represented an important step forward in its usage of artificial light to illuminate and visualize an internal cavity [14, 18]. This idea was further refined by Antoin Desormeaux of France, who used a combination of a kerosene lamp along with a 45 degree mirror to improve visualization [13].

Shortly thereafter, Max Nitze, a German physician, developed a fairly advanced endoscope which utilized electric light from a platinum filament lamp and a series of lenses to magnify images in 1879 [13]. Nitze's scope had the ability to take intraoperative photographs [13]. However, heat from the platinum filament was problematic

and was later replaced by Edison's incandescent bulb in 1883 [13].

Modern endoscopy was made possible by two major advancements: the invention of the rod-lens system in 1959 by Harold Hopkins, PhD, and the introduction of fiber-optic light transmission by Karl Storz in 1970 [16]. The rod-light system allowed for wider viewing angles with a smaller diameter endoscope, and the fiber-optic lighting solved the issue of poor or inadequate lighting [13]. Still, early endoscopes could not project their images onto a screen or TV monitor until the addition of a colored image projection by Oka et al. in 1990 [13, 19]. While further refinements in endoscopic design have occurred since, most of these changes have represented incremental improvement on an existing design with improved lighting, resolution, and instrument access. Indeed, the key components of modern endoscopic equipment are well established, and a discussion of their theoretical underpinnings is required.

## 34.3 The Scientific Foundations of the Modern Spinal Endoscope

### 34.3.1 Transmission of Light

In endoscopy, the surgical working window is illuminated by high-powered light source and visualized digitally. Light is transmitted to the surgical field from the light source through a fiber-optic cable causing total internal reflection [20]. The light must reflect off the fiber wall with an angle greater than the critical angle (with respect to the normal) to ensure sufficient light intensity as it returns through the fiber-optic canal and is ultimately digitalized. For total internal reflection to occur, the refractive index of the medium through which light propagates must be greater than the refractive index of the boundary medium [21]. The principle of total internal reflection occurs both in the transmission of light from the source to the surgical field and from the surgical field back through the aperture to the camera.

This system allows the image to be transported from its origin inside the body over a large number of individual components to the screen. Only if all individual components are coordinated with each other, a high-quality image is produced. The amount of light energy directed on the target is controlled by the width of each individual component [22]. Dilation of the light apertures of the endoscopic system increases the amount light energy reaching the target, and thus increases the illumination, defined as the light power per unit area of image [22].

### 34.3.2 Image Visualization and Processing

A brief discussion of image transmission within an endoscope is also instructive. The lens is at the distal end of the endoscope. The image that a lens produces from an object is a real image, but the image must be transported via intermediate images through a series of lenses within the rod lens. The image quality of an endoscope can be varied by features such as light intensity, focal length, viewing angle, and field of view. The field of view is described as the cone of visualization from the camera (Fig. 34.1) [23]. Field of view may also be represented as the two-dimensional visible area that is visualized at the focal length distance from camera [23, 24]. Although the term field of view is sometimes used interchangeably with angular field of view and angle of view, standardization of nomenclature helps to lend clarity to the terminology [23].

The optical angle of the endoscope refers to the angle between the middle axis of the camera and the axis of the endoscope. In general, the optical angle of spine endoscopes varies from 0 to 30° due to differences in manufacturing company, appropriate degrees of freedom for different spinal levels, and the purpose of the endoscopic instrument [25]. Typically, endoscopes designed for use in the cervical spine have a lower optical angle than endoscopes designed for use in the thoracic and lumbar spine. Larger optical angles allow for a larger surgical working window, as endoscopic rotation permits different viewpoints

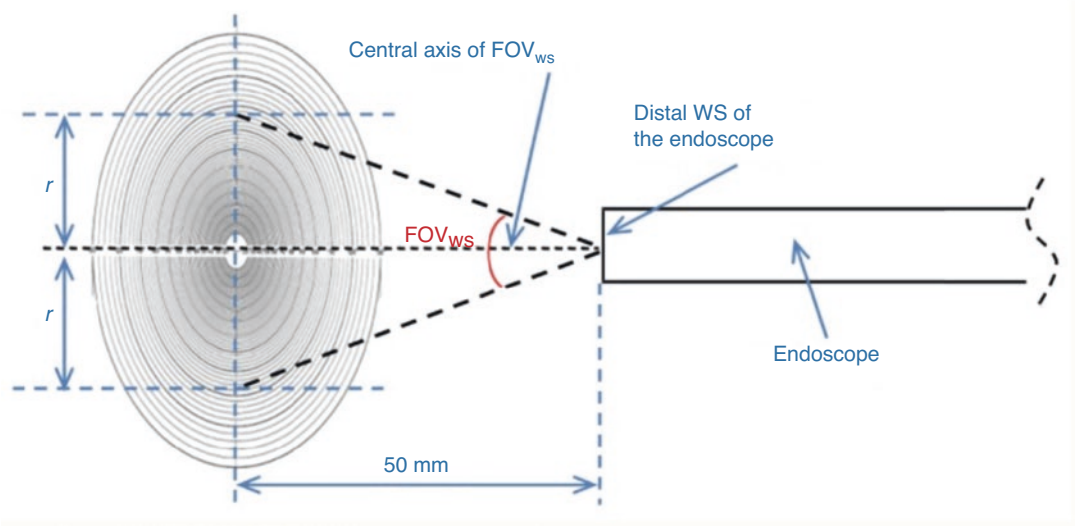


**Fig. 34.1** Endoscopic field of view (FOV) measurement from the window surface WS of an endoscope from Wang et al. [23]

of areas within the target tissue [26]. Furthermore, a greater optical angle prevents the field of view from being obstructed by instruments. But the unassisted human eye views the world through a 0° optical angle, and more degrees of freedom can lead to visual disorientation.

Focal length, usually represented in millimeters, is a calculation of the optical distance where the light rays converge to form a sharp image before transmitted through the endoscope to the digital interface. In most endoscopes, the focal length can be manually adjusted 10–40 mm by changing the distance between adjacent lenses. Longer focal lengths can provide narrow angles of view with higher magnification, allowing for less reposition to maintain appropriate visualization of target tissue [27].

In modern endoscopic surgery, the light images are digitalized and processed to be displayed on a screen, allowing for manipulation and recording. Video quality is determined by image resolution, rate of image refreshes, minimum luminance, and the signal to noise ratio. Image resolution, broadly, refers to the details an image holds. The term is measured by pixel count on a digital image, often in pixels per inch. Higher resolution correlates to greater image detail and sharpness. Most standard definition endoscope camera systems have a resolution of 1920 × 1080, with high-definition systems having resolutions up to 3480 × 2160. Image refresh rate is a measure of the number of distinct images captured and joined to produce a fluid video, with most systems having refresh rates of 50–60 Hz. Each camera system has a minimum brightness at which the target must be illuminated to be detected, known as the minimum luminance [28]. A lower minimum required luminance corresponds to a better camera system. Finally, the signal to noise ratio compares the magnitude in intensity of the detected image relative to the uncertainty in image transmission through the camera system [29]. A higher signal to noise ratio is indicative of a higher quality image.

## 34.4 Methods of Enhanced Visualization

Having discussed the basic scientific principles of modern endoscopes, potential targets of enhanced visualization begin to become clear. Firstly, we will discuss simple yet novel transformative means of enhancing visualization.

These techniques do not rely upon advanced endoscopic technology, but rather manipulation of a patient's tissue. Having established these techniques, we will then discuss more advanced means of enhanced visualization including optical manipulation and imaging processing.

## 34.5 Methods of Direct Tissue Manipulation

### 34.5.1 Topical Chromoendoscopy

Chromoendoscopy and endoscopic tattooing are two techniques which have been pioneered by general surgeons, but that have clear applications to neurosurgical practice. Chromoendoscopy refers to the use of topical stains or dyes or, more recently, the use of optic technologies such as narrow-band imaging (NBI; **Olympus** Medical Systems Corporation, Tokyo, Japan) to improve tissue visualization during endoscopic surgery [30, 31]. Dye-based chromoendoscopy utilizes various agents such as methylene blue and indigo carmine to preferentially stain pathologic tissue [30, 31]. This preferential staining can then be observed and acted upon by the practitioner under direct endoscopic visualization [30].

In reference to spinal surgery, this technique is referred to as "chromoendoscopic nucleotomy" and involves the use of indigo carmine to improve visualization of degenerated nucleus pulposus [32]. Indigo carmine is a "contrast stain" (i.e., it is not absorbed into the cells themselves, but rather accumulates in the intercellular spaces, highlighting the surface architecture) [32]. This is in contrast to a "vital stain," such as methylene blue, which is absorbed intracellularly [32]. Indigo carmine is ideally suited for spine surgery as it has been shown to be especially reactive with the acidic extracellular matrix seen in degenerated disks [32].

In practice, chromoendoscopic nucleotomy is accomplished via percutaneous access to the disk space with a spinal needle under fluoroscopic guidance [33]. Once the disk space has been entered, a solution of indigo carmine mixed with contrast media is injected and fluoroscopy is used to confirm successful infiltration [33]. The surgeon can then introduce a guide wire and proceed in a usual fashion with an endoscopic discectomy guided by the blue staining of degenerated disk material which is easily visualized using standard, un-enhanced endoscopic equipment (Fig. 34.2) [34].

This technique, however, is limited in its ability to truly identify the offending tissue—namely because indigo carmine does not discriminate between normal senescent disk and pathologic degenerated disk material causing symptomatology [32]. Therefore, while chromendoscopic nucleotomy will aid the practitioner in identifying the nucleus pulposus, it does little to inform how much of the stained nuclear material to

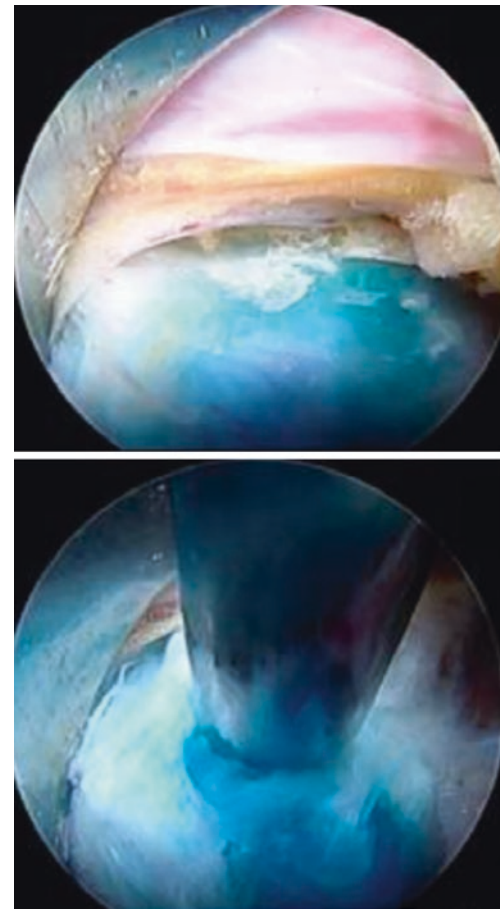

**Fig. 34.2** Intraoperative endoscopic photographs from Wu et al. study demonstrating bluish hue of degenerated disk material stained with indigo carmine [34]

remove, nor in which anatomic location it should be preferentially removed. Much like the topical chromoendoscopy utilized in general surgery, this technique therefore represents a simple, low-tech means of enhancing visualization.

### 34.5.2 Endoscopic Tattooing

Much like topical chromoendoscopy, endoscopic tattooing relies upon local tissue manipulation under standard endoscopic illumination. Specifically, this technique utilizes a locally applied tattoo agent (usually carbon-based) to allow re-identification of pathologic tissue at a later date [35]. Endoscopic tattooing is conceptually unique from other methods of tissue identification and enhanced visualization discussed in this chapter, as it does not attempt to identify pathologic tissue in and of itself, but rather serves as a marker for a surgeon to resume previous work. Specifically, it has been used to help tag abnormal tissue identified on endoscopy for subsequent surgical intervention [35].

While the medium used for endoscopic tattooing varies, carbon-based tattooing agents such as India Ink are most commonly cited in the literature [35, 36]. More recently, due to side effects associated with these compounds (including infection and local tissue ulceration) other tattoo agents such as indocyanine green (ICG) have shown promise [37, 38]. A major and well-recognized limitation of endoscopic tattooing is the short life of the tattoo mark on the biologic tissue. In one study, a number of stains were investigated, with only ICG and India Ink lasting longer than 48 h and with ICG persisting for only 7 days [39]. These findings are notable, as they limit the efficacy of this technique for long-term tissue marking.

Although this technique has not yet been applied to neurosurgical practice, it represents an interesting conceptual avenue worthy of further exploration. Specifically, this technique offers a means of aiding a spine surgeon in maintaining anatomic orientation—a common problem resulting from an interplay between a limited field of view, an unnatural optical angle, and patient/scope orientation. A more detailed discussion of its potential application is contained later in this manuscript.

## 34.6 Methods of Light Transformation

### 34.6.1 Optical Chromendoscopy

Perhaps more compelling than the aforementioned techniques is optical chromoendoscopy: the usage of optical imaging technology to enhance visualization [31]. The term "optical chromendoscopy" does not refer to one specific technology but rather a family of techniques including NBI, flexible spectral color imaging enhancement (FICE, Fujinon), and i-scan (Pentax) [31]. To understand how these new technologies serve to enhance imaging, we must compare them to traditional endoscopic imaging, which as previously discussed, encompasses the full visible wavelength (~400–700 nm). This "white light," however, is produced using various methodologies.

Indeed, technology developed over the past half century has relied almost solely upon choosing from naturally available light spectra. Historically, lamps relied on different metal (carbon, tungsten) filaments for illumination, but as the technology behind luminance advanced, we have shifted toward using plasma arcs for illumination within operative microscopes. Initially developed lamps with carbon filaments had the disadvantage of a low vaporization temperature of the filament, necessitating operation at a lower voltage, resulting in emission of a yellow light [40]. Tungsten filaments have the advantage of a higher vaporization temperature, allowing application of a greater voltage and generation of brighter light from the source [40]. However, the downside to tungsten filaments is that their use over time results in the formation of a blue-black soot deposit along the inside of the bulb [41]. Lamps with carbon and tungsten filaments generate light output with a continuous spectrum of wavelengths, extending from the ultraviolet (<400 nm) to infrared

(>700 nm). Fortunately, with the utilization of light energy from plasma arc lamps such as high pressure mercury HBO lamps, we are able view objects up to 100 times brighter than incandescent bulbs [42]. HBO lamps remain a workhorse in fluorescence microscopy and are still considered a great source of illumination over specific wavelengths. Xenon arc lamps (XBO) generate significant light energy and subsequently fail to produce prominent emission lines, and thus are more suitable for quantitative electron microscopy (Fig. 34.3) [43].

Alternatively, the usage of NBI has the potential to highlight mucosal aberrations without changing the physical medium with staining agents (as described above) [31]. Instead of using a broader light spectrum, NBI illuminates tissue surfaces using special filters that enhance the relative intensity of the blue band [31]. In doing so, the resulting narrow, high-intensity blue band only penetrates the mucosa superficially and scatters less, thus enhancing the color contrast between diseased and normal tissue [31]. Enhanced visualization of subtle anatomic differences has clear oncologic applications, and has been used broadly across multiple subspecialties (Fig. 34.4) [44–46].

In the neurosurgical area, NBI has been praised for its ability to enhance the visualization of very fine vessels and its ability to contrast abnormal from normal architecture in a more detailed manner than conventional modes [45]. The optical filter allows two narrow wavelength bands. The first blue band, emitted at 450 nm, will have a more superficial penetration, and will therefore function to highlight surface architecture. The second emitted green band (540 nm) will provide better imaging of deeper tissue [45]. Each individual image compiled from both bands will be integrated and processed to produce a single, sharp image [45]. FICE and i-scan result in similar image outputs NBI, but process reflected photons to reconstruct virtual images, rather than using optical filters [31]. Regardless of the mechanism, however, each of these technologies represents a means of altering visual perception by manipulating light output.

### 34.6.2 LASER as a Light Source

Advances and modification in the endoscope light source have the potential to be the next step to enhance visualization of the surgical field. Traditional endoscopic spine surgery relies on white light produced by a xenon light source. Using other alternatives can result in higher quality images. Although the application of optical chromoendoscopy produces sharply distinctive images of microstructures because of a narrow bandwidth by using an optical filter, one disadvantage of this technique is the production of darker images limiting the observation of distal anatomic structures [47]. Understanding the physical properties of light amplification by the stimulated emission of radiation or laser technology is key for the successful utilization of this method as a potential light source to overcome the limitations of conventional light sources and the use of optical filters. Laser light is by definition predominantly monochromatic and of a narrower bandwidth (2 nm), compared to the bandwidth of NBI (30 nm) [48]. This narrower bandwidth translates into higher spectral resolution. Endoscopic laser imaging is accomplished by combining two laser sources of different wavelengths (410 nm and 450 nm), thereby producing a brighter and higher-resolution image when compared to the conventional endoscope system using a xenon light source [47, 49]. This technology is being employed in other endoscopic specialties [50] and seems promising to endoscopic spine area.

## 34.7 A Culmination of Methods: Tissue Manipulation with Light Transformation

As previously mentioned, the term “fluorescence” describes the emission of light which occurs after the absorption of higher energy light. This property is present in certain chemical substrates and has been used in multiple surgical arenas—perhaps most pertinently in cranial neurosurgery. In this regard, a number of agents

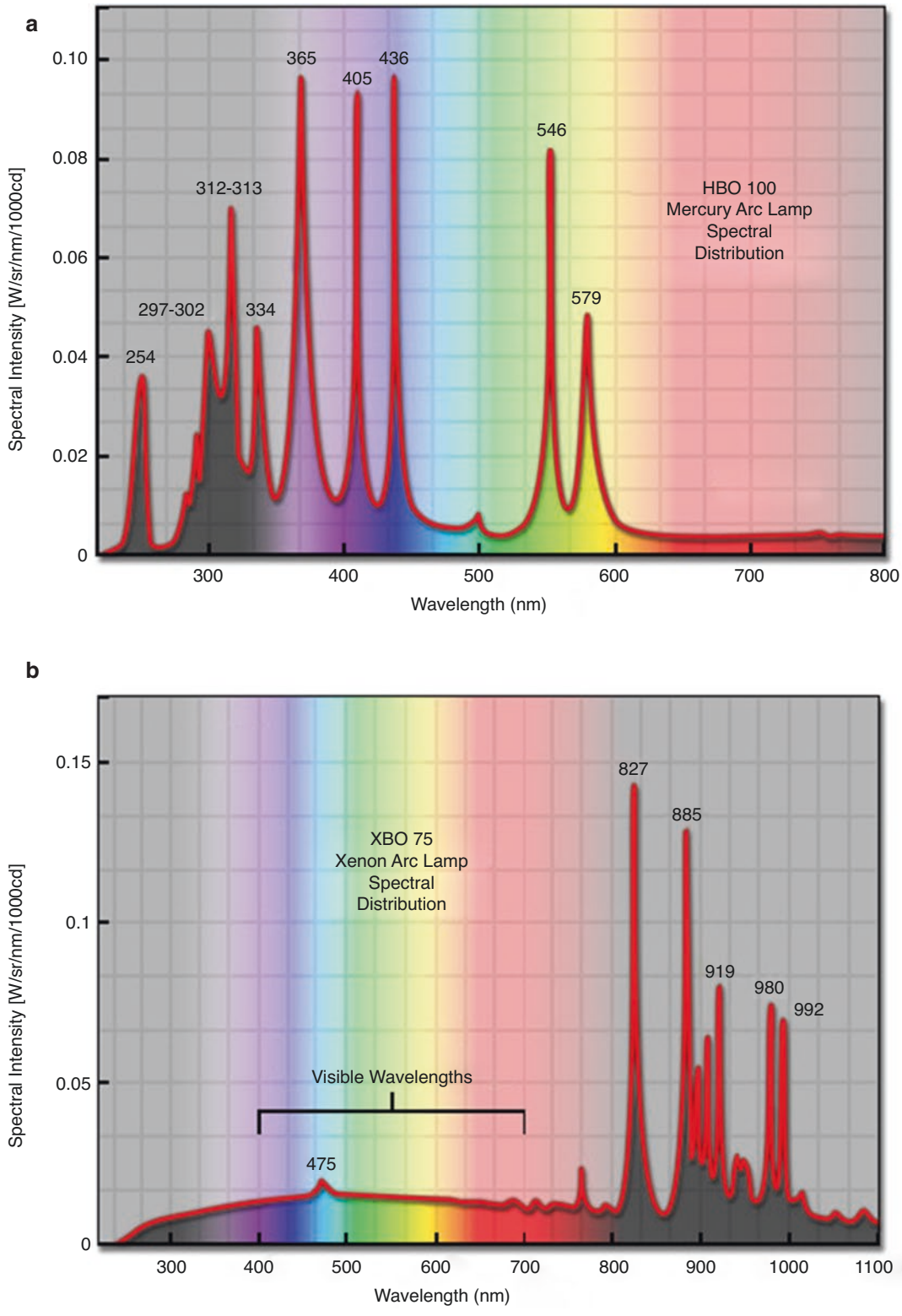


**Fig. 34.3** Spectral distribution of a 100 W high pressure mercury arc lamp (HBO) [42] (**a**) and xenon arc lamp (XBO) [43] (**b**)

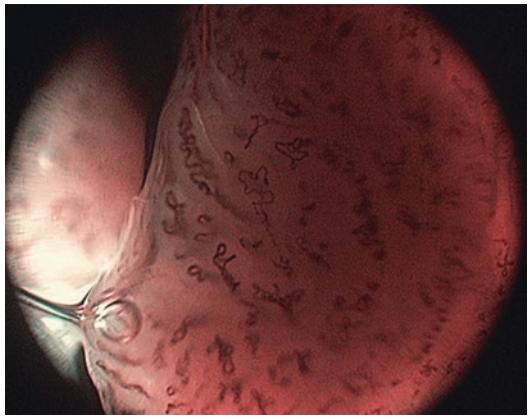

**Fig. 34.4** Intraoperative photo from Piazza et al. demonstrating contact endoscopy with narrow-band imaging [44]. Perpendicular vascular patterns with regularly distributed loops with wide-angled turning points in the right vocal cord

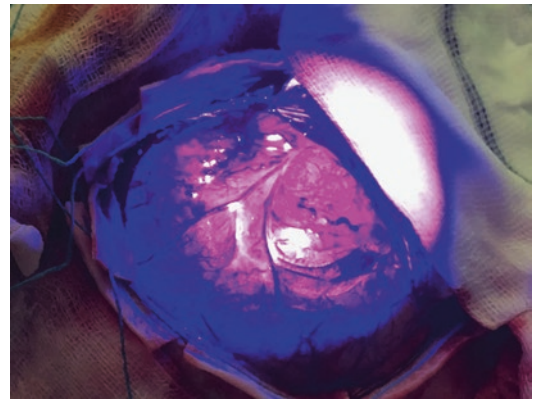

**Fig. 34.5** Intraoperative photo from Verburg et al. demonstrating 5-ALA-guided resection of superficial glioblastoma with clear pink fluorescence of the tumor with the surrounding normal tissue appearing blue [54]

are commonly used, including 5-aminolevulinic, indocyanine green, and fluorescein.

### 34.7.1 5-ALA

Fluorescence-based imaging to guide cranial surgery, especially within the realm of glioblastoma resection, has been clearly described within the pertinent literature [51–53]. This technique harnesses the natural precursor to hemoglobin, 5-aminolevulinic (5-ALA), which elicits synthesis and concentration of fluorescent porphyrins within malignant glioma cells [52, 53]. In clinical practice, 5-ALA is given prior to surgery, and a modified neurosurgical microscope is used intraoperatively to visualize residual malignant glioma tissue to aid in tumor resection [52]. Such diseased tissue will emit red/pink fluorescence in contrast to normal architecture (Fig. 34.5) [54]. This technique is thought to be more precise than simply administering fluorescent agents through a disrupted blood–brain barrier, as the malignant tissue produces the fluorescent porphyrins endogenously [52].

### 34.7.2 Indocyanine Green

Indocyanine green (ICG), a near-infrared dye, has proven extremely valuable to contemporary neurovascular surgery [55]. Several important and unique biochemical properties of ICG make it an attractive operative aid when administered intravenously. First, the ICG remains intravascular due to its affinity for globulins. Secondly, the specific absorption and emission peaks of ICG are unlikely to be absorbed by other endogenous chromophores [55]. Thus, ICG will only fluoresce when the surgical field is illuminated by a light source within the specific absorption band of ICG [55]. This fluorescence can then be visualized using a microscope equipped with a specialized filter (Fig. 34.6) [56].

Interestingly, due to ICG's previously described binding affinity for intervascular globulins, it can be utilized to identify the vascular vaso nervorum within peripheral nerves. This property has been described in application to intraoperative peripheral nerve visualization. For example, the superior cluneal nerve is classically challenging to identify and decompress within surgery due to its small cali-

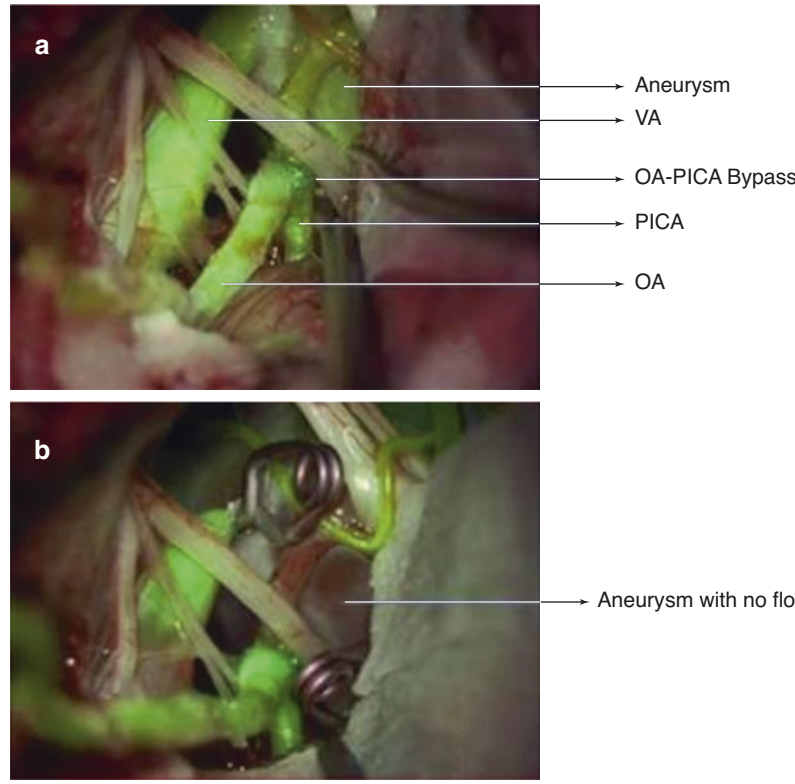


**Fig. 34.6** Intraoperative photos from Balaji et al. demonstrating (**a**) dual image video angiography (DIVA) with ICG assistance showing filling of the aneurysm, occipital artery (OA)-posterior inferior cerebellar artery (PICA) bypass completed. (**b**) Post-trapping DIVA shows no flow in the aneurysm and good flow in the OA-PICA. *VA* vertebral artery [56]

ber and anatomic location within lipomatous tissue [57]. ICG can therefore be used to aid not only in nerve identification, but also to assess the degree and adequacy of surgical decompression [57]. Similar applications can be conceived for endoscopic spinal decompression surgery, where neural decompression is often the primary surgical objective.

### 34.7.3 Fluorescein

Intrathecal fluorescein is especially advantageous within endoscopic skull base surgery, as its ability to cause a yellow pigmentation of CSF allows the surgeon to assess for CSF leaks. It is typically injected intrathecally at a low dose to identify fistulous points. Under ambient lighting fluorescein has a bright yellow color, and therefore is typically easily distinguishable from other secretions which may otherwise be confused for CSF. This property of fluorescein, however, is only one facet of its full potential.

In recent years, there have been technological advances to harness the full capacity of the fluorescent properties of fluorescein [58]. For example, Carl Zeiss Meditec has developed a modified microscope which contains properties that allow the user to visualize fluorescence in contrast to normal surrounding tissue [58]. This module, coined YELLOW 560 (Carl Zeiss Meditec, Oberkochen, Germany), employs certain wavelength ranges that perfectly align with fluorescence stimulation (460–500 nm) and detection (540–690 nm), thus fully optimizing the fluorescent properties of fluorescein [58]. The future potential of this technology within spinal endoscopic neurosurgery can allow for better identification of the thecal sac, exiting nerve root, and other neural structures.

### 34.7.4 Laser Scanning Confocal Endomicroscopy

Laser scanning confocal endomicroscopy (LSCE) represents a final additional avenue of interest with regard to endoscopic approaches to the spine. To date, this technology has been applied to intraoperative tissue diagnosis in cranial neurosurgery, and leverages fluorescent tumor labeling as previously discussed [59]. LSCE relies upon laser scanning confocal microscopy (LSCE) which uses a laser of a specific wavelength to cause fluorophore excitation within tissues [59]. The emitted photons are then passed through two filters: (1) an objective filter and (2) a pinhole (confocal) aperture which allows for visualization of thin tissue sections [59]. This technology obviates the need for frozen sections taken intraoperatively (Fig. 34.7) [60].

As with other fluorescent technologies discussed, LSCE requires the presence of fluorophores within the tissue being examined [59]. We have previously discussed commonly used fluorescent agents in the neurosurgical arena, and they include fluorescein, ICG, and 5-ALA [59]. While the application of this technology to neurosurgery is still in the early stages, it has been described in the literature with respect to differentiating normal tissue from neoplastic tissue using ICG, and the in vivo visualization of areas of hypercellularity and necrosis [59, 61–63].

## 34.8 Methods of Image Processing

### 34.8.1 Three-Dimensional Endoscopy

The use of three-dimensional endoscopy has become increasingly more prevalent in numerous surgical specialties. 3-D endoscopes have been used in cardiothoracic procedures such as coronary artery bypass surgery, ENT procedures including ear and lateral skull base surgery, and neurosurgical procedures such as transsphenoidal endonasal skull base surgeries [64–67]. A major benefit of 3-D endoscopy, when compared to 2-D, is the ability for a surgeon to utilize depth perception to approximate distances without hav-

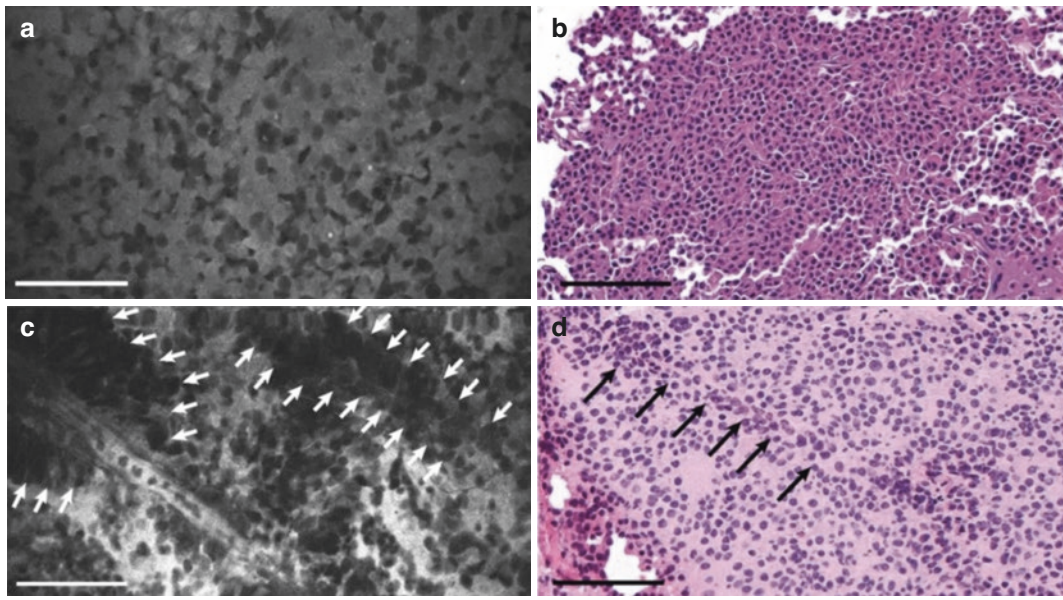


**Fig. 34.7** Photomicrographs of a pituitary adenoma from Belykh et al. demonstrating (**a**) Confocal laser endomicroscopy (CLE) image and (**b**) hematoxylin and eosin (H&E) stain of the same tumor showing sheets of uniform nonlobulated cells with prominent nuclei. (**c**) CLE image and (**d**) H&E image showing perivascular sheets of the cells (arrows). Bar = 100 μm [60]

ing to move the endoscope, as needed in traditional 2-D endoscopy [65].

In traditional 2-D endoscopy, images are displayed on a monitor through capturing and processing, as described before. 3-D imaging requires a more complicated process to obtain and visualize images, termed stereoscopic encoding. Two distinct cameras within the 3-D endoscope, oriented at different angles to converge on a point equidistant to the focal lengths of both, are used to produce two separate images. The images are processed identically and visualized with the image from the left camera projected to the left eye and the right camera projected to the right eye. The user is then able to view the combined image through either a virtual reality headset or 3-D glasses [64].

Stereoscopic encoding is not without pitfalls. For instance, because the point of convergence of the two endoscopic cameras must match the focal length of both lenses, tissues within the periphery of the image can appear out of focus and blurry. This difference can cause intraoperative disorientation. One group overcame this obstacle by using a diffractive optical element (DOE), which utilizes a projector to scatter a laser light, identifying the distance of the endoscope from tissues to determine optimal focus length [68].

## 34.9 Looking Forward: The Future of Endoscopic Spinal Surgery

While spinal endoscopy has improved dramatically from its humble beginnings, it has yet to undergo a fundamental paradigm shift with regard to light manipulation and enhanced visualization. Indeed, higher quality camera systems with improved digital displays represent marginal improvements on an existing technology. The expansion of the indications for endoscopic spine surgery and the proliferation of its practice necessitates investigation and integration of existing enhanced visualization technologies utilized outside this field.

In order to justify widespread adoption in any endoscopic practice, new or enhanced imaging technology must have the following qualities: (1) the risk of harm to the patient must be exceedingly low; (2) it must be economically reasonable and scalable; and (3) it must result in minimal prolongation of total operative time. Therefore, as we review the abovementioned techniques and attempt to apply them to neuro-endoscopy of the spine, we will do so using these three qualities as a framework for understanding their utility.

An important facet for the novice learner within endoscopic surgery is the ability to correctly identify important neurovascular structures. Such challenges are heightened with respect to reoperations or cancerous tissue, where anatomy may be scarred or distorted. While we have discussed existing technologies such as the use of indigo carmine to visualize pathology, these technologies fail to identify normal neural tissue. We can utilize the fact that low-dose fluorescein is safely used to detect cerebrospinal fluid leaks in neurosurgical patients, and re-purpose this property for endoscopic spine cases [69, 70]. For example, the YELLOW 560 module could be utilized in conjunction with injected fluorescein to illuminate important neural structures such as the nerve root sleeve and thecal sac. The technical challenges of this application, however, must carefully be considered.

The usage of technologies such as NBI and FICE also appear to offer significant promise for endoscopic spine surgeons. While they have not yet been tested expressly for this purpose, it seems evident that the vasculature of the dura and surrounding musculature and connective tissue will differ significantly, and these technologies *should* therefore be able to provide improved contrast between these two media. In addition, the use of more potent light sources, as it is the case with laser technology, could translate into enhanced visualization of the surgical field. While cadaveric and in vivo testing would be required to validate this, this technology seems ideally suited for spinal neuro-endoscopy, as it offers the promise of improved tissue differentiation without the need to access the subarachnoid space.

We can also begin to think about novel ways in which these technologies may make surgery safer and more effective. As an example, if we revisit

the concept of endoscopic tattooing, we can conceive re-purposing this technology for spinal neuro-endoscopy. Specifically, if a surgeon were to "tattoo" the edges of the annulus, there would be numerous advantages: (1) the landmarks would allow a surgeon to maintain a defined orientation as the endoscopic procedure frequently requires endoscope (and therefore image) rotation, which can be disorienting; (2) having a stable landmark of reference will help surgeons know if they have successfully completed the surgical procedure (e.g., removal of concealed disk herniations behind the dura can be inferred from the altered location of the landmark); (3) automated removal of pathology is more reliable and secure with a fixed anatomic frame of reference proximate to the pathology; and (4) finally, as a teaching method it would allow trainees to more safely work unassisted [71–74].

Additionally, as the scope of endoscopic surgery inevitably expands, one could envision a role for laser confocal endomicroscopy in an endoscopic tumor debulking and possible endoscopic tumor biopsy. The usage of 3-D endoscopy in spine surgery in synergy with other existing technologies is compelling. For example, an intradiscal carmine blue injection could be used in conjunction with fluorescence imaging. While one would identify clearly pathologic tissue, the other would highlight normal neural anatomy, providing an additive and synergistic contrast effect. The reality of being able to clearly identify the surgical target and also the tissues most at risk for iatrogenic injury will enhance the safety of spinal endoscopy, leading to greater adoption.

## References


1. Yang Y, Liu ZY, Zhang LM, et al. Microendoscopy-assisted minimally invasive versus open transforaminal lumbar interbody fusion for lumbar degenerative diseases: 5-year outcomes. World Neurosurg. 2018;116:e602–10.
2. Kolcun JPG, Brusko GD, Basil GW, Epstein R, Wang MY. Endoscopic transforaminal lumbar interbody fusion without general anesthesia: operative and clinical outcomes in 100 consecutive patients with a minimum 1-year follow-up. Neurosurg Focus. 2019;46(4):E14.
3. Ahn Y, Youn MS, Heo DH. Endoscopic transforaminal lumbar interbody fusion: a comprehensive review. Expert Rev Med Devices. 2019;16(5):373–80.
4. Kafadar A, Kahraman S, Akboru M. Percutaneous endoscopic transforaminal lumbar discectomy: a critical appraisal. Minim Invasive Neurosurg. 2006;49(2):74–9.
5. Wang H, Huang B, Li C, et al. Learning curve for percutaneous endoscopic lumbar discectomy depending on the surgeon's training level of minimally invasive spine surgery. Clin Neurol Neurosurg. 2013;115(10):1987–91.
6. Wang H-Z, He H-X, Feng J, Chen X-D, Lin W. The actual nature of light (I) reveal the mystery about the actual nature of light from Newton, Einstein to the recent mistakes. J Quantum Inf Sci. 2011;1(02):54.
7. Born M, Wolf E. Principles of optics: electromagnetic theory of propagation, interference and diffraction of light. Elsevier; 2013.
8. Aspect A. From Huygens' waves to Einstein's photons: Weird light. Comptes Rendus Physique. 2017;18(9–10):498–503.
9. Huygens C, Huygens C. Traité de la lumière (Bruxelles): Culture et civilisation. 1967.
10. Worrall J. The pressure of light: the strange case of the vacillating 'crucial experiment'. Stud Hist Phil Sci Part A. 1982;13(2):133–71.
11. Saleski CG. Color, light, and shade matching. J Prosthet Dentistry. 1972;27(3):263–8.
12. Guilbault GG. Practical fluorescence, vol. 3. CRC Press; 1990.
13. Di Ieva A, Tam M, Tschabitscher M, Cusimano MD. A journey into the technical evolution of neuroendoscopy. World Neurosurg. 2014;82(6):e777–89.
14. Zada G, Liu C, Apuzzo ML. "Through the looking glass": optical physics, issues, and the evolution of neuroendoscopy. World Neurosurg. 2013;79(2 Suppl):S3–13.
15. Spaner SJ, Warnock GL. A brief history of endoscopy, laparoscopy, and laparoscopic surgery. J Laparoendosc Adv Surg Tech A. 1997;7(6):369–73.
16. Linder TE, Simmen D, Stool SE. Revolutionary inventions in the 20th century. The history of endoscopy. Arch Otolaryngol Head Neck Surg. 1997;123(11):1161–3.
17. Bush RB, Leonhardt H, Bush IV, Landes RR. Dr. Bozzini's Lichtleiter. A translation of his original article (1806). Urology. 1974;3(1):119–23.
18. Shah J. Endoscopy through the ages. BJU Int. 2002;89(7):645–52.
19. Oka K, Ohta T, Kibe M, Tomonaga M. A new neurosurgical ventriculoscope–technical note. Neurol Med Chir (Tokyo). 1990;30(1):77–9.
20. Cheng D, Wang Y, Yu L, Liu X. Optical design and evaluation of a 4 mm cost-effective ultra-high-definition arthroscope. Biomed Opt Express. 2014;5(8):2697–714.
21. Zhang YJ, Hsu JC, Tsao JH, Sun YS. Fabrication of a bare optical fiber-based biosensor. Micromachines (Basel). 2019;10(8)

22. Liu CY, Wang MY, Apuzzo ML. The physics of image formation in the neuroendoscope. Childs Nerv Syst. 2004;20(11–12):777–82.
23. Wang Q, Khanicheh A, Leiner D, Shafer D, Zobel J. Endoscope field of view measurement. Biomed Opt Express. 2017;8(3):1441–54.
24. Van Gompel JJ, Tabor MH, Youssef AS, et al. Field of view comparison between two-dimensional and three-dimensional endoscopy. Laryngoscope. 2014;124(2):387–90.
25. Klein SM, Nielsen KC, Ahmed N, Buckenmaier CC, Steele SM. In situ images of the thoracic paravertebral space. Reg Anesth Pain Med. 2004;29(6):596–9.
26. Kwak JM, Kholinne E, Gandhi M, et al. Improvement of arthroscopic surgical performance using a new wide-angle arthroscope in the surgical training. PLoS One. 2019;14(3):e0203578.
27. Schulz-Hildebrandt H, Pieper M, Stehmar C, et al. Novel endoscope with increased depth of field for imaging human nasal tissue by microscopic optical coherence tomography. Biomed Opt Express. 2018;9(2):636–47.
28. Laparra V, Berardino A, Balle J, Simoncelli EP. Perceptually optimized image rendering. J Opt Soc Am A Opt Image Sci Vis. 2017;34(9):1511–25.
29. Xia W, Chen ECS, Peters T. Endoscopic image enhancement with noise suppression. Healthc Technol Lett. 2018;5(5):154–7.
30. Committee AT, Wong Kee Song LM, Adler DG, et al. Chromoendoscopy. Gastrointest Endosc. 2007;66(4):639–49.
31. Buchner AM. The role of chromoendoscopy in evaluating colorectal dysplasia. Gastroenterol Hepatol (N Y). 2017;13(6):336–47.
32. Kim IS, Kim KH, Shin SW, Kim TK, Kim JI. Indigo carmine for the selective endoscopic intervertebral nuclectomy. J Korean Med Sci. 2005;20(4):702–3.
33. Kim MJ, Lee SH, Jung ES, et al. Targeted percutaneous transforaminal endoscopic diskectomy in 295 patients: comparison with results of microscopic diskectomy. Surg Neurol. 2007;68(6):623–31.
34. Wu PH, Kim HS, Jang IT. Intervertebral disc diseases PART 2: A review of the current diagnostic and treatment strategies for intervertebral disc disease. Int J Mol Sci. 2020;21(6)
35. Committee AT, Kethu SR, Banerjee S, et al. Endoscopic tattooing. Gastrointest Endosc. 2010;72(4):681–5.
36. Nizam R, Siddiqi N, Landas SK, Kaplan DS, Holtzapple PG. Colonic tattooing with India ink: benefits, risks, and alternatives. Am J Gastroenterol. 1996;91(9):1804–8.
37. Ashida R, Yamao K, Okubo K, et al. Indocyanine green is an ideal dye for endoscopic ultrasound-guided fine-needle tattooing of pancreatic tumors. Endoscopy. 2006;38(2):190–2.
38. Dell'Abate P, Iosca A, Galimberti A, Piccolo P, Soliani P, Foggi E. Endoscopic preoperative colonic tattooing: a clinical and surgical complication. Endoscopy. 1999;31(3):271–3.
39. Hammond DC, Lane FR, Welk RA, Madura MJ, Borreson DK, Passinault WJ. Endoscopic tattooing of the colon. An experimental study. Am Surg. 1989;55(7):457–61.
40. Worthing AG. Atomic heats of tungsten and of carbon at incandescent temperatures. Phys Rev. 1918;12(3):199–225.
41. Taylor JH, Rupert CS, Strong J. An incandescent tungsten source for infrared spectroscopy. J Opt Soc Am. 1951;41(9):626–9.
42. Davidson MW. Fundamentals of mercury arc lamps. 2020. http://zeiss-campus.magnet.fsu.edu/articles/lightsources/mercuryarc.html. Accessed 19 Apr 2020.
43. Davidson MW. Fundamentals of xenon arc lamps. Education in microscopy and digital imaging web site. 2020. http://zeiss-campus.magnet.fsu.edu/articles/lightsources/xenonarc.html. Accessed 19 Apr 2020.
44. Piazza C, Del Bon F, Peretti G, Nicolai P. Narrow band imaging in endoscopic evaluation of the larynx. Curr Opin Otolaryngol Head Neck Surg. 2012;20(6):472–6.
45. Sasagawa Y, Akai T, Nakada S, et al. Narrow band imaging-guided endoscopic biopsy for intraventricular and paraventricular brain tumors: clinical experience with 14 cases. Acta Neurochir (Wien). 2014;156(4):681–7.
46. Diorio GJ, Canter DJ. Adjunctive use of narrow band imaging during transurethral resection/vaporization of bladder tumors to aid In identifying mucosal and sub-mucosal hypervascularity. Can J Urol. 2015;22(2):7763–6.
47. Osawa H, Yamamoto H. Present and future status of flexible spectral imaging color enhancement and blue laser imaging technology. Dig Endosc. 2014;26(Suppl 1):105–15.
48. Yoshida N, Hisabe T, Inada Y, et al. The ability of a novel blue laser imaging system for the diagnosis of invasion depth of colorectal neoplasms. J Gastroenterol. 2014;49(1):73–80.
49. Suzuki T, Kitagawa Y, Nankinzan R, Yamaguchi T. Early gastric cancer diagnostic ability of ultrathin endoscope loaded with laser light source. World J Gastroenterol. 2019;25(11):1378–86.
50. Shimoda R, Sakata Y, Fujise T, et al. The adenoma miss rate of blue-laser imaging vs. white-light imaging during colonoscopy: a randomized tandem trial. Endoscopy. 2017;49(2):186–90.
51. Sexton K, Davis SC, McClatchy D III, et al. Pulsed-light imaging for fluorescence guided surgery under normal room lighting. Opt Lett. 2013;38(17):3249–52.
52. Stummer W, Pichlmeier U, Meinel T, et al. Fluorescence-guided surgery with 5-aminolevulinic acid for resection of malignant glioma: a randomised controlled multicentre phase III trial. Lancet Oncol. 2006;7(5):392–401.
53. Stummer W, Stocker S, Wagner S, et al. Intraoperative detection of malignant gliomas by 5-aminolevulinic

acid-induced porphyrin fluorescence. Neurosurgery. 1998;42(3):518–25. discussion 525-516
54. Verburg N, de Witt Hamer PC. State-of-the-art imaging for glioma surgery. Neurosurg Rev. 2020;
55. Raabe A, Nakaji P, Beck J, et al. Prospective evaluation of surgical microscope-integrated intraoperative near-infrared indocyanine green videoangiography during aneurysm surgery. J Neurosurg. 2005;103(6):982–9.
56. Balaji A, Rajagopal N, Yamada Y, Teranishi T, Kawase T, Kato Y. A retrospective study in microsurgical procedures of large and giant intracranial aneurysms: an outcome analysis. World Neurosurg X. 2019;2:100007.
57. Kim K, Isu T, Chiba Y, et al. The usefulness of ICG video angiography in the surgical treatment of superior cluneal nerve entrapment neuropathy: technical note. J Neurosurg Spine. 2013;19(5):624–8.
58. Rey-Dios R, Cohen-Gadol AA. Technical principles and neurosurgical applications of fluorescein fluorescence using a microscope-integrated fluorescence module. Acta Neurochir (Wien). 2013;155(4):701–6.
59. Mooney MA, Zehri AH, Georges JF, Nakaji P. Laser scanning confocal endomicroscopy in the neurosurgical operating room: a review and discussion of future applications. Neurosurg Focus. 2014;36(2):E9.
60. Belykh E, Ngo B, Farhadi DS, et al. Confocal laser endomicroscopy assessment of pituitary tumor microstructure: a feasibility study. J Clin Med. 2020;9(10)
61. Martirosyan NL, Cavalcanti DD, Eschbacher JM, et al. Use of in vivo near-infrared laser confocal endomicroscopy with indocyanine green to detect the boundary of infiltrative tumor. J Neurosurg. 2011;115(6):1131–8.
62. Foersch S, Heimann A, Ayyad A, et al. Confocal laser endomicroscopy for diagnosis and histomorphologic imaging of brain tumors in vivo. PLoS One. 2012;7(7):e41760.
63. Sankar T, Delaney PM, Ryan RW, et al. Miniaturized handheld confocal microscopy for neurosurgery: results in an experimental glioblastoma model. Neurosurgery. 2010;66(2):410–7. discussion 417-418
64. Endo Y, Nakamura Y, Kuroda M, Ito Y, Hori T. The utility of a 3D endoscope and robot-assisted system for MIDCAB. Ann Thorac Cardiovasc Surg. 2019;25(4):200–4.
65. Bernardeschi D, Lahlou G, De Seta D, Russo FY, Mosnier I, Sterkers O. 3D endoscopic ear surgery: a clinical pilot study. Eur Arch Otorhinolaryngol. 2018;275(2):379–84.
66. Chen CK, Hsieh LC, Hsu TH. Novel three-dimensional image system for endoscopic ear surgery. Eur Arch Otorhinolaryngol. 2018;275(12):2933–9.
67. Altieri R, Tardivo V, Pacca P, et al. 3D HD endoscopy in skull base surgery: from darkness to light. Surg Technol Int. 2016;29:359–65.
68. Furukawa R, Sanomura Y, Tanaka S, et al. 3D endoscope system using DOE projector. Conf Proc IEEE Eng Med Biol Soc. 2016;2016:2091–4.
69. Placantonakis DG, Tabaee A, Anand VK, Hiltzik D, Schwartz TH. Safety of low-dose intrathecal fluorescein in endoscopic cranial base surgery. Neurosurgery. 2007;61(3 Suppl):161–5. discussion 165-166
70. Felisati G, Bianchi A, Lozza P, Portaleone S. Italian multicentre study on intrathecal fluorescein for craniosinusal fistulae. Acta Otorhinolaryngol Ital. 2008;28(4):159–63.
71. Basil G, Brusko G, Brooks J, Wang MY. The value of a synthetic model-based training lab to increase proficiency with endoscopic approaches to the spine. Cureus. 2020;12(3)
72. Wang B, Lu G, Patel AA, Ren P, Cheng I. An evaluation of the learning curve for a complex surgical technique: the full endoscopic interlaminar approach for lumbar disc herniations. Spine J. 2011;11(2):122–30.
73. Park SM, Kim HJ, Kim GU, et al. Learning curve for lumbar decompressive laminectomy in biportal endoscopic spinal surgery using the cumulative summation test for learning curve. World Neurosurg. 2019;122:e1007–13.
74. Sharif S, Afsar A. Learning curve and minimally invasive spine surgery. World Neurosurg. 2018;119:472–8.

# MIS-TLIF with 3D Navigation and Augmented Reality Enhanced

35

Fabian Sommer, Jacob L. Goldberg, Sertac Kirnaz, Lynn McGrath, Cameron Rawanduzy, Franziska Schmidt, Branden Medary, and Roger Härtl

## 35.1 Introduction

The continuous advancements in treatments for degenerative spine disease have seen translumbar interbody fusion (TLIF) via a posterior approach become a mainstay procedure that achieves excellent results [1–3]. The advent of minimally invasive surgery (MIS) and the development of MIS-TLIF has produced additional benefits such as reductions in intraoperative blood loss and decreased hospital length of stay, among others [4]. However, an MIS approach can present challenges to the surgeon and a learning curve exists in the initial experiences. There is a more limited visual field in MIS compared to an open technique that requires adjusting to the intraoperative orientation [2, 5].

In MIS-TLIF, identifying anatomical landmarks is paramount to success. The use of image-guided spinal surgery (IGSS) is commonly incorporated to facilitate proper orientation within the narrow surgical field [6]. One of the most established IGSS techniques is 3D navigation, and more recently augmented reality (AR) has been introduced as an add-on to this [7]. AR is defined as an augmentation or enhancement of the real world obtained by superimposing computer-generated images into the user's field of view. The technology offers many possibilities to improve IGSS as AR can perfectly integrate with 3D navigation [7]. This can be particularly useful in MIS-TLIF.

### 35.1.1 Preoperative Planning

Intraoperative 3D navigation can be employed without relevant preoperative planning, while thorough planning is required for AR. A high-resolution MRI or CT is necessary for AR, but because these are usually performed as part of the preoperative diagnostics, they are available in most cases without additional organizational effort or radiation exposure.

Preoperative planning for AR-enhanced IGSS can be completed with the appropriate software developed by the manufacturer (in the example, images of the planning software of the company Brainlab (Brainlab AG, Munich, Germany)). The preoperative MRI or CT data sets are imported into the software program and then relevant structures are marked and labeled using a drawing tool function (Smartbrush). The recom-

F. Sommer (✉) · J. L. Goldberg · S. Kirnaz
L. McGrath · C. Rawanduzy · F. Schmidt · B. Medary
Department of Neurological Surgery, New York-Presbyterian Hospital/Weill Cornell Medical Center, New York, NY, USA
e-mail: fjv4001@med.cornell.edu

R. Härtl
Department of Neurological Surgery, Weill Cornell Medicine Center for Comprehensive Spine Care New York Presbyterian OCH SPINE, New York, NY, USA



J.-S. Kim et al. (eds.), *Technical Advances in Minimally Invasive Spine Surgery*,
https://doi.org/10.1007/978-981-19-0175-1_35

mended structures to identify and overlay with AR for MIS-TLIF are:

1. Lamina of vertebral arch (upper corresponding vertebra).
2. Pars interarticularis (upper corresponding vertebra).
3. Ipsilateral pedicles.
4. Disc space.
5. Contralateral pedicles (optional).

In the current version of the software, automatic pedicle identification is already possible and only the lamina, the pars interarticularis, and the disc space have to be separately and manually highlighted. This may change in future versions where all recommended structures could be automatically identified.

AR should not be seen as a replacement for 3D navigation, but rather as a complementary visual guide to support the identification of the critical anatomy.

### 35.1.2 Procedure Steps

The MIS-TLIF technique is dependent on the stepwise identification of key anatomical landmarks and therefore follows a tailored workflow that is standardized for almost every case [5]. The steps for MIS-TLIF with combined 3D navigation and AR support are described below [6].

Intraoperative low dose CT: At the start of the case, intraoperative low-dose CT is performed to generate an imaging dataset that corresponds to the patient's actual spinal anatomy while on the operating table. Prior to this CT, a reference array is placed as close to the target spinal segment as possible. Maximizing the accuracy of surgical access is essential due to the mobility of the spine; so for this reason, in MIS-TLIF, the reference array is usually placed at the iliac crest. This also ensures it does not interfere with the procedure or contaminate the field. An example of an operating room setup is shown in (Fig. 35.1).

1. Level orientation: Once the patient is positioned and CT is obtained for navigation, the target spinal segment is located using 3D imaging and a navigated pointer. No additional fluoroscopic images are required at this time, thus reducing the further radiation exposure for the surgical team and the patient. The patient is then marked on the skin to map out incision sites for the implantation of the pedicle screws and the surgical approach (Fig. 35.2).
2. Image fusion: The preoperative imaging data used to plan landmarks that are going to be superimposed with AR must be fused with the intraoperative scans. This is known as elastic image fusion. Because the preoperative images are typically taken with the patient in the supine position and the surgery is performed via a dorsal approach with the patient prone, the different alignments of the spine would result in an inaccurate representation of the planned structures. An important step to consider when merging the image data sets is that the target segments for MIS-TLIF should be the segments that are most closely aligned to minimize the digital correction necessary. After completion of the elastic image fusion, the accuracy of the combined data set should be verified using navigated pointers (Fig. 35.3).
3. Pedicle screw placement and preparation of tubular approach: The pedicle screw trajectory and placement can either be planned at this time intraoperatively, or the surgeon can use preoperatively planned screw placements from before the elastic image fusion. However, when performing a TLIF on a single segment, the time advantage of using preoperatively planned screws is usually marginal. Once accuracy is confirmed, the pedicle screws can be placed under navigation guidance, and to minimize tissue damage, the tubular retractor can be placed through the same skin incisions. The exact anatomical localization of the position of the tubular retractor and any potential readjustments of the tube are performed using a 3D navigated pointer (Fig. 35.4).
4. Calibration of the microscope and verification of the anatomical landmarks: When the tubular retractor position is finalized, the microsurgical dissection can proceed with utilization of the surgical microscope. The

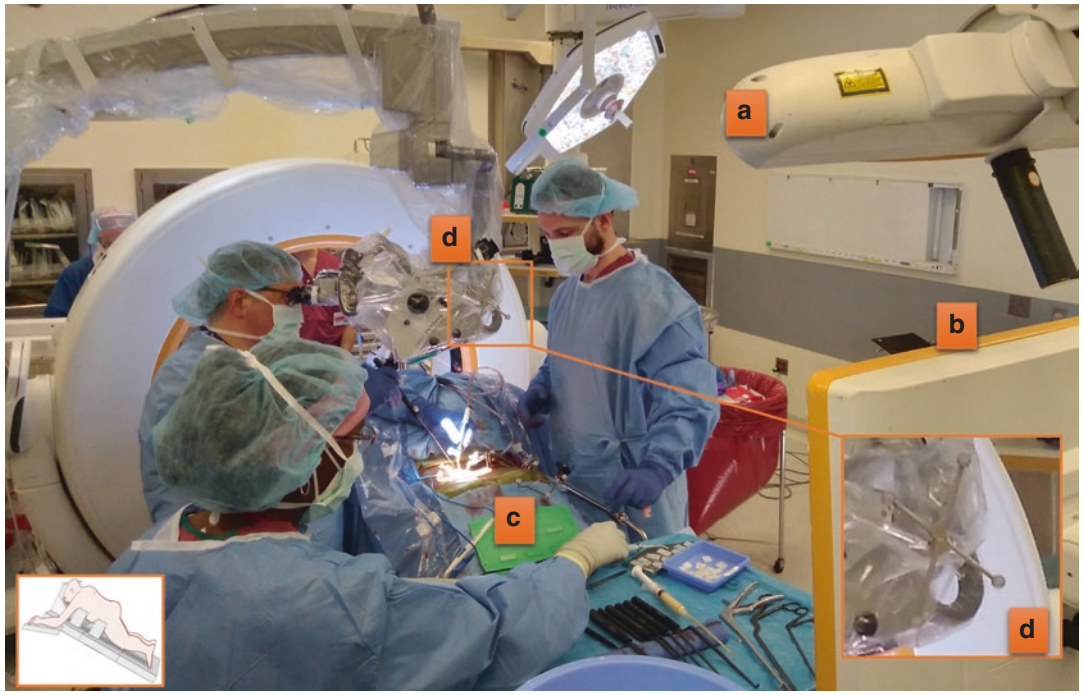


**Fig. 35.1** OR setup for AR navigation for a left sided TLIF approach with AR support. (**a**) Navigation Camera. (**b**) Navigation Screen. (**c**) Patient reference array. (**d**) Microscope reference array

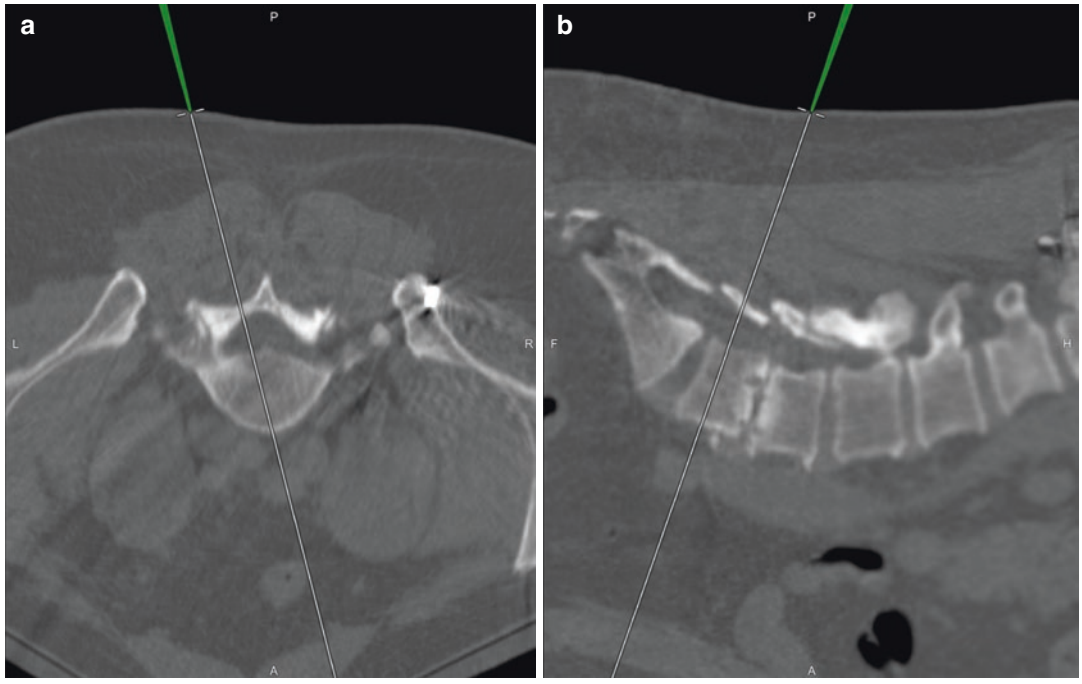


**Fig. 35.2** Axial (**a**) and sagittal (**b**) view of the navigation screen during spinal level orientation and planning of the approach trajectory using a navigated pointer and 3D navigation (green)

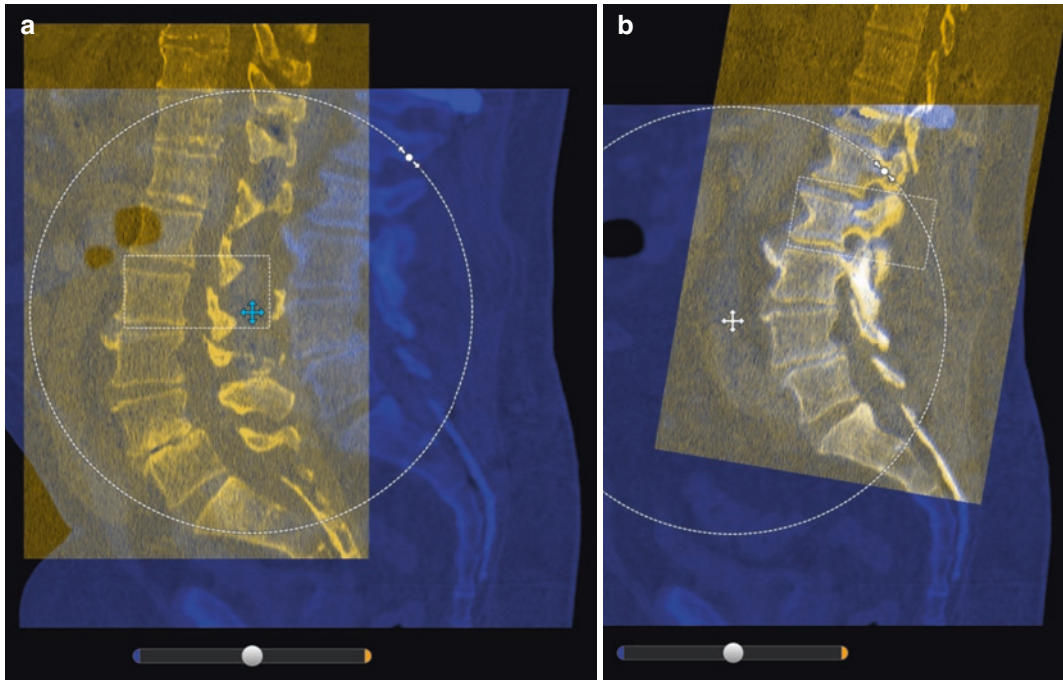


**Fig. 35.3** Screen view of elastic image fusion of the preoperative CT (yellow) and the intraoperative CT (blue) of a lumbar spine. The level to be operated on (L4/L5) is matched on both scans manually before the digital image fusion can be achieved accurately. Image (**a**): Screen view before manual matching; Image (**b**): Screen view after manual matching

microscope is put into position, which entails detection by the navigation system of its location with respect to the patient on the operating table. To accomplish this, another reference array is now attached to the microscope, and it is then calibrated to the reference array on the patient. At this point, the AR is fully operational, and the pre-identified landmarks can be projected onto the microscope's field of view during soft tissue dissection. To verify the approach, a navigated pointer confirms the bony landmarks. When verifying the lower edge of the medial lamina where the resection of the inferior facet starts, the correct position of the AR projection is simultaneously matched (Fig. 35.5).

5. Resection of the inferior articular process: The first step in the actual MIS-TLIF is the resection of the inferior facet of the corresponding superior vertebrae. This begins at the medial inferior edge of the ipsilateral lamina, and it is performed toward the ipsilateral pars interarticularis, which is the end point. The medial inferior edge of the ipsilateral lamina is highlighted by AR support to make it easier for the surgeon to find and then a high-speed drill is used for bone resection. Because of the narrow field of view, the end point of the resection at the edge of the pars interarticularis is also highlighted using AR to assist in showing the correct direction of the bone resection. An additional advantage of AR is the ability to display the position of landmarks, such as the pars, even when it is still outside the actual field of view of the tubular retractor. This in turn contributes to better orientation when performing bony resection. After the bone has been cut between these two landmarks, the inferior facet can be removed (Fig. 35.6).
6. Resection of the superior articular process: The next surgical step is resection of the superior facet to achieve exposure to the spinal canal. The anatomical landmark that this

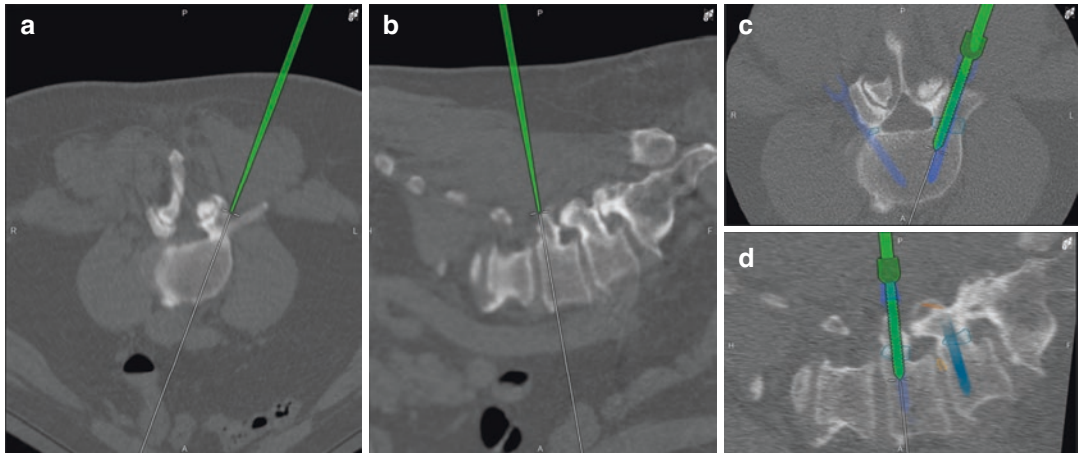


**Fig. 35.4** Axial (**a**) and sagittal (**b**) View of the navigation screen during verification of the position of a left L4 pedicle screw. Axial (**c**) and sagittal (**d**) view of the navigation screen during screw implantation in the left L4 pedicle. Preplanned screw positions are visible as blue shapes of screws

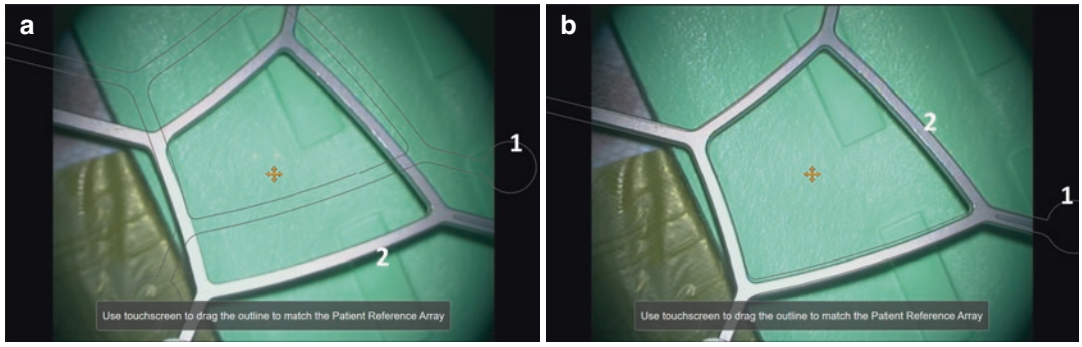


**Fig. 35.5** Microscope view of the calibration of the AR module of the surgical microscope. The digital border (1) of the patient's reference array (2) is projected in the microscope and has to be matched manually to the actual position of the array. Image (**a**): microscope view before calibration, the digital shape of the array and the actual position of the array do not match. Image (**b**): After manual calibration the digital shape matches the actual position of the reference array

resection is oriented on is at the ipsilateral pedicle of the lower corresponding vertebra. The exact level is determined by highlighting the pedicle using AR. Resection is performed using a high-speed drill again (Fig. 35.7).

7. Resection of the ligamentum flavum and mobilization of the dural sac: After the facet joint is removed, the ligamentum flavum and epidural fat are dissected so the dural sac can be sufficiently mobilized for subsequent discectomy and implantation of the expandable cage. During ligamentum flavum resection, the disc space is not visible yet due to tissue obstruction, so AR can help the surgeon to estimate the actual position of the disc space (Fig. 35.8).
8. Discectomy and cage placement: After sufficient mobilization of the dural sac, the intervertebral disc is exposed. The disc space is highlighted with AR to reinforce its location in the limited field of view. The disc is then incised using a scalpel and the discectomy is performed to create sufficient space for the cage. The depth of the discectomy space is verified using a 3D-navigated probe. When sufficient space is available, a cage filled

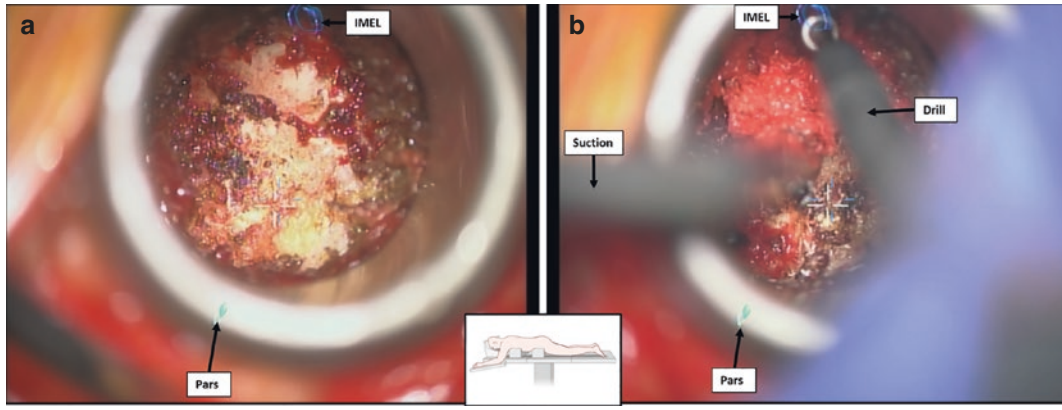


**Fig. 35.6** (**a**) Microscope view of the exposed anatomy of the inferior articular process (IAP) of the facet joint, the AR highlighted landmarks pars interarticularis (green) and inferior medial edge of the lamina (IMEL; blue) are visible. (**b**) Drilling of the bone during resection of the inferior facet between medial inferior edge of the lamina (blue) and the pars interarticularis (green)

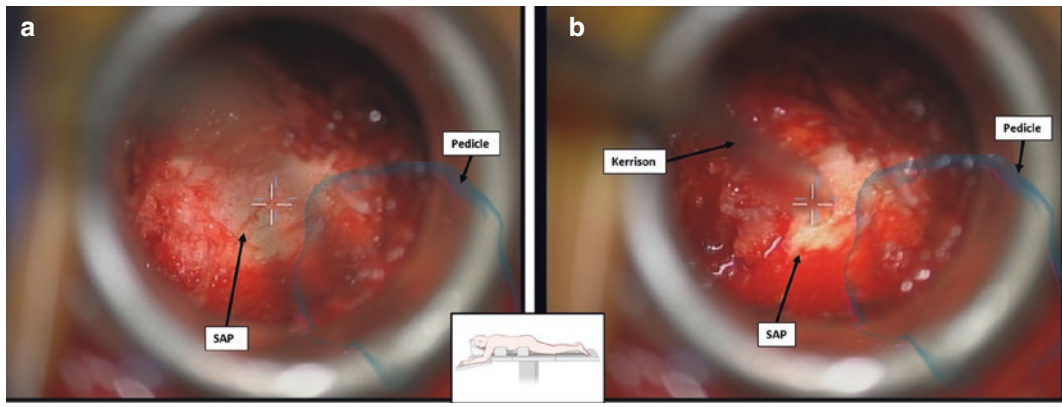


**Fig. 35.7** Microscope view of the resection of the superior articular process (SAP) of the facet joint. (**a**) Exposed anatomy of the superior facet after resection of IAP (**a**). The AR highlighted ipsilateral (left) L5 pedicle (blue) shows the anatomical level of the resection of the SAP. Image (**b**) Resection of the superior facet with Kerrison

with autologous bone graft is placed and, if necessary, expanded to achieve sufficient lordosis (Fig. 35.9).

9. Optional additional decompression of the spinal canal in "over the top" technique: The last step of the operation is only required if there is additional stenosis on the same segment. Here, the "over-the-top" technique is used to decompress the spinal canal. In this specialized MIS technique, the operating table is tilted slightly away from the surgeon to allow access to the contralateral side of the spinal canal. For better orientation, the pedicles of the contralateral side are highlighted by AR. This allows the surgeon to more easily estimate how much decompression is complete on the contralateral side of the spinal canal. If the anatomy is particularly difficult to visualize, additional confirmation using a navigated pointer is recommended (Fig. 35.10).
10. After implantation of the cage and possible decompression of the contralateral side of the spinal canal, the rods for stabilizing the spinal segments are inserted, connected to the pedicle screws, and locked in place. Final imaging verifies the implant position, then wound closure is performed.

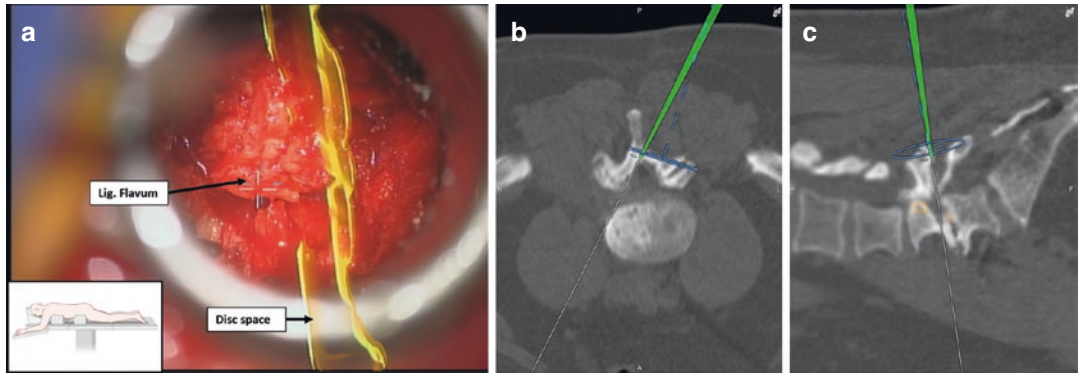


**Fig. 35.8** Image (**a**): Microscope view of the resection of the ligamentum flavum. The highlighted disc space (yellow) supports the orientation in the narrow field of view. Image (**b**)+(**c**): Axial (**b**) and View of the navigation screen during verification of the correct anatomical position using a navigated pointer (green). The round blue structure with the dashed line shows the focus plane and the angulation of the microscope

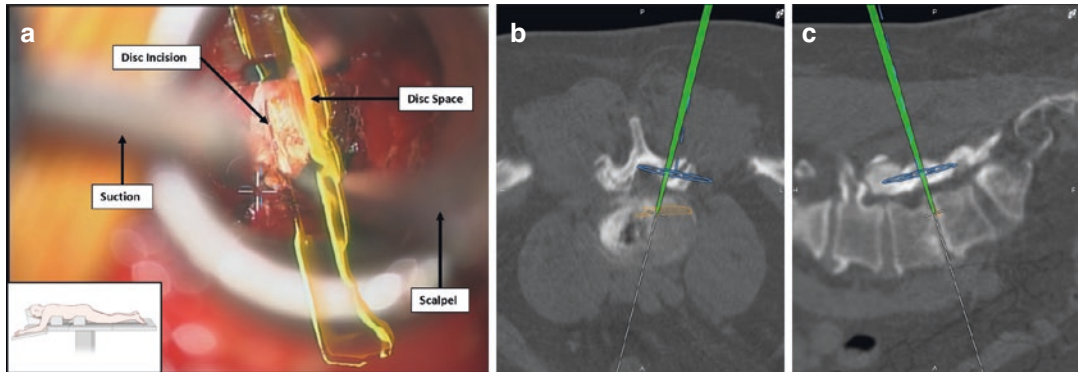


**Fig. 35.9** Image (**a**): Intraoperative view of the discectomy. The disc space is highlighted yellow using AR. Image (**b**)+(**c**): Axial (**b**) and sagittal (**c**) cuts of the navigation CT on the Navigation screen during evaluation of discectomy progress using a navigated pointer (green)

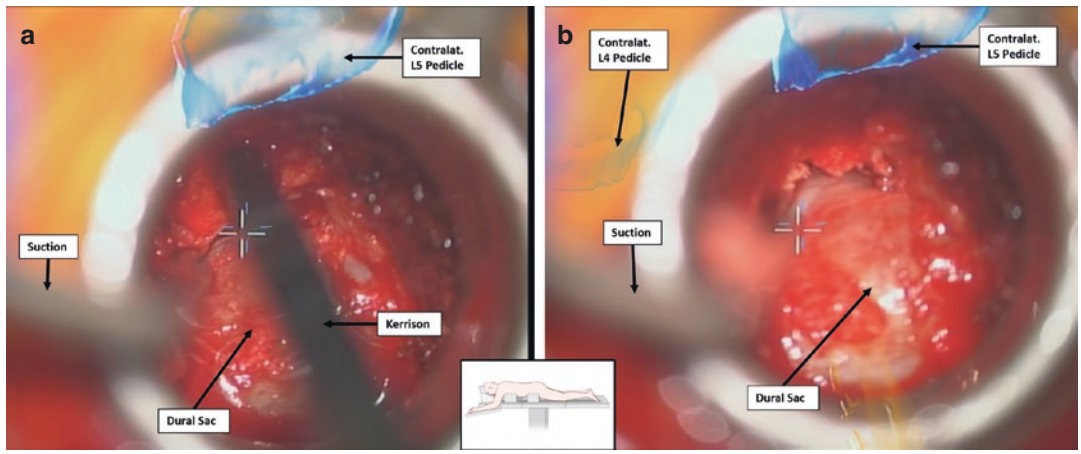


**Fig. 35.10** Image (**a**)+(**b**): Microscope view of an "over the top"-decompression of the contralateral side of the spinal canal. To facilitate the orientation, the contralateral pedicles are projected in the microscope

## 35.2 Summary

Minimally invasive surgical procedures have an inherently limited field of view, and they benefit from intraoperative navigation techniques. 3D navigation is an already popularly used IGSS system to facilitate correct intraoperative orientation, while augmented reality is a relatively new technique in the field of spinal surgery that has great potential to complement navigation. Rather than replace established methods, the goal when introducing AR into spine procedures should be to enhance the workflow. 3D navigation techniques allow for precise orientation of the surgical field, but surgery is frequently interrupted by the use of the navigated pointer. AR displays the targeted structures continuously during the actual surgery and improves the detailed orientation in the narrow field of view without interrupting the surgeon's workflow.

Ultimately, augmented reality can be incorporated into MIS without significant modification to the standard steps of the procedure. The only additional procedure steps are elastic image fusion and calibrating the microscope for AR, and considering the total duration of the operation, the time expenditure is insignificant and can possibly be accounted for in time saved during the course of the whole procedure by using AR.

Since the development of AR is currently still in its initial stages, further developments remain to be seen. One of these could be in the field of education. For example, AR could support surgeons in training by walking them through complex surgical procedures and highlighting the integral surgical landmarks of the current step as well as displaying the next procedure step. This could potentially help to improve the learning curve. At this time, the technology is a useful extension of 3D navigation, but there are many possible exciting applications in the future.

## References

1. Mobbs RJ, Phan K, Malham G, Seex K, Rao PJ. Lumbar interbody fusion: techniques, indications and comparison of interbody fusion options including PLIF, TLIF, MI-TLIF, OLIF/ATP, LLIF and ALIF. J Spine Surg (Hong Kong). 2015;1(1):2–18. https://doi.org/10.3978/j.issn.2414-469X.2015.10.05.
2. Avila MJ, Baaj A, Navarro-Ramirez R, Härtl R. Transforaminal lumbar interbody fusion (TLIF). In: Lumbar Interbody Fusions E-Book; 2018. p. 59.
3. Wu RH, Fraser JF, Härtl R. Minimal access versus open transforaminal lumbar interbody fusion: meta-analysis of fusion rates. Spine (Phila Pa 1976). 2010;35(26):2273–81. https://doi.org/10.1097/BRS.0b013e3181cd42cc.
4. McGirt MJ, Parker SL, Mummaneni P, et al. Is the use of minimally invasive fusion technologies associated with improved outcomes after elective interbody lumbar fusion? Analysis of a nationwide prospective patient-reported outcomes registry. Spine J. 2017;17(7):922–32. https://doi.org/10.1016/j.spinee.2017.02.003.
5. Härtl R, Gelb D, Nov NC. Step-by-step guide: key steps in a MIS TLIF procedure. 2015:1–9.
6. Lian X, Navarro-Ramirez R, Berlin C, et al. Total 3D Airo® navigation for minimally invasive transforaminal lumbar interbody fusion. Biomed Res Int. 2016;2016 https://doi.org/10.1155/2016/5027340.
7. Sommer F, Goldberg JL, McGrath L Jr, Kirnaz S, Branden Medary RH. Image guidance in spinal surgery: a critical appraisal and future directions. Int J Spine Surg.

# 36 Application of Extended Reality to MIS Lumbar Fusion

Daiuke Sakai, Wataru Narita, and Tokumi Kanemura

Minimally invasive spine surgery (MISS) is becoming increasingly utilized for spinal surgery given smaller exposure sites, postoperative pain reduction, and fewer complications [1]. With reduced exposure, visualization is compromised, increasing reliance on surface anatomy and computed tomography (CT) imaging to guide surgeons. Thus, the market for navigation systems for spinal surgery is expanding to address this need, which is estimated to grow at 4.4% compound annual growth rate to $780 million by 2024 [2].

Navigation systems have begun to incorporate virtual, augmented, and mixed reality technologies into MISS procedures. Virtual reality (VR) integrates positional information from surgical instruments and translates them into three-dimensional (3D) virtual images based on previous CT or magnetic resonance imaging (MRI). This modality has been installed in education centers to train surgeons in simulations; however, these systems are traditionally expensive to acquire with no outcomes data on benefit to surgical training [3, 4]. Augmented reality (AR) combines a computer-generated virtual image based on prior imaging projected onto the surgical field. This gives the user direct visualization of the relevant anatomy with accurately perceived depth through a head-mounted display (HMD) to guide the surgeon, allowing the surgeon to maintain focus on the surgical field rather than reverting to a monitor. This differs from VR, as VR blends two virtual images in a virtual space whereas AR blends a virtual image into the user's real environment.

To further this integration of the real environment and virtual technologies, mixed reality (MR) platforms are now in development. This technology concept enables the user to interact with and manipulate both real and virtual components of their environment [5, 6]. With MR technologies, a surgeon can access anatomical information of the patient in real time, overlaying virtual holographic elements on the surface anatomy of the patient. MR is powered by the amount of input data received and output modalities available. For example, further variable input data such as patient positioning during spine surgery can be used to update and reposition virtual images, while the positional data in virtual images can guide the surgeon through various anatomic structures with haptic feedback in the

D. Sakai
Department of Orthopaedic Surgery, Surgical Science, Tokai University School of Medicine, Isehara, Kanagawa, Japan
e-mail: daisakai@is.icc.u-tokai.ac.jp

W. Narita
Department of Orthopedic Surgery, Kameoka Municipal Hospital, Kameoka, Kyoto, Japan

T. Kanemura (✉)
Department of Orthopedic Surgery, Spine Center, Konan Kosei Hospital, Konan, Aichi, Japan
e-mail: spinesho@vmail.plala.or.jp



J.-S. Kim et al. (eds.), *Technical Advances in Minimally Invasive Spine Surgery*,
https://doi.org/10.1007/978-981-19-0175-1_36

surgical instruments. These increased inputs and outputs aim to further blur the line between real and virtual to allow seamless navigation in MISS. VR, AR, and MR are collectively referred to as extended reality (XR) [7]. XR is being developed in combination with robotic-assisted surgery with the aim of alleviating surgeon fatigue and increasing precision of spinal realignment and stabilization. Increasing precision and consistency has become a primary objective of studies evaluating these technologies with the secondary aim of reducing surgical time and supporting fine motor control in MISS.

Since 1997, AR has been used in spine surgery through a system that superimposed a fluoroscopy-generated representation of the vertebra onto the surgeon's field of vision [8]. However, this innovative approach to visualization exposes patients and surgeons to considerably higher levels of ionizing radiation [9]. Modern AR navigation systems strive to lower patient and occupational exposure to ionizing radiation. Optimized imaging protocols utilizing AR now boast 0.01% exposure to radiation versus disease reported using other imaging modalities [10].

While various iterations of AR technologies have used CT [11], MRI [12–14], and X-ray [15], CT has gained favor given its fast acquisition high-resolution capabilities. MRI is limited by increased imaging times and the need for investment and physical space in a specialized metal-free OR, despite eliminating radiation exposure. MRI also requires permanent fixture installment and has a larger physical footprint in the OR. Multi-slice (32 and 64 slice) CT scanners have replaced cone-beam CT scanners with an increase in slice specification, reducing scan times [16–18]. Microsoft HoloLens is the most cited HMD device in spinal surgery [19–22], offering features beneficial to AR surgery such as gaze and eye tracking capabilities, gesture control, and user positional tracking. Infrared network device interface camera tracking systems (Xvision—Augmedics) enable uninterrupted device connection and feedback [23].

AR visualization is powered by the software it is built upon, including image processing and 3D rendering. The accuracy, precision, and resolution of these representations are crucial for optimal guidance with representative anatomy, depth perception, and tactile responses. Medtronic, Philips, and other MedTech companies are competing to develop state-of-the-art 3D rendering to integrate into their existing OR workflows to capture this growing market. Therefore, much of the source algorithms and imaging software are now proprietary, despite an initial open-source approach in the field. Image overlay and superposition of 3D rendering is dependent upon reference points. Some studies have superimposed 3D anatomical models onto the patient using localization by superficial skin markers [24, 25]. Using superficial markers, a maximum error of 1.8 mm across all three planes was recorded; however, rotational error was not recorded. Despite the promising results, this non-invasive point of reference is subject to distortion and increased margin of error, especially in obese patients versus reference points on bony landmarks such as the spinous process or iliac crest.

AR has been used in percutaneous vertebroplasty studying five patients with osteoporotic vertebral fractures [17]. Error of the insertion (EIA) angle was 2.09° ± 1.3° and 1.98° ± 1.8° in axial and sagittal planes on postoperative imaging. Pedicle screw placement has been the major focus of AR studies, exemplified by Elmi-Terander et al., undertaking a prospective cohort study of pedicle screw placement in patients [16]. Results demonstrated 94.1% overall accuracy of pedicle screw placement determined by Gertzbein Grade A or B. AR navigation has also been used in the planning and approach of intracranial tumor resection [26]. This has the benefit of reducing radiation exposure by 70% boasting a mean registration error of 1 mm. Neurosurgical procedures such as intracranial tumor resections have reported greater accuracy than spinal procedures reports [27–29], possibly due to the natural rigidity of the skull to retain the position of fiducial markers and the use of contrast imaging modalities with high resolution.

Most studies to date have investigated the precision and accuracy of AR systems in MISS, mostly focused on pedicle screw placement or

guide wire insertion. AR approaches have been used in MIS discectomy, localization for intracranial targets, and facet joint injections. CT-based imaging is most commonly employed in combination with Microsoft HoloLens which appears to be the HMD of choice. Output parameters include recorded registration error, angular deviation of the instrument path, and pedicle screw placement using a placement grading system (Gertzbein grade). Other measured parameters were variably included such as registration times, procedure time, successful screw insertion, and other specific parameters to individual procedures.

The aim of these preclinical, cadaveric, and first-in-man trials is to demonstrate the precision, accuracy, and reliability of these systems to facilitate widespread adoption across secondary care centers for less skilled users. In response to this growing technology, the FDA has laid strict approval criteria for procedures involving instrument approach, such as a pedicle screw, in accordance with Standard Practice for Measurement of Positional Accuracy of Computer Assisted Surgical Systems. This specifies registration error of less than 3 mm screw tip deviation and 3° angular deviation [30]. This approval criteria will help to standardize reporting for these systems given the heterogeneous and sometimes haphazard choice of parameters that have been reported to date. Meeting this standard and future of iterations of such systems will further the benefit and economic potential of this application of AR to attract capital investment, legislative approval, and widespread adoption.

There is a clear trend toward AR in an HMD system integrated with sensitive deep fiducial markers for image superposition. The benefits of AR implementation are apparent: visualization of deep anatomy in percutaneous approaches, simulated surgical training, and reduced learning curve for complex procedures facilitating more MISS. The further advantage of 3D rendering in AR visualization is the STL, OBJ 3D printable format, which can produce a physical construct identical to the original patient anatomy for surgery planning and simulation [31].

This technology is currently limited by variable inaccuracy and lack of comprehensive authorization standards by regulatory bodies. In addition, visual fatigue along with the need for re-registration and recalibration of equipment may deter users. Above all, installment costs, adaptation in OR workflow, and training of staff remain the biggest challenges in adopting such systems. These organizational and economic barriers can be reasonably offset with the guarantee of increased surgical accuracy, reduced revision rates, and a reduction in staff radiation exposure.

Given the trend toward HMD inclusion, it is important to recognize the current limitations of available devices. At present, image latency, low resolution, poor brightness, and contrast are all considered relative issues. Further to this, wireless devices may suffer from short battery lives, some failing to last the duration of the intended surgery. The best specifications of devices on the market today include 50 MB 3D rendering models, 2 K resolution per eye (47 pixels per degree of viewing angle) (Microsoft HoloLens 2), 16.8 million colors, and a 20 Hz refresh rate. Some battery lives also report beyond 5 h of continuous use. While these specifications reflect devices currently available, we anticipate substantial improvement in these systems in the coming years, expecting 4 K–8 K resolution and 60 Hz refresh rate, while rendering far more complex models, powered by advancements in other tech industries such as gaming.

Although these systems aim to reduce the learning curve of complex procedures, there is a steep learning curve in integrating this technology in itself, especially for those unaccustomed to AR. This entails a high cost of employee training in a market dominated by few providers. In addition, with future adoption there is a risk of producing a generation of trainees reliant on AR navigation without the capability of switching to free-hand instrumentation should the system fail, although this is speculative. The current challenges this technology faces result in an unclear value proposition for investors and adopters; however, increased precision, accuracy, and safety will establish its clinical relevance in the

most challenging applications such as tumor resections and complex deformities in MIS procedures.

## 36.1 Single Position Lateral Surgery with 3D Navigation Enhanced by XR

Applying XR to spine surgery, the author has developed a simulator for lateral lumbar interbody fusion (LIF) in the single position and an imaging assistant device that allows users to confirm the anatomy of each patient during surgery. The simulator represents the surgical table and three-dimensional anatomy in a virtual field, and the user can insert screws while moving freely in the field and observing the necessary anatomy at any cross section.

In the intraoperative image support system, the surgeon can set the screw trajectory before the operation and then project it onto the surgical field during the operation. Besides improving the surgeon's three-dimensional (3D) recognition of anatomy and spatial orientation, these technologies also provide medical education on surgical techniques. Moreover, they can simultaneously share the motions of surgical staff and the spatial background, along with medical images and medical record information. In this way, several people with head-mounted displays (HMDs) can enter the same virtual space and communicate in real time. Although the support system currently has limited positioning accuracy, it is expected to become a practical surgical support device as technology advances in the near future.

## 36.2 Extended Reality (XR)

XR and similar information technologies embrace human–machine interactions and the complex environment of physical and virtual realities generated by computer technologies and wearables (Fig. 36.1).

Recently, high-specification computers and smart devices, along with versatile applications and cloud services, have become readily available. The presented digital information is no longer limited to planar viewing on flat monitors and

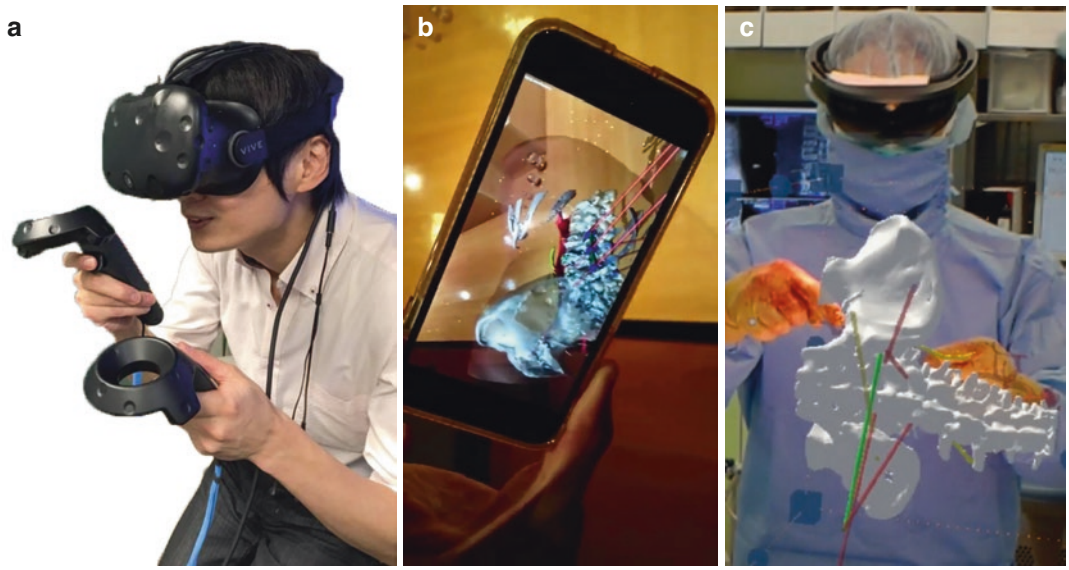


**Fig. 36.1** Extended reality (VR, AR, and MR): (**a**) Virtual reality (VR) uses a head-mounted device and a controller. Information from outside the device is completely shielded. (**b**) Augmented reality (AR) displays a spine model on a smartphone screen in real time. (**c**) Mixed reality (MR) simultaneously confirms the surgical field and model during the operation

smart tablets; now, it can also be viewed and experienced through wearable headsets, goggles, smart glasses, and other information terminals with built-in sensors. In clinical practice, these devices are widely used for surgical planning, surgical assistance, surgical training simulations, academic research, and education [6, 14, 32]. Recent advances in computer technology have changed the process of calculating images and delivering them to the visual fields of users. XR is a recently coined term for "reality technologies" that are often combined with other similar technologies; as such, they defy a distinct description.

## 36.3 Single Position Lumbar Interbody Fusion in VR Technology

VR technology has been determined to artificially stimulate the user's senses, generating an environment that is not seen in front of our eyes but which functionally resembles physical reality [33]. The non-delayed images displayed on an HMD impart a high level of immersion by real-time tracking of the angle and position of the HMD worn by the user. Moreover, by tracking the information of multiple controllers and providing feedback of this information through visuals and physical action such as vibrations, a VR system imparts the "feel" of the use.

LIF is an efficient, minimally invasive approach for anterior fusion of the lumbar spine using a specially designed retractor. LIF uses a large intervertebral cage with an approximate diameter of 50 mm, which is equivalent to the lateral diameter of the vertebral body. The minimally invasive LIF technique allows anterior column reconstruction, restoration of intervertebral height, and associated indirect decompression of the nerve, which previously required a relatively large skin incision and a broad surgical field. In addition to the conventional posterior approach methods (such as posterior and transforaminal LIF), the anterior minimally invasive LIF technique has become a useful option for spinal fusion surgery. Anterior surgery by the LIF technique is usually performed in the lateral decubitus position, followed by a posterior procedure with the patient placed in the supine position. When direct decompression of the nerve is not required, posterior fusion is commonly performed with percutaneous pedicle screws (PPS). Although the cortical bone trajectory technique is also deemed effective and minimally invasive for spinal fusion, it requires repositioning between the anterior and posterior fixations, which then increases the occupation time of the operating room and requires repeated procedures to create a sterile surgical field. We believe that safe PPS insertion while the patient is lying prone after the LIF procedure would be advantageous [34, 35]. From this viewpoint, we carefully selected the indications for spinal fusion using PPS in a single lateral decubitus position. However, users of this surgical technique must learn the spatial recognition and orientation of screw insertion, which may be difficult for surgeons who are familiar with PPS fixation in the supine position.

In 2016, the authors developed a VR simulation system for surgical planning and training [36]. In this system, the point cloud data must be converted into surface models (polygons) such as contour surfaces and cross sections that visualize the three-dimensional shapes of vertebrae, peripheral vessels, and ureters at the level of the vertebral body constructed from CT images. Here, the polygons were created using the medical mage analysis application OsiriX® (Pixmeo).

The files were modified by Meshmixer® (Autodesk, Inc.) (Fig. 36.2) and transferred to Unity® (Unity Technology, Inc.), a gaming image development platform. A Vive® (HTC Inc.) headset was used as the HMD. This simulator displays the surgical table and three-dimensional anatomy of the patients in the virtual space. The user is able to insert screws into the simulated body, while the user moves freely in the created space and the users can observe the desired anatomy at any cross section (Fig. 36.3). The screw in the virtual simulation is shaped identically to the actual screw because the computer-aided design data of the actual screw in clinical practice are imported into the Unity® system. The operating room equipment and anesthesiology data can

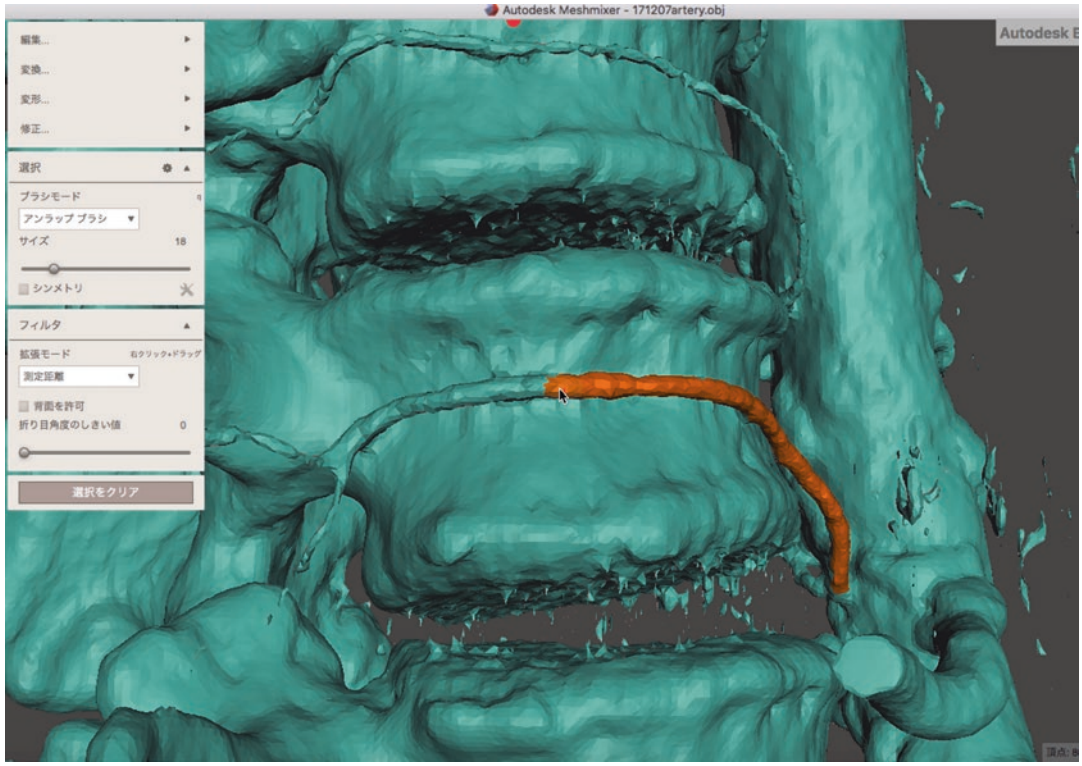


**Fig. 36.2** Extraction of segmental arteries using Meshmixer®

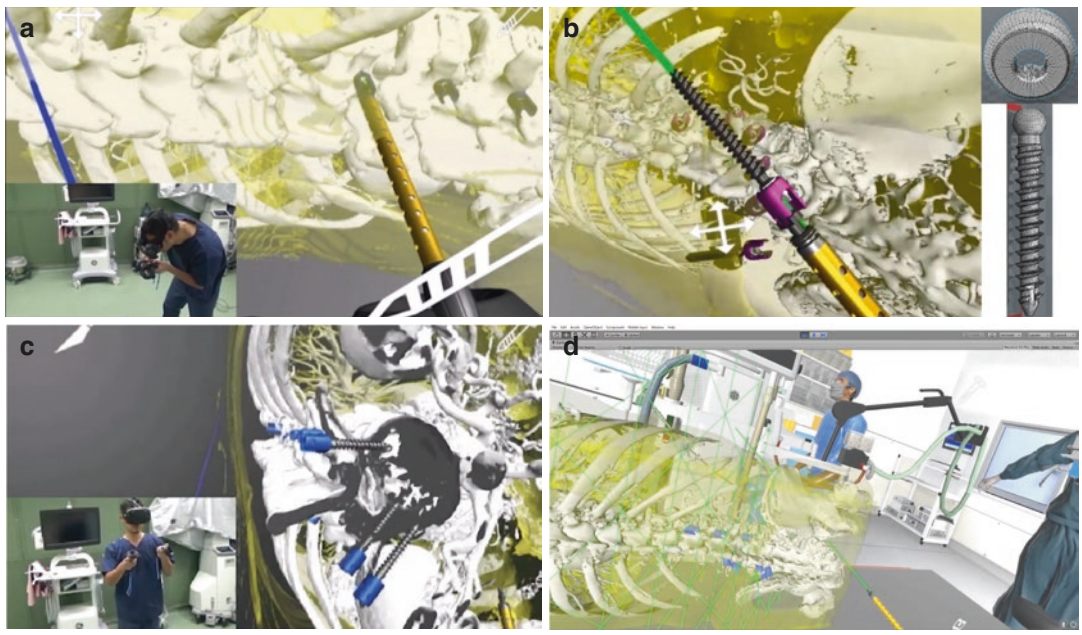


**Fig. 36.3** VR simulator: (**a**) The user can move freely in the virtual space while observing the three-dimensional anatomy. (**b**) The actual screw data are installed. (**c**) The user can observe any cross-sectional area using the controller. (**d**) Equipment and anesthesiologist in the operating room are displayed

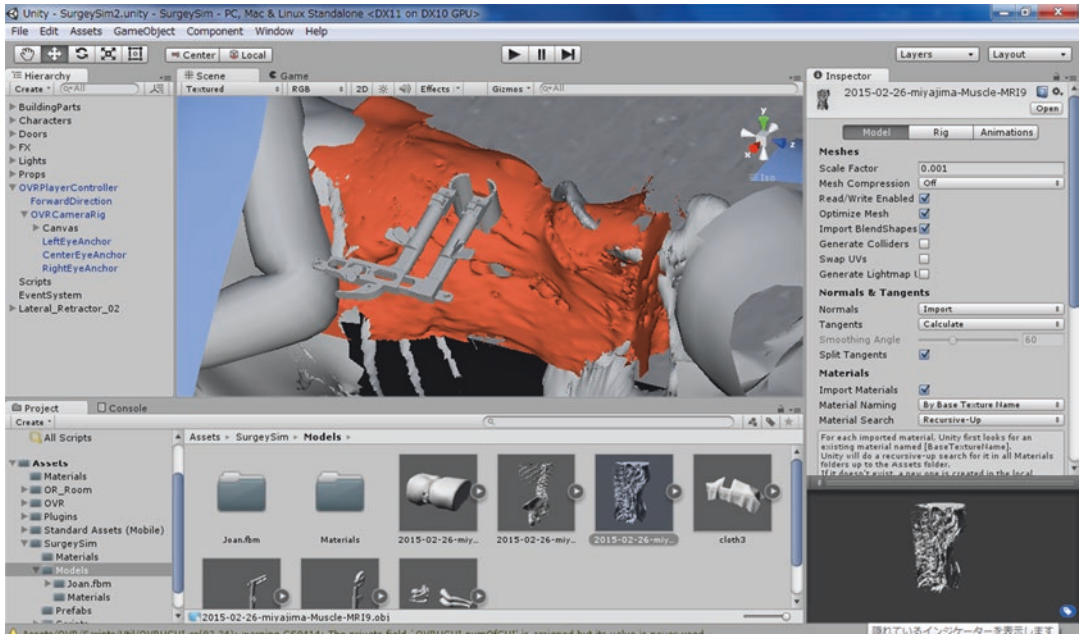


**Fig. 36.4** Unity supports the import of various modeling data (provided by Dr. Yuichiro Abe)

also be inputted into this simulation system. The Unity® technology then enables the visualization of surgical instruments and various other LIF devices in the VR simulation (Fig. 36.4).

## 36.4 Utility of Augmented Reality (AR) in Spinal Surgery

AR is identified as a general term for technologies that add real-time information to video recordings of real objects [37]. For example, software that adds computer-generated (CG) illustrations to the faces captured by smartphone cameras (which have remarkably developed in recent years) has been gaining popularity. In the field of spine surgery, Abe et al. [17] reported a surgical assistance device using AR and an HMD for percutaneous vertebroplasty (see Fig. 36.5). Although the AR system is compatible with non-transmissive HMDs, Abe et al. employed a transmissive-type HMD to superimpose the display on the user's visual field. Our MR specification (as described below) is based on a similar concept. Transmissive HMD and AR differ in one major aspect: whereas AR projects a 2D image of the stereoscopic space into the field of view, HMD performs 3D spatial positioning. Briefly, because AR measures the coordinates in 2D images, it is considered as a measurement technology rather than a display technology. In the prototype AR application developed by the authors, the spine model inputted by Unity is displayed in real time on the smartphone screen (Fig. 36.5).

## 36.5 Intraoperative MR Assistance for PPS in the Lateral Position

MR technology combines the real and virtual spaces, creating a new space in which the objects in both original spaces affect each other in real time [36, 38, 39]. MR includes the features of both VR and AR. Real views and CG images are synthesized in a transmissive HMD. The HoloLens® (Microsoft) version for developers, launched in 2016, is a leading MR device [40–43]. Although MR-implemented transmissive HMD systems (MR-HMD) existed before 2016, they were expensive (costing tens of thousands of

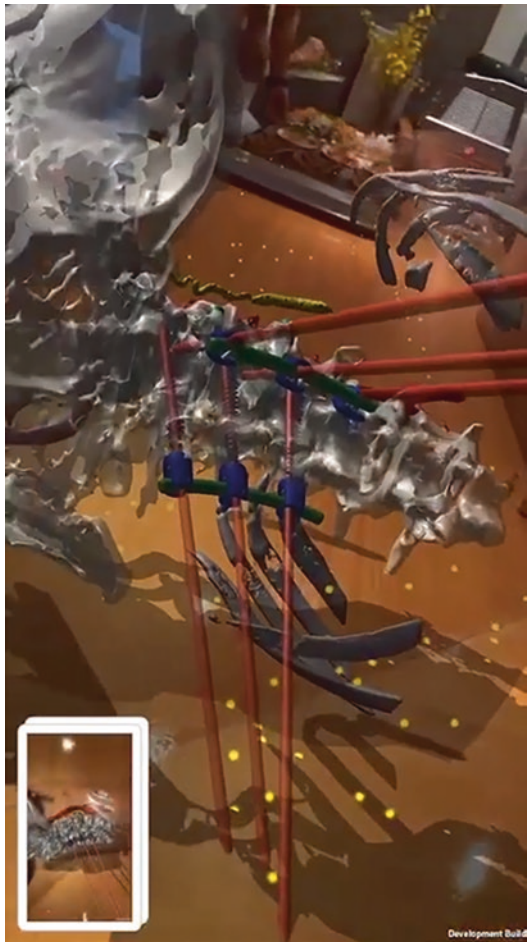


**Fig. 36.5** AR application running on a smartphone. Apple ARKit provides a spine model display on the screen

dollars), required wired connections to workstations, and weighed more than 1 kg. Therefore, they were deemed inaccessible to most users. The HoloLens® weighs only 579 g, lowering the physical effort of users, and its built-in battery allows approximately 5 h of operation. The HoloLens® is also equipped with four built-in environmentally aware cameras and an infrared projection device. Because position measurements are autonomously made by a special depth camera in the center of the device, no additional devices such as cameras or sensors are required outside of the user. Using the parallax of a half-mirror screen installed in front of the user's eyes, the system can update and display position- and time-consistent VR information in real space. The display frequency is 60–90 times per second. In addition, users of the same Wi-Fi system can share their spatial position information, meaning that multiple HMDs can simultaneously display the same spine 3D model.

In our system, the 3D surface models of the vertebrae, surrounding blood vessels, and ureter are extracted at the vertebra level from the CT image data and are inputted into Unity®. The screws, rods, and cages are synthesized following the surgical plan (Fig. 36.6). After installing the program on HoloLens®, we confirmed that MR-assisted surgery clearly depicts the vertebral bodies, blood vessels, ureter, and trajectories of the screws created in the preoperative planning while correcting the position of the 3D spine model superimposed on the surgical field in real time. Moreover, these capabilities were preserved when the surgeon moved within the MR field (Fig. 36.7). Besides improving the surgeon's understanding of 3D anatomy and spatial orientation, these techniques can also enhance medical education of surgical techniques.

The medical imaging software Holoeyes MD (Holoeyes, Inc.) is now commercially available as the "General Diagnostic Imaging Workstation Program." Certified as a medical device (Class II), this software can process and display the 3D image information obtained by diagnostic imaging equipment on an HMD (Oculus-Quest) and transmissive MR wearable glasses (Hololens2, Magic Leap 1, etc.). This software and display devices are used in surgical planning and intraoperative surgical assistance.

## 36.6 Remote Conferencing Using XR Technology (Teleconferencing)

The spread of the novel coronavirus has become a worldwide social problem; moreover, it has driven the shift toward non-contact and remote operations [44, 45].Meanwhile, the fifth-generation mobile communication system (5G) promises to cope with the increasing volume of information distribution. 5G is highly compatible with XR technology, and the research and

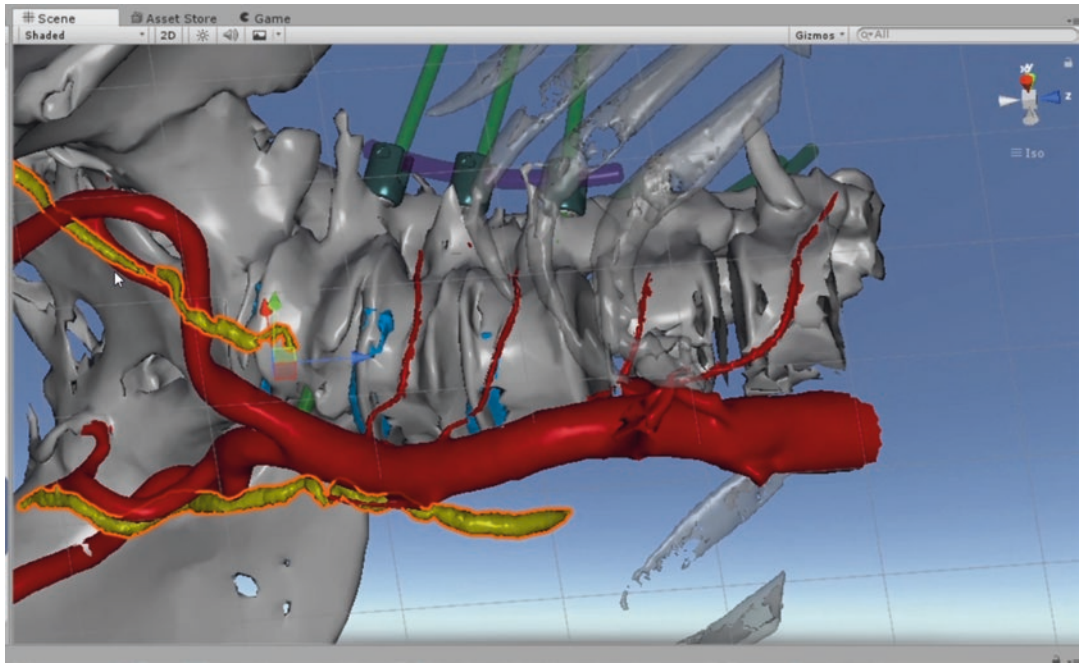


**Fig. 36.6** Model reconstruction by Unity®, showing blood vessels, ureter, and the LLIF cage

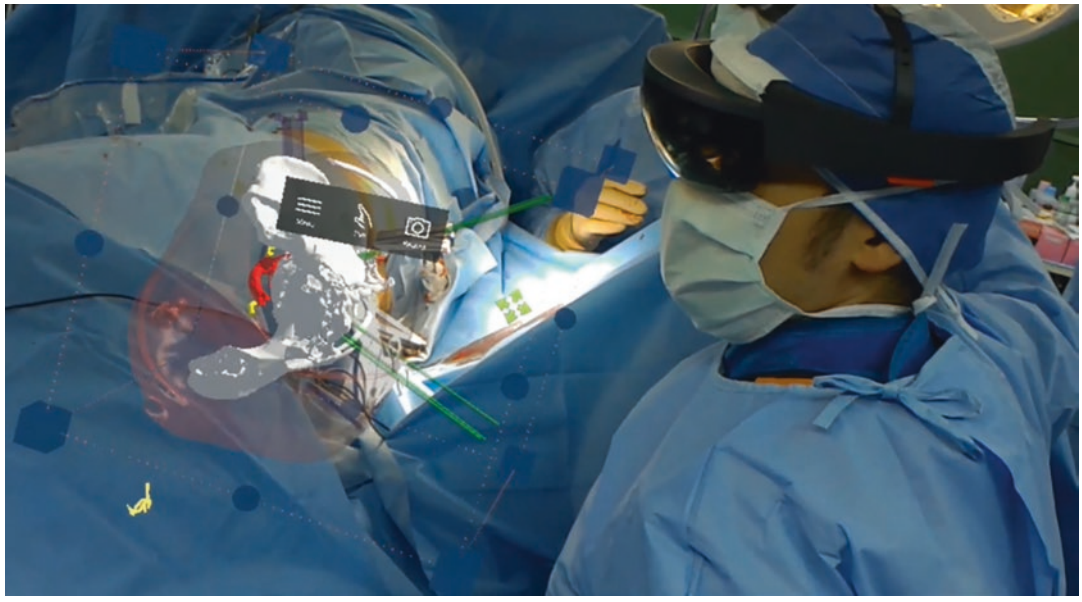

**Fig. 36.7** MR intraoperative image assistance for L3/4/5 LLIF

development of high-resolution, high-definition image transmission, stereophonic sound, and haptic (touch) communication are well underway. Besides transmitting patients' medical information, XR technology also captures the motions of doctors and patients as avatars, thus benefiting the doctor–doctor and doctor–patient communications. In our system, multiple sur-

geons wearing HoloLens® or other HMDs can enter the same VR space and communicate in real time by simultaneously sharing their physical movements and spatial backgrounds along with medical images and patient information. Telepresence, demonstrated as a remote-space-sharing tool in an XR conference by Holoeyes XR (Holoeyes, Inc.), has now been adopted in medical education (Fig. 36.8). Spatial (Spatial Systems) creates a 3D avatar model from a 2D photograph within a few seconds. The avatar model then appears in a VR chat room, in which presentations and 3D models are shared in the same virtual space.

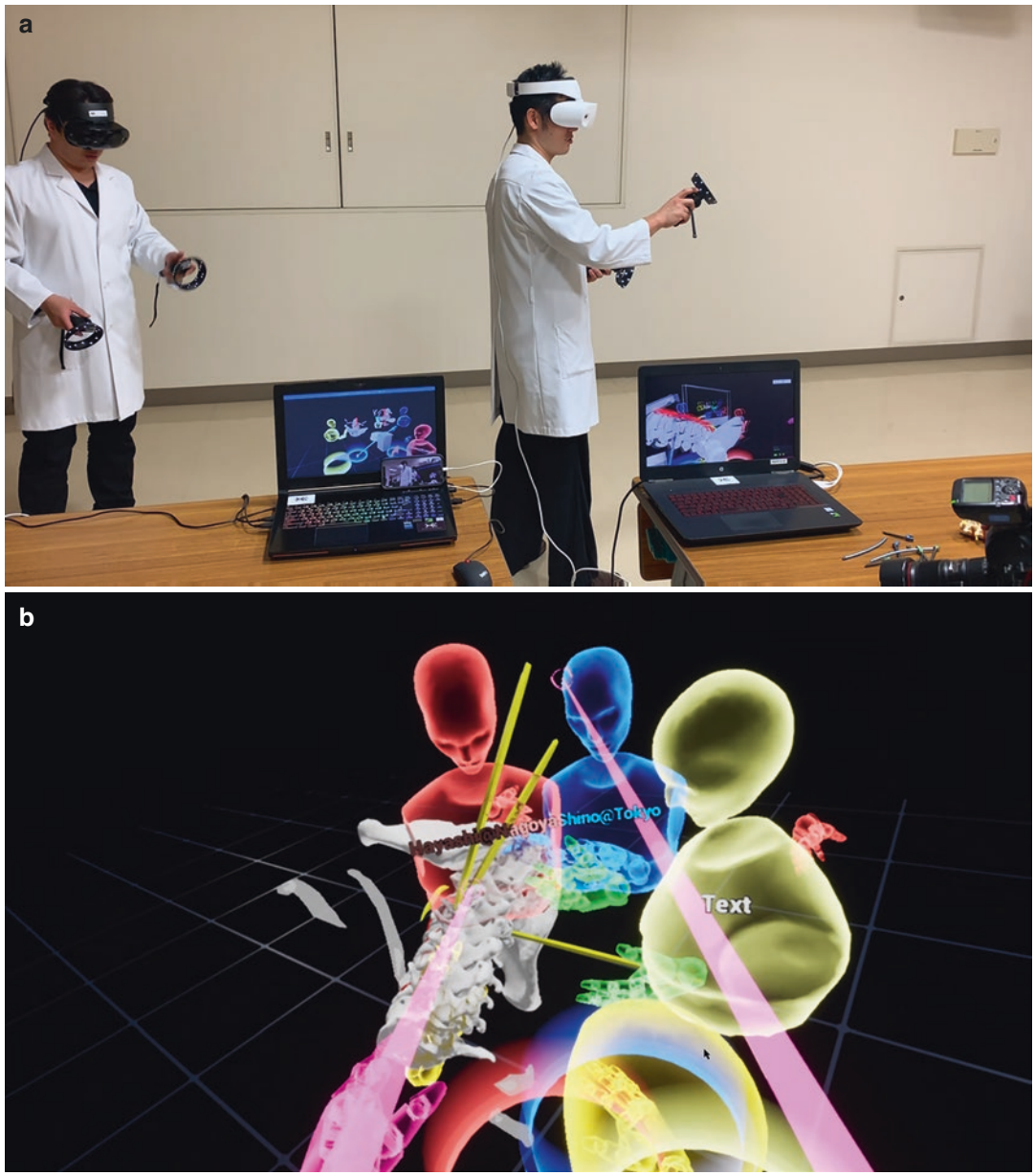


**Fig. 36.8** Teleconference using Holoeyes XR (Holoeyes, Inc.) (**a**) VR meeting with an HMD connected to PC. (**b**) Remote space sharing where the screw trajectory is displayed three-dimensionally by multiple surgeons wearing HMDs

## 36.7 Future Prospects and Challenges of Reality Technology

The main difference between VR and AR/MR is the presence or absence of interaction with the real space. AR and MR technologies aim to add information to the real space, whereas VR provides visual information in a non-real space. Because the virtual space can be disconnected from the real space, VR in medicine is often targeted at the educational arena. It is also important to note that under the current Japan's Pharmaceutical Affairs Law, simulation programs for educational purposes are excluded from medical devices and require no approval by the Pharmaceutical Affairs Bureau. We believe that besides providing intraoperative imaging assistance in clinical settings, our MR device will enhance education and communication through its positional information and line-of-sight sharing function (Fig. 36.9). In teleconferences, multiple users wearing HMD-MR devices can consult the anatomy constructed from patient imaging examinations and discuss a detailed surgical plan. Such collaboration is especially useful in cases of advanced spinal degeneration and body parts with complex anatomical structures. In addition, we believe that the simultaneous sharing of images with medical staff and patients will support explanations of the surgery (Fig. 36.10). Finally, the system can potentially be developed as a simulator through which young doctors can understand anatomical structures and perform safe surgical operations.

Current MR technology has been found to have several limitations. The available MR-HMD devices measure the surrounding area with infrared sensors and correct the position when projected into real space. Although this technique is low cost and removes the need for registration and spatial recognition markers, the virtual model is vulnerable to accuracy degradation because it lacks a reference point in real space [40]. Reality technology devices can also be affected by radio waves and infrared rays generated by other

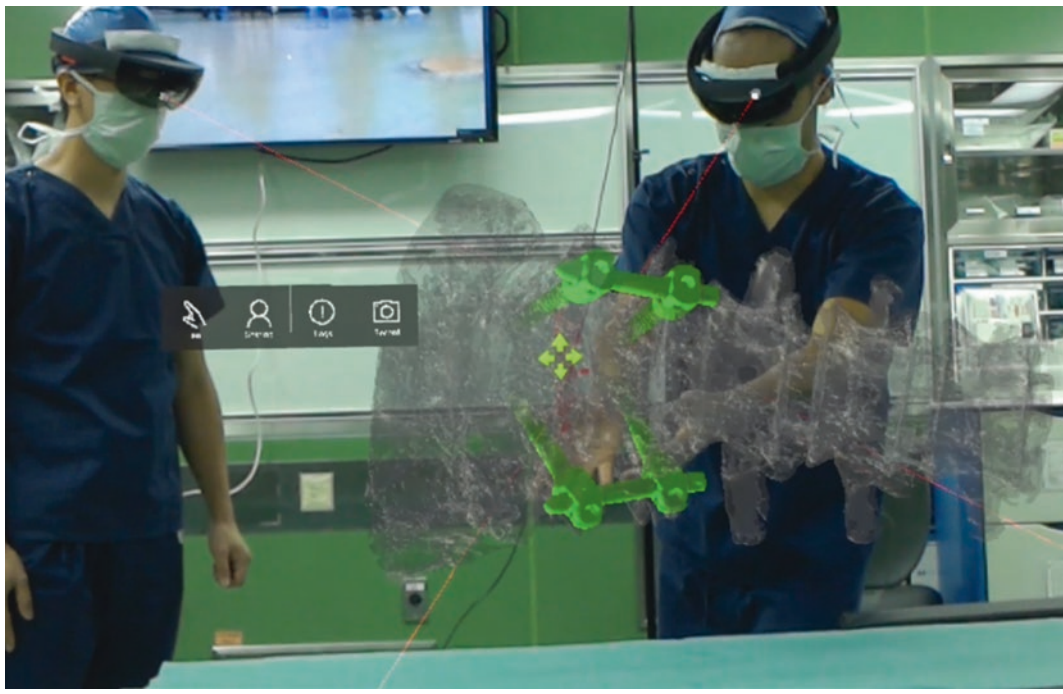

**Fig. 36.9** Preoperative discussion in the operating room: The shared view function (enclosed by red lines) facilitates communication between users

**Fig. 36.10** Application to patient explanation: A doctor gives informed consent to a patient by sharing a 3D image

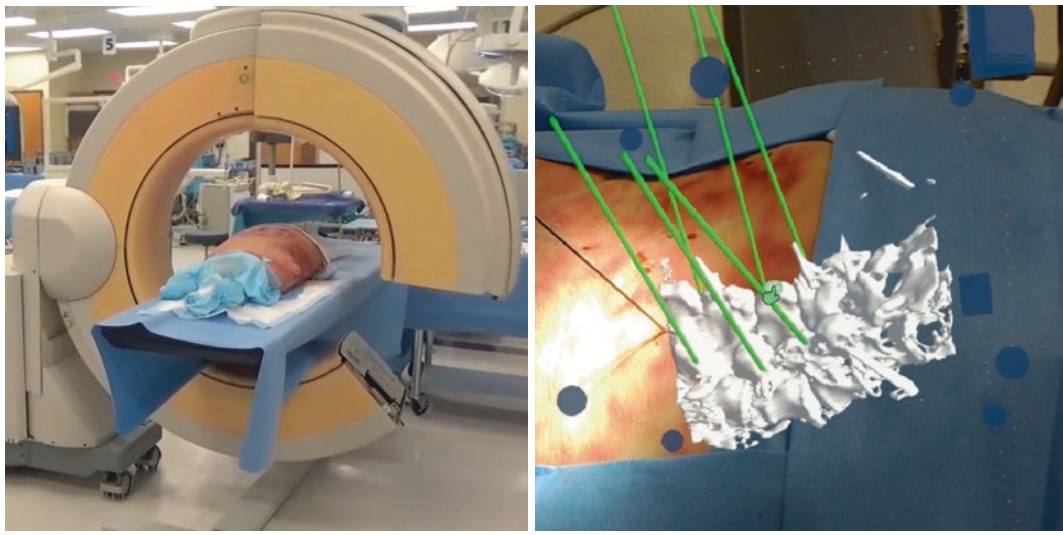

**Fig. 36.11** Mixed reality application on a cadaver with intraoperative CT imaging (O-arm)

medical devices in the operating room. To improve the accuracy of the simulated images, we proposed synchronization of MR-HMD device with intraoperative CT imaging and measured the accuracy of screw insertion in a cadaver using an O-arm (Medtronic, USA). However, the accuracy of the MR-HMD device was insufficient for safe practice (Fig. 36.11). These problems could be mitigated by developing a navigation device, adding a reference point during CT imaging, or specifying a solid reference frame (as done in current navigation systems).

Besides improving the surgeon's 3D understanding of anatomy and spatial orientation, VR technologies are useful educational tools for students of surgical techniques. At present, these technologies are limited by their positional accuracy, but future advancements are expected to realize practical image support devices.

**Acknowledgments** We express our deepest gratitude to Maki Sugimoto and Naoji Taniguchi of Holoeyes, Inc., for their cooperation in developing this device.

## References


1. Al Jammal OM, Delavar A, Maguire KR, et al. National trends in the surgical management of lumbar spinal stenosis in adult spinal deformity patients. Spine. 2019;44:E1369–78.
2. LLC MSR. Orthopedic navigation system market size. Industry Report, 2018–2025. 2019.
3. Iannessi A, Marcy PY, Clatz O, et al. A review of existing and potential computer user interfaces for modern radiology. Insights Imaging. 2018:599–609.
4. Ahern DP, Gibbons D, Schroeder GD, et al. Image-guidance, robotics, and the future of spine surgery. Clinical spine surgery. Lippincott Williams and Wilkins; 2019.
5. Yoshida S, Sugimoto M, Fukuda S, et al. Mixed reality computed tomography-based surgical planning for partial nephrectomy using a head-mounted holographic computer. Int J Urol. 2019:681–2.
6. Saito Y, Sugimoto M, Imura S, et al. Intraoperative 3D hologram support with mixed reality techniques in liver surgery. Ann Surg. 2020;271:E4–7.
7. Jantz J, Molnar A, Alcaide R. A brain-computer interface for extended reality interfaces. In: ACM SIGGRAPH 2017 VR Village [internet]. New York, NY, USA: Association for Computing Machinery; 2017 [cited 2020 Nov 8]. p. 1–2. (SIGGRAPH '17). Available from: https://doi.org/10.1145/3089269.3089290.
8. Peuchot B, Tanguy A, Eude M. Augmented reality in spinal surgery. Stud Health Technol Inform. 1997;37:441–4.
9. Theocharopoulos N, Perisinakis K, Damilakis J, et al. Occupational exposure from common fluoroscopic projections used in orthopaedic surgery. J Bone Joint Surg - Series A. 2003;85:1698–703.
10. Edström E, Burström G, Omar A, et al. Augmented reality surgical navigation in spine surgery to minimize staff radiation exposure. Spine. 2019:1.
11. Moore J, Clarke C, Bainbridge D, et al. Image guidance for spinal facet injections using tracked ultrasound. In: Lecture notes in computer science (including subseries Lecture notes in artificial intelligence and lecture notes in bioinformatics). 2009, p. 516–23.
12. Bisson M, Cheriet F, Parent S. 3D visualization tool for minimally invasive discectomy assistance. In: Studies in health technology and informatics 2010. IOS Press. p. 55-60
13. Weiss CR, Marker DR, Fischer GS, et al. Augmented reality visualization using image-overlay for MR-guided interventions: system description, feasibility, and initial evaluation in a spine phantom. Am J Roentgenol. 2011;196:W305–7.
14. Fritz J, Paweena U, Thainual, Ungi T, et al. MR-guided vertebroplasty with augmented reality image overlay navigation. Cardiovasc Intervent Radiol. 2014:1589–96.
15. Navab N, Heining SM, Traub J. Camera augmented mobile C-arm (CAMC): calibration, accuracy study, and clinical applications. IEEE Trans Med Imaging. 2010;29:1412–23.
16. Elmi-Terander A, Burström G, Nachabe R, et al. Pedicle screw placement using augmented reality surgical navigation with intraoperative 3D imaging: a first in-human prospective cohort study. Spine. 2019;44:517–25.
17. Abe Y, Sato S, Kato K, et al. A novel 3D guidance system using augmented reality for percutaneous vertebroplasty. J Neurosurg Spine. 2013;19:492–501.
18. Elmi-Terander A, Burström G, Nachabé R, et al. Augmented reality navigation with intraoperative 3D imaging vs fluoroscopy-assisted free-hand surgery for spine fixation surgery: a matched-control study comparing accuracy. Sci Rep. 2020;10:1–8.
19. Urakov TM, Wang MY, Levi AD. Workflow caveats in augmented reality–assisted pedicle instrumentation: Cadaver Lab. World Neurosurg. 2019;126:e1449–55.
20. Liebmann F, Roner S, von Atzigen M, et al. Pedicle screw navigation using surface digitization on the Microsoft HoloLens. Int J Comput Assist Radiol Surg. 2019;14:1157–65.
21. Gibby JT, Swenson SA, Cvetko S, et al. Head-mounted display augmented reality to guide pedicle screw placement utilizing computed tomography. Int J Comput Assisted Radiol Surg. 2019:525–35.
22. Müller F, Roner S, Liebmann F, et al. Augmented reality navigation for spinal pedicle screw instrumentation using intraoperative 3D imaging. Spine J. 2019.
23. Molina CA, Theodore N, Karim Ahmed A, et al. Augmented reality-assisted pedicle screw insertion: a cadaveric proof-of-concept study. J Neurosurg Spine. 2019;31:139–46.
24. Wu JR, Wang ML, Liu KC, et al. Real-time advanced spinal surgery via visible patient model and augmented reality system. Comput Methods Prog Biomed. 2014;113:869–81.
25. Sugimoto M, Yasuda H, Koda K, et al. Image overlay navigation by markerless surface registration in gastrointestinal, hepatobiliary and pancreatic surgery. J Hepatobiliary Pancreat Sci. 2010;17:629–36.
26. Carl B, Bopp M, Saß B, et al. Implementation of augmented reality support in spine surgery. Eur Spine J. 2019;28:1697–711.
27. Carl B, Bopp M, Saß B, et al. Reliable navigation registration in cranial and spine surgery based on intraoperative computed tomography. Neurosurg Focus. 2019;47:E11.
28. Inoue D, Cho B, Mori M, et al. Preliminary study on the clinical application of augmented reality neuronavigation. J Neurol Surg Part A: Central Eur Neurosurg. 2013;74:71–6.
29. Tabrizi LB, Mahvash M. Augmented reality-guided neurosurgery: accuracy and intraoperative application of an image projection technique. J Neurosurg. 2015;123:206–11.

30. International A. ASTM F2554 - 10 standard practice for measurement of positional accuracy of computer assisted surgical systems. 2010.
31. Sugimoto M. Augmented tangibility surgical navigation using spatial interactive 3-D hologram zSpace with OsiriX and bio-texture 3-D organ modeling. In: Proceedings - 2015 international conference on computer application technologies, CCATS 2015 2016. Institute of Electrical and Electronics Engineers Inc. p. 189–94.
32. Chuang M-F, Tung H-H, Clinciu DL, Huang J-S, Iqbal U, Chang C-J, et al. The effect of an integrated education model on anxiety and uncertainty in patients undergoing cervical disc herniation surgery. Comput Methods Prog Biomed. 2016;133:17–23.
33. Lanier J. Virtual reality: the promise of the future. Interact Learn Int. 1992;8(4):275–9.
34. Blizzard DJ, Thomas JA. MIS single-position lateral and oblique lateral lumbar interbody fusion and bilateral pedicle screw fixation. Spine. 2018;43(6):440–6.
35. Quiceno E, Hartman C, Godzik J, Pacult MA, Hemphill C, Uribe JS. Single position spinal surgery for the treatment of grade II spondylolisthesis: a technical note. J Clin Neurosci. 2019;65:145–7.
36. Sakai D, Joyce K, Sugimoto M, Horikita N, Hiyama A, Sato M, et al. Augmented, virtual and mixed reality in spinal surgery: a real-world experience. J Orthop Surg. 2020;28(3):2309499020952698.
37. Milgram P, Takemura H, Utsumi A, Kishino F. Augmented reality: a class of displays on the reality-virtuality continuum. In: Telemanipulator and telepresence technologies. International Society for Optics and Photonics; 1995. p. 282–92.
38. Milgram P, Kishino F. A taxonomy of mixed reality visual displays [Internet]. 1994 [cited 2020 Nov 9]. Available from: https://search.ieice.org/bin/summary.php?id=e77-d_12_1321
39. Williams T, Szafir D, Chakraborti T. The reality-virtuality interaction cube. In: Proceedings of the 2nd international workshop on virtual, augmented, and mixed reality for HRI. 2019.
40. Vassallo R, Rankin A, Chen ECS, Peters TM. Hologram stability evaluation for Microsoft HoloLens. In: Medical Imaging 2017: Image perception, observer performance, and technology assessment [Internet]. International Society for Optics and Photonics; 2017 [cited 2020 Nov 9]. p. 1013614. Available from: https://www.spiedigitallibrary.org/conference-proceedings-of-spie/10136/1013614/Hologram-stability-evaluation-for-Microsoft-HoloLens/10.1117/12.2255831.short
41. Vovk A, Wild F, Guest W, Kuula T. Simulator sickness in augmented reality training using the Microsoft HoloLens. In: Proceedings of the 2018 CHI conference on human factors in computing systems [Internet]. New York, NY, USA: Association for Computing Machinery; 2018 [cited 2020 Nov 8]. p. 1–9. (CHI '18). Available from: https://doi.org/10.1145/3173574.3173783
42. Augmented Reality Technology Using Microsoft HoloLens in Anatomic Pathology | Archives of Pathology & Laboratory Medicine | Allen Press [Internet]. [cited 2020 Nov 9]. Available from https://meridian.allenpress.com/aplm/article/142/5/638/194343/Augmented-Reality-Technology-Using-Microsoft
43. Evaluating the Microsoft HoloLens through an augmented reality assembly application [Internet]. [cited 2020 Nov 9]. Available from: https://www.spiedigitallibrary.org/conference-proceedings-of-spie/10197/101970V/Evaluating-the-Microsoft-HoloLens-through-an-augmented-reality-assembly-application/10.1117/12.2262626.short?webSyncID=9a0ce46e-9e6e-c7a4-9dab-6a0cbad05932&sessionGUID=9ad883c9-d902-bc99-93ce-d268bead49a2&SSO=1
44. Kwok AOJ, Koh SGM. COVID-19 and extended reality (XR). Curr Issues Tour. 2020;0(0):1–6.
45. Nuriman H, Sabana S, Mutiaz IR, Kusmara RA. From real to virtual: adaptation model of performance arts during covid-19 period. J Sosioteknologi. 2020;19(2):162–9.

# Technical Feasibility of Augmented Reality in Spinal Tumor Surgery

37

Erik Edström, Gustav Burström, Oscar Persson, and Adrian Elmi-Terander

## 37.1 Introduction

For decades, 3D navigation has been the norm in intracranial tumor surgery [1]. Consequently, the inclusion of AR solutions has been a natural step, reflecting the gradual technical advances in the field of navigated cranial surgery. In fact, microscope-based AR has been implemented in cranial neurosurgery since the 1990s [2]. In contrast, navigation in spine surgery remains a topic of some debate without uniform adoption [3, 4]. Pedicle screw placement, rather than tumor surgery, is the predominant application of image-guided spinal navigation, and the data on AR navigation in spine tumor surgery are limited [5–8]. However, like the success seen in spinal fixation surgery, the combination of AR navigation and MISS techniques in spine tumor surgery promises increased accuracy, better patient outcomes, and reduced staff radiation exposure.

MISS has revolutionized spinal surgery. Although initially popularized for degenerative spinal disease and trauma, these techniques have also become widely applied in spinal tumor and deformity surgery. MISS provides several advantages in treating spinal tumors. Minimal damage to muscles and bony structures in benign tumor cases may reduce the risk of structural instability and the need for fusion surgery. Reduced surgical trauma minimizes blood loss, recovery times, and both initial and chronic pain. Consequently, MISS techniques allow the start of radiotherapy and chemotherapy for malignant tumors with minimal delay. The diminished systemic surgical stress in MISS is also beneficial for patients with comorbidity. By minimizing the postoperative complications compared to open surgery, MISS lets patients return home more quickly.

## 37.2 Spinal Tumor Surgery

Obtaining tumor control, decompressing the spinal cord, and restoring the mechanical stability of the spine are the main indications for spinal tumor surgery. The surgical intent can be curative for primary tumors and palliative for metastatic lesions. Using the umbrella term spinal tumors to describe all tumors affecting the spine creates a large and diverse group of medical conditions ranging from strictly intramedullary lesions to wholly extravertebral tumors with secondary effects on the vertebral column. For most of these conditions, a potential benefit of AR navigation is apparent. Arguably, any intraoperative imaging technique or navigational aid used in intradural tumor surgery can help confirm the right spinal levels for operation. Using AR to accomplish this

E. Edström · G. Burström · O. Persson
A. Elmi-Terander (✉)
Department of Clinical Neuroscience, Karolinska Institute and Department of Neurosurgery, Karolinska University Hospital, Stockholm, Sweden
e-mail: adrian.elmi.terander@ki.se



J.-S. Kim et al. (eds.), *Technical Advances in Minimally Invasive Spine Surgery*,
https://doi.org/10.1007/978-981-19-0175-1_37

allows 3D confirmation of the relation of the tumor to the surrounding bony anatomy, which may enhance and facilitate surgical decision making for spinal tumor surgery.

For simplicity, two broad categories of tumors will be used as a basis for the discussion when illustrating the role of AR in spinal tumor surgery. These categories are intradural tumors (where the bony anatomy of the spinal column remains unaffected) and extradural tumors (where the structural integrity of the spine is a key aspect of surgery).

## 37.3 Intradural Tumors

Intradural tumors are primarily accessed through posterior laminotomy-based approaches. Reasons for this include the relatively low morbidity and simplicity of this approach and, when the tumor is intramedullary, the preferred direct midline access between the dorsal columns. The shallow spinal canal is often filled with tumor and compressed spinal cord or nerve roots, providing limited space for microsurgical manipulation. Thus, the laminotomy must include a sufficient number of levels to provide a direct line of sight to the cranial and caudal tumor margins and be wide enough to ensure maximal access without unnecessarily removing structural elements. To simplify this problem, AR navigation can provide the surgeon with a visualization of the relevant anatomy as well as the outline of the tumor. Optimally, the relevant structures are automatically segmented based on intraoperative imaging. Commercially available software solutions for automatic tumor segmentation of spine tumors are not fully developed, and soft tissue tumors may be poorly visualized using CT-based imaging techniques. However, several solutions for automatic spine segmentation on intraoperative 3D scans are available, and efforts have been made to solve the challenge of automatic tumor segmentation in several surgical disciplines [7, 9–11]. For instance, in neurosurgery and radiooncology, great progress has been made to develop segmentation algorithms for CT and MRI data [12–14]. In contrast to segmentation of the bony spine where the normal anatomy is known, and imaging produces well-defined structural borders, tumor segmentation is complicated due to the lack of standard anatomy and difficulty in defining the tumor borders [15–17]. However, it is important to note that tumor segmentation also poses a challenge for the trained clinician. In radiation oncology, clinically relevant inter-observer and intra-observer inconsistencies have been reported in the segmentation of the target and organs at risk [13, 18–21]. Within this field, deep learning algorithms have successfully been applied to auto-segment targets in the thorax, abdomen, pelvis, head and neck, and brain. These algorithms sometimes outperform their clinical counterparts with lower inter-observer and intra-observer variability [13]. Thus, it seems reasonable to expect automatic tumor segmentation algorithms to be included in the upcoming generations of navigational software.

Currently, manual segmentation on preoperative imaging combined with intraoperative fusion to the registration scan is the best option available. Manual tumor delineation for 3D representation is a standard feature of most commercially available navigation packages, including Brainlab, Stealth Station, and NAV3i. Smart functions in these software packages help the surgeon complete the task of tumor delineation rapidly (Fig. 37.1). However, only Brainlab elements provide this feature that has been designed for spinal tumor surgery. A problem specific to the spine arises when preoperative images (typically in the supine position) are fused to intraoperative images (typically in the prone position) for registration. The normal movements of the spine need to be compensated for to allow image fusion. Carl et al. have presented a solution based on non-linear matching with excellent results [7].

When AR is used to simplify the macroscopic part of access surgery, the use of a head-up display (HUD) or monitor interface would be the most suitable. In the application of AR for spinal navigation, HMD solutions have received a great deal of attention due to their simplicity [22–28]. However, HMD systems are comparatively newer and have an additional tracked object (the HMD itself), thereby increasing the complexity and

**Fig. 37.1** The Artis zeego imaging system (Siemens) during intraoperative use. Image originally published by Pireau et al. [50]. Republished with permission by Springer Nature

**Fig. 37.2** Microsoft's HoloLens. Image courtesy of Microsoft

potential for errors. These systems typically rely on optical matching with manual fine-tuning for registration. One such device, the Microsoft HoloLens, reached an accuracy ranging from 9 to 45 mm depending on the distance to the object in non-medical models ([29]; Fig. 37.2). In a spine phantom study, accuracy of roughly 5 mm was achieved [25]. For intradural tumor surgery, this level of accuracy is inadequate. Alternatively, direct or indirect projection techniques would serve the same function. Thus far, projection solutions have been mostly used for interventional procedures such as spinal injections, and there are no reports of any clinical use in surgery.

Once soft tissue dissection, bone removal, and dural access are satisfactory, the subsequent intradural surgery is typically performed under a microscope. Care must be taken in the positioning of dynamic reference frames since they may interfere with the positioning of the surgical microscope. At the same time, placing reference frames too distant to the tumor may lead to reduced navigational accuracy [4]. It is often impractical to place dynamic reference frames or skin fiducials before the access part of the surgery has been performed. DRF clamps are often attached to spinous processes, requiring some degree of skin opening, and markers on the skin may be dislodged due to skin deformation at this stage of the surgery. Thus, in many AR-guided spine surgery workflows, navigation is started only after adequate exposure of the relevant anatomy. Microscope-based AR is the most obvious solution for intradural tumor surgery. Microscope-based AR is provided through HUD in the eyepieces of a surgical microscope, a technology developed in the 1980s [30, 31]. A separate monitor could be used for AR display but would require a shift of the surgeon's focus from the microscope to the screen whenever consulted. HMD solutions, however, are not feasible for this part of surgery since they cannot be efficiently combined with the surgical microscope. For HMD-based AR to work, the technology must become accurate enough and provide sufficient magnification to serve as head-mounted microscopes with AR functionality. A possible solution would involve the use of HMD in combination with novel visualization solutions such as exoscopes (Orbeye, Artevo, DSM). These tools have been used for ophthalmic, ENT, neurologic, and general surgery [32–34]. They are navigated high-resolution camera systems designed to replace a microscope with a camera head small

enough to be placed in proximity to the surgical field without being too obtrusive. The view is presented on a monitor. In theory, the same view could be provided in an HMD-display solution. However, a normal microsurgical microscope has the benefit of providing a line of sight matching that of the surgeon. Hence, the movements performed by the surgeon will be matched visually in all directions. With a different perspective, the surgeon must retrain and adjust their movements to avoid manual errors.

In a study of 10 patients scheduled for intradural tumor surgery, Carl et al. evaluated the use of microscope-based AR [7] using the commercially available spinal navigation suite "Elements" from Brainlab. Preoperative 3D imaging included CT angiography and MRI scanning. Tumors and other structures of interest, such as blood vessels, were manually segmented with the aid of a smart brush feature (Figs. 37.3 and 37.4). The vertebrae were automatically segmented, and corrections were made manually before the images were fused. When needed, the spine curvature correction functionality of the software suite was employed. Automatic registration was based on intraoperative 3D radiology using the AIRO scanner and a dynamic reference frame [35, 36]. To avoid cluttering of the surgical field, the dynamic reference frame was either placed on the carbon fiber Mayfield head clamp for cervical cases or taped to the skin caudal to the area of interest for thoracolumbar cases. The initial part of the surgery was performed before registration was started. Skin fiducials that were not part of the navigation were added and subsequently used for accuracy measurements. The AIRO incorporated a low-dose protocol for registration [36]. AR was shown when desired by the surgeon as a see-through 3D object or an outline using HUD in the eyepieces of a Zeiss Pentero900 microscope. Additional views were displayed continuously on monitors in the OR. Tumor outline and the relevant surrounding anatomy were visualized.

The authors concluded:

Microscope-based AR can be successfully applied to intradural spine tumor surgery, providing an intuitive intraoperative visualization of the tumor extent and surrounding structures. Automatic low-dose intraoperative computed tomography registration ensures high accuracy. Thus, all advanced multi-modality options of cranial AR can now also be applied to spinal surgery [7].

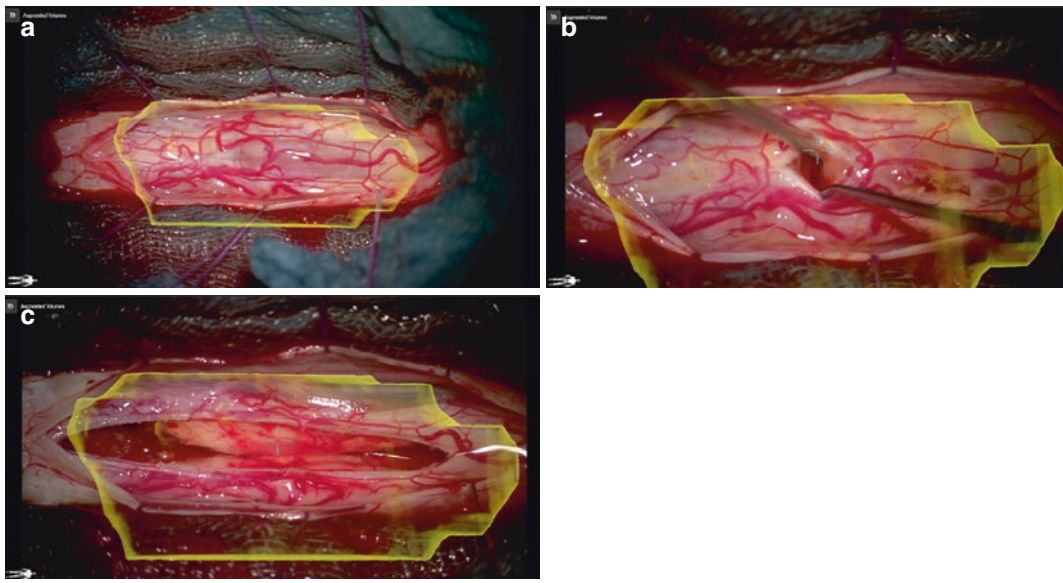


**Fig. 37.3** The surgeon's view during microscope-based augmented reality navigation. The yellow field outlines the tumor boundaries (**a**, immediately after dural opening; **b**, at the beginning of resection; **c**, at the end of resection). Image originally published by Carl et al. [7]. Republished with permission by Springer Nature

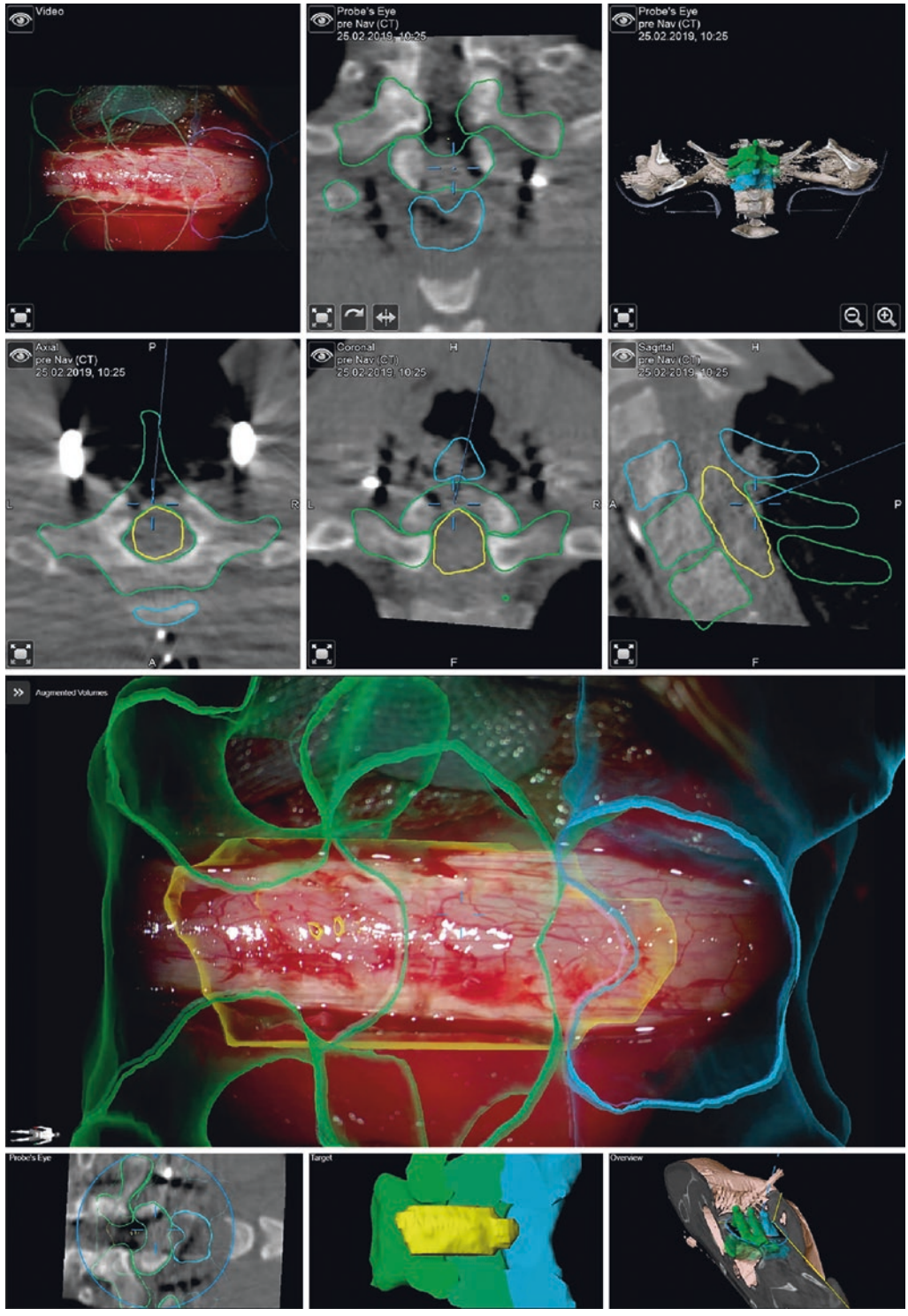


**Fig. 37.4** The planning (top two rows) and surgeon's view (bottom half) during microscope-based augmented reality navigation. Yellow field outlines the tumor boundaries. Green and blue outline vertebral boundaries. Image originally published by Carl et al. [7]. Republished with permission by Springer Nature

The reported target registration error was 0.72 ± 0.24 mm, which is needed for safe intradural surgery. This should not be confused with navigation accuracy, which also includes the inbound error of the navigation system and the surgeon's ability to adhere to the planned path. In brain tumor surgery, accuracy in soft tissue navigation has a short half-life. When soft tissues are manipulated (e.g., when parts of the tumor have been removed) accuracy is quickly lost [37]. The same phenomenon will occur in intradural spine tumor surgery, even if the space for soft tissue movement is much more limited. Currently, the best available solution to this problem is intraoperative ultrasound [38]. Unfortunately, there are no commercially available clinical systems using US, and the only reported system combining US and AR is experimental [39].

## 37.4 Extradural Tumors

Even though navigation in orthopedic and spinal tumor surgery has become more commonplace, the literature does not offer publications on image-guided extradural tumor surgery using AR technology [40]. Early publications have investigated image-guided surgery for benign cervical bone tumors [41], osteoid osteoma of the spine [42–44], metastatic disease of the spine [45, 46], and en bloc resection and subsequent fixations to treat a giant cell tumor in the thoracic spine [47]. More recent publications have described the use of a navigated ultrasonic osteotome to add precision to en bloc resections of chordomas in the thoracic and lumbar spine [48]. Navigation in these cases simplifies surgical planning, tumor removal, and subsequent fixation [40, 49].

Nonetheless, AR solutions designed for pedicle screw placement provide an excellent starting point for extradural spine tumor surgery. The technology, which typically includes automatic spine segmentation, needs to be combined with manual or automated tumor recognition and segmentation algorithms to provide the surgeon with 3D representations of the relevant anatomy. This would simplify the process of surgical planning for tumor removal and subsequent fixation. Ideally, software solutions should include functions to plan not only the tumor resection but also the reconstruction and fixation of the spine. A predictable problem in the removal of large tumor masses in the spinal column involves the degree of destruction to, or removal of, weight-bearing structures exceeding what was planned. In this context, intraoperative 3D scanning and ultrasound would provide added benefits by allowing repeated examinations of the bony and soft tissue anatomy during the different stages of tumor removal [38].

For extradural tumor surgery, a combination of AR display technologies would be most effective. On the one hand, microscope-based AR is optimal for delicate dissection and removal of the tumor. HUD or monitor-based solutions, on the other hand, lend themselves to the initial tumor access surgery and possible fixation surgery. In this scenario, a headset would need to be removed during the use of the microscope.

## References

1. Maciunas RJ. Computer-assisted neurosurgery. Clin Neurosurg. 2006;53:267–71.
2. King A, Edwards P, Maurer Jr C, De Cunha D, Hawkes D, Hill D, et al. A system for microscope-assisted guided interventions 1999;72(2–4):107–11.
3. Hussain I, Cosar M, Kirnaz S, Schmidt FA, Wipplinger C, Wong T, et al. Evolving navigation, robotics, and augmented reality in minimally invasive spine surgery. Global Spine J. 2020;10(2 Suppl):22S–33S.
4. Burström G, Nachabe R, Homan R, Hoppenbrouwers J, Holthuizen R, Persson O, et al. Frameless patient tracking with adhesive optical skin markers for augmented reality surgical navigation in spine surgery. Spine (Phila Pa 1976). 2020.
5. Jarvers J-S, Katscher S, Franck A, Glasmacher S, Schmidt C, Blattert T, et al. 3D-based navigation in posterior stabilisations of the cervical and thoracic spine: problems and benefits. Results of 451 screws. 2011;37(2):109–19.
6. Rampersaud YR, Pik JH, Salonen D, Farooq SJS. Clinical accuracy of fluoroscopic computer-assisted pedicle screw fixation: a CT analysis. 2005;30(7):E183-E90.
7. Carl B, Bopp M, Sass B, Pojskic M, Nimsky C. Augmented reality in intradural spinal tumor surgery. Acta Neurochir. 2019;161(10):2181–93.

8. Bandiera S, Ghermandi R, Gasbarrini A, Brodano GB, Colangeli S, Boriani SJESJ. Navigation-assisted surgery for tumors of the spine 2013;22(6):919–24.
9. Burström G, Buerger C, Hoppenbrouwers J, Nachabe R, Lorenz C, Babic D, et al. Machine learning for automated 3-dimensional segmentation of the spine and suggested placement of pedicle screws based on intraoperative cone beam computer tomography. J Neurosurg Spine. 2019;31(1):147–54.
10. Carl B, Bopp M, Sass B, Nimsky C. Microscope-based augmented reality in degenerative spine surgery: initial experience. World Neurosurg. 2019;
11. Carl B, Bopp M, Sass B, Pojskic M, Voellger B, Nimsky C. Spine surgery supported by augmented reality. Global Spine J. 2020;10(2 Suppl):41S–55S.
12. Wadhwa A, Bhardwaj A, Verma VSJMri. A review on brain tumor segmentation of MRI images 2019;61:247–259.
13. Cardenas CE, Yang J, Anderson BM, Court LE, Brock KB, editors. Advances in auto-segmentation. Semin Radiat Oncol; 2019.
14. Angulakshmi M, Lakshmi Priya G. Technology. Automated brain tumour segmentation techniques—a review. Int J Imaging Syst. 2017;27(1):66–77.
15. Ben Rabeh A, Benzarti F, Amiri H. Segmentation of brain MRI using active contour model. Int J Imaging Syst. 2017;27(1):3–11.
16. Kamnitsas K, Ledig C, Newcombe VF, Simpson JP, Kane AD, Menon DK, et al. Efficient multi-scale 3D CNN with fully connected CRF for accurate brain lesion segmentation. 2017;36:61–78.
17. Vaishnavee K, Amshakala K, editors. An automated MRI brain image segmentation and tumor detection using SOM-clustering and proximal support vector machine classifier. 2015 IEEE International Conference on Engineering and Technology (ICETECH). IEEE; 2015.
18. Hong TS, Tomé WA, Harari PMJR. Oncology. Heterogeneity Head Neck IMRT Target Des Clin Pract. 2012;103(1):92–8.
19. Li XA, Tai A, Arthur DW, Buchholz TA, Macdonald S, Marks LB, et al. Variability of target and normal structure delineation for breast cancer radiotherapy: an RTOG multi-institutional and multiobserver study. Int J Radiat Oncol Biol Phys. 2009;73(3):944–51.
20. Eminowicz G, McCormack M. Variability of clinical target volume delineation for definitive radiotherapy in cervix cancer. Radiother Oncol. 2015;117(3):542–7.
21. Ng SP, Dyer BA, Kalpathy-Cramer J, Mohamed ASR, Awan MJ, Gunn GB, et al. A prospective in silico analysis of interdisciplinary and interobserver spatial variability in post-operative target delineation of high-risk oral cavity cancers: does physician specialty matter? Clin Transl Radiat Oncol. 2018;12:40–6.
22. Abe Y, Sato S, Kato K, Hyakumachi T, Yanagibashi Y, Ito M, et al. A novel 3D guidance system using augmented reality for percutaneous vertebroplasty. J Neurosurg-Spine. 2013;19(4):492–501.
23. Agten CA, Dennler C, Rosskopf AB, Jaberg L, Pfirrmann CWA, Farshad M. Augmented reality-guided lumbar facet joint injections. Investig Radiol. 2018;53(8):495–8.
24. Deib G, Johnson A, Unberath M, Yu K, Andress S, Qian L, et al. Image guided percutaneous spine procedures using an optical see-through head mounted display: proof of concept and rationale. J Neurointerv Surg. 2018;10(12):1187–91.
25. Gibby JT, Swenson SA, Cvetko S, Rao R, Javan R. Head-mounted display augmented reality to guide pedicle screw placement utilizing computed tomography. Int J Comput Assist Radiol Surg. 2019;14(3):525–35.
26. Liebmann F, Roner S, von Atzigen M, Scaramuzza D, Sutter R, Snedeker J, et al. Pedicle screw navigation using surface digitization on the Microsoft HoloLens. Int J Comput Assist Radiol Surg. 2019;14(7):1157–65.
27. Molina CA, Theodore N, Ahmed AK, Westbroek EM, Mirovsky Y, Harel R, et al. Augmented reality-assisted pedicle screw insertion: a cadaveric proof-of-concept study. J Neurosurg Spine. 2019:1–8.
28. Yoon JW, Chen RE, Kim EJ, Akinduro OO, Kerezoudis P, Han PK, et al. Augmented reality for the surgeon: systematic review. Int J Med Robot. 2018;14(4):e1914.
29. Hubner P, Clintworth K, Liu Q, Weinmann M, Wursthorn S. Evaluation of HoloLens tracking and depth sensing for indoor mapping applications. Sensors (Basel). 2020;20(4).
30. Kelly PJ, Alker GJ Jr, Goerss S. Computer-assisted stereotactic laser microsurgery for the treatment of intracranial neoplasms. Neurosurgery. 1982;10(3):324–31.
31. Roberts DW, Strohbehn JW, Hatch JF, Murray W, Kettenberger H. A frameless stereotaxic integration of computerized tomographic imaging and the operating microscope. J Neurosurg. 1986;65(4):545–9.
32. Langer DJ, White TG, Schulder M, Boockvar JA, Labib M, Lawton MT. Advances in intraoperative optics: a brief review of current exoscope platforms. Operat Neurosurg. 2020;19(1):84–93.
33. Corcione F, Silvestri V, Merola G, Dambra M, Lionetti R, Pirozzi N, et al. Use of the ORBEYETM exoscope in general surgery: the advent of video-assisted open surgery. Surg Innov. 2020;
34. Kanzaki S, Takahashi S, Toda M, Yoshida K, Ogawa K. Pros and cons of the exoscope for otologic surgery. Surg Innov. 2020.
35. Hecht N, Kamphuis M, Czabanka M, Hamm B, Konig S, Woitzik J, et al. Accuracy and workflow of navigated spinal instrumentation with the mobile AIRO((R)) CT scanner. Eur Spine J. 2016;25(3):716–23.
36. Weir VJ, Zhang J, Bruner AP. Dosimetric characterization and image quality evaluation of the AIRO mobile CT scanner. J X-Ray Sci Technol. 2015;23(3):373–81.
37. Kuhnt D, Bauer MH, Nimsky C. Brain shift compensation and neurosurgical image fusion using intraop-

erative MRI: current status and future challenges. Crit Rev Biomed Eng. 2012;40(3).
38. Ungi T, Greer H, Sunderland K, Wu V, Baum ZM, Schlenger C, et al. Automatic spine ultrasound segmentation for scoliosis visualization and measurement. 2020.
39. Ma L, Zhao Z, Chen F, Zhang B, Fu L, Liao H. Augmented reality surgical navigation with ultrasound-assisted registration for pedicle screw placement: a pilot study. Int J Comput Assist Radiol Surg. 2017;12(12):2205–15.
40. Kelly PD, Zuckerman SL, Yamada Y, Lis E, Bilsky MH, Laufer I, et al. Image guidance in spine tumor surgery. Neurosurg Rev. 2020;43(3):1007–17.
41. Moore T, McLain RF. Image-guided surgery in resection of benign cervicothoracic spinal tumors: a report of two cases. Spine J. 2005;5(1):109–14.
42. Nagashima H, Nishi T, Yamane K, Tanida A. Case report: osteoid osteoma of the C2 pedicle: surgical technique using a navigation system. Clin Orthop Relat Res. 2010;468(1):283.
43. Rajasekaran S, Kamath V, Shetty AP. Intraoperative Iso-C three-dimensional navigation in excision of spinal osteoid osteomas. Spine (Phila Pa 1976). 2008;33(1):E25–E9.
44. Van Royen BJ, Baayen JC, Pijpers R, Noske DP, Schakenraad D, Wuisman PI. Osteoid osteoma of the spine: a novel technique using combined computer-assisted and gamma probe-guided high-speed intralesional drill excision. Spine (Phila Pa 1976). 2005;30(3):369–73.
45. Arand M, Hartwig E, Kinzl L, Gebhard F. Spinal navigation in tumor surgery of the thoracic spine: first clinical results. Clin Orthop Relat Res. 2002;399:211–8.
46. Gebhard F, Kinzl L, Hartwig E, Arand M. Navigation of tumors and metastases in the area of the thoracolumbar spine. Unfallchirurg. 2003;106(11):949–55.
47. Smitherman SM, Tatsui CE, Rao G, Walsh G, Rhines LD. Image-guided multilevel vertebral osteotomies for en bloc resection of giant cell tumor of the thoracic spine: case report and description of operative technique. Eur Spine J. 2010;19(6):1021–8.
48. Towner JE, Piper KF, Schoeniger LO, Qureshi SH, Li YM. Use of image-guided bone scalpel for resection of spine tumors. AME case reports. 2018;2.
49. Barzilai O, Robin AM, O'Toole JE, Laufer I. Minimally invasive surgery strategies: changing the treatment of spine tumors. Neurosurg Clin. 2020;31(2):201–9.
50. Pireau N, Cordemans V, Banse X, Irda N, Lichtherte S, Kaminski L. Radiation dose reduction in thoracic and lumbar spine instrumentation using navigation based on an intraoperative cone beam CT imaging system: a prospective randomized clinical trial. Eur Spine J. 2017;26(11):2818–27.

# 38 Future Perspective of Augmented Reality in Minimally Invasive Spine Surgery

Adrian Elmi-Terander, Gustav Burström, Oscar Persson, and Erik Edström

## 38.1 Introduction

Surgical accuracy results from a combination of factors. The most important one—and often overlooked—is the surgical understanding of anatomy. A screw placed exactly according to plan may still be placed poorly if the original plan was flawed. Augmented reality can project the relevant segmented anatomy into the perspective of the surgeon to improve real-time understanding of surgical anatomy and trajectories. This provides a new dimension of navigated MISS. Image fusion and segmentation algorithms need to provide a seamless combination of CT and MRI imaging data. Software solutions must be tailored or customizable to the intended use so that they assist in creating the best surgical plans rather than forcing the surgeon to adjust the surgical technique to compensate for technological flaws [1].

Live video tracking of motion requires custom-built systems to avoid lagging and mismatched alignment. Modern navigation systems also offer the possibility of additional intraoperative imaging to be merged with preoperative plans. In the future, systems might even add AI solutions to adapt the surgical plan to changes during the surgery. Hence, there is—and will most likely continue to be—a counterbalance between having systems as lightweight and portable as possible and providing more advanced features for accurate AR navigation [2, 3].

However, neither the surgeon nor the navigational system can see inside the body, and no amount of preoperative planning or imaging can solve this inherent problem. While tracking the reference markers, the navigational system does not provide true feedback on where the tip of an instrument is inside the body. Thus, the bending of instruments that are pushed against dense bone is only felt by the surgeon and not seen by the navigational system [4]. Similarly, small movements of the spine may go undetected. These problems are compounded if control of the surgical instruments is relinquished to a surgical robot. Navigated robotic placement of pedicle screws can be performed with excellent accuracy. Nonetheless, robots carry the potential to do great harm if the navigational data is inaccurate or force-feedback systems are misinterpreted. Novel technologies and solutions must be incorporated to address these issues.

In the following sections, key aspects in the development of AR in MISS applications will be discussed.

A. Elmi-Terander (✉) · G. Burström · O. Persson
E. Edström
Department of Clinical Neuroscience, Karolinska Institute and Department of Neurosurgery, Karolinska University Hospital, Stockholm, Sweden
e-mail: adrian.elmi.terander@ki.se


J.-S. Kim et al. (eds.), *Technical Advances in Minimally Invasive Spine Surgery*,
https://doi.org/10.1007/978-981-19-0175-1_38

## 38.2 Segmentation

Operating room (OR) time is an expensive commodity. The increasing use of navigation technologies results in valuable OR time being spent on planning navigation trajectories [5]. This perceived increase in OR time is one of the main obstacles to the wide implementation of navigation technology [6]. Several approaches have been adopted for automating the identification of vertebral levels [7]. Recent efforts have focused on segmentation (building a virtual 3D reconstruction) of entire sections of the spine on preoperative or intraoperative images to facilitate surgical planning [8–12]. Solutions for intraoperative segmentation to improve surgical navigation usability in the OR are commercially available [13]. The most recent advances have addressed the issue of automatic screw-path planning [14]. Ultrasound segmentation technologies are rapidly developing and could be a valuable addition for intraoperative planning and updating [15].

## 38.3 Hybrid OR and AR

The hybrid OR is the result of combining the functionality of a fully equipped, modern OR with that of an interventional radiology suite. The integration of state-of-the-art radiological equipment into the OR provides new dimensions to surgery. For navigated surgery, immediate access to high-quality 3D imaging capability means that it can become an integral part of the navigational setup. As the image quality of intraoperative solutions improves with time, intraoperative imaging can replace preoperative examinations and provide an accurate basis for patient registration. In addition, repeated examinations can be performed to ensure surgical results are achieved without error before finishing a surgery. Exploring these possibilities, Philips has developed an AR navigation system for the spine built around a hybrid OR (Fig. 38.1). Published results indicate a fully integrated and simplified workflow, including initial 3D CBCT scanning for registration, tracking, and navigation, as well as repeat scanning to ensure the correct placement of pedicle screws [5]. Combining this solution with an integrated robotic arm has produced high accuracy in cadaveric experiments [16]. Similarly, the integration of intraoperative ultrasound and endoscopy functionality would further expand the imaging capabilities of the AR-navigated hybrid OR [17]. Moreover, complex approaches could be envisioned in which angiography could be used to image the vasculature or even perform combined endovascular and surgical treatments (e.g., in treating spinal vascular malformations

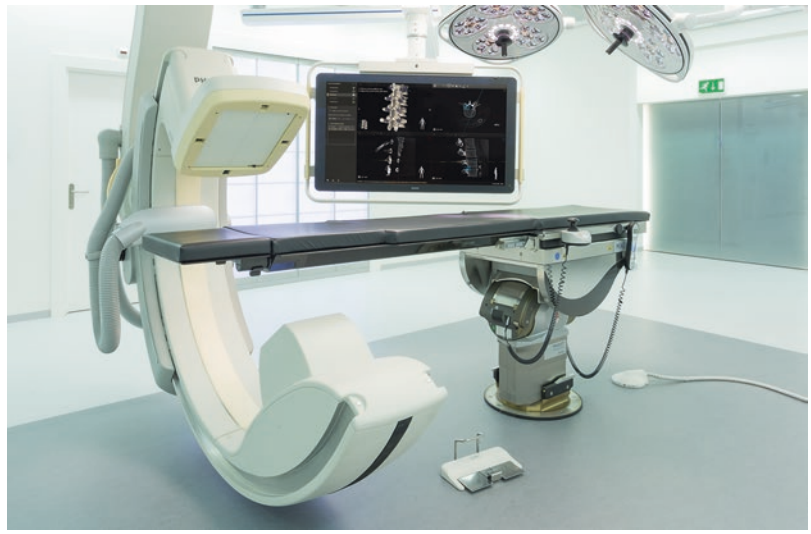

**Fig. 38.1** OR setup of the augmented reality surgical navigation system (ClarifEye) with four patient tracking cameras integrated into the C-arm. The AR view is presented on the monitor. Photo courtesy of Philips Healthcare

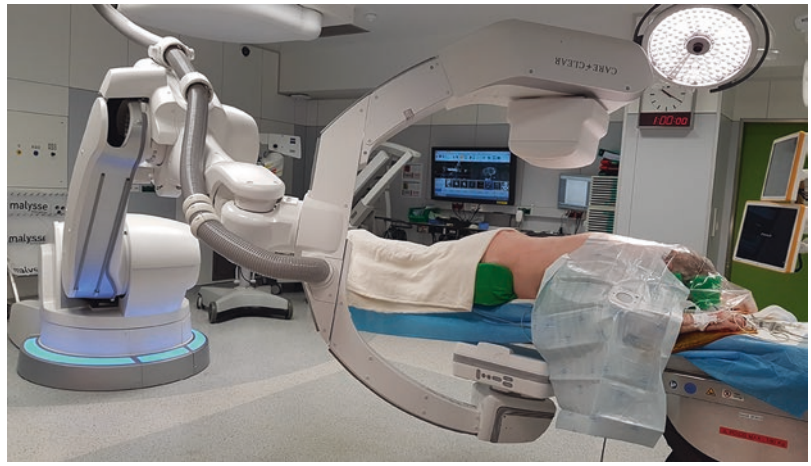

**Fig. 38.2** The Artis zeego imaging system (Siemens) during intraoperative use. Image originally published by Pireau et al. [18]. Republished with permission by Springer Nature

and fistulas). A hybrid OR with robotic capability is also offered by Siemens and can be combined with AR solutions from third-party providers (Fig. 38.2).

## 38.4 Tracking Technologies

Accurate and uninterrupted tracking of the patient is essential for navigated surgery. The most common tracking solution used currently is the DRF, which is often designed as a metal star or cross with reflective spheres at the points. The three-dimensional relation between the spheres is recognized by the navigational system, and their position in space is fixed in relation to the patient and the imaging data during patient registration. However, the metal star must be positioned in the vicinity of the surgical field; if it is dislodged, accuracy may be lost. Alternatives, such as adhesive markers, reduce the problems associated with a bulky DRF but still add to the complexity of performing a navigated surgery. Future solutions should implement marker-free alternatives where the eye of the navigational system sees the patient and continuously tracks both the patient and the instruments within the surgical field. In this context, AR technology is well suited since it can provide visual feedback on the accuracy of the alignment of real-world and virtual objects.

What if the cameras of a navigational system could visualize the patient's spinal anatomy rather than the spheres or markers of a reference system? To explore this idea, Manni et al. applied a computer vision framework to process spine images [2]. Using common algorithms in image processing, spine features could be detected and used for 3D triangulation, reaching less than an 0.5-mm error of the matched features. Spine feature tracking offers an extension and an improvement of current tracking systems, aiming for optimal patient motion compensation and reliable surgical guidance. A tracking technique that relies on features directly related to each vertebra in the surgical field has the potential to be more accurate than dynamic reference frames, which only provide tracking of a single vertebra, or patient-tracking techniques with an indirect relationship to the movements of the spine [2, 19, 20].

Despite the high accuracy obtained using spine feature detection, this technology can only be employed in open surgical cases where the spine is exposed. However, the same algorithms could be used for marker-less skin feature detection to aid in MISS cases. A recent study, applying these methods in combination with hyperspectral imaging of the skin, showed promising results while obtaining a TRE below 0.5 mm [3].

## 38.5 Intraoperative Imaging to Realign Co-registration

Perhaps the easiest way to realign the intraoperative situation with the preoperative imaging and plan would involve the use of 2D fluoroscopy to obtain at least two different image views, followed by using these to adjust or renew the co-registration. The strategy, already used for the first generations of the Mazor robot, has been further developed by several companies and should soon be available for commercial use [21, 22].

A CT or CBCT update provides the possibility of a 3D realignment, offering higher accuracy since the updated images can align better with the previously planned paths and surgical course. As a prerequisite for this functionality, the navigation plan from the start of the procedure can be fused with new intraoperative images without the need for replanning or manual realignment.

The use of MRI and US for updating surgical navigation plans will persist in the future. While MR images would add valuable detailed anatomical information, the problem remains of adapting the whole OR, instruments, and staff to work in proximity of MR. New MR sequences requiring shorter imaging time may also be an important game-changer regarding the use of intraoperative MR images in relation to OR time [23].

Ultrasound offers fast and easy image updates, and efforts to integrate US into navigation solutions are already ongoing. Clinical spine applications may soon be on the market.

## 38.6 Robotics and AR

Surgical accuracy could be markedly improved by replacing the human hand with a robotic arm. Initial studies on AR navigation combined with robotics have demonstrated a significantly higher accuracy than AR without the robot [16, 24]. Automatization of parts of the process using AI or machine learning could both improve workflow and simplify robotic integration [14]. For spine surgery, a robotic system for pedicle screw placement needs to be quick and simple to set up, sterile within the surgical field, and as unobtrusive as possible without being unstable. Thus, a sweet spot needs to be found to create a robotic arm that is stable enough to maintain accuracy while reaching targets and angles of approach within a large enough area, without occupying too much of the OR space. Similarly, the surgeon should be able to move the robotic arm rapidly out of the way if necessary. A robotic arm should be integrated with the navigation system used or itself be fully navigated to avoid having multiple systems running in parallel. Surgical robots designed for navigation are already on the market, and the transition to AR navigation solutions would likely provide the greatest benefit to MISS procedures where visualization and accuracy are vital. For pedicle screw placement, the combination of robotics and AR navigation promises to reach the goal of minimizing clinically unacceptable pedicle breaches, which exceed 2 mm [25, 26].

However, robots do not have proprioception and cannot anticipate dangerous situations. Anatomical structures are rarely flat, and the risk of skewing and deflection must be considered. Rigorous force-feedback systems, which can warn for force vectors moving a robotic-guided instrument away from the planned path and notify the attending surgeon, will be mandatory before the transitions from passive robots to intelligent and active robots can be made.

## 38.7 Machine Learning Technology

The promise of machine learning to improve the AR navigation experience has already yielded results in the form of an improved workflow [14]. Using machine learning to automate processes such as the planning of pedicle screws or rod placements are already within the grasp of current technologies and will help reduce the impact of navigation on OR time [14, 27, 28]. However, the vast majority of potential uses have yet to be explored. One way of improving the AR experience could involve combining the preoperative plan with the intraoperative visible changes to the surgical field. For example, when a part of a

tumor is removed, the use of advanced visual machine learning techniques and vast amounts of training data could help adapt the virtual tumor representation to the surgical progress by removing parts of it. However, this option is relegated to the future, as suitable algorithms for 3D reconstruction are still lacking and the computational power would most likely exceed the limits of today's AR systems.

## 38.8 Tissue Recognition for MISS and AR Navigation

Different tissues have various cellular and extracellular compositions. Consequently, tissues can be separated based on their physical properties besides their appearance in a microscope to allow real-time differentiation of tissue types. AR navigation could be combined with sensing technologies such as impedance probes or optical probes that rely on diffuse reflectance spectroscopy (DRS; [29, 30]). These and similar technologies, such as hyperspectral imaging (HIS), could provide direct feedback on the tissue type at the tip of the surgical tool and possibly offer an additional layer of safety in an automated workflow [31–33].

## References


1. Dixon BJ, Daly MJ, Chan HH, Vescan A, Witterick IJ, Irish JC. Inattentional blindness increased with augmented reality surgical navigation. Am J Rhinol Allergy. 2014;28(5):433–7.
2. Manni F, Elmi-Terander A, Burström G, Persson O, Edström E, Holthuizen R, et al. Towards optical imaging for spine tracking without markers in navigated spine surgery. Sensors (Basel). 2020;20(13).
3. Manni F, van der Sommen F, Zinger S, Shan CF, Holthuizen R, Lai M, et al. Hyperspectral imaging for skin feature detection: advances in markerless tracking for spine surgery. Appl Sci-Basel. 2020;10(12)
4. Yeh M, Wickens CD. Display signaling in augmented reality: effects of cue reliability and image realism on attention allocation and trust calibration. Hum Factors. 2001;43(3):355–65.
5. Edström E, Burström G, Nachabe R, Gerdhem P, Elmi-Terander A. A novel augmented-reality-based surgical navigation system for spine surgery in a hybrid operating room: design, workflow, and clinical applications. Oper Neurosurg (Hagerstown). 2020;18(5):496–502.
6. Hartl R, Lam KS, Wang J, Korge A, Kandziora F, Audige L. Worldwide survey on the use of navigation in spine surgery. World Neurosurg. 2013;79(1):162–72.
7. Otake Y, Schafer S, Stayman JW, Zbijewski W, Kleinszig G, Graumann R, et al. Automatic localization of vertebral levels in x-ray fluoroscopy using 3D-2D registration: a tool to reduce wrong-site surgery. Phys Med Biol. 2012;57(17):5485–508.
8. Kim Y, Kim D. A fully automatic vertebra segmentation method using 3D deformable fences. Comput Med Imaging Graph. 2009;33(5):343–52.
9. Klinder T, Ostermann J, Ehm M, Franz A, Kneser R, Lorenz C. Automated model-based vertebra detection, identification, and segmentation in CT images. Med Image Anal. 2009;13(3):471–82.
10. Huang J, Jian F, Wu H, Li H. An improved level set method for vertebra CT image segmentation. Biomed Eng Online. 2013;12(48)
11. Mandell JG, Langelaan JW, Webb AG, Schiff SJ. Volumetric brain analysis in neurosurgery: part 1. Particle filter segmentation of brain and cerebrospinal fluid growth dynamics from MRI and CT images. J Neurosurg Pediatr. 2015;15(2):113–24.
12. Byrnes TJ, Barrick TR, Bell BA, Clark CA. Semiautomatic tractography: motor pathway segmentation in patients with intracranial vascular malformations. Clinical article J Neurosurg 2009;111(1):132–140.
13. Goerres J, Uneri A, De Silva T, Ketcha M, Reaungamornrat S, Jacobson M, et al. Spinal pedicle screw planning using deformable atlas registration. Phys Med Biol. 2017;62(7):2871–91.
14. Burström G, Buerger C, Hoppenbrouwers J, Nachabe R, Lorenz C, Babic D, et al. Machine learning for automated 3-dimensional segmentation of the spine and suggested placement of pedicle screws based on intraoperative cone beam computer tomography. J Neurosurg Spine. 2019;31(1):147–54.
15. Ungi T, Greer H, Sunderland K, Wu V, Baum ZM, Schlenger C, et al. Automatic spine ultrasound segmentation for scoliosis visualization and measurement. 2020.
16. Burström G, Balicki M, Patriciu A, Kyne S, Popovic A, Holthuizen R, et al. Feasibility and accuracy of a robotic guidance system for navigated spine surgery in a hybrid operating room: a cadaver study. Sci Rep. 2020;10(1):7522.
17. Lai M, Skyrman S, Shan C, Babic D, Homan R, Edstrom E, et al. Fusion of augmented reality imaging with the endoscopic view for endonasal skull base surgery; a novel application for surgical navigation based on intraoperative cone beam computed tomography and optical tracking. PLoS One. 2020;15(1):e0227312.

18. Pireau N, Cordemans V, Banse X, Irda N, Lichtherte S, Kaminski L. Radiation dose reduction in thoracic and lumbar spine instrumentation using navigation based on an intraoperative cone beam CT imaging system: a prospective randomized clinical trial. Eur Spine J. 2017;26(11):2818–27.
19. Houten JK, Nasser R, Baxi N. Clinical assessment of percutaneous lumbar pedicle screw placement using the O-arm multidimensional surgical imaging system. Neurosurgery. 2012;70(4):990–5.
20. Uehara M, Takahashi J, Ikegami S, Kuraishi S, Shimizu M, Futatsugi T, et al. Are pedicle screw perforation rates influenced by distance from the reference frame in multilevel registration using a computed tomography-based navigation system in the setting of scoliosis? Spine J. 2017;17(4):499–504.
21. Lieberman IH, Togawa D, Kayanja MM, Reinhardt MK, Friedlander A, Knoller N, et al. Bone-mounted miniature robotic guidance for pedicle screw and translaminar facet screw placement: Part I—Technical development and a test case result. 2006;59(3):641–50.
22. Togawa D, Kayanja MM, Reinhardt MK, Shoham M, Balter A, Friedlander A, et al. Bone-mounted miniature robotic guidance for pedicle screw and translaminar facet screw placement: part 2--Evaluation of system accuracy. Neurosurgery. 2007.;60(2 Suppl 1):ONS129–39; discussion ONS39.
23. Delgado AF, Kits A, Bystam J, Kaijser M, Skorpil M, Sprenger T, et al. Diagnostic performance of a new multicontrast one-minute full brain exam (EPIMix) in neuroradiology: a prospective study. J Magn Reson Imaging. 2019;50(6):1824–33.
24. Balicki M, Kyne S, Toporek G, Holthuizen R, Homan R, Popovic A, et al. Design and control of an image guided robot for spine surgery in a hybrid OR. Int J Med Robot Comput Assist Surg. 2020;
25. Gertzbein SD, Robbins SE. Accuracy of pedicular screw placement in vivo. Spine (Phila Pa 1976). 1990;15(1):11–4.
26. Rampersaud YR, Simon DA, Foley KT. Accuracy requirements for image-guided spinal pedicle screw placement. Spine (Phila Pa 1976). 2001;26(4):352–9.
27. Wanivenhaus F, Neuhaus C, Liebmann F, Roner S, Spirig JM, Farshad M. Augmented reality-assisted rod bending in spinal surgery. Spine J. 2019;19(10):1687–9.
28. Auloge P, Cazzato RL, Ramamurthy N, de Marini P, Rousseau C, Garnon J, et al. Augmented reality and artificial intelligence-based navigation during percutaneous vertebroplasty: a pilot randomised clinical trial. Eur Spine J. 2019;
29. Burström G, Swamy A, Spliethoff JW, Reich C, Babic D, Hendriks BH, et al. Diffuse reflectance spectroscopy accurately identifies the pre-cortical zone to avoid impending pedicle screw breach in spinal fixation surgery. Biomed Opt Express. 2019;10(11):5905–20.
30. Guillen PT, Knopper RG, Kroger J, Wycliffe ND, Danisa OA, Cheng WK. Independent assessment of a new pedicle probe and its ability to detect pedicle breach: a cadaveric study. J Neurosurg Spine. 2014;21(5):821–5.
31. Fabelo H, Halicek M, Ortega S, Shahedi M, Szolna A, Piñeiro JF, et al. Deep learning-based framework for in vivo identification of glioblastoma tumor using hyperspectral images of human brain. Sensors (Basel). 2019;19(4):920.
32. Martinez B, Leon R, Fabelo H, Ortega S, Piñeiro JF, Szolna A, et al. Most relevant spectral bands identification for brain cancer detection using hyperspectral imaging. Sensors (Basel). 2019;19(24):5481.
33. Huang J, Halicek M, Shahedi M, Fei B, editors. Augmented reality visualization of hyperspectral imaging classifications for image-guided brain tumor resection. Medical Imaging 2020: Image-Guided Procedures, Robotic Interventions, and Modeling; 2020: International Society for Optics and Photonics.

# Part V

# Augmented and Virtual Reality in Spine Surgery Training

# History and Application of Virtual Reality in Spinal Surgery

39

Gustav Burström, Erik Edström, Oscar Persson, and Adrian Elmi-Terander

## 39.1 Historical Overview of Surgical Simulation

Surgical simulation has comprised an integral part of surgical training for centuries, relying on animal models, cadavers, and recent synthetic models of organs or body parts. This chapter will focus on the more recent history of surgical simulation using mannequins, computer models, and VR. Traditionally, the primary aim of simulation has been to train medical professionals for anatomical understanding and general aptitude regarding the techniques in question rather than patient-specific cases. The use of simulation as patient-specific "surgical rehearsal," equivalent to the military use of "mission rehearsal," is a newly developing area [1]. This chapter will treat both forms of simulation, sharing the aim of helping surgeons master their surgical techniques for future cases.

Current surgical simulation technologies largely owe their existence to the pioneering work done in the 1970s, 1980s, and early 1990s. Simple forms of mannequin simulation have been widely used in orthopedic surgery in the form of imitation bones and joints. The AO Foundation began hosting annual surgical training courses in Davos, Switzerland in 1960. These surgical courses encompassed simulated surgeries for teaching the use of new surgical instruments and implants [2]. The initial surgical simulations focused on fracture fixation, arthroscopic techniques, and joint replacement. Likewise, basic surgical technique simulation was employed in otolaryngology for microscopic surgery training [2]. The advent of minimally invasive procedures brought a need to train surgeons differently. Complex technical skills with an extended learning curve had to be taught. Initial simulators emphasized the need to practice hand–eye coordination in the laparoscopic environment. Sackier et al. presented a training device in 1991 with the intent of improving depth perception, hand–eye coordination, and team cooperation during laparoscopic cholecystectomy ([3]; Fig. 39.1). A variety of laparoscopic training boxes facilitated knot tying, precise moving of objects, and precision pointing [4].

## 39.2 Historical Overview of Virtual Reality in Surgery

The foundations of VR systems began in the late 1950s and early 1960s. Filmmaker Morton Heilig was a pioneer of VR who promoted the use of multiple sensory inputs to create an immersive cinematographic experience. His first commercial

G. Burström · E. Edström · O. Persson
A. Elmi-Terander (✉)
Department of Clinical Neuroscience, Karolinska Institute and Department of Neurosurgery, Karolinska University Hospital, Stockholm, Sweden
e-mail: adrian.elmi.terander@ki.se



J.-S. Kim et al. (eds.), *Technical Advances in Minimally Invasive Spine Surgery*,
https://doi.org/10.1007/978-981-19-0175-1_39

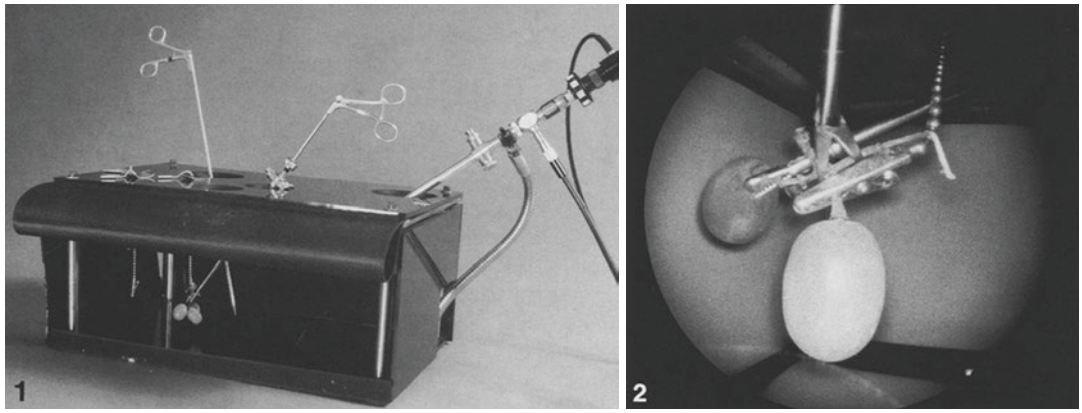


**Fig. 39.1** A cholecystectomy training box (left) and view through the telescope showing the removal of a grape (right). Image originally published by Sackier et al. [3]. Republished with permission by Springer Nature

product, the *Sensorama*, combined smell, wind, 3D imaging in the form of a prerecorded film, and vibrations to create a VR experience of riding a motorcycle through the streets of Brooklyn, New York [5]. Numerous VR projects and virtual products were presented in the years that followed. *The Sword of Damocles,* created by Ivan Sutherland, was the first VR system that incorporated a head-mounted display that tracked head orientation and updated the stereoscopic view according to the user to create a sense of being inside the virtual world [6]. Jaron Lanier and Thomas Zimmerman developed the Power Glove and Data Glove; these wired gloves that could register hand and finger movements and incorporate them into a virtual world. These were followed by the CyberGlove, a commercial version of a wired glove [7]. BOOM, commercialized in 1989 by Fake Space Labs, consisted of a small box with two CRT monitors that the user viewed through eye holes to create a 3D picture [8]. The box was mounted on a mechanical arm that sensed the position and orientation of the box, representing one of the first commercial systems that enabled movement in a VR simulation.

Despite the early development of VR solutions for other uses, computer-based surgical simulation initially focused on simple case scenarios using text and images that were answered in a stepwise fashion to solve surgical problems, using Bayesian methodology [1]. It was not until the late 1980s that surgical VR environments were introduced. Scott Delph and Joseph Rosen developed one of the first medical VR simulators, which consisted of a leg simulator that was used to practice Achilles' tendon repair and simulate the effect that such a procedure would have on gait [9]. In this sense, it was one of the first examples of using VR simulation as "surgical rehearsal," where patient-specific anatomical conditions could help simulate surgical outcomes and find an optimal treatment strategy.

Around the same time, a general surgery VR simulator was developed by Lanier and Satava. It combined the CyberGlove with a head-mounted display to enable training surgeons to interact with virtual images [1]. Although they viewed their invention as crude, it could serve as a demonstration of the possibilities of VR education in medicine and surgery. Next, a wound simulator focused on debridement and suturing was developed at the Massachusetts Institute of Technology (MIT).

The MIST-VR (minimally invasive surgery trainer–VR) was one of the first commercially successful surgical simulators (Fig. 39.2). It coupled a low-fidelity representation of a surgical image to a mechanical box trainer. Although the VR experience was exceedingly abstract by today's standards, a reduction in operating time and error rates during cholecystectomies was demonstrated in a randomized controlled trial, where surgical residents completed typical residency training with and without MIST-VR [10].

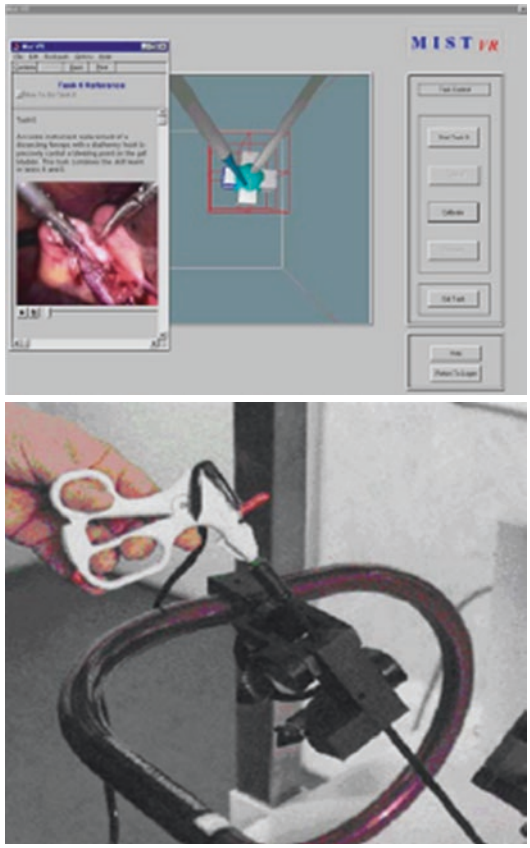


**Fig. 39.2** MIST-VR simulator. Photo courtesy Mentice, Inc. and originally published by Satava [1]. Republished with permission by Springer Nature

Yet another example of early successful VR simulators was the ENT Sinus Surgery Simulator, which was developed by the Lockheed-Martin Corporation ([11]; Fig. 39.3). The tool's creation was influenced by experience gained from the development of aviation simulators, and it was considered highly sophisticated at the time and validated in several studies [11, 12].

In parallel to simulators for general surgery, the first interventional simulation training systems were launched. Two of the earliest examples were the Simsuite by Medical Simulation Corporation and the Interventional Cardiology Training System by Mitsubishi Electric. These tools included virtual simulation of fluoroscopy, haptics, catheter physics, and hemodynamics [13].

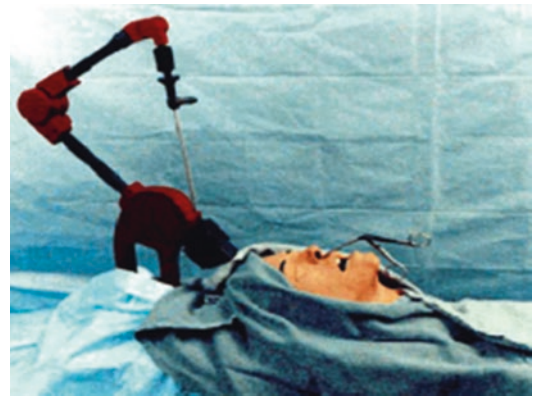

**Fig. 39.3** ENT simulator. Photo courtesy of Lockheed Martin and originally published by Satava [1]. Republished with permission by Springer Nature

Since the start of the 2000s, numerous VR simulators have entered the market. Hybrid simulators—surgical instruments that are used as part of the simulator (e.g., an endoscope)—meant that most of the surgical setup around the surgeon reflected the surgical situation, except for the virtual images being displayed. Around this time, the addition of hand or instrument tracking was also popularized. These tracking devices provide procedure-related data such as path length, economy of motion, precision, and time for the procedure. Datta et al. even showed that the motion signature captured by these tracking devices can be used to determine the surgical skill of the user ([14]; Fig. 39.4).

Whereas VR simulators began with the advent of minimally invasive procedures, a new surgical paradigm was introduced in the form of robotic surgery in the early 2000s. The da Vinci robot system, which supports intraabdominal surgery generally and prostatectomy and hysterectomy in particular, consists in part of a free-standing workstation where the surgeon sits to control the robot. The da Vinci Skills Simulator was introduced in 2007 and simulates entire surgeries using the da Vinci surgeon console ([15]; Fig. 39.5). With this development, VR surgical simulation has become even more true to surgical reality in the sense that the simulation can function on the same surgical console that is later used for the procedure.

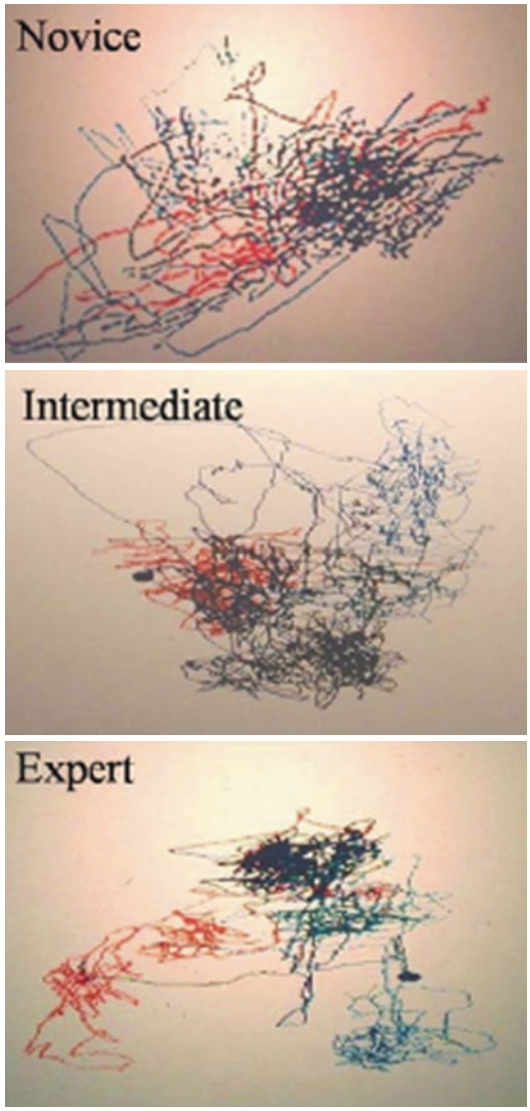


**Fig. 39.4** The hand motion signature of a novice, intermediate, and expert surgeon during laparoscopic surgery. Courtesy of Sir Ara Darzi, MD, Imperial College of London, 2001. Originally published by Satava [1]. Republished with permission by Springer Nature

## 39.3 First Publications on Spinal Surgery and VR

Only in the 2010s did VR simulation extend to spine surgical applications. In 2011, Luciano et al. investigated the learning retention of thoracic pedicle screw placement using the ImmersiveTouch workstation, a VR system developed at the University of Illinois that combines stereoscopic VR with haptic feedback [16]. In this study, one cohort underwent two separate sessions on the workstation: a practice and a test session. Between the sessions, they showed an increase in accuracy but no significant difference in failure rates. In a similar but controlled study by Gasco et al., the same workstation was used [17]. In this study, the test group trained on the ImmersiveTouch workstation, while the control group learned from traditional verbal and visual instructions. Participants in both groups then placed two pedicle screws each in lumbar sawbones. The VR-trained group performed better in all aspects tested, including the average number of errors per screw, breaches, and trajectory errors.


**Fig. 39.5** The da Vinci surgical console with the da Vinci Skills Simulator (dVSS) attached. Image courtesy of dVSS, Intuitive Surgical, Sunnyvale, USA and originally published by Bric et al. [19]. Republished with permission by Springer Nature

The early studies on spine surgical VR simulation rarely involved residents or attendings, and they were not blinded, randomized, or controlled. The first high-level evidence for the usefulness of this technology was not produced until 2015 by Gottschalk et al. The researchers grouped residents into a VR simulation group, which underwent VR training, and a control group. All residents then placed lateral mass screws at C3–C7, and all screws were rated according to trajectory adherence in a blinded fashion. This randomized controlled study showed that residents trained in VR significantly improved their insertion of lateral mass screws [18].

## References


1. Satava RM. Historical review of surgical simulation—a personal perspective. World J Surg. 2008;32(2):141–8.
2. MacIntyre I, Munro A. Simulation in surgical training. Br Med J. 1990;300(6732):1088.
3. Sackier JM, Berci G, Paz-Partlow M. A new training device for laparoscopic cholecystectomy. Surg Endosc. 1991;5(3):158–9.
4. Cozzi P, McCall J, Jorgensen J, Morris D. Laparoscopic vs open ultrasound of the liver: an in vitro study. HPB Surg. 1996;10(2):87–9.
5. Pimentel K, Teixeira K. Virtual reality through the new looking glass. 1993.
6. Srivastava K, Das R, Chaudhury S. Virtual reality applications in mental health: challenges and perspectives. Ind Psychiatry J. 2014;23(2):83.
7. Kessler GD, Hodges LF, Walker N. Evaluation of the CyberGlove as a whole-hand input device. ACM Trans Comput-Hum Interact (TOCHI). 1995;2(4):263–83.
8. Veron H, Hezel P, Southard DA, editors. Head-mounted displays for virtual reality. Helmet-and head-mounted displays and symbology design requirements; 1994: International Society for Optics and Photonics.
9. Delp SL, Loan JP, Hoy MG, Zajac FE, Topp EL, Rosen JM. An interactive graphics-based model of the lower extremity to study orthopaedic surgical procedures. IEEE Trans Biomed Eng. 1990;37(8):757–67.
10. Seymour NE, Gallagher AG, Roman SA, O'brien MK, Bansal VK, Andersen DK, et al. Virtual reality training improves operating room performance: results of a randomized, double-blinded study. Ann Surg. 2002;236(4):458.
11. Edmond CV Jr, Wiet GJ, Bolger LB. Virtual environments: surgical simulation in otolaryngology. Otolaryngol Clin N Am. 1998;31(2):369–81.
12. Satava RM, Fried MP. A methodology for objective assessment of errors: an example using an endoscopic sinus surgery simulator. Otolaryngol Clin N Am. 2002;35(6):1289–301.
13. Cotin S, Dawson S, Meglan D, Shaffer D, Ferrell M, Bardsley R, et al. ICTS, an interventional cardiology training system. Stud Health Technol Inform. 2000:59–65.
14. Datta V, Mackay S, Mandalia M, Darzi A. The use of electromagnetic motion tracking analysis to objectively measure open surgical skill in the laboratory-based model. J Am Coll Surg. 2001;193(5):479–85.
15. Kelly DC, Margules AC, Kundavaram CR, Narins H, Gomella LG, Trabulsi EJ, et al. Face, content, and construct validation of the da Vinci skills simulator. Urology. 2012;79(5):1068–72.
16. Luciano CJ, Banerjee PP, Bellotte B, Oh GM, Lemole M Jr, Charbel FT, et al. Learning retention of thoracic pedicle screw placement using a high-resolution augmented reality simulator with haptic feedback. Neurosurgery. 2011;69(1 Suppl Operative):ons14–9; discussion ons9.
17. Gasco J, Patel A, Ortega-Barnett J, Branch D, Desai S, Kuo YF, et al. Virtual reality spine surgery simulation: an empirical study of its usefulness. Neurol Res. 2014;36(11):968–73.
18. Gottschalk MB, Yoon ST, Park DK, Rhee JM, Mitchell PM. Surgical training using three-dimensional simulation in placement of cervical lateral mass screws: a blinded randomized control trial. Spine J. 2015;15(1):168–75.
19. Bric JD, Lumbard DC, Frelich MJ, Gould JC. Current state of virtual reality simulation in robotic surgery training: a review. Surg Endosc. 2016;30(6):2169–78.

# The Impact of Virtual Reality on Surgical Training

40

Ufuk Aydinli, Umut Elestekin, and Sinan Vural

Surgical complications cost lives, and the economic impact of only the annual one million training-related orthopedic complications is $5 billion per year. There is no standardization in surgical training worldwide. Democratization is also needed and is currently not achievable. The measurement and assessment in medical education cannot be done objectively, as there are no standard metrics available. Finally, there is a need to reinforce the learning before and after advanced surgery courses. We tend to forget 80% of what we learn in 3 days, but unfortunately, we cannot help young surgeons repeat what they learn [1–3].

Simulation is not new. For instance, pilots are training with simulators since the 1980s. Simulators also started to become a part of surgical training at that time, but they were expensive and not easy to reach at all. However, the swift technological advances of the twenty-first century enable us to create portable, feasible, and reachable virtual-reality simulators with tactile feedback to use in medical education [3–5].

Virtual reality creates an immersive environment in which the users experience a stereoscopic visual environment and auditory signals. As a user, you have stereoscopic depth perception and six degrees of freedom as you move within the environment. This means however you move your head, the headset will show you whatever you are looking at just like the real world, only the rendering quality might not be as realistic. Of course, it is very objective and every single person must experience it to get the full immersiveness provided by the VR headsets, even watching a video of it would not be enough.

Most important aspect of VR is spatial tracking. The headset's position and rotation in space are tracked in three dimensions. This is done either by external sensors or from inside out by sensors on the headset itself. As the users move their heads, the positional and rotational data is tracked and a camera is positioned in the 3D environment to replicate what each eye should see. The view from these cameras is rendered in real time with smaller than 10 ms of delay and displayed on the screens in front of each eye. Thus, the user has a cohesive visual representation in the virtual environment.

The immersive experience is visual initially but it is further enhanced by utilizing auditory feedback. Modern virtual reality head-mounted systems also support 3D audio rendering. When you are at a movie theater, surround sound systems create a realistic audio experience. With the VR headset, the sounds of the environment are rendered separately for each of the ears.

U. Aydinli (✉)
Verom Spine and Tumor Center, Bursa, Turkey

U. Elestekin
NOYA Enterprise, Istanbul, Turkey

S. Vural
NOYA Enterprise, Oslo, Norway



J.-S. Kim et al. (eds.), *Technical Advances in Minimally Invasive Spine Surgery*,
https://doi.org/10.1007/978-981-19-0175-1_40

Like stereoscopic images, you are served stereo audio that reacts to the way you move your head.

In surgical simulations, you can hear the sounds from a real-life surgical operation. Like surgeons talking to each other, ambient sounds in the operating theater. On top of this, real-time data can be presented as audio, the rate of breathing, the heartbeat can be represented as sound and give the user feedback about the status of the patient. Add on top of this the interactive sounds of medical instruments being used, the hum of the burr, buzz of the saw, sounds of the screwdriver, tools being dropped on the tray and you see and hear the operating room.

One of the most important feedbacks comes from the tactile or haptic interfaces. Haptic feedback has been shown to improve the fidelity, realism, and thus the training effect of VR simulators [6].

Our surgical simulator makes use of an entry-level haptic device, balancing the cost of equipment and the outcome of the experience. Our implementation of the haptic force feedback allows the user to register if they are operating on hard tissue like bone or soft tissue like muscle and fat. As our simulator focuses on the procedural training method and not on psychomotor skill development, a more strong form of haptic input was not necessary.

With this new generation of simulators, simulation-based training can be used to design structured learning experiences, measure outcomes of targeted teamwork exercises, and oversee learning objectives. Simulation-based training allows learning and relearning as often as needed to correct mistakes, enabling the trainee to perfect steps and fine-tune skills to optimize clinical outcomes. It is possible to filter and select trainees for further procedural competency-based training. Simulation-based medical education protects patients from unnecessary risks while developing health professionals' knowledge, skills, and attitudes. It also is a valuable tool for a trainee for understanding ethical issues and overcome practical dilemmas. Moreover, the trainee has the advantage of being in a familiar environment and does not need to take days off and travel, which means saving money and time [7–10].

Simulation by VR in orthopedic surgery and neurosurgery for educational, preoperative planning, and intraoperative utilization continues to improve with technological advances in computer processing [2, 11]. VR utilizes a computer processing unit with a head-mounted display to provide visual and auditory cues coupled with haptics to provide an immersive, multisensory experience with the creation of touch, vibration, and motion [3–5].

In our study design, 25 (20 orthopedic, 5 neurosurgeon) junior surgeons who have no previous experience in posterior cervical spine instrumentation procedures were involved. Before all practical procedures, all surgeons received a 2-h lecture about cervical spine anatomy, C1–C2 Lateral mass-Cervical pedicle screw application methods, and video demonstration by expert senior surgeons who have more than 20 years of spine surgery experience. Then they were divided into two groups, Group 1 (10 surgeons) underwent VR simulation with haptic feedback posterior cervical instrumentation training (Fig. 40.1), Group 2 (15 surgeons) only applied C1–2 screw with Harm's technique, C3–4-5 lateral mass screw with Magerl Technique, and C6–7 cervical pedicle screws with Abumi technique to the sawbones without any instruction (Fig. 40.2). Group 1 did the same sawbone instrumentation procedures after VR simulation training. All sawbones underwent CT imaging and all screw pathways were analyzed (Fig. 40.3). For the statistical analysis, the student's T-test (unpaired t-test) was used and $p$-value of $<0.05$ is regarded as statistically significant. All sawbones which were screws implanted were sent to the radiology department and axial CT images were taken and reformatted in sagittal and coronal planes. Independent radiologist interpreted all CT images and screw misplacements were reported. The number of screws implanted was 70 in Group 1 and 105 in Group 2. The screw misplacement ratio was 12% in Group 1 and 19% in Group 2. The p-value was 0.0263 which was statistically significant. Within the 19% misplaced screws in Group 2, 4% directly were hitting the vertebral

**Fig. 40.1** VR simulation with haptic feedback posterior cervical instrumentation training

**Fig. 40.2** Applications of C1–2 screw with Harm's technique, C3–4-5 lateral mass screw with Magerl Technique, and C6–7 cervical pedicle screws with Abumi technique to the sawbones without any instruction

artery. The short questionnaire taken from all surgeons after the workshop reported that using the simulation was easy and very helpful for their training. In this study; we provide a virtual reality and haptic enabled simulator for spine surgeons wishing to train in posterior cervical instrumented spine surgery (Fig. 40.4). It provides an entirely immersive, multisensory operating room environment for training. A surgeon using this simulator can do pedicle screw, lateral mass screw placement in the posterior cervical spine with unlimited repetition.

In medicine, there is an ancient rule: "Primum non nocere," meaning "First do no harm," while attending a patient. For this rule, it is essential to get the necessary training and experience.

WHO reports that 60% of surgical complications are due to not following surgical protocols.

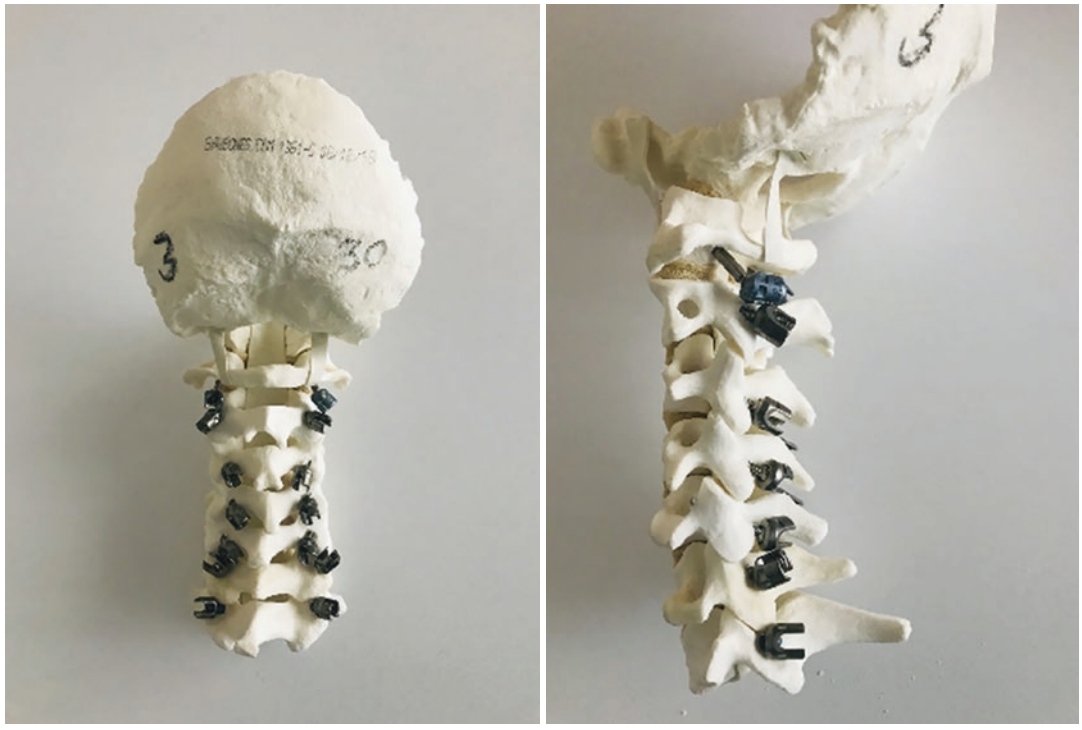

**Fig. 40.3** All sawbones underwent CT imaging and all screw pathways were analyzed

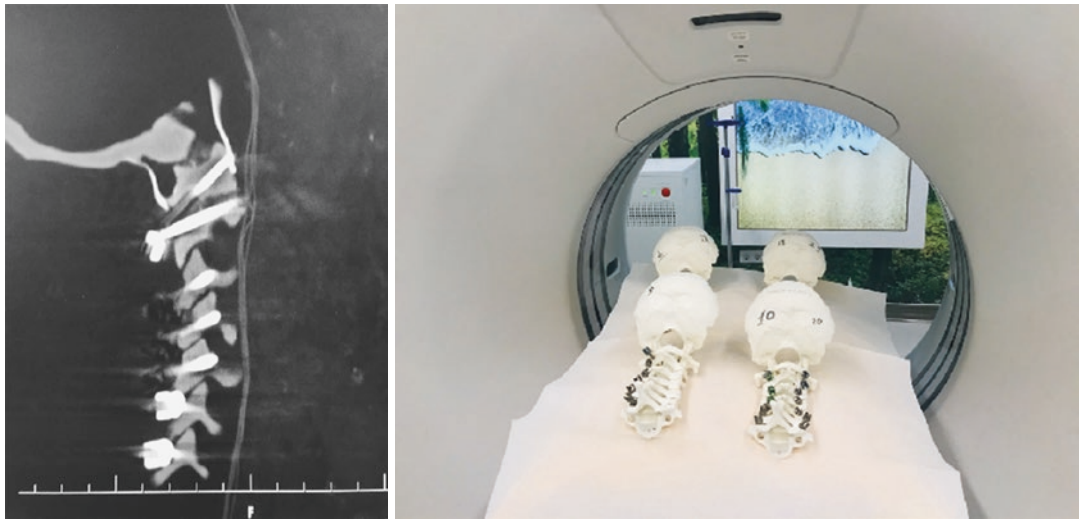

**Fig. 40.4** Virtual reality and haptic enabled simulator for spine surgeons wishing to train in posterior cervical instrumented spine surgery

In order to not break the ancient rule, surgeons need to be trained intensively, and comprehensively. A survey of general surgery residency programs in the USA found that 86% had specific curricula for teaching "book knowledge," but only 45% had curricula for surgical technique.

Medical professionals need to be trained so that they follow medical procedures step by step

that need to be repeated many times to engrain them into their memories. We, therefore, need a practical, easy to reach, and low-cost training method [10].

Professional development is an ongoing process in all walks of life. Unlike most, medical education and training not only require vast amounts of knowledge but also interaction with patients. Briefly, education/training is the act and systemic instruction process of imparting or acquiring and validating particular competencies. These learned competencies are factual knowledge, know-how, operational skills, and overall attitude toward patient treatment.

Repetition is a crucial part of learning. It solidifies new skills, improves speed, increases confidence, and strengthens the connections in the brain. Most importantly, it draws attention to minor details. So, practice is the best way to solidify data that you need to keep in your mind and retrieve when required [12].

Reports of high complication rates in early adaptation in spine surgery may adversely steer established surgeons from performing these procedures. As the evidence grows for simulation training techniques in this field, it will reverse the current practice and training behaviors [2]. Those simulators should be commercially available and unique for every person.

Simulation-based training allows learning and relearning as often as needed to correct mistakes, enabling the trainee to perfect steps and fine-tune skills to optimize clinical outcomes. It is possible to filter and select trainees for further procedural competency-based training. Simulation-based medical education protects patients from unnecessary risks while developing health professionals' knowledge, skills, and attitudes. Future studies should attempt standardization of these simulation training techniques, clinical outcomes, supporting well-conducted randomized trials of simulators use in spine surgery field. These outcomes should be combined with radiographic parameters with patient-reported outcome measures.

## References

1. Aim F, Lonjon G, Hannouche D, Nizard R. Effectiveness of virtual reality training in orthopaedic surgery. Arthroscopy. 2016;32:224–32.
2. Lohre R, Wang JC, Lewandrowski KU, Goel DP. Virtual reality in spinal endoscopy: a paradigm shift in education to support spine surgeons. J Spine Surg. 2020;6(Suppl 1):208–23.
3. Lohre R, Warner JP, Athwal GS, Goel DP. The evolution of virtual reality in shoulder and elbow surgery. JSES Int. 2020;4:215–23.
4. Kalun P, Wagner N, Yan J, Nousiainen MT, Sonnadara RR. Surgical simulation training in orthopedics: current insights. Adv Med Educ Pract. 2018;9:125–31.
5. Lohre R, Bois A, Athwal G, Goel DP. Improved complex skill acquisition by immersive virtual reality training. J Bone Joint Surg Am. 2020;102:26.
6. Bernardo A. Virtual reality and simulation in neurosurgical training. World Neurosurg. 2017;106:1015–29.
7. Konakondla S, Fong R, Schirmer CM. Simulation training in neurosurgery: advances in education and practice. Adv Med Educ Pract. 2017;8:465–73.
8. Oliveira LM, Figueiredo EG. Simulation training methods in neurological surgery. Asian J Neurosurg. 2019;14:364–70.
9. Pfandler M, Lazarovici M, Stefan P, et al. Virtual reality- based simulators for spine surgery: a systematic review. Spine J. 2017;17:1352–63.
10. Rangarajan K, Davis H, Pucher PH. Systematic review of virtual haptics in surgical simulation: a valid educational tool? J Surg Educ. 2020;77(2):337–47.
11. Vaughan N, Dubey VN, Wainwright TW, et al. A review of virtual reality based training simulators for orthopaedic surgery. Med Eng Phys. 2016;38:59–71.
12. Hu Z, Li X, Cui J, et al. Significance of preoperative planning software for puncture and channel establishment in percutaneous endoscopic lumbar discectomy. A study of 40 cases. Int J Surg. 2017;41:97–103.

# 41 Mixed and Augmented Reality Simulation for Minimally Invasive Spine Surgery Education

Simon Weidert and Philipp Stefan

## 41.1 Introduction

Spine surgery, like most surgical disciplines, is a highly tactile and visual specialty that requires a fundamental understanding of the spatial relationship of anatomical structures to each other, with respect to surgical instrumentation and their representation in medical imaging [1].

Operative competency in surgery is attained through years of practice and exposure to challenging situations [2]. While training and assessment in the surgical workplace, i.e., the operating room, is desirable and a cornerstone of surgical education, there are limitations imposed by factors such as patient safety concerns, non-standardized settings, and case mixes, the infrequency of clinical situations, and cost of operating room time [3]. Surgical education must therefore continue to rely on simulation complementing workplace-based educational activities [3].

Simulation enables training and assessment of targeted interventions and related skills in a safe environment. It further allows standardizing conditions across trainees and the range of relevant cases, procedures, and clinical contexts that can be modified to emphasize fundamental techniques and alternative approaches, and infrequent but critical tasks [3, 4]. Simulation thus provides a structured training experience and fair assessment conditions [4]. While the history of simulation goes back centuries [5], digital simulation modalities have seen much development over the last decade. Two prominent simulation modalities are virtual reality (VR) and augmented reality (AR) [1].

## 41.2 VR and AR Simulation

VR enables real-time immersion in a completely virtual environment (see also the previous chapter). Thus, the success of VR applications is determined by their ability to entirely block out real-world stimuli and replace them with digitally rendered graphics and, in many cases, simulated haptics [1]. However, computer graphics and, in particular, computer-generated haptics are often unrealistic [1]. Furthermore, with growing technological sophistication and a focus on increasing fidelity toward total immersion, VR simulation risks losing touch with the real environments they intend to replicate [6].

By contrast, AR is situated between reality and VR. To illustrate this, Milgram et al. [7] have over two decades ago proposed the reality-virtuality continuum that locates AR in the spectrum of mixed reality (MR) techniques between

S. Weidert (✉)
Musculoskeletal University Center of LMU Munich, Munich, Germany
e-mail: simon.weidert@med.uni-muenchen.de

P. Stefan
Medability GmbH, Munich, Germany


J.-S. Kim et al. (eds.), *Technical Advances in Minimally Invasive Spine Surgery*,
https://doi.org/10.1007/978-981-19-0175-1_41

the extremes of reality and virtuality.[1] Not entirely real or virtual, AR mixes digital information with real-world stimuli to create a mixed reality environment allowing the user to interact with virtual information in the context of their real-world surroundings" [1, p. 1].

Despite this fundamental difference, AR and VR are often confused within the literature [1]. Furthermore, much of the discussion of AR centers on the devices used for implementation in applications [8]. However, AR is not tied to specific technologies. Instead, following Ronald Azuma [10], it is defined as meeting the following three characteristics:

1. Combines real and virtual.
2. Is interactive in real time.
3. Is registered in three dimensions.

It is these characteristics that allow AR to combine virtual and real-world content seamlessly and in correct spatial alignment, making AR an ideal tool for simulation as defined by David Gaba, the godfather of simulation: "a technique (not a tool or technology) for replacing, augmenting, or amplifying reality with guided experiences, often immersive in nature, that evoke or replicate essential aspects of the real world in an interactive manner" [11].

## 41.3 AR in Spine Surgery Simulation

AR applications have been broadly defined as "augmenting natural feedback to the operator with simulated cues" [7, p. 283]. On the one hand, AR allows us to naturally integrate supplemental information into real-world experiences [12], i.e., to use AR to *supplement* simulation. On the other hand, AR may be used to replace substantial parts of reality with virtual representations blended in seamlessly and thus help to *implement* simulation.

In a surgical simulation, two major applications of using AR to *supplement* simulation have emerged. First, AR has been used to provide guidance content that is visualized in-situ, i.e., in the simulated operating field. Such guidance in simulation-based training can be anatomy-related or performance-related. Anatomy-related content may include virtual representations of the patient anatomy shown as an overlay on the patient model, e.g., 3D models and volumetric renderings [13] or CT slice data superimposed on the anatomy [14]. Another approach is to overlay (real) imaging data with virtual content. Moult et al. [15], for example, show a virtual spine model superimposed on real ultrasound images to support training of the interpretation of sonographic images and ultrasound-guided facet joint injection.

Performance-related guidance content may include, for example, optimal entry points or instrument trajectories [16] or instructions on the performance of the workflow steps of a procedure.

Second, AR has been used for telementoring in surgical simulation training to integrate remote instructors or faculty in training. In addition to audio communication, AR telementoring allows remote instructors to provide real-time visual instruction in direct spatial alignment with the surgical field. This may take the form of annotations, e.g., cutting paths, target points, or text labels, drawn or placed into the surgical field [17]. Alternatively, it can include the demonstration of workflow step performance, which is then displayed in the surgical field on the trainee's side, e.g., as semi-transparent "ghost" instruments [18, 19].

Furthermore, AR has been used to *implement* simulation in the field of spine surgery. Where VR aims at complete immersion replacing reality entirely, AR allows replacing real-world elements selectively. One of the key strengths of simulation is the patient-specific replication of real-world cases. Compared to OR-based or

[1]Note: For the purpose of this article, we use techniques within the MR spectrum including AR under the term "augmented reality," as the more general term MR is variably used in literature, in addition to its intention as an umbrella term, to describe extensions of AR, combinations of VR and AR or seen as a marketing term [8, 9].

cadaver lab training, patient-specific simulation allows a structured selection of patient cases with the anatomical and pathological characteristics relevant for the targeted intervention and repetition of cases [20]. While VR and AR simulation are both suited for the implementation of patient-specific simulation, VR is constrained to virtual representations of patient models and therefore bound to the capabilities of computer graphics and haptic device hardware.

Relevant elements of AR in spine surgery

Visual elements

- Spinal bone.
- Soft tissue.
- Fluids (blood, water).
- Foreign bodies (instruments, devices).
- Medical imaging (X-ray fluoroscopy, Computed Tomography, Computer Navigation, endoscopic and microscopic imaging).

Haptic elements

- Spinal bone (vertebrae).
- Soft tissue.
- Instruments.
- Implants.

However, with today's hardware capabilities, it is close to impossible to create the complex haptics of spine surgery instrumentation authentically. VR haptic simulation is furthermore limited to instrument–tissue interaction and does not allow the user to touch and feel the anatomy, which is a sensory input essential in spine surgery. If hands-on operative competency is a teaching objective, spine surgery simulation must rely on physical patient anatomy models treated with real surgical instruments for the foreseeable future.

Recent advances in 3D printing allow the low-cost production of patient-specific spine models based on CT data that closely resemble the haptics of real human bone [21]. AR allows integration of such physical models and real instruments into simulations and seamlessly mix them with virtual content in real time and correct spatial alignment.

Currently, the use of AR to implement simulation in spine surgery is focused on replacing X-ray imaging, i.e., fluoroscopy or CT, with simulated, virtual imaging. C-arm X-ray imaging is still one of the most commonly used intraoperative imaging modalities in spine surgery. However, the use of real C-arms in education is limited by availability and cost. Simulation of X-ray imaging is therefore of particular relevance for surgical education. Furthermore, it avoids exposing learners and educators to ionizing radiation.

A number of studies investigate simulators integrating physical models and simulated radiation-free imaging. Harrop et al. used an AR simulator for simulation-based training and assessment of posterior cervical decompression [22]. They created patient-specific spine models from CT data using 3D printing and used the same CT data to implement simulated CT imaging of anatomy and surgical tools. Hollensteiner et al. utilized AR to simulate X-ray imaging of patient anatomy (synthetic foam models and synthetic muscle tissue) and surgical instruments [23]. Stefan et al. implemented a patient-specific simulation of facet-joint injection, using patient CT data for 3D printing of spine models and X-ray imaging simulation [24]. They used AR to simulate X-ray imaging of patient anatomy and instruments using a real, physical C-arm, which provided completely radiation-free simulated X-ray images. They could demonstrate that simulated imaging can replicate real imaging with high accuracy within the tolerable error range (<2 mm) for spine surgery.

## 41.4 AR in Simulation-Based Assessment

Frequent performance assessment in authentic settings is a cornerstone of competency-based medical education that is continuing to replace traditional education models worldwide [25]. When making educational decisions based on assessments or providing feedback on learner's performance, it is crucial to ensure that assessment scores measure what they intend to measure, i.e., that there is sufficient validity evidence for their intended use. While the concept of validity thus does not apply to the simulator itself, an assessment conducted in a simulation has implications for validity.

Any assessment can be characterized by its stimulus format (the task performed) and response format (how it captures responses) [26]. What empirical research has shown is that validity is primarily determined by the stimulus format and that authenticity of the stimulus is essential for validity [26]. Suppose a simulation is used as a format for authentic assessment of surgical performance, in that case, it is paramount that simulated tasks reflect clinical reality in the facets that are relevant to the competencies constituting such performance.

Earlier, we highlighted that the strength of AR simulation is the seamless integration of reality and virtual content and that AR, in particular, may accommodate patient-specific physical anatomy models. Empirical research has shown that such content is drawn from real life. In particular, the physical presence of a simulated patient is a significant factor constituting the authenticity of simulation [27]. This is further supported by situative theory which argues for the importance of the complex interplay between participants and their environment (physical context) for knowledge, thinking, and learning [28]. Situativity theory also emphasizes the importance of participants interacting with each other [28]. To this end, and in contrast to VR, AR enables real face-to-face interaction between participants to occur. The occurrence of authentic team performance and interaction is a prerequisite for the assessment of non-technical skills such as communication and teamwork skills.

Taking an example from spine surgery, Pfandler et al. used AR techniques to implement a full-scale OR simulation of vertebroplasty involving a full surgical team and used this simulation as a format for technical and non-technical competency assessment [29]. Study results showed that surgeons' non-technical skills correlated significantly with their technical performance.

## 41.5 Discussion

### 41.5.1 The Goal of the Simulation

There are two main objectives that surgical simulators have to accomplish. First, it is to support learners to acquire the competencies required for practice and facilitate the seamless transfer to the operating theater. Simulators have to do the job by inviting the trainee on a structured educational journey, adjusted to 'learners' needs, and allow the repetitive practice of relevant procedures and cases.

The second objective is tightly intertwined with the first—the assessment of the trainee by using meaningful metrics and thus allowing to rate the trainee and give supportive feedback on where the skill gaps are. This information can now be used for the first objective in formative assessment (also called *assessment for learning*) to provide feedback and developmental guidance. Ideally, this will reduce or even eliminate the need for a faculty supervisor for the most of the educational journey.

Furthermore, performance evaluation can also be used for summative assessment (also called *assessment of learning*) for educational or certification related decisions, such as graduation, readiness for practice certification or Maintenance of Certification (MoC).

### 41.5.2 The Case for AR

VR simulation systems have recently become popular due to the availability of consumer-grade low-cost devices, such as head-mounted displays and the advances in computer graphics. These technologies allow the users to enter a virtual world, usually an operating theater, and perform tasks under virtual guidance. The main weakness of these systems is that they either provide no haptics at all or provide simplistic feedback using haptic devices, often using abstracted pen-like tools as an interface instead of real surgical instruments. As mentioned above, spine surgery is a specialty that poses high demands on haptic perception abilities, be it regarding instrumentation or manual feeling, to explore the anatomy and to interact with it in complex ways. Existing haptic device technology is far from meeting those requirements. Considering that haptic devices have seen decades of research and development already, it is doubtful to see fundamental improvements in the foreseeable future.

In comparison, synthetic phantoms, while offering a highly realistic haptic and visual appearance and even case specificity, have one major drawback. They usually do not include the capacity to gather data and thus are entirely ignorant of what the trainee is doing or what the training goals even are. While they can be used for rehearsal under supervision, their capabilities are somewhat limited when it comes to deriving metrics and providing structured feedback. Thus, what is clearly missing, compared to digital simulation systems, is the potential to generate meaningful feedback from data that could be used to evaluate progress or improve training.

Therefore, the future of spinal surgery simulators is undoubtedly the combination of synthetic models with high haptic fidelity with digital technology able to augment the trainee's perception with meaningful guidance as well as tapping the potential of data analysis with its many possible future applications as mentioned above.

While for long, high fidelity was the top goal of simulator design, the focus has shifted now toward educational utility. To achieve the desired learning effects, visual, haptic, and functional representation must be aligned with the learning objectives and demands of surgical practice. Highly artificial VR environments, for instance, risk that what is learned is not readily transferable to live, work-based settings. Worse, learned material might "have to be unlearned before authentic learning can take place in a specific context" [6, p. 154].

For training, AR simulators yield a number of advantages compared to alternative approaches. Regarding haptics, AR simulators benefit from the capability to integrate physical models that offer a high degree of authenticity and are close to the haptic properties of real tissue. Moreover, it is possible to integrate additional physical components used in actual surgical practice into the simulation, e.g., imaging devices such as C-arms and real surgical instruments. Besides, in contrast to fully immersive VR, AR allows face-to-face communication with team members or instructors, enabling natural training situations such as those found in the cadaver lab or the operating room. Using AR telementoring, remote instructors or faculty can be involved in simulation training. This helps to make training location-independent and to counteract the scarcity of locally available instructors. Automated AR guidance can support training when instructors are not available. Further, it helps to standardize and structure training content, if required.

Assessment benefits from the increased authenticity of AR simulation and the ability to create structured and standardized scenario portfolios including patient-specific cases.

### 41.5.3 Current Status of AR Spine Simulation

So why don't we see an abundance of AR simulators on the market today? Combining virtual and real elements seamlessly is not a trivial task. For instance, an open surgical approach would require the simulator to precisely track soft tissues as well as bone tissue as they are manipulated manually or with the help of instruments. This is true in particular because any incoherence of virtual and real world due to non-detected

alterations of reality would be immediately visible in the AR display. This problem can be compared to computer-assisted surgery with navigation systems that do not reflect tissue manipulation. Thus, unless tracking becomes more precise and capable of tracking relevant tissue in real-time, AR simulators will likely focus on minimally invasive applications before advancing into the open field.

### 41.5.4 Skills Transfer

AR simulation is still in its relative infancy. To facilitate a more comprehensive implementation, a central question arises: To what extent does AR simulation fulfill its purpose of supporting training and assessment of surgical learners? Providing strong evidence of transfer of what is learned in AR simulation into surgical practice is not a simple task and requires prospective controlled studies. Weidert et al. recently showed that clinical students trained on an AR spine surgery simulator were able to place percutaneous pedicle screws on a cadaver without any help and even outperformed the control group that was trained on the cadaver [30]. However, prospective controlled studies are still rare, and most publications do not provide extensive evidence for transfer to practice settings.

**From training cases to training for a case:**

In order to allow an effective transfer of skills into the OR, it is mandatory that the training cases reflect the variations of anatomy and pathology that can be encountered in real-life situations. This will lead to an ever-growing library of cases, ideally derived from actual patient data. Those will have to be well-structured and curated for targeted skill training. As in other forms of training, simple cases and skills have to be mastered first before moving on to more complex lessons and integrated competencies. Ideally, case libraries will be compiled by societies and training centers or experts in the field willing to contribute cases, allowing for democratizing educational content.

As the variety, quality, and complexity of training cases increase, the use of spine surgery simulators can evolve from basic skill training to Maintenance of Certification (MoC) and ultimately just-in-time training on a specific dataset prior to the real surgery. This may eventually lead to rehearsing a case on a simulator using its preoperative data before entering the OR.

### 41.5.5 Economics

While VR and synthetic phantoms are comparably cheap and easy to use, AR is more expensive and difficult to set up due to more complex system designs often requiring several working components. Most of those are not yet consumer goods nor are they cheaply available. Modern AR HMDs, for instance, range from 3500 € (Hololens 2) to $38.000 (Canon MREAL S1).

It can be expected that with the cost of components steadily decreasing, AR simulators will become increasingly affordable for training institutions such as university skills labs and societies' course curricula.

## 41.6 Conclusion

Assessment of surgeons' performance, formative feedback, and realistic case libraries are key strengths of digital simulation for spine surgery education. As a result, cadaver, as well as synthetic phantom training, will decrease in their importance for training programs. AR spine surgery simulation is destined to be the training and assessment modality of future due to its inherent strengths and capabilities.

## References

1. Williams MA, McVeigh J, Handa AI, Lee R. Augmented reality in surgical training: a systematic review. Postgrad Med J. 2020;96(1139):537–42.
2. Azari D, Greenberg C, Pugh C, Wiegmann D, Radwin R. In search of characterizing surgical skill. J Surg Educ. 2019;76(5):1348–63.

3. Brydges R, Hatala R, Zendejas B, Erwin PJ, Cook DA. Linking simulation-based educational assessments and patient-related outcomes: a systematic review and meta-analysis. Acad Med. 2015;90(2):246–56.
4. Cook DA, Hatala R. Validation of educational assessments: a primer for simulation and beyond. Adv Simul. 2016;1(1):31.
5. Owen H. Early use of simulation in medical education. Simul Healthc. 2012;7(2):102–16.
6. Bleakley A, Bligh J, Browne J. Learning by simulation and the simulation of learning. In: Bleakley A, Bligh J, Browne J, editors. Medical education for the future: identity, power and location. Dordrecht: Springer; 2011. p. 153–69.
7. Milgram P, Takemura H, Utsumi A, Kishino F. In: Das H, editor. Augmented reality: a class of displays on the reality-virtuality continuum. Boston, MA; 1995. p. 282–92.
8. Brigham TJ. Reality check: basics of augmented, virtual, and mixed reality. Med Ref Serv Q. 2017;36(2):171–8.
9. Speicher M, Hall BD, Nebeling M. What is mixed reality? In: Proceedings of the 2019 CHI conference on human factors in computing systems. New York: Association for Computing Machinery; 2019. p. 1–15.
10. Azuma RT. A survey of augmented reality. Presence Teleop Virt. 1997;6(4):355–85.
11. Gaba DM. The future vision of simulation in health care. BMJ Q Safety. 2004;13(Suppl 1):i2–10.
12. Linte CA, White J, Eagleson R, Guiraudon GM, Peters TM. Virtual and augmented medical imaging environments: enabling technology for minimally invasive cardiac interventional guidance. IEEE Rev Biomed Eng. 2010;3:25–47.
13. Sutherland C, Hashtrudi-Zaad K, Sellens R, Abolmaesumi P, Mousavi P. An augmented reality haptic training simulator for spinal needle procedures. IEEE Trans Biomed Eng. 2013;60(11):3009–18.
14. Yeo CT, Ungi T, U-Thainual P, Lasso A, McGraw RC, Fichtinger G. The effect of augmented reality training on percutaneous needle placement in spinal facet joint injections. IEEE Trans Biomed Eng. 2011;58(7):2031–7.
15. Moult E, Ungi T, Welch M, Lu J, McGraw RC, Fichtinger G. Ultrasound-guided facet joint injection training using perk tutor. Int J CARS. 2013;8(5):831–6.
16. Abe Y, Sato S, Kato K, Hyakumachi T, Yanagibashi Y, Ito M, et al. A novel 3D guidance system using augmented reality for percutaneous vertebroplasty: technical note. J Neurosurg Spine. 2013;19(4):492–501.
17. Rojas-Muñoz E, Cabrera ME, Andersen D, Popescu V, Marley S, Mullis B, et al. Surgical Telementoring without encumbrance: a comparative study of see-through augmented reality-based approaches. Ann Surg. 2019;270(2):384–9.
18. Andersen D, Popescu V, Cabrera ME, Shanghavi A, Gomez G, Marley S, et al. Medical telementoring using an augmented reality transparent display. Surgery. 2016;159(6):1646–53.
19. Vera AM, Russo M, Mohsin A, Tsuda S. Augmented reality telementoring (ART) platform: a randomized controlled trial to assess the efficacy of a new surgical education technology. Surg Endosc. 2014;28(12):3467–72.
20. Ryu WHA, Dharampal N, Mostafa AE, Sharlin E, Kopp G, Jacobs WB, et al. Systematic review of patient-specific surgical simulation: toward advancing medical education. J Surg Educ. 2017;74(6):1028–38.
21. Stefan P, Pfandler M, Lazarovici M, Weigl M, Navab N, Euler E, et al. Three-dimensional–printed computed tomography–based bone models for spine surgery simulation. Simul Healthc. 2020;15(1):61–6.
22. Harrop J, Rezai AR, Hoh DJ, Ghobrial GM, Sharan A. Neurosurgical training with a novel cervical spine simulator: posterior foraminotomy and laminectomy. Neurosurgery. 2013;73(Suppl 1):S94–9.
23. Hollensteiner M, Fuerst D, Schrempf A. Artificial muscles for a novel simulator in minimally invasive spine surgery. In: 2014 36th annual international conference of the IEEE engineering in medicine and biology society. 2014. p. 506–9.
24. Stefan P, Habert S, Winkler A, Lazarovici M, Fürmetz J, Eck U, et al. A radiation-free mixed-reality training environment and assessment concept for C-arm-based surgery. Int J CARS. 2018;13(9):1335–44.
25. Lockyer J, Carraccio C, Chan M-K, Hart D, Smee S, Touchie C, et al. Core principles of assessment in competency-based medical education. Med Teach. 2017;39(6):609–16.
26. van der Vleuten CPM, Schuwirth LWT, Scheele F, Driessen EW, Hodges B. The assessment of professional competence: building blocks for theory development. Best Pract Res Clin Obstet Gynaecol. 2010;24(6):703–19.
27. Lavoie P, Deschênes M-F, Nolin R, Bélisle M, Blanchet Garneau A, Boyer L, et al. Beyond technology: a scoping review of features that promote fidelity and authenticity in simulation-based health professional education. Clin Simul Nurs. 2020;42:22–41.
28. Durning SJ, Artino AR. Situativity theory: a perspective on how participants and the environment can interact: AMEE guide no. 52. Med Teach. 2011;33(3):188–99.
29. Pfandler M, Stefan P, Mehren C, Lazarovici M, Weigl M. Technical and nontechnical skills in surgery: a simulated operating room environment study. Spine. 2019;44(23):E1396.
30. Weidert S, et al. The unfair advantage of hybrid spine surgery simulation for percutaneous pedicle screw placement makes it as effective as training on a cadaver: a prospective randomized study with novice volunteers. Eur Spine J. 2020;29:2853–939.

# 42 Immersive Virtual Reality of Endoscopic and Open Spine Surgery Training

Danny P. Goel, Ryan Lohre, Jeffrey C. Wang, and Jin-Sung Kim

## 42.1 Introduction

Simulation in surgical education provides trainees with an opportunity to acquire or retain skills. Skill in spine surgery may be defined as technical or non-technical – procedural knowledge and understanding. As trainees begin to acquire skill, task recall gradually improves until it is autonomous. Fitts and Posner described a well-recognized skill acquisition from novice to levels of expertise in this manner [1]. The ultimate goal of a simulator is to provide training scenarios that graduate a trainee to replicate a skill or task to a level of proficiency in a clinical environment. This skill transfer, or transfer validity, of a simulator is dependent on the inherent capabilities or simulator traits, as well as the circumstances and temporality of its use. Research into the effectiveness of simulator training shows that initial and incremental improvements eventually plateau [2]. The ability of the simulator to provide efficient and effective training correlative to real-world experiences defines the simulator's transfer effectiveness of skills [3].

Simulator research combines subjective and objective assessments to validate the realism, teaching capacity, and ability to distinguish and differentiate the skills of the user. These validation schemas are termed face, content, and construct validity, respectively [4]. Face and content validity are evaluated using subjective questionnaires while construct validity may be examined by simulated task performance, simulator performance metric scales, or by using machine learning and artificial intelligence algorithms. An ideal surgical simulator would provide a realistic learning environment, capable of distinguishing novice from advanced users and provide a teaching curriculum in line with the expectations of each level of learner to provide measurable skill improvements when evaluated in a real operative scenario. In achieving this, a simulator would satisfy all aspects of validity measures. With computing power, simulators are able to now track user performance and provide metric data. These feedback systems should provide consistent, reliable information that is valid and correlative to

D. P. Goel (✉)
UBC Department of Orthopedic Surgery, Vancouver, BC, Canada

PrecisionOS, Vancouver, BC, Canada
e-mail: danny@precisionostech.com

R. Lohre
University of British Columbia Department of Orthopaedics, Vancouver, BC, Canada

J. C. Wang
Orthopaedic Spine Service, USC Spine Center, Los Angeles, CA, USA

Orthopaedic Surgery and Neurosurgery, USC Spine Center, Los Angeles, CA, USA

J.-S. Kim
Department of Neurosurgery, Seoul St Mary's Hospital, The Catholic University of Korea, College of Medicine, Seoul, Korea (Republic of)



J.-S. Kim et al. (eds.), *Technical Advances in Minimally Invasive Spine Surgery*,
https://doi.org/10.1007/978-981-19-0175-1_42

real operative scenarios. This information should also be easily accessible and interpretable to aid in user understanding of areas of deficiency. Finally, training should be efficient and enjoyable as determined by the user via subjective assessment methods. Study quality in simulator use is best evaluated by quality assessments such as the Medical Education Research Study Quality Instrument (MERSQI), Best Medical Education Evaluation global scale, and Newcastle–Ottawa Scale [5–7]. Kirkpatrick described a hierarchy of measuring educational outcomes as (1) reaction - focusing on perceptions of the intervention; (2) learning - evaluating knowledge, skills, and attitudinal changes; (3) behavior; and (4) results - focuses on the organizational benefits obtained [8]. The MERSQI framework has the largest body of evidence on these scales and adopts a methodological assessment that satisfies Kirkpatrick's framework for simulator effectiveness [9]. Carter et al. devised a modified Oxford Centre for Evidence-Based Medicine (OCEBM) level of evidence and recommendation format for simulators [10]. These research instruments have been used to assess immersive virtual reality (iVR) simulators used in spine surgery education and their use should be continued to provide clear study descriptors.

Realistic simulator use is particularly of interest in spine surgery training due to the high procedural learning curve and potentially catastrophic complications from error. Simulators used in spine surgery have been of varying fidelity, or realism, extending from simple bone composite models, three-dimensional printed patient-specific models, low-fidelity virtual training systems, mixed reality (MR) simulators including iVR and augmented reality (AR), to fresh frozen cadaveric specimens. Anders Ericsson described the concept of deliberate practice as directly attributable to gaining expertise [11]. For an individual learning scenario to provide an opportunity for deliberate practice, it must be immersive, provide personalized feedback, and must permit repetitive and productive failure. Most recently, novel (iVR) simulators have been developed with these advanced learning concepts in mind. Systems provide uninterrupted and immersive practice to surgeons devoid of patient harm. Research into the transfer of skill of these systems is currently limited given their novelty, but the theoretic applicability of these systems stands to disrupt the concept of spine simulation training.

## 42.2 Immersive Virtual Reality

Improvements in computing power have aided the development of high-fidelity simulators. Most recently, simulators have been developed that utilize consumer-level electronics to provide realistic audiovisuals coupled with additional tactile sensory input. A trainee interacts with a simulated operating room through software installed on a head-mounted display (HMD) which houses the hardware and operating system. Three-dimensional, interactive imaging is displayed through the HMD via stereoscopic imaging – one monitor per eye. Immersion, or the sense of being inside of the computer-generated world, is a result of both the quality and number of sensory dimensions experienced by the user simultaneously. Figure 42.1 provides an example of a surgical trainee using a contemporary iVR system. For the operating rooms to be truly immersive in iVR simulators, the visuals must be to a life-size scale and accommodate perspective changes [12]. The computing power of the HMD allows for trainees to seamlessly change their virtual perspective by moving their heads or changing their gaze, overcoming noticeable monitor latency and frame rate. Speakers situated on the HMD near the user's ears provide shifting audio depending on the operative environment. Users for example would hear pitch change when striking hardware with a mallet, or the sounds of a drill as it advances from cortical to cancellous bone. Controllers are utilized in these iVR simulators that provide tactile feedback in response to simulated environmental cues. The unique process of simulated force feedback and responsive translation of digital touch is termed haptics [13]. Coupling haptics through intuitive user control schemes with realistic visual perspectives provides unparalleled immersion compared to previous iterations of virtual reality

**Fig. 42.1** A surgical trainee using a contemporary immersive virtual reality simulator. The hardware is comprised of the Oculus Quest system, complete with head-mounted display and hand-based controllers. The software is produced by Precision OS Technology (Vancouver, Canada)

(VR) simulators used in spine surgery training. Using position-tracked controllers with haptics, a trainee would be able to palpate the spinous processes of a simulated patient and similarly feel the soft tissue and bone of the spinal canal with needle localization. The realism experienced in a simulator as described by the user is a method of determining the face validity of the simulator. This is typically studied using subjective Likert-scale questionnaires. The combined experience of stereoscopic visuals, auditory cues, and haptic feedback lends iVR systems in providing highly realistic environments.

Software capabilities also allow user input tracking. Task completion may be tracked to provide users with individualized module feedback. Recently, a virtual feedback and performance metric termed the Precision Score™ has been shown to strongly correlate with real-world performance in shoulder arthroplasty, including implant positioning [14]. Feedback may include a number of correct or erroneous actions by the user which can be used as stepwise progression to proficiency. Erroneous actions could include an incorrect sequence of procedural steps, incorrect needle or screw placement, plunging while drilling, or soft tissue destruction. A recent study comparing iVR to video-based training in shoulder arthroplasty demonstrated a significant reduction of errors in surgical technique and hardware implantation by those trained in iVR [14]. Head and eye as well as hand movements may be tracked to determine the efficiency of movement. Cumulative score reports are provided that delineate actionable learning points for continued skill improvement. Internet connectivity allows for data storage and retrieval by the user through multiple personal computing options and similarly may be provided to training committees for progress oversight. Given the complex regional anatomy in spinal surgery, consistent metric feedback in the virtual training space offers learners iterative knowledge and skill improvement, safely.

Simulator use and adoption is dependent on learner and instructor experiences. The experience of using an iVR simulator should provide efficient, reproducible, and enjoyable learning experiences that are aligned with learner expectations. Immersive VR simulators should also provide an intuitive user interface. Hardware and software should be readily available, understandable, scalable, reasonably priced, and upgradeable. Studies of iVR simulators have shown significantly greater enjoyment and ease of use as compared to traditional learning formats such as reading or watching videos [14, 15]. These novel iVR simulators have also demonstrated clear face, content, and construct validity [15]. In orthopedic surgery, there are currently eight studies of high (MERSQI >10) methodological quality, level of evidence of 1b (randomized controlled trials of good quality and of adequate sample size/power) providing an overall level of recommendation of 1 [14–21]. There are additionally two studies in obstetrics and gynecology (high quality) [22, 23], one study in general surgery (moderate quality) [24], and two unspeci-

fied, general skill-based studies (low quality) [25, 26]. In spine surgery, there are two randomized controlled trials (high-quality, MERSQI 12.5 and 13.5 out of 18) examining the success rate and accuracy of pedicle screw placement [27, 28]. One of these studies examines outcomes on real patients and is the only currently published evidence for direct transfer of skill from iVR simulation training to the operating room (OR) [27].

The unique ability of iVR to provide immersive OR environments affords a user-free educational and erroneous enterprise. Numerous reports have delineated medical errors to occur due to inexperience or overworked trainees [29]. Current educational systems do not afford ethical learning on real patients, necessitating realistic simulator experiences such as iVR. In spine surgery, complications of dural tear, infection, epidural hematoma, dysesthesias, spinal root, or cord injury have significant long-term effects on patient quality of life. Pedicle screw insertion has an estimated quantified value of 80 screw placements to reach an asymptote of technical skill [30]. This has been further estimated to be around 25 cases involving posterior spinal instrumentation [30]. Minimally invasive spine surgery (MISS) and endoscopic spine surgery are nearing equivalency of procedural numbers per year to open equivalents for common conditions of spinal stenosis, degenerative disk disease, or compression fracture management [31]. Similar to open surgery, endoscopic procedures require exacting three-dimensional awareness of the spinal column in localization, cannulization, and neural element visualization. Safe percutaneous endoscopic lumbar discectomy (PELD) is a moving target, with continued improvements in surgical time and outcomes demonstrated over multi-center, multi-year analyses [32]. Thus, additional learning in a controlled, immersive environment in which a surgeon is able to make an error and learn from safe, productive failure stands to greatly benefit the spine surgery community. Lohre et al. recently published a systematic review on the evidence for iVR in minimally invasive and endoscopic spine surgery training [33]. They describe a sample training workflow for an established spine surgeon, delineating virtual stock case or imported patient-specific case practice, repetition, analysis of performance, and real-life execution. Through this circle of experience, the spine surgeon can develop a better understanding and experience in 3D localization for minimally invasive techniques through a Kolb experiential learning cycle [34]. It is through immersion, individualized feedback, and learning from mistakes that iVR embodies principles of deliberate practice.

### 42.2.1 Haptics and Spine Surgery Training with Immersive Virtual Reality

Haptics has been defined as the interaction between the kinesthetic and cutaneous sensory channels and the tactile stimulation provided to them by one's environment [35]. Motor coordination and performance is predominantly affected by visual and haptic feedback [36]. Determining the compliance of an object, whether in the OR or in a simulator is thus dependent on the amount and quality of sensory information from the environment and the ability to integrate this information by the user. Limitations of human perception exist in domains of tactile and kinesthetic sensory systems. Fingertips are able to distinguish 0.15 mm point stimulus, 1 mm two-point discrimination, and vibration sequences up to 1 kHz [37]. The just noticeable difference (JND) of kinesthetic sensations is approximately 2.5 degrees for finger joints, 2 degrees for wrist and elbow joints, and 0.8 degrees for the shoulder [36]. The motor system similarly is limited by mode of operation, for example, up to 5 Hz for learned motor trajectories [38]. Incorporating instruments or barriers to cutaneous sensors attenuates sensory channels and can negatively impact haptic feedback loops. Haptic devices (hardware) thus attempt to create realistic environments at the threshold of perception, though sometimes in non-natural environments. For example, spinal level localization using a needle and fluoroscopy in real life may be replicated by iVR systems using hand-based controllers with joysticks. Combined active touch of sensory, kinesthetic,

and motor channels are actualized through realistic audio, video, and output by these non-natural devices. As a surgeon would pierce skin, fascia, and muscle, virtually a user would be able to feel varying sensory outputs through vibrational cues simulating varying tissue elasticity. Figure 42.2a, b show a representative iVR training scenario for spinal level localization with simulated fluoroscopy. As the user moves between Fig. 42.2a, b, the controllers provide tactile and kinesthetic feedback through vibratory output, simulating the feel of piercing skin and fascia. The realistic visuals, auditory cues of the OR, and tactile feedback lend to a significant sense of presence by the user.

Types of haptic controls available in iVR include commercially available hand controllers, specific force-feedback devices with multiple degrees of freedom (DOF), or exoskeletal/body-based devices such as flexible gloves or rigid linkages. Immersive VR systems used in spine surgery training and research have largely used commercially available controllers or specific force-feedback devices. Theoretic benefits of flexible gloves include improved sensory output to the user and motor input by the user [39]. Microelectrochemical systems can be used as electrostatic actuators to provide individual finger, high-resolution tactile and kinesthetic output, and technological advances are continuing in this field. Thermal stimuli may also be provided through these haptic interfaces. Evaluation of the performance of haptic devices through research is limited by generalizability [40]. There are currently no measurable, standardized performance measures of haptic devices that allow the determination of reproducibility, performance, efficiency, and realism as most previous research is highly task dependent.

Haptic devices should also be comfortable and ergonomic to use, resisting user strain with repetitive motions. A recent systematic review of neurosurgeons showed high rates of musculoskeletal strain involving the neck, lower back, shoulders, hands, and wrists compared to the general population, increasing in use of endoscopy, and an overall correlation of work hours with carpal tunnel symptoms [41]. Ergonomic simulation outside of the operating room is thus important. Overt studies into the ergonomics of iVR in surgical training have not been performed; however, Lohre et al. asked eight post-graduate year 4 and 5 orthopedic surgery residents and four experienced shoulder surgeons about their experiences with a commercially available hand-based controller haptic user interface [15]. No significant differences were seen between novices and experts in their evaluation of the realism, control interface, and comfort. Novices and experts rated the ergonomics as very ergonomic (mean 4.6 ± 0.6) on a 5-point Likert scale [15]. Bugdadi et al. analyzed perspectives of seven users of varying haptic control devices on the NeuroVR platform. There was an equal performance in the iVR subpial brain tumor resection task though clear user preference was seen, with the authors

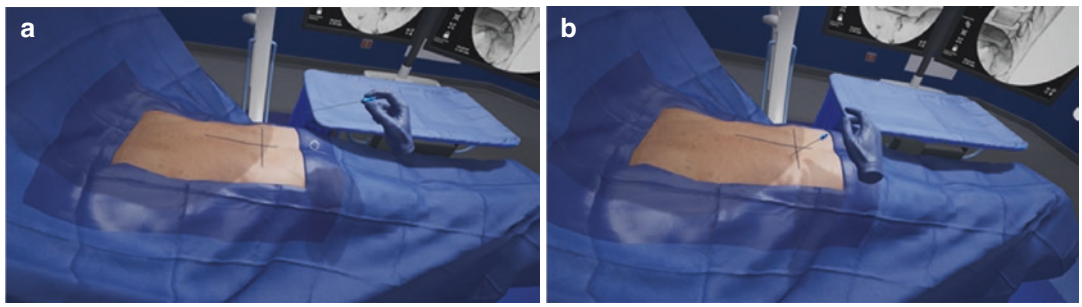


**Fig. 42.2** A representative immersive virtual reality training scenario for localization of spinal level and exiting nerve roots. (**a**) The user is able to move the spinal needle in an immersive, scaled operating room environment and with the assistance of simulated fluoroscopic guidance and superficial landmarking, (**b**) insert a spinal needle with provided haptic feedback to determine depth and endpoint tissue

recommending that presence and realism may be improved with enjoyable controllers [42]. Immersive VR is theoretically advantageous over 3D models or benchtop low fidelity systems since performing virtual tasks may be done in any environment and repositioning is easy. Eye strain or nausea has been previously described using HMD; however, newer and commercially available systems utilize high frame rates, mitigating these sensations [43]. All available studies using contemporary iVR technology in surgical trainees did not report any of these symptoms.

Differentiating novice from expert surgeons in technical skill performance can be attributable to improved haptic feedback loops developed over time. This is readily demonstrated in a systematic review examining learning curves of minimally invasive procedures including lumbar decompression, transforaminal lumbar interbody fusion, percutaneous pedicle screw insertion, laparoscopic anterior lumbar interbody fusion, and cervical procedures. All of the procedures demonstrated learning curves with a mean of 20–30 consecutive cases. An initial complication rate of 11% was seen during the first 30 procedures during decompressive surgery incorporating six publications and 528 procedures. Durotomy (80.6%), nerve root injury (9.7%), and incorrect level operation (6.4%) were the most common complications during the early learning curve. Similar complication rates were observed for pedicle screw insertion and interbody fusion [44].

## 42.3 Endoscopic Spine Surgery Training and Immersive Virtual Reality

### 42.3.1 Skill Acquisition

Minimally invasive spine surgery (MISS) volume is increasing, evidenced by a 41-fold rate of increase in publications from 1997 to 2017 [45]. Recently, the volume of MISS procedures has paralleled that of open procedures [46]. Despite potential benefits of faster patient recovery, reduced blood loss, shorter hospital stays, and ability to perform these procedures in outpatient settings, adoption by practicing surgeons may be limited [31]. Evidence of steep learning curves for MISS procedures may limit practicing surgeons from transitioning elements of their practice. Percutaneous endoscopic lumbar discectomy (PELD) multi-center studies have shown continuous improvements in surgical time as the number of cases performed increases [32]. Early learning curve complications have included dural tear, infection, epidural hematoma, and dysesthesias [47–49]. Successful endoscopic spinal procedures require specialized, distinct surgical skill sets from open procedures. Endoscopic spinal procedures rely on correct localization, canulation, and various portal or endoscope docking techniques with continuous irrigation to visualize neural elements and local anatomy. Improper visualization because of unfamiliarity can lead to complications, increased operating time, and increased fluoroscopic usage and radiation exposure [33]. Surgical trainees may be limited in their exposure and technical experience due to training centers, course offerings and access, simulator access, and instructor comfort.

Learning strategies for MISS procedures should provide consistent experiences in cognitive and technical skill acquisition, tailored to the level of experience and understanding. More novice trainees for example require a stepwise approach of anatomy understanding and deformity and pathology recognition, working toward developing surgical approaches and treatment plans. Traditionally, trainees were shown or provided a spinal model to understand the location of exiting and traversing nerve roots, foraminal pathology, disc herniations, or surgical techniques such as laminectomy. These are cumbersome and usually provided for multiple trainees and do not afford the instructor to alter the anatomy to show distinct pathology, for example, various scoliotic patterns, differing regions of disc herniations, or stable and unstable fracture patterns. Separate 3D printed spine phantoms have been promoted to overcome these limitations; however, they require costly materials and multiple printings for various pathologies [50]. Similarly, cadaveric specimens have been considered a gold standard in anatomic instruction and tissue haptics despite

the lack of translative evidence for use. In an iVR training platform, deformity, degeneration, or fracture can be modeled through stock examples or uploaded patient-specific datasets from CT scan DICOM imaging. High-resolution CT scans are required for this conversion to minimize artifacts [33]. Three-dimensional images can then be interacted with, rotated, placed in or out of patients positioned for operating room exposures and better aid in anatomic understanding. Actual procedural planning and performance can then be undertaken in iVR complete with localization fluoroscopy and MISS techniques [51]. The majority of studied iVR simulators are proprietary combinations of hardware and software utilizing HMDs and forms of haptic controllers. A recent systematic review of immersive training in spine surgery showed that out of 38 studies included for analysis, 14 specified types of simulator as VR, 11 as AR, and 10 as mixed reality (MR). Fifty-seven percent used unspecified or proprietary products. Commercial entities studied included Simulation and Visualization Research Group, NeuroSIM VR (Calgary, AB, Canada), ImmersiveTouch (San Francisco, CA, USA), Boholo Fengsuan Inc. (Shanghai, China), and NeuroVR (Montreal, Canada) [33]. Additional platforms that are commercially available include Fundamental Surgery (London, UK) pedicle screw and facetectomy modules, and Precision OS Technology (Vancouver, BC, Canada) percutaneous spinal localization module.

Simulated procedures studied using VR in MISS include microsurgical endoscopic assisted transpedicular corpectomy of the thoracic spine, lumbar puncture, cervical lateral mass screw via Magerl technique, percutaneous endoscopic lumbar discectomy (PELD), cervical, thoracic, and lumbar pedicle screw placement, general microsurgical sills, percutaneous transforaminal endoscopic discectomy (PTED), kyphoplasty and vertebroplasty, and facet joint injection.

### 42.3.2 Medical Student

Medical and undergraduate university students have been used as participants to learn technical skills in MISS procedures, particularly that of spinal localization such as lumbar puncture and lumbar face joint injections. Three studies provide evidence for the use of VR simulators in MISS skills for this population [52–54]. Validity assessments including face and content were performed in two while one study examined the transfer of skills to a real task. Kulcsar et al. randomized 27 medical students to receive VR training versus conventional (in-person technical workshop using an orange) [52]. A robust assessment protocol of knowledge (written multiple-choice examination) and skill through overall real-world performance (global ratings scale, task-specific checklist, and repeat video review by examiners) was employed. Knowledge did not differ between groups, though the VR-trained group outperformed the control via the global ratings scale of performance. Interestingly, the video review did not show a significant difference in performance between groups, though overall assessor rating agreement was seen to be low and between 68.2% and 73.8%. The additional studies only assessed participants on the simulator to track performance [52]. Farber at el. demonstrated improved performance over three sessions, though no significant testing was performed [53]. Moult et al. showed that undergraduate students learning L3/4 and L4/5 facet injections with a VR simulator (Perk Tutor (Kingston, Canada)) outperformed a control with a success rate of 61.5% compared to 38.5% when performed on a simulated phantom spine [54]. Overall study quality shows a MERSQI score between 10.5 and 12.5, indicating high methodological quality and level of evidence of 2a. The studied systems are traditional VR format and not immersive VR. There are no current studies available for the use of iVR in training this population in spine surgery.

### 42.3.3 Resident

Literature on resident training in MISS using VR simulators focuses on lumbar puncture and percutaneous pedicle screw placement. The majority of studies examining residents as participants are

for open procedures and pedicle screw insertion into cervical, lumbar, and thoracic vertebra [55–57]. Through a VR/MR (3D Slicer) platform, Yu et al. showed that residents learning transforaminal endoscopic surgical system (THESSYS) technique with 3D anatomic visualization of the spine was superior to conventional 2D (fluoroscopic) learning when analyzed by outcomes of puncture time, task total completion times, and overall fluoroscopy times. Outcomes were measured by repeat performance on a spine phantom model. The authors additionally developed a questionnaire for face validity of the system and showed that participants' view of the use of VR/MR in training increased following the surgical task. Interestingly, opinions on the importance of preoperative planning for PTED increased for all residents after performing the training and task [55]. Considering combinations of improved task-specific performance and cognitive behaviors, VR/MR may provide significant learning opportunities for inexperienced surgeons or residents. Keri et al. showed in an intervention-control group study design that residents trained using a VR/MR system for learning lumbar puncture localization showed significantly reduced task-specific parameters of needle path length, tissue damage, and time to needle insertion, though no differences in overall success rates [56]. Chitale et al. similarly examined eight residents learning percutaneous pedicle screw placement by an MR simulator. Residents received pre- and post-tests and VR/MR training coupled with a didactic learning session. Non-significant improvements were seen following the educational structure in an overall fluoroscopic score (number of images and overall fluoroscopic time), computer tomography score (time, start point and trajectory), and written scores. Evaluation of the results is limited by the lack of power [57].

Study quality ranged from moderate to high (MERSQI range 9.5–12.5) with levels of evidence from 3-2a. Overall, VR trainers incorporated into resident educational tasks appear to influence early learning curves when outcome measurements include task-specific items such as completion times and fluoroscopic use. Described disadvantages of MISS in practice include reliance on fluoroscopy, with novice surgeons producing far greater amounts of radiation per case than those more experienced. These studies show promise in reducing this operative variable. Translational evidence of acquired skill or knowledge to real operative scenarios remains lacking in this group, as does evaluation with more global skill assessments such as global ratings scale or OSATS scores. Furthermore, the entirety of study is based on traditional VR trainers and not iVR systems. Further research is required in this group to quantify skill improvement and the effects of iVR systems.

### 42.3.4 Surgeons

The majority of instructional literature on the use of VR in MISS training focuses on surgeon participants. Because of this, studies have examined the effects of training on actual patient outcomes and thus provide greater evidence of knowledge and skill translation. The majority of study lends evidence to preoperative planning and improved task-specific outcome measures, though intraoperative evidence for MR format simulators is also available with patient-reported outcomes. Archavlis et al. produced a pilot, feasibility study of the use of VR in preoperative planning for endoscopic and mini-open transpedicular corpectomy. Seven cases were described, two unstable burst fractures, and five metastatic oncologic cases performed by trained spine surgeons. The VR system used allowed for preoperative planning to determine area of resection, surgical distance from critical structures, and implant sizing. The authors showed that the VR system and volume-rendered spine was accurate in all measured parameters and that the use of VR in preoperative planning in endoscopic assisted spine surgical cases may be beneficial [58]. Hu et al. used a VR simulator to plan PELD in 20 patients receiving L4/5 or L5/S1 PELD and compared this to a matched traditional planning group. Both task-specific and patient-related outcomes were measured. Task-specific outcomes included time to establish channels, total operative time, and overall fluoroscopic

time, while patient outcomes included a 10-point visual analog scale (VAS) for pain, Oswestry disability index (ODA), modified Macnab's criteria for satisfaction, and overall complication rates. Technically, all parameters were significantly reduced for the group that planned in VR. Patient follow-up occurred for 6 months with no differences in any time point for VAS, ODI, or modified Macnab's criteria. One complication (transient dysesthesia) occurred in the VR group and two complications (residual disc fragments and residual neuropathic pain) occurred in the conventional planning group. The authors concluded that the benefits of the VR planning software in learning patient-specific puncture and cannula insertion for PELD was beneficial [51]. Liu et al. demonstrated in their pilot study of one group, single case design, that using their unspecified "Minimally invasive spine system training" (MISST), providing volume-rendered virtual spine models that an MISS lumbar pedicle screw insertion improved screw trajectory by the experienced surgeon. The score provided was a computer-calculated score of proprietary design that was not explicitly described [59]. Zhou et al. designed a pilot study incorporating four surgeons using an unspecified volume-rendered spine in VR for preoperative planning of lumbosacral PTED. Levels included L3/4, L4/5, and L5/S1 and were performed on cadavers following preoperative VR planning. Isocentric navigation was used and outcomes of puncture channel time and radiation exposure times were calculated showing reduced radiation exposure for all lumbar levels, though puncture time was only reduced at L4/5 and L5/S1 levels [60]. Koch et al. used an unspecified VR vertebroplasty simulator with haptic controllers and simulated fluoroscopy with 13 orthopedic trauma surgeons and neurosurgeons with an average practice duration of 5.9 years. Surgeons were trained on the VR platform and their feedback was collected during use to establish an open-ended method of face validity. Technical aspects of the virtual procedure including path length, motion smoothness, and fluoroscopy were obtained as well as overall performance metrics via OSATS and a pass/fail rating by a single expert surgeon. Only 53.8% of surgeons were seen to pass based on two evaluative sessions though scored the system favorably in mentioning realism and visuals. The lowest scored aspects of the simulator were in the category of haptic feedback, mentioned negatively by 63% [61]. Though this study does not track training efficacy or performance, it provides evidence for the applicability of these systems in training surgeons and the ability to provide outcome measures that easily track hand movements and technical performance. The authors did not correlate these variables to the human-derived OSATS score; however, composite and correlative scores should be further examined in the future.

Utilizing intraoperative MR via volume-rendered spine (Baholo, Shanhai Front Computing Company, China), Wei et al. analyzed technical and patient-specific outcomes for 40 cases of osteoporotic vertebral compression fractures treated with percutaneous vertebroplasty and randomized to treatment with MR or traditional fluoroscopy. The MR guidance group had improvements in all measured technical parameters (operation time, fluoroscopy time, PMMA volume, relative vertebral height measured by anterior/posterior height ratio, central vertebral height measured by center/posterior height ratio, change in vertebral kyphotic angle, and cement-both-endplates-contact). Lower incidence of height loss and re-collapse occurred in the MR treated cohort at 1-year follow-up. Patient VAS and ODI scores were improved compared to the control at follow-up at all intervals to 1 year [62]. The authors comment that intraoperative fluoroscopy is still required and that hardware errors required the use of fluoroscopy in some cases. This study is also limited by small sample size, inadequate power, and short interval follow-up though provides insight into the promise of improved visualization and local anatomic understanding provided by HMDs and VR/MR technology.

Wucherer et al. designed an MR/VR training environment allowing for task disruptions during vertebroplasty and demonstrated face and content validity though only through a single experienced user [63]. Weigl et al. subsequently designed a study to determine the effects of surgical disrup-

tion (telephone calls and patient discomfort intraoperatively) on spine surgical fellows measured by SURG-TLX scores (mental workload metrics), performance outcomes, and overall fluoroscopy on the same MR/VR platform [64]. Though the VR system used was not involved in surgical training or examined in terms of effectiveness, this study demonstrates the ability of these technologies to aid in understanding other aspects of surgical training that would otherwise be difficult to study.

Overall methodologic quality of studies using VR for surgeon education ranges from low (5.5) to high (13.5) by MERSQI scoring. The levels of evidence similarly range from 3 to 2a by the modified OCEBM criteria. The spectrum of MR, incorporating immersive VR visualization creates challenging categorical descriptions for unfamiliar users; however, these systems incorporate technology through HMDs allowing for more interactive virtual anatomy. Mixed reality and iVR in this group have shown both training improvements and beneficial treatment effects in patient populations. The studies however lack long-term follow-up of patients and are limited in their descriptions of devices used, availability, and cost structure thus hampering the overall impact of incorporation. As with other trainee populations, further study is required.

### 42.3.5 Summary

Evidence exists of varying methodologic quality and levels of evidence for the use of VR in spine surgical training. Studies of VR in spine training focus in general on task-specific outcomes such as procedural times, implant locations, or fluoroscopy use. Validity measurements were variably reported, at most defining realism (face validity) or ability to instruct what the simulator intended to instruct (content validity) through subjective questioning. There are studies of higher methodologic quality that determine patient-reported outcomes, with VR demonstrating improved technical performance and patient outcome measures to up to 1-year follow-up in recent studies [51]. Studies beyond 2018 utilized more contemporary immersive VR formats than earlier studies. This is an important distinction, as the level of realism in iVR training formats coupled with ongoing iterative improvements in haptic user integration may mean greater or more consistent skill improvement when studied. Figure 42.3 demonstrates visual learning capabilities of iVR technology. A patient's spine, specific to their anatomy may be volume rendered and may be interacted with in virtual space for improved regional anatomy understanding.

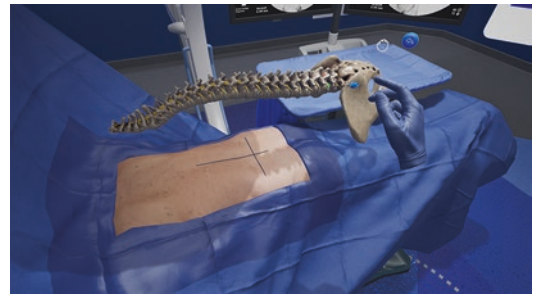

**Fig. 42.3** Immersive virtual reality systems allow for virtual interaction with patient-specific anatomy. In this case, the patient's spine is able to be removed from the body to visualize needle trajectory. Practicing in this manner may assist in learning cognitive and technical aspects of procedures thereby reducing operative time or fluoroscopic use

Delineating evidence in training subtypes from novice (medical student, resident, fellow or junior surgeon) to experienced surgeon shows distinctive themes of improvement. Novice trainees appear to benefit from the use of haptic instruction to perform successful tasks when evaluated, compared to more experienced users which gain value from the ability to preoperatively plan three dimensionally for surgical performance. Coupling VR preoperative planning with intraoperative use in an MR format continues to extend the three-dimensional understanding and has been shown to have accurate constructs with improved patient-related outcomes [51].

Further adequately powered study is required to determine the training efficiency and effectiveness of contemporary iVR simulators in endoscopic and MISS. Simulation study suffers from convenience sampling given the availability and time constraints of participants, though this may be improved by larger scale, multi-center efforts.

Studies moving away from simple technical outcome measures should incorporate more global assessments such as GRS, OSATS, or the Ottawa Surgical Competency Operating Room Evaluation (O-SCORE) as well as objectively measured training outcomes such as transfer of training ratios and transfer effectiveness ratios [14, 34]. Given learning curves have been numerically estimated for procedures, these training ratios can be used to provide evidence for alteration of learning curves. The majority of simulators studied appear to be proprietary and institutional for MISS and efforts to produce available, accessible, and intuitive systems for larger-scale training should be undertaken. Similarly, the cost of these simulators should be clearly described to ascertain the cost-effectiveness of inclusion in training for surgical educators, training programs, and practicing surgeons. Only recently have commercialized and easily accessible iVR simulators become available, with many training programs in North America and Europe using this technology at the graduate training level. Current evidence in the use of iVR is lacking given the use of proprietary training formats previously available. As incorporation has increased, so too will study into this technology.

## 42.4 Open Spine Surgery Training and Immersive Virtual Reality

### 42.4.1 Medical Student

For purposes of our review, pedicle screw training unless specified as minimally invasive will be designated as an open procedure. Study into medical student learning of pedicle screw insertion is limited to lumbar pedicle screw insertion [65]. Gasco et al. performed an intervention-control group designed pilot study of 26 neurosurgically interested medical students randomized to using the ImmersiveTouch (San Francisco, USA) VR simulator or conventional visual/verbal instruction. Participants from both groups performed two lumbar pedicle screw insertions each into a phantom model which was subsequently CT scanned to determine pedicle insertion parameters of coronal entry point, axial and sagittal deviations, length error, and pedicle breaches. Error criteria were defined as deviations in each plane of coronal, sagittal, and axial, breach, or suboptimal length. Average errors per screw were reduced from 2.08 to 0.96 with VR training. The most improved criteria were screw length (86.7%), coronal errors (71.4%), and pedicle breach (66.7%) [65]. The study design was of high quality (MERSQI score 13.5) with a level of evidence of 2a.

### 42.4.2 Resident

Research focus on VR simulation for surgical resident training focuses on the placement of pedicle screws in cervical, thoracic, and lumbar spine regions. The majority of available literature uses non-immersive VR simulators lacking HMD though incorporating realistic visuals and haptic feedback. Commercially available simulators studied for use in resident training include ImmersiveTouch and NeuroVR while the remainder are unspecified or institutional, proprietary devices and software.

Gottschalk et al. designed a study incorporating VR/MR simulated drill navigation using the Stealth 3D Navigation Unit (Medtronic, USA) and PixelStick (Plum Amazing LLC, USA) software. Fifteen orthopedic residents (PGY1–6) were given an informational packet on how to place a lateral mass screw through the Magerl technique. Baseline performance of screw insertion was determined. One group received no additional training, another received training on Sawbones with navigation, and the third group received training on cadavers using the navigation system. Repeat assessment of placement of C3-C7 screws for each participant on cadavers using navigation showed an improvement in performance for both the sawbones and cadaver groups in screw trajectory and starting point. Overall errors were reduced in the navigation trained group including nerve root injuries [66]. The use of navigation is essentially a VR/MR solution to pedicle screw placement with

sawbones and cadavers acting as haptic devices for novice residents in this study. The use of the VR system despite the lower or higher fidelity training model resulted in improved repeat performance compared to a control group that only underwent cognitive rehearsal, demonstrating the importance of 3D visualization for conceptual understanding and skill translation for trainees. Shi et al. utilized a non-immersive, unspecified VR system to train five residents in lumbar pedicle screw insertion and compared screw placement parameters to a control group receiving conventional instructional training. Pedicle screws were graded on a system described by the authors relative to penetration of the pedicle wall measured in millimeters. Residents trained using VR had higher numbers of acceptable screw placement (in pedicle or <2 mm medial wall penetration) [67]. Xin et al. utilized an unspecified, contemporary immersive VR simulator to instruct eight surgical residents in thoracolumbar pedicle screw insertion. They used an intervention-control group, randomized trial design to answer the hypothesis of whether immersive VR training was efficacious in teaching pedicle screw insertion for trainees compared to an instructional video and training session. Both groups trained for a total of 50 min before each placing six screws in T11-L4 of cadavers prior to CT scans to determine pedicle screw placement. The immersive VR-trained cohort had faster completion times and acceptable screw placement of all (100%) of screws, compared to 79.2% of screws in the control group [28]. Though small sample sizes and no overt discussion of previous experience between groups, efficiency and improved implant positioning were provided by the immersive VR system. Further study is required with larger, diverse cohorts to determine efficacy.

### 42.4.3 Surgeon

A recent study by Xin et al. using an institutionally derived immersive VR spine trainer provides evidence for the use of immersive VR in learning pedicle screw insertion in real clinical scenarios on patients [27]. Twenty-four surgeons, recently graduated from training programs and in their first year of practice were randomized to 40-minute training sessions of either a video of pedicle screw insertion technique, or performing virtual pedicle screw insertion using an immersive VR simulator. The authors used a pre- and post-test, randomized intervention-control study design to assess the efficacy of immersive VR training for spine surgeons. Measured outcomes included screw placement parameters measured in numerical and lettered grades based on the location of pedicle screws on radiographs and CT scans and placement accuracy. For a screw to be considered accurate, it required a grade of 1 and position of grade A or B when measured on radiographs (denoting appropriate trajectory and start point). Baseline performance for screw placement was not significantly different between the groups. Following training, the immersive VR trained cohort showed improved screw accuracy and number of acceptable screws compared to control. Screw accuracy improved by 22.1% and number of acceptable screws increased by 13.7%, both values being statistically significantly different [27]. The quality of study is high (13.5) by MERSQI scoring with a level of evidence of 2b by the modified OCEBM criteria. Very little has been published on the use of immersive VR simulators in providing translational skill to real operating rooms given the novelty and ethical barriers of this avenue of study. A pending publication of the use of immersive VR simulation to revise a failed hip fixation in a pediatric patient with slipped capital femoral epiphysis (SCFE) provides some of the only other translational evidence of the use of this technology. In this example, the resident performing the case was able to place two cannulated screws using significantly less fluoroscopy than the initial treating surgeon after four independent study sessions using an immersive VR simulator (Precision OS Technology, Canada). To date, the highest quality study in immersive VR literature is by Lohre et al. in their quantification of training effectiveness of immersive VR on learning reverse shoulder arthroplasty, with a MERSQI score of 14.5 [14]. The Precision OS immersive VR system provided improved learn-

ing efficiency and improved measurable performance metrics while offering a VR ratings scale of performance that correlated to real-world ability. The work by Xin et al. and other authors into translational evidence of iVR into real-world application is important for further incorporation of this technology.

## 42.5 Future Directions

Evidence for the use of VR simulators in spine surgery training is present for both MISS and open procedures in varying levels of trainee experience. Improving on realism and immersion of the training experience, immersive VR provides similar haptic interaction that may improve training experiences for trainees and spine surgeons. These devices may also assist in preoperative planning by providing interactive and patient-specific anatomy. The use of immersive VR in spine surgery is likely to evolve through study in key areas of: (1) evidence of training effectiveness for trainees and established surgeons (2) skill retention studies (3) improved haptic user interfaces (4) cost analyses and commercial availability (5) integrative efforts with the spectrum of AR and MR for preoperative planning, skill acquisition, and intraoperative virtual assistance and (6) longitudinal studies of patient-reported outcome measures.

### 42.5.1 Evidence of Training Effectiveness

The validity of immersive VR trainers in domains of face, content, construct, and transfer validity is dependent on each respective software and hardware system. Established criteria for simulators by working groups have been established and research should clearly describe these validity domains with particular focus on the transfer of acquired skill to real, or nearly equivalently real, operating room procedures. Studies designed around these validity considerations as well as MERSQI scoring will provide improved study quality and generalizability of outcomes. The study by Xin et al. is the only available study examining the effect of immersive VR training on learning pedicle screw insertion with evidence of skill translation to real patient care [27]. Training effectiveness should also be quantified through measures of skill transfer ratios based on measurable outcomes, training time, and evaluative task completion times. This information provides quantifiable evidence of transfer of skill utilized for decades in military and aviation literature and only recently studied in general surgery and orthopedic surgery for MIST-VR and Precision OS simulators [3, 14, 68]. These ratios include the transfer of training and transfer effectiveness ratios. The Precision OS immersive VR simulator used in learning reverse shoulder arthroplasty currently has the highest described transfer effectiveness at 0.79, meaning that training using the simulator for 60 minutes can account for up to 47 minutes of real operative experience. These ratios coupled with novel VR performance tracking metrics allow for direct numerical representation of where an individual is on a procedural learning curve and may thus be tracked over time to improvement with a combined real and virtual experience. Though simulation study suffers inherently from convenience sampling, efforts should be made to increase sample sizes to provide adequately powered studies with participants of various demographics and abilities and experiences. Novel applications of immersive VR to study training effectiveness in spine surgery that take advantage of system capabilities such as remote, multiple user training should be undertaken in the future. In plastic surgery, for example, remote surgeons in the USA utilized an AR training program to proctor surgeons in Peru for the treatment of cleft palate [69]. Improvements in diagnosis, counseling, technique, decision making, and operative efficiency were seen, with no tertiary care referrals required for all children treated remotely at 30-month follow-up. Global spine professional organizations may similarly utilize this technology for remote instruction.

### 42.5.2 Skill Retention

Skill retention measured through objective formats at time intervals beyond initial training sequences is the next step in evaluative literature on spine surgical VR training. Given the novelty of highly immersive VR technology, evidence of skill retention remains unpublished. This avenue of study is hampered by an inability to control for confounding variables such as adjunctive training. Little evidence exists for retention of simulation skills in general, with follow-up periods typically around 6 months [70]. In many circumstances, skill was not retained for these time periods and similarly is reflected in off-duty periods in military literature [71]. Despite this, evidence for trainees and practicing surgeons for the acquisition and longitudinal retention of gained cognitive and motor skills through immersive VR simulation would provide powerful evidence for its use.

### 42.5.3 Improved Haptic Interfaces, Commercial Availability, and Cost Analyses

Further incorporation of immersive VR technology as a training platform in institutional training programs, continuing medical education courses, training for ancillary OR staff, and industry teaching by device representatives will spur further development of enhanced user interfaces of designed VR software with haptic hardware. The limits of perception in human tactile and kinesthetic systems are known and can theoretically be reproduced in real time with available consumer-grade computing power [40]. Only recently have commercial companies realized the disruptive nature of this technology in surgical training and as evidence for added value to health care systems increases, so too will research and development.

Cost of systems is not provided for surgical VR or immersive VR training systems studied in the literature as a whole despite this being a crucial piece of information for institutional adoption. Lohre et al. demonstrated through the use of a cost-effectiveness ratio based on the comparative cost of the Precision OS system and improved task performance relative to a control (traditional course structure including flight, attendance fees, and accommodation) for a surgical trainee and found that the iVR system was 34× more cost-effective [14]. With limited institutional funding, surgeon educators and publicly funded systems require quantifiable evidence for both skill and cost-effectiveness for incorporation to mitigate opportunity costs. With costs of OR time estimated at greater than $37 per minute, adjunctive training avenues that mitigate patient risk are extremely valuable [72]. The majority of spine VR and immersive VR systems studied are not commercially available or are unspecified in the literature. With more companies producing systems, return on investment evidence increasing, the availability of these systems for training institutions, professional organizations, or individual surgeons will likely considerably increase.

### 42.5.4 Integrative Immersive VR, AR, and MR and Longitudinal Patient Study

The spectrum of MR incorporating VR and AR systems lends to a new generation of surgeons proficient in virtual technology. Use can extend from training, through preoperative planning, to intraoperative and postoperative utilization. It is important that surgeons proficient in the use of MR technology not succumb to reliance but rather leverage the benefits. Immersive VR has demonstrable improvements in technical and cognitive skill acquisition and may benefit surgeons in preoperative planning using patient-specific, interactive 3D renderings. Augmented reality has been shown to provide reliable assistance in instrumentation, though surgeon anatomical understanding and tactile expertise will remain the fundamental platform of skill that these virtual technologies help to refine. Evidence for the use of immersive VR systems in chronic and neuropathic type pain exists and maybe an adjunctive postoperative treatment strategy for cord or root injured patients [73]. Using these technologies on

real patients should be extended to high-quality studies involving prospective and long-term follow-up with validated patient-reported outcome measures to better inform patient outcomes for the utilization of this technology.

## References


1. Fitts P, Posner M. Human performance. Belmont, CA: Brooks/Cole; 1967.
2. Roscoe SN. Incremental transfer effectiveness. Tech Rep ARL-70-5/AFOSR-70-1. 1971.
3. Korteling JEH, Oprins EAPBE, Kallen VL. Measurement of effectiveness for training simulations. NATO RTO. 2009;SAS-095(2005):1–12.
4. Gallagher AG, O'Sullivan GC. How to develop metrics from first principles. In: Apell P, editor. Fundamentals of surgical simulation: principles and practices. Springer US; 2012. p. 133–40.
5. Reed D, Cook D, Beckman T. Association between funding and quality of published medical education research. JAMA. 2007;298:1002–9.
6. Hammick M, Dornan T, Steinert Y. Conducting a best evidence systematic review. Part 1: from idea to data coding. BEME guide no. 13. Med Teach. 2010;32(1):3–15.
7. Wells G, Brodksy L, O'Connell D, Shea B, Henry D, Mayank S, et al. Evaluation of the Newcastle-Ottawa Scale (NOS): an assessment tool for evaluating the quality of non-randomized studies. XI Cochrane Colloquium: Evidence, Health Care and Culture. Barcelona, Spain; 2003.
8. Yardley S, Dornan T. Kirkpatrick's levels and education "evidence". Med Educ. 2012;46(1):97–106.
9. Cook DA, Reed DA. Appraising the quality of medical education research methods: the medical education research study quality instrument and the Newcastle-Ottawa scale-education. Acad Med. 2015;90(8):1067–76.
10. Carter FJ, Schijven MP, Aggarwal R, Grantcharov T, Francis NK, Hanna GB, et al. Consensus guidelines for validation of virtual reality surgical simulators. Simul Healthc. 2006;1(3):171–9.
11. Ericsson KA. Deliberate practice and the acquisition and maintenance of expert performance in medicine and related domains. Acad Med. 2004;79(10 Suppl):S70–81.
12. Slater M, Wilbur S. A framework for immersive virtual environments (FIVE): speculations on the role of presence in virtual environments. PRESENCE Virtual Augment Real. 1997;6(6):603–16.
13. Robles de la Torre G. The importance of the sense of touch in virtual and real environments. IEEE Multimed. 2006;13(3):24–30.
14. Lohre R, Bois A, Pollock J, Lapner P, McIlquham K, Athwal GS, et al. Effectiveness of immersive virtual reality for orthopaedic surgical skills and knowledge acquisition: a randomized controlled trial. JAMA Netw Open. 2020;3(12):e2031217.
15. Lohre R, Bois A, Athwal GS, Goel DP, (CSES) TCS and ES. Improved complex skill acquisition by immersive virtual reality training: a randomized controlled trial. J Bone Jt Surg. 2020;102(6):e26.
16. Arroyo-Berezowsky C, Jorba-Elguero P, Altamirano-Cruz MA, Quinzaños-Fresnedo J. Usefulness of immersive virtual reality simulation during femoral nail application in an orthopedic fracture skills course. J Musculoskelet Surg Res. 2019;3(4):326–33.
17. Blumstein G, Zukotynski B, Cevallos N, Ishmael C, Zoller S, Burke Z, et al. Randomized trial of a virtual reality tool to teach surgical technique for tibial shaft fracture intramedullary nailing. J Surg Educ. 2020;310:1–9.
18. Hooper J, Tsiridis E, Feng JE, Poulsides L, Macaulay W, The NYU Virtual Reality Consortium. Virtual reality simulation facilitates resident training in total hip arthroplasty: a randomized controlled trial. J Arthroplast. 2019;34(10):2278–83.
19. Logishetty K, Rudran B, Cobb JP. Virtual reality training improves trainee performance in total hip arthroplasty: a randomized controlled trial. Bone Jt J. 2019;101-B(12):1585–92.
20. Logishetty K, Wade GT, Rudran B, Beaule PE, Gupte CM, Cobb JP. A multicenter randomized controlled trial evaluating the effectiveness of cognitive training for anterior approach total hip arthroplasty. J Bone Jt Surg. 2020;102(2):pe7.
21. Racy M, Barrow A, Tomlinson J, Bello F. Development and validation of a virtual reality haptic femoral nailing simulator. J Surg Educ. 2021;78(3):1013–23.
22. Bing E, Parham G, Cuevas A. Using low-cost virtual reality simulation to build surgical capacity for cervical cancer treatment. J Glob Oncol. 2019;5:1–7.
23. Frederiksen J, Sorensen S, Konge L. Cognitive load and performance in immersive virtual reality versus conventional virtual reality simulation training of laparoscopic surgery: a randomized trial. Surg Endosc. 2020;34(3):1244–52.
24. Barre J, Michelet D, Truchot J. Virtual reality single-port sleeve gastrectomy training decreases physica and mental workload in novice surgeons: an exploratory study. Obes Surg. 2019;29(4):1309–16.
25. Chaudhary A, Bukhari F, Iqbal W, Nawaz Z, Malik M. Laparoscopic training exercises using HTC VIVE. Intell Autom Soft Co. 2020;26(1):53–9.
26. Sankaranarayanan G, Odlozil C, Wells K. Training with cognitive load improves performance under similar conditions in a real surgical task. Am J Surg. 2020;220(3):620–9.
27. Xin B, Huang X, Wan W, Lv K, Hu Y, Wang J, et al. The efficacy of immersive virtual reality surgical simulator training for pedicle screw placement: a randomized double-blind controlled trial. Int Orthop. 2020;44(5):927–34.
28. Xin B, Chen G, Wang Y, Bai G, Gao X, Chu J, et al. The efficacy of immersive virtual reality surgical

simulator training for pedicle screw placement: a randomized double-blind controlled trial. World Neurosurg. 2019;124:e324–30. https://doi.org/10.1016/j.wneu.2018.12.090.
29. Dyer C. Bristol inquiry. BMJ. 2001;323(7306):181.
30. Gonzalvo A, Fitt G, Liew S, de la Harpe D, Turner P, Ton L, et al. The learning curve of pedicle screw placement: how many screws are enough? Spine (Phila Pa 1976). 2009;34(21):E761–5.
31. Butler AJ, Alam M, Wiley K, Ghasem A, Iii AJR, Wang JC. Endoscopic lumbar surgery: the state of the art in 2019. Neurospine. 2019;16(1):15–23.
32. Shi R, Wang F, Hong X, Wang Y-T, Bao J-P, Liu L, et al. Comparison of percutaneous endoscopic lumbar discectomy versus microendoscopic discectomy for the treatment of lumbar disc herniation: a meta-analysis. Int Orthop. 2019;43(4):923–37.
33. Lohre R, Wang JC, Lewandrowski K-U, Goel DP. Virtual reality in spinal endoscopy: a paradigm shift in education to support spine surgeons. J Spine Surg. 2020;6(1):S208–23.
34. Lohre R, Athwal GS, Warner JP, Goel DP. The evolution of virtual reality in shoulder and elbow surgery. JSES Int. 2020;4(2):215–23.
35. Leleve A, McDaniel T, Rossa C. Haptic training simulation. Front Virtual Real. 2020;1:1–3.
36. Durlach NI, Mavor AS, editors. Committee on Virtual Reality Research and Development. Virtual reality: scientific and technological challenges. Washington, D.C.: National Academy Press; 1995. p. 161–87.
37. Tan H, Srinivasan M, Eberman B, Cheng B. Human factors for the design of force-reflecting haptic interfaces. In: Proceedings of ASME winter annual meeting. ASME; 1994.
38. Brooks T. Telerobotic response requirements. In: Proceedings of the IEEE international conference on systems, man and cybernetics. Report No. STX/ROB/90-03. Los Angeles: STX Corporation; 1990.
39. Zhu M, Sun Z, Zhang Z, Shi Q, He T, Liu H, et al. Haptic-feedback smart glove as a creative human-machine interface (HMI) for virtual/augmented reality applications. Sci Adv. 2020;6(19):eaaz8693.
40. Hayward V, Astley OR. Performance measures for haptic interfaces. In: Giralt G, Hirzinger G, editors. Robotics research. London: Springer; 1996. p. 195–206.
41. Lavé A, Gondar R, Demetriades AK, Meling TR. Ergonomics and musculoskeletal disorders in neurosurgery: a systematic review. Acta Neurochir. 2020;162(9):2213–20. https://pubmed.ncbi.nlm.nih.gov/32705353
42. Bugdadi A, Sawaya R, Bajunaid K, Olwi D, Winkler-Schwartz A, Ledwos N, et al. Is virtual reality surgical performance influenced by force feedback device utilized? J Surg Educ. 2019;76(1):262–73.
43. Weech S, Kenny S, Barnett-Cowan M. Presence and cybersickness in virtual reality are negatively related: a review. Front Psychol. 2019;10:158. https://pubmed.ncbi.nlm.nih.gov/30778320
44. Sclafani JA, Kim CW. Complications associated with the initial learning curve of minimally invasive spine surgery: a systematic review. Clin Orthop Relat Res. 2014;472(6):1711–7. https://pubmed.ncbi.nlm.nih.gov/24510358
45. Iprenburg M, Wagner R, Godschalx A, Telfeian AE. Patient radiation exposure during transforaminal lumbar endoscopic spine surgery: a prospective study. Neurosurg Focus. 2016;40(2):E7.
46. Wewel JT, Godzik J, Uribe JS. The utilization of minimally invasive surgery techniques for the treatment of spinal deformity. J Spine Surg (Hong Kong). 2019;5(Suppl 1):S84–90.
47. Marappan K, Jothi R, Paul RS. Microendoscopic discectomy (MED) for lumbar disc herniation: comparison of learning curve of the surgery and outcome with other established case studies. J Spine Surg (Hong Kong). 2018;4(3):630–7.
48. Nowitzke AM. Assessment of the learning curve for lumbar microendoscopic discectomy. Neurosurgery. 2005;56(4):755–62.
49. Soliman HM. Irrigation endoscopic discectomy: a novel percutaneous approach for lumbar disc prolapse. Eur Spine J. 2013;22(5):1037–44. https://www.ncbi.nlm.nih.gov/pubmed/23392557
50. Bohl MA, McBryan S, Nakaji P, Chang SW, Turner JD, Kakarla K. Development and first clinical use of a novel anatomical and biomechanical testing platform for scoliosis. J Spine Surg. 2019;5(3):329–36.
51. Hu Z, Li X, Cui J, He X, Li C, Han Y, et al. Significance of preoperative planning software for puncture and channel establishment in percutaneous endoscopic lumbar DISCECTOMY: a study of 40 cases. Int J Surg. 2017;41:97–103. https://doi.org/10.1016/j.ijsu.2017.03.059.
52. Kulcsár Z, Shorten G. Preliminary evaluation of a virtual reality-based simulator for learning spinal anesthesia. J Clin Anesth. 2013;25(2):98–105.
53. Färber M, Hummel F, Gerloff C, Handels H. Virtual reality simulator for the training of lumbar punctures. Methods Inf Med. 2009;48(5):493–501.
54. Moult E, Ungi T, Welch M, Lu J, McGraw R, Fichtinger G. Ultrasound-guided facet joint injection training using Perk Tutor. Int J Comput Assist Radiol Surg. 2013;8(5):831–6.
55. Yu H, Zhou Z, Lei X, Liu H, Fan G, He S. Mixed reality-based preoperative planning for training of percutaneous transforaminal endoscopic discectomy: a feasibility study. World Neurosurg. 2019;129:e767–75. https://doi.org/10.1016/j.wneu.2019.06.020.
56. Keri Z, Sydor D, Ungi T, Holden MS, McGraw R, Mousavi P, et al. Computerized training system for ultrasound-guided lumbar puncture on abnormal spine models: a randomized controlled trial. Can J Anaesth. 2015;62(7):777–84.
57. Chitale R, Ghobrial GM, Lobel D, Harrop J. Simulated lumbar minimally invasive surgery educational model with didactic and technical components. Neurosurgery. 2013;73(4):107–10.

58. Archavlis E, Schwandt E, Kosterhon M, Gutenberg A, Nimer A, Giese A, et al. A modified microsurgical endoscopic assisted transpedicular corpectomy of the thoracic spine based on virtual 3D planning, technical note. World Neurosurg. 2016; https://doi.org/10.1016/j.wneu.2016.04.043.
59. Liu X, Bai H, Guoli S, Zhao Y, Han J. Augmented reality system training for minimally invasive spine surgery. IEEE; 2017.
60. Zhou Z, Hu S, Zhao Y, Zhu Y, Wang C, Gu X, et al. Feasibility of virtual reality combined with isocentric navigation in transforaminal percutaneous endoscopic discectomy: a cadaver study. Orthop Surg. 2019;11:493–9.
61. Koch A, Pfandler M, Stefan P, Wucherer P, Lazarovici M, Navab N, et al. Say, what is on your mind? Surgeons' evaluations of realism and usability of a virtual reality vertebroplasty simulator. Surg Innov. 2019;26(2):234–43.
62. Wei P, Yao Q, Xu Y, Zhang H, Gu Y, Wang L. Percutaneous kyphoplasty assisted with/without mixed reality technology in treatment of OVCF with IVC: a prospective study. J Orthop Surg Res. 2019;14(68):1–9.
63. Wucherer P, Stefan P, Abhari K, Fallavollita P, Weigl M, Lazarovici M, et al. Vertebroplasty performance on simulator for 19 surgeons using hierarchical task. Analysis. 2015;34(8):1730–7.
64. Weigl M, Stefan P, Abhari K, Wucherer P, Fallavollita P, Lazarovici M, et al. Intra-operative disruptions, surgeon' s mental workload, and technical performance in a full-scale simulated procedure. Surg Endosc. 2016;30(2):559–66.
65. Gasco J, Patel A, Ortega-barnett J, Branch D, Kuo YF, Luciano C, et al. Virtual reality spine surgery simulation: an empirical study of its usefulness virtual reality spine surgery simulation: an empirical study of its usefulness. Neurol Res. 2014;36(11):968–73.
66. Gottschalk MB, Yoon ST, Park DK, Rhee JM, Mitchell PM. Surgical training using three-dimensional simulation in placement of cervical lateral mass screws: a blinded randomized control trial. Spine J. 2015;15(1):168–75. https://doi.org/10.1016/j.spinee.2014.08.444.
67. Shi J, Hou Y, Lin Y, Chen H, Yuan W. Role of visuohaptic surgical training simulator in resident education of orthopedic surgery. World Neurosurg. 2017;111:e98–e104. https://doi.org/10.1016/j.wneu.2017.12.015.
68. Gallagher AG, O'Sullivan GC. Fundamentals of surgical simulation: principles and practices. New York: Springer; 2012. p. 1–372.
69. Vyas RM, Sayadi LR, Bendit D, Hamdan US. Using virtual augmented reality to remotely proctor overseas surgical outreach: building long-term international capacity and sustainability. Plast Reconstr Surg. 2020;146(5):622e–9e. https://journals.lww.com/plasreconsurg/Fulltext/2020/11000/Using_Virtual_Augmented_Reality_to_Remotely.40.aspx
70. Atesok K, Satava RM, Van Heest A, Hogan MV, Pedowitz RA, Fu FH, et al. Retention of skills after simulation-based training in orthopaedic. J Am Acad Orthop Surg. 2016;24(8):505–14.
71. Perez RS, Skinner A, Weyhrauch P, Niehaus J, Lathan C, Schwaitzberg SD, et al. Prevention of surgical skill decay. Mil Med. 2013;178(10):76–87.
72. Childers PC, Maggard-Gibbons M. Understanding costs of care in the operating room. JAMA Surg. 2018;153(4):e176233.
73. Mallari B, Spaeth EK, Goh H, Boyd BS. Virtual reality as an analgesic for acute and chronic pain in adults: a systematic review and meta-analysis. J Pain Res. 2019;12:2053–85.

# 43 Future Applications of Virtual Reality in Spinal Surgery

Gustav Burström, Oscar Persson, Erik Edström, and Adrian Elmi-Terander

Although studies have already shown the benefits of using VR as part of spine surgical training, widespread use is still lacking. The ideal application of VR in surgical training is probably yet to be found, and the same can be said for the ideal type of VR solution. Most likely, the most significant innovative steps in spine surgical VR simulation have not yet occurred.

The most obvious direction of innovation seeks to improve upon the existing systems. With an increasingly lifelike VR experience, tactical feedback, and adaptive tissue simulation, VR simulation in everyday surgical training could become the norm. The experience could also be extended to include multiple people in the same VR experience so that multiple VR headsets are tracked and positioned accordingly. This would simulate a surgical setup in which students and experts alike can see and interact in the same virtual space, facilitating discussion and teaching during the VR experience. This could also be used in high-level discussions among surgeons for determining the best approach to specific surgical cases.

One potential field of innovation involves the use of VR simulation for distance education. Up until today, surgical training has been performed in person by a teacher and one or more students. With evolving VR simulation technologies, spine surgery could be taught at a distance. This "telementoring" may be especially suited for beginners in surgical training when basic hand–eye coordination and procedures taught through step-by-step instructions are the main goals of the training. Additionally, it can create an unprecedented level of preparedness in spine surgery residents when they enter the operating theater.

In the future, VR simulation could also support advanced spine surgical training by placing stereoscopic wide-angle cameras in the operating room to mimic the view of an assisting surgeon. The prospect of having masterclasses for new spine surgeons, delivered as fully immersive VR simulations of real surgeries performed by expert surgeons, could allow surgical professionals to learn from the best members of their field all over the world. Whereas expert courses are used today to further a person's surgical skills, VR simulation could potentially make complex or rare surgeries available for spine surgeons worldwide to participate in and learn from.

The opposite situation might also be suited for VR distance learning: for example, a junior spine surgeon would like assistance or guidance from a senior colleague. In this situation, VR could be used for remote guidance during surgeries where

G. Burström · O. Persson · E. Edström
A. Elmi-Terander (✉)
Department of Clinical Neuroscience, Karolinska Institute, Stockholm, Sweden

Department of Neurosurgery, Karolinska University Hospital, Stockholm, Sweden
e-mail: gustav.burstrom@ki.se; oscar.persson.1@ki.se; erik.edstrom.1@ki.se; adrian.elmi.terander@ki.se



J.-S. Kim et al. (eds.), *Technical Advances in Minimally Invasive Spine Surgery*,
https://doi.org/10.1007/978-981-19-0175-1_43

the combination of stereoscopic imagery and the ability to look around improves the experience beyond a mere video call. However, the technology would not necessarily consist of a VR video feed from inside the operating room; instead, segmented preoperative or intraoperative CT or MRI results could be discussed. This would facilitate profound discussions about surgical approaches and strategies just before or during surgery.